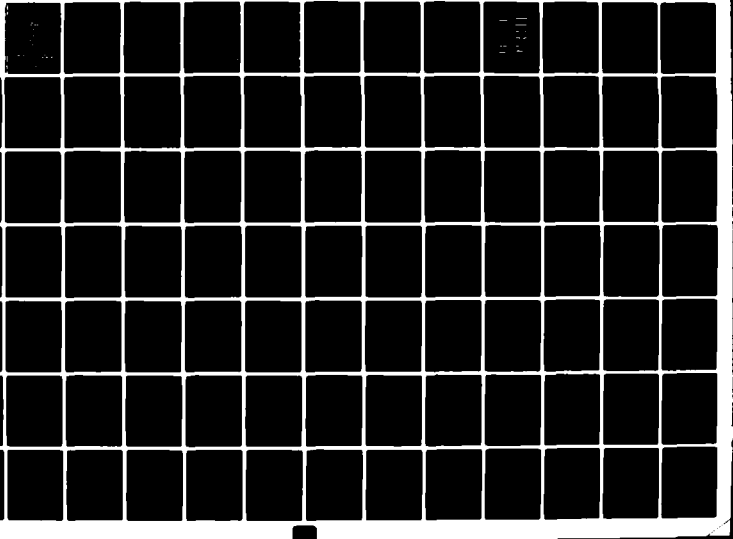
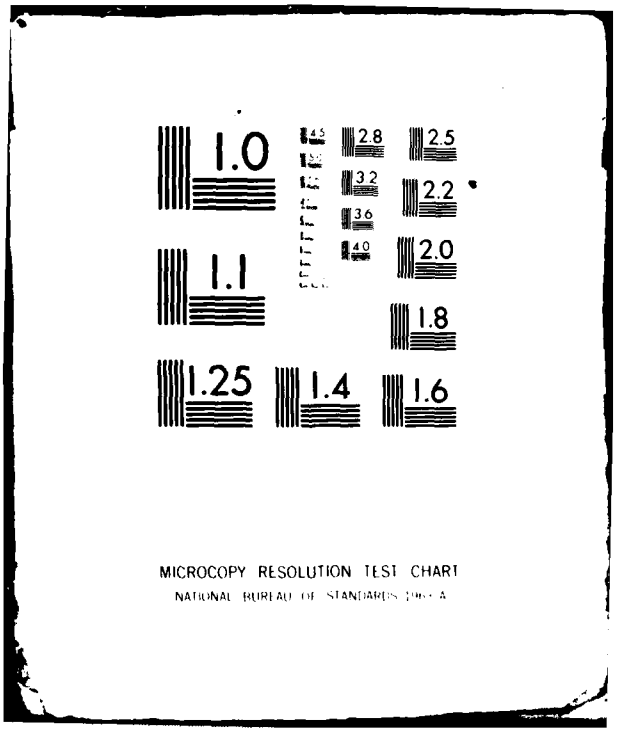
AD-A097 394 SOUTHEASTERN CENTER FOR ELECTRICAL ENGINEERING EDUCAT--ETC F/G 5/1
USAF SUMMER FACULTY RESEARCH PROGRAM, 1980, RESEARCH REPORTS, V--ETC(U)
OCT 80 W D PEELE F49620-79-C-0038

UNCLASSIFIED AFOSR-TR-81-0193 NL




1.0
1.1
1.25
1.4
1.6
1.8
2.0
2.2
2.5
2.8
3.2
3.6
4.0
MICROCOPY RESOLUTION TEST CHART
NATIONAL BUREAU OF STANDARDS 1963-A

AFOSR-TR-81-0178

AD A097394

AFOSR SCEEE

# USAF SUMMER FACULTY RESEARCH PROGRAM

1980

## RESEARCH REPORTS
## VOLUME 2

CONDUCTED BY
THE SOUTHEASTERN CENTER FOR
ELECTRICAL ENGINEERING EDUCATION

DTIC
APR 7 1981
A

DTIC FILE COPY

PROF. WARREN B. PEELE
PROGRAM DIRECTOR, SCEEE

[redacted]

[redacted]

81 4 7 036

AFOSR-TR- 81-0193

AIR FORCE OFFICE OF SCIENTIFIC RESEARCH (AFSC)
NOTICE OF TRANSMITTAL TO DDC
This technical report has been reviewed and is
approved for publication IAW AFR 190-12 (7b).
Distribution is unlimited.
A. D. Blose
Technical Information Officer

Approved for public release;
distribution unlimited.

# DISCLAIMER NOTICE

THIS DOCUMENT IS BEST QUALITY PRACTICABLE. THE COPY FURNISHED TO DTIC CONTAINED A SIGNIFICANT NUMBER OF PAGES WHICH DO NOT REPRODUCE LEGIBLY.

UNCLASSIFIED

SECURITY CLASSIFICATION OF THIS PAGE (When Data Entered)

# REPORT DOCUMENTATION PAGE

READ INSTRUCTIONS BEFORE COMPLETING FORM

| 1. REPORT NUMBER | 2. GOVT ACCESSION NO. | 3. RECIPIENT'S CATALOG NUMBER |
|---|---|---|
| AFOSR-TR-81-0193 | AD-A097394 | |

4. TITLE (and Subtitle)

USAF SUMMER FACULTY RESEARCH PROGRAM, ~~VOLUME II~~ 1980 Research Reports, Volume II of

5. TYPE OF REPORT & PERIOD COVERED

FINAL rpt.

6. PERFORMING ORG. REPORT NUMBER

7. AUTHOR(s)

Prof. Warren D. Peele

8. CONTRACT OR GRANT NUMBER(s)

F49620-79-C-0038

9. PERFORMING ORGANIZATION NAME AND ADDRESS

Southeastern Center for Electrical Engineering Education, 11th Massachusetts Ave.
St. Cloud, Florida 32769

10. PROGRAM ELEMENT, PROJECT, TASK AREA & WORK UNIT NUMBERS

61102F 2305/D5

11. CONTROLLING OFFICE NAME AND ADDRESS

AFOSR/XO
Bolling AFB, DC 20332

12. REPORT DATE

October ~~1~~ 1980

13. NUMBER OF PAGES

1123 (1125)

14. MONITORING AGENCY NAME & ADDRESS (if different from Controlling Office)

15. SECURITY CLASS. (of this report)

UNCLASSIFIED

15a. DECLASSIFICATION/DOWNGRADING SCHEDULE

16. DISTRIBUTION STATEMENT (of this Report)

Approved for public release; distribution unlimited.

17. DISTRIBUTION STATEMENT (of the abstract entered in Block 20, if different from Report)

18. SUPPLEMENTARY NOTES

19. KEY WORDS (Continue on reverse side if necessary and identify by block number)

20. ABSTRACT (Continue on reverse side if necessary and identify by block number)

The United States Air Force Summer Faculty Research Program (USAF-SFRP) is a program designed to introduce university, college, and technical institute faculty members to Air Force research. This is accomplished by the faculty members being selected on a nationally advertised competive basis for a ten-week assignment during the summer intercession to perform research at Air Force Laboratories/centers. Each assignment is in a subject area and at an

DD FORM 1 JAN 73 1473 EDITION OF 1 NOV 65 IS OBSOLETE

294958

UNCLASSIFIED

SECURITY CLASSIFICATION OF THIS PAGE (When Data Entered)

Air Force facility mutually agreed upon by the faculty member and the Air Force. In addition to compensation and travel expenses, a cost of living allowance is also paid. The USAF-SFRP is sponsored by the Air Force Office of Scientific Research/Air Force Systems Command, United States Air Force, and is conduted by the Southeastern Center for Electrical Engineering Education, Inc.

AFOSR-TR-81-0193

# 1980 USAF/SCEEE SUMMER FACULTY RESEARCH PROGRAM

Conducted by

Southeastern Center for

Electrical Engineering Education

under

USAF Contract Number F49620-79-C-0038

## RESEARCH REPORTS

Volume II of II

Submitted to

Air Force Office of Scientific Research

Bolling Air Force Base

Washington, D.C.

by

Southeastern Center for
Electrical Engineering Education

October 1980

Accession For
NTIS GRA&I
DTIC TAB
Unannounced
Justification
By
Distribution/
Availability Codes
Dist | Avail and/or Special
A

**Approved for public release; distribution unlimited.**

AIR FORCE OFFICE OF SCIENTIFIC RESEARCH (AFSC)
NOTICE OF TRANSMITTAL TO DDC
This tech[illegible] has been reviewed and is
approved [illegible] IAW AFR 190-12 (7b).
Distribution is unlimited.
A. D. BLOSE
Technical Information Officer

# PREFACE

The United States Air Force Summer Faculty Research Program (USAF-SFRP) is a program designed to introduce university, college, and technical institute faculty members to Air Force research. This is accomplished by the faculty members being selected on a nationally advertised competitive basis for a ten-week assignment during the summer intercession to perform research at Air Force laboratories/centers. Each assignment is in a subject area and at an Air Force facility mutually agreed upon by the faculty member and the Air Force. In addition to compensation and travel expenses, a cost of living allowance is also paid. The USAF-SFRP is sponsored by the Air Force Office of Scientific Research/ Air Force Systems Command, United States Air Force, and is conducted by the Southeastern Center for Electrical Engineering Education, Inc.

The specific objectives of the 1980 USAF-SFRP are:

(1) To develop the basis for continuing research of interest to the Air Force at the faculty member's institution.

(2) To further the research objectives of the Air Force.

(3) To stimulate continuing relations among faculty members and their professional peers in the Air Force.

(4) To enhance the research interests and capabilities of scientific and engineering educators.

In the 1979 summer program, 70 faculty members participated, and in the 1980 program, 87 faculty members participated. These researchers were assigned to 25 USAF laboratories/centers across the country. This three-volume document is a compilation of the final reports written by the assigned faculty members about their summer research efforts.

Pages iii thru xiv deleted
per AFOSR

8 May 81

| NAME/ADDRESS | DEGREE, SPECIALTY & LABORATORY ASSIGNMENT |
|---|---|
| Dr. David Williams<br>Assistant Professor<br>University of Texas/El Paso<br>Dept. of Electrical Engineering<br>El Paso, TX 79968<br>(915) 747-5470 [redacted] | Degree: PhD, Electrical Engineering, 1977<br>Specialty: Digital Image<br>Assigned: AFWL (Kirtland)<br>[redacted] |
| Dr. Paul Williams<br>Assistant Professor<br>University of Wisconsin/ Superior<br>Superior, WI 54880<br>(715) 392-8101 [redacted] | Degree: PhD, Professional Studies, 1976<br>Specialty: Research & Evaluation<br>Assigned: AFLC (Wright-Patterson)<br>[redacted] |
| Dr. Edward Winkofsky<br>Assistant Professor<br>Virginia Polytechnic Institute & State Univ.<br>Dept. of Business Administration<br>Blacksburg, VA 24061<br>(703) 961-5083 [redacted] | Degree: PhD, Business, 1977<br>Specialty: Quantitative Analysis, Mathematical Optimization<br>Assigned: AFAL (Wright-Patterson)<br>[redacted] |
| Dr. George Worm<br>Associate Professor<br>Clemson University<br>Dept. of Industrial Management<br>Sirrine Hall<br>Clemson, SC 29631<br>(803) 656-3499 [redacted] | Degree: PhD, Management Sciences, 1970<br>Specialty: Operations Research, Management Sciences, Math, & Statistics<br>Assigned: AFBRMC (Wright-Patterson)<br>[redacted] |
| Dr. Daniel Yannitell<br>Associate Professor<br>Louisiana State University<br>Dept. of Mechanical Engineering<br>Baton Rouge, LA 70803<br>(504) 388-5792 [redacted] | Degree: PhD, Theoretical & Applied Mech. 1967<br>Specialty: Applied Math, Fluid Mechanics Dynamics<br>Assigned: AFRPL (Edwards)<br>[redacted] |
| Dr. Yehoshua Zeevi<br>Associate Professor<br>Massachusetts Institute of Technology<br>Dept. of Aeronautics & Astronics<br>Cambridge, MA 02139<br>(617) 253-7759 [redacted] | Degree: PhD, Electronics Engineering,<br>Specialty: Eye Movement Technology<br>Assigned: AFHRL (Williams)<br>[redacted] |

PARTICIPANT LABORATORY ASSIGNMENT

1980 USAF/SCEEE SUMMER FACULTY RESEARCH PROGRAM

APL AERO PROPULSION LABORATORY
([redacted] Force Base)
1. Dr. Leslie Fishler - Oklahoma State University
2. Dr. James Lawler - University of [redacted]
3. Dr. Albert Menard - Washington & Jefferson College
4. Dr. Dasara Rathnamma - US Naval Academy

AMRL AEROSPACE MEDICAL RESEARCH LABORATORY
([redacted] Air Force Base)
1. Dr. Inez Bacon - University of the [redacted]bia
2. Dr. Thiruvenkatasamy Govindaraj - Purdue University
3. Dr. Vernon Henderson - Grambling State University
4. Dr. Timothy Hight - Duke University
5. Dr. John Petersik - Southeast Missouri State University

AD [redacted] ARMAMENT DIVISION
(Eglin Air Force Base)
1. Dr. Stanley Benton - Tulane University
2. Dr. Karen Frair - Virginia Polytechnic Institute/State University
3. Dr. Lester Frair - Virginia Polytechnic Institute/State University
4. Dr. Royce Harbor - University of West Florida
5. Dr. James Sinclair - Rice University

AEDC [redacted] ARNOLD ENGINEERING DEVELOPMENT CENTER
(Arnold Air Force Station)
1. Dr. Arend Hagedoorn - University of Central Florida
2. Dr. Robert Kerce - David Lipscomb College

AL AVIONICS LABORATORY
(Wright-Patterson Air Force Base)
1. Dr. Frank Brown - University of Kentucky
2. [redacted] Wright State University
3. Dr. Max Mintz - University of Pennsylvania
4. Prof. Harry Nienhaus - University of South Florida
5. Dr. Edward Winkofsky - Virginia Polytechnic Institute/State University

[redacted]
BRMC BUSINESS RESEARCH MANAGEMENT CENTER
(Wright-Patterson Air Force Base)
1. Dr. Frederick Bear - Western Carolina University
2. Dr. Sallye Benoit - Nicholls State University
3. Dr. Richard Burton - Duke University
4. Dr. George Worm - Clemson University

ESMC EASTERN SPACE & MISSILE CENTER
(Patrick Air Force Base)
1. Dr. Venkateswararao Vemuri - State University of New York/ Binghamton

PARTICIPANT LABORATORY ASSIGNMENT (Continued)

ESD — ELECTRONIC SYSTEMS DIVISION
(Hanscom Air Force Base)
1. Dr. John Papageorgiou - University of Massachusetts/Boston

ESC — ENGINEERING & SERVICES CENTER
(Tyndall Air Force Base)
1. Dr. Thomas Baseheart - University of Cincinnati
2. Dr. James Gossett - Cornell University
3. Dr. Thomas Higgins - Arizona State University
4. Dr. Thomas Mason - Florida A&M University
5. Dr. Lawrence Rude - Virginia Polytechnic Institute/State University

FDL — FLIGHT DYNAMICS LABORATORY
(Wright-Patterson Air Force Base)
1. Dr. Franklin Eastep - North Carolina State University
2. Dr. Arthur Grainger - Atlanta University
3. Dr. Sherif Noah - Texas A&M University
4. Dr. Louise Raphael - Clark College
5. Dr. Kuldip Rattan - Wright State University
6. Dr. Shiva Singh - University of Kentucky
7. Dr. Akhouri Sinha - Purdue University

FJSRL — FRANK J. SEILER RESEARCH LABORATORY
(USAF Academy)
1. Dr. Richard Beckro - Virginia Polytechnic Institute/State University
2. Dr. Howard Sherwood - University of Central Florida
3. Dr. Almon Turner - University of Detroit

GL — GEOPHYSICS LABORATORY
(Hanscom Air Force Base)
1. Dr. Robert Armstrong - New Mexico State University
2. Dr. Stephen Berman - University of Oklahoma
3. Dr. David Cooke - University of Utah
4. Dr. Peter Hierl - Kansas University
5. Dr. George Peace - College of the Holy Cross
6. Dr. William Tucker - Florida A&M University

HRL/ASD — HUMAN RESOURCES LABORATORY/ADVANCED SYSTEMS DIVISION
(Wright-Patterson Air Force Base)
1. Dr. Larry Wall - New Mexico State University
2. Dr. Richard Warren - State University College/Buffalo

HRL/FTD — HUMAN RESOURCES LABORATORY/FLYING TRAINING DIVISION
(Williams Air Force Base)
1. Prof. Marshall Waller - George Washington University
2. Dr. Yehoshua Zeevi - Massachusetts Institute of Technology

HRL/PRD — HUMAN RESOURCES LABORATORY/PERSONNEL RESEARCH DIVISION
(Brooks Air Force Base)
1. Dr. Howard Alford - Morgan State University
2. Dr. Richard Christ - New Mexico State University
3. Dr. Philip Tolin - Central Washington University

PARTICIPANT LABORATORY ASSIGNMENT (Continued)

HRL/TTD — HUMAN RESOURCES LABORATORY/TECHNICAL TRAINING DIVISION
(Lowry Air Force Base)
1. Dr. Barbara Lindauer - Miami University

LMDC — LEADERSHIP & MANAGEMENT DEVELOPMENT CENTER
(Maxwell Air Force Base)
1. Dr. Edward Conlon - Georgia Institute of Technology
2. Dr. Thomas Petrie - University of Nebraska/Omaha

LC — LOGISTICS COMMAND
(Wright-Patterson Air Force Base)
1. Dr. Paul Williams - University of Wisconsin/Superior

LMC — LOGISTICS MANAGEMENT CENTER
(Gunter Air Force Station)
1. Dr. Andrew Hargrove - Tuskegee Institute
2. Dr. James Patterson - Clemson University

ML — MATERIALS LABORATORY
(Wright-Patterson Air Force Base)
1. Dr. Billy Covington - Sam Houston State University
2. Dr. Charles Falkner - University of Wisconsin
3. Dr. Michael Hyer - Virginia Polytechnic Institute/State University
4. Dr. Francis Loo - Clarkson College of Technology
5. Dr. Joseph Schmidt - Memphis State University

RPL — ROCKET PROPULSION LABORATORY
(Edwards Air Force Base)
1. Dr. Joseph Chiang - State University of New York College/Oneonta
2. Dr. Chong Jin Park - San Diego State University
3. Dr. Daniel Yannitell - Louisiana State University

RADC — ROME AIR DEVELOPMENT CENTER
(Griffiss Air Force Base)
1. Dr. Caroline Eastman - Florida State University
2. Dr. Edward Lee - Wayne State University
3. Dr. Lonnie Ludeman - New Mexico State University
4. Dr. Francis Merat - Case Western Reserve University
5. Dr. Eugene Moriarty - San Jose State University

RADC/ET — ROME AIR DEVELOPMENT CENTER
(Hanscom Air Force Base)
1. Dr. Timothy Anderson - University of Florida
2. Dr. Charles Smith - University of Texas/Arlington

SAM — SCHOOL OF AEROSPACE MEDICINE
(Brooks Air Force Base)
1. Dr. Craig Daniels - University of Hartford
2. Dr. Howard Duncan - North Carolina Central University
3. Dr. Walter Kuklinski - Texas A&M University
4. Dr. Leland Morgans - University of Arkansas/Little Rock
5. Dr. Marvin Riedesel - University of New Mexico

## PARTICIPANT LABORATORY ASSIGNMENT (Continued)

WL — WEAPONS LABORATORY
(Kirtland Air Force Base)

1. Dr. Richard Fragaszy - San Diego State University
2. Dr. Rafael Jimenez-Perez - University of Puerto Rico
3. Dr. Richard McCluskey - Clarkson College
4. Dr. Gerald McIvor - Illinois Institute of Technology
5. Dr. James Steelman - New Mexico State University
6. Dr. David Williams - University of Texas/El Pasco

RESEARCH REPORTS

1980 USAF-SCEEE SUMMER FACULTY RESEARCH PROGRAM


| Volume I Report No. | Title | Research Associate |
|---|---|---|
| 1 | The Human Resources Laboratory Management Model for Increasing R&D Productivity | Dr. Howard L. Alford |
| 2 | Influence of Reaction Variables on the Electrical Properties of Homoepitaxial InP in the Hydride System | Dr. Timothy J. Anderson |
| 3 | Molecular Absorption in the Far Wings | Dr. Robert L. Armstrong |
| 4 | Teratologic Evaluation of a Model Perfluorinated Acid, NDFDA | Dr. Inez R. Bacon |
| 5 | The Response of Reinforced Concrete Structures to Near Field Explosions | Dr. Thomas M. Baseheart |
| 6 | Incentives for Defense Industry Investment | Dr. Frederick T. Bear |
| 7 | Improving Information Management Skills of the Air Force Business Research Management Center Personnel to Achieve Optimum Extension and Productivity of Research Services | Dr. Sallye S. Benoit |
| 8 | Response Surface Fitting for Missile Endgame Models | Dr. Stanley H. Benton |
| 9 | Parameterizing Boundary-Layer Processes for General Circulation Models | Dr. Stephen Berman |
| 10 | Inferential Processor | Dr. Frank M. Brown |
| 11 | Manpower Allocation in ASD's Matrix Organization | Dr. Richard M. Burton |
| 12 | Fourier Transform Infrared Spectoscopy Analysis of MNA | Dr. Joseph F. Chiang |
| 13 | An Alternative to Existing Strategies for Personnel Selection and Classification | Dr. Richard E. Christ |
| 14 | Investigations of Behavioral Consultation in the Air Force | Dr. Edward J. Conlon |
| 15 | Investigation of Aspects of the Cosmic Ray Penumbra | Dr. David J. Cooke |
| 16 | Infrared Study of Silicon: Indium, NTD Silicon, and Silicon-Germanium Alloys | Dr. Billy C. Covington |

RESEARCH REPORTS (Continued)

| Report No. | Title | Research Associate |
|---|---|---|
| 17 | Measurement of Coronary-Prone Behavior and Autonomic Reactivity | Dr. Craig E. Daniels |
| 18 | Modeling Network Disruption | Dr. Richard F. Deckro |
| 19 | Serologic Evaluation of Chagas' Disease in Nonhuman Primates | Dr. Howard B. Duncan |
| 20 | Nonlinear Oscillations of a Fluttering Panel in a Transonic Airstream | Dr. Franklin E. Eastep |
| 21 | Search Problems in Logic-Based Systems | Dr. Caroline M. Eastman |
| 22 | Operations Research Strategies for Manufacturing Control | Dr. Charles H. Falkner |
| 23 | Modeling Turbulence with a Five-Equation Reynolds Stress Closure | Dr. Leslie S. Fishler |
| 24 | A Research Program for Blast-Induced Liquefaction | Dr. Richard J. Fragaszy |
| 25 | A Theoretical Review of Detonation Waves with Possible Applications to Dispersed High Explosives | Dr. Karen L. Frair |
| 26 | Air Base Survivability--An Initial Investigation | Dr. Lester C. Frair |
| 27 | Packed Tower Air Stripping of Trichloroethylene From Dilute Aqueous Solution | Dr. James M. Gossett |
| 28 | Modeling Human Attention Allocation Strategies in Situations with Competing Criteria | Dr. Thiruvenkatasamy Govindaraj |
| 29 | Multi Dimensional Linear Interpolation | Dr. Arthur D. Grainger |
| 30 | An Interactive Command System for Building Finite Element Models | Dr. A. Henry Hagedoorn |
| 31 | An Investigation of Selected Observations Noted in Implementing Optimal Guidance in Air-to-Air Ballistic Missiles | Dr. Royce D. Harbor |
| 32 | An Assessment of Air Force Maintenance Scheduling Procedures | Dr. Andrew Hargrove |
| 33 | Effects of Hydrazine on the Morphology and Physical Development in Rainbow Trout (Salmo Gairdneri) Eggs | Dr. Vernon Henderson |

RESEARCH REPORTS (Continued)

| Report No. | Title | Research Associate |
|---|---|---|
| 34 | Translational Energy Dependence of Selected Ion-Molecule Reaction Cross Sections | Dr. Peter M. Hierl |
| 35 | Treatment of Plating Wastewater by Sulfide Precipitation, Coagulation and Upflow Filtration | Dr. Thomas E. Higgins |
| 36 | Long-Bone Injury Criteria for Use with the ATB Model | Dr. Timothy K. Hight |
| 37 | Unsymmetric Laminates | Dr. Michael W. Hyer |
| 38 | Postcracking Model for Finite Element Analysis of Reinforced Concrete | Dr. Rafael Jimenez-Perez |
| 39 | Laser Velocimeter Signal Processing | Dr. Robert H. Kerce |
| 40 | A Fast Walsh Transform Electrocardiogram Data Compression Algorithm Suitable for Microprocessor Implementation | Dr. Walter S. Kuklinski |
| 41 | Finite Difference Calculation of a Gas Heated from a Time-Dependent Horizontal Downward Facing Hot Spot | Dr. James H. L. Lawler |
| 42 | Testability Considerations for Distributed Fault-Tolerant Computer Systems | Dr. Edward T. Lee |
| 43 | On Training Mnemonics: The Role of Metacognition | Dr. Barbara K. Lindauer |
| 44 | Radiation Damage Profiles and Annealing Effects of 120 keV Sulfur Implants in GaAs | Dr. Samuel C. Ling |
| 45 | Finite Element Modeling of Elastic-Plastic Crack Growth | Dr. Francis T. C. Loo |
| 46 | Optimum Sampling Times for Spectral Estimation | Dr. Lonnie C. Ludeman |
| 47 | Generation of Singlet Delta Oxygen | Dr. Richard J. McCluskey |

RESEARCH REPORTS (Continued)

| Volume II Report No. | Title | Research Associate |
|---|---|---|
| 49 | An Investigation of the Informational Needs of the Engineering and Services Laboratory | Dr. Thomas W. Mason |
| 50 | Transient Heat Transfer in Coated Superconductors | Dr. Albert R. Menard |
| 51 | Fast Algorithms for Target Location and Identification | Dr. Francis L. Merat |
| 52 | Several Applications of Game Theory, Markov Chains, and Time Series Models to Tactical and Strategic Fire Control Systems | Dr. Max Mintz |
| 53 | The Effects of Different Environments on Auditory Canal and Rectal Temperatures | Dr. Leland F. Morgans |
| 54 | Side-Lobe Modulation | Dr. Eugene M. Moriarty |
| 55 | Automatic Fault Diagnosis of a Switching Regulator | Prof. Harry A. Nienhaus |
| 56 | Dynamic Analysis of Coupled Structures and Relationship to Test Procedures | Dr. Sherif T. Noah |
| 57 | An Application of GERT (Graphical Evaluation and Review Technique) to Air Force Systems Development Planning | Dr. John C. Papageorgiou |
| 58 | The Estimation of Decay Coefficient in Pulsed Transient Signal | Dr. Chong J. Park |
| 59 | A Preliminary Analysis of Alternative Forecasting Techniques for the Standard Base Supply System (SBSS) | Dr. J. Wayne Patterson |
| 60 | Quantitative Determination of Odd-Chlorine Species | Dr. G. Earl Peace |
| 61 | The Effects of Image Motion and Rotation on Contrast Sensitivity in a Letter Detection and Identification Task | Dr. J. Timothy Petersik |
| 62 | The Relationship of the Three Component Model of Leadership to the Development of Action Plans and Levels of Leadership | Dr. Thomas A. Petrie |
| 63 | Report I: Fitting NACA Cambered Airfoil Data by Splines<br>Report II: Inclusion Theorems for Summable Abel and Stieltjes Methods for Improper Integrals | Dr. Louise A. Raphael |

RESEARCH REPORTS (Continued)

| Report No. | Title | Research Associate |
|---|---|---|
| 64 | Evaluation of Method and Technique for Fast Estimation of Antioxidants in Turbine Engine Lubricants | Dr. Dasara V. Rathnamma |
| 65 | Digitalization of Existing Continuous-Data Control Systems | Dr. Kuldip S. Rattan |
| 66 | Physiological Responses to Wearing Fire Fighter's Ensemble on the Treadmill | Dr. Marvin L. Riedesel |
| 67 | Evaluation of the Bomb Damage Repair Computer Code | Dr. Lawrence C. Rude |
| 68 | Crack Tip Velocity Measurements During Brittle Fracture | Dr. Joseph H. Schmidt |
| 69 | Products of Fuzzy Subgroups | Dr. Howard Sherwood |
| 70 | Characterization of Quasi-Correlated Mux Bus Traffic in a Guided Weapon | Dr. James B. Sinclair |
| 71 | Vortex Breakdown and Instability | Dr. Shiva N. Singh |
| 72 | An Application of Invariance Principle to Pilot Model for NT-33 Aircraft with Variable Coefficients and Delays | Dr. Akhouri S. C. Sinha |
| 73 | A Model and Polder Tensor for Magnetostatic Wave Interactions with Metal Strips | Dr. Charles V. Smith |
| 74 | Optimal Control of the HEL Beam | Dr. J. Eldon Steelman |
| 75 | A Study of Selected Factors Relating to Human Resource Management in the Air Force | Dr. Philip Tolin |
| 76 | Proton Induced Nuclear Events in Silicon | Dr. William P. Tucker |
| 77 | A Model for the Thermal Decomposition of TNT; Theoretical Reaction Profiles | Dr. Almon G. Turner |
| 78 | Improvement of Trajectory Tracking Accuracy of Instrumentation Ships: A Feasibility Study | Dr. Venkateswararao Vemuri |
| 79 | A Comparative Study of Organizational Structures in Air Force Maintenance Organizations Using a Macro Model: POMO VRS 66-1 | Dr. Larry C. Wall |
| 80 | Evaluation of R&D Program on Computation for Simulation | Prof. Marshall Waller |

RESEARCH REPORTS (Continued)

| Report No. | Title | Research Associate |
|---|---|---|
| 81 | The Assessment of Human Factors in Command Control and Communication Systems: Application of Non-Parametric Relative Operating Characteristics | Dr. Richard Warren |
| 82 | The Effect of Rotation, Noise and Similitude on Image Moments and Moment Invariants | Dr. David H. Williams |
| 83 | Evaluation of Depot Maintenance Cost Allocation in VAMOSC II | Dr. Paul L. Williams |
| 84 | An Analysis of the Planned Multifunction-Multiband Airborne Radio System (MFBARS) Operational Impact Study: A Marketing Perspective | Dr. Edward P. Winkofsky |
| 85 | Application of Risk Analysis in the Acquisition of Major Weapon Systems | Dr. George H. Worm |
| 86 | Pulsed Plasma Plume Modeling Study | Dr. Daniel W. Yannitell |
| 87 | Analysis of Eye Movements in Target Tracking and Detection Tasks | Dr. Yehoshua Y. Zeevi |

1980 USAF - SCEEE SUMMER FACULTY RESEARCH PROGRAM

Sponsored by the

AIR FORCE OFFICE OF SCIENTIFIC RESEARCH

Conducted by the

SOUTHEASTERN CENTER FOR ELECTRICAL ENGINEERING EDUCATION

# FINAL REPORT

# AN INVESTIGATION OF THE INFORMATIONAL NEEDS OF THE ENGINEERING AND SERVICES LABORATORY


| | |
|---|---|
| Prepared by: | Dr. Thomas W. Mason |
| Academic Rank: | Associate Professor |
| Department and University: | Department of Data Processing<br>Florida A&M University |
| Research Location: | Engineering and Services Laboratory/RDX |
| USAF Research Colleague: | Lt. Col. James Morrow |
| Date: | September 5, 1980 |
| Contract No: | F49620-79-C-0038 |

# AN INVESTIGATION OF THE INFORMATIONAL NEEDS OF THE ENGINEERING AND SERVICES LABORATORY

by

Thomas W. Mason

## ABSTRACT

The general task of management is to know: "WHAT is done by WHOM, HOW and WHEN." A description is given of the current management reporting systems that are used at the Engineering and Services Laboratory -- MASIS, Manhour accounting, Status of Resources and CMIS-LS. These systems furnish the basic reports for the Technical Management Review (TMR).

The TMR can be significantly improved by having local access to locally produced data. Since the current database is about 3 megabytes in size, a variety of computing alternatives are available and are discussed. It is recommended that a computer be acquired with a suitable complement of terminals and be geared for the use of Project Officers.

## ACKNOWLEDGMENTS

The author thanks the Air Force Systems Command, the Air Force Office of Scientific Research and the Southeastern Center for Electrical Engineering Education for the opportunity to spend a very fruitful summer at the Engineering and Services Center, Tyndall AFB, FL. He acknowledges the hospitality shown by the entire Center as well as specific aknowledgment of the officers and staff of the Engineering and Services Laboratory.

The author would like to thank Lt. Col. Morrow for suggesting this area of investigation and for his helpfulness and guidance. He is also very appreciative of the help proffered by Maj. Rice, Capt. Fleming and Sgts. Ali, Rast and Tittle.

## I. INTRODUCTION:

A general formulation of the task of Research and Development managers can be stated as knowing, at any given time, as much as possible about:

WHAT is done by WHOM, HOW and WHEN.

WHAT refers to the definition of effort -- from Program Element to Work Unit. WHO includes information on both the performer and the monitor. HOW is a definition of all resources, both monetary and manpower, and WHEN is a measure of completion. The appropriate data include all timetables, milestone charts and measures of actual versus planned progress.

This formulation is, of course, applicable to any managerial situation. The focus of this effort, however, is to consider methods useable at the Engineering and Services Laboratory. The Laboratory is charged with providing managerial information to three reporting systems -- MASIS, Manhour Accounting and CMIS(-LS). In addition, a Status of Resources document is provided Project Officers which has data similar to the local Accounting and Finance systems.

The origin of most data is the Project Officer. His problem, generally stated, is:

> "Given a statement of the task and the funding level, accomplish the task within a fixed time period using an internal or external workforce."

The steps taken by the Project Officer to accomplish this feat are beyond the scope of this study. Of pertinent interest, however, is the process of local project management -- the Technical Management Review (TMR). This process is described more fully in a later section.

## II. OBJECTIVES:

Laboratory management is acutely aware of the shortcomings of the current informational processes. Although the system is awash with data and data requirements, there is an overriding need to unload paperwork from the Project Officers, to have a single entry point for data to be sent to external systems and to use data that has been

captured in a timely fashion. This all points to the potential for developing a laboratory-based information system.

## III. THE CURRENT PROCEDURE:

### MASIS

AFSC Regulation 80-14 establishes MASIS (Management and Scientific Information System) as the reporting system for all scientific and technical work units. MASIS is not a generalized data base management system. The data elements are categorized as follows:

Record identification
Work Unit identification
Monitor
Performer
Descriptors of Work
Procurement and Status
Resource Data
Funding identification
Fiscal Control
Duration
Man-Years

In terms of the WHAT-WHO-HOW-WHEN structuring, the MASIS categories can be aligned as follows:

WHAT
- Work Unit
- Descriptors of Work

WHO
- Monitor
- Performer

HOW
- Resource Data
- Funding identification
- Fiscal Control

WHEN
- Duration
- Man-Years

The Laboratory currently uses 61 of the 136 MASIS elements. They are shown below with 11 other elements, shown in parentheses, which were not defined in the official MASIS documentation:

WHAT
- Title

Work Unit Program Element
Work Unit Project
Work Unit Task
Work Unit Serial Number
End Product Code I, II, III
COSATI Code I, II, III
Primary Technical Need
Primary Technical Need Category
General Operational Requirement
Technical Planning Objectives
Job Order Number, JON
JON Short Title
(Job Category)
JON Work Category
System Relationship
Prime Customer
Priority Code
Work Phase Code
Benefit Code I, II
Security Classification of Work
Environmental Impact Code
Contractor Access to DD1498 Information
Invention Probability Code
Distribution Limitation Code
Patent Rights Clause
(Remarks)
(Objective)
(Approach)

WHO

Monitor Name
Office Symbol
(Phone Number)
(Grade)
Institution Sort Code
Contractor Security Access Code
Principal Investigator

HOW

Total Amount of Contract Effort
(Reimbursable Code)
(Funding Document)
(Amount)
Procurement Method
Fiscal Year of Funds
Purchase Request Number
Funding Project
Funding Task
Funding Start Date
Funding End Date
Committed Date

Committed Dollars
Obligated Date
Obligated Dollars
Direct S&E Man-Years
S&E Contract Monitor
Source of Funds

WHEN
(Begin Date)
Final Product Due Date
Estimated Completion Date
Completion Date
Informal Environmental Assessment
Formal Environmental Assessment
(Progress)

The primary data are compiled from the follwing Forms:

Program Management Directive
Program Authorization/Budget Authorization Allotment (Form AFSC 115-5)
Cost Estimates and Financial Forecast (Form 282)
Program Schedule (Form 103)

The elements are input to MASIS by the Project Officer (using the form shown in Figure 1) and the Finance Officer (using the form shown in Figure 2). The system produces a report of the type shown in Figure 3.

JON Control and Manhour Accounting

The Job Order Cost Accounting System (JOCAS) was designed to determine the total cost of accomplishing an R&D job. The Laboratory uses only the Manhour Accounting section of this system. The MASIS input form is also used for this data. Figure 4 shows the data fields which are transmitted to JOCAS only (J), MASIS only (M), or both MASIS and JOCAS (M/J).

Status of Resources

This report gives a monthly status of laboratory R&D funds at the work unit level. A sample report is shown in Figure 5. The report is prepared from the documents submitted by the Project Officers to fund work units and the manual records of obligated funds maintained

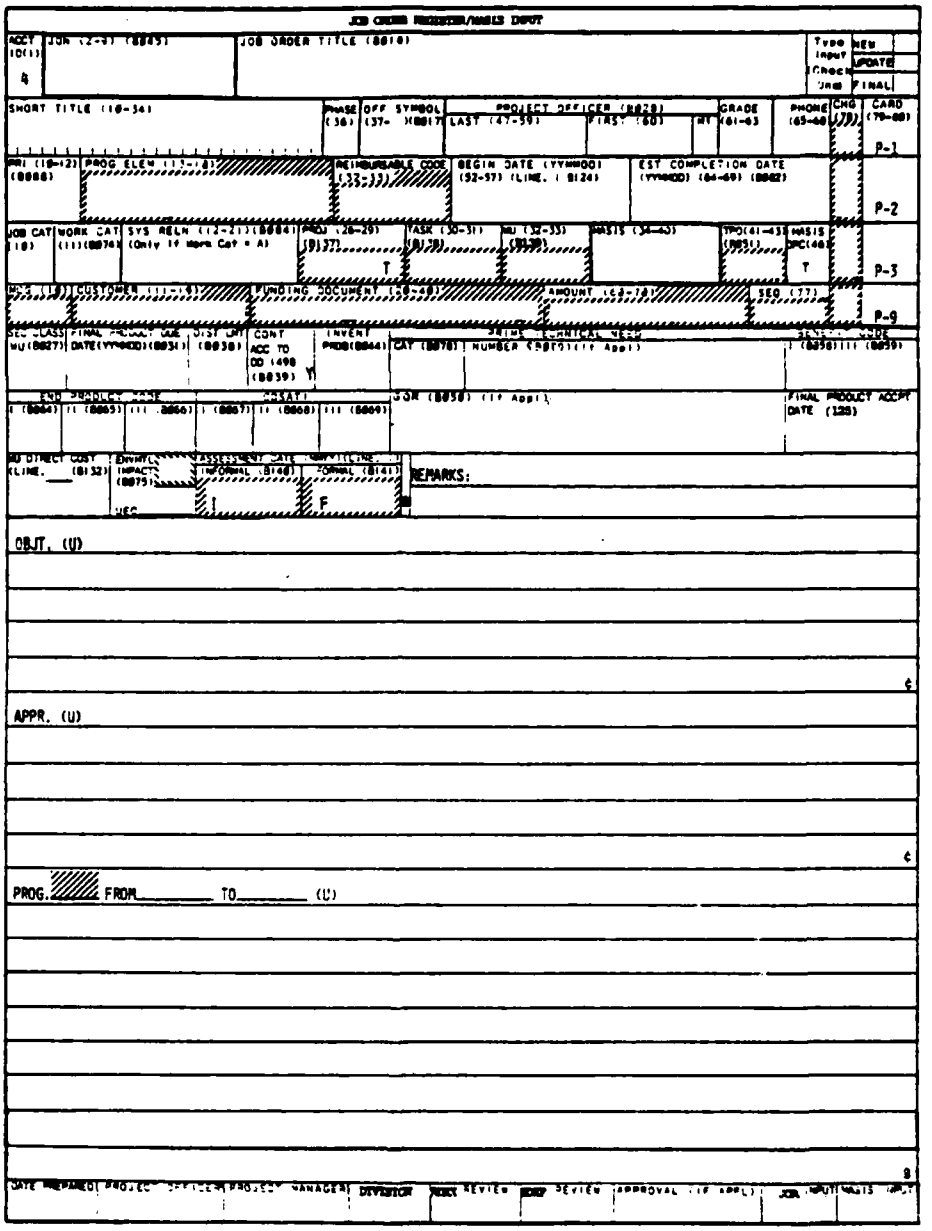



Figure 1. MASIS input form (Project Officer)

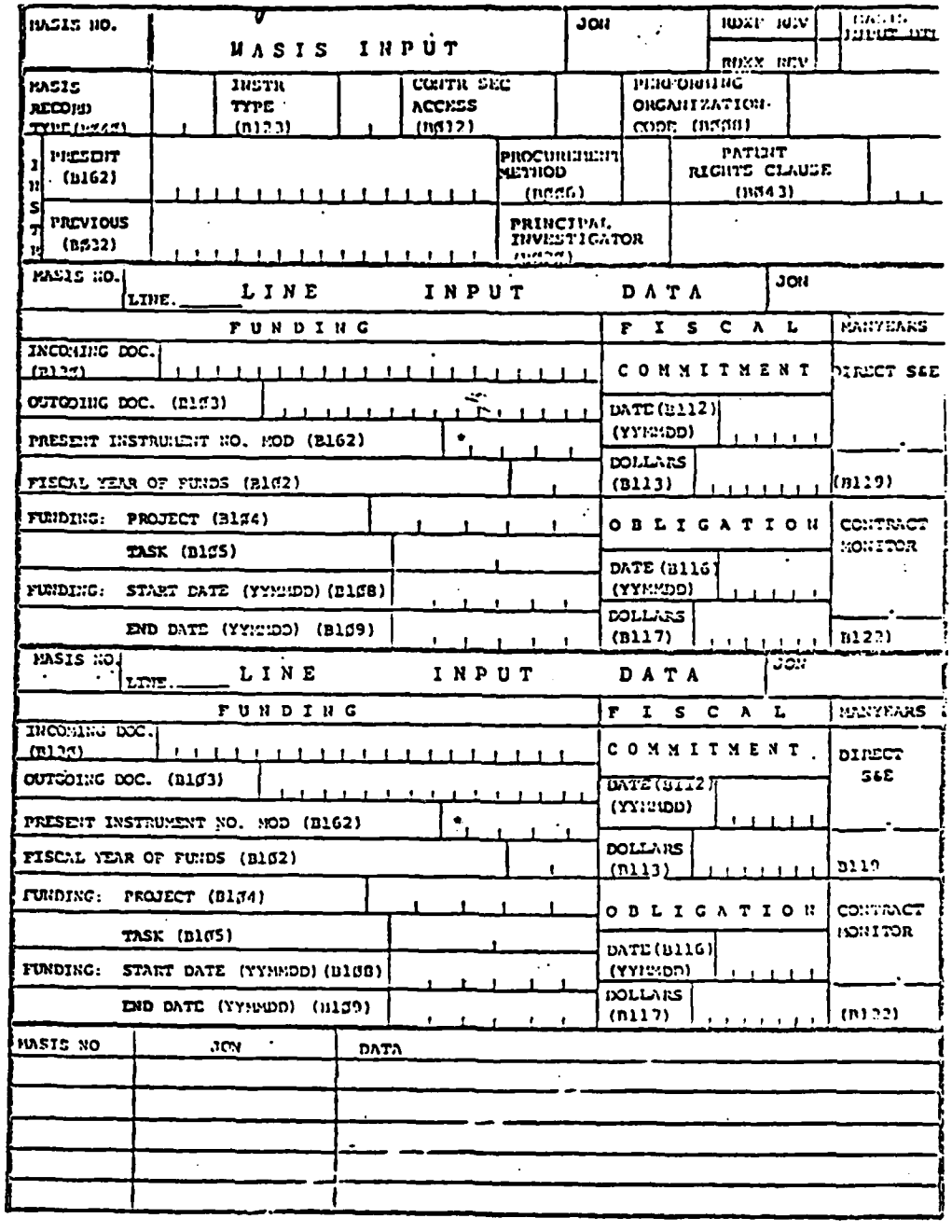
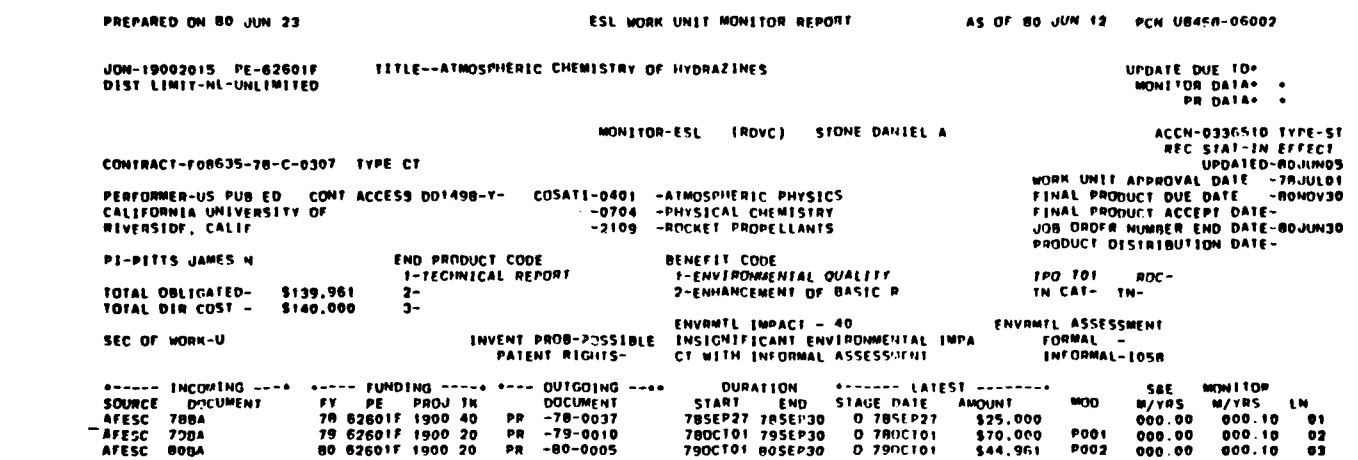



Figure 2. MASIS input form (Financial)



PREPARED ON 80 JUN 23 ESL WORK UNIT MONITOR REPORT AS OF 80 JUN 12 PCN UB458-06002

JON-19002015 PE-62601F TITLE--ATMOSPHERIC CHEMISTRY OF HYDRAZINES
DIST LIMIT-NL-UNLIMITED

UPDATE DUE TO*
MONITOR DATA* *
PR DATA* *

MONITOR-ESL (RDVC) STONE DANIEL A

ACCN-033G510 TYPE-ST
REC STAT-IN EFFECT
UPDATED-80JUN05

CONTRACT-F08635-78-C-0307 TYPE CT

WORK UNIT APPROVAL DATE -78JUL01
FINAL PRODUCT DUE DATE -80NOV30
FINAL PRODUCT ACCEPT DATE-
JOB ORDER NUMBER END DATE-80JUN30
PRODUCT DISTRIBUTION DATE-

PERFORMER-US PUB ED CONT ACCESS DD1498-Y- COSATI-0401 -ATMOSPHERIC PHYSICS
CALIFORNIA UNIVERSITY OF -0704 -PHYSICAL CHEMISTRY
RIVERSIDE, CALIF -2109 -ROCKET PROPELLANTS

PI-PITTS JAMES N

END PRODUCT CODE
1-TECHNICAL REPORT
2-
3-

BENEFIT CODE
1-ENVIRONMENTAL QUALITY
2-ENHANCEMENT OF BASIC R

TPO TOI ROC-
TN CAT- TN-

TOTAL OBLIGATED- $139,961
TOTAL DIR COST - $140,000

ENVRMTL IMPACT - 40
INSIGNIFICANT ENVIRONMENTAL IMPA
CT WITH INFORMAL ASSESSMENT

ENVRMTL ASSESSMENT
FORMAL -
INFORMAL-105R

SEC OF WORK-U

INVENT PROB-POSSIBLE
PATENT RIGHTS-

| INCOMING | | FUNDING | | | | OUTGOING | DURATION | | LATEST | | | S&E | MONITOR | |
|---|---|---|---|---|---|---|---|---|---|---|---|---|---|---|
| SOURCE | DOCUMENT | FY | PE | PROJ | TK | DOCUMENT | START | END | STAGE DATE | AMOUNT | MOD | M/YRS | M/YRS | LN |
| AFESC | 788A | 78 | 62601F | 1900 | 40 PR | -78-0037 | 78SEP27 | 78SEP30 | O 78SEP27 | $25,000 | | 000.00 | 000.10 | 01 |
| AFESC | 798A | 79 | 62601F | 1900 | 20 PR | -79-0010 | 78OCT01 | 79SEP30 | O 78OCT01 | $70,000 | P001 | 000.00 | 000.10 | 02 |
| AFESC | 808A | 80 | 62601F | 1900 | 20 PR | -80-0005 | 79OCT01 | 80SEP30 | O 79OCT01 | $44,961 | P002 | 000.00 | 000.10 | 03 |

OBJECTIVE - 79 JAN 16

(U) TO INVESTIGATE THE GAS PHASE REACTIONS OF SELECTED HYDRAZINES IN THE POLLUTED AND NATURAL TROPOSPHERE, INCLUDING KINETIC AND MECHANISTIC STUDIES. THE RESEARCH IS BEING CONDUCTED IN SUPPORT OF THE ENVIRONMENTAL QUALITY ASSESSMENT FUNCTION OF THE AIR FORCE. THIS FUNCTION IS CURRENTLY DEFICIENT WITH REGARD TO NECESSARY DETAILED KINETIC KNOWLEDGE OF THE ATMOSPHERIC REACTIONS OF HYDRAZINE BASED FUELS. THIS WORK WILL PROVIDE DATA ESSENTIAL TO AN ACCURATE ASSESSMENT OF THE ENVIRONMENTAL FATE OF THESE FUELS IN SUPPORT OF THE SPACE TRANSPORTATION SYSTEM AND F-16 FOR MISSION ACCOMPLISHMENT AND READINESS.

APPROACH - 78 MAY 04

(U) TWO AREAS OF STUDY WILL BE INVOLVED - ATMOSPHERIC SIMULATION EXPERIMENTS USING ENVIRONMENTAL CHAMBERS, AND INSTRUMENTAL STUDIES. THESE TWO AREAS WILL PROVIDE DATA ON PHOTOCHEMICAL REACTION RATES AND PRODUCTS, AND, RELATIVE REACTIVITIES, RADICALS FORMED AND MOLECULAR REACTION KINETICS RESPECTIVELY.

PROGRESS- I 80 JAN 15 TO 80 FEB 15 (INTERIM-1)

(U) THE OUTDOOR CHAMBER HAS BEEN SUCCESSFULLY USED TO TEST THE REACTIVITY OF HYDRAZINE WITH OZONE. HYDRAZINE HALF-LIFE IN THE CHAMBER IN PURIFIED AIR VARIED FROM ABOUT 250 MINUTES IN DRY AIR, TO ABOUT 100 MINUTES IN HUMID AIR. WHEN 1.64 PPM HYDRAZINE WAS COMBINED WITH 1.5 PPM OZONE, THE HYDRAZINE CONCENTRATION HAD DECREASED BY 90 PERCENT WITHIN 30 MINUTES, WITH HYDROGEN PEROXIDE AND NITROUS OXIDE FORMED AS PRINCIPAL REACTION PRODUCTS.

PCN UB458-06002 PAGE 1

Figure 3. Sample MASIS report

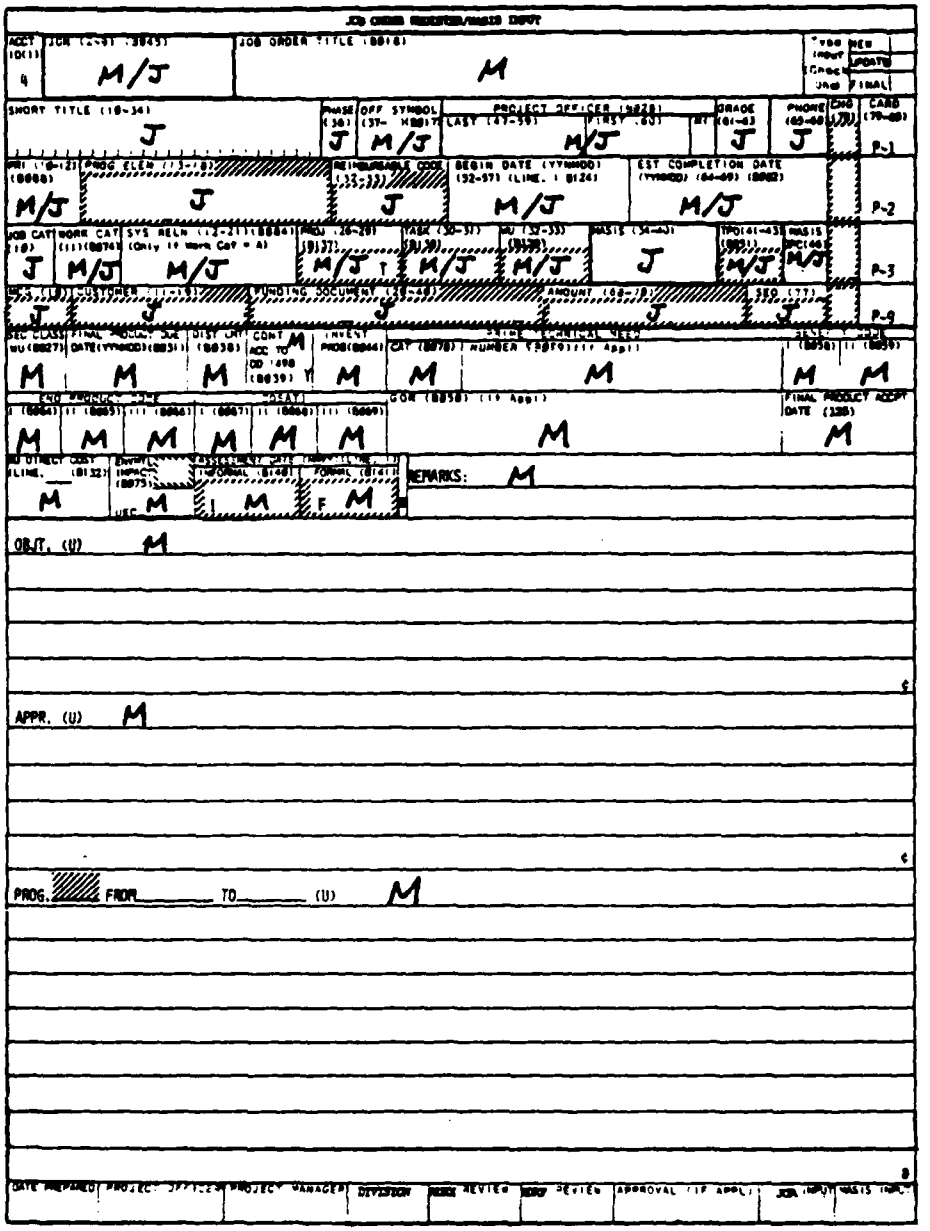



Figure 4. JOCAS input form

STATUS OF R&D FUNDS — AS OF: 31 Mar 80 — Page 8

| PROJECT JON | 2104 Civil Engineering DESCRIPTION | ANNUAL PROGRAM | INITIATIONS | COMMITMENTS | OBLIGATIONS | BALANCE | REMARKS |
|---|---|---|---|---|---|---|---|
| 2B49 | Alternate Launch and Recovery Surface Concept | 20,000 | | 25,000 | 585 | (5,585) | TOC |
| 2B50 | Tensile Structure Concept | 50,000 | | | 46,013 | 3,987 | |
| 2B51 | Small Crater Repair Manual | 40,000 | | 40,000 | | 0 | TOC |
| 2B52 | HAVE BOUNCE Simulation Support | 100,000 | | 25,000 | 74,000 | 1,000 | |
| 2B53 | Alternate Launch and Recovery Study | 105,000 | | | 102,270 | 2,730 | |
| 2B54 | C-141 Surface Roughness Simulation | 185,000 | | 84,500 | | 100,500 | |
| 4S03 | EMP Shelter Specifications | 60,000 | | 59,570 | 720 | (290) | |
| 4S04 | New Panel Designs | 90,000 | | 87,125 | 3,625 | (750) | |
| 4S05 | Foam Wall System for Expedient Facilities | 0 | | | 40,000 | (40,000) | |
| 4S06 | Advance Shelter Development | 150,000 | | 150,000 | | 0 | |
| XXXX | Surface Roughness Reserve | 45,000 | | | | 45,000 | |
| XXXX | 2104 Reserve | 205,000 | | | | 205,000 | |
| | Total | 2,400,000 | | 1,151,172 | 662,512 | 586,316 | |
| | Percent of Program | | | 48.0 | 27.6 | 24.4 | |
| | | | | | | | |
| | | | | | | | |
| | | | | | | | |
| | | | | | | | |

Figure 5. Monthly Status of Resources report

by RDXF.

CMIS

Air Force Systems Command has utilized a series of automated systems, each of which is oriented toward a specialized managerial need:

| Management Need | System |
|---|---|
| Division (Program) Management | Automation of SPO management (AUTOSPO) |
| Center Management | FIMS (Facilities Information Management System) |
| People Management | Manpower/Personnel |
| Laboratory Management | Management and Scientific Information System (MASIS) |
| Contract Management | Procurement Management Reporting System |

In an effort to unify these systems in accordance with current database management methodology, a "global" Command Management Information System (CMIS) has been proposed. CMIS, however, is to be built in sections and the initial portion is the system to support the AFSC laboratories -- CMIS-L.

CMIS-L is to provide "effective and flexible management information systems with the capability to implement advanced management concepts within HQ AFSC/DL organizations at both the headquarters and field levels." It is to consist of a headquarters-DL MIS (CMIS-LH) and a variety of field level MIS. CMIS-L is to ultimately include all current MIS in use by all organizational elements under DL. Thus, all of the systems mentioned above -- financial/accounting, procurement tracking, work unit management and personnel -- will ultimately be a part of CMIS-L.

The existing portion of this ambitious project is an interim version of the headquarters-DL system -- CMIS-LS. The system has been implemented in System 2000; its structure is shown in Figure 6.

The next step in the development of CMIS is to define CMIS-LH and to provide communication to and from all activities with appropriate terminals to access and update data. A very tentative version

CMIS-LS

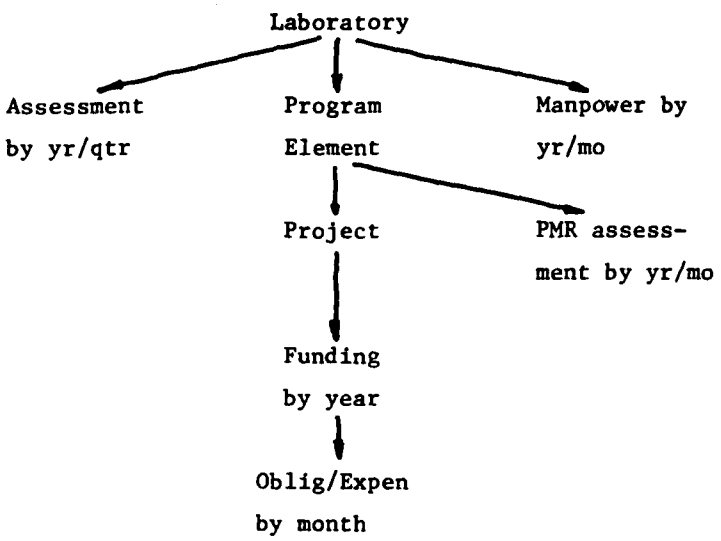



Figure 6. System 2000 structure of CMIS-LS

of CMIS-LH has been promulgated and its structure is shown in Figure 7 (only for comparative purposes with CMIS-LS).

Technical Management Review (TMR)

The TMR represents the major local use of the work unit data. The Project Officer is to supply:

a. the latest MASIS output report (Figure 3),
b. a Summary Sheet (Figure 8) showing an overall assessment, problem areas and major events,
c. a more detailed Assessment Sheet (Figure 9) which uses color and arrows to denote the betterment or worsening of conditions, and
d. a graph of actual versus forecast costs (Figure 10) as a measure of project progress.

An informal survey of Project Officers revealed that they did not consider the time necessary to prepare for the TMR to be excessive or wasted.

## IV. POTENTIAL FOR FUTURE DEVELOPMENTS:

The Laboratory does not find itself in an extreme situation in regard to informational practices. That is, the current system is not on the verge of collapse. Therefore, the analysis of what might be done to improve the local information system becomes a matter of exploring what is possible with current technology.

The basic need is to establish a local database with a suitable management system. This need arises primarily from the difficulty of entering and extracting data from the MASIS system. On the average it takes four to six weeks from the time a data element is entered to the time it appears on a MASIS report. This negates the timely use of MASIS reports for local use, particularly for the TMR.

Furthermore, a local database management system can easily be produced to automatically extract data from the local database, convert it to an appropriate format, and ship the data to various exter-

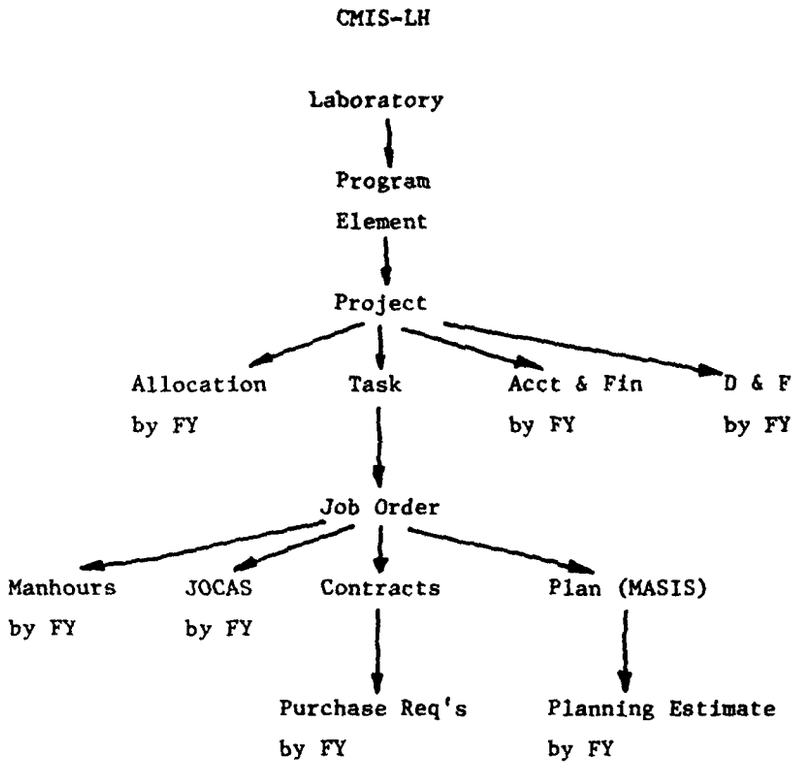



Figure 7. System 2000 structure of CMIS-LH (tentative)

# SUMMARY

**PROJECT NO.** 2054 **TITLE:** AEROSPACE FACILITIES ENG. DEV. **AS OF:** 5 AUGUST 1980

**ASSESSMENT EVALUATION:** SATISFACTORY

**PROBLEM AREAS:** NONE

**MAJOR EVENTS:**
1. VISIT BY HQ AFSC/SDNE/MR. MURAD TO PREPARE FY80 PMD. 7-8 AUG.
2. C-130 HAVE BOUNCE TESTS. 1-31 AUG.
3. NORTH FIELD TEST. 9-23 AUG.

Figure 8. TMR Summary Sheet

# PROJECT MANAGER'S ASSESSMENT

PROJECT NO: 2054 TITLE: AEROSPACE FACILITIES ENG DEV AS OF: 5 AUGUST 1980

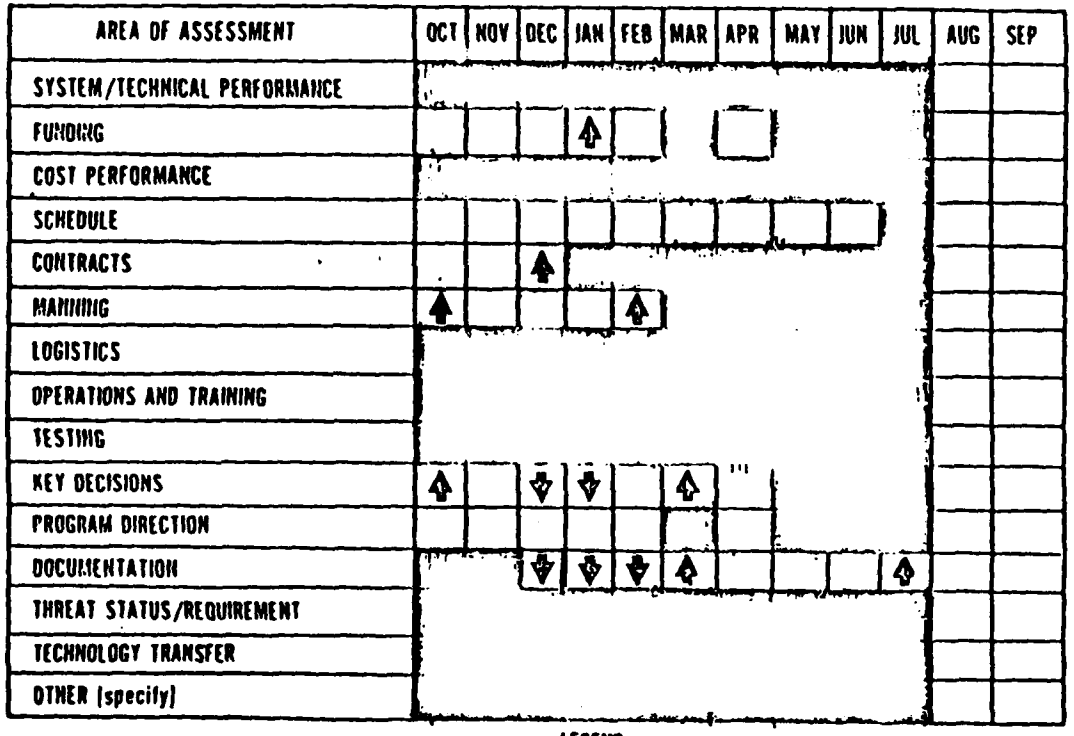



Figure 9. TMR Assessment Sheet

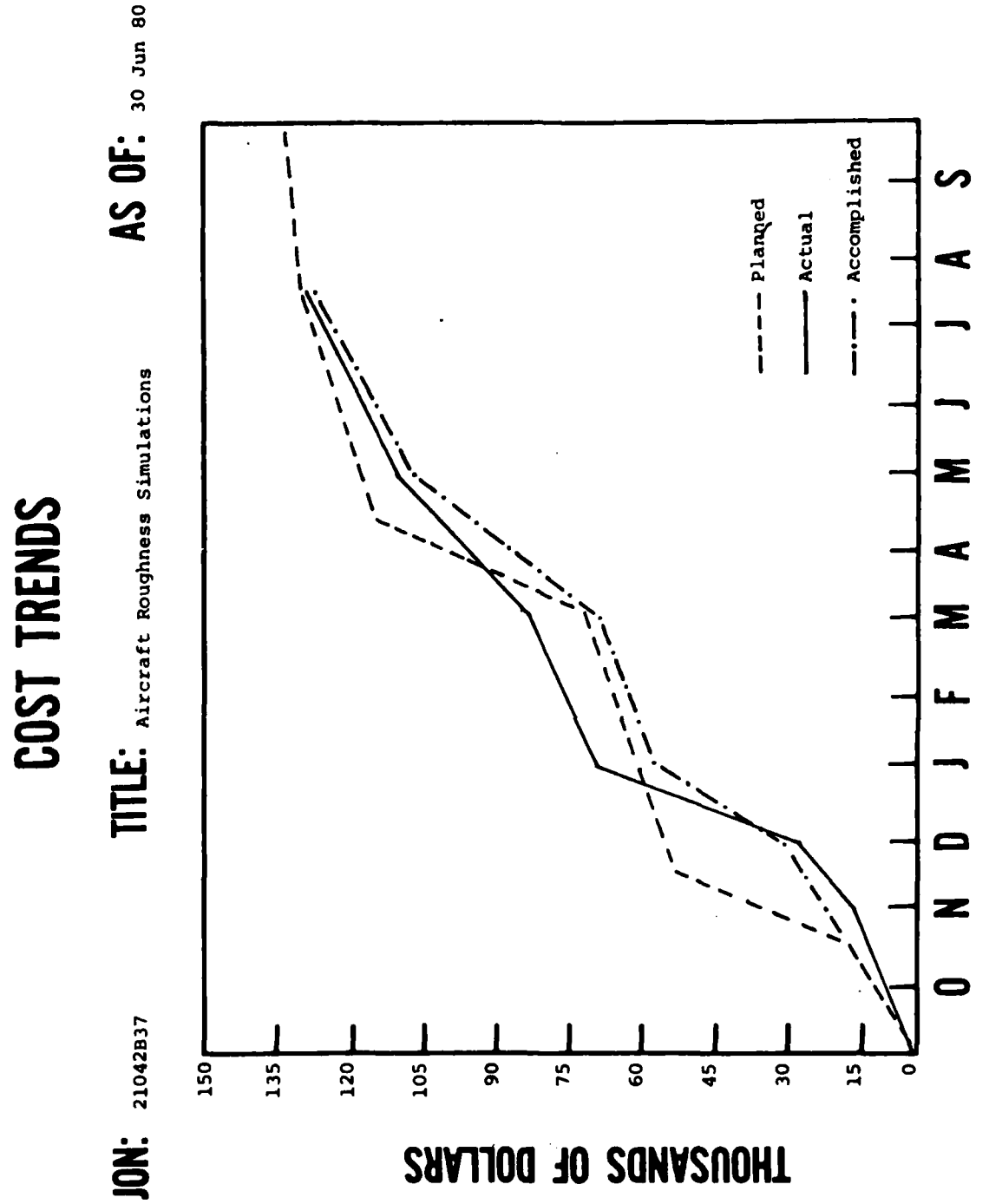



Figure 10. TMR Cost Performance Chart

nal systems. This feature will be increasingly important as the various CMIS systems grow in number and size.

It should be noted that the local database in of moderate size. A generous estimate of the size of the database is:

200 work units to be documented
300 data elements per work unit
50 characters (bytes) per data element
database size = 200 x 300 x 50 bytes = 3 megabytes

Thus, the database of 3 megabytes is even within the capacity of microcomputers as well as larger computers.

Furthermore, the entries are relatively static, although some financial data will change monthly. Also, the data for any given work unit is essentially independent of the data for any other work unit. This means that the database could even be distributed over several floppy diskettes or data cartridges rather than requiring a large disk.

In summary, then, we have a moderate (3 megabytes) database that is to satisfy external data requirements and provide internal management information. The important questions are:

a. How can a database be established locally to service external systems?
b. How can a local database help in improving the management of work units?

## V. ESTABLISHMENT OF THE DATABASE:

Particular details of the implementation of a database are, of course, dependent upon the specific hardware system to be used. So far, that decision has not been made. The system that is installed should have some processing power and storage capability. This is a minimum requirement for the Laboratory to handle current and future informational requirements. The processing power can be a microcomputer or larger. Data entry should be through terminals with graphics capability (color graphics would be even better) for output. The sys-

tem should have the capacity to store 3 megabytes of data either residentially or segmented over a reasonable number of data cartridges or diskettes.

If a minicomputer were acquired, then the processing and storage requirements would be met with ease. Graphics terminals would still be necessary -- such as Tektronix 4016's or microcomputers.

There is some chance that the acquisition of increased computing power would be coupled with the demand for sharing this resource with the operating units. This situation was discussed with Environics personnel since they are performing the bulk of in-house research. It was found that Environics has moved to acquire its own microcomputers -- HP System 4685, Tektronix 4054 and an Intel system. The only potential candidates for transfer to a local minicomputer are the Air Quality Assessment, Fuel Dump, and Dispersion models with are currently running at Eglin.

VI. LOCAL USE OF THE DATABASE ELEMENTS:

The primary R&D management tool is a presentation by the Project Officer of current management/financial status and the progress of a work unit. Thus, any local database system must have the capability of augmenting the review process.

a. Presentation

   The MASIS work unit report and the Cost Performance Chart could both be produced with the most current data. Conversations with both RDX and the Project Officers indicate this would represent a significant improvement.

b. Extensions of the TMR

   1. A paper-less TMR could be provided by presenting the presentation elements directly on the terminal.
   2. Analysis packages could be provided for more sophisticated interpretations of the contractor's cost data. The intent is to discern trends in contractor performance as early as possible.

3. An analysis of the procurement process can also be provided. By using the project milestone chart and standard estimates for the time necessary to complete the procurement paperwork, an augmented milestone chart can be produced integrating bureaucratic constraints with the regular project components. This should be very useful in the early detection of excess end-of-year funds.
4. Television and computing can be combined in the TMR. If a microcomputer is acquired with an output monitor, then it is possible to videotape part of the presentation and combine it with the computed presentation elements.

VII. RECOMMENDATIONS:

The most obvious recommendation, of course, is that the Laboratory continue its inexorable march toward a computer-based information system. The optimal strategy for acquiring processing power is moot. One can "buy into" a large remote system or one can acquire more modest, but local, capability.

My personal recommendation is for the acquisition of a local computer housed in the Laboratory. This should be accompanied by an array of terminals either clustered in one area or distributed about the Project Officers. It is important to remember that the objective of the entire effort is to significantly assist the Project Officers while simultaneously increasing managerial efficiency. This objective will be greatly enhanced by having terminals readily available for the use of the Project Officers.

The computerization of the TMR and its various components should be viewed as but the first step in the Laboratory's development. With the advent of the VANGUARD system by AFSC, the Laboratory is placed in a difficult "marketing" position. In order for programs to be funded, they must either be an obvious component of a weapon system or

or items of apparent critical importance. This implies that future budget cycles will become even more hectic as R&D projects attempt to fit within the VANGUARD scheme.

A possible solution to this problem is the development of a "what-if" system. This is a computer-based system which will allow rapid reformulation of basic data to accommodate alternative scenarios. In the trade, these are called decision support systems. The design of such a system for ESL will be the subject of my mini-grant proposal.

## REFERENCES


1. Laboratory Program Managers Guide (AFSC TR 75-02) Headquarters Air Force Systems Command
2. AFSC Regulation 80-14
3. Working papers of ESC/RDX, particularly the file on the CMIS sytems.

1980 USAF - SCEEE SUMMER FACULTY RESEARCH PROGRAM

Sponsored by the

AIR FORCE OFFICE OF SCIENTIFIC RESEARCH

Conducted by the

SOUTHEASTERN CENTER FOR ELECTRICAL ENGINEERING EDUCATION

FINAL REPORT

# TRANSIENT HEAT TRANSFER IN COATED SUPERCONDUCTORS


| | |
|---|---|
| Prepared by: | Albert Menard |
| Academic Rank: | Assistant Professor |
| Department and University: | Physics Department<br>Saginaw Valley State College |
| Research Location: | Air Force Wright Aeronautical Laboratories,<br>Aerospace Power Division, Power Systems Branch |
| USAF Research Colleague: | Dr Charles E. Oberly |
| Date: | August 11, 1980 |

# TRANSIENT HEAT TRANSFER IN COATED SUPERCONDUCTORS

by

Albert Menard

## ABSTRACT

The effect of coatings on the transient (of the order of one millisecond) heat transfer from superconductors to the surrounding helium bath is investigated. A computer model for calculating the response of a superconductor to pulses of heating is developed. This model permits the evaluation of the effectiveness of coatings in promoting heat transfer as a function of the properties of the coatings, particularly the specific heat and thermal conductivity of the coatings, the thickness of the coating, and the properties of the superconductor. A comparison of the predications of this model with existing experimental data is given. The experimental test apparatus, built to verify the predictions of the model is described. Suggestions for future research in this area is offered.

## Acknowledgement

The author would like to thank the Air Force Systems Command, the Air Force Office of Scientific Research, and the Southeastern Center for Electrical Engineering Education for providing him with the opportunity to spend a productive and interesting summer at the Air Force Wright Aeronautics Laboratory at Wright-Patterson AFB, Ohio. He would like to express his appreciation to the Power Systems Branch of the laboratory for its hospitality and helpfulness.

In particular the author wishes to thank Dr Charles Oberly for suggesting this problem and guiding the research despite other commitments on his time; Lt Scott Holmes for his hard work, knowledge, and skill in computer programming which contributed immeasurably to this project; Dr James Ho for his assistance with experimental aspects of this problem and general encouragement; and Marty Marcum and Price Thomas for technical assistance.

## I. INTRODUCTION:

The Air Force has long been interested in superconducting systems for power generation and energy storage on-board aircraft.[1] Many of the uses of the energy stored in a superconducting magnet demand that the magnet be pulsed. Pulsed magnets generate more heat energy than do steady state magnets since the eddy current heating depends on dB/dt which is much larger for the rapidly changing fields of a pulsed magnet. If the superconductor is to be kept below its transition temperature, this heat must be dissipated into the helium bath. Superconductors have a low specific heat and poor thermal conductivity, thus their temperature rises rapidly for small amounts of heating. When the temperature of the superconductor exceeds its transition temperature, it goes "normal". The "normal" superconductor heats up very rapidly due to Joule heating since it is now resistive. Such a quench as it is called leads to failure of the superconducting system and a degradation of the properties of the superconductor. Traditionally the superconductor has been stabilized by surrounding it with a copper matrix which has a high thermal conductivity and a high specific heat which absorbs and distributes any heat which is generated. Copper is relatively heavy, adding weight which is undesirable for aircraft systems. In addition the presence of copper substantially increases the eddy current heating, thus increasing the amount of energy which must be dissipated. Seeking to solve this problem Lake Shore Cryotronics of Westerville Ohio working under an Air Force contract, has recently (1979-80) developed a series of ceramic material called "Laketite" which have high thermal conductivity and/or high specific heat at low temperatures. These materials are electrical insulators. Since they are electrical insulators, they do not contribute to the eddy current heating, which arises from currents which are induced in conductors by rapidly changing magnetic fields. Also because the coatings are insulators, they could replace both the copper and the epoxy insulation in superconducting applications. These materials are less dense than copper; thus they could reduce the weight of the superconducting system - a prime concern of the Air Force. In addition the wide range of properties of

these materials creates the possibility that they could be "tailored" for specific applications. Improvement in the thermal properties of superconductors, would permit faster pulses, and higher power levels in superconducting systems. A method is needed to evaluate the performance of these materials and to allow the Air Force to select the material(s) from the group of Laketite materials that have the best set of physical properties for further testing and development.

## II. OBJECTIVES

The objective of this program is to develop a computer model that would simulate the thermal behavior of both coated and uncoated superconducting wires. Such a computer model would allow specification of the optimum properties for a coating material and the optimum thickness for a coating if it were shown that coatings enhance the thermal properties of superconductors. The model would also reveal whether the coatings would alter the heat transfer in the manner that is anticipated. Computer models must always be verified by comparison with actual experimental data. For the case of uncoated wires and surfaces, some experimental data exists. The predictions of this computer model are compared with existing experimental data. Since data for these coatings is non-existent, an experimental test facility was constructed to make measurements on coated and uncoated samples, for the purpose of comparison with the results of the computer model.

## III. THEORY

Before presenting the actual computer program, the general physical background and physical assumptions that underlie the model will follow. Since atoms in a solid are fixed, there are only two modes of heat transfer - radiation and conduction. At the low temperatures necessary for superconductivity, radiation is a very inefficient mode of heat transfer. The maximum transfer of energy by radiation is given by

$$\dot{Q}/A = \sigma \, (T_1^4 - T_2^4) \qquad (1)$$

Assuming $T_2$ = 4.2 K, the normal boiling temperature of the helium bath, and $T_1$ = 30 K a temperature well above the transition temperature of any currently known superconductor, then $\dot{Q}/A = 4.59 \times 10^{-6}$ W/cm$^2$. Any thermal disturbance of a superconductor sufficient to drive it normal would require heating power levels of the order of magnitude of Watts/square centimeters. Since the heating levels are several orders of magnitude greater than the maximum radiative heat transfer, radiative heat transfer will be ignored in this model.

For a uniformly heated cylindrical wire, heat can be conducted both radially and axially. If one considers a cylinder in which heat is transferred uniformly to the bath, i.e. equal amounts per unit surface area, then the ratio of axial to radial heat transfer is given by the ratio of the area of the ends to the area of the sides. This ratio is r/l where r is the radius of the cylinder and l is its length. For wires this ratio typically is less than .01 which means that axial heat flow is less than 1% of radial heat flow and can be ignored. However, with a copper stabilized superconductor and a low thermal conductivity electrically insulating coating, it is possible that the axial heat flow would be significant because of the much greater thermal conductivity in the axial direction along the copper, than in the radial direction across the coating. For simplicity the present model ignores axial heat transfer.

Most experimental work on heat transfer at low temperatures is done with flat plates. For a flat plate

$$\dot{Q}/A = K_m (T_o - T_i)/x \qquad (2)$$

where $K_m (T_o - T_i) = \int_{T_o}^{T_i} K(T)dT$ the integral of the thermal conductivity and x is the thickness of the plate. The integral is necessary since the thermal conductivity of materials at low temperatures is a strongly varying function of temperature. The other simple geometry that can be solved analytically is the cylindrical tube. For this case the equation for conductive heat transfer[2] is given by

$$Q/A = -2\pi LK_m(T_o - T_i)/\ \ln(r_o/r_i) \qquad (3)$$

where L is the length of the tube, $r_o$ and $r_i$ are respectively the outer and inner radius of the tube and $K_m$ is the same as the previous equation. A solid cylinder or wire can be constructed from a series of such rings. To eliminate the mathematical singularity that would occur for the innermost ring when $r_i = 0$, $r_i$ is taken at the midpoint of each ring and $r_o$ at the midpoint of the next ring except for the outermost ring where $r_o = r_s$ the radius of the surface of the wire. It can be shown that the average distance from an atom in one ring to an atom in the next ring is 8/9 of the distance between the midpoint of the two rings. Thus very little error is introduced by this procedure. By this procedure one can calculate the conductive heat transfer through a wire if the thermal conductivity and the dimensions of the wire are known.

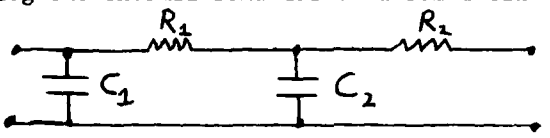
In a steady state situation this is the only contribution to heat transfer. However, for transient conditions the material is being heated by the energy passing through it. Some of the thermal energy passing through the material is absorbed. The amount of heat that is absorbed is given by

$$Q = \rho VC_p\ T \qquad (4)$$

where $\rho$ is the density of the material, V its volume, $C_p$ is the specific heat of the material, and $\Delta T$ is the temperature rise of the material. Because heat transfer is a diffusive process similar to electrical conduction, equations 2 & 4 are formally identical to the electric circuit equations for a electric current through a resistor, and the charge on a capacitor. Because electrical engineers have developed extensive computer codes such as SCEPTRE for studying the transient behavior of electric circuits, these analogy between heat flow and electric current will be exploited in developing a computer model for transient heat transfer. The complete analogies are:

| Electric | Thermal |
|---|---|
| Voltage V | Temperature T |
| Current I | Heat Flow Q |
| Charge Q | Total Heat Energy Q |
| Capacitance C | Thermal Capacity $VC_p$ |
| Resistance R | Thermal Resistance $\Delta x/K_m$ for flat plate<br>$\ln(r_o/r_i)/2\pi LK_m$<br>for the hollow tube |

Two problems arise in "translation": the units must be a completely consistent set on both sides of the analogy, and the analogy must now be carried beyond the equations it refers to, for example there is no thermal equivalent of electrical ground, or electrical energy. With this analog the thermal behavior of a solid can be modeled by an electric network:




where the subscripts represent different segments of the solid. For a wire $C_1$ is determined by the volume from 0 - $r_1$ and the density and specific heat of the material. $R_1$ is determined by the ratio of the radii of the midpoints of the first two segments and the thermal conductivity of the material. Since both the heat capacity and thermal conductivity vary significantly with temperature at low temperatures, the capacitance and resistance of the equivalent circuit are functions of the voltage across them. Coatings can be represented in the same fashion. Since both the coating and the wire are solids with similiar densities and stiffness, it is anticipated that the thermal boundary resistance between the coating and the wire would be negligible. This point should be checked experimentally, a most formidable experiment for which there is no obvious approach. This report will assume that this resistance is negligible.

The greatest problem in this approach is how to model, the heat transfer from the solid to the liquid helium bath. Because of the sharply different densities (common solids are 15-70 times as dense as liquid helium)

and very different sound velocities (solids have sound velocities 10-30 times that of helium), there is a substantial barrier to the transmission of mechanical vibrations including heat between solids and liquid helium. This thermal barrier, called the Kapitza resistance exists because of the differences in the phonon spectra between solid and helium. The general form of the Kapitza resistance from theoretical considerations[3] is

$$R_k = C\ (T_{ref}/T)^3 \qquad (5)$$

Experimentally the exponent is between 2.7 & 3.3. The coefficient varies somewhat with material. The value of 1.42 obtained by Steward[4] for Carbon films at 4K seems to be the most representative data. This report assumes that the Kapitza resistance is given by $R_k = 1.42\ (4/T)^3$.

Because helium is a fluid it can transport heat by convection and other fluid motions as well as by conduction and radiation. As in most fluids, the fluid motion terms will dominate the heat transfer. In addition liquid helium is usually at 4.2 K the normal boiling point, which means that minor changes in temperature will induce boiling. Furthermore helium at 4.2K and 1 atmosphere is close to its critical point of 5.2K and 2.2 atmospheres. This causes the thermophysical properties of helium to vary rapidly in the temperature range of greatest interest. Finally for short heat pulses it is doubtful that the liquid is in thermal equilibrium. Despite these complexities it is possible to model most of the physical processes that occur; just as it is possible to experimentally measure transient heat transfer to helium despite the formidable problems of thermometry.

There are five basic modes of heat transfer in helium. While more than one mode is usually present, normally one mode of heat transfer dominates for any given set of conditions. Which mode dominates depends on the amount of power applied to the surface - customarily called the wall and referred to by a subscript w - and the length of time that the

heating has been taking place. The modes are conduction, convection, nucleate boiling, transition, and film boiling.

For the very shortest times - less than 10 microseconds - the liquid helium is virtually stationary, and can be treated as a solid. Convection is repressed because horizontal motions of the fluid are stopped by the roughness of the surface. Without horizontal motion convection cells can not form. Since heat propagates at a finite speed, for sufficiently short periods of time the heat has not penetrated far enough into the fluid to start convection. Using a model of heat penetration into a solid[5], the penetration depth at 1 microsecond would be approximately $10^{-5}$cm. at typical value for the surface roughness of an ordinary solid. In the conductive mode the heat transfer is proportional to the difference in temperature between the wall (the surface of the wire plate etc.) and the bath

$$\dot{Q}/A \propto T_w - T_\ell \qquad \Delta T \tag{6}$$

Because of the extremely short times and small distances involved there are no measurements of the conductive mode.

As soon as the heat penetrates beyond the boundary layer, convection will begin. The heat transferred by convection is given by

$$\dot{Q}/A = h \Delta T \tag{7}$$

where h is the heat transfer coefficient. For static fluid h is about 4 times larger than the corresponding coefficient for conduction. Since both conduction and convection have the same dependence on T, it is impossible to distinguish them on the customary plots of $\dot{Q}/A$ versus $\Delta T$. The conductive/convection regime will last until there is sufficient energy per unit volume in the layer of helium adjacent to the wall to initiate nucleate boiling. At low power levels this can be a long time but at the heating power levels of interest the time for this to occur

is of the order 100 microseconds and decreases rapidly with increased power levels. Since experimentation is difficult for such short time periods, very little data exists in this region. For low power levels and short times Steward's data[4] does have a linear region suggestive of conduction of convection. In his data the onset of nucleate boiling seems to occur at a fixed energy per unit volume, but the data is not conclusive. A calculation of the thermal resistance of a layer of helium $10^{-5}$cm across transporting heat solely by conduction yields a figure of .26 compared with a Kapitza resistance of 1.2 at 4.2K. Convection would lower the thermal resistance by a factor of four. This justifies trating the Kapitza resistance as the dominant thermal resistance in this regime. A warning of the proceeding results are valid only for normal helium (He I) and are not valid for superfluid helium (He II).

The most important mode of heat transfer is nucleate boiling. Bubbles of vapor form at preferred sites; being less dense than the surrounding fluid they rise. Each bubble carries off the latent heat of vaporization of the amount of the fluid required to form the bubble, just as each parcel of convecting fluid carries off the specific heat required to heat it to the lower density required for convection. Because the latent heat of vaporization is much greater than the specific heat, nucleate boiling is a more efficient mode of heat transfer than convection. Despite the complexities of nucleate boiling, in particular its dependence on surface properties, helium as well as other cryogenic fluids follow a modified Kutateladze correlation[6] which predicts that

$$\dot{Q}/A \propto (T_w - T_l)^{2.5} \qquad (8)$$

where $T_w$ and $T_l$ are respectively the temperature of the wall and the liquid. The coefficient of this equation depends soley on the properties of the fluid. Actual experimental data[7] suggests that the exponent of equation 7 should lie between 1.9 and 2.1. This probably reflects the fact that convection whose exponent is one exists simultaneously with

nucleate boiling occupying the space between the bubbles. For this report an equation

$$\dot{Q}/A\ (T_w - T_l)^2 \qquad (9)$$

will be used as representing the mean of the experimental data. Nucleate boiling continues until a peak flux is reached. The peak flux depends strongly on the nature of the surface that is producing the heat. Values for the peak flux range from .3 - 1W/cm$^2$. The experimental values for systems most similar to ours clusters around the values used in this report $\dot{Q}/A$ = .75 W/cm$^2$ with T = .6K .

At the peak flux, the bubbles merge to form a continuous layer of gas. Because the thermal conductivity of the vapor is much lower than that of the liquid- a factor of five for helium - a large thermal resistance builds up. The amount of heat transported drops rapidly. If a constant heat flux is applied to the wall, the temperature of the wall rises very rapidly. Due to the rapidity of the temperature rise - typically less than a millisecond, the exact form of heat transfer in this transition region is unknown. From measurements [6,7] made with the temperature of the surface controlled, it is known that the heat flux drops to a value of .3 W/cm$^2$ at T = 5 K. Lacking any better correlation, it will be assumed that this change is linear even though, the curve appears to fall more steeply than that. After the transition, the heat transfer is dominated by film boiling. As with the transition from convection to nucleate boiling, this transition seems to require a fixed amount of energy per unit volume in the helium close to the surface.

In film boiling the heat transfer is dominated by the properties of the vapor film. The high thermal resistance of the film causes the wall temperature to rise sharply; values of 30 to 100 K above the bath temperature are common. Because of the large rises in temperature, the thermophysical properties of the film vary significantly across the range of film boiling. If the surface of the wall is curved e.g. a wire the heat transfer is strongly effected, being enhanced because the curvature creates instabilities in the film layer. These instabilities cause parts

of the film layer to break off requiring extra energy to reform the layer. Also the instabilities cause the film layer to locally thicken which absorbs extra energy to create the additional film. Theoretical treatment [8] of film boiling gives a correlation of

$$\dot{Q}/A \propto T^{0.75} \tag{10}$$

This correlation is in good agreement with experimental values. However, the coefficient of T contains fluid properties that are strongly temperature dependent. To simplify the fit to the experimental data on empirical equation

$$\dot{Q}/A = 0.0146\ (T)^{1.3} + 0.1816 \tag{11}$$

was used for flat surfaces. Curved surfaces would change the coefficient and the constant but not the exponent. The increased exponent accounts for the increasing thermal conductivity of the film layer with increasing temperature and the constant reflects the existence of other modes of heat transfer which prevent the correlation from passing through the origin. The preceeding analysis assumes that the film is in equilibrium. For very fast pulses the film is not in equilibrium but is changing its thickness. These changes in thickness absorb additional heat. Iwasa[9] has shown both theoretically and experimentally that this effect can be accounted for by adding an additional term to the film boiling correlation of the form

$$\dot{Q}/A = C\ d(T)/dt \tag{12}$$

For flat copper plates the value of C is

$$C = 5 + 0.53((T) - 0.5)^2\ Jm^{-2}K^{-1} \tag{13}$$

C is strongly dependent on surface conditions but such variation changes the overall heat transfer function by only a small amount.

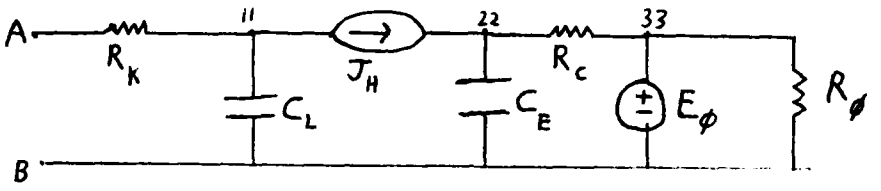
By fitting all these correlations together i.e. requiring that the values by continuous at the juncture points, a complete description of heat transfer into liquid helium can be constructed. When this is combined with the previous thermal model of the surface a complete heat transfer model is constructed. The next section will describe in detail the computer model that was constructed.

## IV. COMPUTER MODELS AND RESULTS

A powerful computer code called SCEPTRE[10] has been developed for solving transient problems in electric circuits. Since SCEPTRE was already implemented on the computer system at Wright-Patterson AFB, it was decided to use this computer code. As explained in the previous section of this report, analogies can be made which permit the translation of a thermal problem into an electric circuit problem, which can be solved with the use of SCEPTRE computer code. The equivalent electric circuit for heat transfer in a solid is simple, a string of resistors and capacitors as previously diagrammed. The liquid helium bath and its associated heat transfer is more difficult to model because of the difference in heat transfer in the different modes.

The model of the liquid helium consisted of an idealized current source(JH) whose value depended on the mode of heat transfer, the temperature difference between the wall and the helium bath, the total amount of energy received by the bath, and the time. A separate FORTRAN subprogram generated the value of the required current. Because of the complicated interrelations among all of these variables, this was the most difficult part of the program to write correctly. To represent the assumed constant temperature of the bulk of the bath - fixed at 4.2K, the normal boiling point of helium - an idealized voltage source (EØ) was added. Under the SCEPTRE code the presence of a voltage source requires an external resistor (RØ) to complete the circuit. Since this resistor is supposed to be large, its value was arbitrarily set at 10,000 ohms. As a test, the value of this resistor was varied from $10^2$ ohms to $10^6$ ohms. No effect on the output of the program was noted at the level of one part in $10^4$. The boundary layer was represented by a small capacitor (CL) whose capacitance was equal to the specific heat of a layer of helium $10^{-5}$cm in depth. As explained previously this is a reasonable value for this quantity for times greater than ten microseconds. This small capacitor serves an additional purpose-measurement of temperature of the helium adjacent to the wall. The SCEPTRE automatically calculates the voltage (equivalent to temperature) across capacitors at each step of its iterative solution to the circuit problem. This voltage can be used

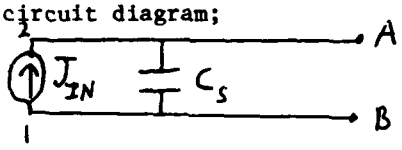
in other parts of the model which are dependent on the temperature. The Kapitza resistance is represented by a resistor (RK) whose value depends on the temperature of the wall surface. An additional resistor RC and capacitor CE were added to allow the temperature of the wall to relax back toward 4.2K after the pulse of heating ended. The values of these quantities were chosen so that the relaxation time constant was 0.1 seconds which roughly agrees with experimental measurements. Detailed studies of the relaxation process may well alter these values. The resistor serves the additional function of monitoring the heat flow into the bath. SCEPTRE automatically computes the current flow across resistors at each step of the solution. These values can be used in other parts of the program or printed out as a check on the behavior of the model. The capacitor does the same thing for measuring the temperature. The equivalent circuit for the helium is




For flat surfaces, it is customary to divide through by the unit area of cross section since this is constant for all subsections of the wall coating, and the bath. This converts resistance into resistivity, current to current density, etc. However, the specific heat must still be multiplied by the thickness of each subelement to convert it into capacitance, since the capacitance depends on volume rather than area. Because it makes comparisons easy, most experimental results are reported this way with the heater power given in Watts/cm$^2$. On the other hand, for curved surfaces such as wires, the surface area is not constant for all subelements. To avoid errors, thermal conductivities must be explicitly multiplied by surface areas and specific heats by the appropriate volume to get the correct resistance and capacitance for the circuit. Also the heating current must represent the total number of watts of energy that

enters the system.

To model the N.B.S. work[4] on transient heat transfer, a heater current source JIN and a small capcitor for measuring the temperature of the sample were added to the helium model resulting in the following circuit diagram;




LIQUID HELIUM MODEL

The N.B.S. used a very thin flat carbon film as both heater and thermometer. The film was thin enough to be isothermal, so that there were no thermal conductivity effects. The capacitance was set at one-tenth of the value of the capacitance of the helium boundary layer even though the film is thicker than the assumed boundary layer. Tests showed that this value could be altered by a factor of ten without altering the results of the program.

Preliminary results from this model were in qualitative agreement with the experimental data. However the ten week period was too short to fully "debug" the program and obtain extensive accurate results. For curved surfaces there is a need to subdivide the wire and/or the coating into separate elements. The program "elements" successfully achieved this goal on the interactive computer system at Wright-Patterson AFB. Since the main program was not fully "debugged" for the simpler flat surface case, no attempt was made to extend it to the more complicated wire case.

## V. EXPERIMENTAL PROCEDURES AND RESULTS

Conceptually the general procedure for the experimental work is simple. A known heat pulse is applied to a material in a helium bath and the resulting temperature rise is measured. The output of the computer model is a plot of temperature versus time for a given power input. A measurement of the temperature history of a sample for a known power input would directly check the predictions of the computer model. For the comparison of model and experiment to work the thermal conductivity and specific

heat of the sample as a function of temperature at low temperature must be known as the model demands this information as input data. Repeating the experiment for different coatings and different thicknesses of coatings, the effectiveness of the coating process and the accuracy of the computer model could be throughly checked.

At low temperatures heat is usually produced by electric resistive heating. A measurement of the current I and voltage V simultaneously during the heater pulse yields the power input directly since P=IV. An integration of the power over the length of the pulse gives the total energy input to the sample. Circuitry for the simultaneous measurement of I and V by use of a four point connection is well-developed, fast and accurate. The main experimental problem is the measurement of the temperature of the sample.

Thermometry always consists of measuring some physical property of a system that varies in a known way with temperature. In the temperature range of greatest interest, 4 to 20K, most properties of nearly all materials are constant with respect to temperature changes. A property that varies by one per cent or less over this entire temperature range is too insensitive to measure the temperature with enough accuracy to fulfill the experimental objectives. An additional problem in this temperature range is the poor thermal contact between materials. Unless a long time is allowed for the sample and the thermometer to come to thermal equilibrium, there is a substantial question whether the thermometer is actually measuring the temperature of the sample or is reading some other unrelated temperature. The required equilibrium times are typically 1 to 10 seconds which is far longer than the transient heat transfer times of $10^{-4}$ to $10^{-2}$ seconds. Furthermore, some properties e.g. length changes occur slowly at these temperatures and/or require slow measurements. The electric resistance is the one thermodynamic property that both varies significantly with temperature, changes rapidly in response to changing temperatures, and can be measured rapidly at these temperatures. If the material that is heated has an electric resistance that varies significantly in this temperature range, then the

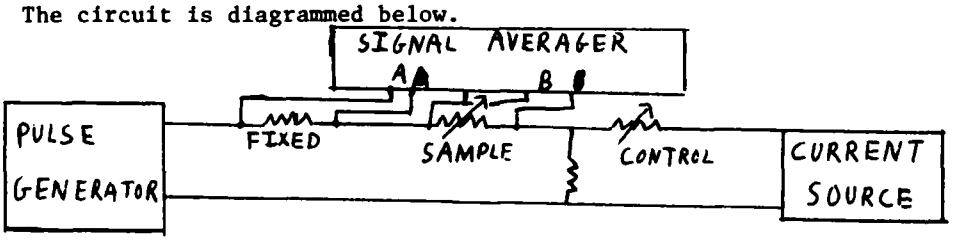
same material can be used both as heater and thermometer, thus eliminating any problems of thermal equilibrium. The most accurate measurements are made by simultaneously measuring the voltage and the current across the resistor by use of a four point connection in a manner similar to the measurement of the input power.

The best material for resistance measurements of temperature at low temperatures is carbon. The standard low temperature thermometers for work in the 4 to 20K range are carbon radio resistors and carbon impregnated glass. A few researchers have used manganin or platinum wire, or thermocouples, but the sensitivity is much lower. The specific heat and thermal conductivity of carbon radio resistors is unknown and varies among different brands depending on the details of the manufacturing process and the past history of the resistor. To avoid this problem samples of high purity, well-characterized graphite were obtained from NASA-Lewis. These samples had numerous mechanical problems; unmachineability, difficulties in attaching electrical leads, and a tendacy to crack and fall apart when cycled between room temperature and liquid helium temperatures. However, the most serious problem was a lack of sensitivity in the appropriate temperature range. Carbon always has a sensitive range, but the exact temperature value of this range is unknown until it is measured at low temperatures because it is strongly dependent on the past history of the sample. The sensitive range of this graphite was well below the temperatures of interest to this project.

To alleviate these and other problems with graphite at low temperatures, Corning glass developed a way to impregnate Vycor glass with Carbon. Corning provided a rod of this material. As part of their contract with the Air Force, Lakeshore Cryogenics measured the thermal conductivity, specific heat, and electric resistance of samples of this material at low temperatures. When it proved suitable in all respects, they coated two pieces of it with different thicknesses of Laketite coating I-SC-1 and performed the tricky job of attaching electric leads to the sample. When tested at Wright-Patterson, both samples cracked apart at the lead attachment upon cooling to liquid Nitrogen temperatures. In addition the coatings

cracked longitudinally indicating unexpectedly severe mechanical stress due to differential contraction upon cooling. The samples were returned to Lakeshore for recoating with the lead attachments left bare to relieve thermal stress. They were scheduled to be returned to W-PAFB the week after this project ended.

To test the experimental apparatus a small piece of uncoated carbon impregnated glass was used. A voltage pulse from a Hewlett-Packard 8012 pulse generator was fed into the sample. The voltage across the sample was digitized and recorded on one of the two inputs of a Nicolet 7021 signal averager. The other input of the signal averager digitized and recorded the voltage across a fixed precision resistor in series with the sample. The current through the sample is equal to the voltage across the fixed resistor divided by its resistance. The voltage across the sample is multiplied by the current through it and the result is integrated over time to provide the total energy input to the sample. The minicomputer on the signal averager will do all these operations automatically except for the multiplication. Because the pulse generator could not provide the steady small current required to measure the changing resistance and hence the temperature of the sample after the application of the pulse, a current source was added to the circuit for this purpose. If a steady current is applied to the sample, the voltage across the sample is proportional to its resistance. This current must be small enough so it does not create any substantial heating in the sample. The circuit is diagrammed below.




The apparatus worked successfully, but the small size of the sample made its resistance so low that the pulse generator was unable to deliver enough power to significantly heat the sample. Thus no useful results were obtained. Nevertheless, if the thermometry problems can be solved the apparatus is capable of producing useful data.

## VI CONCLUSIONS AND RECOMMENDATIONS

The computer model gave results that were qualitatively in agreement with experimental results. As explained in this report every section of the model is based on sound physical principles. For this project to be useful the computer program needs to be fully "debugged" and ran extensively to test its validity in a wide range of situations that can be compared with experimental results. Thus validated, the program could be run at length simulating wires both with and without coatings, with different types of coatings, and with the different thicknesses of coatings. This will provide the information necessary to evaluate the usefulness of these coatings for the Air Force. Clearly such a project will require additional time and effort. The experimental test rig works and will produce results if the thermometry and mechanical cracking problems can be solved. Such results are vital for validating the computer model since these new coatings may have characteristics that are not properly modeled because they have never been used before in any experimental system. Also direct experimental testing is necessary to properly evaluate new products. As indicated in the report, Lakeshore is attempting to repair and recoat the broken Carbon-impregnated glass rods. In addition the N.B.S. is sending some of its thin film specimens for use in the experimental test rig. Recent[11] literature indicates that a French group has sucessfully used a superconductor as a thermometer. Since this is a more realistic representation of the actual situation of interest - coating of superconductors, this approach should be investigated. As the sudden appearance of this paper indicates work in the field of transient heat transfer is badly fragmented and the literature is widely scattered. A thorough review of the literature plus the results of this project, assuming there is more computer and experimental work, would make a good technical report which could bring order to this field and indicate areas where the performance of superconducting systems could be enhanced by better means of transient heat transfer.

## BIBLIOGRAPHY


1. James S. Bower, SCEPTRE,"A Computer Program for Circuit and Systems Analysis", Prentice-Hall, N.Y. 1969.

2. B.P. Breen & J.W. Westwater, "Film Boiling Correlations", Chemical Engineering Progress 58 #7, pg 67, 1962.

3. E.G. Brentari & R.V. Smith, "Nucleate and Film Pool Boiling Design Correlations for $O_2$, $N_2$, $H_2$ and He", in Advances in Cryogenic Engineering Vol 10, Plenum Press N.Y., 1965 pg 325.

4. Walter Frost, editor Heat Transfer at Low Temperature Plenum Press N.Y. 1975.

5. D. Gentile, W. Hassenzahl, & M. Polak, "A Method for determining Temperatures and Heat Transfer Coefficients with a Superconducting Sample", Journal of Applied Physics 51 (5) 2758, 1980.

6. Y. Iwasa & B.A. Apgar, "Transient Heat Transfer in Liquid Helium From Bare Copper Surfaces in a Vertical Orientation - 1 Film Boiling", Cyrogenics 18, 267 1978.

7. J. Jackson, "Transient Heat Transfer and Stability of Superconducting Composites", Cryogenics 9 103, 1969.

8. H. Merte & J.A. Clark, "Boiling of Nitrogen on Smooth Spherical Surface", in Advances in Cryogenic Engineering Vol 7 Plenum Press N.Y. 1962, pg. 546

9. C.E. Oberly, "Air Force Applications of Lightweight Superconducting Machinery",in Applications of Cryogenic Technology, Vol 7, pg. 293, 1978.

10. Warren M. Rosenhow, "Heat Mass and Momentum Transfer, Prentice-Hall N.Y. 1961.

11. W.G. Steward, "Transient Helium Heat Transfer Phase I - Static Cooling" International Journal of Heat and Mass Transfer 21, 863, 1978.

12. O. Tsukamoto & T. Kubayashi, "Transient Heat Transfer Characteristics of Liquid Helium", Journal of Applied Physics 46 (3), 1359, 1975.

## FOOTNOTES


1. C.E. Oberly, Applications of Cryogenic Technology, Vol 7, pg. 293, 1978.

2. Walter Frost editor, Heat Transfer at Low Temperatures, pg 12, 1975.

3. Ibid pg. 328 - 336.

4. W.G. Steward, International Journal of Heat and Mass Transfer 21, 863, 1978.

5. W.M. Rosenhow, Heat Mass and Momentum Transfer, pg. 121, 1961.

6. E.G. Brentari & R.V. Smith in Advances in Cryogenic Engineering, Vol 10 pg. 325, 1965.

7. H. Merte & J.A. Clark in Advances in Cryogenic Engineering, Vol 7, pg. 546 1962.

8. B.P. Breen & J.W. Westwater, Chem. Engineering Progress 58, #7, pg. 67, 1962.

9. Y. Iwasa & B.A. Apgar, Cryogenics 18, pg. 267, 1978.

10. James S. Bower, SCEPTRE, A Computer Program For Circuit and Systems Analysis, 1969.

11. D. Gentile, W. Hassenzahl, & M. Polak, J. Appl. Phys. 51, #5, pg. 2758 1980.

1980 USAF - SCEEE SUMMER FACULTY RESEARCH PROGRAM

Sponsored by the

AIR FORCE OFFICE OF SCIENTIFIC RESEARCH

Conducted by the

SOUTHEASTERN CENTER FOR ELECTRICAL ENGINEERING EDUCATION

FINAL REPORT

# FAST ALGORITHMS FOR TARGET LOCATION AND IDENTIFICATION


| | |
|---|---|
| Prepared by: | Dr. Francis L. Merat |
| Academic Rank: | Assistant Professor |
| Department and University: | Department of Electrical Engineering and Applied Physics, Case Western Reserve University |
| Research Location: | Rome Air Development Center, Intelligence and Reconaissance Division, Image Exploitation Section |
| USAF Research Colleague: | Mr. Ellsworth Hicks |
| Date: | August 28, 1980 |
| Contract No: | F49620-79-C-0038 |

# FAST ALGORITHMS FOR TARGET LOCATION AND IDENTIFICATION

by

Dr. Francis L. Merat

## ABSTRACT

Methods for target location and identification in digitized aerial imagery are investigated. Template matching is shown to be suitable for implementation under the RADC Automatic Feature Extraction System. Template image similarity and algorithms are examined which can recognize image similarity in fewer calculations than correlation. These sequential similarity detection algorithms have been implemented on the RADC PDP-11/70 and partial results are reported. A fast correlation algorithm has been developed but not tested. Suggestions for further research in fast similarity detection algorithms are offered.

ACKNOWLEDGEMENTS

The author would like to thank the Air Force Systems Command, the Air Force Office of Scientific Research and the Southeastern Center For Electrical Engineering Education for providing him with the opportunity to spend a very worthwhile and interesting summer at Rome Air Development Center (Griffiss AFB, New York). He would like to acknowledge RADC and, in particular, the Image Exploitation Section of the Intelligence and Reconaissance Division, for providing the opportunity to carry out the research described herein.

Special acknowledgements are in order to Mr. Ellsworth Hicks and Mr. Don Bush for numerous discussions, guidance and assistance which helped make this author's summer a worthwhile experience. Appreciation is also due Mr. John Huss, Mr. John Boland and Mr. Fred Rahrig of RADC for their thoughtful assistance.

## I. INTRODUCTION

There is a significant interest within the United States Air Force in the identification of objects within aerial imagery. As an example, it would be invaluable to locate airplanes, tanks, and other objects of military interest in aerial photography automatically. The automatic qualifier is very important as the inputs from the wide range of sensors available can produce too much data to be analyzed by skilled personnel.

Perhaps the simplest computer approach to locating and/or identifying objects is template matching in which a template (a replica of an object of interest) is compared to all objects in an image. If the template matches any object in the image, that image object is labeled as being the template object. This technique is fine in principle but difficult in practice because real objects never match the template (which is usually an ideal object). A general procedure used in template matching is to define a function which expresses the difference between the template and the image field. If this difference function is less than some threshold the template object has been found in the image.

However, this method requires the evaluation of the similarity function at all points in the image - a typical image might be 512x512 points - which requires a large number of calculations, say P. In addition, there is the number of calculations needed to evaluate the similarity function over the template, say Q calculations. The total number of calculations required to search one image for a particular template is then PxQ - often a huge number for real images. What is needed are algorithms which can reduce P and/or Q. Symbolic coding can be used to reduce the dimensionality of the image and, consequently, P. Feature extraction, theme encoding, and region growing are but some of the more popular methods of image coding. On the other hand, very little work has been done to reduce Q, the number of calculations needed to establish similarity between the image and the template. Precise methods for reducing Q are the subject of this report and will be described in later sections.

## II. OBJECTIVES

The main objective of this project was to add target identification capabilities to the RADC Automatic Feature Extraction System. Practical considerations included the development of fast algorithms for target identification, i.e. template matching. Specifically, the project objectives were:

(1) To define and implement target identification methods compatable with existing RADC software.

(2) To determine the fundamental limitations of suitable target identification algorithms. This includes the criterion of computational efficiency.

## III. COMPUTATIONAL ENVIRONMENT

Before discussing various target identification algorithms it is reasonable to review the computing environment in which these algorithms will operate. Specifically, algorithms are desired which will operate under the Automatic Feature Extraction System (AFES) developed by Pattern Analysis and Recognition Corp. The AFES system is written in C and operates under UNIX on a Digital Equipment Corporation PDP-11/70. Intrinsically, C offers excellent I/O and file capabilities but very little mathematically. There are no intrinsic functions such as square root, trigonometric functions, and the like. AFES contains a set of C programs called the "window code" which may be added to any C program and provides a sub-image of user definable size which moves through an input image in a row by row fashion. Such a code is particularly well suited to template matching algorithms. Additional features of AFES are the ability to classify aerial photography via region growing and the ability to train pattern classifiers, i.e. them encoding.

## IV. MATHEMATICAL FORMULATION OF TEMPLATE MATCHING

To provide a basis for discussing template matching it is necessary to develop the appropriate background for expressing object similarity.

Let the image field (the search area) S by a LxM discrete image and let the template (commonly called a window) W by a KxJ discrete image [See Figure 1] where each picture element is quantized to k grey levels. Note that W is wholly contained in S and any measure of similarity (or dissimilarity) must be a function of where W is positioned within S. Let

$$S^{i,j}$$

denote the location of the origin of W within S, i.e. $S^{i,j}$ denotes that subset of S which is congruent with W. (i,j) is known as the reference point and is allowed to span the range

$$0 \leq i \leq K - M + 1$$

$$0 \leq j \leq J - L + 1$$

In keeping with later references it is useful to define a measure of dissimilarity. Using the above notation the dissimilarity function d(i,j) can be expressed as

$$d(i,j) = \sum_{k=1}^{J} \sum_{\ell=1}^{K} f(S^{i,j}(k,\ell) = W(k,\ell)) \qquad (1)$$

If d(i,j) < T [where T is a preset threshold] a match is said to occur. This is the classical template matching problem which has been analyzed at great length (See [1] for a review of template matching.) The major problems in target identification via template matching are:

* the differences between the target and the mask image, i.e. scaling, rotations, noise, and
* computational inefficiencies.

The last point is particularly important for template matching as computational times can easily exceed several hours per image on even large computers.

The first problem can be overcome by the use of appropriate transforms. A cross-correlation (defined later in this section) is insensitive to translation and rotation. Doyle [2] has demonstrated a double

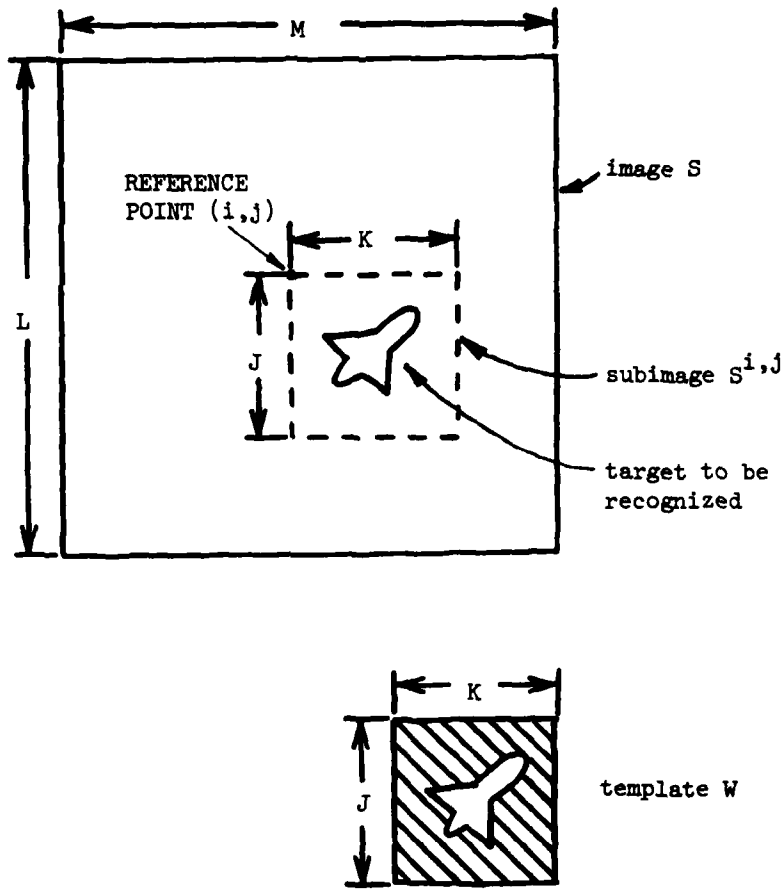



Figure 1. Image and template conventions for template matching.

correlation technique which also compensates for energy and scale difference. In most all cases tolerance to various image-template differences can be achieved only at the expense of the second problem in template matching - computation times.

The large computational requirements of template matching are prohibitive for many applications, hence, the interest in fast correlation via optics [3], etc. The exact computational requirements are dependent upon many parameters. An examination of (1) reveals an obvious dependence upon L and M and the dissimilarity function f.

The function f has traditionally been restricted to $f(x) = |x|$, corresponding to the L1 difference between the subimage $S^{i,j}$ and the window W, for $f(x) = x^2$ which is the usual squared error measure of similarity. The classical correlation function is a special form of $f(x) = x^2$ (See [1]),

$$R(i,j) = \frac{\sum S^{i,j}(k,\ell)W(k,\ell)}{\sqrt{\sum S^{i,j}(k,\ell)}\sqrt{\sum W(k,\ell)}} \qquad (2)$$

Although the correlation function (2) is a common measure of image (dis) similarity it is computationally inefficient because of the presence of the normalization terms in the denominator (more will be said about these terms later). For any choice of the function f in (1) there are (K-M+1)(J-L+1) possible registration points. If JK operations are required to evaluate the dissimilarity function we have the awesome total of JK(K-M+1)(J-L+1) operations. To give this expression some real meaning consider the case where L=M=512 and J=K=32 then the number of operations is

$$(32)\ (32)\ (512-32+1)^2 \approx 2.36\text{x}10^8 .$$

This particular example was chosen to be representative of the aerial imagery in routine use at RADC/IRRE.

The general problem has been to find an algorithm which is insensitive to rotation, translation, scale, etc. and is computationally efficient. Barnea and Silverman [4] recognized that the total dissimilarity function need not be calculated, instead it is sufficient to examine the rate at which the dissimilarity d(i,j) increases. If d(i,j) increases rapdily a template match is not likely at this point (i,j) and the search continues. Other authors [5] have recognized the utility of sub-templates. In this scheme the template is broken into several sub-templates of reduced size. If a sub-template shows a high degree of similarity, other sub-templates will be compared and only if all sub-templates show high correlation will a match be confirmed. This is essentially identical to coarse-fine template matching.

Both examples show that it is not necessary to evaluate the complete dissimilarity function for each (i,j), i.e. summing over all points within the template, and, thus, drastically reduce computational requirements. Barnea and Silverman's algorithm has often been cited but has not often been implemented. Two-stage template matching can be regarded as another form of Barnea and Silverman's algorithm [6]. Very little unified work has been done in the area of reducing the computational requirements of dissimilarity functions, and , in particular, little has been done with coded images (i.e. images described not in terms of pixels, but rather in terms of boundaries, regions, etc.). This will be discussed further in Section V.

## V. TEMPLATE MATCHING VIA CORRELATION

The correlation function is a classic measure of similarity. As mentioned in Section VI it is related to the squared difference (the L2 difference) and is the cross term in the expansion of the square. At this point it is appropriate to distinguish between normalized and unnormalized correlation functions. The unnormalized correlation function

$$\hat{R}(i,j) = \sum_{k=1}^{J} \sum_{\ell=1}^{K} S^{i,j}(k,\ell)W(k,\ell) \qquad (3)$$

is not very useful for template matching because it is difficult to compare values of the function at different locations in the image within any meaningful context. To illustrate this point, the cross-correlation can become large, even in a mismatch situation, if the elements in S have large amplitudes. On the other hand, a correct match could occur but if the elements in S are small the correlation function will be small. It is the variation of energy represented by

$$\sum_{k=1}^{J} \sum_{\ell=1}^{K} S^{i,j}(k,\ell)$$

that must be used to normalize (3) to allow meaningful comparisons of image correlation across an entire image S. Without this normalization there is no meaningful measure of what the correlation function means. With normalization a value of zero indicates no correlation and no match, one indicates a perfect match.

A program to compute the normalized correlation coefficient was developed and tested under the RADC AFES system. The test image S was a 512x512 pixel digitized aerial photo of the Schnedectady, New York airport with a plane sitting on the runway. A 32x32 element subimage containing the airplane was taken from S to serve as the template. As indicated in Section IV this brute force correlation required approximately 10 calculations and took approximately 15,000 seconds (about 4 hours) of CPU time on a PDP-11/70 to compute the normalized correlation function for the entire image S. The initial template retained a portion of the runway with the plane on it and resulted in an overall high correlation with the runway segments in S. This suggests that exclusion of the template background from the correlation would increase the target discrimination and, because of the reduced size of the template, reduce computation time. (Note: an unfortunate hardware failure prevented inclusion of these results and copies of the images used at this time. A RADC report which will include this information is anticipated by November 1980 and will be available upon request

from the author.) It is this idea of selecting a subset of the template for correlation which provides the basis for fast template matching as will be seen in the next section.

## VI. FAST SIMILARITY DETECTION ALGORITHMS

As indicated in Section V it is not necessary to evaluate the correlation function over an entire sub-image to determine if sufficient dissimilarity exists that the sub-image cannot match the template. A general class of algorithms based on this observation was proposed by Barnea and Silverman [6] in 1971. Their observations were restricted to the similarity function $f(x) = |x|$. Consider the evaluation of (1) for this similarity function. When the template closely matches the sub-image the value of the dissimilarity function is small; conversely, a mis-match generates a large error. The class of Sequential Similarity Detection Algorithms (SSDA's) advocated by Barnea and Silverman describe a template matching algorithm which does not necessarily require computations over the entire JxK element sub-image. In its simplest implementation the partial sum

$$d(i,j;p,q) = \sum_{k=1}^{p} \sum_{\ell=1}^{q} | S^{i,j}(k,\ell) - W(k,\ell) | \qquad (4)$$

$$p \leq J \ , \quad q \leq K$$

is compared to a fixed threshold T. If $d(i,j;p,q) > T$ a mixmatch is declared and the evaluation proceeds to the next reference point. Unfortunately, there is no simple method to predict exactly how many computations will be needed before a mismatch can be declared. Intuitively, this number (pq) should be lower than the JK computations required for correlation at each reference point. Note that the number of possible reference points is fixed - only the number of computations per reference point is reduced. Barnea et al [4] report that for a 32x32 pixel template 10-15 partial sums were often sufficient to establish registration.

It is interesting to note that the SSDA algorithm worked well for the airport and plane template matching problem described earlier for nearly all values of the threshold T. It is particularly encouraging that low threshold values seemed to provide an optimum distinction of the correct registration from the background. Such programs executed on the RADC PDP-11/70 in approximately 2-8 minutes (depending on T) as compared to the 4 hours for conventional correlation. It was hoped that the SSDA would show a broad maximum near the correct registration point permiting one to compute the dissimilarity function at multiple pixel spacings (thereby reducing computational requirements) and still be assured of finding the correct registration. Unfortunately, the SSDA showed very narrow peaks for all low values of T and only began to broaden for T's too large to be useful.

## VII. A NEW SIMILARITY DETECTION ALGORITHM

These results have motivated a new algorithm (which has not been tested due to problems with the RADC PDP-11/70 but which will be described in the forthcoming RADC report). This new algorithm is a SSDA based upon correlation as the correlation function typically had broader peaks than the SSDA for $f(x) = |x|$. This algorithm may be developed from (1), (2) and (4) by recalling that the correlation is related to the squared error; hence, the SSDA can be applied to correlation. Specifically, let

$$d(i,j) = 1 - R(i,j) \tag{5}$$

The second term in the denominator of R(i,j) is a constant and need only be computed once. The first term in the same denominator is the sub-image energy and must be computed for each sub-image so as to normalize R(i,j). If $S^{i,j}$ and W were closely matched R will approach one and d will go to zero, i.e. the dissimilarity will be a minimum. As R(i,j) can be represented as a set of partial sums in the manner of (4) a SSDA algorithm for (5) might set a threshold T and count the number of steps required for d(i,j) to become larger than T. Because

there is no square root function in C and for computational simplicity the squared correlation function can be computed instead. Note that $R^2(k,j;p,q)$ is a monotonically increasing function of p and q. If the dissimilarity d(i,j) is greater than T before N interations that sub-image can be rejected as a possible match. Conversely, one can evaluate just $R^2(i,j;p,q)$ and, if $R^2 > T$ for $(p\ q) < JK$, a match is probable. More specifically, one might determine how many iterations are necessary to reach a certain similarity (correlation). This may be regarded as a gradient and, if the rate of similarity increase is small, anticipate the final correlation as being insignificant.

## VIII. RECOMMENDATIONS

At this point it is obvious that much faster algorithms than direct correlation are reasonable for target identification. This is exemplified by the four hour run time for correlation versus the 2-8 minutes for SSDA's. Execution times will be further decreased by parallel computing as each row of an image can be evaluated for similarity independent of the other rows. If all 512 rows were evaluated in parallel a six minute run time would reduce to approximately 0.7 seconds. This number could be further reduced by the higher speed of the dedicated hardware.

The deterministic nature of the data used is not representative of real world problems. Real images are noisy, cloudy, etc. Barnea et al [4] observe that a SSDA algorithm appears to be tolerant of clouds, etc. whereas the correlation is not and may require additional processing. This may somewhat defeat the advantage of the fast correlation algorithm developed in the previous section and suggests using a SSDA algorithm where $f(x) = x^2$.

The most important factor in future work is to determine if fast similarity algorithms can be extended to rotational invariance. The correlation function is somewhat adaptable to this end; hence, the interest in developing the fast correlation algorithm. It is not clear at this time that scale invariance is particularly important -

the scale of aerial photographs is usually known or can be computed.

A second recommendation for additional research is the ordering of the points used for matching within the sub-image. Barnea and Silverman used a random ordering of points. A grid of evenly spaced points was used for the work described in this report. However, the most promising approach is to use an edge detection algorithm and a set of points along the edges of the template object(s). Previous work [7,8] suggest the use of edge features for template matching can significantly improve the matching process in terms of accuracy and that there may indeed be an optimum ordering [9]. A final observation is that although the RADC AFES system was unable to produce any theme-encoded images during the period this report covers, there is no reason why symbolic (abstract) data cannot be matched with a SSDA algorithm. The problems are mathematically the same except for the meaning of the symbols.

## REFERENCES


1. William K. Pratt, Digital Image Processing, (Wiley-Interscience, New York, 1978), pp. 551-553.
2. W. Doyle, "Operations Useful for Similarity-Invarient Pattern Recognition," J. ACM, Vol. 9, pp. 259-267, 1962.
3. H. J. Caufield, R. Haimes, D. Casasent, "Beyond Matched Filtering," Optical Engineering, Vol. 19, No. 2, pp. 152-156, March/April 1980.
4. D. Barnea, H. Silverman, "A Class of Algorithms for Fast Digital Image Registration," IEEE Transactions on Computers, Vol. C-21, No. 2, pp. 179-186, February 1972.
5. G. Vanderbrug, A. Rosenfeld, "Two Stage Template Matching," IEEE Transactions on Computers, Vol. C-26, No. 4, April 1977.
6. Daniel Barnea, Harvey Silverman, The Class of Sequential Similarity Detection Algorithms (SSDA's) for Fast Digital Image Registration," IBM Technical Report RC-3356, May 10, 1971.
7. M. Svedlow, C. McGillen, P. Anuta, "Image Registration: Similarity Measure and Preprocessing Method Comparisons," IEEE Transactions on Aerospace and Electronic Systems," Vol. AES-14, No. 1, pp. 141-149, January 1978.
8. Robert Wong, Ernest Hall, "Performance Comparison of Scene Matching Techniques," IEEE Transactions on Pattern Analysis and Matching Intelligence, Vol. PAMI-1, No. 3, pp. 325-330, July 1979.
9. Ernest Hall, David Davis, Michael Casey, "The Selection of Critical Subsets for Signal, Image and Scene Analysis," IEEE Transactions on Pattern Analysis and Machine Intelligence, Vol. PAMI-2, No. 4, July 1980.

1980 USAF - SCEEE SUMMER FACULTY RESEARCH PROGRAM

Sponsored by the

AIR FORCE OFFICE OF SCIENTIFIC RESEARCH

Conducted by the

SOUTH EASTERN CENTER FOR ELECTRICAL ENGINEERING EDUCATION

FINAL REPORT

# SEVERAL APPLICATIONS OF GAME THEORY, MARKOV CHAINS, AND TIME SERIES MODELS TO TACTICAL AND STRATEGIC FIRE CONTROL SYSTEMS


Prepared by: Dr. Max Mintz

Academic Rank: Associate Professor

Department and University: Department of Systems Engineering, University of Pennsylvania

Research Location: Air Force Avionics Laboratory/AART-4

USAF Research Colleagues: Dr. H. M. Dobbins & Mr. Michael Noviskey



Date: September 1980

Contract No: F49620-79-C-0038

# SEVERAL APPLICATIONS OF GAME THEORY, MARKOV CHAINS, AND TIME SERIES MODELS TO TACTICAL AND STRATEGIC FIRE CONTROL SYSTEMS

by

Dr. Max Mintz

## ABSTRACT

In this report we have briefly delineated a range of practical applications of three distinct classes of mathematical models to tactical and strategic fire control problems. The focus of the research effort reported here is the application of game theory, markov chains, and time series models in an integrated study for determining techniques to generate and/or evaluate evasive maneuvers for defensive fire control scenarios.

The applications paradigms include: Evasive Maneuvering Against GCI and Airborne EW Radar Systems; Evasive Maneuvering Against Enhanced AAA Fire Control; Evasive Maneuvering Against a Multiple Missile Threat.

A portion of this report summarizes research results obtained todate; the remainder of the report suggests avenues for further research effort.

## ACKNOWLEDGMENT

The author wishes to thank the Air Force Office of Scientific Research, the Air Force Systems Command, and Southeastern Center for Electrical Engineering Education for an interesting summer. The author also wishes to acknowledge the following individuals and organizations for their generous advice, assistance, encouragement, and support:

AFWAL/AART-4: Mrs. J. Allswede, Dr. H. Dobbins, Mr. J. May, Mr. L. McFawn, Mr. R. Nieter, Mr. M. Noviskey, Capt. D. Van Liere, Mr. J. Zingg.

AFWAL/AART-2: Mr. R. Bryan, Mr. A. Duke, Mr. P. Hannen.

AFWAL/XRPA: Lt. Col. J. Taylor.

AFWAL/FIGL: Mr. E. Rachovitsky.

AFWAL/FIGX: Mr. T. Neighbor.

AFIT: Maj. G. Reid, Capt. J. Silverthorn.

AFOSR/XPO: Maj. R. Kopka.

SCEEE: Mr. M. Danishek, Dr. W. Peele.

The author wishes to thank his SFRP research colleagues Mike Dobbins and Mike Noviskey for their insight and guidance which made this work possible.

# I. INTRODUCTION

## 1.0 Background

In order to synthesize effective weapon systems or achieve more effective use of current systems, designers, analysts, and operations personnel must continually consider the conflicting roles of offense and defense in seeking a means of evaluating new designs, proposed modifications, or operational tactics. These individuals must continually seek to understand the interaction, often complex, frequently time-varying, between the offensive capabilities of a given weapon system and potential defensive systems or tactics to be employed against this given system. As an illustration we observe that in virtually all aspects of defensive and offensive operations of fire control systems, as well as the related sensor, data processing, and battle management subsystems, it is necessary to consider the effect of target maneuvers in order to properly assess overall system performance.

## 1.1 Focus

In this report we have briefly delineated a range of practical applications of three distinct classes of mathematical models to tactical and strategic fire control problems. The focus of the research effort reported here is the application of game theory, markov chains, and time series models in an integrated study for determining

techniques to generate and/or evaluate evasive maneuvers for defensive fire control scenarios.

A portion of this report summarizes research results obtained to date; the remainder of the report suggests avenues for further research efforts.

## 1.2 Philosophy

The underlying philosophy of the research reported here is threefold:

i) We have emphasized practical applications as opposed to pure theory. The fire control environment is inherently a real-time environment. Hence, rather than following a path developing a global theory which leads to algorithms which are not consistent with our real-time objectives, we have sought instead to develop suitable heuristics to achieve significant improvements in the state of the art, while at the same time achieving the underlying requirement of computability in real time.

ii) We have sought to identify a suitable degree of model complexity to achieve the desired applications oriented results. Where closed form or analytical results were not achievable, digital computer simulation techniques were used judiciously.

iii) We have sought to develop generic models wherever possible. Although actual flight test data provided some substantial insight into the behavior of some aspects of system performance, it is felt that this insight can reasonably be generalized to encompass other aircraft.

In certain instances characteristic parameters for specific aircraft and missiles were used to provide truth models to evaluate algorithm performance. Once again, the insights gained from these specific models are felt to be indicative of a range of aircraft and missiles. Varying these parameters would lead to variations in performance envelopes as opposed to the refutation of a specific concept.

### 1.3 Presentation

Since the purpose of this report is to summarize an integrated study of applications oriented mathematical modeling techniques for defensive fire control, the presentation will emphasize brevity at the expense of copious detail. The interested reader is referred to recent reports [1,2,3], by the author and his colleagues, which contain complete details of the earlier work summarized herein, and to a forthcoming technical report [4] which emphasizes the integrated aspects of this modeling research. The presentation of the remainder of this report is couched in a fashion which assumes that the reader is familiar with certain basic results of game theory and stochastic processes. References [1,2,3,5,6] provide an overview of the basic concepts which are used in the sequel.

## II. OBJECTIVES

### 2.0 Primary Considerations

The major objective of this report is to identify and

briefly illustrate a variety of interrelated practical applications of game theory, markov chains, and time series models to defensive fire control technology. The primary thrust of this integrated study is the determination of techniques to generate and/or evaluate evasive maneuvers of aircraft in both tactical and strategic conflict environments. The specific arenas and applications areas include:

(Section III) Evasive Maneuvering Against GCI and Airborne EW Radar Systems

(Section IV) Evasive Maneuvering Against Enhanced AAA Fire Control

(Section V) Evasive Maneuvering Against A Multiple Missile Threat.

The concepts and algorithms delineated in sections III, IV, and V have been motivated by or have potential impact on the following USAF programs: Integrated Defensive Operations Systems Technology (IDOST); Integrated Flight/Fire Control (IFFC); Integrated Flight/Weapon Control (IFWC); Missile Evaluation (MISVAL). These programs are cited to suggest representative related applications areas and do not constitute a complete list of possibilities.

## 2.1 Section III Objectives

The first objective of section III is to summarize new probabilistic relations which characterize the effect of evasive maneuvering on the performance of return-to-track correlation algorithms (RTCA) which could be employed by a

GCI network or by an airborne EW radar system as part of an automatic track initiation (ATI) function. These probabilistic relations represent new results in this applications area. The second objective of section III is to indicate how one can apply game theoretic techniques and markov chain concepts in conjunction with these new relations to synthesize a family of evasive maneuvers to blunt the effectiveness of GCI and EW radar tracking systems.

2.2 Section IV Objectives

The first objective of section IV is to briefly summarize our recent research [1,2] integrating game theoretic, markov chain, and time series models to obtain enhanced filtering and prediction capability in AAA fire control. The second objective of section IV is to indicate how this development of enhanced AAA fire control capability provides insight into the development of evasive maneuvers to blunt the effectiveness of such AAA systems. The connection between these new concepts and the USAF IFFC and IFWC programs is highlighted.

2.3 Section V Objectives

The first objective of section V is to briefly summarize our recent research [3] developing real-time heuristic algorithms for multiple missile evasion based on game theoretic techniques. The second objective of section V is to indicate avenues of exploration expected to enhance

these real-time algorithms. Finally, the connection between these new concepts and several USAF programs is highlighted.

## III. EVASIVE MANEUVERING AGAINST GCI AND AIRBORNE EW RADAR SYSTEMS

### 3.0 Introduction

A review of the recent literature [5,6,7,8,9] pertaining to return-to-track correlation algorithms (RTCA) as well as algorithms for automatic track initiation (ATI) reveals the existence of a universal assumptiom which is crucial in the evaluation of algorithm performance. Specifically, it is universally assumed that the underlying truth model for the discrete time stochastic process representing the observation residuals, i.e., the one scan prediction errors associated with the TWS function, is a zero mean stochastic process. This pivotal assumption is equivalent to the assertion that the target maneuver process is adequately modelled as an uncorrelated or white noise process with zero or known mean. This latter assumption would be reasonable if, for example, the tracking process was carried out in an X-Y coordinate frame and the target aircraft followed a nearly constant velocity path except for occasional maneuver acceleration inputs modelled by white noise. It is important to note that while the assumption that the observation residuals constitute a zero mean stochastic process seems to be universally adopted for the purposes of analysis and performance evaluation, it is,

nonetheless, recognized in the literature that this assumption could preclude the proper analysis of the effect of evasive target maneuvers.

Since the contribution of this portion of our research effort focuses on the effect of evasive maneuvers in degrading the performance of GCI and airborne EW radar systems, it is necessary to reconsider the choice of underlying assumptions, particularly those which relate to target maneuver models. Next, we present the probabilistic relations which capture the effect of evasive maneuvering on RTCA. These relations contain as special cases the previously known results [5,6] for nonmaneuvering targets. We conclude this section with some remarks indicating how game theoretic techniques and markov chain concepts can be used to design evasive maneuvers to degrade GCI and EW radar system performance by exploiting the functional form of the probabilistic relations presented in the following subsection.

### 3.1 Degradation of Tracking Performance Due to Evasive Maneuvering

We begin this subsection by introducing some notation and by defining and illustrating a RTCA. Consider a TWS radar system with scan time T. Let z(n) denote an N-vector which characterizes the observation of a radar return at "time nT". Here nT refers to the nth scan of a "localized" surveillance volume which is "predicted" to contain the next or nth return from a target currently being tracked, or the

next or nth return from a potential target being considered for track status. We remark that the radar system is gated so that the surveillance volume associated with the location of the predicted return can be limited. We assume the TWS radar system employs some generic type of one step (one scan ahead) predictor such as an alpha-beta predictor or a Kalman filter. In order to make the RTCA problem interesting we assume that we are faced with "returns" due to clutter, false alarms, and radio frequency interference (RFI), as well as real targets. In order to accomplish the return-to-track correlation process, we shall adopt the following generic [5,6] approach. For each return $z_i(n)$, i=1,2,..,s, within a "rectangular" gate centered at the predicted location of the nth return, we compute the following "distance"

$$d(y_i) = y_i' V^{-1} y_i \quad . \tag{3.1}$$

Here V denotes a covariance matrix to be defined subsequently and $y_i$ denotes the vector difference (observation residual) between the ith return and the predicted location of the target based on one scan ahead prediction. The covariance matrix V is defined to be the covariance matrix for the observation residuals based on an assumed target model (which is generally not the truth model) and a one step prediction algorithm, e.g., a given Kalman filter. The RTCA operates as follows: the distance $d(y_i)$ is computed for each i, i = 1,2,..,s. The residual $y_k$

associated with the minimum value of d( ) is associated with the (true) return from the desired target. Several remarks are in order:

(a) If s = 0, i.e., there are no returns in the gate, the system is allowed to "coast" and a two step prediction is generated based on the last correlated return.

(b) If s = 1, the track is declared correlated with this return.

(c) If s > 1, the track is declared correlated with the return which has the minimum value of d( ).

(d) This correlation algorithm is equivalent to a maximum likelihood selection process under the assumption that the observation residuals from the true target are gaussian with zero mean and covariance matrix V.

In what follows we will assume that the actual errors in one step prediction based on the actual target truth model and the given TWS predictor (which is generally not matched to the target truth model) is adequately modeled by a conditionally gaussian stochastic process $\{y(n): n = 1,2,..\}$ with moments defined by:

$$E[y(n)] = m(n)$$

$$E[(y(n)-m(n))(y(k)-m(k))'] = W(n,k) \qquad (3.2)$$

$$n,k = 1,2,... \quad .$$

Several remarks are in order:

(a) The stochastic process $\{y(n)\}$ is said to be conditionally gaussian, since the process is gaussian

"conditioned" on a given set of moments (3.2).

(b) The moments (3.2) generally will depend on the (as yet unspecified) maneuver process which characterizes the target motion.

(c) In what follows we shall assume m(n) depends on n (the scan index) but that W(n,n) does not.

(d) In our subsequent discussion in this subsection we will have no need to consider W(n,k) for $n \neq k$.

The following parameters are employed in the sequel to characterize the probabilistic expressions which relate to RTCA performance:

(a) G denotes the "rectangular" gate associated with the TWS radar system and the RTCA. The gate G denotes a volume in the N-dimensional coordinate space associated with the observation residuals. The jth axis in this space is measured in units of $\sigma_j$, where $\sigma_j^2 = V_{jj}$.

(b) The normalized half width of the gate G in the jth coordinate is denoted by $K_j$.

(c) L denotes the average number of false returns (clutter returns, false alarms, and RFI) per unit surveillance volume. We assume in any scan of a given surveillance volume, the number of false returns has a Poisson distribution (with parameter L per unit volume) and the spatial distribution of these false returns is further assumed to be locally uniform.

(d) $P_D$ denotes the probability of detecting a return from the target aircraft.

(e) $P_G$ denotes the probability that a correlation will be declared. (N.B. This return-to-track correlation may be either correct or incorrect.)

(f) $P_C$ denotes the probability that a correlation will be correct given that a correlation is declared.

(g) P(correct/det) denotes the probability that the return from the aircraft target on the nth scan will be properly associated (correlated) with the actual track, conditioned on the event that a return from the target aircraft is detected on the nth scan. We simplify the language here by saying P(correct/det) denotes the probability that a proper return is correlated given a proper return is detected.

(h) P(none/det) denotes the probability that no correlation is declared given a proper return is detected.

(i) P(false/det) denotes the probability that a false (incorrect) correlation is declared given a proper return is detected.

(j) P(none/no det) denotes the probability that no correlation is declared given a proper return is <u>not</u> detected.

(k) P(false/no det) denotes the probability that a false (incorrect) correlation is declared given a proper return is not detected.

The following expressions delineate the relevant probabilities which characterize the correlation performance of the generic RTCA adopted in this study:

$$P(\text{correct/det}) = \tag{3.3.1}$$

$$a \int_G \exp[-b(y'V^{-1}y)^{N/2} - (1/2)(y-m)'W^{-1}(y-m)]dy \ ,$$

where

$$a = [(2\pi)^N \text{Det}(W)]^{-1/2} \ ,$$

$$b = (LC_N \pi \text{Det}(V)^{1/2})/(2\sigma_1 . 2\sigma_2 .. 2\sigma_N) \ ,$$

$$C_N = 2C_{N-1}\int_0^{2\pi} \cos^N(t)dt \ ,$$

$C_1 = 2/\pi$ , and m, W refer to moments (3.2).

$$P(\text{none/det}) = \tag{3.3.2}$$

$$[1 - a \int_G \exp[-(1/2)(y-m)'W^{-1}(y-m)]dy]\exp[-LK_1K_2..K_N] \ .$$

$$P(\text{false/det}) = 1 - P(\text{correct/det}) - P(\text{none/det}) \ . \tag{3.3.3}$$

$$P(\text{none/no det}) = \exp[-LK_1K_2..K_N] \ . \tag{3.3.4}$$

$$P(\text{false/no det}) = 1 - \exp[-LK_1K_2..K_N] \ . \tag{3.3.5}$$

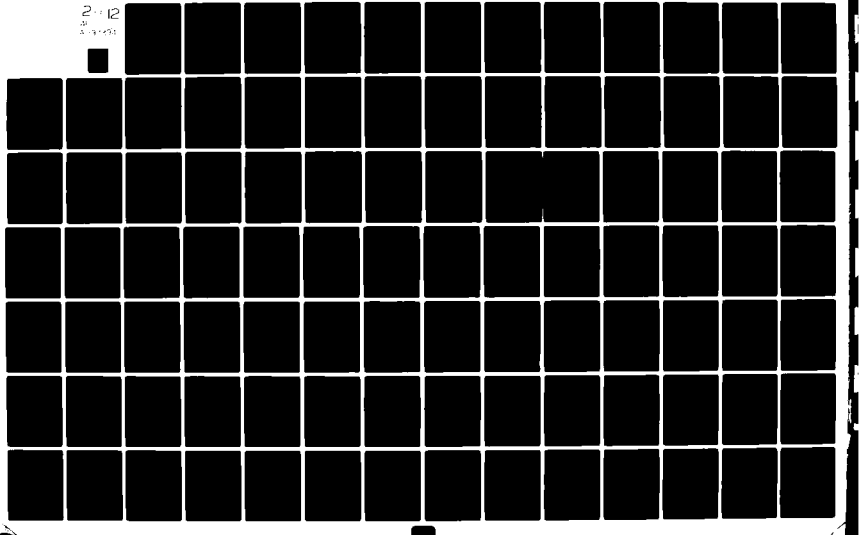
$$P_C = P_D P(\text{correct/det})/P_G \ . \tag{3.3.6}$$

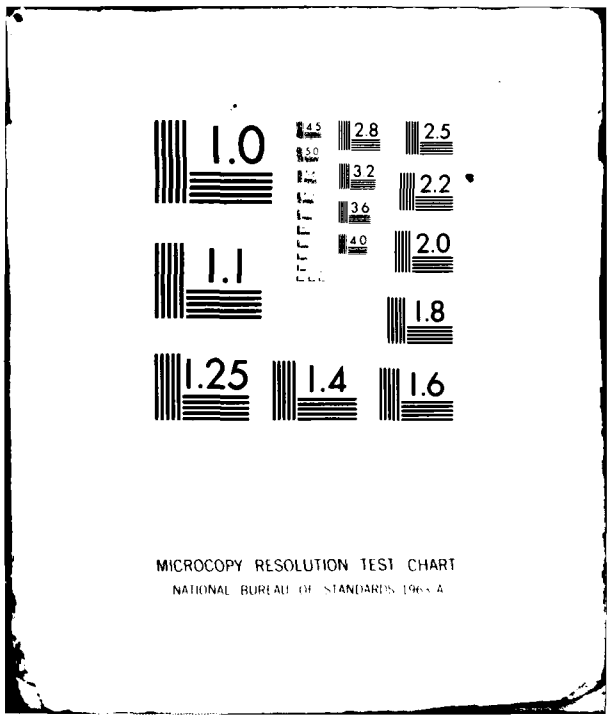
$$P_G = 1 - P(\text{none/det})P_D - P(\text{none/no det})(1-P_D) \ . \tag{3.3.7}$$

A complete derivation of these previous probabilistic expressions characterizing the RTCA appears in [4]. The probabilistic relations (3.3.1), (3.3.2), (3.3.3), (3.3.6), and (3.3.7) depend on the mean m of the observation residual associated with the nth scan. When the mean vector m is

AD-A097 394 SOUTHEASTERN CENTER FOR ELECTRICAL ENGINEERING EDUCAT--ETC F/G 5/1
USAF SUMMER FACULTY RESEARCH PROGRAM, 1980, RESEARCH REPORTS, V--ETC(U)
OCT 80 W D PEELE F49620-79-C-0038

UNCLASSIFIED AFOSR-TR-81-0193 NL




1.0
1.1
1.25
1.4
1.6
1.8
2.0
2.2
2.5
2.8
3.2
3.6
4.0
4.5
5.0
MICROCOPY RESOLUTION TEST CHART
NATIONAL BUREAU OF STANDARDS 1963 A

zero these expressions reduce to the previously known results obtained in [5,6]. The probabilistic relations (3.3.4) and (3.3.5) do not depend on the mean vector m, i.e., these probabilities do not depend explicitly on the target maneuver process, and hence are identical to the related expressions previously obtained in [5,6].

It is enlightening to consider the behavior of the RTCA in a special but very practical case where N = 2. When N = 2, we could be considering our observables to be range and azimuth, or X and Y. In the following, we evaluate explicitly the expression for P(correct/det) for the limiting case where G is infinite.

INFINITE GATE EXAMPLE:

If N = 2, and $K_1 = K_2 = \infty$, then P(correct/det) becomes:

$$P(\text{correct/det}) = c\exp[-(1/2)m'Am] \ , \qquad (3.3.8)$$

where:

$$c = \text{Det}[I + 2rWV^{-1}]^{-1/2},$$

$$r = (1/2)L\pi(1-\rho)^{1/2},$$

$$A = W^{-1} - W^{-1}BW^{-1},$$

$$B = (1/2)[rV^{-1} + (1/2)W^{-1}]^{-1},$$

and $\rho$ denotes the estimated coefficient of correlation between the two observables on the nth scan, i.e., the coefficient of correlation of V. Here m and W refer to the moments (3.2). Expression (3.3.8) collapses to the

previously known result [6] when m = 0. We remark that the matrix A is positive definite when L > 0.

A second special case not presented here but considered in [4] concerns the explicit functional form of P(correct/det) when the gate G is finite, there is *no* correlation between observables, and the second moment statics of the tracking filter and the actual residuals are equal.

Several remarks are in order:

(a) The derivation of (3.3.1) - (3.3.8) assumes that there is no interference between separate tracks, i.e., gates for different tracks do not overlap. Such overlap could lead to ambiguity in applying the generic RTCA.

(b) The derivation of (3.3.1) assumes that the hyperellipsoidal volume D, D = [u: $u'V^{-1}u$ < dmin ], where dmin denotes the minimum value of (3.1) evaluated for all returns within the gate, lies entirely within G. This approximation is good for practical gates which are suitably large, and becomes exact in the infinite case.

## 3.2 Conclusions and Avenues for Further Research

We have examined how the existence of a non-zero mean m(n), which characterizes the behavior of the discrete time stochastic process $\{ y(n): n=1,2,..\}$ representing the observation residuals of a TWS radar, degrades the performance of the tracking system by affecting the values of P(correct/det) over a given sequence of scans.

We have presented specific probabilistic relations (3.3.1) - (3.3.8) which delineate the effect of the process mean m(n) on the RTCA. An examination of (3.3.1) indicates that P(correct/det) achieves its maximum value over m when m = 0. This functional behavior is particularly evident in the special case of the infinite gate (3.3.8).

3.2.1 Markov Chains and Game Theory

Our ongoing research effort is concerned with the effect of the target maneuver process on the performance of the RTCA. Here we are exploiting the functional dependence of P(correct/det) on m(n) as well as V, and W. Several remarks are in order:

(a) The actual maneuvering behavior of the target determines the values of of the mean vectors $\{ m(n): n=1,2,...\}$ . Based on an elementary analysis of stochastic systems, it can be shown [4] that the values of the sequence $\{m(n): n=1,2,...\}$ are <u>not</u> generally independent. Hence we can view the choice of a target control law or maneuver process in the following way. We can seek a choice of maneuver process to maximize the probability of loss of track. This is a sequential decision problem which is modelled in terms of a finite markov chain [4].

(b) The counter strategies of the GCI or EW radar systems designers must also be considered. Specifically, the choice of tracking filter affects the behavior of V -- which is generally not known exactly by the evasive target. This

leads to a game theoretic analysis of a choice of tracking filter versus a choice of target maneuver process. The evaluation of these strategy pairs is made in terms of RTCA performance [4].

## IV. EVASIVE MANEUVERING AGAINST ENHANCED AAA FIRE CONTROL

### 4.0 Summary

In a recent study [1] we have described practical applications of an integrated modeling technique which combines game theory, markov chains, and multivariate time series models to obtain enhanced filtering and prediction capability for AAA fire control systems. This study was in turn an outgrowth of an earlier study [2] which applied game theory and univariate time series analysis to problems in AAA fire control. This unified approach lead to the development of enhanced filters and predictors and simultaneously provided insight into the nature of successful maneuver processes to blunt the effectiveness of AAA systems. The game theoretic techniques lead to the development of (i) robust filters and predictors to be used against evasive targets and (ii) a technique for designing a class of "worst case" maneuver processes. The application of markov chains and multivariate time series models has lead to an enhanced understanding of the effective attributes of evasive maneuvering by attack aircraft in an air-to-ground weapon delivery environment. The models developed in studies [1] and [2] were based on actual flight

test data.

### 4.1 Further Research

Studies [1] and [2] provide a useful conceptual framework and simulation test bed for evaluating the effectiveness and survivability of air-to-ground attack strategies generated by proposed IFFC and IFWC systems. We suggest that further research effort relating to the conceptual approach and algorithm development of studies [1] and [2] be focused on data sets generated by IFFC and IFWC simulations and actual flight tests.

## V. EVASIVE MANEUVERING AGAINST A MULTIPLE MISSILE THREAT

### 5.0 Summary

In a recent study [3], we have presented four real-time heuristic algorithms for determining aircraft evasion strategies against a multiple missile threat. Algorithms 1 and 2 are based on a "myopic" saddle-point calculation which apportions the projection of the instantaneous aircraft acceleration among the normals to the individual maneuver or guidance planes defined by each missile and its target. Algorithms 3 and 4 are also based on "myopic" saddle-point calculations. These latter two algorithms apportion the projection of the instantaneous aircraft acceleration into the individual maneuver planes so as to maximize the minimum of a function which is related to the line of sight rate of each missile threat. These latter two algorithms are

motivated by the concept of anti-proportional navigation.

Each algorithm has the following properties: i) each requires relatively minimal dynamic and parametric information; ii) each provides capability against an N missile threat; iii) each generates aerodynamically feasible aircraft maneuvers which meet both structural and pilot stress limitations; iv) each is computable using foreseeable hardware; v) each exhibits markovian behavior, i.e., each is restartable from present state information.

Simulation results using each algorithm with generic F-4 and AIM-9 truth models, characterized by nonlinear differential equations, including lift, drag, gravity, 3-dimensional point mass dynamics, aircraft load factor and roll rate limits, and missile autopilot dynamics and load factor limits are presented.

All four heuristic algorithms are motivated by a formal game theoretic model for multiple missile evasion. This formal game theoretic analysis is included as part of this study.

## 5.1 Further Research

Study [3] is the first reported research on the development of real-time algorithms for multiple missile evasion. We propose to continue the algorithm development initiated in [3]. This research to achieve enhanced algorithm performance will focus on the effects of i) engagement geometry; ii) maneuver initiation timing; iii) simultaneous programming of bank angle and load

factor decision variables; iv) thrust modulation and drag modulation; v) evasive maneuver smoothing via short term prediction. The results of this research could potentially impact USAF programs such as MISVAL and the Advanced Fighter Technology Integration (AFTI) program.

## VI. RECOMMENDATIONS

Our recommendations for further research on the application of game theory, markov chains, and time series models to tactical and strategic fire control systems, which were presented in sections 3.2, 4.1, and 5.1, represent an integrated program of research with substantial potential for useful impact on a variety of USAF programs. We cite AFWAL related programs such as IDOST, IFFC, IFWC, MISVAL, and AFTI as realistic examples.

## REFERENCES


1. E. B. Pate, M. Mintz, S. A. Goodman, and W. Dziwak, "Robust AAA Prediction Based On Finite Markov Chains and Multivariable Time Series Models," to appear as an invited paper in the Proceedings of the 1981 Southcon Conference.

2. S. F. Huling, and M. Mintz, "ENHANCED FILTERING & *PREDICTION FOR AAA FIRE CONTROL:* An Application of Game Theory and Time Series Analysis," Final Report on Contract No. DAAK10-78-C-0186, Submitted to US Army ARRADCOM, May 1980.

3. M. S. Sheketoff, S. F. Huling, and M. Mintz, "A SIMULATION STUDY OF FOUR REAL-TIME HEURISTIC ALGORITHMS FOR MULTIPLE MISSILE EVASION: A Game Theoretic Approach," Final Report on Grant No. 77-3327, Submitted to US Air Force AFOSR, June 1979.

4. M. Mintz, "Applications of Game Theory, Finite Markov Chains, and Multivariate Time Series Models to Tactical and Strategic Fire Control Systems," forthcoming *Air Force Avionics* Laboratory Technical Report.

5. R. G. Sea, "An Efficient Suboptimal Decision Procedure for Associating Sensor Data With Stored Tracks in Real-Time Surveillance Systems," Proceedings of the IEEE Conference on Decision and Control, 1971, pp. 33-37.

6. R. A. Singer, and R. G. Sea, "New Results in Optimizing Surveillance System Tracking and Data Correlation Performance in Dense Multitarget Environments," IEEE Transactions On Automatic Control, Vol. AC-18, No. 6, December 1973, pp. 571-582.

7. H. B. Driessen, "Design Considerations for Radar Tracking in Clutter," STC Professional Paper PP-110, SHAPE Technical Centre, The Hague, The Netherlands, 1975.

8. Conference Proceedings: Strategies for Automatic Track Initiation, NATO Advisory Group for Aerospace Research and Development, AGARD-CP-252, June 1979.

9. Conference Proceedings: Modeling and Simulation of Avionics Systems and Command, Control and Communication Systems, NATO Advisory Group for Aerospace Research and Development, AGARD-CP-268, January 1980.

1980 USAF - SCEEE SUMMER FACULTY RESEARCH PROGRAM

Sponsored by the

AIR FORCE OFFICE OF SCIENTIFIC RESEARCH

Conducted by the

SOUTHEASTERN CENTER FOR ELECTRICAL ENGINEERING EDUCATION

FINAL REPORT

# THE EFFECTS OF DIFFERENT ENVIRONMENTS ON AUDITORY CANAL AND RECTAL TEMPERATURES


| | |
|---|---|
| Prepared by: | Dr. Leland F. Morgans |
| Academic Rank: | Professor |
| Department and University: | Department of Biology, University of Arkansas at Little Rock |
| Research Location: | School of Aerospace Medicine, Crew Technology Division, Crew Protection Branch |
| USAF Research Colleague: | Dr. Sarah A. Nunneley |



| | |
|---|---|
| Date: | August 6, 1980 |
| Contract No: | F49620-79-C-0038 |

# THE EFFECTS OF DIFFERENT ENVIRONMENTS ON AUDITORY CANAL AND RECTAL TEMPERATURES

by

Leland F. Morgans

## ABSTRACT

The effects that different inflight and preflight environments have on auditory canal and rectal temperatures were investigated. The various types of environments included the donning and removal of a flight helmet, different ambient temperatures, the type of material that was used to pack and cover the auditory canal, and whether or not a breeze was blowing past the subjects. Results obtained from these experiments have shown that: (1) the ambient temperatures had a significant effect upon both auditory canal and rectal temperatures; (2) the donning and removal of a flight helmet and whether or not a breeze was blowing past the subject had a significant effect on auditory canal but not rectal temperatures; (3) and the type of material used to pack and cover the auditory canal did not significantly affect either auditory canal or rectal temperatures.

## Acknowledgement

The author would like to thank the Air Force Systems Command, the Air Force Office of Scientific Research, and the Southeastern Center for Electrical Engineering Education for providing him with the opportunity to spend a very worthwhile and interesting summer at the School of Aerospace Medicine, Brooks AFB, TX.

The author would also like to thank Dr. Sarah A. Nunneley for suggesting this area of research and for her collaboration and guidance. Acknowledgments should be given to Dr. Loren G. Myhre for his helpful suggestions concerning this and future areas of research and to MSgt Tom Crosby and Mr. Don Tucker for teaching me the research techniques that were used during the summer. Stephanie Malloy deserves a special word of praise for performing all of the statistical analyses on the data. Finally, I would like to thank Capt Richard F. Stribley who provided me with some of the raw data that he collected in experiments which he conducted during the previous year (1979).

## I. INTRODUCTION

It has been known for some time that heat stress adversely affects human performance.[1,2,3] Cockpit temperatures of fighter aircraft can become quite warm.[4,5,6,7,8,9] For example, cockpit temperatures in fighter aircraft have been found to remain above 30°C during low-level flight in hot weather[10,11,12] and peaks of 45°C or more have been recorded in the F-4.[11] Also, radiant heating due to sunlight has been found to produce black globe temperatures 8-12°C above dry bulb temperatures.[10,12] Therefore, since cockpit tempeartures do become quite high, it should come as no surprise that these temperatures can produce adverse effects on the pilot.[10,11,12,7,13,14]

One of the best ways to measure the effects of heat stress within an individual is to monitor his core temperature.[15,16] However, many factors can affect core temperature such as exercise,[17,18] surrounding ambient temperatures,[19,20] hyperventilation and muscle tensing,[21] donning a flight helmet,[22] applying heat to the head,[23,24,25] cooling the head,[26,27] etc. The preflight and inflight recording of core temperature usually uses one of two methods: rectal (Tre) and auditory canal (Tac) temperatures. Rectal temperatures are rarely recorded because of the reluctance of aircrews to use this method. For these reason, Tac is used in both the laboratory and field environment to measure core temperature. However, the problem with using Tac as an indicator of core temperature is that environmental changes may cause Tac to fluctuate rapidly whereas Tre remains more stable and changes that do take place occur more slowly.[25,26,28] Thus, Tre may be a better indicator of true core temperature than Tac.

## II. OBJECTIVES

One of the primary objectives of this research project was to study the combined effects of various preflight and inflight environmental conditions on auditory canal and rectal temperatures. The various environmental conditions were: ambient temperatures, types of ear packing and covering material, donning and removal of a flight helmet and whether or not a breeze was blowing.

Another objective of this study was to determine what effect central core temperature changes had on auditory canal and rectal temperatures. A third objective was to determine which of the two temperature recordings, i.e., Tre or Tac, is more stable and thus gives a better indication of true core temperature.

## III. MATERIALS AND METHODS

All of the eleven subjects used in this study were either military personnel or civilians who worked for the Air Force at the School of Aerospace Medicine (Brooks AFB) in San Antonio, Texas. Five of the subjects were used in the first experiment that was conducted in the summer of 1979 while the other six individuals were used in the second experiment that was carried on in the summer of 1980. All of the subjects were informed of the nature of the experiments before they agreed to participate and they all signed the proper consent forms.

The experiments were conducted in environmental chambers which were set at 22°C (cool environment) or 35°C (warm environment). Temperatures were measured using rectal and ear thermistors (YSI, 700 series). The tympanic membrance was examined with an otoscope before the ear probe was inserted so that one could be certain the ear was free of infection or any other potentially hazardous condition. The auditory canals were either packed with cotton or they were packed with cotton and covered with a sheet of plastic. Thus, the first experiments consisted of the following four runs: (1) the environmental chamber was set at 22°C and the auditory canal was packed with cotton; (2) the environmental chamber was set at 22°C and the auditory canal was packed with cotton which in turn was covered by plastic; (3) the environmental chamber was set at 35°C and the auditory canal was packed with cotton; and (4) the environmental chamber was set at 35°C and the auditory canal was packed with cotton which in turn was covered with plastic. Each subject participated in all four runs in a randomized order. No more than one run was performed on a subject/day and each subject did not participate in more than two runs/week. A minimum of one day elapsed between each run with every subject.

After the ear and rectal thermistors were inserted and the individual was in the environmental chamber, the probes were attached to a temperature recorder and printer (Westronics, Inc.) that was located outside the chamber.

While the subjects were in the environmental chamber, five experimental conditions were performed on them, always in the same sequence: (1) fan off, helmet off; (2) fan off, helmet on; (3) fan off, helmet off; (4) fan on, helmet off; and (5) fan off, helmet on. The helmets used were standard flight helmets. The fan created an air flow which was measured at 3m/sec by an anemometer (Datametrics). Once a subject's Tac and Tre had reached a steady

state ($\pm$0.05°C over a five minute period) in a particular stage, he was moved on to the next stage. This procedure was repeated until the subject had completed all five stages.

Because of the results obtained in the first experiment, a second experiment was performed that was very similar to the first. However, in the second experiment, the ear canals were only packed with cotton, i.e., they were never covered with plastic, and the subjects pedaled a bicycle ergometer when the environmental chamber was at 22°C. The subjects pedaled the bicycle at a load of 50W with a frequency of 50cpm. Five-minute work periods alternated with five-minute rest periods throughout the experiment.

The data were statistically analyzed by two to six way ANOVA and paired t-tests. Differences were considered significant if $p<.05$ and highly significant if $p<.01$.

## IV. RESULTS

The results of the first experiment are graphically shown in Fig. 1 and 2. Highly significant differences were found between Tac and Tre. The average temperatures within the auditory canal (36.34°C) were lower than those of the rectum (36.97°C). Highly significant differences also existed between the trends of Tre and Tac. Rectal temperatures showed a trend toward a slight fall or rise depending upon whether the experiment was performed in a cool or warm environment whereas auditory canal temperatures tended to fluctuate more with the external environmental changes such as donning or removing the flight helmet or whether or not a breeze was blowing.

The two different dry bulb temperatures (Tdb) had a significant effect on Tac in that the average auditory canal temperatures were lower (35.88°C) when the surrounding Tdb was 22°C than they were when Tdb was 35°C (36.66°C). Auditory canal packing and covering material (ear coverings) did not have a significant effect on Tac, i.e., it didn't matter whether the auditory canal was packed with cotton only or whether, in addition to the cotton, the external ear was covered with a sheet of plastic. The different experimental conditions had highly significant effects on Tac. Donning of a flight helmet produced a rise in Tac whereas flight helmet removal caused a fall in Tac. If a breeze was blowing, it produced a further drop in Tac at 22°C Tdb but not at 35°C Tdb. These fluctuations in Tac were more

pronounced in 22°C than they were in 35°C. Within those experimental conditions, stations 1 and 3 (fan off, helmet off) were the same as were stations 2 and 5 (fan off, helmet on). In order to answer the question as to whether or not stations 1 and 3 and 2 and 5 had similar Tac, paired t-tests were conducted. These tests showed that highly significant differences existed between conditons 1 and 3 and significant differences existed between 2 and 5.

Since there was a significnat fall in Tre when the experiment was performed in a cool environment, a question arose, viz., were the fluctuations that one observed in Tac at 22°C due solely to the different experimental conditions or did the decline in Tre play some role in Tac fluctuations. In order to answer that question, an experiment (experiment II, described in Materials and Methods) was designed in which the fall in Tre was prevented by having the subject perform a minimal amount of work (pedaling a bicycle ergometer) when the Tdb was 22°C. The experiment was also carried out in 35°C Tdb so that the first experiment could be duplicated as well as possible. However, no work was done in 35°C Tdb because one did not have to be concerned about a fall in Tre, as was demonstrated in the first experiment. Also, in the second experiment, two different ear coverings were not used because the results of experiment I showed that ear coverings had no significant effect on Tac or Tre. In the second experiment, then, the auditory canals were always packed with cotton and were not covered with plastic. The results of experiment II are shown in Fig. 3 and 4.

Even though fall in Tre was factored out of the experiment, the two different Tdb (22°C and 35°C) still had a significant effect on Tac, at least while the wind was blowing. Also, the different conditions still had a highly significant effect on Tac. The Tre was not significantly affected by Tdb.

## V. DISCUSSION

The results of the first experiment have shown that (1) highly significant differences exist between Tac and Tre, (2) highly significant differences exist between the trends of Tac and Tre, (3) the two different ambient temperatures had a significant effect on Tac and Tre, (4) the ear coverings did not have a significant effect on Tac or Tre and (5) the experimental conditions had a highly significant effect on Tac but no Tre.

Tac temperatures were consistently lower than Tre.[19,20] The tympanic membrane lies closer to the surrounding environment than the site where Tre was recorded which was 10 cm from the anal sphincter. Therefore, Tac should be more readily influenced by the ambient temperature. Proof of that observation can be seen by comparing Tac and Tre temperatures in a cool and warm environment (Fig. 1 and 2). When the experiment was carried out in a cool environment, Tac was 0.9°C lower than Tre. However, when the experiment was performed in a warm environment, Tac was only 0.4°C lower than Tre.

Highly significant differences existed between the trends of Tac and Tre. Rectal temperatues tended to drop slightly when the experiment was run in a cool environment whereas they tended to increase slightly when the experiment was performed in a warm environment. This general observation has been seen many times (Nunneley, personal communication). Ambient temperatures more quickly affect Tac than they do Tre.[25,26,28] Nevertheless, over an extended period of time the environmental temperatures do have an effect on core temperatures as measured by Tre. All of the runs of each of these experiments lasted three to four hours which means that the environment would have enough time to cuase changes in Tre. The more dramatic changes in Tac that occurred during the experiments probably reflect the different experimental conditions; e.g., donning and removal of the flight helmet, rather than the surrounding temperatures although one cannot rule out the possible effects that ambient temperature may have had on Tac.

Different ambient temperatures had a significant effect on Tac and Tre.[19,20,23,24,25,26,27] For example, in the first experiment Tac was lower in a cool environment than it was in warm environment (35.9°C vs. 36.7°C). The same phenomenon was observed in Tre (36.8°C vs. 36.7°C). At 22°C the gradient between skin temperature and ambient temperature is higher than it is at 35°C. Thus, more body heat would be lost by convection and radiation in a cool environment than a warm environment.[29] Consequently, the core temperature is lower in a cool environment than it is in a warm environment.

Ear coverings did not have a significant effect on Tac or Tre. The theory behind the two different coverings was that the extra sheet of plastic may have acted as a windbreaker when the fan was blowing and as an extra layer of insulation to help prevent dissipation of heat from the auditory canal. The effect, then, would have been a more stable Tac

when the sheet of plastic was used. Such was not the case because Tac remained the same (36.3°C) whether cotton or cotton plus plastic was used as a covering which indicates that the small extra layer had no effect on Tac. The plastic was, of course, not expected to have an effect on Tre since it covered the auditory canal and not the rectum.

The experimental conditions, viz., donning and removal of a flight helmet and whether or not a breeze was blowing, had a highly significant effect on Tac but not Tre. Donning of a flight helmet always resulted in an increase in Tac while removal of that helmet always resulted in a decrease in Tac.[22] The fluctuations were greater when the Tdb was 22°C than it was when it was 35°C. Donning of the flight helmet decreased the amount of convective heat loss from the auditory canal and the head region to the external environment and thus Tac rose. Removal of the flight helmet had the opposite effect. The fluctuations of Tac were greater in 22°C Tdb than they were in 35°C Tdb because of the differences in thermal gradient between skin temperature and Tdb.[29] When the experiment was performed in a cool environment, a breeze caused a reduction in Tac whereas Tac remained the same when the experiment was carried out in a warm environment. The reason for this phenonemon is that when the body surface temperature is warmer than the environmental air temperature, which it would be if Tdb was 22°C, then there is a net flow of heat from the body to the surrounding air. As this air is heated, it rises and is replaced by more dense, cooler air. Thus, cool air moves continuously up to the body surface, is warmed by the body heat, and then flows away, resulting in a net heat loss from the surface (convection). What the breeze does then, when Tdb is 22°C, is to increase the amount of convective heat loss which results in an even cooler Tac.[32] Conversely, when Tdb is 35°C, the thermal gradient is negligible between the body surface and Tdb. Under these conditions, the blowing of a breeze does not increase the amount of convective heat loss from the body to the surrounding environment and thus Tac remains the same. One would not expect the breeze to have an effect on Tre since the fan was blowing primarily on the head area. It would have been interesting to note what effect the breeze might have had if the fan had blown over the entire body. In that regard, one can note from the two appropriate graphs (Fig. 1 and 2) that there was slight drop in Tre when a cool breeze was blowing and a slight increase in Tre when a warm breeze was blowing.

The results of experiment II have shown (1) that the two different ambient temperatures had no effect on Tac or Tre but (2) that the experimental conditions had a highly significant effect on Tac and Tre (Fig. 3 and 4).

The second experiment was carried out in order to determine whether or not the gradual fall that occurred in Tre when the first experiment was performed at 22°C Tdb had any effect on Tac or were the various temperature fluctuations in Tac due entirely to the different experimental conditions. This question was answered by effectively factoring out Tre, i.e., preventing a decline in Tre at 22°C Tam by having the subjects perform a minimal amount of work (see both results and materials and methods). If, after having factored out Tre, Tac was still significantly affected by the experimental conditions, one could conclude that the fluctuations in Tac were due solely to the experimental conditions. On the other hand, if the experimental conditions no longer had a significant effect on Tac, then one would know that the fluctuations were due to changes in Tre. The actual results obtained, which are depicted in Fig. 2 and 3, proved that the experimental conditions still had an effect on Tac.

The fact that Tre was factored out of the experiment explains why Tdb had no effect on Tac or Tre. The sequence of events would be as follows: (1) by pedaling a bicycle in a cool environment one increases the amount of body heat produced; (2) the increase in body heat is reflected in an increase in core temperature; (3) an increase in body temperature produces a core temperature that is closer to the core temperature when the experiment was performed at 35°C; (4) thus, in effect, Tdb would have no effect on Tac or Tre.

## VI. RECOMMENDATIONS

### a. Implementation of these experiments

Based upon the results of these experiments, the following recommendations can be made:

1. Rectal temperature is the best measure of true core temperature, particulatrly in a steady state condition. Environmental changes produce rapid fluctuations in auditory canal temperatures. This phenomenon is especially true with respect to donning and removal of a flight helmet and the presence or absence of a wind. Therefore, if one wants a true measure steady state core temperature one should use rectal temperatures or, if auditory canal temperatures must be used, then the flight helmet should remain

on at all times pertaining to a flight (even the preflight) because removal of the helmet causes too many fluctuations in auditory canal temperatures.

2. If one wants to measure the rapid effects of transient environmental situations on core temperature, then auditory canal temperatures would be a better choice. Even though rectal temperatures represent a better measuremetn of steady state conditons, they exhibit too much of a lagging response pattern with respect to transitory environmental changes.

b. Follow-on research

Since cockpit temperatures do become hot, especially during low level flights, one of the problems that the Air Force faces, it seems to me, is how to acclimate their pilots and other aircraft personnel to the various stresses of heat. Studies have shown that physical training in a cool environment improves tolerance to exercise in the heat and the rate of heat acclimitization.[31,32,33] The retention of heat acclimatization responses also appears improved in physically trained individuals.[34] The classic description of the physiological changes associated with improved exercise heat tolerance or the heat acclimatized iandividual performing exercise in the heat are the maintenacne of high level of sweating, lowered heart rate, and lowered internal body temperature. One can produce these physiological changes by engaging in training programs that (1) increase the heart rate (to at least 60% of the maximum heart rate reserve) and (2) cause high levels of body hyperthermia.[33,34,35]

My own recent interests have been in the area of exercise physiology, particularly sports physiology. Within the past year, I have begun some studies on racquetball players which I believe could serve as an excellent model with respect to the whole area of acclimation to heat stress. Our studies have shown that racquetball has a tremendous training effect (results available upon request since they are still in the process of being published). During a match, which lasts an hour, these individuals average using approximately 75% of their maximum heart rate reserve (MHRR). At no time does the MHRR drop below 60%. By personally observing these individuals during a match, I feel there must be a tremendous increase in body heat because these people sweat profusely. Therefore, racquetball represents an excellent method of studying acclimation to heat stress because the sport produces an excellent training effect (which would result in a lower heart rate) and a possible increase in core temperature. In addition, racquetball seems to exhibit a rapid learning curve so that one does not have to possess athletic ability

or spend long hours practicing in order to develop the skills necessary to play the game.

The effects of racquetball and other sports on heat acclimation could be performed in the following two stages:

Stage I

Since my previous experiments indicate that a large increase in heart rate occurs during a racquetball match, one now needs to determine if the sport also increases body temperature which in turn would have a positive effect on heat acclimation. This stage would the basis of a mini-grant. The possibility does exist that racquetball may not increase core temperature because the subject may respond to the increase in body temperature by evaporation, sweating , vasomotor response, etc. in such a proficient manner that there may be no increase (in body temperature). Rectal probes and skin thermisters attached to a Medi-log recorder would be used to record changes in body temperature. Sweat rates could also be measured using standard techniques.

Stage II

The purpose of these experiments would be to determine if tennis, played outdoors, would increase core temperature more than racquetball and therefore act as a better heat acclimator. This stage would be the basis of a follow-on unsolicited proposal. Tennis was chosen because it provides additional heat stress factors, viz., radiant heat from the sun and a possible higher environmental temperature depending on what time of the year the match was played. One would have to repeat my original racquetball experiments on tennis players in order to determine the training effect of tennis. In order to study which sport better acclimated the individual to heat stress one could perform standard heat tolerance tests (HTT) on the participants of the two sports. A student population would be used as a control. Runners might also be compared because they are known to perform very well to HTT.

Fig. 1. Experiment performed in cool ($22^{o}C$) environment. Each point represents the Mean (n=5) with the vertical lines showing $\pm 1$ S.E.M.

Fig. 2. Experiment performed in warm ($35^{o}C$) environment. Symbols as in Fig. 1.

Fig. 3. Experiment performed in cool environment while pedaling a bicycle ergometer. Each point represents the Mean (n=6) with other symbols as in Fig. 1.

Fig. 4. Experiment performed in warm environment. No pedaling of the bicycle ergometer. Mean as in Fig. 3 and other symbols as in Fig. 1.

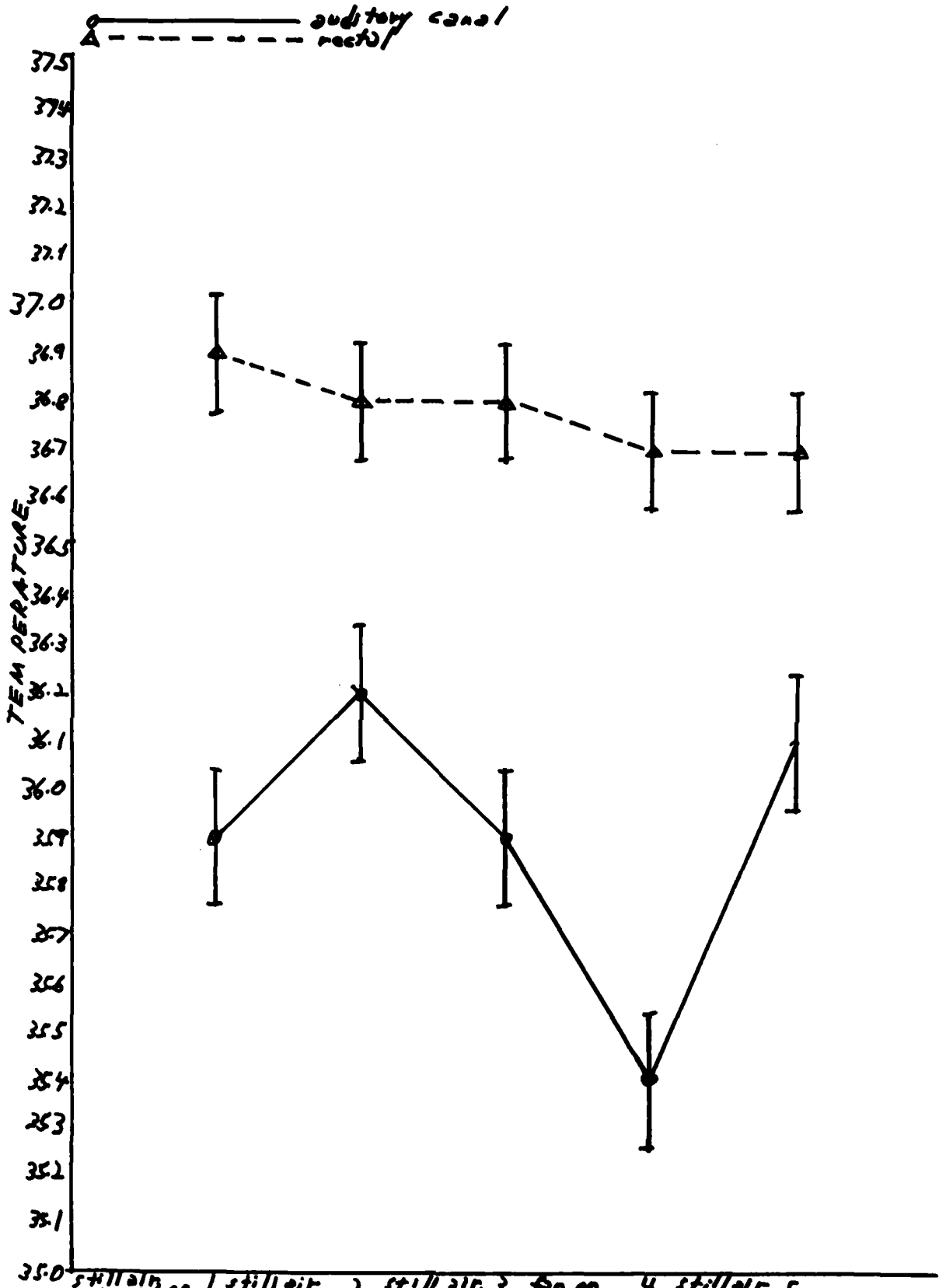



Fig. 1 Experiment performed in the cold (-1.4°C) environment

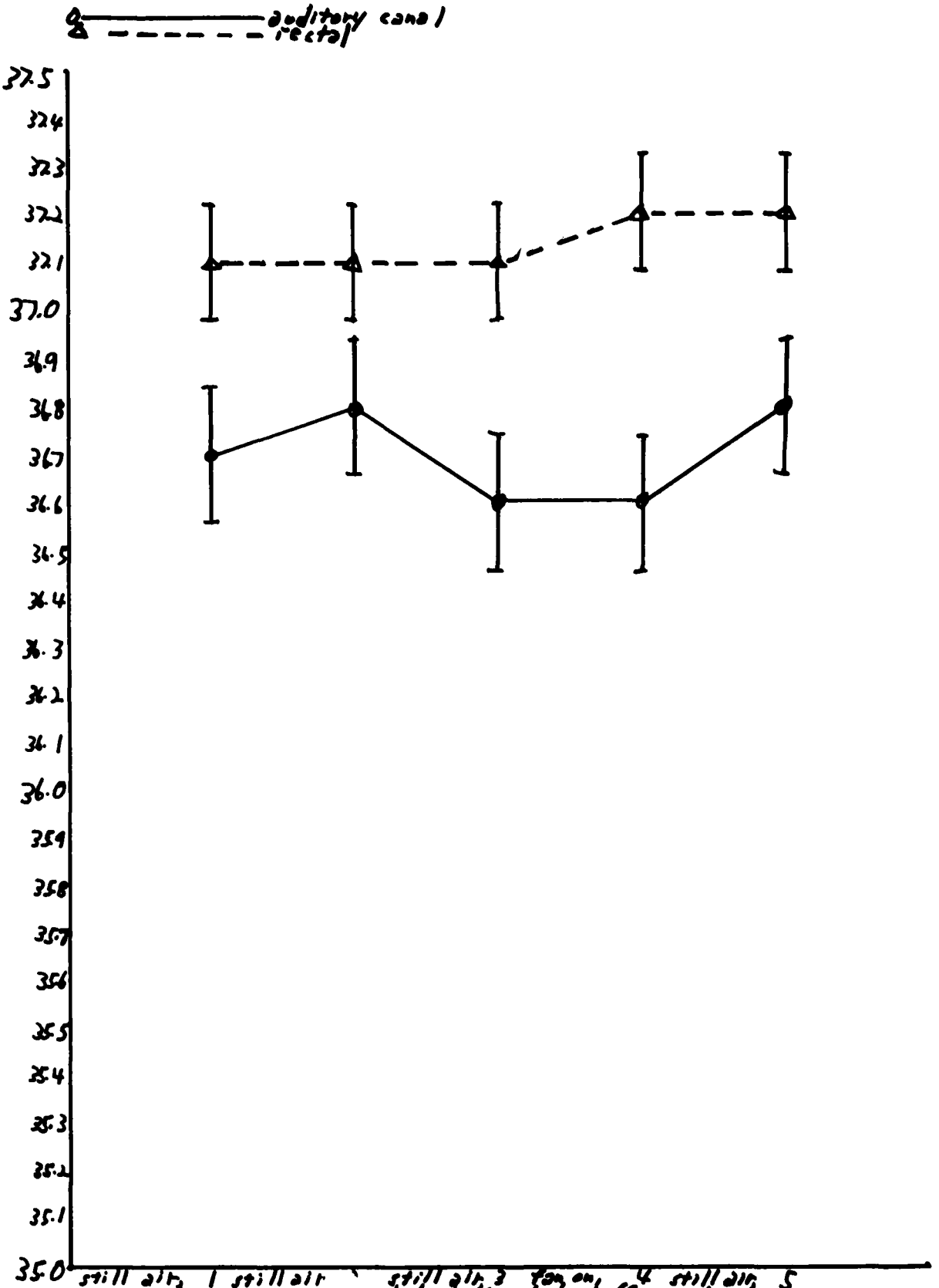



Fig. 2 Experiment performed in warm (35°C) environment

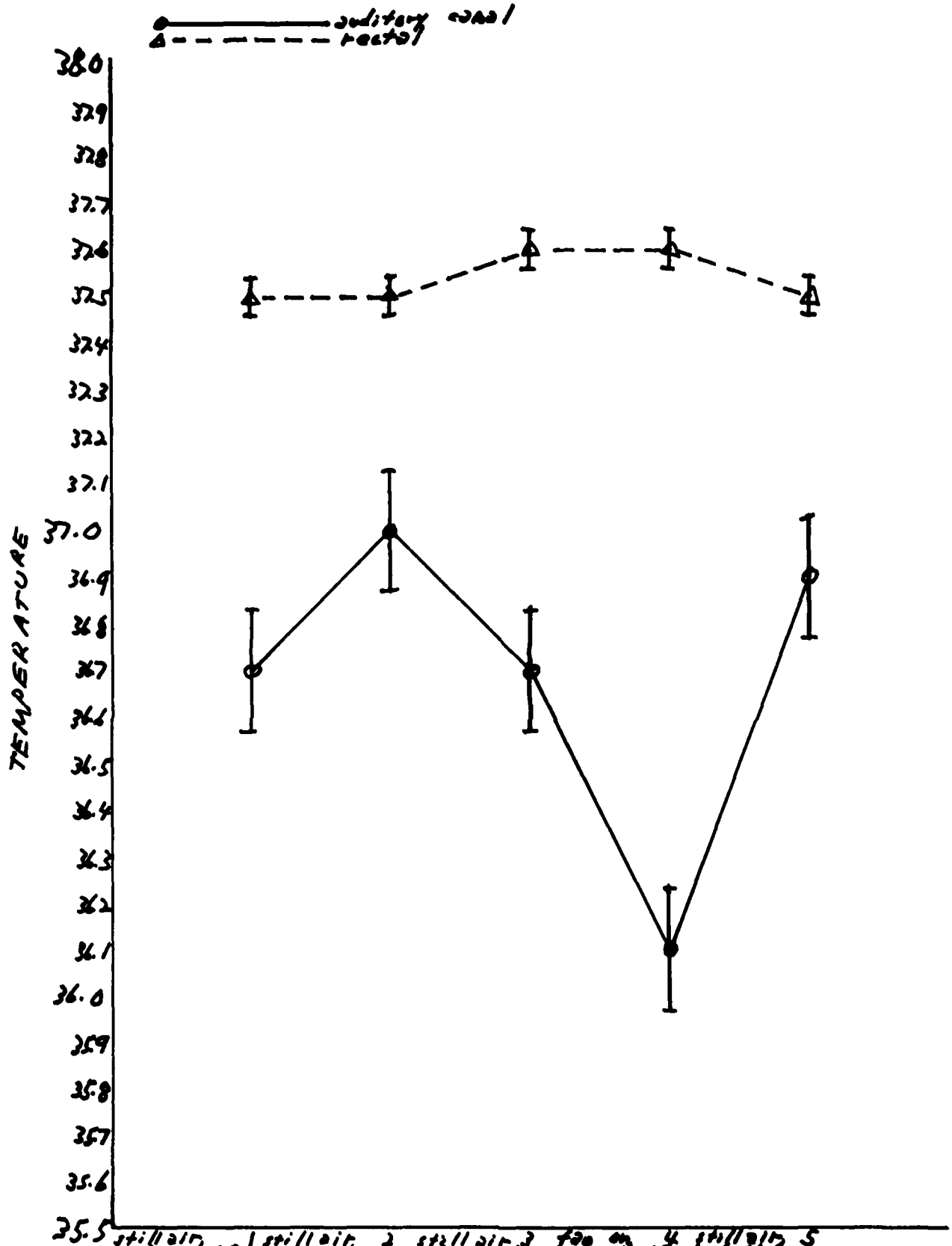



Fig. 3 Experiment performed in cool (24°C) environment

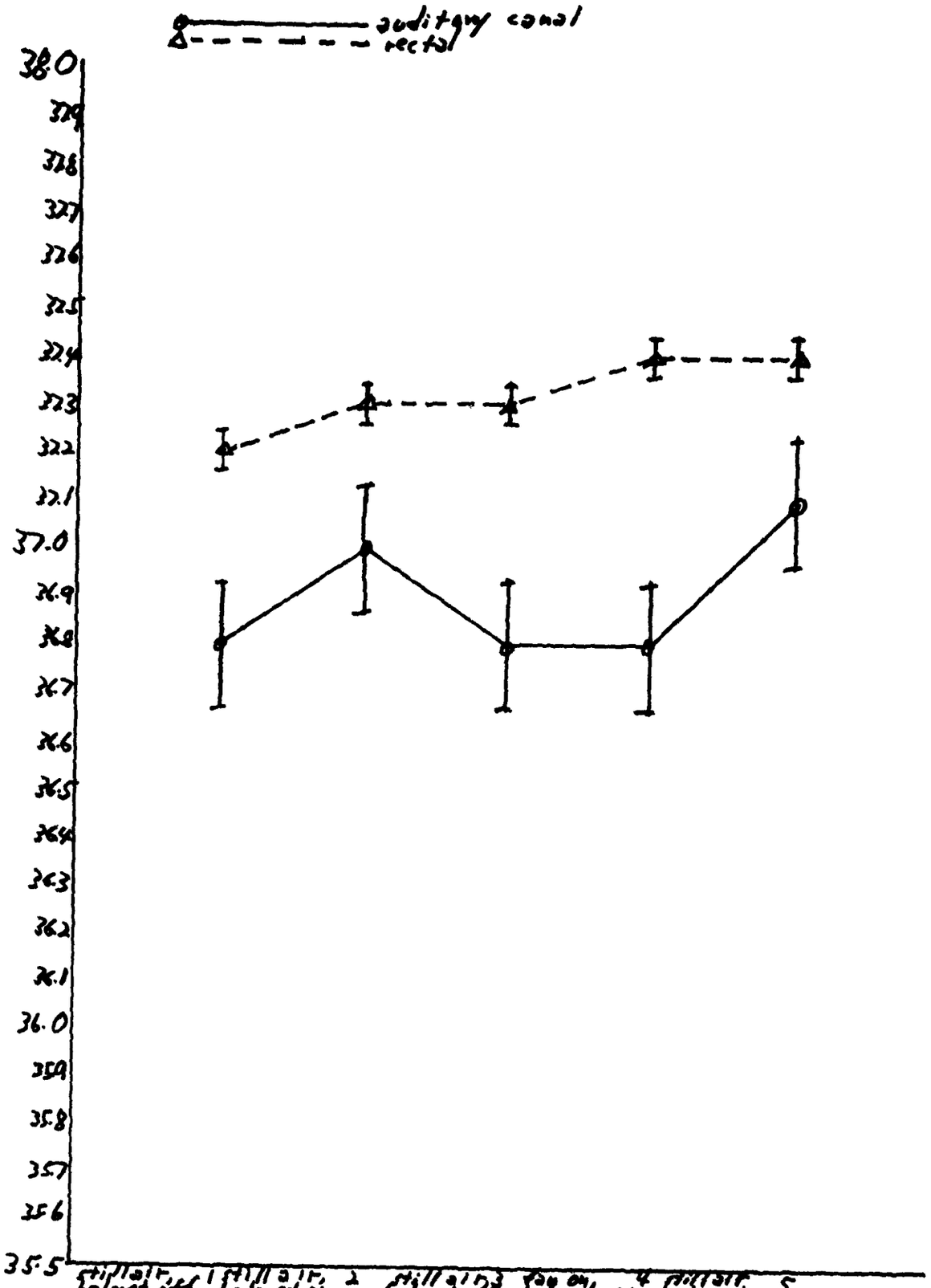



Fig. 4 Experiment performed in warm (35°C) environment

## REFERENCES


1. Allnutt, M. F., and J. R. Allan, "The Effects of Core Temperature Elevation and Thermal Sensation on Performance," Ergonomics, Vol. 16, pp. 189-196, 1973

2. Ramsey, J. D., D. Dayal, and B. Ghahramani, "Heat Stress Limits for the Sedentary Worker," Am. Indust. Hyg. Assoc. J., Vol. 36, pp. 259-265, 1975.

3. Wing, J. R., "Upper Thermal Tolerance Limits for Unimpaired Mental Performance," Aerospace Med., Vol. 36, pp. 960-963, 1965.

4. Clifford, J. M., "Head Ventilation," Flying Personnel Research Committee, RAF Institute of Aviation Medicine, p. 30, 1965.

5. Hughes, R. L., "Cabin Air Requirements for Crew Comfort in Military Aircraft," RAF Institute of Aviation Medicine, IAM TR-68-304, 1968.

6. Joy, R. J. T., "Heat Stress in Army Pilots Flying Combat Missions in the Mohawk Aircraft in Vietnam," Aerospace Med., Vol. 38, pp. 389-900, 1967.

7. Nunneley, S. A. and L. G. Myhre, "Physiological Effects of Solar Heat Load in a Fighter Cockpit," Aviat. Space Environ. Med., Vol. 47(9), pp. 969-973, 1976.

8. Nunneley, S. A., P. J. Dowd, L. G. Myhre, and R. F. Stribley, "Physiological and Psycological Effects of Heat Stress Simulating Cockpit Conditions," Aviat. Space Environ. Med., Vol. 49(6), pp. 763-767, 1978.

9. Nunneley, S. A. and C. F. Flick, "Heat Stress in the A-10 Cockpit: Flight Over Desert," in preparation.

10. Allan, J. R., M. H. Harrison, C. Higenbottam, R. Ridgem, and C. Saxton, "In-Flight Thermal Data from Harrier, Phantom, Buccaneer, Gazelle, and Scout Aircraft," RAF Institute of Aviation Medicine, Aircrew Equipment Group Report No. 401, 1976.

11. Bollinger, R. R. and G. R. Carwell, "Biomedical Cost of Low-Level Flight in a Hot Environment," Aviat. Space Environ. Med., Vol. 46, pp. 1221-1226, 1975.

12. Nunneley, S. A. and G. R. James, "Cockpit Thermal Conditions and Crew Skin Temperatues Measured in Flight," Aviat. Sapce Environ. Med., Vol. 48, pp. 44-47, 1977.

13. Goldman, R. F., "Assessment of Thermal Comfort in Flight and its Effects on Performance," In: AGARD Conference Proceedings No. 40, 1968.

14. Larsson, L. E., H. Nilsson, B. Andrae and O. Wilson, "Determination of Pilot Performance During Heat Stress in a Flight Simulator," Swedish Institute of Aviation Medicine, Report 72-7, 1972.

15. Cooper, K. E., W. I. Cranston, and E. S. Snell, "Temperature in the External Auditory Meatus as an Index of Central Temperature Changes," J. Appl. Physiol., Vol. 19(5), pp. 1032-1035, 1964.

16. Kerslake, D. Mck., The Stress of Hot Environments, Cambridge University Press, p. 128.

17. Aikas, E., M. Karvonen, P. Piironen, and R. Ruosteenoja, "Intramuscular, Rectal and Oesophageal Temperatue During Exercise," Acta Physiol. Scand, Vol. 54, pp. 366-370, 1962.

18. Saltin, B. and Hemansen, "Esophageal, Rectal, and Muscle Temperature During Exercise," J. Appl. Physiol., Vol. 21(6), pp. 1747-1762, 1966.

19. Nadel, E. R. and S. M. Horvath, "Comparison of Tympanic Membrane and Deep Body Temperatures in Man," Life Sciences, Vol. 9(1), pp. 869-875, 1970.

20. Piironen, P. and E. Aikas, "Temperature of the Human Body During Rapid Alternate Heating and Cooling," Institute of Occupational Health, Report No. AMRL-TR-64-131. 1964.

21. Cranston, W. I., J. Gerbrandy, and E. S. Snell, "Oral, Rectal and Oesophageal Temperatures and Some Factors Affecting Them in Man," J. Physiol., Vol. 126, pp. 347-358, 1954.

22. Edwards, R. J., A. Belyavin, and M. H. Harrison, "Core Temperature Measurements in Man," Aviat. Space Environ. Med., Vol. 49(11), pp. 1289-1294, 1978.

23. Marcus, P., "Some Effects of Cooling and Heating Areas of the Head and Neck on Body Temperature Measurement at the Ear," Aerospace Med., Vol. 44(4), pp. 397-402, 1973.

24. Marcus, P., "Some Effects of Radiant Heating of the Head on Body Temperature Measurement at the Ear," Aerospace Med., Vol. 44(4), pp. 403-406, 1973.

25. McCaffrey, T. V., G. S. Geis, J. M. Chung, and R. D. Wurster, "Effect of Isolated Head Heating and Cooling on Sweating in Man," Aviat. Space Environ. Med., Vol. 46, pp. 1353-1357, 1975.

26. Nunneley, S. A., S. J. Troutman, Jr., and P. Webb, "Head Cooling in Work and Heat Stress," Aerospace Med., Vol. 42(1), pp. 64-68, 1971.

27. Williams, B. A. and A. Shitzer, "Modular Liquid-Cooled Helmet Liner for Thermal Comfort," Aerospace Med., Vol. 45(9), pp. 1030-1036, 1974.

28. Piironen, P., "Effects of Exposures to Extremely Hot Environments on Temperatures of the Tympanic Membrane, the Oesophagus, and the Rectum of Men," Technical Documentary Report, No. AMRL-TDR-63-85, 1963.

29. Nadel, R. R., "Control of Sweating Rate While Exercising in the Heat," Med. Sci. Sports, Vol. 11(1), pp. 31-35, 1979.

30. Ruch, T. C. and H. D. Patton, Physiology and Biophysics, Philadelphia, PA, W. B. Saunders, 19th edition, p. 1052, 1965.

31. Gisolfi, C. V., "Work-Heat Tolerance Derived From Interval Training," J. Appl. Physiol., Vol. 35, pp. 349-354, 1973.

32. Gisolfi, C. V. and J. S. Cohen, "Relationships Among Training, Heat Acclimation, and Heat Tolearnce in Men and Women: the Controversy Revisited," Med. Sci. Sports, Vol. 11(1), pp. 56-59, 1979.

33. Henane, R., R. Flandrois, and J. P. Charbonnier, "Increase in Sweating Sensitivity by Endurance Conditioning in Man," J. Appl. Physiol., Vol. 43, pp. 822-828, 1977.

34. Pandolf, K. B., R. L. Burse, and R. F. Goldman, "Role of Physical Fitness in Heat Acclimatization, Decay and Reinduction," Ergonomics, Vol. 20, pp. 399-408, 1977.

35. Shvartz, Y. S., A. Maganik, A. Meroz, H. Birnfeld, A. Mechtinger, and S. Shibolet, "Heat Acclimation, Physical Fitness, and Responses to Exercise in Temperature and Hot Environment," J. Appl. Physiol., Vol. 43, pp. 678-683, 1977.

1980 USAF - SCEEE SUMMER FACULTY RESEARCH PROGRAM

Sponsored by the

AIR FORCE OFFICE OF SCIENTIFIC RESEARCH

Conducted by the

SOUTHEASTERN CENTER FOR ELECTRICAL ENGINEERING EDUCATION

FINAL REPORT

# SIDE-LOBE MODULATION


| | |
|---|---|
| Prepared by: | Dr. Gene Moriarty |
| Academic Rank: | Assistant Professor |
| Department and University: | Department of Electrical Engineering<br>San Jose State University |
| Research Location: | Rome Air Development Center<br>Surveillance Division<br>Surveillance Technology Branch<br>Signal Processing Section |
| USAF Research Colleague: | Mr. Paul Van Etten |
| Date: | August 1, 1980 |
| Contract No: | F49620-79-C-0038 |

# SIDE-LOBE MODULATION

by

Gene Moriarty

## ABSTRACT

This research effort considers the possibility of time-modulating an antenna's aperture such that, in the far-field pattern, the sidelobes are severely modulated while the main beam remains unmodulated. A number of different approaches are investigated. A method of time averaging of sub-arrays is found to produce the most significant results. The theoretical details as well as examples to illustrate this method are presented. Directions for further research in this area are suggested.

## ACKNOWLEDGEMENT

The author would like to thank the Air Force Systems Command, Air Force Office of Scientific Research, Rome Air Development Center, and the Southeastern Center for Electrical Engineering Education for providing the opportunity to carry out the research described herein. Special acknowledgement is made to Paul Van Etten of RADC, the effort's focal point, for suggesting this research area and for his generous assistance and expert guidance throughout the author's ten week stay at RADC.

Appreciation is also extended to John Huss, Clarence Silfer, Russ Brown, John McNamara, Carmen Malagisi, Cheri Christy and Jeff Guernier, all of RADC, for their assistance in various aspects of this project.

## I. INTRODUCTION:

Radar is an indispensible link in many Air Force systems. This research effort is in the service of improving certain features of radar operation. Array antennas which are formed by a combination of individual radiators are receiving increased attention in modern radar systems. They will be emphasized in this research. Array antennas have a distinct advantage over antennas of the lens or reflector type: the radar beam can be steered without mechanically moving the entire array antenna structure. It is only necessary to vary electronically the relative phase between the radiating elements. This advantage increases as the size of the antenna increases.

Array antennas are characterized by the geometric position of the individual radiators and by the amplitude and phase of their excitation. The excitation distribution is related to the far-field radiation pattern by the Fourier transform. Among the parameters of the far-field of interest in radar design are beam-width, directivity, power gain, impedance and sidelobe level. Low sidelobes, for example, are generally desired in most radar designs. This research focuses on the effective reduction of sidelobe levels by time-modulating the array excitation distribution. A number of different time-modulation schemes will be investigated.

It is well known that a uniform radar current distribution produces a far-field pattern whose first sidelobe level is 13.5 dB down from the mainbeam. To achieve lower sidelobe levels many clever schemes have been devised [1,4]. Most of these employ a nonuniform current excitation across the antenna's radiating elements. The binomial distribution, for example, produces zero sidelobes but at the expense of a very wide main beam. The Dolph-Chebyshev current distribution yields a far-field pattern which has minimum beamwidth for a specified sidelobe level. In theory, these distributions can produce zero or very low sidelobes. In practice, however, for a single array antenna, a sidelobe level of around 40 dB is minimum. This is because very low sidelobe levels require very large current ratios across the aperture distribution and these large current ratios are impossible to maintain with the presently available construction technologies.

Now, if the excitation distribution of an array antenna is time-modulated, then the far-field radiation pattern will also be time-modulated. By proper choice of a modulation function, a far-field pattern can be produced which has a fairly steady mainbeam and sidelobes which when averaged over a period of time are effectively very low. Time-modulation schemes will be investigated in this research effort as a way of overcoming the practical 40 dB limitation on minimum sidelobe levels.

## II. OBJECTIVES:

The objectives of this project were:

(1) To investigate various modulation schemes in order to achieve effectively very low sidelobe levels while maintaining a fairly steady mainbeam.

(2) To develop the theory of the "sub-array" approach to sidelobe modulation (this approach proved most effective of all the approaches considered).

(3) To generate some examples to illustrate the "sub-array" approach to sidelobe modulation.

## III. MOTIVATION:

A planar array antenna produces a three-dimensional far-field pattern. An RADC programming package is available to generate far-field plots for a wide variety of aperture current distributions [3]. For a current distribution which is spatially thinned to yield 30 dB sidelobes, the far-field pattern appears as in Figure 1.

Now, if this spatially thinned antenna were rotated at a fixed angular rate, then the pattern of Figure 1 would rotate as well. Consider a particular point off the mainbeam, say at $(\theta_o, \phi_o)$, in the rotating far-field. Over a period of time, T, a time signal could be observed at $(\theta_o, \phi_o)$. The average value of this waveform would be much lower than any of the particular sidelobes indicated in Figure 1.

However, the prospect of rotating a large planar array of, for example, one thousand elements is not attractive. How can a similar result occur without needing to rotate a large antenna? Answer: by time-modulating the antenna elements in such a way that in the far-field at $(\theta_o, \phi_o)$ a time signal appears which is similar to the time signal mentioned above. What kind of time-modulation to employ is the question addressed by this research effort.

Further motivation is provided by a consideration of the advantages of low sidelobe levels. A particular case of interest is the situation in which a jammer is present. How can a jammer be prevented from detecting the presence of the radar signal? Of course, this is impossible to do if the jammer is right in the mainbeam. However, if the jammer is at an angle sufficiently away from the mainbeam, then he will see only the sidelobes. If the sidelobes are severely modulated, then the jammer will not be able to distinguish between the signal he detects and his own receiver noise.

The jammer problem is currently handled by adaptive radar techniques. The presence of the jammer must first be determined at a specific $(\theta_o, \phi_o)$. Then, via an adaptive feedback loop, a notch is placed in the far-field pattern at $(\theta_o, \phi_o)$. Since the mechanism for this process is rather involved, it is anticipated that sidelobe modulation techniques might serve as an alternative to adaptive processing. An obvious advantage of sidelobe modulation is that the presence of the jammer at a specific angle need not be determined, eliminating the need for a feedback loop.

## IV. AMPLITUDE AND PHASE MODULATION:

If a number of the elements in the array that produced the pattern of Figure 1 were randomly blinked off and on, then the sidelobes would appear to jump around in a random fashion. This is the desired result. However, what kind of randomness to employ on what percentage of the elements is not easy to discern, especially in a large planar array.

To get a better grasp of the problem, a simple linear array antenna was considered. The first array investigated had five elements spaced one-half wavelength apart. The amplitudes were arranged in an edge distribution: $A_0$, 0, 0, 0, $A_4$, where $A_i$ is the amplitude weighting of the ith element. Also, $A_o + A_4 = 2$ was fixed as a constraint to give a constant total power to the antenna. This guarantees at least a constant value in the far-field maximum power level.

The far-field equation for this case can be written:

$$E(\psi) = A_o + A_4 e^{j4\psi} \qquad (1)$$

where $\psi = \pi \sin\theta$ and $\theta$ is the angle off broadside. Employing the constraint, the far-field becomes

$$E(\psi) = A_o + (2 - A_o) e^{j4\psi} \qquad (2)$$

and the power becomes

$$|E(\psi)|^2 = (4A_c - 2A_o^2)(\cos A\psi - 1) + 4 . \tag{3}$$

$|E(\psi)|^2$ is plotted in Figure 2 for $A_o$ = 1.0, 0.5, 0.25, 0.0. These values could represent four points in time over which the time-modulation occurs. Obviously, if $A_o$ is blinked off and on, the whole pattern is severely modulated. However, no effective sidelobe reduction is achieved in this case. Similar results occur if the end elements are modulated with noise sources or with some other time functions, like $\sin^2 t$ and $\cos^2 t$. The indication here was that a more complicated distribution must be considered.

Next, an eight element Dolph-Chebyshev distribution was considered. From [5] the following weights produce 26 dB sidelobes: 1.0, 1.7, 2.6, 3.1, 3.1, 2.6, 1.7, 1.0. If the first and last elements are modulated with $\sin^2\omega_o t$ and $\cos^2\omega_o t$ respectively, then the far-field modulated power becomes:

$$\begin{aligned} |E|^2 = {} & \sin^2\omega_o t + 1.7\cos\psi + 2.6\cos 2\psi + 3.1\cos 3\psi + 3.1\cos 4\psi + 2.6\cos 5\psi \\ & + 1.7\cos 6\psi + \cos^2\omega_o t \cos 7\psi + 1.7\sin\psi + 2.6\sin 2\psi + 3.1\sin 3\psi \\ & + 3.1\sin 4\psi + 2.6\sin 5\psi + 1.7\sin 6\psi + \cos^2\omega_o t \sin 7\psi \end{aligned} \tag{4}$$

If $|E_u|^2$ is the unmodulated far-field power, then the relationship between $E_u$ and E is:

$$|E|^2 = |E_u|^2 - \cos^2\omega_c t - \sin^2\omega_c t\,(\cos 7\psi + \sin 7\psi) \tag{5}$$

At a fixed value of $\psi$, say $\psi = \psi_o$:

$$|E|^2 = |E_u|^2 - f(t) \tag{6}$$

These expressions are actually the square of the amplitude of the total sinusoidal voltage signal transmitted or received by this particular antenna. Thus, what is seen at $\psi_o$ is a sinusoid of the form A sin $(\omega_c t + \phi)$, where $\omega_c$ is the CW frequency and $\phi$ its phase. The amplitude, A, is the square root of the expression in (6) which can be written:

$$A = k + g(t) \tag{7}$$

Note that this amplitude is a linear combination of a constant term and a time-varying term. If a jammer, for example, detects the signal A sin $(\omega_c t + \phi)$ and computes its spectrum, what does he see? There will be impulses in the spectrum due to the constant term, k, located at $\omega = \pm\omega_c$. This is precisely the information necessary to discern the presence of the radar signal. If the expression (7) were purely a time function, then there would be no impulses and the presence of the radar signal would be concealed. The preliminary observation, then, is that not just the end elements, but all the array elements will have to be modulated.

Before considering a more total modulation, a slightly different approach was taken: modulation of the phase instead of the amplitude was investigated. For three and five element arrays with one or two elements phase modulated, the sidelobes were severely modulated, but the mainbeam was also severely modulated. This implied that larger arrays needed to be considered. But, again, with larger arrays where a few elements were phase modulated, the same problem arose which plagued the amplitude modulation schemes: to effectively swamp out the carrier signal it appeared necessary to modulate all elements of the array. A total modulation scheme which employs a set of sub-arrays did prove effective. It will be examined shortly.

## V. PAIRED-ECHOES

The concept of paired-echoes [2,4] can be employed to reduce sidelobe levels. Let $f(x)$ be the current distribution function and $F(\theta)$ be the far-field function, then F.T. $\{f(x)\} = F(\theta)$. For discrete linear arrays $f(x)$ is sampled and the discrete Fourier transform is the proper operator. However, the paired-echo concept is more easily presented with continuous functions. If $f(x) \leftrightarrow F(\theta)$, then $f(x) + a f(x)\cos bx \leftrightarrow F(\theta) + \frac{a}{2}\left(F(\theta+\theta_0) + F(\theta-\theta_0)\right)$. The term $a f(x)\cos bx$ can be viewed as a distortion term added to the original $f(x)$. The transform is the original undistorted $F(\theta)$ plus two "echoes" similar in shape to $F(\theta)$ but displaced from it on either side by $\theta_0$.

Sidelobe reduction can be achieved by adjusting $F(\theta \pm \theta_0)$ such that $\theta_0$ occurs at the center of a sidelobe and $\frac{a}{2}$ is adjusted to be equal in magnitude and opposite in sign to the sidelobe level. As an example, consider the familiar uniform distribution which yields the familiar $\sin\theta/\theta$ far-field pattern. Adding the distortion term, the results are as in Figure 3.

The reduction of the first sidelobe level is dramatic. However, the other sidelobes are still a problem. These could each be cancelled by adding more cosines to the original $f(x)$. The resultant far-field might then have very low overall sidelobes, say 80 dB down. But the resulting current distribution function would then be a distribution, like perhaps a Dolph-Chebychev, which yields 80 dB sidelobes and the same problem occurs as before: large current ratios across the aperture are required and these are impossible to maintain.

The paired-echo concept, though not directly applicable to the issue of sidelobe modulation, does prove useful in illustrating some general ideas relevant to sidelobe reduction. In fact, almost every current distribution function may be viewed as a uniform distribution with some "distortion" term superimposed and this distortion term may always be expressed as a summation of cosine terms. This follows directly from the theory of Fourier series.

## VI. THE SUB-ARRAY APPROACH

A sub-array approach to sidelobe modulation has proved most effective. In this approach a set of M sub-arrays is designed. Each of these sub-arrays is required to be implementable in the sense that each yields a far-field pattern with a first sidelobe level of 40 dB or less. The average value of this set of M sub-arrays is required to be an array which yields a far-field pattern with very low sidelobes, for example, 80 dB or more. The modulation comes about due to switching from one sub-array to the next over a period of M time points. In general, all elements of the sub-arrays are modulated.

To explicate this sub-array approach a number of terms are defined:

$N$ = the number of elements in each array.

$M$ = the number of sub-arrays.

$k$ = the desired dB attenuation.

$\bar{k}$ = the realizable dB attenuation of the sub-arrays.

$I_i$ = the weight of the ith element of the array that achieves the desired dB attenuation ($i = 1, 2, \ldots, N$).

$I_{ij}$ = the weight of the ith element of the jth sub-array ($i = 1, 2, \ldots$ N and $j = 1, 2, \ldots, M$).

$W = \sum_{i=1}^{N} I_i$, the sum of all the weights of the desired array, the value to which the sub-array summed weights are adjusted to keep the main lobe constant.

$\eta_j$ = the scale factor of the jth sub-array.

For specified values of W, $I_i$, N, M, k and $\bar{k}$, the task is to determine $I_{ij}$ and $\eta_j$. The sum of all elements of each sub-array, multiplied by the proper scale factor, must equal W:

$$\eta_j \sum_{i=1}^{N} I_{ij} = W \quad \text{for } j = 1,2,\ldots,M \tag{8}$$

Also, it must be true that the average value of a given element in every sub-array must equal the corresponding element value in the desired array:

$$\frac{1}{M} \sum_{j=1}^{M} \eta_j I_{ij} = I_i \quad \text{for } i = 1,2,\ldots,N \tag{9}$$

Equation (8) will be called the scaling equation and equation (9) the modulation equation. Due to the symmetries in the problem, it will not be necessary to use all N of the modulation equations. This will be seen shortly.

The modulation and scaling equations need to be solved subject to some constraints on the sidelobe levels. A particularly useful formulation, from [6] , for the far-field power equations is as follows:

$$P_o(y) = \prod_{i=1}^{(N-1)/2} (y + c_i)^2 \quad \text{for N odd}, \tag{10}$$

and

$$P_e(y) = (y+2) \prod_{i=1}^{(N-2)/2} (y + c_i)^2 \quad \text{for N even}. \tag{11}$$

These equations describe the far-field power in terms of $y$ and $c_i$, where $y = 2\cos\left[\frac{2\pi d}{\lambda} (\cos\theta - \cos\theta_o)\right]$ , $\lambda$ = the free-space wavelength of the radiating signal, d = the distance between two adjacent elements, $\theta$ = the angle between the line of the linear array and a line through the center of the array, $\theta_o$ = the position of the principal maximum and $c_i$ = the terms which constitute the weights of the array elements.

Also from [6] :

$$E_o(z) = \prod_{i=1}^{(N-1)/2} \left(1 + c_i z^{-1} + z^{-2}\right) \quad \text{for N odd} \tag{12}$$

and

$$E_e(z) = (1+z^{-1}) \prod_{i=1}^{(N-2)/2} \left(1 + c_i z^{-1} + z^{-2}\right) \quad \text{for N even}. \tag{13}$$

These are called the array polynomials. The $c_i$ terms are the same as before and $z$ is related to y by: $y = z + z^{-1}$ . Expansion of $E_o$ or $E_e$ yields polynomials in $z^{-i}$, where the coefficients of $z^{-i}$ are the array weights, symmetrical with respect to the middle of the array. For example, for a five element array: $E_o(z) = 1 + (c_1 + c_2)Z^{-1} + (2 + c_1c_2)Z^{-2} + (c_1 + c_2)Z^{-3} + Z^{-4}$, which implies that the relative weights are 1, $c_1 + c_2$, $2 + c_1c_2$, $c_1 + c_2$, 1. Because of this symmetry, it is only necessary to consider equations (9), the modulation equations, for i = 1, 2,..., N/2 for N even and i = 1, 2,.... $\frac{N+1}{2}$ for N odd.

Now, to obtain the constraint equation on the first sidelobe level, the roots of $\frac{d}{dy}P(y)=0$ are obtained, excluding y = -2 and y = $-c_i$ since these values are identified as nulls of the P(y) equation. Let y = y* be the root of $\frac{d}{dy}P(y)=0$ . Then

$$\frac{P(y^*)}{P(2)} \geq \frac{1}{k_o} \tag{14}$$

becomes the constraint relation. P(2) is the maximum of P(y) and $k_o$ is found from $\bar{k}$ = 10 log $k_o$. A value typically used here is $\bar{k}$ = 40 dB. This implies $k_o = 10^4$. Thus, the constraint

$$\frac{P(y^*)}{P(2)} \geq \frac{1}{10^4} \tag{15}$$

is typically used to make sure that the first sidelobe level does not get unreasonably low in the sub-arrays to be designed.

With this as background, an algorithm can now be postulated for the sub-array approach to sidelobe modulation:

1. Specify k, $\bar{k}$, N and M.
2. Using any well known techniques, synthesize the array which in theory achieves the k dB pattern.
3. Calculate W.
4. Choose P(y) and E(Z) based on N.
5. Determine the sidelobe constraint relation from (14).
6. Express $I_{ij}$ in terms of $c_i$ from E(Z).
7. Write and solve (8) and (9) for $\eta_j$ and $I_{ij}$ subject to the constraint of step five.

## VII. EXAMPLES

As a first example, two sub-arrays each producing a first sidelobe level of 40 dB are averaged to yield an array producing 68 dB sidelobes. The two subarrays and the resultant array are seven element arrays. Although

one of the sub-arrays was actually a five elemen_ array, it can be viewed as a seven element array with zero weights on the first and last elements. The weights for the first sub-array were 1.00, 3.02, 5.29, 6.31, 5.29, 3.02, 1.00. The first scale factor was 1.00. The weights for the second sub-array were 0.00, 1.00, 2.95, 4.02, 2.95, 1.00, 0.00. The scale factor here was 1.74. The weights for the resultant array were 0.50, 2.38, 5.21, 6.66, 5.21, 2.38, 0.50. The scale factor here was 1.00. Note that the scaled weights for these arrays were not quite all the same: 24.9 for sub-array 1, 20.8 for sub-array 2 and 22.9 for the resultant array. Thus, the mainbeam will vary slightly. This is simply because with only two sub-arrays, there are not enough parameters available to be adjusted to achieve the desired result. The scaled array weights are presented in Figure 4 and the relative far-field intensities are presented in Figure 5.

In the second example, four sub-arrays each producing a first sidelobe level of 40 dB or less are averaged to yield an array producing 80 dB sidelobes. The four sub-arrays and the resultant array are all seven element arrays. Again, two of the sub-arrays are actually five element arrays, viewed as seven element arrays with zero weights on the first and last elements. The scaled array weights for the four sub-arrays are presented in Figure 6 and the far-field intensities for the four sub-arrays are presented in Figure 7. Finally, in Figure 8 is presented the array weights and the far-field intensities for the resultant array which has sidelobes that are 80 dB down. In this example, the mainbeam is kept fixed in magnitude. This can be seen by summing the scaled weights. For the four sub-arrays, as well as the resultant array, the sum of the scaled weights is 51.5.

## VIII. RECOMMENDATIONS:

A method of sidelobe modulation involving a process of time-averaging of sub-arrays has been presented. The results look promising for a couple of simple cases. However, many issues remain unresolved.

The general theory behind sidelobe modulation requires much more development. It is anticipated that some of the results of time-varying systems theory will be useful in this regard. One aspect of the sub-array approach to sidelobe modulation developed in this research that needs further study is the constraint relation (14). It is not yet clear whether such a constraint on the first sidelobe is the best approach. Another approach that bears consideration is to generate a set of specific far-field

pattern shapes which the sub-arrays would be required to produce. Such an approach to array synthesis is developed in [6] and involves approximation and interpolation theories.

The computational aspect of the problem also bears further consideration. The sub-array approach to sidelobe modulation requires the solution of a large number of nonlinear algebraic equations in many unknowns (14 equations in 14 unknowns for the second example involving four sub-arrays presented above). The standard subroutines available to perform these calculations are very sensitive to the initial starting point. Some of the results of modern nonlinear programming theory should be useful in attaining more efficient convergence.

Some final recommendations are to study the extention of the sub-array approach to sidelobe modulation to the case of planar arrays, to consider the advantages of nonuniformly spaced arrays and to explore not just modulation of the amplitudes of the array elements, but modulation of both amplitudes and phases.

## REFERENCES


1. Collin, R.E. and F.T. Zucker, Antenna Theory, (McGraw-Hill Book Co., New York, 1969).

2. Goldman, S., Frequency Analysis, Modulation and Noise, (McGraw-Hill book Co., New York., 1948).

3. Hancock, R.J. and J.R. Fricke, Parametric Antenna Analysis Software Package, Final Technical Report, RADC-TR-78-147, September 1978.

4. Klauder, J.R., et. al., "The Theory and Design of Chirp Radars", The Bell Systems Technical Journal, Vol. XXXIX, No. 4, July 1960, pp. 745-808.

5. Kraus, J.D., Antennas, (McGraw-Hill Book Co., New York, 1950).

6. Ma, M.T., Theory and Application of Antenna Arrays, (John Wiley and Sons, New York, 1974).

7. Skolnik, M.I. Introduction to Radar Systems, (McGraw-Hill Book Co., New York, 1962).

8. Skolnik, M.I., ed., Radar Handbook, (McGraw-Hill Book Co., New York, 1970).

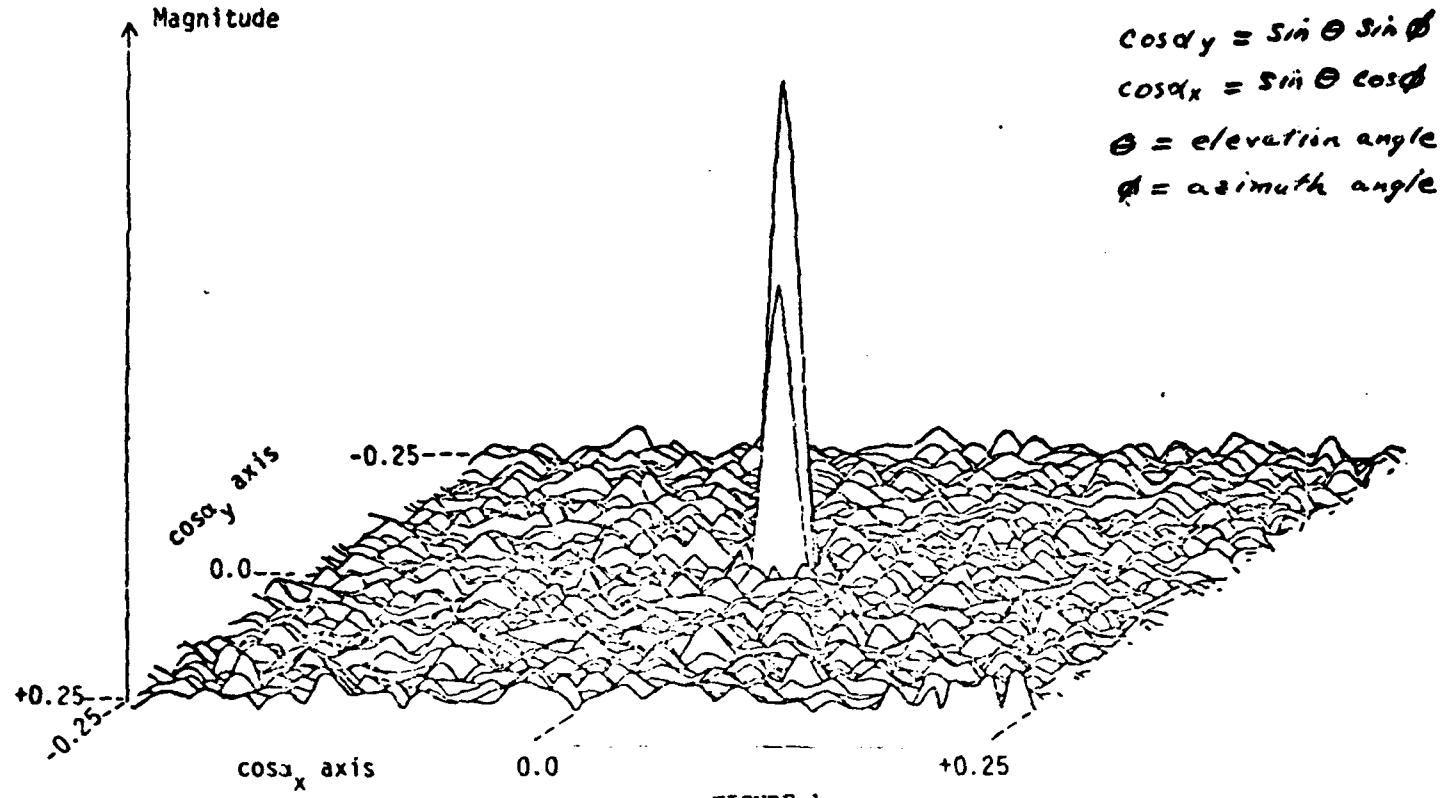



FIGURE 1
FAR-FIELD PATTERN WITH
30 dB SIDELOBES FROM A
SPATIALLY THINNED PLANAR ARRAY

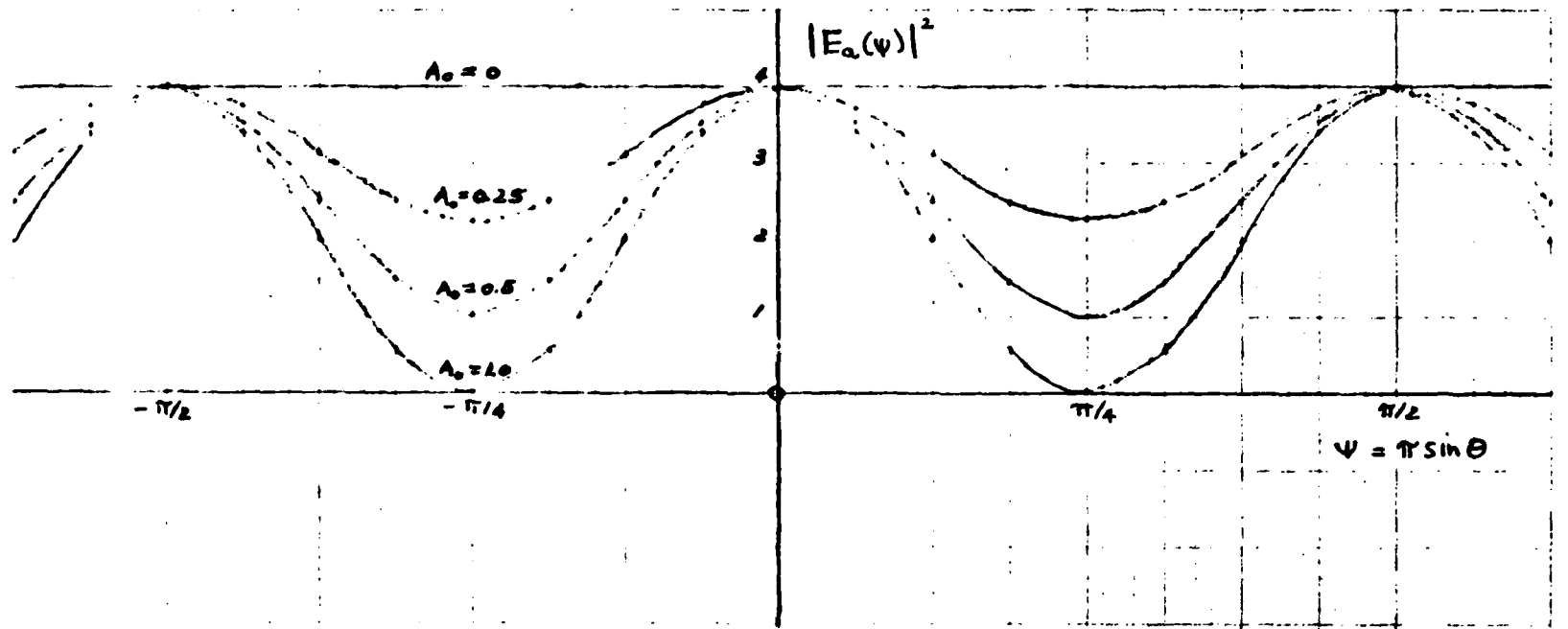



FIGURE 2

FAR-FIELD POWER PATTERN VS. $\psi$ FOR FOUR VALUES OF $A_0$

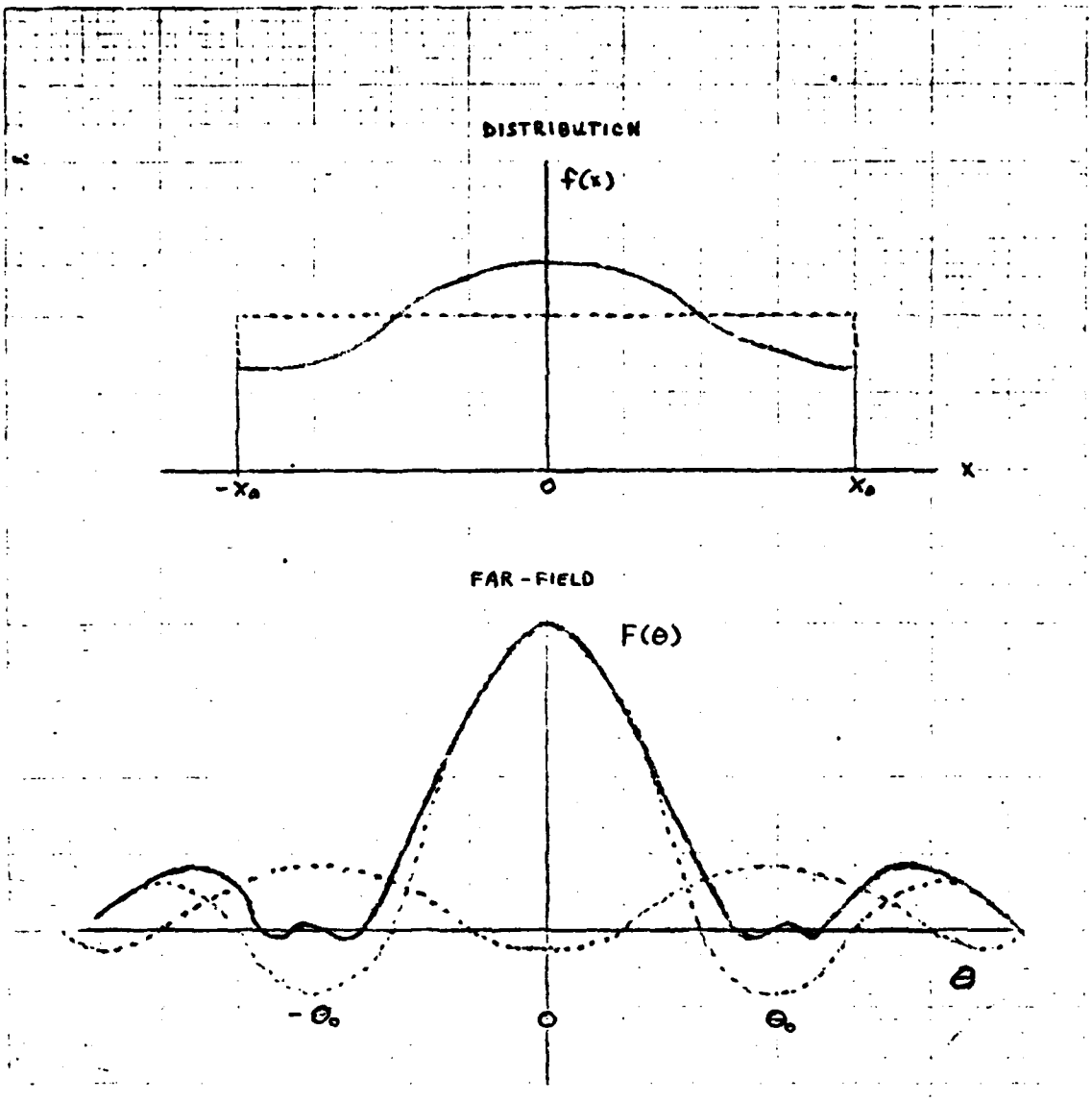



FIGURE 3
DISTORTED UNIFORM
DISTRIBUTION AND
RESULTING FAR-FIELD
PATTERN

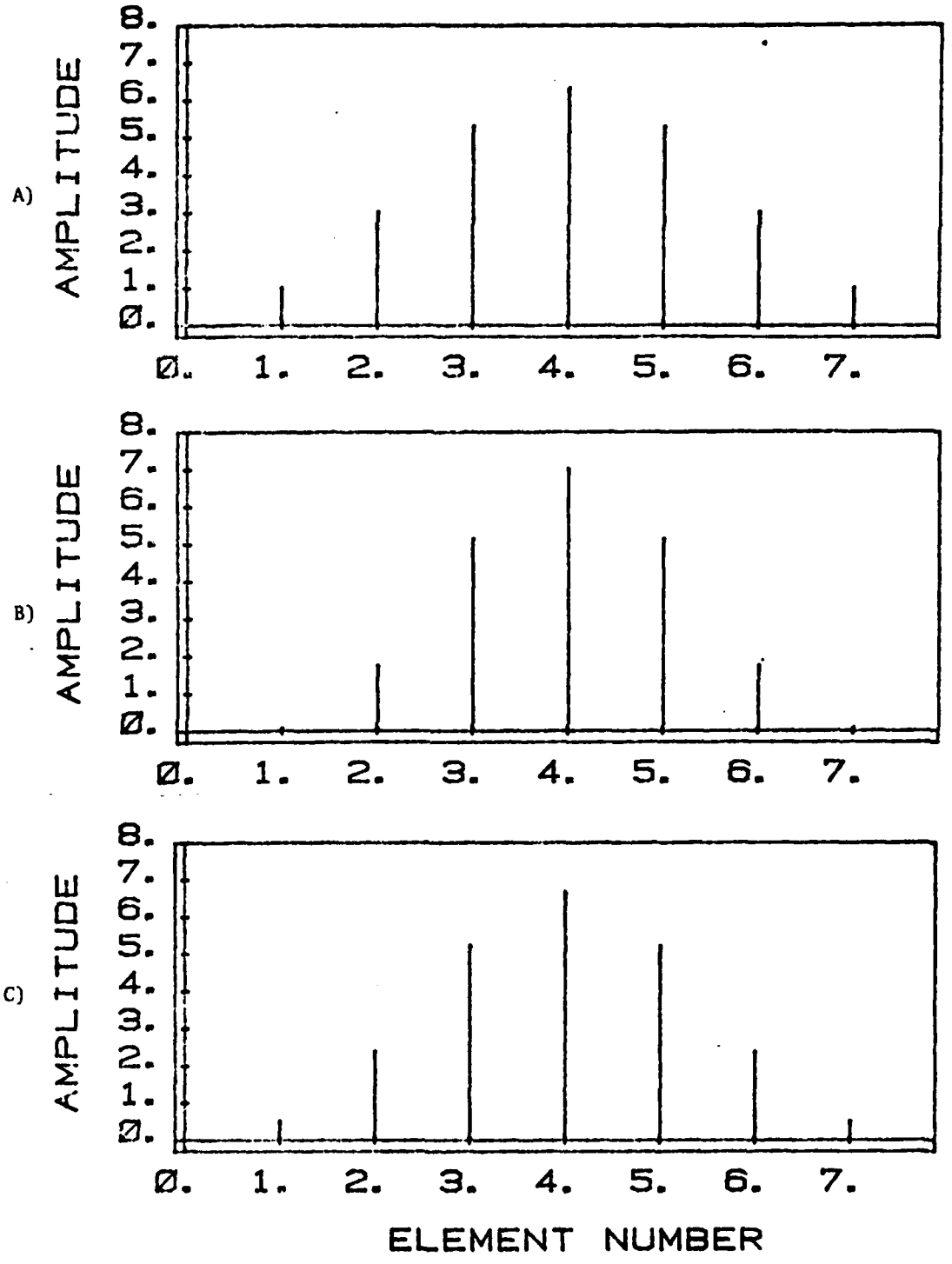



FIGURE 4
CURRENT DISTRIBUTION OF THE
A: FIRST SUB-ARRAY, B: SECOND SUB-ARRAY, C: RESULTANT ARRAY

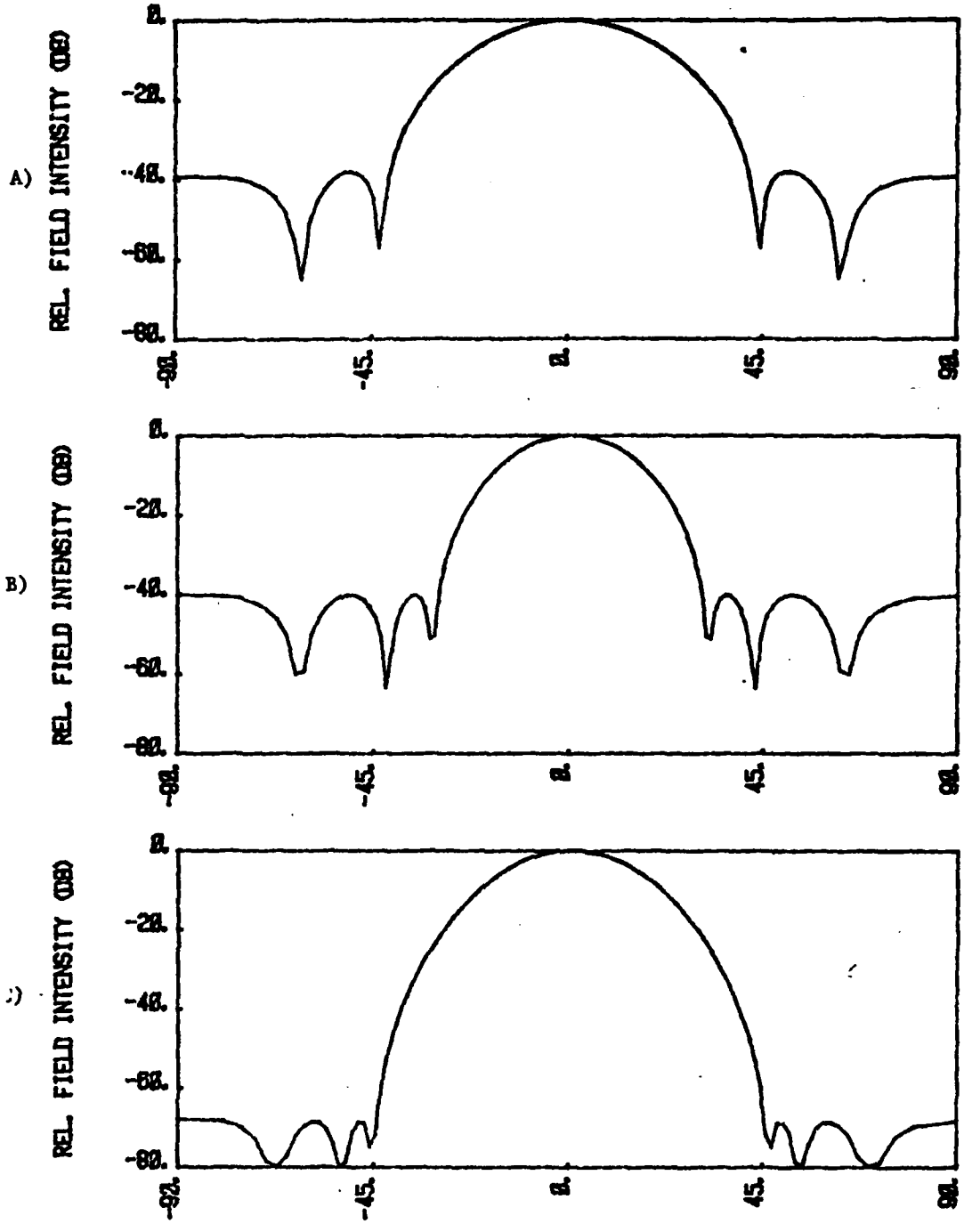



FIGURE 5
FAR-FIELD INTENSITIES PRODUCED BY THE
A:) FIRST SUB-ARRAY, B:) SECOND SUB-ARRAY, C:) RESULTANT ARRAY

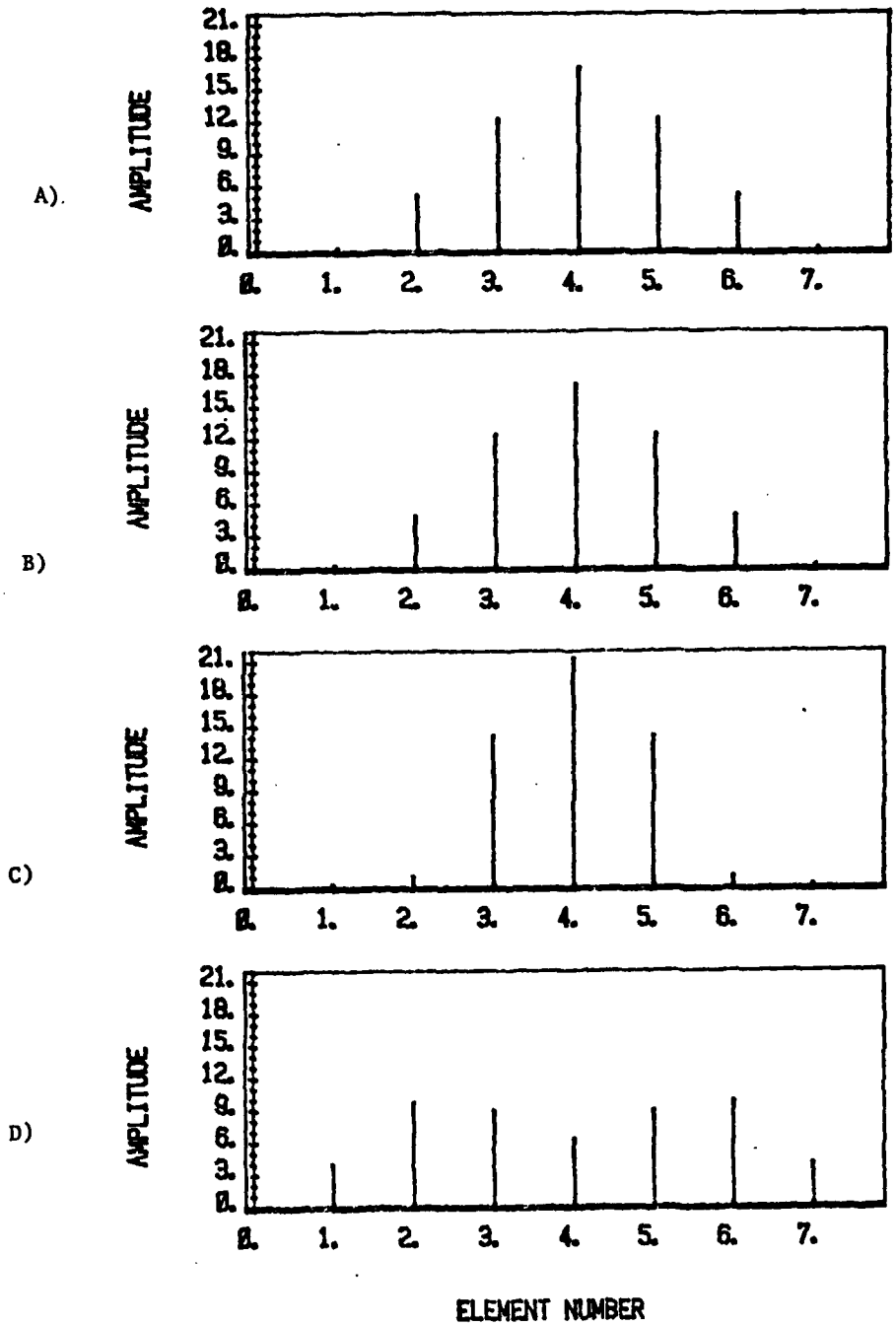



FIGURE 6

CURRENT DISTRIBUTIONS OF THE

A: FIRST SUB-ARRAY, B: SECOND SUB-ARRAY

C: THIRD SUB-ARRAY, D: FOURTH SUB-ARRAY

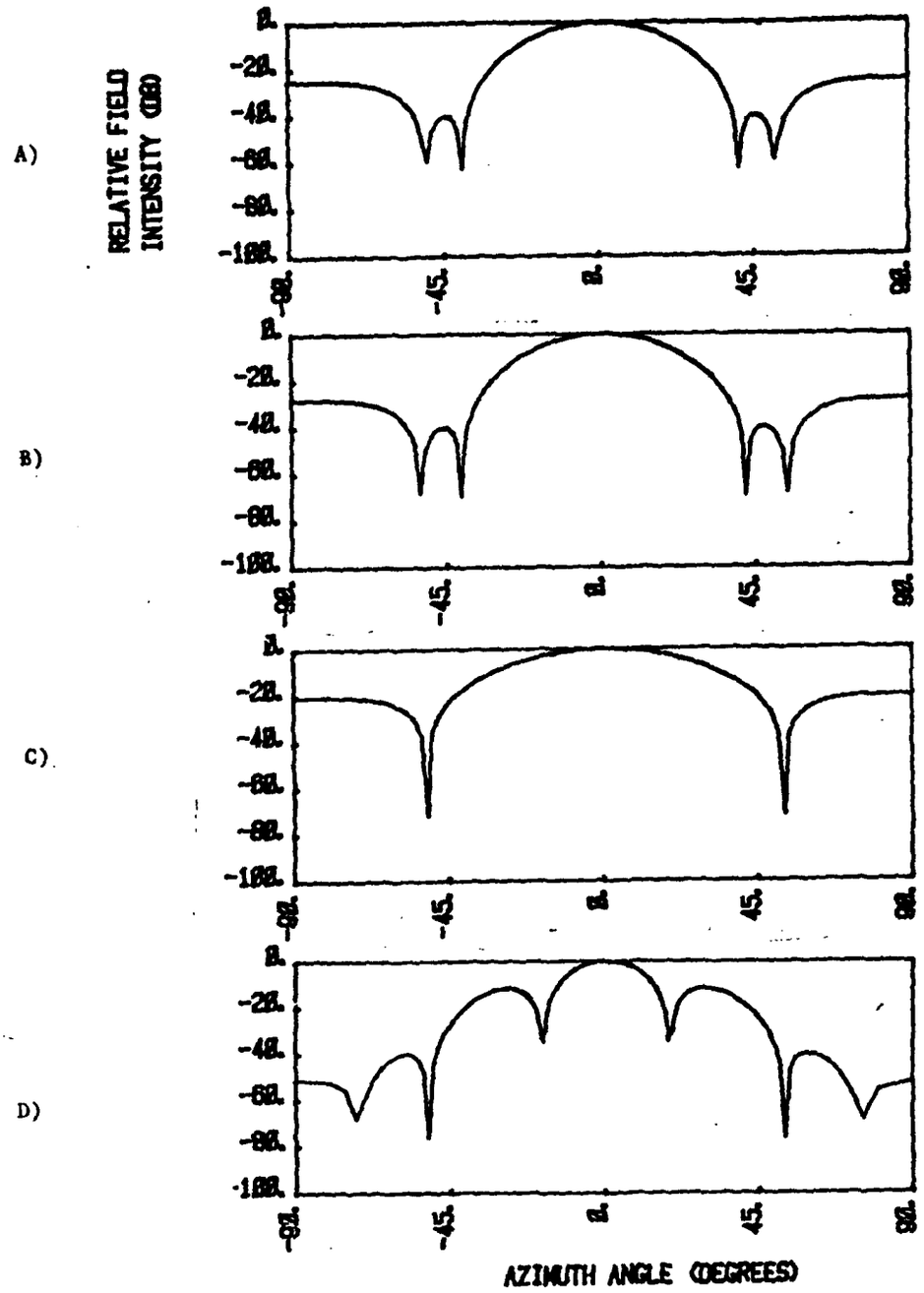



FIGURE 7

FAR-FIELD INTENSITIES PRODUCED BY THE

A: FIRST SUB-ARRAY B: SECOND SUB-ARRAY

C: THIRD SUB-ARRAY D: FOURTH SUB-ARRAY

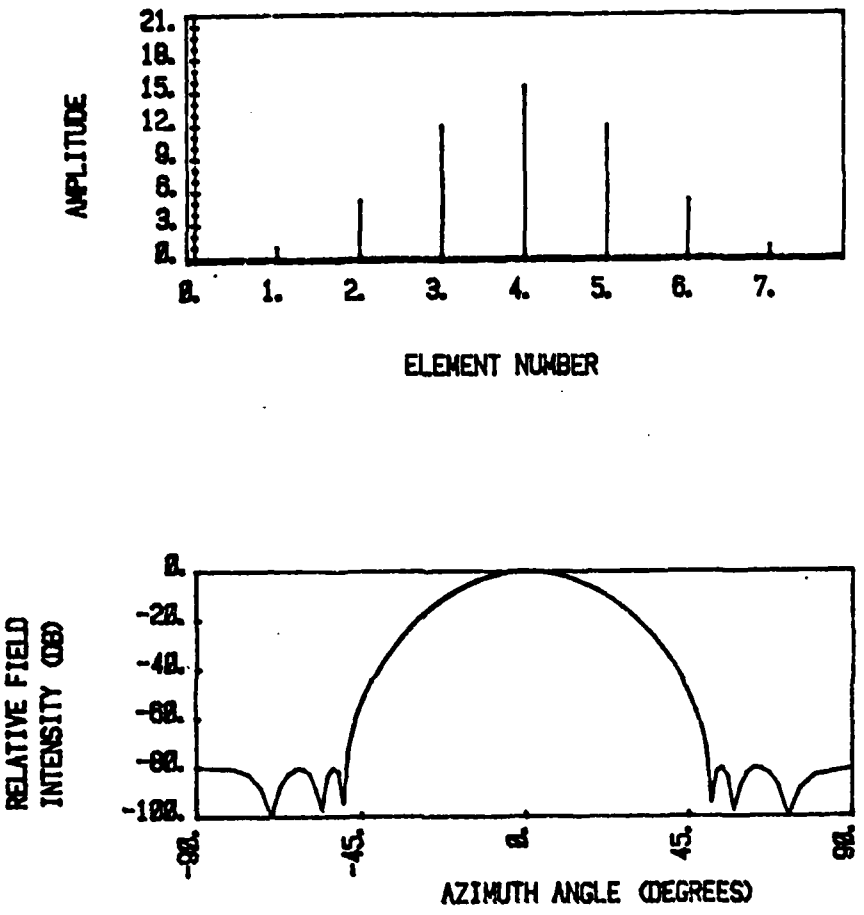



FIGURE 8

RESULTANT CURRENT DISTRIBUTION

AND FAR-FIELD INTENSITIES FROM

THE CASE OF FOUR SUB-ARRAYS

1980 USAF - SCEEE SUMMER FACULTY RESEARCH PROGRAM

Sponsored by the

AIR FORCE OFFICE OF SCIENTIFIC RESEARCH

Conducted by the

SOUTHEASTERN CENTER FOR ELECTRICAL ENGINEERING EDUCATION

FINAL REPORT

# AUTOMATIC FAULT DIAGNOSIS OF A SWITCHING REGULATOR


Prepared by: Harry A. Nienhaus

Academic Rank: Associate Professor

Department and University: Electrical Engineering Department
University of South Florida

Research Location: AFWAL, Avionics Laboratory, System Avionics Division, System Integration Branch, Concepts and Evaluation Group

USAF Research Colleague: 2Lt Donald E. Palmer



Date: August 1980

Contract No.: F49620-79-C-0038

# AUTOMATIC FAULT DIAGNOSIS OF A SWITCHING REGULATOR

by

Harry A. Nienhaus

## ABSTRACT

This report describes a microprocessor-based system for the automatic fault diagnosis of a switching regulator. It covers the system development from a test philosophy to a working breadboard that correctly identifies single simulated faults in the switching regulator. In addition to open circuit, short circuit, and stuck at faults, the system is capable of diagnosing faults due to excessive leakage, drift in critical components, and system instability. The basic approach taken was to program the microprocessor to make the same logical decisions to isolate faults that the writer would make in troubleshooting a circuit. Self checking procedures for the automatic test equipment are also proposed. Suggestions for further research in this area are offered.

## Acknowledgement

The author would like to thank the Air Force Systems Command, the Air Force Office of Scientific Research, and the Southeastern Center for Electrical Engineering Education for providing him with the opportunity to spend a worthwhile and interesting summer at the Avionics Laboratory, Wright-Patterson Air Force Base, Ohio. He would also like to thank the Avionics Laboratory, in particular the Systems Integration Branch, for its hospitality and excellent working conditions. Finally, he would like to thank Lt Don Palmer for his support on this project.

## I. INTRODUCTION:

Many modern electronic systems in aircraft and missiles are powered by switching regulators. A significant percentage of electronic system failures can be attributed to these devices. Automatic fault diagnosis is extremely important to the Air Force for several reasons.

a. Human fault diagnosis is a tedious and time consuming process, requiring many skilled technician manhours. Automatic fault diagnosis means that more equipment can be maintained in a state of readiness with the same amount of technician manhours.

b. Intermittent faults that occur in flight but not during ground maintenance can be automatically diagnosed, recorded, and later repaired.

c. Certain faults (e.g., a leaky capacitor or transistor) can be automatically diagnosed and corrected before they become catastrophic.

To underscore the importance of this problem, Air Force Project #2003-02-49 was underway at the Avionics Laboratory to investigate automatic fault diagnosis long before the writer arrived on the scene. Several key hardware components had been ordered for automatic fault diagnosis of a switching regulator, but a viable test philosophy had not been established. The writer was chosen for this project primarily because of an extensive background in electronic circuit and system design, including switching regulators.

Human fault diagnosis of a switching regulator is a relatively straightforward problem if it is done in a logical manner. A power supply is somewhat unique in that external test signals do not have to be applied in order to diagnose faults. Logical human fault diagnosis involves gathering data and using deductive reasoning to interpret this data in order to isolate faults to a particular functional block or component. A microprocessor is well suited for gathering data (with the aid of a data acquisition system) and making logical decisions. Because of its relatively slow speed, it is not well suited for analyzing periodic waveshapes except at very low frequencies. However, with the aid of external hardware, it can gather data on important characteristics of periodic waveforms such as frequency, average value, and peak-to-peak value. Fortunately, this is sufficient for a switching regulator. The basic approach taken to solve the fault diagnosis problem was to program the microprocessor to make the same logical decisions to isolate faults

that the writer would make in troubleshooting a circuit.

Beginning with this basic approach, a complete microprocessor based automatic fault diagnosis system has been designed and breadboarded that correctly identifies single simulated faults in the switching regulator. In addition to open, short, and stuck at faults, it also diagnoses faults due to excessive leakage, drift in critical components, and instability (or excessive ripple). In fact, the microprocessor has been programmed to diagnose every significant single fault that the writer could anticipate and simulate. In the event that a single significant fault does exist that was not anticipated, it should be a simple matter to change the EPROM program to accommodate it.

It is also shown how the fault diagnosis program for the switching regulator can be expanded to diagnose open circuit faults in the data acquisition multiplexors. A self checking software procedure for the microprocessor system is also proposed.

This project has shown that automatic fault diagnosis of a switching regulator is technically feasible. In the writer's judgment, it is also economically feasible, not only because of the technician manhours that can be saved but also because early fault detection could improve the probability of mission success and save airplanes.

## II. OBJECTIVES:

Originally, the objectives agreed upon by the writer and his effort focal point were necessarily vague and modest because of the limited time available to investigate the fault diagnosis problem. Unlike other areas, the literature on analog fault diagnosis, while extensive, is disappointingly of little practical value. However, after beginning the project, it soon became apparent that the specific problem of automatic fault diagnosis of a switching regulator could be solved from test philosophy to working breadboard. Consequently, this became the writer's sole objective during this project. This objective was met.

It should be noted that no attempt was made to solve the general problem of analog fault diagnosis, although many of the techniques used to solve the specific problem could be applied to other systems, both analog and digital.

## III. SWITCHING REGULATOR FAULT ANALYSIS:

A schematic of the switching regulator used in this project is shown

in Figure 1. It is a standard +5V, 10A buck converter. A functional block diagram which more clearly illustrates the major system components is shown in Figure 2. Here, the fold-over short circuit protection is not shown for simplicity. Nine fault diagnosis test points are indicated by a circled X in Figure 1. These were chosen because they correspond to the inputs and outputs of each of the functional blocks shown in Figure 2. Omission of any of these test points makes it impossible to distinguish between faults in adjacent components.

The switching regulator utilizes two IC's; the SG1524 regulating pulse width modulator (PWM) and the PIC645 power integrated circuit. A computer fault analysis of the circuit requires development of accurate computer models for these devices. It should be noted that existing computer models for devices, that are perfectly valid under normal operating conditions, are not necessarily valid under fault conditions. Because of the time consuming nature of I.C. computer model development, a computer fault analysis of the circuit was not attempted.

Instead, the approach that was adopted was to decompose the system into functional blocks that are more readily analyzed, using both spec sheet and experimental data. The major criteria for defining a fault in a functional block is that the block is no longer satisfactorily performing the system function for which it was intended. In the switching regulator we can distinguish 8 different types of functional blocks (See Figure 2).

(1) Reference Regulator
(2) Voltage Dividers
(3) Error Amplifier
(4) Sawtooth Oscillator
(5) PWM
(6) DC Power Chopper
(7) Average LC Filter
(8) Compensation Network

The effects of faults in each of these functional blocks is considered in the succeeding paragraphs. In general, the diagnostic technique used is dependent upon, among other things, the type of functional block and type of fault being diagnosed.

1. Reference Regulator

The +5VDC reference regulator is wholly contained in I.C. U2, with only the input (U2-15) and output (U2-16) terminals accessible. This

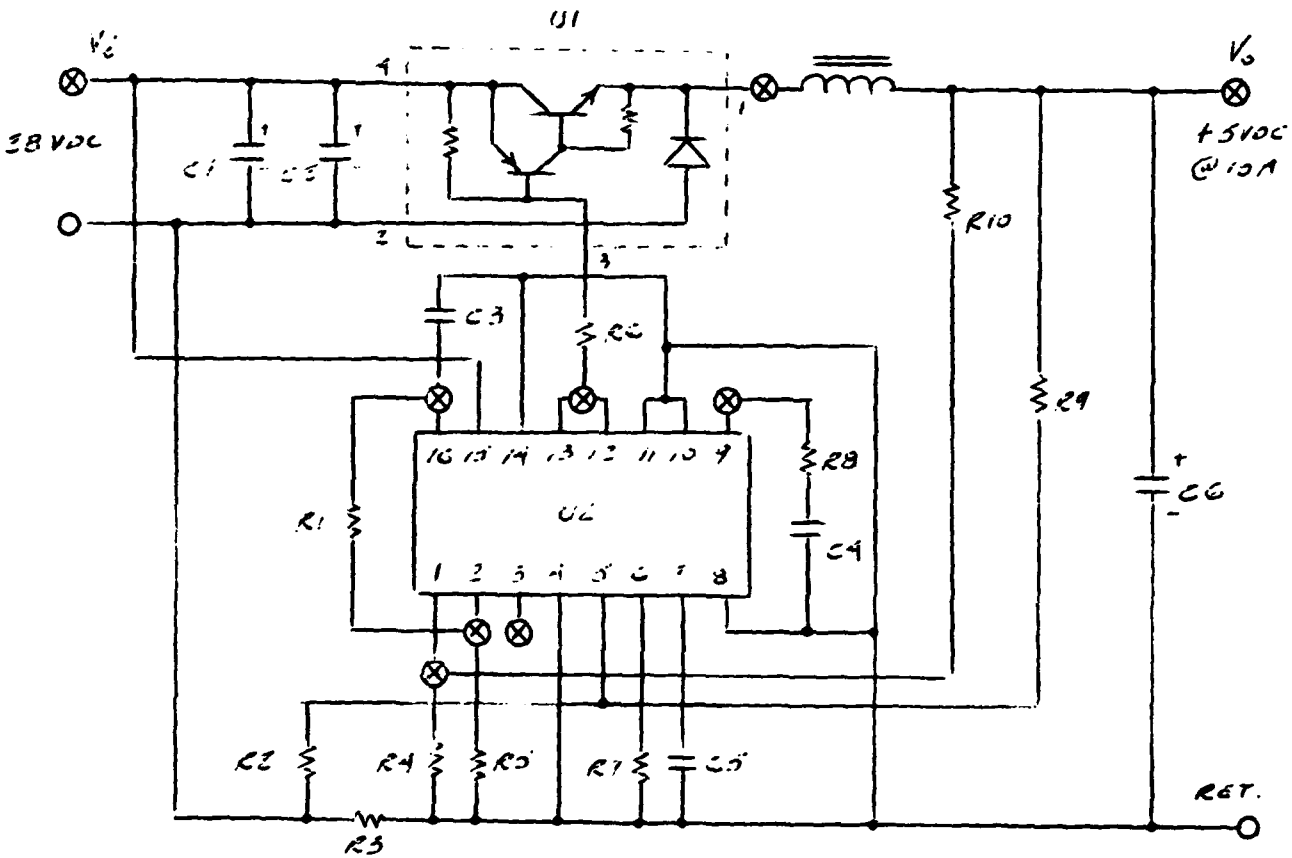



FIGURE 1. SWITCHING REGULATOR SCHEMATIC.

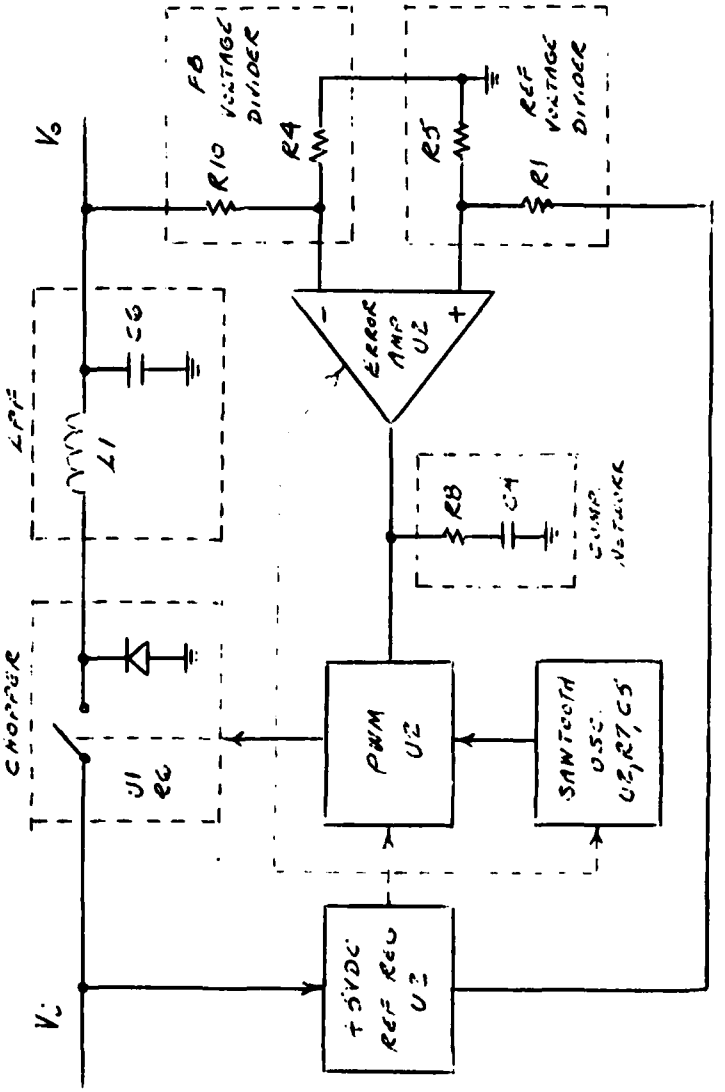



FIGURE 2. SWITCHING REGULATOR BLOCK DIAGRAM.

regulator provides a stable DC reference voltage, $V_R$, for the switching regulator as long as the input voltage, $V_i$, is in the range 8 to 40V. This reference voltage is virtually independent of any other voltage in the system. However, other voltages in the system are heavily dependent upon it not only because the system feedback (FB) forces the output voltage, $V_o$, to closely follow the reference, but also because the reference supplies power for the sawtooth oscillator, error amp, and PWM. Meaningful fault diagnosis of these components is not possible unless the reference is in tolerance.

Fault diagnosis of the reference regulator is very simple. As long as the input voltage is within its specified range of 8 to 40V, then any sample of the reference output must lie within the specified range of 4.8 to 5.2V. If not, the reference is bad and U2 must be replaced. An exception to this is a $V_R = 0$ condition which could be caused by a faulty reference regulator or a short in capacitor C3, which is connected across its output. It is impossible to diagnose the exact cause automatically. It should be noted that the reference regulator has short circuit protection in the event that capacitor C3 shorts.

Experimentally it was determined that open circuiting capacitor C3 has no noticeable effect on the system. The system is also extremely tolerant of leaky or drift faults in this component.

In the succeeding paragraphs, it is assumed that both the input and reference voltages are in tolerance. Faults in these voltages should be corrected before fault diagnosis of other system components is attempted. All of the concepts developed in this section have been incorporated into the fault diagnosis flow diagram described in Section V.

2. Voltage Dividers

Consider the voltage divider network shown in Figure 3. At any instant of time, the terminal voltages are related by,

$$V_2 = \frac{Rb\ V_1}{Ra + Rb} \qquad (1)$$

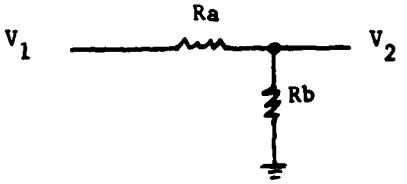



Figure 3. Voltage Divider.

Hence, a simple diagnostic test for a voltage divider is to simultaneously sample the input and output voltages and compare the two to determine if the voltage divider ratio is in tolerance. This test will identify a voltage divider fault, regardless of the waveforms or magnitudes of $V_1$ and $V_2$, as long as $V_1$ is non-zero.

Standard MSI data acquisition systems have only one S/H network, and a custom data acquisition system is required for simultaneous sampling of two signals. One might think that since the voltage divider signals in the switching regulator are essentially DC, that simultaneous sampling of the input and output is not required. This may be marginally true if faults that produce excessive ripple or system instability are diagnosed first. However, worst case full load ripple, which is in tolerance (unspecified), might cause a fault to be misdiagnosed as a voltage divider fault if simultaneous sampling is not employed.

Critical voltage dividers normally employ 1% film resistors. A practical problem is that component drift may cause the voltage divider ratio to be slightly out of tolerance without causing the output voltage to be out of tolerance. This is true since drift in one functional block may cancel the effect of drift in another. Diagnosing such conditions as faults would be counterproductive. Consequently, the voltage divider ratios should not be tested unless it has first been established that the output voltage is out of tolerance. This same criteria applies to drift in other critical components such as the error amp. In the case of drift in the voltage divider, it is impossible to distinguish between a high value of Rb and a low value of Ra, or vice versa.

For diagnostic purposes, it is convenient to categorize switching regulator faults according to the effect they have on the output voltage. These are divided into 3 classes with symptoms; $V_o = 0$, $V_o$ low, and $V_o$ high. In the case of the FB and reference voltage dividers, we can distinguish 8 distinct faults in these 3 categories.

(1) $V_o = 0$: R1 open, and R5 open (or very high)

(2) $V_o$ low: R4 open, R4 high or R10 low, and R1 high or R5 low

(3) $V_o$ high: R10 open (or very high), R5 high or R1 low, and R10 high or R4 low

Except for the R5 open (or very high) fault, all of these classifications are easily verified by linear analysis. As R5 increases significantly, it moves from the $V_o$ high to the $V_o = 0$ category. This is because a very high value of R5 causes the error amplifier to operate

above its common mode input range. This causes the error amplifier to invert, changing the system FB from negative to positive, and driving the PWM completely off.

Unlike the case of drift faults, voltage divider ratios that are significantly out of tolerance can be attributed to a single resistor, which is open circuited or has a very high resistance. This follows from the fact that reliability studies show that a short circuit in a film resistor is an improbable failure mode. A poor solder connection, which is a common fault in electronic circuits, also causes the apparent resistance to increase.

3. Error Amplifier

The error amplifier is wholly contained in I.C. U2 with both the differential inputs (U2-1,2) and the output (U2-9) accessible. The function of the error amplifier is to maintain the error voltage (the differential input voltage) at a small level in comparison to the reference voltage, in spite of changes in the PWM duty cycle. Simple application of Kirchhoff's Voltage Law to Figure 1 reveals that the switching regulator output voltage, $V_o$, is related to the reference voltage, $V_R$, and the error voltage, $V_E$, by,

$$V_o = V_R - 2V_E \qquad (2)$$

Arbitrarily specifying a maximum error voltage of 40 mv will force the regulator output to track the reference within 80 mv, exclusive of other tolerances. Faults that can cause the error voltage to become excessive include low error amplifier gain or excessive input current or voltage offset. These can be detected by simultaneous sampling of both differential inputs and comparing the magnitude of the difference to 40 mv. However, this test is not valid unless the output of the error amplifier is within the linear input range of the PWM comparator (1 to 3.5V). If it is not, then the system FB loop is open due to a stuck at fault somewhere in the system.

In the event of a system stuck at fault that causes the FB loop to open, the error amplifier is functioning properly if the voltage at U2-1 is greater than the voltage of U2-2 and the error amplifier output is less than 1V, or if the voltage at U2-1 is less than the voltage at U2-2 and the error amplifier output is greater than 3.5V. If the opposite is true, then the system fault is due to a stuck at fault in the error amplifier itself.

4. Sawtooth Oscillator

The block diagram of a typical I.C. sawtooth oscillator is shown in Figure 4. Here a constant current source linearly charges external timing capacitor C5 until the voltage across it reaches the UTL of the Schmitt trigger. This causes the output of the Schmitt trigger to go high, turning on the reset transistor which quickly discharges the capacitor to the LTL of the Schmitt trigger. This causes the Schmitt trigger output to go low, turning off the reset transistor and the cycle repeats itself.

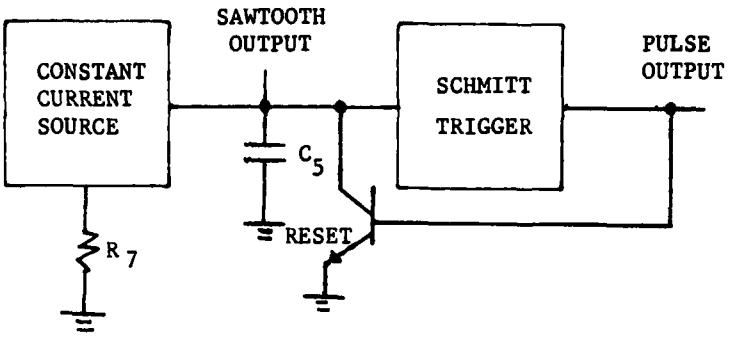



Figure 4. Sawtooth Oscillator.

If the reset period is small compared to the charging period, the period of oscillation is given by,

$$T = \frac{1}{f} = C\,\frac{(UTL - LTL)}{I} \simeq R7C5 \qquad (3)$$

where I = constant current source value. This is adjustable with external timing resistor R7.

Except for the external timing resistor and capacitor, all of the sawtooth oscillator circuitry is contained in U2, with both the sawtooth output (U2-7) and pulse output (U2-3) accessible. Although the exact details of the circuitry are unknown, the operation fits the block diagram described previously.

Because of the negative FB and high loop gain, the system is virtually insensitive to non-linearities in the sawtooth waveform. For diagnostic purposes, the most important characteristic of this oscillator is its frequency rather than its waveshape. If the frequency is too high, excessive switching losses can occur in the chopper. If it is too

low, excessive ripple will result. This is true even if the DC output voltage is within tolerance. However, this frequency is not overly critical, and an arbitrarily wide range from 17.9 Khz to 35.5 Khz is allowed before a fault is defined.

We can identify 9 distinct sawtooth oscillator faults in 4 diagnostic categories.

(1) f high: C5 open

(2) f low: C5 leaky, U2-7 leaky, R7 very high

(3) f = 0, Vo nom: R7 open, C5 very leaky, U2-7 very leaky

(4) f = 0, Vo high: C5 short, U2-7 short

Note that the only catastrophic faults, are the C5 or U2-7 (reset transistor) shorts. These cause one input to the PWM comparator to be clamped at ground, forcing the PWM to turn on continuously, and the output voltage to approach the input voltage. While the other faults do not result in an out of tolerance DC output, they should be diagnosed, not only because of their harmful effect on the output ripple and chopper power dissipation, but also in the case of leaky components because they indicate degradation which can only worsen with time and become catastrophic.

If timing capacitor C5 opens, the sawtooth oscillator operates at a much higher frequency since the constant current source has only stray circuit capacitance to charge. On the breadboard model this frequency was about 2Mhz at light loads. At full loads the excessive power dissipation produced by this fault could destroy or fatigue chopper U1.

If the timing capacitor C5, the constant current source, or the reset transistor is leaky, the sawtooth output increases exponentially, rather than linearly with time. This results in a longer period to charge the capacitor to the Schmitt trigger UTL. Hence, the oscillator frequency decreases. Also, a high value of R7 decreases the constant current output which results in a decrease in frequency.

If C5, the constant source, or the reset transistor is very leaky, C5 cannot charge up to the UTL of the Schmitt trigger and the sawtooth oscillations cease. Also, if R7 opens, the constant current source output is zero and oscillations cease. Intuitively, one might expect that the PWM would have either 0 or 100% duty cycle for these faults with the output being catastrophically out of tolerance. However, this

is not the case, at least at light loads. Experimentally it was determined that with R7 open, the sawtooth oscillator frequency goes to zero but the switching regulator itself free runs at a frequency of 125 Khz with the DC output voltage in tolerance. A similar result was obtained simulating a very leaky C5 fault with a fixed shunt resistor. The distinction between a leaky and very leaky C5 fault is necessary because the non-linearities in the constant current source place these in separate diagnostic categories.

5. Pulse Width Modulator

The pulse width modulator (PWM) is wholly contained in I.C. U2. Its output consists of 2 open collector transistors which are connected in parallel externally (U2-12 and U2-13). These are driven by 2 NOR gates. A flip-flop driven by the pulse output of the sawtooth oscillator, alternately inhibits one or the other NOR gates, so that each output transistor is turned on only every other cycle of the sawtooth oscillations. The output of the PWM comparator is also applied to each NOR gate to control the pulse width of the turn-on periods. The pulse output of the sawtooth oscillator is also applied directly to the NOR gate to limit the maximum duty cycle that can be obtained. The PWM control input is the error amplifier output (U2-9). Meaningful fault diagnosis of the PWM and chopper must assume that no fault exists in the sawtooth oscillator.

The fact that the comparator, flip-flop, and NOR gate outputs are inaccessible is not a detriment to fault diagnosis. Any stuck at faults in these components will cause the output transistors to be stuck open or short. An internal static fault which is not stuck-at will show up as a leaky output transistor.

It should be noted that similar faults in both the PWM and chopper produce the same symptoms at the chopper output (U1-1) and switching regulator output, $V_o$. These include open, short, and leaky faults. These faults can be isolated to one of these two functional blocks by examining the PWM input (U2-9) and the switching regulator and/or chopper output. Consequently, it is convenient to lump fault analysis of the PWM with that of the chopper, which is covered in succeeding paragraphs. In order to distinguish between a fault in the PWM and a similar fault in the chopper, it is also necessary to examine the PWM output (U2-12). While a human would have little difficulty interpreting the waveform at this terminal, this is much more difficult for the

microprocessor without adding significantly to the complexity of the data acquisition system.

Major practical problems associated with reading data from terminal U2-12 are:

(1) Some type of interface circuit is required to reduce the voltages at this test point to safe levels for the data acquisition system.

(2) This test point is capable of sinking a moderate amount of current from an interface circuit, but it cannot act as a significant current source without turning the chopper partially on when it should be off.

(3) Unless multiple interface circuits and inputs are used, only one characteristic of the waveform can be examined (e.g., average value, frequency, etc.).

(4) The low level of the rectangular waveform at this terminal varies as the input voltage varies. This is because the PWM output transistors are not driven into saturation except when the input is below about 20V.

A practical interface circuit that is a solution to some of these problems is described in Section IV. This makes it possible to distinguish between all short circuit faults and some open circuit faults in the PWM or the chopper. Essentially, it reads the average value of that portion of the waveform below 5 volts.

If only one of the two PWM output transistors is open circuited, the chopper frequency is cut in half and the PWM duty cycle is limited to a maximum of 45% (instead of 90%). As long as the nominal 28V input does not fall below about 12V the only effect on the system is that the output ripple doubles. If the input falls to 8V, the DC output voltage also falls out of tolerance. The fault diagnosis program, described in Section V, will not recognize the former condition as a fault, but it will diagnose the latter condition as a type TFL fault. A separate diagnostic test for this condition is not considered practical because of the additional hardware required.

6. DC Power Chopper

The DC power chopper is an I.C. containing a NPN power transistor, a PNP driver transistor, emitter-base resistors for each of these, and a power rectifier. External resistor R6, which is connected between the

base of the PNP transistor (U1-3) and the output of the PWM driver is also considered to be part of the chopper.

The most significant characteristic of the PWM waveform at the output of the DC power chopper (U1-1) is its instantaneous average value. This is equal to the product of the peak amplitude and the duty cycle of the waveform. Since the voltage of U1-1 alternately switches between the input (+28VDC) and ground, it must be low pass filtered before being applied to the data acquisition system. Connecting an RC network from this terminal to ground will not interfere with the switching regulator operation. The low pass filter not only extracts the average value of the voltage at U1-1, but also suppresses high voltage transients that can appear at this terminal and damage the data acquisition system.

If a single short circuit or excessive leakage exists in either the PWM or chopper, the output voltage will be high and the system FB will command the PWM input to turn completely off (U2-9<1V). The fact that there is no response to this command is sufficient proof that a short circuit or excessive leakage exists in one of these components. A PWM short exists if U2-12=0. If this is not the case, either a chopper short or leaky fault exists or, less probably, the PWM has excessive leakage. Leaky faults can most easily be detected at no load. At heavy loads the switching regulator can tolerate more leakage without showing significant symptoms. Early detection of leaky faults could prevent damage to equipment being powered by the switching regulator. Leaky faults may be intermittent (e.g., they may occur only when a component heats up).

If a single open circuit exists in either the PWM or chopper, the output voltage is zero and the system FB will command the PWM input to turn completely on (U2-9>3.5V). The fact that there is no response to this command is sufficient proof that an open circuit exists in one of the components.

If U2-12≈0, the PWM is on most of the time, indicating that R6 or U1 is open circuited. If the average value of U2-12<4V, the PWM is on at least part of the time, indicating the open circuit is in the chopper. If not, the PWM is open if Vi<20V, since the PWM "on" voltage is close to zero for this case. If Vi>20V, the PWM comes out of saturation and its "on" voltage cannot be reliably predicted or detected with the interface circuit. Hence, further fault isolation is not possible.

If the rectifier in U1 opens and the switching regulator is operating under normal load, the large voltage transient at U1-1 will most probably burn an open circuit between terminals 1 and 4 of U1. If this rectifier shorts, the excessive current will burn an open circuit between terminals 1 and 4 of U1 also. This corresponds to an open chopper fault. Because of the destructive nature of these faults, they have not been simulated experimentally.

7. Average LC Filter

The low pass LC filter section functions as a PWM detector. Except for the DC IR drop across the inductor, its average or DC output is equal to the instantaneous average value of its input, which is the product of the peak input amplitude and the duty cycle. It is also designed to attenuate the relatively high chopper frequency to a low level ripple component.

A simple functional DC check of this filter is to compare simultaneous samples of Vo and the average value of the voltage at U1-1. Excessive ripple due to out of tolerance components is not as easy to detect. However, excessive ripple is more likely to occur because of reduced oscillator frequency, which is easily detected. It is also difficult to determine whether a large AC component on the output is due to excessive ripple or to switching regulator instability, without resorting to an additional frequency measurement. The problem of detecting large AC components at the output of the switching regulator is considered in detail in Section V.

8. Compensation Network

The lag-lead compensation network consists of R8 in series with C4 connected across the output of the error amplifier. This network is designed to make the feedback control system stable under all operating conditions. If the system is designed properly, it should be highly tolerant of drift in these components. Experimentally it was determined that the system functioned properly even with C4 shorted. However, open circuiting either R8 or C4 caused the switching regulator to become unstable. At no load the oscillation frequency is about 3 Khz, and the amplitude is only about 70 mv p to p. The oscillations are more apparent at the output of the error amplifier (U2-9) where the peak to peak amplitude is about 2.5V.

One method of detecting an excessive AC component at the error

amplifier output, due to either instability or a defective LC filter, is to measure the peak to peak value of the voltage at U2-9. A detailed technique for accomplishing this is covered in Section V.

9. Fold-Over Short Circuit Protection

The fold-over short circuit protection circuitry consists of resistors R3, R2, and R9 plus a comparator in U2-9. While the fold-over feature of this circuit reduces the maximum output current in the event of a short circuit, it increases it in the event of an over-voltage fault. Since over-voltage faults can destroy digital equipment being powered by the switching regulator, the fold-over feature may do more harm than good. For this reason, it is recommended that the fold-over voltage divider (R2 and R9) be removed. In any event, open circuiting, either R2 or R9, has no noticeable effect on the normal switching regulator operation.

Although separate diagnostic tests for the short circuit protection circuitry was not considered practical, major faults will be detected by the fault diagnosis program of Section V. For example, if R3 is open circuited, loss of input voltage results. This will be diagnosed as a Vi low fault. A stuck at fault in the short circuit comparator is indistinguishable from a stuck at fault in the error amplifier. Since these two are both located in U2, there is no need to isolate them. Finally, an output short has the same symptoms and diagnosis as an error amp stuck at 0 fault.

## IV. DATA ACQUISITION SYSTEM:

A simplified block diagram of the data acquisition system is shown in Figure 5. In addition to interface networks, it consists of an 8 bit frequency counter to measure the frequency of the sawtooth oscillator and an 8 bit A to D converter for voltage measurements. Two 4 input analog multiplexors (MUX 1 and 2) and sample and hold networks make it possible to select and sample two voltages simultaneously. A 2 input multiplexor (MUX 3) is used to select which of the two samples is to be converted to digital. Tri-state buffer latches are used to store the data until it can be read and stored in RAM by the 6802 microprocessor (MPU). Multiplexor select, sample and hold, A to D conversion start, and buffer latch enable are controlled by the MPU via the B (output) port of a peripheral interface adaptor (PIA). Data is read into the MPU via the A (input) port of the PIA. The enable inputs on the buffer

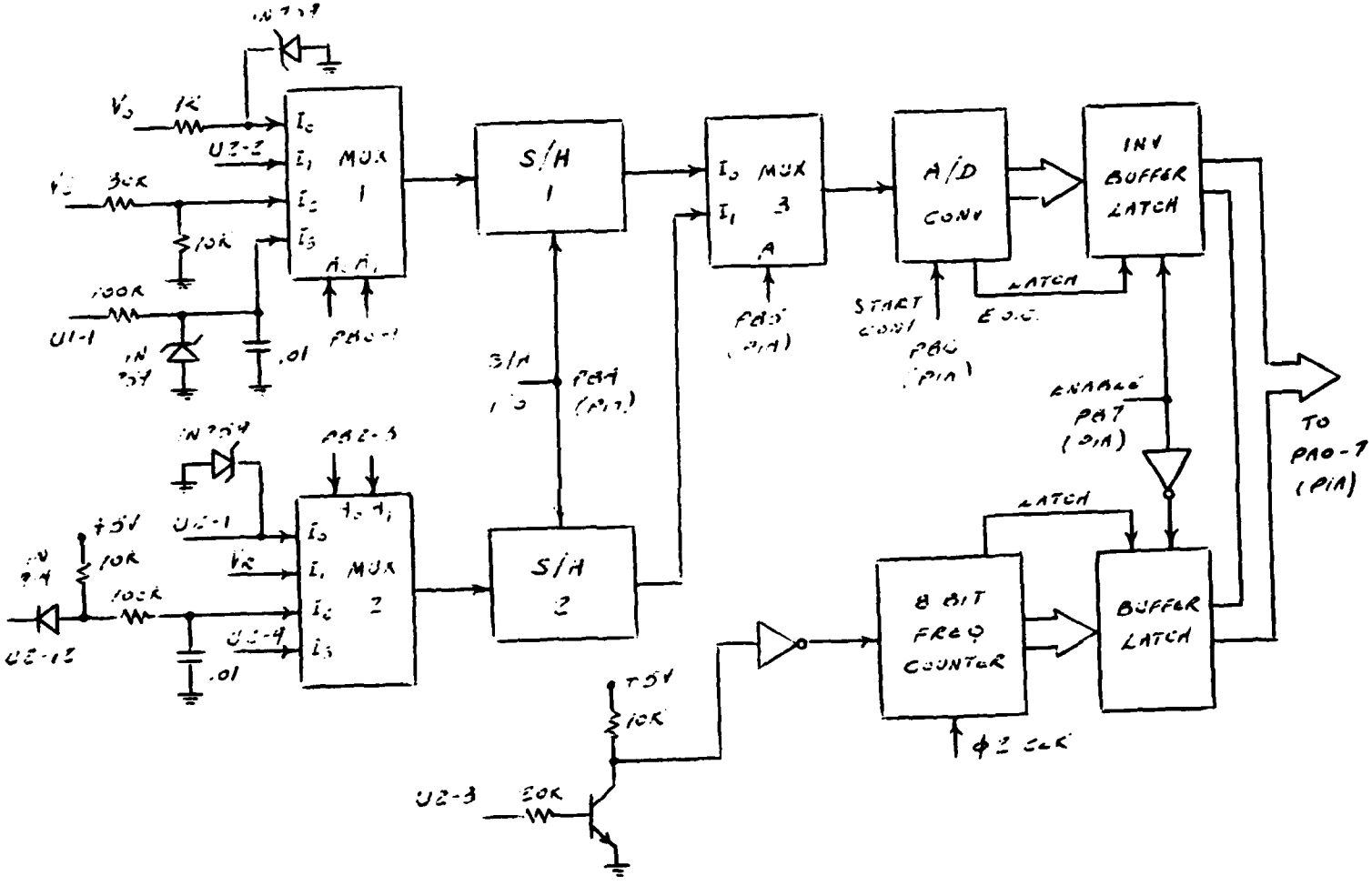



FIGURE 5. DATA ACQUISITION SYSTEM BLOCK DIAGRAM.

latches allow selection of either to be read into a single PIA port.

The A/D converter in the breadboard is a short-cycled Datel ADC-AZ12B with a buffered input. A less expensive unit would suffice in this application. Specified conversion time is 7 μsec. An 8.8 μsec MPU software delay occurs after the start conversion pulse and before data is read into the MPU to insure that conversion is complete. Hence, data acquisition times are wholly dependent on the MPU. The A/D converter output is complementary unipolar, 0 to +10V, which is converted to normal unipolar binary by the inverting buffer latch. Key A/D conversion values are listed in Table 1.

The S/H networks used in the breadboard are Analog Devices SHA1134. MUX 3 consists of AD7510DI CMOS switches with a TTL inverter decoder, and MUX 1 and 2 are AD7501 8 input analog multiplexors.

A detailed block diagram of the frequency counter, which uses standard TTL components is shown in Figure 6. In this circuit the MPU 894.8 Khz Ø2 clock is divided by counters to a 559.25 hz square wave. This is further divided into 279.6 hz and 139.8 hz square waves by two J-K flip-flops. The 139.8 hz square wave provides a 3.58 MS read time for the 8 bit counter. All three square waves are anded to provide a clear signal for the 8 bit counter and a latch signal for the buffer latch in the proper sequence as shown in the timing diagram of Figure 7. The most significant bit (MSB) of the 8 bit counter is used to inhibit the count after it has reached a maximum value of hex 80 to prevent overflow due to a high frequency fault. The MPU is programmed to diagnose a fault if the sawtooth oscillator frequency is above hex 7F or below hex 40. These correspond to frequencies of 35.5 Khz and 17.88 Khz, respectively, with the 3.58 MS read time. Note that sawtooth oscillator frequency data is continuously available to the MPU but it is updated only once every 7.16 MS.

Next, consider the interface networks at the inputs to the data acquisition system. To begin with the MUX's, S/H networks, and A/D converter can withstand input voltages of up to 15V without sustaining damage. The switching regulator input voltage can be as high as 40V. This voltage is divided down by a factor of 4 before it is applied to MUX 1-$I_2$. Certain switching regulator faults can produce over-voltage conditions at other test points in excess of 15V that do not occur in normal operation. Where this is the case, 1N759 12 volt zener diodes are used to protect the data acquisition system. In the case of the

TABLE 1. A/D OUTPUT, UNIPOLAR, 0 TO =10V

| Input Voltage | Output Binary | Hex |
|---|---|---|
| 0.000 | 0000 0000 | 0 0 |
| 0.039 | 0000 0001 | 0 1 |
| - | | |
| 0.507 | 0000 1101 | 0 D |
| - | | |
| 1.014 | 0001 1010 | 1 A |
| - | | |
| 1.989 | 0011 0011 | 3 3 |
| 2.028 | 0011 0100 | 3 4 |
| - | | |
| 2.496 | 0100 0000 | 4 0 |
| - | | |
| 3.510 | 0101 1010 | 5 A |
| - | | |
| 4.048 | 0110 1000 | 6 8 |
| - | | |
| 4.758 | 0111 1010 | 7 A |
| 4.797 | 0111 1011 | 7 B |
| - | | |
| 4.992 | 1000 0000 | 8 0 |
| 5.031 | 1000 0001 | 8 1 |
| - | | |
| 5.187 | 1000 0101 | 8 5 |
| 5.226 | 1000 0110 | 8 6 |
| 5.265 | 1000 0111 | 8 7 |
| - | | |
| 9.945 | 1111 1111 | F F |

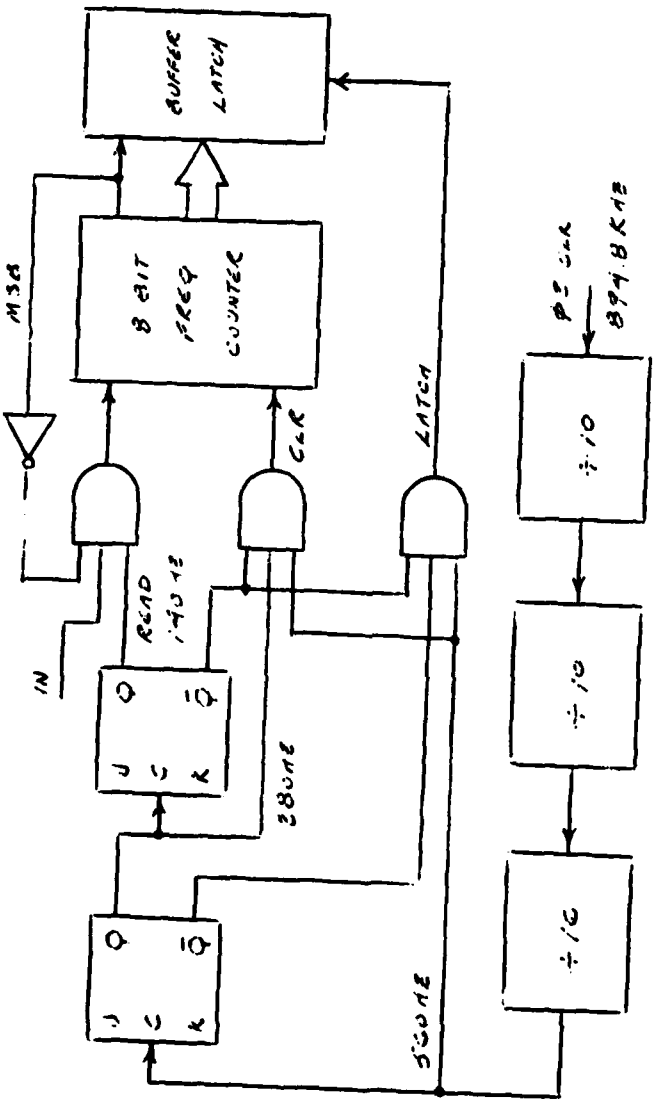



FIGURE 6. FREQUENCY COUNTER BLOCK DIAGRAM.

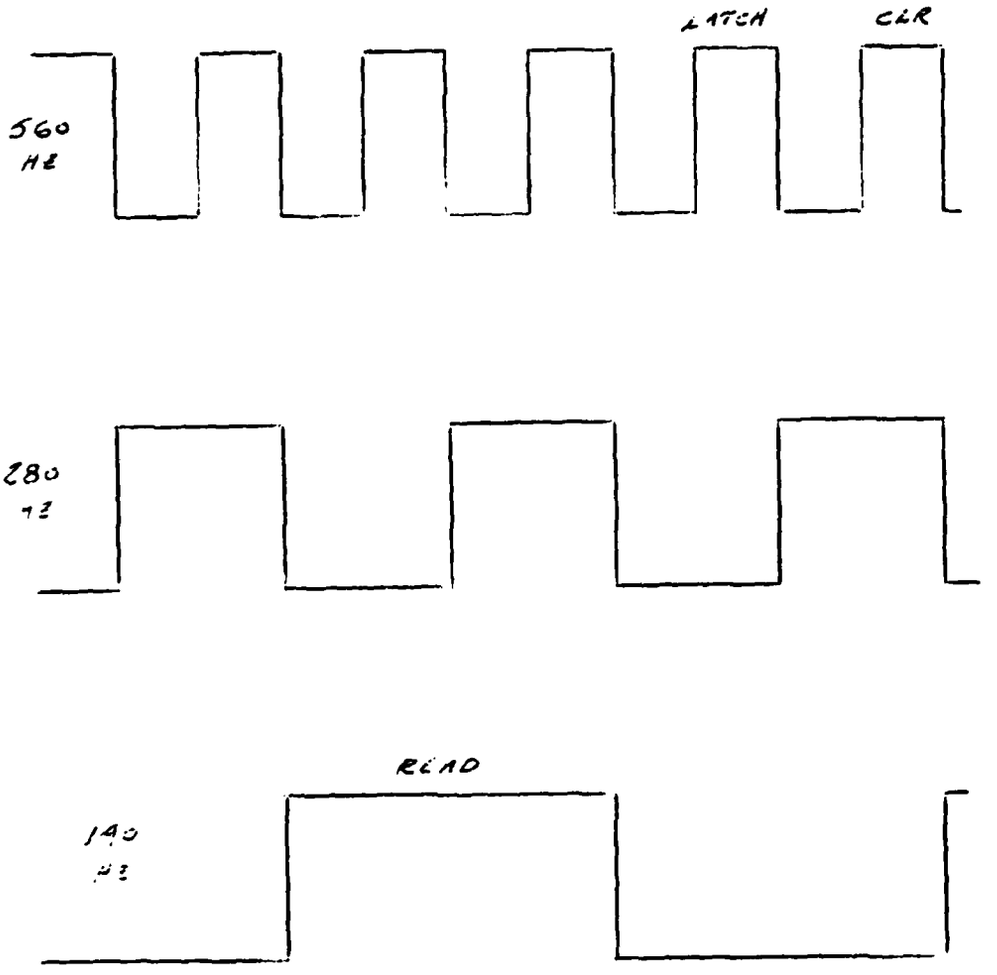



FIGURE 7. FREQUENCY COUNTER TIMING DIAGRAM.

low impedance Vo test point, a 1K resistor is used to limit the zener current under over-voltage fault conditions. An RC low pass filter with a 1MS time constant is used to measure the average value of the U1-1 test point before it is applied to MUX 1-$I_3$.

The U2-3 test point has an ideal pulse waveform for the frequency counter. Unfortunately, it has a 2K impedance to ground and is incapable of sinking even a single TTL load. Consequently, a discrete component transistor inverter is used to interface this test point with the frequency counter.

The most difficult interface problem is with test point U2-12 between the PWM output and R6. This test point can act as a current sink but it cannot act as a current source without interfering with the switching regulator operation. The IN914 diode referenced to +5V, at the input to the interface network, allows the PWM output to sink current when it is on and below about 4.4V but it does not allow R6 to act as a current source under any conditions. Furthermore, as long as the input voltage is above 5V, R6 cannot act as a current sink for the diode. The voltage at the anode of the diode is low pass filtered before it is applied to MUX 2-$I_2$, to make the test voltage independent of the sampling time. This interface network gives a reliable indication to distinguish between a PWM short and a chopper short condition. It also gives a reliable indication to distinguish between a PWM open and an R6 open condition. However, it cannot distinguish between a PWM open and a chopper open condition unless the switching regulator input voltage is below about 20V. When the input voltage is raised above about 20V, the PWM output transistors come out of saturation because of internal current limiting. When the PWM "on" output rises above +4.4V, the interface network can no longer tell whether it is on or off. This problem does not have an easy solution.

The data acquisition system is easily expandable to acquire test data from two positive output switching regulators in sequence. Inputs are already available on analog MUX 1 and 2 to accommodate 8 additional test points from another switching regulator. A 2 input digital MUX must be added at the input to the frequency counter to accommodate another frequency test point. Finally, a buffer latch must be added at the output of PIA port B to select one or the other of the switching regulators.

## V. FAULT DIAGNOSIS FLOW DIAGRAM:

The switching regulator fault diagnosis flow diagram is shown in Figures 8 through 11. This is a logical structure that systematically identifies and isolates faults to one of the functional blocks shown in Figure 2 or to a particular component. It is the key to the success of this project. It is capable of detecting every fault in the switching regulator that causes the output voltage to go out of tolerance as well as certain faults that occur before the output voltage goes out of tolerance. It is capable of diagnosing 30 distinct single faults in the 14 key components of the switching regulator. These include open, short, stuck at, excessive leakage, critical component drift, and instability; essentially every major fault that the writer could anticipate. These faults are coded for identification purposes and listed in Table 2. Three additional faults, TFO, TFL, and TFH, are included in the event that the microprocessor detects a Vo = 0, Vo low, and Vo high fault, respectively but is unable to diagnose it. This could occur if an out of tolerance fault exists that the writer did not anticipate. If this happens, it would be a simple matter to expand the flow diagram to cover this unforeseen case.

The 6802 machine language program that implements the fault diagnosis flow diagram is listed at the end of this section. It consists of 361 bytes burned on a 2716 EPROM. This does not include initialization of the PIA. Referring to the major fault diagnosis loop of Figure 8, the program begins by clearing memory locations E0 through EF. These are used to store the fault codes from 16 independent diagnostic checks. Data is then acquired and stored in memory locations C1 through DF as shown in Table 3. After the data is acquired, the major diagnostic tests begin. These include, in sequence, an input voltage test, reference regulator voltage tests, sawtooth oscillator frequency tests, an exesssive ripple test, and finally output voltage tests. The sequence in which each diagnostic test is performed is very important to the logical structure of the flow diagram. For example, if the input voltage is below 8 volts, no conclusions can be drawn about any other test. Consequently, this test must precede all others.

If the major diagnostic tests do not indicate a fault, then a new set of data is acquired and the sequence is repeated. If a fault is indicated, it may be immediately diagnosed, or additional diagnostic

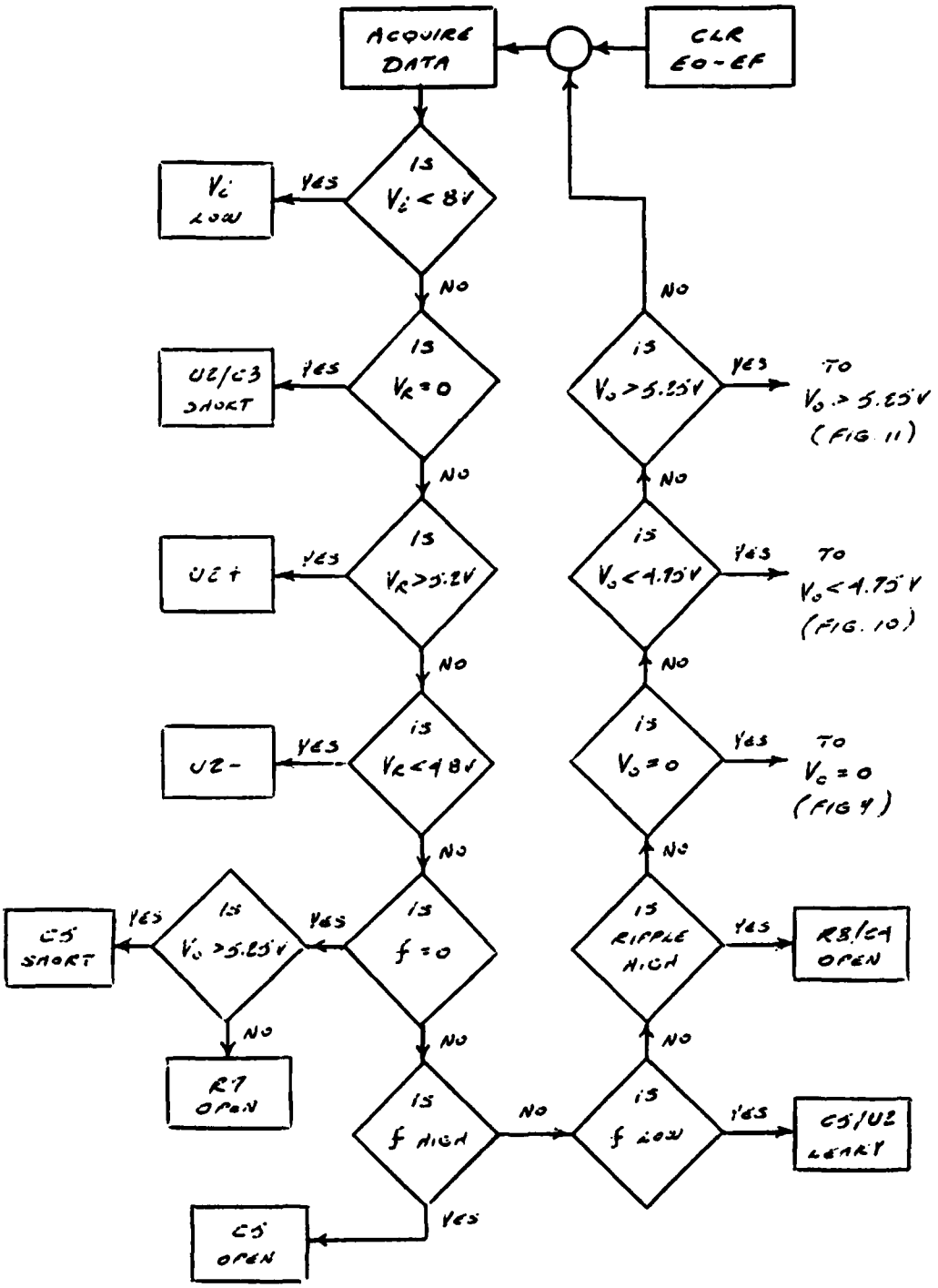



FIGURE 8. FAULT DIAGNOSIS FLOW DIAGRAM.

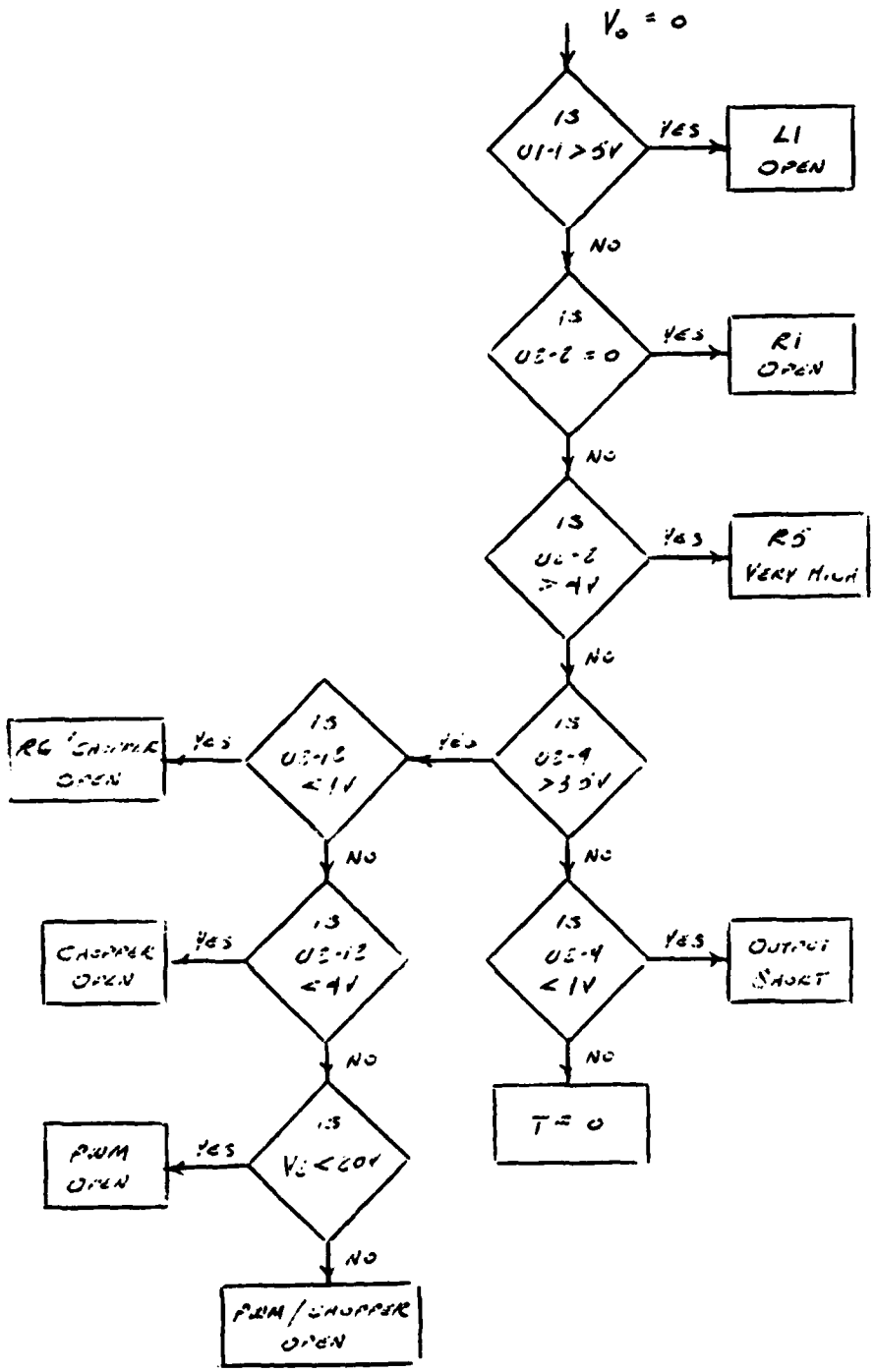



FIGURE 9. FAULT DIAGNOSIS FLOW DIAGRAM ($V_o$=0).

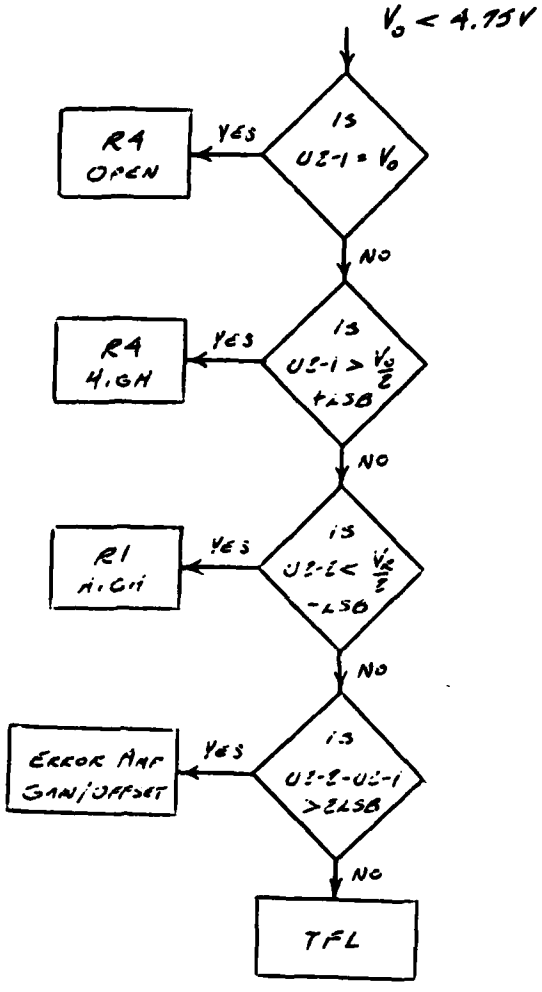



FIGURE 10. FAULT DIAGNOSIS FLOW DIAGRAM ($V_o$<4.75V).

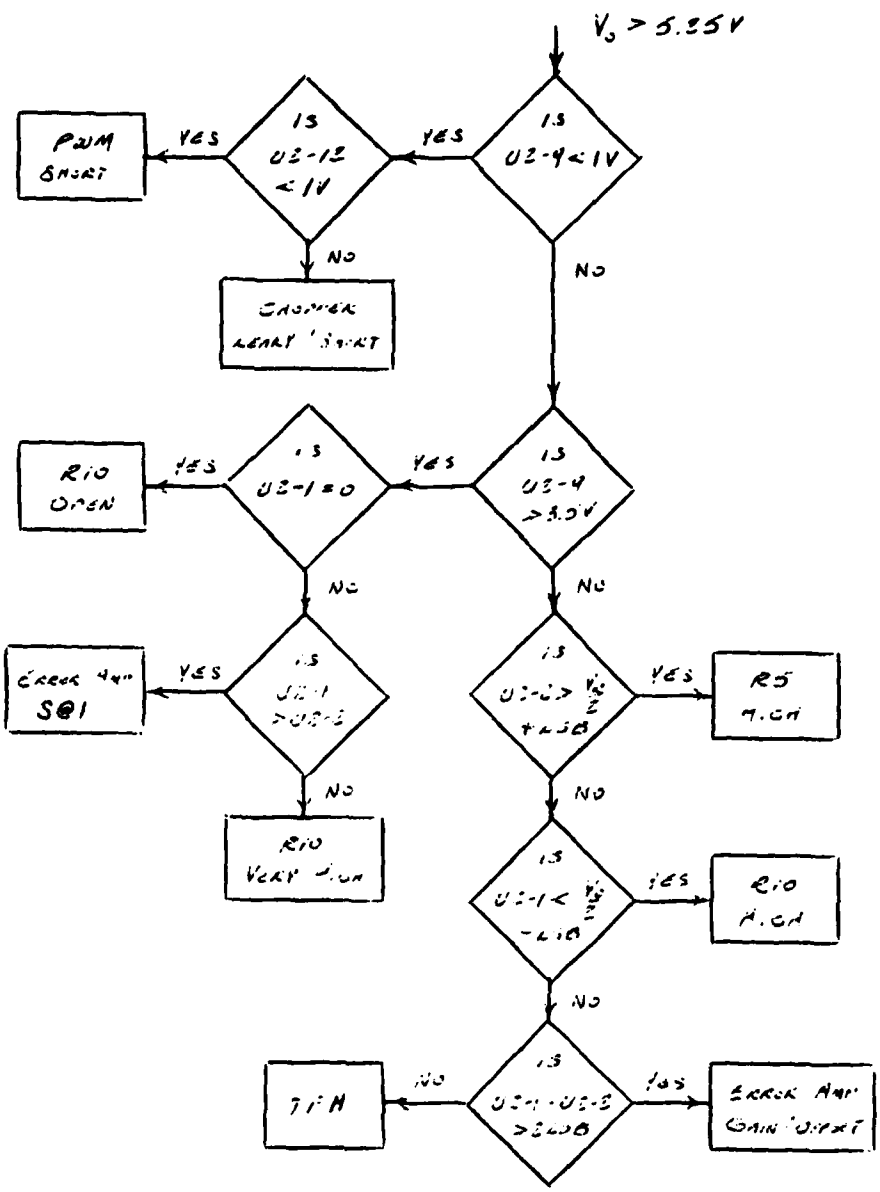



FIGURE 11. FAULT DIAGNOSIS FLOW DIAGRAM ($V_O$>5.25V).

TABLE 2. FAULT CODES

| Code | Fault |
|---|---|
| 00 | No Fault |
| 01 | $V_i$ Low |
| 02 | $V_R$ High (U2) |
| 03 | $V_R$ Low (U2) |
| 04 | $V_R$=0, U2, C3 Short |
| 05 | f High, C5 Open |
| 06 | f Low, C5/U2 Leaky, R7 High |
| 07 | f=0-, R7 Open |
| 08 | f=0+, C5 Short |
| 10 | Excessive Ripple, C4/R8 Open, C6 Open |
| A0 | L1 Open |
| A1 | R1 Open |
| A2 | R5 Very High |
| A3 | R6/Chopper Open |
| A4 | Chopper Open |
| A5 | PWM Open |
| A6 | Chopper/PWM Open |
| A7 | Output/C6 Short, Error Amp S@0 |
| A8 | TFO |
| A9 | R10 Open |
| AA | R10 Very High |
| AB | Error Amp S@1 |
| AC | R5 High, R1 Low |
| AD | R10 High, R4 Low |
| AE | TFH |
| AF | Error Amp + Offset/Gain |
| B0 | PWM Short |
| B1 | Chopper Leaky/Short |
| B2 | R4 Open |
| B3 | R4 High, R10 Low |
| B4 | R1 High, R5 Low |
| B5 | TFL |
| B6 | Error Amp - Offset/Gain |

TABLE 3. DATA MEMORY ADDRESSES

| Address | Data | Normal Reading |
|---|---|---|
| C1 | $V_o$ | 80 (Hex) |
| C2 | U2-1 | 40 |
| C3 | U2-2 | 40 |
| C4 | U2-1 | 40 |
| C5 | $V_i$ | - |
| C6 | U2-1 | 40 |
| C7 | U1-1 | 80 |
| C8 | U2-1 | 40 |
| C9 | $V_o$ | 80 |
| CA | $V_R$ | 80 |
| CB | U2-2 | 40 |
| CC | $V_R$ | 80 |
| CD | $V_i$ | - |
| CE | $V_R$ | 80 |
| CF | U1-1 | 80 |
| D0 | $V_R$ | 80 |
| D1 | $V_o$ | 80 |
| D2 | U2-12 | - |
| D3-DF | U2-9 | - |

tests may be required to diagnose it. Once it is identified, the fault code is stored in memory beginning at location E0. A new set of data is acquired and the sequence is repeated until 16 independent diagnostic checks indicate that a fault is present.

A major problem in analog fault diagnosis is that critical components such as voltage dividers and error amplifiers can drift out of tolerance without causing the important system parameters to drift outside of tolerance. It is desirable to ignore such "soft" faults. A major advantage of the fault diagnosis flow diagram is that faults due to component drift are not tested unless the output voltage is out of tolerance and not equal to zero and then only after all other possible causes have been eliminated. On the other hand, more serious faults in the sawtooth oscillator are identified even if the output voltage is in tolerance.

Although the flow diagram logic was designed to diagnose single faults, all multiple faults can be detected and some of these can be diagnosed and repaired sequentially. For example, if the reference regulator is out of tolerance and the chopper is open circuited, the former fault will first be diagnosed. If this is repaired, the latter fault will then be diagnosed. This does not imply that all multiple faults can be diagnosed in this manner. It is possible that the flow diagram logic can be expanded to diagnose all double faults, but this is beyond the present scope of this project.

In most cases the fault diagnosis program is a straightforward implementation of the fault diagnosis flow diagram. However, the excessive ripple block and the data acquisition block require some explanation. A detailed flow diagram of the excessive ripple subprogram (A0A1-A0C5) is shown in Figure 12. This subprogram finds the largest and smallest samples of U2-9 (stored in memory locations D3 through DF) and temporarily stores these in the A and B registors, respectively. A fault is defined whenever the difference between these is greater than 1 volt. Note that this difference is an estimate of the peak to peak value of the waveform. The accuracy of this estimate is dependent on the relationship between the sampling period and the period of the waveform under test.

The sampling period is wholly dependent on the microprocessor. Exactly 46 machine cycles elapse between successive samples of U2-9. This includes a deliberate 4 machine cycle (NOP) delay to insure that

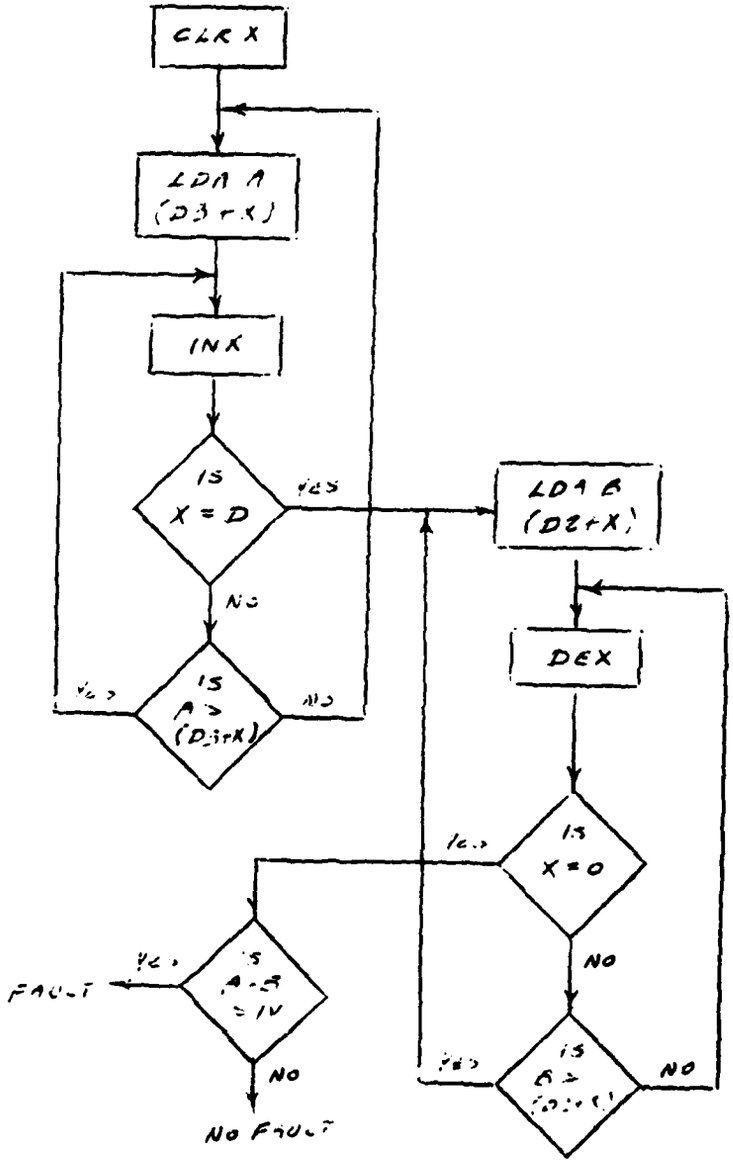



FIGURE 12. EXCESSIVE RIPPLE FLOW DIAGRAM.

the A to D conversion process is complete before data is read. The Ø2 clock frequency is 894.8 Khz, which corresponds to a 1.1176 μsec cycle time. Hence, the sampling period is 51.4 μsec. If this is an exact multiple of the period of the waveform under test, then all samples are identical and an estimate of the peak to peak value cannot be obtained. If the periods of the waveforms under test are known, this problem can be overcome as follows.

For illustrative purposes, suppose that the sampling period, $T_s$, is exactly equal to the test period, T. For a periodic waveform, $f(t) = f(t+T)$. If $T_s$ is increased to 1.1T by adding machine cycle (NOP) delays, then if the first sample is $f(t_1)$, the second sample is $f(t_1 + 1.1T) = f(t_1 + 0.1T)$, the third sample is $f(t_1 + 2.2T) = f(t_1 + 0.2T)$, etc. Hence, the sampling is equivalent to taking 10 samples of one period of the waveform.

In the switching regulator our interest is in finding excessive peak to peak ripple due to instability or due to a faulty LC filter. (Excessive ripple due to a very low sawtooth oscillator frequency is diagnosed in a prior test.) Experimentally it was determined that instability due to an R8/C4 open circuit occurred with a jittery period of about 300 μsec. It is expected that this will be somewhat a function of temperature and load. With the present sampling period, at least 6 distinct samples and possibly more can be obtained. The normal ripple period is the same as the sawtooth oscillator period. This is in the range, 42.8 μsec to 46.7 μsec, which corresponds to $T_s = 1.2T$ and 1.1T, respectively. Again, at least 5 distinct samples and possibly more can be obtained. Experimentally the excessive ripple subprogram was able to diagnose instability due to an R8/C4 open circuit consistently. Excessive ripple due to a faulty filter is less probable and more difficult to simulate.

In the data acquisition subprogram, initially 9 pairs of simultaneous samples are taken and stored sequentially in memory locations C1 through D2 as shown in Table 3. Exactly 79 machine cycles or 88.3 μsec elapse between successive sample pairs. This is followed by 13 successive samples of U2-9 stored in memory locations D3 through DF. Total data acquisition time is 1.4685 MS.

During ground maintenance the program could be initiated by a technician to reliably diagnose faults already present in the switching

## DATA ACQUISITION PROGRAM

| Address | Op Code | Comments | |
|---|---|---|---|
| A000 | CE,00,EF | LDX # $ 00EF | CLR E0-EF |
| A003 | 6F,00 | CLR $ 00, X | |
| A005 | 09 | DEX | |
| A006 | 8C,00,DF | CPX # $ 00DF | |
| A009 | 26,F8 | BNE (03) | |
| A00B | DF,A0 | STX $ A0 | |
| A00D | CE,00,C0 | LDX # $ 00C0 | ACQ DATA |
| A010 | 5F | CLR B | |
| A011 | 86,10 | LDA A # $ 10 | |
| A013 | 1B | ABA | |
| A014 | B7,40,06 | STA A PIA-B | |
| A017 | 8B,30 | ADD A # $ 30 | |
| A019 | B7,40,06 | STA A PIA-B | |
| A01C | 80,40 | SUB A # $ 40 | |
| A01E | B7,40,06 | STA A PIA-B | |
| A021 | 08 | INX | |
| A022 | 01 | NOP | |
| A023 | 01 | | |
| A024 | B6,40,04 | LDA A PIA-A | |
| A027 | A7,00 | STA A $ 00, X | |
| A029 | 86,60 | LDA A # $ 60 | |
| A02B | B7,40,06 | STA A PIA-B | |
| A02E | 86,20 | LDA A # $ 20 | |
| A030 | B7,40,06 | STA A PIA-B | |
| A033 | 08 | INX | |
| A034 | 01 | NOP | |
| A035 | 01 | | |
| A036 | B6,40,04 | LDA A PIA-A | |
| A039 | A7,00 | STA $ 00, X | |
| A03B | 5C | INC B | |
| A03C | C1,09 | CMP B # $ 09 | |
| A03E | 26,D1 | BNE (11) | |
| A040 | 86,3C | LDA A # $ 3C | |
| A042 | B7,40,06 | STA A PIA-B | |

## DATA ACQUISITION PROGRAM (Cont.)

| Address | Op Code | Comments |
|---|---|---|
| A045 | 86,6C | LDA A # $ 6C |
| A047 | B7,40,06 | STA A PIA-B |
| A04A | 86,2C | LDA A # $ 2C |
| A04C | B7,40,06 | STA A PIA-B |
| A04F | 08 | INX |
| A050 | 01 | NOP |
| A051 | 01 | |
| A052 | B6,40,04 | LDA A PIA-A |
| A055 | A7,00 | STA A $ 00, X |
| A057 | 8C,00,DF | CPX # $ 00DF |
| A05A | 26,E4 | BNE (40) |

## FAULT DIAGNOSIS PROGRAM

| Address | Op Code | Comments | |
|---|---|---|---|
| A05C | 5F | CLR B | |
| A05D | 96,C5 | LDA A $ C5 | |
| A05F | 81,34 | CMP A # $ 34 | |
| A061 | 25,2B | BCS | Vi low |
| A063 | 96,CA | LDA A $ CA | |
| A065 | 27,24 | BEQ | $V_R = 0$ |
| A067 | 81,86 | CMPA # $ 86 | |
| A069 | 22,22 | BHI | $V_R$ high |
| A06B | 81,7B | CMPA # $ 7B | |
| A06D | 25,1D | BCS | $V_R$ low |
| A06F | 86,80 | LDA A # $ 80 | |
| A071 | B7,40,06 | STA A PIA-B | |
| A074 | B6,40,04 | LDA A PIA-A | |
| A077 | 2B,11 | BMI | f high |
| A079 | 27,06 | BEQ | f = 0 |
| A07B | 81,40 | CMPA # $ 40 | |
| A07D | 2B,0A | BMI | f low |
| A07F | 20,20 | BRA | |
| A081 | 96,C1 | LDA A $ C1 | f = 0 |
| A083 | 81,87 | CMPA # $ 87 | |
| A085 | 2B,01 | BMI | |
| A087 | 5C | INC B | f = 0+ |
| A088 | 5C | | f = 0- |
| A089 | 5C | | f low |
| A08A | 5C | | f high |
| A08B | 5C | | $V_R = 0$ |
| A08C | 5C | | $V_R$ low |
| A08D | 5C | | $V_R$ high |
| A08E | 5C | | $V_i$ low |
| A08F | DE,A0 | LDX $ A0 | |
| A091 | E7,01 | STA B $ 01, X | |
| A093 | 08 | INX | |
| A094 | DF,A0 | STX $ A0 | |

## FAULT DIAGNOSIS PROGRAM (Cont.)

| Address | Op Code | Comments | |
|---|---|---|---|
| A096 | 8C,00,EF | CPX # $ 00EF | |
| A099 | 27,03 | BEQ | |
| A09B | 7E,A0,0D | JMP to D.A. | |
| A09E | 7E,F8,57 | JMP to PROMPT | |
| A0A1 | CE,00,00 | LDX # $ 0000 | Check Ripple |
| A0A4 | A6,D3 | LDA A $ D3, X | |
| A0A6 | 08 | INX | |
| A0A7 | 8C,00,0D | CPX # $ 000D | |
| A0AA | 27,06 | BEQ | |
| A0AC | A1,D3 | CMP A $ D3, X | |
| A0AE | 2B,F4 | BMI | |
| A0B0 | 2A,F4 | BPL | |
| A0B2 | E6,D2 | LDA B $ D2, X | |
| A0B4 | 09 | DEX | |
| A0B5 | 27,06 | BEQ | |
| A0B7 | E1,D2 | CMP B $ D2, X | |
| A0B9 | 2A,F7 | BPL | |
| A0BB | 2B,F7 | BMI | |
| A0BD | 10 | SBA | |
| A0BE | 81,1A | CMP A # $ 1A | |
| A0C0 | 2B,04 | BMI | Ripple O.K. |
| A0C2 | C6,10 | LDA B # $ 10 | Excessive Ripple |
| A0C4 | 20,C9 | BRA (8F) | |
| A0C6 | 5F | CLR B | Ripple O.K. |
| A0C7 | 96,C1 | LDA A $ C1 | |
| A0C9 | 27,76 | BEQ | $V_o = 0$ |
| A0CB | 81,7A | CMP A # $ 7A | |
| A0CD | 25,3D | BCS | $V_o < 4.75V$ |
| A0CF | 81,87 | CMPA # $ 87 | |
| A0D1 | 22,03 | BH1 | $V_o > 5.25V$ |
| A0D3 | 7E,A0,0D | JMP $ A00D | $V_o$ is O.K. |
| A0D6 | 96,D3 | LDA A $ D3 | $V_o > 5.25V$ |
| A0D8 | 81,1A | CMP A # $ 1A | |

## FAULT DIAGNOSIS PROGRAM (Cont.)

| Address | Op Code | Comments | |
|---|---|---|---|
| A0DA | 25,28 | BCS | PWM/Chopper |
| A0DC | 81,5A | CMPA # $ 5A | |
| A0DE | 25,0A | BCS | Linear |
| A0E0 | 96,C4 | LDA A $ C4 | |
| A0E2 | 27,4F | BEQ | R10 Open |
| A0E4 | 91,C3 | CMP A $ C3 | |
| A0E6 | 25,4A | BCS | R10 Very High |
| A0E8 | 20,47 | BRA | Error Amp S@I |
| A0EA | 96,CC | LDA A $ CC | Linear |
| A0EC | 44 | LSRA | |
| A0ED | 4C | INCA | |
| A0EE | 91,CB | CMP A $ CB | |
| A0F0 | 2B,3E | BMI | R5 High |
| A0F2 | 96,C1 | LDA A $ C1 | |
| A0F4 | 44 | LSRA | |
| A0F5 | 4A | DEC A | |
| A0F6 | 91,C2 | CMP A $ C2 | |
| A0F8 | 22,35 | BHI | R10 High |
| A0FA | 96,C4 | LDA A $ C4 | |
| A0FC | 90,C3 | SUB A $ C3 | |
| A0FE | 81,02 | CMP A # $ 02 | |
| A100 | 2B,2C | BMI | TF+ |
| A102 | 20,29 | BRA | Error Amp + |
| A104 | 96,D2 | LDA A $ D2 | PWM/Chopper |
| A106 | 81,1A | CMP A $ 1A | |
| A108 | 25,22 | BCS | PWM Short |
| A10A | 20,1F | BRA | Chopper Leaky/Short |
| A10C | 91,C2 | CMP A $ C2 | $V_o$ < 4.75V |
| A10E | 27,1A | BEQ | R4 Open |
| A110 | 44 | LSR A | |
| A111 | 4C | INC A | |
| A112 | 91,C2 | CMP A $ C2 | |
| A114 | 2B,13 | BMI | R4 High |

## FAULT DIAGNOSIS PROGRAM (Cont.)

| Address | Op Code | Comments | |
|---|---|---|---|
| A116 | 96,CC | LDA A $ CC | |
| A118 | 44 | LSR A | |
| A119 | 4A | DEC A | |
| A11A | 91,CB | CMP A $ CB | |
| A11C | 2E,0A | BGT | R1 High |
| A11E | 96,C3 | LDA A $ C3 | |
| A120 | 90,C4 | SUB A $ C4 | |
| A122 | 81,02 | CMP A # $ 02 | |
| A124 | 2B,01 | BMI | TF- |
| A126 | 5C | INC B | Error Amp - |
| A127 | 5C | | TF- |
| A128 | 5C | | R1 High |
| A129 | 5C | | R4 High |
| A12A | 5C | | R4 Open |
| A12B | 5C | | Chopper Leaky/Short |
| A12C | 5C | | PWM Short |
| A12D | 5C | | Error Amp + |
| A12E | 5C | | TF+ |
| A12F | 5C | | R10 High |
| A130 | 5C | | R5 High |
| A131 | 5C | INC B | Error Amp S@1 |
| A132 | 5C | | R10 Very High |
| A133 | 5C | | R10 Open |
| A134 | 5C | | TFO |
| A135 | 5C | | Output Short |
| A136 | 5C | | PWM/Chopper Open |
| A137 | 5C | | PWM Open |
| A138 | 5C | | Chopper Open |
| A139 | 5C | | R6/Chopper Open |
| A13A | 5C | | R5 Very High |
| A13B | 5C | | R1 Open |
| A13C | CB,A0 | ADD B # $ A0 | L1 Open |
| A13E | 7E,A0,8F | JMP $ A08F | |

## FAULT DIAGNOSIS PROGRAM (Cont.)

| Address | Op Code | Comments | |
|---|---|---|---|
| A141 | 96,C7 | LDA A $ C7 | Vo = 0 |
| A143 | 2B,F7 | BMI | L1 Open |
| A145 | 96,C3 | LDA A $ C3 | |
| A147 | 27,F2 | BEQ | R1 Open |
| A149 | 81,68 | CMP A # $ 68 | |
| A14B | 22,ED | BHI | R5 Very High |
| A14D | 96,D3 | LDA A $ D3 | |
| A14F | 81,5A | CMP A # $ 5A | |
| A151 | 22,06 | BH1 | |
| A153 | 81,1A | CMP A # $ 1A | |
| A155 | 25,DE | BCS | Output Short |
| A157 | 20,DB | BRA | TFO |
| A159 | 96,D2 | LDA A $ D2 | |
| A15B | 81,1A | CMP A $ 1A | |
| A15D | 25,DA | BCS | R6/Chopper Open |
| A15F | 81,7A | CMP A # $ 7A | |
| A161 | 25,D5 | BCS | Chopper Open |
| A163 | 96,C5 | LDA A $ C5 | |
| A165 | 2B,DO | BMI | PWM/Chopper Open |
| A167 | 20,CD | BRA | PWM Open |

regulator. However, if the fault occurs while the program is running, the fault code stored in the first memory location (E0) may not be accurate for two reasons.

a. If the fault occurs during the data acquisition period, then part of the data is acquired before the fault occurs and part afterwards.

b. Because of the finite time constant associated with the low pass filter interface circuits, the first set of data acquired may not reflect steady state conditions for these test points.

The complete fault diagnosis system has been breadboarded and tested in the lab at room temperature and with the switching regulator operating at light loads. Virtually every fault listed in Table 2 that could be practically simulated was consistently identified by the MPU.

## VI. AUTOMATIC SELF CHECKING PROCEDURES

In general, diagnosing a test unit fault where one does not exist can be more disastrous than ignoring or misdiagnosing an actual fault. For this reason it is desirable to incorporate self checking procedures into the automatic test circuitry to insure that a test equipment fault is not diagnosed as a test unit fault. This section takes a preliminary look at this problem and proposes some partial solutions. Because of the limited time available for this portion of the project, it is impossible to formulate a complete solution or to incorporate the limited solutions into the breadboard system. Since adding hardware for self checking purposes can be counterproductive, this preliminary study considers only software approaches to this problem.

For self checking purposes it is convenient to divide the automatic test equipment into 3 major groups.

a. MPU, EPROM, and RAM

b. PIA

c. Data Acquisition System

Self checking procedures for each of these is considered in the following paragraphs.

A relatively straightforward software procedure can be used to insure that that portion of the MPU, EPROM, and RAM used for fault diagnosis is functioning properly. This is as follows.

a. Load data into memory locations C1 through DF to simulate one of the 33 faults listed in Table 2.

b. Run the fault diagnosis portion of the program.

c. Compare contents of memory locations E0 through EF to insure that fault code stored corresponds to the fault defined by the simulated data set.

d. Repeat Steps (a), (b), and (c) for each of the 33 faults listed in Table 2.

A PIA initialization subprogram should be inserted into the fault diagnosis loop of Figure 8 prior to acquiring data. This insures that a momentary power loss or glitch that resets the PIA does not interfere with the system operation.

The following procedure can be used to check the data acquisition system and PIA's ability to load data into the MPU.

a. Clear memory locations C1 through DF.

b. Check to insure that all memory locations have been cleared.

c. Run data acquisition subprogram and check contents of D2. If it is zero, the system is unable to load data into the MPU.

Note that the contents of D2 comes from U2-12 via an interface circuit. Because of the diode and +5V reference in this interface circuit, this data is non-zero even if all test unit voltages are zero. If a load data fault is indicated, the PIA's control registers are first examined for a fault, then the data direction registers are checked, and finally data is loaded into peripheral data register (PDR) B and checked. However, a fault in PDR A cannot be isolated.

Certain faults in the data acquisition system can be isolated by making use of inconsistencies in the acquired data set. In addition to discrepancies between two samples of the same test point, these include:

(1) Vi < Vo
(2) Vi < $V_R$
(3) U2-1 > Vo
(4) U2-2 > $V_R$
(5) U1-1 < Vo
(6) U2-9 > $V_R$
(7) U2-12 = 0
(8) U2-12 > 87 hex
(9) f > 80 hex

To illustrate this, consider an expansion of the test unit fault diagnosis flow diagram that enables the MPU to detect and partially isolate any single open circuit fault in the data acquisition system's

multiplexors (or interface networks). This can be accomplished at a cost of a few hundred bytes of EPROM.

Experimentally an open circuit between any test point and the output of MUX 1 or 2 gives a zero data reading for that test point. An open circuit at the output gives a zero data reading for all 4 test points interfaced to that MUX. An open circuit at the output of MUX 3 gives a zero reading for all 8 test points.

An open circuit at either input to MUX 3 is more complex because of the sequential sampling scheme used to acquire data and the slow discharge times of CMOS capacitances under open circuit conditions. Memory locations C1 through D2 are loaded alternately with data samples from MUX 1 and 2. If one input, say $I_1$, of MUX 3 opens, the data from MUX 1 is still valid. The data from MUX 2 is lost, but the slow capacitor discharge time makes the apparent data read into the A/D converter dependent upon the data previously obtained from MUX 1. Consequently, two apparent data samples from the same test point will differ markedly in a predictable manner. This fact is used to identify this fault.

The expanded fault diagnosis flow diagram that utilizes the previous symptoms to isolate MUX open circuit faults, as well as PIA and test unit faults, is shown in Figure 13, 14, and 15. This is a revision of the main fault diagnosis loop of Figure 8. Those portions of the fault diagnosis loop shown in Figures 9, 10, and 11 are unaffected by the expansion.

Implementing this expanded fault diagnosis diagram with EPROM software is a straightforward, if time consuming, task. However, this is intended as only one example of how software expansion can be used to isolate faults in the data acquisition system. If additional time was available, other fault isolation tests could be developed and incorporated into the fault diagnosis flow diagram.

It should be noted that the test unit fault diagnosis program itself provides a limited check of the data acquisition system. For example, if it is established that $V_R$ is within its $\pm 4\%$ tolerance, it is improbable that any major fault exists in either S/H2, the A/D converter, or the PIA.

## VII. RECOMMENDATIONS:

This project has shown that automatic fault diagnosis of a switching

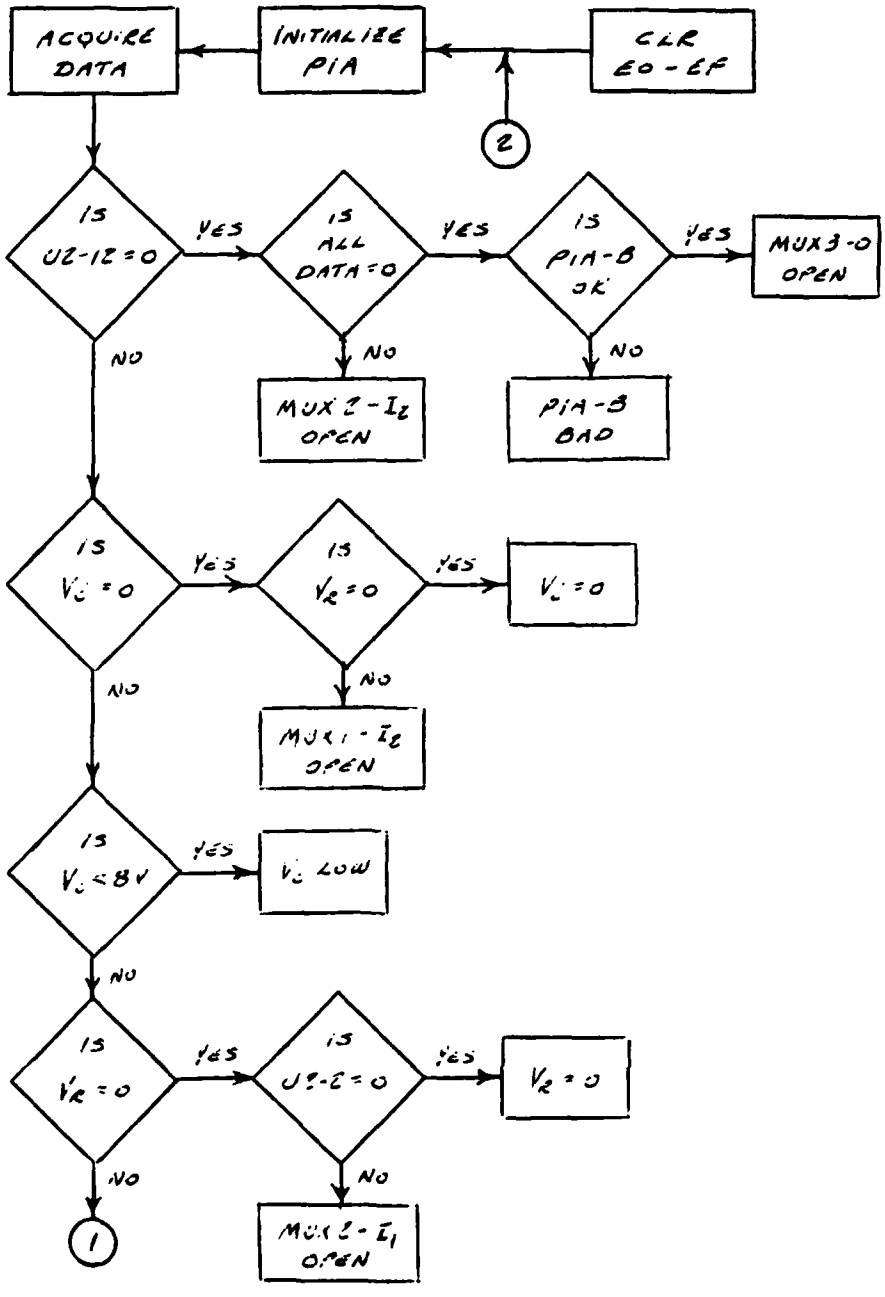
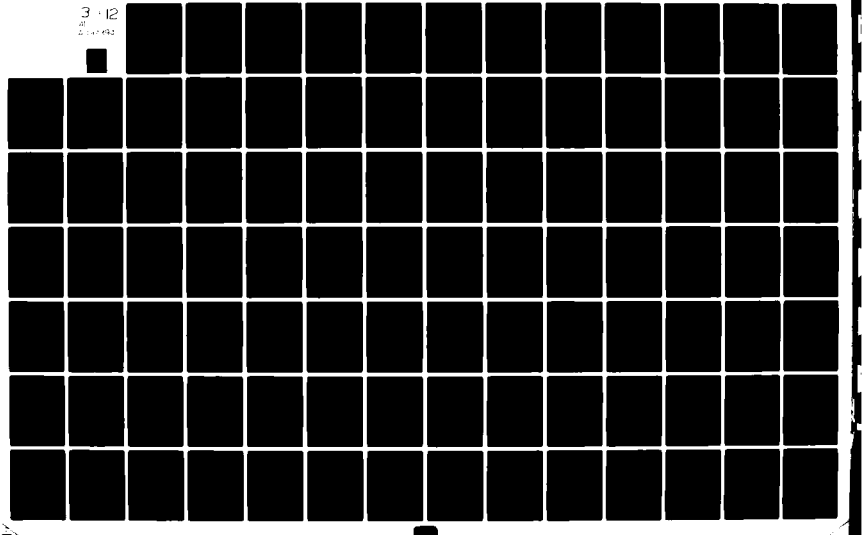


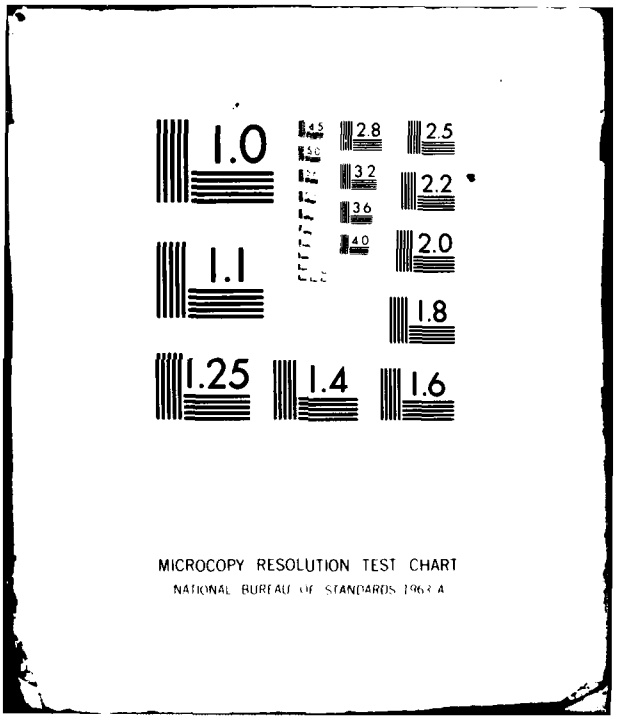

FIGURE 13. EXPANDED FAULT DIAGNOSIS FLOW DIAGRAM.

AD-A097 394 SOUTHEASTERN CENTER FOR ELECTRICAL ENGINEERING EDUCAT--ETC F/G 5/1
USAF SUMMER FACULTY RESEARCH PROGRAM, 1980, RESEARCH REPORTS, V--ETC(U)
OCT 80 W D PEELE F49620-79-C-0038

UNCLASSIFIED AFOSR-TR-81-0193 NL

3 12




1.0
1.1
1.25
1.4
1.6
1.8
2.0
2.2
2.5
2.8
3.2
3.6
4.0
4.5
5.0
MICROCOPY RESOLUTION TEST CHART
NATIONAL BUREAU OF STANDARDS 1963 A

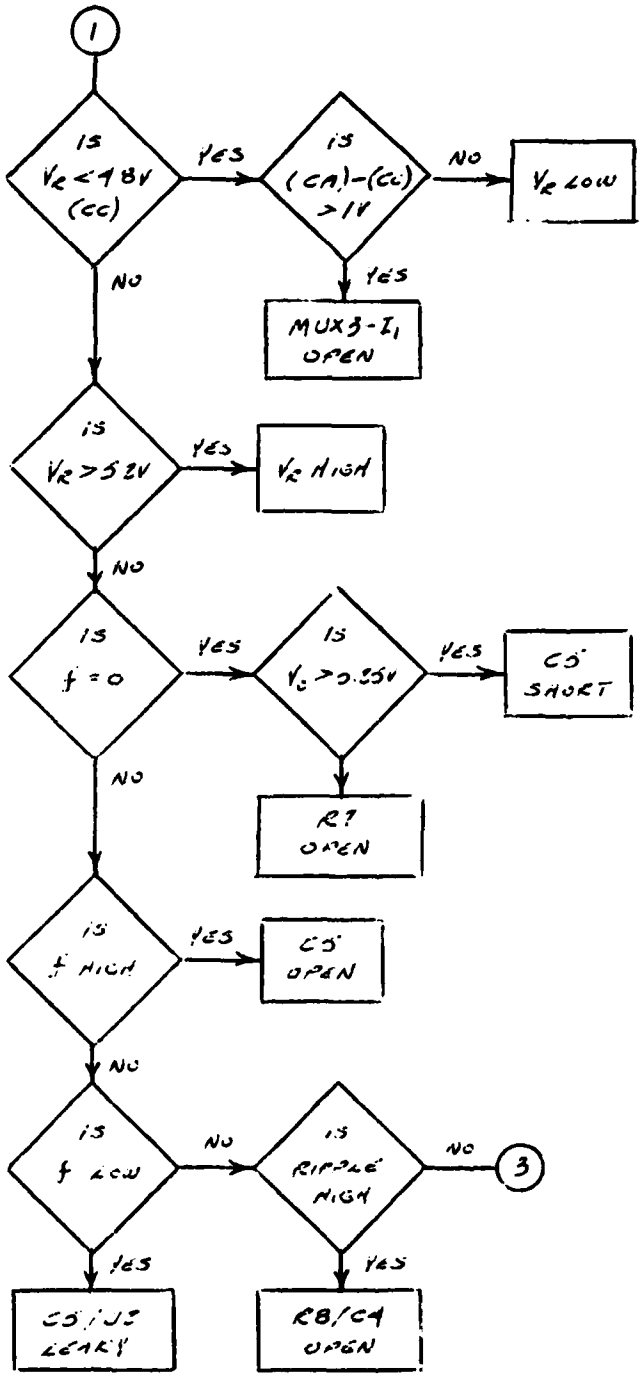



FIGURE 14. EXPANDED FAULT DIAGNOSIS FLOW DIAGRAM (CONT'D).

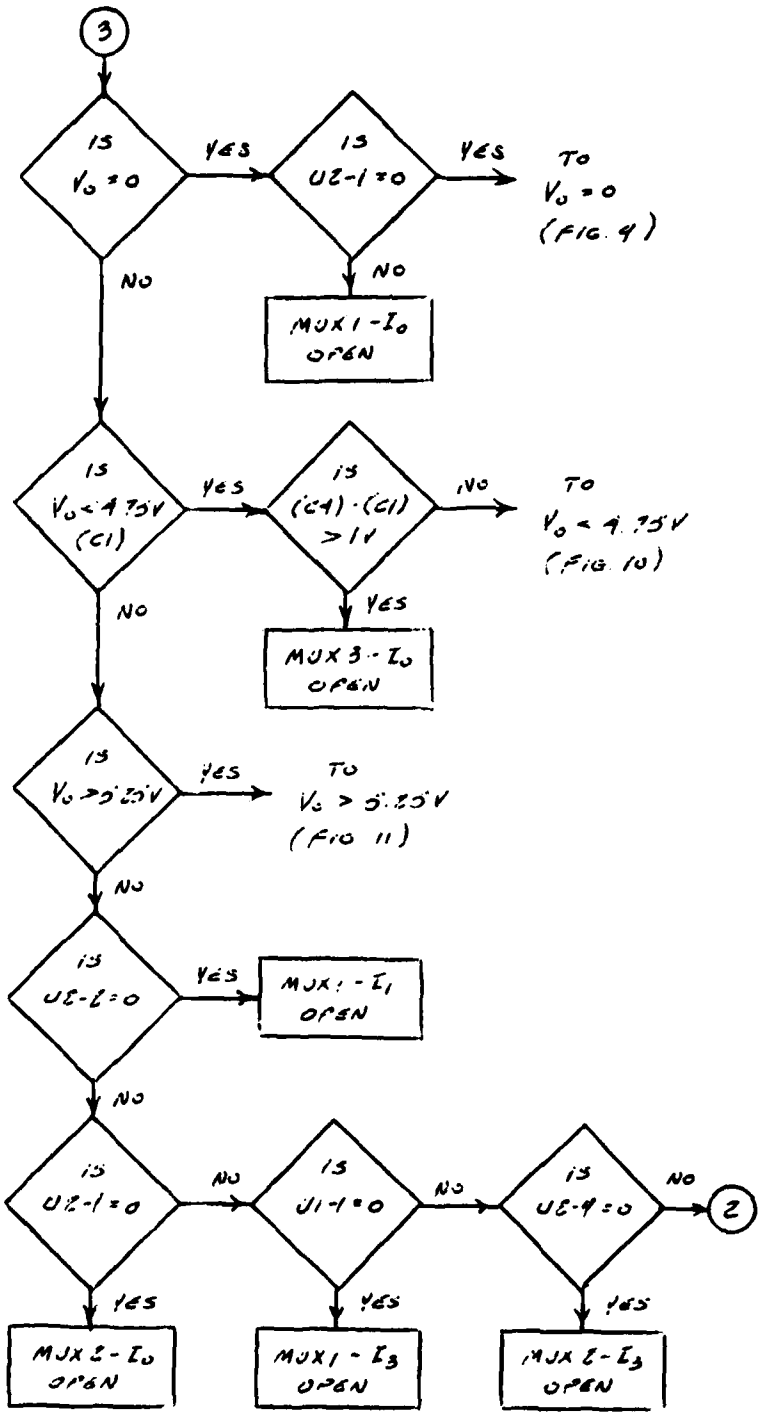



FIGURE 15. EXPANDED FAULT DIAGNOSIS FLOW DIAGRAM (CONT'D).

regulator is technically feasible. There is no reason to believe that this is not the case for other avionic subsystems, both analog and digital. It is recommended that these efforts be pursued until finally a single microprocessor and data acquisition system can be used to sequentially diagnose faults in every piece of avionics hardware in an aircraft. Ideally, the MPU can also check itself and the data acquisition system to insure that test equipment faults are not misdiagnosed as test unit faults. This is an ambitious goal that can best be accomplished in small steps.

Having a working breadboard of an automatic fault diagnosis system for a switching regulator is an important first step, since it restores credibility to the automatic fault diagnosis concept. This credibility has been seriously weakened by poor implementations of the concept in the past. In order to accomplish this in the limited time available, it was necessary to begin with a relatively simple system such as a switching regulator. However, a switching regulator does not present a sufficiently broad spectrum of fault diagnosis problems to infer that the approach taken can be generalized.

Since the switching regulator automatic fault diagnosis system is practical in itself, it is recommended that this be updated from fragile breadboard to prototype status. This should be subjected to further testing at full load and under expected environmental conditions. The test equipment self checking procedures outlined in Section VI should be incorporated into the system. Other self checking software should be developed and incorporated into the system.

A suggested next step is this: Apply techniques developed during this project and develop additional techniques as required to automatically diagnose faults in a second avionics subsystem. This should be more complex and utilize different functional blocks than a switching regulator, but it should not be so complex that tangible results cannot be obtained in a reasonable amount of time. Since the switching regulator is an analog system, at least some of these functional blocks should be digital. As in the present project, the MPU and EPROM software should be utilized as much as possible to minimize off board hardware.

A problem that is applicable only to analog fault diagnosis is this: Although canned computer programs exist for analyzing non-linear analog systems, modern analog systems utilize complex integrated circuits

for which a known computer model does not exist. Even where computer models do exist, in most cases these are not valid under certain fault conditions. Unless computer fault models are developed for analog integrated circuits, computer fault simulation of systems that utilize these is impossible. The alternative breadboard fault simulation approach is not always practical. For this reason it is recommended that commonly used analog I.C.'s in avionics systems be identified and computer fault models be developed for these.

## REFERENCES


1. Bishop, Ron, Basic Microprocessors and the 6800, Rochelle Park, New Jersey, Hayden Book Co., Inc., 1979.

2. Duhamel, P. and J. C. Rault, "Automatic Test Generation Techniques for Analog Circuits and Systems: A Review," IEEE Transactions on Circuits and Systems, Volume CAS-26, Number 7, pp. 411-440, July, 1979.

3. Report AD-B040 586L, Failure Rates, Naval Fleet Analysis Center, Corona, California, February, 1976.

1980 USAF - SCEEE SUMMER FACULTY RESEARCH PROGRAM

Sponsored by the

AIR FORCE OFFICE OF SCIENTIFIC RESEARCH

Conducted by the

SOUTHEASTERN CENTER FOR ELECTRICAL ENGINEERING EDUCATION

# FINAL REPORT

# DYNAMIC ANALYSIS OF COUPLED STRUCTURES AND RELATIONSHIP TO TEST PROCEDURES


| | |
|---|---|
| Prepared By: | Sherif T. Noah |
| Academic Rank: | Assistant Professor |
| Department and University: | Department of Mechanical Engineering<br>Texas A&M University |
| Research Location: | Air Force Flight Dynamics Laboratory<br>Structures and Dynamics Division<br>Structural Vibrations Branch |
| USAF Research Colleague: | Otto F. Maurer |
| Date: | September 17, 1980 |
| Contract No: | F49620-79-C-0038 |

# DYNAMIC ANALYSIS OF COUPLED STRUCTURES AND RELATIONSHIP TO TEST PROCEDURES

by

Sherif T. Noah

ABSTRACT

The problems arising in modal synthesis based on experimentally derived dynamic characteristics of separated structural components are investigated. A comprehensive review of existing synthesis techniques is presented and the relationship to test procedures is examined. It is concluded that the synthesis methods with the best potential for achieving experimental compatibility are those employing truncated sets of free-interface modes of the components plus an appropriate account for the effects of deleted modes. Feasibility of extending the free-interface component mode synthesis methods to enable utilization of complex modes is demonstrated. Recommendations for further research efforts are made.

## ACKNOWLEDGEMENTS

The author is grateful to the Air Force Systems Command, the Air Force Office of Scientific Research and the Southeastern Center for Electrical Engineering Education for providing him with the unique opportunity of spending a very fruitful and gratifying summer at the Air Force Flight Dynamics Laboratory, Wright-Patterson Air Force Base, Ohio. He would also like to acknowledge the laboratory, in particular the Structural Vibration branch of the Structures and Dynamics Division, for its fine facilities and pleasant working conditions.

The author wishes to express special appreciation to Mr. Otto Maurer for suggesting the research area, for many fruitful discussions and for making his stay a very enriching and stimulating experience. The author is grateful to Mr. R. Bingman and Mr. C. Thomas for their help in securing every resource needed for the completion of the research. The author would also like to thank Dr. C. Keller for interesting discussions and for furnishing the author with a copy of his most recent work being prepared for publication.

## I. INTRODUCTION

The dynamic analysis of structures is increasingly becoming a requirement in the design and testing of most modern applications involving structural systems. A vital part of the design effort is the analysis of analytical models of the structures. The parameters of the model are usually derived from the finite element formulation and, in many cases, are experimentally verified once the hardware becomes available.

Recent advances in structural applications, coupled with a drive toward more stringent requirements of safety, reliability and cost effectiveness have created a need for greater accuracy and speed in the dynamic analysis of structures. This is particularly the case in aerospace applications, where efficient lightweight structures are designed for reliable and safe operation in severe environments.

With the requirement for higher accuracy, more detailed models defined by a large number of generalized coordinates become necessary. A direct solution using all of the coordinates of the total structure may exceed the capability of a given computer facility, lead to numerical errors and/or result in prohibitively costly long run times. Furthermore, the design process often requires several cycles of reanalysis to arrive at improved configurations. Also, desirable modifications and additions might necessitate additional analysis of the altered structures. The implication of cost and time involved in the repeated analysis of detailed models of the structures is self evident.

During the past two decades, a growing effort has been devoted to the development of subsystem techniques to avert the inadequacies discussed above. In these methods a complex structure is treated as an assembly of connected components (or substructures) whose dynamic characteristics are used to arrive at a description of the total structure. Most of the methods are developed around the idea of utilizing a set of modes or displacement shapes constructed for the separated components which, through appropriate coupling procedure, are used to define a set of generalized coordinates describing the complete structures. In the majority of these methods, the normal modes of the separated components are used to synthesize those of the complete structure. These methods therefore, came to be known as "modal synthesis" techniques.

Significant advantages resulting from the use of the substructure approach in the design and analysis of structures may be readily envisaged. The approach parallels the design process of complex structures and allows for flexibility of the analysis. Different levels of detail in modeling the structures and its components may be employed. Also the dynamic characteristics of some of the substructures may be determined from experimental test data while those of the other substructures are derived from finite element formulations. Furthermore, most of the component synthesis techniques utilize truncated sets of the significant modes of each substructure. This permits the development of a substantially smaller number of equations for adequate description of the complete structure.

In recognition of the component synthesis approach as an emerging design tool of vital significance, several symposia were devoted entirely to the subject (see for example reference 1). Various synthesis techniques are being incorporated in large general purpose finite element computer programs such as that of NASTRAN[2,30]. More recently, Clough and Wilson[3] demonstrated the benefits derived from employing a modal synthesis technique for the analysis of a structure with local nonlinearity. Synthesis techniques are also being applied to problems involving fluid-structure interactions[4].

At the present time modal synthesis techniques based on analytical formulations are fairly developed. However, further effort is needed to extend the applicability of existing techniques to more general types of structures. In particular, studies are needed for the representation of the various damping mechanisms in component mode synthesis. The potential of the synthesis methods for dealing with nonconservative structural systems and with systems possessing nonlinearities should also be explored.

Unfortunately, a major limitation on the use of the modal synthesis approach as an effective design tool is the lack of demonstrated compatibility with practical experimental procedures. The need for experimental parameter identification of complex structures has been recently emphasized. This is particularly the case with some of the parameters, such as those related to damping, which are virtually impossible to estimate other than by test data. In other cases where the structure is of

extremely large dimensions, as in space applications, testing of the complete structure would be practically unfeasible.

In general, full scale testing of complex structures is both costly and time consuming. This is particularly the case in the ground vibration tests (GVT) of aircraft structures and appended components. An experimentally compatible subsystem synthesis technique would prove extremely valuable in avoiding repeated testing of the total structure with every addition or alteration of various components. An important application of such synthesis technique would be the determination of the dynamic characteristics of aircraft with attached stores in various arrangements.

## II OBJECTIVES

The main objective of this research effort was to investigate the problems arising in modal synthesis based on experimentally derived dynamic characteristics of separated components. The work would be directed toward the development of a sound combined experimental/analytical procedure for the synthesis of the dynamic characteristics of complex structures. An initial effort toward meeting the above goal was to fulfill the following specific objectives:

(1) To review existing modal synthesis and other subsystem techniques of dynamic analysis of structures.

(2) To assess major synthesis approaches and their derivatives with regard to their relationship to experimental test procedure and potential for further development or modification to achieve test compatability.

(3) To explore the relationship of synthesis techniques to methods of experimental system identification of stuctural components.

(4) To identify specific future research efforts needed for the development of experimentally compatible synthesis techniques which would be particularly effective in applications of relevance to the Air Force such as that of synthesizing the dynamic characteristics of aircraft/stores assemblies.

## III. REVIEW OF SYNTHESIS TECHNIQUES AND RECENT DEVELOPMENTS

The early work on modal synthesis was motivated by the need for an economic representation of substructures in analog computer solutions of structures as combined with aeroelastic and control system models. Representation of the subsystems was done in terms of electrical analogies (see for example reference 5).

The first applications to digital computers were simple extensions of the analog techniques and proved highly restrictive and limited in accuracy. Numerous synthesis approaches have recently been developed, resulting in increased accuracy and more generality as applied to large-order and complex structure dynamics problems.

In what follows, a brief account of the existing synthesis techniques is presented. Several reviews of some of these techniques are also available in the literature[6,7,15]. The review presented by Craig and Chang[7] is particularly comprehensive, covering reported techniques and applications to 1977.

It was Hurty[8,9] who developed the first general modal synthesis* method capable of coupling substructures with redundant interface connections. Fixed-interface normal modes, rigid-body modes, and redundant constraint modes** of the substructures are used in that method to define generalized coordinates of the assembled structure. In addition, Hurty[10,11] devised a convergence criterion for the system's normal frequencies. The criterion serves as a guide in selecting the proper component modes to be included in the synthesis provided the upper frequency for the system is known.

---

* The term "modal synthesis" is used here generically to refer to any analytical process whereby the normal modes of a system of structural components are synthesized from the modes of the individual components. Other terms used are "component mode synthesis", "modal coupling", and "dynamic substructure coupling". These terms are used interchangeably throughout the report depending on the particular techniques discussed.

** Exposition of Hurty's method is presented in a later section where the meaning of these modes will become apparent.

Bamford[12] added another type of displacement modes called "attachment modes" to Hurty's procedure. These modes are "static" displacement shapes of a substructure corresponding to concentrated forces at the substructure's interfaces due to attachment to other substructures. The attachment modes may be used to complement normal modes of a restrained substructure obtained with its interfaces free.

Craig and Bampton[13] pointed out that the rigid body modes and the redundant constraint static displacement modes in Hurty's formulation need not be treated separately. They modified Hurty's method accordingly so that the generalized coordinates of the substructures would consist only of "constraint modes" and "fixed-interface normal modes". A method similar to that of Craig and Bampton was reported by Bajan and Feng[14] where an algorithm was added to the procedure in order to assist in optimizing the choice of the component modes.

An alternative modal synthesis approach based on the normal modes of separate components with their interfaces free was pursued by Hou[15]. Hou developed a method of synthesis which utilizes truncated sets of these component modes. The method is appropriately called a "free-interface component mode method". For a proper choice of component modes, he proposed an error index based on convergence of the system's frequencies. In order to improve the representation of substructures by truncated sets of free-interface modes, MacNeal[16] proposed the use of statically derived modes to account, in an approximate manner, for the missing flexibility due to truncation. This missing static contribution is called residual flexibility. MacNeal* also presented a hybrid synthesis method which allows some substructure interface coordinates to be restrained while others are free.

Benfield and Hruda[17] introduced the new idea of interface loading in which approximate mass and stiffness effects of neighboring components may be added to each component of the structure before obtaining the component's modes. The modes would then be more representative of the actual deformation shapes of the assembled structure.

---

* The methods of Hou and MacNeal are described in sufficient detail in a later section.

While in a synthesis technique a reduction in the size of a system is usually achieved through a reduction in the subsystems representation, Kuhar and Stahle[18] introduced a method in which the reduction is performed after the system equations are developed. A frequency-dependent approximation of the effect of the truncated modes is used as the basis of the reduction. System's modes with frequencies close to that employed for the approximation are thereby improved in accuracy. This approach, however, appears to be of questionable practical value since it requires knowledge of the deleted mode shapes of the components.

Goldenberg and Shapiro[19] employed a procedure similar to that due to Hou but provided for arbitrary mass loading of interface points to improve the representation of substructures by fewer free-interface modes. Their procedure may also be adopted for fixed interface mode methods such as that of Hurty. A different technique for methods was developed by Rubin[20] who extended MacNeal's method to include second-order residual effects of the truncated set of component modes. Craig and Chang[21] provided results of test problems for comparisons of the free-interface mode methods of Hou, MacNeal and Rubin.

Recently, Hintz[22] described two statically complete mode sets which he labelled "attachment modes" and "constraint modes". The former set may be used with both free-interface and fixed interface normal modes while the latter may be only combined with fixed-interface mode methods. Hintz investigated the convergence associated with several variations of these two methods and concluded that the method of attachment modes with unconstrained normal modes yielded system frequencies of comparable accuracy to Hurtz type methods. Craig and Chang[23] reformulated the free-interface mode methods of Hintz, MacNeal and Rubin, focussing on the various attachment modes involved. It was also concluded that the free-interface mode synthesis examined are of comparable accuracy, when augmented by attachment modes, to that of fixed-interface mode methods.

Although for a given number of component normal modes, the fixed interface mode method of Hurty is known to be very accurate, the method requires retaining constraint coordinates equal in number to those at the interface. This feature would be a handicap in cases involving large interface points. In order to overcome this problem, Craig and

Chang[24] described three techniques of reducing the number of the interface coordinates.

A free-interface component mode method utilizing Lagrange multipliers to enforce constraints between the structural components was presented by Dowell[25]. The method leads to an unusual form of the eigenvalue problem of the complete system. Utilizing a different formulation based on the use of Lagrange multipliers, Craig and Chang[26] attempted to describe some of the pertinent synthesis methods by a single comprehensive formulation.

Flannelly, et al.[27] developed a subsystem approach utilizing measured modal based modility matrices of the separated subsystems. The method yields the frequency response of the combined systems rather than the modal information sought by other methods. Another subsystem approach utilizing physical rather than modal coordinates was presented by Berman[28]. The coupling method in that approach involves the frequency response of the substructure. The method performs an exact reduction of the substructure to the interface coordinates. This leads to a representation of the entire system where the influence of the substructures is exactly present. Again, the analysis performed in this manner yields responses rather than natural frequencies and modes.

Recently, Berman[29] presented a general synthesis procedure capable of coupling structural components which are presented by either modal or physical coordinates. The method relies on forming transformation matrices relating the component coordinates to those of the total system. As stated by Berman, the mathematical basis of the method is closely related to that of Hurty[9], Przemieniecki[30], and others. Efforts towards developing general coupling methods of substructures which are described by physical or modal coordinates have also been reported by Herting and Hoesly[31] within the frame work of NASTRAN.

The structures in most of the references cited above are assumed to be undamped. In a few cases, proportional damping was included in the analysis[32]. Limited efforts have been directed in recent years towards incorporating more general forms of damping in appropriate synthesis techniques. Hasselman and Kaplan[33] extended the fixed-interface modal synthesis formulation of Craig and Bampton to accomodate complex modes and eigenvalues. However, as was pointed out in reference 31,

the effects of left-hand eigenvalues occurring with nonsymmetric matrices were omitted in the development of the complex mode synthesis. Glasgow and Nelson[34] observed that the formulations of Hasselman and Kaplan also did not include consideration of the components constraint modes which are used in the Hurty type approach. They proceeded to further develop the complex modal synthesis to include the component constrain modes, thus allowing the full transformation incorporated in the fixed-interface mode method. In a recent paper, Dowell[35] presented a study with the objective of demonstrating the potential for extending the component mode synthesis techniques utilizing Lagrange multipliers to the analysis of nonconservative and nonlinear systems.

Almost all of the studies cited above were primarily concerned with the use of subsystem techniques in the analytical determination of modes and frequencies of structures. Correlation with test procedures was briefly discussed in a few of these references. The synthesis techniques developed pre-suppose the knowledge of the necessary component parameters. Limited studies[27], however, explored the use of experimental test data as input to the synthesis procedure.

Klosterman[36] reported on a comprehensive study of the experimental determination of modal characteristics of substructures and their use in synthesizing those of the total structure. Based on the results of that study, Klosterman[37] presented two different methods of synthesis. One method, which resembles that of Bamford, was called "component mode synthesis". The other method, labelled "general impedance method", makes use of transfer functions of the substructures. In two subsequent publications, Klosterman, et al.[38,39] presented a synthesis procedure which is particularly suited to the analysis of two structural components where one component is represented by its experimentally determined modal parameters and the other by a finite element model.

Despite the limited efforts which have been devoted to the development of experimentally compatible synthesis techniques, complete correlation between test and analysis is far from being achieved. The presence of general damping mechanisms is obviously one of the complicating factors. Limited studies, however, have been reported on the development of experimentally based damping synthesis procedures.

Kana and Huzar[40] developed a semi-empirical energy approach for

determining the damping of a space shuttle model in terms of damping measurements performed on the separate components and described by the total dissipative energy. Due to lack of resolution in the energy approach, Kana and Huzar proposed grouping of the structural modes so as to form several energy curves for a given substructur . A readily recognized shortcoming in that scheme is the need for a judgement on the grouping of the modes. Hasselman[41] utilized the more familiar modal matrix formulation in developing a perturbation technique to describe component damping. Hasselman[42] also discussed the implications of basing the damping synthesis on fixed-interface, free-interface or mass loaded-interface component mode methods.

Recently, Jezequel[43] discussed the relationship of some of the reported modal synthesis techniques to test procedures. He then proposed a Ritz-Galerkin based method in which fixed-interface modes, complemented by mass loaded-interface component modes were used for the synthesis. The method was applied to a system of elastic plates to demonstrate synthesizing of the system's damping from substructure test data.

## IV. DESCRIPTION OF BASIC MODAL SYNTHESIS PROCEDURES

Consider the components (substructures) of a structural system which are connected to each other at the junction (interface) points as shown in Figure 1 below.

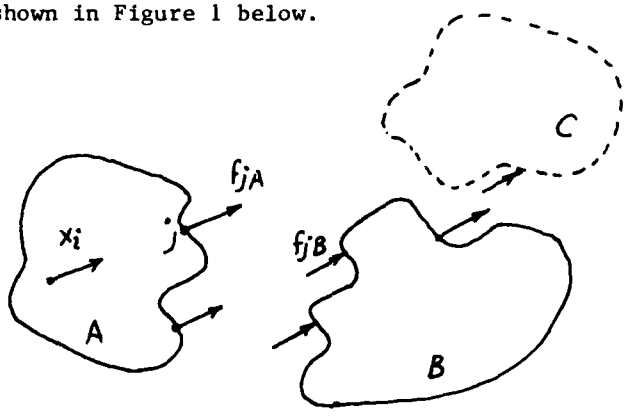



Figure 1. STRUCTURAL SYSTEM ABC.

The equations of motion for any of the substructures when executing undamped free vibration while being connected to other substructures may be written in the matrix form

$$[m]\{\ddot{x}\} + [K]\{x\} = \{f\} \tag{1}$$

or in the partitioned form, using the notation of reference 24, as

$$\begin{bmatrix} m_{ii} & m_{ij} \\ m_{ji} & m_{jj} \end{bmatrix} \begin{Bmatrix} \ddot{x}_i \\ \ddot{x}_j \end{Bmatrix} + \begin{bmatrix} K_{ii} & K_{ij} \\ K_{ji} & K_{jj} \end{bmatrix} \begin{Bmatrix} x_i \\ x_j \end{Bmatrix} = \begin{Bmatrix} 0 \\ f_j \end{Bmatrix} \tag{2}$$

where $\{x_j\}$ represents the junction physical coordinates of the interface points and $\{x_i\}$ denotes those interior to the substructure. The forces $\{f_j\}$ contains forces at junction points of the connected (coupled) substructure. In what follows, the fixed-interface component modes method of Hurty, as modified by Craig and Bampton, and the free-interface mode methods of Hou[15], MacNeal[16], and Rubin[20] are described. The exposition of the methods closely parallel those of References 19 and 24.

(a) Fixed-Interface Component Mode Synthesis

In this procedure, the displacement of any point within a structure is defined by superimposing the displacement relative to the substructure interfaces on that produced by displacing the interface connections. This may be experssed as

$$\{x_i\} = \{x_n\} + \{x_c\} \tag{3}$$

where $\{x_n\}$ is a set of displacements relative to fixed interface connections and $\{x_c\}$ is a set of displacements produced by motion of the interface connections. The displacements $\{x_n\}$ are defined in terms of the normal mode shapes of the substructure with all interface degrees of freedom fixed so that

$$\{x_n\} = [\psi_n]\{P_n\} \tag{4}$$

The column vectors of $[\psi_n]$ are the mode shapes of the free vibration of the substructures with its interfaces fixed (i.e., the solution of the equations in the upper partition of equation (2) with $\{x_j\} = 0$), and $\{P_n\}$ is a vector of generalized displacements.

The displacements $\{x_c\}$ can be obtained from the static force-displacement equations for the substructure. This is achieved by

dropping the inertia terms from equation (2) yielding

$$\begin{bmatrix} K_{ii} & K_{ij} \\ K_{ji} & K_{jj} \end{bmatrix} \begin{Bmatrix} x_c \\ x_j \end{Bmatrix} = \begin{Bmatrix} 0 \\ f_j \end{Bmatrix} \tag{5}$$

The displacements $\{x_j\}$ would produce displacements of the interior points, $\{x_c\}$, as given by the upper partition of equation (5), or

$$\{x_c\} = -[K_{ii}]^{-1}[K_{ij}]\{x_j\} = [\psi_c]\{x_j\} \tag{6}$$

where

$$[K_{ii}][\psi_c] = -[K_{ij}] \tag{7}$$

The transformation matrix $[\psi_c]$ is called the "constraint mode" matrix, where it may be noted that the procedure employed to obtain this matrix is equivalent to applying a Guyan[44] reduction to all interior coordinates. Using equations (3), (4), and (6), the motion of the substructure can be expressed, replacing $x_j$ by $p_c$ , as

$$\begin{Bmatrix} x_i \\ x_j \end{Bmatrix} = \begin{bmatrix} [\psi_c] & [\psi_c] \\ [0] & [I] \end{bmatrix} \begin{Bmatrix} p_n \\ p_c \end{Bmatrix} \tag{8}$$

or

$$\{x\} = [\Psi]\{p\} \tag{9}$$

The equations of motion (1) of the connected substructure may be transformed to the new generalized coordinates $\{p\}$ as

$$[\bar{m}]\{\ddot{p}\} + [\bar{K}]\{p\} = \{g\} \tag{10}$$

where

$$[\bar{m}] = [\Psi]^T[m][\Psi] \tag{11}$$

$$[\bar{K}] = \begin{bmatrix} \bar{K}_{ii} & 0 \\ 0 & \bar{K}_{jj} \end{bmatrix} = [\Psi]^T[K][\Psi] \tag{12}$$

and

$$\{g\} = [\Psi]^T\{f\} \tag{13}$$

The null partitions of $[\bar{K}]$ is a consequence of the relations given by equation (7).

To illustrate the procedure of modal synthesis utilized in this method, the structure is assumed to consist of only two substructures, A and B. Following the development utilized by Craig and Chang[24], the

total set of the generalized coordinates of the assembled structure is written as

$$\{q\} = \begin{Bmatrix} q_i \\ q_j \end{Bmatrix} \tag{14}$$

where $\{q_i\}$ contains all of the retained normal modes of the substructures and $\{q_j\}$ is a set of all junction coordinates. The substructure coordinates are related to those of the structure by transformation matrices $[L]$ which identify substructure coordinates with those of the structure. This relation may be written in the form

$$\{p\} = \begin{Bmatrix} p_{iA} \\ p_{jA} \\ p_{iB} \\ p_{jB} \end{Bmatrix} = \begin{bmatrix} L_{iA} & 0 & 0 \\ 0 & 0 & L_{jA} \\ 0 & L_{iB} & 0 \\ 0 & 0 & L_{jB} \end{bmatrix} \begin{Bmatrix} q_{iA} \\ q_{iB} \\ q_j \end{Bmatrix} \tag{15}$$

Utilizing equation (15), the system matrices may be formed using an appropriate assembly procedure to yield the system equations in the form

$$[\bar{M}]\{\ddot{q}\} + [\bar{K}]\{q\} = \{\bar{F}\} \tag{16}$$

or, in absence of any external forces, in the partitioned form as

$$\left[\begin{array}{cc:c} \bar{M}_{iiA} & 0 & \bar{M}_{ijA} \\ 0 & \bar{M}_{iiB} & \bar{M}_{ijB} \\ \hdashline \bar{M}_{jiA} & \bar{M}_{jiB} & \bar{M}_{jjA}+\bar{M}_{jjB} \end{array}\right] \begin{Bmatrix} \ddot{q}_{iA} \\ \ddot{q}_{iB} \\ \ddot{q}_j \end{Bmatrix} + \left[\begin{array}{cc:c} \bar{K}_{iiA} & 0 & 0 \\ 0 & \bar{K}_{iiB} & 0 \\ \hdashline 0 & 0 & \bar{K}_{jjA}+\bar{K}_{jjB} \end{array}\right] \begin{Bmatrix} q_{iA} \\ q_{iB} \\ q_j \end{Bmatrix} = 0 \tag{17}$$

The eigenvalue problem associated with the above equations of motion may then be solved for the natural frequencies and mode shapes of the assembled structure.

(b) Free-Interface Component Mode Synthesis

The free, undamped vibration of any of the uncoupled (not connected) substructures is described by equation (1), with their right hand side set to zero. The associated modal matrix may be employed to transform the equation of free vibration of the connected substructure to the form

$$[M_j]\{\ddot{p}\} + [K_j]\{p\} = [\phi]^T \begin{Bmatrix} 0 \\ f_j \end{Bmatrix} = [\phi_j]^T \{f_j\} \tag{18}$$

where $\{p\}$ are the generalized coordinates, so that $\{x\} = [\phi]\{p\}$

$$[M_n] = [\phi]^T[m][\phi] \quad ,$$

and $$[K_n] = [\phi]^T[K][\phi] = [\Omega^2 M_n] \quad ,$$

where $\Omega$ is the natural frequency of the uncoupled substructure. The matrix $[\phi_{jn}]$ is the partition of the modal matrix associated with the junction (interface) coordinates.

It should be noted that a truncated set of modes and associated frequencies are usually utilized so that equation (18) is written in terms of a reduced number of generalized coordinates and parameters.

Following the development of substructure coupling as presented by Goldenberg and Shapiro[19], the equations of motion of the two uncoupled substructures A and B are first assembled in the partitioned form

$$\begin{bmatrix} [M_{An}] & 0 \\ 0 & [M_{Bn}] \end{bmatrix} \begin{Bmatrix} \ddot{P}_A \\ \ddot{P}_B \end{Bmatrix} + \begin{bmatrix} [K_{An}] & 0 \\ 0 & [K_{Bn}] \end{bmatrix} \begin{Bmatrix} P_A \\ P_B \end{Bmatrix} = \begin{bmatrix} [\phi_{jA}]^T & \\ & [\phi_{jB}]^T \end{bmatrix} \begin{Bmatrix} f_{jA} \\ f_{jB} \end{Bmatrix} \quad (19)$$

where $$\{f_{jA}\} = -\{f_{jB}\} \quad (20)$$

To obtain the equations of motion for the coupled system, displacement compatibility at the interfaces of the two substructures has to be enforced. The compatibility conditions are

$$\{x_{jA}\} - \{x_{jB}\} = \{0\} \quad (21)$$

or, in terms of the generalized coordinates

$$\left[[\phi_{jA}] \;\vdots\; -[\phi_{jB}]\right] \begin{Bmatrix} P_A \\ P_B \end{Bmatrix} = \{0\} \quad (22)$$

or $$[\phi_{jn}]\{P\} = \{0\} \quad (23)$$

Equation (22) represents constraint conditions involving the generalized coordinates of the two substructures. To obtain a set of independent coordinates for the system, the matrices of equation (22) are arbitrarily partitioned as

$$\left[\left[\phi_j^s\right] \vdots \left[\phi_j^r\right]\right]\left\{\begin{matrix} p^s \\ \cdots \\ p^r \end{matrix}\right\} = \left\{0\right\} \tag{24}$$

where $s$ denotes a square, non-singular partition of $[\phi_j]$, and $r$ denotes the remaining partition. This implies that the total number of the retained modes of the two substructures is greater than the number of interface coordinates. Solving for $\{p^s\}$ results in the following transformation, where $\{p^r\}$ are the independent system coordinates,

$$\left\{\begin{matrix} p^s \\ \cdots \\ p^r \end{matrix}\right\} = \left[\begin{matrix} -\left[\phi_j^s\right]^{-1}\left[\phi_j^s\right] \\ \cdots\cdots\cdots\cdots \\ [I] \end{matrix}\right]\left\{p^r\right\} = [T]\{p\} \tag{25}$$

Use of the above transformation in conjunction with (19) yields the equations of motion for the assembled structure as

$$[\bar{M}_p]\{\ddot{p}\} + [\bar{K}_p]\{p\} = [T]^T\left[\begin{matrix} [\phi_{jA}]^T & 0 \\ \cdots & \cdots \\ 0 & [\phi_{jB}]^T \end{matrix}\right]\left\{\begin{matrix} f_{jA} \\ \cdots \\ f_{jB} \end{matrix}\right\} = \{0\} \tag{26}$$

where it is noted (as proved in reference 19) that the right hand side vanishes. This is a consequence of the fact that the interface forces are internal forces to the assembled structure. Equation (26) yields the natural frequencies and mode shapes $\{\bar{\phi}\}$ of the total structure in terms of the generalized coordinates of the structure. The system modal shapes expressed in terms of the physical coordinates may be readily shown to take the form

$$[\phi]_{sys.} = \left[\begin{matrix} [\phi_A] & \vdots & 0 \\ \cdots & \vdots & \cdots \\ 0 & \vdots & [\phi_B] \end{matrix}\right][T][\bar{\phi}]$$

The method proposed by MacNeal to account for the residual affects of the deleted modes in the above procedure is outlined next, using a slightly different formulation from that of Craig and Bampton[24].

The modal matrix $[\phi]$ associated with the free vibration of an <u>unconnected</u> substructure can be expressed as

$$[\phi] = \left[\begin{matrix} \phi_{iK} & \phi_{ia} \\ \phi_{jK} & \phi_{ja} \end{matrix}\right] \tag{27}$$

where "$K$" and "$a$" stand for kept and approximated, respectively. If the assembled structure is executing harmonic oscillation in one of its

natural modes with frequency $\omega$ , the forces at the interface $\{f_j\}$ will also be harmonic and of the same frequency. Using equation (18), the resulting response of a connected substructure acting within the system may be written as

$$\left[-\omega^2[M_\cdot]+[\Omega^2 M_\cdot]\right]\{\bar{P}\} = [\Phi_{j\cdot}]^T\{\bar{f}_{j\cdot}\} \tag{28}$$

where a bar over a symbol indicates the magnitude. The amplitudes of the physical coordinates can be related to those of the generalized coordinates

$$\{\bar{x}\} = \left[\Phi_K \;\vdots\; \Phi_a\right]\left\{\begin{matrix}\bar{P}_K \\ \cdots \\ \bar{P}_a\end{matrix}\right\} \tag{29}$$

For the substructure modes in which $\Omega_n \gg \omega$ , a static approximation of these modes may be achieved as follows. Eliminating the inertia terms from equation (1) results in

$$[k]\{\bar{x}\}^{(s)} = \{\bar{f}_j\} \tag{30}$$

or

$$\{\bar{x}\}^{(s)} = [G]\{\bar{f}_j\} \tag{31}$$

where $[G]$ is the flexibility matrix and the superscript $s$ denotes a static approximation to the response. The pseudo-static response may be written in a form analogous to (29) as

$$\{\bar{x}\}^{(s)} = \left[\Phi_K \;\vdots\; \Phi_a\right]\left\{\begin{matrix}\bar{P}_K \\ \cdots \\ d_a'^{(s)}\end{matrix}\right\} \tag{32}$$

Substitution of (32) into (30), premultiplying the resulting equations by $\begin{bmatrix}[\Phi_K]^T \\ [\Phi_a]^T\end{bmatrix}$ and making use of orthogonality of the modes, yields

$$\{d_a^{(s)}\} = \left[\frac{1}{\Omega_K^2 M_K}\right][\Phi_K]^T\{\bar{f}_j\} \tag{33}$$

Use of equations (31), (32), and (33) yields

$$\{\bar{x}\}^{(s)} = [\Phi_K]\{\bar{P}_K\} + [G]^{(f)}\{\bar{f}_{j\cdot}\} \tag{34}$$

where

$$[G]^{(f)} = [G] - [G_K] \tag{35}$$

and

$$[G_K] = [\Phi_K]\left[\frac{1}{\Omega_K^2 M_K}\right][\Phi_K]^T \tag{36}$$

For a coupled substructure, the following equations are used for the synthesis

$$\left[-\omega^2\left[M_K\right]+\left[\Omega_K^2 M_K\right]\right]\left\{\bar{P}_K\right\}=\left[\Phi_j\right]^T\left\{\bar{f}_j\right\} \tag{37}$$

$$\left\{\bar{x}_j\right\}^{(s)}=\left[\Phi_{jK}\right]\left\{\bar{P}_K\right\}+\left[G_{jj}^{(f)}\right]\left\{\bar{f}_j\right\} \tag{38}$$

where, as before, "$j$" stands for junction coordinates and $\left[G_{jj}^{(s)}\right]$ is the residual flexibility at junction coordinates and is formed from the appropriate columns of $\left[G\right]^{(f)}$. For coupling with another substructure, the following compatibility conditions must be enforced between the two substructures

$$\left\{\bar{x}_{jA}\right\}=\left\{\bar{x}_{jB}\right\}\quad,\quad\left\{\bar{f}_{jA}\right\}=-\left\{\bar{f}_{jB}\right\}$$

where $A$ and $B$ denote the two substructures.

Utilizing equations (37) and (38) for each of substructures $A$ and $B$ together with the compatability conditions, one obtains the eigenvalue problem for determining the modes and frequencies $\omega_n$ of the coupled structure. An illustration for using this method is included in Appendix A.

A further refinement of the method presented above was proposed by Rubin[20]. As before, if the system is vibrating in one of its normal modes with frequency $\omega$, the response of the substructure acting within the system may be obtained from (2) as

$$\left[K\right]\left\{\bar{x}\right\}=\left\{\bar{f}_j\right\}+\omega^2\left[m\right]\left\{\bar{x}\right\}$$

The refinement of Rubin was achieved by substituting for the pseudo-static response $\left\{x\right\}^{(s)}$ in the right hand side of the above equation and solving for $\left\{\bar{x}\right\}$ on the left hand side. After considerable manipulation, Rubin arrived at equations analogous to those of (38) as

$$\left\{\bar{x}\right\}^R=\left[\Phi_K\right]\left\{\bar{P}_K\right\}+\left[G^{(R)}\right]\left\{\bar{f}_j\right\}$$

where $$\left[G^{(R)}\right]=\left[G^{(f)}\right]+\omega^2\left[H\right]^{(f)}$$

where $$\left[H\right]^{(f)}=\left[G^{(f)}\right]\left[m\right]\left[G^{(f)}\right]$$

The above approximation results in higher accuracy for a given number of substructure modes but requires considerable computation, involving inversion of large numbers of matrices.

It should be noted that the above methods of MacNeal and Rubin are presented for substructures restrained against any rigid body motion. The formulation involving unrestrained substructures may be found in References 16, 20 and 24.

## V. Relationship to Test Procedures

Compatibility of a synthesis method with practical test procedures requires that the method be formulated so that test data may be used, directly or indirectly, to form or verify the synthesis. The data required for most of the synthesis techniques includes modal properties of the different components obtained with the components' interfaces, either free, fixed, or with some of the interface points free and some fixed. However, since any of these support conditions at the interfaces will not be those occuring when the component is acting within the structural system, information in addition to those of the modal characteristics are usually needed for better representation of the components. The nature of the additional information depends on the synthesis technique used and is usually the source of problems which arise when attempting to utilize the technique in conjunction with a test procedure.

In fixed-interface component synthesis methods, such as that of Hurty[9], Craig and Bampton[13] or Jezequel[43], use is made of component normal modes obtained with its interfaces clamped. Since clamping causes local deformations of the component parts near the interfaces, fewer number of the lower normal modes can be used for accurate representation of the component.

Determination of only a few of the lower modes is clearly a desirable feature in standard modal survey tests. However, clamping of the component interfaces may be difficult or cumbersome to use, particularly when substructures of large dimensions or with large numbers of interface points are involved. Also, synthesis techniques of the above type require knowledge of the so-called "constant modes." One scheme for determining these modes (suggested by the form of equation (5)) would be to apply a unit displacement at each of the interfaces, one at a time, while holding all of the others fixed and record the displacements at the

components' interior degrees of freedom. Another scheme would be to determine the stiffness matrices of analytical models of the components in conjunction with a reliable, experimentally-based system identification technique (yet to be found). The constraint modes would then be determined from equation (7).

Experimental determination of the static constraint modes is obviously another handicap of the above synthesis techniques. Nevertheless, with components of small dimensions and few interface degrees of freedom, the above problems might be tolerated.

The free-interface component techniques, such as that due to Hou, employ normal modes of the components with their interfaces free. This eliminates the experimental difficulties associated with clamping. In many applications, however, a large number of free-interface modes has to be used to adequately represent local deformation near the interfaces of the connected substructures. The number of modes employed would, of course, depend on the type of substructures.

An elementary two degrees of freedom model, whose parameters are carefully selected, is utilized in Appendix A to demonstrate the effect of component mode truncation on the calculated system frequencies using Hou's method. The model may be considered as a very crude representation for an aircraft wing with a rigid store attached to it through a relatively flexible pylon. As would be expected, the results show a large error in the calculated frequency. This is due to the fact that the free-interface lower mode of substructure A utilized in the synthesis does not contain any significant information about the local deformation near the interface. The effect of local deformation could have been accounted for if a properly selected mass was attached to the interface of the substructure when determining the first mode. This type of interface loading proposed by Goldenberg and Shapiro[19], however, poses the problems of selecting appropriate values for the masses and of attaching them to the substructures.

The residual flexibility technique proposed by MacNeal[16] to compensate for the effects of mode truncation does not require any substructure interface loading or much extra testing. However, experimental determination of the residual flexibility coefficients may pose other problems related to errors resulting from the subtraction of usually very small

numbers (see equation 35). Nevertheless, MacNeal's method and, more generally, methods utilizing attachment modes to complement free-interface component modes, appear to hold the highest promise for development of sound, experimentally-based, modal synthesis techniques. Efforts toward the development of MacNeal's method, for example, would be directed toward examination of the sensitivity of the residual flexibility coefficients. Alternatively, in cases where approximate representation of local flexibility may suffice, techniques could be developed to produce the same compensating effects of residual flexibility. This is demonstrated in Appendix A by replacing the residual flexibility at the interface of substructure A by the local flexibility. The resulting system frequency is seen to be comparable to that determined by accounting for the residual flexibility of the total substructure.

## VI. DAMPING SYNTHESIS AND PARAMETER IDENTIFICATION

The presence of damping might be significant in determining the coupled response of substructures in many structural applications. It was shown in reference (41) that allowing for representation of a general form of damping for substructures is essential for obtaining meaningful results through synthesis. This may be true even if representation by a special form of damping (such as that of proportional damping) for the substructure would suffice in describing the dynamic behavior of the uncoupled substructure. This points to the need for developing reliable experimentally-based parameter identification techniques and for extending the capability of some of the more promising synthesis methods to account for the presence of damping.

A possible approach for extending the synthesis techniques is through the use of complex modal parameters in the synthesis formulation, as is done in References 33 and 34 in conjunction with the fixed-interface component mode method of Hurty. An additional handicap of the fixed-interface methods which becomes apparent at this point is that it would be impossible to determine the damping effects associated with the static constraint modes.

To demonstrate the feasibility of complex modal formulation in conjunction with free-interface component mode methods, an extension of Hou's method is briefly outlined in what follows.

The equations of motion of a coupled substructure may be written as

$$[m]\{\ddot{x}\} + [c]\{\dot{x}\} + [k]\{x\} = \{f\} \tag{39}$$

where $[c]$ is a general, symmetric damping matrix. The above equation, written in state vector form, becomes

$$\begin{bmatrix} [I] & [0] \\ [0] & [m] \end{bmatrix} \begin{Bmatrix} \dot{x} \\ \ddot{x} \end{Bmatrix} + \begin{bmatrix} [0] & -[I] \\ [k] & [c] \end{bmatrix} \begin{Bmatrix} x \\ \dot{x} \end{Bmatrix} = \begin{Bmatrix} 0 \\ f \end{Bmatrix} \tag{40}$$

or

$$[A]\{\dot{h}\} + [B]\{h\} = \begin{Bmatrix} 0 \\ f \end{Bmatrix} \tag{41}$$

The equations of motion for two uncoupled substructures I and II may be written in the partitioned form

$$\left[\begin{array}{c|c} [A]_I & 0 \\ \hline 0 & [A]_{II} \end{array}\right] \begin{Bmatrix} \dot{h}_I \\ \dot{h}_{II} \end{Bmatrix} + \left[\begin{array}{c|c} [B]_I & 0 \\ \hline 0 & [B]_{II} \end{array}\right] \begin{Bmatrix} h_I \\ h_{II} \end{Bmatrix} = \begin{Bmatrix} 0 \\ f_I \\ \hline 0 \\ f_{II} \end{Bmatrix} \tag{42}$$

The space vectors for the two substructures may be written in terms of the right-hand complex modal matrix $[U]$ associated with the *free vibration of each of the substructures as follows*

$$\begin{Bmatrix} h_I \\ h_{II} \end{Bmatrix} = \left[\begin{array}{c|c} [U_I] & 0 \\ \hline 0 & [U_{II}] \end{array}\right] \begin{Bmatrix} \xi_I \\ \xi_{II} \end{Bmatrix} \tag{43}$$

Substitution from (43) into (42) and pre-multiplication by the matrix formed from the left-hand complex modal matrices of the two substructures, yields

$$\left[\begin{array}{c|c} [a_I] & 0 \\ \hline 0 & [a_{II}] \end{array}\right] \begin{Bmatrix} \dot{\xi}_I \\ \dot{\xi}_{II} \end{Bmatrix} + \left[\begin{array}{c|c} [-a_I\lambda_I] & 0 \\ \hline 0 & [-a_{II}\lambda_{II}] \end{array}\right] \begin{Bmatrix} \xi_I \\ \xi_{II} \end{Bmatrix} = \left[\begin{array}{c|c} [V_I] & 0 \\ \hline 0 & [V_{II}] \end{array}\right] \begin{Bmatrix} 0 \\ f_I \\ \hline 0 \\ f_{II} \end{Bmatrix} \tag{44}$$

where for each of the substructures

$$[a] = [V]^T [A] [U] \tag{45}$$

$$[-a\lambda] = [V]^T[B][U] \tag{46}$$

The compatibility conditions may be expressed as

$$\{h_I^j\} - \{h_{II}^j\} = \{0\} \tag{47}$$

which, upon using equation (43), take the form

$$\left[[U_I^j] \;\vdots\; -[U_{II}^j]\right] \left\{\begin{matrix} f_I \\ \hline f_{II} \end{matrix}\right\} = \{0\} \tag{48}$$

In an analogous fashion to the development presented earlier, with real normal modes, it can be shown that the generalized coordinates of the two substructures may be experssed in terms of those of the system such that

$$\left\{\begin{matrix} \bar{\xi} \\ \hline \hat{\xi} \end{matrix}\right\} = \left[\begin{matrix} -[\bar{U}_j]^{-1}[\hat{U}_j] \\ \hline [I] \end{matrix}\right] \{\hat{\xi}\} = [T]\{\hat{\xi}\} \tag{49}$$

where, as before, $[\bar{U}_j]$ is an arbitrary square partition of $[U_j]$. Utilizing the above transformaion in conjunction with equation (44) yields the equations of motion of the coupled system in the form

$$[\hat{A}]\{\ddot{\hat{\xi}}\} + [\hat{B}]\{\hat{\xi}\} = \{0\} \tag{50}$$

Similar procedures such as that employed above may be utilized for extension of the methods of MacNeal and Rubin. Rubin's method appears to be more of a necessity rather than a refinement when damping is considered since dissipative effects could be accounted for through the residual flexibility formulation. Research efforts directed toward assessing the merits of extended versions of the above two methods may prove beneficial.

In conjunction with studies of complex mode synthesis procedures, appropriate system identification techniques should also be sought. Several promising identification methods are being developed[45,46].

## VII. RECOMMENDATIONS

### Conclusions

The following conclusions are based on this study and on results, not reported here, obtained during the course of the study:

(1) Synthesis techniques with the best potential for achieving complete compatibility with test procedures are those utilizing an appropriate set of attachment modes.

(2) Damping should be completely represented in the analytical models of the substructures in order to arrive at meaningful results for the assembled structure.

(3) In some applications, representation of the residual flexibility at the interfaces of a substructure may be replaced by the local flexibility near the interfaces. The local flexibility may be determined by means of an appropriate system identification technique. This might lead to better synthesis accuracy than that obtained using experimentally determined residual flexibility based on the characteristics of the total substructure.

### Future research efforts

Considerable research efforts are needed toward the development of experimentally compatible synthesis techniques which would be particularly effective in applications of relevance to the Air Force.

In what follows, specific studies to be carried out towards achieving the above goal are briefly outlined.

(1) To develop experimental procedures for the determination of the additional information utilized in conjunction with free-interface component mode synthesis techniques. In particular, a study of the sensitivity of MacNeal's residual flexibility coefficients to measurement errors would be beneficial.

(2) To extend the capability of free-interface mode methods to the analysis of damped structures. This may be achieved by extending the synthesis formulations to allow the use of complex modal parameters for the substructures. Special attention would be payed to unrestrained substructures.

(3) To apply the methods developed in (2) to the analysis of structural systems of sufficient generality to demonstrate the applicability of the method to real structures.

## APPENDIX A

Consider a simple model of a system, shown in Fig. 2(a), to be assembled from the two components, A and B, shown in Fig. 2(b). The unity assigned to the mass and stiffness values are arbitrary.

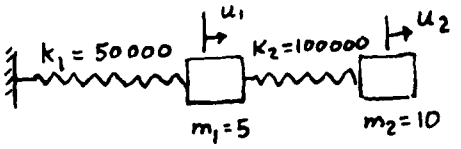



Figure 2(a). The assembled system.

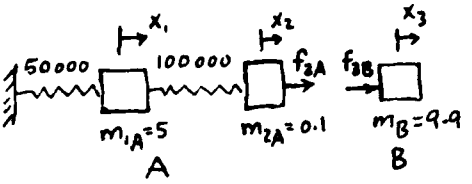



Figure 2(b). Components A and B.

Modal parameters of the system:

The two natural frequencies and mode shapes of free vibration are

$$\omega_1 = 51.8 \text{ rad/sec}, \quad \begin{Bmatrix} \phi_1 \\ \phi_2 \end{Bmatrix}^{(1)} = \begin{Bmatrix} 1 \\ 1.366 \end{Bmatrix}$$

$$\omega_2 = 193.2 \text{ rad/sec}, \quad \begin{Bmatrix} \phi_1 \\ \phi_2 \end{Bmatrix}^{(2)} = \begin{Bmatrix} 1 \\ -.368 \end{Bmatrix}$$

Modal parameters of component A

$$\Omega_1 = 99 \text{ rad/sec}, \quad \begin{Bmatrix} \phi_1 \\ \phi_2 \end{Bmatrix}^{(1)} = \begin{Bmatrix} 1 \\ 1.01 \end{Bmatrix}$$

$$\Omega_2 = 1010.1 \text{ rad/sec}, \quad \begin{Bmatrix} \phi_1 \\ \phi_2 \end{Bmatrix}^{(2)} = \begin{Bmatrix} 1 \\ -49.5 \end{Bmatrix}$$

The generalized mass and stiffness matrices of component A, based on the modal shapes given above, are

$$\left[M_A\right] = \begin{bmatrix} 5.1 & 0 \\ 0 & 250.1 \end{bmatrix}, \quad \left[K_A\right] = \begin{bmatrix} 50010 & 0 \\ 0 & 255125503 \end{bmatrix}$$

In what follows, the natural frequencies and modal shapes of the structure are obtained using two of the free-interface synthesis techniques described in this report.

Synthesis using Hou's method

Utilizing a single mode to represent component A, the equations of the assembled system may be written as (see equation 19)

$$\left[\begin{array}{c|c} 5.1 & 0 \\ \hline 0 & 9.9 \end{array}\right] \begin{Bmatrix} \ddot{P}_{1A} \\ \hline \ddot{x}_3 \end{Bmatrix} + \left[\begin{array}{c|c} 50010 & 0 \\ \hline 0 & 0 \end{array}\right] \begin{Bmatrix} P_{1A} \\ \hline x_3 \end{Bmatrix} = \begin{Bmatrix} 1.01\, f_{2A} \\ \hline f_{3B} \end{Bmatrix} \tag{A1}$$

in which $f_{2A} = -f_{3B}$ and where

$$\begin{Bmatrix} x_1 \\ x_2 \\ x_3 \end{Bmatrix} = \left[\begin{array}{c:c} 1.0 & 0 \\ 1.01 & 0 \\ \hdashline 0 & 1 \end{array}\right] \begin{Bmatrix} P_{1A} \\ \cdots \\ X_3 \end{Bmatrix} \tag{A2}$$

The compatibility condition is $X_2 - X_3 = 0$, which yields the following upon using (A2)

$$\left[\begin{array}{c:c} 1.01 & -1 \end{array}\right] \begin{Bmatrix} P_{1A} \\ \cdots \\ X_3 \end{Bmatrix} = 0$$

leading to the transformation

$$\begin{Bmatrix} P_{1A} \\ X_3 \end{Bmatrix} = \begin{Bmatrix} 1 \\ 1.01 \end{Bmatrix} P_{1A} \tag{A3}$$

Substitution from (A3) into (A1), premultiplying by (1 1.01), gives

$$15.2\ \ddot{P}_{1A} + 50010\ P_{1A} = 0$$

This yields for the lowest natural frequency of the system

$$\omega_1 = 57.4 \text{ rad/sec}, \tag{A4}$$

where the associated mode shape of the system is obviously fixed by the ration $P_{1A}$: $X_2 = X_1 : X_2 = 1 : 1.01$.

Synthesis Using MacNeal's Method

Utilizing only the first normal mode, the motion of component A may be written, using equation (28), as

$$\left(-\omega^2\ 5.1 + 50\ 010\right)\ P_{1A} = 1.01\ \bar{f}_{2A} \tag{A5}$$

The residual flexibility matrix of the component is calculated from equations (35), using (36), to give

$$[G]_A^{(f)} = \begin{bmatrix} 150{,}000 & -100{,}000 \\ -100{,}000 & 100{,}000 \end{bmatrix}^{-1} - \begin{Bmatrix} 1 \\ 1.01 \end{Bmatrix} \left[\frac{1}{50010}\right] \begin{pmatrix} 1 & 1.01 \end{pmatrix}$$

$$= \begin{bmatrix} 0.00002 & 0.00002 \\ 0.00002 & 0.00003 \end{bmatrix} - \begin{bmatrix} 0.00002 & 0.0000202 \\ 0.0000202 & 0.00002039 \end{bmatrix}$$

or $$[G]_A^{(f)} = \begin{bmatrix} 0 & -2 \times 10^{-7} \\ -2 \times 10^{-7} & 0.961 \times 10^{-5} \end{bmatrix} \tag{A6}$$

so that at the interface,

$$0.961 \times 10^{-5} \tag{A7}$$

Utilizing equation (37), the approximated displacement amplitude at the interface is then given by

$$\bar{x}_2 = 1.01\ \bar{P}_{1A} + 0.961 \times 10^{-5}\ \bar{f}_{2A} \tag{A8}$$

The response amplitude of component B is

$$-9.9\omega^2\ \bar{x}_3 = -\bar{f}_{3B} \tag{A9}$$

The compatibility conditions take the form

$$\bar{f}_{2A} = -\bar{f}_{3B} \text{ and } \bar{x}_2 = \bar{x}_3 \tag{A10}$$

Use of equations (A5), (A8), (A9) and (A10) yields the eigenvalue problem of the system as

$$\begin{bmatrix} 30625 & -20619 \\ -10626 & 10522 \end{bmatrix} \begin{Bmatrix} \bar{P}_{1A} \\ \bar{x}_2 \end{Bmatrix} = \begin{bmatrix} \omega^2 & 0 \\ 0 & \omega^2 \end{bmatrix} \begin{Bmatrix} \bar{P}_{1A} \\ \bar{x}_2 \end{Bmatrix} \tag{A11}$$

Solution of equation (A11) results in the two system frequencies

$$\omega_1 = 51.8 \text{ rad/sec} \quad \text{and} \quad \omega_2 = 196.1 \text{ rad/sec}$$

where it may be observed that the magnitude of the first natural frequency is that of the exact value. Using equation (A11) above, the mode shapes are calculated to be (recalling that $\bar{P}_{1A} = \bar{x}_1$ ),

$\begin{Bmatrix} 1 \\ 1.355 \end{Bmatrix}$ and $\begin{Bmatrix} 1 \\ -0.38 \end{Bmatrix}$ , which are also very close to the exact values.

It should be noted that the above formulation would obviously yield the same results as those obtained using Hou's method if the residual term was not included in equation (A8).

If the residual flexibility term in equation (A8) is replace by the local flexibility at the interface, or

$$G^{(f)}_{22A} = 10^{-5}$$

the procedure outlined above will yield the following values for the natural frequencies of the system; $\omega_1 = 51.6$ rad/sec and $\omega_2 = 193$ and corresponding mode shapes of $\begin{Bmatrix} 1 \\ 1.37 \end{Bmatrix}$ and $\begin{Bmatrix} 1 \\ -0.377 \end{Bmatrix}$ .

## REFERENCES


1. V.H. Neubert and J.P. Raney, ed., "Synthsis of Vibrating Systems," ASME Winter Annual Meeting, Washington, D.C., 1971.

2. R.H. MacNeal, ed., Special Modeling Techniques, NASTRAN Theoretical Manual, NASA SP-221(1), Ch. 14, 1972.

3. R.W. Clough and E.L. Wilson,"Dynamic Analysis of Large Structural Systems with Local Nonlinearities," Comp. Meth. Appl. Mech. & Engr., 17/18, pp. 107-129, 1979.

4. R.H. MacNeal, R. Citerley and M. Chargin, "A Symmetric Model Formulation of Fluid - Structure Interaction, Including a Static Approximation to Higher Order Fluid Modes," Paper No. 80-C2/PVP- 116, ASME Century 2 Pressure Vessels & Piping Conf., San Francisco, CA, 1980.

5. R.H. MacNeal, "Vibrations of Composite Systems," Office of Scientific Research, Report OSR TN-55-120, 1954.

6. W.C.Hurty , J.D. Collins, and G.C. Hart, "Dynamic Analysis of Large Structures by Modal Synthesis Techniques, Computers and Stru., Vol.1, No 4, pp. 535-563, 1971.

7. R.R. Craig, Jr., "Methods of Component Mode Synthesis," Shock Vib. Digest, U.S. Naval Research Lab., Vol. 9 , No.11, pp.3-10, 1977.

8. W.C. Hurty, "Vibrations of Structural Systems by Component Mode Synthesis, "Proc. ASCE, Vol. 85, No. EM4, pp. 51-69, 1960.

9. W.C. Hurty, Dynamic Analysis of Structural Systems Using Component Modes," AIAA J., Vol.3, No.4, pp. 678-685, 1965.

10. W.C. Hurty, "A Criterion for Selecting Realistic Natural Modes of a Structure," Tech. Memo. 33-364, Jet Propulsion Lab., Pasadena, CA, 1967.

11. W.C. Hurty, "Truncation Errors in Natural Frequencies as Computed by the Method of Component Mode Synthesis," Proc. First Conf. Matrix Meth. in Stru. Mech., WPAFB, OH, AFFDL-TR-66-80, pp. 803-821, 1966.

12. R.M. Bamford, "A Modal Combination Program for Dynamic Analysis of Structures," Tech. Memo. 33-290, Jet Propulsion Lab., Padasena, CA 1967.

13. R.R. Craig, Jr., and M.C. Bampton, "Coupling of Substructures for Dynamic Analyses, AIAA J., Vol. 6, No.7, pp. 1313-1319, 1968.

14. R.L. Bajan and C.C. Feng, "Free Vibration Analysis by the Modal Substitution Method," Paper No. 68-8-1, American Astro Soc. Symposium on Space Projections from the Rocky Mountain Region, Denver, CO, 1968.

15. S. Hou, "Review of Modal Synthesis Techniques and a New Approach," Shock Vib. Bull., U.S. Naval Res. Lab., Vol.40, part 4, pp. 25-39, 1969.

16. R.H. MacNeal, "A Hybrid Method of Component Mode Synthesis," J. Comp. & Struc., Vol.1 , No. 4, pp. 581-601, 1971.

17. W.A. Benfield and R.F. Hruda, "Vibration Analysis of Structures by Component Mode Substitution," AIAA J., Vol. 9, No.7, 1971.

18. E.J. Kuhar and C.V. Stahle, "A Dynamic Transformation Method for Modal Synthesis," AIAA J., Vol. 12, No.5, pp. 672-678, 1974.

19. S. Goldenberg and M. Shapiro, "A Study of Modal Coupling Procedures," Grumman Aerospace Corp., NASA CR-112252, 1972.

20. S. Rubin, "An Improved Component-Mode Representation," AIAA J., Vol.13, No. 8, pp. 995-1006, 1975.

21. R.R. Craig, Jr. and C-J Chang, "Free-Interface Methods of Substructure Coupling for Dynamic Analysis," AIAA J., Vol.14, No. 11, pp. 1633-1635, 1976.

22. R.M. Hintz, "Analytical Methods in Component Modal Synthesis," AIAA J., Vol.13, No. 8, pp. 1007-1016, 1975.

23. R.R. Craig, Jr. and C-J. Chang, "On the Use of Attachment Modes in Substructure Coupling for Dynamic Analysis," Paper 77-405, AIAA/ASME 18th Struc., Struc Dyn., and Materials Conf., San Diego, pp.89-99, 1977.

24. R.R. Craig, Jr. and C-J. Chang, "Substructure Coupling for Dynamic Analysis and Testing," NASA CR-2781, 1977.

25. E.H. Dowell, "Free Vibrations of an Arbitrary Structure in Terms of Component Modes," J. Appl. Mech., Trans. ASME, Vol.39, No.3, pp. 727-732, 1972.

26. R.R. Craig, Jr., and C-J. Chang, "A Review of Substructure Coupling Methods for Dynamic Analysis," NASA, Conf. Publ. CP-2001, Vol.2, pp.393-408, 1976.

27. W.G. Flannelly, A. Berman, and N. Giansante, "Research on Structural Dynamic Testing by Impedance Methods, Kaman Aerospace Corporation; USAAMRDL Tecnical Report 72-63, U.S. Army Mobility Research and Develop. Lab., Virginia, 1972.

28. A. Berman, "Vibration Analysis of Structural Systems Using Virtual Substructures," Shock Vib. Bull., U.S. Naval Res. Lab., Proc., Vol. 43, part 2, pp. 13-22, 1973.

29. A. Berman, "A Generalized Coupling Technique for the Dynamic Analysis of Structural Systems," AIAA/ASME/ASCE/AHS 20th Struc., and Materials Conf., St. Louis, MO, 1979.

30. J.S. Przemieniecki and L. Berke, "Digital Computer Program for the Analysis of Aerospace Structures by the Matrix Displacement Method," AFDL Report No.FDLTDR 64-18, 1965.

31. D.N. Herting and R.L. Hoesly, "Development of an Automated Multi-Stage Modal Synthesis System for NASTRAN," NASA, Conf. Publ., CP-2018, pp. 435-448, 1977.

32. L.R. Klein and E.H. Dowell, "Analysis of Modal Damping by Component Modes Method Using Lagrange Multipliers," J. Appl. Mech., Trans. ASME, Vol. 41, No. 2, pp. 527-528, 1974.

33. T.K. Hasselman and A. Kaplan, "Dynamic Analysis of Large Systems by Complex Mode Synthesis," J. Dyn. Sys., Measur., and Control, pp. 327-333, 1974.

34. D.A. Glasgow and H.D. Nelson, "Stability Analysis of Rotor-Bearing Systems Using Component Mode Synthesis," Paper No. 79-DET-63, ASME Design Engg. Tech. Conf., St. Louis, MO , 1979.

35. E.H. Dowell, "Component Mode Analysis of Nonlinear and Non-Conservative Systems," J. Appl. Mech., Trans. ASME, Vol. 47, pp. 172-176, March 1980.

36. A.L. Klosterman, "On the Experimental Determination and Use of Modal Representations of Dynamic Characteristics," Ph.D. Dissertation, University of Cincinnati, 1971.

37. A.L. Klosterman, "A Combined Experimental and Analytical Procedure for Improving Automotive System Dynamics," Paper No. 720093, Soc. Auto. Engrs., Auto. Engg Cong., Detroit, MI, 1972.

38. A.L. Klosterman and W. A. McClelland, "Combining Experimental and Analytical Techniques for Dynamic System Analysis," presented at the 1973 Tokyo Seminar on Finite Element Analysis, 1973.

39. A.L. Klosterman, W.A. McClelland and J.E. Sherlock, "Dynamic Simulation of Complex Systems Utilizing Experimental and Analytical Techniques," Paper No. 75-WA/Aero-9, ASME Winter Annual Meeting, Houston, TX , 1975

40. D.D. Kana and S. Huzar, "Synthesis of Shuttle Vehicle Damping Using Substructure Test Results," J. Spacecraft and Rockets, Vol. 10, No. 12, pp. 790-797, 1973.

41. T.K. Hasselman, "Study of Modal Coupling Procedures for the Shuttle: A Matrix Method for Damping Synthesis," NASA CR-112253, 1972.

42. T.K. Hasselman, "Damping Synthesis from Substructure Tests," AIAA J., Vol. 14, No. 10, pp. 1409-1418, 1976.

43. L. Jesequel, "A Method of Damping Synthesis from Substructure Tests," J. Mechanical Design, Trans. ASME, Vol. 102, pp. 286-294, April 1980.

44. R.J. Guyan, "Reduction of Stiffness and Mass Matrices," AIAA J., Vol. 3, No. 2, p. 380, 1965.

45. C. L. Keller, "Methods for Determining Modal Parameters and Mass, Stiffness and Damping Matrices," Tech. Report AFFDL-TR-78-59, 1978.

46. M. Link and A. Vollan, "Identification of Structural System Parameters from Dynamic Response Data," Z. Flugwiss., Weltraum 2, pp. 165-174, 1978.

1980 USAF - SCEEE SUMMER FACULTY RESEARCH PROGRAM

Sponsored by the

AIR FORCE OFFICE OF SCIENTIFIC RESEARCH

Conducted by the

SOUTHEASTERN CENTER FOR ELECTRICAL ENGINEERING EDUCATION

FINAL REPORT

# AN APPLICATION OF GERT (GRAPHICAL EVALUATION AND REVIEW TECHNIQUE) TO AIR FORCE SYSTEMS DEVELOPMENT PLANNING


| | |
|---|---|
| Prepared by: | Dr. John C. Papageorgiou |
| *Academic Rank:* | *Professor and Chairman* |
| Department and | Department of Management Sciences, |
| University: | University of Massachusetts at Boston |
| Research Location: | Air Force Systems Command, Electronics Systems Division, Deputy for Development Plans |
| USAF Research Colleague: | Dr. Donald B. Brick |
| Date: | September 10, 1980 |
| Contract No.: | F49620 - 79 - C - 0038 |

# AN APPLICATION OF GERT(GRAPHICAL EVALUATION AND REVIEW TECHNIQUE) TO AIR FORCE SYSTEMS DEVELOPMENT PLANNING

by

Dr. John C. Papageorgiou

## ABSTRACT

Gantt charting is currently being used for planning the development of the different Air Force systems in association with established deadlines for reaching certain milestones. Given the complexity of the projects and the inherent uncertainty regarding their outcome, the GERT network modeling technique was tried as an alternative for their systematic planning and control. GERT is an improvement over PERT in allowing looping and probabilistic branching among its other features.

The Assault Breaker program was chosen as a case study and it was broken down into approximately five hundred activities. Taking into account the precedence relationship of the activities, the GERT network was constructed. Then, the parameters of the activity time distributions were estimated together with the activity realization probabilities and the network was simulated using a prewritten simulation software package.

The results of the simulation such as probabilities and time probability distributions for the realization of different events in the network or different paths of it and other kinds of statistics are considered valuable for planning and control. The benefits also derived from drawing the network were significant as people had to think and agree on a particular structure of the project and the interfacing of its component parts. Similar cost information could also be derived but it was not considered important for this case study.

## ACKNOWLEDGEMENTS

I would like to thank the Air Force Systems Command, the Air Force Office of Scientific Research, and the Southeastern Center for Electrical Engineering Education for providing me with the opportunity to carry out this research project. I am at least as thankful to the Deputy for Development Plans, Electronics Systems Division, for their hospitality and help in actually carrying out my research. In particular I would like to mention Dr. Donald B. Brick, Scientific Director, Col. Ernest L. Hatchell, Jr., Head of the Deputy, Col. Anthony Napoli, Director of Tactical Planning, and Lt. Col. Charles T. Jaglinski, Assault Breaker Program Director, without whose cooperation I wouldn't have been able to accomplish my goal. I would like also to thank in particular Mr. Albert E. Ward of MITRE Corporation who collaborated with me and provided me with all the information to carry out my research project. I would like to acknowledge the collaboration of Col. William M. Smith, Jr., Lt. Col. John M. Jasinski, Mr. Otto A. Wech, Major John A. Harvey, Mr. Charles W. Hunter, and Mr. Joseph R. Russo. Finally a word of appreciation also for Col. William F. H. Page, Col. Lloyd L. Moir, Jr., and Lt. Col William H. Niles for their briefings and my secretary at the University of Massachusetts at Boston, Toni Shatzman, for typing this report.

## I. INTRODUCTION

The Electronics Systems Division, Air Force Systems Command, has as a mission to plan, acquire, manage and conduct technological development (research, exploratory, advanced and engineering) for command, control, communications and intelligence systems ($C^3I$). It is divided into a number of deputies, one of which is the Deputy for Development Plans, coded as ESD/XR. This deputy is responsible for development planning and more specifically mission area analysis, $C^3I$ architecture, interoperability planning, investment strategy, technology guidance, and system acquisition planning. It is subdivided into four directorates: Technological and Functional Area Planning; Strategic Planning; Tactical Planning; and Communications Planning.

Planning is carried out through the recently introduced VANGUARD planning system. Its objective is to analyze available capabilities; compare them with what is required; synthesize programs to make up the difference; and provide a means for integrating these programs into a cohesive and meaningful whole which is tied to the real world of equipment and operations.

To this end, seven master mission areas have been identified: Strategic offense; strategic defense; air-to-surface; counterair; reconnaisance; command, control, communications ($C^3$); and mobility. These mission areas are analyzed along with a consideration of functional areas and major force elements to achieve integration in the planning process. As a result, about forty plans have been identified. Most of them are mission area plans and the rest are functional or force element plans. An office of primary responsibility has been assigned to each of these plans.

From a consideration of national goals and security objectives, military missions are identified within a plan and they are further broken down into functions and tasks. Comparisons are then made with current forces, they are assessed against current and future needs, deficiencies are identified, and prioritized goals are established. As a result, alternatives are proposed for correcting the identified deficiencies.

The system acquisition process, which aims at the satisfaction of identified mission needs, is divided into four major phases demarcated by respective major decision points called milestones. They are as follows:
Milestone I - Demonstration and Validation. A mission need, as documented in

the Mission Element Need Statement (MENS), is determined to be essential, it is reconciled with other Department of Defense capabilities, and it is approved by the Secretary of Defense. Following this approval, technological solutions are proposed and developed; technological, military and economic bases for acquisition are established; a program manager is designated; and competing contractor efforts are started and brought to the point when approval is required for a hardware and software demonstration and validation of both technological and economic considerations of one or more proposed system concepts.

Milestone I - Demonstration and Validation. The recommendations developed in the previous phase and documented in the so called Decision Coordination Paper (DCP) are reviewed by the Defense System Acquistion Review Council (DSARC), and the Secretary of Defense approves one or more selected alternatives for competitive demonstration and validation. Following this approval, the approved concepts are developed into hardware and software for testing; field demonstrations take place; and studies are carried out towards improving and advancing the system performance definition and cost/schedule data.

Milestone II - Full-Scale Engineering Development. The recommendations for full scale engineering development, based on the outcome of the demonstration and validation phase and documented in an updated Decision Coordination Paper, are reviewed by the Defense System Acquisition Review Council. The Secretary of Defense will then approve the full-scale engineering development of one of the alternative systems. This approval will include procurement of long lead production items and also limited production for operational test and evaluation.

It should be noted that the task of the Deputy for Development Plans, Electronics Systems Division, ends at this point with the recommendation for production and deployment of the system, incorporated in an updated Decision Coordination Paper.

Milestone III - Production and Deployment. The recommendation for production at a certain rate and deployment to the using agency, based on the outcome of the operational test and evaluation and documented in an updated Decision Coordination Paper, is reviewed by the Defense System Acquisition Review Council and approved by the Secretary of Defense.

## II. OBJECTIVES

The Deputy for Development Plans is currently involved with the develop-

ment planning of a number of programs ranging from programs that they are just being conceived to such that are going through their full scale engineering development (FSED) stage. Each of these programs consists of hundreds of activities that have to be completed with a certain precedence relationship among them. Because of the nature of the planned systems there is some uncertainty associated with the different activities regarding their realization and their outcome if they are performed. A number of reasons contribute to frequent revisions of the conceptual and mechanical configuration of the planned systems which cause revisions of the number and type of activities that have to be performed as well as their precedence relationship. As a result, the planning process becomes very complex. At the same time, however, good planning is absolutely necessary, given the fact that technology advances exponentially, the world scenario changes very fast, and that a delay in the production of a system may render it outdated by the time it reaches the user.

A systematic and scientific planning approach is therefore necessary to help the managers of these programs with their planning task. Operations research has made significant contributions during the last three decades in helping managers in industry, business, government and the military with their planning problems. It was, therefore, the objective of this project to introduce operations research and more specifically the network planning approach called Graphical Evaluation and Review Technique (GERT) into the planning process of Air Force Systems. The limited time available did not allow for the actual and realistic planning of any of these systems. It was possible however to show through a case study the usefulness of the approach, the way it can be applied and implemented, and to create an interest on behalf of the staff involved to look into approaches different than the ones already used.

## III. THE GERT APPROACH

Application of network analysis to the planning and control of large projects started in the late 1950's with the development of PERT and CPM. Today these methods are being applied in all kinds of organizations throughout the world and they are among the most well known and commonly used operations research approaches. They have found applications particularly in the planning and control of construction and research and development projects; A very brief review of PERT follows:

A project is broken down into detailed tasks and their precedence relation-

ship is determined. They are then represented by a network consisting of nodes, standing for the events, and directed branches, standing for the activities.

The events represent significant accomplishments at recognizable points in time and they can be thought of as significant "milestones" in a project. They signal the start and completion of one or more activities. An activity represents the actual performance of a task and consumes time and resources. Activity times are of primary interest and they are usually represented by the Beta distribution with estimates for the most likely, optimistic and pessimistic times. On the basis of this information earliest expected times, latest allowable expected times and slack times can be computed for each activity and event. Thus schedules are made and probabilities of meeting these schedules are computed. Finally a detailed scheduling of the activities takes place with specific start and completion times, taking into account the limited resources available and the duration and criticality of the specific activities.

Although PERT has been applied extensively, it has a number of limitations that render it inflexible in modeling complex projects such as research and development and other complex planning projects. Its basic limitations are [1]:

1. Every activity must be completed in order for the network to be realized.
2. Every activity leading to a node must be completed in order for the node to be realized.
3. Each node can be realized once only; looping is not allowed.
4. The activity times can be represented by a constant or the Beta distribution only.
5. There is only sink node (terminal event) representing completion of the project.
6. The critical path is the longest path on the basis of expected activity times which may not materialize.

Because of these limitations, more flexible networking approaches have been developed and GERT is one of them. It possesses none of the above limitations of PERT and it has found numerous applications particularly in the planning of research and development projects (see Bibliography). It is characterized by the following improvements over PERT [2].

1. An activity has associated with it a probability that it will be selected, ranging from zero to one. The nodes are, therefore, constructed differently to denote their nature as deterministic or probabilistic; Figure 1 gives examples of the output side of a node in which Node 12 is deterministic and all activities emanating from it start when the node is released;

Node 20 is probabilistic and one only of the activities emanating from it will be selected according to the given probabilities.




Figure 1. Examples of Deterministic and Probabilistic Output Sides of Nodes.

2. The realization of a node may be specified to occur upon the realization of one or more of the activities leading to it, it may be realized one or more times, and the first time it is realized the number of activities to be completed may be different from subsequent repeats. Examples of possible input sides of a node are given in Figure 2. Figure 3 gives examples of both sides of a node.

| Input Side of Node | MEANING |
|---|---|
|   | Three incident activity completions are needed to release the node the first time and two such completions any subsequent time. Multiple completions of the same activity count as separate completions. |
|   | Like in the previous case but the completions must be of <u>different</u> activities. Multiple completions of the same activity count as one. |
|   | Like in the first case, but all the other on-going incident activities will be halted when the node is released. |
|   | Like in the second case, but all the other incident activities will be halted when the node is released. |

Figure 2. Examples of the Input Side of Nodes.

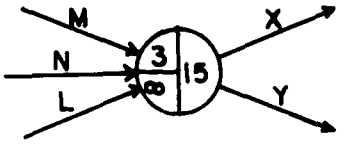
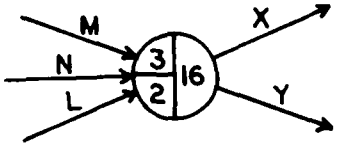
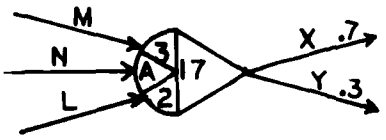
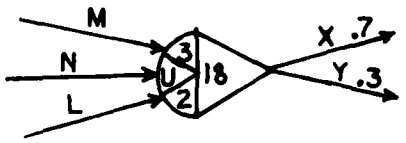
| NODE | MEANING |
|---|---|
|  | Node 15 is deterministic and it will be released the first time when any three completions occur (MNL, MMN, NMM, MNN, etc.). It cannot be released a second time. When released, both activities X and Y can start. |
|  | Like node 15 above, but subsequent releases are allowed when any two completions occur (MN, ML, MN, MM, NN, or LL). |
|  | Node 17 is probabilistic. It will be released the first time only when all three activities M, N, and L are completed. Subsequent releases will occur when any two of the three activities are completed (MN, ML, NL). When released, then either X can start with a probability of 0.70 or Y with probability of 0.30. |
|  | Like Node 17 above, but in subsequent completions the third activity is halted when the node is realized upon the completion of the two activities. |

Figure 3. Examples of Nodes

3. Looping is allowed as shown in Figure 4. It shows that there is

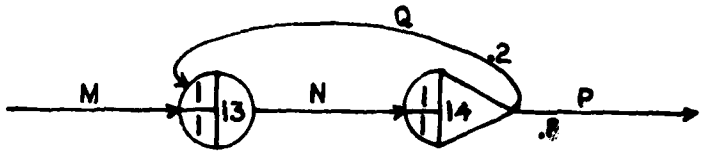



Figure 4. Looping Example

a 0.20 chance that activity Q will be chosen upon realization of Node 14 which is incident to Node 13 and will cause activity N to be repeated. More complex forms of looping are also allowed.

4. The network can have more than one source node.
5. The network can have more than one sink node (eg. success, failure, postponement, etc. of a project).
6. Modifications of the network can be incorporated which take place upon the completion of a certain activity for each one of them. Figure 5 shows such a modification. It shows that as soon

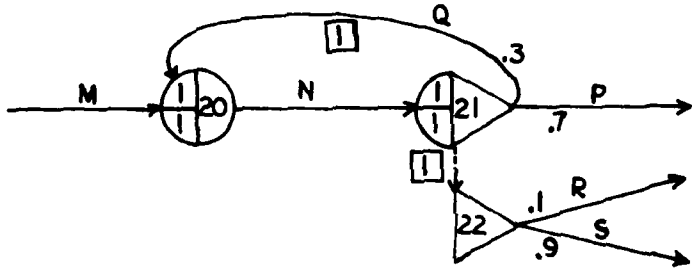



Figure 5. Example of Network Modification

as activity 1 is completed (indicated next to the dotted arrow), the output side of Node 21 is replaced by the output side of Node 22.

7. The following types of probability distributions can be used to represent activity times:
   a) Constant; b) Normal; c) Uniform; d) Erlang; e) Lognormal; f) Poisson; g) Beta; h) Gamma; i) Beta fitted to three parameters (as in PERT).

8. Cost can be assigned to each activity in terms of a fixed component and a variable per unit of time component.
9. Statistics can be collected for designated nodes and the sink nodes on time, cost, and activity counts for specified activities. For each of these nodes information is provided regarding the mean, standard deviation, minimum, maximum, number of observations, probability of realization, and time and cost frequency distributions accompanied by their respective histograms. The above statistics are generated through simulation of the network using a prewritten software package called GERT IIIZ* and they can be collected on the following alternatives:

| Statistics Code for Specific Node | Description |
|---|---|
| F | Time and cost statistics on first release of the node |
| A | Time and cost statistics on all releases of the node |
| B | Time and cost statistics on between releases of the node |
| I | Time and cost statistics on the interval between a previous node designated as "mark node" (M) and the node in question (I). |
| D | Time and cost statistics on the delay from the first incident activity completion for a node to the release of the node. |

*The program has been developed by Pritsker and Associates, Inc., P.O. Box 2413, West Lafayette, Indiana 47906. It is written in FORTRAN IV and can be operated using any FORTRAN compiler.

## IV. SELECTION OF THE PROGRAM FOR APPLYING GERT

As it was mentioned above, the Deputy for Development Plans is engaged in a number of programs of which some are more complicated than others. As they usually last ten, fifteen, or even more years, they are characterized by considerable uncertainty regarding the possible turns of events, the time and cost for reaching the different milestones, and the establishment of schedules. It was judged that GERT would prove useful in helping the program directors with their planning tasks.

Any of the programs would be a good candidate for applying GERT. For the application to be successful, however, it was considered critical that the program director had some understanding of the approach and that he was willing to try it and devote the necessary time and resources. The approach was therefore explained to the staff through both a written document and a number of oral presentations. As a result, two program directors expressed their interest in trying it. One of them, however, was not able to devote the necessary time due to other on-going activities and commitments. It therefore left one candidate for further analysis, namely the Assault Breaker program.

## V. THE ASSAULT BREAKER PROGRAM

The Assault Breaker program [3] is a joint project between the Air Force and the Army and aims at the fulfillment of the goal of developing systems that could detect, locate, and strike enemy armor at ranges well beyond the forward edge of the battle area. Its concept includes a surveillance-strike system consisting of an airborne radar to sense second echelon armor and then guide an aircraft and/or air-to-surface missiles against that armor.

The objective of the Assault Breaker program is to plan Air Force participation in a series of field technology demonstrations and to accomplish the development planning necessary to support a milestone II decision, i.e. potential follow-on Full Scale Engineering Development of the Ground Target Attack Control System.

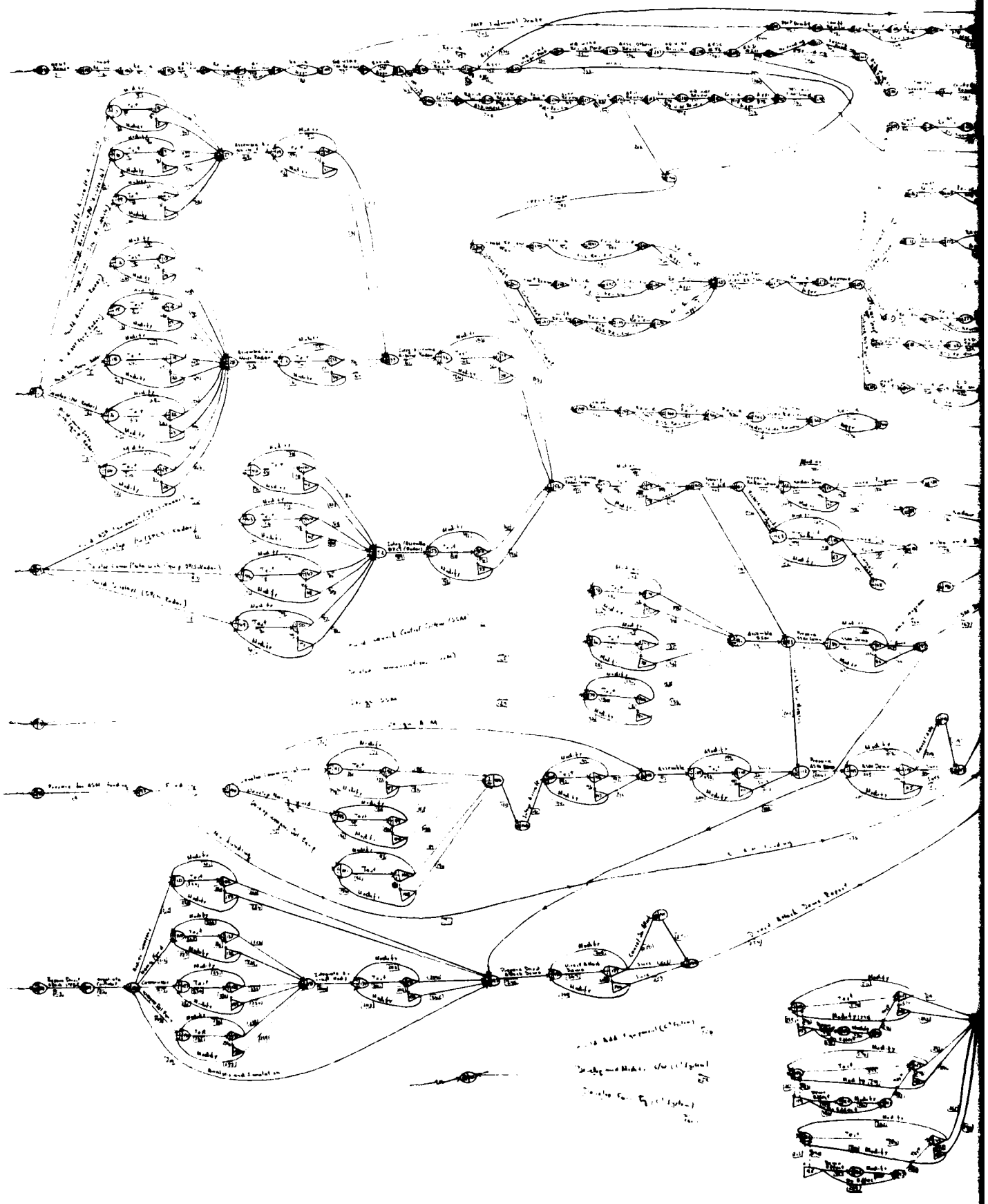
The Air Force has developed an airborne moving target indicator and synthetic aperature radar (Pave Mover) capable of locating armor and guiding munitions against the target. This is a segment of the Ground Target Attack Control System which aims at an integrated force management capability to manage and direct friendly forces against second echelon enemy forces. The

other segments include the ground target attack control element that aims at real time operational control, weapon and target pairing, and aircraft and weapon guidance, the integration and interface segment that aims at incorporating this control center with existing and planned control and communications elements; and the aircraft/weapons interface segment that aims at developing the hardware that interface between the radar platform/aircraft and the weapons and direct attack aircraft. The Air Force has also developed air-to-surface munitions while the Army has developed a surface-to-surface missile which is interoperable with the Pave Mover radar.

Complexity has been added to the Assault Breaker program by the fact that it is an accelerated program and the different segments have not followed the normal route of planning and development. For example, the radar and the control and communications segments will meet their first official milestone at milestone II without having gone through the approval decisions at milestones 0 and I. Another complexity was mentioned above regarding the inter-agency character of the program that requires integration, coordination and monitoring of the different aspects of the program and all the activities of the participating agencies.

## VI. THE GERT NETWORK FOR THE ASSAULT BREAKER PROGRAM

As in any other case of network modeling, one of the major benefits derived from the application of GERT is the fact that the people involved are forced to organize their perceptions of the structure of the project and the interfacing of the activities in a systematic way. This was particularly true in the case of the Assault Breaker project. Although at the beginning the detailed structure of the project was nebulous in the minds of the people involved, they were forced through the networking process to think about it, clarify their perceptions, cross-verify them, and arrive at some kind of a consensus. As a result, the original draft of the network went through a number of revisions with each one of them approaching closer the modeled reality. The final draft of the network is presented in Figure 6 and it gives a good approximation of reality. It is not possible here to discuss in detail the network but an explanation of some of its features will help in better understanding it.



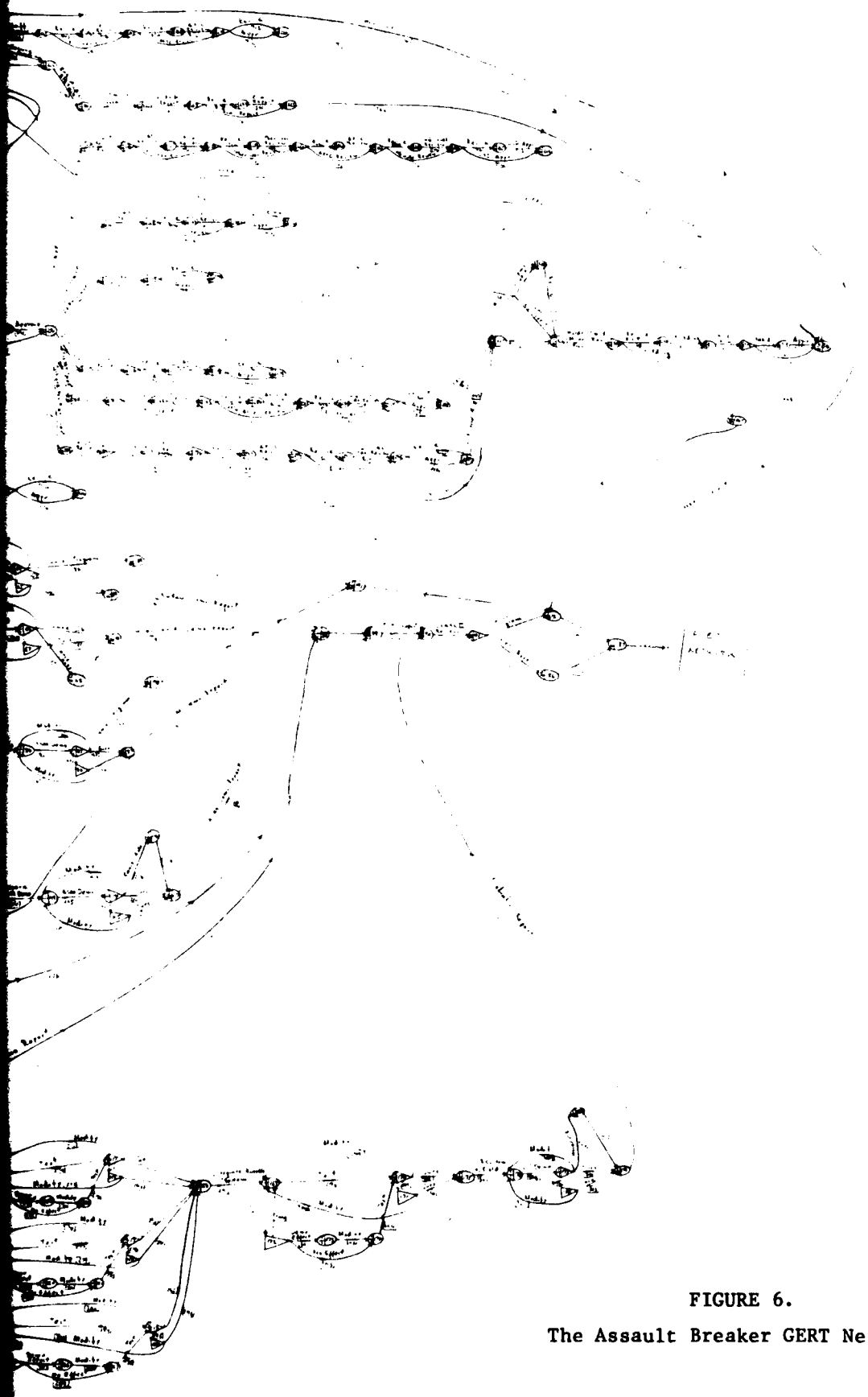


FIGURE 6.

The Assault Breaker GERT Network

A common feature of the network is the network modification used to indicate that after a test and subsequent modification of a component, the chance of further modifications of the component will be different than that before the first modification. As a result, the picture represented in Figure 7 occurs very frequently throughout the network. This says that after the test (activity a)

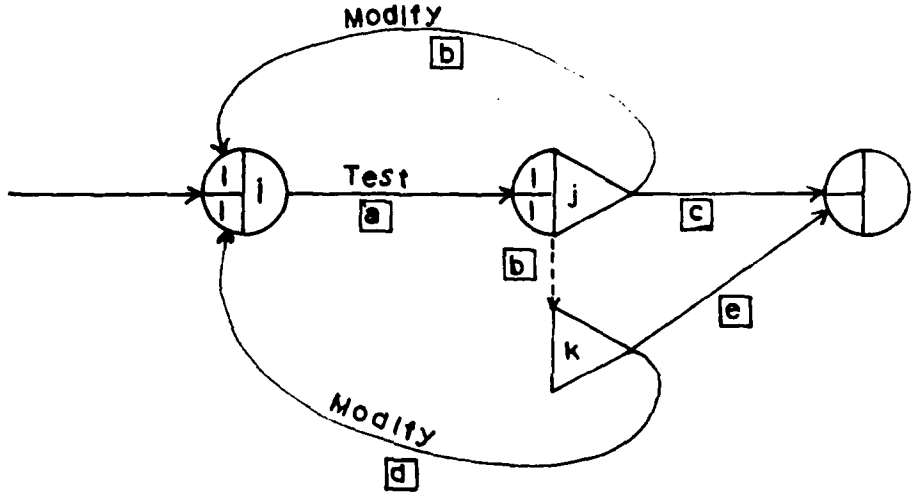



Figure 7. A Common Feature of the Assault Breaker Network

there is a 0.40 chance that the component will have to be modified (activity b). But if this happens, then the output side of node j is replaced by the output side of node k, and after the test (activity a) is repeated, the chance that the component will have to be modified again is 0.20 (activity d).

Another part of the network that needs some explanation is that represented in Figure 8. In addition to the network modification explained above, additional

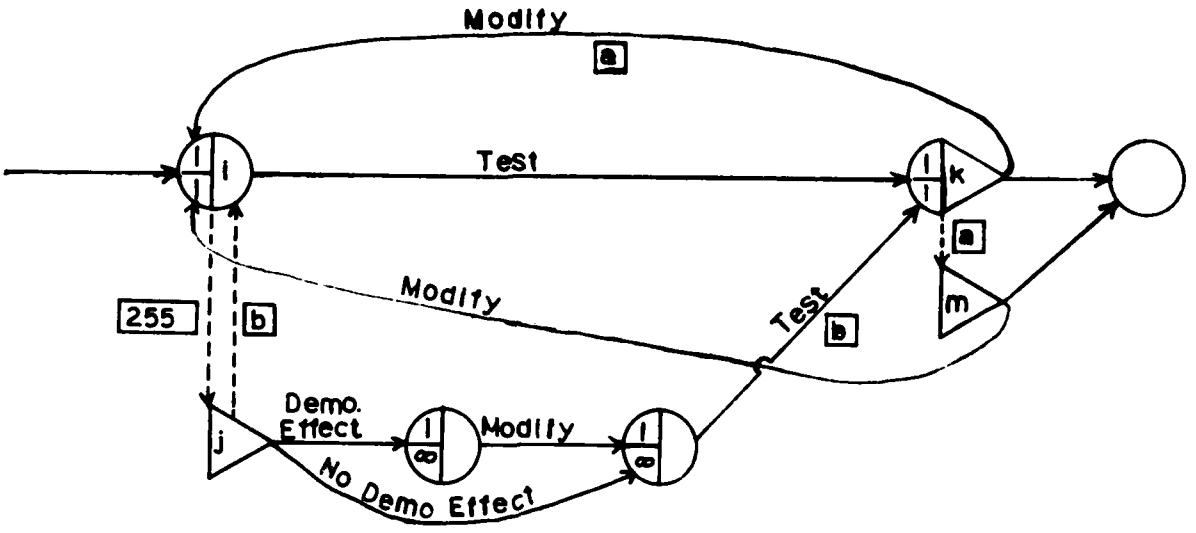



Figure 8. An Example Part of the Network with More Than One Modification

modifications are introduced in response to the outcome from a field demonstration (activity 255) upon the Ground Target Attack Control System. Thus, as soon as a report on a field demonstration is issued (activity 255), the output side of node i is replaced by node j. If this path is followed, upon its completion (activity b) the network returns to its previous format (node j is replaced by node i).

Following these explanations and the previous general discussion of the GERT approach, the reader should be able to understand the network represented in Figure 6.

## VII. INPUT DATA ESTIMATION

Three kinds of data have to be estimated for each activity in order to simulate the network: probability of selection, time and probably cost. As there are approximately five hundred activities, few of which only are infor-

mation transfer activities not involving time and cost, it would be impossible within the time limitations of this study to systematically derive the most suitable probability distribution for each activity and estimate with relative precision its parameters. It was also felt by the program director that cost estimates would not be of much interest at this stage of the analysis although they would have been if the analysis had been done at an earlier stage.

A rough estimation process of activity probabilities and times was therefore judged adequate at this stage of the analysis in demonstrating the usefulness of the approach. The Beta distribution fitted to three parameters (as in the case of PERT) was mainly used to represent the time distribution for each activity, or a constant. The parameters of the distribution together with the selection probability for each activity were roughly estimated. As parts of the network had already been completed or contracted for completion with a promised delivery date, a constant time was assigned to that part of the network equal to the time still remaining until the completion deadline. The input data is presented in Appendix I.

Appendix I consists of two parts. The first describes the activities and the second gives the parameter values for the Beta distribution (most likely, optimistic, pessimistic). Each activity is defined by a start and an end node and a distribution type (10=constant time equal to the value given in the "parameter number" column; 9=Beta distribution whose parameters are given in the second part of Appendix I for the particular parameter number). If a track is kept of the number of times that particular activity was completed, then a "count type" is associated with it. Finally a probability of selection is given for each activity. As it was mentioned above, cost data were not employed at this stage of the analysis and they are equal to zero in the respective columns.

## VIII. SIMULATION RESULTS

In order to simulate the network we used the prewritten software package supplied by Pritsker & Associates, Inc. after some modifications so that it would accomodate the particular size of our network. Although at the time of this writing there are still some problems with the reporting of the results of the simulation, the program has worked for all practical purposes. We sumulated the network 500 times on the MITRE Corporation IBM 370 computer and it took 4.8 minutes CPU time. The statistics collected are given in Appendix II. Appendix II consists

of two parts: In the first part, summary statistics are given for the nodes for which statistics were collected. If a node was never realized, like node 307, the message "no values recorded" is given. The same message is given for the row in which cost data should be reported for each statistics node. The information provided includes probability of realization of a node; mean, standard deviation, minimum and maximum values for time; number of observations; and type of statistics collected. The count statistics refer to activity completions with a specific counter type with respect to releases of the particular node for which the specific statistics are collected.

As an example take the summary statistics for Node 186 (Program approved for full scale engineering development). There is a .5320 chance that the program will be approved for full scale engineering development (according to the roughly estimated input data). As an average it will take 18.222 months. The minimum observed completion time out of the 266 observations was 70.3394 months. and the maximum was 205.4856 months. With respect to releases of Node 186, the average number of activity completions with counter type 1 (Activities 276, 283, 290, and 304 according to the activity description data of Appendix I) is .4398 with standard deviation .7951, a minimum value of 0 and a maximum of 3.000. Analagous is the interpretation of statistics for the other count types.

The second part of Appendix II gives the relative frequency and cumulative relative frequency distributions of time for each of the statistics nodes together with their respective histograms (*for relative frequencies and C for cumulative relative frequencies). If the network had been simulated for a larger number of times more smooth distributions would have been obtained for some of the nodes.

Although the results of the simulation are of limited usefulness due to the fact that the input data are rough estimates, nevertheless they fullfill the objective of the study in demonstrating the usefullness of the GERT approach for planning purposes. The above statistics are not only useful at the stage of initial planning but also at any other later stage for controlling the program. For example if it has been scheduled to reach Node 186 by a specific date, say March 31, 1982, that is 19 months from the date of the simulation, the probability of meeting this schedule according to the cumulative relative frequency statistics for Node 186 (Appendix II) is zero (based on the input information). This information would be extremely valuable to the program manager in designing his future strategy.

As it is obvious, the accuracy of these results depends on the accuracy of the input data. This simulation was performed for demonstration purposes only and therefore rough estimates of the input data were used. If the GERT approach was to be adopted for actual planning, then more careful and precise estimates should be made of the input data. Also sensitivity analysis should be performed to judge the sensitivity of the results to the accuracy of the input data and to establish ranges of statistics within which the program director would base his actual planning.

## IX. RECOMMENDATIONS

Operations research approaches have proved to be useful in solving problems in business, industry, government, and the military. Network modeling techniques like PERT/CPM have facilitated the planning and control of large projects and they have become wellknown and popular in their use. However, due to some disadvantages they present in the modeling of complex projects, more flexible network techniques like GERT have been developed during the last few years.

GERT was applied as a demonstration in the planning of the Assault Breaker project, a cooperative effort between the Air Force and the Army, directed by the Air Force. The network model was developed and, on the basis of rough estimates of the relevant parameters, it was simulated using a prewritten software package. The benefits derived from this analysis were significant. The network development process itself helped the people involved with the project gain a better understanding of its structure and the interfacing of its component parts. The derived network can now serve as a basis for further refinements; briefings on the project of new staff or any people that have an involvement with the project; and further simulation for planning and control.

The simulation showed the value of the derived output that can prove extremely helpful to the program director in planning the future course of the program, estimating the possibility of meeting deadlines, and systematically documenting proposed plans. Given the difficulties involved in estimating the values of the input parameters, sensitivity analysis can be carried out to test the sensitivity of the results to the accuracy of the data. Also, given the uncertainty that surrounds such programs, experimentation can be carried out by modifying the network and observing the effect of the modifications upon the plans.

The approach should not be viewed as a static tool used at the beginning

of the planning process only but as a dynamic one used frequently as the project progresses, new information is added, and perceptions about the project change. By modifying the network and/or the data, the plans can be updated, the possibility of meeting schedules can be reevaluated and appropriate corrective actions can possibly be taken. It should be emphasized that it will still be the program director who will be making plans and decisions but this systematic analysis will help him do all this in a systematic way and on the basis of analysis rather than on pure or educated guessing.

In view of the above benefits and usefulness of the GERT approach, it is recommended that it is adopted as a regular approach throughout the Air Force, the Army and the Navy, in planning major systems. It could also prove equally useful in the planning or R & D projects.

More specifically, it is recommended that ESD/XR further refines the Assault Breaker program GERT network and the estimates of the relevant input parameters and uses the results to evaluate the feasibility of already established schedules. It should then use the approach in programs that are at their conceptual stage to prove its equal usefulness as an initial planning device. The general adoption of the approach as a planning device throughout ESD/XR should be preceded by a proper training of the staff on the approach itself, its capabilities and the use of the results in planning and decision making. In spite of the fact that expert advice should be used during the implementation of the approach it is absolutely necessary that the particular staffs involved are completely familiar with the approach.

Similar steps can be taken to introduce the approach throughout similar agencies in the Air Force, Army and Navy. Other quantitative approaches should also be considered in resolving other difficult problems like prioritization of alternative projects and goals, and selection of the best alternatives in each case. The world scenario has become so competitive and changeable, and technology advances at such a fast and exponential rate that systematic analytical management techniques are deemed absolutely necessary. The Air Force, therefore, as well as the other agencies, should consider introducing such approaches to a larger extent than it has done so far.

## REFERENCES


1. Wiest, J. D. and F. K. Levy, A Management Guide to PERT/CPM, Englewood Cliffs, N. J., Prentice-Hall, 1969.

2. Clayton, E. R. and L. J. Moore, "PERT Versus GERT", Journal Of Systems Management, Vol. 23, No. 2, February 1972, pp. 11 - 19.

3. Jaglinski, T., Program Management Plan for Ground Target Attack Control System Assault Breaker (3rd Draft), unpublished document, HQ Electronics Systems Division, Hanscomb AFB, Bedford, Mass., April 1980.

4. Moore, L. J. and B. W. Taylor, III, "Multiteam, Multiproject Research and Development Planning with GERT", Management Science, Vol. 24, No. 4, December 1977, pp. 401 - 410.

5. Taylor, B. W. III and L. J. Moore, " R & D Project Planning With Q-GERT Network Modeling and Simulation", Management Science, Vol. 26, No. 1, January 1980, pp. 44 - 59.

6. Pritsker, A. A. B., Modeling and Analysis Using Q-GERT Networks (Second Edition), New York, N. Y., John Wiley/Halsted Press, 1979.

7. Whitehouse, G. E., Systems Analysis and Design Using Network Techniques, Englewood Cliffs, N. J., L973.

8. Moore, L. J. and Clayton, E. R., GERT Modeling and Simulation: Fundamentals and Applications, New York, N. Y., Petrocelli - Charter, 1976.

9. Pritsker, A. A. B. and C. E. Sigal, The GERT-IIIZ User's Manual,W. Lafayette, Indiana, Pritsker & Associate, Inc., 1974.

APPENDIX I
**ACTIVITY DESCRIPTION**

| START NODE | END NODE | PARAMETER NUMBER | DISTRIBUTION TYPE | COUNT TYPE | ACTIVITY NUMBER | PROBABILITY | SETUP COST | VARIABLE COST |
|---|---|---|---|---|---|---|---|---|
| 2 | 3 | 0 | 10 = CONSTANT | 0 | 1 | 1.0000 | 0.0 | 0.0 |
| 2 | 6 | 0 | 10 | 0 | 2 | 1.0000 | 0.0 | 0.0 |
| 2 | 9 | 0 | 10 | 0 | 3 | 1.0000 | 0.0 | 0.0 |
| 2 | 12 | 0 | 10 | 0 | 13 | 1.0000 | 0.0 | 0.0 |
| 2 | 15 | 0 | 10 | 0 | 14 | 1.0000 | 0.0 | 0.0 |
| 2 | 18 | 0 | 10 | 0 | 15 | 1.0000 | 0.0 | 0.0 |
| 2 | 21 | 0 | 10 | 0 | 16 | 1.0000 | 0.0 | 0.0 |
| 2 | 24 | 0 | 10 | 0 | 17 | 1.0000 | 0.0 | 0.0 |
| 3 | 4 | 0 | 10 | 0 | 4 | 1.0000 | 0.0 | 0.0 |
| 4 | 27 | 0 | 10 | 0 | 33 | 1.0000 | 0.0 | 0.0 |
| 4 | 3 | 0 | 10 | 0 | 5 | 0.0 | 0.0 | 0.0 |
| 5 | 27 | 0 | 10 | 0 | 34 | 1.0000 | 0.0 | 0.0 |
| 5 | 3 | 0 | 10 | 0 | 6 | 0.0 | 0.0 | 0.0 |
| 6 | 7 | 0 | 10 | 0 | 7 | 1.0000 | 0.0 | 0.0 |
| 7 | 27 | 0 | 10 | 0 | 35 | 1.0000 | 0.0 | 0.0 |
| 7 | 6 | 0 | 10 | 0 | 8 | 0.0 | 0.0 | 0.0 |
| 8 | 27 | 0 | 10 | 0 | 36 | 1.0000 | 0.0 | 0.0 |
| 8 | 6 | 0 | 10 | 0 | 9 | 0.0 | 0.0 | 0.0 |
| 9 | 10 | 0 | 10 | 0 | 10 | 1.0000 | 0.0 | 0.0 |
| 10 | 27 | 0 | 10 | 0 | 37 | 1.0000 | 0.0 | 0.0 |
| 10 | 9 | 0 | 10 | 0 | 11 | 0.0 | 0.0 | 0.0 |
| 11 | 27 | 0 | 10 | 0 | 38 | 1.0000 | 0.0 | 0.0 |
| 11 | 9 | 0 | 10 | 0 | 12 | 0.0 | 0.0 | 0.0 |
| 12 | 13 | 0 | 10 | 0 | 18 | 1.0000 | 0.0 | 0.0 |
| 13 | 28 | 0 | 10 | 0 | 39 | 1.0000 | 0.0 | 0.0 |
| 13 | 12 | 0 | 10 | 0 | 19 | 0.0 | 0.0 | 0.0 |
| 14 | 29 | 0 | 10 | 0 | 40 | 1.0000 | 0.0 | 0.0 |
| 14 | 12 | 0 | 10 | 0 | 20 | 0.0 | 0.0 | 0.0 |
| 15 | 16 | 0 | 10 | 0 | 21 | 1.0000 | 0.0 | 0.0 |
| 16 | 29 | 0 | 10 | 0 | 41 | 1.0000 | 0.0 | 0.0 |
| 16 | 15 | 0 | 10 | 0 | 22 | 0.0 | 0.0 | 0.0 |
| 17 | 28 | 0 | 10 | 0 | 42 | 1.0000 | 0.0 | 0.0 |
| 17 | 15 | 0 | 10 | 0 | 23 | 0.0 | 0.0 | 0.0 |
| 18 | 19 | 0 | 10 | 0 | 24 | 1.0000 | 0.0 | 0.0 |
| 19 | 28 | 0 | 10 | 0 | 43 | 1.0000 | 0.0 | 0.0 |
| 19 | 18 | 0 | 10 | 0 | 25 | 0.0 | 0.0 | 0.0 |
| 20 | 28 | 0 | 10 | 0 | 44 | 1.0000 | 0.0 | 0.0 |
| 20 | 18 | 0 | 10 | 0 | 26 | 0.0 | 0.0 | 0.0 |
| 21 | 22 | 0 | 10 | 0 | 27 | 1.0000 | 0.0 | 0.0 |
| 22 | 28 | 0 | 10 | 0 | 45 | 1.0000 | 0.0 | 0.0 |
| 22 | 21 | 0 | 10 | 0 | 28 | 0.0 | 0.0 | 0.0 |
| 23 | 25 | 0 | 10 | 0 | 46 | 1.0000 | 0.0 | 0.0 |
| 23 | 21 | 0 | 10 | 0 | 29 | 0.0 | 0.0 | 0.0 |
| 24 | 25 | 0 | 10 | 0 | 30 | 1.0000 | 0.0 | 0.0 |
| 25 | 28 | 0 | 10 | 0 | 47 | 1.0000 | 0.0 | 0.0 |
| 25 | 24 | 0 | 10 | 0 | 31 | 0.0 | 0.0 | 0.0 |
| 26 | 28 | 0 | 10 | 0 | 48 | 1.0000 | 0.0 | 0.0 |
| 26 | 24 | 0 | 10 | 0 | 32 | 0.0 | 0.0 | 0.0 |
| 27 | 29 | 1 | 9 = BETA | 0 | 49 | 1.0000 | 0.0 | 0.0 |
| 28 | 32 | 6 | 9 | 0 | 53 | 1.0000 | 0.0 | 0.0 |
| 29 | 30 | 2 | 9 | 0 | 50 | 1.0000 | 0.0 | 0.0 |
| 30 | 29 | 3 | 9 | 0 | 51 | 0.7000 | 0.0 | 0.0 |
| 30 | 35 | 5 | 9 | 0 | 57 | 0.3000 | 0.0 | 0.0 |
| 31 | 29 | 4 | 9 | 0 | 52 | 0.5000 | 0.0 | 0.0 |
| 31 | 35 | 5 | 9 | 0 | 58 | 0.5000 | 0.0 | 0.0 |
| 32 | 33 | 7 | 9 | 0 | 54 | 1.0000 | 0.0 | 0.0 |
| 33 | 32 | 8 | 9 | 0 | 55 | 0.7000 | 0.0 | 0.0 |
| 33 | 35 | 5 | 9 | 0 | 59 | 0.3000 | 0.0 | 0.0 |
| 34 | 32 | 8 | 9 | 0 | 56 | 0.5000 | 0.0 | 0.0 |
| 34 | 35 | 5 | 9 | 0 | 60 | 0.5000 | 0.0 | 0.0 |
| 35 | 36 | 1 | 9 | 0 | 61 | 1.0000 | 0.0 | 0.0 |
| 36 | 37 | 9 | 9 | 0 | 62 | 1.0000 | 0.0 | 0.0 |
| 37 | 36 | 10 | 9 | 0 | 63 | 0.7000 | 0.0 | 0.0 |
| 37 | 56 | 11 | 9 | 0 | 93 | 0.3000 | 0.0 | 0.0 |
| 38 | 36 | 10 | 9 | 0 | 64 | 0.5000 | 0.0 | 0.0 |
| 38 | 56 | 11 | 9 | 0 | 94 | 0.5000 | 0.0 | 0.0 |
| 39 | 40 | 2 | 10 | 0 | 65 | 1.0000 | 0.0 | 0.0 |
| 39 | 43 | 0 | 10 | 0 | 66 | 1.0000 | 0.0 | 0.0 |
| 39 | 46 | 0 | 10 | 0 | 67 | 1.0000 | 0.0 | 0.0 |
| 39 | 49 | 0 | 10 | 0 | 68 | 1.0000 | 0.0 | 0.0 |
| 40 | 41 | 0 | 10 | 0 | 69 | 1.0000 | 0.0 | 0.0 |

| | | | | | | | | |
|---|---|---|---|---|---|---|---|---|
| 41 | 52 | 0 | 10 | 0 | 81 | 1.0000 | 0.0 | 0.0 |
| 41 | 40 | 0 | 10 | 0 | 70 | 0.0 | 0.0 | 0.0 |
| 42 | 52 | 0 | 10 | 0 | 82 | 1.0000 | 0.0 | 0.0 |
| 42 | 40 | 0 | 10 | 0 | 71 | 0.0 | 0.0 | 0.0 |
| 43 | 44 | 0 | 10 | 0 | 72 | 1.0000 | 0.0 | 0.0 |
| 44 | 52 | 0 | 10 | 0 | 83 | 1.0000 | 0.0 | 0.0 |
| 44 | 43 | 0 | 10 | 0 | 73 | 0.0 | 0.0 | 0.0 |
| 45 | 52 | 0 | 10 | 0 | 84 | 1.0000 | 0.0 | 0.0 |
| 45 | 43 | 0 | 10 | 0 | 74 | 0.0 | 0.0 | 0.0 |
| 46 | 47 | 0 | 10 | 0 | 75 | 1.0000 | 0.0 | 0.0 |
| 47 | 52 | 0 | 10 | 0 | 85 | 1.0000 | 0.0 | 0.0 |
| 47 | 46 | 0 | 10 | 0 | 76 | 0.0 | 0.0 | 0.0 |
| 48 | 52 | 0 | 10 | 0 | 86 | 1.0000 | 0.0 | 0.0 |
| 48 | 46 | 0 | 10 | 0 | 77 | 0.0 | 0.0 | 0.0 |
| 49 | 50 | 0 | 10 | 0 | 78 | 1.0000 | 0.0 | 0.0 |
| 50 | 52 | 0 | 10 | 0 | 87 | 1.0000 | 0.0 | 0.0 |
| 50 | 49 | 0 | 10 | 0 | 79 | 0.0 | 0.0 | 0.0 |
| 51 | 52 | 0 | 10 | 0 | 88 | 1.0000 | 0.0 | 0.0 |
| 51 | 49 | 0 | 10 | 0 | 80 | 0.0 | 0.0 | 0.0 |
| 52 | 53 | 12 | 9 | 0 | 89 | 1.0000 | 0.0 | 0.0 |
| 53 | 54 | 13 | 9 | 0 | 90 | 1.0000 | 0.0 | 0.0 |
| 54 | 53 | 14 | 9 | 0 | 91 | 0.7000 | 0.0 | 0.0 |
| 54 | 56 | 15 | 9 | 0 | 95 | 0.3000 | 0.0 | 0.0 |
| 55 | 53 | 14 | 9 | 0 | 92 | 0.5000 | 0.0 | 0.0 |
| 55 | 56 | 15 | 9 | 0 | 96 | 0.5000 | 0.0 | 0.0 |
| 56 | 57 | 16 | 9 | 0 | 97 | 1.0000 | 0.0 | 0.0 |
| 57 | 58 | 17 | 9 | 0 | 98 | 1.0000 | 0.0 | 0.0 |
| 58 | 57 | 18 | 9 | 0 | 99 | 0.7000 | 0.0 | 0.0 |
| 58 | 60 | 19 | 9 | 0 | 101 | 0.3000 | 0.0 | 0.0 |
| 59 | 57 | 18 | 9 | 0 | 100 | 0.5000 | 0.0 | 0.0 |
| 59 | 60 | 19 | 9 | 0 | 102 | 0.5000 | 0.0 | 0.0 |
| 60 | 61 | 20 | 9 | 0 | 140 | 1.0000 | 0.0 | 0.0 |
| 60 | 83 | 23 | 9 | 0 | 159 | 1.0000 | 0.0 | 0.0 |
| 61 | 62 | 21 | 9 | 0 | 141 | 1.0000 | 0.0 | 0.0 |
| 61 | 63 | 22 | 9 | 0 | 142 | 1.0000 | 0.0 | 0.0 |
| 62 | 64 | 24 | 9 | 6 | 143 | 1.0000 | 0.0 | 0.0 |
| 63 | 66 | 30 | 9 | 5 | 149 | 1.0000 | 0.0 | 0.0 |
| 64 | 69 | 28 | 9 | 0 | 147 | 0.6000 | 0.0 | 0.0 |
| 64 | 62 | 25 | 9 | 0 | 144 | 0.3000 | 0.0 | 0.0 |
| 64 | 189 | 27 | 9 | 0 | 146 | 0.1000 | 0.0 | 0.0 |
| 65 | 69 | 28 | 9 | 0 | 148 | 0.8000 | 0.0 | 0.0 |
| 65 | 62 | 26 | 9 | 0 | 145 | 0.2000 | 0.0 | 0.0 |
| 66 | 70 | 32 | 9 | 0 | 153 | 0.6000 | 0.0 | 0.0 |
| 66 | 63 | 31 | 9 | 0 | 150 | 0.3000 | 0.0 | 0.0 |
| 66 | 68 | 33 | 9 | 0 | 154 | 0.1000 | 0.0 | 0.0 |
| 67 | 70 | 34 | 9 | 0 | 155 | 0.8000 | 0.0 | 0.0 |
| 67 | 63 | 31 | 9 | 0 | 152 | 0.2000 | 0.0 | 0.0 |
| 68 | 70 | 0 | 10 | 0 | 157 | 1.0000 | 0.0 | 0.0 |
| 69 | 88 | 29 | 9 | 0 | 156 | 1.0000 | 0.0 | 0.0 |
| 70 | 89 | 35 | 9 | 0 | 158 | 1.0000 | 0.0 | 0.0 |
| 72 | 73 | 6 | 10 | 0 | 121 | 1.0000 | 0.0 | 0.0 |
| 72 | 76 | 0 | 10 | 0 | 125 | 1.0000 | 0.0 | 0.0 |
| 72 | 79 | 0 | 10 | 0 | 129 | 1.0000 | 0.0 | 0.0 |
| 73 | 74 | 0 | 10 | 0 | 122 | 1.0000 | 0.0 | 0.0 |
| 74 | 82 | 0 | 10 | 0 | 133 | 1.0000 | 0.0 | 0.0 |
| 74 | 73 | 0 | 10 | 0 | 123 | 0.0 | 0.0 | 0.0 |
| 75 | 82 | 0 | 10 | 0 | 134 | 1.0000 | 0.0 | 0.0 |
| 75 | 73 | 0 | 10 | 0 | 124 | 0.0 | 0.0 | 0.0 |
| 76 | 77 | 0 | 10 | 0 | 126 | 1.0000 | 0.0 | 0.0 |
| 77 | 82 | 0 | 10 | 0 | 135 | 1.0000 | 0.0 | 0.0 |
| 77 | 76 | 0 | 10 | 0 | 127 | 0.0 | 0.0 | 0.0 |
| 78 | 82 | 0 | 10 | 0 | 136 | 1.0000 | 0.0 | 0.0 |
| 78 | 74 | 0 | 10 | 0 | 128 | 0.0 | 0.0 | 0.0 |

| | | | | | | | | |
|---|---|---|---|---|---|---|---|---|
| 79 | 80 | 0 | 10 | 0 | 130 | 1.0000 | 0.0 | 0.0 |
| 80 | 82 | 0 | 10 | 0 | 137 | 1.0000 | 0.0 | 0.0 |
| 80 | 79 | 0 | 10 | 0 | 131 | 0.0 | 0.0 | 0.0 |
| 81 | 82 | 0 | 10 | 0 | 138 | 1.0000 | 0.0 | 0.0 |
| 81 | 79 | 0 | 10 | 0 | 132 | 0.0 | 0.0 | 0.0 |
| 82 | 83 | 39 | 9 | 0 | 139 | 1.0000 | 0.0 | 0.0 |
| 83 | 112 | 37 | 9 | 0 | 203 | 1.0000 | 0.0 | 0.0 |
| 83 | 84 | 40 | 9 | 0 | 160 | 1.0000 | 0.0 | 0.0 |
| 84 | 85 | 41 | 9 | 4 | 161 | 1.0000 | 0.0 | 0.0 |
| 85 | 84 | 42 | 9 | 0 | 162 | 0.5000 | 0.0 | 0.0 |
| 85 | 87 | 43 | 9 | 0 | 165 | 0.4000 | 0.0 | 0.0 |
| 85 | 190 | 44 | 9 | 0 | 164 | 0.1000 | 0.0 | 0.0 |
| 86 | 87 | 43 | 9 | 0 | 166 | 0.6000 | 0.0 | 0.0 |
| 86 | 84 | 42 | 9 | 0 | 163 | 0.4000 | 0.0 | 0.0 |
| 87 | 137 | 38 | 9 | 0 | 168 | 1.0000 | 0.0 | 0.0 |
| 87 | 88 | 45 | 9 | 0 | 167 | 1.0000 | 0.0 | 0.0 |
| 88 | 89 | 0 | 10 | 0 | 255 | 1.0000 | 0.0 | 0.0 |
| 89 | 90 | 110 | 9 | 0 | 256 | 1.0000 | 0.0 | 0.0 |
| 90 | 91 | 111 | 9 | 0 | 510 | 1.0000 | 0.0 | 0.0 |
| 91 | 186 | 112 | 9 | 0 | 512 | 0.9000 | 0.0 | 0.0 |
| 91 | 185 | 112 | 9 | 0 | 511 | 0.1000 | 0.0 | 0.0 |
| 92 | 93 | 46 | 9 | 0 | 169 | 1.0000 | 0.0 | 0.0 |
| 93 | 94 | 47 | 9 | 0 | 170 | 0.5000 | 0.0 | 0.0 |
| 93 | 89 | 0 | 10 | 0 | 171 | 0.5000 | 0.0 | 0.0 |
| 94 | 108 | 48 | 9 | 0 | 172 | 1.0000 | 0.0 | 0.0 |
| 94 | 95 | 49 | 9 | 0 | 173 | 1.0000 | 0.0 | 0.0 |
| 94 | 98 | 54 | 9 | 0 | 174 | 1.0000 | 0.0 | 0.0 |
| 94 | 101 | 58 | 9 | 0 | 175 | 1.0000 | 0.0 | 0.0 |
| 95 | 96 | 50 | 9 | 0 | 176 | 1.0000 | 0.0 | 0.0 |
| 96 | 104 | 53 | 9 | 0 | 185 | 0.7000 | 0.0 | 0.0 |
| 96 | 95 | 51 | 9 | 0 | 177 | 0.3000 | 0.0 | 0.0 |
| 97 | 104 | 53 | 9 | 0 | 186 | 0.8000 | 0.0 | 0.0 |
| 97 | 95 | 52 | 9 | 0 | 178 | 0.2000 | 0.0 | 0.0 |
| 98 | 99 | 55 | 9 | 0 | 179 | 1.0000 | 0.0 | 0.0 |
| 99 | 104 | 57 | 9 | 0 | 187 | 0.7000 | 0.0 | 0.0 |
| 99 | 98 | 56 | 9 | 0 | 180 | 0.3000 | 0.0 | 0.0 |
| 100 | 104 | 57 | 9 | 0 | 188 | 0.8000 | 0.0 | 0.0 |
| 100 | 98 | 56 | 9 | 0 | 181 | 0.2000 | 0.0 | 0.0 |
| 101 | 102 | 59 | 9 | 0 | 182 | 1.0000 | 0.0 | 0.0 |
| 102 | 104 | 61 | 9 | 0 | 189 | 0.7000 | 0.0 | 0.0 |
| 102 | 101 | 60 | 9 | 0 | 183 | 0.3000 | 0.0 | 0.0 |
| 103 | 104 | 61 | 9 | 0 | 190 | 0.8000 | 0.0 | 0.0 |
| 103 | 101 | 60 | 9 | 0 | 184 | 0.2000 | 0.0 | 0.0 |
| 104 | 146 | 0 | 10 | 0 | 151 | 1.0000 | 0.0 | 0.0 |
| 105 | 106 | 63 | 9 | 0 | 192 | 1.0000 | 0.0 | 0.0 |
| 106 | 105 | 65 | 9 | 0 | 195 | 0.7000 | 0.0 | 0.0 |
| 106 | 105 | 64 | 9 | 0 | 193 | 0.3000 | 0.0 | 0.0 |
| 107 | 108 | 65 | 9 | 0 | 196 | 0.8000 | 0.0 | 0.0 |
| 107 | 105 | 64 | 9 | 0 | 194 | 0.2000 | 0.0 | 0.0 |
| 108 | 109 | 66 | 9 | 0 | 197 | 1.0000 | 0.0 | 0.0 |
| 109 | 110 | 67 | 9 | 0 | 198 | 1.0000 | 0.0 | 0.0 |
| 110 | 112 | 69 | 9 | 0 | 201 | 0.7000 | 0.0 | 0.0 |
| 110 | 109 | 68 | 9 | 0 | 199 | 0.3000 | 0.0 | 0.0 |
| 111 | 112 | 69 | 9 | 0 | 202 | 0.8000 | 0.0 | 0.0 |
| 111 | 109 | 68 | 9 | 0 | 200 | 0.2000 | 0.0 | 0.0 |
| 112 | 113 | 70 | 9 | 0 | 204 | 1.0000 | 0.0 | 0.0 |
| 113 | 114 | 71 | 9 | 3 | 205 | 1.0000 | 0.0 | 0.0 |
| 114 | 117 | 74 | 9 | 0 | 210 | 0.6000 | 0.0 | 0.0 |
| 114 | 113 | 72 | 9 | 0 | 206 | 0.3000 | 0.0 | 0.0 |
| 114 | 116 | 73 | 9 | 0 | 208 | 0.1000 | 0.0 | 0.0 |
| 115 | 117 | 74 | 9 | 0 | 211 | 0.8000 | 0.0 | 0.0 |
| 115 | 113 | 72 | 9 | 0 | 207 | 0.2000 | 0.0 | 0.0 |
| 116 | 117 | 0 | 10 | 0 | 209 | 1.0000 | 0.0 | 0.0 |

| | | | | | | | | |
|---|---|---|---|---|---|---|---|---|
| 117 | 88 | 75 | 9 | 0 | 212 | 1.0000 | 0.0 | 0.0 |
| 118 | 119 | 76 | 9 | 0 | 213 | 1.0000 | 0.0 | 0.0 |
| 119 | 120 | 76 | 9 | 0 | 214 | 1.0000 | 0.0 | 0.0 |
| 120 | 121 | 77 | 9 | 0 | 215 | 1.0000 | 0.0 | 0.0 |
| 120 | 124 | 81 | 9 | 0 | 216 | 1.0000 | 0.0 | 0.0 |
| 120 | 127 | 87 | 9 | 0 | 217 | 1.0000 | 0.0 | 0.0 |
| 120 | 130 | 92 | 9 | 0 | 218 | 1.0000 | 0.0 | 0.0 |
| 120 | 137 | 97 | 9 | 0 | 219 | 1.0000 | 0.0 | 0.0 |
| 121 | 122 | 78 | 9 | 0 | 220 | 1.0000 | 0.0 | 0.0 |
| 122 | 121 | 79 | 9 | 0 | 221 | 0.5000 | 0.0 | 0.0 |
| 122 | 137 | 80 | 9 | 0 | 223 | 0.5000 | 0.0 | 0.0 |
| 123 | 137 | 80 | 9 | 0 | 224 | 0.6000 | 0.0 | 0.0 |
| 123 | 121 | 79 | 9 | 0 | 222 | 0.4000 | 0.0 | 0.0 |
| 124 | 125 | 82 | 9 | 0 | 225 | 1.0000 | 0.0 | 0.0 |
| 125 | 124 | 83 | 9 | 0 | 226 | 0.5000 | 0.0 | 0.0 |
| 125 | 133 | 85 | 9 | 0 | 228 | 0.5000 | 0.0 | 0.0 |
| 126 | 133 | 86 | 9 | 0 | 229 | 0.6000 | 0.0 | 0.0 |
| 126 | 124 | 84 | 9 | 0 | 227 | 0.4000 | 0.0 | 0.0 |
| 127 | 128 | 88 | 9 | 0 | 230 | 1.0000 | 0.0 | 0.0 |
| 128 | 127 | 89 | 9 | 0 | 231 | 0.5000 | 0.0 | 0.0 |
| 128 | 133 | 91 | 9 | 0 | 233 | 0.5000 | 0.0 | 0.0 |
| 129 | 133 | 91 | 9 | 0 | 234 | 0.6000 | 0.0 | 0.0 |
| 129 | 127 | 90 | 9 | 0 | 232 | 0.4000 | 0.0 | 0.0 |
| 130 | 131 | 93 | 9 | 0 | 235 | 1.0000 | 0.0 | 0.0 |
| 131 | 130 | 94 | 9 | 0 | 236 | 0.5000 | 0.0 | 0.0 |
| 131 | 133 | 96 | 9 | 0 | 238 | 0.5000 | 0.0 | 0.0 |
| 132 | 133 | 96 | 9 | 0 | 239 | 0.6000 | 0.0 | 0.0 |
| 132 | 130 | 95 | 9 | 0 | 237 | 0.4000 | 0.0 | 0.0 |
| 133 | 134 | 98 | 9 | 0 | 240 | 1.0000 | 0.0 | 0.0 |
| 134 | 135 | 99 | 9 | 0 | 241 | 1.0000 | 0.0 | 0.0 |
| 135 | 137 | 102 | 9 | 0 | 244 | 0.7000 | 0.0 | 0.0 |
| 135 | 134 | 100 | 9 | 0 | 242 | 0.3000 | 0.0 | 0.0 |
| 136 | 137 | 102 | 9 | 0 | 245 | 0.8000 | 0.0 | 0.0 |
| 136 | 134 | 101 | 9 | 0 | 243 | 0.2000 | 0.0 | 0.0 |
| 137 | 139 | 103 | 9 | 0 | 246 | 1.0000 | 0.0 | 0.0 |
| 138 | 139 | 104 | 9 | 2 | 247 | 1.0000 | 0.0 | 0.0 |
| 139 | 142 | 108 | 9 | 0 | 252 | 0.6000 | 0.0 | 0.0 |
| 139 | 138 | 105 | 9 | 0 | 248 | 0.3000 | 0.0 | 0.0 |
| 139 | 141 | 107 | 9 | 0 | 250 | 0.1000 | 0.0 | 0.0 |
| 140 | 142 | 108 | 9 | 0 | 253 | 0.8000 | 0.0 | 0.0 |
| 140 | 138 | 106 | 9 | 0 | 249 | 0.2000 | 0.0 | 0.0 |
| 141 | 142 | 0 | 10 | 0 | 251 | 1.0000 | 0.0 | 0.0 |
| 142 | 88 | 109 | 9 | 0 | 254 | 1.0000 | 0.0 | 0.0 |
| 143 | 150 | 113 | 9 | 0 | 258 | 1.0000 | 0.0 | 0.0 |
| 143 | 156 | 114 | 9 | 0 | 259 | 1.0000 | 0.0 | 0.0 |
| 143 | 162 | 115 | 9 | 0 | 260 | 1.0000 | 0.0 | 0.0 |
| 144 | 239 | 203 | 9 | 0 | 383 | 1.0000 | 0.0 | 0.0 |
| 145 | 90 | 0 | 10 | 0 | 506 | 1.0000 | 0.0 | 0.0 |
| 146 | 105 | 62 | 9 | 0 | 191 | 1.0000 | 0.0 | 0.0 |
| 150 | 151 | 116 | 9 | 0 | 270 | 1.0000 | 0.0 | 0.0 |
| 151 | 168 | 120 | 9 | 0 | 291 | 0.7000 | 0.0 | 0.0 |
| 151 | 150 | 117 | 9 | 0 | 271 | 0.3000 | 0.0 | 0.0 |
| 152 | 168 | 120 | 9 | 0 | 292 | 0.8000 | 0.0 | 0.0 |
| 152 | 150 | 118 | 9 | 0 | 272 | 0.2000 | 0.0 | 0.0 |
| 153 | 154 | 123 | 9 | 0 | 273 | 0.5000 | 0.0 | 0.0 |
| 153 | 155 | 124 | 9 | 0 | 275 | 0.5000 | 0.0 | 0.0 |
| 154 | 155 | 119 | 9 | 0 | 274 | 1.0000 | 0.0 | 0.0 |
| 155 | 151 | 116 | 9 | 1 | 276 | 1.0000 | 0.0 | 0.0 |
| 156 | 157 | 121 | 9 | 0 | 277 | 1.0000 | 0.0 | 0.0 |
| 157 | 156 | 122 | 9 | 0 | 278 | 0.7000 | 0.0 | 0.0 |
| 157 | 168 | 129 | 9 | 0 | 293 | 0.3000 | 0.0 | 0.0 |
| 158 | 156 | 122 | 9 | 0 | 279 | 0.6000 | 0.0 | 0.0 |
| 159 | 158 | 129 | 9 | 0 | 294 | 0.4000 | 0.0 | 0.0 |

| | | | | | | | | |
|---|---|---|---|---|---|---|---|---|
| 159 | 160 | 125 | 9 | 0 | 280 | 0.5000 | 0.0 | 0.0 |
| 159 | 161 | 127 | 9 | 0 | 282 | 0.5000 | 0.0 | 0.0 |
| 160 | 161 | 126 | 9 | 0 | 281 | 1.0000 | 0.0 | 0.0 |
| 161 | 151 | 128 | 9 | 1 | 283 | 1.0000 | 0.0 | 0.0 |
| 162 | 163 | 130 | 9 | 0 | 284 | 1.0000 | 0.0 | 0.0 |
| 163 | 169 | 137 | 9 | 0 | 295 | 0.7000 | 0.0 | 0.0 |
| 163 | 162 | 131 | 9 | 0 | 285 | 0.3000 | 0.0 | 0.0 |
| 164 | 168 | 137 | 9 | 0 | 296 | 0.8000 | 0.0 | 0.0 |
| 164 | 162 | 132 | 9 | 0 | 286 | 0.2000 | 0.0 | 0.0 |
| 165 | 167 | 135 | 9 | 0 | 289 | 0.7000 | 0.0 | 0.0 |
| 165 | 166 | 133 | 9 | 0 | 287 | 0.3000 | 0.0 | 0.0 |
| 166 | 167 | 134 | 9 | 0 | 288 | 1.0000 | 0.0 | 0.0 |
| 167 | 163 | 136 | 9 | 1 | 290 | 1.0000 | 0.0 | 0.0 |
| 168 | 169 | 138 | 9 | 0 | 297 | 1.0000 | 0.0 | 0.0 |
| 169 | 170 | 139 | 9 | 0 | 298 | 1.0000 | 0.0 | 0.0 |
| 170 | 175 | 146 | 9 | 0 | 305 | 0.7000 | 0.0 | 0.0 |
| 170 | 169 | 140 | 9 | 0 | 299 | 0.3000 | 0.0 | 0.0 |
| 171 | 175 | 146 | 9 | 0 | 306 | 0.8000 | 0.0 | 0.0 |
| 171 | 169 | 141 | 9 | 0 | 300 | 0.2000 | 0.0 | 0.0 |
| 172 | 173 | 142 | 9 | 0 | 301 | 0.5000 | 0.0 | 0.0 |
| 172 | 174 | 144 | 9 | 0 | 303 | 0.5000 | 0.0 | 0.0 |
| 173 | 174 | 143 | 9 | 0 | 302 | 1.0000 | 0.0 | 0.0 |
| 174 | 170 | 145 | 9 | 1 | 304 | 1.0000 | 0.0 | 0.0 |
| 175 | 176 | 147 | 9 | 0 | 307 | 1.0000 | 0.0 | 0.0 |
| 176 | 177 | 148 | 9 | 1 | 308 | 1.0000 | 0.0 | 0.0 |
| 177 | 179 | 151 | 9 | 0 | 311 | 0.6000 | 0.0 | 0.0 |
| 177 | 176 | 149 | 9 | 0 | 309 | 0.3000 | 0.0 | 0.0 |
| 177 | 180 | 152 | 9 | 0 | 312 | 0.1000 | 0.0 | 0.0 |
| 178 | 179 | 151 | 9 | 0 | 313 | 0.8000 | 0.0 | 0.0 |
| 178 | 176 | 150 | 9 | 0 | 310 | 0.2000 | 0.0 | 0.0 |
| 179 | 90 | 153 | 9 | 0 | 314 | 1.0000 | 0.0 | 0.0 |
| 180 | 179 | 0 | 10 | 0 | 515 | 1.0000 | 0.0 | 0.0 |
| 185 | 187 | 0 | 10 | 0 | 513 | 1.0000 | 0.0 | 0.0 |
| 185 | 187 | 0 | 10 | 0 | 513 | 1.0000 | 0.0 | 0.0 |
| 186 | 187 | 0 | 10 | 0 | 514 | 1.0000 | 0.0 | 0.0 |
| 189 | 191 | 0 | 10 | 0 | 507 | 1.0000 | 0.0 | 0.0 |
| 190 | 191 | 0 | 10 | 0 | 508 | 1.0000 | 0.0 | 0.0 |
| 191 | 185 | 0 | 10 | 0 | 509 | 1.0000 | 0.0 | 0.0 |
| 192 | 193 | 154 | 9 | 0 | 315 | 1.0000 | 0.0 | 0.0 |
| 193 | 194 | 155 | 9 | 0 | 316 | 1.0000 | 0.0 | 0.0 |
| 194 | 195 | 156 | 9 | 0 | 317 | 1.0000 | 0.0 | 0.0 |
| 195 | 196 | 157 | 9 | 0 | 318 | 1.0000 | 0.0 | 0.0 |
| 196 | 197 | 158 | 9 | 0 | 319 | 0.7000 | 0.0 | 0.0 |
| 196 | 198 | 159 | 9 | 0 | 321 | 0.3000 | 0.0 | 0.0 |
| 197 | 198 | 159 | 9 | 0 | 320 | 1.0000 | 0.0 | 0.0 |
| 198 | 199 | 160 | 9 | 0 | 322 | 0.7000 | 0.0 | 0.0 |
| 198 | 199 | 161 | 9 | 0 | 323 | 0.3000 | 0.0 | 0.0 |
| 199 | 200 | 162 | 9 | 0 | 324 | 1.0000 | 0.0 | 0.0 |
| 199 | 213 | 0 | 10 | 0 | 343 | 1.0000 | 0.0 | 0.0 |
| 200 | 201 | 163 | 9 | 0 | 325 | 0.7000 | 0.0 | 0.0 |
| 200 | 201 | 164 | 9 | 0 | 326 | 0.3000 | 0.0 | 0.0 |
| 201 | 202 | 0 | 10 | 0 | 327 | 1.0000 | 0.0 | 0.0 |
| 201 | 226 | 191 | 9 | 0 | 363 | 1.0000 | 0.0 | 0.0 |
| 202 | 203 | 165 | 9 | 0 | 328 | 1.0000 | 0.0 | 0.0 |
| 203 | 204 | 168 | 9 | 0 | 331 | 0.4000 | 0.0 | 0.0 |
| 203 | 202 | 166 | 9 | 0 | 329 | 0.3000 | 0.0 | 0.0 |
| 203 | 185 | 167 | 9 | 0 | 330 | 0.3000 | 0.0 | 0.0 |
| 204 | 314 | 0 | 10 | 0 | 333 | 1.0000 | 0.0 | 0.0 |
| 204 | 205 | 169 | 9 | 0 | 334 | 1.0000 | 0.0 | 0.0 |
| 205 | 206 | 170 | 9 | 0 | 335 | 1.0000 | 0.0 | 0.0 |
| 206 | 207 | 171 | 9 | 0 | 336 | 1.0000 | 0.0 | 0.0 |
| 207 | 208 | 172 | 9 | 0 | 337 | 1.0000 | 0.0 | 0.0 |
| 208 | 209 | 173 | 9 | 0 | 338 | 1.0000 | 0.0 | 0.0 |

| | | | | | | | | |
|---|---|---|---|---|---|---|---|---|
| 209 | 210 | 174 | 9 | 0 | 339 | 1.0000 | 0.0 | 0.0 |
| 209 | 213 | 0 | 10 | 0 | 344 | 1.0000 | 0.0 | 0.0 |
| 209 | 237 | 0 | 10 | 0 | 380 | 1.0000 | 0.0 | 0.0 |
| 209 | 144 | 0 | 10 | 0 | 261 | 1.0000 | 0.0 | 0.0 |
| 210 | 211 | 175 | 9 | 0 | 340 | 0.5000 | 0.0 | 0.0 |
| 210 | 212 | 177 | 9 | 0 | 342 | 0.5000 | 0.0 | 0.0 |
| 211 | 212 | 176 | 9 | 0 | 341 | 1.0000 | 0.0 | 0.0 |
| 212 | 221 | 186 | 9 | 0 | 356 | 1.0000 | 0.0 | 0.0 |
| 213 | 214 | 178 | 9 | 0 | 345 | 1.0000 | 0.0 | 0.0 |
| 214 | 215 | 179 | 9 | 0 | 346 | 1.0000 | 0.0 | 0.0 |
| 215 | 216 | 180 | 9 | 0 | 347 | 0.7000 | 0.0 | 0.0 |
| 215 | 217 | 181 | 9 | 0 | 349 | 0.3000 | 0.0 | 0.0 |
| 216 | 217 | 181 | 9 | 0 | 348 | 1.0000 | 0.0 | 0.0 |
| 217 | 218 | 182 | 9 | 0 | 350 | 0.7000 | 0.0 | 0.0 |
| 217 | 219 | 183 | 9 | 0 | 352 | 0.3000 | 0.0 | 0.0 |
| 218 | 219 | 183 | 9 | 0 | 351 | 1.0000 | 0.0 | 0.0 |
| 219 | 220 | 184 | 9 | 0 | 353 | 0.7000 | 0.0 | 0.0 |
| 219 | 220 | 185 | 9 | 0 | 354 | 0.3000 | 0.0 | 0.0 |
| 220 | 314 | 0 | 10 | 0 | 355 | 1.0000 | 0.0 | 0.0 |
| 221 | 222 | 187 | 9 | 0 | 357 | 1.0000 | 0.0 | 0.0 |
| 222 | 223 | 188 | 9 | 0 | 358 | 1.0000 | 0.0 | 0.0 |
| 223 | 224 | 189 | 9 | 0 | 359 | 0.7000 | 0.0 | 0.0 |
| 223 | 225 | 190 | 9 | 0 | 361 | 0.3000 | 0.0 | 0.0 |
| 224 | 225 | 190 | 9 | 0 | 360 | 1.0000 | 0.0 | 0.0 |
| 225 | 314 | 0 | 10 | 0 | 362 | 1.0000 | 0.0 | 0.0 |
| 226 | 227 | 192 | 9 | 0 | 364 | 1.0000 | 0.0 | 0.0 |
| 227 | 228 | 193 | 9 | 0 | 365 | 0.7000 | 0.0 | 0.0 |
| 227 | 229 | 194 | 9 | 0 | 367 | 0.3000 | 0.0 | 0.0 |
| 228 | 229 | 194 | 9 | 0 | 366 | 1.0000 | 0.0 | 0.0 |
| 229 | 230 | 195 | 9 | 0 | 368 | 0.7000 | 0.0 | 0.0 |
| 229 | 231 | 196 | 9 | 0 | 370 | 0.3000 | 0.0 | 0.0 |
| 230 | 231 | 196 | 9 | 0 | 369 | 1.0000 | 0.0 | 0.0 |
| 231 | 232 | 197 | 9 | 0 | 371 | 0.7000 | 0.0 | 0.0 |
| 231 | 232 | 208 | 9 | 0 | 373 | 0.3000 | 0.0 | 0.0 |
| 232 | 233 | 198 | 9 | 0 | 372 | 1.0000 | 0.0 | 0.0 |
| 232 | 144 | 0 | 10 | 0 | 262 | 1.0000 | 0.0 | 0.0 |
| 233 | 234 | 199 | 9 | 0 | 374 | 0.7000 | 0.0 | 0.0 |
| 233 | 235 | 200 | 9 | 0 | 376 | 0.3000 | 0.0 | 0.0 |
| 234 | 235 | 200 | 9 | 0 | 375 | 1.0000 | 0.0 | 0.0 |
| 235 | 236 | 201 | 9 | 0 | 377 | 0.7000 | 0.0 | 0.0 |
| 235 | 237 | 207 | 9 | 0 | 379 | 0.3000 | 0.0 | 0.0 |
| 236 | 237 | 207 | 9 | 0 | 378 | 1.0000 | 0.0 | 0.0 |
| 237 | 238 | 202 | 9 | 0 | 381 | 1.0000 | 0.0 | 0.0 |
| 238 | 314 | 0 | 10 | 0 | 382 | 1.0000 | 0.0 | 0.0 |
| 239 | 240 | 204 | 9 | 0 | 384 | 1.0000 | 0.0 | 0.0 |
| 239 | 243 | 211 | 9 | 0 | 455 | 1.0000 | 0.0 | 0.0 |
| 239 | 298 | 222 | 9 | 0 | 465 | 1.0000 | 0.0 | 0.0 |
| 240 | 241 | 205 | 9 | 0 | 385 | 0.9000 | 0.0 | 0.0 |
| 240 | 242 | 206 | 9 | 0 | 387 | 0.1000 | 0.0 | 0.0 |
| 241 | 242 | 206 | 9 | 0 | 386 | 1.0000 | 0.0 | 0.0 |
| 242 | 251 | 209 | 9 | 0 | 388 | 0.9000 | 0.0 | 0.0 |
| 242 | 251 | 210 | 9 | 0 | 389 | 0.1000 | 0.0 | 0.0 |
| 243 | 244 | 212 | 9 | 0 | 456 | 1.0000 | 0.0 | 0.0 |
| 243 | 247 | 217 | 9 | 0 | 460 | 1.0000 | 0.0 | 0.0 |
| 244 | 245 | 213 | 9 | 0 | 457 | 0.8000 | 0.0 | 0.0 |
| 244 | 246 | 214 | 9 | 0 | 459 | 0.2000 | 0.0 | 0.0 |
| 245 | 246 | 214 | 9 | 0 | 458 | 1.0000 | 0.0 | 0.0 |
| 246 | 251 | 215 | 9 | 0 | 390 | 0.7000 | 0.0 | 0.0 |
| 246 | 251 | 216 | 9 | 0 | 391 | 0.3000 | 0.0 | 0.0 |
| 247 | 249 | 218 | 9 | 0 | 461 | 1.0000 | 0.0 | 0.0 |
| 248 | 249 | 219 | 9 | 0 | 462 | 0.7000 | 0.0 | 0.0 |
| 248 | 250 | 220 | 9 | 0 | 464 | 0.3000 | 0.0 | 0.0 |
| 249 | 250 | 220 | 9 | 0 | 463 | 1.0000 | 0.0 | 0.0 |

| | | | | | | | | |
|---|---|---|---|---|---|---|---|---|
| 250 | 251 | 221 | 9 | 0 | 392 | 0.7000 | 0.0 | 0.0 |
| 250 | 251 | 0 | 10 | 0 | 393 | 0.3000 | 0.0 | 0.0 |
| 251 | 252 | 230 | 9 | 0 | 394 | 1.0000 | 0.0 | 0.0 |
| 252 | 253 | 231 | 9 | 0 | 395 | 0.9000 | 0.0 | 0.0 |
| 252 | 254 | 233 | 9 | 0 | 397 | 0.1000 | 0.0 | 0.0 |
| 253 | 254 | 232 | 9 | 0 | 396 | 1.0000 | 0.0 | 0.0 |
| 254 | 255 | 234 | 9 | 0 | 488 | 1.0000 | 0.0 | 0.0 |
| 254 | 267 | 248 | 9 | 0 | 404 | 1.0000 | 0.0 | 0.0 |
| 254 | 272 | 254 | 9 | 0 | 399 | 1.0000 | 0.0 | 0.0 |
| 254 | 305 | 0 | 10 | 0 | 398 | 1.0000 | 0.0 | 0.0 |
| 254 | 275 | 257 | 9 | 0 | 412 | 1.0000 | 0.0 | 0.0 |
| 254 | 280 | 263 | 9 | 0 | 420 | 1.0000 | 0.0 | 0.0 |
| 254 | 289 | 276 | 9 | 0 | 434 | 1.0000 | 0.0 | 0.0 |
| 255 | 256 | 235 | 9 | 0 | 489 | 1.0000 | 0.0 | 0.0 |
| 256 | 257 | 236 | 9 | 0 | 490 | 0.5000 | 0.0 | 0.0 |
| 256 | 258 | 237 | 9 | 0 | 492 | 0.5000 | 0.0 | 0.0 |
| 257 | 258 | 237 | 9 | 0 | 491 | 1.0000 | 0.0 | 0.0 |
| 258 | 259 | 238 | 9 | 0 | 493 | 0.5000 | 0.0 | 0.0 |
| 258 | 260 | 240 | 9 | 0 | 495 | 0.5000 | 0.0 | 0.0 |
| 259 | 260 | 239 | 9 | 0 | 494 | 1.0000 | 0.0 | 0.0 |
| 260 | 261 | 241 | 9 | 0 | 496 | 0.5000 | 0.0 | 0.0 |
| 260 | 262 | 243 | 9 | 0 | 498 | 0.5000 | 0.0 | 0.0 |
| 261 | 262 | 242 | 9 | 0 | 497 | 1.0000 | 0.0 | 0.0 |
| 262 | 263 | 244 | 9 | 0 | 499 | 0.5000 | 0.0 | 0.0 |
| 262 | 264 | 245 | 9 | 0 | 501 | 0.5000 | 0.0 | 0.0 |
| 263 | 264 | 245 | 9 | 0 | 500 | 1.0000 | 0.0 | 0.0 |
| 264 | 265 | 246 | 9 | 0 | 502 | 0.5000 | 0.0 | 0.0 |
| 264 | 266 | 247 | 9 | 0 | 504 | 0.5000 | 0.0 | 0.0 |
| 265 | 266 | 247 | 9 | 0 | 503 | 1.0000 | 0.0 | 0.0 |
| 266 | 314 | 0 | 10 | 0 | 505 | 1.0000 | 0.0 | 0.0 |
| 267 | 268 | 249 | 9 | 0 | 405 | 1.0000 | 0.0 | 0.0 |
| 268 | 269 | 250 | 9 | 0 | 406 | 0.5000 | 0.0 | 0.0 |
| 268 | 270 | 251 | 9 | 0 | 408 | 0.5000 | 0.0 | 0.0 |
| 269 | 270 | 251 | 9 | 0 | 407 | 1.0000 | 0.0 | 0.0 |
| 270 | 271 | 253 | 9 | 0 | 410 | 0.7000 | 0.0 | 0.0 |
| 270 | 271 | 252 | 9 | 0 | 409 | 0.3000 | 0.0 | 0.0 |
| 271 | 305 | 0 | 10 | 0 | 411 | 1.0000 | 0.0 | 0.0 |
| 272 | 273 | 255 | 9 | 0 | 400 | 1.0000 | 0.0 | 0.0 |
| 273 | 274 | 256 | 9 | 0 | 401 | 0.5000 | 0.0 | 0.0 |
| 273 | 274 | 0 | 10 | 0 | 402 | 0.5000 | 0.0 | 0.0 |
| 274 | 305 | 0 | 10 | 0 | 403 | 1.0000 | 0.0 | 0.0 |
| 275 | 276 | 258 | 9 | 0 | 413 | 1.0000 | 0.0 | 0.0 |
| 276 | 277 | 259 | 9 | 0 | 414 | 0.5000 | 0.0 | 0.0 |
| 276 | 278 | 260 | 9 | 0 | 416 | 0.5000 | 0.0 | 0.0 |
| 277 | 278 | 260 | 9 | 0 | 415 | 1.0000 | 0.0 | 0.0 |
| 278 | 279 | 261 | 9 | 0 | 417 | 0.5000 | 0.0 | 0.0 |
| 278 | 279 | 262 | 9 | 0 | 418 | 0.5000 | 0.0 | 0.0 |
| 279 | 305 | 0 | 10 | 0 | 419 | 1.0000 | 0.0 | 0.0 |
| 280 | 281 | 264 | 9 | 0 | 421 | 1.0000 | 0.0 | 0.0 |
| 281 | 283 | 267 | 9 | 0 | 424 | 0.7000 | 0.0 | 0.0 |
| 281 | 282 | 265 | 9 | 0 | 422 | 0.3000 | 0.0 | 0.0 |
| 282 | 283 | 266 | 9 | 0 | 423 | 1.0000 | 0.0 | 0.0 |
| 283 | 284 | 268 | 9 | 0 | 425 | 0.7000 | 0.0 | 0.0 |
| 283 | 285 | 270 | 9 | 0 | 427 | 0.3000 | 0.0 | 0.0 |
| 284 | 285 | 269 | 9 | 0 | 426 | 1.0000 | 0.0 | 0.0 |
| 285 | 287 | 273 | 9 | 0 | 430 | 0.7000 | 0.0 | 0.0 |
| 285 | 286 | 271 | 9 | 0 | 428 | 0.3000 | 0.0 | 0.0 |
| 286 | 287 | 272 | 9 | 0 | 429 | 1.0000 | 0.0 | 0.0 |
| 287 | 289 | 275 | 9 | 0 | 432 | 0.7000 | 0.0 | 0.0 |
| 287 | 288 | 274 | 9 | 0 | 431 | 0.3000 | 0.0 | 0.0 |
| 288 | 305 | 0 | 10 | 0 | 433 | 1.0000 | 0.0 | 0.0 |
| 289 | 290 | 277 | 9 | 0 | 435 | 1.0000 | 0.0 | 0.0 |
| 290 | 291 | 278 | 9 | 0 | 436 | 0.5000 | 0.0 | 0.0 |

| | | | | | | | | |
|---|---|---|---|---|---|---|---|---|
| 290 | 292 | 282 | 9 | 0 | 438 | 0.5000 | 0.0 | 0.0 |
| 291 | 292 | 279 | 9 | 0 | 437 | 1.0000 | 0.0 | 0.0 |
| 292 | 294 | 283 | 9 | 0 | 441 | 0.7000 | 0.0 | 0.0 |
| 292 | 293 | 280 | 9 | 0 | 439 | 0.3000 | 0.0 | 0.0 |
| 293 | 294 | 281 | 9 | 0 | 440 | 1.0000 | 0.0 | 0.0 |
| 294 | 296 | 285 | 9 | 0 | 444 | 0.7000 | 0.0 | 0.0 |
| 294 | 295 | 284 | 9 | 0 | 442 | 0.3000 | 0.0 | 0.0 |
| 295 | 296 | 285 | 9 | 0 | 443 | 1.0000 | 0.0 | 0.0 |
| 296 | 297 | 0 | 10 | 0 | 446 | 0.7000 | 0.0 | 0.0 |
| 296 | 297 | 286 | 9 | 0 | 445 | 0.3000 | 0.0 | 0.0 |
| 297 | 305 | 0 | 10 | 0 | 447 | 1.0000 | 0.0 | 0.0 |
| 298 | 299 | 223 | 9 | 0 | 466 | 1.0000 | 0.0 | 0.0 |
| 299 | 300 | 224 | 9 | 0 | 467 | 0.6000 | 0.0 | 0.0 |
| 299 | 301 | 225 | 9 | 0 | 469 | 0.4000 | 0.0 | 0.0 |
| 300 | 301 | 225 | 9 | 0 | 468 | 1.0000 | 0.0 | 0.0 |
| 301 | 302 | 226 | 9 | 0 | 470 | 0.6000 | 0.0 | 0.0 |
| 301 | 303 | 227 | 9 | 0 | 472 | 0.4000 | 0.0 | 0.0 |
| 302 | 303 | 227 | 9 | 0 | 471 | 1.0000 | 0.0 | 0.0 |
| 303 | 304 | 228 | 9 | 0 | 473 | 0.5000 | 0.0 | 0.0 |
| 303 | 304 | 229 | 9 | 0 | 474 | 0.5000 | 0.0 | 0.0 |
| 304 | 305 | 0 | 10 | 0 | 475 | 1.0000 | 0.0 | 0.0 |
| 305 | 306 | 0 | 10 | 0 | 476 | 1.0000 | 0.0 | 0.0 |
| 306 | 309 | 288 | 9 | 0 | 480 | 1.0000 | 0.0 | 0.0 |
| 307 | 306 | 0 | 10 | 0 | 477 | 0.5000 | 0.0 | 0.0 |
| 307 | 308 | 0 | 10 | 0 | 478 | 0.5000 | 0.0 | 0.0 |
| 308 | 306 | 287 | 9 | 0 | 479 | 1.0000 | 0.0 | 0.0 |
| 309 | 310 | 289 | 9 | 0 | 481 | 0.5000 | 0.0 | 0.0 |
| 309 | 311 | 290 | 9 | 0 | 483 | 0.5000 | 0.0 | 0.0 |
| 310 | 311 | 290 | 9 | 0 | 482 | 1.0000 | 0.0 | 0.0 |
| 311 | 312 | 291 | 9 | 0 | 484 | 1.0000 | 0.0 | 0.0 |
| 312 | 314 | 293 | 9 | 0 | 487 | 0.7000 | 0.0 | 0.0 |
| 312 | 313 | 292 | 9 | 0 | 485 | 0.3000 | 0.0 | 0.0 |
| 313 | 314 | 293 | 9 | 0 | 486 | 1.0000 | 0.0 | 0.0 |
| 314 | 145 | 0 | 10 | 0 | 263 | 1.0000 | 0.0 | 0.0 |

**ACTIVITY PARAMETERS**

| PARAMETER NUMBER | PARAMETERS 1 | 2 | 3 |
|---|---|---|---|
| 1 | 2.0000 | 1.0000 | 4.0000 |
| 2 | 1.0000 | 0.5000 | 2.0000 |
| 3 | 1.2000 | 1.0000 | 2.0000 |
| 4 | 1.2000 | 1.0000 | 2.0000 |
| 5 | 0.5000 | 0.2000 | 1.0000 |
| 6 | 2.0000 | 1.0000 | 4.0000 |
| 7 | 1.0000 | 0.5000 | 2.0000 |
| 8 | 1.5000 | 1.0000 | 3.0000 |
| 9 | 1.0000 | 0.5000 | 2.0000 |
| 10 | 1.5000 | 1.0000 | 3.0000 |
| 11 | 0.5000 | 0.2000 | 1.0000 |
| 12 | 2.0000 | 1.0000 | 4.0000 |
| 13 | 1.0000 | 0.5000 | 2.0000 |
| 14 | 1.5000 | 1.0000 | 3.0000 |
| 15 | 0.5000 | 0.2000 | 1.0000 |
| 16 | 2.0000 | 1.0000 | 4.0000 |
| 17 | 2.0000 | 1.0000 | 3.0000 |
| 18 | 1.5000 | 1.0000 | 3.0000 |
| 19 | 1.0000 | 0.4000 | 2.0000 |
| 20 | 2.0000 | 0.5000 | 3.0000 |
| 21 | 1.0000 | 0.5000 | 3.0000 |
| 22 | 2.0000 | 1.0000 | 4.0000 |
| 23 | 0.5000 | 0.0 | 1.0000 |
| 24 | 7.0000 | 5.0000 | 9.0000 |
| 25 | 3.0000 | 2.0000 | 5.0000 |
| 26 | 2.0000 | 1.0000 | 3.0000 |
| 27 | 0.6000 | 0.5000 | 1.0000 |
| 28 | 0.5000 | 0.2000 | 1.0000 |
| 29 | 2.0000 | 1.0000 | 4.0000 |
| 30 | 3.0000 | 2.0000 | 5.0000 |
| 31 | 2.0000 | 1.0000 | 3.0000 |
| 32 | 0.5000 | 0.2000 | 1.0000 |
| 33 | 0.6000 | 0.5000 | 1.0000 |
| 34 | 0.5000 | 0.2000 | 1.0000 |
| 35 | 3.0000 | 2.0000 | 5.0000 |
| 37 | 6.0000 | 6.0000 | 8.0000 |
| 38 | 1.0000 | 0.5000 | 3.0000 |
| 39 | 3.0000 | 2.0000 | 4.0000 |
| 40 | 4.0000 | 2.0000 | 6.0000 |
| 41 | 12.0000 | 9.0000 | 18.0000 |
| 42 | 4.0000 | 2.0000 | 6.0000 |
| 43 | 0.5000 | 0.2000 | 1.0000 |
| 44 | 0.6000 | 0.5000 | 1.0000 |
| 45 | 2.0000 | 1.0000 | 4.0000 |
| 46 | 6.0000 | 4.0000 | 8.0000 |
| 47 | 1.5000 | 1.0000 | 2.0000 |
| 48 | 12.0000 | 8.0000 | 18.0000 |
| 49 | 6.0000 | 4.0000 | 8.0000 |
| 50 | 2.0000 | 1.0000 | 6.0000 |
| 51 | 2.0000 | 0.5000 | 4.0000 |
| 52 | 2.0000 | 0.5000 | 4.0000 |
| 53 | 0.5000 | 0.2000 | 1.0000 |
| 54 | 6.0000 | 4.0000 | 8.0000 |
| 55 | 2.0000 | 1.0000 | 6.0000 |
| [illegible] | [illegible] | [illegible] | [illegible] |
| 57 | 0.5000 | 0.2000 | 1.0000 |
| 58 | 6.0000 | 4.0000 | 8.0000 |
| 59 | 2.0000 | 1.0000 | 6.0000 |
| 60 | 2.0000 | 0.5000 | 4.0000 |
| 61 | 0.5000 | 0.2000 | 1.0000 |
| 62 | 2.0000 | 1.0000 | 4.0000 |
| 63 | 2.0000 | 1.0000 | 4.0000 |
| 64 | 1.5000 | 1.0000 | 2.0000 |
| 65 | 0.5000 | 0.2000 | 1.0000 |
| 66 | 1.0000 | 0.5000 | 2.0000 |
| 67 | 1.0000 | 0.5000 | 1.5000 |
| 68 | 1.0000 | 0.5000 | 2.0000 |
| 69 | 0.5000 | 0.2000 | 1.0000 |
| 70 | 2.0000 | 1.0000 | 4.0000 |
| 71 | 8.0000 | 6.0000 | 12.0000 |
| 72 | 2.0000 | 1.0000 | 4.0000 |
| 73 | 0.5000 | 0.2000 | 1.0000 |
| 74 | 0.5000 | 0.2000 | 1.0000 |
| 75 | 3.0000 | 2.0000 | 4.0000 |
| 76 | 2.0000 | 1.0000 | 3.0000 |
| 77 | 4.0000 | 2.0000 | 6.0000 |
| 78 | 4.0000 | 2.0000 | 6.0000 |
| 79 | 2.0000 | 1.0000 | 4.0000 |
| 80 | 0.5000 | 0.2000 | 1.0000 |
| 81 | 6.0000 | 4.0000 | 8.0000 |
| 82 | 4.0000 | 2.0000 | 8.0000 |
| 83 | 2.0000 | 1.0000 | 4.0000 |
| 84 | 2.0000 | 1.0000 | 4.0000 |
| 85 | 0.5000 | 0.2000 | 1.0000 |
| 86 | 0.5000 | 0.2000 | 1.0000 |
| 87 | 6.0000 | 4.0000 | 8.0000 |
| 88 | 4.0000 | 2.0000 | 8.0000 |
| 89 | 2.0000 | 1.0000 | 4.0000 |
| 90 | 2.0000 | 1.0000 | 4.0000 |
| 91 | 0.5000 | 0.2000 | 1.0000 |
| 92 | 6.0000 | 4.0000 | 8.0000 |
| 93 | 4.0000 | 2.0000 | 8.0000 |
| 94 | 2.0000 | 1.0000 | 4.0000 |
| 95 | 2.0000 | 1.0000 | 4.0000 |
| 96 | 0.5000 | 0.2000 | 1.0000 |
| 97 | 8.0000 | 6.0000 | 12.0000 |
| 98 | 1.0000 | 0.5000 | 2.0000 |
| 99 | 1.0000 | 0.5000 | 2.0000 |
| 100 | 1.0000 | 0.5000 | 2.0000 |
| 101 | 1.0000 | 0.5000 | 2.0000 |
| 102 | 0.5000 | 0.2000 | 1.0000 |
| 103 | 1.0000 | 0.5000 | 1.5000 |
| 104 | 4.0000 | 3.0000 | 6.0000 |
| 105 | 1.5000 | 1.0000 | 3.0000 |
| 106 | 1.0000 | 0.0 | 2.0000 |
| 107 | 0.5000 | 0.5000 | 1.0000 |
| 108 | 0.5000 | 0.2000 | 1.0000 |
| 109 | 3.0000 | 2.0000 | 5.0000 |
| 110 | 4.0000 | 2.0000 | 6.0000 |
| 111 | 4.0000 | 3.5000 | 5.0000 |
| 112 | 0.7000 | 0.5000 | 1.0000 |
| 113 | 8.0000 | 6.0000 | 12.0000 |
| 114 | 10.0000 | 8.0000 | 14.0000 |
| 115 | 6.0000 | 4.0000 | 10.0000 |
| 116 | 4.0000 | 2.0000 | 8.0000 |
| 117 | 2.0000 | 1.0000 | 4.0000 |
| 118 | 1.5000 | 1.0000 | 2.0000 |

| | | | | | | | |
|---|---|---|---|---|---|---|---|
| 120 | 0.5000 | 0.2000 | 1.0000 | 183 | 1.5000 | 0.7000 | 3.0000 |
| 121 | 4.0000 | 2.0000 | 8.0000 | 184 | 1.0000 | 0.7000 | 1.5000 |
| 122 | 2.0000 | 1.0000 | 4.0000 | 185 | 0.5000 | 0.2000 | 0.7000 |
| 123 | 1.5000 | 1.0000 | 2.0000 | 186 | 2.0000 | 1.0000 | 2.5000 |
| 124 | 0.5000 | 0.2000 | 1.0000 | 187 | 2.0000 | 1.0000 | 2.5000 |
| 125 | 2.0000 | 1.0000 | 4.0000 | 188 | 8.0000 | 6.0000 | 12.0000 |
| 126 | 1.5000 | 1.0000 | 2.0000 | 189 | 3.0000 | 2.0000 | 5.0000 |
| 127 | 0.5000 | 0.2000 | 1.0000 | 190 | 3.0000 | 2.0000 | 4.0000 |
| 128 | 1.5000 | 1.0000 | 2.0000 | 191 | 5.0000 | 4.0000 | 8.0000 |
| 129 | 0.5000 | 0.2000 | 1.0000 | 192 | 1.0000 | 0.5000 | 2.0000 |
| 130 | 2.0000 | 1.0000 | 5.0000 | 193 | 0.5000 | 0.3000 | 2.0000 |
| 131 | 2.0000 | 1.0000 | 4.0000 | 194 | 0.5000 | 0.3000 | 1.0000 |
| 132 | 2.0000 | 1.0000 | 4.0000 | 195 | 0.5000 | 0.3000 | 2.0000 |
| 133 | 2.0000 | 1.0000 | 4.0000 | 196 | 1.0000 | 0.5000 | 2.0000 |
| 134 | 1.5000 | 1.0000 | 2.0000 | 197 | 0.5000 | 0.3000 | 2.0000 |
| 135 | 0.5000 | 0.2000 | 1.0000 | 198 | 1.0000 | 0.5000 | 2.0000 |
| 136 | 1.5000 | 1.0000 | 2.0000 | 199 | 1.0000 | 0.5000 | 2.0000 |
| 137 | 0.5000 | 0.2000 | 1.0000 | 200 | 1.0000 | 0.5000 | 2.0000 |
| 138 | 3.0000 | 2.0000 | 5.0000 | 201 | 0.7000 | 0.5000 | 1.5000 |
| 139 | 3.0000 | 2.0000 | 5.0000 | 202 | 1.5000 | 1.0000 | 2.5000 |
| 140 | 2.0000 | 1.0000 | 4.0000 | 203 | 6.0000 | 4.0000 | 10.0000 |
| 141 | 2.0000 | 1.0000 | 4.0000 | 204 | 2.0000 | 1.0000 | 4.0000 |
| 142 | 1.0000 | 0.5000 | 2.0000 | 205 | 3.0000 | 2.0000 | 5.0000 |
| 143 | 1.0000 | 0.5000 | 2.0000 | 206 | 1.5000 | 0.5000 | 2.0000 |
| 144 | 0.5000 | 0.2000 | 1.0000 | 207 | 0.7000 | 0.5000 | 1.5000 |
| 145 | 2.0000 | 1.0000 | 4.0000 | 208 | 0.6000 | 0.3000 | 1.5000 |
| 146 | 0.5000 | 0.2000 | 1.0000 | 209 | 2.0000 | 1.0000 | 4.0000 |
| 147 | 3.0000 | 2.0000 | 4.0000 | 210 | 1.0000 | 0.5000 | 2.0000 |
| 148 | 6.0000 | 4.0000 | 8.0000 | 211 | 2.0000 | 1.0000 | 3.0000 |
| 149 | 2.0000 | 1.0000 | 4.0000 | 212 | 1.0000 | 0.5000 | 2.0000 |
| 150 | 2.0000 | 1.0000 | 4.0000 | 213 | 1.0000 | 0.5000 | 2.0000 |
| 151 | 0.5000 | 0.2000 | 1.0000 | 214 | 0.5000 | 0.3000 | 1.0000 |
| 152 | 0.5000 | 0.2000 | 0.6000 | 215 | 1.0000 | 0.5000 | 1.5000 |
| 153 | 3.0000 | 2.0000 | 6.0000 | 216 | 0.5000 | 0.2000 | 1.0000 |
| 154 | 1.0000 | 0.5000 | 2.0000 | 217 | 0.5000 | 0.2000 | 1.0000 |
| 155 | 0.5000 | 0.2000 | 2.0000 | 218 | 0.3000 | 0.1000 | 0.6000 |
| 156 | 1.0000 | 0.5000 | 2.0000 | 219 | 0.3000 | 0.1000 | 0.6000 |
| 157 | 0.5000 | 0.2000 | 2.0000 | 220 | 0.3000 | 0.1000 | 0.6000 |
| 158 | 1.0000 | 0.5000 | 2.0000 | 221 | 0.2000 | 0.1000 | 0.4000 |
| 159 | 0.5000 | 0.2000 | 2.0000 | 222 | 1.0000 | 0.5000 | 2.0000 |
| 160 | 1.0000 | 0.5000 | 2.0000 | 223 | 0.2000 | 0.1000 | 0.5000 |
| 161 | 0.5000 | 0.2000 | 2.0000 | 224 | 0.3000 | 0.1000 | 0.6000 |
| 162 | 1.5000 | 1.0000 | 3.0000 | 225 | 0.2000 | 0.1000 | 0.5000 |
| 163 | 1.5000 | 1.0000 | 2.0000 | 226 | 0.3000 | 0.2000 | 0.6000 |
| 164 | 0.5000 | 0.2000 | 1.5000 | 227 | 0.6000 | 0.2000 | 1.0000 |
| 165 | 1.0000 | 0.5000 | 2.0000 | 228 | 0.3000 | 0.2000 | 0.6000 |
| 166 | 1.0000 | 0.5000 | 2.0000 | 229 | 0.3000 | 0.1000 | 0.6000 |
| 167 | 1.0000 | 0.5000 | 3.0000 | 230 | 2.0000 | 1.0000 | 4.0000 |
| 168 | 0.3000 | 0.2000 | 0.5000 | 231 | 2.0000 | 1.0000 | 4.0000 |
| 169 | 4.0000 | 2.0000 | 7.0000 | 232 | 1.0000 | 0.5000 | 2.0000 |
| 170 | 2.0000 | 1.0000 | 4.0000 | 233 | 1.0000 | 0.5000 | 3.0000 |
| 171 | 1.5000 | 1.0000 | 3.0000 | 234 | 6.0000 | 4.0000 | 8.0000 |
| 172 | 1.0000 | 0.6000 | 1.5000 | 235 | 1.0000 | 0.5000 | 2.0000 |
| 173 | 1.0000 | 0.6000 | 1.5000 | 236 | 2.0000 | 1.0000 | 3.0000 |
| 174 | 0.6000 | 0.2000 | 1.5000 | 237 | 1.0000 | 0.5000 | 2.0000 |
| 175 | 1.0000 | 0.5000 | 2.0000 | 238 | 1.0000 | 0.5000 | 2.0000 |
| 176 | 2.0000 | 1.5000 | 4.0000 | 239 | 2.0000 | 1.0000 | 3.0000 |
| 177 | 1.0000 | 0.5000 | 2.0000 | 240 | 1.0000 | 0.5000 | 2.0000 |
| 178 | 4.0000 | 3.0000 | 6.0000 | 241 | 1.0000 | 0.5000 | 2.0000 |
| 179 | 1.0000 | 0.5000 | 2.0000 | 242 | 1.0000 | 0.5000 | 2.0000 |
| 180 | 1.5000 | 1.0000 | 3.0000 | 243 | 2.0000 | 1.0000 | 3.0000 |
| 181 | 1.0000 | 0.5000 | 2.0000 | 244 | 1.0000 | 0.5000 | 2.0000 |
| 182 | 0.6000 | 0.3000 | 1.5000 | 245 | 1.0000 | 0.5000 | |

| | | | |
|---|---|---|---|
| 246 | 2.0000 | 1.0000 | 3.0000 |
| 247 | 1.0000 | 0.5000 | 2.0000 |
| 248 | 2.0000 | 1.0000 | 3.0000 |
| 249 | 0.5000 | 0.2000 | 1.0000 |
| 250 | 1.0000 | 0.5000 | 2.0000 |
| 251 | 0.5000 | 0.2000 | 1.0000 |
| 252 | 1.0000 | 0.5000 | 2.0000 |
| 253 | 0.5000 | 0.2000 | 1.0000 |
| 254 | 0.5000 | 0.2000 | 1.0000 |
| 255 | 0.5000 | 0.2000 | 1.0000 |
| 256 | 0.5000 | 0.2000 | 1.0000 |
| 257 | 6.0000 | 4.0000 | 9.0000 |
| 258 | 1.5000 | 1.0000 | 3.0000 |
| 259 | 3.0000 | 2.0000 | 5.0000 |
| 260 | 1.5000 | 1.0000 | 3.0000 |
| 261 | 2.0000 | 1.0000 | 4.0000 |
| 262 | 1.0000 | 0.5000 | 2.0000 |
| 263 | 6.0000 | 4.0000 | 10.0000 |
| 264 | 2.0000 | 1.0000 | 4.0000 |
| 265 | 3.0000 | 2.0000 | 5.0000 |
| 266 | 1.0000 | 0.5000 | 1.5000 |
| 267 | 0.5000 | 0.2000 | 1.0000 |
| 268 | 3.0000 | 2.0000 | 5.0000 |
| 269 | 1.0000 | 0.5000 | 1.5000 |
| 270 | 0.5000 | 0.2000 | 1.0000 |
| 271 | 2.0000 | 1.0000 | 4.0000 |
| 272 | 1.0000 | 0.5000 | 1.5000 |
| 273 | 0.5000 | 0.2000 | 1.0000 |
| 274 | 1.0000 | 0.5000 | 2.0000 |
| 275 | 0.5000 | 0.2000 | 1.0000 |
| 276 | 3.0000 | 2.0000 | 5.0000 |
| 277 | 1.0000 | 0.5000 | 2.0000 |
| 278 | 2.0000 | 1.0000 | 3.0000 |
| 279 | 1.0000 | 0.5000 | 2.0000 |
| 280 | 1.0000 | 0.5000 | 1.5000 |
| 281 | 1.0000 | 0.5000 | 1.5000 |
| 282 | 0.5000 | 0.2000 | 1.0000 |
| 283 | 0.5000 | 0.2000 | 1.0000 |
| 284 | 1.0000 | 0.5000 | 1.5000 |
| 285 | 0.5000 | 0.2000 | 1.0000 |
| 286 | 0.5000 | 0.2000 | 1.0000 |
| 287 | 6.0000 | 4.0000 | 8.0000 |
| 288 | 3.0000 | 2.0000 | 5.0000 |
| 289 | 3.0000 | 2.0000 | 5.0000 |
| 290 | 3.0000 | 2.0000 | 4.0000 |
| 291 | 3.0000 | 2.0000 | 4.0000 |
| 292 | 5.0000 | 4.0000 | 8.0000 |
| 293 | 4.0000 | 2.0000 | 6.0000 |

SERT SIMULATION PROJECT - [illegible]
DATE 8/ 6/ 1980

**FINAL RESULTS FOR 500 SIMULATIONS**

| NODE | PROBABILITY | | MEAN | STD. DEV. | NO. OF OBS. | MIN. | MAX. | TYPE |
|---|---|---|---|---|---|---|---|---|
| 187 | 1.0000 | | 61.1076 | 39.2100 | 500. | | | 6 |
| | | 1 | 0.2580 | 0.6575 | 500. | 0.0 | 0.0 | |
| | | 2 | 0.3240 | 0.8778 | 500. | 0.0 | 1.0000 | |
| | | 3 | 0.3700 | 0.6943 | 500. | | | |
| | | 4 | 1.2340 | 1.3253 | 500. | 0.0 | 2.0000 | |
| | | 5 | 0.3100 | 0.7634 | 500. | 0.0 | 2.0000 | |
| | | 6 | 0.9540 | 0.9453 | 500. | 0.0 | 1.0000 | |
| | | 7 | 0.9000 | 0.9239 | 500. | 0.0 | 2.0000 | |
| 89 | 0.5920 | | 54.5169 | 27.7616 | 291. | 13.4393 | 100.004 | 0 |
| | | 0 | NO VALUES RECORDED | | | | | |
| | | 1 | 0.4261 | 0.7772 | 291. | 0.0 | 0.0 | |
| | | 2 | 1.4158 | 0.6965 | 291. | 1.0000 | 3.0000 | |
| | | 3 | 0.6136 | 0.8151 | 291. | 2.0000 | 0.0 | |
| | | 4 | 2.0309 | 1.3035 | 291. | 3.0000 | 0.0 | |
| | | 5 | 1.3162 | 0.6123 | 291. | 1.0000 | 2.0000 | |
| | | 6 | 1.4605 | 0.4988 | 291. | 1.0000 | 1.0000 | |
| | | 7 | 1.2371 | 0.6743 | 291. | 2.0000 | 2.0000 | |
| 314 | 0.5820 | | 10.4321 | 3.1195 | 291. | 14.6793 | 0.0 | 1 |
| | | 0 | NO VALUES RECORDED | | | | | |
| | | 1 | 0.4399 | 0.8136 | 291. | 0.0 | 0.0 | |
| | | 2 | 0.9553 | 0.7691 | 291. | 0.0 | 2.0000 | |
| | | 3 | 0.6049 | 0.7556 | 291. | 1.0000 | 1.0000 | |
| | | 4 | 1.0240 | 0.6946 | 291. | 2.0000 | 2.0000 | |
| | | 5 | 1.3162 | 0.6123 | 291. | 2.0000 | 2.0000 | |
| | | 6 | 1.4433 | 0.4934 | 291. | 1.0000 | 1.0000 | |
| | | 7 | 1.3677 | 0.6315 | 291. | 2.0000 | 0.0 | |
| 307 | | 0 | NO VALUES RECORDED | | | | | |
| 305 | 0.5900 | | 14.7114 | 2.4613 | 295. | 9.2339 | 22.4449 | 1 |
| | | 0 | NO VALUES RECORDED | | | | | |
| | | 1 | 0.3966 | 0.7251 | 295. | 0.0 | 3.0000 | |
| | | 2 | 0.4136 | 0.6377 | 295. | 0.0 | 3.0000 | |
| | | 3 | 0.4339 | 0.6532 | 295. | 0.0 | 3.0000 | |
| | | 4 | 1.0949 | 0.6306 | 295. | 0.0 | 2.0000 | |
| | | 5 | 1.2881 | 0.6144 | 295. | 0.0 | 4.0000 | |
| | | 6 | 1.3119 | 0.5312 | 295. | 0.0 | 3.0000 | |
| | | 7 | 1.1017 | 0.6725 | 295. | 0.0 | 4.0000 | |
| 251 | 0.6680 | | 14.7499 | 1.6153 | 334. | 9.8069 | 19.2476 | 1 |
| | | 0 | NO VALUES RECORDED | | | | | |
| | | 1 | 0.0479 | 0.2134 | 334. | 0.0 | 1.0000 | |
| | | 2 | 0.0 | 0.0 | 334. | 0.0 | 0.0 | |
| | | 3 | 0.6180 | 0.1330 | 334. | 0.0 | 1.0000 | |
| | | 4 | 0.1048 | 0.3067 | 334. | 0.0 | 1.0000 | |
| | | 5 | 0.5856 | 0.6576 | 334. | 0.0 | 4.0000 | |
| | | 6 | 0.4521 | 0.5277 | 334. | 0.0 | 2.0000 | |
| | | 7 | 0.2395 | 0.4493 | 334. | 0.0 | 2.0000 | |

| NODE | PROBABILITY | | MEAN | STD. DEV. | NO. OF OBS. | MIN. | MAX. | TYPE |
|---|---|---|---|---|---|---|---|---|
| 225 | 0.6360 | | 17.3493 | 1.9477 | 315. | 13.6953 | 21.7772 | 1 |
| | | 0 | NO VALUES RECORDED | | | | | |
| | | 1 | 0.1206 | 0.4085 | 315. | 0.0 | 3.0000 | |
| | | 2 | 0.0254 | 0.1576 | 315. | 0.0 | 1.0000 | |
| | | 3 | 0.1048 | 0.3067 | 315. | 0.0 | 1.0000 | |
| | | 4 | 0.3397 | 0.4744 | 315. | 0.0 | 1.0000 | |
| | | 5 | 0.6419 | 0.6803 | 315. | 0.0 | 4.0000 | |
| | | 6 | 0.3556 | 0.5502 | 315. | 0.0 | 2.0000 | |
| | | 7 | 0.2111 | 0.4594 | 315. | 0.0 | 2.0000 | |
| 234 | 0.6880 | | 11.2491 | 1.4527 | 344. | 7.4139 | 17.0012 | |
| | | 0 | NO VALUES RECORDED | | | | | |
| | | 1 | 0.0 | 0.0 | 344. | 0.0 | 0.0 | |
| | | 2 | 0.0 | 0.0 | 344. | 0.0 | 0.0 | |
| | | 3 | 0.0 | 0.0 | 344. | 0.0 | 0.0 | |
| | | 4 | 0.0 | 0.0 | 344. | 0.0 | 0.0 | |
| | | 5 | 0.0 | 0.0 | 344. | 0.0 | 0.0 | |
| | | 6 | 0.0 | 0.0 | 344. | 0.0 | 0.0 | |
| | | 7 | 0.0 | 0.0 | 344. | 0.0 | 0.0 | |
| 191 | 0.1060 | | 43.1775 | 0.3741 | 53. | 42.4739 | 44.1213 | |
| | | 1 | 0.0189 | 0.1374 | 53. | 0.0 | 1.0000 | |
| | | 2 | 0.0 | 0.0 | 53. | 0.0 | 0.0 | |
| | | 3 | 0.0943 | 0.2951 | 53. | 0.0 | 1.0000 | |
| | | 4 | 0.4906 | 0.5047 | 53. | 0.0 | 1.0000 | |
| | | 5 | 1.0755 | 0.2447 | 53. | 1.0000 | 2.0000 | |
| | | 6 | 1.0000 | 0.0 | 53. | 1.0000 | 1.0000 | |
| | | 7 | 0.6604 | 0.5001 | 53. | 0.0 | 2.0000 | |
| 190 | 0.0520 | | 40.2513 | 7.5274 | 26. | 29.6037 | 44.1477 | |
| | | 0 | NO VALUES RECORDED | | | | | |
| | | 1 | 0.0335 | 0.1961 | 26. | 0.0 | 1.0000 | |
| | | 2 | 0.0 | 0.0 | 26. | 0.0 | 0.0 | |
| | | 3 | 0.1923 | 0.4019 | 26. | 0.0 | 1.0000 | |
| | | 4 | 1.0000 | 0.0 | 26. | 1.0000 | 1.0000 | |
| | | 5 | 1.1154 | 0.3258 | 26. | 1.0000 | 2.0000 | |
| | | 6 | 1.0000 | 0.0 | 26. | 1.0000 | 1.0000 | |
| | | 7 | 0.6538 | 0.5616 | 26. | 0.0 | 2.0000 | |
| 189 | 0.0540 | | 40.2064 | 7.8779 | 27. | 25.7734 | 44.1123 | |
| | | 1 | 0.0 | 0.0 | 27. | 0.0 | 0.0 | |
| | | 2 | 0.0 | 0.0 | 27. | 0.0 | 0.0 | |
| | | 3 | 0.0 | 0.0 | 27. | 0.0 | 0.0 | |
| | | 4 | 0.0 | 0.0 | 27. | 0.0 | 0.0 | |
| | | 5 | 1.0370 | 0.1925 | 27. | 1.0000 | 2.0000 | |
| | | 6 | 1.0000 | 0.0 | 27. | 1.0000 | 1.0000 | |
| | | 7 | 0.3704 | 0.6293 | 27. | 0.0 | 2.0000 | |
| 186 | 0.5320 | | 91.1450 | 18.2232 | 266. | 75.3334 | 206.4550 | |
| | | 1 | 0.4398 | 0.7951 | 266. | 0.0 | 3.0000 | |
| | | 2 | 1.4173 | 0.7574 | 266. | 1.0000 | 4.0000 | |
| | | 3 | 0.6090 | 0.8150 | 266. | 0.0 | 4.0000 | |
| | | 4 | 2.0150 | 1.3231 | 266. | 1.0000 | 9.0000 | |
| | | 5 | 1.3233 | 0.6210 | 266. | 1.0000 | 4.0000 | |
| | | 6 | 1.4474 | 0.6494 | 266. | 1.0000 | 4.0000 | |
| | | 7 | 1.3947 | 0.6311 | 266. | 1.0000 | 4.0000 | |

| NODE | PROB./COUNT | | MEAN | STD.DEV. | VAR. 095. | MIN. | MAX. | |
|---|---|---|---|---|---|---|---|---|
| 185 | 0.4480 | | 2e+9836 | 2e+7457 | 234. | 3e+915 | 131e+11 | F |
| | | 1 | 0.0513 | 0.3551 | 23e. | 0.0 | | |
| | | 2 | 0.1496 | 0.e711 | 23e. | 0.0 | | |
| | | 3 | 0.0953 | 0.3635 | 23e. | 0.0 | | |
| | | 4 | 0.1e12 | 0.7362 | 23e. | 0.0 | | |
| | | 5 | 0.1741 | 0.5745 | 23e. | 0.0 | | |
| | | 6 | 0.1976 | 0.6902 | 23e. | 0.0 | | |
| | | 7 | 0.2607 | 0.5601 | 23e. | 0.0 | | |
| 188 | 0.0740 | | 45.3649 | 9.2117 | 37. | 3e+7571 | 71.6723 | F |
| | | 1 | 0.3514 | 0.6755 | 37. | 0.0 | | |
| | | 2 | 0.0911 | 0.3e3[illegible] | 37. | 0.0 | | |
| | | 3 | 0.2432 | 0.4354 | 37. | 0.0 | | |
| | | 4 | 0.5135 | 0.[illegible] | 37. | 0.0 | | |
| | | 5 | 1.1e22 | 0.7270 | 37. | 0.0 | | |
| | | 6 | 0.9135 | 0.5e66 | 37. | 0.0 | | |
| | | 7 | 1.0000 | 0.0 | 37. | 1.0000 | | |
| 179 | 0.6200 | | 47.4115 | 11.3652 | 310. | 23.7314 | 7e+541e | F |
| | | 1 | 0.4129 | 0.7947 | 310. | 0.0 | | |
| | | 2 | 0.2230 | 0.5112 | 310. | 0.0 | | |
| | | 3 | 0.2452 | 0.4800 | 310. | 0.0 | | |
| | | 4 | 0.6226 | 0.6557 | 310. | 0.0 | | |
| | | 5 | 1.0355 | 0.7029 | 310. | 0.0 | | |
| | | 6 | 0.9137 | 0.7192 | 310. | 0.0 | | |
| | | 7 | 1.3710 | 0.6151 | 310. | 1.0000 | | |
| 169 | 0.6700 | | 29.7933 | 9.6591 | 315. | 15.[illegible] | [illegible] | |
| | | 1 | 0.1126 | 0.3963 | 315. | 0.0 | | |
| | | 2 | 0.0753 | 0.1745 | 315. | 0.0 | | |
| | | 3 | 0.0943 | 0.2071 | 315. | 0.0 | | |
| | | 4 | 0.1194 | 0.3247 | 315. | 0.0 | | |
| | | 5 | 0.3226 | 0.5665 | 315. | 0.0 | | |
| | | 6 | 0.2239 | 0.5036 | 315. | 0.0 | | |
| | | 7 | 0.0 | 0.0 | 315. | 0.0 | 0.0 | |
| 145 | 0.5820 | | 75.6139 | 5.0e+7 | 291. | 6e+1e+9 | [illegible] | F |
| | | 1 | 0.4594 | 0.3330 | 291. | 0.0 | | |
| | | 2 | 0.0955 | 0.2521 | 291. | 0.0 | | |
| | | 3 | 0.e549 | 0.2556 | 291. | 0.0 | | |
| | | 4 | 1.6229 | 0.6946 | 291. | 0.0 | | |
| | | 5 | 1.3162 | 0.6126 | 291. | 1.0000 | | |
| | | 6 | 1.4433 | 0.6534 | 291. | 1.0000 | | |
| | | 7 | 1.3e77 | 0.6315 | 291. | 0.0 | | |
| 142 | 0.5920 | | 71.9833 | 25.7506 | 291. | 39.6126 | 193.3705 | F |
| | | 0 | NO VALUES RECORDED | | | | | |
| | | 1 | 0.3914 | 0.4915 | 291. | 0.0 | | |
| | | 2 | 1.6153 | 0.4955 | 291. | 1.0000 | | |
| | | 3 | 0.5567 | 0.6593 | 291. | 0.0 | | |
| | | 4 | 2.0369 | 1.3035 | 291. | 1.0000 | | |
| | | 5 | 1.3162 | 0.6121 | 291. | 1.0000 | | |
| | | 6 | 1.4296 | 0.6251 | 291. | 1.0000 | | |
| | | 7 | 1.1821 | 0.6741 | 291. | 0.0 | | |
| 141 | 0.0530 | | 60.4085 | 19.2840 | 25. | 39.6126 | 110.5313 | F |
| | | 0 | NO VALUES RECORDED | | | | | |
| | | 1 | 0.4330 | 0.7702 | 25. | 0.0 | | |
| | | 2 | 1.0000 | 0.0 | 25. | 1.0000 | | |
| | | 3 | 0.4400 | 0.5831 | 25. | 0.0 | | |
| | | 4 | 1.4400 | 0.9660 | 25. | 1.0000 | | |
| | | 5 | 1.2000 | 0.5000 | 25. | 1.0000 | | |
| | | 6 | 1.2400 | 0.4359 | 25. | 1.0000 | | |
| | | 7 | 0.9600 | 0.6110 | 25. | 0.0 | | |

| NODE | PROB./COUNT | | MEAN | STD.DEV. | VAR. 095. | MIN. | MAX. | |
|---|---|---|---|---|---|---|---|---|
| 116 | 0.0360 | | 47.e+77 | [illegible] | 11e. | 3e+[illegible] | [illegible] | |
| | | 1 | [illegible] | [illegible] | 15e. | [illegible] | [illegible] | |
| | | 2 | [illegible] | 0.2357 | 15e. | 0.0 | 1.0 | |
| | | 3 | 1.0000 | [illegible] | 15e. | 1.0 | 1.0 | |
| | | 4 | [illegible] | [illegible] | 15e. | [illegible] | [illegible] | |
| | | 5 | 1.1111 | [illegible] | 15e. | 1.0 | [illegible] | |
| | | 6 | 1.1667 | 0.3e35 | 15e. | 1.0000 | 2.0000 | |
| | | 7 | 0.8333 | 0.7959 | 15e. | 0.0 | 2.0000 | |
| 113 | 0.3160 | | 39.2407 | 6.4e+15 | 157. | 2e+83e5 | [illegible] | F |
| | | 1 | 0.0317 | [illegible] | 157. | [illegible] | [illegible] | |
| | | 2 | 0.0 | 0.0 | 157. | [illegible] | [illegible] | |
| | | 3 | 0.0 | 0.0 | 157. | [illegible] | [illegible] | |
| | | 4 | [illegible] | [illegible] | 157. | [illegible] | [illegible] | |
| | | 5 | 1.0000 | [illegible] | 157. | [illegible] | [illegible] | |
| | | 6 | [illegible] | [illegible] | 157. | [illegible] | [illegible] | |
| | | 7 | [illegible] | [illegible] | 157. | [illegible] | [illegible] | |
| 108 | 0.3200 | | 6.0092 | 2.7978 | 1e0. | 3.25e3 | 17.[illegible] | I |
| | | 1 | 0.0125 | 0.1115 | 1e0. | 0.0 | 1.0 | |
| | | 2 | 0.0 | 0.0 | 1e0. | 0.0 | 0.0 | |
| | | 3 | 0.0 | 0.0 | 1e0. | 0.0 | 0.0 | |
| | | 4 | [illegible] | [illegible] | 1e0. | [illegible] | [illegible] | |
| | | 5 | [illegible] | [illegible] | 1e0. | [illegible] | 1. | |
| | | 6 | [illegible] | [illegible] | 1e0. | [illegible] | 1. | |
| | | 7 | [illegible] | [illegible] | 1e0. | [illegible] | 1. | |
| 104 | [illegible] | | 13.[illegible] | [illegible] | 1e0. | [illegible] | [illegible] | I |
| | | 1 | 0.0 | 0.0 | 1e0. | [illegible] | [illegible] | |
| | | 2 | 0.0 | 0.0 | 1e0. | [illegible] | [illegible] | |
| | | 3 | 0.0 | 0.0 | 1e0. | [illegible] | [illegible] | |
| | | 4 | 0.0 | 0.0 | 1e0. | 0.0 | 0.0 | |
| | | 5 | [illegible] | [illegible] | 1e0. | [illegible] | [illegible] | |
| | | 6 | [illegible] | [illegible] | 1e0. | [illegible] | [illegible] | |
| | | 7 | [illegible] | [illegible] | 1e0. | [illegible] | [illegible] | |
| 50 | [illegible] | | [illegible] | [illegible] | [illegible] | [illegible] | [illegible] | I |
| | | 1 | [illegible] | [illegible] | [illegible] | [illegible] | [illegible] | |
| | | 2 | [illegible] | [illegible] | [illegible] | [illegible] | [illegible] | |
| | | 3 | [illegible] | [illegible] | [illegible] | [illegible] | [illegible] | |
| | | 4 | [illegible] | [illegible] | [illegible] | [illegible] | [illegible] | |
| | | 5 | [illegible] | [illegible] | [illegible] | [illegible] | [illegible] | |
| | | 6 | [illegible] | [illegible] | [illegible] | [illegible] | [illegible] | |
| | | 7 | [illegible] | [illegible] | [illegible] | [illegible] | [illegible] | |
| 68 | [illegible] | | [illegible] | [illegible] | [illegible] | [illegible] | [illegible] | |
| | | 1 | 0.0 | 0.0 | [illegible] | [illegible] | [illegible] | |
| | | 2 | 0.0 | 0.0 | [illegible] | [illegible] | [illegible] | |
| | | 3 | 0.0 | 0.0 | [illegible] | [illegible] | [illegible] | |
| | | 4 | 0.0 | 0.0 | [illegible] | 0.0 | 0.0 | |
| | | 5 | [illegible] | 0.0 | [illegible] | [illegible] | 1. | |
| | | 6 | [illegible] | [illegible] | [illegible] | [illegible] | [illegible] | |
| | | 7 | [illegible] | [illegible] | [illegible] | [illegible] | [illegible] | |

TIME STAT HISTOGRAM FOR NODE 68 ( REALIZATION OF EVENT 68 )

| OBSV FREQ | RELA FREQ | CUML FREQ | UPPER BOUND OF CELL |
|---|---|---|---|
| 0 | 0.0 | 0.0 | 12.00 |
| 0 | 0.0 | 0.0 | 13.00 |
| 0 | 0.0 | 0.0 | 14.00 |
| 0 | 0.0 | 0.0 | 15.00 |
| 0 | 0.0 | 0.0 | 16.00 |
| 0 | 0.0 | 0.0 | 17.00 |
| 0 | 0.0 | 0.0 | 18.00 |
| 0 | 0.0 | 0.0 | 19.00 |
| 0 | 0.0 | 0.0 | 20.00 |
| 0 | 0.0 | 0.0 | 21.00 |
| 1 | 0.023 | 0.023 | 22.00 |
| 1 | 0.023 | 0.045 | 23.00 |
| 1 | 0.023 | 0.068 | 24.00 |
| 1 | 0.023 | 0.091 | 25.00 |
| 2 | 0.045 | 0.136 | 26.00 |
| 0 | 0.0 | 0.136 | 27.00 |
| 0 | 0.0 | 0.136 | 28.00 |
| 1 | 0.023 | 0.159 | 29.00 |
| 4 | 0.091 | 0.250 | 30.00 |
| 2 | 0.045 | 0.295 | 31.00 |
| 5 | 0.114 | 0.409 | 32.00 |
| 2 | 0.045 | 0.455 | 33.00 |
| 3 | 0.068 | 0.523 | 34.00 |
| 1 | 0.023 | 0.545 | 35.00 |
| 2 | 0.045 | 0.591 | 36.00 |
| 1 | 0.023 | 0.614 | 37.00 |
| 4 | 0.091 | 0.705 | 38.00 |
| 0 | 0.0 | 0.705 | 39.00 |
| 2 | 0.045 | 0.750 | 40.00 |
| 2 | 0.045 | 0.795 | 41.00 |
| 1 | 0.023 | 0.818 | 42.00 |
| 8 | 0.182 | 1.000 | +INF |

TOTAL 44.

TIME STAT HISTOGRAM FOR NODE 90 ( REALIZATION OF EVENT 90 )

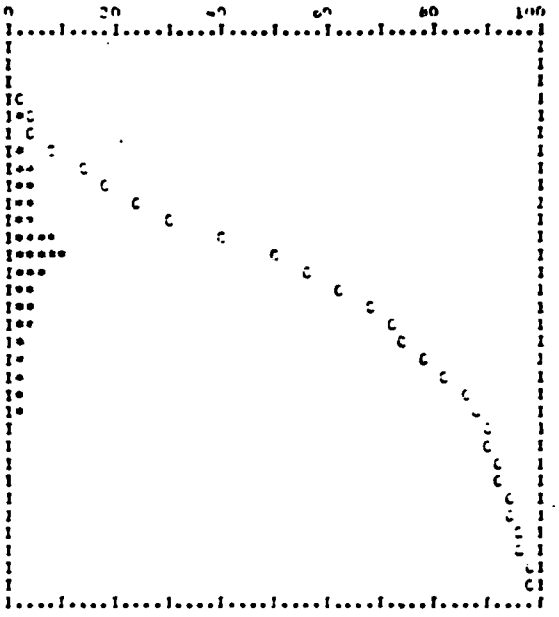
| OBSV FREQ | RELA FREQ | CUML FREQ | UPPER BOUND OF CELL |
|---|---|---|---|
| 0 | 0.0 | 0.0 | 37.00 |
| 0 | 0.0 | 0.0 | 38.00 |
| 0 | 0.0 | 0.0 | 39.00 |
| 0 | 0.0 | 0.0 | 40.00 |
| 0 | 0.0 | 0.0 | 41.00 |
| 0 | 0.0 | 0.0 | 42.00 |
| 0 | 0.0 | 0.0 | 43.00 |
| 0 | 0.0 | 0.0 | 44.00 |
| 0 | 0.0 | 0.0 | 45.00 |
| 0 | 0.0 | 0.0 | 46.00 |
| 0 | 0.0 | 0.0 | 47.00 |
| 0 | 0.0 | 0.0 | 48.00 |
| 0 | 0.0 | 0.0 | 49.00 |
| 0 | 0.0 | 0.0 | 50.00 |
| 0 | 0.0 | 0.0 | 51.00 |
| 0 | 0.0 | 0.0 | 52.00 |
| 0 | 0.0 | 0.0 | 53.00 |
| 0 | 0.0 | 0.0 | 54.00 |
| 0 | 0.0 | 0.0 | 55.00 |
| 0 | 0.0 | 0.0 | 56.00 |
| 0 | 0.0 | 0.0 | 57.00 |
| 0 | 0.0 | 0.0 | 58.00 |
| 0 | 0.0 | 0.0 | 59.00 |
| 0 | 0.0 | 0.0 | 60.00 |
| 0 | 0.0 | 0.0 | 61.00 |
| 0 | 0.0 | 0.0 | 62.00 |
| 0 | 0.0 | 0.0 | 63.00 |
| 0 | 0.0 | 0.0 | 64.00 |
| 291 | 1.000 | 1.000 | +INF |

TOTAL 291.

TIME STAT HISTOGRAM FOR NODE 113 ( REALIZATION OF EVENT 113 )

| OBSV FREQ | RELA FREQ | CUML FREQ | UPPER BOUND OF CELL |
|---|---|---|---|
| 0 | 0.0 | 0.0 | 25.00 |
| 0 | 0.0 | 0.0 | 26.00 |
| 3 | 0.019 | 0.019 | 27.00 |
| 1 | 0.006 | 0.025 | 28.00 |
| 4 | 0.025 | 0.051 | 29.00 |
| 1 | 0.006 | 0.057 | 30.00 |
| 4 | 0.025 | 0.083 | 31.00 |
| 9 | 0.057 | 0.140 | 32.00 |
| 9 | 0.057 | 0.197 | 33.00 |
| 8 | 0.051 | 0.248 | 34.00 |
| 9 | 0.057 | 0.306 | 35.00 |
| 15 | 0.096 | 0.401 | 36.00 |
| 16 | 0.102 | 0.503 | 37.00 |
| 12 | 0.076 | 0.580 | 38.00 |
| 8 | 0.051 | 0.631 | 39.00 |
| 8 | 0.051 | 0.682 | 40.00 |
| 7 | 0.045 | 0.726 | 41.00 |
| 5 | 0.032 | 0.759 | 42.00 |
| 6 | 0.038 | 0.796 | 43.00 |
| 6 | 0.038 | 0.834 | 44.00 |
| 5 | 0.032 | 0.866 | 45.00 |
| 4 | 0.025 | 0.892 | 46.00 |
| 2 | 0.013 | 0.904 | 47.00 |
| 2 | 0.013 | 0.917 | 48.00 |
| 2 | 0.013 | 0.930 | 49.00 |
| 0 | 0.0 | 0.930 | 50.00 |
| 3 | 0.019 | 0.949 | 51.00 |
| 0 | 0.0 | 0.949 | 52.00 |
| 2 | 0.013 | 0.962 | 53.00 |
| 0 | 0.0 | 0.962 | 54.00 |
| 3 | 0.019 | 0.981 | 55.00 |
| 3 | 0.019 | 1.000 | +INF |

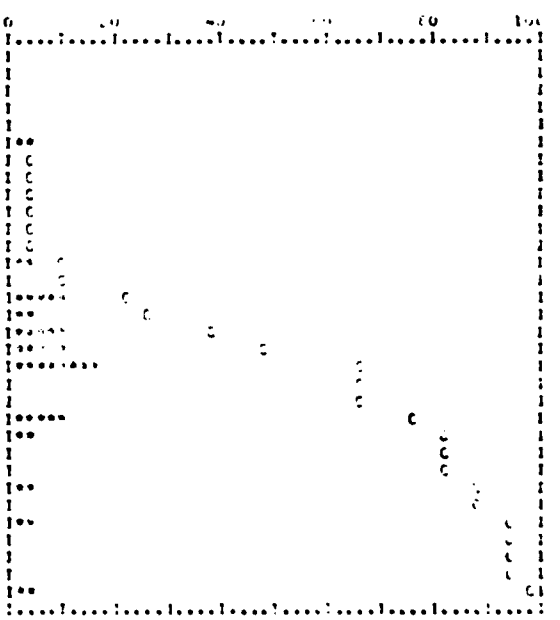
TOTAL 157.




TIME STAT HISTOGRAM FOR NODE 116 ( REALIZATION OF EVENT 116 )

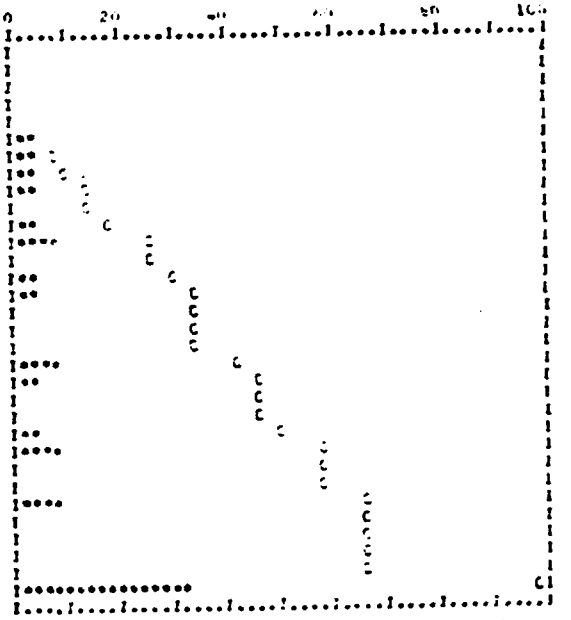
| OBSV FREQ | RELA FREQ | CUML FREQ | UPPER BOUND OF CELL |
|---|---|---|---|
| 0 | 0.0 | 0.0 | 30.00 |
| 0 | 0.0 | 0.0 | 31.00 |
| 0 | 0.0 | 0.0 | 32.00 |
| 0 | 0.0 | 0.0 | 33.00 |
| 0 | 0.0 | 0.0 | 34.00 |
| 1 | 0.056 | 0.056 | 35.00 |
| 0 | 0.0 | 0.056 | 36.00 |
| 0 | 0.0 | 0.056 | 37.00 |
| 0 | 0.0 | 0.056 | 38.00 |
| 0 | 0.0 | 0.056 | 39.00 |
| 0 | 0.0 | 0.056 | 40.00 |
| 0 | 0.0 | 0.056 | 41.00 |
| 1 | 0.056 | 0.111 | 42.00 |
| 0 | 0.0 | 0.111 | 43.00 |
| 2 | 0.111 | 0.222 | 44.00 |
| 1 | 0.056 | 0.278 | 45.00 |
| 2 | 0.111 | 0.389 | 46.00 |
| 2 | 0.111 | 0.500 | 47.00 |
| 3 | 0.167 | 0.667 | 48.00 |
| 0 | 0.0 | 0.667 | 49.00 |
| 0 | 0.0 | 0.667 | 50.00 |
| 2 | 0.111 | 0.778 | 51.00 |
| 1 | 0.056 | 0.833 | 52.00 |
| 0 | 0.0 | 0.833 | 53.00 |
| 0 | 0.0 | 0.833 | 54.00 |
| 1 | 0.056 | 0.889 | 55.00 |
| 0 | 0.0 | 0.889 | 56.00 |
| 1 | 0.056 | 0.944 | 57.00 |
| 0 | 0.0 | 0.944 | 58.00 |
| 0 | 0.0 | 0.944 | 59.00 |
| 0 | 0.0 | 0.944 | 60.00 |
| 1 | 0.056 | 1.000 | +INF |

TOTAL 18.



TIME STAT HISTOGRAM FOR NODE 141 ( REALIZATION OF EVENT 141 )

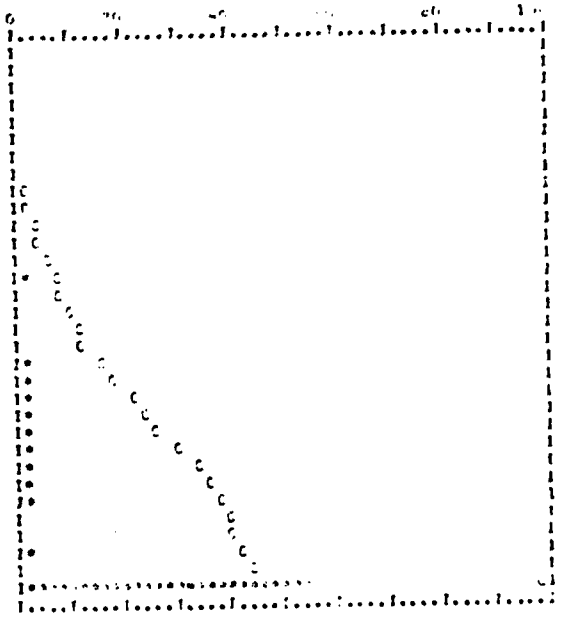
| OBSV FREQ | RELA FREQ | CUML FREQ | UPPER BOUND OF CELL |
|---|---|---|---|
| 0 | 0.0 | 0.0 | 33.00 |
| 0 | 0.0 | 0.0 | 34.00 |
| 0 | 0.0 | 0.0 | 37.00 |
| 0 | 0.0 | 0.0 | 38.00 |
| 0 | 0.0 | 0.0 | 39.00 |
| 1 | 0.040 | 0.040 | 40.00 |
| 1 | 0.040 | 0.080 | 41.00 |
| 1 | 0.040 | 0.120 | 42.00 |
| 1 | 0.040 | 0.160 | 43.00 |
| 0 | 0.0 | 0.160 | 44.00 |
| 1 | 0.040 | 0.200 | 45.00 |
| 2 | 0.080 | 0.280 | 46.00 |
| 0 | 0.0 | 0.280 | 47.00 |
| 1 | 0.040 | 0.320 | 48.00 |
| 1 | 0.040 | 0.360 | 49.00 |
| 0 | 0.0 | 0.360 | 50.00 |
| 0 | 0.0 | 0.360 | 51.00 |
| 0 | 0.0 | 0.360 | 52.00 |
| 2 | 0.080 | 0.440 | 53.00 |
| 1 | 0.040 | 0.480 | 54.00 |
| 0 | 0.0 | 0.480 | 55.00 |
| 0 | 0.0 | 0.480 | 56.00 |
| 1 | 0.040 | 0.520 | 57.00 |
| 2 | 0.080 | 0.600 | 58.00 |
| 0 | 0.0 | 0.600 | 59.00 |
| 0 | 0.0 | 0.600 | 60.00 |
| 2 | 0.080 | 0.680 | 61.00 |
| 0 | 0.0 | 0.680 | 62.00 |
| 0 | 0.0 | 0.680 | 63.00 |
| 0 | 0.0 | 0.680 | 64.00 |
| 0 | 0.0 | 0.680 | 65.00 |
| 8 | 0.320 | 1.000 | +INF |




TOTAL 25.

TIME STAT HISTOGRAM FOR NODE 142 ( REALIZATION OF EVENT 142 )

| OBSV FREQ | RELA FREQ | CUML FREQ | UPPER BOUND OF CELL |
|---|---|---|---|
| 0 | 0.0 | 0.0 | 33.00 |
| 0 | 0.0 | 0.0 | 34.00 |
| 0 | 0.0 | 0.0 | 37.00 |
| 0 | 0.0 | 0.0 | 38.00 |
| 0 | 0.0 | 0.0 | 39.00 |
| 1 | 0.003 | 0.003 | 40.00 |
| 2 | 0.007 | 0.010 | 41.00 |
| 2 | 0.007 | 0.017 | 42.00 |
| 3 | 0.010 | 0.027 | 43.00 |
| 3 | 0.010 | 0.038 | 44.00 |
| 3 | 0.010 | 0.048 | 45.00 |
| 3 | 0.010 | 0.059 | 46.00 |
| 2 | 0.007 | 0.065 | 47.00 |
| 6 | 0.021 | 0.086 | 48.00 |
| 1 | 0.003 | 0.089 | 49.00 |
| 4 | 0.014 | 0.103 | 50.00 |
| 5 | 0.017 | 0.120 | 51.00 |
| 5 | 0.017 | 0.137 | 52.00 |
| 8 | 0.027 | 0.165 | 53.00 |
| 10 | 0.034 | 0.199 | 54.00 |
| 7 | 0.024 | 0.223 | 55.00 |
| 8 | 0.027 | 0.251 | 56.00 |
| 6 | 0.021 | 0.271 | 57.00 |
| 9 | 0.031 | 0.302 | 58.00 |
| 11 | 0.038 | 0.340 | 59.00 |
| 7 | 0.024 | 0.364 | 60.00 |
| 8 | 0.027 | 0.392 | 61.00 |
| 5 | 0.017 | 0.409 | 62.00 |
| 3 | 0.010 | 0.419 | 63.00 |
| 6 | 0.021 | 0.440 | 64.00 |
| 7 | 0.017 | 0.457 | 65.00 |
| 156 | 0.543 | 1.000 | +INF |




TOTAL 291.

TIME STAT HISTOGRAM FOR NODE 145 ( REALIZATION OF EVENT 145 )

| OBSV FREQ | RELA FREQ | CUML FREQ | UPPER BOUND OF CELL |
|---|---|---|---|
| 0 | 0.0 | 0.0 | 35.00 |
| 0 | 0.0 | 0.0 | 36.00 |
| 0 | 0.0 | 0.0 | 37.00 |
| 0 | 0.0 | 0.0 | 38.00 |
| 0 | 0.0 | 0.0 | 39.00 |
| 0 | 0.0 | 0.0 | 40.00 |
| 0 | 0.0 | 0.0 | 41.00 |
| 0 | 0.0 | 0.0 | 42.00 |
| 0 | 0.0 | 0.0 | 43.00 |
| 0 | 0.0 | 0.0 | 44.00 |
| 0 | 0.0 | 0.0 | 45.00 |
| 0 | 0.0 | 0.0 | 46.00 |
| 0 | 0.0 | 0.0 | 47.00 |
| 0 | 0.0 | 0.0 | 48.00 |
| 0 | 0.0 | 0.0 | 49.00 |
| 0 | 0.0 | 0.0 | 50.00 |
| 0 | 0.0 | 0.0 | 51.00 |
| 0 | 0.0 | 0.0 | 52.00 |
| 0 | 0.0 | 0.0 | 53.00 |
| 0 | 0.0 | 0.0 | 54.00 |
| 0 | 0.0 | 0.0 | 55.00 |
| 0 | 0.0 | 0.0 | 56.00 |
| 0 | 0.0 | 0.0 | 57.00 |
| 0 | 0.0 | 0.0 | 58.00 |
| 0 | 0.0 | 0.0 | 59.00 |
| 0 | 0.0 | 0.0 | 60.00 |
| 0 | 0.0 | 0.0 | 61.00 |
| 0 | 0.0 | 0.0 | 62.00 |
| 0 | 0.0 | 0.0 | 63.00 |
| 0 | 0.0 | 0.0 | 64.00 |
| 2 | 0.007 | 0.007 | 65.00 |
| 289 | 0.993 | 1.000 | +INF |

TOTAL 291.

TIME STAT HISTOGRAM FOR NODE 169 ( REALIZATION OF EVENT 169 )

| OBSV FREQ | RELA FREQ | CUML FREQ | UPPER BOUND OF CELL |
|---|---|---|---|
| 0 | 0.0 | 0.0 | 15.00 |
| 2 | 0.006 | 0.006 | 16.00 |
| 10 | 0.030 | 0.036 | 17.00 |
| 17 | 0.051 | 0.087 | 18.00 |
| 17 | 0.051 | 0.137 | 19.00 |
| 15 | 0.045 | 0.182 | 20.00 |
| 16 | 0.048 | 0.230 | 21.00 |
| 10 | 0.030 | 0.260 | 22.00 |
| 19 | 0.054 | 0.313 | 23.00 |
| 18 | 0.054 | 0.367 | 24.00 |
| 23 | 0.069 | 0.436 | 25.00 |
| 25 | 0.075 | 0.511 | 26.00 |
| 18 | 0.054 | 0.565 | 27.00 |
| 6 | 0.018 | 0.583 | 28.00 |
| 9 | 0.027 | 0.610 | 29.00 |
| 4 | 0.012 | 0.622 | 30.00 |
| 13 | 0.039 | 0.661 | 31.00 |
| 10 | 0.030 | 0.691 | 32.00 |
| 10 | 0.030 | 0.721 | 33.00 |
| 8 | 0.024 | 0.745 | 34.00 |
| 9 | 0.027 | 0.772 | 35.00 |
| 3 | 0.009 | 0.781 | 36.00 |
| 10 | 0.030 | 0.811 | 37.00 |
| 5 | 0.015 | 0.826 | 38.00 |
| 11 | 0.033 | 0.859 | 39.00 |
| 3 | 0.009 | 0.868 | 40.00 |
| 5 | 0.015 | 0.883 | 41.00 |
| 0 | 0.0 | 0.883 | 42.00 |
| 3 | 0.009 | 0.892 | 43.00 |
| 6 | 0.018 | 0.910 | 44.00 |
| 4 | 0.012 | 0.922 | 45.00 |
| 27 | 0.078 | 1.000 | +INF |

TOTAL 337.

TIME STAT HISTOGRAM FOR NODE 179 ( REALIZATION OF EVENT 179 )

| OBSV FREQ | RELA FREQ | CUML FREQ | UPPER EQUIV OF CELL |
|---|---|---|---|
| 0 | 0.0 | 0.0 | 25.00 |
| 0 | 0.0 | 0.0 | 26.00 |
| 0 | 0.0 | 0.0 | 27.00 |
| 0 | 0.0 | 0.0 | 28.00 |
| 1 | 0.003 | 0.003 | 29.00 |
| 4 | 0.013 | 0.016 | 30.00 |
| 6 | 0.019 | 0.035 | 31.00 |
| 5 | 0.016 | 0.052 | 32.00 |
| 10 | 0.032 | 0.084 | 33.00 |
| 0 | 0.0 | 0.084 | 34.00 |
| 4 | 0.013 | 0.097 | 35.00 |
| 11 | 0.035 | 0.132 | 36.00 |
| 19 | 0.061 | 0.194 | 37.00 |
| 14 | 0.045 | 0.239 | 38.00 |
| 6 | 0.019 | 0.258 | 39.00 |
| 15 | 0.048 | 0.306 | 40.00 |
| 7 | 0.023 | 0.329 | 41.00 |
| 9 | 0.029 | 0.358 | 42.00 |
| 14 | 0.045 | 0.403 | 43.00 |
| 13 | 0.042 | 0.445 | 44.00 |
| 10 | 0.032 | 0.477 | 45.00 |
| 18 | 0.058 | 0.535 | 46.00 |
| 7 | 0.023 | 0.558 | 47.00 |
| 7 | 0.023 | 0.581 | 48.00 |
| 8 | 0.026 | 0.606 | 49.00 |
| 7 | 0.023 | 0.629 | 50.00 |
| 8 | 0.026 | 0.655 | 51.00 |
| 13 | 0.042 | 0.697 | 52.00 |
| 3 | 0.010 | 0.706 | 53.00 |
| 7 | 0.023 | 0.729 | 54.00 |
| 6 | 0.019 | 0.748 | 55.00 |
| 78 | 0.252 | 1.000 | +INF |

TOTAL 310.

TIME STAT HISTOGRAM FOR NODE 180 ( REALIZATION OF EVENT 180 )

| OBSV FREQ | RELA FREQ | CUML FREQ | UPPER EQUIV OF CELL |
|---|---|---|---|
| 0 | 0.0 | 0.0 | 25.00 |
| 0 | 0.0 | 0.0 | 26.00 |
| 0 | 0.0 | 0.0 | 27.00 |
| 0 | 0.0 | 0.0 | 28.00 |
| 0 | 0.0 | 0.0 | 29.00 |
| 0 | 0.0 | 0.0 | 30.00 |
| 1 | 0.027 | 0.027 | 31.00 |
| 1 | 0.027 | 0.054 | 32.00 |
| 1 | 0.027 | 0.081 | 33.00 |
| 0 | 0.0 | 0.081 | 34.00 |
| 0 | 0.0 | 0.081 | 35.00 |
| 1 | 0.027 | 0.108 | 36.00 |
| 4 | 0.108 | 0.216 | 37.00 |
| 2 | 0.054 | 0.270 | 38.00 |
| 2 | 0.054 | 0.324 | 39.00 |
| 2 | 0.054 | 0.378 | 40.00 |
| 0 | 0.0 | 0.378 | 41.00 |
| 1 | 0.027 | 0.405 | 42.00 |
| 0 | 0.0 | 0.405 | 43.00 |
| 2 | 0.054 | 0.459 | 44.00 |
| 1 | 0.027 | 0.486 | 45.00 |
| 4 | 0.108 | 0.595 | 46.00 |
| 0 | 0.0 | 0.595 | 47.00 |
| 0 | 0.0 | 0.595 | 48.00 |
| 3 | 0.081 | 0.676 | 49.00 |
| 2 | 0.054 | 0.730 | 50.00 |
| 1 | 0.027 | 0.757 | 51.00 |
| 2 | 0.054 | 0.811 | 52.00 |
| 0 | 0.0 | 0.811 | 53.00 |
| 1 | 0.027 | 0.838 | 54.00 |
| 1 | 0.027 | 0.865 | 55.00 |
| 5 | 0.135 | 1.000 | +INF |

TOTAL 37.

TIME STAT HISTOGRAM FOR NODE 185 ( REALIZATION OF EVENT 185 )

| OBSV FREQ | RELA FREQ | CUML FREQ | UPPER BOUND OF CELL |
|---|---|---|---|
| 0 | 0.0 | 0.0 | 5.00 |
| 0 | 0.0 | 0.0 | 8.00 |
| 75 | 0.321 | 0.321 | 11.00 |
| 79 | 0.338 | 0.658 | 14.00 |
| 2 | 0.009 | 0.667 | 17.00 |
| 0 | 0.0 | 0.667 | 20.00 |
| 0 | 0.0 | 0.667 | 23.00 |
| 0 | 0.0 | 0.667 | 26.00 |
| 2 | 0.009 | 0.675 | 29.00 |
| 2 | 0.009 | 0.684 | 32.00 |
| 6 | 0.026 | 0.709 | 35.00 |
| 7 | 0.030 | 0.739 | 38.00 |
| 6 | 0.026 | 0.765 | 41.00 |
| 8 | 0.034 | 0.799 | 44.00 |
| 4 | 0.017 | 0.816 | 47.00 |
| 4 | 0.017 | 0.833 | 50.00 |
| 7 | 0.030 | 0.863 | 53.00 |
| 3 | 0.013 | 0.876 | 56.00 |
| 2 | 0.009 | 0.885 | 59.00 |
| 2 | 0.009 | 0.893 | 62.00 |
| 0 | 0.0 | 0.893 | 65.00 |
| 0 | 0.0 | 0.893 | 68.00 |
| 0 | 0.0 | 0.893 | 71.00 |
| 1 | 0.004 | 0.897 | 74.00 |
| 2 | 0.009 | 0.906 | 77.00 |
| 3 | 0.013 | 0.919 | 80.00 |
| 2 | 0.009 | 0.927 | 83.00 |
| 5 | 0.021 | 0.949 | 86.00 |
| 3 | 0.013 | 0.962 | 89.00 |
| 1 | 0.004 | 0.966 | 92.00 |
| 1 | 0.004 | 0.970 | 95.00 |
| 7 | 0.030 | 1.000 | +INF |

TOTAL 234.

TIME STAT HISTOGRAM FOR NODE 186 ( REALIZATION OF EVENT 186 )

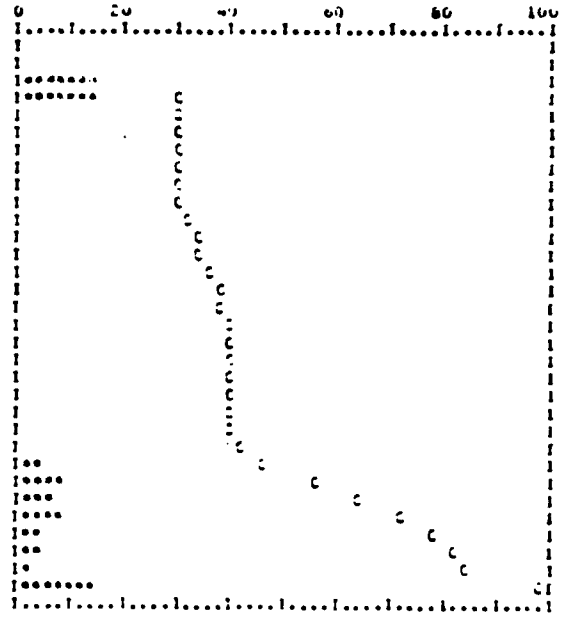
| OBSV FREQ | RELA FREQ | CUML FREQ | UPPER BOUND OF CELL |
|---|---|---|---|
| 0 | 0.0 | 0.0 | 35.00 |
| 0 | 0.0 | 0.0 | 38.00 |
| 0 | 0.0 | 0.0 | 41.00 |
| 0 | 0.0 | 0.0 | 44.00 |
| 0 | 0.0 | 0.0 | 47.00 |
| 0 | 0.0 | 0.0 | 50.00 |
| 0 | 0.0 | 0.0 | 53.00 |
| 0 | 0.0 | 0.0 | 56.00 |
| 0 | 0.0 | 0.0 | 59.00 |
| 0 | 0.0 | 0.0 | 62.00 |
| 0 | 0.0 | 0.0 | 65.00 |
| 0 | 0.0 | 0.0 | 68.00 |
| 0 | 0.0 | 0.0 | 71.00 |
| 0 | 0.0 | 0.0 | 74.00 |
| 0 | 0.0 | 0.0 | 77.00 |
| 0 | 0.0 | 0.0 | 80.00 |
| 0 | 0.0 | 0.0 | 83.00 |
| 0 | 0.0 | 0.0 | 86.00 |
| 0 | 0.0 | 0.0 | 89.00 |
| 0 | 0.0 | 0.0 | 92.00 |
| 0 | 0.0 | 0.0 | 95.00 |
| 0 | 0.0 | 0.0 | 98.00 |
| 0 | 0.0 | 0.0 | 101.00 |
| 0 | 0.0 | 0.0 | 104.00 |
| 0 | 0.0 | 0.0 | 107.00 |
| 0 | 0.0 | 0.0 | 110.00 |
| 0 | 0.0 | 0.0 | 113.00 |
| 0 | 0.0 | 0.0 | 116.00 |
| 0 | 0.0 | 0.0 | 119.00 |
| 0 | 0.0 | 0.0 | 122.00 |
| 0 | 0.0 | 0.0 | 125.00 |
| 0 | 0.0 | 0.0 | 128.00 |
| 0 | 0.0 | 0.0 | 131.00 |
| 0 | 0.0 | 0.0 | 134.00 |
| 0 | 0.0 | 0.0 | 137.00 |
| 0 | 0.0 | 0.0 | 140.00 |
| 0 | 0.0 | 0.0 | 143.00 |
| 0 | 0.0 | 0.0 | 146.00 |
| 0 | 0.0 | 0.0 | 149.00 |
| 0 | 0.0 | 0.0 | 152.00 |
| 0 | 0.0 | 0.0 | 155.00 |
| 0 | 0.0 | 0.0 | 158.00 |
| 0 | 0.0 | 0.0 | 161.00 |
| 0 | 0.0 | 0.0 | 164.00 |
| 0 | 0.0 | 0.0 | 167.00 |
| 0 | 0.0 | 0.0 | 170.00 |
| 0 | 0.0 | 0.0 | 173.00 |
| 0 | 0.0 | 0.0 | 176.00 |
| 0 | 0.0 | 0.0 | 179.00 |
| 0 | 0.0 | 0.0 | 182.00 |
| 0 | 0.0 | 0.0 | 185.00 |
| 0 | 0.0 | 0.0 | 188.00 |
| 0 | 0.0 | 0.0 | 191.00 |
| 0 | 0.0 | 0.0 | 194.00 |
| 0 | 0.0 | 0.0 | 197.00 |
| 0 | 0.0 | 0.0 | 200.00 |
| 266 | 1.000 | 1.000 | +INF |

TOTAL 266.

TIME STAT HISTOGRAM FOR NODE 187 ( REALIZATION OF THE NETWORK )

| OBSV FREQ | RELA FREQ | CUML FREQ | UPPER BOUND OF CELL |
|---|---|---|---|
| 0 | 0.0 | 0.0 | 5.00 |
| 0 | 0.0 | 0.0 | 8.00 |
| 75 | 0.150 | 0.150 | 11.00 |
| 79 | 0.158 | 0.308 | 14.00 |
| 2 | 0.004 | 0.312 | 17.00 |
| 0 | 0.0 | 0.312 | 20.00 |
| 0 | 0.0 | 0.312 | 23.00 |
| 0 | 0.0 | 0.312 | 26.00 |
| 2 | 0.004 | 0.316 | 29.00 |
| 2 | 0.004 | 0.320 | 32.00 |
| 6 | 0.012 | 0.332 | 35.00 |
| 7 | 0.014 | 0.346 | 38.00 |
| 6 | 0.012 | 0.358 | 41.00 |
| 8 | 0.016 | 0.374 | 44.00 |
| 4 | 0.008 | 0.382 | 47.00 |
| 4 | 0.008 | 0.390 | 50.00 |
| 7 | 0.014 | 0.404 | 53.00 |
| 3 | 0.006 | 0.410 | 56.00 |
| 2 | 0.004 | 0.414 | 59.00 |
| 2 | 0.004 | 0.418 | 62.00 |
| 0 | 0.0 | 0.418 | 65.00 |
| 0 | 0.0 | 0.418 | 68.00 |
| 1 | 0.002 | 0.420 | 71.00 |
| 9 | 0.018 | 0.438 | 74.00 |
| 21 | 0.042 | 0.479 | 77.00 |
| 47 | 0.094 | 0.572 | 80.00 |
| 39 | 0.078 | 0.650 | 83.00 |
| 41 | 0.082 | 0.732 | 86.00 |
| 25 | 0.050 | 0.782 | 89.00 |
| 21 | 0.042 | 0.824 | 92.00 |
| 17 | 0.034 | 0.858 | 95.00 |
| 71 | 0.142 | 1.000 | +INF |

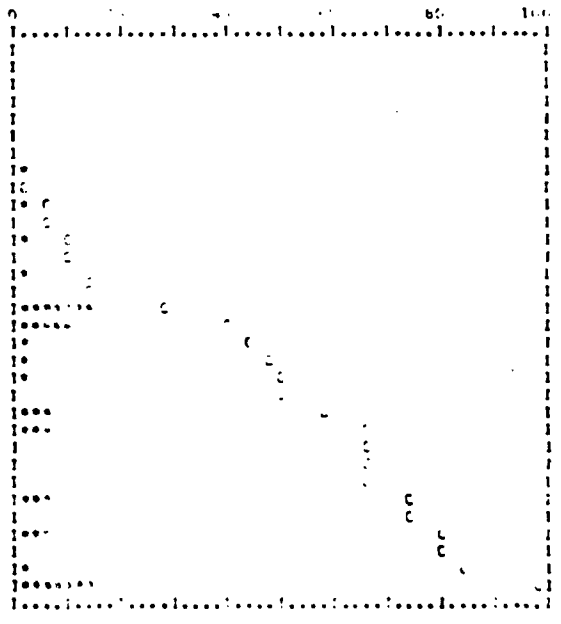
TOTAL 500.




TIME STAT HISTOGRAM FOR NODE 189 ( REALIZATION OF EVENT 189 )

| OBSV FREQ | RELA FREQ | CUML FREQ | UPPER BOUND OF CELL |
|---|---|---|---|
| 0 | 0.0 | 0.0 | 5.00 |
| 0 | 0.0 | 0.0 | 11.00 |
| 0 | 0.0 | 0.0 | 17.00 |
| 0 | 0.0 | 0.0 | 23.00 |
| 0 | 0.0 | 0.0 | 29.00 |
| 0 | 0.0 | 0.0 | 35.00 |
| 1 | 0.037 | 0.037 | 41.00 |
| 0 | 0.0 | 0.037 | 47.00 |
| 1 | 0.037 | 0.074 | 53.00 |
| 0 | 0.0 | 0.074 | 59.00 |
| 1 | 0.037 | 0.111 | 65.00 |
| 0 | 0.0 | 0.111 | 71.00 |
| 1 | 0.037 | 0.148 | 77.00 |
| 0 | 0.0 | 0.148 | 83.00 |
| 4 | 0.148 | 0.296 | 89.00 |
| 3 | 0.111 | 0.407 | 95.00 |
| 1 | 0.037 | 0.444 | 101.00 |
| 1 | 0.037 | 0.481 | 107.00 |
| 1 | 0.037 | 0.519 | 113.00 |
| 0 | 0.0 | 0.519 | 119.00 |
| 2 | 0.074 | 0.593 | 125.00 |
| 2 | 0.074 | 0.667 | 131.00 |
| 0 | 0.0 | 0.667 | 137.00 |
| 0 | 0.0 | 0.667 | 143.00 |
| 0 | 0.0 | 0.667 | 149.00 |
| 2 | 0.074 | 0.741 | 155.00 |
| 0 | 0.0 | 0.741 | 161.00 |
| 2 | 0.074 | 0.815 | 167.00 |
| 0 | 0.0 | 0.815 | 173.00 |
| 1 | 0.037 | 0.852 | 179.00 |
| 4 | 0.148 | 1.000 | +INF |

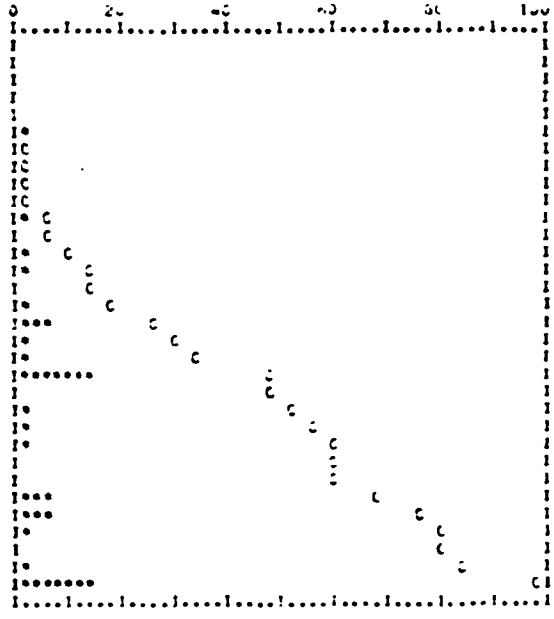
TOTAL 27.



TIME STAT HISTOGRAM FOR NODE 190 ( REALIZATION OF EVENT 190 )

| OBSV FREQ | RELA FREQ | CUML FREQ | UPPER BOUND OF CELL |
|---|---|---|---|
| 0 | 0.0 | 0.0 | 25.00 |
| 0 | 0.0 | 0.0 | 26.00 |
| 0 | 0.0 | 0.0 | 27.00 |
| 0 | 0.0 | 0.0 | 28.00 |
| 0 | 0.0 | 0.0 | 29.00 |
| 1 | 0.038 | 0.038 | 30.00 |
| 0 | 0.0 | 0.038 | 31.00 |
| 0 | 0.0 | 0.038 | 32.00 |
| 0 | 0.0 | 0.038 | 33.00 |
| 0 | 0.0 | 0.038 | 34.00 |
| 1 | 0.038 | 0.077 | 35.00 |
| 0 | 0.0 | 0.077 | 36.00 |
| 1 | 0.038 | 0.115 | 37.00 |
| 1 | 0.038 | 0.154 | 38.00 |
| 0 | 0.0 | 0.154 | 39.00 |
| 1 | 0.038 | 0.192 | 40.00 |
| 2 | 0.077 | 0.269 | 41.00 |
| 1 | 0.038 | 0.308 | 42.00 |
| 1 | 0.038 | 0.346 | 43.00 |
| 4 | 0.154 | 0.500 | 44.00 |
| 0 | 0.0 | 0.500 | 45.00 |
| 1 | 0.038 | 0.538 | 46.00 |
| 1 | 0.038 | 0.577 | 47.00 |
| 1 | 0.038 | 0.615 | 48.00 |
| 0 | 0.0 | 0.615 | 49.00 |
| 0 | 0.0 | 0.615 | 50.00 |
| 2 | 0.077 | 0.692 | 51.00 |
| 2 | 0.077 | 0.769 | 52.00 |
| 1 | 0.038 | 0.808 | 53.00 |
| 0 | 0.0 | 0.808 | 54.00 |
| 1 | 0.038 | 0.846 | 55.00 |
| 4 | 0.154 | 1.000 | +INF |

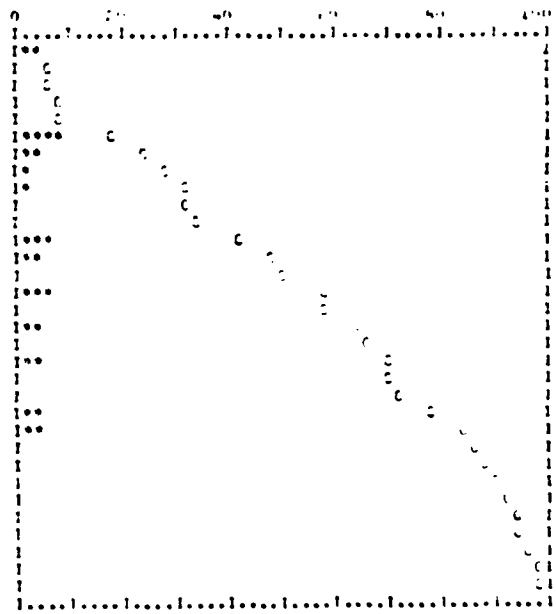
TOTAL 26.



TIME STAT HISTOGRAM FOR NODE 191 ( REALIZATION OF EVENT 191 )

| OBSV FREQ | RELA FREQ | CUML FREQ | UPPER BOUND OF CELL |
|---|---|---|---|
| 3 | 0.057 | 0.057 | 30.00 |
| 1 | 0.019 | 0.075 | 31.00 |
| 0 | 0.0 | 0.075 | 32.00 |
| 1 | 0.019 | 0.094 | 33.00 |
| 0 | 0.0 | 0.094 | 34.00 |
| 5 | 0.094 | 0.189 | 35.00 |
| 3 | 0.057 | 0.245 | 36.00 |
| 2 | 0.038 | 0.283 | 37.00 |
| 2 | 0.038 | 0.321 | 38.00 |
| 1 | 0.019 | 0.340 | 39.00 |
| 1 | 0.019 | 0.358 | 40.00 |
| 4 | 0.075 | 0.434 | 41.00 |
| 3 | 0.057 | 0.491 | 42.00 |
| 1 | 0.019 | 0.509 | 43.00 |
| 4 | 0.075 | 0.585 | 44.00 |
| 0 | 0.0 | 0.585 | 45.00 |
| 3 | 0.057 | 0.642 | 46.00 |
| 1 | 0.019 | 0.660 | 47.00 |
| 3 | 0.057 | 0.717 | 48.00 |
| 0 | 0.0 | 0.717 | 49.00 |
| 1 | 0.019 | 0.736 | 50.00 |
| 3 | 0.057 | 0.792 | 51.00 |
| 3 | 0.057 | 0.849 | 52.00 |
| 1 | 0.019 | 0.868 | 53.00 |
| 1 | 0.019 | 0.887 | 54.00 |
| 1 | 0.019 | 0.906 | 55.00 |
| 1 | 0.019 | 0.925 | 56.00 |
| 1 | 0.019 | 0.943 | 57.00 |
| 0 | 0.0 | 0.943 | 58.00 |
| 1 | 0.019 | 0.962 | 59.00 |
| 1 | 0.019 | 0.981 | 60.00 |
| 1 | 0.019 | 1.000 | +INF |

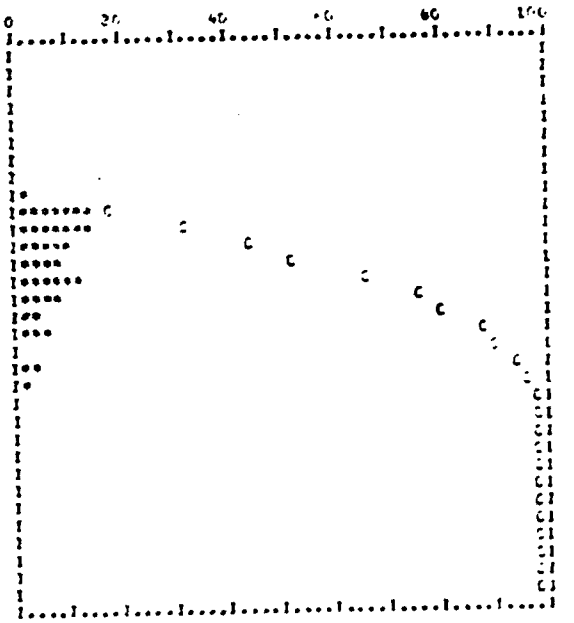
TOTAL 53.



TIME STAT HISTOGRAM FOR NODE 104 ( PART OF THE NETWORK BETWEEN NODES 104 AND 94 )

| OBSV FREQ | RELA FREQ | CUML FREQ | UPPER BOUND OF CELL |
|---|---|---|---|
| 0 | 0.0 | 0.0 | 1.00 |
| 0 | 0.0 | 0.0 | 2.00 |
| 0 | 0.0 | 0.0 | 3.00 |
| 0 | 0.0 | 0.0 | 4.00 |
| 0 | 0.0 | 0.0 | 5.00 |
| 0 | 0.0 | 0.0 | 6.00 |
| 0 | 0.0 | 0.0 | 7.00 |
| 0 | 0.0 | 0.0 | 8.00 |
| 5 | 0.031 | 0.031 | 9.00 |
| 24 | 0.150 | 0.181 | 10.00 |
| 24 | 0.150 | 0.331 | 11.00 |
| 18 | 0.112 | 0.444 | 12.00 |
| 13 | 0.081 | 0.525 | 13.00 |
| 22 | 0.137 | 0.662 | 14.00 |
| 16 | 0.100 | 0.762 | 15.00 |
| 8 | 0.050 | 0.812 | 16.00 |
| 12 | 0.075 | 0.887 | 17.00 |
| 3 | 0.019 | 0.906 | 18.00 |
| 7 | 0.044 | 0.950 | 19.00 |
| 4 | 0.025 | 0.975 | 20.00 |
| 1 | 0.006 | 0.981 | 21.00 |
| 2 | 0.012 | 0.994 | 22.00 |
| 0 | 0.0 | 0.994 | 23.00 |
| 0 | 0.0 | 0.994 | 24.00 |
| 1 | 0.006 | 1.000 | 25.00 |
| 0 | 0.0 | 1.000 | 26.00 |
| 0 | 0.0 | 1.000 | 27.00 |
| 0 | 0.0 | 1.000 | 28.00 |
| 0 | 0.0 | 1.000 | 29.00 |
| 0 | 0.0 | 1.000 | 30.00 |
| 0 | 0.0 | 1.000 | 31.00 |
| 0 | 0.0 | 1.000 | +INF |

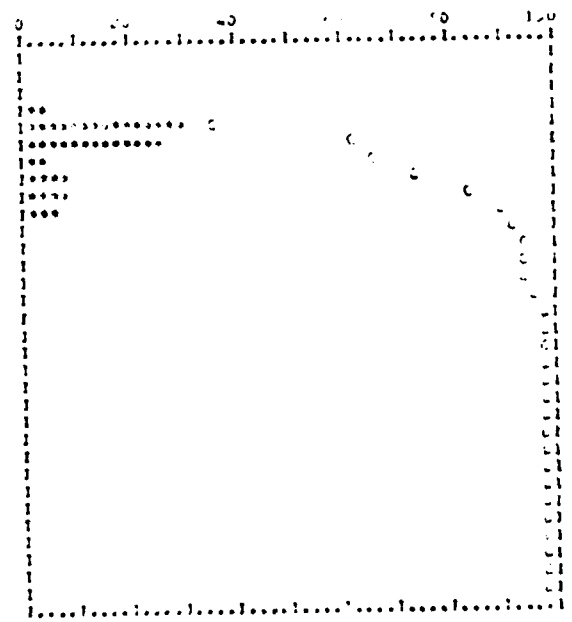
TOTAL 160.




TIME STAT HISTOGRAM FOR NODE 108 ( PART OF THE NETWORK BETWEEN NODES 146 AND 108 )

| OBSV FREQ | RELA FREQ | CUML FREQ | UPPER BOUND OF CELL |
|---|---|---|---|
| 0 | 0.0 | 0.0 | 1.00 |
| 0 | 0.0 | 0.0 | 2.00 |
| 0 | 0.0 | 0.0 | 3.00 |
| 3 | 0.050 | 0.050 | 4.00 |
| 50 | 0.333 | 0.382 | 5.00 |
| 42 | 0.262 | 0.645 | 6.00 |
| 7 | 0.044 | 0.689 | 7.00 |
| 13 | 0.081 | 0.770 | 8.00 |
| 14 | 0.100 | 0.870 | 9.00 |
| 11 | 0.069 | 0.939 | 10.00 |
| 3 | 0.019 | 0.957 | 11.00 |
| 1 | 0.006 | 0.963 | 12.00 |
| 0 | 0.0 | 0.963 | 13.00 |
| 2 | 0.013 | 0.976 | 14.00 |
| 3 | 0.019 | 0.995 | 15.00 |
| 1 | 0.006 | 0.981 | 16.00 |
| 2 | 0.013 | 0.994 | 17.00 |
| 1 | 0.006 | 1.000 | 18.00 |
| 0 | 0.0 | 1.000 | 19.00 |
| 0 | 0.0 | 1.000 | 20.00 |
| 0 | 0.0 | 1.000 | 21.00 |
| 0 | 0.0 | 1.000 | 22.00 |
| 0 | 0.0 | 1.000 | 23.00 |
| 0 | 0.0 | 1.000 | 24.00 |
| 0 | 0.0 | 1.000 | 25.00 |
| 0 | 0.0 | 1.000 | 26.00 |
| 0 | 0.0 | 1.000 | 27.00 |
| 0 | 0.0 | 1.000 | 28.00 |
| 0 | 0.0 | 1.000 | 29.00 |
| 0 | 0.0 | 1.000 | 30.00 |
| 0 | 0.0 | 1.000 | 31.00 |
| 0 | 0.0 | 1.000 | +INF |

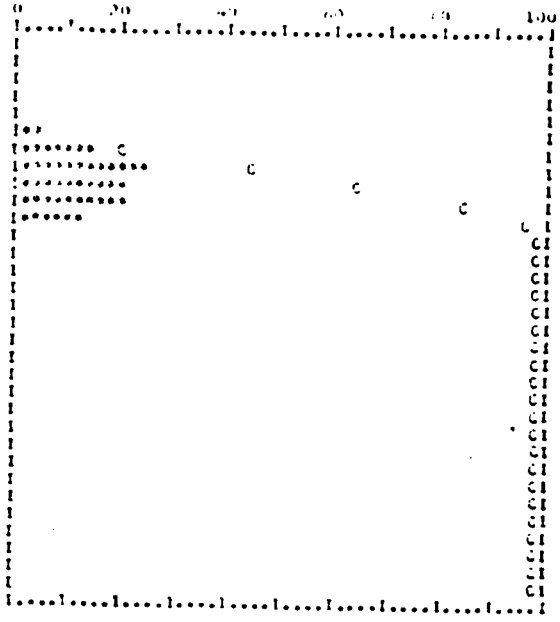
TOTAL 160.



TIME STAT HISTOGRAM FOR NODE 204 ( REALIZATION OF EVENT 204 )

| OBSV FREQ | RELA FREQ | CUML FREQ | UPPER BOUND OF CELL |
|---|---|---|---|
| 0 | 0.0 | 0.0 | 4.00 |
| 0 | 0.0 | 0.0 | 5.00 |
| 0 | 0.0 | 0.0 | 6.00 |
| 0 | 0.0 | 0.0 | 7.00 |
| 3 | 0.009 | 0.009 | 8.00 |
| 17 | 0.049 | 0.058 | 9.00 |
| 49 | 0.142 | 0.201 | 10.00 |
| 83 | 0.241 | 0.442 | 11.00 |
| 74 | 0.215 | 0.657 | 12.00 |
| 69 | 0.201 | 0.858 | 13.00 |
| 42 | 0.122 | 0.980 | 14.00 |
| 5 | 0.015 | 0.994 | 15.00 |
| 2 | 0.006 | 1.000 | 16.00 |
| 0 | 0.0 | 1.000 | 17.00 |
| 0 | 0.0 | 1.000 | 18.00 |
| 0 | 0.0 | 1.000 | 19.00 |
| 0 | 0.0 | 1.000 | 20.00 |
| 0 | 0.0 | 1.000 | 21.00 |
| 0 | 0.0 | 1.000 | 22.00 |
| 0 | 0.0 | 1.000 | 23.00 |
| 0 | 0.0 | 1.000 | 24.00 |
| 0 | 0.0 | 1.000 | 25.00 |
| 0 | 0.0 | 1.000 | 26.00 |
| 0 | 0.0 | 1.000 | 27.00 |
| 0 | 0.0 | 1.000 | 28.00 |
| 0 | 0.0 | 1.000 | 29.00 |
| 0 | 0.0 | 1.000 | 30.00 |
| 0 | 0.0 | 1.000 | 31.00 |
| 0 | 0.0 | 1.000 | 32.00 |
| 0 | 0.0 | 1.000 | 33.00 |
| 0 | 0.0 | 1.000 | 34.00 |
| 0 | 0.0 | 1.000 | +INF |

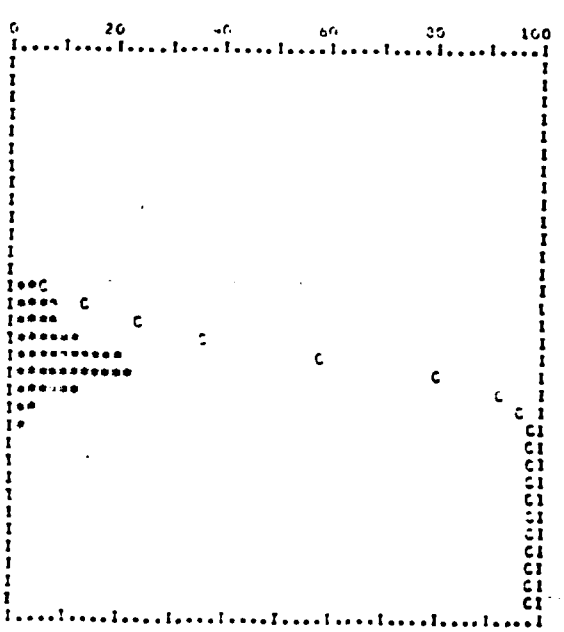
TOTAL 344.




TIME STAT HISTOGRAM FOR NODE 225 ( PART OF THE NETWORK BETWEEN NODES 225 AND 212 )

| OBSV FREQ | RELA FREQ | CUML FREQ | UPPER BOUND OF CELL |
|---|---|---|---|
| 0 | 0.0 | 0.0 | 1.00 |
| 0 | 0.0 | 0.0 | 2.00 |
| 0 | 0.0 | 0.0 | 3.00 |
| 0 | 0.0 | 0.0 | 4.00 |
| 0 | 0.0 | 0.0 | 5.00 |
| 0 | 0.0 | 0.0 | 6.00 |
| 0 | 0.0 | 0.0 | 7.00 |
| 0 | 0.0 | 0.0 | 8.00 |
| 0 | 0.0 | 0.0 | 9.00 |
| 0 | 0.0 | 0.0 | 10.00 |
| 0 | 0.0 | 0.0 | 11.00 |
| 0 | 0.0 | 0.0 | 12.00 |
| 3 | 0.010 | 0.010 | 13.00 |
| 18 | 0.057 | 0.067 | 14.00 |
| 28 | 0.089 | 0.156 | 15.00 |
| 29 | 0.092 | 0.248 | 16.00 |
| 40 | 0.127 | 0.375 | 17.00 |
| 65 | 0.206 | 0.581 | 18.00 |
| 70 | 0.222 | 0.803 | 19.00 |
| 42 | 0.133 | 0.937 | 20.00 |
| 13 | 0.041 | 0.978 | 21.00 |
| 7 | 0.022 | 1.000 | 22.00 |
| 0 | 0.0 | 1.000 | 23.00 |
| 0 | 0.0 | 1.000 | 24.00 |
| 0 | 0.0 | 1.000 | 25.00 |
| 0 | 0.0 | 1.000 | 26.00 |
| 0 | 0.0 | 1.000 | 27.00 |
| 0 | 0.0 | 1.000 | 28.00 |
| 0 | 0.0 | 1.000 | 29.00 |
| 0 | 0.0 | 1.000 | 30.00 |
| 0 | 0.0 | 1.000 | 31.00 |
| 0 | 0.0 | 1.000 | +INF |

TOTAL 315.



TIME STAT HISTOGRAM FOR NODE 251 ( PART OF THE NETWORK BETWEEN NODES 144 AND 251 )

| OBSV FREQ | RELA FREQ | CUML FREQ | UPPER BOUND OF CELL |
|---|---|---|---|
| 0 | 0.0 | 0.0 | 0.00 |
| 0 | 0.0 | 0.0 | 5.50 |
| 0 | 0.0 | 0.0 | 9.00 |
| 0 | 0.0 | 0.0 | 9.50 |
| 1 | 0.003 | 0.003 | 10.00 |
| 1 | 0.003 | 0.006 | 10.50 |
| 4 | 0.012 | 0.018 | 11.00 |
| 2 | 0.006 | 0.024 | 11.50 |
| 11 | 0.033 | 0.057 | 12.00 |
| 12 | 0.036 | 0.093 | 12.50 |
| 21 | 0.063 | 0.156 | 13.00 |
| 20 | 0.060 | 0.216 | 13.50 |
| 26 | 0.078 | 0.293 | 14.00 |
| 37 | 0.111 | 0.404 | 14.50 |
| 53 | 0.159 | 0.563 | 15.00 |
| 40 | 0.120 | 0.683 | 15.50 |
| 32 | 0.096 | 0.779 | 16.00 |
| 26 | 0.078 | 0.856 | 16.50 |
| 24 | 0.072 | 0.928 | 17.00 |
| 12 | 0.036 | 0.964 | 17.50 |
| 6 | 0.018 | 0.982 | 18.00 |
| 3 | 0.009 | 0.991 | 18.50 |
| 2 | 0.006 | 0.997 | 19.00 |
| 1 | 0.003 | 1.000 | 19.50 |
| 0 | 0.0 | 1.000 | 20.00 |
| 0 | 0.0 | 1.000 | 20.50 |
| 0 | 0.0 | 1.000 | 21.00 |
| 0 | 0.0 | 1.000 | 21.50 |
| 0 | 0.0 | 1.000 | 22.00 |
| 0 | 0.0 | 1.000 | 22.50 |
| 0 | 0.0 | 1.000 | 23.00 |
| 0 | 0.0 | 1.000 | +INF |

TOTAL 334.

TIME STAT HISTOGRAM FOR NODE 305 ( PART OF THE NETWORK BETWEEN NODES 254 AND 305 )

| OBSV FREQ | RELA FREQ | CUML FREQ | UPPER BOUND OF CELL |
|---|---|---|---|
| 0 | 0.0 | 0.0 | 2.00 |
| 0 | 0.0 | 0.0 | 3.00 |
| 0 | 0.0 | 0.0 | 4.00 |
| 0 | 0.0 | 0.0 | 5.00 |
| 0 | 0.0 | 0.0 | 6.00 |
| 0 | 0.0 | 0.0 | 7.00 |
| 0 | 0.0 | 0.0 | 8.00 |
| 0 | 0.0 | 0.0 | 9.00 |
| 1 | 0.003 | 0.003 | 10.00 |
| 3 | 0.010 | 0.014 | 11.00 |
| 10 | 0.034 | 0.047 | 12.00 |
| 20 | 0.068 | 0.115 | 13.00 |
| 34 | 0.115 | 0.231 | 14.00 |
| 52 | 0.176 | 0.407 | 15.00 |
| 56 | 0.190 | 0.597 | 16.00 |
| 41 | 0.139 | 0.736 | 17.00 |
| 24 | 0.081 | 0.817 | 18.00 |
| 21 | 0.071 | 0.888 | 19.00 |
| 12 | 0.041 | 0.929 | 20.00 |
| 7 | 0.024 | 0.953 | 21.00 |
| 8 | 0.027 | 0.980 | 22.00 |
| 4 | 0.014 | 1.000 | 23.00 |
| 0 | 0.0 | 1.000 | 24.00 |
| 0 | 0.0 | 1.000 | 25.00 |
| 0 | 0.0 | 1.000 | 26.00 |
| 0 | 0.0 | 1.000 | 27.00 |
| 0 | 0.0 | 1.000 | 28.00 |
| 0 | 0.0 | 1.000 | 29.00 |
| 0 | 0.0 | 1.000 | 30.00 |
| 0 | 0.0 | 1.000 | 31.00 |
| 0 | 0.0 | 1.000 | 32.00 |
| 0 | 0.0 | 1.000 | +INF |

TOTAL 295.

TIME STAT HIST [illegible] 314 ( PART OF THE NETWORK BETWEEN NODES 306 AND 314 )

| OBSV FREQ | REL FREQ | CUML FREQ | UPPER BOUND OF CELL |
|---|---|---|---|
| 0 | 0.0 | [illegible] | [illegible] |
| 0 | 0.0 | [illegible] | [illegible] |
| 0 | 0.0 | [illegible] | [illegible] |
| 0 | 0.0 | [illegible] | [illegible] |
| 0 | 0.0 | [illegible] | [illegible] |
| 0 | 0.0 | [illegible] | [illegible] |
| 0 | 0.0 | [illegible] | [illegible] |
| 0 | 0.0 | [illegible] | [illegible] |
| 0 | 0.0 | [illegible] | [illegible] |
| 1 | 0.003 | [illegible] | [illegible] |
| 10 | 0.034 | [illegible] | [illegible] |
| 32 | 0.110 | 0.144 | 13.00 |
| 34 | 0.134 | 0.278 | 14.00 |
| 24 | 0.082 | 0.371 | 15.00 |
| 31 | 0.107 | 0.478 | 16.00 |
| 34 | 0.124 | [illegible] | 17.00 |
| 28 | 0.096 | [illegible] | [illegible] |
| 28 | 0.096 | [illegible] | 19.00 |
| 19 | 0.065 | 0.858 | 20.00 |
| 12 | 0.041 | 0.899 | 21.00 |
| 15 | 0.052 | 0.952 | 22.00 |
| 7 | 0.024 | 0.976 | 23.00 |
| 5 | 0.017 | 0.993 | 24.00 |
| 2 | 0.007 | 1.000 | 25.00 |
| 0 | 0.0 | 1.000 | 26.00 |
| 0 | 0.0 | 1.000 | 27.00 |
| 0 | 0.0 | 1.000 | 28.00 |
| 0 | 0.0 | 1.000 | 29.00 |
| 0 | 0.0 | 1.000 | 30.00 |
| 0 | 0.0 | 1.000 | 31.00 |
| 0 | 0.0 | 1.000 | 32.00 |
| 0 | 0.0 | 1.000 | +INF |

TOTAL 291.

TIME STAT HISTOGRAM FOR NODE 89 ( DELAY BETWEEN FIRST AND LAST FIELD DEMONSTRATION )

| OBSV FREQ | REL FREQ | CUML FREQ | UPPER BOUND OF CELL |
|---|---|---|---|
| 1 | 0.003 | 0.003 | 12.00 |
| 2 | 0.007 | 0.010 | 13.00 |
| 1 | 0.003 | 0.014 | 14.00 |
| 3 | 0.010 | 0.024 | 15.00 |
| 5 | 0.017 | 0.041 | 16.00 |
| 2 | 0.007 | 0.048 | 17.00 |
| 3 | 0.010 | 0.058 | 18.00 |
| 5 | 0.017 | 0.076 | 19.00 |
| 4 | 0.014 | 0.089 | 20.00 |
| 4 | 0.014 | 0.103 | 21.00 |
| 3 | 0.010 | 0.113 | 22.00 |
| 6 | 0.021 | 0.134 | 23.00 |
| 6 | 0.021 | 0.155 | 24.00 |
| 1 | 0.003 | 0.158 | 25.00 |
| 2 | 0.007 | 0.165 | 26.00 |
| 2 | 0.007 | 0.172 | 27.00 |
| 2 | 0.007 | 0.179 | 28.00 |
| 2 | 0.007 | 0.186 | 29.00 |
| 3 | 0.010 | 0.196 | 30.00 |
| 6 | 0.021 | 0.216 | 31.00 |
| 3 | 0.010 | 0.227 | 32.00 |
| 3 | 0.010 | 0.237 | 33.00 |
| 3 | 0.010 | 0.247 | 34.00 |
| 5 | 0.017 | 0.265 | 35.00 |
| 6 | 0.021 | 0.285 | 36.00 |
| 5 | 0.017 | 0.302 | 37.00 |
| 0 | 0.0 | 0.302 | 38.00 |
| 4 | 0.014 | 0.316 | 39.00 |
| 6 | 0.021 | 0.337 | 40.00 |
| 1 | 0.003 | 0.340 | 41.00 |
| 3 | 0.010 | 0.351 | 42.00 |
| 189 | 0.649 | 1.000 | +INF |

TOTAL 291.

1980 USAF - SCEEE SUMMER FACULTY RESEARCH PROGRAM

Sponsored by the

AIR FORCE OFFICE OF SCIENTIFIC RESEARCH

Conducted by the

SOUTHEASTERN CENTER FOR ELECTRICAL ENGINEERING EDUCATION

FINAL REPORT

# THE ESTIMATION OF DECAY COEFFICIENT IN PULSED TRANSIENT SIGNAL


| | |
|---|---|
| Prepared by: | Dr. C. J. Park |
| Academic Rank: | Professor |
| Department and University: | Department of Mathematical Sciences<br>San Diego State University |
| Research Location: | Air Force Rocket Propulsion Laboratory,<br>Propulsion Analysis Division, Combustion<br>Technology Branch and Data Branch |
| USAF Research Colleague: | Mr. Wilbur Andrepont and<br>Dr. Tae-Woo Park |
| Date: | August 1, 1980 |
| Contract No: | F49620-79-C-0038 |

# THE ESTIMATION OF DECAY COEFFICIENT IN PULSED TRANSIENT SIGNAL

by

C. J. Park

## ABSTRACT

The estimation and interpretation of decay coefficient in pulsed transient signal are considered. Two methods are proposed in estimating the decay coefficient of pulse decay transient data. The methods are derived through a spectral analysis for a parametric model of impulse response function with a single frequency. Suggestions for further research in this area are offered. The estimation procedures proposed in this project can be extended to the case of multiple frequencies in an impulse response function and time dependent decay or growth coefficient.

## Acknowledgement

The author would like to thank the Air Force Systems Command, the Air Force Office of Scientific Research and the Southeastern Center for Electrical Engineering Education for providing him with the opportunity to work at the Air Force Rocket Propulsion Laboratory, Edwards AFB, CA. He would like to acknowledge the Laboratory, in particular the Combustion Technology Branch and the Data Branch, for their support and hospitality.

Finally, he would like to thank Mr. W. Andrepont and Dr. T. Park for their collaboration and for their suggestions, and he would like to acknowledge many helpful discussions with Mr. J. Levine.

## I. INTRODUCTION:

The determination of pulse decay and growth rates of data from motors and combustion burns has long been an outstanding problem. In particular, the determination of damping coefficients of multiple acoustic modes from a single motor pulse signal is very useful information in experimentally determining the actual stability characteristics of solid motors and validating the stability predictive methods.

The present project considers the problem of estimation and interpretation of decay coefficient in pulsed transient signal using the spectral analysis method. More specifically, the transient pulse signals induced by combustion burns of rocket motors can be represented as a solution of a linear system [1] [5],

$$y(t) = \int_0^\infty h(u)\ \chi(t-u)\ du,\ 0 < t < \infty,$$

where $\chi(t)$ is an input, $h(u)$ an impulse response function, and $y(t)$ is an output signal. In this paper, the methods of estimating the decay coefficient are derived using a spectral analysis [7] for the case of a simple impulse response function [5] given by

$h(t) = A_o e^{-\alpha_o t} \cos(2\pi f_o t + \theta_o)$, where the parameter $\alpha_o$ denotes the decay coefficient corresponding to the frequency $f_o$, the initial amplitude is denoted by $A_o$ and the initial phase shift is denoted by $\theta_o$. The input $\chi(t)$ is a unit impulse and the output of the pulsed signal data $y(t)$ is a sum of $h(t)$ and a possible noise $n(t)$. The methods developed in this paper can be extended to a more general case of impulse response function with multiple frequencies given by

$$h_K(t) = \sum_{k=o}^{K} A_k\ e^{-\alpha_k t} \cos(2\pi\ f_k t + \theta_k).$$

## II. OBJECTIVES:

The objective of this project was to develop techniques for analyzing transient data. In particular, the methods are derived, through a spectral analysis, to determine the decay coefficient of the pulsed data of a simple impulse response function with a single frequency. The methods developed can handle the more general case of impulse response function with multiple frequencies.

## III. THE ESTIMATION OF DECAY COEFFICIENT:

In the derivation of the estimate of decay coefficient, it is assumed that the observed pulse signal data y(t) is a sum of the impulse response function $h(t) = e^{-\alpha_o t} (\cos 2\pi f_o + \theta_o)$ and a possible noise n(t), i.e., $y(t) = h(t) + n(t)$. Since the estimates of $\alpha_o$ and $f_o$ will be derived in the frequency domain of y(t), it is also assumed that the influence of noise n(t) is negligible in estimating $f_o$. Before presenting the methods, it is necessary to define the terms that are used in the derivation. The total energy of the impulse response function h(u) in the time interval $(t, \infty)$ is defined by

$$P_t(f_o) = \int_t^\infty h^2(u)\, du \text{ and assume that } P_t(f_o) < \infty. \tag{1}$$

Let $H_t(f)$ be the Fourier transform of $\{h(u), t < u < \infty\}$, then

$$H_t(f) = \int_t^\infty h(u)\, e^{-j2\pi fu}\, du, \quad -\infty < f < \infty, \text{ and the power spectral}$$

density

$$|H_t(f)|^2 = H_t(f) \times H_t^*(f), \text{ where } H_t^*(f) \tag{2}$$

is the conjugate of $H_t(f)$. Note that from Parseval theorem it follows that

$$P_t(f_o) = \int_{-\infty}^\infty |H_t(f)|^2\, df.$$

After some tedious algebra, it can be shown [8] that

$$P_t(f_o) = \frac{e^{-2\alpha_o t}}{4\alpha_o\,(\alpha_o^2 + w_o^2)} \times (w_o^2 + \alpha_o^2\,(1 + \cos(2\theta_o + 2w_o t)) - \alpha_o w_o \sin(2\theta_o + 2w_o t), \tag{1'}$$

and

$$|H_t(f_o)|^2 = \frac{e^{-2\alpha_o t}}{\alpha_o^4 + \alpha_o^2\,(2w_o)^2} \tag{2'}$$

$$\times \{w_o^2 + \alpha_o^2\,((\cos\theta_o)^2\,(\cos w_o t)^4 + (\sin\theta_o)^2\,(\sin w_o t)^4$$

$$+ (\cos w_o t)^2\,(\sin w_o t)^2$$

$$+ 2\alpha_o w_o\,(\sin w_o t)\,(\cos w_o t)\,((\sin\theta o)^2 - (\cos\theta_o)^2)\},$$

where $w_o = 2\pi f_o$.

From (1′) and (2′) it can be easily shown [8] that when $\alpha_o << f_o$ tends to infinity

$$P_t(f_o)/|H_t(f_o)|^2 \to \alpha_o, \text{ and} \tag{3}$$

$$|H_{t_2}(f_o)|^2/|H_{t_1}(f_o)|^2 \to 2\alpha_o(t_2-t_1),\ t_1 < t_2. \tag{4}$$

These relations were used in the derivation of the methods in estimating the decay coefficient $\alpha_o$.

Assume that $\theta = o$ in (1′) and (2′), then it can be shown that

$$\ell n\ \underline{B}(\gamma_o) \le \ell n\ \{|H_{t_2}(f_o)|^2/|H_{t_1}(fo)|^2\} + 2\alpha_o(t_2-t_1) \le \ell n\ \bar{B}\ (\gamma_o), \tag{5}$$

where $\bar{B}\ (\gamma_o) = [\underline{B}(\gamma_o)]^{-1} = \dfrac{2\alpha_o{}^2 + 1 + \sqrt{2}\ (\frac{1}{2} + \gamma_o)}{2\alpha_o{}^2 + 1 - \sqrt{2}\ (\frac{1}{2} + \gamma_o)}$, $\gamma_o = 2\pi f_o/\alpha_o$

and as $f_o$ tends to infinity,

$$\frac{P_t(f_o)}{|H_t(f_o)|^2} = \alpha_o + o\ (\frac{\alpha_o}{2\pi f_o}). \tag{6}$$

In view of equations (3), (4), (5), and (6), along with the assumption that the contribution of the noise to the power spectral density at $f_o$ is negligible, the following methods are proposed in estimating the decay coefficient of pulse data y(t) when the input is a unit impulse. Suppose that the signal record y(t) is available in time interval $(t_o, T)$. Choose the time points $t_1, t_2, \ldots, t_n$ in $(t_o, T)$ such that $t_\ell < t_{\ell+1}$. Using the Fast Fourier Transform program compute $P_{t_\ell}(f_o)$ and $|H_{t_\ell}(f_o)|^2$. Because the methods in estimating $\alpha_o$ and $f_o$ are heavily dependent on the estimate of the total energy $P_t(f_o)$ and the power spectral density $|H_t(f_o)|^2$, the numerical method for computing them must be carefully scrutinized [2], [3], [4], and [6].

The first method of estimating $\alpha_o$ is based on the estimate of spectral density and equation (5) and given by

$$\hat{\alpha}_o\ (\Delta t_\ell) = \frac{1}{2\Delta t_\ell}\ \ell n\ \{\ |H_{t_{\ell+1}}(f_o)|^2/|H_{t_\ell}(f_o)|^2\}, \tag{7}$$

for $\ell = o, 1, \ldots, n-1$, where $f_o$ is the frequency that gives the maximum spectral density estimate $|H_t(f_o)|^2$ and $\Delta t_\ell = t_{\ell+1} - t_\ell$. The formula (7) will be referred to as H-method in the sequel.

The second method is based on the estimate of the spectral density, the total energy and equation (6), and given by

$$\hat{\alpha}(t_\ell) = P_{t_\ell}(f_o)/[|H_{t_\ell}(f_o)|^2 \times BW(t_\ell) X(T-T_\ell)] \qquad (8)$$

for $\ell = o, 1, \ldots, n$, where $BW(t_\ell)$ denotes the band width used in the calculation of $|H_{t_\ell}(f_o)|^2$. The formula (4) will be referred to as PH-method in the sequel. Because the output signal y(t) is influenced by a possible noise, and the spectral densities and the total powers are computed from the digitized continuous signal, these point estimates are subject to a certain degree of variations. The other sources of variations can be due to the departure from the underlying assumption such as the correctness of $h_o(t)$ and time independency of $\alpha_o$. Thus, when there are undue variations among the point estimates, one should examine the sources of variations more carefully.

When the variations among the point estimates are reasonable, a smoothing technique for an effective way of pooling the point estimates is considered. First, the following smoothing technique for the H-method estimates is proposed. From (5) it is reasonable to assume that $\ell n\,[|H_{t_{\ell+1}}(f_o)|^2/|H_{t_\ell}(f_o)|^2]$ can be well approximated by a linear function of $(t_{\ell+1} - t_\ell)$, namely

$$\ell n\,[|H_{t_{\ell+1}}(f_o)|^2/|H_{t_\ell}(f_o)|^2] = \beta_o + \beta_1 (t_{\ell+1} - t_\ell) + \text{error}.$$

Hence for $\ell = o, 1, \ldots, n-1$, fit $\ell n\,[|H_{t_\ell}(f_o)|^2/|H_o(f_o)|^2]$ to $\beta_o + \beta_1 X t_\ell$ by the least square method. Let $\hat{\beta}_1$ be the least square estimate of the slope $\beta_1$. The pooled estimate of $\alpha_o$, using H-method estimates, is given by

$$\hat{\alpha}_o(H) = \hat{\beta}_1/2. \qquad (9)$$

This method deserves an additional usage in detecting a possible departure from the assumption that $\alpha_o$ is independent of time. More specifically, the dependence of $\alpha_o$ on time can be detected by inspecting the "goodness of fit" of $\ell n\,[|H_{t_\ell}(f_o)|^2]$ to a linear function of time. If the linear fit is "poor" this might suggest that $\alpha_o$ may be dependent on t or possible phase shift; however, it requires a further study to correctly ascertain such departure. Another important merit of this estimate is the fact that it provides a meaningful interpretation of decay coefficient. More precisely, let $\Delta|H_t(f_o)|^2$ denote the power

spectral in the time interval (t, t + Δt), i.e.,

$\Delta|H_t(fo)|^2 = |H_t(f_o)|^2 - |H_{t+\Delta t}(f_o)|^2$, then the estimate $2\hat{\alpha}(H)\Delta t$ is a reasonable estimate of $\Delta|H_t(f_o)|^2/|H_t(f_o)|^2$.

The pooling technique for the PH-method estimates is as follows. By the least square method fit $\ell n\, P_t(f_o)$ and $\ell n\, |H_t(f_o)|^2$, separately, to a linear function of time and let $\hat{\ell n}\, P_t(f_o)$ and $\hat{\ell n}\, |H_t(f_o)|^2$ be the fitted values. Then the smoothed estimates of $\alpha_o$ is given by

$$\hat{\alpha}_o(PH) = \frac{1}{\sum_{\ell=o}^{n} (T-t_\ell)^2} \sum_{\ell=o}^{n} \frac{(T-t_\ell)\, \exp\left[\hat{\ell n}\, P_{t_\ell}(f_o) - \hat{\ell n}\, |H_{t_\ell}(f_o)|^2\right]}{BW(t_\ell)} . \qquad (10)$$

The methods developed in this project are tested for some synthesized data and several pulsed data firm T-burner tests. Their performance was good for the cases reported in [8].

IV. RECOMMENDATION:

The methods developed in this project can be extended to a more general case of impulse response function with multiple frequencies. It is recommended that the methods should be tried for the multiple frequencies. The methods developed are based on the parametric model of impulse response function and the sensitivity study of the estimates with respect to the departure from the assumed model deserve a further consideration, even though the methods can be used as an approximation in the case where the impulse response function is tried as an exploratory model. By detail investigation of the influence of the noise term, the statistical properties of the estimates can be studied, [4], [7].

## REFERENCES


1. Bendat, J. S., and Piersall, A. G., Measurement and Analysis of Random Data, John Wiley & Sons, Inc., New York (1966).

2. Blackman, R. B., and Tukey, J. W., The Measurement of Power Spectra, Dover Publications, Inc., New York (1958).

3. Brigham, E. O., The Fast Fourier Transform, Prentice-Hall, Inc., Englewood Cliffs, New Jersey (1974).

4. Brillinger, D. R., Time Series Data Analysis and Theory, Holt, Rinehart and Winston, Inc., New York (1965).

5. Culick, F. E. C., Combustion Instability in Solid Rocket Motors: Vol. II, CPIA Publication 290 (1980).

6. Jenkin, G. M., and Watts, D. G., Spectral Analysis and Its Applications, Holden-Day, San Francisco (1968).

7. Koopmans, L. H., The Spectral Analysis of Time Series, Academic Press, New York (1974).

8. Andrepont, W., Park, T., and Park, C. J., "The Estimation of Decay Coefficient in Pulsed Transient Signal," to be submitted to JANNAF.

1980 USAF - SCEEE SUMMER FACULTY RESEARCH PROGRAM

Sponsored by the

AIR FORCE OFFICE OF SCIENTIFIC RESEARCH

Conducted by the

SOUTHEASTERN CENTER FOR ELECTRICAL ENGINEERING EDUCATION

FINAL REPORT

# A PRELIMINARY ANALYSIS OF ALTERNATIVE FORECASTING TECHNIQUES FOR THE STANDARD BASE SUPPLY SYSTEM (SBSS)


Prepared by: Dr. J. Wayne Patterson

Academic Rank: Assistant Professor

Department and University: Department of Industrial Management, Clemson University

Research Location: Air Force Logistics Management Center, Gunter AFS, Alabama

USAF Research Colleague: Major Richard A. Lombardi



Date: August 8, 1980

Contract No: F49620-79-C-0038

# A PRELIMINARY ANALYSIS OF ALTERNATIVE FORECASTING TECHNIQUES FOR THE STANDARD BASE SUPPLY SYSTEM (SBSS)

by

J. Wayne Patterson

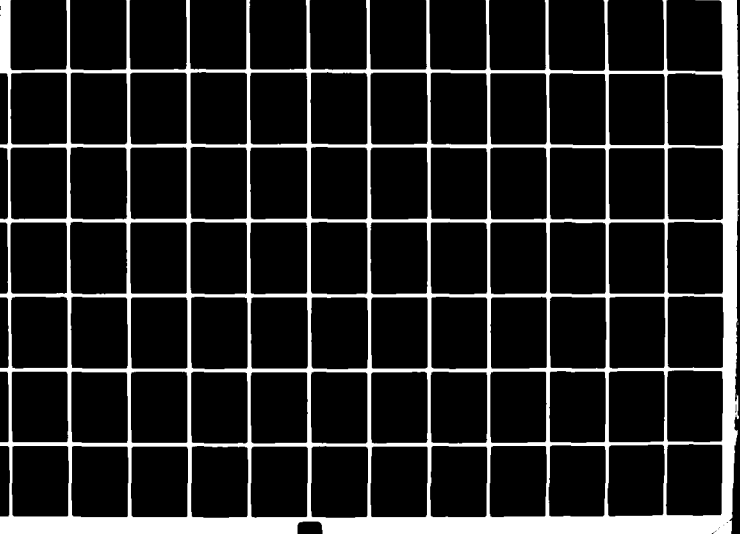
## ABSTRACT

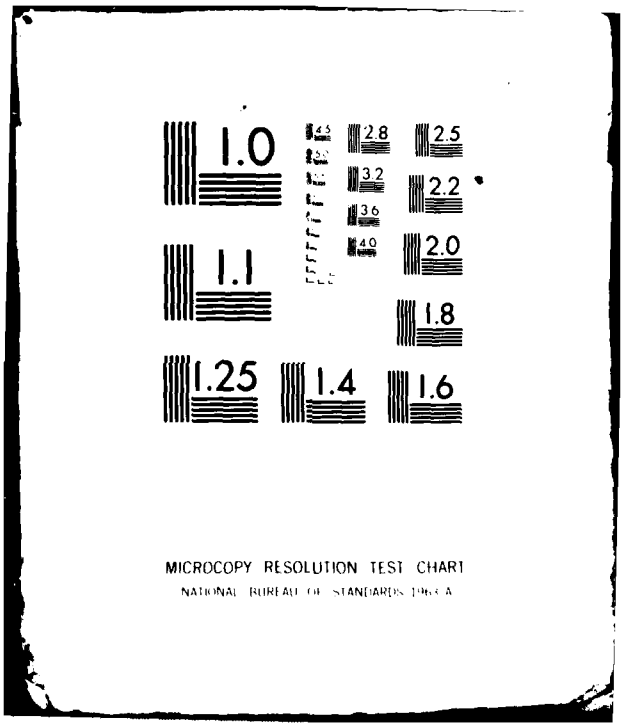
The purpose of this research is to investigate alternative approaches to forecasting demand for expendable items in the Standard Base Supply System (SBSS). The forecasting models studied include single, double and adaptive exponential smoothing. Samples were selected from Dover AFB, Delaware and analysis of the various smoothing models was performed by a FORTRAN program written for each model. Comparison of the forecasting models was made on the basis of forecast error as measured by mean absolute deviation (MAD). The forecast error was also measured for the current forecasting model used by the SBSS. Single exponential smoothing, with small smoothing constants, proved to be the model with the lowest forecast error rate. Program activity was also studied as a possible tool to be used in demand prediction. Flying hours correlated with demand levels for some federal stock classes. Suggestions for further study are included.

AD-A097 394 SOUTHEASTERN CENTER FOR ELECTRICAL ENGINEERING EDUCAT--ETC F/G 5/1
USAF SUMMER FACULTY RESEARCH PROGRAM, 1980. RESEARCH REPORTS. V--ETC(U)
OCT 80 W D PEELE F49620-79-C-0038

UNCLASSIFIED AFOSR-TR-81-0193 NL

4 12




1.0
1.1
1.25
1.4
1.6
1.8
2.0
2.2
2.5
2.8
3.2
3.6
4.0
MICROCOPY RESOLUTION TEST CHART
NATIONAL BUREAU OF STANDARDS 1963 A

## ACKNOWLEDGEMENT

The author would like to express his sincere appreciation to the Air Force Systems Command, the Air Force Office of Scientific Research and the Southeastern Center for Electrical Engineering Education for providing him with the opportunity to spend a very worthwhile, interesting and rewarding summer at the Air Force Logistics Management Center, Gunter AFS, Alabama. The Logistics Management Center has provided excellent support and working conditions during my stay at Gunter.

Special thanks to Major Richard A. Lombardi for suggesting this area of research and for his guidance and colloboration on the project. Thanks also to Mr. Ron Hare for his helpful comments and suggestions and to Mr. Willie Hahn for his assistance in data preparation and in running the simulation model.

## I. INTRODUCTION

The USAF Standard Base Supply System (SBSS) is an automated inventory accounting system used by all Air Force bases to control their supply functions. Seppanen indicates in his technical planning study that SBSS can be categorized as a multi-item, single-echelon, continuous review inventory system with stochastic, multiple unit demands, backordering and an annual budget constraint.[15]

The SBSS was designed to facilitate the flow of materials from a multitude of sources to the base user organizations. The SBSS inventory is stocked by the arrival of material from Air Force depots, GSA, DSA as well as through local purchase. As such the SBSS is a retail organization in much the same sense as a local merchant, interfacing the wholesale level with the final consumer.

The SBSS is driven by demand action. When an item is needed, at base level, a requisition is submitted to SBSS. Typically, the request is filled from available stock. If the requested item is not available, the requisition is logged as a due-out for later filling. The request may be filled through the normal operating cycle or in some instances special orders may be required. In general, orders for resupply of the SBSS are logged as due-ins and are maintained until the material is received.

SBSS EOQ requirements computation may be divided into two components the range model and the depth model. The use of the term range model refers to the procedure employed by inventory planners to determine if an item is to be stocked. Specific criteria are available in AFM 67-1, Vol II, Part Two, to indicate whether new items should be added to the stock list or currently stocked items should be retained on the stock list.

The EOQ depth model of SBSS is used to determine how much and when to order. The depth model is based on the Economic Order Quantity (EOQ) formula:

$$EOQ = \sqrt{2DA/IP} \qquad (1)$$

Where D is the annual demand rate, A is the cost per order (currently used figure, $5.00), I is the annual inventory carrying rate (currently used figure, 50%) and P is the item unit price. The EOQ formula balances the cost of ordering with the cost of holding inventory so that total variable cost will be minimized. Although the SBSS depth model is EOQ based only in a few instances is the exact EOQ used. A modified version of (1) is used as follows to vary the stockage level in accordance with the requisition objective.

$$EOQ_{VSO} = \sqrt{2 \cdot DDR \cdot VSO \cdot A/(I \cdot P)} \qquad (2)$$

Where A, I and P are the same as described above, DDR is the daily demand rate and VSO represents the number of days demand to be considered in the EOQ computation. The variable stockage objective (VSO) is a function of stockage priority code, number of demands in 365 days and total number of recorded demands, number of days since the first demand and the daily demand rate. Chapter 11, attachment A-16 of AFM 67-1, Vol II, Part Two contains the necessary lookup table to determine the VSO for a particular item.

In addition to the EOQ computation, which is modified by VSO, the reorder point is also an important part of SBSS. The reorder point is a combination of the order and ship time quantity (OSTQ) and safety level quantity (SLQ). The OSTQ is given by

$$OSTQ = DDR \cdot OST \qquad (3)$$

Using an average order and ship time (OST) in days based on the item source and priority. The SLQ is given by

$$SLQ = C\sqrt{3 \cdot OSTQ} \qquad (4)$$

Where C, the safety factor (is typically set to 1 which implies an 84% service effectiveness) and 3 has been historically determined as the lead time demand variance/mean ratio. The reorder point (RP) is then given by

$$RP = OSTQ + SLQ \qquad (5)$$

The requisition objective (RO) is the maximum desired inventory position and is given by

$$RO = INT(EOQ_{VSO} + OSTQ + SLQ + 0.999) \qquad (6)$$

Notice that each of the three variables included in the requisition objective computation are to some extent a function of the daily demand rate. In essence the DDR is the forecast measurement for the SBSS. Unless accurate estimates are available for the DDR considerable errors may result.

Each time a particular item is demanded the DDR is revised. SBSS maintains the cumulative recurring demand (CRD) and the date of first demand (DOFD). Each time an item is demanded, the number of units requisitioned is added to the CRD. The revised DDR is then calculated as

$$DDR = CRD/MAX(180, \text{Current Date} - DOFD) \qquad (7)$$

A minimum of 180 days usage is assumed so as not to overstock items that have just been added to the stockage list.

In addition to these routine revisions of the DDR, the CRD and DOFD are adjusted at six month intervals so as to reflect the most recent usage data. The adjustments are as follows:

$$CRD = DDR \cdot MIN(365, \text{Current Date} - DOFD) \qquad (8)$$

$$DOFD = MAX(DOFD, \text{Current date} - 365) \qquad (9)$$

These adjustments assure that the DDR computation is based on at most the past 540 days demand history. The net effect of this adjustment is to convert the forecasting model to a modified exponential smoothing with a variable smoothing parameter. Seppanen states that during the six month intervals between adjustments, new demands enter the forecast with a smoothing constant

$$\alpha = N/(365+N) \qquad (10)$$

Where N is the number of days since the last adjustment.[15]

This research is concerned with the forecasting model in the SBSS. It is not clear that the current DDR computation provides the best approach to estimating demand. Alternative approaches to forecasting which were considered in this study are limited to consumable supplies. The AFLMC, however intends to review forecasting approaches for reparables as well as consumable items.

## II. OBJECTIVES

This research is the first activity of a multiphase project to study demand forecasting procedures in the SBSS. The primary objectives of this study is to investigate alternative approaches to demand forecasting for SBSS. The forecasting models which may lead to improvement in estimating DDR will be studied in detail in later phases of the project. The criteria for recommending forecasting models for further study is based on the level of forecast error. It was decided that the mean absolute deviation (MAD) would provide an acceptable measure of forecast error to be used in comparing alternative models.

A secondary objective is to analyze, to the extent possible, the use of program activity (flying hours, sorties, etc.) as a demand prediction tool. Although some studies have been conducted, it is not clear as to how program activity can be incorporated into demand prediction procedures.

In this study analysis is limited to expendable (consumable) inventory items. The data analyzed are from Dover AFB, Delaware, for a one year period from April 1978 through March 1979.

## III. METHODOLOGY

In order to select appropriate forecasting models for a particular situation careful consideration must be given to the underlying characteristics of the organization. In many instances these characteristics may rule out some potential forecasting approaches and allow more detailed analysis of the

practical techniques. Such is the case with the SBSS. The typical base may stock 20,000 or more items and demand history is available for at most 540 days. The sheer number of items for which forecasts must be made would rule out forecasting models which require extensive computations. In addition the available demand history of approximately 1½ years also precludes the use of several advanced statistical techniques. For these reasons it was decided that, as an overall approach, time series analysis (decomposition), econometric methods, and correlation and regression analysis were inappropriate for consideration.[13,18] Correlation and regression analysis will be considered for only a small portion of items when program activity is studied.

The distribution of demand patterns also poses an interesting problem in the SBSS. Although some research has been done on this problem there is still no concensus on the appropriate distribution.[11, 16] This should not be surprising if one considers the number of bases and the difference in mission from one base to another. Although the demand distribution is unknown one can get a feel for the forecasting problem from a look at selected item histories as presented in Table 1 below.

TABLE 1

MONTHLY DEMAND FOR EIGHT SELECTED ITEMS IN FEDERAL STOCK CLASS 28, APRIL 1978 - MARCH 1979, DOVER AFB

| Month | Item | | | | | | | |
|---|---|---|---|---|---|---|---|---|
| | 1 | 2 | 3 | 4 | 5 | 6 | 7 | 8 |
| A | 1 | 0 | 3 | 0 | 1 | 0 | 0 | 0 |
| M | 1 | 0 | 4 | 0 | 7 | 303 | 6 | 12 |
| J | 0 | 0 | 3 | 0 | 3 | 190 | 6 | 0 |
| J | 0 | 0 | 5 | 0 | 11 | 120 | 6 | 0 |
| A | 0 | 1 | 0 | 0 | 11 | 51 | 6 | 0 |
| S | 2 | 0 | 7 | 1 | 2 | 180 | 14 | 12 |
| O | 0 | 0 | 9 | 0 | 12 | 343 | 20 | 0 |
| N | 0 | 4 | 4 | 0 | 3 | 0 | 0 | 12 |
| D | 3 | 0 | 6 | 0 | 3 | 250 | 0 | 0 |
| J | 3 | 0 | 3 | 0 | 11 | 542 | 6 | 0 |
| F | 0 | 0 | 2 | 0 | 3 | 12 | 6 | 8 |
| M | 1 | 0 | 4 | 0 | 4 | 45 | 6 | 0 |

The agreement among analysts familiar with this problem is strong that demand patterns are at best erratic. Cohen summarizes the situation best by posing the question, what is 30 days supply of an item with 3 demands in the last 2 years?[6]

One might raise the question of what forecasting techniques fit the situation described above which have not been ruled out already. The models left for consideration include both moving averages and exponential smoothing. The current SBSS forecasting model is a mixture of these techniques. It is a moving average in the sense that the DDR is a quotient of cumulative demands over time divided by the length of time for which these demands were accumulated. It includes exponential smoothing by the manner in which updates to CRD and DOFD are performed. Although the net effect of the current SBSS is a "hybrid" of moving averages and exponential smoothing, it is not apparent that this approach provides the best estimate of future demand. In short an approach to forecasting which reduces forecast error should provide a more accurate estimate of future demand and result in improved performance for the SBSS. The techniques which are considered in this study are single exponential smoothing, double exponential smoothing, adaptive exponential smoothing and moving averages.

The criteria for comparison of the various forecasting techniques will be based on their accuracy as measured by forecast error. The most commonly used measures of forecast error are the mean squared error (MSE) and the mean absolute deviation (MAD). Although the MSE is more tractable for statistical analysis, it's giving additional penalty to large errors make it less attractive. The most straightforward measure of error is MAD since it treats over estimates and under estimate equally by taking the magnitude of error, regardless of sign and averaging it.[1]

In addition to the measurement of forecast error for the various techniques, it is desirable to analyze the impact of the potential models on the entire system. Feeney and Sherbrooke point out that optimization on an item basis is short sighted and that a systems approach must be used to evaluate overall impact on the system.[7] In order to accomplish this analysis, the EOQ Federal Simulation Model (FEDSIM) will be used to assess the overall impact of proposed models when possible. FEDSIM is a model of SBSS and includes options to test the impact of changes within the supply system. At present an option is available to test single exponential smoothing models.

Some research has already been conducted to study the potential use of program activity as a demand prediction tool.[6, 9, 10] In general these studies have been focused at the wholesale level rather than the base level. Also these studies have been performed on reparable items as opposed to the expendable items which will be studied here. Correlation and regression analysis will be used to explore the use of program activity as a potential demand prediction tool.

The data analyzed in the current study were selected from Dover AFB, Delaware, for a one year period from April 1978 to March 1979. Units demanded monthly were tabulated from the transaction history file providing 12 data points for each selected item. The major portion of this study, evaluating alternative forecasting models, was accomplished using four samples of 200 items each from selected federal stock classes. The selected stock classes were 28, 47, 59, and 66.

In the study of program activity the monthly demand levels as well as flying hours, sorties and aircraft population from Dover AFB, Delaware, for the same time period as above were used. Samples of 200 items each were selected from federal stock classes 15, 16, 28, 29, 31 and 47.

Before any analysis was begun the data were scanned in order to detect potential outliers. The data displayed in Table 1 is representative of the demand patterns present. Only one item had an obvious outlier which was discarded from the analysis thus leaving only 199 items in federal stock class 47. In that case there were eleven months in which zero units were demanded but in one month 6,160 units were requested. This item was dropped from the sample as a potential data entry error.

## IV. COMPARISON OF FORECASTING MODELS

Once the data were selected for analysis the testing of the various models was performed by developing a FORTRAN program for each technique. The programs were designed to measure the forecast error for the last ten periods, using the first two periods for initialization of the model. Since each forecasting model was tested using the same data, comparisons of their accuracy may be based on the level of forecast error. The forecast error for prospective models as well as the current SBSS forecasting model are presented in Table 2. Statistics for the several models are placed into Table 2 to facilitate comparison of the models. A detailed description of each model and analysis of results follows.

Single exponential smoothing is one of the simplest, and perhaps most popular, forecasting techniques applied to multi-item inventories.[2,13,18] It is a form of weighted average designed to smooth random variations in demand by averaging the most recent forecast with the most recent actual demand

TABLE 2

MEAN ABSOLUTE DEVIATION FOR ALTERNATIVE FORECASTING MODELS AND SBSS BY FEDERAL STOCK CLASS

| MODEL | FEDERAL STOCK CLASS 28 | 47 | 59 | 66 | AVERAGE |
|---|---|---|---|---|---|
| Single Exponential Smoothing | | | | | |
| $\alpha$ = .1 | 3.51 | 3.29 | .60 | 1.12 | 2.13 |
| $\alpha$ = .2 | 3.72 | 3.46 | .63 | 1.15 | 2.24 |
| $\alpha$ = .3 | 3.83 | 3.62 | .65 | 1.18 | 2.32 |
| $\alpha$ = .4 | 3.95 | 3.78 | .67 | 1.22 | 2.41 |
| $\alpha$ = .5 | 4.03 | 3.90 | .68 | 1.25 | 2.47 |
| Double Exponential Smoothing | | | | | |
| $\alpha$ = .1 | 3.82 | 3.52 | .63 | 1.16 | 2.28 |
| $\alpha$ = .2 | 4.14 | 3.91 | .70 | 1.26 | 2.50 |
| $\alpha$ = .3 | 4.36 | 4.19 | .74 | 1.35 | 2.66 |
| Adaptive Exponential Smoothing | | | | | |
| Chow | | | | | |
| Initial $\alpha$ = .1 | 3.82 | 3.48 | .63 | 1.17 | 2.27 |
| Initial $\alpha$ = .2 | 4.03 | 3.91 | .69 | 1.28 | 2.48 |
| Trigg and Leach | | | | | |
| Initial $\alpha$ = .1, $\beta$ = .2 | 3.73 | 3.69 | .60 | 1.22 | 2.31 |
| Moving Average 3-Month | 4.28 | 4.87 | .71 | 1.35 | 2.80 |
| SBSS | 3.59 | 3.72 | .70 | 1.35 | 2.34 |

experienced. The forecast for period t ($F_t$) is given by

$$F_t = \alpha X_{t-1} + (1-\alpha) F_{t-1} \qquad (11)$$

Where $X_{t-1}$ is the actual demand in the prior period and $\alpha$ is the smoothing constant. The smoothing constant represents the weight given to the most recent actual demand data and is in a range $0 < \alpha < 1$. The selection of the smoothing constant for a particular set of items is performed through trial and error. Typically a common set of data is used to test the forecasting accuracy with alternative values of the smoothing constant. The forecast error is measured for each set of forecasts and the superior smoothing constant is determined. Forecast errors reported in Table 2 were measured as follows:

$$MAD = \frac{\Sigma |X_t - F_t|}{n} \qquad (12)$$

where the error measurement MAD is determined for n periods. In each federal stock class the overall measure of error was determined by averaging the MAD for all items in the group. For example in federal stock class 66, the MAD for the 200 items using an $\alpha = .1$ was 1.12, an $\alpha = .2$ was 1.15 and so forth. The average forecast error for all four groups using an $\alpha = .1$ was 2.13, an $\alpha = .2$ was 2.24 and so on.

For the samples studied it is clear that the best smoothing constant is $\alpha = .1$ since this value gives the lowest forecast error in each of the four samples. The general pattern indicated is that as one increases the smoothing constant and the forecast error increases. This finding that small smoothing constants are preferable for SBSS data is consistent with the research reported in references 8, 11, and 20.

In order to forecast using single exponential smoothing a limited amount of information is required. Technically one needs only an initial forecast, an initial measurement of actual demand and a smoothing constant. The only data that need be retained to continue forecasting using single exponential smoothing are the forecast and actual demand for the preceding period. In this study the models were initialized by using the first month's actual demand as the forecast for the second month, then forecasts were made for the last ten months.

Double exponential smoothing is an extension of single smoothing and is typically applied to items that exhibit a trend pattern.[13,18] Since both single and double smoothed values lag actual data when a trend exists, the difference between the single and double smoothed values can be added to the single smoothed values and adjusted for trend. This approach is also referred to as linear exponential smoothing. The calculations required for double smoothing as presented by Makridakis and Wheelwright are as follows:[13]

$$S_t' = \alpha X_t + (1-\alpha)S_{t-1}' \qquad (13)$$

$$S_t'' = \alpha S_t' + (1-\alpha)S_{t-1}'' \qquad (14)$$

where $S_t$ and $S_t$ are single and double smoothed values respectively.

$$a_t = 2\,S_t' - S_t'' \qquad (15)$$

$$b_t = \alpha/(1-\alpha)\,(S_t' - S_t'') \qquad (16)$$

and the forecast for period t+1 is

$$F_{t+1} = a_t + b_t \qquad (17)$$

In order to use this approach only three data values and a smoothing constant are required. Initialization of this model was accomplished by setting $S_2'$ and $S_2''$ equal to $X_1$, the actual demand in the first month. Then forecasts were prepared for the last ten months using three different smoothing constants

$\alpha$ =.1, $\alpha$ =.2 and $\alpha$ =.3. The results presented in Table 2 demonstrate that as is increased the forecast error tends to also rise. Furthermore the double smoothing model produced a higher degree of forecast error than did single exponential smoothing for these four samples. In none of the four groups was double smoothing superior to single smoothing. This may also indicate that as a general rule trend does not exist in SBSS items. Due to the erratic nature of demand patterns, it is not surprising that adjusting for trend did not reduce forecast error. With the variation present in SBSS items there may well be more than random variability in demand data. In order to test this phenomena adaptive models will be considered.

When forecast are required for several thousand items as in the SBSS it seems reasonable that more than one smoothing parameter should be used. That is the weight given to most recent data should be greater when a persistent demand pattern exists and should be reduced when highly erratic demand patterns occur. The cost associated with studying each item separately to determine the appropriate smoothing constant to minimize forecast error would be extremely high, whether single or double smoothing is to be used. It was hoped that some criteria such as essentiality codes could be used to at least study groups of items but these data were not available during the term of this research. Adaptive forecasting models were studied since they are self-regulating based on forecast error and thus bypass the problems of item by item analysis and stratification.

The first adaptive model tested in this study was developed by Chow in 1965.[5,13,18] The Chow model is designed to allow the smoothing constant to adapt in small increments in order to minimize forecast error. The model assumes that the time ordered data contains all or some of the following:

trend; cyclical movements, including seasonal; and random variation. The equations necessary for employing this method are as follows:

$$S_t = \alpha_t X_t + (1-\alpha_t)S_{t-1} \qquad (18)$$

$$b_t = \alpha_t (S_t - S_{t-1}) + (1-\alpha_t)b_{t-1} \qquad (19)$$

and the forecast is

$$F_{t+1} = S_t + \frac{(1-\alpha_t)b_t}{\alpha_t} \qquad (20)$$

At the outset the forecaster is required to have initial values for S, b and $\alpha_t$ as well as an increment to be used in changing the smoothing parameter. Initialization employed in this study was to set $S_1$ equal to $X_1$ and $b_1$ equal to zero. The forecast for the second month ($F_2$) was set equal to $X_1$ and therefore comparable to the start-up values for single and double smoothing models described above. Since small values of the smoothing parameter provided best results in the models already studied the Chow model was tested with initial values of $\alpha_t = .1$ and $\alpha_t = .2$. The increment for changing the smoothing constant was set at .05. Overall limits for the smoothing constant were set so that it remained in the range $.05 \leq \alpha_t \leq .95$.

The revision of the smoothing constant is the unique feature of Chow's model. At each time period three values of $\alpha$ must be considered; a "nominal" value, a low value and a high value. The forecast for the next period is always derived using the "nominal" value but dependent on the forecast error measured in the current period the "nominal" value for next period may either increase or decrease by the amount of the pre-determined increment. This allows the smoothing constant to respond to changes in demand patterns but at the same time limits its responsiveness to the amount of the increment.

In comparison to single and double smoothing models the Chow model requires more recordkeeping so that the smoothing constant can be revised. Since in each time period three forecasts must be made, the necessary data to continue the procedure must be available. One might note that in addition to the current smoothing value and the three forecasts for the last period, three values must be kept for both $S_t$ and $b_t$. Thus it is clear that the overhead for maintaining the Chow model exceeds that for previously described models.

The results from the Chow model are presented in Table 2. The lowest forecast error was obtained when the initial smoothing constant was set at .1. The average figure of 2.27 indicates that this model performed about as well as the double smoothing model but was not superior to single smoothing.

One other adaptive model was tested, the Trigg and Leach model.[13,18] It differs from the Chow model by using the ratio of two forecast error measurements to calculate the smoothing constant. The equations required in the model are given by Makridakis and Wheelwright[13] as follows:

$$F_{t+1} = \alpha_t X_t + (1-\alpha_t)F_t \qquad (21)$$

Where

$$\alpha_{t+1} = \left|\frac{E_t}{M_t}\right| \qquad (22)$$

$$E_t = \beta e_t + (1-\beta)\, E_{t-1} \qquad (23)$$

$$M_t = \beta |e_t| + (1-\beta) M_{t-1} \qquad (24)$$

$$e_t = X_t - F_t \qquad (25)$$

$\beta$ is a constant used to smooth the forecast error in the equations for $E_t$, the smoothed error, and $M_t$, the absolute smoothed error. It is set in the range $0 < \beta < 1$ and in the current study $\beta$ was set equal to .2. Forecasting was begun by setting $E_1$, $M_1$ and $e_1$ to zero and $F_2$ was set equal to $X_1$, making

initialization comparable to the previously discussed models. The initial value of $\alpha$ was set equal to .1 and this value was used until the adaptive feature of the model could take over. One should recognize that the calculation of $\alpha_{t+1}$ does not begin until the actual demand is less than the forecast since $E_t$ and $M_t$ will be equal until $e_t$ takes on a negative value. The forecast error resulting from this model is shown in Table 2. The forecast error did not prove less than in previously tested models, but was comparable to the Chow model and the double smoothing model.

The data which must be kept to employ the Trigg and Leach model includes the forecasted value, the smoothed error, the absolute smoothed error and the value of $\alpha_{t+1}$. $\beta$ may be included in programming as a constant and of course actual demand ($X_t$) must be kept as in any forecast model. Less storage space is required for the Trigg and Leach model than for the Chow model but of course more data is required than for the single or double smoothed models.

In addition to the smoothing models described above, moving averages were considered. Due to limited available data only a 3 month moving average was considered. Of all the models tested it is perhaps the simplest. The forecast for a particular period is simply the average of the last 3 periods actual demand.

$$F_{t+1} = (X_t + X_{t-1} + X_{t-2})/3 \qquad (26)$$

Since only 12 data points were available, forecast for the last nine months were derived. Forecast error was measured by MAD as in the other models tested. This approach provided the highest degree of forecast error of any of the models studied as is indicated in Table 2.

One question that remains to be addressed is a comparison of the forecast error in the current forecasting model employed by SBSS. A FORTRAN program was written to forecast the last ten months of the sample period and measure its forecast error. The results are presented in Table 2. Single smoothing with an $\alpha$ =.1 was the only model which had a lower forecast error in each sample. But from the average of all four groups it appears that forecast error can be reduced by other techniques as well. Additional study through simulation is required to assess the overall impact of forecasting on the SBSS.

It is interesting to note that in the test of forecasting models the forecast error differ substantially between groups. It is not surprising that forecast error varies with item activity as was reported by Kaplan.[12] It would appear that the federal stock classes selected for this study provide a cross section of SBSS items.

## V. SIMULATION RESULTS

At present single exponential smoothing is the only forecasting model which could be tested using the FEDSIM model and compared to SBSS data. The default option of FEDSIM was used to select a stratified sample of 5000 items from the demand data on Dover AFB, Delaware for a one year period April 1978 - March 1979. The single exponential smoothing option was run for =.1 and =.2 with quarterly forecasts. The year end results are shown in Table 3 along with the current SBSS forecasting results.

TABLE 3

SBSS SIMULATION RESULTS USING THE CURRENT FORECASTING

MODEL AND SINGLE EXPONENTIAL SMOOTHING

| Effectiveness Measure | Current System | Single Smoothing $\alpha$ = .1 | Single Smoothing $\alpha$ = .2 |
|---|---|---|---|
| Line Item Fill Rate (%) | 85.40 | 84.43 | 83.86 |
| Net Line Item Fill Rate (%) | 89.68 | 88.77 | 87.73 |
| Units Fill Rate (%) | 84.60 | 82.61 | 80.83 |
| Net Units Fill Rate (%) | 86.75 | 85.06 | 82.85 |
| Avg. On-Hand Inventory ($) | 772,033 | 754,032 | 721,855 |
| Avg. On-Order Inventory ($) | 245,638 | 244,193 | 236,933 |
| Avg. Due-Out Inventory ($) | 35,474 | 37,563 | 38,910 |

In comparing these results consider the change in the net line item fill rate and the average on-hand inventory level. The net line item fill rate is a measure of effectiveness considering only items which are stocked by SBSS. This rate is lower in both simulations of single smoothing than for the current system, however, the average on-hand inventory is reduced as well. The fact that lower inventory levels reduce issue effectivenss is not surprising. The decision that must be made is whether the reduction in issue effectivenss is worth the savings which result. For example the simulation of single smoothing with $\alpha$=.1 shows roughly a one percent reduction in the net line item fill rate and approximately a $28,000 reduction in the average on-hand inventory. Keeping in mind that this simulation is for only 5,000 items at one base, the potential savings Air Force wide would be a significant amount if this relationship exists as a general rule. Clearly a one year simulation at one base does not provide

sufficient evidence to reach an optimal decision. If these patterns are found to exist on other bases, the trade-off between issue and asset effectivenss must be considered if the SBSS forecasting model is to be revised.

## VI. PROGRAM ACTIVITY AND DEMAND PREDICTION

It is realized that program activity (flying hours, sorties, etc.) has limited potential as a general approach to demand prediction. That is, only a small portion of items in SBSS are likely to be directly affected by program factors. In addition prior studies have focused on the wholesale rather than base level to consider the effects of program activity on the demand for selected reparable items.[6,9,10,16] In this study the demand activity of expendable items from selected federal stock classes were analyzed along with program factors. Units demanded monthly in federal stock classes 15, 16, 28, 29, 31, and 47, for samples of 200 items in each class, were determined. Monthly data were also obtained for the following program factors: flying hours, sorties flown and possessed aircraft. Statistical analysis was then performed using the stepwise regression program available in the Honeywell 6000 timesharing system. Measures of correlation between program factors and demand levels are shown in Table 4.

TABLE 4

CORRELATIONS BETWEEN PROGRAM FACTORS AND UNITS DEMANDED BY FEDERAL STOCK CLASS

| FEDERAL STOCK CLASS | PROGRAM FACTOR | | |
|---|---|---|---|
| | FLYING HOURS | SORTIES FLOWN | POSSESSED AIRCRAFT |
| 15 | -.620* | -.479 | .079 |
| 16 | -.297 | -.452 | .315 |
| 28 | -.155 | .045 | -.618* |
| 29 | -.633* | -.619* | .092 |
| 31 | -.627* | -.238 | -.372 |
| 47 | -.427 | -.283 | .138 |

*Significant at .05 level.

In three of the federal stock classes flying hours correlate significantly with units demanded. This finding is consistent with the prior studies on reparable items.[9,10] However, it is still not clear as to how these results can be used to predict demand on an item basis at base level. Each of the significant correlation coefficients are negative which indicates an inverse relationship between the program factors and units demanded. One possible explanation for this is that during extensive program activity some maintenance is postponed thereby creating a lag in parts demand. Available data prevented further study to determine if such a lag actually exists.

Multiple regression equations were also determined for units demanded in each federal stock class using program factors as independent variables. Analysis of the residuals showed high errors in prediction and that the use of more than one program factor did not improve the prediction of demand levels. In short no useful results were obtained from the regression analysis, perhaps due to the way in which demand was measured. It appears that the use of program activity in predicting the demand for expendable items is still questionable.

## VI. RECOMMENDATIONS

The purpose of this research was to investigate alternative approaches to demand forecasting for the SBSS. From the measurement of forecast error (MAD) single exponential smoothing, with small smoothing constants, emerged as the technique with the lowest error rate. In addition simulation results indicated that potential savings exist through a reduction of average inventory. It is clear that these findings can only be considered preliminary and that the analysis of larger samples from several bases will be required before substantive conclusions can be reached.

The double exponential smoothing model and the adaptive models tended to produce about the same level of forecast error. Since it is not likely that all items have a trend pattern, perhaps adaptive models should be considered as the second choice for further study. The time period in the present study may have been too short to allow the adaptive models to overcome the initialization conditions employed. Analysis of adaptive models for a longer time period may be required to adequately test its forecasting performance. However, considering the large number of items to be forecast at each base, the additional data requirements for adaptive models must be studied carefully.

Another consideration for further study is the stratification of items into homogenous groups in order to reduce forecast error. This grouping might be on the basis of item activity (high, medium and low volume) or item essentiality. Given the large number of items it would appear that this approach could reduce forecast error. This does not necessarily require completely different approaches to forecasting. For example the general approach to forecasting might be single exponential smoothing but with different smoothing constants for each strata.

Due to the limited data base available, monthly demand data were studied. For many items a large number of months were observed to have zero demands. Further study of demand data may be enhanced by the analysis of quarterly rather than monthly data. Given the large number of items at each base and the available computer facilities, as a practical matter quarterly forecast may be preferable.

In regard to program activity as a demand prediction tool for expendable items, this study does not provide any substantive conclusions. Although flying hours were correlated to demand level for some federal stock classes, the inverse relationship present could not be adequately explained. Since program activity is likely to be used for a very small number of items, further study should concentrate on a well defined group of items.

## REFERENCES


1. William Ascher, Forecasting: An Appraisal for Policy-Makers and Planners, (The John Hopkins University Press, Baltimore, 1978).

2. R.G. Brown and R.F. Meyer, "The Fundamental Theorem of Exponential Smoothing," Operations Research, Vol. 9, No. 5, pp. 673-685, 1961.

3. J.L. Buffay; C.J. Christianson; J.M. Meyer; J.A. Scanga; H.D. Sheets and D.E. Smith, "Demand Data Analysis Applied to Repair-Parts Supply Management," Technical Paper RAC-TP-426, June 1971.

4. H.S. Campbell, "Concept and Measurement of Demand for Recoverable Components," Rand Corporation RM 3824-PR, September 1963.

5. W.M. Chow, "Adaptive Control of the Exponential Smoothing Constant," Journal of Industrial Engineering, Vol. 16, No. 5, pp. 314-317, 1965.

6. Martin Cohen, "Demand Forecasting with Program Factors," USAMC Inventory Research Office, IRO Report No. 182, September 1975.

7. G.J. Feeney and C.C. Sherbrooke, "Systems Analysis and Supply Management," Rand Corporation RM-4054-PR, April 1974.

8. D.C. Fischer, Jr. and P.S. Gibson, "The Application of Exponential Smoothing to Forecasting Demand for Economic Order Quantity Items," unpublished Masters Thesis, United States Air Force, Air University, Air Force Institute of Technology, Wright-Patterson AFB, Ohio, January 1972.

9. O.A. Goldfarb and W.A. Smiley, "An Evaluation of Program Activity as a Demand Prediction Tool," Unpublisehd Masters Thesis, United States Air Force, Air University, Air Force Institute of Technology, Wright-Patterson AFB, Ohio, August 1967.

10. T.A. Goldman, "Relationships Between Program Elements and System Demand for Airframe Spare Parts," Rand Corporation RM-1858, January 1957.

11. D. Gross and R.J. Craig, "A Comparison of Maximum Likelihood, Exponential Smoothing and Bayes Forecasting Procedures in Inventory Modeling," The George Washington University, Serial T-261, April 1972.

12. A.J. Kaplan, "Estimation of Demand Variability Parameters," USAMC Inventory Research Office, IRO Report No. 183, May 74.

13. S. Makridakis and S.C. Wheelwright, Forecasting: Methods and Applications (John Wiley and Sons, New York, 1978).

14. M. Nerlove and S. Wage, "On the Optimality of Adaptive Forecasting," Management Science, Vol. 10, No. 2, pp. 207-224, 1964.

15. M.S. Seppanen, "Technical Planning for the USAF Standard Base Supply System (SBSS); RIMSTOP and Beyond," Unpublished Report 1978 USAF-ASEE Summer Faculty Research Program.

16. H. Solomon, "A Summary of the Logistics Research Project's Experience with Problems of Demand Prediction," The George Washington University, Serial T-139/62, April 1962.

17. H. Theil and S. Wage, "Some Observations on Adaptive Forecasting," Management Science, Vol. 10, No. 2, pp. 198-206, 1964.

18. N.T. Thomopoulos, Applied Forecasting Methods, (Prentice-Hall, Englewood Cliffs, New Jersey, 1980).

19. P.R. Winters, "Forecasting Sales by Exponentially Moving Averages," Management Science, Vol. 6, No. 3, pp. 324-342, 1960.

20. P.W. Zehna and C.F. Taylor, Jr. "Comparing Inventory Demand Forecasts," Naval Postgraduate School, Report No. NPS55ZE75051, May 1975.

1980 USAF - SCEEE SUMMER FACULTY RESEARCH PROGRAM

Sponsored by the

AIR FORCE OFFICE OF SCIENTIFIC RESEARCH

Conducted by the

SOUTHEASTERN CENTER FOR ELECTRICAL ENGINEERING EDUCATION

FINAL REPORT

# QUANTITATIVE DETERMINATION OF ODD CHLORINE SPECIES


| | |
|---|---|
| Prepared by: | Dr. G. Earl Peace, Jr. |
| Academic Rank: | Associate Professor |
| Department and University: | Department of Chemistry<br>College of the Holy Cross |
| Research Location: | Air Force Geophysics Laboratory,<br>Aeronomy Division, Composition Branch |
| USAF Research Colleague: | Charles C. Gallagher |
| Date: | September 15, 1980 |
| Contract No: | F49620-79-C-0038 |

# QUANTITATIVE DETERMINATION OF ODD-CHLORINE SPECIES

by

G. Earl Peace, Jr.

## ABSTRACT

The feasibility of an analytical method yielding the sum of the concentrations of odd-chlorine species is investigated. The procedure would involve first reacting these odd-chlorine species with a strong, organic Lewis acid, which would be adsorbed onto the filter medium, to form HCl. The HCl would then be determined in aqueous solution using an ion-selective electrode. A quantitative, reproducible aqueous extraction procedure by which the HCl may be removed from the filter medium is described. The use of an integrating digital voltmeter and a programmable calculator to eliminate short-term noise fluctuations through a signal averaging technique allowed the ion-selective electrode to be used with good precision and reasonable accuracy well below its suggested lower limit. The Lewis acids could not be tested directly due to a lack of suitable filter media.

## Acknowledgement

The author would like to thank the Air Force Systems Command, the Air Force Office of Scientific Research and the Southeastern Center for Electrical Engineering Education for affording him the opportunity to engage in such interesting and personally rewarding research with the Aeronomy Division, Air Force Geophysics Laboratory, Hanscom AFB, MA.

Special thanks are due Mr. Charles C. Gallagher for his assistance, guidance and cooperation. I would also like to thank Dr. Rocco Narcisi, Mr. Charles Forsberg and Col. Alan Mason for their helpful discussions.

I. INTRODUCTION:

The stratospheric ozone layer, although its concentration is at most only a few parts per million, is responsible for absorbing most of the high energy ultraviolet radiation that would otherwise prove harmful to most life forms on earth. Therefore, any mechanism by which its concentration might be lowered is of primary importance. Unfortunately, there now appear to be several compounds which are capable of catalyzing the destruction of ozone as illustrated by the following examples:

$$NO + O_3 \longrightarrow NO_2 + O_2 \qquad (1)$$

$$NO_2 + O \longrightarrow NO + O_2 \qquad (2)$$

net: $$O_3 + O \longrightarrow 2\,O_2 \qquad (3)$$

$$Cl + O_3 \longrightarrow ClO + O_2 \qquad (4)$$

$$ClO + O \longrightarrow Cl + O_2 \qquad (5)$$

net: $$O_3 + O \longrightarrow 2\,O_2 \qquad (6)$$

The former set of reactions (1-3) is important because of the oxides of nitrogen ($NO_x$) emitted by aircraft operating at or above the tropopause. The latter set of reactions (4-6) is important because of the confirmed photochemical decomposition of chlorofluorocarbons (also known as "freons") to yield atomic chlorine. It is apparent, however, from reactions (3) and (6) above that the net effects of these two reaction schemes are identical and, therefore, are supplementary and indistinguishable.

In order to be able to predict the effects of the injection of additional $NO_x$, it is necessary to develop a budget for the odd Cl constituents - so called because the various chemical forms transform relatively rapidly from one to another. The chlorine atoms eventually form hydrogen chloride by reaction with such species as methane, molecular hydrogen, hydrogen peroxide or hydrogen peroxy radicals[1].

Lazrus and colleagues[1] have reported quantitative values for the HCl and particulate Cl. Gallagher and colleagues[2] have reported quantitative values for $CFCl_3$ (freon-11) and $CF_2Cl_2$ (freon-12). These data, however, are insufficient to completely characterize the

odd Cl budget. Quantitative values for HOCl, $HO_2Cl$, HCl, $ClO_x$ and $ClONO_2$ in addition to the previously mentioned species would effectively complete the data so that the odd Cl budget can be more precisely determined.

## II. OBJECTIVES

The main objective of this project was to develop an analytical procedure which is specific for the odd Cl species. Rather than trying to identify each and every one of these chemical forms individually, it was decided to attempt to devise a procedure which would yield the sum of their respective concentrations. The specific goals may be stated as follows:

(1) to develop an aqueous extraction procedure which is both quantitative and reproducible in removing soluble chloride compounds from filter media.

(2) to compare and contrast the use of a chloride ion-selective electrode and the fluorescence quenching ability of chloride ion as to their suitability as methods of analyzing the aqueous extract.

(3) to study the effectiveness of certain strong secondary Lewis acids, e.g., cumene (isopropyl benzene), in reacting with the various odd Cl species to form water soluble hydrogen chloride.

## III. AQUEOUS EXTRACTION PROCEDURE

An aqueous extraction procedure is desirable for several reasons. First, the procedures for making extremely pure water are well documented and relatively simple. Second, the solvent should be polar to dissolve the polar chlorine compounds, and should have a relatively low vapor pressure at room temperature to minimize losses due to evaporation during analysis. Third, there must be an unambiguous method by which the purity (absence of ions) can be determined. The conductivity of the water can be used to satisfy this last criterion. Lastly, low concentration standards can be prepared simply and accurately by dilution.

Samples of suspended particulates were collected over a 24-hour period on three occasions using a high-volume air sampler (General Metal Works) equipped with glass-fiber filter (BGI, Inc., Catalog #25/810). Each filter was then cut into quarters. Diagonally opposite quarters were then cut into smaller strips, placed in 75 ml. of distilled/deionized $H_2O$, and heated to approximately 75°C. with continuous stirring. This digestion process

was continued until the filter strips were completely decomposed and homogeneous, a process which took about five hours. This viscous solution was then filtered through Whatman #41 quantitative filter paper into a 100 ml. volumetric flask. The residue was washed repeatedly with distilled/deionized water and the washings were used to dilute to volume. Tests of subsequent washings with the ion-selective electrode showed the chloride ion concentration to be well below the minimum detection limits.

To make sure that chloride ions were not being adsorbed by the glass fibers, one quarter sheet of unexposed glass fiber filter was digested in 75 ml. of distilled/deionized water to which was added 0.05845 g. of reagent grade NaCl. After filtering as described above, 10.00 ml. of the filtrate was diluted to the mark in another 100 ml. volumetric flask. This solution was then analyzed with the ion-selective electrode and was found to contain 35.4 ppm (theoretical value would be 35.45 ppm). The average value of five such trials was also 35.4 ppm, corresponding to a 99.9% recovery. The use of a digital voltmeter with a four or five digit readout would allow a refinement of this percent recovery, but the goal of a simple, quantitative and reproducible extraction appears to have been attained.

## IV. USE OF ION-SELECTIVE ELECTRODE

The recommended lower limit of detection for the Orion Model 94-17 chloride ion-selective electrode is approximately 1-10 ppm. Lazrus et al have reported the total inorganic chlorine concentration to be approximately 0.75 ppbm. Therefore, in order to have enough sample to prepare a 1.00 ppm solution $\frac{1.00 \times 10^{-5}\text{g}}{10.0\text{ ml}}$ of chloride ion in a 10.0 ml volumetric flask,

$$\frac{1.00 \times 10^{-5}\text{g}}{0.75 \times 10^{-9}\text{g/g of air}} = 1.33 \times 10^{4}\text{g of air} \qquad (7)$$

The density of air at 20 km (65,600 ft.) is 92.13 $g/m^3$ so that that the volume of air which must be drawn through a filter in order to collect the required $1.00 \times 10^{-5}$g of chloride is given by

$$1.33 \times 10^{4}\text{g}/92.13\text{g}/\text{m}^3 = 1.45 \times 10^{2}\text{m}^3 \qquad (8)$$

A larger volume would be required at higher altitudes due to the lower density. Since the time required to collect this amount of material would

be excessive, the major effort of this project was spent on evaluating the quantitative utility of this electrode at concentrations down to 1.00 ppb.

The minimum detection limit (or background) of the chloride ion is determined by the chloride concentration of the solvent. In this study, distilled water was passed through a 75 cm mixed-bed cation/anion exchange resin column in order to remove ionic impurities. The measured conductivity of the resulting water was measured and found to be no more than $2 \times 10^{-7}$ $ohm^{-1}$ $cm^{-1}$, at a pH of 5.5. If it is assumed that all of the conductance is due to dissolved sodium chloride, hydronium ions and hydroxide ions, then the maximum possible concentration of chloride ion is calculated to be 40 ppb. Since there is no basis for this underlying assumption, however, the actual chloride ion concentration of this water is certainly much lower than this calculated maximum.

A solution containing 99.97 ppm chloride ion was prepared by dissolving 0.1648 g of reagent grade sodium chloride in enough distilled/deionized water to make exactly one liter of solution. In all subsequent calculations, the concentration of this solution is taken to be 100.ppm.

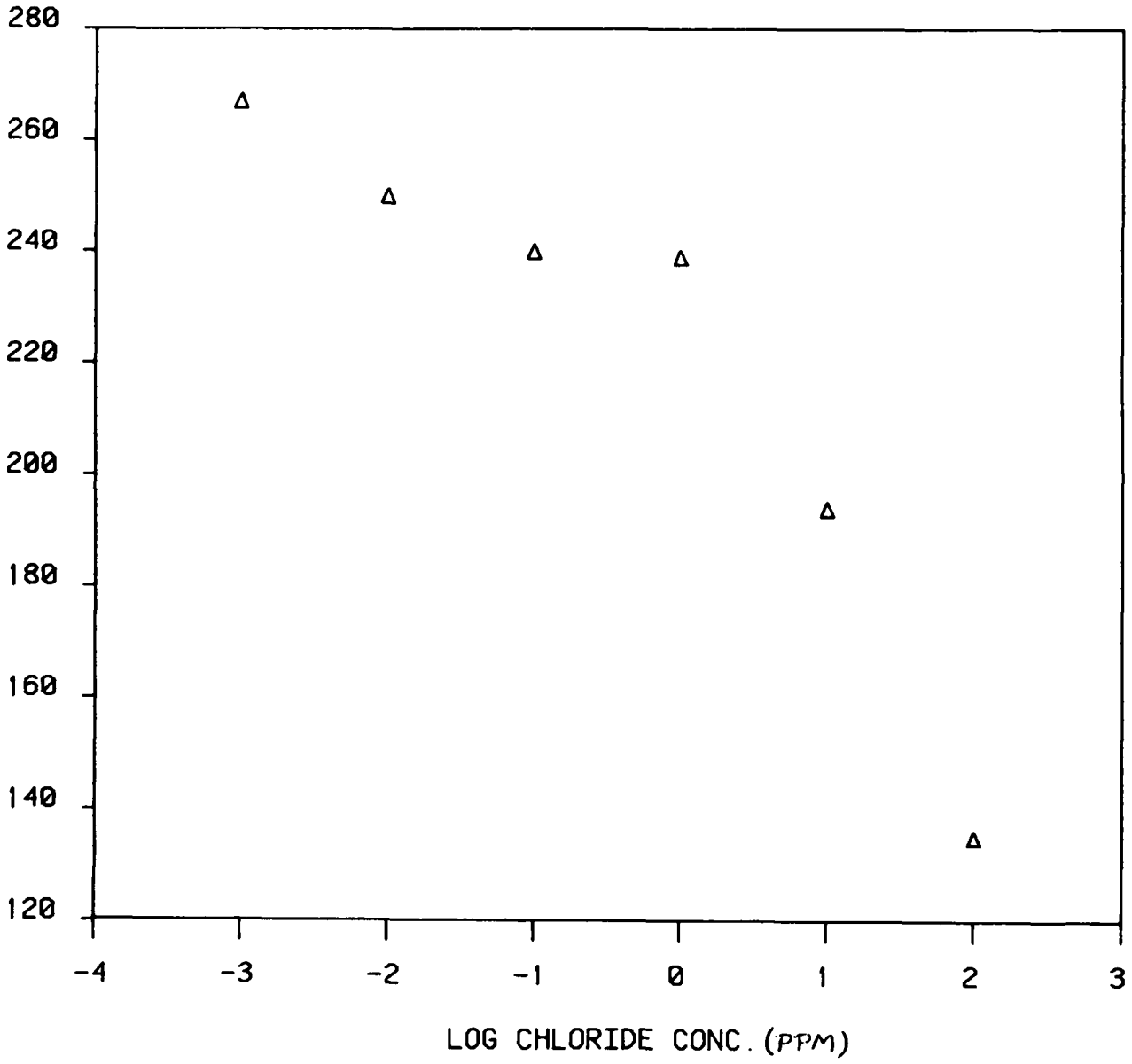
A series of standard solutions was prepared by serial dilution of the 100. ppm stock solution. The 10.0ppm standard was prepared by making a 1/10 dilution of the 100.ppm solution. Each successive standard was prepared by making a 1/10 dilution of the preceding standard until, after four such dilutions, the final standard(1.00ppb chloride) was prepared.

The electrode was then checked for proper Nernstian behavior. The potential measured by the electrode should theoretically decrease by 59.1 millivolts for each tenfold increase in the concentration of the chloride ion. As shown by the following table, this behavior was, in fact, observed.

| Log $Cl^-$(ppm) | Millivolts |
|---|---|
| 2.00 | 135.0 |
| 1.00 | 194.0 |
| 0.00 | 247.0 |

The data obtained when all of the standard solutions were measured are shown in Figure 1. The change in the measured potential becomes markedly non-Nernstian below 1 ppm, with tenfold changes in concentration producing differences of only 25% of the theoretical ones, as shown in the following table:

FIGURE 1


280
260
240
220
200
180
160
140
120
MILLIVOLTS
-4
-3
-2
-1
0
1
2
3
LOG CHLORIDE CONC. (PPM)

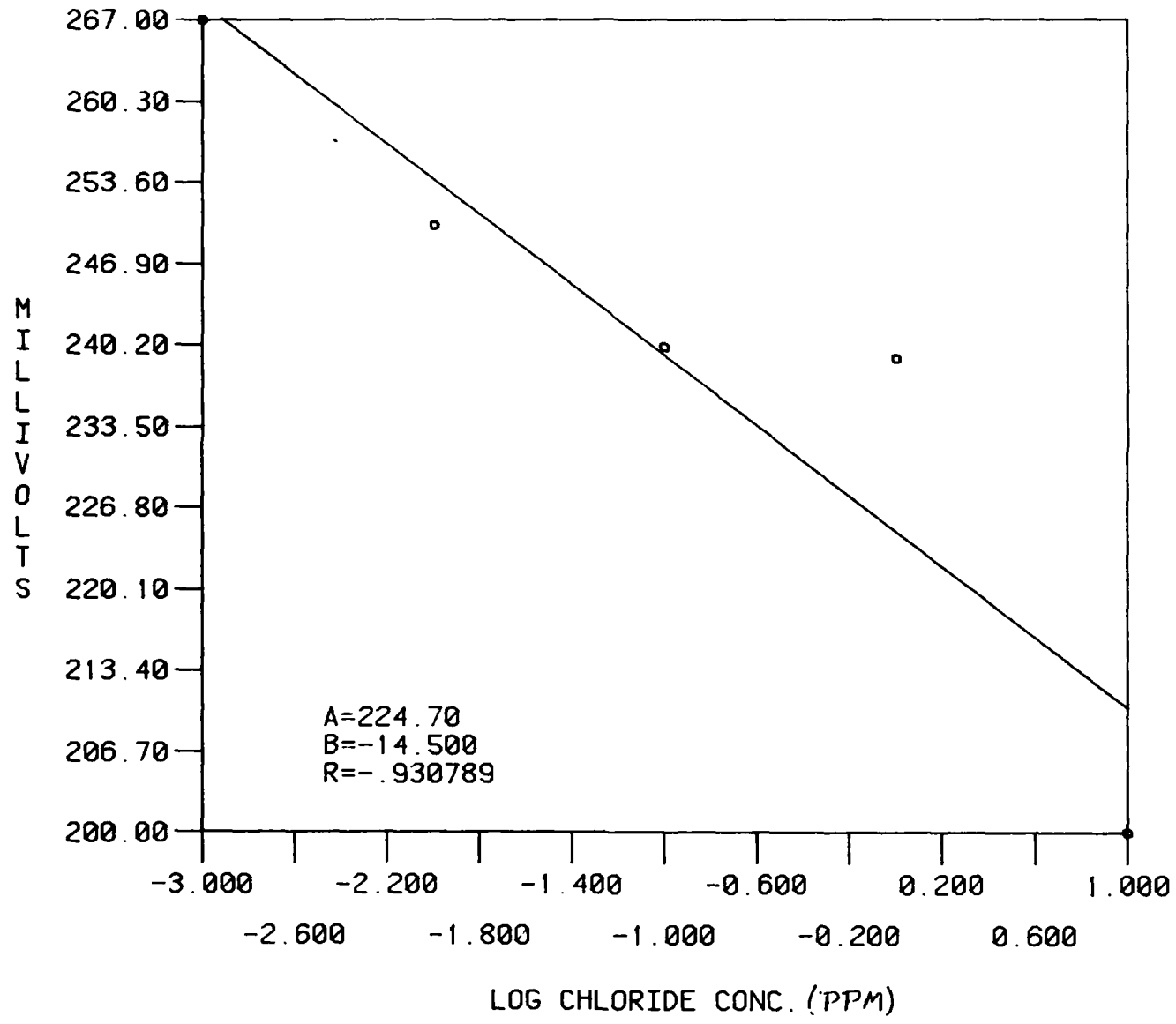
| Log $Cl^-$ (ppm) | Millivolts |
|---|---|
| 1.00 | 200 |
| 0.00 | 239 |
| -1.00 | 240 |
| -2.00 | 250 |
| -3.00 | 267 |

Nevertheless, it was decided to test the low concentration range for linearity, with the results shown in Figure 2. The resulting correlation coefficient of -0.931 (a value of -0.993 is obtained if one assumes the point at (0.00,239) to be in error) does not truly indicate the difficulties encountered in obtaining these data. At such low concentrations, the electrode potential exhibited both a rapid, random noise fluctuation and a long-term drift. This long-term drift was measured for several solutions over a period of 90-120 minutes, and was consistently found to be approximately 0.1 millivolts/minute. Surprisingly, this rate of drift is identical to that reported by Baumann[3] in a study involving a fluoride ion-selective electrode at concentrations below the stated lower limit of utility.

A second series of standard solutions was prepared using the same general procedure described above, but with one important change. Each solution also contained 2.5 ml of 5.00 M sodium nitrate per 250 ml. of solution. The purpose of the added sodium nitrate was to act as an ionic strength "buffer", so that the background ionic strength of each solution is constant. When these "buffered" solutions were measured, however, there was no significant difference in the measured potentials of any of the solutions below 1ppm. This indicates that an impurity of chloride ion in the sodium nitrate although stated to be "less than 0.001%" on the label, is still large enough at these concentrations to exert a levelling effect on all of these solutions. It was then decided to proceed with the original set of standard solutions rather than attempt to purify the sodium nitrate.

The next several days were then spent attempting to isolate and eliminate the cause of this long-term drift in electrode potentials. The various components of the system, i.e., the pH/specific ion meter, the digital voltmeter and the recorder were all checked and found to be operating within their respective manufacturer's specifications. This drift was also observed when the temperature of the standard solution was maintained in a water bath, although the short-term noise fluctuations were reduced. It was also discovered

FIGURE 2




60-10

that the magnitude of the measured potential changed slightly with changes in the stirring rate of the magnetic stirrer. This problem was eliminated by leaving the stirring rate set at a mid-range setting even when changing samples. The short-term noise fluctuations and long-term drift were both reduced somewhat by insulating the beaker containing the sample from the warm surface of the magnetic stirrer by means of a square styrofoam block with a small circular area removed so that the beaker would fit.

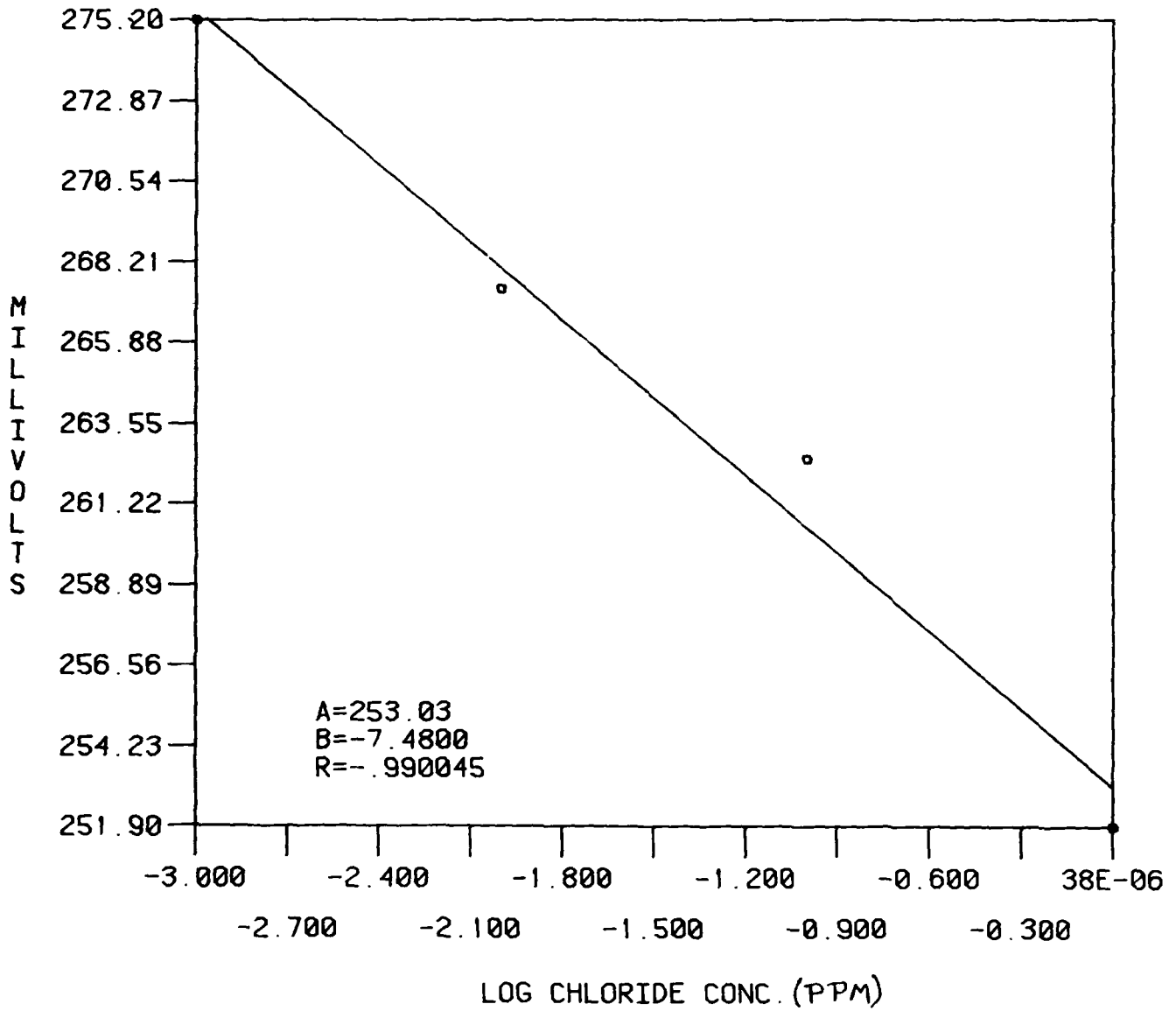
Since the drift could not be completely eliminated, it was decided to at least eliminate the short-term noise fluctuations by means of signal averaging. An integrating digital voltmeter was first used to accomplish this, but the lack of any permanent record of these average values offered little overall advantage. This integrating voltmeter was then replaced by the orginal digital voltmeter, but the output of this voltmeter was then fed into a Hewlett-Packard 982A0 programmable calculator. This calculator was programmed to sum and average the output of the voltmeter for one minute intervals (342 values per minute) and print this average value. The system was now automated, once the electrode was inserted into a sample, to record the behavior of the electrode potential over time on the recorder, while printing average values of this potential at one minute intervals.

When this system was used to remeasure all of the low concentration standards, it was found that for each solution the rate of the long-term drift seemed minimal between 35 and 45 minutes after beginning the measurement, although it then began again at a slightly slower rate. From this information, the optimum value of the potential for each solution was taken to be the forty-fifth printed value. A plot of these results for one trial of the low concentration solutions is shown in Figure 3. Three subsequent trials all gave correlation coefficients between -0.97 and 0.99, thus indicating that, despite all of the attendant problems, a chloride ion-selective electrode can be used below its suggested lower limit with reasonable accuracy and good precision.

## V. STUDY OF LEWIS ACIDS

While attempting to measure the inorganic (soluble) chlorine content in samples of suspended particulates collected as previously described, it was discovered that the glass-fiber filters used have a significant and highly variable chloride ion content. All atempts to wash these filters prior to use resulted in such a loss of structural integrity that the filters were easily torn. The Lewis acids to be studied could thus not be directly compared or contrasted in actual sample collection tests using suspended particulates.

FIGURE 3


275.20
272.87
270.54
268.21
265.88
263.55
261.22
258.89
256.56
254.23
251.90
MILLIVOLTS
A=253.03
B=-7.4800
R=-.990045
-3.000
-2.700
-2.400
-2.100
-1.800
-1.500
-1.200
-0.900
-0.600
-0.300
38E-06
LOG CHLORIDE CONC. (PPM)

## VI. RECOMMENDATIONS

In order to accomplish the initial goals of this project, two additional studies should be completed. The first of these is to attempt to react the secondary Lewis acids to be investigated with samples of such compounds as $NO_2Cl$, $Cl_2$, ClO, freon-11 and freon-12. If, at temperatures approximating those found above 20 km, hydrochloric acid is found to be a product of the reaction for any of these Lewis acids, then a method for quantatively determining stratospheric concentrations of odd-chlorine species is possible.

The second study which must be completed is a comparison of different brands and types of filters to determine which one, if any, has a low enough chloride ion content to serve as a substrate for the application of the secondary Lewis acid. Alternatively, any filter which will stand up structurally to repeated washings to remove chloride ions would also suffice.

## REFERENCES


1. A. L. Lazrus, B. W. Gandrud, R. N. Woodard and W. A. Sedlacek, "Direct Measurements of Stratospheric Chlorine and Bromine," J. Geophys. Res, Vol. 81, pp. 1067-1070, 1976.

2. C. C. Gallagher, R. V. Pieri and P. D. Goldan, "Stratospheric Measurements of $N_2O$, $CFCl_3$ and $CF_2Cl_2$," J. Atmos. Sci., Vol. 34, pp. 1481-1482, 1977.

3. E. W. Baumann, "Sensitivity of the Fluoride-Selective Electrode Below the Micromolar Range," Anal. Chim. Acta., Vol. 54, pp. 189-197, 1971.

1980 USAF - SCEEE SUMMER FACULTY RESEARCH PROGRAM

Sponsored by the

AIR FORCE OFFICE OF SCIENTIFIC RESEARCH

Conducted by the

SOUTHEASTERN CENTER FOR ELECTRICAL ENGINEERING EDUCATION

FINAL REPORT

# THE EFFECTS OF IMAGE MOTION AND ROTATION ON CONTRAST SENSITIVITY IN A LETTER DETECTION AND IDENTIFICATION TASK


| | |
|---|---|
| Prepared by: | Dr. J. Timothy Petersik |
| Academic Rank: | Instructor |
| Department and University: | Department of Psychology<br>Southeast Missouri State University |
| Research Location: | Air Force Aerospace Medical Research Laboratory, Human Engineering Division, Visual Display Systems Branch, Aviation Vision Laboratory |
| USAF Research Colleague: | Capt Arthur P. Ginsburg, Ph.D. |
| Date: | August 10, 1980 |
| Contract No: | F49620-79-C-0038 |

# THE EFFECTS OF IMAGE MOTION AND ROTATION ON CONTRAST SENSITIVITY IN A LETTER DETECTION AND IDENTIFICATION TASK

by

J. Timothy Petersik

## ABSTRACT

The effects of image motion and rotation are examined in a task in which subjects adjusted the contrast required to just detect and just recognize various stimuli consisting of (1) sine-wave gratings of various spatial frequencies and (2) Snellen letters of various sizes and rotations relative to the frontoparallel plane. Results show that motion enhances sensitivity in both tasks, but generally only with (1) low-frequency gratings and, paradoxically, with (2) small Snellen-letter targets. The advantage produced by motion generally depended upon velocity, target size, and target rotation. Other findings include the fact that sensitivity in the detection task always exceeded that in the identification task, the slope of the line relating sensitivity to target size increased with rotation, and sensitivity to small, moving targets increased with the energy of the targets. Suggestions for extending the results of this research are offered.

## Acknowledgement

The author would like to thank the Air Force Systems Command, the Air Force Office of Scientific Research, and the Southeastern Center for Electrical Engineering Education for making possible his summer visit to the Air Force Aerospace Medical Research Laboratory, Wright-Patterson AFB, OH. He also extends his gratitude to the Aviation Vision Laboratory and the Visual Display Systems Branch for their hospitality and assistance.

The author especially wishes to thank Capt Arthur P. Ginsburg for the intellectual stimulation and encouragement he provided and for the technical and material support he made available. Certain other individuals deserve special thanks: Mr. Steve Fullenkamp, Lt Dave Evans, and Dr. Mark Cannon for showing the author "the ropes" around the laboratory, Mr. Brian Bennett for lending his technical expertise, Lt Don Wallquist for his photographic assistance, Mrs. Pamela Porter for her competent typing, Ms. Jacqueline Hickman for secretarial assistance, and P.K., M.J.H., K.S., D.S., B.F., and others for their valuable moral support.

## I. INTRODUCTION:

The solution of many problems that are of interest to the Air Force requires a thorough understanding of the processing capabilities and organizational principles of the human visual system. Such problems include, but are not limited to, display design, windscreen design, image processing, pattern recognition, visual tracking, etc. A new approach to understanding the human visual system has involved the concept of filtering, within the context of linear systems analysis. This approach seeks to determine how spatial information about objects is physically filtered and transmitted in the visual system. The present project is an attempt to extend our understanding of visual filtering to include stimuli not heretofore examined, namely moving complex objects and rotated images.

The simplest stimuli available for testing the operating characteristics of the visual system are sine-wave gratings, i.e., luminance distributions whose profiles are sinusoidal. In general, sine-wave gratings are described by three to four parameters, spatial frequency (the rate of luminance changes over space, usually in units of cycles per degree of visual angle, or cpd), contrast (defined as $L_{max} - L_{min} / L_{max} + L_{min}$, where $L_{max}$ and $L_{min}$ refer to the maximum and minimum luminances of the grating, respectively), phase (the location of peaks and troughs of the distribution relative to some fixed point), and orientation. Recent studies using such stimuli[1,2] suggest that the human visual system behaves like a bandpass filter with respect to spatial frequency. Furthermore, studies suggest that the visual system is linear to a first approximation, both at threshold contrasts[2] and at suprathreshold contrasts[3]. These findings render the human visual system open to linear-systems types of analyses.

Other experiments[4,5] have examined the human contrast sensitivity function (CSF) in more detail. CSF relates the reciprocal of threshold contrast to spatial frequency, and for most normal observers is an inverted-U shaped function. Adaptation of the visual system to individual spatial frequencies[4,5] results in a localized depression in the CSF, centered at the adapting spatial frequency and about 1.5 octaves in width. These results strongly suggest that the normal CSF is an envelope of the CSFs of several narrower spatial channels, each of which can be thought of as a bandpass filter.

Ginsburg[6] has argued that, under certain conditions, the visual system can be considered as passing spatial information through roughly seven distinct channels or filters, each of which is tuned differently. The evidence for Ginsburg's proposal includes many demonstrations, one of which warrants detailed discussion: A portrait of a human face was filtered through eight distinct channels whose center spatial frequencies were one octave apart and whose bandwidths were two octaves. Each successive filtered portrait revealed information useful to successively more refined perceptual tasks - the lowest filtered portrait passed only gradual contrast changes; the next, an elliptical shape; next, generalized facial information; information regarding age, sex, etc.,; information required for identification; details of hair, eyes, etc.,; and so on.

In an example that is especially relevant to the present research, Ginsburg[6] compared the CSF to the more traditional method of assessing visual performance (i.e., Snellen acuity) in an effort to elucidate the filter concept. He began by determining the number of spatial frequencies required for identification of two common Snellen letters, E and L. He filtered each of the letters with successively broader low-frequency band-pass filters and showed that about 2.5 cycles per object (cycles per object, or cpo, is a relative measure that does not depend upon viewing distance as does cpd) are required for identification of the E, and about 1.5 cpo are required for identification of the L. It was suggested that a spatial filter with a bandwidth of 1.5-2.5 cpo is required for Snellen letter recognition in general. This means that, given Snellen-type letters of any size (i.e., of any fundamental spatial frequency), the spatial information required for identification of the letter will be contained in a range of spatial frequencies about 1.5 to 2.5 times the fundamental spatial frequency. Thus, for Snellen letters of various sizes, Ginsburg was able to identify the band of spatial frequencies that would be required for identification. Further, after obtaining the CSFs of several individuals, Ginsburg was able to predict Snellen acuity on the basis of the above analysis.

As important, however, is Ginsburg's criticism of the adequacy of Snellen acuity as a measure of visual performance. First of all, Snellen acuity is a undimensional measure. That is, it tests only sensitivity to <u>high contrast</u> letters of varying size. On the other hand, sine-wave testing varies both contrast and size (i.e., spatial

frequency). Furthermore, the CSF can sometimes reveal visual deficits that are not detected by conventional Snellen testing. As an example, suppose an individual attempts to recognize a Snellen letter that subtends 5' visual angle. The fundamental spatial frequency of this letter will be about 12 cpd (5' = $.08333^{o}$; $1/.08333^{o}$ = 12 cpd) and, by the analysis of the preceding paragraph, the information required for identification will lie in the region from 18-30 cpd. As long as the person's visual system passes information from 18-30 cpd normally, identification of the letter will be accomplished and acuity will be judged to be normal. However, if, as was the case with one of Ginsburg's subjects, the individual has a loss of sensitivity outside the 18-30 cpd region, that loss will go undetected by the Snellen method. The individual will nonetheless suffer from some visual degradation. As Ginsburg showed, the CSF would reveal such a loss.

Although Ginsburg's determination of the spatial bandwidth required to recognize Snellen letters and his subsequent prediction of Snellen acuity based upon the CSF represents a major advance in visual science, it is incomplete inasmuch as the stimuli he used were stationary and were always perpendicular to the observer's line of sight. Since most of the visual world is glimpsed under conditions of movement (either of the observers or of the observed objects themselves) and since not all objects face the observer directly, it was thought to be beneficial to extend Ginsburg's analysis to include such conditions.

The pioneering psychophysical studies of Kulikowski and Tolhurst[7] and of Tolhurst[8] have shown that with moving sine-wave gratings, most combinations of spatial frequency and velocity give rise to two perceptual thresholds. One of these is a "movement" or "flicker" threshold, and the other is a "pattern" threshold. It has since been postulated that the visual system actually consists of two broad classes of channels and that each class has its own spatio-temporal response properties (see Brietmeyer and Ganz[9] and Petersik[10] for a review of these properties). The transient channel responds best to moving or flickering stimuli and provides little information about the detailed structure of a stimulus. On the other hand, the "sustained channel" prefers relatively stationary stimuli and does provide information regarding pattern detail. This

distinction has recently found support in the physiological literature (see Sekuler, Pantle and Levinson[11] for a review). Presumably, the Snellen letter recognition studies of Ginsburg cited above make use almost solely of the sustained system. Depending upon their contrast, moving targets may be analyzed only by transient mechanisms or by both transient and sustained mechanisms. Thus, there is a good reason to replicate the studies of Ginsburg under conditions in which both gratings and targets move.

Projective geometry shows that the two-dimensional image on the picture plane (in this case, the retinal image) changes both in shape and size as the object giving rise to the image is rotated about the vertical axis (Petersik[12]). The geometric analysis suggests that as an object rotates relative to the observer, its spatial frequency spectrum on the picture plane must also change. How this change in the spectrum of the object affects target acquisition and recognition is not known. However, the question is of practical importance, since, for example, most of the stimuli approaching a pilot will not be perpendicular to his or her line of sight. The type of analysis previously employed by Ginsburg should determine how rotation affects visual performance.

Finally, Ginsburg[6] has suggested that the crucial processing of a complex visual scene could be analyzed through the activity of approximately seven visual filters, each selective for a different range of spatial frequencies. The output of one of these filters would account for the detection of a stimulus, another for its classification as an object, another for its identification, etc. Similarly, visual performance on tasks involving moving and rotated stimuli ought to reveal corresponding channels or filters. A knowledge of the biological data regarding motion filters will allow Ginsburg's theory to be applied to the vast majority of real-world visual scenes. The specific aims of the proposed experiments are described below.

## II. OBJECTIVES:

The main objective of this project was to provide preliminary data which can ultimately be used to extend Ginsburg's[6] filtering model of visual processing to cases involving moving visual stimuli and stimuli rotated with respect to the observer's frontoparallel plane. The stimuli included sine-wave gratings and complex images, namely four Snellen letters,

B, E, V, & L. The specific objectives included:

(1) Design modification of a pre-existing variable-contrast visual stimulation system to include the presentation of both stationary and moving (variable velocity) stimuli.

(2) To collect contrast sensitivity data for both moving and stationary sine-wave gratings over a range of visible spatial frequencies.

(3) To collect contrast sensitivity data at both "detection" and "identification" thresholds for both stationary and moving Snellen letters of various sizes (i.e., fundamental spatial frequencies).

(4) To relate the basic CSFs obtained with stationary and moving sine-wave gratings to the detection and identification thresholds obtained with stationary and moving Snellen letters.

## III. METHODS:

### A. Stimuli and Apparatus

High contrast photographic slides (Kodak 35mm High Contrast Copy Film) of sine-wave gratings of various spatial frequencies that had been generated on a display monitor were prepared. The specific spatial frequencies used were: 0.46, 0.96, 1.79, 3.50, 7.17, 12.00, and 18.33 cpd. High contrast photographic slides (Kodak 35mm Kodalith film) of Snellen letters of three different sizes and four rotations were also prepared. The particular letters chosen were B, E, V, and L, and at $0^{\circ}$ rotation the letter-widths for the small, medium and large letters were $.34^{\circ}$, $68^{\circ}$ and $1.00^{\circ}$ visual angle, respectively. For each size, each letter was photographed at an angle of $0^{\circ}$, $30^{\circ}$, $45^{\circ}$, and $60^{\circ}$ relative to the frontoparallel plane. As a letter of a single size is rotated, its spatial-frequency content changes correspondingly. This fact is reflected in the present Results section.

Stimuli were presented through a dual-channel cross-polarizing system. This system places orthogonally oriented filters in front of each of two slide projectors, (a) the stimulus projector, and (b) the luminance projector (which contains no stimulus). The beams from both projectors are next passed through a polarizing analyzer and superimposed upon a screen. Rotation of the analyzer allows the relative contribution of the luminance from each projector to vary while maintaining overall luminance at an approximately fixed level. In practice, this allows the observer to

to manipulate stimulus contrast. To produce image motion, the summed beams were reflected from a front-surfaced mirror, then passed through the analyzer, through a mask, and finally onto a screen. The mirror was situated on a scanner that was driven by a waveform generator. The waveform generator controlled the frequency and amplitude of the rotation of the scanner, and therefore also of the mirror and stimulus image. With respect to the observer, stimulus images moved at velocities of either 0, 1.2, or 3.6 degrees of visual angle/sec.

The average luminance of the display varied from stimulus to stimulus, but was in the range of 2.25 - 3.50 fL.

B. Subjects

Two subjects served in the present experiments. Viewing was monocular with the preferred eye. Subject NDP was naive with respect to the purpose of the project, had corrected-to-normal vision, and viewed the displays with the right eye. Subject JTP was the author, had corrected-to-normal vision, and viewed with the left eye.

C. Procedure

All sessions were conducted in a semi-dark room whose only ambient illumination was provided by a desk lamp situated near the subject and by the slide projectors themselves. To prevent subject fatigue, trials were run in 50-min blocks. On any trial, the subject was seated 444.5cm from the display screen. The subject viewed a $6^{o}$ x $6^{o}$ (visual angle) area of the screen through a "window" located 36cm from his nose. The purpose of the window and its masking background was to prevent observation of any potentially distracting stimuli. The window's background was illuminated from behind by a desk lamp and was roughly matched to the stimulus luminance.

On each trial, the subject adjusted (1) a "detection" threshold, and (2) an "identification" threshold. The observer always began a trial at a randomly pre-set level of contrast well below threshold and proceeded to increase contrast until threshold was reached. The experimenter, hidden from view, recorded the read-out of a digital display which varied with the rotation of the polarizing analyzer. From this, the physical contrast of the stimulus could be recovered.

For stationary stimuli, the observer was allowed to adjust contrast ad lib. However, the observer only viewed the leftward-moving half of a motion cycle, the rightward motion being masked by a shutter in order

to reduce transients produced by motion reversal. Thus, the observer only adjusted contrast during one-half of a motion cycle.

For each combination of spatial frequency and velocity, the subject made 11 settings of each type of threshold. These trials were conducted in randomized blocks with each condition being displayed within a block. For the Snellen-letter stimuli, trials were run in randomized blocks with letter size held constant within a block. Each combination of velocity, angle of rotation, and letter was presented in each block.

## IV. RESULTS AND DISCUSSION

### A. Contrast Sensitivity Functions

Figures 1 and 2 respectively show the "detection threshold" CSFs for each of our two subjects. The task in setting these thresholds was to detect any inhomogeneity of contrast in the display. Each separate curve in each figure shows the contrast sensitivity for gratings of different velocities, 0 deg/sec, 1.2 deg/sec, or 3.6 deg/sec. As can be seen in the figures, with stationary gratings sensitivity peaks at or near a spatial frequency of 3 cpd. For subject NDP, successively greater velocities had the effect of shifting the peak spatial frequency to lower values. For both subjects, successively greater velocities produced corresponding increases in sensitivity at spatial frequencies below about 3 cpd.

Figures 3 and 4 respectively show the "identification threshold" CSFs for each of our two subjects. The task in setting these thresholds was to detect the presence of bars on the screen (as opposed to <u>any</u> spatial inhomogeneity). For subject JTP, velocity did not influence the shape or position of the CSF except for at the lowest frequencies tested. In general, the effects of velocity are somewhat less noticeable with the identification-threshold data. Velocity produced some elevation in sensitivity at spatial frequencies below 7 cpd for subject NDP.

The contrast sensitivity data obtained with moving gratings suggest that image motion should not affect the detectability or identifiability of complex images whose crucial frequencies (for detection and identification) lie above 3-7 cpd. On the other hand, within limits, increases in movement velocity should produce corresponding increases in contrast sensitivity for a detection task involving larger (i.e., low frequency) complex targets. Evidence from one subject suggests that increasing motion velocity might also enhance contrast sensitivity in an identification task involving larger complex images.

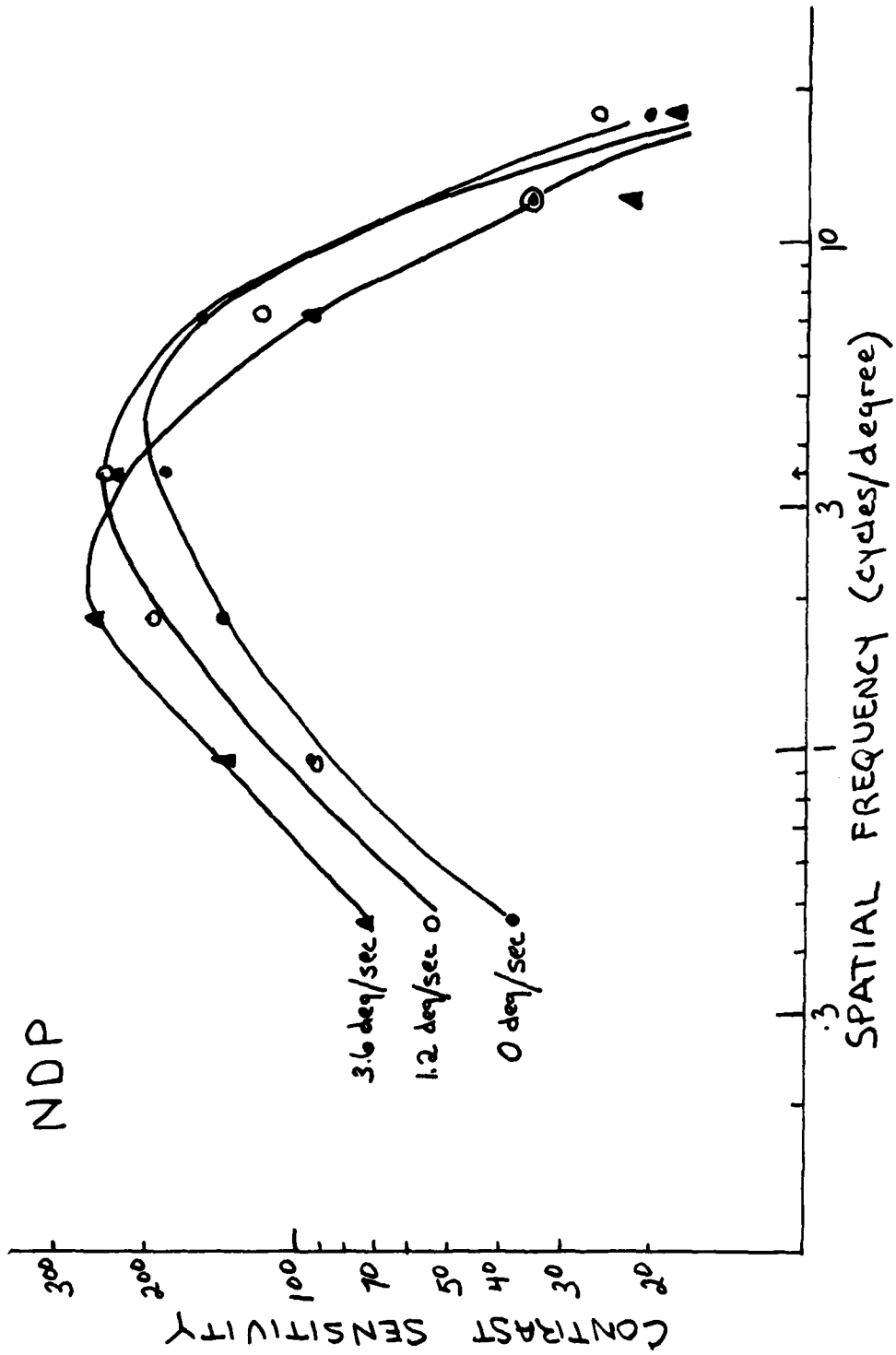



FIGURE 1. Detection-threshold CSFs, subject NDP.

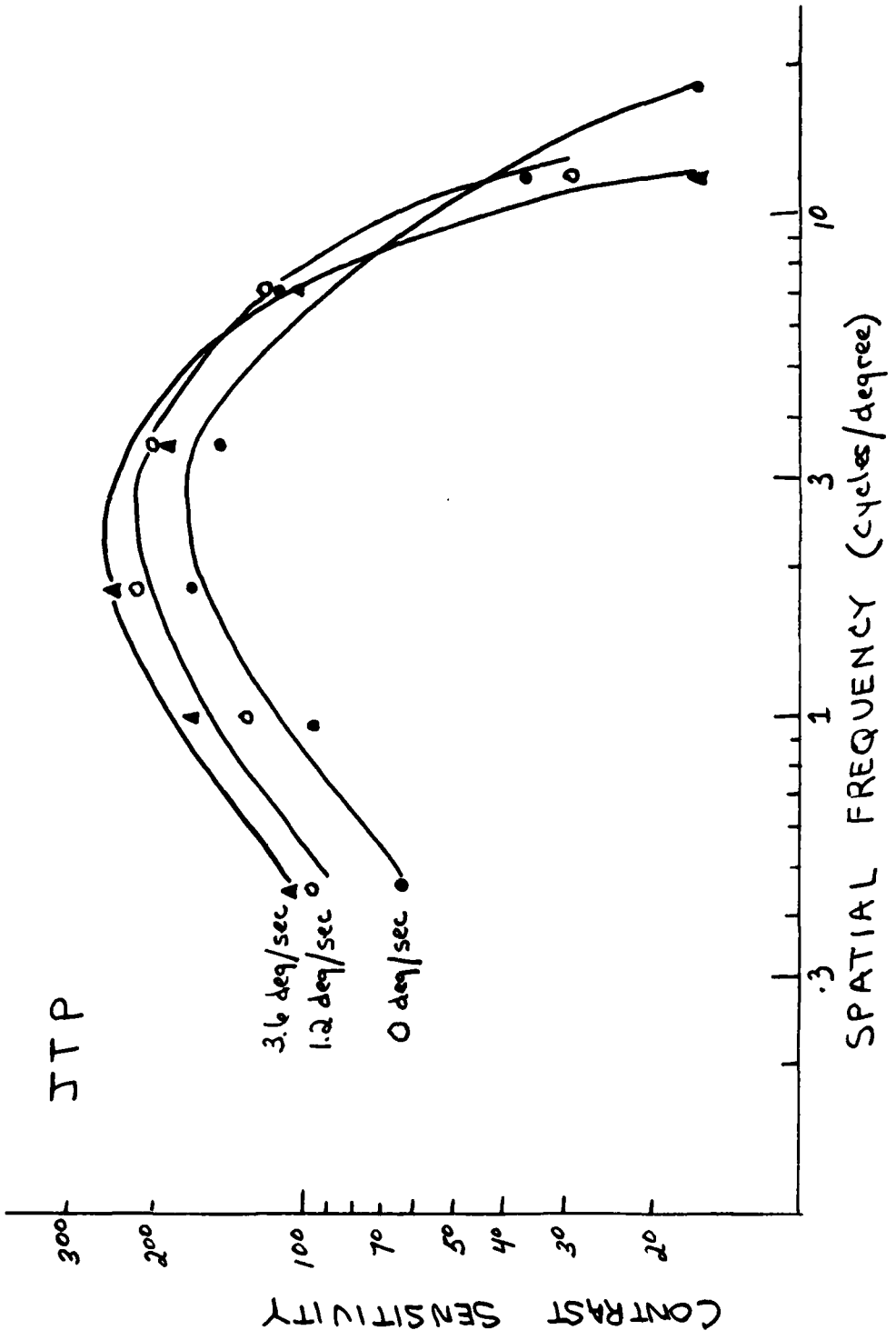



FIGURE 2. Detection-threshold CSFs, subject JTP.

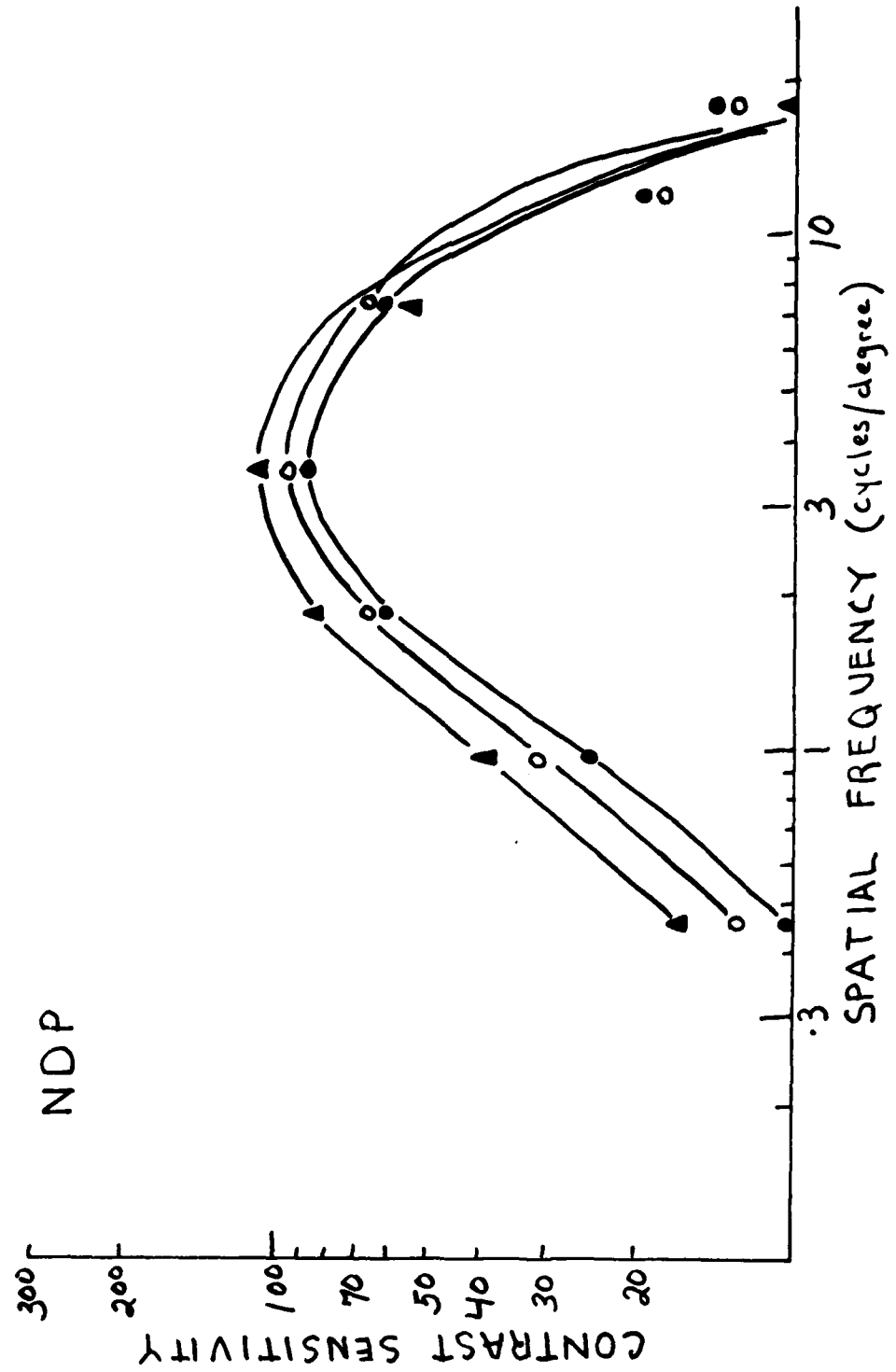



FIGURE 3. Identification-threshold CSFs, subject NDP.

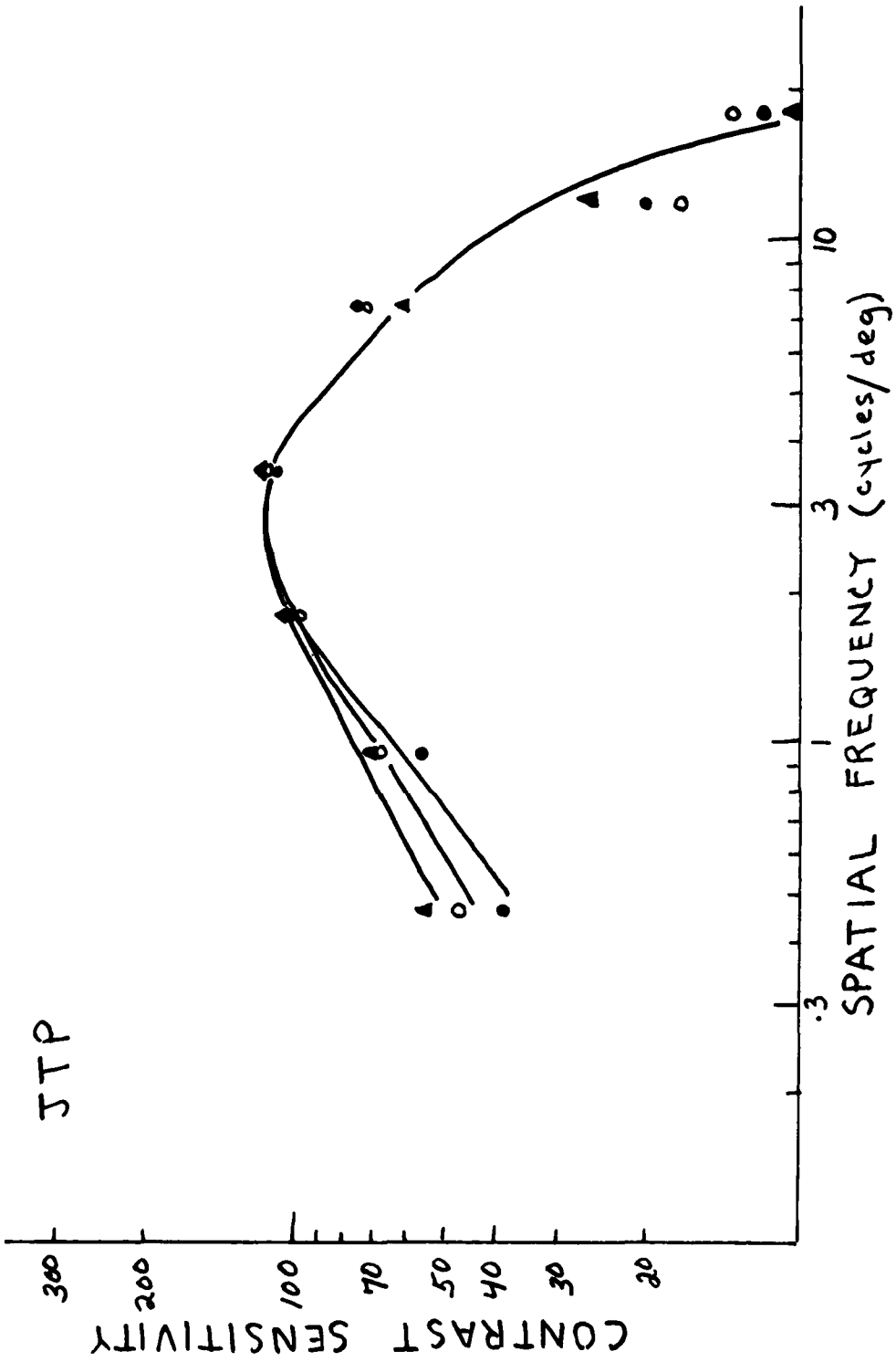



FIGURE 4. Identification-threshold CSFs, subject JTP.

B. Effects of Motion and Letter Size on Detection and Identification of Snellen Letters

Figures 5 and 6, respectively, show the effects of motion and letter size on the detection and identification contrast sensitivity of subject NDP. Since the results of the various letters were similar, letters are collapsed in these figures. Maximum standard errors are also shown alongside the curves. Figures 7 and 8, respectively, show the comparable effects for subje-t JTP. The first finding was that sensitivity on both tasks declined with decreasing letter size. However, within any letter size changes in spatial frequency (the result of successive rotations, as shown in the figures) had only modest effects on sensitivity. For subject NDP, the 3.6 deg/sec motion had the effect of producing successively greater relative increases i:: sensitivity as one compares the curves for the three target sizes from large to small. One reason for this finding may be that a "ceiling effect" is observed with the largest stimuli, i.e., sensitivity is already so great with the large stationary targets that movement cannot enhance it much. The effect of velocity was not as straightforward for subject JTP, whose data differed from those of NDP in at least one other respect: JTP's sensitivity to Snellen targets can be predicted (within bounds set by experimental error) from his initial CSFs, whereas NDP's sensitivities cannot be related to his CSFs as easily. Further research should be conducted with both trained and naive observers as well as with a greater range of velocities in order to adequately assess the effects of velocity.

Figure 9 shows the relative influence of image size, image rotation, and image velocity on both detection and identification contrast sensitivity. Data are for a representative letter, V. Since NDP and JTP's data were qualitatively similar results are shown for JTP only. For the sake of clarity, curves for the 1.2 deg/sec velocity are omitted. The size of the typical standard error is shown in four locations in the figure. Notice also that results are shown only for the two extreme rotations, data for the other rotations being intermediate. The interesting points to be gleaned from this figure and which can be generalized to other data not shown are:

(1) Observers were always more sensitive in the detection task than in the identification tasks, despite variations in image size, image velocity, and image rotation.

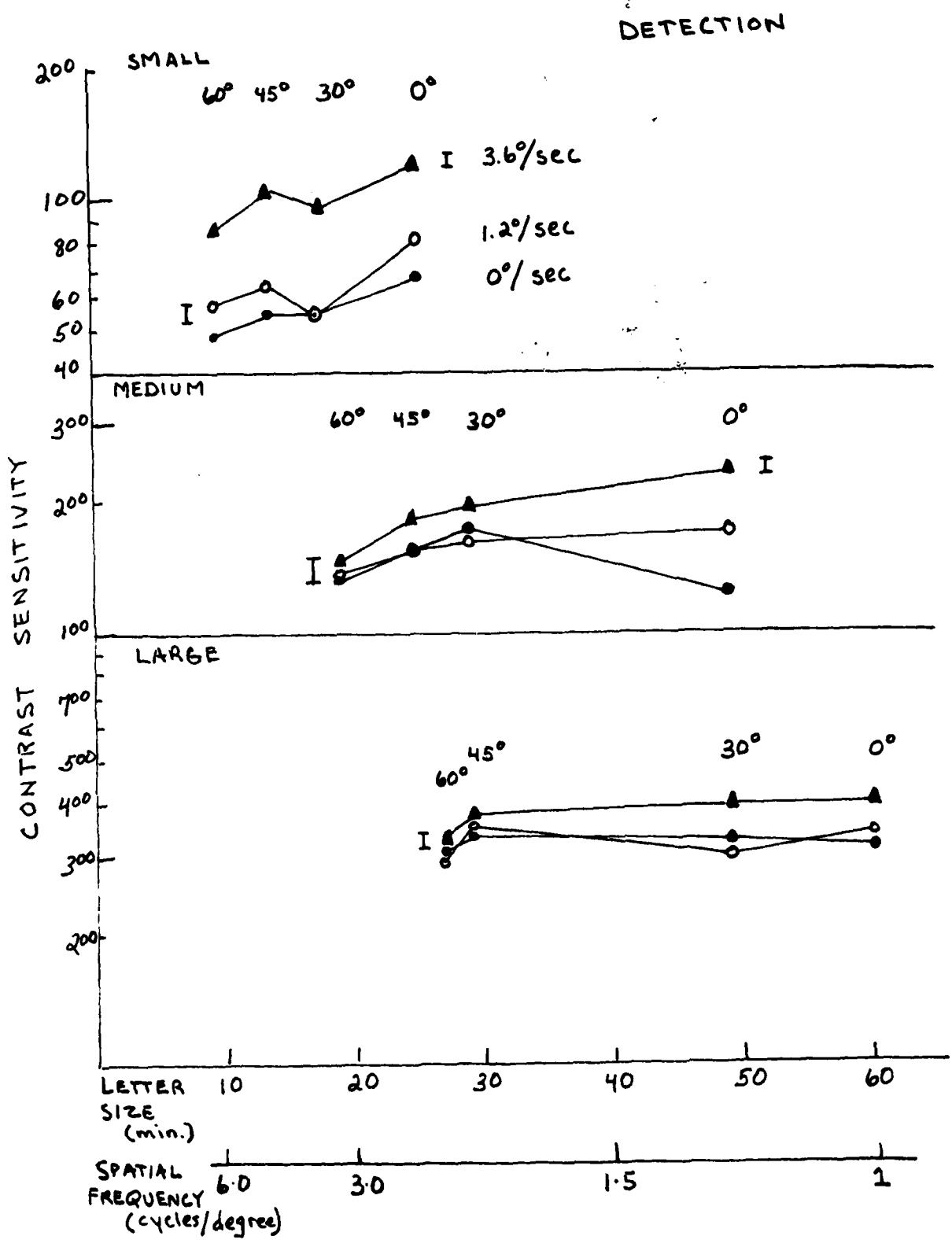



Figure 5. Contrast sensitivity to Snellen letters in the detection task, subject NDP. Brackets: largest standard errors; numbers above curves: letter rotations.

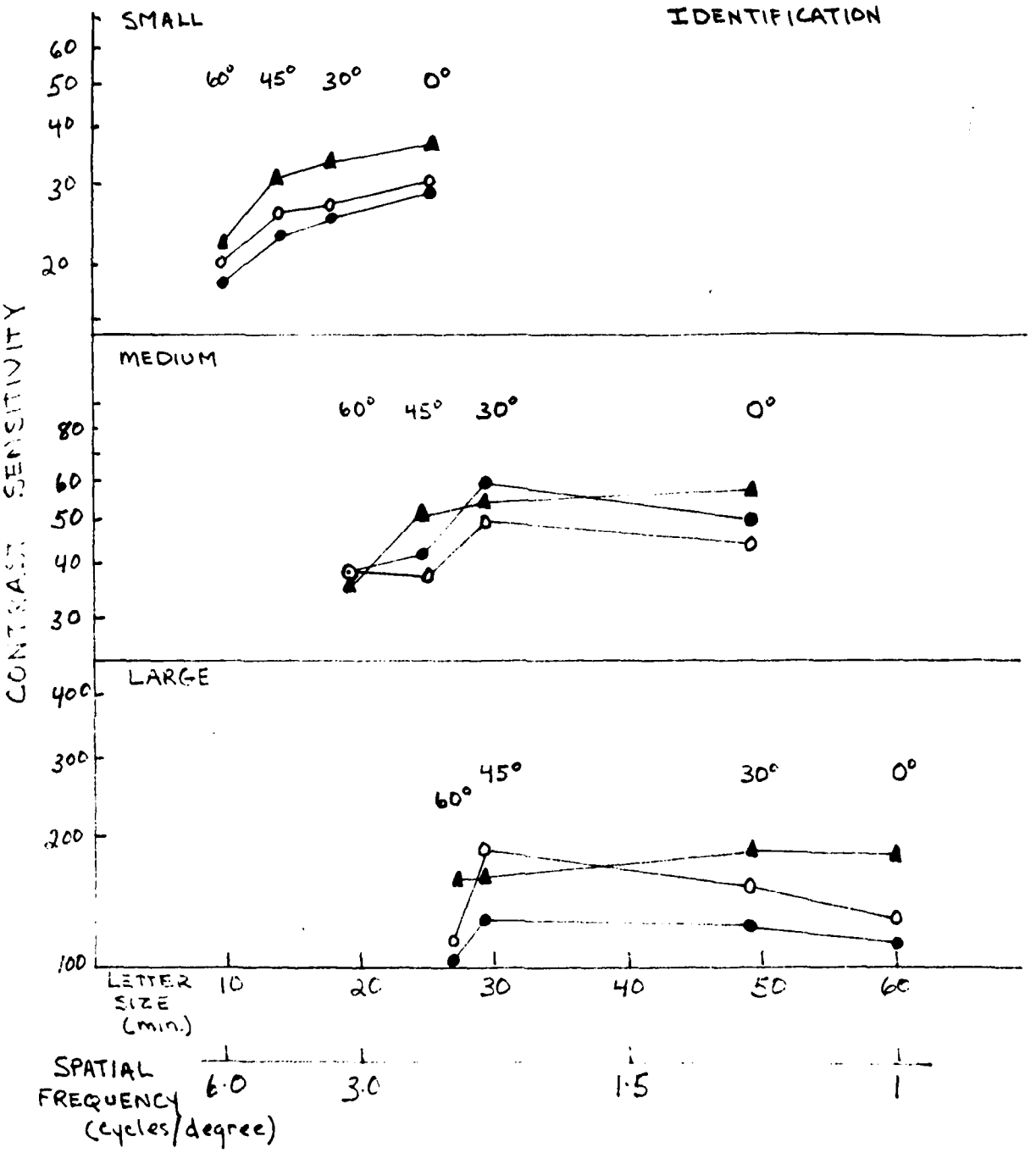



Figure 6. Contrast sensitivity to Snellen letters in the identification task, subject NDP. Conventions as in Figure 5.

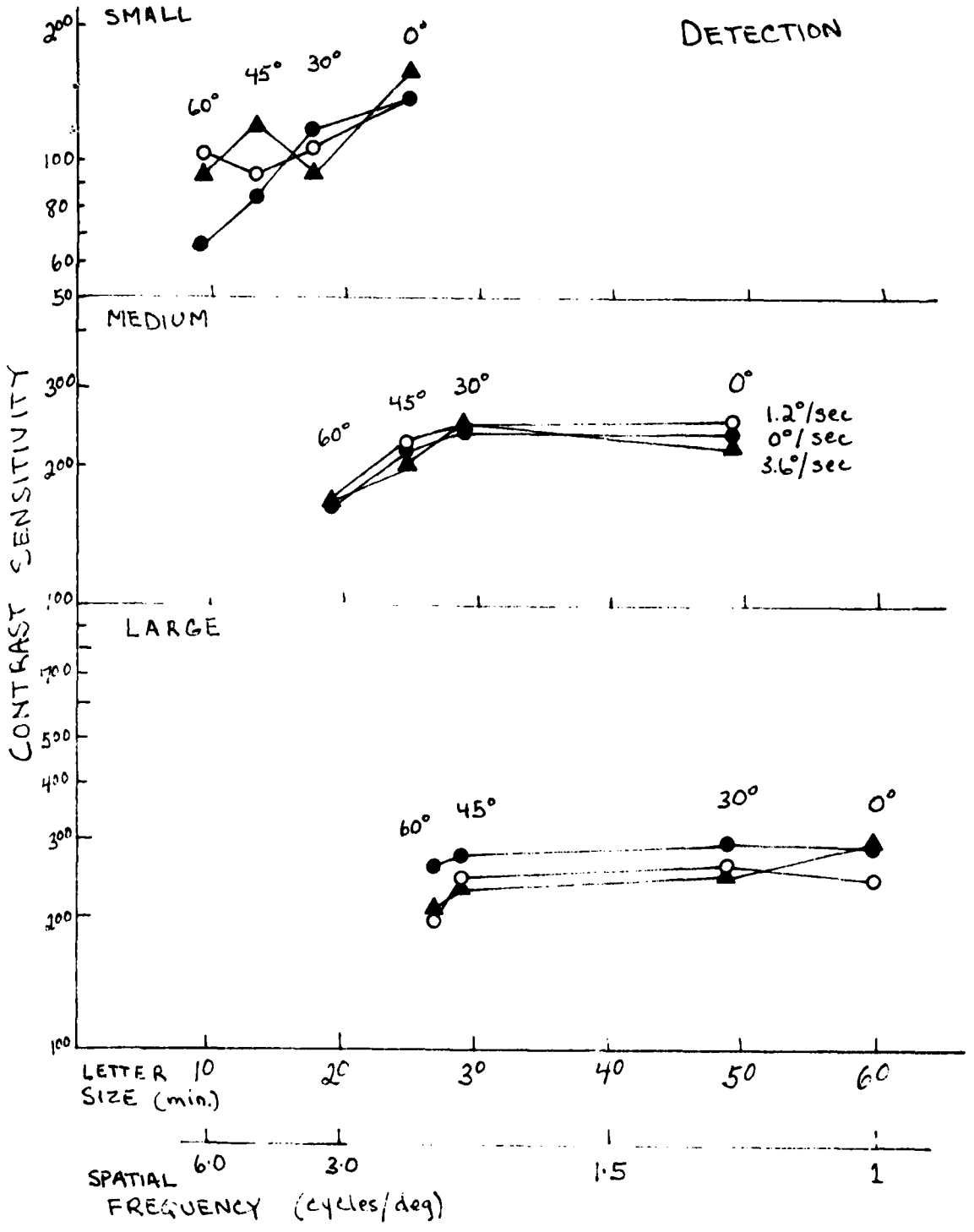



Figure 7. Contrast sensitivity to Snellen letters in the detection task, subject JTP.

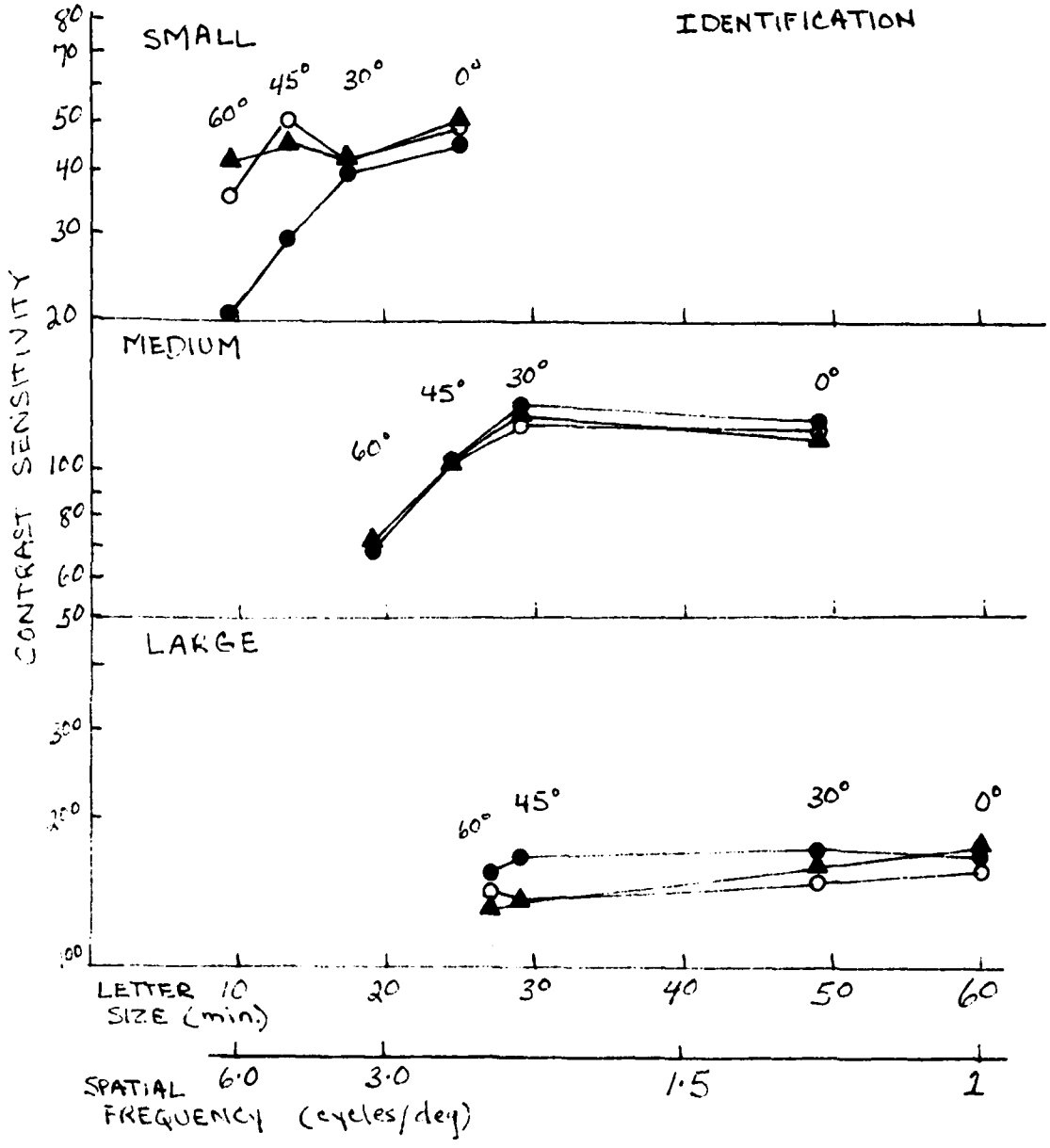



**Figure 8. Contrast sensitivity to Snellen letters in the identification task, subject JTP.**

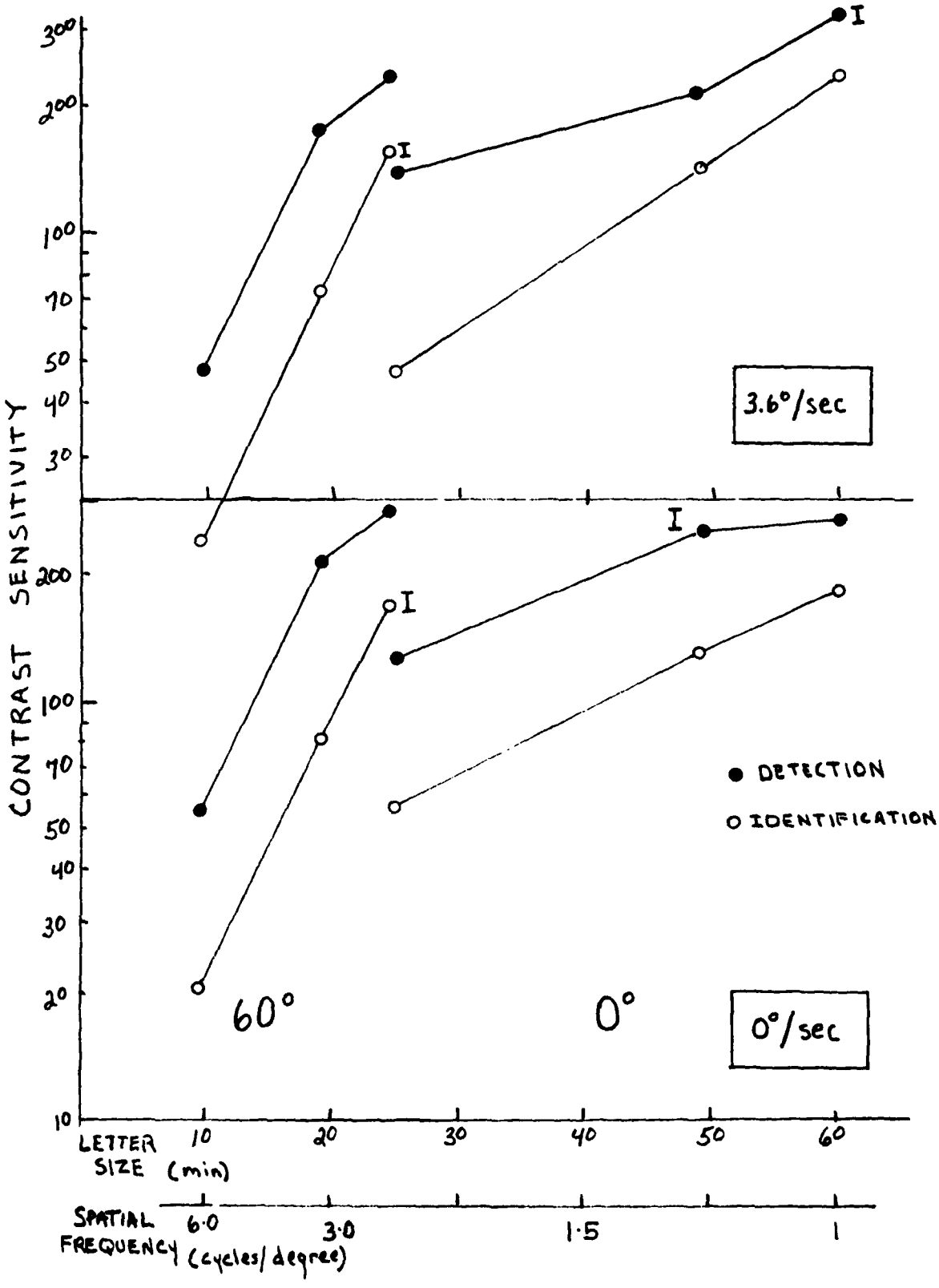



Figure 9. Relationship between detection and identification sensitivities, subject JTP.

(2) Between sets of stimuli at given rotations, the largest image sizes always yielded comparable sensitivities, despite differences in size that sometimes exceeded a factor of two. For example, as shown in Figure 9 for the letter V, a large image at $60^{o}$ subtended roughly 22 min visual angle whereas at $0^{o}$ the large image subtended 60 min. Yet, as can be seen, sensitivities to these images at both velocities shown are comparable.

(3) With increasing rotation of the Snellen-letter image, the slope of the line relating image size to contrast sensitivity increases, indicating that changes in size have greater effects on rotated stimuli. Hence, the slope of the $0^{o}$ curves in Figure 9 is approximately 3.4; of the $60^{o}$ curves, 10.5.

Ginsburg[6] determined the ratio of the contrast required for detection versus identification of stationary non-rotated Snellen letters and found that the function relating the ratio to spatial frequency was a straight line with negative slope. Ginsburg explained this finding as follows:

... the contrast sensitivity function decreases exponentially from peak to minimum sensitivity with increasing spatial frequency when plotted on log contrast sensitivity versus log spatial frequency scale. If the ratio of spatial frequencies used for the detection and identification of Snellen letters remains the same for all different size letters and the detection and identification thresholds are a function of the shape of the contrast sensitivity function, then the ratio should be a straight line when plotted on a linear ratio versus log spatial frequency scale.

In an effort to determine whether the ratios of identification to detection contrasts for rotated letters also decline linearly as a function of spatial frequency, we calculated these values for each subject with the stationary stimuli only. The results of these calculations are shown for subject NDP and subject JTP in Table 1 and Table 2 respectively. These tables show, for each test letter, the detection/identification contrast ratio as a function of spatial frequency. Additionally, each row adjacent to a test letter shows the ratios for images of the three basic sizes. Notice again that for a given size letter, spatial frequency changes as a function of rotation. Hence, in Table 1, the ratio for a large B at $60^{o}$ is .33; at $45^{o}$, .42; at $30^{o}$, .38; and so on. NDP's data give little evidence for a decline in the detection/identification ratio

TABLE 1. Detection/Identification Threshold Contrast Ratios as a Function of Letter Size and Spatial Frequency. Subject NDP.

| LETTER SIZE: | | | | | | | | | | | | |
|---|---|---|---|---|---|---|---|---|---|---|---|---|
| SMALL | | | | | | | 2.93 | | 3.88 | 4.39 | 6.28 | SPATIAL FREQUENCY |
| MEDIUM | | | 1.47 | | 2.05 | | 2.44 | 3.14 | | | | |
| LARGE | 1.00 | 1.22 | | 2.05 | | 2.20 | | | | | | |
| LETTER: | | | | | | | | | | | | |
| | | | | | | | 0.42 | | 0.46 | 0.50 | 0.32 | |
| | | | 0.28 | | 0.35 | | 0.30 | 0.27 | | | | |
| B | 0.33 | 0.42 | | 0.38 | | 0.43 | | | | | | |
| | | | | | | | 0.42 | | 0.44 | 0.35 | 0.34 | |
| | | | 0.25 | | 0.31 | | 0.22 | 0.24 | | | | |
| E | 0.38 | 0.33 | | 0.44 | | 0.34 | | | | | | |
| | | | | | | | 0.39 | | 0.47 | 0.37 | 0.41 | |
| | | | 0.27 | | 0.21 | | 0.30 | 0.50 | | | | |
| V | 0.35 | 0.44 | | 0.30 | | 0.37 | | | | | | |
| | | | | | | | 0.52 | | 0.52 | 0.49 | 0.52 | |
| | | | 0.33 | | 0.26 | | 0.16 | 0.23 | | | | |
| L | 0.37 | 0.33 | | 0.33 | | 0.38 | | | | | | |
| $\bar{X}$ SM | | | | | | | 0.43 | | 0.47 | 0.42 | 0.38 | |
| $\bar{X}$ MD | | | 0.28 | | 0.28 | | 0.23 | 0.28 | | | | |
| $\bar{X}$ LG | 0.36 | 0.38 | | 0.35 | | 0.38 | | | | | | |

TABLE 2. Detection/Identification Threshold Contrast Ratios as a Function of Letter Size and Spatial Frequency. Subject JTP.

| LETTER SIZE: | | | | | | | | | | | | |
|---|---|---|---|---|---|---|---|---|---|---|---|---|
| SMALL | | | | | | | 2.93 | | 3.88 | 4.39 | 6.28 | } SPATIAL |
| MEDIUM | | | 1.47 | | 2.05 | | 2.44 | | 3.14 | | | FREQUENCY |
| LARGE | 1.00 | 1.22 | | 2.05 | | 2.20 | | | | | | |
| LETTER: | | | | | | | | | | | | |
| | | | | | | | 0.24 | | 0.30 | 0.28 | 0.30 | |
| | | | 0.59 | | 0.57 | | 0.43 | | 0.52 | | | |
| B | 0.53 | 0.63 | | 0.62 | | 0.61 | | | | | | |
| | | | | | | | 0.24 | | 0.21 | 0.26 | 0.21 | |
| | | | 0.50 | | 0.56 | | 0.45 | | 0.35 | | | |
| E | 0.60 | 0.50 | | 0.66 | | 0.57 | | | | | | |
| | | | | | | | 0.44 | | 0.43 | 0.50 | 0.37 | |
| | | | 0.51 | | 0.49 | | 0.65 | | 0.38 | | | |
| V | 0.68 | 0.66 | | 0.54 | | 0.59 | | | | | | |
| | | | | | | | 0.46 | | 0.50 | 0.51 | 0.50 | |
| | | | 0.54 | | 0.55 | | 0.41 | | 0.45 | | | |
| L | 0.52 | 0.53 | | 0.68 | | 0.62 | | | | | | |
| $\bar{X}$ SM | | | | | | | 0.31 | | 0.32 | 0.35 | 0.31 | |
| $\bar{X}$ MD | | | 0.53 | | 0.54 | | 0.47 | | 0.42 | | | |
| $\bar{X}$ LG | 0.57 | 0.57 | | 0.62 | | 0.60 | | | | | | |

with increasing contrast. On the other hand, JTP's data do show such a trend, but the results are not as straightforward as we would like. The safest conclusion we can draw at this point is that image size, image rotation, and image energy enter into a complex interaction in the determination of the detection/identification ratio.

Next, we sought to determine what effect the individual test letters themselves had upon detection and identification contrast sensitivity. Thus, for subject NDP, Figure 10 and Figure 11, respectively, show contrast sensitivity as a function of test letters (arranged in order of decreasing energy). Letter set-size and velocity are parameters. For the detection task, it is clear that individual letters influenced sensitivity only when image motion was at $3.6^{o}$/sec, and then only for the small and medium sizes (as would be expected). There is little evidence for such a relationship, except perhaps with the small letter-size, in the identification task.

As a final analysis, for several of the experimental conditions reported here and for each of our two subjects, we plotted both detection and identification contrast sensitivity as a function of linear spatial frequency. Regression lines were next determined, and the ratio of the spatial-frequency intercept for the detection sensitivity vs. the spatial-frequency intercept for the identification sensitivity was found in order to estimate the bandwidth of the identification-to-detection threshold ratio (see Ginsburg[6], p. 87, for rationale). Since the pattern of results was exceptionally similar for both subject NDP and subject JTP, the results of this analysis are shown in Table 3 for NDP only:

| | LETTER | | | |
|---|---|---|---|---|
| | B | | L | |
| Rotation: | $0^{o}$ | $60^{o}$ | $0^{o}$ | $60^{o}$ |
| VELOCITY | | | | |
| $0^{o}$/sec | 1.28 | 1.50 | 1.17 | 1.28 |
| $3.6^{o}$/sec | 1.96 | 1.87 | 1.52 | 1.54 |

TABLE 3. Identification-to-detection threshold ratio bandwidths. Subject NDP.

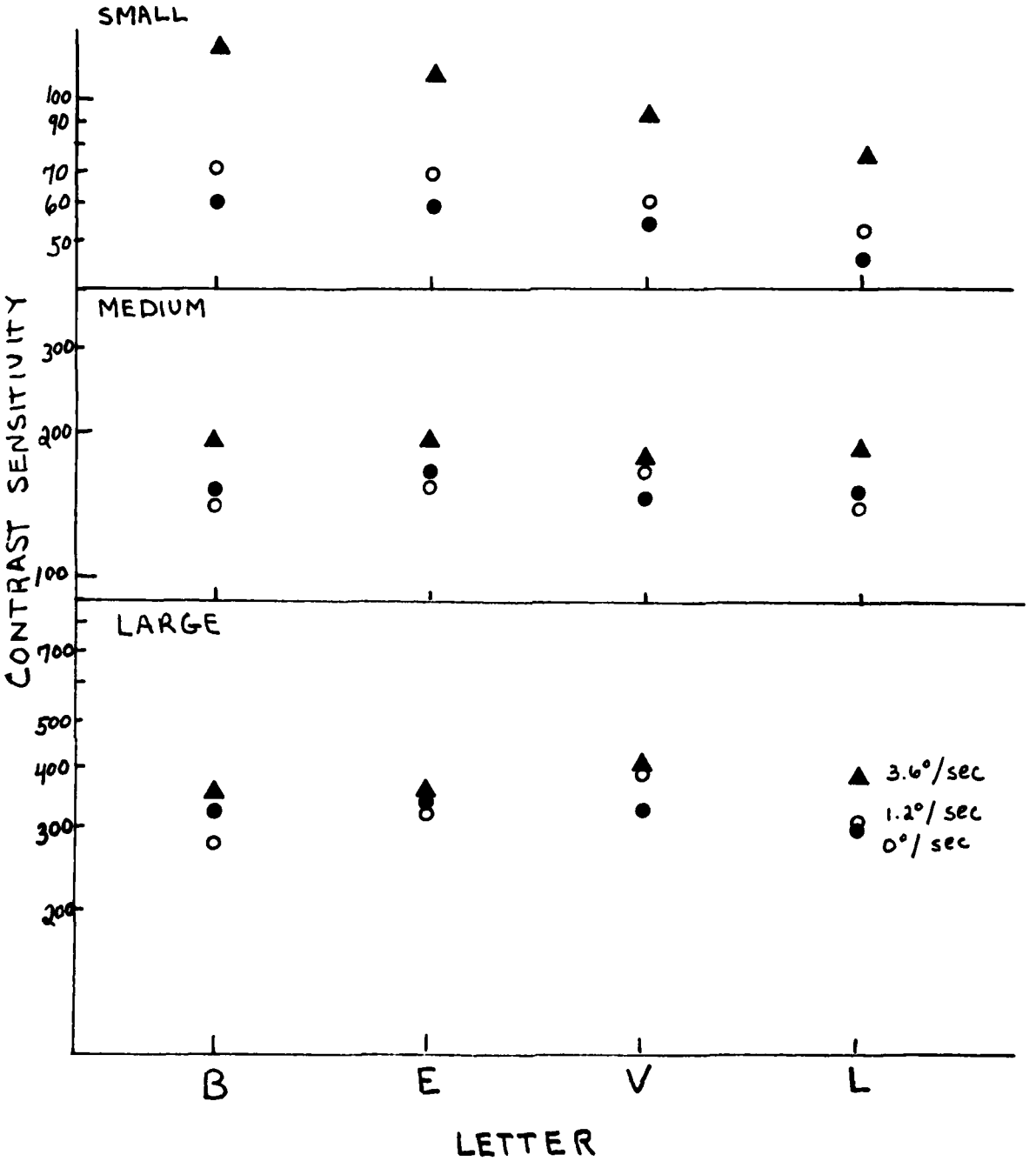



Figure 10. Contrast sensitivities to individual Snellen letters in the detection task, angles collapsed, subject NDP.

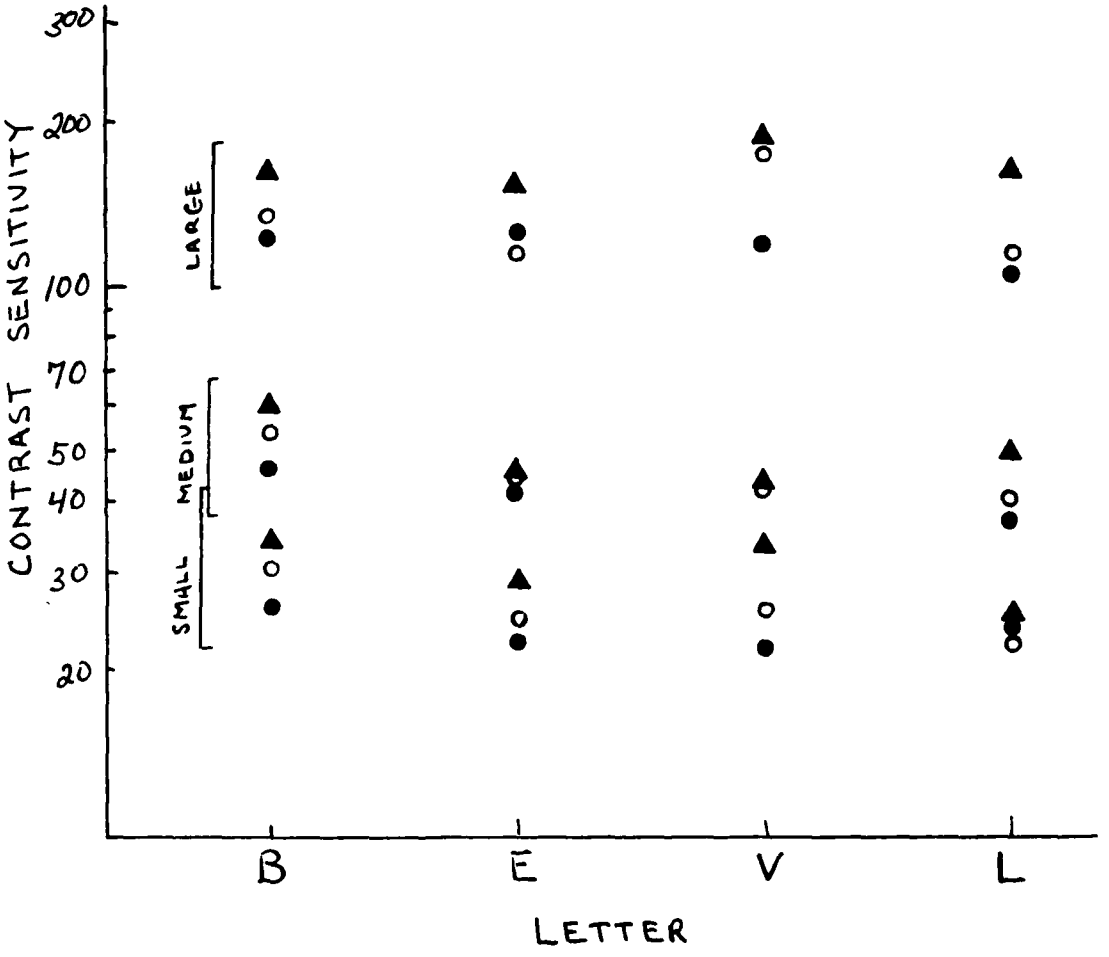



Figure 11. Contrast sensitivities to Snellen letters in the identification task, angles collapsed, subject NDP. Conventions as in Figure 8.

As can be seen in Table 3, the bandwidth increased by a factor of 1.2-1.5 with stimulus movement. For stationary stimuli only, the bandwidth increased by a factor of 1.1-1.2 as the letter was rotated from $0^{o}$ to $60^{o}$ relative to the frontoparallel plane. In general, the bandwidths for the high-energy (relatively speaking) letter B were larger than for the low-energy letter L. Why the bandwidths change under such conditions should be considered in future research of this type.

## V. CONCLUSIONS

Despite the limited ranges of target size and velocity we were able to employ in the present project, it is evident that image motion reveals information about the processing characteristics of the visual system that cannot be deduced from the study of static images alone. We suggest that the following conclusions be replicated in future research and that they be extended to conditions not studied in the present experiment:

(1) Relatively slow movements of sine-wave gratings produce successive elevations in the low-frequency portion (less than 3-7 cpd) of both detection and identification CSFs.
(2) As previously shown by Ginsburg[6] for static stimuli, contrast sensitivity to moving targets is always higher in the detection task than in the identification task.
(3) In both detection and identification tasks, contrast sensitivity was generally, though not always, higher in response to moving targets than to stationary targets.
(4) Identification-to-detection threshold ratio bandwidths increased by a factor of 1.2-1.5 with stimulus movement and, for stationary targets, by a factor of 1.1-1.2 with image rotation.
(5) The advantage produced by motion described above (conclusion #3) is

a monotonically decreasing function of target size. There is some suggestion (Figures 5, ) that it is also a decreasing function of image rotation.

(5) For stimuli at the various rotations (i.e., $0^{o}$, $30^{o}$, $45^{o}$, $60^{o}$), the largest target sizes always yielded comparable contrast sensitivities, despite differences in absolute size that sometimes exceeded a factor of two.

(6) With increasing rotation of targets, the slope of the line relating contrast sensitivity to target size increases, indicating that changes in size of similar magnitude have larger effects on successively rotated targets.

(7) The ratio of detection to identification threshold contrast changes little, if at all, with changes in target spatial frequency (i.e., with changes in the interaction between target set-size and target rotation).

(8) At least in the detection task, contrast sensitivity monotonically increased with the power of the Snellen-letter spatial frequencies. This advantage is a monotonically decreasing function of target size and an increasing function of target velocity.

## VI. RECOMMENDATIONS

The results of the present project have strengthened our initial conjecture that image motion and image rotation may further reveal fundamental filtering and processing capabilities of the human visual system. However, because of technical limitations in the velocities available to us and in the available letter sizes, our conclusions have been confined to intermediate cases, i.e., those which are not at the limits of either the CSF or the motion-processing capabilities of the visual system. Therefore, the primary recommendation is to replicate the present investigation with the following modifications:

(1) Extend the range of target velocities to include those which fall at or below the production of "retinal smear."

(2) Extend the range of target sizes to include fundamental spatial frequencies at both the high (i.e., 20-60 cpd) and low (about .2 cpd) extremes of the CSF.

(3) Study subjects whose CSFs differ in at least one significant way and relate this difference to differences in letter detection and

identification.

I hope to adopt these recommendations in follow-on research which is being proposed under the AFOSR mini-grant program.

## REFERENCES


1. O. H. Schade, "Optical and Photoelectric Analog of the Eye," J. Opt. Soc. Am., Vol. 46, pp. 721-739, 1956.

2. F. W. Campbell and J. G. Robson, "Application of Fourier Analysis to the Visibility of Gratings," J. Physiol. (Lond.), Vol. 197, pp. 551-556, 1968.

3. A. P. Ginsburg, M. Cannon, and M. Nelson, "Suprathreshold processing of Complex Visual Stimuli: Evidence for Linearity in Contrast Perception," Science, Vol. 208. pp. 619-621, 1980.

4. C. Blakemore and F. W. Campbell, "On the Existence of Neurones in the Human Visual System Selectively Sensitive to the Orientation and Size of Retinal Images," J. Physiol. (Lond.), Vol. 203, pp. 237-260, 1969.

5. A. J. Pantle and R. Sekuler, "Size-detecting Mechanisms in Human Vision," Science, Vol. 162, pp. 1146-1148, 1968.

6. A. P. Ginsburg, Visual Information Processing Based on Spatial Filters Constrained by Biological Data. Unpublished Ph.D. dissertation, University of Cambridge, 1978. (In press as AMRL-TR-78-129).

7. J. J. Kulikowski and D. J. Tolhurst, "Psychophysical Evidence for Sustained and Transient Detectors in Human Vision," J. Physiol. (Lond.), Vol. 232, pp. 149-162, 1973.

8. D. J. Tolhurst, "Separate Channels for the Analysis of the Shape and the Movement of a Moving Visual Stimulus," J. Physiol. (Lond.), Vol. 231, pp. 231-248, 1973.

9. B. Breitmeyer and L. Ganz, "Implications of Sustained and Transient Channels on Visual Pattern Masking, Saccadic Suppression, and Information Processing," Psychol. Rev., Vol. 83, pp. 1-31, 1976.

10. J. T. Petersik, "Possible Role of Transient and Sustained Visual Mechanisms in the Determination of Similarity Judgments," Perceptual and Mot. Skills, Vol. 47, pp. 683-698, 1978.

11. R. S. Sekuler, A. J. Pantle, and E. Levinson, "Physiological Basis of Motion Perception." In R. Held, H. W. Leibowitz, and H.-L. Teuber (Eds.), Handbook of Sensory Physiology, Vol. VIII: Perception. New York: Springer-Verlag, 1978.

12. J. T. Petersik, Mechanisms Controlling the Sensations of Depth and Direction in Moving Perspective-transformation Displays. Unpublished Ph.D. dissertation, Miami University, 1978.

1980 USAF - SCEEE SUMMER FACULTY RESEARCH PROGRAM

Sponsored by the

AIR FORCE OFFICE OF SCIENTIFIC RESEARCH

Conducted by the

SOUTHEASTERN CENTER FOR ELECTRICAL ENGINEERING EDUCATION

Final Report

# THE RELATIONSHIP OF THE THREE COMPONENT MODELS OF LEADERSHIP TO THE DEVELOPMENT OF ACTION PLANS AND LEVELS OF LEADERSHIP


| | |
|---|---|
| Prepared by: | Dr. Thomas A. Petrie |
| Academic Rank: | Professor |
| Department and University: | Department of Educational Administration and Foundations<br>University of Nebraska at Omaha |
| Research Location: | Leadership Management and Development Center, Maxwell AFB, Alabama |
| USAF Research Colleague: | Dr. Kenneth Hamilton, Lt. Col., USAF |



| | |
|---|---|
| Date: | September 15, 1980 |
| Contract No.: | F49620-79-C-0038 |

# The Relationship of the Three Component Model of Leadership to the Development of Action Plans and Levels of Leadership

by

Dr. Thomas A. Petrie

This study analyzes the three component leadership model and its relationship to a hierarchial model of leadership. First, the Organizational Assessment Package designed to measure the three components of leaderships, situations and outcomes was analyzed to determine the congruence with the levels of leadership and potential contribution to order the data and direct the development of action plans. The face validity of this effort was confirmed by the consultants. Second, a factor analysis of the data revealed a congruence between the theoretical structure of leadership and the factor structure of leadership. Subsequent recommendations to study the longitudinal development of leaders would provide insights for the training of leaders.

## ACKNOWLEDGEMENTS

This investigator would like to thank the Air Force Systems Command, the Air Force Office of Scientific Research and the Southeastern Center for Electrical Engineering Education for providing the opportunity to spend a productive summer at the Leadership Management and Development Centers, Maxwell AFB, Alabama. He would particularly like to acknowledge the support of Col. Guy Winstead, Commander of the IMD for the insightful use of research outcomes in the continuous development of Center strategies.

I also wish to thank Lt. Col. Kenneth Hamilton, Ph.D.; Lt. Col. David Wilkerson, DBA; Major Larry Short, Ph.D.; and to Jeffery Austin for the helpful discussions and professional support necessary to bring such an inquiry to fruition.

## I. INTRODUCTION

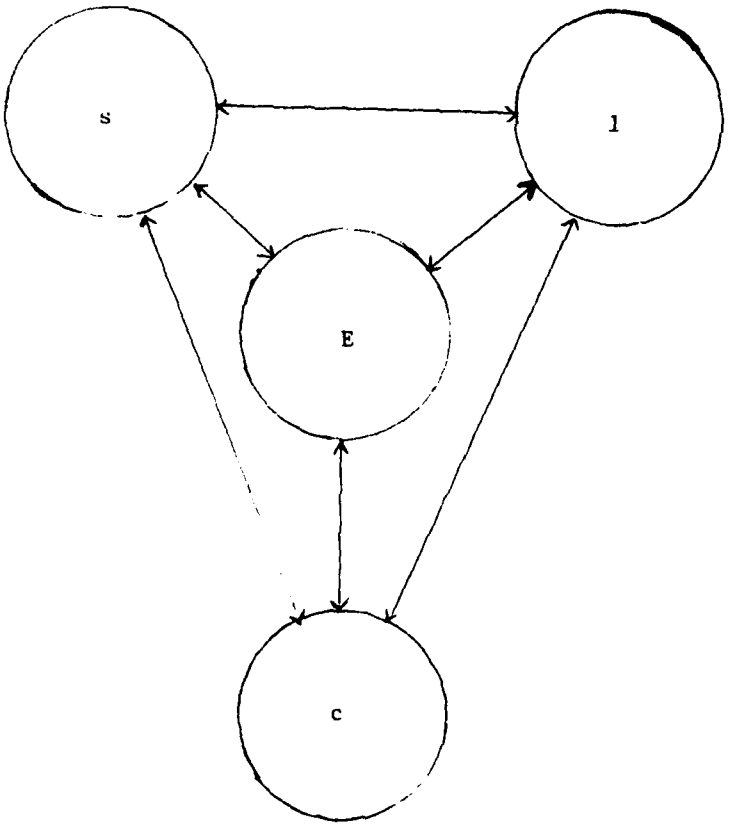
The three component leadership effectiveness model[1] provides a descriptive framework for depicting the phenomenon of leadership in the United States Air Force. The model depicts leadership effectiveness as the function of three interdependent components (see Figure 1): the leadership, situation and criterion.

The utility of the model is to be evaluated for: (1) its usefulness as a descriptive framework; (2) its capability for depicting the leadership, and (3) its testability.

Work in LMDC after explicating the model[2] concentrated upon developing an instrument, the Organizational Assessment Package (OAP), to assess the three components of the model. Items theoretically or experientially related to the components were identified and reduced by factor analysis. Seventeen demographic factors and 93 dependent or independent variables have been identified. The OAP now provides a data base for assisting leaders to empirically quantify and reflect upon the perceptions of their followers about the situation, leadership and the outcomes or productivity. The usefulness of the OAP data for assessment and decision making needs further review and interpretation.

The three component leadership model was designed to assess and relate leadership style to the situation and outputs. A particular important point and part of the rationale is that leaders with more skills have a broader range of styles than less skillful leaders. A broader range of styles involves more ability to combine information. For example, OAP Variable 404 ("My supervisor is a good planner") may reflect the supervisor's ability to organize the many activities of management efficiently. With efficiency as the guiding principle, the supervisor, through trial and error, could eventually identify and efficiently plan activities that are basic to success. While a trial and error style may result in identifying efficient procedures, it is limited to the experiential style. It is more complex for a supervisor to effectively plan by establishing work procedures (OAP

Figure 1




The three component leadership effectiveness model.

Legend:

E = Effectiveness
c = Criterion
l = Leadership Style
s = Situational Environment

Variable 412). Effective planning is more complex than delegation. In turn, delegation is more effective if it includes seeking a member's feedback, i.e., "My supervisor asks members for their ideas or task improvement" (variable 426). In short, categorizing the OAP variables and relating them to the complex skills of leadership makes it possible to analyze the variables (and subsequently the client's scores) for the meanings they have for decision making and application to any leadership style. For skills and conceptual rules or schema's job-combining information are building blocks of leadership and provide leaders with more ways of doing things. When these skills and processes are acquired the leader possesses more resources for effective leadership.

## II. OBJECTIVES

The main objective of this project was to investigate the three component leadership model and the Organizational Assessment Package for logical contingency to leadership technology and the identification of action plans. To accomplish the above objective the following procedures were used.

1. An analysis of the contingency model for leadership assumptions.
2. An ordering of the variable according to their relationship to levels of leadership.
3. A relevance of the variables according to leadership technology.
4. A testing of the face validity of the ordering with the LMDC consultants.
5. A factor analysis of the date to determine the of the levels of leadership with the factors generated by the OAP data.

The second objective was to create a consultant tool for the development of action plans.

III. Building Blocks of Leadership

What are the functional building blocks of leadership? The most basic process of leadership is communication. Organizational members constantly communicate and attribute verbally and nonverbally that what leaders do is important. Leaders can do their job in such a way so that the members can perceive a sense of order. Therefore the leader's responsibility is to organize. Through creating order and efficient routines, others are able to identify priorities. This basic leadership process is found among the individuals whose routines generate a sense of continuity, reflect order and demonstrate the capacity of the leader to take charge of their life. It is through the routine use of skills of time management, planning and written communication that the leader mobilizes the use of valuable time, space, technology, personnel and other resources.

The leader's second responsibility is to establish clear and specific job goals. Leaders use job descriptions and rules to provide a structure in which individuals can do their jobs and meet their obligations. In short, coordination of effort is initiated through clearly stated rules and job descriptions that outline activity and authority.

The leader's third responsibility is to evaluate what is done and clarify how what is done contributes to the goals, directions and organizational mission. Feedback clarifies the relationship between actions and goals. These three cumulative processes of organizing, delegating, and evaluation constitute a basic leadership structure. These three processes provide a structure of expectations necessary for growth of the members.

To this point leadership has been described as a maintenance, management or administration process. However, the leadership skills of long range planning, programming and job enrichment can be mobilized to enable the leader to provide opportunities for members to develop status, esteem and prestigue. The fourth responsibility of leadership involves capitalizing upon the individuality of the

members through problem solving in order to find ways to use available talents and resources. Problem solving initiates training needs to increase the skills, prestige and value of the member.

The fifth responsibility is to integrate and clarify the meaning of individual and/or collective activity. The skill of clarification make explicit the relationship between chosen means and ends. For, leaders tho constantly clarify and integrate motivate each individual to reflect upon their activity and beliefs and the way they contribute to the support of organizational goals.

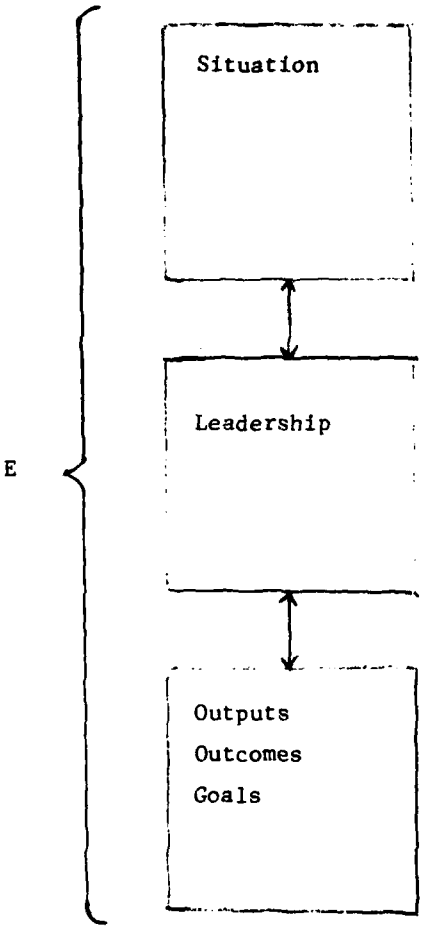
In summary, the rationale presented above conceives of communication as the basic process that enables leaders and individuals to share human experiences and collaborate to achieve organizational goals. This occurs when leaders are sufficiently disciplines and experienced to contribute a sense of efficiency, coordination, direction, competence and integrity. Leaders are perceived as more competent as they develop the skills necessary to organize, delegate, evaluate, develop and integrate. Furthermore, these processes serve as functional means for categorizing the skills of leadership. They point to skills that increase the alternatives available to leaders, whatever their style. They constitute a hierarchy of processes and a structure for categorizing leadership factors and variables.

The organizational decision making model outlined in Figure 1 is an interactive and interdependent model. From a leadership perspective the emphasis is upon the leader and the leader's capacities and/or styles. While followers are part of the situation and the criterion of effectiveness are important components, it is the leader who skillfully acts or decides that is the subject for further discussion.

The three component leadership model has been re-diagrammed (Figure 2) to emphasize the logical relationship between the situation, leadership and the output. It is assumed that the most dynamic aspect of the model is the leadership component, for it is leadership that influences the relationships between the interdependent parts. For example, as a decision making model, there are a number of decisions that must be made by the leader. Given an assessment of the situation,

Figure 2

Three Component Leadership Model



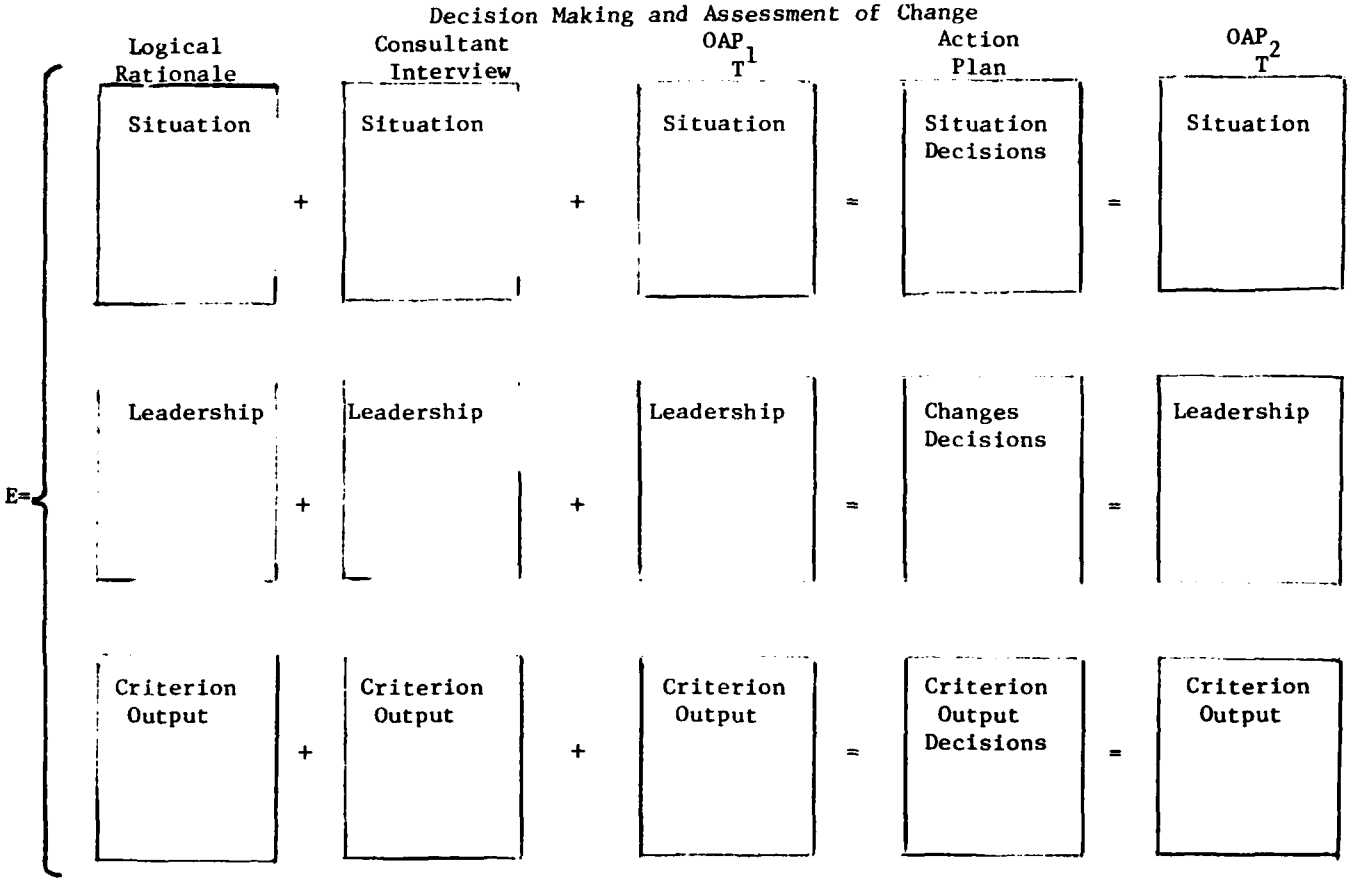
and an assessment of the goals or the objectives or the criterion, it is the leader who must plan, organize and initiate a leadership strategy to accomplish the goals. It is the leader who maintains and initiates the logical strategies. It is the leader who skillfully or not organizes efficiently. The following sections relate the model to the unit or base and illustrate the use of the model and leadership relationships to the situation and output.

The three component leadership model, as diagrammed in Figure 3, illustrates the relationships between the organizational components, and the respective emphasis of base commanders and the consultants. This figure illustrates the common and the unique responsibilities for leader decision making, however the character of decision making changes with particular Air Force unit. For example, the base commanders' invitation to the LMDC for consultation, initiates a systematic process of data collection by open-ended questionnaire, personal interviews, and the OAP (see column 2 and 3, Figure 3). As this data is collected it is categorized as situational, leadership or output. From the base commander's perspective, the primary concern about the data is "What does it mean?" The meaning is derived from analyzing the logical relationships between the components. Next the OAP data reveals indicators of problems or organizational health. This data is congruent or descrepant with the consultant or interview data and consequently is verified or rejected. This analysis reveals a best guess about the actions necessary to bring about change. From the recommended actions the commander or unit leader selects and develops an action plan. The consultant then provides training or other help as requested and necessary to make the action plan work.

The power of the three component model to increase understanding about leadership is shown in Figure 4. The OAP data and the consultant data is entered in column 2 and 3. From this information the consultant and base leaders may logically develop an action plan that includes an intended leadership strategy for improving the situation and outcomes. Subsequently an assessment of change in the situation,

Figure 3

Decision Making and Assessment of Change



leadership and output (the action plan) may be made with the OAP at Time Two.

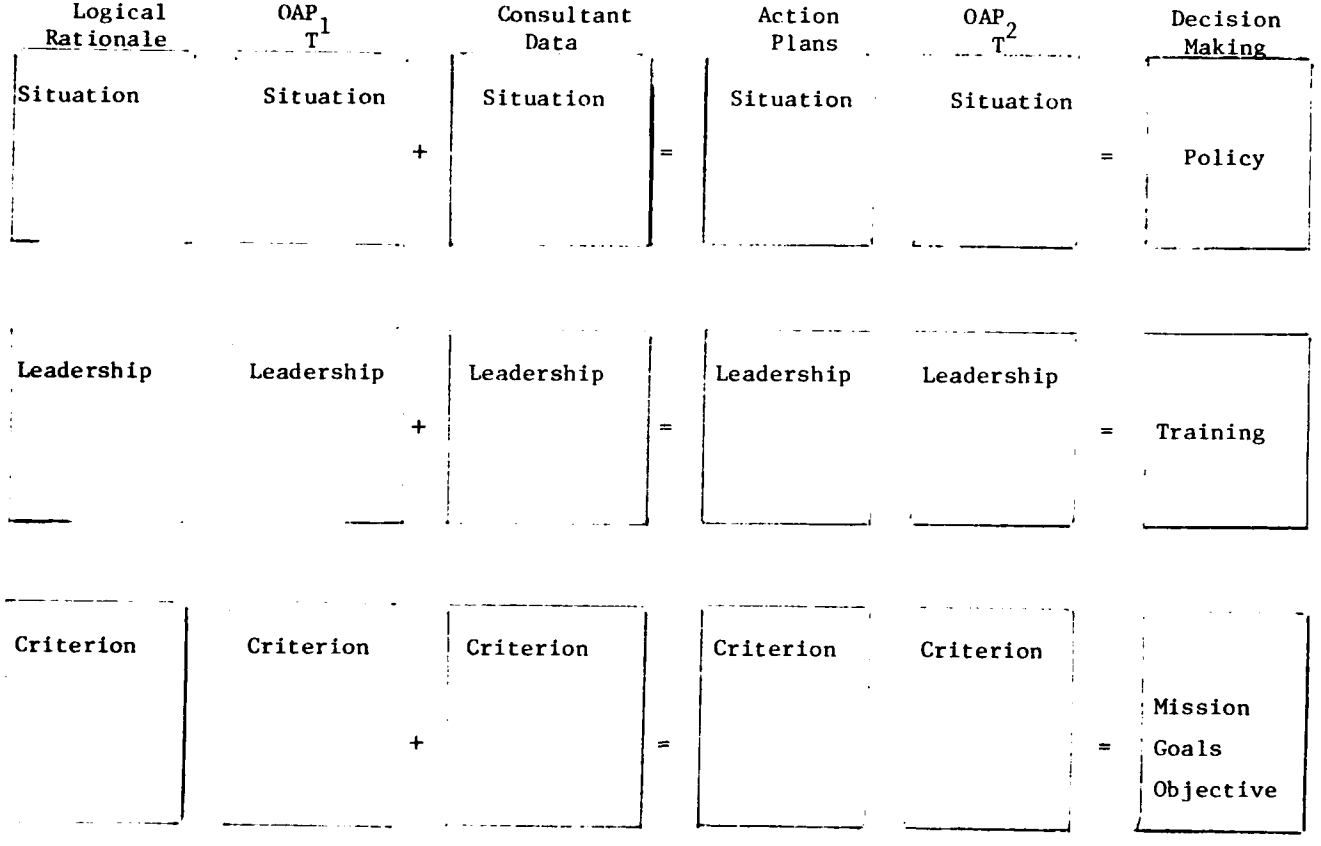
As the data cumulates in the data bank, the data is coded to include such factors as major command, base, supervisory unit and career fields. The $T^1$ data cumulatively reflects the Air Force situation, leadership and output. The $T^2$ data cumulatively reflects change. The data is then amenable to a wide range of analyses. The potential analyses pertain to decisions about Air Force policy, training and/or tactics. Finally, the action plan contains the elements of an action research design for the further study of leadership effectiveness.

To this point, this paper has elaborated on the three component model, and explored a developmental perspective of leadership that communicates the dynamic role of leadership in the organization. Ths usefulness of the three component model has been discussed and illustrated in Figures 2 through 4. The usefulness of the model is important for both the local commander as they design action plans and Air Force commanders as they design, train and develop policy. The remainder of this paper will be to describe the relationships of the Organizational Assessment Package (OAP) to assess the three components of the model as a consulting tool. This relationship will particularly emphasize the usefulness of the OAP data for local decision making, leadership training and consulting.

A review of the OAP reveals that 49 of the items are classified situational variables. Forty items are leadership variables, and 30 are criterion variables. Generally speaking, the leadership variables are most amenable to planned change. The situational variables may be receptive to limited planned changes. More often than not, the situation is not easily changed by consultants or commanders. Rather, situational matters are generally Air Force policy or allocation decisions. The outputs variables tend to be dependent upon situational matters and leadership strategies. Of considerable import is that the situation is often outside of the local commander's leaderships' control.

Figure 4

Decision Making Matrix



Often the goals or objectives are decided. The leader influences the outputs only by the degree. However many of the OAP leadership variables contain a wide range of acceptable skills and behaviors. These can be manipulated as the commander deems appropriate. Therefore, the focus of this analysis will be upon the leadership variables in order to analyze them for their logical relationship to developmental leadership perspective.

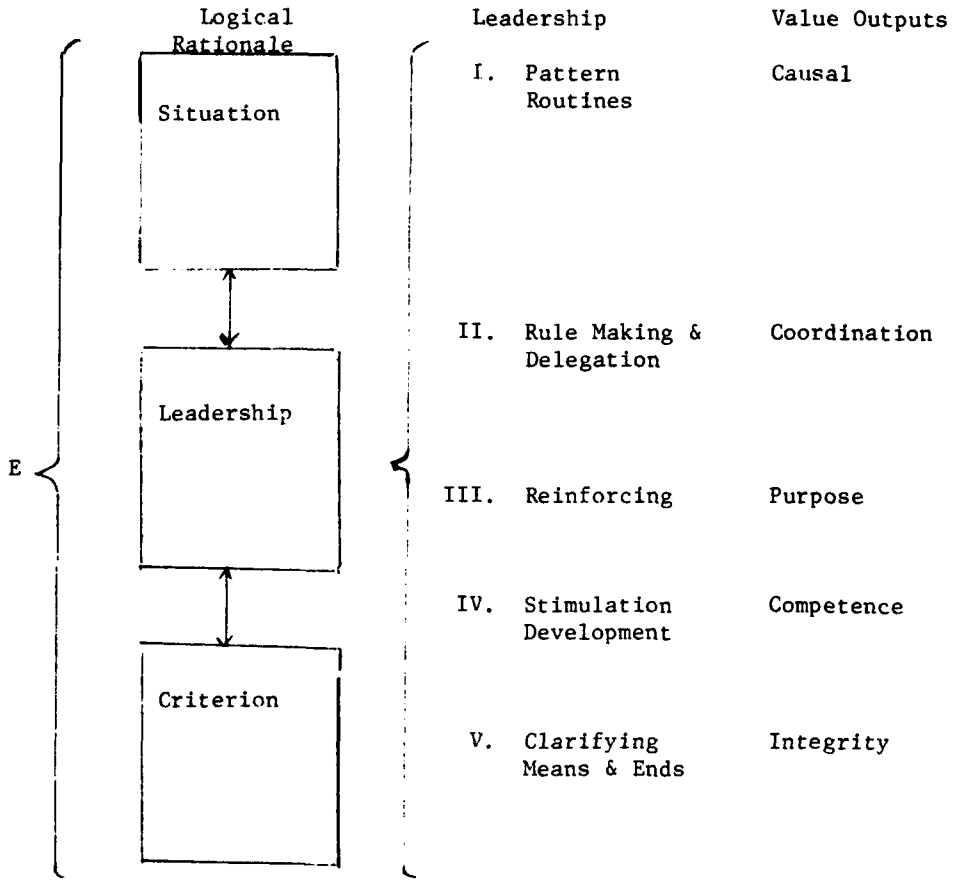
The five levels of leadership previously described will be used to categorize the OAP variables (see Figure 5). The variables will also be related to the technology that is available to develop the skills called for if the leader is to take charge and influence the organization. As previously stated, the first level process is the leader's patterned routines or regularities designed to set the tempo for efficiency. Based upon tradition there are efficient methods for getting things organized and done. When used, the methods reveal to followers that the leaders activities make sense, that hinderances are reduced, and that this is a good place to be and to work. The OAP assess this as follows:

I. Pattern routines for efficiency and casuality

| TECHNOLOGY | OAP ITEMS |
|---|---|
| a. Planner | 404 Good Planning |
| b. Communicator | 301 Adequate Information |
| | 302 Adequate Information to Group |
| | 309 Information Widely Shared |
| | 318 Accurate Information |
| | 413 Responsibilities Clear |
| | 305 Organization is Interested |
| c. Time Manager | 279 Bottleneck |

Figure 5

Levels of Leadership



Level two leadership reflects the leader-followers relationships. These relationships are necessary for the coordination of effort. Therefore, rules are made and job descriptions structure activity, feelings and deference. The OAP assesses this process as follows:

II. Rules and Delegation for Coordination

| TECHNOLOGY | OAP ITEMS |
|---|---|
| a. Communicator | 217 Knows What's Expected |
| | 303 Work Group Aware of Events |
| | 428 Explains My Job |
| | 445 Supervisor Explains Procedures |
| b. Goal Setting | 218 Performs Goals |
| | 221 Performance Goals Realistic |
| | 274 Job Performance Goals Specific |
| | 273 Job Performance Goals Clear |
| | 314 Clear Cut Goals |
| | 317 Goals Reasonable |
| | 405 Sets High Performance Standards |
| | 412 Establishes Good Work Procedure |
| c. Assistor | 424 Takes Time to Help Me |
| | 435 Helps Me Improve Performance |

Level three leadership reflects the leader's conceptualization of the information flow and the influence of evaluation. The OAP assess this process as follows:

III. Reinforcements for Maintaining Purposes

| TECHNOLOGY | OAP ITEMS |
|---|---|
| a. Goal Setter | 431 Helps Me Set Goals |
| b. Communicator | 016 Frequency of Meetings |
| | 017 Meets to Solve Problems |
| | 410 Encourages Teamwork |
| | 439 Go to Supervisor for Advice |
| c. Reinforcer | 437 Performance Improves with Feedback |
| | 442 Supervisor Gives Me Feedback |
| | 310 Personal Recognition |
| | 316 Rewards Individuals |
| | 433 Lets Me Know Good Job |
| | 434 Lets Me Know Poor Job |
| d. Listener | 304 Complaints are Aired |
| | 316 Organization is Interested in My Welfare |

Level four leadership reflects the leader's conceptualization of the use of new technology and the unused talents of members.

IV. Stimulating Individual Development and the Development of Competence.

| TECHNOLOGY | OAP ITEMS |
|---|---|
| a. Programmer | 436 Assures That I Get Training |
| b. Motivator | 426 Asks for Ideas |
| | 300 Ideas are Accepted |
| | 241 Performance is Recognized |
| c. Expert | 311 Opportunity to Demonstrate Skills |
| | 416 Performs Well Under Pressure |

Level five leadership demonstrates the leader's capacity to conceptualize and integrate means and ends. As unique talents and technologies are found work they are integrated as new activities or

decision making processes. The OAP assess clarifying means and ends as follows:

V. Clarifying Behavior Indicators of Value

| TECHNOLOGY | OAP ITEMS |
|---|---|
| a. Clarifier | 411 Represents Group |

To this point this report has emphasized the analysis of the LMDC consultation and research process. The ideas taken from the model lend themselves to three cells for categorizing the leadership, outcomes and situational dimensions of organizations. Furthermore, these three categories appear to be useful for both consulting and research purposes. The information needed by the practicing commanders, consultants and researchers can be mingled in such a manner that it remains of value to all concerned. However, the usefulness of the model and the OAP data to the consultant and the practitioners is to be found in the connections between the data and recommended strategies. These connections are to be found in the consultant's and commander's practitioners recognition that the OAP scores on selected items are indicators of organizational health or disorders. As indicators of health or disorder they point to the need of leaders to maintain or initiate and thereby exercise leadership or which sustains or develops organizational health. The following section identifies and further describes the connections between the OAP and leadership resources available for improvement. However, before describing the relationships between OAP items and leadership improvement, it may be helpful to place the consultants' interview and the researchers' more-empirical-data-orientation into perspective. The researcher's perspective necessarily includes answering a series of questions about theoretical construets, item analyses, instrument reliability, instrument validity and generalizability of the findings. Concerns about assessment methods are governed by a rather rigorous if not regimented set of procedures to ensure that generalizations can be made and that the

"garbage in, garbage out" syndrome is reduced if not eliminated. For the researcher, meaning is derived from generalizations that must apply to the totality of the universe represented by the sample studied. The researchers generalizations or findings must meet the challenge of chance. Events of life are more than an accident. In a universe of relationships events must be understood. Some happenings may be predicted. The researcher is invested in identifying these predictions and making generalizations that leaders can depend upon and use for decision making and action.

On the other hand, the consultant must glean particularistic meaning from data. This gleaning occurs in the complexity of an ebb and flow of daily decision making. Organizations are people with all their joys, delights and contributions. Organizations are people with all their cuts, burns, bruises and scratches derived from daily living. Bringing order to the complexities of organizational life involves more variables and data than can ever be supplied by an OAP. However, through interview and participant observation the consultant may screen a flood of feelings, activities, attitudes and predispositions. These have meaning to the holder. Collectively, they hold rich meaning and constitute expectations of the membership. Collectively, these data are related to decision making, power, prestige and productivity. The OAP assesses a significant part of these expectations as indicators of organizational health. However, the OAP data must be supplemented if the meanings of the data and recommended changes are to make sense to local commanders, their men or their women. The OAP data reveals tentative generalization about the organizational leadership. OAP scores screen for the relative strength and wekanesses. However, understanding the meaning and rich use for decision making involves using interview data and participant observation data. The best and the brightest already implicitly know how to lead better than theories, data or researchers' generalizations can reveal. The data base researcher systematically taps the leadership, constructs, measures a limited number of performance variables and recommends that which tests out to be related to productivity.

The consultant-participant observer is needed to sort through the observed or participant observational data imbedded in the particular context and recommend or collaborately develop a logically relevant action plan. Undoubtedly, experienced leaders functioning as peer consultants often approach this process in a rather unconventional manner. That is, there are less predetermined conventions or procedures that must be observed. When treating data the consultant must deal with multiple sets of conventions or procedures. Bringing order to information is often guided by the less explicit procedures that form the core of the consultants' style, habit or personality. It is a necessary means for bringing order to information and creating mutual understandings between the consultants and the commanders.

In summary, OAP data and consultant data serve complimentary purposes. The OAP generates structured data or indicators for empirically identifying needs for change. The consultant data contributes the personal richness necessary for the relevant and full understanding needed for decision making. This richness enables the investigator, consultant and practitioners to answer the complementary questions about how organizations work and why things are as they are. The OAP information identifies that an issue or discrepancy exists. Consultant clarify the meanings and understandings of leaders. In conclusion, the OAP data gathering and consultant interview processes compliment the other in the search for organizational understandings. This section will continue with an ordering and a description of the resources consultants have for using OAP data.

It was noted in the introduction to this paper that persons entering an organization looks for the cues that enable them to make sense about what goes on. Members were described as working in such a way as to develop predictable patterns of work. Over time the members come to know who they are and engage in patterned procedures or habitual ways of acting. They engage in their roles, jobs and responsibilities almost without thinking. Others come to expect them to know certain things and to do certain things. Much of organized life becomes routinized. This routinized activity and ways of thinking enable the

member to function smoothly and efficiently. Collectively, they enable the organization to function smoothly and efficiently. Furthermore, unless a substantial proportion of organizational behavior is routinized there is no structural cement to hold the organization together. Every day cannot be a new day. Every day must be in the context of every other day. Organizational activity has an ebb and flow. Every organization has a history. Leaders influence if not control a substantial proportion of this patterned activity. The leader's work is perceived to be important and unless demonstrated otherwise, it is important. As members work with a leader they are constantly alert to the signals that enable them to predict the leader's patterned activity and decision making. The importance which followers give, to being tuned into the work patterns of leaders, is not to be underestimated. Followers recognize that the leader is the controller of the reward system. They know that leaders govern and influence policies, work conditions and resources. How do they exercise this control? They exercise it primarily through the skill they bring to policy making, planning and time management. Currently three sets of OAP data relate to the leaders' patterned work of policy making, planning and time management. The OAP variables listed below assess the leaders' patterned routines of work.

| Patterned Activity | Relevant OAP Variable |
|---|---|
| Planning | #404 Good Planning |
| Policy Making | #301 Adequate information |
| | #307 Adequate information Grp |
| | #303 Information shared |
| | #318 Accurate information |
| | #413 Responsibilities |
| Time Management | #279 Bottleneck |
| Visibility | #305 Organizational interest |
| | #306 Organizational interest |

Planning is a powerful variable in the leadership (818) factor. Subordinates perceive whether the leader's activities are complete and sensible. Through planning the leader communicates that organizational matters have been thought out and anticipated. If the leader plans and organizes with due regard to the work setting and professional values, the leader reveals the intensity and relevance of their work. They reveal that they are invested in making the organization work sensible. With respect to this, leaders have considerable freedom to organize time, space, resources, personnel and technology to accomplish organizational objectives or purposes. The way the leader schedules work, influences the accomplishment of purposes. Scheduling communicates a

TABLE 1

Organizational Planning Matrix

| Time | Space | Resources | Technology | Personnel |
|---|---|---|---|---|
| Scheduling | Functional | Budgeting | Discipline | Specialization |
| Calendar | Proximity | Equipment | | Socialized Professional |
| Deadlines | Mood | Facilities | Activities | Values |

sense of timeliness associated with the daily or weekly or monthly calendar. The leader's space arrangement of office space may communicate a mood and function. The allocation of resources can expedite work of some or impede the work of others. Comprehension of the way the technology of the banker, priest or Air Force dictates that performance is revealed by the leaders organized activities. Finally, personnel can be used in such a way that specializations organizationally relevant values are supported. In short, the leader has many opportunities to communicate credibility through their planning. For this planning influences the life of every member through the use of scarce allocation of resources time, space and technology.

The second cluster of variables pertain to policy communications. OAP items assess to adequacy of communications; (V301 & 302) sharing (V303) and accuracy (V318) of information assesses the leader's planning and policy implementation. Thoughtful planning makes it possible to have information available as needed. Planning guided by policy dictates that information be adequate and shared. Policies are made in order to reduce the nuisance of making the same decision over and over again or make the expectations explicit. Policy streamlines the routine decision making process. However, for policy to work, an adequate and accurate information flow must exist.

A third item relevant to the leader's patterned routine is the bottleneck Variable #279. The neck of a bottle is usually found at the top. A bottleneck occurs when information needed is not processed and planning is chaotic. Generally, bottlenecks indicate an absence of planning skills. Apparently a vicious cycle spins out of control if policy does not guide decision making and planning. If planning does not result in the accurate and adequate dissemination of information the cycle becomes more destructive. Together policy and planning make for efficiency and shared communications. The basic skills of policy implementation and planning communications are learned from the technology of time management, writing and program evaluation and review techniques (PERT). A final routine management variable of fundamental importance is that of organizational interest (variables 305 to 306). This variable is primarily a reflection of the leader's visibility and willingness to personally chat and glean information from persons of various ranks and statuses. As previously noted, how the leader uses resources (time) influences if not controls follower's perceptions about the use of resources. A visible leader communicates not only interest but also respect for the ideas and contributions of others.

The OAP variables relevant to the leader's patterned activity, and over which, the leader may exercise considerable control has been identified and related to the technology of planning, communications,

time management and visibility. In Table 2 this technology is further ordered as concrete, relational and conceptual. For example, planning may be according to the traditional way it has always been done. Planning can be guided by forms to be filled out; deadlines to be anticipated, and the seasons that come and go. Planning may be in relation to others or according to standard operating procedures (SOP) and policy. This requires a relational perspective in addition to an understanding of linear tasks. Finally, on a conceptual level, program evaluation review and technique is used to relate goals, policies and resources identified in Table 1. In the same way the technology of communication or the role of communicator includes work scheduling, correspondence and policy formulation. Time management can be used to get increased

Table 2

Level I Leadership

| Technology | Concrete | Relational | Conceptual |
|---|---|---|---|
| Planner | Traditional | S.O.P. | P.E.R.T. |
| Communication | Activity Scheduling | Correspondence | Policy Formation |
| Time Management | Routine | Priorities "To Do" | 80/20 |
| Visible | Tour | Chat | Inquiry |

efficiency. To take control of one's life a priority "to do" list may be helpful. On the other hand, following the 80/20 rule conceptually establishes higher order to daily work.

At this point it may be important to note that communication cuts across leadership. To create or maintain expectations and interactions, leaders must communicate. For good or ill, leaders constantly communicate. Their every activity communicates. This constant communication can be anticipated. On the other hand, whether anticipated or not, messages are perceived from every leadership act.

Rule making and delegating leadership occur as the division of labor demands a structure for coordinated work and authority. Understandings about who does what, who decides what and how do members feel about it are necessary. The OAP assesses the division of labor through the leaders' involvement in such things as developing job descriptions, communications goal setting and technical assistance. The OAP assesses delegation through such variables as performance standards (Variable 405) and establishing good work procedures (Variable 412). Standards and procedures are generally included in the job descriptions. The OAP assesses how job information is communicated through work groups aware of events (Variable 303), information shared (V309), explains my job (V428), and supervisor explains procedures (V444). The goals of the job are assessed by OAP items, performance goals are realistic (V218), specific (V270), clear (V273), and reasonable (V317). Communication about job related matters are measured by variable, information is shared (V309), explains my job (V428) and explains procedures (V444). The supervision in some instances follows up the delegation and communication with technical assistance by taking time to help me (V424) and helps me improve performance (V435). The OAP assessment screens for patterns and comparative indicators. On the basis of comparison data tentative areas of excellence or areas of deficiency are revealed. From comparative data observers are apt to infer from low or high scores that something is amiss or positive.

Table 3

Delegation Level 2

| Technology | Concrete | Relational | Conceptual |
|---|---|---|---|
| Job Descriptions | Qualifications | Expectations | Goals |
| Communication | Telling | Explaining | Listening |
| Goal Setting | To be done | PERT | Solving Problems |
| Technician | Telling | Explaining | Training |

Leaders generally perceive that they have a responsibility to reward appropriate and correct inappropriate behavior (Level III). The extensic motivation system is supported by the consistency of the leader's rewarding patterns. As noted previously, the delegation processes include communicating job responsibilities and clarifying expectations with respect to activity, authority and feeling. Situationally, describing all the activity, all the authority and all the feeling are impossible. It also may be undesirable. For specifying all the authority and activity would reduce the worker's areas of freedom and eliminate discretionary behavior. The day by day leadership responsibility to clarify is used to maintain purposeful direction.

It is the leader's reinforcement that follows the subordinate act that makes the difference. Actions speak louder than words. Don's underestimate the effects of words, words of praise are desirable and necessary. But actions must be also congruent words. Merit pay, commendations, desks, passes, carpets, keys to the washroom, and other accoutrements of status speak concretely to the issue of status and success. These have to do with reinforcement and (again) commendation.

The previously level dealt with the division of labor. The division of labor is a process of delegating things to be done. Once done the subordinate deserves clarification of how their contribution measures up.

Table 4

Clarify And Reinforcing

| Technology | Concrete | Relationship | Conceptual |
|---|---|---|---|
| Goal Setter | Roles | Norms | Problem Behavior |
| Communication | Descriptive | + - | Use Ideas |
| Reinforcement | Specific Task | Praise | Recognition |
| Listening | Clarifying | Conferences | Meetings |

The relevant technology has been organized into four categories. Goal setting, communicating, reinforcement and listening. The categories are assessed by the OAP items. Goal setting is measured by variable 431, helps set goals. Communicating is measured by the variable frequency of meetings (016), meets to solve problems (V017), encourages teamwork (V410) and goes to supervisor for advice (V439). Reinforcement is assessed by six variables pertaining to rewards and informational feedback, (V437, 442, 310, 316, 433, and 434). Finally the category of listening is assessed by three variables that measure the interest and willingness of the leader to hear complaints and express interest (V304, 305, and 306).

STIMULATING INDIVIDUAL DEVELOPMENT:

Leadership responsibility for initiating the use of new talent and technology becomes possible as the expectations or SOP are reasonably understood and operationally efficient. In a technological

Table 6

Stimulating Individual Development

| Technology | Concrete | Relationship | Conceptual |
|---|---|---|---|
| Programmer | Technological Resource | Brainstorming | Problem Solving |
| Motivator | Listening | Using Ideas | Recognizing Merit |
| Expert | Technological | Representational | Authority |

society, skilled craftsmen, skill technicians and competent men and women often have talents that are unused. New technology of great worth will be revealed. Better ways of getting the job done will be discovered. Personnel and technical break throughs are resources to be used. Leaders influence if not control the followers opportunity to use this new technology and personal talents.

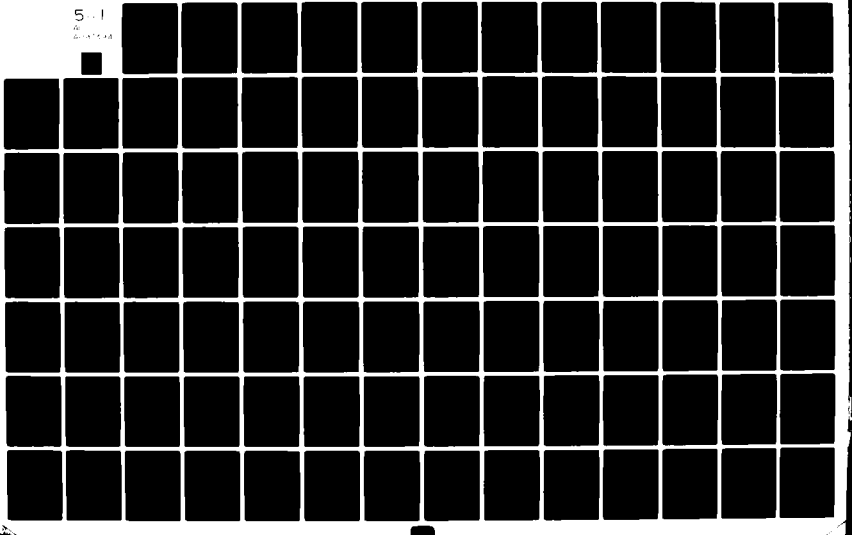
Table 6 reports the roles and ways leaders may view their technological roles. The OAP variable measuring programming to use technology and talent are assuring that I get training (V436). The motivating variables are, asking for ideas (V426), ideas are accepted (V300), performance recognized (V241), and personal performance recognized (V310). The role of the expert appears to be measured by - performs well under pressure (V416).

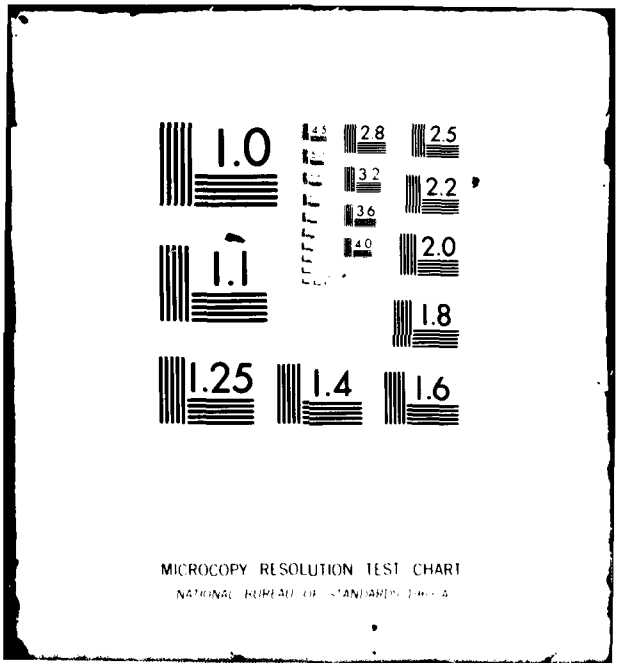
The fifth level of leadership - to clarify means and ends, may be somewhat tapped by the OAP variable, the leader represents the group (V411). Otherwise, the leadership processes of reflection and introspection seems to be untapped.

This section of the paper has traced the relationship of leadership to the OAP. The levels of leadership have been used to

AD-A097 394 SOUTHEASTERN CENTER FOR ELECTRICAL ENGINEERING EDUCAT--ETC F/G 5/1
USAF SUMMER FACULTY RESEARCH PROGRAM, 1980. RESEARCH REPORTS, V--ETC(U)
OCT 80 W D PEELE F49620-79-C-0038

UNCLASSIFIED AFOSR-TR-81-0193 NL




1.0
2.8
2.5
3.2
2.2
3.6
4.0
2.0
1.1
1.8
1.25
1.4
1.6
MICROCOPY RESOLUTION TEST CHART
NATIONAL BUREAU OF STANDARDS 1963-A

categorize the OAP variables. Within each level of leadership there are important roles such as planner, amanger, and commincator. The role of communicator cuts across all levels for whatever the leader does communicates by word and deed. Can the leaders role be developed through training and practice? We think so. However, it may be necessary to develop the more fundamental skills first is the more complex processes are to be relevant. If the more fundamental are not perfected, the more complex skills and processes may not be attainable. If the less complex is not perfected, dealing with the more complex tasks may result in mechanisms that are desctructive to self and others.

There are many implications of this ordering for both research and training. Foremost are the training implications derived from the OAP assessment. The OAP scores are indicators of organizational health. As indicators, they can be best verified and interpreted when compliemented by the consultant interview data. As problems are verified consultant intervention alternatives may be developed and described in the action plans. A second implication is that the leadership levels point to getting to basic matters before attempting to change more complex matters. Improving one's own act may be necessary before commanding a subordinate to "shape up" makes any sense. Logically delegating follows organizing, reinforcement follows delegating and program development follows once the organizational maintenance processes of organizing, delegating and reinforcing are in place. Within each of these levels are some rather specific skills and responsibilities. The complexity of the responsibilities are illustrated in figures two thru five. The OAP assessment then directs the consultants to order and make decisions about the place or programs they have to offer for improvement.

The implications for research are both analytical and descriptive. Of most importance is to understand the consultant process. This understanding may initially be descriptive. Descriptions of what consultants do may reveal differences that affect leadership and organizational outcomes. Subsequently, analysis of collected information

will be helpful to identify the consultant interventions that are most productive. This assessment of consultant treatment is necessary to understand if there are contexts and processes that are more productive than others. This is not a control process. Rather it is an open process of data based briefing, debriefing and analysis in order to understand the ways consultants influence the quality of leadership.

Another implication is to understand the LMDC influences the quality of leadership. If leadership has a hierarchial structure it is feasible to develop a resource for guiding the development of action plans. The tables and figures contained in this paper outline and relate levels of leadership, conventional roles of leadership, and the OAP variables. This resource could serve as a screening tool to order the OAP data and guide the organizing of action plan? Table 7 is an example of how this could be done by combining the levels of leadership and the conventional leadership roles. If the preliminary ordering in Table 7 has face validity a form or several forms may be developed to guide the creation of an action plan and identify the questions that should be raised to make decisions about the content of the action plan?

## IV. ASSESSMENT OF LEADERSHIP STRUCTURES

To assess the power of the described leadership structure for ordering the Organizational Assessment Package (OAP) variables, and developing action plans, three procedures were used. The first procedure was to test the relationship between high scores on the Management-Supervisor Factor 818 and selected output variables. The second procedure was to test the face validity of the logically ordered leadership variables according to the respective leadership levels and operational leadership roles. This face validity was assessed by obtaining the judgements of the Leadership Management Development Center Consultants. The third procedure was to factor the leadership variables.

The relationship between the Management-Supervisor Factor 818 and selected output variables was assessed by contrasting high rated leaders and low rated leaders with selected output variables of career intent and the leadership process variable of holding problem solving meetings. Leader rates 6.25 or above were compared with leaders rated 3.88 or below. Fifty-four percent of the leaders rated high were reported as holding meetings to solve problems about half the time or all the time. Twelve percent of the low rated leaders were reported to hold meetings for problem solving. Of the low rated leaders, forty-nine percent were reported as never using meetings for problem solving (see Table 7). The career intent of the followers of high rated leaders was significantly different than followers of low rated leaders. Forty-five percent of the high rated leader's personnel intended to continue. Twenty-nine percent of the low rated leader's men intended to continue. The intent to separate response was eight percent and nineteen percent respectively (see Table 8). It is apparent that there are important output differences related to the patterns of high rated leaders.

The second procedure - to establish the face validity of the theoretical structure was to circulate the preliminary description and classification of the leadership variable to the Leadership and Management Development Center Consultants. The consultants were requested to judge the appropriateness of the classification with the fitness of their experience. In the opinions of the consultants all classifications reported on Table 1 were judged appropriately.

The third procedure was to factor analysis the Organizational Assessment Package (OAP) leadership variable to determine the congruence between the theoretical factor structure and the empirical factor structure. Forty-five leadership variables selected as independent variables over which leaders exercise considerable power if not control. These were included in the analysis. Three factor analyses were computed. The first included three cuts of officers and three cuts of enlisted men according to whether the leader was perceived by

Table 7

How Often Are Meetings Used to Solve Problems

| Response | Low Rated Leaders N=8715 | % | High Rated Leaders N = 11290 | % |
|---|---|---|---|---|
| Never | 4293 | 49.3 | 1096 | 9.6 |
| Occasionally | 3305 | 37.9 | 4113 | 36.4 |
| About Half the Time | 709 | 8.1 | 2293 | 20.3 |
| All the Time | 408 | 4.7 | 3800 | 33.6 |

Table 8

Followers' Career Intent

| | Low Rated Leaders N = 8500 | % | High Rated Leaders N= 10944 | % |
|---|---|---|---|---|
| Retire | 443 | 5.2 | 720 | 6.6 |
| Will Continue | 2472 | 29.1 | 4982 | 45.5 |
| Most Likely Continue | 1358 | 16.0 | 1789 | 16.3 |
| May Continue | 1469 | 17.3 | 1604 | 14.7 |
| Most Likely Not | 1152 | 13.6 | 986 | 9.0 |
| Separate | 1606 | 18.9 | 863 | 7.9 |

followers to be in the upper, middle or lower third on the Management-Supervising 818 factor. The initial factor analysis used on the twelve factors identified during the previous analysis of the OAP.[2] The second and third analysis used the same cuts. However, the varimax rotations included only those factors with an initial equinvalue of 1.0 or greater.

The factor analysis revealed loadings on a generalized leadership factor of information processing that is necessary for the maintenance of work structures and interaction. The initial analysis included from twenty eight to thirty three variables with loading exceeding .4. The generalized nature of the factor was further affirmed by the marginal loadings of ten to thirteen variables ranging between .2 and .399.

The specific factors were identified and interpreted after verimax rotation. Three major analyses were computed. The first included the twelve factors previously computed on the basis of the ninety three OAP variables. When the forty five leadership variables were computed on a sample of lower rated officers the primary factor consisted of the supervision management variable, consisting of nine variables. These variables generally reflect an attitude toward the supervisor, however, since the factor occurs as the primary factor among lower rated supervisors it may be labeled as perceptions of the manager's communications and technical expertise. When considered in light of the 404 Planer and the 405 performance standard variables the 400 variables can be labeled as the followers' perceptions of the manager's skill.

The other five analysis based upon the twelve factor structure revealed that the"three hundred"variables pertaining to communication or organizational climate was the primary factor. Seventeen variable uniformity load on this factor at .40 or greater. The naming variables were those of adequately information .86 and accuracy of information .75. Interestingly, the factor was the secondary factors of lower rated leaders and included only five of the variables. The third factor consisted of job expectations, (217); goals realistic, (221); goals clear, (273); and goals specific, (274). This factor is best characterized as goal clarity. The fourth leadership factor

included reinforcement or motivation. Three variables are related to the factor. They are recognition for performance, (V241); personnel recognition for performance, (V310); and organization reward individuals on performance, (V316).

The fifth factor in supervisory assistance variables 424 and 428, supervisor takes time to help me and superior explains my job relationship to mission, load for the higher rated supervisors. Two other factors emerge from the data these are planning and problem solving. The higher rated supervisor load on planning V404 and rate high performance standard as a unique variable. All analyses included the two meeting variables as loading at .60 or higher.

The factor analysis computed on factors having an equivalent of 1.0 or greater and including varimax rotation revealed a slightly pattern. The primary factor was uniformly a generalized leadership communication factor on leadership-communication of seventeen 300 variables. The secondary factor was the division of labor or supervisory management factor. However, interesting differences are evident. High rated supervisors, load on the 426-445 service variables while lower rated supervisor load negatively also on planning and performance variables V410, 411, and 412. These loadings are high yet it is evident that follows rate their supervisor low in these matters.

The respective analysis reveals that there is a generalized factor of leadership. This factor parallels the global process of communications and work appropriate for maintaining structures for expectations and interaction. The supervisor through the management of their work creates the structure through which communications are perceived and attitudes about work are developed. The varimax rotation of the factors reveals that in conducting their work leaders communicate expectations about job performance goals in their many dimensions (see Table10). Knowledge about the goals, clarity of goals and specificity of goals parallel the division of labor. A third factor pertains to recognition of performance. This factor parallels the reinforcement of relevant behavior. The higher rated

Table 9

Leadership Structure

| Theoretical Model Levels of Leadership | OAP Factor Structure High Rated Leaders | |
|---|---|---|
| | Factor # | Label |
| 1. Patterned Routines | 1 | Generalized Leadership Behavior |
| 2. Rules and Delegation | 2 | Division of Labor |
| 3. Reinforcement of Relevant Behavior | 3 | Goal Clarity |
| 4. Stimulating Individual Development | 4 | Goal Setting |
| | 5 | Recognition |
| 5. Classification Values | 6 | Problem Solving |

leaders enact two factors parallel to stimulating individual development. The high loading on (V435) helps me improve my performance and supplies feedback about how well I'm doing (V442) load highly on the fourth specific factor. Another factor is the cooperate problem solving factor (V016 and 017). Combined these two factors of assistance and problem solving characterize the pattern of higher rated leaders.

Another interesting contrast between the higher and lower rated leaders is clear. The loading of the recognition for performance variables (241, 210 and 316) account for a higher proportion of the variance among lower rated supervisors. It is conjectured that this difference is based upon the possibility that lower rated supervisors use recognition as an extrensic motivator. While, higher rated supervisors use recognition as an intrensix motivator. In short, it is apparent that the factors support the conclusion that the theoretical levels of leadership are congruent with the factors structure of more mature and higher rated leaders (see Table 10).

The factor analysis reveals that the structure of leadership roughly parallels the levels of leadership. Before rotation the correlation of .40 or greater on a generalized leadership factor include thirty two of the variables. The factor of the highest loading are the communication variables of accuracy of information and adequacy of information. Apparently the leader's behavioral patterns reflect a consistency and continuity of information. Furthermore, these patterns communicate standards of relevance and articulation. The verimax rotation reveals a factor structure that is more different and systematically elaborate for higher rated leaders. Their structure pertains to leadership communication, division of labor, goal clarity, goal setting, recognition and problem solving. Considering this structure and the apparent meaning the variables bring to the factors the format for ordering OAP data and the development of action plans dictated some revision from that outlined in Table 7. The format (Appendix A) for the development of action plans is recommended further testing.

Table 10

Leadership Factor Analysis

| Factor 1 - Generalized Leadership - Communication | | Higher Rated Leaders | | Lower Rated Leaders | |
|---|---|---|---|---|---|
| Variable # | Statement | Officers | Enlisted | Officers | Enlisted |
| 300 | Ideas developed by my work group are readily accepted by management personnel above my supervisor. | 5941 | 6456 | 5435 | 5707 |
| 301 | My organization provides all the necessary information for me to do my job effectively. | 7119 | 7511 | 5835 | 6978 |
| 302 | My organization provides adequate information to my work group. | 7975 | 7984 | 6333 | 7629 |
| 303 | My work group is usually aware of important events and situations. | 6957 | 7362 | 5886 | 6338 |
| 304 | My complaints are aired satisfactorily. | 6929 | 7323 | 6340 | 5711 |
| 305 | My organization is very interested in the attitudes of the group members toward their jobs. | 7723 | 8041 | 6339 | 6672 |
| 306 | My organization has a very strong interest in the welfare of its people. | 7656 | 8112 | 6347 | 6949 |
| 309 | The information in my organization is widely shared so that those needing it have it available. | 7865 | 8017 | 6399 | 7234 |

Table 10 (Continued)

| Factor 1 - Generalized Leadership - Communication | | Higher Rated Leaders | | Lower Rated Leaders | |
|---|---|---|---|---|---|
| Variable # | Statement | Officers | Enlisted | Officers | Enlisted |
| 310 | Personnel in my unit are recognized for outstanding performance. | 6609 | 7205 | 6343 | 5454 |
| 311 | I am usually given the opportunity to show or demonstrate my work to others. | 5629 | 5819 | 5879 | 4401 |
| 312 | There is a higher spirit of teamwork among my co-workers. | 6033 | 5178 | 5279 | 4322 |
| 313 | There is outstanding cooperation between work groups of my organization. | 6732 | 7119 | 5747 | 6017 |
| 314 | My organization has clear-cut goals. | 6363 | 7417 | 5034 | 5898 |
| 315 | I feel motivated to contribute my best efforts to the mission of my organization. | 5790 | 6875 | 5034 | 5268 |
| 316 | My organization rewards individuals based on performance. | 6911 | 7525 | 6669 | 5946 |
| 317 | The goals of my organization are reasonable. | 6472 | 7266 | 5405 | 6017 |
| 318 | My organization provides accurate information to my work group. | 8129 | 8296 | 6709 | 7516 |

Table 10 (Continued)

| *Factor 2 - Division of Labor - Management* | | Higher Rated Leaders | | Lower Rated Leaders | |
|---|---|---|---|---|---|
| Variable # | Statement | Officers | Enlisted | Officers | Enlisted |
| 404 | My supervisor is a good planner. | | | | 4960 |
| 410 | My supervisor encourages teamwork. | | | | 4837 |
| 411 | My supervisor represents the group at all times. | | | | 4838 |
| 412 | My supervisor establishes good work procedures. | | | | 5949 |
| 413 | My supervisor has made his responsibilities clear to the group. | | | | 4151 |
| 416 | My supervisor performs well under pressure. | | | | 4829 |
| 424 | My supervisor takes time to help me when needed. | | | 4558 | 6246 |
| 428 | My supervisor explains how my job contributes to the overall mission. | 4819 | 4625 | | 5906 |
| 431 | My supervisor helps me set specific goals. | 5502 | 5784 | 4423 | 6831 |
| 433 | My supervisor lets me know when I am doing a good job. | 6895 | 6835 | 4301 | 6250 |
| 434 | My supervisor lets me know when I am doing a poor job. | 5218 | 4996 | 5119 | |
| 435 | My supervisor always helps me improve my performance. | 7527 | 7379 | | 7494 |

Table 10 (Continued)

| Factor 2 - Division of Labor - Management | | Higher Rated Leaders | | Lower Rated Leaders | |
|---|---|---|---|---|---|
| Variable # | Statement | Officers | Enlisted | Officers | Enlisted |
| 436 | My supervisor insures that I get job-related training when needed. | 5736 | 6139 | | 5714 |
| 437 | My job performance has improved due to feedback received from my supervisor. | 6957 | 6699 | 4541 | 6626 |
| 439 | When I need technical advice, I usually go to my supervisor. | 4091 | | | 4980 |
| 442 | My supervisor frequently gives me feedback on how well I am doing my job. | 7546 | 6659 | 4402 | 6296 |
| 445 | My supervisor fully explains procedures to each group member. | | | | 5665 |
| Factor 3 - Goal Clarity | | | | | |
| 217 | To what extent do you know exactly what is expected of you in performing your job? | 6267 | 5787 | 4751 | 5729 |
| 221 | To what extent are your job performance goals realistic? | / 6295 | 5973 | 4485 | 5990 |
| 273 | To what extent are your job performance goals clear? | 8706 | 8441 | 7458 | 8569 |
| 274 | To what extent are your job performance goals specific? | 7905 | 8482 | 7107 | 8422 |

Table 10 (Continued)

| Factor 4 - Goal Setting | | Higher Rated Leaders | | Lower Rated Leaders | |
|---|---|---|---|---|---|
| Variable # | Statement | Officers | Enlisted | Officers | Enlisted |
| 404 | My supervisor is a good planner. | 5522 | 4369 | | |
| 405 | My supervisor sets high performance standards. | 5145 | 4398 | | |
| 412 | My supervisor establishes good work procedures. | 4538 | 6160 | | |
| 413 | My supervisor has made his responsibilities clear to the group. | | 4139 | | |
| Factor 5 - Recognition - Competence | | | | | |
| 241 | To what extent do people who perform well receive recognition? | 4643 | 4216 | | 4429 |
| 310 | Personnel in my unit are recognized for outstanding performance. | 4701 | | | 5180 |
| 316 | My organization rewards individuals based on performance. | 4016 | | | 4391 |
| Factor 6 - Problem Solving - Clarification | | | | | |
| 016 | How often does your supervisor hold group meetings? | 4595 | 6037 | 4039 | 6168 |
| 017 | How often are group meetings used to solve problems and establish goals? | 5675 | 6834 | | 6108 |

## V. RECOMMENDATIONS

Two sets of recommendations are relevant to this study. The first has to do with the consultant use of the OAP data in the formulation of action plans. The second pertains to further investigations. The OAP assesses the structure of leadership. The generalized leadership patterns include a complex of skills, habits and values. These skills, habits and values are sustained by the leader almost without thinking. They are institutionalized in the individual and generally accepted by the membership. The quality of leadership depends upon the skillfulness, relevance and consistency of leader behavior. The OAP reveals that low rated leaders behavior is less skillful, relevant and systematic. Since every subsequent leadership act is grounded in the leaders generalized or routine behavior, attention must be given to strengthen the fundamental leadership skills related to routine matters. Therefore, it is recommended that the OAP data be systematically organized according to the levels of leadership and action plans be developed that treat the most basic problems or deficiencies before plans include the treatment of higher order concerns is initiated.

As action plans are developed and initiated it is recommended that the implementation process be documented. This documentation will be helpful for understanding the change process and the unique problems or habits that must also be overcome. Undoubtedly, every individual responds rationally, from their perspective, to the leaders' expectations. Initiating a rational model is fraught with many problems. Understanding these problems may depend upon documentation as change is planned and initiated.

The second set of recommendations pertains to the continuous study of leadership. To the extent that there is a generic structure of leadership, "leadership style" will begin to have less meaning. Undoubtedly the matching of leadership and followers "style" has much meaning. However, change is based upon skills and habits that are

relevant to task accomplishment. Regardless of the leader's style certain skills improve the quality of life individually and collectively. Therefore, it is recommended that continued study of the generic leadership skills be continued. Second, it is recommended that the forty-five leadership variables be studied for the relationships they have to the situational and output variables. (We know that the Supervisory Management 818 factor is related to problem solving behavior and intent to continue in the service). Continued study of the specific leadership variables and the relationship to output variables would be of continued value.

The final recommendation is to study a sample of superior, excellent and average leaders. This study could serve as a beginning of a longitudinal study of leadership development in the Air Force. A stratified sample of Air Force ranks would enable the investigator to understand the dynamics of leadership development and the career pattern of superiors, excellent and average leaders from the perspective of both the position sampled and the perspective of the individual.

## References


1. Hendrix, W.H. "Contingency approaches to leadership: A review and synthesis." AFHRL-TR-76-17, AD-A028 485. Lackland AFB, TX: Occupation and Manpower Research Division, Air Force Human Resources Laboratory, June 1976.

2. Hendrix, W.H. & Halverson, V.B. "Organizational survey assessment package for Air Force organizations." AFHRL-TR-78-93, AD-A068 476. Brooks AFB, TX: Occupation and Manpower Research Division, Air Force Human Resources Laboratory, February 1979. (a)

3. Petrie, T.A. & Burton, Barry. "Levels of Leadership", Educational Leadership, May 1980, pp. 628-631.

Appendix A

Leadership and Management Development Center
Maxwell Air Force Base
Maxwell, Alabama

Action Plan Guide

OAP Variable Relationships

| Factor #1 | | Relevant to Output | | Training Alternatives |
|---|---|---|---|---|
| Variable | Mean | Variable | Mean | |
| 300 | ____ | 210 | ____ | |
| 301 | ____ | 250 | ____ | Visibility |
| 302 | ____ | 239 | ____ | Time Management |
| 303 | ____ | 705 | ____ | Listening Skills |
| 304 | ____ | 709 | ____ | Hygenic Motivation |
| 304 | ____ | | | Communications |
| 304 | ____ | | | Organizational Skills |
| 309* | ____ | | | Officership |
| 310 | ____ | | | Brainstorming |
| 311 | ____ | | | Management by Objectives |
| 312 | ____ | | | |
| 313 | ____ | | | |
| 314 | ____ | | | |
| 315 | ____ | | | |
| 316 | ____ | | | |
| 317 | ____ | | | |
| 318* | ____ | | | |

Action Plan Guide - Continued

| Factor #2 | | Relevant to Output | | Training Alternatives |
|---|---|---|---|---|
| Variable | Mean | Variable | Mean | |
| 428 | ____ | 250 | ____ | Organizational/ Assessment |
| 431 | ____ | 251 | ____ | |
| 433 | ____ | 252 | ____ | Delegation |
| 434 | ____ | 253 | ____ | Human Resource Mgr. |
| 435* | ____ | 216 | ____ | |
| 436 | ____ | 259 | ____ | Managing the Technical Worker |
| 437 | ____ | 260 | ____ | |
| 439 | ____ | 264 | ____ | Human Resource Mgr. |
| 442* | ____ | 265 | ____ | |

| Factor #3 | | | | |
|---|---|---|---|---|
| Variable | Mean | Variable | Mean | Training Alternatives |
| 217 | ____ | | | Motivational Models |
| 221 | ____ | | | Goal Setting |
| 273* | ____ | 019 | ____ | MBO |
| 274* | ____ | | | Targeting |
| | | | | Job Descriptions |

Action Plan Guide - Continued

Factor #4

| Variable # | Mean | Variable | Mean | Training Alternatives |
|---|---|---|---|---|
| 404* | ____ | 251 | ____ | |
| 405* | ____ | 209 | ____ | Team Building |
| 410 | ____ | 238 | ____ | Leadership Style |
| 412 | ____ | 240 | ____ | |
| 413 | ____ | 109 | ____ | Conferencing |
| 416 | ____ | | | |
| 424 | ____ | | | |
| 426 | ____ | | | |

Factor #5

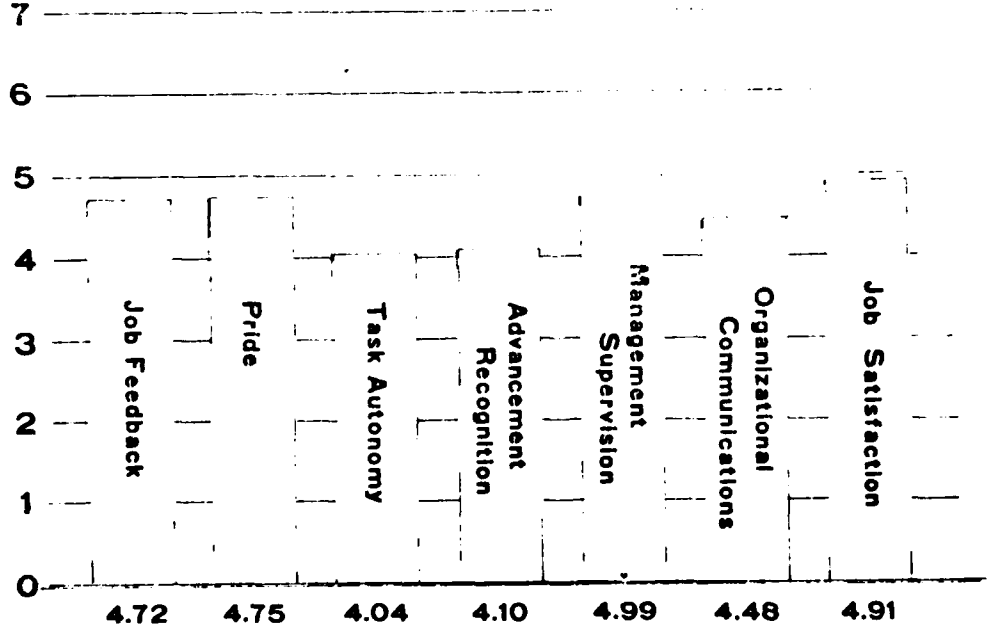
| Variable | Mean | Variable | Mean | Training Alternatives |
|---|---|---|---|---|
| 241* | ____ | 215 | ____ | *Recognition* |
| 310* | ____ | 275 | ____ | Organizational Assessment |
| 316* | ____ | 239 | ____ | Job Enrichment |

Factor #6

| Variable | Mean | Variable | Mean | Training Alternatives |
|---|---|---|---|---|
| 016* | ____ | 109 | ____ | Problem Solving |
| 017* | ____ | 307 | ____ | Meeting that Matter |
| | | 308 | ____ | Conflict Resolution |

*Naming variables

# ORGANIZATIONAL ASSESSMENT PACKAGE OUTPUT




Prepared by:
MSgt George R. Christ
LMDC/Directorate of Research
Maxwell AFB AL 36112
AV 875-7302

## ORGANIZATIONAL ASSESSMENT PACKAGE OUTPUT

The Organizational Assessment Package (OAP) was developed for use by the Air Force Leadership and Management Development Center (LMDC), Maxwell AFB, Alabama. The LMDC mission includes (a) providing management consultation services to Air Force commanders, (b) providing leadership and management training to Air Force personnel in their work environment, and (c) performing research in support of (a) and (b). The consultative role involves organizational problem area identification and recommendations for resolving problems identified.

The OAP was designed to support the mission objectives of LMDC. First, the OAP provides a means of identifying existing strengths and weaknesses within organizational work groups and aggregated work groups, such as directorates. Second, research results can be fed back into Professional Military Education curricula, other leadership and management training courses; and when action is required, to Air Staff and functional offices of primary responsibility. Third, the OAP data base established can be used for research to strengthen the overall Air Force organizational effectiveness program.

### EXTERNALLY [illegible] DESCRIPTORS

62-49

Batch Number

Julian Date of Survey

Major Air Command

Base Code

Consultation Method

Consultant Code

Survey Version

### FACTORS

Survey Version: OAP 14 Feb 79

FACTOR: DEMOGRAPHIC (NOT A STATISTICAL FACTOR)

SECTION A

| VARIABLE NUMBER | STATEMENT NUMBER | STATEMENT |
|---|---|---|
| - | - | Supervisor's Code |
| - | - | Work Group Code |
| - | - | Sex |
| - | - | Your age is |
| - | - | You are (officer, enlisted, GS,etc.) |
| - | - | Your pay grade is |
| - | - | Primary AFSC |
| - | - | Duty AFSC |

SECTION B

| VARIABLE NUMBER | STATEMENT NUMBER | STATEMENT |
|---|---|---|
| 003 | 1 | Total years in the Air Force:<br>1. Less than 1 year<br>2. More than 1 year, less than 2 years<br>3. More than 2 years, less than 3 years<br>4. More than 3 years, less than 4 years<br>5. More than 4 years, less than 8 years<br>6. More than 8 years |

| VARIABLE NUMBER | STATEMENT NUMBER | STATEMENT |
|---|---|---|
| 004 | 2 | Total months in present career field:<br>1. Less than 1 month<br>2. More than 1 month, less than 6 months<br>3. More than 6 months, less than 12 months<br>4. More than 12 months, less than 18 months<br>5. More than 18 months, less than 24 months<br>6. More than 24 months, less than 36 months<br>7. More than 36 months |
| 005 | 3 | Total months at this station:<br>1. Less than 1 month<br>2. More than 1 month, less than 6 months<br>3. More than 6 months, less than 12 months<br>4. More than 12 months, less than 18 months<br>5. More than 18 months, less than 24 months<br>6. More than 24 months, less than 36 months<br>7. More than 36 months |
| 006 | 4 | Total months in present position:<br>1. Less than 1 month<br>2. More than 1 month, less than 6 months<br>3. More than 6 months, less than 12 months<br>4. More than 12 months, less than 18 months<br>5. More than 18 months, less than 24 months<br>6. More than 24 months, less than 36 months<br>7. More than 36 months |
| 007 | 5 | Your Ethnic Group is:<br>1. American Indian or Alaskan Native<br>2. Asian or Pacific Islander<br>3. Black, not of Hispanic Origin<br>4. Hispanic<br>5. White, not of Hispanic Origin<br>6. Other |
| 008 | 11 | Which of the following "best" describes your marital status?<br>0. Not married.<br>1. Married: Spouse is a civilian employed outside home.<br>2. Married: Spouse is a civilian employed outside home - geographically separated.<br>3. Married: Spouse not employed outside home.<br>4. Married: Spouse not employed outside home - geographically separated.<br>5. Married: Spouse is a military member.<br>6. Married: Spouse is a military member - geographically separated.<br>7. Single parent. |

NOTE: *Variable 008, statement 11 was added to the OAP on 19 Jan 80 and replaced variable 014 which* [illegible] *Variable 014 is still shown* [illegible] *this variable is* [illegible]

| VARIABLE NUMBER | STATEMENT NUMBER | STATEMENT |
|---|---|---|
| 009 | 6 | Your highest education level obtained is:<br>1. Non-high school graduate<br>2. High school graduate or GED<br>3. Less than two years college<br>4. Two years or more college<br>5. Bachelors Degree<br>6. Masters Degree<br>7. Doctoral Degree |
| 010 | 7 | Highest level of professional military education (residence or correspondence):<br>0. *None or not applicable*<br>1. NCO Orientation Course or USAF Supervisor Course (NCO Phase 1 or 2)<br>2. NCO Leadership School (NCO Phase 3)<br>3. NCO Academy (NCO Phase 4)<br>4. Senior NCO Academy (NCO Phase 5)<br>5. Squadron Officer School<br>6. Intermediate Service School (i.e., ACSC, AFSC)<br>7. Senior Service School (i.e., AWC, ICAF, NWC) |
| 011 | 8 | How many people do you directly supervise?<br>1. None 5. 4 to 5<br>2. 1 6. 6 to 8<br>3. 2 7. 9 or more<br>4. 3 |
| 012 | 9 | For how many people do you write performance reports?<br>1. None 5. 4 to 5<br>2. 1 6. 6 to 8<br>3. 2 7. 9 or more<br>4. 3 |
| 013 | 10 | Does your supervisor actually write your performance reports?<br>1. Yes 2. No 3. Not sure |

| VARIABLE NUMBER | STATEMENT NUMBER | STATEMENT |
|---|---|---|
| 014 | 11 | Your work requires you to work primarily:<br><br>1. Alone<br>2. With one or two people<br>3. As a small work group (3-5 people)<br>4. As a large work group (6 or more people)<br>5. Other |
| 015 | 12 | What is your usual work schedule?<br><br>1. Day shift, normally stable hours<br>2. Swing shift (about 1600-2400)<br>3. Mid shift (about 2400-0800)<br>4. Rotating shift schedule<br>5. Day or shift work with irregular/unstable hours<br>6. Frequent TDY/travel or frequently on-call to report to work<br>7. Crew schedule |
| 016 | 13 | How often does your supervisor hold group meetings?<br><br>1. Never 4. Weekly<br>2. Occasionally 5. Daily<br>3. Monthly 6. Continuously |
| 017 | 14 | How often are group meetings used to solve problems and establish goals?<br><br>1. Never 3. About half the time<br>2. Occasionally 4. All of the time |
| 018 | 15 | What is your aeronautical rating and current status?<br><br>1. Nonrated, not on aircrew<br>2. Nonrated, now on aircrew<br>3. Rated, in crew/operations job<br>4. Rated, in support job |

| VARIABLE NUMBER | STATEMENT NUMBER | STATEMENT |
|---|---|---|
| 019 | 16 | Which of the following best describes your career or employment intentions?<br><br>1. Planning to retire in the next 12 months<br>2. Will continue in/with the Air Force as a career<br>3. Will most likely continue in/with the Air Force<br>4. May continue in/with the Air Force<br>5. Will most likely not make the Air Force a career<br>6. Will separate/terminate from the Air Force as soon as possible |

FACTORS, MULTIPLE ITEM SCALES: Each factor series consists of two or more variables which correspond to statements in the JOE. A mean score can be derived for each factor except 805, 807, 811, and 825 by using a "straight average." The formula for computing the exceptions is indicated.

FACTOR 800: SKILL VARIETY

| VARIABLE NUMBER | STATEMENT NUMBER | STATEMENT |
|---|---|---|
| 201 | 17 | To what extent does your job require you to do many *different things*, using a variety of your talents and skills? |
| 212 | 29 | To what extent does your job require you to use a number of complex skills? |

FACTOR 801: TASK IDENTITY

| VARIABLE NUMBER | STATEMENT NUMBER | STATEMENT |
|---|---|---|
| 202 | 18 | To what extent does your job involve doing a *whole* task or unit of work? |
| 211 | 28 | To what extent does your job provide you with a chance to finish completely the piece of work you have begun? |

FACTOR 802: TASK SIGNIFICANCE

| VARIABLE NUMBER | STATEMENT NUMBER | STATEMENT |
|---|---|---|
| 203 | 19 | To what extent is your job significant in that it affects others in some important way? |
| 210 | 27 | To what extent does doing your job well affect a lot of people? |

FACTOR 803 (NOT USED)

FACTOR 804: JOB FEEDBACK

| VARIABLE NUMBER | STATEMENT NUMBER | STATEMENT |
|---|---|---|
| 272 | 22 | To what extent are you able to determine how well you are doing your job without feedback from anyone else? |
| 209 | 26 | To what extent does your job provide the chance to know for yourself when you do a [illegible] to be responsible for your [illegible]? |

FACTOR 805: WORK SUPPORT

| VARIABLE NUMBER | STATEMENT NUMBER | STATEMENT |
|---|---|---|
| 206 | 23 | To what extent do additional duties interfere with the amount of your energy |
| 207 | 24 | To what extent do you have enough time to do and what you want to accomplish your job? |
| 208 | 25 | To what extent is the amount of work space provided adequate? |

Formula (8-206+207+208)/3

FACTOR 806: NEED FOR ENRICHMENT INDEX (JOB DESIRES)

| VARIABLE NUMBER | STATEMENT NUMBER | STATEMENT |
|---|---|---|
| (In my job, I would like to have the characteristics described ---from "not at all" to "an extremely large amount") | | |
| 249 | 51 | Opportunities to have independence in my work |
| 250 | 52 | A job that is meaningful |
| 251 | 53 | The opportunity for personal growth in my job |
| 252 | 54 | Opportunities in my work to use my skills |
| 253 | 55 | Opportunities to perform a variety of tasks |

FACTOR 807: JOB MOTIVATION INDEX

Index is computed using the following factors:

| | |
|---|---|
| 800 | Skill variety |
| 801 | Task identity |
| 802 | Task significance |
| 805 | Performance barriers/blockages |
| 813 | Task autonomy |
| 804 | Job Feedback |

Formula ( (800+801+802+805)/4)*813*804

FACTOR 808: OJI TOTAL SCORE

Score is computed using the variables in the following formula:

(V201+V202+V203+V270+V271+V272
+8-V206+V207+V208+V209+V210
+V211+V212+V213)

FACTOR 809: JOB MOTIVATION INDEX ---- ADDITIVE

Index is computed using the following factors:

| | |
|---|---|
| 800 | Skill Variety |
| 801 | Task Identity |
| 802 | Task Significance |
| 805 | Performance Barriers/Blockages |
| 813 | Task Autonomy |
| 804 | Work Repetition |

FORMULA: ( (800+801+802+805)/4)+813+804

FACTOR 810: JOB PERFORMANCE GOALS

| VARIABLE NUMBER | STATEMENT NUMBER | STATEMENT |
|---|---|---|
| 217 | 34 | To what extent do you know exactly what is expected of you in performing your job? |
| 218 | 35 | To what extent are your job performance *goals difficult to accomplish*? |
| 273 | 36 | To what extent are your job performance goals clear? |
| 274 | 37 | To what extent are your job performance goals specific? |
| 221 | 38 | To what extent are your job performance goals realistic? |

FACTOR 811: PRIDE

| VARIABLE NUMBER | STATEMENT NUMBER | STATEMENT |
|---|---|---|
| 215 | 32 | To what extent are you proud of your job? |
| 275 | 46 | To what extent does your work give you a feeling of pride? |

FACTOR 812: TASK CHARACTERISTICS

| VARIABLE NUMBER | STATEMENT NUMBER | STATEMENT |
|---|---|---|
| 201 | 17 | To what extent does your job require you to do many different things, using a variety of your talents and skills? |
| 202 | 18 | To what extent does your job involve doing a whole task or unit of work? |
| 203 | 19 | To what extent is your job significant, in that it affects others in some important way? |
| 272 | 22 | To what extent are you able to determine how well you are doing your job without feedback from anyone else? |
| 209 | 26 | To what extent does your job provide the chance to know for yourself when you do a good job, and to be responsible for your own work? |
| 210 | 27 | To what extent does doing your job well affect a lot of people? |
| 211 | 28 | To what extent does your job provide you with a chance to finish completely the piece of work you have begun? |
| 212 | 29 | To what extent does your job require you to use a number of complex skills? |

FACTOR 813: TASK AUTONOMY

| VARIABLE NUMBER | STATEMENT NUMBER | STATEMENT |
|---|---|---|
| 270 | 20 | To what extent does your job provide a great deal of freedom and independence in scheduling your work? |
| 271 | 21 | To what extent does your job provide a great deal of freedom and independence in selecting your own procedures to accomplish it? |
| 213 | 30 | To what extent does your job give you freedom to do your work as you see fit? |
| 214 | 31 | To what extent are you allowed to make the major decisions required to perform your job well? |

FACTOR 814: WORK REPETITION

| VARIABLE NUMBER | STATEMENT NUMBER | STATEMENT |
|---|---|---|
| 226 | 39 | To what extent do you perform the same tasks repeatedly within a short period of time? |
| 227 | 40 | To what extent are you faced with the same type of problem on a weekly basis? |

FACTOR 815 (NOT USED)

FACTOR 816: DESIRED REPETITIVE EASY TASKS

| VARIABLE NUMBER | STATEMENT NUMBER | STATEMENT |
|---|---|---|
| 255 | 56 | A job in which tasks are repetitive. |
| 258 | 57 | A job in which tasks are relatively easy to accomplish. |

FACTOR: JOB INFLUENCES (NOT A STATISTICAL FACTOR)

| VARIABLE NUMBER | STATEMENT NUMBER | STATEMENT |
|---|---|---|
| 216 | 33 | To what extent do you feel accountable to your supervisor in accomplishing your job? |
| 238 | 42 | To what extent do workers in your work group maintain high standards of performance? |

FACTOR 817: ADVANCEMENT/RECOGNITION

| VARIABLE NUMBER | STATEMENT NUMBER | STATEMENT |
|---|---|---|
| 214 | 41 | To what extent are you aware of promotion/advancement opportunities that affect you? |
| 239 | 43 | To what extent do you have the opportunity to progress up your career ladder? |
| 240 | 44 | To what extent are you being prepared to accept increased responsibility? |
| 241 | 45 | To what extent do people who perform well receive recognition? |
| 276 | 47 | To what extent do you have the opportunity to learn skills which will improve your promotion potential? |

FACTOR 818: MANAGEMENT - SUPERVISION (A)

| VARIABLE NUMBER | STATEMENT NUMBER | STATEMENT |
|---|---|---|
| 404 | 58 | My supervisor is a good planner |
| 405 | 59 | My supervisor sets high performance standards |
| 410 | 60 | My supervisor encourages teamwork |
| 411 | 61 | My supervisor represents the group at all times |
| 412 | 62 | My supervisor establishes good work procedures. |
| 413 | 63 | My supervisor has made his responsibilities clear to the group |
| 435 | 64 | My supervisor fully explains procedures to each group member |
| 416 | 65 | My supervisor performs well under pressure |

FACTOR: MANAGEMENT - SUPERVISION (B) (NOT A STATISTICAL FACTOR)

| VARIABLE NUMBER | STATEMENT NUMBER | STATEMENT |
|---|---|---|
| 124 | 66 | My supervisor takes time to help me when needed |
| 434 | 71 | My supervisor lets me know when I am doing a poor job |
| 439 | 75 | When I need technical advice, I usually go to my supervisor |

FACTOR 819: SUPERVISORY COMMUNICATION CLIMATE

| VARIABLE NUMBER | STATEMENT NUMBER | STATEMENT |
|---|---|---|
| 426 | 67 | My supervisor asks members for their ideas on task improvements |
| 428 | 68 | My supervisor explains how my job contributes to the overall mission |
| 431 | 69 | My supervisor helps me set specific goals |
| 433 | 70 | My supervisor lets me know when I am doing a good job |
| 435 | 72 | My supervisor always helps me improve my performance |
| 436 | 73 | My supervisor insures that I get job related training when needed |
| 437 | 74 | My job performance has improved due to feedback received from my supervisor |
| 442 | 76 | My supervisor frequently gives me feedback on how well I am doing my job |

FACTOR 820: ORGANIZATIONAL COMMUNICATIONS CLIMATE

| VARIABLE NUMBER | STATEMENT NUMBER | STATEMENT |
|---|---|---|
| 300 | 82 | Ideas developed by my work group are readily accepted by management personnel above my supervisor |
| 301 | 83 | My organization provides all the necessary information for me to do my job effectively |
| 302 | 84 | My organization provides adequate information to my work group |
| 303 | 85 | My work group is usually aware of important events and situations |
| 304 | 86 | My complaints are given satisfactorily |
| 309 | 91 | The information in my organization is widely shared so that those needing it have it available |
| 314 | 96 | My organization has clear-cut goals |
| 317 | 99 | The goals of my organization are reasonable |
| 318 | 100 | My organization provides accurate information to my work group |

FACTOR 821: WORK GROUP EFFECTIVENESS

| VARIABLE NUMBER | STATEMENT NUMBER | STATEMENT |
|---|---|---|
| 259 | 77 | The quantity of output of your work group is very high |
| 260 | 78 | The quality of output of your work group is very high |
| 261 | 79 | When high priority work arises, such as short suspenses, crash programs, and schedule changes, the people in my work group do an outstanding job in handling these situations |
| 263 | 80 | Your work group always gets maximum output from available resources (e.g., personnel and materials) |
| 265 | 81 | Your work group's performance in comparison to similar work groups is very high |

FACTOR: WORK INTERFERENCES (NOT A STATISTICAL FACTOR)

| VARIABLE NUMBER | STATEMENT NUMBER | STATEMENT |
|---|---|---|
| 277 | 48 | To what extent do you have the necessary supplies to accomplish your job? |
| 278 | 49 | To what extent do details (task not covered by primary or additional duty descriptions) interfere with the performance of your primary job? |
| 279 | 50 | To what extent does a bottleneck in your organization seriously affect the flow of work either to or from your group? |

FACTOR 822: JOB RELATED SATISFACTION

| VARIABLE NUMBER | STATEMENT NUMBER | STATEMENT |
|---|---|---|
| 705 | 101 | Feeling of Helpfulness<br>The chance to help people and improve their welfare through the performance of my job. The importance of my job performance to the welfare of others. |
| 709 | 102 | Co-worker Relationships<br>My amount of effort compared to the effort of my co-workers, the extent to which my co-workers share the load, and the spirit of teamwork which exists among my co-workers. |
| 710 | 103 | Family Attitude Toward Job<br>The recognition and the pride my family has in the work I do. |
| 717 | 106 | Work Schedule<br>My work schedule; flexibility and regularity of my work schedule; the number of hours I work per week. |
| 718 | 107 | Job Security |
| 719 | 108 | Acquired Valuable Skills<br>The chance to acquire valuable skills in my job which prepare me for future opportunities. |
| 723 | 109 | My Job as a Whole |

FACTOR 823: JOB RELATED TRAINING

| VARIABLE NUMBER | STATEMENT NUMBER | STATEMENT |
|---|---|---|
| 711 | 104 | On-the-Job Training (OJT)<br>The OJT instructional methods and instructors' competence. |
| 712 | 105 | Technical Training (Other than OJT)<br>The technical training I have received to perform my current job. |

FACTOR 824: GENERAL ORGANIZATIONAL CLIMATE

| VARIABLE NUMBER | STATEMENT NUMBER | STATEMENT |
|---|---|---|
| 305 | 87 | My organization is very interested in the attitudes of the group members toward their jobs. |
| 306 | 88 | My organization has a very strong interest in the welfare of its people. |
| 307 | 89 | I am very proud to work for this organization. |
| 308 | 90 | I feel responsible to my organization in accomplishing its mission. |
| 310 | 92 | Personnel in my unit are recognized for outstanding performance. |
| 311 | 93 | I am usually given the opportunity to show or demonstrate my work to others. |
| 312 | 94 | There is a high spirit of teamwork among my co-workers. |
| 313 | 95 | There is outstanding cooperation between work groups of my organization. |
| 315 | 97 | I feel motivated to contribute my best efforts to the mission of my organization. |
| 316 | 98 | My organization rewards individuals based on performance. |

FACTOR 825: MOTIVATION POTENTIAL SCORE

Score is computed using the following factors:

| | |
|---|---|
| 800 | Skill variety |
| 801 | Task identity |
| 802 | Task significance |
| 804 | Job feedback |
| 813 | Task autonomy |

Formula ( (800+801+802)/3)*813*804

Value range will be from 1 to 343.

1980 USAF - SCEEE SUMMER FACULTY RESEARCH PROGRAM

Sponsored by the

AIR FORCE OFFICE OF SCIENTIFIC RESEARCH

Conducted by the

SOUTHEASTERN CENTER FOR ELECTRICAL ENGINEERING EDUCATION

TWO FINAL REPORTS

REPORT 1: FITTING NACA CAMBERED AIRFOIL DATA BY SPLINES

REPORT 2: INCLUSION THEOREMS FOR ABSOLUTELY ABEL AND STIELTJES METHODS FOR IMPROPER INTEGRALS

Prepared by: Dr. Louise A. Raphael

Academic Rank: Professor

Department and University: Department of Mathematics, Clark College

Research Location: Flight Dynamics Laboratory, Structures and Dynamics Division, Analysis and Optimization Branch, Applied Mathematics Group

USAF Research Advisor: Dr. Paul J. Nikolai

USAF Research Colleague: Dr. Dennis W. Quinn, AFIT

Date: August 9, 1980

Contract Number: F49620-79-C-0038

REPORT 1

# FITTING NACA CAMBERED AIRFOIL DATA BY SPLINES

By

Louise A. Raphael

"... the experience should stiffen your backbone - you might call it splining your spine."

Anon

ABSTRACT

The question of finding the approximating function which best fits NACA cambered airfoil data and gives accurate information about the first and second derivatives is investigated. It was found that if the data is noisy, the best algorithm is the IMSL least squares approximation by cubic splines for variable knots. Cubic splines and derivatives have been calculated for the NACA data. To insure that users of the IMSL or Hewlett-Packard codes understand the basics of spline theory, an expository report on splines has been included. Finally, suggestions for further research is offered.

## Acknowledgement

I would like to thank Dr. Paul J. Nikolai of the Wright-Patterson Flight Dynamics Laboratory, the Air Force Systems Command, the Air Force Office of Scientific Research and the Southeastern Center for Electrical Engineering Education for providing the opportunity to spend a mathematically productive and interesting summer at the Air Force Flight Dynamics Laboratory, Wright Patterson, Ohio. I would like to acknowledge the laboratory, in particular, the Applied Mathematics Group of the Analysis and Optimization Branch, for mathematical conversation, hospitality and direction for future research projects of interest to the Air Force.

In particular, I would like to especially thank Dr. Dennis W. Quinn for suggesting the application of splines to airfoil data and for his collaboration. I wish to thank Dr. Nikolai for his encouragement and guidance to pursue both basic and applied research. I must acknowledge many helpful and enjoyable discussions with the super friendly mathematicians and engineers at the Flight Dynamics Laboratory and AFIT. Finally, I thank Miss Mary Lipik, who cheerfully and quickly transformed illegible manuscript into typed reports.

ACTIVITIES AT FLIGHT DYNAMICS LABORATORY, WRIGHT-PATTERSON

Applied Research: Writing Technical Memorandum for AFFDL on Splines with Professor Dennis Quinn, AFIT.

Basic Research: Submitting Report 2 for publication in a mathematics journal.

AFIT Seminar: Gave a talk to the AFIT Department of Mathematics on "Summing Sturm-Liouville Expansions"

## I. INTRODUCTION:

Numerous families of airfoils have been constructed by the National Advisory Committee for Aeronautics (NACA) to study the characteristics of airfoils in order to determine the shapes that are best suited for specific aerodynamic purposes. These airfoils have been tested in wind tunnel and computer experiments.

The airfoils are composed of a thickness envelope wrapped about a mean camber line as shown in Figure 1. The mean camber line is halfway between the upper and lower surfaces of the airfoil and intersects the chord (horizontal) line at the leading and trailing edge.

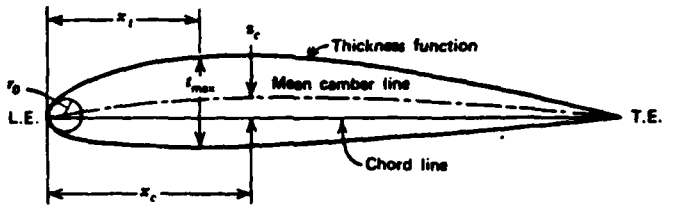



Fig. 1 Important geometrical variables.

Some of the geometrical variables of the airfoil include the maximum camber $z_c$ of the mean camber line; its distance $x_c$ behind the leading edge (LE); the maximum thickness $t_{max}$ and its distance behind the leading edge. Varying the geometrical variables affects the angle of attack and consequently the lift and drag. These various families of airfoils are specifically designed to show the effects of varying the geometrical variables on the aerodynamic characteristics. The experiments verify the effects of these variables. Thus a specific shape can be chosen for a specific purpose.

After the airfoil has been selected for a specific purpose, it is necessary to fit curves to this data in order to study other aerodynamical

phenomena. For example, airfoil coordinates and slopes are used to generate transonic oscillatory pressure distributions for transonic unsteady aerodynamic analysis. So the immediate concern of finding functions which give a best fit to NACA airfoil data generates the more fundamental question: What is the best algorithm for fitting curves through noisy data which gives accurate information about slopes and curvatures at the data and interpolative points?

The answer is found in the theory of splines. In particular, for noisy data an answer is the algorithm for the least squares approximation by cubic splines wtih variable knots.

## II. OBJECTIVES

The main objectives of this project are threefold:

(1) To apply modern and classical spline theory to determine the best approximating function to fit cambered airfoil data, and to calculate the first and second derivatives at the data points. The airfoil data used was compiled by the National Advisory Committee for Aeronautics (NACA).

(2) To determine which computer code of the IMSL library for cubic splines is best suited for the noisy NACA data, and to note the limitations of that code.

(3) To write an expository report on the basics of modern and classical spline theory, so that the users of the code at the Air Force Laboratories understand the mathematical ideas involved.

## III. SPLINES

### III. A. Heuristic Motivation

The age old problem of data fitting is based on two information components of the data $(x_n, f(x_n))$. The first is the trend of $f(x)$, and the second is the error or noise in the data. The goal is to fit the data by some function $F(x)$ such that $F(x)$ represents most of the information about $f(x)$ contained in the data and as little of the error as possible. Usually a set of functions $[u_i]_{i=1}^{k}$ is selected. The funtion F depends on parameters $[c_i]_{i=1}^{k}$ to be determined. The art is to select $F(x)$ so that F depends linearly on the parameters, where k is both large enough so that the data is represented by a proper choice of the $[c_i]_{i=1}^{k}$ and at the same time k is too small for reproduction of the error or noise.

Least squares approximation is a popular technique in defining the approximating function F. Although F may fit the data points closely, it may oscillate between these points so that the numbers it gives for the slopes are totally unreliable. To overcome this inherent deficiency, it is both accurate and efficient to fit a set of data points by splines!

There are two ways to define spline functions. In the beginning of spline theory (1946), a spline of order k was defined to be a piecewise polynomial function of degree k-1 on some (finite or infinite) interval, agreeing with the data and having k-2 continuous derivatives there. So, under these constraints, a cubic spline is a piecewise cubic polynomial function on an interval, agreeing with the data points, and having both first and second derivatives continuous. In section V, we construct the cubic spline from this viewpoint and apply it to curve fitting of cambered airfoil data, but the bias of the expository report is strongly directed to

the usefulness of splines being defined as a linear combination of B-splines. B-splines are basic. Studying B-splines means looking at piecewise polynomial functions. The principal advantage is that if a B-spline has multiple knots (points at which the behavior of the approximating function F is constrained), then it can be replaced by a B-spline similar to it with simple knots. In other words, B-splines are stable under sufficiently small changes in the positions of the knots.

On the other hand while spline interpolation is, in general, more accurate than some standard polynomial interpolations, there are cases where this is not so. For example, cubic Hermite or cubic Bessel interpolations, with their less restrictive constraints, could be preferred to a cubic spline. B-splines generate both classes of curves - the cubic splines and the cubic Hermite, Bessel interpolations.

From a practical standpoint, B-splines are efficiently coded for computer use. For example, Professor David Lee of the Department of Mathematics of the Air Force Institute of Technology has developed a B-spline code for a maximum of 200 data points.

III. B. BACKGROUND DEFINITIONS AND EXAMPLES:

In this section, we review the basic definitions needed to understand the concept of a B-spline. Let k be a positive integer and let $t_o < t_1 < t_2 < \ldots < t_n$ be a non-decreasing sequence of points for which a function f is defined. First, we review the definition of the kth divided difference for a function f.

1st divided difference: $f[t_o, t_1] = \dfrac{f(t_1) - f(t_o)}{t_1 - t_o}$

2nd divided difference: $f[t_o, t_1, t_2] = \dfrac{\dfrac{f(t_2) - f(t_1)}{t_2 - t_1} - \dfrac{f(t_1) - f(t_o)}{t_1 - t_o}}{t_2 - t_o}$

. . .

k-th divided difference: $f[t_o, t_1, \ldots, t_k] = \dfrac{f[t_1, t_2, \ldots, t_k] - f[t_o, t_1 \ldots t_{k-1}]}{t_k - t_o}$

The polynomial $(x-a)^k$ is called a power function. A truncated power function, denoted by $(x-a)_+^k$, is defined as follows:

$(x-a)_+^k = \max((x-a)^k, 0)$. For K add, this can be written as:

$$(x-a)_+^k = \begin{cases} (x-a)^k, & \text{if } x=a \\ 0, & \text{otherwise.} \end{cases}$$

The function $f(x) = (x-a)_+^k$ is a piecewise polynomial with one breakpoint at 'a'. The derivative of $(x-a)_+^k$ equals $k(x-a)_+^{k-1}$. So $(x-a)_+^k$ has k-1 continuous derivatives, with a jump in the kth derivative at 'a' equal to k.

Throughout this chapter, the function $f(x) = (t-x)_+^k[t_o, t_1, \ldots, t_k]$ denotes the k-th divided difference of the function $(t-x)_+^k$ evaluated at $t_o, t_1, \ldots, t_k$ for the variable t.

The theory and FORTRAN programs to evaluate B-splines and splines are elegantly and completely presented in Carl de Boor's A

Practical Guide to Splines [3]. The rudiments of B-splines and spline theory is presented herein, so that anyone using an IMSL code to fit a spline curve through a set of finite two dimensional data points understands the basics.

The knots of an approximating function f is the set of points at which the behavior of the approximating function f is constrained. The knots are, in general, unequally spaced and may appear more than once. An example of such a knot sequence is {0,0,0,1,4,4,6,9,9,9}. In basic terms, a B-spline is a scaled k-th divided difference of a truncated power function $(x-t)_+^{k-1}$ evaluated at the knot sequence.

We remark that if one is using a cubic spline to fit some data and has the need to calculate the slopes and the curvatures of the approximating function, then all the knots are simple (i.e. appear only once), except possibly for the endpoints.

Let $\{t_i\}_{i=0}^{n}$ be a finite non-decreasing sequence of real numbers. Let k, a positive integer, denote the order of the B-spline. The i-th B-spline of order k for the knot sequence $\{t_i\}_{i=0}^{n}$ is denoted by $B_{i,k}(x)$ and is defined as follows:

$$k = 2: \quad B_{i,2}(x) = (t_{i+2} - t_i)(t - x)_+[t_i, t_{i+1}, t_{i+2}]$$

$$k = 3: \quad B_{i,3}(x) = (t_{i+3} - t_i)(t - x)_+^2[t_i, t_{i+1}, t_{i+2}, t_{i+3}]$$

$$\vdots \qquad \vdots \qquad \vdots$$

$$k: \quad B_{i,k}(x) = (t_{i+k} - t_i)(t - x)_+^{k-1}[t_i, t_{i+1}, \ldots, t_{i+k}].$$

We now present the linear and quadratic B-splines on a knot sequence (which has been added to i.e., if $\{t_i\}_{i=0}^{n}$ is our sequence for a B-spline of order k,

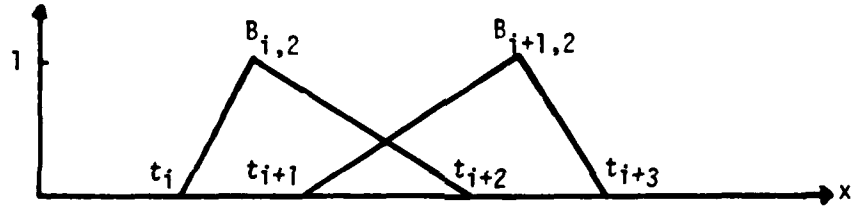
then one adds k points and defines the B-splines on the knot sequence $\{t_i\}_{i=0}^{n+k}$.

EXAMPLE 1: Let k = 2. By definition, the i-th linear B-spline is

$$B_{i,2}(x) = (t - x)_+[t_{i+1}, t_{i+2}] - (t - x)_+[t_i, t_{i+1}]$$

$$= \begin{cases} (t_{i+2} - x)/(t_{i+2} - t_{i+1}) & \text{on } t_{i+1} \le x \le t_{i+2} \\ (x - t_i)/(t_{i+1} - t_i) & \text{on } t_i \le x \le t_{i+1} \\ 0 & \text{otherwise} \end{cases}$$

So evaluating $B_{i,2}(x)$ at $t_i$, $t_{i+1}$, $t_{i+2}$, we see that $B_{i,2}(t_{j+1}) = \delta_{ij}$, where $\delta_{ij}$ is the ever popular Knonecker delta (i.e., $\delta_{ij} = 1$ if $i = j$ and $\delta_{ij} = 0$, otherwise). Moreover, the graph of $B_{i,2}(x)$ is the hat function.




EXAMPLE 2: Let k=3. By definition, the i-th parabolic B-spline is

$$B_{i,3}(x) = (t-x)_+^2[t_{i+1}, t_{i+2}, t_{i+3}] - (t-x)_+^2[t_i, t_{i+1}, t_{i+2}^2]$$

$$= \begin{cases} (t_{i+3} - x)^2/(t_{i+3} - t_{i+2})(t_{i+3} - t_i & \text{on } t_{i+2} \le x \le t_{i+3} \\ \dfrac{}{(t_{i+3}-t_{i+})(t_{i+}-t_{i+1})} - \dfrac{}{(t_{i+2}-t_{i+1})(t_{i+}-t_i} & \text{on } t_{i+1} \le x \le t_{i+2} \\ \dfrac{(x - t_i)^2}{(t_{i+2} - t_i)(t_{i+1} - t_1)} & \text{on } t_i \le t \le t_{i+1} \\ 0 & \text{otherwise} \end{cases}$$

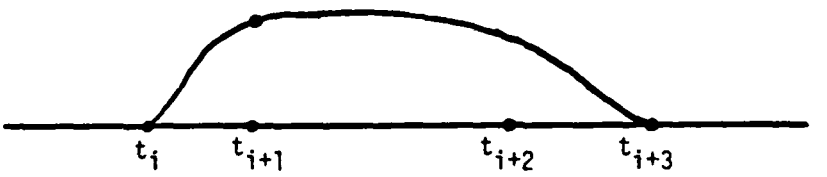
Evaluating $B_{i,3}$ at $t_i$, $t_{i+1}$, $t_{i+2}$, $t_{i+3}$

we have $B_{i,3}(t_i) = B_{i,3}(t_{i+3}) = 0$;

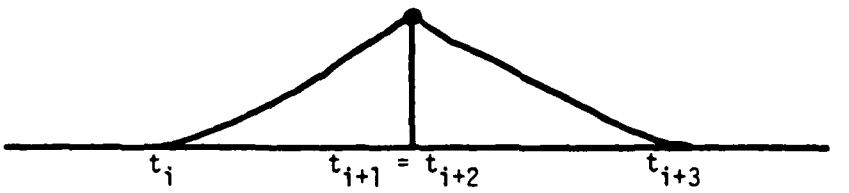
$$B_{i,3}(t_{i+2}) = \frac{t_{i+3} - t_{i+2}}{t_{i+3} - t_{i+1}}, \text{ and}$$

$$B_{i,3}(t_{i+1}) = \frac{t_{i+1} - t_i}{t_{i+2} - t_i}$$

The graph of $B_{i,3}$ on $[t_i, t_{i+3}]$ is parabolic, and for simple knots would be of the following shape




The graph of $B_{i,3}$ for multiple knots could be of the following shape




Before we exhibit the i-th cubic B-splines, we state some useful properties of B-splines.

PROPERTY(i): $B_{i,k}$ has small support. $B_{i,k}(x) = 0$ for $x < t_i$ or $x > t_{i+k}$.

PROPERTY(ii): $B_{i,k}$ is positive on its support. $B_{i,k}(x) > 0$ for $t_i < x < t_{i+k}$.

PROPERTY(iii): The $B_{i,k}$'s are a partition of unity (with (i) and (ii)).

$$\Sigma_i B_{i,k}(x) = \sum_{i=r+1-k}^{s-1} B_{i,k}(x) = 1 \quad \text{for} \quad t_r < x < t_s.$$

PROPERTY(iv): Recurrence Relation for B-splines.

$$B_{i,1} = \begin{cases} 1 & t_1 \leqq x \leqq t_{i+1} \\ 0 & \text{otherwise} \end{cases}$$

and

$$B_{i,k} = \frac{(x - t_i)}{t_{i+k-1} - t_i} B_{i,k-1}(x) + \frac{t_{i+k} - x}{t_{i+k} - t_{i+1}} B_{i+1,k-1}(x)$$

As constructing the cubic B-spline by definition would be extremely tedious, we exhibit the *i-th cubic spline by using* the recursive relation property (iv) for B-splines. So when k = 4,

$$B_{i,4}(x) = \frac{(x-t_i)}{t_{i+3}-t_i} B_{i,3}(x) + \frac{(t_{i+4}-x)}{t_{i+4}-t_{i+1}} B_{i+1,3}(x).$$

For equally spaced knots, the B-splines are pleasing to write down. For a clear exposition of this case, see Prenter [5].

III. C. SPLINES

Finally, we come to the definition of a SPLINE. A spline function of order k with knot sequence $t = \{t_i\}_i$ is a linear combination of B-splines of order k. The collection of all such rewarding functions is denoted by $\$_k = \{\sum_i a_i B_{i,k}(x) | a_i \text{ is real for all } i\}$. In other words, $\$_k$ is a linear span of B-splines of order k.

So we finally see why B-splines are basic (!). They are the standard functions to express a spline function. But also they enable us to differentiate and integrate spline functions with ease.

PROPERTY (v): Derivative of a spline. The first derivative of a spline function $\sum_i a_i B_{i,k}$ is found by differencing its B-spline coefficients.

$$D\left[\sum_{i=r}^{s} \alpha_i B_{i,k}\right] = \sum_{i=r}^{s+1} (k-1) \frac{a_i - a_{i-1}}{t_{i+k-1} - t_i} B_{i,k-1} \quad \text{where } a_{r-1} = a_{s+1} = 0.$$

The j-th derivative of a spline:

$$D^j\left[\sum_i a_i B_{i,k}\right] = \sum_i a_i^{(j+1)} B_{i,k-j}$$

with

$$a_r^{(j+1)} = \begin{cases} a_r & \text{for } j = 0 \\ \dfrac{a_r^{(j)} - a_{r-1}^{(j)}}{(t_{r+k-j} - t_r)/(k-j)} & \text{for } j > 0 \end{cases}$$

PROPERTY (vi): Integration of a spline:

$$\int_{t_1}^{x} \sum_{i=1}^{n} a_i B_{i,k}(s)\,ds = \sum_{i=1}^{s-1} \left[\sum_{j}^{i} a_j (t_{j+k} - t_j)/k\right] B_{i,k+1}(x) \text{ on } t_1 \leq x \leq t_s.$$

Now, we identify the class of spline functions of order k defined on a

knot sequence t with the space, $P_{k,w,c}$, of piecewise polynomial functions of degree k-1 defined on a breakpoint sequence w from which the knot sequence t is constructed. The subspace $P_{k,w,c}$ consists of those piecewise polynomials which satisfy continuity conditions, c, at the breakpoints of w (those points at which a new piecewise polynomial function is defined).

Speaking in layman's terms, we first choose a strictly increasing sequence w of real numbers such that $w_1 < \ldots < w_\ell$. This is our breakpoint sequence. We then have a space of piecewise polynomials of degree k-1 (order k) defined on the breakpoint sequence w. At each of the points $w_2$, $\ldots$, $w_{\ell-1}$, f has a continuity condition. For example it might be that $f_n$ must have both continuous first and second derivatives at the breakpoint $w_3$. Let $c_i$ ($i = 2, \ldots, \ell-1$) denote the number of continuity conditions on f at $w_i$. In our example, if f has continuous first and second derivatives at $w_3$ then $c_3 = 2$.

Let k be a positive integer and n denote the dimension of $P_{k,w,c}$. By [3] we know

$$n = \dim P_{k,w,c} = k\ell - \sum_{i=1}^{\ell-1} \nu_i.$$

This n is the number of linear parameters needed to best approximate the data.

Next a knot sequence $\{t_i\}_{i=1}^{n+k}$ is constructed as follows:

$$\underbrace{t_1 \le \ldots \le t_k}_{k \text{ elements}} \le w_1 < t_{k+1} \le \ldots \le t_n \le w_{\ell-1} < w_\ell \le \underbrace{t_{n+1} \le \ldots t_{n+k}}_{k \text{ elements}}$$

The relation between the occurrences of knots and number of continuity points is that the number of knots at $w_i$ equals the order k minus the number of continuity conditions at $w_i$.

Finally it can be proved that the set of k-th order B-splines, $B_{1,k}, \ldots, B_{n,k}$ constructed from the knot sequence $\{t_i\}_{i=0}^{n+k}$ is a basis for <u>both</u> $\$_k$ and

$P_{k,w,c}$ considered as functions on $[t_{k-2}, t_{n+1}] \subset [w_0, w_\ell]$. Thus

$$\$_k = P_{k,w,c} \text{ on } [t_{k-2}, t_{n+1}].$$

To convert a B-spline representation to a $P_{k,w,c}$ representation and conversely see de Boor [3].

We now know that the spline coefficients are linear combinations of B-splines. That is any spline function $s_k \in \$_k$ can be expressed as

$$s_k(x) = \sum_{j=1}^{n} a_j B_{j,k}(x)$$

where the real numbers $a_i$ are to be found as follows. Let $L_i$ be the linear functional defined on the space of all functions whose k-1 derivatives exist by

$$L_i f = \sum_{r=0}^{k-1} (-1)^{k-1-r} G^{k-1-r}(x_i) D^r f(x_i) \text{ for all } f$$

with

$G(x) = (t_{i+1} - x) \ldots (t_{i+k} - x)/(k-1)!$ and $x_i \in (t_i, t_{i+k})$. In particular

$$L_i(B_{j,k}) = \delta_{ij} \text{ for all } j.$$

So

$$L_i s_k(x) = L_i \sum_{j=1}^{n} a_j B_{j,k}(x) = \sum_{j=1}^{n} a_j L_i B_{j,k}(x)$$

$$= \sum_{j=1}^{n} a_j \delta_{ij} = a_i$$

$$= \sum_{r=0}^{k-1} (-1)^{k-1-r} G^{k-1-r}(x_i) D^r s_k(x_i)$$

where $D^r s_k(x)$ is obtained from property (v).

III. D. NOISY DATA AND IMSL SUBROUTINES.

There are various algorithms for constructing approximating functions by spline functions. The IMSL library codes include the cubic spline interpolation, approximation, and smoothing routines. The interpolation routines are used only if the data is accurate and it is assumed that a smooth curve passes through the data. The smoothing routines were developed to be used with contaminated data. The user can specify conditions for detecting and correcting points that are in error (of about 10%) and compute new values that give a smooth curve.

Finally, the least squares approximation by cubic spline is the code which is used for noisy data. The calculated data values F(I) are assumed to contain small random errors. The code selects the spline function S which minimize the least squares error

$$\sum_{I=1}^{NX} [F(I) - S(X(I)]^2 WT(I)$$

where WT(I) is a weight function and NX is the number of data points.

In the IMSL codes the knots $X(1) = XK(1) < XK(2) < \ldots < XK(NXK) = X(NX)$ are distinct and define a partition on the domain [X(1), X(NX)] of the function F. The NXK denotes the number of knots. In these codes, a cubic spline function is any function S defined on [X(1), X(NX)] which is continuous, has continuous first and second derivatives, and is equal to a third degree polynomial on each of the subintervals defined by the knots.

In our research, we used the ICSVKU and DCSEVC subroutines. The ICSVKU computes the least squares approximation to a given set of points by cubic splines with a given number of knots. The placement of knots is critical. ICSVKU starts with a given set of knots and varies them one by

one in order to determine the knot locations that minimize the least squares error. The subroutine DCSEVU evaluates the first and second derivatives of a cubic spline.

The following cubic spline representation is used by the IMSL subroutines:

$$S(P) = C(I,3)*(P-XK(I))^3 + C(I,2)*(P-XK(I))^2 + C(I,1)*(P-XK(I)) + Y(I)$$

where $XI(I) \leq P \leq XK(I+1)$ and where the vector Y of length NXK - 1 and the NXK - 1 by 3 matrix C uniquely define a cubic spline function S.

An illustration where the number of knots NXK is 4, giving 3 subintervals now follows:

OUTPUT

(Least Squares) ERROR = .023

WE'RE THE KNOTS

0.0 .57 .8 1

Y(I) WE'RE THE SPLINE COEFFICIENTS

.12 -.2 -3.1 5.6

.32 .66 2.6 -9.3

.41 1.4 -4.5 6.2

So for a point $P \in [.57, .8]$ the spline approximation gives

$$S(P) = -9.3(P-.57)^3 + 2.6(P-.57)^2 + .66(P-.57) + .32$$

A word of caution, if at an endpoint b the slope of the approximating function f is arbitrarily large, one counteracts this by adding a data point where x is sufficiently close to b. This has the effect of not permitting the spline to zoom off, for it forces the spline to fit the actual path. Also, one should place the knots closer to the point b.

In fitting the spline curve to the cambered airfoil data, it was sufficient to place the knots closer to the leading edge, in order to

significantly reduce the error between the actual data and the calculated values.

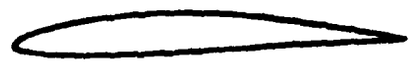
Moreover, one must be cautious in how many knots are being used in the code. Although the IMSL code, *ICSVICU*, states a maximum number of twenty-eight knots, it was found for cambered airfoil data that if more than sixteen knots were used, bizairre results were obtained. For example, when 26 knots were used for the NACA 64A010 data, the interpolations points between the calculated data points oscillated between positive and negative values.

If an experiment needs more knots than allowed, the scientist-engineer is encouraged to contact Professor David Lee of AFIT's Department of Mathematics, who has a B-spline program for a maximum number of two hundred knots. But this would mean a different spline function for each subinterval determined by two adjacent knots.

## IV. IMSL OUTPUT FOR NACA 64 A410 AIRFOIL

An IMSL least squares cubic spline computer program was written especially to determine the best approximating function for the shape of cambered airfoil data. But, it is emphasized that this program will work in general for any set of noisy data. The program accepts tabulated values of X(I) and F(I). It first places the knots so that the least squares error is minimized. It then solves for the spline coefficients and then calculates the new F(I), denoted by CF(I); the error between F(I) and CF(I), denoted by E(I); the first and second derivatives denoted by DS(I) and DDS(I) respectively.

Table 1 gives the input data for the NACA 64 A410 airfoil upper and lower surface. Tables 2 and 3 list the output for the airfoil using sixteen and four knots respectively. We knon that the least squares error for the sixteen knots is $4.9348 \times 10^{-6}$ and for the four knots is $4.2962 \times 10^{-4}$. As the data is noisy and it is easier to calculate the spline function for four knots, it is both practical and efficient to choose the four knot program.



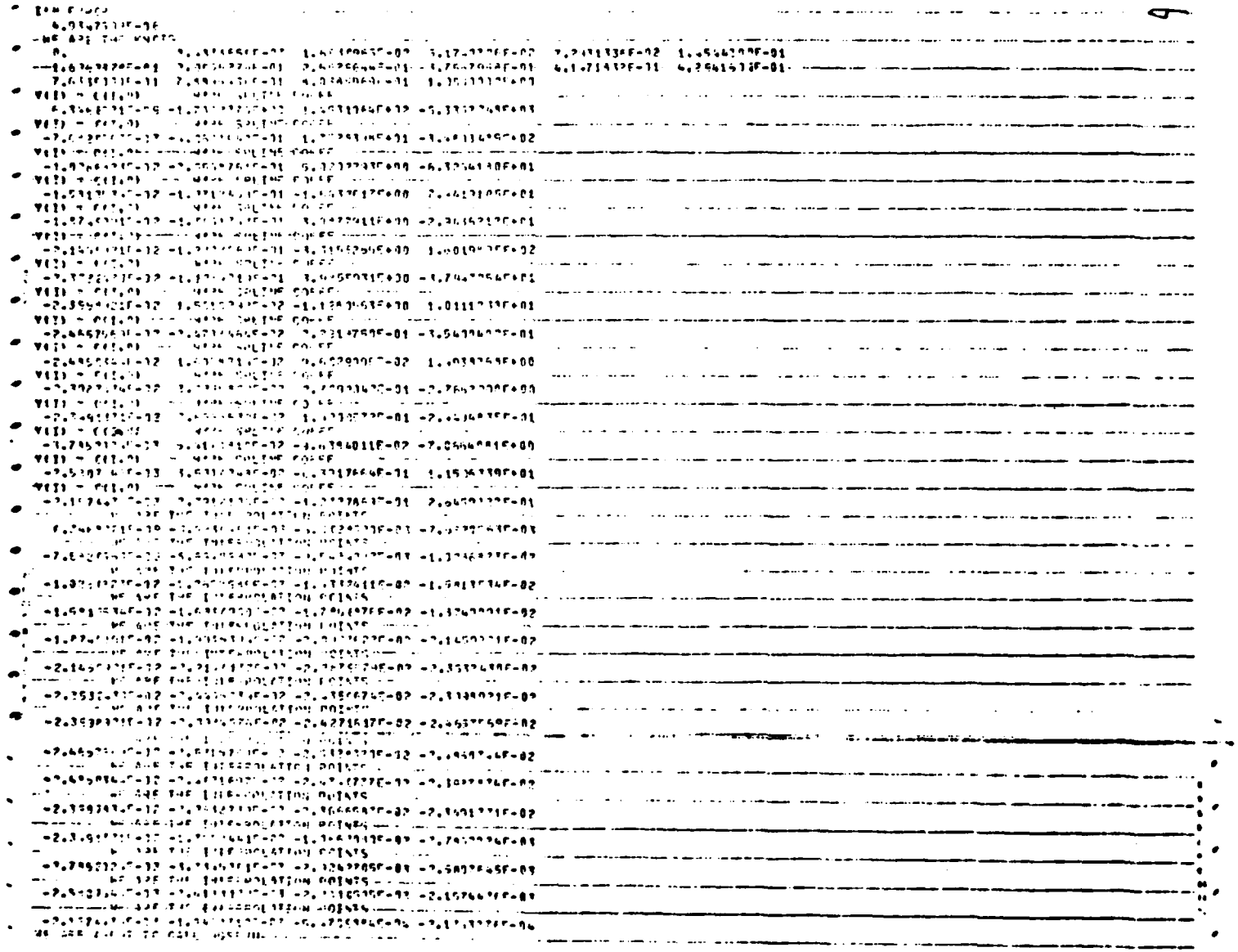
NACA 64A410 Airfoil

**Figure 2. Airfoil Used for Applications**

Table 1. Coordinates for NACA 64A410 Airfoil

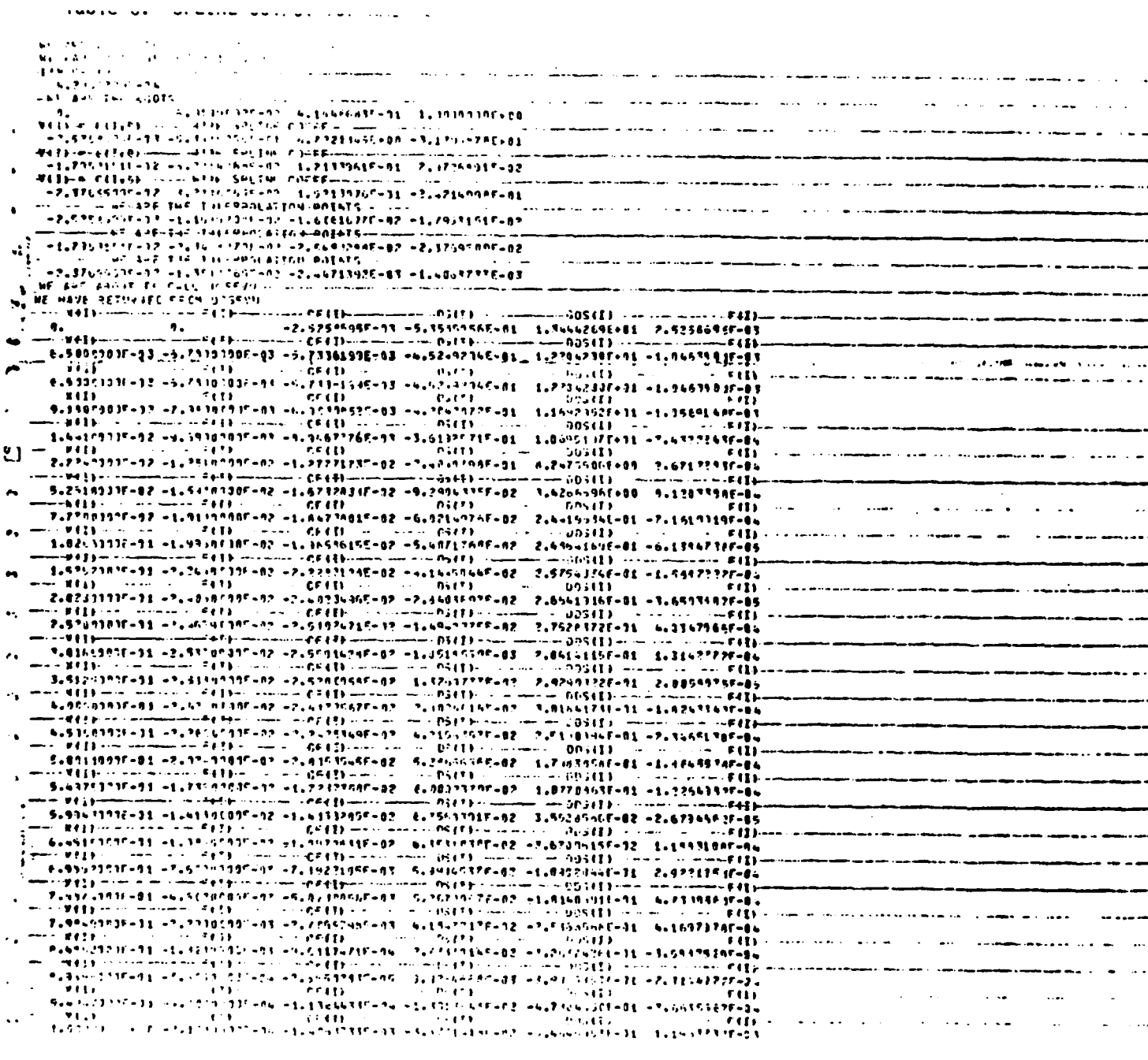
| Upper Surface | | Lower Surface | |
|---|---|---|---|
| x | F(x) | x | F(x) |
| 0.0 | 0.0 | 0.0 | 0.0 |
| .00350 | .00902 | .00650 | -.00678 |
| .00582 | .01112 | .00918 | -.00796 |
| .01059 | .01451 | .01441 | -.00969 |
| .02276 | .02095 | .02724 | -.01251 |
| .04749 | .03034 | .05251 | -.01592 |
| .07230 | .03865 | .07770 | -.01919 |
| .09737 | .04380 | .10263 | -.01996 |
| .14748 | .05366 | .15252 | -.02244 |
| .19770 | .06126 | .20230 | -.02406 |
| .24800 | .06705 | .25200 | -.02499 |
| .29834 | .07131 | .30166 | -.02537 |
| .34871 | .07414 | .35129 | -.02518 |
| .39910 | .07552 | .40090 | -.02436 |
| .44950 | .07522 | .45050 | -.02266 |
| .49989 | .07344 | .50011 | -.02024 |
| .55025 | .07040 | .54975 | -.01736 |
| .60057 | .06624 | .59943 | -.01418 |
| .65085 | .06106 | .64915 | -.01086 |
| .70108 | .05490 | .69892 | -.00760 |
| .75126 | .04780 | .74874 | -.00460 |
| .80151 | .03967 | .79849 | -.00229 |
| .85148 | .03018 | .84852 | -.00132 |
| .90104 | .02038 | .89896 | -.00076 |
| .95053 | .01028 | .94947 | -.00048 |
| 1.0 | .00021 | 1.0 | -.00021 |

Table 2. SPLINE OUTPUT for NACA 64A410 LOWER SURFACE with SIXTEEN KNOTS



## Table 2. SPLINE OUTPUT for NACA 64A410 LOWER SURFACE WITH SIXTEEN KNOTS (cont'd)

| X(I) | Y(I) | CF(I) | DS(I) | DDS(I) | F(I) |
|---|---|---|---|---|---|
| 3.5125000E-01 | -2.5119000E-02 | -2.5179942E-02 | 1.0732756E-02 | 2.6186275E-01 | -1.7932917E-08 |
| 4.0000000E-01 | -2.6[illegible]000E-02 | -2.6[illegible]052E-02 | 2.3[illegible]516E-02 | 4.1918781E-01 | 5.1961779E-08 |
| 4.5000000E-01 | -2.7550000E-02 | -2.7556176E-02 | 4.2525316E-02 | 2.6782453E-01 | -3.6233717E-06 |
| 5.0000000E-01 | -2.[illegible]000E-02 | -2.8246813E-02 | 5.3957758E-02 | 1.9411320E-01 | 8.0129690E-06 |
| 5.4975000E-01 | -1.7[illegible]000E-02 | -1.7168056E-02 | 6.1799787E-02 | 1.2115778E-01 | 5.3931858E-06 |
| 5.9967000E-01 | -1.4110000E-02 | -1.4173007E-02 | 6.5946779E-02 | 4.8143579E-02 | -9.8933025E-06 |
| 6.4915000E-01 | -1.0910000E-02 | -1.0862273E-02 | 6.6571333E-02 | -2.4329413E-02 | 2.7330043E-07 |
| 6.9992000E-01 | -7.6010000E-03 | -7.6[illegible]917E-03 | 6.3518346E-02 | -9.8075889E-02 | 8.0917257E-06 |
| 7.4974000E-01 | -4.6010000E-03 | -4.5961091E-03 | 5.6800296E-02 | -1.7129545E-01 | -1.9980114E-06 |
| 7.9965000E-01 | -2.2910000E-03 | -2.2923100E-03 | 2.6256093E-02 | -6.2081161E-01 | 2.2799514E-06 |
| 8.4952000E-01 | -1.3210000E-03 | -1.3124161E-03 | 1.4491862E-02 | -1.7571964E-01 | -7.5818744E-06 |
| 8.9996000E-01 | -7.6010000E-04 | -7.7106744E-04 | 7.6673000E-03 | -9.5648634E-02 | 1.1862474E-05 |
| 9.4994000E-01 | -4.6010000E-04 | -4.7263087E-04 | 4.9417490E-03 | -1.5451496E-02 | -7.5819258E-06 |
| 1.0000000E+00 | -2.1[illegible]000E-04 | -2.1361276E-04 | 6.8877657E-03 | 6.4769391E-02 | 3.6[illegible]759E-06 |



V. CLASSICAL CUBIC SPLINES:

A draftsman spline is a long thin strip of flexible wood used for constructing a smooth curve between selected points. The classical mathematical spline is the abstraction of the draftsman spline. The mathematical cubic spline is a piecewise cubic polynomial which is continuous and has both a continuous first derivative and continuous second derivative. This idea to force fit piecewise curves, which are smooth in slopes and curvatures at the common points, has given rise to the theoretical and pratical art of fitting data by splines. In this section, working formulas (CS-31) for computing a cubic spline based on agreement of data and derivatives are derived in the standard way [2]. Then programming (CS-31) in BASIC on a Hewlett-Packard 9830, a cubic spline is constructed through cambered airfoil data.

First, let denote the mesh $a=x_0 < x_1 < \ldots, < x_n = b$ and $S_\Delta(x)$ denote the spline with respect to the mesh. A table of data is to be fitted by cubic polynomial splines so that there is a different spline for each subinterval of $\Delta$. These subintervals are not necessarily of equal length. For each subinterval the following four constraints are imposed on the j-th cubic spline $S_{\Delta_j}(x)$ on $[x_{j-1},x_j]$ for each (j=0, 1...,N).

$$
\begin{aligned}
&S_{\Delta_j}(x_{j-1}) = y_{j-1} \\
&S_{\Delta_j}(x_j) = y_j \\
&S'_{\Delta_{j-1}}(x_{j-1}^-) = S'_{\Delta_j}(x_{j-1}^+) \\
&S''_{\Delta_{j-1}}(x_{j-1}^-) = S''_{\Delta_j}(x_{j-1}^+)
\end{aligned}
\qquad \text{(CS-1)}
$$

As there are four constraints, a polynomial with four parameters, namely a cubic polynomial, is required for each subinterval. As $S_{\Delta_j}(x)$ is a cubic polynomial, $S''_{\Delta_j}(x_j)$ is a linear polynomial. Let

$$M_j = S''_{\Delta_j}(x_j), \text{ and} \qquad \text{(CS-2)}$$

$$h_j = x_j - x_{j-1} \qquad \text{for } (j=o, 1, 2, \ldots, N)$$

Then the linear equation of $S''_{\Delta_j}(x)$ on $[x_{j-1}, x_j]$ passing through $(x_{j-1}, M_{j-1})$ and $(x_j, M_j)$ is

$$S''_{\Delta_j}(x) = M_{j-1}(x_j-x)/h_j + M_j(x-x_{j-1})/h_j. \qquad \text{(CS-3)}$$

Integrating (CS-3) twice gives

$$S_{\Delta_j}(x) = M_{j-1}(x_j-x)^3/(6h_j) + M_j(x-x_{j-1})^3/6h_j) + a_j(x_j-x) + b_j(x-x_{j-1}) \qquad \text{(CS-4)}$$

where the linear terms are expressed as the last two terms of (CS-4) so that $S''_{\Delta_j}(x)$ can be put into standard form.

[Cf: Ahlberg, Nelson, Walsh; eq (2.1.2), p 10]

To solve for $A_j$, let $S''_{\Delta_j}(x_{j-1}) = y_{j-1}$ and solving (CS-4) yields

$$y_{j-1} = M_{j-1}(x_j-x_{j-1})^2/6 + a_j(x_j-x_{j-1}). \qquad \text{(CS-5)}$$

So

$$a_j = y_j/h_{j+1} - M_{j-1}h_{j+1}/6. \qquad \text{(CS-6)}$$

To solve for $b_j$, let $S_{\Delta_j}(x_j) = y_j$ and substitute in (CS-4) and find

$$b_j = y_j/h_j - M_jh_j/6 \qquad \text{(CS-7)}$$

Now the crux of the development of the construction of $S_{\Delta_j}(x)$ remains in satisfying the continuity of the first derivative at each $x_{j-1}$.

Namely, we need

$$S'_{\Delta_j}(x_{j-1}+) = S'_{\Delta_{j-1}}(x_{j-1}-) \qquad \text{(CS-8)}$$

where

$$S'_{\Delta_j}(x_{j-1}+) = -M_{j-1}h_j/3 - M_j h_j/6 + (y_j - y_{j-1})/h_j \qquad \text{(CS-9)}$$

and

$$S'_{\Delta_{j-1}}(x_{j-1}-) = M_{j-1}h_{j-1}/3 + M_{j-2}h_{j-1}/6 + (y_{j-1} - y_{j-2})/h_{j-1} \qquad \text{(CS-10)}$$

Thus the continuity at $x_{j-1}$ yields by means of (CS-9) and (CS-10)

$$(y_j - y_{j-1})/h_j - (y_{j-1} - y_{j-2})/h_{j-1} = M_{j-2}h_{j-1}/6 + (h_j + h_{j-1})M_{j-1}/3 + M_j h_j/6 \qquad \text{(CS-11)}$$

So equations (CS-11) for $j = 2, 3, \ldots, N$ gives N-1 simultaneous equations in the N+1 quantities $M_0, M_1, M_2, \ldots, M_N$. So two additional conditions must be determined. In particular the end conditions must be specified. Let $S'_{\Delta}(a+) = y'_0$ and $S'_{\Delta}(b-) = y'_n$. So from (CS-9) (j=1)

$$S'_{\Delta_1}(a+) = y'_0 = -M_0 h_1/3 - M_1 h_1/6 + (y_1 - y_0)h_1, \qquad \text{(CS-12)}$$

giving

$$2M_0 + M_1 = 6[(y_1 - y_0)h_1 - y'_0]/h_1. \qquad \text{(CS-13)}$$

In general, (CS-13) is written as

$$2M_0 + \lambda_0 M_1 = d_0. \qquad \text{(CS-14)}$$

Similarly by (CS-10) where $S'_{\Delta_N}(b-) = y'_N$, the following is obtained for $j-1 = N$.

$$M_{N-1} + 2M_N = 6(y'_N - (y_N - y_{N-1})/h_N]/h_N \qquad \text{(CS-15)}$$

This in turn is expressed in the general form

$$\mu_N M_{N-1} + 2M_N = d_N \qquad \text{(CS-16)}$$

Introducing the notation

$$\lambda_{j-1} = h_j/(h_j + h_{j-1}) \text{ and } \mu_{j-1} = 1 - \lambda_{j-1} \text{ for } (j = 2,3, \ldots, N), \qquad \text{(CS-17)}$$

the continuity requirement (CS-11) becomes

$$\mu_{j-1}M_{j-2} + 2M_{j-1} + \lambda_{j-1}M_j = 6[[(y_j - y_{j-1})/h_j] - [(y_{j-1} - y_{j-2})/h_{j-1}]]/(h_j + h_{j-1}) \qquad \text{(CS-18)}$$

For this spline, the defining equations (CS-17) and (CS-18) are written in matrix form as

$$A\,M = \begin{bmatrix} 2 & \lambda_0 & 0 & \cdots & 0 & 0 & 0 \\ \mu_1 & 2 & \lambda_1 & \cdots & 0 & 0 & 0 \\ 0 & \mu_2 & 2 & \cdots & 0 & 0 & 0 \\ \vdots & \vdots & \vdots & & \vdots & \vdots & \vdots \\ 0 & 0 & 0 & \cdots & 2 & \lambda_{N-2} & 0 \\ 0 & 0 & 0 & \cdots & \mu_{N-1} & 2 & \lambda_{N-1} \\ 0 & 0 & 0 & \cdots & 0 & \mu_N & 2 \end{bmatrix} \begin{bmatrix} M_0 \\ M_1 \\ M_2 \\ \vdots \\ M_{N-2} \\ M_{N-1} \\ M_N \end{bmatrix} = \begin{bmatrix} d_0 \\ d_1 \\ d_2 \\ \vdots \\ d_{N-2} \\ d_{N-1} \\ d_N \end{bmatrix} = D \qquad \text{(CS-19)}$$

where $d_j (j = 2,3, \ldots, N)$ represents the right-hand side of (CS-18).

For the periodic spline, the derivative,

$$S_\Delta^{(P)}(A+) = S_\Delta^{(P)}(b-) \quad \text{for} \quad P = 0,1,2 \qquad \text{(CS-20)}$$

and $y_0 = y_N$, $M_0 = M_N$. The defining equations for the periodic case are

$$\begin{bmatrix} 2 & \lambda_1 & 0 & \cdots & 0 & 0 & \mu_1 \\ \mu_2 & 2 & \lambda_2 & \cdots & 0 & 0 & 0 \\ 0 & \mu_3 & 2 & \cdots & 0 & 0 & 0 \\ \vdots & \vdots & \vdots & & \vdots & \vdots & \vdots \\ 0 & 0 & 0 & \cdots & 2 & \lambda_{N-1} & 0 \\ 0 & 0 & 0 & \cdots & \mu_{N-1} & 2 & \lambda_N \\ \lambda_N & 0 & 0 & \cdots & 0 & \mu_N & 2 \end{bmatrix} \begin{bmatrix} M_1 \\ M_2 \\ M_3 \\ \vdots \\ M_{N-1} \\ M_N \\ M_N \end{bmatrix} = \begin{bmatrix} d_1 \\ d_2 \\ d_3 \\ \vdots \\ d_{N-1} \\ d_N \\ d_N \end{bmatrix}. \qquad \text{(CS-21)}$$

In the matrix equations (CS-19) and (CS-21), the coefficient matrix is tridiagonal. To find $M_j$ in (CS-19) efficiently on the computer, the tridiagonal coefficient matrix A is written as a product LU of a lower triangular matrix L and an upper triangular matrix U. The entries of L on the main diagonal are 1's; below the diagonal, they are the multiples $l_{ij}$ of row j which are subtracted from row i during Gaussian elimination. U is the coefficient matrix which appears after Gaussian elimination and before back-substitution. [For details, see Gilbert Strang's, Linear Algebra And Its Applications, Chapter 1, Academic Press, 1976]

So the (N+1) by (N+1) matrix A is factored as follows:

$$A = \begin{bmatrix} 2 & \lambda_0 & 0 & \cdots & 0 & 0 & 0 \\ \mu_1 & 2 & \lambda_1 & \cdots & 0 & 0 & 0 \\ 0 & \mu_2 & 2 & \cdots & 0 & 0 & 0 \\ \vdots & \vdots & \vdots & & \vdots & \vdots & \vdots \\ 0 & 0 & 0 & \cdots & 2 & \lambda_{N-2} & 0 \\ 0 & 0 & 0 & \cdots & \mu_{N-1} & 2 & \lambda_{N-1} \\ 0 & 0 & 0 & \cdots & 0 & \mu_N & 2 \end{bmatrix} = \begin{bmatrix} 1 & 0 & 0 & \cdots & 0 & 0 & 0 \\ L_1 & 1 & 0 & \cdots & 0 & 0 & 0 \\ 0 & L_2 & 1 & \cdots & 0 & 0 & 0 \\ & \ddots & \ddots & & & & \\ & & \ddots & \ddots & & & \\ & & & \ddots & \ddots & & \\ & & & & L_{N-1} & 1 & 0 \\ 0 & & & & & L_N & 1 \end{bmatrix} \begin{bmatrix} u_0 & \lambda_0 & 0 & \cdots & 0 & 0 & 0 \\ 0 & U_1 & \lambda_1 & \cdots & 0 & 0 & 0 \\ 0 & 0 & U_2 & \lambda_2 & 0 & 0 & 0 \\ & & \ddots & \ddots & & & \\ & & & \ddots & \ddots & & \\ & & & & U_{N-2} & \lambda_{N-2} & \\ 0 & & & & 0 & U_{N-1} & \lambda_{N-1} \\ & & & & & 0 & U_N \end{bmatrix} \qquad \text{(CS-22)}$$

The following equations are obtained from equating the respective entries in (CS-22).

Entry

(1,1): $u_o = 2$

(2,2): $\lambda_o L_1 + u_1 = 2 \qquad u_1 = 2-\lambda_o L_1$ (CS-23)

(3,3): $\lambda_1 L_2 + u_2 = 2 \qquad u_2 = 2-\lambda_1 L_2$

$\vdots \qquad \vdots \qquad \vdots$

(N+1, N+1): $\lambda_{N-1} L_N + u_N = 2 \qquad u_N = 2-\lambda_{N-1} L_N$

So in general, $u_j = 2-\lambda_{j-1} L_j$ (j=1, ..., N). (CS-24)

Also,

Entry

(2,1): $L_1 u_o = \mu_1 \qquad L_1 = \mu_1/u_o = \mu_1/2$ (CS-25)

(3,2): $L_2 u_1 = \mu_2 \qquad L_2 = \mu_2/u_1 = \mu_2/(2-{}_1L2)$

$\vdots \qquad \vdots \qquad \vdots \quad \vdots$

(N+1, N): $L_N u_{N-1} = \mu_N \qquad L_N = \mu_N/u_{N-1}$

So, thus far the equations (since all other entries give identities) are

$$u_o = 2$$

$$L_j = \mu_j/u_{j-1} \qquad \text{(CS-26)}$$

$$u_j = 2-\lambda_{j-1} L_i \qquad \text{for } (j = 1, \ldots., N).$$

Now let M denote the column vector of $M_j$'s and D denote the column vector of $d_j$'s, (j = o, 1, ...., N). So the matrix equation

AM = D becomes LUM = D. So

$UM = L^{-1}D = T$ and $LT = D$

$$\begin{bmatrix} 1 & 0 & 0 & \cdots & 0 \\ L_1 & 1 & 0 & \cdots & 0 \\ 0 & L_2 & 1 & 0 \cdots & 0 \\ 0 & 0 & L_3 & 1 \cdots & 0 \\ & & & & 0 \\ & & & L_N & 1 \end{bmatrix} \begin{bmatrix} t_0 \\ t_1 \\ t_2 \\ \vdots \\ t_N \end{bmatrix} = \begin{bmatrix} d_0 \\ d_1 \\ d_2 \\ \vdots \\ d_{N-1} \\ d_N \end{bmatrix} \qquad \text{(CS-27)}$$

By equating entries,

$$t_o = d_o$$

$$t_j = d_j - L_j\, t_{j-1} \qquad (j = 1, \ldots, N) \qquad \text{(CS-28)}$$

Now to find the column vector M, use backward substitution for UM = T.

That is,

$$\begin{bmatrix} U_o & \lambda_o & 0 & \cdots & 0 & 0 & 0 \\ 0 & U_1 & \lambda_1 & \cdots & 0 & 0 & 0 \\ 0 & 0 & U_2 & \lambda_2 \cdots & 0 & 0 & 0 \\ & & & & \vdots & & \\ & & U_{N-2} & & \lambda_{N-2} & & 0 \\ & & & & U_{N-1} & & \lambda_{N-1} \\ & & & & & & U_N \end{bmatrix} \begin{bmatrix} M_0 \\ M_1 \\ M_2 \\ \vdots \\ M_{N-1} \\ M_N \end{bmatrix} = \begin{bmatrix} t_0 \\ t_1 \\ t_2 \\ \vdots \\ t_{N-1} \\ t_N \end{bmatrix} \qquad \text{(CS-29)}$$

So

Entry

(N+1, N+1): $U_N M_N = T_N \longrightarrow M_N = T_N / U_N$

(N, N): $U_{N-1} M_{N-1} + \lambda_{N-1} M_N = T_{N-1} \longrightarrow M_{N-1} = (T_{N-1} - \lambda_{N-1} M_N) / U_{N-1}$

(N-1, N-1): $U_{N-2} M_{N-2} + \lambda_{N-2} M_{N-1} = T_{N-2} \longrightarrow M_{N-2} = (T_{N-2} - \lambda_{N-2} M_{N-1}) / U_{N-2}$

So, in general,

$$M_{N-j} = (T_{N-j} - \lambda_{N-j} M_{N-j+1})/U_{N-j} \quad (J = 1,2, \ldots, N) \qquad \text{(CS-30)}$$

So finaly, the general working formulas are

$$\begin{aligned} U_0 &= 2 \\ L_j &= \mu_j / u_{j-1} \\ U_j &= 2 - \lambda_{j-1}, L_j \\ t_j &= d_j - L_j t_{j-1} \\ M_{N-j} &= (T_{N-j} - \lambda_{N-j} M_{N-j+1})/U_{N-j} \quad (j = 1, 2, \ldots, N). \end{aligned} \qquad \text{(CS-31)}$$

Remark. These equations are equivalent to (2.1.20) and (2.1.21) derived in Ahlberg, Nelson and Walsh. The derivation of analogous working equations for the non-periodic case (CS-21) is similar.

A code for formulas (C-31), written by Professor Dennis Quinn of AFIT for the Hewlett-Packard 9830, was used to fit international airfoil data. This data is presented in the next section.

## VI. OUTPUT FOR NACE 64 A410 AIRFOIL

A computer program for the Hewlett-Packard 98-30 was written to determine the cubic spline which best fits the cambered airfoil data. In this case all twenty six of the X values were used as the knots. The plot of each of the cubic splines was accurate. The program accepts tabulated values of X(I) and F(I). It solves for the spline coefficients and then calculates new F(I) and the first derivative DS(I).

Table 4 lists the output for the NACA 64 A410 airfoil upper surface using the twenty six points as the knots.

Table 4: SPLINE OUTPUT for NACA 64A410 UPPER SURFACE with TWENTY SIX KNOTS

SPLINE COEFFICIENTS

| X(I) | New F(I) | Derivative |
|---|---|---|
| | -1.00000E-14 | 2.577142857 |
| 2.50000E-03 | 9.02000E-03 | 1.692722672 |
| 5.00000E-03 | 0.0112 | 0.606010743 |
| 7.50000E-03 | 0.014510000 | 0.693377622 |
| 1.00000E-02 | 0.02095 | 0.427814566 |
| 1.50000E-02 | 0.030340000 | 0.361714295 |
| 2.00000E-02 | 0.038660000 | 0.289228645 |
| 2.50000E-02 | 0.0438 | 0.183581585 |
| 3.14748 | 0.053660000 | 0.182923677 |
| 4.1977 | 0.061260000 | 0.129097136 |
| 5.248 | 0.067050000 | 0.100033719 |
| 6.29834 | 0.071310000 | 0.068982534 |
| 7.34871 | 0.0741+0000 | 0.042470783 |
| 8.3993 | 0.075520000 | 0.010351616 |
| 9.4465 | 0.075220000 | -0.021571660 |
| 10.49489 | 0.073440000 | -0.043818189 |
| 11.54025 | 0.070400000 | -0.071911680 |
| 12.58857 | 0.066240000 | -0.093072555 |
| 13.63915 | 0.061000000 | -0.112866015 |
| 14.69103 | 0.054900000 | -0.132561047 |
| 15.75126 | 0.0478 | -0.150053304 |
| 16.80151 | 0.039670 | -0.177254199 |
| 17.85148 | 0.03018 | -0.196134968 |
| 18.90104 | 0.020080000 | -0.201162159 |
| 19.95053 | 0.01028 | -0.204695031 |

## VII. RECOMMENDATIONS

Whether we used the least squares approximation by cubic splines or the interpolation cubic spline routine to fit the cambered airfoil data, the curve fits are exact. In particular, contaminated data was not smoothed out by the spline routines. So one avenue of research would be to see the effect of first applying a smoothing spline routine as a preprocessor (to get rid of the contaminated data) and then apply the least squares approximation by cubic splines.

A second avenue of follow-through research on wings, of use to the Air Force, would be to write a technical memorandum on three dimensional surface fitting by splines of aerodynamical data such as mode shape of wings in computer graphics.

## REFERENCES


1. I. H. Abbott and A. E. von Doenhoff, Theory of Wing Sections, Including a Summary of Airfoil Data. Dover (paperback) 1959.

2. J. H. Ahlberg, E. N. Nilson, and J. L. Walsh, The Theory of Splines and Their Applications. Academic Press, 1967.

3. de Boor, Carl, A Practical Guide to Splines. Springer Verlag, 1978.

4. A. M. Kuethe and C-Y Chow, Foundations of Aerodynamics, 3rd edition, 1976.

   G. Strang, Linear Algebra And Its Application, Academic Press, 1976.

5. P. M. Prenter, Splines and Variational Methods, John Wiley and Sons, 1975.

REPORT 2

# Inclusion Theorems for Absolutely Summable Abel and Stieltjes Methods for Improper Integrals

Louise A. Raphael[2]

## Abstract

The Stieltjes summability method for divergent integrals, whose Stieltjes means are of bounded variation on the half line, is defined. This method is said to be absolutely summable Stieltjes. The main results prove inclusion theorems between two absolutely summable Abel methods and the absolutely summable Stieltjes method.

1) This paper will be jointly submitted for publication with Professor Harvey Diamond of West Virginia University.

2) Research supported by Air Force Office of Scientific Research at Wright Patterson AFB.

1. Introduction. Let $\{x_n\}_0^\infty$ be a non-negative, monotonically increasing unbounded sequence. The infinite series $\sum_n^\infty f_n$ is said to be Abel summable to the sum L, if the sum function $\phi(s) = \sum_n^\infty f_n \exp(-x_n s)$ converges for every $s > 0$ and its sum function $\phi(s) \to L$ as $s \to 0+$. A classical theorem due to Hardy [2] states that Abel summability for $\{x_n\}_0^\infty$ is weaker than Abel summability for $\{\ln(x_n)\}_0^\infty$, $x_0 \geq 1$. D. Rath [7] proved an analogous inclusion theorem for these Abel summability methods where the sum functions $\Sigma_n f_n \exp(-x_n s)$ are of bounded variation on the half-line $(0,\infty)$.

In [8] Tikhonov introduced a regularization operator to sum Fourier-like series whose coefficients were perbturbed. The summability method associated with this operator was studied by Hudak [3]. In deriving a stable method for summing eigenfunction expansions under the $L^2(0,\infty)$ pertubation of the coefficients, Raphael [6] extended this new summability method to divergent integrals. This summability method is now called Stieltjes summability, because of its close relationship with the Stieltjes transform.

This paper is solely concerned with Abel and Stieltjes summability methods for divergent integrals whose summability means are of bounded variation on $(0,\infty)$. These methods are called absolutely summable.

There are three inclusion results. The first proves that absolutely summable Abel plus convergence of the Stieltjes means implies absolutely summable Stieltjes to the same sum. The second states that absolutely summable Stieltjes and convergence of the Mellin transform implies abolutely summable Abel with respect to ln x to the same sum. The third is an immediate corollary of these theorems. It is an extension of Rath's result [7] for absolutely summable Abel methods for infinite series to absolutely summable Abel methods for divergent integrals.

2. Basic Definitions and Results. So that this paper is self contained, definitions and results needed in the proofs are stated in this section. All functions are Lebesque measurable, locally integrable real valued functions defined on the half line $[o,\infty]$. The integral $\int_0^\infty f(x)dx$ means $\lim_{a\to\infty} \int_0^a f(x)dx$ provided the limit exists, or equals infinity.

First we define Abel and Stieltjes summability methods for divergent integrals and state the propositions in [6] needed in our proofs.

Definition 1. The integral $\int_0^\infty f$ is summable by the Abel method A(x) to the sum L, if the Laplace transform of f, $\int_0^\infty \exp(-xs)f(x)dx$, converges for $s > 0$ and $\lim_{s\to 0} \int_0^\infty f(x)\exp(-xs)dx = L$. We write $\int_0^\infty f = L\ A(x)$ and say $\int_0^\infty f$ is Abel summable to L.

Similarly, $\int_0^\infty f$ is summable by the Abel method A(ln x) to the sum L, if the Mellin transform of f, $\int_0^\infty f(x)x^{-s}dx = \int_0^\infty f(x)\exp(-s\ln x)dx$, converges for $s > 0$ and $\lim_{s\to 0} \int_0^\infty f(x)x^{-s}dx = L$. Here we write $\int_0^\infty f = L\ A(\ln x)$.

Definition 2. The integral $\int_0^\infty f$ is summable by the Stieltjes method S(x) to the sum L, if $\int_0^\infty f(x)(1 + bx)^{-1}dx$ exists for $b > 0$ and $\lim_{b\to 0} \int_0^\infty f(x)(1 + bx)^{-1}dx = L$. We write $\int_0^\infty f = L\ S(x)$.

Propositions 3 and 5 state inclusion results between Abel and Stieltjes summability.

Proposition 3. If $\int_0^\infty f = L\ A(x)$ and $\int_0^\infty (1 + bx)^{-1}f$ converges for $b > 0$, then $\int_0^\infty f = S(x,1)$.

In the proof of Proposition 3, the Stieltjes mean $\int_0^\infty f(x)(1 + bx)^{-1}dx =$ expressed as a twice iterated Laplace transform $\int_0^\infty f(x)(1 + bx)^{-1}dx = (1/b)\int_0^\infty \exp(-s/b)\int_0^\infty f(x)\exp(-xs)dxds$. The next proposition was needed in the proof of Proposition 5 and will be used in the proof of our main results.

Proposition 4. If the integral $\int_0^\infty f(x)\exp(-s\ln x)dx$ converges for s, $0 < s < 1$, then $\int_0^\infty f(x)\exp(-s\ln x)dx = [(\sin \pi s)/\pi]\int_0^\infty b^{s-1}\int_0^\infty f(x)(1 + bx)^{-1}dxdb$ for $0 < s < 1$.

Proposition 5. If $G(s) = \int_0^\infty f(x)\exp(-s\ln x)dx$ converges for $0 < s < 1$ and $\int_0^\infty f = L$ $S(x,1)$, then $\int_0^\infty f = L$ $A(\ln x)$.

We recall the definition of a function f to be of bounded variation on $(0,\infty)$. Let a function f be defined and finite on the interval $[a,b]$. The interval $[a,b]$ is subdivided into subintervals by means of the points $x_0 = a < x_1 < x_2 \ldots < x_n = b$, and we form the finite series sum

$$V = \sum_k |f(x_{k+1}) - f(x_k)|, \quad (k = 0, \ldots, n)$$

We denote the least upper bound of the set of all possible sums V by $\overset{b}{\underset{a}{V}}(f)$. If $\overset{b}{\underset{a}{V}}(f) < \infty$, then f is of bounded variation on $[a,b]$. Now let f be defined for all x, $0 < x < \infty$. If $\overset{b}{\underset{a}{V}}(f) < \infty$ for all $a < b$, and if $\sup\overset{b}{\underset{a}{V}}(f)$, for $a < b$, is finite, then f is of bounded variation on $(0,\infty)$. The number $\sup\overset{b}{\underset{a}{V}}(f) = \overset{\infty}{\underset{0}{V}}(f)$, for $a < b$, is said to be the bounded variation of f.

We let $BV(o,\infty)$ denote the class of functions of bounded variation on $(o,\infty)$ [4].

Definition 6. The integral $\int_0^\infty f$ is absolutely summable Abel to the sum L, if $\int_0^\infty f = L$ $A(x)$ and $\int_0^\infty f(x)\exp(-xs)dx \in BV(o,\infty)$. Here we write $\int^\infty f = L$ $|A(x)|$.

Similarly, absolutely summable Stieltjes is defined.

Definition 7. The integral $\int_0^\infty f$ is absolutely summable Stieltjes to the sum L, if $\int_0^\infty f = L$ $S(x)$ and $\int_0^\infty f(x)(1 + bx)^{-1}dx \in BV(o,\infty)$. We write $\int_0^\infty f = L$ $|S(x)|$.

The following Lemma is Rath's [7] version of a classical result due to Knopp [4][3]. This lemma is true for functions of $BV(o,c)$, $c$ finite.

Lemma 8. (Knopp) Suppose that

1. $g(s) \in BV(o,\infty)$
2. $\int_0^\infty h(b,s)ds = F(b)$ exists for $b > 0$

3) Knopp's basic research was supported by AFOSR.

and

3. $\int_t^\infty h(b,u)du \in BV(o,\infty)$, uniformly for $t \geq 0$.

Then $$F(b) = \int_0^\infty h(b,s)g(s)ds \in BV(o,\infty).$$

Proposition 9. If $\int_0^\infty f = L\ |A(x)|$ and $\int_0^\infty f(x)(1 + bx)^{-1}dx$ converges for all $b > 0$, then $\int_0^\infty f = L\ |S(x)|$.

Proof. By virtue of Proposition 3, $\int_0^\infty f = L\ S(x)$. So it remains to show that the Stieltjes means $\int_0^\infty f(x)(1 + bx)^{-1}dx$ belong to the class $BV(o,\infty)$ for all $b > 0$. We do this by showing the hypotheses of Knopp's lemma are satisfied.

The integral $\int_0^\infty f(x)(1 + bx)^{-1}dx = b^{-1}\int_0^\infty \exp(-s/b)\int_0^\infty f(x)\exp(-xs)dxdx$. By assumption $g(s) = \int_0^\infty f(x)\exp(-xs)dx$ belongs to $BV(o,\infty)$. The second hypothesis is satisfied as $b^{-1}\int_0^\infty \exp(-s/b)ds = 1$ for all $b > 0$.

Now, let

$$K_b(t) = b^{-1}\int_0^\infty \exp(- /b)du = e^{-t/b}$$

We now show that $K_b(t) \in BV(o,\infty)$ uniformly in $t$ for $b > 0$.

$$\int_0^x \left|\frac{dK_b(t)}{db}\right| db = \int_0^x tb^{-2}\exp(-t/b)db = c^{-t/b}\Big]_0^x = e^{-t/x}$$

which is uniformly bounded by one for $t > 0$ and $x \in (o,\infty)$. So for each $b > 0$, $K_b(t) \in BV(o,\infty)$ uniformly for $t \geq 0$.

Proposition 10. If $\int_0^\infty f = L\ |S(x)|$ and $\int_0^\infty f(x)x^{-s}dx$ converges for $0 < s < c$, then $\int_0^\infty f = L\ |A(\ln x)|$, $0 < s \leq c - \varepsilon < c$ where $\varepsilon > 0$ is arbitrary.

Proof. Define $h(s) = \int_0^\infty f(x)x^{-s}dx$, $0 < s < c$. By Proposition 5, $\int_0^\infty f = L\ A(\ln x)$ so we need only show that $h(s) \in BV\ (0,c - \varepsilon]$. Given any $a,b$ satisfying $0 < a < b < c$, it is easy to prove that $h(s)$ is infinitely differentiable for $s \in [a,b]$. This in turn implies the boundedness of $h'(s)$ on $[a,b]$ so that $h(s) \in BV\ [a,b]$ follows. It remains then to show that $h(s) \in BV\ (0,a]$ for some $a < c$. In what follows, we let $\underline{a}$ be any number satisfying $4a < \min(1,c)$.

Under the assumption $\int_0^\infty f = L\ |s(x)|$ and the existence of $\int_0^\infty f(x)x^{-s}dx$, $0 < s < c$, we have

$$\int_0^\infty f(x)x^{-s}dx = \frac{\sin\pi s}{\pi}\int_0^\infty b^{s-1}\left[\int_0^\infty \frac{f(x)}{1+bx}\,dx\right]db$$

$$= \frac{\sin\pi s}{\pi}\int_0^\infty \frac{b^{s-1}}{(1+b)^{2a}}\left[(1+b)^{2a}\int_0^\infty \frac{f(x)}{1+bx}\,dx\right]db,\quad 0 < s < c$$

To apply Knopp's Theorem we must show first that $g(b) \equiv (1+b)^{2a}\int_0^\infty \frac{f(x)}{1+bx}\,dx \in BV(0,\infty)$. By assumption, $\int_0^\infty \frac{f(x)}{1+bx}\,dx \in BV(0,\infty)$ so $g(b) \in BV(0,\beta]$ for any finite $\beta > 0$. We will show that $g(b) \in BV\ [1,\infty)$ by proving that $\int_1^\infty |g'(b)|db < \infty$. Differentiating,

$$g'(b) = \frac{2a(1+ba)^{2a}}{(1+b)}\int_0^\infty \frac{f(x)}{1+bx}\,dx - (1+b)^{2a}\int_0^\infty \frac{xf(x)}{(1+bx)^2}\,dx \qquad (1)$$

We rewrite the first integral as $\int_0^\infty f(x)x^{-3a}\left(\frac{x^{3a}}{1+bx}\right)dx$. Since $3a < c$, $\int_0^\infty f(x)x^{-3a}dx$ exists. We also have $\frac{x^{3a}}{1+bx} < \frac{1}{b^{3a}}$ and for each $b$, the function has a unique maximum. Applying Bonnet's second mean value theorem, we can obtain

$$\left|\int_0^\infty \frac{f(x)}{1+bx}\,dx\right| \le \frac{1}{b^{3a}} \sup_{0 < x_1 < x_2 < \infty} \left|\int_{x_1}^{x_2} f(x)x^{-3a}dx\right| < \frac{M}{b^{3a}} \text{ for some constant M.}$$

The first term in (1) is then bounded in absolute value by $4aM/b^{1+a}$ for $b \ge 1$. The second integral in (1) may be treated in a similar fashion, so that we obtain $\left|\int_0^\infty \frac{xf(x)}{(1+bx)^2}\,dx\right| < M/b^{1+3a}$ and can then bound the second term in (1) to be less than $2M/b^{1+a}$ in absolute value for $b \ge 1$. Finally, we have $|g'(b)| < 3M/b^{1+a}$, proving that $\int_1^\infty |g'(b)|db < \infty$ and hence that $g(b) \in BV(0,\infty)$, using the arguments above.

As it is clear that $\frac{\sin\pi s}{\pi}\int_0^\infty b^{s-1}(1+b)^{-2a}db$ exists, to complete the proof using Knopp's theorem, we must show that $\frac{\sin\pi s}{\pi}\int_t^\infty \frac{b^{s-1}}{(1+b)^{2a}}\,db \in BV(0,a]$ uniformly for $t \ge 0$. Integrating by parts gives

$$\frac{\sin\pi s}{\pi}\,\frac{t^s}{(1+t)^{2a}} + 2a\,\frac{\sin\pi s}{\pi s}\int_t^\infty \frac{b^s}{(1+b)^{1+2a}}\,db \qquad (2)$$

Clearly, $(\sin\pi s)/\pi s \in BV[0,a]$. Next, it is easily seen that $t^s/(1+t)^{2a} \le 1$ for $(s,t) \in [0,a] \times [0,\infty)$; and furthermore, for any fixed $t \in [0,\infty)$, the function is either non-increasing or non-decreasing in s. Thus the total variation of $t^s/(1+t)^{2a}$ is less than 1, uniformly in $t \ge 0$. We show next that the integral in (2) is of bounded variation on [0,a] uniformly in t by showing that its derivative is uniformly bounded:

$$\left|\frac{d}{ds}\int_t^\infty \frac{b^s}{(1+b)^{1+2a}}\,db\right| \le \int_t^\infty \frac{|\ln b|b^s}{(1+b)^{1+a}(1+b)^a}\,db \le \int_0^\infty \frac{|\ln b|}{(1+b)^{1+a}}\,db$$

where the last step follows from the bound $b^s/(1+b)^a \le 1$ for $s \in (0,a)$ and all $b \ge 0$. The final integral exists and its value is of course the required bound. This completes the proof.

As an immediate corollary, we have the divergent integral analogue of Hardy's and Rath's inclusion theorem for absolutely summable Abel methods.

Corollary 11. If $\int_0^\infty f = L\ |A(x)|$ and $\int_0^\infty f(x)(1+bx)^{-1}dx$ converges for all $b > 0$, then $\int_0^\infty f = L\ |A(\ln x)|$.

Proof. The proof follows immediately from the statements of Propositions 9 and 10.

Acknowledgement. The author wishes to thank the Applied Mathematics Group of the Flight Dynamics Laboratory at Wright Patterson for their hospitality, and Professor Billy E. Rhoades of Indiana University for encouragement to continue to study the problem.

Clark College
Atlanta, Georgia

## Bibliography

[1] I. S. Gradshteyn and I. M. Ryzhik. Table of Integrals, Series and Products (Academic Press, 1965, 4th edition).

[2] G. H. Hardy, Divergent Series (Oxford 1949).

[3] Ju. Hudak, "Two Inclusion Theorems for a Method of Generalized Summation of $T\{\lambda_k\}$ Series". Soviet Math. Dokl. 13 (1972), pp 304-308.

[4] K. Knopp, "Norlund Method for Functions", Math Z, 63 (1955), 39-52.

[5] I. P. Natanson, Theory of Functions of a Real Variable (Ungar 1955)

[6] L. A. Raphael, "The Stieltjes Summarbility Method and Summary Sturm-Liouville Expansions", to be published SIAM Journal of Mathematical Analysis.

[7] D. Rath, "An Inclusion Theorem on Summability", J. London Math. Soc. (2), 16 (1977), 483-489.

[8] A. N. Tikhonov, "Stable Methods for the Summation of Fourier Series", Soviet Math. Dokl. 5 (1964), 641-644.

[9] A. Zygmund, "On Certain Integrals", Trans. Amer. Math. Soc. 55 (1944), 170-204.

1980 USAF - SCEEE SUMMER FACULTY RESEARCH PROGRAM

Sponsored by the

AIR FORCE OFFICE OF SCIENTIFIC RESEARCH

Conducted by the

SOUTHEASTERN CENTER FOR ELECTRICAL ENGINEERING EDUCATION

FINAL REPORT

# EVALUATION OF METHOD AND TECHNIQUE FOR FAST ESTIMATION OF ANTIOXIDANT IN TURBINE ENGINE LUBRICANTS


| | |
|---|---|
| Prepared by: | Dasara V. Rathnamma |
| Academic Rank: | Associate Professor |
| Department and University: | Chemistry<br>U.S. Naval Academy (79-80) |
| Research Location: | Aero Propulsion Laboratory<br>Lubrication Branch<br>Wright-Patterson Air Force Base, Ohio |
| USAF Research Colleague: | Mr. Phillip Centers, Summer<br>Major George F. Uhlig, Pre-program and Technical Facility |
| Date: | September 7, 1980 |
| Contract No.: | F49620-79-C-0038 |

# EVALUATION OF METHOD AND TECHNIQUE FOR FAST ESTIMATION OF ANTIOXIDANTS IN TURBINE ENGINE LUBRICANTS

by

DASARA V. RATHNAMMA

## ABSTRACT

The present work describes setting up of an equipment and evaluation of the technique and method. Apparatus for determining the total effective concentration of chain stopping antioxidant species present in lubricants, described by Mahoney[1], et al, was set up, made leakproof, and calibrated. Using this equipment, the method of estimating the antioxidant by titration with peroxy radicals released at a constant rate by the thermal decomposition of a free radical initiator was standardized. It was confirmed that the time required for the start of the rapid oxidation of the hydrocarbon substrate of the lubricant is proportional to the concentration of the antioxidant additive in the lubricant. The method can be applied to the study of new and used lubricants and predict possibly a chemical model for the useful lifetimes of aircraft lubricants.

## ACKNOWLEDGEMENTS

The author would like to thank the Air Force Systems Command, The Air Force Office of Scientific Research and the Southeastern Center for Electrical Engineering Education for providing her with the opportunity to spend a worthwhile summer in the Lubrication Branch Fuels and Lubrication Division of the Aero Propulsion Laboratory at Wright-Patterson Air Force Base, Ohio.

She would like to thank Major George F. Uhlig, Ph.D., Chief of the Technical Facilities Division, for suggesting this area of research and for continuous encouragement; Mr. Phillip W. Centers, the effort focal point, for his collaboration, and Mr. Howard F. Jones, Chief of the Lubrication Branch, for his cooperation and support.

She would also like to thank technicians Stephen R. Jackson and John T. Fisher for their help in setting up the apparatus.

## I. INTRODUCTION:

The standard methods for testing the oxidative and thermal degradation of lubricants are very time-consuming. A new and fast method reported in literature[1] in recent years was chosen for study and comparison with the traditional methods. The new method is based upon the measurement of the time required for the reaction of the antioxidant in the lubricant with the free radicals formed at a constant rate from a free radical initiator injected into the system.

The apparatus required for this determination was set up during this summer. A lubricant substrate like cyclohexene in a reaction cell is mixed with a solution of an antioxidant in n-hexadecane as solvent and equilibrated with oxygen. A free radical initiator in chlorobenzene is injected into the cell. The antioxidant concentration is reduced to a minimum due to its reaction with the free radicals released from the initiator. The time required for this reaction is recorded on a strip chart recorder. Then follows the oxidation of the substrate which consumes oxygen. The oxygen pressure falls. A pressure transducer transmits this pressure differential to an indicator and the input from the indicator is traced on the strip chart. The reaction is carried out at a constant temperature of $60^{o}C$. The time elapsed before the start of the oxidation of the substrate evaluates the antioxidant capacity of the lubricant.

This method is based upon the kinetics of the reaction between the molecules of the antioxidant present in the additive package of the lubricant and the peroxy radicals formed at a constant rate from the free radical initiator. As a physical chemist, this kinetics problem interested me. My specialty in surface chemistry enables me to look into the allied problems in lubrication for further investigations in the near future using the facilities at the Air Force laboratory.

II. OBJECTIVES OF THE RESEARCH EFFORT:

It was possible to accomplish the first part of the effort set out during the pre-program visit. After all the components were received, work was started to construct the apparatus for the antioxidant determination The apparatus was made leakproof and calibrated.

The goals arrived at during the pre-program visit and goals added later on according to the letter dated June 30, 1980 from SCEEE are as follows:

"Present techniques used to study the thermal and oxidative degradation of lubricants can be extremely time-consuming. The Squires test method, for example, required 196 hours for completion. On the other hand, the complete oil breakdown rate analyzer determines the status of an oil in a few seconds. However, it is difficult to correlate the COBRA reading with what has actually occurred within the lubricant. A simple laboratory method has been developed for the determination of the total effective concentration of chain stopping antioxidant species present in new and used lubricants. The technique has been demonstrated for additive packages formulated in mineral base automotive lubricants. The principle of the method is based upon the titration of antioxidant species by peroxy radicals formed at a constant rate from the decomposition of a free radial initiator. Past work has applied this method to the analysis of variety of pure and commercial antioxidants and samples of new and aged lubricants derived from laboratory and service tests. These experiments have shown the decay of antioxidant species takes place in used samples before significant changes in other properties of the lubricant occur. Rapid degradation of the lubricant takes place only when the antioxidant species decays to a low level. The types of additive packages used with mineral oil lubricants are different from those used in turbine engine synthetic lubricants.

The suggested program will last about ten weeks. It will involve setting up experimental apparatus according to conversations with Dr. Lee Mahoney of the Ford Motor Company, Dearborn MI. The work done by Dr. Mahoney was funded by AFOSR and should prove suitable for following additive depletion in synthetic turbine engine oils and will represent a transition from Air Force basic

research to Air Force exploratory development. Once the experimental apparatus is constructed, experiments will be run on base stock with no additives as well as fully formulated lubricants and lubricants that have been degraded using the Squires technique. Correlation between the results obtained from this very simple laboratory method and the COBRA instrument and Squires will be made. Sufficient data should be obtained to result in a scientific publication concerning the use of this new technique for the evaluation of gas turbine engine lubricants and the additive degradation which occurs because of high thermal and oxidative environments."

The major objective namely setting up and standardizing the equipment was accomplished. Now by the use of this apparatus, progress on the second objective of estimating the antioxidant capacity of new and used lubricants can be made.

III. APPROACH:

The approach taken in realizing each of the above objectives was first to construct the apparatus required and then to carry out the measurements. Accordingly, the parts needed to set up the equipment were secured. Once all the parts and the help of technicians were available, the apparatus was constructed as outlined in literature[1], made leakproof, and checked with a helium leak detector. A trip to the Engineering Research Division of the Ford Motor Company was undertaken to visit the laboratory where the apparatus was in use and to hold discussions with the scientists who had published the paper on the apparatus and its applications.

The next section contains detailed description of the apparatus and its operation. Chemicals were purified as noted. The apparatus and glassware for distillation, recrystallization, drying, and columns for solvent drying were collected from different buildings. After all the chemicals were received, they were purified and dried. A miniature chemistry laboratory was set up for purifying chemicals, making up solutions and for preserving the solutions and chemicals in stable and safe conditions.

MATERIALS and Purification:

n-hexadecane

Aldrich - Distilled over $CaH_2$ fraction boiling at 280°C collected and passed over activated silica gel. Mesh 60-200; Davison Grade H

Chlorobenzene

Baker Analyzed #1-9179 Lot 842416

Dried over anhydrous $CaSO_4$. Distilled through short glass beads packed column. Fraction boiling at 128°collected and passed through activated alumina.

Cyclohexene

Fisher Scientific Company Purified Lot 796058 C-94

Distilled from calcium hydride

Fraction boiling at 82°C was collected and passed through activated alumina immediately before use.

AIBN

2-2' - AZobis (isobutyronitrile)

Recrystallized twice from methanol $(CH_3)_2C(CN)-N=N-CN(C)(CH_3)_2$ are in a dessicator in a refrigerator. Methanol HPLC Grade, Fisher certified.

Antioxidant

DuPont No. 29; 2,6-di-tert- butyl, 4-methyl phenol. Recrystallized twice from methanol (HPLC grade Fisher certified) and dried in a dessicator in a refrigerator.

IV. DETERMINATION OF THE ANTIOXIDANT CAPACITY OF NEW AND USED LUBRICANTS: METHOD AND APPLICATIONS

APPARATUS AND DETAILED PROCEDURE:[4]

Apparatus and Equipment: The apparatus, shown schematically in Figures 1.A and 1.B consists of the following components:

1. Glass reaction cell consisting of a sample area (28 mm i.d. x 30 mm), 1, an inlet closeable with a serum cap, 2, and a side arm connected to the measuring system by a coupling (Cajon #SS-4-UT-1-2).

2. Measuring system constructed with coiled 1/8" stainless steel tubing, 5, and handle, 6, which allows the reaction cell to be raised above the bath and removed for cleaning; a set of valves, $S_7$ - $S_9$, and $S_6$; and a differential pressure transducer, 7, (Validyne Model DP15) range $\pm$ 1 psi, connected via transducer indicator (Validyne Model CP12), 8, to a strip chart recorder (Hewlett Packard Model 7100B), 9.

3. Vacuum and gas supply system shich includes stopcocks $S_1$ - $S_5$ and $S_{10}$, 10 (Swaglok B-200-4 Unioncross), mercury pressure relief valve, 11, mercury manometer, 12, and an outlet for a cpaillary pipet, 13, used for flushing the reaction cell.

4. Submersible magnetic stirrer (Troemner Model 700), 14, and stirrer controller, 15, for stirring the reactant mixture in the reaction cell.

5. Constant temperature bath, 16, Cannon Model H-1 with stirrer, 17, and temperature control system.

Procedure:

1. Flushing and filling the system with oxygen.

   a. Close Valves $S_2$, $S_3$, and $S_5$ except when required to be open.

      $S_2$ Manometer

      $S_3$ Vacuum

      $S_5$ Mercury Relief Valve

   b. Open $S_1$, $S_4$, and $S_6$ - $S_9$

      $S_1$ Oxygen Inlet and fill the system with oxygen. Keep the pressure in the oxygen supply line only slightly higher than atmospheric pressure.

      $S_4$ Entry to system

      $S_6$ - $S_9$ (Valves immersed in the bath)

   c. Flush the coil and cell with oxygen having the inlet, 2, open.

   d. Open $S_{10}$, flush and insert the capillary pipet, 13, through inlet 2 all the way to the bottom of the cell in order to flush the sample area, 1.

e. Close $S_6$ and $S_9$ and maintain flushing through the capillary (Close $S_1$, keep $S_{10}$ open).

2. Charging the reactants to the cell.

a. Charge the required amounts of hexadecane, cyclohexene and sample into the cell using syringes with long needles (20 cm); maintain oxygen flushing near the top of the reaction cell.

b. Start magnetic stirring in the cell.

c. Remove the flushing capillary and quickly close the inlet, 2, with a serum cap.

d. Open $S_9$, close $S_7$ and $S_8$.

e. Allow the temperature to equilibrate for about 15 minutes.

3. Adding the initiator.

a. Start the recorder (chart speed - 0.25 cm/min; full scale - 1V).

b. Inject 0.5 ml of AIBN in chlorobenzene (0.2M) through the serum cap using a 1 ml syringe with a long needle.

c. Open $S_7$ and $S_8$ momentarily to allow equilibration of pressure on both sides of the transducer; reclose.

4. Measurement.

a. Open the measuring side of the transducer - open $S_7$ or $S_8$.

b. Record oxygen uptake, i.e., pressure decrease, versus time until the final linear portion of the curve is sufficiently long to determine the final rate of oxygen uptake.

c. Open $S_7$, stop recording, close $S_9$; discontinue stirring, lift up, disconnect and clean the reaction cell.

d. Determine the inhibition time, $\tau$, graphically.

5. Typical Charge.

a. 9.0 ml hexadecane

b. 1.0 ml cyclohexene

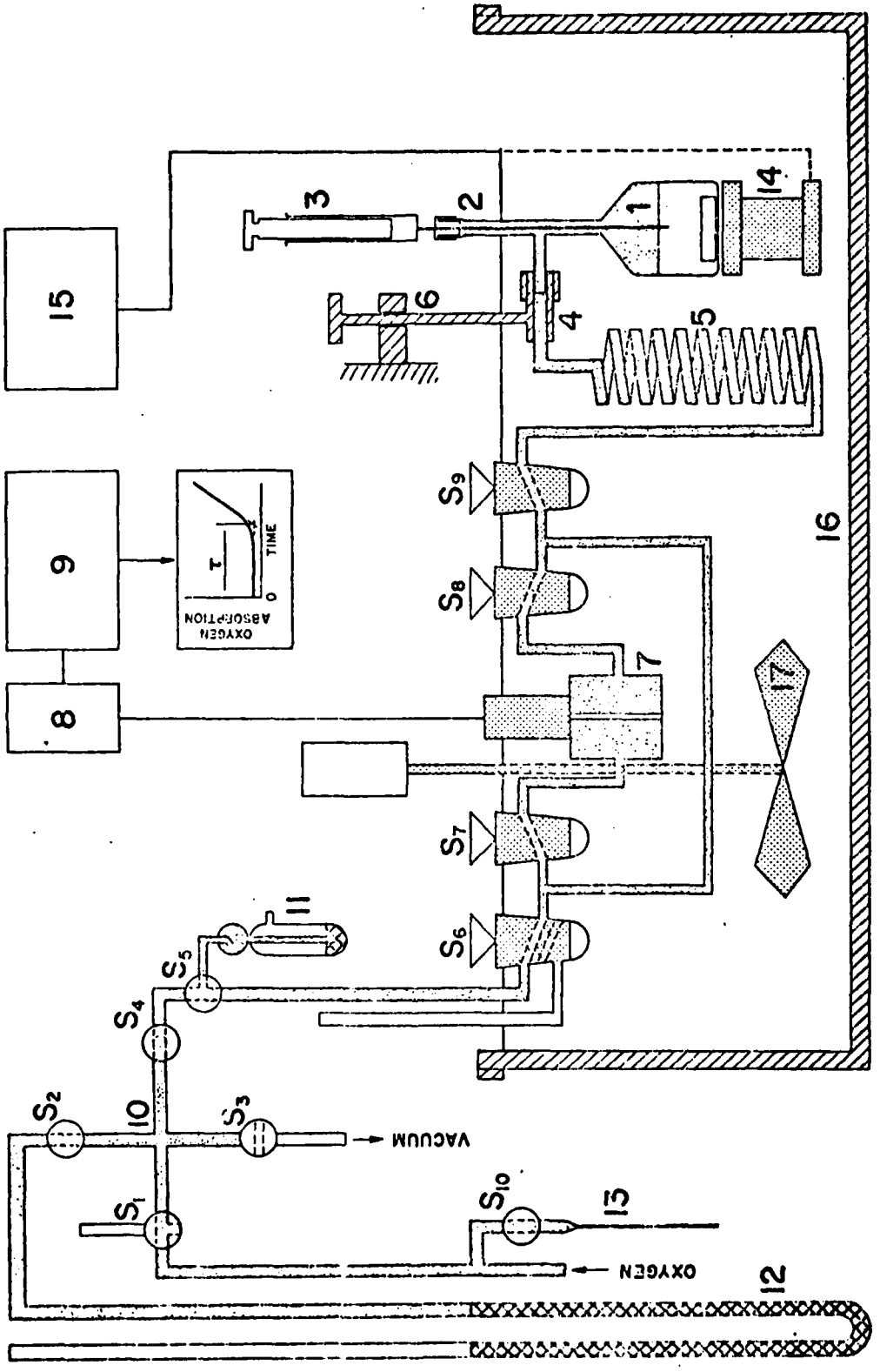
c. 0.5 ml sample, diluted in hexadecane such that n(AH) is approximately $3.5 \times 10^{-3}$. This will give a final n(AH) in the cell of about $1.6 \times 10^{-4}$ and an inhibition time of approximately 45 minutes for pure antioxidant[4].

d. 0.5 ml of AIBN in chlorobenzene (0.2M).

All tubing used was stainless steel.

All valves: Brass Swagelok #BOGS 2 (brass toggle switch valves and brass joints)

All Tees: Brass Swagelok Cat #200-3. Swagelok reducers 1/8" - 1/4" Cat 200-R-4 union cross.


SCHEMATIC DIAGRAM OF APPARATUS FOR MEASURING ANTIOXIDANT CAPACITY
FIG 1A
1
2
3
4
5
6
7
8
9
10
11
12
13
14
15
16
17
$S_1$
$S_2$
$S_3$
$S_4$
$S_5$
$S_6$
$S_7$
$S_8$
$S_9$
$S_{10}$
VACUUM
OXYGEN
OXYGEN ABSORPTION
TIME
T
0

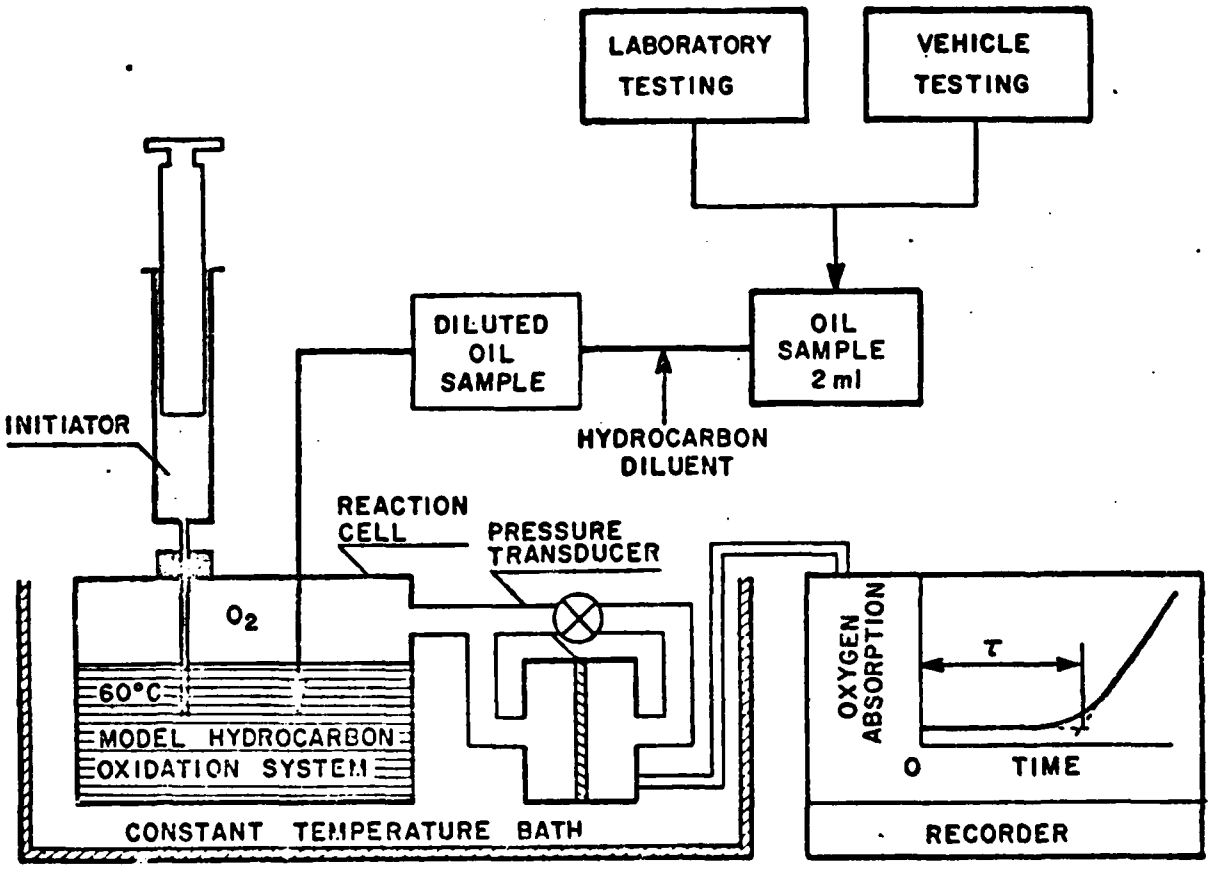



Fig. 1.B Peroxy radical titration of antioxidants.

## V. RESULTS AND DISCUSSIONS 1-18

The apparatus was to be tested and the method standardized. The concentrations of antioxidant in the standards were as follows (moles/liter):

Antioxidant used: 2, 6 Di-Tertiary Butyl 4 Methyl phenol

DuPont # 29

Solvent: N hexadecane

| | Concentration | Time Run #1 | Time Run #2 |
|---|---|---|---|
| $C_1$ (Stock): | $6.954 \times 10^{-3}$M | | |
| $C_2$ ..... | $3.477 \times 10^{-3}$M | | 130' |
| $C_3$ ..... | $2.318 \times 10^{-3}$M | | 76' |
| $C_4$ ..... | $1.159 \times 10^{-3}$M | 34' | 32½' |
| $C_5$ ..... | $5.795 \times 10^{-4}$M | 15' | |
| $C_0$ ..... | No Antioxidant | 6' | 8' |

It is evident from the curves traced by the strip chart recorder that the time elapsed before the oxidation of the substrate cyclohexene begins, is directly proportional to the concentration of the antioxidant in the standard.

In the oxidation apparatus , the antioxidant species reacts with the peroxy radicals.

$$AH + nRO_2 \longrightarrow \text{Inactive Products}$$

When the antioxidant is depleted, the substrate cyclohexene is oxidized rapidly.




Cyclohexene

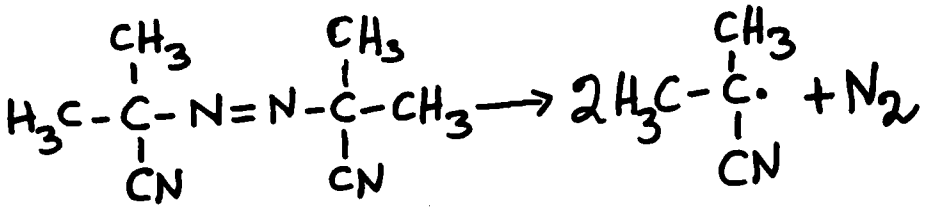
Hydroperoxides of Cyclohexene

These products are formed[1] via a free radical chain reaction as shown here.

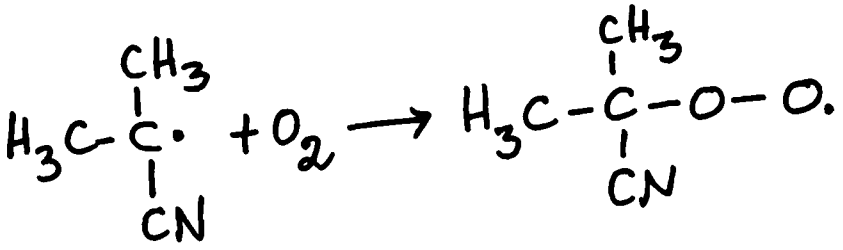
### Definitions

The antioxidant capacity of the oil is defined as the product of this antioxidant concentration in the oil, (AH) in moles per liter and the stoichiometric factor, n, given by the number of peroxy radicals terminated per molecule of a given antioxidant.

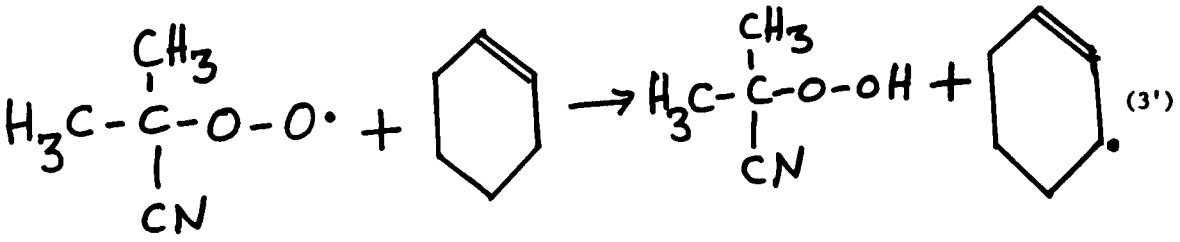
AIBN $\xrightarrow[\text{at } 60^{\circ}C]{\text{Thermal Decomposition}}$ Free Radicals



(1)

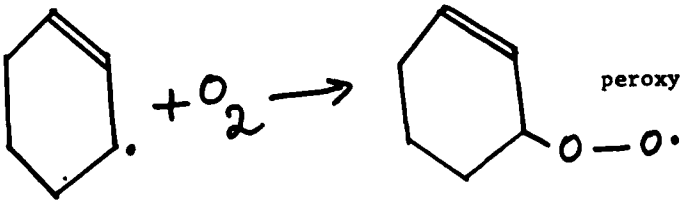


(2')

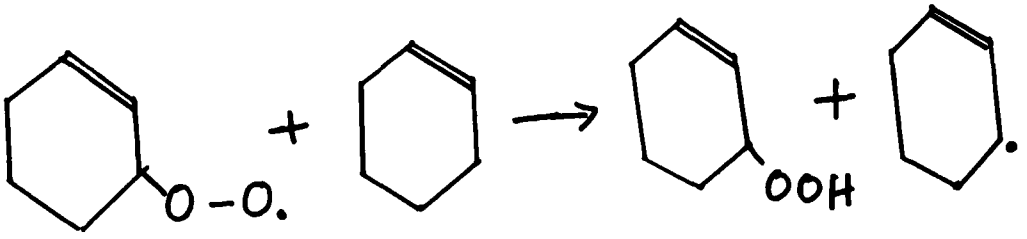


(3')

Chain propogation reactions are shown by (2) and (3).

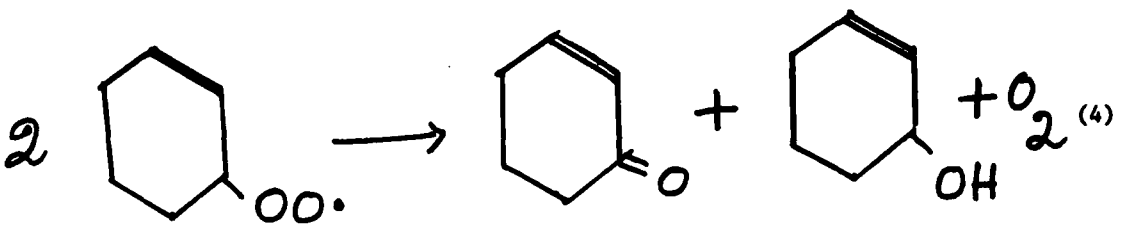


peroxy radical (2)



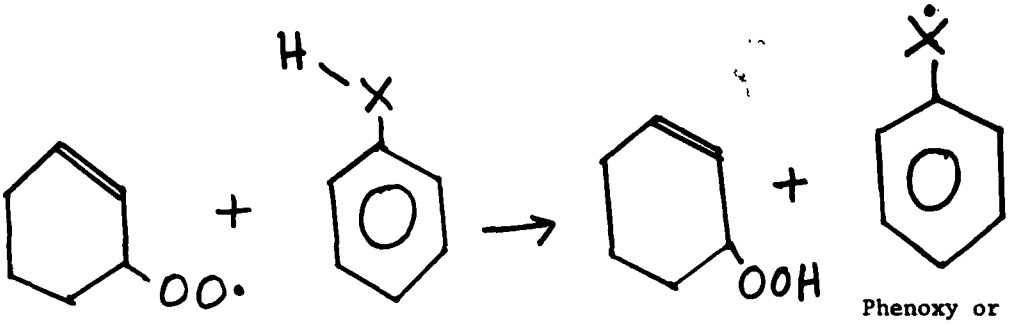
(3)

Absence of Antioxidants



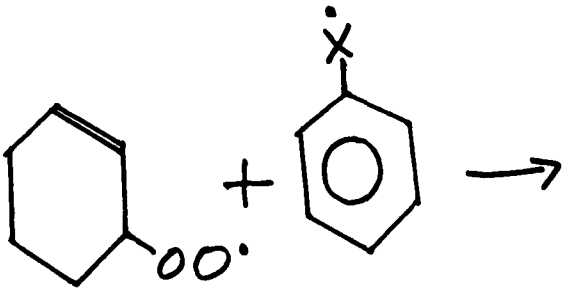

(4)

With Added Antioxidant




Phenoxy or
Amino Radical

(5)




Nonradical Products

(6)

In the Antioxidant

X represents the oxygen in the phenolic or > NR in the amino

Rate Equations:

Rate of free radical formation from the decomposition of AIBN:

$$= 2\varepsilon\kappa_1 (AIBN) = -n \left[\frac{d(AH)}{dt}\right]_t \quad \text{..... I}$$

$\varepsilon$ = efficiency of the free radical formation

$\kappa_1$ = first order rate constant

n = total number of peroxy radicals consumed by reaction with a total molecule of AH.

Integration of the above equation gives the relationship between the total number of free radicals produced and the initial concentration of the antioxidant.

$$2\varepsilon(AIBN)_o (1-\varepsilon^{\kappa_1 \tau}) = n (AH)_o \quad \text{..... II}$$

When $\tau$ is very small, decomposition of AIBN is neligible, $e^{-\kappa_1 \tau} \sim 1$ and

$$2 \kappa_1 \varepsilon (AIBN)_o \tau = n(AH)_o \quad \text{..... III}$$

n for the antioxidant 2, 6-di tert-butyl - 4-Methyl phenol is 4. $2\kappa_1\varepsilon$ is equal to the slope of the line (Figure 2) obtained by plotting the experimental valves of $\tau$ (AIBN) vs $(AH)_o$.

For the n-hexadecane-cyclohexene-AIBN system at 60°C, $2\kappa_1\varepsilon = 6.0 \times 10^{-6}$ Sec$^{-1}$ (Mahoney[1]). Our valve of $2\kappa_1\varepsilon = 10^{-6}$ sec$^{-1}$.

By knowing the valve of $2\kappa_1\varepsilon$ for a system, the quantity n(AH) for an unknown system may then be determined from equation III by determining $\tau$ for a given concentration of AIBN.

Calculation of $2\kappa_1\varepsilon$ for our System using Commercial Antioxidant DuPont #29

$2\kappa_1\varepsilon (AIBN)_o\tau = n (AH)_o$

n = 4 from literature

From Figure 2 $\frac{4(AH)_o}{(AIBN)_o\tau} = 4.4 \times 10^{-6}$ Sec$^{-1}$ for our system

Mahoney and Korcek report $6.0 \times 10^{-6}$ Sec$^{-1}$ for their system

Limitations of the Method

This method measures only the chain breaking antioxidants. It does not measure peroxide decomposing inhibitors or metal deactivators. Korcek etal are of the opinion that still it is a very useful method since it evaluates oxidative degradation of engine oils in the early stages of use before changes in the other oil properties are measurable. Also, chain breaking inhibitors are a very important type of inhibitors in the current engine oils.

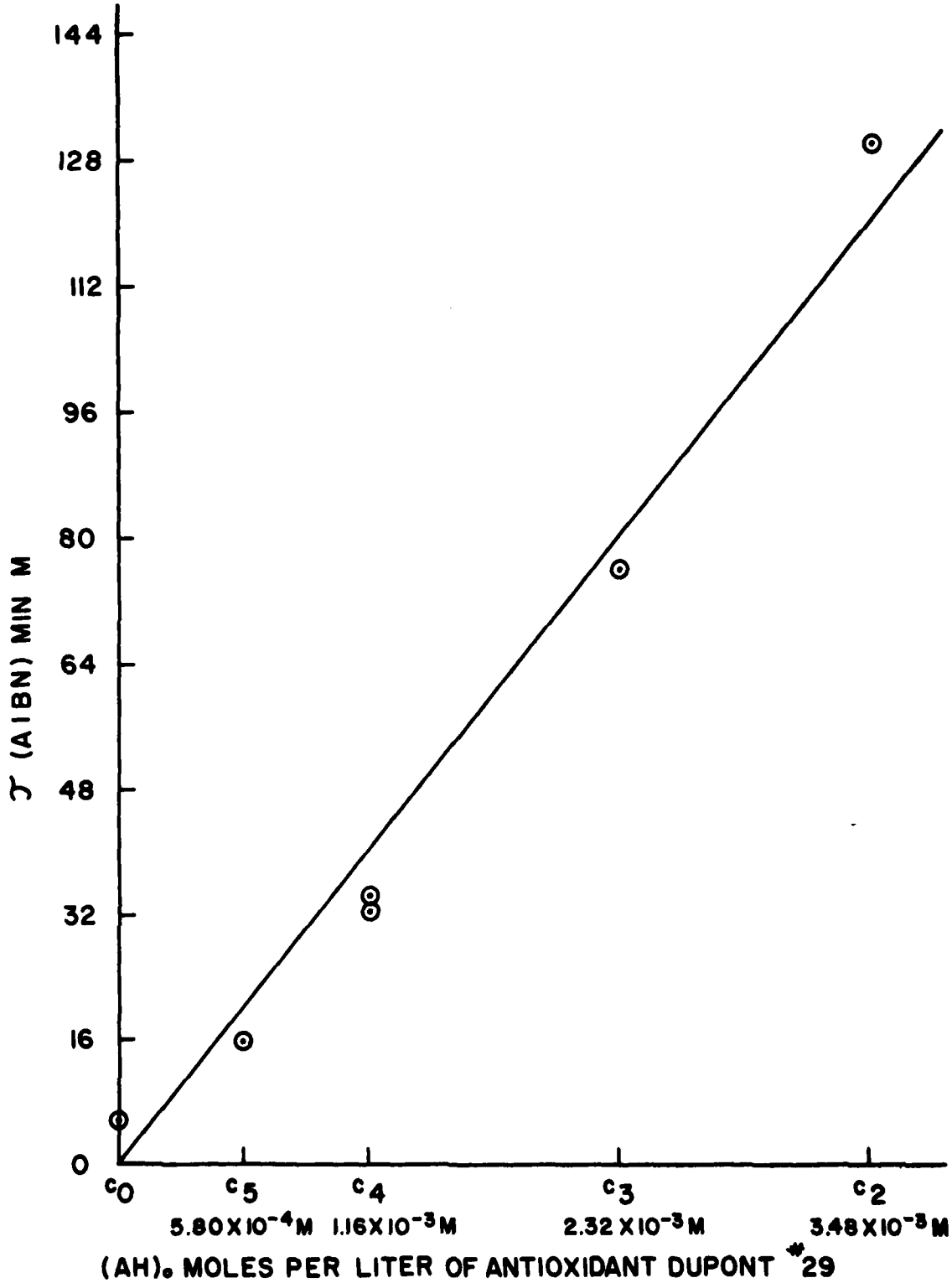

144
128
112
96
80
64
48
32
16
0
τ (AIBN) MIN M
C0
C5
C4
C3
C2
5.80X10-4M
1.16X10-3M
2.32X10-3M
3.48X10-3M
(AH)o MOLES PER LITER OF ANTIOXIDANT DUPONT #29

FIG 2
64-16

## VI. RECOMMENDATIONS:

It took more time than was anticipated to set up the equipment, eliminate leaks and other problems, and get a stable working system. Some delay due to certain factors, if eliminated, could have provided some time for a few experiments on base stocks with no additives and fully formulated lubricants that have been degraded using the Squires technique. However, each test by this new technique requires two and one-half hours. In order to compare the data with the data from other methods, a reasonably large number of estimations are required. Ten-week summer period was not sufficient for such data collection especially after a major part of the time was required for constructing and standardizing the equipment. These measurements can be undertaken during the mini-grant period.

It would be worthwhile exploring methods for the estimation of antioxidants in engine oils by employing other chemical reactions and techniques with and without involving reaction rate measurements.

Although it might appear ambitious, a more general method for the estimation of all of the antioxidants including the chain stopping antioxidants, if developed, would be more useful. Experimental technique improvement could be attempted.

It would be worthwhile taking up a study of the data available to find out the pattern, if any, that exists among the various properties of lubricants and write a computer program showing these correlations.

## REFERENCES


1. Mahoney, L. R., Korcek, S., Hoffman, S., Willermet, P. A., Ind. Eng. Chem. Prod. Res. Dev., Vol. 17, p. 250, 1978.

2. Korcek, S., Mahoney, L. R., Johnson, M. D., Hoffman, S., SAE Trans., Vol. 87, p. 3588, 1979.

3. Mahoney, L. R., Otto, K., Korcek, S., Johnson, M. D., Ind. Eng. Chem. Prod. Res. Dev., Vol. 19, p. 111, 1980.

4. Korcek, S., Mahoney, L. R., Johnson, M. D., Otto, K., to be published in the proceedings of the conference, NBS Special Publication, U.S. Department of Commerce, 1980.

5. Boozer, C. E., Hammond, G. S., Hamilton, C. E., Sen. J.N., J. Am. Chem. Soc., Vol. 77, p. 3233, 1955.

6. Burn, A. J., Terahedron, Vol. 22, p. 2153, 1966.

7. Hammone, G. S., Mahoney, L. R., Nandi, U. S., J. Am. Chem. Soc., Vol. 85, p. 737, 1963.

8. Howard, J. A., Ohkatsu, Y., Chenier, J. H. G., Ingold, K. U., Can. J. Chem. Vol. 51, p. 1543, 1973.

9. Ingold, K. U., in "Free Radicals", Vol. I, Chapter 2, Kocki, J. K., E., Wiley, New York, NY, 1973.

10. Kagler, S. H., "Spectroscopic and Chromatographic Analysis of Mineral Oil", Wiley, New York, NY, 1973.

11. Koenig, T., Fischer, H., in "Free Radicals", Vol. I, Chapter 4, J. K. Kocki, Ed., Wiley, New York, NY, 1973.

12. Mahoney, L. R., Angew. Chem. Int. Ed. Engl., Vol. 8, p. 547, 1969.

13. Mahoney, L. R., DaRooge, M. A., J. Am. Chem. Soc., Vol. 97, p. 422, 1975.

14. Mahoney, L. R., Korcek, S., Jenson, R. K., Zinbo, M., Am. Chem. Soc. Div. Pet. Chem., Prepr., 21, No. 4, p. 852, 1976.

15. Masson, J. C., in "Polymer Handbook:, 2nd ed. p II-4, J. Brandup and E. H. Immergut, Ed., Wiley, New York, NY, 1975.

16. Rowe, C. N., Dickert, J. J., Jr., ASLE Trans., Vol 10, p. 85, 1967.

17. Shkhiyants, I. V., Dzyubina, M. A., Sher, V. V., Sanin, P. I., Pet Chem. USSR, Vol. 13, p. 161, 1973.

18. Willermet, P. A., Mahoney, L. R., Haas, C. M., "The Effects of Antioxidant Reactions on the Wear Behavior of a Zinc Dialkyldithiophosphate", presented at the 1978 Annual ASLE Meeting, Dearborn, Michigan, Paper No. 78-AM-1B-1, Apr 17-20, 1978.

19. Gunderson, Reigh C., Hart, Andrew W., Ed., "Synethtic Lubricants", Reinhold Publishing Corporation, New York, 1962.

20. Proceedings of the Air Force-Navy-Industry, Propulsion Systems Lubricants Conference, November 15, 16, 17, 1960; An Air Research and Development Command Presentation, April 1961, Co-sponsored by Wright Air Development Division and Southwest Research Institute.

1980 USAF - SCEE SUMMER FACULTY RESEARCH PROGRAM

Sponsored by the

AIR FORCE OFFICE OF SCIENTIFIC RESEARCH

Conducted by the

SOUTHEASTERN CENTER FOR ELECTRICAL ENGINEERING EDUCATION

FINAL REPORT

# *DIGITALIZATION OF EXISTING CONTINUOUS-DATA CONTROL SYSTEMS*


| | |
|---|---|
| Prepared by: | Kuldip S. Rattan |
| Academic Rank: | Assistant Professor |
| Department and University: | Department of Engineering<br>Wright State University<br>Dayton, OH 45435 |
| Research Location: | Flight Dynamics Laboratory,<br>Flight Control Division,<br>Control Dynamics Branch,<br>Control Analysis Group,<br>Wright-Patterson Air Force Base<br>Dayton, OH |
| USAF Research Colleague: | Capt. Dennis Didaleusky |
| Date: | September 17, 1980 |
| Contract No: | F49620-79-C-0038 |

# DIGITALIZATION OF EXISTING CONTINUOUS-DATA CONTROL SYSTEMS

by

Kuldip S. Rattan

## ABSTRACT

A computer-aided method for converting existing multiloop continuous-data control systems into digital control systems is presented. Digital controllers are synthesized by matching the frequency responses of the digital control system to that of the continuous control system with a minimum weighted mean square error. Formulas for computing the parameters of the digital controllers are obtained as a result. An example of digitalizing existing continuous flight controller for the longitudinal YF-16 aircraft is considered and the results obtained are compared with those obtained by the Tustin transform.

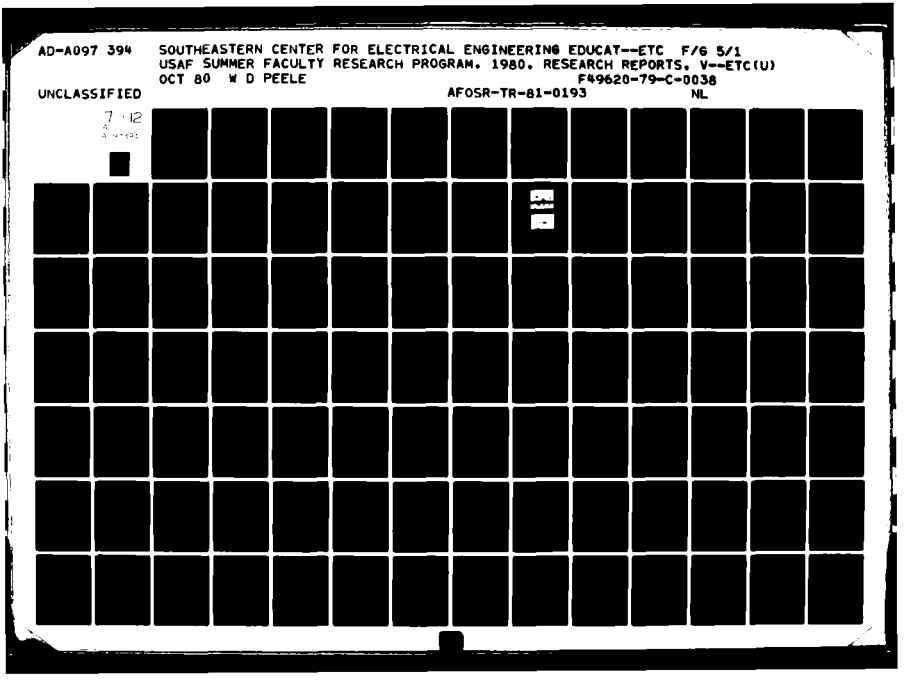
## ACKNOWLEDGMENTS

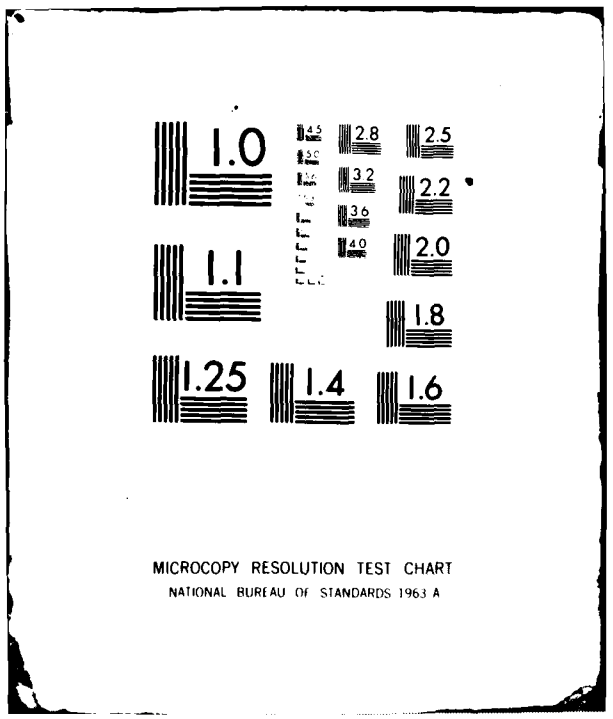
The author would like to thank the Air Force Systems Command, the Air Force Office of Scientific Research and the Southeastern Center for Electrical Engineering Education for providing him with the opportunity to spend a very worthwhile and exciting summer at the Air Force Flight Dynamics Laboratory, Wright-Patterson AFB, Dayton, Ohio. He would like to acknowledge the laboratory, in particular the Control Analysis Group, for its hospitality and excellent working conditions.

The author wishes to thank Captain Dennis Didaleusky for his collaboration and guidance. Finally, he would like to thank Lt. Stan Larimer and Dr. Robert Schwanz for many helpful discussions.

AD-A097 394 SOUTHEASTERN CENTER FOR ELECTRICAL ENGINEERING EDUCAT--ETC F/G 5/1
USAF SUMMER FACULTY RESEARCH PROGRAM, 1980, RESEARCH REPORTS, V--ETC(U)
OCT 80 W D PEELE F49620-79-C-0038

UNCLASSIFIED AFOSR-TR-81-0193 NL




1.0
1.1
1.25
1.4
1.6
1.8
2.0
2.2
2.5
2.8
3.2
3.6
4.0
MICROCOPY RESOLUTION TEST CHART
NATIONAL BUREAU OF STANDARDS 1963 A

The results of the study are shown on the chart in Figure 11. The horizontal axis of the graph depicts the ratio of the static deflection of an F-4 located at the center of the repair to the static deflection of the same aircraft on the undamaged runway. The vertical axis represents the depth of push back, $d_3$, to the depth of the crater, R. $d_3/R$ equal to 0 represents the situation where the crater is completely filled with compacted limestone. $d_3/R$ equal to one would represent the situation where only push back material was used to completely fill the crater.

For the two subgrade soils shown, the least deflections correspond to compacted material completely filling the crater. The greatest deflections corresponds to 12 inches of crushed stone over 108 inches of loose push back. The increase deflections due to the repair are significant. For the crater completely filled with compacted stone the deflections increase 10.8 times the deflection in the originial pavement for a medium clay subsoil and 14.3 times increase of deflections for a hard clay subsoil.

For a special repair consisting of 4 inches of a special quick drying concrete, 68 inches of compacted stone, 48 inches of push back material over 24 inches of hard clay the maximum deflections are greatly reduced. For a hard clay subsoil the static deflection of the repair were only 2.64 those of the undamaged runway. For a medium clay subsoil the deflections only increased by a factor of 2.28. Geofabrics have been used in recent years in earth retaining structures and in pavements in remove areas for oil field construction. Some rutting is necessary to develop the tensile strength in the fabric but if a special concrete repair is not feasible, a fabric reinforced crater repair could reduce the acculation of the rutting phenomena. At present the BDR code does not have the capability of such an analyses.

Summary

Computer calculations performed during this project have been presented. They fall into three basic categories: (1) comparison with elastic solutions, (2) variational studies and (3) parameter studies. The results of the first category indicates that good accuracy is obtainable with the program. The second category of calculations serves as a reminder that the procedures adopted for the prismatic elements are

a semi-analytic process and the results are very dependent of the characteristic length and the number of terms used in the Fourier series. The parameter studies illustrate the design and creative capability of the program.

## VI. RECOMMENDATIONS

In general, the Bomb Damage Repair Computer Code is a good finite element program. It idealizes the repaired crater, pavement system, or alternate launch and recovery surface as well as any finite element computer program. The program computes the stresses and displacements due to the application of prescribed load. Reasonable caution should be used when using the prismatic elements since the use of the Fourier series qualifies the method as semi-analytic.

The following recommendations are presenting for the improvement of the BDR code.

(1) Modify the axisymmetric solution by a Fourier series function or other semi-analytic method so non-symmetric loads can be applied to the mesh surface to represent multiwheel aircraft.

(2) Install a routine to compute residual deflections due to unloading and reloading.

(3) Install new elements to represent F.O.D. covers and membranes.

(4) Introduce the capability for multilayer soil systems outside the crater boundary.

(5) New material laws may have to be introduced if consolidation or undrained behavior of push back and other material is a problem at a particular air base.

(6) Flexibility should be added to the program regarding to positioning of the wheel loads.

(7) Greater control is needed over the quantity of output listing.

(8) New material laws should be added to represent the behavior of non-linear materials not represented by Hardin's laws.

(9) Interaction between the crater and existing pavements should be considered, especially when a rigid cap is placed over the crater.

(10) Verify the current use of the KHARDN parameter.

(11) Write a system manual, a users manual and an engineering manual for the use of the code.

(12) Verify the program by well instrumented field tests.

## REFERENCES

**Technical publications:**


1. John Crawford, Finite Element Analysis of Pavement Structures Using AFPAV Code (Nonlinear Elastic Analysis), AFWL-TR-74-71, Kirtland Air Force Base, New Mexico, April, 1975.

2. John Crawford and James B. Forrest, A Structural Evaluation of Rapid Methods of Backfilling for Bomb Damage Repair -- Phase II, AFWL-TR-74-272, Kirtland Air Force Base, New Mexico, August, 1975.

3. James B. Forrest, A Structural Evaluation of Rapid Methods of Backfilling for Bomb Damage Repair, AFWL-TR-73-29, Kirtland Air Force Base, New Mexico, March, 1974.

4. Bobby O. Hardin, Characterization and Use of Shear - Strain Relations for Airfield Subgrade and Base Course Materials, AFWL-TR-71-60, Kirtland Air Force Base, New Mexico, July, 1971.

5. Bobby O. Hardin, Effects of Strain Amplitude on the Shear Modulus of Soils, UKY TR63-72-CE23 College of Engineering, University of Kentucky, Lexington, Kentucky, November, 1972.

6. Bobby O. Hardin, Shear Modulus of Gravels, UKY TR74-73-CE19, College of Engineering, University of Kentucky, Lexington, Kentucky, September, 1973.

7. John P. Nielsen, AFPAV Computer Code for Structural Analysis of Airfield Pavements, AFWL-TR-75-151, Kirtland Air Force Base, New Mexico, October, 1975.

8. Raman Pichumani, Theoretical Analysis of Airfield Pavement Structure, AFWL-TR-71-26, Kirtland Air Force Base, New Mexico, July, 1971.

9. Raman Pichumani, Finite Element Analysis of Pavement Using AFPAV Code (Linear Elestic Analysis), AFWL-TR-72-186, Kirtland Air Force Base, New Mexico, May, 1973.

10. Program Management Plan (PMP) for Rapid Runway Repair (RRR), Engineering and Services Laboratory, Air Force Engineering and Services Center, Tyndall Air Force Base, Florida, March, 1980.

Books:


1. Joseph E. Bowles, Foundation Analysis and Design, New York: McGraw Hill Book Company, 1977.

2. Chandrabant S. Desai and John T. Christian, Numerical Methods in Geotechnical Engineering, New York, McGraw Hill Book Company, 1977.

3. O. C. Zienkiewicz, The Finite Element Method, Maiden Head, Berkshire, England: McGraw Hill Book Company (UK) Limited, 1977.

1980 USAF - SCEEE SUMMER FACULTY RESEARCH PROGRAM

Sponsored by the

AIR FORCE OFFICE OF SCIENTIFIC RESEARCH

Conducted by the

SOUTHEASTERN CENTER FOR ELECTRICAL ENGINEERING EDUCATION

FINAL REPORT

# CRACK TIP VELOCITY MEASUREMENTS DURING BRITTLE FRACTURE


| | |
|---|---|
| Prepared by: | Dr. Joseph H. Schmidt |
| Academic Rank: | Assistant Professor |
| Department and University: | Department of Mechanical Engineering<br>Memphis State University |
| Research Location: | AFWAL/MLLP, WPAFB, Ohio |
| USAF Research Colleague: | Dr. Thomas J. Moran |
| Date: | August 1, 1980 |
| Contract No: | F49620-79-C-0038 |

# CRACK TIP VELOCITY MEASUREMENTS

# DURING BRITTLE FRACTURE

by

Joseph H. Schmidt

## ABSTRACT

A comprehensive review of the literature concerning elastodynamic stress fields in the crack tip neighborhood of a running crack and methods of measuring crack tip velocities has been conducted. Experiments have been suggested that should answer questions of fundamental importance and give insight to the running crack and its arrest.

ACKNOWLEDGEMENT

The author wishes to express his deep gratitude to the Air Force Systems Command, the Air Force Office of Scientific Research, and the Southeastern Center for Electrical Engineering Education for an enlightening summer at the Materials Laboratory at Wright-Patterson Air Force Base, Ohio. In particular he would like to acknowledge the Nondestructive Evaluation Branch of the AFWAL/Materials Laboratory for its excellent working conditions.

Additional acknowledgements are due Drs. T. Moran and R. Crane for suggesting this area of research and answering many questions. Acknowledgement is extended the technical personnel of the Systems Research Laboratories (SRL) in general and Dr. N. Batra in particular for the design and assembly of ultrasonic test equipment.

## I. INTRODUCTION:

The measurement of crack tip velocity is an important step in verifying the validity of fracture models on which the prediction of failure probability during the service life of structures in general and aircraft structures in particular is based.

This present work is an attempt to measure crack velocities in brittle materials via a technique utilizing high power (on the order of 1 kw) ultrasonics, the ultrasonic ripple technique of Kerkhof, [1-7] and to relate these velocities to crack arrest material parameters. This ultrasonic method resembles fatigue striation techniques and provides an after the fact means of determining crack velocities. Unlike other velocity measurement techniques (eg. high speed photographic and electrical methods), it records the crack front shape (of particular importance in composite fracture studies) and velocities ranging from 1 m/sec to 1600 m/sec. In the process of recording the above information the technique provides a permanent record.

According to Green[1] the technique has been used to measure velocities in silicon, germanium, glass, perspex, tungsten, and magnesium oxide. In addition to the above materials, Clark and Irwin[2] obtained velocity measurements in Hysol 4290, Hysol 4264, Homolite 100, and plexiglas II (polymethylmethacrylate). However, velocity measurements in these later materials remain suspect because of modifications (introduced by Clark and Irwin) in the Kerkhof ultrasonic technique.

## II. OBJECTIVES

The main objective of this work is the establishment and evaluation of the Kerkhof ultrasonic ripple technique in measuring velocities in brittle material. More specific objectives are:

1) A comprehensive review of the running crack problem,
2) A review of crack tip velocity measuring techniques in general and the ultrasonic technique of Kerkhof in particular,
3) The experimental determination of the effects of ultrasonic waves on crack tip stress fields (the result of theoretical investigations of this question are explored in section II), and

4) The identification of parameters, if any, that are involved in crack arrest, and to what extent they are dependent on crack tip velocity and crack length (parameters obtainable by the ultrasonic technique of Kerkhof).

## III. LINEAR ELASTIC FRACTURE MECHANICS

An understanding of linear elastic fracture mechanics (LEFM) should prove helpful in the recognition of important crack initiation and arrest material parameters. Toward this end we shall follow with a brief review of both stationary and running cracks.

For the stationary mode I (opening mode) crack it can be shown[8] that the stresses, $\sigma_{ij}$,

$$\sigma_{ij} = \frac{K_I}{\sqrt{2\pi r}} f_{ij}(\theta) \tag{1}$$

as $r \to 0$ j $i,j \in \{1,2\}$ are the asymototic solutions of the stress fields for the elastostatic problem. Where $(r,\theta)$ are the polar coordinates associated with the two-dimensional or plane problem (see Figure 1) and $K_I$ the static stress intensity factor. The static stress intensity factor, $K_I$ may be obtained through

$$K_I = \lim_{\substack{r \to 0 \\ \theta = 0}} \sigma_y \sqrt{2\pi r} \tag{2}$$

and is dependent upon geometry and loading and independent of coordinate representation.[9] We denote, for the static case, a critical value of $K_I$ after which fracture (failure) occurs as $K_{Ic}$, i.e. fracture occurs whenever $K_I \quad K_{Ic}$. This critical value of stress intensity factor is called the plane strain fracture toughness or critical stress intensity factor, and it is reasonable to assume that it is a material parameter or property.[10] For example, consider the case of a finite length crack of length "a" located in an infinite sheet with loads "$\sigma$" uniformly applied to the sheet at infinity in a direction perpendicular to the plane of the crack. Then, the stress intensity factor is given by[10]

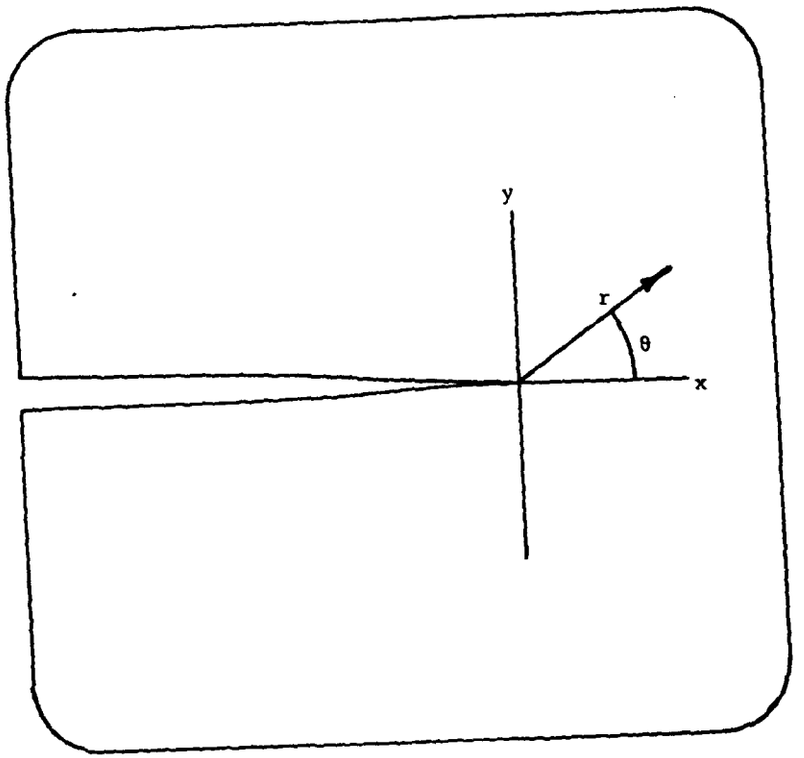



FIGURE 1. CROSS-SECTION OF AN IDEALIZED CRACK

$$K_I = \sigma\sqrt{\pi a}. \tag{3}$$

While for plates of finite width $K_I$ may be written

$$K_I = \sigma\sqrt{\pi a}\ \ f\ (\tfrac{a}{w}) \tag{4}$$

where a and $\sigma$ are as before and $f(\frac{a}{w})$ is determined from elastic analysis.[10,11] For a given crack length, a, $K_{I_c} = \sigma_c\sqrt{\pi a}\ f(a/w)$ may be determined provided f(a/w) is known. Indeed, in principle if f(a/w) is known one could load a specifmen and record the $\sigma_c$ required to initiate fracture.

Experimentally, photoelastic techniques are commonly employed in determining stress intensity factors through isochromatic fringe pattern tilting in problems with a small Barenblatt-Dugdale (failure, cohesive, damage) zone. However, isochromatic fringe pattern tilting effects can be shown[13] to exist due solely to the Barenblatt-Dugdale zone indicating caution should be followed when ignoring the zone. Another method used in obtaining critical stress intensity factors in high toughness materials is the crack opening displacement (COD) concept. In this method the displacements between the crack surfaces are measured and related to a material parameter associated with fracture initiation, viz the critical crack opening displacement.

The elastodynamic state corresponding to the running crack is obtained by solving the equations of motion with appropriate boundary conditions. Broek[14] indicates the crack tip must obtain velocities on the order of one-third of the Rayleigh wave speed in order to appreciably alter the elastodynamic state from a comparable elastostatic state. Clark and Irwin[2] among others, eg. Freund[15], indicate the Rayleigh wave speed is the inertial limitation of the crack speed. Similarly, using energy considerations we may conclude the maximum obtainable crack velocity is that of the Rayleigh wave speed.[3,16,17] These energy balance criteria require the energy rates (internally released and/or externally added) to be greater than the rate of stored and dissipated energies per unit increase of fracture surface. This maximum crack tip velocity should not be confused with supervelocities recorded by Schardin.[7] Schardin found that under some loading conditions secondary fractures may be initiated continuously some distance in front of the crack tip. These secondary cracks give the appearance of a higher

velocity than one would expect. It is this higher velocity that is sometimes called the supervelocity crack speed. The actual crack tip velocity of the running crack is considerably less than the Rayleigh wave speed and we may, therefore, conclude that it is the dampening process rather than the material inertia that is dominant in determining maximum velocity.[2]

In Reference 2, Clark and Irwin use Yoffe's[18] solution for the constant length crack to investigate the problem of a growing crack by requiring $\sigma\sqrt{a}$ to remain constant. Adhering to the accepted definition for dynamic stress intensity factor, viz

$$K_D = \lim_{r \to 0} \sigma_y\sqrt{2\pi r} \qquad \text{along } \theta = 0$$

$\sigma_y$, r as before

(we have here, and will continue to, suppressed the mode I designation as we shall only be concerned with mode I in this work). Clark and Irwin[2] find that the dynamic and static stress intensity factors are the same regardless of velocity except for dynamic unloading effects. As noted in Reference 2 one cannot conclude this result for angles other than $\theta = 0^\circ$. Contrasting the rather mild dependence of dynamic stress intensity factor on velocity recorded by[2], Freund[19] found a rather marked dependence of the dynamic stress intensity factor on velocity for the case of a two dimensional crack in an infinite sheet sufficiently loaded at the boundaries to cause constant crack extension (see Figure 3 of Reference 19). In addition, it can be shown[2,14] that the maximum values of tensile stress for the running crack no longer lie perpendicular to the crack plane as is the case for the stationary crack.

Freund[15,20] finds the form of $K_D$ is given by

$$K_D(vt,v) = \left(\frac{2}{\pi}\right)^{\frac{1}{2}} k(v) \int_0^{vt} (vt - x)^{-\frac{1}{2}} p(x)dx \qquad (5)$$

where p(x) is the normal stress exerted in the damage zone region and v is the crack velocity. Freund concludes that the form of the stress intensity factor for both the opening mode (mode I) and the inplane shear mod (mode II) is given by

$$K_D\left[\ell(t),\ v(t)\right] = k\left[v(t)\right]\ K\left[\ell(t),0\right] \tag{6}$$

where $v(t) = \frac{d}{d_t}\ \ell(t)$ and $K\left[\ell(t),0\right]$ is the static stress intensity factor corresponding to a stationary crack of length $\ell(t)$.

Nilsson[21] shows the angular distribution of the singularity in the neighborhood of the crack tip (moving with arbitrary velocity in an elastic media) is only dependent on the instantaneous crack tip velocity. Nilsson further proves that Freund's relation between stress intensity factor and strain energy release rate is given by[19,21]

$$G = \frac{K_D^2(t)}{2\mu}\quad \frac{\beta_1(\beta_2^2 - 1)}{(1 + \beta_2^2) - 4\beta_1\beta_2} \tag{7}$$

where

$\mu$ is the shear modulus

$\beta_1^2 = 1 - (\frac{\dot{a}(t)}{C_1})^2$

$\beta_2^2 = 1 - (\frac{\dot{a}(t)}{C_2})^2$

$\dot{a}(t)$ is the crack tip velocity

$C_1$ is the dilatational wave speed

$C_2$ is the shear wave speed

G is the dynamic energy released per unit growth, i.e., the dynamic energy release rate.

Carlson et al[22] solve the problem of a cracked infinite strip subjected to uniform boundary displacements $v_o$ and find the form of the stress intensity factor as

$$K_{\infty D} = v_o\ E\left[\ \ \right]_{1,2}\left[(\frac{1}{h})\ \frac{4\beta_1\beta_2 - (1 + \beta_2^2)}{\beta_1(1 - \beta_2^2)}\ \right]^{\frac{1}{2}} \tag{8}$$

where

$$[\ ]_1 = \frac{\sqrt{1 - v}}{(\sqrt{1 - 2v})(1 + v)} \qquad \text{(plane strain)}$$

$$[\ ]_2 = \frac{\sqrt{1 - v}}{(1 - v^2)} \qquad \text{(plane stress)}$$

$2h$ is the strip height

$v$ is the poison's ratio

$E$ is Young's modulus

$\beta_1, \beta_2$ as before.

Carlson et al then assume the following relation between dynamic stress intensity factor and velocity for a finite strip,

$$K_D = \frac{K_{\infty D}}{K_{\infty S}} K_S \qquad (9)$$

where

$K_D$ is the dynamic stress intensity factor for the finite strip

$K_{\infty D}$ as per equation (8)

$K_{\infty S}$ is the static stress intensity factor for the infinite strip and

$K_S$ is the statis stress intensity factor for the finite strip.

Because crack tip velocity appears as a crucial parameter throughout this section we shall now focus attention on a crack tip velocity measuring technique, namely the Kerkhof ultrasonic ripple technique.

## IV. THE KERKHOF ULTRASONIC RIPPLE TECHNIQUE

Of the four major experimental techniques used to measure crack velocities[3] (velocity gages, impedence method, high-speed photography, and ultrasonic) we shall concentrate on the ultrasonic technique of Kerkhof.

The ultrasonic method developed by Kerkhof[4] is a clever application of the well-known Wallner lines, i.e., those lines produced on a running crack surface by wave reflections off of specimen surface imperfections. The Kerkhof ultrasonic ripple technique modifies this rather random phenomena by purposely modulating the specimen surface with a continuous ultrasonic wave of known frequency.[4] Though the beginning of the Kerkhof ultrasonic method lies in Wallner lines, Carlsson et al[22] claim wave reflections are minor significance compared to the induced modulations. In Carlsson's work velocity measurements of 700 m/sec are obtained by the electric impedence method (0.718 $C_2$ --A velocity considerably above the predicted velocity for branching of 0.629 $C_2$) occurred without branching for a running crack in PMMA.

In plexiglas there appears to be no well-defined maximum for crack velocity. This is supported by the works of Carlsson et al[22] and Schardin[7] and is in direct contrast to velocities occurring in more brittle materials, e.g. glass.

The most effective modulation of the crack surface is obtained when the crack surface is modulated by a transverse wave running either perpendicular or parallel to the crack surface.[4-6] In addition, Kuppers[6] proves that the effect of transverse waves on crack tip velocities appears only in higher order terms. In determining the effect of longitudinal ultrasonic waves on crack tip velocities, Kuppers[5,6] employed two ultrasonic waves, one transverse at a frequency of 1 MHz and one longitudinal at a frequency of 160 KHz, on a precut specimen under a tensile load. The transverse and longitudinal waves both modulate the crack surface. Since the higher frequency transverse waves have only secondary effects on the crack tip velocity, any crack tip velocity change is due primarily to the longitudinal wave. Indeed, the frequency of the longitudinal wave can be observed in the experiments (see Figure 2 of Reference 6) conducted by Kuppers. It was found that the longitudinal waves vary the crack tip velocity between 15-30 m/sec. At maximum velocities (approximately 1500 m/sec in glass) the influence of longitudinal waves appears negligible. While Kuppers found definite preferred directions exists for marking with transverse waves (0° and 90° to the plane of the crack, see $\alpha$ in Figure 2) he found longitudinal waves exhibit no such preferred direction.

Kerkhof[4] further shows, for both waves, the crack tip velocity is given by

$$v_b = \frac{1}{\frac{f}{\lambda_b} + \frac{\cos \alpha}{v_{\ell,t}}} \tag{10}$$

where

$f$ is the frequency of the modulating wave

$\lambda_b$ is the wavelength of the surface ripple

$v_{\ell,t}$ is either the longitudinal or transverse ultrasonic wave velocity, and

$\alpha$ is the angle of incidence of the modulating ultrasonic wave as per Figure 2.

Equation (10) reduces to

$$v_b = \frac{\lambda_b}{f} \tag{11}$$

whenever $\alpha = \pm \pi/2$.

Kerkhof[4] also finds

$$v_{b,max} = 2 \frac{\alpha_s}{\rho \bar{r}_o} . \tag{12}$$

where

$\alpha_s$ is the crack surface energy

$\rho$ is the density of the specimen, and

$\bar{r}_o$ is the mean ionic distance,

to be a satisfactory relationship, within 10% of measured velocities, for the greater part of 42 different glasses that were tested. The glass specimen had maximum velocities ranging from 700-2150 m/sec. In contrast,

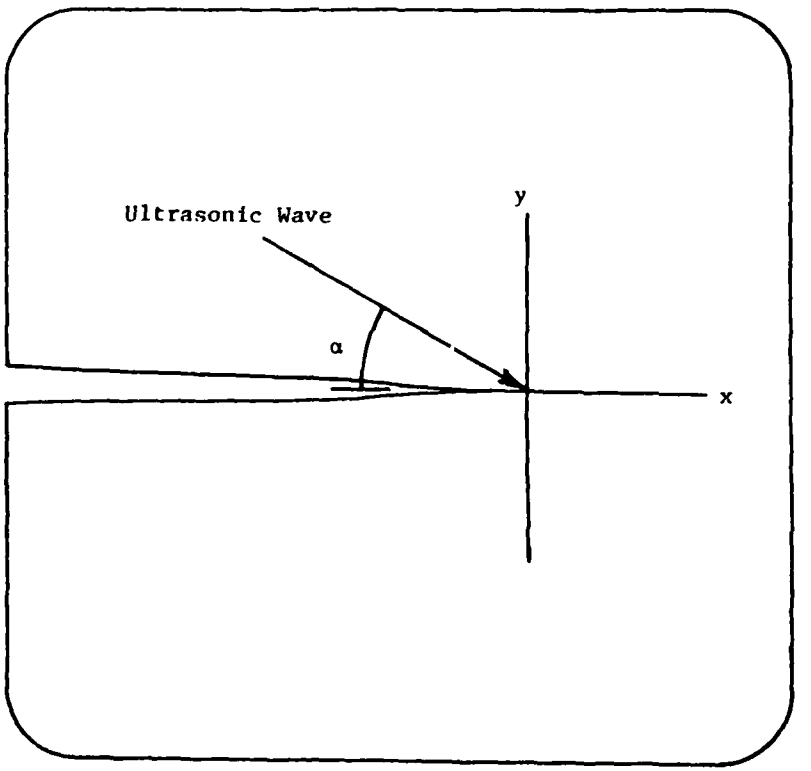



FIGURE 2. A RUNNING CRACK MODULATED BY ULTRASONIC WAVES

Schardin[7] found the maximum velocity in glass to be approximately 1500 m/sec.

The calculations of Kerkhof are based in part on Andersson's work and the Erdogen-Sih criterion that a crack advances in a direction perpendicular to the principle stress direction.[4] As reported by Knauss in the discussion following reference 4, an alternative to the Erdogen-Sih criterion has been suggested by Palaniswany and Knauss based on the maximum energy release rate. In addition, Knauss indicates there are some unfortunate errors in the work of Andersson. However, Knauss argues that these errors are insignificant provided the angle of crack deviation from the main axis is less than 20 degrees.

This summer a water cooled Transducer has been designed and constructed by SRL (Figures 3 and 4). However, due to continued difficulties in obtaining necessary electronic equipment (some orders date back approximately six months) construction of the power supply for the ultrasonic transducer isn't complete.

Ultimately we seek crack arrest mechanisms. To help achieve this goal we shall now turn our attention to crack arrest.

## V. CRACK INSTABILITY AND ARREST

Fracture instability occurs when the strain energy release rate G is greater than the crack resistance R. The excess energy released by the material is converted into dynamic or kinetic energy. This conversion into kinetic energy is manifested through rapid crack growth.

Closely aligned with the idea of maximum crack speed is that of crack bifurcations or branching. Since the strain energy release rate is proportional to crack length; for a constant or slowly increasing crack resistance, the difference between the strain energy release rate and the crack resistance increases with crack size. As the crack tip speed approaches the Rayleigh wave speed, sufficient energy becomes available to support two cracks. At this point two cracks appear, each absorbing part of the available energy. This phenomena is often observed in practice, eg., the shattering of window pane or the exploding of a pressure vessel into many pieces after over pressurization.

On the other hand, suppose a specimen is subjected to constant displacement after crack growth initiates. In many cases, R increases and/or G

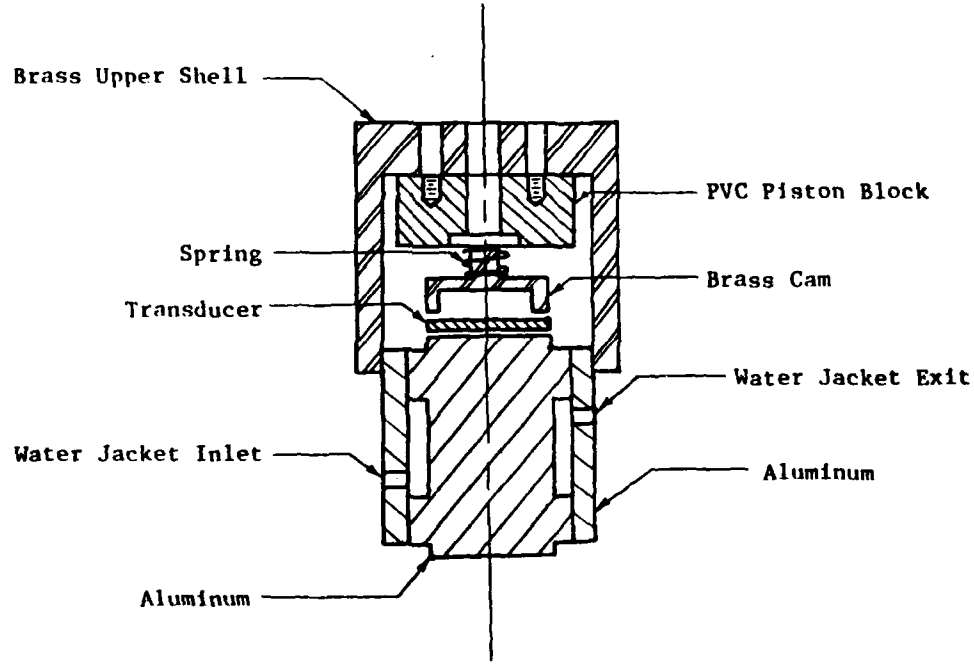
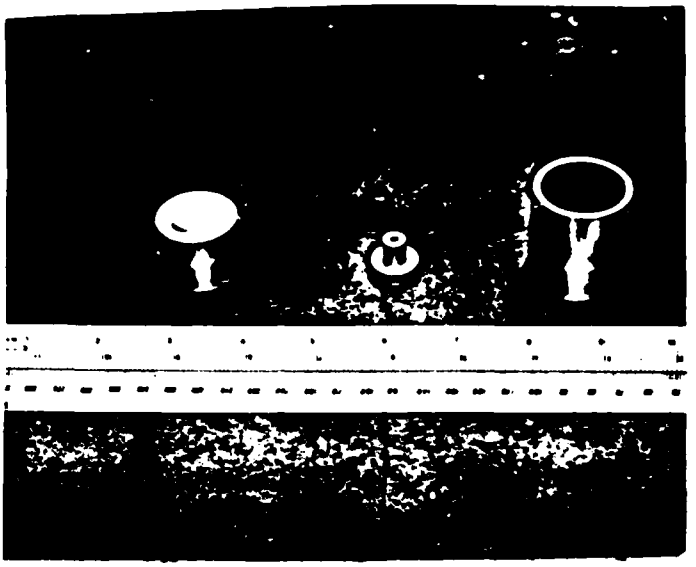
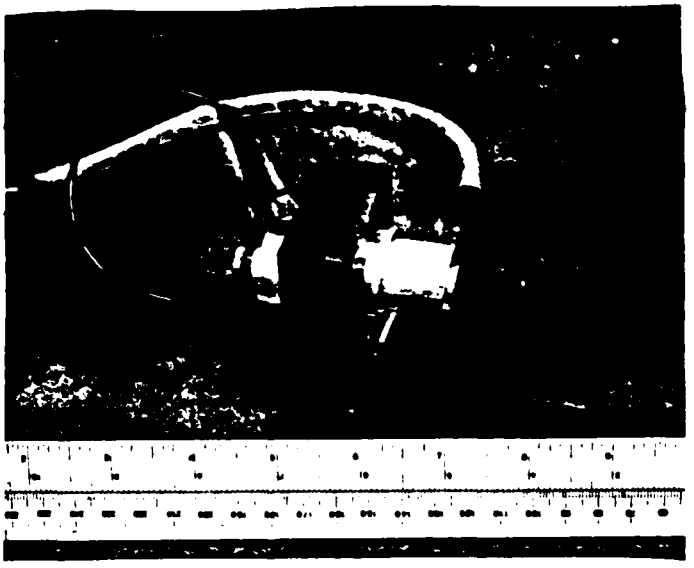



FIGURE 3. TRANSDUCER ASSEMBLY SCHEMATIC



a)



b)

FIGURE 4. a) TRANSDUCER COMPONENTS, b) ASSEMBLED TRANSDUCER

decreases. In any case, G may become smaller than R. G less than R is a necessary but not sufficient condition for crack arrest. Indeed, available kinetic energy may continue to drive the crack as can be seen by a decrease in crack tip velocity. For example, Hahn et al (Reference 26 in Reference 14) has shown that 85 per cent of the kinetic energy associated with a dynamic crack in DCB (double cantilever beam) specimens is consumed as crack driving energy. This leads one to believe, in contrast to the static or stationary crack, there may be no unique arrest value or dynamic fracture toughness property.[14] However, there remains some controversy over the existance of this property.[23]

Since flaws are inherent in most if not all structures, crack arrest mechanisms are in many cases built into structures. A common method of increasing R is through the introduction of heterogeneities as in composite laminates, while one method of reducing stain energy release rate is through crack arrest strips.

There remain other controversies on crack arrest. For example, Schardin[7] found for both glass and plexiglas that no continuous decrease in crack velocity occurs, i.e., the crack abruptly stops. While, in agreement with Schardin's results for polymers (relatively pronounced strain-rate sensitive materials), Clark and Irwin[2] found the ripple markings in glass (a relatively strain-rate in sensitive material) during crack arrest suggests, in appearance, a mathematical limit point.

## VI. RECOMMENDATIONS

Though the applicability of the ultrasonic technique in ceramics has been well established [1-7] there remain some questions as to applicability of the technique in other materials of interest to the Air Force, eg., structural aluminum alloys. It is recommended that tests be conducted on structural aluminum alloys to ascertain applicability of the technique to these alloys. Further, it is suggested that tests be conducted on ceramic specimen using transverse waves of different intensities. This would be used to verify the theoretical results of Kuppers, viz the independence of crack tip velocity on transverse ultrasonic waves. Finally, an investigation of arrest mechanisms in particulate composites by evaluation of crack velocity and shape in the vicinity of particles should be conducted.

## REFERENCES


1. Green, D. J., Ph.D. Thesis, McMasters University, Hamilton (October 1976).

2. Clark, A. B. J. and Irwin, G. R., "Crack-Propagation Behavior," Exp. Mech., 6, January-June, 1966, pp. 321-330.

3. Erdogen, F., "Crack-Propagation Theories," Fracture, An Advanced Treatise, Academic Press, 2, 1968, pp. 497-590.

4. Kerkhof, F., "Wave Fractographic Investigation of Brittle Fracture Dynamics," Proceedings of an International Conference on Dynamic Crack Propagation, G. C. Sig (ed), Noordhoff, 1972, pp. 3-35.

5. Kuppers, H., "The Initial Course on Crack Velocity in Glass Plates," Int. J. Fract., 3, 1967, pp. 13-17.

6. Kuppers, H., "Der Einflub von Ultraschall auf die Bruchgeschwindig keit," Z. Angew. Phys., 20, 1965, pp. 88-92.

7. Schardin, H., "Velocity Effects in Fracture," Fracture, Averbach, Felback, Hahn, and Thomas (ed), John Wiley, 1959, pp. 297-330.

8. Williams, M. L., "On the Stress Distribution at the Base of a Stationary Crack," J. Applied Mech., 24, 1957, pp. 109-114.

9. Paris, P. C. and Sih, G. C., "Stress Analysis of Cracks," Fracture Toughness Testing and its Application, ASTM, STP 381, 1965, pp. 30-83.

10. Caddell, R. M., Deformation and Fracture of Solids, Prentice-Hall, 1980.

11. Tada, H., Paris, P. C., and Irwin, P. C., The Stress Analysis of Cracks Handbook, Del Research Corporation (Hellertown, Penn.), 1973.

12. Kobayashi, A. S., "Photoelastic Studies of Fracture," Fracture, An Advanced Treatise, Academic Press, 3, 1971, pp. 311-369.

13. Schmidt, J. H., Maddux, G. E., and Schapery, R. A., "Some Observations on the Effect of Nonlinearities in Particulate Composites Containing a Large Crack," (Submitted for publication to SESA, 1980).

14. Broek, D., Elementary Engineering Fracture Mechanics, Noordhoff, The Netherlands (1978).

15. Freund, L. B., "The Motion of a Crack in an Elastic Solid Subjected to General Loading," Proceedings of an International Conference on Dynamic Crack Propagation, G. C. Sih (Ed.), Noordhoff (1972), pp.553-562.

16. Baker, B. R., "Dynamic Stresses Created by a Moving Crack," J. Appl. Mech., 29, 1962, pp. 449-458.

17. Craggs, J. W., "On the Propagation of a Crack in an Elastic-brittle Material," J. Mech. Phys. Solids, 8, 1960, pp. 66-75.

18. Yoffe, E. H., "The Moving Griffth Cracks," Phil. Mag., 42, 1951, pp. 739-750.

19. Freund, L. B., "Crack Propagation in an Elastic Solid Subjected to General Loading--I. Constant Rate of Extension," J. Mech. Phys. Solids, 20, 1972, pp. 129-140.

20. Freund, L. B., "The Analysis of Elastodynamic Crack Tip Stress Fields," Mechanics Today, III, S. Nemat-Nasser (ed.), Pergamon, New York (1976), pp. 55-91.

21. Nilsson, F., "A Note on the Stress Singularity at a Non-uniformly Moving Crack Tip," J. of Elasticity, 4 No. 1, 1974, pp. 73-75.

22. Carlsson, J., Dahlberg, L., and Nilsson, F., "Experimental Studies of the Unstable Phase of Crack Propagation in Metals and Polymers," Proceedings of an International Conference on Dynamic Crack Propagation, G. C. Sih (ed.), Noordhoff, 1972, pp. 663-677.

23. "Response of Metals and Metallic Structures to Dynamic Loadings," National Materials Advisory Board, NMAB-341, National Academy of Sciences (Washington, DC) 1978.

1980 USAF - SCEEE SUMMER FACULTY RESEARCH PROGRAM

Sponsored by the

AIR FORCE OFFICE OF SCIENTIFIC RESEARCH

Conducted by the

SOUTHEASTERN CENTER FOR ELECTRICAL ENGINEERING EDUCATION

FINAL REPORT

# PRODUCTS OF FUZZY SUBGROUPS


Prepared by: Dr. Howard Sherwood

Academic Rank: Professor

Department and University: Department of Mathematics and Statistics, University of Central Florida

Research Location: Frank J. Seiler Research Laboratory, USAF Academy, CO 80840

USAF Research Colleague: Captain James D. Ledbetter



Date: August 22, 1980

Contract No: F49620-79-C-0038

# PRODUCTS OF FUZZY SUBGROUPS

by

H. Sherwood

## ABSTRACT

Products of fuzzy subgroups are defined and investigated. Some expected results are proved: the product of fuzzy subgroups is a fuzzy subgroup; products with the same, but permuted, factors are isomorphic; there is a natural isomorphism from any factor into the product. Functions called t-norms, are used to construct products of fuzzy subgroups--different t-norms giving rise to different products. A fuzzy subgroup must satisfy, among other things, a certain inequality; the strength of that inequality is important. Results are given relating the t-norm used in forming the product to the strength of the ensuing inequality. Some results indicate when a fuzzy subgroup can be expressed as a product of simpler ones. Suggestions are made for further research and a possible area of application to an important aspect of pattern recognition.

## Acknowledgement

The author would like to thank the Air Force Systems Command, the Air Force Office of Scientific Research and the Southeastern Center for Electrical Engineering Education for giving him the privilege of spending a very rewarding summer at the Frank J. Seiler Research Laboratory, USAF Academy, CO. He would like to thank the personnel of the laboratory for their warm hospitality.

He would like to thank Major R. Warren Langley and Major Richard Evans and his wife, Mary, for their kindnesses, Major Roger Salters for stimulating discussions, and Captain James Ledbetter for valuable suggestions, words of encouragement and assistance with this report.

Finally, he would like to thank his family for the personal sacrifices each made to join him for the summer. In particular he wants to thank his wife, Joan, for her continual support and his daughter, Gwen, for her excellent typing assistance.

## I. INTRODUCTION:

Pattern recognition is an important discipline as evidenced by the diversity of its users and contributors including biologists, climatologists, computer scientists, doctors, engineers, mathematicians, physicists, psychologists, statisticians, etc. Since it plays a central role in developing the intelligent image processing capabilities of electro-optical trackers, pattern recognition takes on special importance to the Air Force.

The fuzzy set theory of L. A. Zadeh[1] is finding application to various problems of pattern recognition.[2,3,4,5] Whenever the patterns of interest possess exact descriptions, the recognition problem becomes much easier. Unfortunately, that ideal is rarely available in any real physical situation. In fact the patterns are usually nondeterministic--not merely random but possessing intrinsic ambiguity (or fuzziness). An appropriate nondeterministic model will take into account not only the randomness but this intrinsic ambiguity as well. This observation helps explain the increasing interest in the fuzzy set approach to various aspects of the pattern recognition problem.

A. Rosenfeld, who has made significant contributions in picture processing[6] and pattern recognition,[3] has also applied the fuzzy set concept to generalize some of the basic concepts of group theory.[7] Others continue to develop the notion of a fuzzy subgroup. In a recent paper,[8] J. M. Anthony and this author applied fuzzy subgroups to an abstract recognition problem. These ties between pattern recognition and fuzzy sets motivate further study of the structure of fuzzy subgroups and their possible application to various aspects of the pattern recognition problem.

## II. OBJECTIVES:

The broad objective of this project was to provide mathematical support for developing pattern recognition concepts to further advance image processing capabilities of electro-optical trackers. To do this, two more-specific objectives were identified.

The desire for a better understanding of fuzzy subgroups motivated the first of these objectives. Since people understand a complicated structure better when they see how it is built from simpler structures, our first objective was to determine when complicated fuzzy subgroups can be expressed as products of simpler ones. Our previous background in both fuzzy subgroups and ordinary groups led us to restrict the problem to an important class of fuzzy subgroups leaving the general problem for future investigation.

The general pattern recognition problem is usually divided into various aspects such as measurement, segmentation, feature selection and classification. The second objective of this project was to become acquainted with these aspects and identify possible applications of fuzzy subgroups to the pattern recognition problem.

## III. PRELIMINARIES:

Some definitions, background information and notational conventions are needed before the results of the project and the methods used can be presented. Some of the proofs are straightforward and are, therefore, omitted entirely. For other proofs, an outline or a short discussion of the method will be provided but not all the details will be given (see reference 11 for more details).

Definition 3.1. A t-norm is a function $T: [0,1]\times[0,1]\to[0,1]$ satisfying, for each $\varepsilon$, $\lambda$, $\xi$, $\eta$ in $[0,1]$,

$$T(\lambda,1) = \lambda = T(1,\lambda); \tag{1}$$

$$T(\varepsilon,\lambda) \leq T(\xi,\eta), \text{ if } \varepsilon \leq \xi \text{ and } \lambda \leq \eta; \tag{2}$$

$$T(\varepsilon,\lambda) = T(\lambda,\varepsilon); \tag{3}$$

$$T(\varepsilon, T(\lambda,\xi)) = T(T(\varepsilon,\lambda),\xi). \tag{4}$$

B. Schweizer and A. Sklar[9] introduced t-norms to generalize the metric triangle inequality into the setting of probabilistic metric spaces. The only specific t-norms needed in the report are Z and M defined by

$$Z(x,y) = \begin{cases} x, & \text{if } x \in [0,1] \text{ and } y = 1, \\ y, & \text{if } x = 1 \text{ and } y \in [0,1], \\ 0, & \text{if } x \in [0,1) \text{ and } y \in [0,1), \end{cases} \tag{5}$$

and

$$M(x,y) = \begin{cases} x, & \text{if } 0 \leq x \leq y \leq 1, \\ y, & \text{if } 0 \leq y \leq x \leq 1. \end{cases} \tag{6}$$

Definition 3.2. Let T' and T be t-norms. T' is <u>stronger than</u> T ($T' \geq T$) if $T'(x,y) \geq T(x,y)$ for all x,y in [0,1]. T' <u>dominates</u> T ($T' >> T$) if, for all a, b, c, d in [0,1],

$$T'(T(a,b),T(c,d)) \geq T(T'(a,c),T'(b,d)). \tag{7}$$

Some discussion of the relations defined above is appropriate. Schweizer and Sklar[9] introduced the "stronger than" relation and proved that for any t-norm T, $M \geq T \geq Z$. The term "dominates" is used in a different but related context by R. M. Tardiff.[10] His relation is between triangle functions which are mappings similar to t-norms defined on pairs of distribution functions rather than pairs of numbers. He needed his relation to discuss products of probabilistic metric spaces; we need our relation to discuss products of fuzzy subgroups. Finally, it is easy to show that for any t-norm T, $M >> T >> T >> Z$.

Since any t-norm, T, is associative, for any sequence $\{x_i\}$ in [0,1], the n-fold product $T(x_1,x_2,\ldots,x_n)$ is well defined. For example, $T(x_1,x_2,x_3)$ means the common value $T(T(x_1,x_2),x_3) = T(x_1,T(x_2,x_3))$.

Throughout this report G (with or without a subscript) always denotes a group whose operation is suppressed and indicated by juxtaposition. The symbol e ($e_i$) denotes the identity in G ($G_i$).

For any x in G, <x> denotes the subgroup generated by x. If H and K are subsets of G the HK denotes the set of all possible products hk with h in H and k in K.

Definition 3.3. A function $\mu$: G → [0,1] is a fuzzy subgroup (briefly, a FS) of G if there is a t-norm T such that for all x,y in G,

$$\mu(xy) \geq T(\mu x, \mu y), \tag{8}$$

$$\mu(x^{-1}) = \mu(x), \tag{9}$$

$$\mu(e) = 1. \tag{10}$$

If for some reason we want to refer to the t-norm, we say $\mu$ is a FS of G under T; otherwise, we merely say $\mu$ is a FS of G.

This definition of a fuzzy subgroup is a modification[8] of the one given by A. Rosenfeld.[7] In condition (8) he used M instead of allowing for the use of any t-norm. Moreover, he did not require condition (10). *

Definition 3.4. For i = 1 or 2, let $\mu_i$ be a FS of $G_i$. If there is a group isomorphism $\phi$ from $G_1$ onto $G_2$ such that $\mu_1 = \mu_2 \circ \phi$, then we say $\mu_1$ and $\mu_2$ are isomorphic.

The following two theorems are needed to obtain some of the results given in the later sections of this report. Since their proofs are straightforward, they are omitted.

Theorem 3.5. If H is a subgroup of G, $\mu$ is a FS of G under T, and $\eta$ is the restriction of $\mu$ to H, then $\eta$ is a FS of H under T.

---

* On 7 August 1980, this author received referee's comments on a paper[8] submitted to the International Journal for Fuzzy Sets and Systems telling him that '... the generalization of fuzzy subgroups, by considering other operations in [0,1] than "min," was first done by Negoita and Ralescu in their book "Applications of fuzzy sets to systems analysis," Halsted Press, New York, 1975.' Time constraints and unavailability of the book have prevented the author from verifying this source, so he did not feel free to cite it directly.

Theorem 3.6. If $\phi$ is an isomorphism from $G_1$ onto $G_2$ and $\mu_2$ is a FS of $G_2$ under T, then $\mu_1 = \mu_2 \circ \phi$ is a FS of $G_1$ under T.

IV. PROPERTIES OF PRODUCTS:

Definition 4.1. For each i = 1,2,...,n, let $\mu_i$ be a FS of $G_i$. Let T' be a t-norm. The T'-product of $\mu_i$ (i = 1,2,...,n) is the function $\mu_1 \times \mu_2 \times \ldots \times \mu_n$ defined on $G_1 \times G_2 \times \ldots \times G_n$ given by

$$\mu_1 \times \mu_2 \times \ldots \times \mu_n(x_1, x_2, \ldots, x_n) = T'(\mu_1 x_1, \mu_2 x_2, \ldots, \mu_n x_n). \qquad (11)$$

Theorem 4.2. For each i = 1,2,...,n, let $\mu_i$ be a FS of $G_i$. Then,

(1) $\mu_1 \times \mu_2 \times \ldots \times \mu_n$ is a FS of $G_1 \times G_2 \times \ldots \times G_n$ under Z;

(2) $\mu_1 \times \mu_2 \times \ldots \times \mu_n$ is isomorphic to $\mu_{k(1)} \times \mu_{k(2)} \times \ldots \times \mu_{k(n)}$ for any permutation k on {1,2,...,n};

(3) The natural map $\phi_i$: $G_i \to G_1 \times G_2 \times \ldots \times G_n$ given by $\phi_i(x) = (e_1, \ldots, e_{i-1}, x, e_{i+1}, \ldots, e_n)$ is an isomorphism between $\mu_i$ and the restriction of $\mu_1 \times \mu_2 \times \ldots \times \mu_n$ to the range of $\phi_i$.

Once it is observed that every t-norm is stronger than Z, the proof of part (1) of this theorem follows directly from Definitions 3.3 and 4.1.

If k is a permutation on {1,2,...,n}, then the mapping $\phi$ from $G_1 \times \ldots \times G_n$ onto $G_{k(1)} \times \ldots \times G_{k(n)}$, defined by

$$\phi(x_1, \ldots, x_n) = (x_{k(1)}, \ldots, x_{k(n)}),$$

is a group isomorphism. The commutativity and associativity of T' guarantee that

$$(\mu_{k(1)} \times \ldots \times \mu_{k(n)}) \circ \phi = \mu_1 \times \ldots \times \mu_n.$$

An application of Definition 3.4 yields the result of part (2).

To verify part (3) it suffices to observe that $\phi_i$ is a group isomorphism from $G_i$ onto the range of $\phi_i$ and $\mu_1 \times \ldots \times \mu_n \circ \phi_i = \mu_i$.

Since $Z(a,b) = 0$ unless $a = 1$ or $b = 1$, the inequality (1) of Definition 3.3 gives no information about $\mu(xy)$ unless $\mu(x) = 1$ or $\mu(y) = 1$. In fact, for greatest information, we would like to have the T in that inequality be as strong as possible. In Theorem 4.2 (1) the strongest t-norm we could justify was Z. If all the $\mu_i$ were fuzzy subgroups under the same T we would hope that the T'-product would also be a FS under T. These observations motivate the next result.

Theorem 4.3. Suppose, for each $i = 1,2,\ldots,n$, $\mu_i$ is a FS of $G_i$ under the t-norm T. Suppose T' is a t-norm which dominates T. Then, the T'-product $\mu_1 \chi \ldots \chi \mu_n$ is a FS of $G = G_1 \chi \ldots \chi G_n$ under T.

To prove this, let $(x_1,\ldots,x_n)$, $(y_1,\ldots,y_n)$ be elements of G. Then, since each $\mu_i$ is a FS of $G_i$ and T' is nondecreasing in each place,

$$\mu_1 \chi \ldots \chi \mu_n((x_1,\ldots,x_n)(y_1,\ldots,y_n))$$

$$= \mu_1 \chi \ldots \chi \mu_n(x_1y_1,\ldots,x_ny_n)$$

$$= T'(\mu_1(x_1y_1),\ldots,\mu_n(x_ny_n))$$

$$\geq T'(T(\mu_1x_1,\mu_1y_1),\ldots,T(\mu_nx_n,\mu_ny_n)).$$

An easy induction argument using (7) shows that

$$T'(T(\mu_1x_1,\mu_1y_1),\ldots,T(\mu_nx_n,\mu_ny_n))$$

$$\geq T(T'(\mu_1x_1,\ldots,\mu_nx_n),T'(\mu_1y_1,\ldots,\mu_ny_n)).$$

These two inequalities and the definition of the T'-product yield

$$\mu_1 \chi \ldots \chi \mu_n((x_1,\ldots,x_n)(y_1,\ldots,y_n))$$

$$\geq T(T'(\mu_1x_1,\ldots,\mu_nx_n),T'(\mu_1y_1,\ldots,\mu_ny_n))$$

$$= T(\mu_1 \chi \ldots \chi \mu_n(x_1,\ldots,x_n),\mu_1 \chi \ldots \chi \mu_n(y_1,\ldots,y_n)).$$

Thus $\mu_1 \chi \ldots \chi \mu_n$ satisfies (8) under T. It is easy to verify that conditions (9) and (10) are satisfied.

Corollary 4.4. Suppose $\mu_i$ is a FS of $G_i$, for each i = 1,2,...,n, under the t-norm, T. The T'-product of $\mu_1,\ldots,\mu_n$ is a FS of $G_1 \chi \ldots \chi G_n$ if T' = T or T' = M or T = Z.

This follows from the preceding theorem and the observation that T >> T, M >> T and T' >> Z.

The following example shows that Theorem 4.3 is best-possible in the sense that if T' does not dominate T, then there are groups $G_1$ and $G_2$ having fuzzy subgroups $\mu_1$ and $\mu_2$ under T whose T'-product is not a FS of $G_1 \chi G_2$ under T.

Example 4.5. Suppose T' does not dominate T. Then there exist $a_1$, $b_1$, $a_2$, $b_2$ such that

$$T'(T(a_1,b_1),T(a_2,b_2)) < T(T'(a_1,a_2),T'(b_1,b_2)).$$

Let $G_1 = G_2 = \{e,x,y,z\}$ be the group with four elements such that $x^2 = y^2 = z^2 = e$. For i = 1 or 2, define $\mu_i$ on $G_i$ via $\mu_i(e) = 1$, $\mu_i(x) = a_i$, $\mu_i(y) = b_i$ and $\mu_i(z) = T(a_i,b_i)$. Verifying that $\mu_i$ is a FS of $G_i$ is easy. Moreover, it is straightforward to verify that

$$\mu_1 \chi \mu_2((x,x)(y,y)) < T(\mu_1 \chi \mu_2(x,x),\mu_1 \chi \mu_2(y,y));$$

so $\mu_1 \chi \mu_2$ is not a FS of $G_1 \chi G_2$ under T.

## V. FUZZY SUBGROUPS AS PRODUCTS:

The well-known fundamental theorem of finite abelian groups states that any finite abelian group can be written as a direct product of cyclic groups of prime power orders. Since any ordinary subgroup of a finite abelian group is again a finite abelian group, it can also be expressed as a direct product of cyclic groups of prime power orders. Can every FS of a finite abelian group be written as a direct product of fuzzy subgroups of cyclic subgroups of prime power orders? This section addresses this question in the context of fuzzy subgroups under M.

Theorem 5.1. Every fuzzy subgroup under M of a direct product of a finite number of cyclic groups of distinct prime power orders can be written as an M-product of fuzzy subgroups of those cyclic groups.

To prove this theorem, let $n_1,n_2,\ldots,n_k$ be positive integers, let $p_1,p_2,\ldots,p_k$ be distinct primes, and let each $G_i$ be the cyclic group whose order is the $n_i^{th}$ power of $p_i$. Suppose $\mu$ is a FS of $F = G_1 \chi \ldots \chi G_k$ under M. For each $j = 1,2,\ldots,k$, define $\mu_j$ via

$$\mu_j(a) = \mu(e_1,e_2,\ldots,e_{j-1},a,e_{j+1},\ldots,e_k)$$

for each a in $G_j$. It can be shown that each $\mu_j$ is a FS of $G_j$ under M and $\mu = \mu_1 \chi \ldots \chi \mu_k$, i.e., for each $(a_1,a_2,\ldots,a_k)$ in G,

$$\mu(a_1,a_2,\ldots,a_k) = M(\mu_1 a_1,\mu_2 a_2,\ldots,\mu_k a_k).$$

To show that $\mu = \mu_1 \chi \ldots \chi \mu_k$ two previous results are used. The first of these says that every FS under M is subgroup generated.[8] The second is the well-known result that every subgroup of a finite cyclic group is cyclic, the order of the subgroup divides the order of the group, and there is exactly one subgroup of each order dividing the order of the group.[12]

The following example shows that any attempt to remove the requirement of distinct primes is doomed if the $\mu_j$ are chosen in the manner suggested in the proof of the preceding theorem.

Example 5.2. Let $G_1 = G_2 = \{-1,1\}$ be the multiplicative group of order two. Let $G = G_1 \chi G_2$. Define $\mu$ via $\mu(1,1) = 1$, $\mu(-1,-1) = 2/3$, and $\mu(1,-1) = \mu(-1,1) = 1/3$. It is easy to verify that $\mu$ is a FS of G under M. Let $\mu_1$ and $\mu_2$ be obtained as in the proof of Theorem 3.1. Then $\mu_i(1) = 1$ and $\mu_i(-1) = 1/3$. Thus $\mu$ is not an M-product of $\mu_1$ and $\mu_2$ because $\mu(-1,-1)$ is strictly larger than $M(\mu_1(-1),\mu_2(-1))$.

In order to prove the next theorem, a lemma is needed. The proof of the lemma is omitted because it is a straightforward modification (using the Hausdorff Maximal Principle) of the proof of a theorem of Anthony and Sherwood.[8]

Lemma 5.3. Suppose $\mu$ is a FS of G under M. Let C be the collection of all subgroups of G. There is a maximal nest L (i.e., L is a subset of C, it is linearly ordered by set inclusion, and there is no other such subset of C which properly contains L) in C and a measure m on a $\sigma$-algebra of subsets of L such that for all x in G,

$$\mu(x) = m\{S \in L: x \in S\}. \tag{12}$$

Theorem 5.4. Let p be a prime and, for each $i = 1,2,\ldots,k$, let $G_i$ be the cyclic group of order p. Let $G = G_1 \times \ldots \times G_k$ and let $\mu$ be a FS of G under M. Then, for each $i = 1,2,\ldots,k$, there is a FS, $\mu_i$, of the cyclic group of order p under M such that $\mu$ is isomorphic to the M-product, $\mu_1 \times \mu_2 \times \ldots \times \mu_k$.

The proof of Theorem 5.4 uses Lemma 5.3 to obtain a maximal nest L in the collection of all subgroups of G and a measure m on a $\sigma$-algebra of subsets of L such that, for all x in G, equation (12) is satisfied. This collection L can be shown to be of the form $L = \{S_0, S_1, \ldots, S_k\}$ where for each $i = 1,2,\ldots,k$,

$$S_i = S_{i-1}\langle a_i \rangle = \langle a_1 \rangle \langle a_2 \rangle \cdots \langle a_i \rangle$$

and each $a_j$ is chosen to be any element of $S_j - S_{j-1}$. From this it follows that for each i, $S_i \subset S_{i+1}$ so that

$$\mu(x) = \begin{cases} 1, & \text{if } x \in S_0, \\ m\{S_i, S_{i+1}, \ldots, S_k\}, & \text{if } x \in S_i - S_{i-1}. \end{cases}$$

For each i, define $\mu_i$ on $\langle a_i \rangle$ via $\mu_i(x) = \mu(x)$. By Theorem 3.5, each $\mu_i$ is a FS of $\langle a_i \rangle$ under M. Next, define $\phi$ on $H = \langle a_1 \rangle \times \ldots \times \langle a_k \rangle$ via

$$\phi(x_1, \ldots, x_k) = x_1 \cdots x_k.$$

Then $\phi$ is a group isomorphism from H onto G and, from Tneorem 3.6,

it follows that $\eta = \mu \circ \phi$ is a FS of H. The proof is completed by showing that $\eta$ is the M-product of $\mu_1, \mu_2, \ldots, \mu_k$.

Will the result of Theorem 5.4 still be true if the requirement that $G_i$ has order p be relaxed to require instead that its order be merely some power of p? The following example answers this question negatively.

Example 5.5. Let G be the abelian group of order 32 generated by a and b where a and b have orders 8 and 4, respectively. Let C be the set of all subgroups of G. Let $S_0 = \langle e \rangle$, $S_1 = \langle a^4 b^2 \rangle$, $S_2 = \langle a^4 b^2 \rangle \langle a^4 \rangle$, $S_3 = \langle a^4 b^2 \rangle \langle a^4 \rangle \langle b \rangle$, $S_4 = \langle a^4 b^2 \rangle \langle a^4 \rangle \langle b \rangle \langle a^2 \rangle$, and $S_5 = G$. Let $L = \{S_0, S_1, \ldots, S_5\}$ and define m on the power set of C such that

$$m\{S\} = \begin{cases} 1/6, & \text{if } S \in L, \\ 0, & \text{if } S \notin C\text{-}L. \end{cases}$$

Notice that L is linearly ordered by set inclusion and m(L) = 1. Anthony and Sherwood[8] showed that under these conditions the function $\mu$ defined on G via $\mu(x) = m\{S \in C: x \in S\}$ is a FS of G under M.

The FS $\mu$ of G is not isomorphic to an M-direct product of fuzzy subgroups with prime power orders. To verify this claim is tedious, so, the details will be omitted. It is well-known[12] that any direct product of cyclic groups which is isomorphic to G can be realized as an internal direct product of subgroups of G; moreover, one of the factors has order 8 and the other has order 4.

To show that $\mu$ is not an M-product of the desired sort, it suffices to show that whenever x and y are elements of orders 8 and 4, respectively, such that $\langle x \rangle \cap \langle y \rangle = \langle e \rangle$ and $G = \langle x \rangle \langle y \rangle$, then $\mu(uv)$ is strictly larger than $M(\mu u, \mu v)$ for some u in $\langle x \rangle$ and some v in $\langle y \rangle$. As mentioned above the details are tedious and, therefore, omitted.

This example shows that not every FS of a finite abelian group under M can be written as an M-direct product of fuzzy

subgroups of cyclic groups of prime power orders. In fact it says even more. Since M is the strongest t-norm it shows that some fuzzy subgroups of finite abelian groups cannot be expressed as a t-product for any t-norm, T.

This example is interesting from another standpoint as well. Experience in probabilistic metric spaces indicates that results in ordinary metric spaces seem to carry over directly to those probabilistic metric spaces in which the triangle inequality is stated in terms of the t-norm, M, while for other t-norms there seems to be a departure from the ordinary metric properties. However, in the realm of fuzzy subgroups this phenomenon does not prevail; for our example was a FS under M, and already the ordinary group property did not carry over.

Theorem 5.6. Let $G = G_1G_2\cdots G_k$ be an internal direct product of subgroups $G_1,G_2,\ldots,G_k$. Let $\mu$ be a FS of G under T, and for each $i = 1,2,\ldots,k$, let $\mu_i$ be the restriction of $\mu$ to $G_i$. Let $\mu_1 \curlywedge \ldots \curlywedge \mu_k$ be the T-product of $\mu_1,\ldots,\mu_k$. Then $\mu(x) > \mu_1 \curlywedge \ldots \curlywedge \mu_k(x_1,\ldots,x_k)$ for any $x = x_1\cdots x_k$ where each $x_i \quad G_i$.

To verify this result, let $x = x_1\cdots x_k$ where each $x_i \in G_i$. From the associativity of T and repeated applications of condition (8), it follows that

$$\mu(x_1\cdots x_k) \geq T(\mu x_1,\ldots,\mu x_k)$$
$$= T(\mu_1 x_1,\ldots,\mu_k x_k) = \mu_1 \curlywedge \cdots \curlywedge \mu_k(x_1,\ldots,x_k).$$

The result of Theorem 5.6 deals with an arbitrary group written as a direct product of a finite number of subgroups. The result is interesting because it shows that even though $\mu$ may not actually be a T'-product of its restrictions to the factors of G, it is greater than or equal to the t-product of those restrictions.

VI. RECOMMENDATIONS:

The dominates relation characterized by (7) should be studied. Not only does that relation promise to play a central role in constructing products of fuzzy subgroups but its importance extends well beyond. To see this, consider the following:

"If $(X_1,d_1)$ and $(X_2,d_2)$ are metric spaces, then in order to define a well-behaved metric on the Cartesian product of $X_1$ and $X_2$ a two place function f mapping $R^+ \times R^+ \to R^+$ is required which satisfies the following properties:

(1) $f(a,0) = a$,

(2) $f(a,b) = f(b,a)$,

(3) $f(a,b) \geq f(c,b)$ whenever $a \geq c$,

(4) $f(a,f(b,c)) = f(f(a,b),c)$,

(5) $f(a_1+ b_1,a_2+ b_2) \leq f(a_1,a_2) + f(b_1,b_2)$.

Note that condition (5) states that f dominates addition. In particular if $f(a,b) = (a^p+ b^p)^{1/p}$, $p > 1$, then (5) is the familiar Minkowski Inequality."[10]

The dominates relation was the condition which yielded Theorem 4.5. Next, Theorem 5.6 says, under reasonable technical conditions, that if a fuzzy subgroup under T can be written as a T'-product then T' is stronger than T. Moreover, whenever $T' >> T$, then $T' \geq T$. Deciding whether $T' \geq T$ is much easier than deciding whether $T' >> T$. All these considerations motivate the following question: could these two relations on t-norms actually be the same? If so, that result should be established; if not, perhaps an additional condition could be imposed which in the presence of $T' \geq T$ would imply $T' >> T$.

I would propose to conduct this study by first considering a one-parameter family of t-norms which are linearly ordered by the stronger than relation to see if the order is preserved by the dominates relation. These studies should lead to further insight concerning the dominates relation and its connection with the stronger than relation.

Finally, comments should be made about possible applications to pattern recognition. The ties between fuzzy subgroups and any

real pattern recognition problems are, frankly, still quite tenuous. One aspect of the pattern recognition problem which may lend itself to modeling by fuzzy subgroups is the selection of an optimal set of feature vectors to describe images. If a fuzzy subgroup can model the set of possible feature vectors, then the decomposition of that fuzzy subgroup into simpler ones may lead to a means of selecting an optimal set of feature vectors.

## REFERENCES


1. L. A. Zadeh, "Fuzzy Sets," Inform. Control, Vol. 8, pp. 338-353, 1965.

2. M. G. Thomason, "Finite Fuzzy Automata, Regular Fuzzy Languages, and Pattern Recognition," Pattern Recognition, Vol. 5, pp. 383-390, 1973.

3. K. S. Fu, Digital Pattern Recognition, (Springer-Verlag, Berlin, Heidelberg, New York, 1976), p. 70.

4. A. Kumar, "A Real-time System for Pattern Recognition of Human Sleep Stages by Fuzzy System Analysis," Pattern Recognition, Vol. 9, pp. 43-46, 1977.

5. S. K. Pal and D. D. Majumder, "Fuzzy Sets and Decision-making Approaches in Vowel and Speaker Recognition," IEEE Trans. on Syst., Man, and Cyber., Vol. SMC 7, pp. 625-629, 1977.

6. A. Rosenfeld, Picture Processing by Computer, (Academic Press, New York, London, 1969).

7. A. Rosenfeld, "Fuzzy Groups," J. of Math. Anal. and Appl., Vol. 35, pp. 512-517, 1971.

8. J. M. Anthony and H. Sherwood, "The Structure of Fuzzy Subgroups," submitted to Inter. J. for Fuzzy Sets and Systems.

9. B. Schweizer and A. Sklar, "Statistical Metric Spaces," Pacific J. Math., Vol. 10, pp. 313-334, 1960.

10. R. M. Tardiff, "Topologies for Probabilistic Metric Spaces," Pacific J. Math., Vol. 65, pp. 233-251, 1976.

11. H. Sherwood, "Products of Fuzzy Subgroups," to be submitted to Inter. J. for Fuzzy Sets and Systems.

12. M. Hall, Jr., The Theory of Groups, (The Macmillan Company, New York, 1959), pp. 35, 41.

1980 USAF - SCEEE SUMMER FACULTY RESEARCH PROGRAM

Sponsored by the

AIR FORCE OFFICE OF SCIENTIFIC RESEARCH

Conducted by the

SOUTHEASTERN CENTER FOR ELECTRICAL ENGINEERING EDUCATION

FINAL REPORT

# Characterization of Quasi-Correlated Mux Bus Traffic in a Guided Weapon


Prepared by: J.B. Sinclair

Academic Rank: Assistant Professor

Department and University: Department of Electrical Engineering, Rice University

Research Location: Digital Technology Laboratory, AFATL/DLMM, Eglin AFB, Florida



Date: 2 August 1980

Contract No: F49620-79-C-0038

# Characterization of Quasi-Correlated Mux Bus Traffic in a Guided Weapon

by

J.B. Sinclair

## ABSTRACT

The characteristics of message traffic in a guided weapon featuring several federated processors communicating over a single time-multiplexed serial bus are analyzed. Data latency is of major concern, especially for weapon systems in which control loop information is transmitted on the bus. Message traffic is periodic in nature, and there is significant correlation between the transmissions of various messages. Three different line protocols are considered. Difficulties in achieving interprocessor synchronization may limit the effectiveness of a pure command-response protocol. Preliminary results from simulations of MIL-STD-1765 (proposed) and MIL-STD-1553B utilized in a dynamic bus allocation mode are presented, using an air-to-surface missile as a model of a typical application.

## ACKNOWLEDGMENTS

This research has been sponsored by the Air Force Systems Command, the Air Force Office of Scientific Research, and the Air Force Armament Laboratory, Eglin AFB, Florida. The author would like to thank the Southeastern Center for Electrical Engineering Education for the opportunity to spend a very interesting and rewarding summer at the Armament Laboratory. He would like also to express his appreciation to the Armament Laboratory and especially to the Mid-Course Guidance Branch for the hospitality he experienced. Finally, he would like to thank Dr. J.W. Jones and the rest of the Digital Technology Team for their help in formulating this research and for their invaluable aid and guidance during the summer.

## 1. INTRODUCTION

Modern guided weapon systems are increasingly relying on on-board computer systems to perform a variety of functions, including navigation, guidance, target seeking, stores management, and autopilot. The increased reliance is accompanied by greater demands on the computational capabilities of the computer system, while the missile environment dictates a number of constraints within which the designer must work. Several options have been considered for meeting these computational demands [1]. These are:

(1) a single, centralized computing element, connected directly to each of the various subsystems of the vehicle through a communication network;

(2) a distributed architecture consisting of several computing elements interconnected with a number of "dumb" subsystems via a communication network which allows flexibility in partitioning the system;

(3) a pure federated system, in which each "dumb" subsystem is directly connected to a dedicated computing element, which themselves communicate through the communication network; and

(4) a pure embedded architecture of "smart" subsystems, each have a computing element embedded in it.

The federated system design approach has been chosen as most suitable for guided weapon applications. The communication network consists of a single time-multiplexed serial bus. A variety of line protocols have been examined for suitability. The choice of an appropiate line protocol depends very much on the performance objectives of the system, and is a subject of much debate.

The Round Robin Passing Protocol (RRPP) is a line protocol which has several appealing characteristics, including low data latencies and relatively simple implementations [2]. Control of the bus is passed from one computing element to another in a cyclical fashion, allowing each processor to transmit messages on the bus once during a bus cycle. If a processor has no data to transmit, it simply broadcasts an end-of-

transmission word to indicate to the next processor in the cycle that it should now take control of the bus. The processor is not directly involved in the bus transactions; instead, each computing element includes a Bus Interface Unit (BIU) which controls all bus functions.

In RRPP a data item which is to be sent from one processor to another will in general be delayed in two ways. First, the message is sent serially (at a data rate of one megabit per second), and thus there is a delay due to the time required to complete the transmission of the message. Second, and potentially more serious, there is a delay due to the fact that a message may be queued up at a BIU waiting to be transmitted, but the BIU must wait for its fixed slot in the round robin cycle before the message transmission may begin. If a message is delivered to the BIU just after one of its alloted slots, it must wait nearly an entire bus cycle, and may be delayed by other message transmissions. If a message transmission is delayed by the transmission of other messages, we say that a collision has occurred.

The length of the interval from the point at which a message is delivered to a BIU for transmission and the point at which the BIU begins to transmit the message is called the wait time. The transmission time is the time required to actually transmit the message on the bus. The message latency is defined as the sum of the message wait time and transmission time. It is important to attempt to minimize both the average and maximum message latencies. This becomes critical when the system designer places control loop information on the bus, so that message latency in effect represents a phase delay in the loop, with potentially disastrous effects on loop stability.

The Round Robin Passing Protocol scheme, also called MIL-STD-1765 (proposed) or the DISMUX bus, has been previously analyzed for message latency, using as a model the MGD (Midcourse Guidance Demonstration) vehicle currently under development at the Air Force Armament Laboratory. This study is inadequate for two reasons. One, it assumes a fixed scenario for message traffic (actually, three scenarios), and as system requirements or implementations details change, these results may no longer be valid. Two, the study assumed that no relationships

existed among the messages being sent on the bus (other than being periodic). Clearly, there is a cause-and-effect nature among the messages which results in a high degree of correlation in bus traffic, and this must be modelled as precisely as possible in order to effectively analyze bus behavior.

A third reason for performing additional analysis of data latency is for purposes of comparison. One may question whether a RRPP scheme is better than, or even as good as, other schemes which have been suggested or implemented in different applications. It is to be hoped that detailed analysis would allow questions of relative performance to be answered, at least within the context of specific system requirements. With an accurate enough model, it should also be possible to determine whether or not a given protocol can even satisfy those requirements.

## II. Objectives

We had several objectives in initiating this research. First, a model of the message traffic in a typical guided weapon system was to be developed. The model should include the timing interrelationships for the transmissions of the various messages, as well as message lengths and frequencies. Second, we wished to investigate the use of a pure command-response line protocol in a federated computer network in which minimization of data latency was of primary importance. Finally, our major objective was to characterize the performance of a RRPP scheme in a guided weapon application, as described by the model previously constructed. Of principal concern was the effect on both average and maximum data latency. This objective was later expanded to include a similar characterization, for purposes of comparison, of a command-response line protocol utilized in a modified round robin mode.

As an adjunct to the last objective, we developed a simulator for the model. The simulator had to be flexible, since many of the implementation details for the chosen system were either unknown or subject to change at the time of the simulator's construction. In addition, we

wished to analyze several different configurations for the same basic system without having to develop a new simulator for each variation. Also, it had to be easily adaptable to different choices of line protocols, since one purpose was to allow comparative analysis of different communication methods.

## III. Command-Response and Data Latency

In a pure command-response protocol, no bus transfer ever occurs on the bus unless commanded by the (single) bus controller. The controller, or supervisor, must have complete knowledge of every message which is to be transmitted and must send a command to the appropiate BIU's which are to transmit and receive each message. The exception to this rule is that a BIU may inform the supervisor of a request for service when reporting status, but since status is reported only as a result of a command from the supervisor, this feature is of little utility when considering messages of a periodic nature.

If the supervisor is exactly synchronized to each of the other processors in the federated system, and if there are no processor-dependent delays within the system of which the supervisor is unaware, then the supervisor could command the transmission of data as soon as it became available, and the message latency would simply be the message transmission time. (This assumes no collisions.) Because of the autonomous nature of the processors in a federated system, however, no two processors can ever be exactly sure of what the other is doing. This might be thought of as the defining characteristic of a distributed system. That is, the system consists a number of cooperative, autonomous processes, and no process has complete, current knowledge of the state of all other processes.

We have examined more reasonable assumptions about amount of synchronization and coordination between the supervisor and the various other federated processing elements. In the following discussion we make two assumptions. (1) All traffic on the bus is periodic. For the

application we have chosen, virtually all messages are transmitted periodically, and any which are not can be ignored. (2) Data is requested at a rate no greater than it is produced. That is, if a given piece of data must be transmitted on the bus n times a second, the supervisor commands that it be transmitted only n times a second. Otherwise, the system begins to acquire the characteristics of a polled bus system, with the associated increase in system overhead, and the analysis which follows is not applicable.

Let T be the random variable which corresponds to the point in the interval $[0,\Delta t]$ at which a message is ready to be transmitted, where $\Delta t \leq \frac{1}{f}$. (We have arbitrarily set $t = 0$ at the start of this interval, which we will call a message interval.) f is the frequency at which the data is produced and, consequently, the frequency at which the message transmission is requested (Fig. 1). Assume that the message transmission is requested at times $x$, $x + \frac{1}{f}$, $x + \frac{2}{f}$, ..., where $0 \leq x \leq \Delta t$. This implies that the supervisor knows the bounds of the message interval, but not the exact point within that interval at which the data becomes available for transmission. Define $D(x)$ to be the delay between the moment that the information becomes available during $[0,\Delta t]$ and the moment that the data is requested after becoming available. Let $F_T(t') = Pr[T \leq t']$ be the cumulative distribution function for T. Then

$$\begin{aligned} E[D(x)] &= \int_0^x (x-t')dF_T(t') + \int_x^{\Delta t} [\tfrac{1}{f} - (t'-x)]dF_T(t') \\ &= x - E[T] + \tfrac{1}{f}\cdot[1 - F_T(x)] \end{aligned} \qquad (1)$$

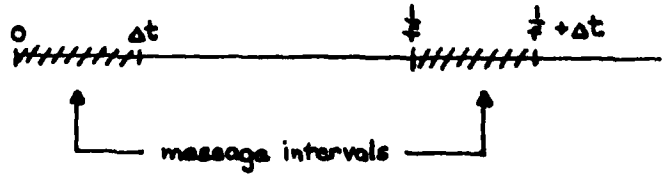



Figure 1. Message Intervals

Evaluating (1) at the endpoints of the interval gives:

$$E[D(0)] = - E[T] + \frac{1}{f}$$

$$E[D(\Delta t)] = - E[T] + \Delta t$$

Differentiating with respect to x and setting the resulting expression equal to 0 gives

$$\frac{d}{dx}[F_T(x)] = f$$

The minimum expected delay occurs at $x = 0$, $x = \Delta t$, or $x = x_{min}$ s.t. $\frac{d}{dx}[F_T(x)]_{x=x_{min}} = f$. Since $\Delta t \leq \frac{1}{f}$, $E[D(x)]$ is bounded by $\frac{1}{f} - E[T]$.

In order to determine the minimum expected delay, the distribution of T must be known. We will make three different assumptions and analyze each. The three distributions chosen are uniform, truncated normal, and truncated exponential.

Assume T is uniformly distributed over the interval $[0,\Delta t]$ (Fig. 2).

$$F_T(t') = \begin{cases} \frac{t'}{\Delta t}, & 0 \leq t' \leq \Delta t \\ 0, & \text{otherwise} \end{cases} \qquad (2)$$

$$E[T] = \frac{\Delta t}{2}$$

This gives

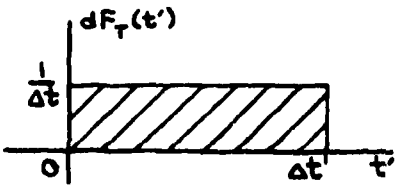



Figure 2. Uniform Distribution for T

$$E[D(x)] = x - \frac{\Delta t}{2} + \frac{\Delta t - x}{f\Delta t}$$

and

$$\frac{d}{dx}\left|E[D(x)]\right| = 1 - \frac{1}{f\Delta t} \neq 0 \quad \text{unless } f = \frac{1}{\Delta t}$$

Hence the minimum expected delay occurs for $x = \Delta t$ and is equal to half the size of the interval $\Delta t$.

A second assumption for the distribution of $\tau$ is that of a truncated exponential, defined by Eq. (3). $G_\tau$ is the cumulative distribution function for an exponentially distributed random variable.

$$G_\tau(t') = \begin{cases} 1 - e^{-\lambda t'}, & t' \geq 0 \\ 0, & \text{otherwise} \end{cases}$$

$$F_\tau(t') = \begin{cases} \dfrac{G_\tau(t')}{\int_0^{\Delta t} G_\tau(t')\,dt'}, & \\ 0 & 0 \leq t' \leq \Delta t \\ 0, & \text{otherwise} \end{cases} \qquad (3)$$

$$= \begin{cases} \dfrac{1 - e^{-\lambda t'}}{1 - e^{-\lambda \Delta t} - \lambda \Delta t e^{-\lambda \Delta t}}, & \\ 0 & 0 \leq t' \leq \Delta t \\ 0, & \text{otherwise} \end{cases}$$

(See Fig. 2). Then

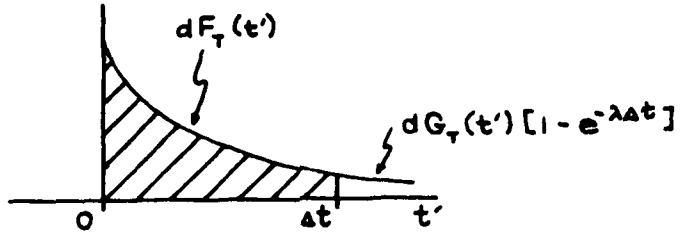



Figure 3. Truncated Exponential Distribution for T

$$E[T] = \frac{1}{\lambda} - \frac{\Delta t e^{-\lambda\Delta t}}{1 - e^{-\lambda\Delta t}}$$

and

$$E[D(x)] = x - \frac{1}{\lambda} + \frac{\Delta t e^{-\lambda\Delta t}}{1 - e^{-\lambda\Delta t}} + \frac{1}{f}\left|1 - \frac{1 - e^{-\lambda x}}{1 - e^{-\lambda\Delta t}}\right|$$

and this is always less than or equal to $\Delta t$.

The third assumption for the distribution of T to be considered is that of a truncated normal random variable with mean $\mu = \frac{\Delta t}{2}$ and variance $\sigma^2$ (before truncation). This is defined in the following equations and illustrated in Fig. 4.

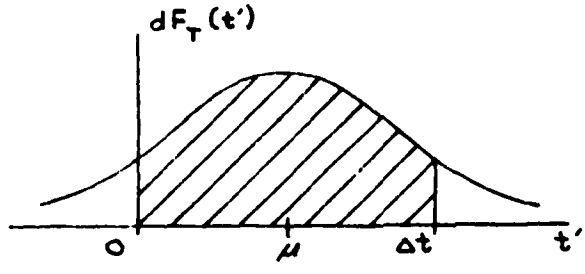



Figure 4. Truncated Normal Distribution for T

$$F_T(t') = \begin{cases} \dfrac{\int_0^{t'} N(\mu,\sigma^2)dx'}{\int_0^{\Delta t} N(\mu,\sigma^2)dx'}, & 0 \le t' \le \Delta t \\ 0, & \text{otherwise} \end{cases} \tag{4}$$

where

$$N(\mu,\sigma^2) = \frac{1}{\sqrt{2\pi}\sigma} e^{-\frac{(x'-\mu)^2}{2\sigma^2}}$$

This gives

$$F_T(t') = \begin{cases} \dfrac{\Phi(\frac{t'}{\sigma} - \frac{\Delta t}{2\sigma}) + \Phi(\frac{\Delta t}{2\sigma}) - 1}{2\Phi(\frac{\Delta t}{2\sigma}) - 1}, & 0 \le t' \le \Delta t \\ 0, & \text{otherwise} \end{cases} \tag{5}$$

Substituting this into Eq. (2) results in

$$E[D(x)] = x - \frac{\Delta t}{2} + \frac{\Phi(\frac{\Delta t}{2\sigma}) - \Phi(\frac{x}{\sigma} - \frac{\Delta t}{2\sigma})}{\Phi[2\Phi(\frac{\Delta t}{2\sigma}) - 1]}$$

Since the distribution is symmetric about its mean, we know that

$$\min_x E[D(x)] \le \frac{\Delta t}{2}$$

One might be tempted to assume that for a distribution of this sort, the optimal point to request data would be at $x = \frac{\Delta t}{2}$, etc., but it is easily shown that

$$E[D(\tfrac{\Delta t}{2})] = \frac{1}{2f}$$

which is a minimum only if $\Delta t = \frac{1}{f}$.

In the above discussion, we have assumed that the supervisor has exact knowledge of the interval during which data will become available, and the processor which generates the data may produce it at any time during that interval. The supervisor requests data transmission at exactly times x, $x + \frac{1}{f}$, $x + \frac{2}{f}$, etc. More realistically, there will be additional uncertainty in attempting to synchronize x to the beginning of the data interval and in maintaining this synchronization during subsequent data intervals. Processors share no common clock, and there are asynchronous processes which may cause interrupts which must be processed at crucial times.

To model this additional uncertainty, let us assume that X is also a random variable, corresponding to the point in the interval $[0,\Delta t]$ at which the supervisor requests a message to be transmitted. Let $F_X(x)$ be the cumulative distribution for X, and assume that X and T are independent events. The expected delay is given by

$$\begin{aligned}\bar{D} &= \int_0^{\Delta t} E[D(x)]dF_Y(x) \\ &= \int_0^{\Delta t} [x - E[T] + \frac{1}{f}[1 - F_T(x)]]dF_Y(x) \qquad (6) \\ &= E[X] - E[T] + \frac{1}{f}\int_0^{\Delta t} F_X(x)dF_T(x)\end{aligned}$$

For distributions of X and T with identical means, this reduces to

$$\bar{D} = \frac{1}{f}\int_0^{\Delta t} F_X(x)dF_T(x) \qquad (7)$$

and if $F_T(\cdot) = F_X(\cdot)$, we arrive at an expected delay of $\frac{1}{2f}$, independently of $\Delta t$. The implication of this is that if there is "similar uncertainty" regarding the point at which data becomes available and the point at which data transmission is requested, the interval during which data is requested should not be allowed to overlap exactly with the interval during which data is produced, since this leads to an average delay which is half the size of the data period.

If the start of the data request interval is delayed by an amount r, then under the same assumptions of independent distributions for X

and T which are symmetric within the respective intervals (i.e., E[X] = E[T]+ ),

$$\overline{D} = E[X] - E[T] + \frac{1}{f}\int_{\tau}^{\Delta t} F_X(x)dF_T(x) \qquad (8)$$

This means that the best that we can do is to delay the request until at least the end of the interval during which the data will become ready, incurring an expected delay of $\Delta t$ in doing so. However, if $\Delta t$ is greater than half of the data period $\frac{1}{f}$, Eq. (7) indicates that the worst case average delay is just $\frac{1}{2f}$.

Clearly, the above analysis leaves many questions unanswered, but it does indicate that in the absence of some synchronization mechanism, command-response is at best a dubious choice when attempting to minimize data latencies in a system with periodic message transmissions. Although nothing has been said about maximum latencies, the average latencies may be very large, on the order of half of the message period.

## IV. Simulation Models

In attempting to answer many of the questions posed earlier, we are forced to used simulation as an analytical tool because of the complexity of the system. Since the answers to the questions will be dependent on the application, it is necessary to describe in detail the models on which the simulations are based.

We have chosen the MCD project as a basis for the simulation model. Three configurations are being considered, based on three different navigation schemes. The first, Unaided Tactical Guidance (UTG), assumes that the vehicle navigation is accomplished using only a low-cost inertial guidance system (LCIGS), with no externally-derived referents. The second, Terrain Contour Matching (TERCOM), uses an LCIGS for navigation between a series of geographical areas used for positional updates via contour matching with reference maps. The third configuration is Tactical Global Positioning System Guidance, and it likewise employs a LCIGS

package, this time in conjunction with a satellite positioning system which supplies reference data at various intervals.

Because of the federated nature of the processing system, the designer has considerable flexibility within any of these configurations in deciding both the number of processors employed and the distribution of tasks to the various processors. Fig. 5 illustrates one possible scenario. This figure shows nine BIU's interfaced to the bus. The simulation actually uses four BIU's for the UTC configuration and five BIU's for both the TERCOM and TCPSC configurations. In each of the configurations, there is an additional slot on the bus which is used for diagnostic purposes. During an actual mission, the additional slot will be unused, and the only effect is to cause an additional delay in the round-robin cycle.

Another major design choice is whether LCIGS data is to be supplied to the requisite processors directly through I/O interfaces in the processors, or be placed on the bus. If it is to be placed on the bus, the bus utilization increases by a large factor, and the effect of data latency on control loop stability is likely to be much more pronounced. The simulation allows the option of specifying whether or not LCIGS data

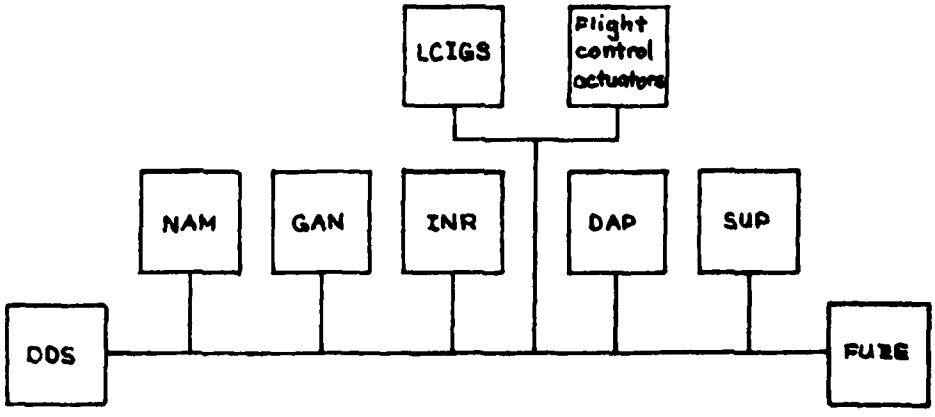



Figure 5. Federated System with Nine BIU's

is transmitted on the bus.

Fig. 6 is a graphical description of the cause-and-effect relationships which may exist among the various messages being transmitted on the bus. The figure indicates message frequencies, computational delays, and precedences. The particular configuration pictured here is UTC without LCIGS data on the bus. Although the description is almost certainly not entirely accurate, it represents a reasonable approximation, and allows relevant comparisons to be made.

The simulation also allows the specification of one of two possible bus protocols. One is MIL-STD-1765 (proposed), also called DISMUX [2]. The major feature of importance is that no single processor acts as a controller, but rather each processor in turn is given control of the bus in a round-robin, cyclical sequence. Messages are source- instead of destination-oriented, so that one message may be received by any number of processors without the knowledge of the transmitting processor. The bus interface is relatively simple and inexpensive.

The other protocol involves the use of MIL-STD-1553B [3] in a dynamic bus allocation mode called Modified Round Robin Passing Protocol [4]. In this mode, the 1553B bus may be thought of as simulating the RPPP of the 1765 standard; however, because of the overhead of the handshaking which must occur, MRRPP is slower than RPPP, by a factor of approximately two. Each BIU must be able to function both as a controller and as a remote terminal, and the requirement of implementing the full 1553B standard makes the BIU relatively more complex and costly.

## V. Simulation Results

Time did not permit extensive simulation runs to be made before the conclusion of the summer appointment. However, some results were obtained, allowing comparison of RPPP and MRPPP for the UTC configuration and for a variety of estimated computational delays. The results from the simulations are summarized in Table 1. Each line of the table

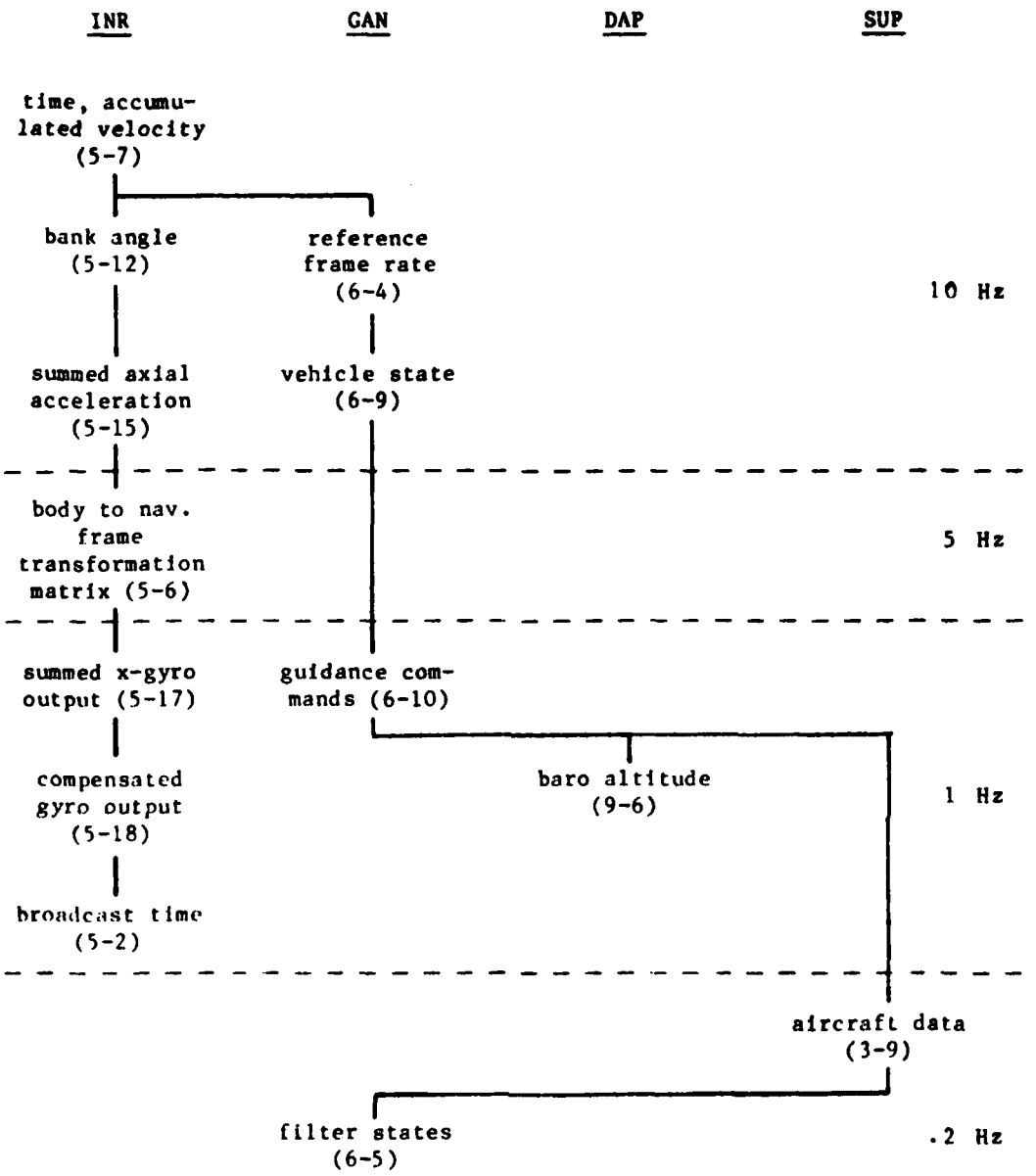



Figure 6. Message Traffic Interrelationships

| Protocol | Message Wait | | Message Latency | | Cycle Length | |
|---|---|---|---|---|---|---|
| RRPP | 82.5 | (311.0) | 153.1 | (530.0) | 123.8 | (583.0) |
| MRRPP | 221.4 | (519.0) | 292.0 | (699.8) | 248.7 | (818.0) |
| RRPP | 83.0 | (266.0) | 153.6 | (524.5) | 123.8 | (583.0) |
| MRRPP | 239.7 | (666.3) | 310.3 | (706.3) | 248.7 | (818.0) |
| RRPP | 80.3 | (214.0) | 150.3 | (499.3) | 123.8 | (543.0) |
| MRRPP | 219.3 | (520.9) | 289.7 | (728.5) | 248.7 | (722.0) |
| RRPP | 116.5 | (263.0) | 152.3 | (504.0) | 125.5 | (548.0) |
| MRRPP | 253.5 | (477.0) | 289.2 | (701.0) | 248.7 | (722.0) |

Table 1.

Results from four simulation runs, comparing Round Robin Passing Protocol (RRPP) with Modified Round Robin Passing Protocol (MRRPP). All times are in microseconds, and are given as "average (maximum)". Configuration is UTG.

corresponds to a different set of computational delays. As expected, the MRRPP results are much poorer than the RRPP results for the same values of computational delays. This is due to two effects. First, as mentioned above, the MRRPP is slower than RRPP because of the overhead of performing handshaking on the bus when transferring control from one BIU to another. Second, as the round robin cycles get longer, the probability of a collision occurring in a cycle increases, further lengthening the average round robin cycle time and hence the average data latency.

As the bus utilization increases, data latency increases rapidly for the MRRPP. This is illustrated in Table 2, which compares the performance of MRRPP when LCIGS data is placed on the bus and when it is not. Note that the average data latency when LCIGS data is being transmitted on the bus is more than .4 milliseconds, while the maximum data latency has increased to well over a millisecond.

| | No LCIGS | | LCIGS | |
|---|---|---|---|---|
| Message wait | 250.8 | (614.4) | 254.8 | (956.5) |
| Message latency | 322.7 | (756.7) | 420.5 | (1136.5) |
| Cycle length | 302.5 | (870.0) | 346.1 | (1126.0) |

Table 2.

Comparison of performance of Modified Round Robin Passing Protocol with and without LCIGS data on bus (TERCOM configuration). All times are in microseconds, and format is "average (maximum)".

## VI. Recommendations

A number of problems remain to be investigated. First, there is the question of model accuracy. Although the models for each configuration were formulated using the best information available from a variety of sources, in many cases the necessary information was not available. Also, as the MGD project evolves, some changes are certain to occur. The success of any attempt to use simulation results to predict performance will of course depend on how realistic the model is. To this end, the simulator was made to be easily adaptable and expandable, so that as changes occur or more information becomes available, the necessary alterations to the model can be incorporated into the simulation in a straightforward, predetermined manner.

A second recommendation, and one in which I have considerable interest, concerns the question of what sort of bus protocol is most suitable for the given applications. Although 1765 is superior to 1553B when using MRRPP, 1553B might be operated in other modes which would improve its performance in terms of reducing data latencies. This should be investigated, and other non-standard bus communication schemes should be considered. In particular, the idea of a carrier sense multiple access broadcast network is intriguing, especially in view of the relatively light bus loading for these applications [5]. In an Ethernet-like approach, one cannot bound maximum latency, but we would expect the average latency to be very low. Also, instances of large

latency may occur only very infrequently, depending on the bus loading, and if these instances are rare, they may have only an insignificant effect on performance. This approach also raises the possibility of incorporating some kind of message priority in the system, such that certain critical messages (control loop information, for instance) could have even lower latency at the expense of other messages less sensitive to delays. Of course, minimizing data latency is not the only criterion for suitability and this should also be considered in judging other communication schemes.

## REFERENCES


1. N. Nathan et. al., "Digital Processing Analyses/Partitioning," Report No. R-1121, Charles Stark Draper Laboratory, Cambridge, MA., November 1977.

2. - , "Proposed Military Standard: Weapon Internal Time Division Multiplex Data Bus," Draft, AFATL/DLMM, Eglin AFB, FL., March 1980.

3. - , "Military Standard: Aircraft Internal Time Division Command/Response Multiplex Data Bus," MIL-STD-1553B, Dept. of Defense, Washington, D.C., September 1978.

4. J.W. Jones, "DISMUX RRPP and 1553 Modified RRPP," Memorandum, AFATL/DLMM, Eglin AFB, FL., January 1980.

5. R.M. Metcalfe and D.R. Boggs, "Ethernet: Distributed Packet Switching for Local Computer Networks," Comm. ACM, Vol. 19, No. 7, July 1976.

1980 USAF - SCEEE SUMMER FACULTY RESEARCH PROGRAM

Sponsored by the

AIR FORCE OFFICE OF SCIENTIFIC RESEARCH

Conducted by the

SOUTHEASTERN CENTER FOR ELECTRICAL ENGINEERING EDUCATION

FINAL REPORT

# VORTEX BREAKDOWN AND INSTABILITY


| | |
|---|---|
| Prepared by: | Dr. Shiva H. Singh |
| Academic Rank: | Associate Professor |
| Department and University: | Department of Mechanical Engineering<br>University of Kentucky |
| Research Location: | Flight Dynamics Laboratory, Aeromechanics Division, Aerodynamics and Airframe Branch, Computational Aerodynamics Group |
| USAF Research Colleague: | Dr. Wilbur L. Hankey |
| Date: | July 31, 1980 |
| Contract No: | F49620-79-C-0038 |

# VORTEX BREAKDOWN AND INSTABILITY

by

Shiva N. Singh

## ABSTRACT

A literature survey on the vortex breakdown phenomenon is presented. Several theoretical and numerical models which have been proposed and applied to explain the experimental observations concerning vortex bursting are reviewed. Required parameters to perform the related stability analysis have been identified. Appropriate criterion where possible are cited to assist engineers in estimating occurrence of vortex bursting. A numerical scheme to compute and verify some of the results for incompressible inviscid unstable modes is programmed on the computer at WPAFB. It is suggested that the influence of adverse pressure gradient on the vortex breakdown be investigated in detail and results thus obtained be compared with experiments under appropriate conditions.

## ACKNOWLEDGEMENT

The author would like to thank the Air Force Systems Command, the Air Force Office of Scientific Research and the Southeastern Center for Electrical Engineering Education for providing him with the opportunity to spend a very worthwhile and interesting summer at the Flight Dynamics Laboratory, Wright-Patterson Air Force Base, Ohio. He would like to acknowledge the Laboratory, in particular the Computational Aerodynamics Group, for its hospitality and excellent working conditions.

He would like to thank Dr. Wilbur Hankey for suggesting this area of research and for his collaboration and guidance. He would like to acknowledge many helpful discussions with Drs. Charles Jobe, Joe Shang and W. Calarese. Finally, the computational help given by Mr. Steve Scherr in programming the instability problem and Mr. Jeff Graham is much appreciated.

## OBJECTIVE

The main objective of this project was to accomplish a literature survey on vortex breakdown and related phenomena and to identify the various nondimensional parameters which govern the vortex breakdown. To study the phenomenon, we wanted to formulate the linear stability analysis and program the problem on the computer. And finally, once this is accomplished, we can point out what additional factors should be taken into consideration to further explain the vortex breakdown.

## SECTION I

## INTRODUCTION

The problem of vortex breakdown occurring over delta wings at large angles of attack and in axisymmetric swirling flows in circular pipes has recently received considerable interest. A number of review articles (Hall[18,19] and Leibovich[31]) on the subject have been written and a symposium on concentrated vortex motions in fluids (KÜchemann[27]) has been arranged.

Peckham and Atkinson[40] were the first to discover the occurrence of vortex breakdown over delta wings with highly swept leading edges, when such wings were set at large angles of incidence. The work of Elle[10], Cox[8], Werle[52], Lambourne and Bryer[28], Hummel[23], Earnshaw[9] and Lowson[33] helped to construct a detailed picture of the flow field near the breakdown. When a slender wing is set at an angle of attack, the flow on the upper surfaces separates from near the leading edges, forming two shear layers. These layers curve upward and inboard and eventually roll up into a core of high vorticity. Most vortex cores have an appreciable axial component of motion and the fluid spirals around and along the axis. In the core of the leading edge vortex over a delta wing, velocities two to three times that of the undisturbed stream have been found. An increase in the angle of attack strengthens the vorticies and eventually there is an abrupt change in the structure of the vortex with a very pronounced retardation of the flow along the axis, followed by reversed flow in a region of limited axial extent. This abrupt change is called "vortex breakdown" or "vortex bursting."

Harvey[20] initiated the study of vortex breakdown through a long cylindrical tube. By varying the amount of swirl that was imparted to the fluid before it entered the tube, he found that the breakdown was the intermediate stage between two basic types of rotating flows, those that do and those that do not exhibit

axial velocity reversal. Since then, Kirkpatrick[24], Chanaud[7], Sarpkaya[42,43,44], Faler and Leibovich[11,12] and Garg[13] performed the more easily controllable experiments in tubes and presented vast data on vortex breakdown. Two forms of vortex breakdown predominate, one called "axisymmetric" or "bubble-like" and the other called "spiral." The type and the shape of the forms depend upon the particular combination of the Reynolds and circulation numbers.

Many analytical and numerical solutions of the Navier-Stokes equations have been attempted to explain the occurrence of vortex breakdown phenomenon. Hall[17] and Stewartson and Hall[48] attempted to solve the Navier-Stokes equations by proposing a simplified model for the vortex core formed over a slender delta wing at incidence by the rolling-up of the shear layer that separates from a leading edge. The incompressible quasi-cylindrical boundary-layer approximate momentum integral equations describing the flow in the viscous core of a wing-tip vortex were solved by Gartshore[14,15], Steiger and Bloom[47] and Mager[37]. Benjamin[3,4] suggested that the inviscid vortex breakdown, like a hydraulic jump is a transition between two conjugate states of flow. Bossel[5,6] analyzed the vortex breakdown flowfield by reducing the equations of motion to simpler sets in four different regions. Solutions of the steady axisymmetric Navier-Stokes equation for vortex breakdown in a confined as well as unconfined viscous vortex have been obtained by Hall[18], Kopecky and Torrance[26] and Grabowski and Berger[16].

Many authors believe that the vortex bursting with a local stagnation of the axial flow is a direct consequence of hydrodynamic instability with respect to axisymmetric, non-axisymmetric or antisymmetric infinitesimal disturbances. Ludweig[35,36] initiated the study of linear hydrodynamic stability concerning swirling flows. Then Leibovich[30,31], Randall and Leibovich[41], Uberoi, Chow and Narain[5], Lessen, Singh and Paillet[32], Lessen and Pailett[33], and Singh and Uberoi[45] carried out detailed stability analysis on the vortex breakdown.

In the forementioned research work concerning various explanations and interpretations of vortex breakdown, there is considerable overlap between theoretical predictions and experimental observations. In the following sections, the mathematical formulation of the vortex flows in cylindrical polar coordinates $(r, \theta, z)$ is given. Solution for the axisymmetric axial flow in trailing line vortices is obtained. This is imposed as the starting condition at $z = 0$, to obtain the solution profiles of full Navier-Stokes equations for $z > 0$. In order to study the linear stability analysis the mean flow is also taken as that of trailing line vortices. Theoretical solutions thus obtained are compared with experimental results and discrepancies pointed out.

## SECTION II

## MATHEMATICAL FORMULATION

Cylindrical polar coordinate system (r, θ, z) are used. The radial, circumferential and axial components of velocity are denoted by u, v and w respectively. The unsteady Navier-Stokes equations for incompressible medium are:

$$\frac{1}{r}\frac{\partial ur}{\partial r} + \frac{1}{r}\frac{\partial u}{\partial \theta} + \frac{\partial w}{\partial z} = 0 \tag{1}$$

$$\frac{\partial u}{\partial t} + u\frac{\partial u}{\partial r} + \frac{u}{r}\frac{\partial u}{\partial \theta} + w\frac{\partial u}{\partial z} - \frac{v^2}{r} = \frac{-1}{\rho}\frac{\partial p}{\partial r} + \nu\left(\nabla^2 u - \frac{u}{r^2} - \left(\frac{2}{r^2}\right)\frac{\partial v}{\partial \theta}\right) \tag{2}$$

$$\frac{\partial v}{\partial t} + u\frac{\partial v}{\partial r} + \frac{v}{r}\frac{\partial v}{\partial \theta} + w\frac{\partial v}{\partial z} + \frac{uv}{r} = \frac{-1}{\rho}\frac{\partial p}{r\partial \theta} + \nu\left(\nabla^2 v - \frac{v}{r^2} + \left(\frac{2}{r^2}\right)\frac{\partial u}{\partial \theta}\right) \tag{3}$$

$$\frac{\partial w}{\partial t} + u\frac{\partial w}{\partial r} + \frac{v}{r}\frac{\partial w}{\partial \theta} + w\frac{\partial w}{\partial z} = -\frac{1}{\rho}\frac{\partial p}{\partial z} + \nu\nabla^2 w, \tag{4}$$

where $\partial^2 \equiv \frac{\partial^2}{\partial r^2} + \frac{1}{r}\frac{\partial}{\partial r} + \frac{1}{r^2}\frac{\partial^2}{\partial \theta 2} + \frac{\partial^2}{\partial_z 2}$

and p, ρ and ν are the pressure, density and kinematic viscosity of the fluid.

Fluid flowing past a lifting wing produces trailing vorticity and this at some distance downstream, eventually concentrates into two trailing line vortices. A characteristic feature of a steady trailing line vortex is the existence of strong axial currents near the axis of symmetry. The link between the azimuthal and the axial components of motion in vorticies is provided by the pressure; the radial pressure gradient balances the centrifugal force, and any change in the azimuthal motion in the axial direction downstream produces an axial pressure gradient and consequently axial acceleration (see Squire[46], Newmann[38], Batchelor[1], Owen[29] and Uberoi[49] for discussion on trailing vorticies).

To derive the expression for the velocity components in the case of trailing line vortices, flow fields are assumed to be steady and axisymmetric, such that the axial variation are smaller than the radial derivatives, i.e.

$$\frac{\partial}{\partial z} << \frac{\partial}{\partial r} , \qquad w >> u . \tag{5}$$

We further approximate that the axial velocity w is nearly equal to the free stream velocity W, then equations (1) to (4) reduce to

$$\frac{1}{r}\frac{\partial}{\partial r}(ru) + \frac{\partial w}{\partial z} = 0 \tag{6}$$

$$-\frac{v^2}{r} = -\frac{1}{\rho}\frac{\partial p}{\partial r} \tag{7}$$

$$W\frac{\partial v}{\partial z} = \nu\left[\left(\frac{\partial^2 v}{\partial r^2}\right) + \frac{1}{r}\frac{\partial v}{\partial r} - \frac{v}{r^2}\right] \tag{8}$$

$$W\frac{\partial w}{\partial z} = -\frac{1}{\rho}\frac{\partial p}{\partial z} + \nu\left(\frac{\partial^2 w}{\partial r^2} + \frac{1}{r}\frac{\partial w}{\partial r}\right) \tag{9}$$

A new independent variable $\zeta$ is introduced in place of r and is defined as

$$\zeta = Wr^2/4\nu z \tag{10}$$

Solution under appropriate conditions is obtained as (see Batchelor[1] and certain comments by Tam[49] and Herron[21])

$$v = \frac{c_o}{r}(1 - e^{-\zeta}), \tag{11}$$

$$w = W - \left(\frac{c_o^2}{8\nu z}\ \mathrm{Log}\ \frac{Wz}{\nu}\right) e^{-\zeta} + \frac{c_o^2}{8\nu z}\ f(\zeta) - \frac{LW^2}{8\nu z}\ e^{-\zeta} \tag{12}$$

$$\frac{P_o - P}{\rho} = \frac{c_{oW}^2}{8\nu z}\left[\frac{(1 - e^{-\zeta})^2}{\zeta} + 2\ ei(\zeta) - 2ei(2\zeta)\right], \tag{13}$$

where

$$f(\zeta) = e^{-\zeta}\{\log \zeta + ei(\zeta) - 0.807\} + 2ei(\zeta) - 2ei(2\zeta),$$

and $$ei(\zeta) = \int_{\zeta}^{\infty} \frac{e^{-\xi}}{\xi}\, d\xi .$$

$c_o$ is the constant circulation at large radius r and L is a constant depending on the induced drag or the initial velocity defect in the presimilarity stage. Uberoi[50] has shown that the expressions (11) to (13) for v, w and p neglect radial and associated axial convection of angular momentum and the radial velocity component is assumed negligibly small. As a result the trailing vortex reduced to a line vortex and thus the approximation may be invalid. Although the solution represented by (11-13) may not be quite accurate, it is generally adequate for many purposes. Further studies have assumed this solution as the starting condition at $z = 0$ to calculate the subsequent development of the vortex breakdown. Also, the experimental measurements of the velocity distribution inside a swirling tube are quite close to those given by (11) and (12) (see Garg[13]).

## SECTION III

## SOLUTIONS OF THE NAVIER-STOKES EQUATIONS

In non-viscous flows, in addition to theorems of Bernoulli and Helmholtz-Kelvin, Crocco[18] developed an interesting result concerning vortex flows. Euler's equation for inviscid compressible gases can be written as

$$(\partial\vec{u}/\partial t) - \vec{u}x(\nabla x\vec{u}) + \nabla(\vec{u}\cdot\vec{u}/2) = -\nabla h + T\nabla s \tag{14}$$

where $\vec{u}$ is the velocity vector, and h, T and s are the enthalpy, temperature and entropy respectively. Making use of Bernoulli theorem equation (14) reduces to (for steady state)

$$\vec{u} \times (\nabla \times \vec{u}) = -T(\nabla s) \tag{15}$$

Two conclusions can be drawn from (15):

1) An irrotational stationary gas flow is an isentropic motion;

2) If there are entropy changes within the field, vortices (vortex sheets) will generally appear. Or the vortex flows are non-isentropic, unless the velocity and vorticity vectors are parallel to each other, a very special case.

On the basis of inviscid theory, Squire[46], Benjamin[3,4], and Bossel[5] considered the following differential equation (see Squire and Benjamin for its derivation)

$$\frac{\partial^2\psi}{\partial r^2} - \frac{1}{r}\frac{\partial\psi}{\partial r} + \frac{\partial^2\psi}{\partial z^2} = r^2\frac{dH}{d\psi} - k\frac{\partial k}{d\psi} \tag{16}$$

where $\psi$ is the Stokes stream function. H is the total head which by Bernoulli's theorem is a function of $\psi$ alone and $k = rv$, the circulation about the z-axis is also a function of $\psi$ alone according to Kelvin's theorem. The above-mentioned authors attempted to obtain solution of (16) in terms of axisymmetric waves. They regarded the vortex breakdown phenomenon as the existence of a critical

state. Vortex flows have been classified as 'supercritical' if the wave can propagate with phase speeds in the downward direction ($c > 0$) or subcritical if the propagation is also possible in the upstream direction ($c < 0$). 'Critical' flow separates the two classes where $c = 0$. Benjamin proposed that vortex breakdown be explained as a transition between two (supercritical and subcritical) conjugate states of axisymmetric swirling flows being much the same in principle as the hydraulic jump in open-channel flow. Leibovich[31] points out that solutions of (16) cannot give much information like the onset or the position of breakdown, or breakdown and transition in the spiral and bubble forms.

Quasi-cylindrical approximations to (1)-(4) have been introduced by Hall[17,18] and Stewartson and Hall[48]. Vortex breakdown was assumed to be similar to the separation of a two-dimensional boundary layer. They used the quasi-cylindrical equations in step-by-step calculations. Gartshore[14,15] and Mager[37] solved the equations by momentum integral methods by neglecting the imposed pressure gradient. When a large axial gradient develops in their solutions, they conclude that the vortex breakdown has occurred. Just as the two-dimensional boundary-layer approximations break down as soon as the separation occurs, similarly the quasi-cylindrical approximation are no longer true the moment infinitely large axial gradients appear. Mager finds that the closed-form transcendental solutions of the quasi-cylindrical momentum-integral equations for the flow in the viscous core of a wing-tip vortex have two separate branches with the same flow force deficiency. Upstream of the discontinuity, the upper branch solution results in a strongly decelerating flow with a rapidly expanding core while the lower branch solution (with the same angular momentum) gives accelerating flow with a rapidly expanding core while the lower branch solution (with the same angular momentum) gives accelerating flow with a substantially larger but slightly contracting core. These facts together with Sarpkaya's[42]

photographs and observations that the axisymmetric bubble is always followed by the spiral breakdown, suggest that the spiral breakdown may be the physical manifestation of the discontinuity while the axisymmetric bubble may be related to the cross-over. However, in words of Leibovich[31], the inference of structural detail from an analysis containing no structure, seems an unusually bold step.

Three sets of investigators attempted to solve numerically the full Navier-Stokes equations. They assumed the flow to be axisymmetric and incompressible. Lavan, Nielsen and Fejer[53] studied the swirling motion in a circular duct, consisting of two smoothly joined sections, (one stationary and the other rotating with a constant angular velocity) for small and large values of the Reynolds numbers. The flow reversal occurs on the axis and near the tube wall and conditions for incipient flow reversal are established. This study deals with a situation much different from those in vortex breakdown. Kopecky and Torrance[26] treated a more realistic problem and imposed initial conditions that resemble vortex breakdown experiments in a tube more closely. An explicit finite difference procedure is used to integrate time dependent transport equations. Their results indicate (a) completely confined eddies can exist even at low Reynolds numbers, (b) sensitivity of eddies to changes in Reynolds number and swirl and (c) some effects of the upstream boundary condition. Calculations performed by Grabowski and Berger[16] in an unconfined region are more extensive and have greater special resolution than those of Kopecky and Torrance. Their solutions exhibit many of the characteristics of vortex breakdown. Taken together the last two results tell us that the Navier-Stokes equations do indeed entertain solutions resembling the axisymmetric bubble form of the vortex breakdown.

## SECTION IV

## HYDRODYNAMIC INSTABILITY

The tip vortex of a laminar flow wing was studied by Singh and Uberoi[51] at a sectional lift-to-drag ratio of 60. Downstream of the wing the jet rapidly dissipated and a wake developed in the core and intensity of turbulent vortices decreased. From 13 to 40 chord length periodic oscillations dominated the velocity fluctuations with little background influence. These instabilities had a symmetric and a helical mode with wavelength of the same order as the core diameter. Garg[13] in his experimental study of the structure of vortex breakdown in a tube observed axial and azimuthal velocity fluctuations at numerous points. It is likely that the oscillations arise from an instability of the mean flow. He measured the mean axial and azimuthal velocity components given by

$$W(r) = W_1 + W_s \exp(-\beta r^2) \tag{17}$$

$$V(r) = \frac{q}{r} [1 - \exp(-\beta r^2)]. \tag{18}$$

The parameters k, $\beta$, and $W_s$ vary slowly with axial distance. Their values have been experimentally determined by Garg (see also Leibovich[31]). The stability of the mean velocity profiles given by (17) and (18) has been analyzed by Howard and Gupta[22], Lessen, Singh and Paillet[32] and Lessen and Paillet[33]. To perform the linear stability analysis, equations (1) to (4) are nondimensionalized with respect to the length scale $r_s$ and the velocity scale $W_s$ given by

$$r_s = (W^2/4\nu z)^{\frac{1}{2}}, \quad W_s = \frac{c_o^2}{8\nu z} \log \frac{Wz}{\nu} + L \frac{W^2}{8\nu z} \tag{19}$$

If we neglect the terms $f(\zeta)$ in equation (12) (Lessen, Singh and Paillet[32] point out that this term is very small under certain conditions), equations (11) and (12) are similar to (17) and (18) when $\beta = \frac{W}{4\nu z}$.

We assume

$$u = u', \quad v = V + v', \quad w = W \text{ " } w', \quad p = \bar{P} + p' \tag{20}$$

and

$$\{u', v', w', p'\} = \{iG, H, F, P\}\,(r)\exp[i(\alpha z - \alpha ct) + ni\theta] \tag{21}$$

where $\bar{P}$ is the mean pressure distribution given by (13) associated with mean velocity distribution W and V. $\alpha$ and n are axial and azimuthal wave numbers, $c = c_r + ic_r$ is the complex phase velocity and F, G, H and P are the complex amplitudes of perturbation. By substituting (20) and (21) into the nondimensionalized and linearized equations (1) to (4), we get (see Lessen and Paillet[33])

$$\alpha rF + (rG)' + nH = 0 \tag{21}$$

$$r^2\gamma G + 2rVH - r^2P' = (iR)^{-1}\,[r(rG')' - (\alpha^2 r^2 + n^2 + 1)\,G - 2nH] \tag{22}$$

$$r^2\gamma H + r(rV)'G + nrP = (iR)^{-1}[r(rH')' - (\alpha^2 r^2 + n^2 + 1)\,H - 2nG] \tag{23}$$

$$r^2\gamma F + r^2W'G + \alpha^2r^2P = (iR)^{-1}\,[r(rF')' - (\alpha^2 r^2 + n^2)F] \tag{24}$$

where a prime denotes d/dr, $R = r_sU_s/\nu$ and $\gamma = \alpha(W - c) + nU/r$.

Batchelor and Gill[2] discuss the boundary conditions required to integrate (21) to (24). These are

$$\begin{aligned} &F(0) = G(0) = H(0) = P(0) = 0 \quad \text{when} \quad n = 0, \neq 1, \\ &F(0) = G(0) = H(0) = P(0) = 0 \quad \text{when} \quad n = 1, 2, 3\ldots(\text{integer}) \end{aligned} \tag{25}$$

$$F(\infty) = F(\infty) = H(\infty) = P(\infty) = 0 \quad \text{for all n.} \tag{26}$$

For the axisymmetric case n = 0, certain general results similar to those of Rayleigh's theorems for the stability of two-dimensional parallel inviscid flows could be established as suggested by Howard and Gupta[23]. Equations (21) to (24) when n = 0 reduce to

$$\frac{d}{dr}\left(\frac{d}{dr} + \frac{1}{r}\right)G = \left[\alpha^2 + \frac{rW'' - W'}{r(W - c)} - \frac{2V(rV' + V)}{r^2(W - c)^2}\right]G \tag{27}$$

Let

$$X = G/(W - c)^{\frac{1}{2}}, \quad \phi = r^{-3}\,D(r^2V^2)$$

$$D = d/dr, \quad D_* = d/dr + 1/r,$$

then (27) becomes

$$D[(W - c)\, D_* X] + \tfrac{1}{2}\left(\frac{W'}{r} - W''\right)X - \tfrac{1}{4}W'^2\,(W - c)^{-1}\,X$$

$$- \alpha^2(W - c)X + \phi(W - c)^{-1}X = 0 \tag{28}$$

Multiplying (28) by $rX^*$ and integrating over $(r_1, r_2)$, we obtain

$$\int_{r_1}^{r_2} (W - c)[|D_* X|^2 + \alpha^2\,|X|^2]\, r\,dr + \tfrac{1}{2}\int_{r_1}^{r_2} (rW'' - W')|X|^2\, dr$$

$$+ \int_{r_1}^{r_2} (W - c^*)[\tfrac{1}{4}W'^2 - \phi]\,\left|\frac{X}{W - c}\right|^2\, r\,dr = 0 \tag{29}$$

Starred quantities denote their corresponding complex conjugate. The imaginary part of (29), if $c_i \equiv I_m\, c > 0$, gives

$$\int_{r_1}^{r_2} [|D_* X|^2 + \alpha^2\,|X|^2]\, r\,dr + \int_{r_1}^{r_2} [\phi - \frac{1}{4}\,W'^2]\,\left|\frac{X}{W - c}\right|^2 r\,dr = 0 \tag{30}$$

which is impossible if $\phi$ is everywhere $\geq \tfrac{1}{4}W'^2$. Thus, a sufficient condition for stability is that $\phi - \tfrac{1}{4}W'^2$ be everywhere non-negative. Defining a local Richardson number J(r) by

$$J(r) = \frac{(r^2V^2)'}{r^3W'^2} \tag{31}$$

the stability condition is $J(r) \geq \tfrac{1}{4}$. This is similar to Rayleigh's point of inflexion theorem for two-dimensional parallel-flow instability. Another result like that of Howard's circle theorem can be established following Kochar and Jain[25]. If we introduce

$$M = G/(W - c)$$

into (27), we have

$$D[(W - c)^2\, D_* M] - \alpha^2(W - c)^2\, M + \phi M = 0 \tag{32}$$

If (32) is multiplied by $M^*$, complex conjugate of M and integrated over $(r_1, r_2)$, then the real and imaginary parts together with certain manipulations introduced by Howard lead the inequality to

$$\left[\left(c_r - \frac{a+b}{2}\right)^2 + c_i^2 - \left(\frac{a-b}{2}\right)^2\right] \int_{r_1}^{r_2} \rho Q \, r\,dr + \int_{r_1}^{r_2} \phi |M|^2 \, r\,dr \leq 0 \quad (33)$$

where $Q = |M'|^2 + \alpha^2 |M|^2$, $\quad a \leq W \leq b$.

The result (33) can be shown such that the complex wave velocity for any unstable mode lies in a semi-ellipse whose major axis coincides with the diameter of Howard's semi-circle while its minor axis depends on the Richardson number J. The following inequality

$$\left[c_r - \tfrac{1}{2}(a+b)\right]^2 + \frac{2c_i^2}{1 + (1 - 4J)^{\frac{1}{2}}} \leq \tfrac{1}{4}(a-b)^2 \quad (34)$$

is satisfied.

The inviscid stability of swirling flows with mean velocity profiles given by (17) and (18) was studied by Lessen, Singh and Paillet with respect to infinitesimal non-axisymmetric disturbances. The flow is characterized by a swirl parameter q which is the ratio of the magnitude of the maximum swirl velocity to that of the maximum axial velocity. It is found that as the swirl is continuously increased from zero, the disturbances die out quickly for a small value of q if n = 1. The results for negative azimuthal modes are very different. For negative values of n, the amplification rate increases and then decreases, falling to negative values at q slightly greater than 1.5 for n = -1. The maximum amplification rate increases for increasingly negative n up to n = -6 (the highest mode investigated) and corresponds to q ≈ 0.85. For viscous stability theory, Lessen and Paillet calculated both time wise and space wise growth rates for the lowest three negative non-axisymmetric modes (n = -1, -2, and -3). The large wave numbers associated with the disturbances at large |n| allow the n = -1 mode to have minimum critical Reynolds

number of 16 (q = 0.60). The other two modes investigated have minimum Reynolds numbers on the neutral curve of 31 (n = -2, q = 0.60) and 57 (n = -3, q = 0.80). For each mode, the neutral stability curve is shown to shift rapidly towards infinite Reynolds numbers one the swirl becomes sufficiently large.

## SECTION V

## CONCLUSION

All the experimental observations indicate that vortex breakdown depend on two dimensionaless numbers (1) the Reynolds $W_s\ r_s/\nu$ and (2) the circulation $\Omega = q/W_s\ r_s$. The axial and swirl velocity components are given by (17) and (18). Starting with these values for the velocity components at a junction $z = 0$, theoretical prediction of the occurrence of axisymmetric 'bubble' like vortex breakdown for $z >> 0$ is in qualitative agreement with experimental observations. Linear stability analysis predicts that all the vortex flows are stable subject to infinitesimal axisymmetric disturbances provided the Richardson number $J = \frac{(r^2V^2)'}{r^3W'^2} \geq \frac{1}{4}$. Breakdown has also been correlated with $\tan \phi = (v_{max}/W)$ such that the maximum value of $\phi$ upstream of breakdown is invaribly greater than about 45°. In the case of non-axisymmetric disturbances, the negative azimuthal modes are more unstable than the positive ones.

Numerical experiments have, however, not been able to predict the spiral form of the breakdown, because it may be excluded by hypothesis by axisymmetric formulation. The effect of adverse pressure gradient on the vortex breakdown has also not been studied.

## SECTION VI

## RECOMMENDATION

Suggestions for follow-up research: We would like to investigate what effect the adverse pressure gradient has on the vortex breakdown. In flows through pipes both Kirkpatrick[24] and Sarpkaya[42] have observed that there is a slight positive pressure gradient upstream of the breakdown and a negative gradient immediately downstream. In flows past ogive cylinders and delta wings at increasing angle of attack the positive pressure gradient seems to accelerate the vortex breakdown. To study this, first the expressions for axial and azimuthal velocity components similar to (17) and (18) have to be obtained as solutions of the Navier-Stokes equations under the imposed pressure gradient. One way is to invoke (16) with (18) and find $\psi$ for given pressure distributions. Once the questions regarding starting values of v and w are decided, then both the solutions of the Navier-Stokes can be attempted and the linear stability analysis subject to axisymmetric and non-axisymmetric disturbances also can be studied.

## REFERENCES


1. Batchelor, G. K., "Axial Flow in Trailing Line Vortices," J. Fluid Mech, Vol. 20, 645-58, 1964.

2. Batchelor, G. K. and Gill, A. E., "Analysis of the Stability of Axisymmetric Jets, J. Fluid Mech. Wol. 14, 528, 1962.

3. Benjamin, T. B., "Theory of of the Vortex Breakdown Phenomenon, J. Fluid Mech, Vol. 14, 593-629, 1962.

4. Benjamin, T. B., "Some Developments in the Theory of Vortex Breakdown, J. Fluid Mech, Vol. 28, 65-84, 1967.

5. Bossel, H. H., "Vortex Breakdown Flow Field, Phys, Fluids, Vol. 12, 498-508, 1969.

6. Bossel, H. H., "Vortex Computation by the Method of Weighted Residuals Using Exponentials, AIAA, Vol. 9, 2027-34, 1971.

7. Chanaud, R. C., "Observations of Oscillating Motion in Certain Swirling Flows, J. Fluid Mech, Vol. 21, 111-27, 1965.

8. Cox, A. P., "Measurements of the Velocity at the Vortex Centre on an A.R.I. Delta Wing by Means of Smoke Observations, RAE, Tech. Note 2634, June 1959.

9. Earnshaw, P. B. and Lawford, J. A., "Low Speed Wind Tunnel Experiments on a Series of Sharp Edged Delta Wings, Part I. Forces, Moments, Normal Force Fluctuations and Positions of Vortex Breakdown," TN Aero 2780, 1961, Royal Aircraft Establishment, Farnborough Hants.

10. Elle, B., "On the Breakdown at High Incidences of the Leading Edge Vorticies on Delta Wings," J. R. Aeronaut. Soc., Vol. 64, 491-93, 1960.

11. Faler, J. H. and Leibovich, S., "Disrupted States of Vortex Flow and Vortex Breakdown," Phys. Fluids, Vol. 20, 1385-1400, 1977.

12. Faler, J. H. and Leibovich, S., "An Experimental Map of the Internal Structure of a Vortex Breakdown," J. Fluid Mech., 1977.

13. Garg, A. K., "Oscillatory Behavior in Vortex Breakdown Flows: An Experimental Study Using a Laser Doppler Anemometer," MS Thesis, Cornell Univ., Ithaca. 255, 1977.

14. Gartshore, I. S., "Recent Work in Swirling Incompressible Flow." NRC Can. Aero. Rep. LR-343, 1962.

15. Gartshore, I. S., "Some Numerical Solutions for the Viscous Core of an Irrotational Vortex," NRC Can. Aero Rep, LR-378, 1963.

16. Grabowski, W. J., Berger, S. A., "Solutions of the Navier-Stokes Equations for Vortex Breakdown," J. Fluid Mech, Vol. 75, 525-44, 1976.

17. Hall, M. G., "The Structure of Concentrated Vortex Cores," Prog. Aeronaut. Sci., Vol 7, 53-110, 1966.

18. Hall, M. G., "A New Approach to Vortex Breakdown," Heat Transfer Fluid Mech. Inst., 319-40, Stanford University Press, 1967.

19. Hall, M. G., "Vortex Breakdown," Ann. Rev. Fluid Mech., Vol. 4, 195-218, 1972.

20. Harvey, J. K., "Some Observations of the Vortex Breakdown Phenomenon," J. Fluid Mech., Vol. 14, 585-92, 1962.

21. Herron, J. H., Comments on a Note on the Flow in a Trailing Vortex, J. Engng. Math., Vol. 8, 339 (1974).

22. Howard. L. N. and Gupta, A. S., "On the Hydrodynamic and Hydromagnetic Stability of Swirling flows," J. Fluid Mech., Vol. 14, 463-76, 1962.

23. Hummel, D., "Untersuchungen über das Aufplatzen der Wirbel an schalnken Deltaflügeln," Z. Flugwiss, Vol. 13, 158-68, 1965.

24. Kirkpatrick, D. L. I., "Experimental Investigation of the Breakdown of a Vortex in a Tube," Aeronaut. Res. Counc. CP, 1964.

25. Kochar, G. T. and Jain, R. K., Note on Howard's Circle Theorem," J. Fluid Mech., Vol. 91, 489, (1979).

26. Kopecky, R. M. and Torrance, K. E., "Initiation and structure of Axisymmetric Eddies in a Rotating Stream," Comput. Fluids, Vol. 1, 289-300, 1973.

27. Küchman, D., IUTAM Symposium of Vortex Motion, Ann Arbor, J. Fluid Mech. Vol. 22, 17 (1964).

28. Lambourne, N. C. and Bryer, D. W., "The Bursting of Leading-Edge Vortices-Some Observations and Discussion of the Phenomenon," Aeronaut. Res. Counc. R & M 3282, (1961).

29. Leibovich, S., "Axisymmetric Eddies Embedded in a Rotational Stream," J. Fluid Mech, Vol. 32, 529-48, 1968.

30. Leibovich, S. and Randall, J. D., "Amplification and Decay of Long Non-linear Waves," J. Fluid Mech, Vol. 52, 481-93, 1973.

31. Leibovich, S., "The Structure of Vortex Breakdown," Ann. Rev. Fluid Mech. Vol. 10, 221-246, 1978. (Also see J. Fluid Mech, Vol 93, 401 [1979]).

32. Lessen, M., Singh, P. J. and Paillet, F., "The Stability of a Trailing Line Vortex, Part 1. Inviscid Theory," J. Fluid Mech, Vol. 63, 753-63, 1974.

33. Lessen, M, and Paillet, F., "The Stability of a Trailing Line Vortex, Part 2. Viscous Theory," J. Fluid Mech., Vol. 65, 769, 1974.

34. Lowson, J. V., "Some Experiments with Vortex Breakdown," Journal of the Royal Aeronautical Society, Vol. 68, No. 621, 343, 1974.

35. Ludwieg, H., "Zur Erklärung der Instabilität der über angestellten Deltaflügeln auftretenden freien Wirbelkerne, Z. Flugwiss, Vol. 10 242-49, 1962.

36. Ludwieg, H., "Erklärung des Wirbelaufplatzens mit Hilfe der Stabilitätstheorie für Strömungen mit schraubenlinienförmigen Stromlinien." Z. Flugwiss, Vol. 13, 437-42, 1965.

37. Mager, A., "Dissipation and Breakdown of a Wing-Tip Vortex," J. Fluid Mech., Vol. 55, 609-28, 1972.

38. Newman, B. G., "Flow in a Viscous Trailing Vortex," Aero. Quart. X, Part 2, 149, 1959.

39. Owen, P. R., "The Decay of a Turbulent Trailing Vortex," Vrit. A.R.C. 25, 818; F.M. 3446, 1964.

40. Peckham, D. H. and Atkinson, S. A., "Preliminary Results of Low Speed Wind Tunnel Tests on a Gothic Wing of Aspect Ratio 1.0," Aeronaut. Rec. Counc. CP 508. 1957.

41. Randall, J. D. and Leibovich, S., "The Critical State: A Trapped Wave Model of Vortex Breakdown," J. Fluid Mech, Vol. 53, 495-515, 1973.

42. Sarpkaya, T. "On Stationary and Travelling Vortex Breakdowns," J. Fluid Mech., Vol. 45, 545-59, 1971.

43. Sarpkaya, T., "Vortex Breakdown in Swirling Conical Flows," AIAA J. Vol. 9, 1979-99, 1971.

44. Sarpkaya, T., "Effect of the Adverse Pressure Gradient on Vortex Breakdown," AIAA J., Vol. 12, 602-7, 1974.

45. Singh, P. I. and Uberoi, M. S., "Experiments on Vortex Stability, Phys. Fluids, Vol. 19, 1858-63, 1976.

46. Squire, H. B., "Analysis of the "Vortex Breakdown" Phenomenon. Part 1," Aero. Dept, Imperial Coll, London, Rep. Vol. 102 (Also in Miszellaneen der Angewandten Mechanik, 306-12, 1962. Berlin: Akademie-Verlag) 1960.

47. Steiger, M. H. and Bloom, M. H., " Axially Symmetric Laminar Free Mixing with Large Swirl," J. Heat Trans. Vol. 4, 370, 1962.

48. Stewartson, K. and Hall, M. G., "The Inner Viscous Solution for the Core of a Leading Edge Vortex," J. Fluid Mech. 15, 306, 1963.

49. Tam, K. K., A Note on the Flow in a Trailing Vortex, J. Engrg. Math. Vol. 7, 1. 1973.

50. Uberoi, M. S., "Mechanisms of Decay of Laminar and Turbulent Vortices, J. Fluid Mech., Vol. 90, 241 (1979).

51. Uberoi, M. S., Chow, C. Y. and Narain, J. P., "Stability of Coaxial Rotating Jet and Vortex of Different Vortices," Phys. Fluids, Vol. 15, 1718,(1972).

52. Werle, H., "Sur l'eclatemant des Tourbillons d'apex d'une aile delta aux faibles vitesses," La Recherche Aeronautique, No. 74, 1960, p. 23.

53. Lavan, Z., Nielsen, H. and Fejer, A. A., "Separation and Flow Reversal in Swirling Flow in Circular ducts," Phys. Fluids, Vol. 12, 1747-57, 1969.

1980 USAF-SCEE SUMMER FACULTY RESEARCH PROGRAM

Sponsored by the

AIR FORCE OFFICE OF SCIENTIFIC RESEARCH

Conducted by the

SOUTHEASTERN CENTER FOR ELECTRICAL ENGINEERING EDUCATION

# FINAL REPORT

# AN APPLICATION OF INVARIANCE PRINCIPLE TO PILOT MODEL FOR NT-33 AIRCRAFT WITH VARIABLE COEFFICIENTS AND DELAYS


| | |
|---|---|
| Prepared by: | Dr. Akhouri S. C. Sinha |
| Academic Rank: | Professor of Electrical Engineering |
| Department: | Division of Engineering |
| University: | Purdue University School of Engineering and Technology, Indianapolis |
| Research Location: | Air Force Wright Aeronautical Laboratories, Control Dynamics Branch |
| USAF Research Colleague: | Dr. Robert Schwanz |



Date: September 12, 1980

Contract No.: F 49620-79-C-0038

# AN APPLICATION OF INVARIANCE PRINCIPLE TO PILOT MODEL FOR NT-33 AIRCRAFT WITH VARIABLE COEFFICIENTS AND DELAYS

by

Akhouri S. C. Sinha

## ABSTRACT

A method for analysing Pilot-induced oscillations (PIO) for NT-33 closed-loop pilot model when the ratardations and coefficients are not constant is proposed. The fact that the retardations and the coefficients are not constant is justified due to the effect of wind shear and the neuromuscular dynamics of the pilot reflected in the available data. The nonlinearities in the model are also considered. The method is based on the use of a new description of such systems in terms of convolution equations. The spectral factorization of the entire functions of the exponential order is used to derive a criterion for the PIO-system with variable coefficients and variable delays under the assumptions of continuity and boundedness of these coefficients and delays. A Lyapunov functional is constructed which gives a criterion on the roots of a certain "quasi-polynomial", i.e., a polynomial in a variable and the exponential of that variable. The largest domain of attraction is obtained from the Invariance Principle. Recommendations for follow-on research in this area are suggested.

## ACKNOWLEDGMENT

The author wishes to acknowledge the Air Force Office of Scientific Research, the Air Force Systems Command, and Southeastern Center for Electrical Engineering Education. The author wishes to express his gratitude to Dr. Robert C. Schwanz for suggesting this area of research and for his guidance and encouragement given him during the course of the project. His able assistance has been invaluable in the preparation of this report and for the presentation of this work in the seminar.

He also wishes to express his sincere thanks to Mr. Frank George for his interest, advise, and discussion of this work.

The author would like to thank the Air Force Control Dynamics Branch for supporting a very worthwhile and interesting summer research program at the Air Force Wright Aeronautical Laboratory, Dayton, Ohio.

Finally, he would like to thank Dr. G. K. Richey, Senior Scientist FICG for his excellent presentation on WPAFB, research activities.

ASCS
Fall 1980

## I INTRODUCTION

The Air Force Flight Dynamics Laboratory (AFWAL/FI) has been conducting research on the effects of control system dynamics on fighter approach and landing longitudinal flying qualities. The objective in the program has been to investigate pilot-induced oscillations (PIO) of the NT-33 aircraft due to significant control system lags, effects of wind shear and the pilot delays. A sharp degradation in flying qualities takes place during this critical phase of the landing task. Severe pilot-induced oscillations during the flare have been reported. The advance digital control schemes add much greater flexibilities and logic capabilities when compared to analog systems. However, this increase in complexity of future aircraft flight control systems also may add larger control systems lags. It has been observed that large control system lags, high pilot gains, pilot-lag due to neuromuscular dynamics and aerodynamic transport lag are all possible causes of pilot-induced oscillation problems. These phenomena all require careful theoretical analysis.

It should be stressed that the use of digital control system is now a reality and its effects on flying qualities of these fighter aircrafts need careful analysis. The variable stability NT-33 is capable of producing a wide range of aircraft and control system characteristics. This was the main reason to select the NT-33 aircraft to test the flying qualities of simulated YF-12 and YF-17 aircraft. The simulation of the YF-17 with the NT-33 aircraft has encountered serious PIO difficulties in flare whereas no such problems have been reported for YF-17 [1]. Some detailed studies of PIO during the NT-33 aircraft simulation can be found in earlier works of USAF/Calspan [2]. Calspan diagnosed the PIO-problem as excessive control lags. They modified the simulated

control system dynamics to reduce the lag contribution to longitudinal dynamics and found that it minimized or reduced the problem. The effects of significant control dynamics on fighter approach and landing longitudinal flying qualities were also investigated in flight using the USAF/Calspan NT-33 aircraft [3]. The pilot-induced oscillations occurred during the landing task. The flight tests as reported in [3] provide a data base for the development of suitable flying qualities requirements which are applicable to aircraft with significant control system dynamics.

The properties of the solutions of the linear differential equations of the retarded type with constant coefficients and constant time-delays for the pilot model has been considered by several authors. However, the formulation when the coefficients and the retardations in the closed-loop pilot model are not constant, has not been considered. Such formulation may now be justified when the effect of wind shear and the neuromuscular system dynamics are included. This extension of the analysis is suggested by the recent measurements that have been cited. A generalized closed-loop nonlinear pilot nodel for NT-33 aircraft, when the retardations and coefficients are not constant is considered herein. The theoretical analysis is developed in the time domain to analyze the pilot-induced oscillations problem in the most general format.

## II OBJECTIVES

The structure of the summer research is as follows. First, a formulation of the closed-loop NT-33 pilot model is introduced. The NT-33 air-frame dynamic equations, linearized about the trim conditions and representing the manual flare and landing of the aircraft, have been used. The pilot dynamics are assumed to have variable gain and variable retardation, possibly due to wind shear and the neuromuscular effects. It is assumed that the pilot forms the closed-loop, thus changing the overall characteristics of the system.

After having introduced the required formulation of the closed-loop NT-33A pilot model, certain theorems dealing with the spectral factorization of the entire functions of the exponential order were used to generate Lyapunov functionals. The reference source for this material is the English translation of the book by Levine [4], which gives a comprehensive treatment of the properties of the zeros of the entire functions and related aspects. The spectral factorization theorems play a central role in constructing the Lyapunov functionals. The emphasis of the spectral factorization will be on the role that these equations play in connection with the generation of Lyapunov functionals for a class of system that represents PIO-systems, rather than on the mathematical proofs. The analysis of the PIO-systems is accomplished by making use of a description of the dynamical systems in terms of convolution equations involving distributions which satisfy assumptions made by Hale and Meyer [5] for the functional equations of the delay type.

## III THE PILOT MODEL

Figure 1 represents a nonlinear pilot model. The NT-33 airframe dynamic equations linearized about the trim condition representing the manual flare and landing of the aircraft have been used. These equations are the same as those given in USAF/CALSPAN [2] and Smith [3], except that only the longitudinal transfer functions have been derived. The longitudinal equations representing the open-loop aircraft dynamics about the trim conditions during the flare and landing manuevers are represented as

$$\begin{bmatrix} \dot{u} \\ \dot{w} \\ \dot{q} \\ \dot{\theta} \end{bmatrix} = \begin{bmatrix} X_u & X_w & -g\cos\theta_o & -w_o \\ Z_u & Z_w & -g\sin\theta_o & u_o \\ M_u & M_w & 0 & M_q \\ 0 & 0 & 0 & 1 \end{bmatrix} \begin{bmatrix} u \\ w \\ q \\ \theta \end{bmatrix} + \begin{bmatrix} X_{\delta_{ES}} \\ Z_{\sigma_{ES}} \\ M_{\delta_{ES}} \\ 0 \end{bmatrix} \delta_{ES} \quad (1)$$

where symbols represent as follows: u, w, q, $\theta$ are perturbation velocity from trim along x-body axis, perturbation velocity from trim along z-body axis, body axis pitch rate and pitch attitude respectively. $\delta_{ES}$ is pitch stick deflection at grip. Also, notationally,

$$X_u = \frac{1}{m}\frac{\partial X}{\partial u}, \quad X_w = \frac{1}{m}\frac{\partial X}{\partial w}, \quad X_{\delta_{ES}} = \frac{1}{m}\frac{\partial X}{\partial \delta_{ES}}$$

$$Z_u = \frac{1}{m}\frac{\partial Z}{\partial u}, \quad Z_w = \frac{1}{m}\frac{\partial Z}{\partial w}, \quad Z_{\delta_{ES}} = \frac{1}{m}\frac{\partial Z}{\partial \delta_{ES}}$$

$$M_u = \frac{1}{I_y}\frac{\partial M}{\partial u}, \quad M_w = \frac{1}{I_y}\frac{\partial M}{\partial w}, \quad M_{\delta_{ES}} = \frac{1}{m}\frac{\partial M}{\partial \delta_{ES}}$$

$X_u$, $X_w$, $Z_u$, $Z_w$ are body axis dimensional x-force derivative and z-force derivatives respectively. $M_u$, $I_x$, $I_y$ are aircraft mass, moment of inertia about body x-axis and body y-axis respectively. $u_o$, $w_o$, $q_o$, and $\theta_o$ are trim valves.

These equations imply that the reference axes are body axes and the wings are always level. For small angles, $u_o \simeq V_T$, the trim true airspeed, and $\alpha_o \simeq W_o/V_T$. The variables u, w ($\alpha$), $\theta$ and $\delta_{ES}$ are all incremental valves from the reference trim conditions.

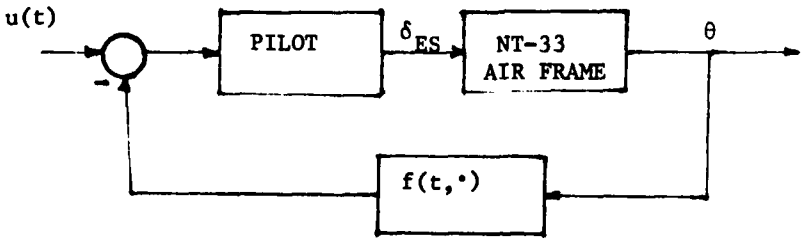



Fig. 1

The transfer function for longitudinal stick input ($\delta_{ES}$) and pitch attitude control output ($\theta$) can be derived from the equations of motion (1) as

$$\frac{\theta}{\delta_{ES}} = \frac{M_{\delta_{ES}} (s + \frac{1}{\tau_{\theta_1}})(s + \frac{1}{\tau_{\theta_2}})}{(s^2 + 2\zeta_{sp} w_{sp} s + w_{sp}^2)(s^2 + 2\zeta_{ph} w_{ph} s + w_{ph}^2)} = \frac{\rho(s)}{\sigma(s)} \qquad (2)$$

where $\tau_{01,2}$ represents airframe lead time constants $\zeta_{sp}$, $w_{sp}$, and $\zeta_{ph}$, $w_{ph}$ are short period damping ratio , short period undamped natural frequency and phugoid damping ratio phugoid undamped natural frequency respectively. $\rho(s)$ and $\sigma(s)$ are polynomials in s. The polynomials $\rho(s)$ and $\sigma(s)$ are such that the degree of $\sigma(s)$ is assumed to exceed to that of $\rho(s)$. An inspection of the data base of ref. [3, 10-12] suggests that a reasonable model for pilot dynamics in pitch tracking would be of the form

$$L(s) = \sum_{i=o}^{m} a_i(t)\, s^i e^{-s\tau(t)} + \sum_{i=o}^{n} b_i(t)\, s^i \; ; \; n > m \qquad (3)$$

where $a_i(t)$, and $b_i(t)$ are bounded coefficients and $\tau(t)$ is a bounded time-delay, the time-delay $\tau(t)$ is unknown and can be assumed due to neuromuscular effect of the pilot. A small transmission lag may also be present. The pilot dynamics is assumed to have variable gains $a_i(t)$, $b_i(t)$ possibly due to wind shear and the neuromuscular effects. It is assumed that the pilot forms the closed-loop, thus changing the overall characteristics of the system.

A closed-loop analysis can be performed by considering the pilot to be controlling to some desired attitude which minimizes the pitch attitude error e. The non-linearities of the artificial feel system are included in the model, as well as the nonlinearities in the stability augmentation systems. Further the nonlinear function $f(t,\theta)$ is such that $df/d\theta$ exists for all $\theta$ and $\theta f(t,\theta) < 0$ for $\theta \neq 0$, or $\theta f(t,0) > K\,\theta^2$.

This completes our formulation of closed-loop nonlinear model with the pilot in the loop. The dynamics of NT-33 airframe, the pilot and the nonlinearities of the artificial feel system as well as the nonlinearities of the stability augumentation system have all been defined. In the next section, we give some notations, theoretical backgrounds and our method of analysis.

## IV APPLICATION OF INVARIANCE PRINCIPLE

The 'invariance principle' of J. P. LaSalle played an important role in the theory of abstract dynamical systems. But it is also particularly useful in solving practical problems. Very few practical applications [7,13] of 'invariance principle' have been attempted because of its complexity. By applying the invariance principle, we are able to derive stability criteria for the dynamical systems which are optimal in a certain sense. Thus the stability results can be improved considerably when the study of the system is based om LaSalle's invariance principle [6].

In this section, we first introduce our notations. This is followed by some lemmas on spectral factorization and its application to the invariance princple. Levin [4] has already given comprehensive treatment of the properties of zeros of the entire functions. The spectral factorization of the entire function plays an important role in studying the properties of solutions as we shall see in our analysis of the pilot-induced oscillation problem.

The following notation from Hale [8] will be used in this paper: $E^n$ is complex Euclidean n-space, and for $x \in E^n$, $|x|$ denotes any vector norm. For a given $\tau(t) \geq \bar{\tau} > 0$, denotes the linear space of continuous functions mapping tne interval $[-\bar{\tau}, 0]$ into $E^n$ and for $\phi \in \mathcal{C}$, $||\phi|| = \sup |\phi(\theta)|$, $-\bar{\tau} \leq \theta \leq 0$.

Of course $\mathcal{C}$ with this norm is a Banach space. For $H > 0$, $\mathcal{C}_H$ denotes the set of $\phi$ in $\mathcal{C}$ for which $|| \phi || < H$, for any continuous function $x(s)$ whose domain is $-\bar{\tau} \leq s \leq \alpha$ $\alpha \geq 0$, and whose range is in $E^n$, and for any $t$, $0 \leq t \leq \alpha$ the symbol $x_t$ will denote $x_t(\theta) = x(t + \theta)$, $-\bar{\tau} \leq \theta \leq 0$; that is $x_t$ is in $\mathcal{C}_H$, and is that segment of the function $x(s)$ defined by letting $s$ range in the interval $t - \bar{\tau} \leq s \leq t$.

Let $G(t,\phi)$ be a function defined on $(0,\infty) \times \mathcal{C}_H$ into $E^n$ and let $\dot{x}(t)$ denote the right hand derivative of $x(s)$ at $s = t$. The system

$$\dot{x}(t) = G(t, x_t), \quad t \geq 0$$

is called functional - differential equation (FDE).

Definition - Let $t_o \geq 0$, and let $\phi$ be any given function in $\mathcal{C}_H$. A function $x(t_o, \phi)(t)$ is said to be solution of FDE with initial function $\phi$ at $t = t_o$ if there exists a number $A \geq 0$ such that

(a) for each $t$, $t_o \leq t \leq t_o + A$, $x_t(t_o, \phi)$ is defined in $\mathcal{C}_H$.

(b) $x_{t_o}(t_o, \phi) = \phi$

(c) $x(t_o, \phi)(t)$ satisfies functional differential equation (FDE) for $t_o \leq t \leq t_o + A$.

To analyze PIO-problem the original model in fig. 1 is redrawn as

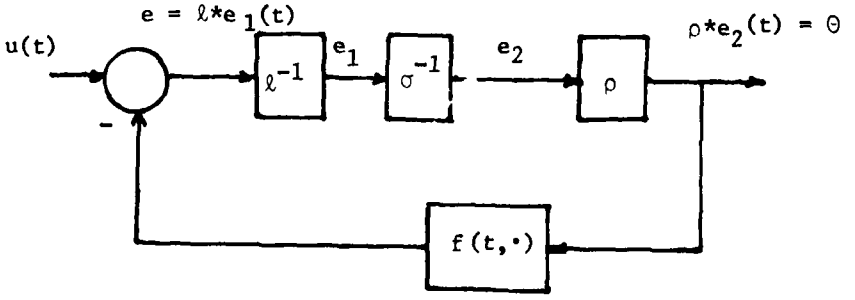



Fig. 2

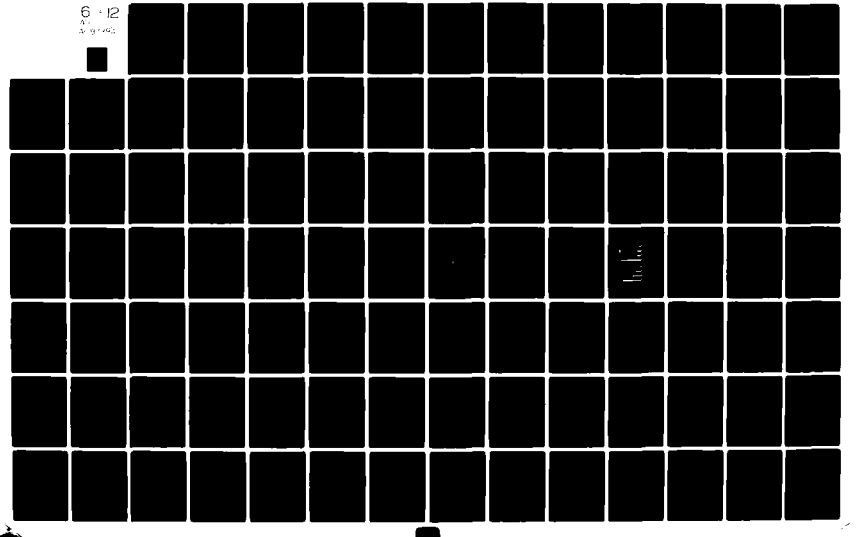
Note that in the block diagram

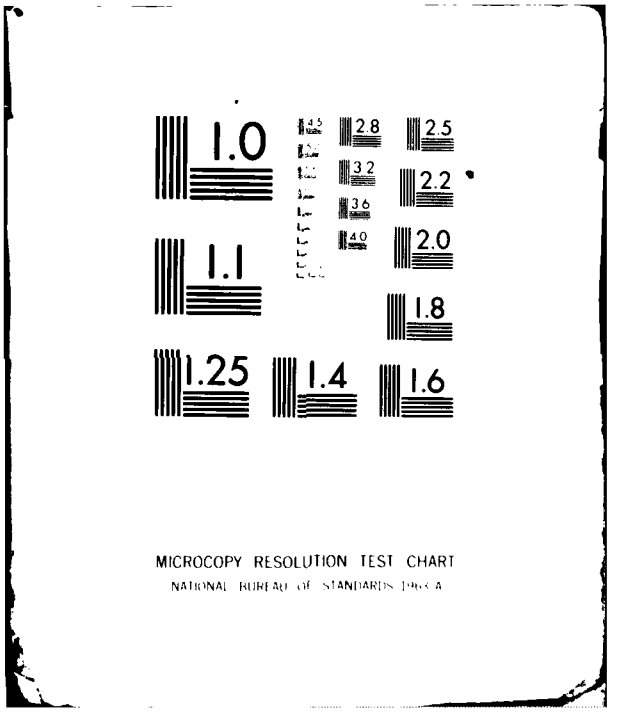
$$\ell * e_1(t) = \left( \sum_{i=o}^{m} a_i(t)\, \delta_{T(t)}^{i} + \sum_{i=o}^{n} b_i(t)\, \delta^i \right) * e_i(t) \qquad (4)$$

AD-A097 394 SOUTHEASTERN CENTER FOR ELECTRICAL ENGINEERING EDUCAT--ETC F/G 5/1
USAF SUMMER FACULTY RESEARCH PROGRAM, 1980, RESEARCH REPORTS, V--ETC(U)
OCT 80 W D PEELE F49620-79-C-0038

UNCLASSIFIED AFOSR-TR-81-0193 NL

6 12




1.0
1.1
1.25
1.4
1.6
1.8
2.0
2.2
2.5
2.8
3.2
3.6
4.0
MICROCOPY RESOLUTION TEST CHART
NATIONAL BUREAU OF STANDARDS 1963 A

## I. INTRODUCTION

Recent developments in microprocessor technology have renewed interest in the analysis and design of sampled-data or digital control systems. For the past few years, digital devices have been incorporated into control systems because they are more compact, reliable and economical in comparison to their analog counterparts. Consequently, new control systems are being designed using digital controllers instead of analog controllers. There is also a need for converting existing continuous-data control systems into digital control systems with similar performances.

Tobak[1] presented a method for converting existing continuous control systems into digital control systems by means of digital controllers. This method converts continuous controllers into digital controllers using bilinear transformation which is also known as the Tustin transform. This method only takes into consideration the frequency responses of the digital controllers, not the overall system. Although the method is straightforward and easy to use, the digital control system obtained by this method approximates the continuous system only if the sampling frequency is sufficiently high compared with the highest frequency of the continuous system. Thus the capabilities of the digital controllers are not fully utilized.

In recent papers, Kuo et al,[2] Yackel et al[3] and Singh et al[4] proposed methods for converting a continuous control system into a sampled-data control system by matching the time response of the systems at all sampling instants or at multiples of sampling instants. The matching requirements are satisfied by changing the input and feedback gains of the system instead of using a digital controller. However, such matching holds only for unit step inputs. Thus the performance of the sampled-data system obtained by their method approximates that of the continuous model only when the input frequency is sufficiently low in comparison with the sampling frequency. For higher input frequencies, the approximation is poor.

Hence there is a need for developing a method which does not require an excessively high sampling frequency and which utilizes the digital controllers to their full capabilities. In this report a computer-aided

method for synthesizing digital controllers is developed by matching the frequency responses of the digital control system with that of the continuous system with maximum weighted mean-square error. The method uses the complex-curve fitting technique of Levy.[5] The design algorithms developed here are based on the parameters of pulse-transfer function of the plant and the closed-loop transfer function of different loops of the continuous system. As a particular application, the digitalization of a flight control system is discussed. The system under consideration is the flight controller for the longitudinal YF-16 aircraft. The results obtained by this method are compared with those obtained by the Tustin transform method.

## II. STATEMENT OF THE PROBLEM

The block diagram of a general multiloop continuous-data control system may be drawn as shown in Figure 1.

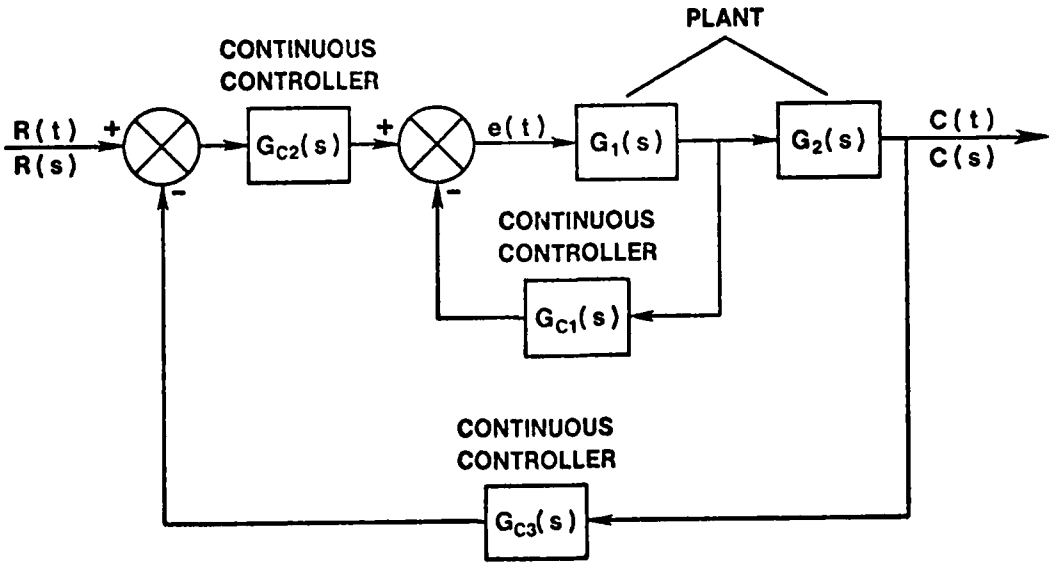



Figure 1. Multiloop continuous-data control system

The continuous model shown in Figure 1 can be digitalized by inserting a sampler at the error input e(t) and replacing the continuous compensators $G_{ci}(s)$ by digital controllers $D_i(z)$ as shown in Figure 2.

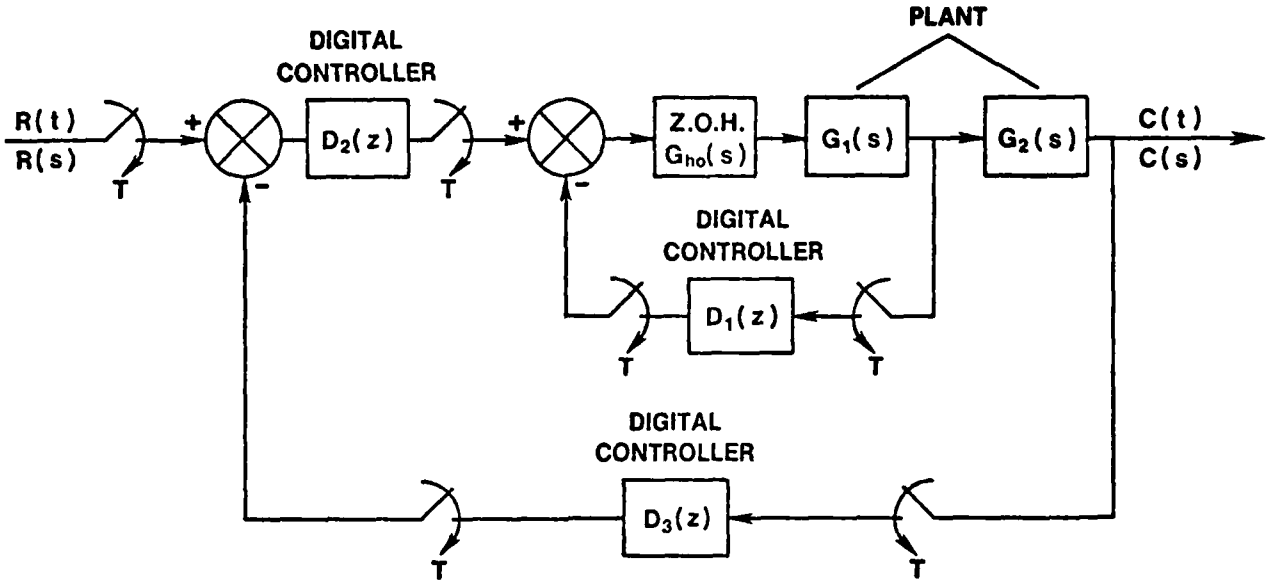



Figure 2. Multiloop digital control system

The general pulse-transfer function of a digital controller may be written as

$$D(z) = \frac{a_0+a_1z^{-1}+a_2z^{-2}+\cdots+a_mz^{-m}}{1+b_1z^{-1}+b_2z^{-2}+\cdots+b_nz^{-n}} \quad , \; m\leq n \qquad (1)$$

where a's and b's are constants. It is required to design digital controllers, i.e., to find a's and b's so that the steady state output of the digital control system at the sampling instants follows the desired output of the continuous model for all sinusoidal inputs within the frequency range. This is done by matching the frequency responses of different loops of the digital control system to the corresponding ideal frequency responses starting from the innermost loop.

Let $G_d^*(j\omega)$ be the frequency characteristic function of a single-loop digital control system with a digital controller either in the feedforward or feedback loop. The error between $G_d^*(j\omega)$ and the transfer function $F(j\omega)$ of the corresponding continuous control system is defined as

$$\epsilon(\omega) = F(j\omega) - G_d^*(j\omega) \tag{2}$$

An optimal set of a's and b's can therefore be obtained by minimizing the mean square of the magnitude of $\epsilon(\omega)$. Let the error function to be minimized be defined as

$$E = \int_0^{\omega_s/2} |F(j\omega) - G_d^*(j\omega)|^2 d\omega \tag{3}$$

where the limit of integration is taken from 0 to 1/2 $\omega_s$ rather than 0 to $\infty$ because of the frequency folding effect of the sampled-data control system. This error function is to be minimized by adjusting the a and b coefficients. This is done by differentiating E with respect to a's and b's and equating the resulting equations to zero. However, due to the presence of unknown constants in the denominator of $G_d^*(j\omega)$, the resulting equations are nonlinear. This nonlinearity may be removed by modifying the error function (3) so that

$$E_m = \int_0^{\omega_s/2} |F(j\omega)M(\omega) - N(\omega)|^2 d\omega \tag{4}$$

where $N(\omega)$ and $M(\omega)$ are the numerator and denominator of $G_d^*(j\omega)$ respectively. This integral differs from that in equation (3) by including $|M(\omega)|^2$ in the integrand as a weighing factor. This modification is not new. It was suggested by Kalman[6] as an identification technique, was used by Levy[5] in complex curve fitting, and by Rao and Lamba[7] for simplifying linear dynamic systems. Mullis and Roberts[8] also discussed the use of this error criterion in the approximation of discrete linear systems.

The weight $M(\omega)$ is zero for some real $\omega$ only if $M(z)$, the characteristic polynomial of the digital control system, has roots on the unit circle in the z-plane. For the stable system, however, all the roots of the

characteristic equation lie inside the unit circle and therefore $M(\omega)$ is nonzero. For a well defined system, the error given by equation (4) is small or nearly zero. Therefore the weighing factor $|M(\omega)|^2$ is approximately equal to a constant times the absolute value of the denominator of $F(j\omega)$. If it is desired to eliminate the effect of the weighing factor, one can further modify equation (4) by dividing the integrand by the square of the magnitude of the denominator of $F(j\omega)$. However the numerical examples considered have shown that this is not necessary.

The transfer function $F(j\omega)$ of the continuous model, and the numerator and denominator of $G_d^*(j\omega)$ can be written in terms of real and imaginary part as

$$F(j\omega) = R(\omega) + jS(\omega) \tag{5}$$

$$N(\omega) = \phi + j\theta \tag{6}$$

$$M(\omega) = \sigma + j\tau \tag{7}$$

Substituting equation (5), (6) and (7) into the integrand of the error function $E_m$ given in equation (4), we get

$$F(j\omega)M(\omega) - N(\omega) = \ell(\omega) + jm(\omega) \tag{8}$$

where

$$\ell(\omega) = R(\omega)\sigma - S(\omega)\tau - \phi \tag{9}$$

$$m(\omega) = R(\omega)\tau + S(\omega)\sigma - \theta \tag{10}$$

By substituting (8), (9) and (10) in (4)

$$E_m = \int_0^{\omega_s/2}\left[\left(R(\omega)\sigma-S(\omega)\tau-\phi\right)^2+\left(R(\omega)\tau+S(\omega)\sigma-\theta\right)^2\right]d\omega \tag{11}$$

Differentiating $E_m$ with respect to a's and b's and equating the resulting equations equal to zero represent $(m+n+1)$ linear equations in $(m+n+1)$ unknowns $a_0$ to $a_m$ and $b_0$ to $b_n$. These equations can be written in the matrix form as

$$\begin{bmatrix}\underline{a}\\ \underline{b}\end{bmatrix} = \begin{bmatrix}A & C\\ C^T & B\end{bmatrix}^{-1}\begin{bmatrix}\underline{I}\\ \underline{J}\end{bmatrix} \tag{12}$$

where A is an (m+1) x (m+1), B an n x n, C an (m+1) x n, I an (m+1) x 1 and J an n x 1 matrix. It is required to find the elements of these matrices for all the digital controllers shown in Figure 1.

## III. DIGITAL CONTROLLERS DESIGN VIA FREQUENCY MATCHING

(A) Inner Loop. The block diagram of the inner loop of the digital control system shown in Figure 2 is redrawn as shown in Figure 3

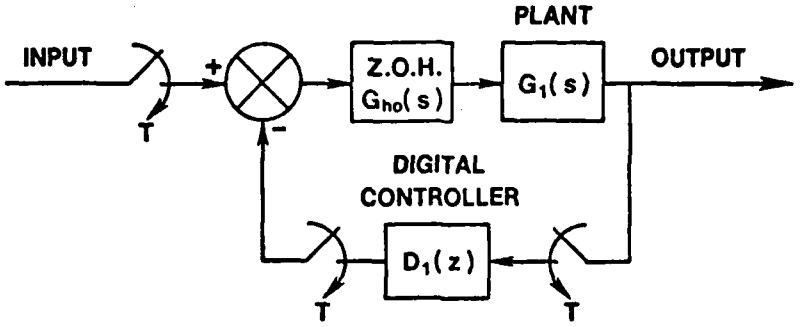



Figure 3. Inner loop of digital control system shown in Figure 2

The frequency characteristic function of the digital control system shown in Figure 3 can be written as

$$G_d^*(j\omega) = \left. \frac{\overline{G_{h0}G_1}(z)}{1 + D_1(z)\,\overline{G_{h0}G_1}(z)} \right|_{z = e^{j\omega T}} \tag{13}$$

where

$$\overline{G_{h0}G_1}(z) = Z\left[G_{h0}G_1(s)\right] \tag{14}$$

$G_{h0}(s)$ and $G_1(s)$ are the transfer function of the zero-order hold and the plant respectively.

Let the pulse transfer function in equation (14) be written in terms of real and imaginary part as

$$\overline{G_{h0}G_1}\,(e^{j\omega T}) = x(\omega) + j\,y(\omega) \tag{15}$$

It can be shown that[9] if

$$\overline{G_{h0}G_1}(z) = \frac{\sum_{i=0}^{n} \alpha_1 z^{-i}}{\sum_{i=0}^{n} \beta_1 z^{-i}} \tag{16}$$

then

$$\text{Re } \overline{G_{h0}G_1}(e^{j\omega T}) = x(\omega) = \frac{\sum_{i=0}^{n} \alpha_i\beta_1 + \sum_{k=1}^{n} \sum_{i=k}^{n} (\alpha_{i-k}\beta_i + \alpha_i\beta_{i-k}) \sin k\omega T}{\sum_{i=0}^{n} \beta_i^2 + 2 \sum_{k=1}^{n} \sum_{i=k}^{n} \beta_{i-k}\beta_i \cos k\omega T} \tag{17}$$

$$\text{Im } \overline{G_{h0}G_1}(e^{j\omega T}) = y(\omega) = \frac{\sum_{k=1}^{n} \sum_{i=k}^{n} (\alpha_{i-k}\beta_i - \alpha_i\beta_{i-k}) \sin k\omega T}{\sum_{i=0}^{n} \beta_i^2 + 2 \sum_{k=1}^{n} \sum_{i=k}^{n} \beta_{i-k}\beta_i \cos k\omega T} \tag{18}$$

These formulas are very useful when the design method is programmed on a digital computer.

Substituting equations (1) and (13) into (11), and after some algebraic manipulation, gives the real and imaginary part of the numerator and denominator of the frequency characteristic function $G_d^*(j\omega)$ as follows

$$\phi = x(\omega) + \sum_{i=1}^{n} b_i \left( x(\omega) \cos i\omega T + y(\omega) \sin i\omega T \right) \tag{19}$$

$$\theta = y(\omega) + \sum_{i=1}^{n} b_i \left( -x(\omega) \sin i\omega T + y(\omega) \cos i\omega T \right) \tag{20}$$

$$\sigma = 1 + \sum_{i=1}^{n} b_i \cos i\omega T + \sum_{i=0}^{m} a_i \left( x(\omega) \cos i\omega T + y(\omega) \sin i\omega T \right) \tag{21}$$

$$\tau = \sum_{i=1}^{n} b_i \sin i\omega T + \sum_{i=0}^{m} a_i \left( -x(\omega) \sin i\omega T + y(\omega) \cos i\omega T \right) \tag{22}$$

After substituting equations (19) - (22) into equation (11), if the first derivatives of $E_m$ with respect to a's and b's are equated to zero, a set of linear algebraic equations for optimal digital controller parameters are obtained. The elements of the matrices given in equation (12) are thus given by

$$A_{ij} = \int_0^{\omega_s/2} \left(R^2(\omega)+S^2(\omega)\right)\left(x^2(\omega)+y^2(\omega)\right) \cos(i-j)\omega T \, d\omega \tag{23}$$

$$B_{ij} = \int_0^{\omega_s/2} \left[R^2(\omega)+S^2(\omega)+x^2(\omega)+y^2(\omega)-2R(\omega)x(\omega)-2S(\omega)y(\omega)\right]\cos(i-j)\omega T \, d\omega \tag{24}$$

$$C_{ij} = \int_0^{\omega_s/2} \left[\left(R^2(\omega)+S^2(\omega)\right)x(\omega)-\left(x^2(\omega)+y^2(\omega)\right)R(\omega)\right] \cos(i-j)\omega T \, d\omega$$

$$+ \int_0^{\omega_s/2} \left[\left(R^2(\omega)+S^2(\omega)\right)y(\omega)-\left(x^2(\omega)+y^2(\omega)\right)S(\omega)\right] \sin(i-j)\omega T \, d\omega \tag{25}$$

$$I_i = -C_{i0} \tag{26}$$

$$J_i = -B_{i0} \tag{27}$$

Equations (11) and (23-27) provide a design algorithm for the digital controller shown in Figure 3 which has been programmed on a digital computer and is available in the form of a subroutine. Note that the order of the digital controller is arbitrary. Therefore using this method, one may try out several digital controllers and select the best design by considering the tradeoff between cost (complexity) and performance. Pulse-transfer function $D_1(z)$ of this controller is then utilized for the synthesis of the digital controllers in the outer loop.

(B) Outer Loop.

(1) Feedforward digital controller. The block diagram (Figure 4) of the digital control system is obtained from Figure 1 after inserting a sampler at the error input e(t), replacing of the continuous compensator $G_{cl}(s)$ by the already designed digital controller $D_1(z)$ and replacing the

continuous controller $G_{c2}(s)$ by the yet to be designed digital controller $D_2(z)$.

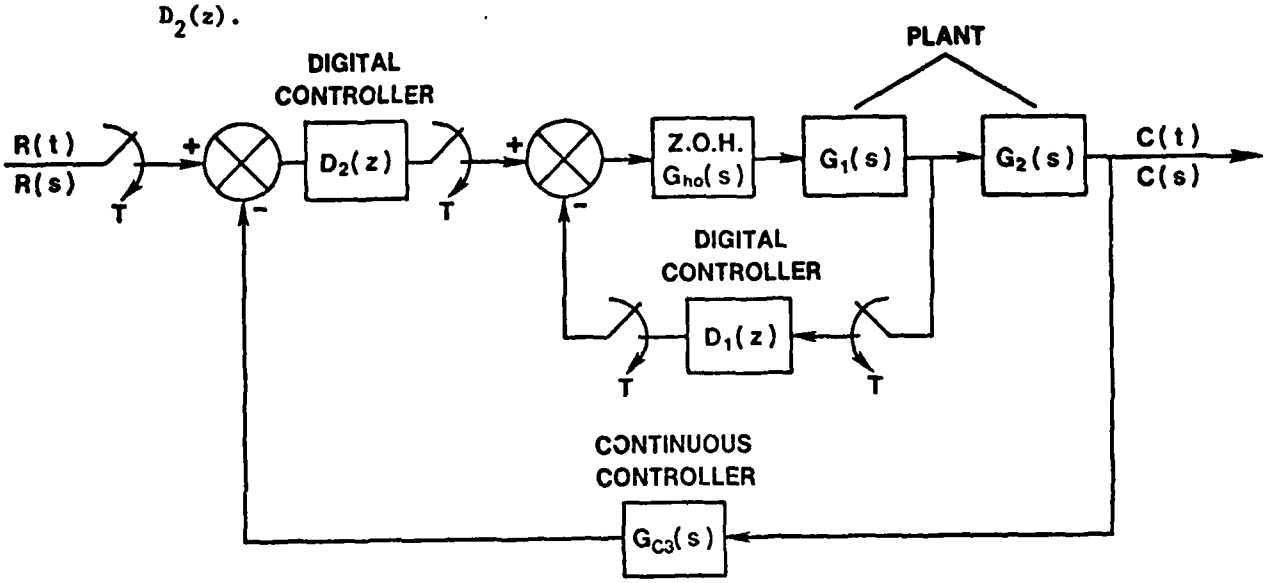



Figure 4. Digital control system with unknown digital controller in the feedforward outer loop.

Let the pulse-transfer function of the digital controller $D_2(z)$ be written as

$$D_2(z) = \frac{a'_0 + a'_1 z^{-1} + a'_2 z^{-2} + \cdots + a'_m z^{-m}}{1 + b'_1 z^{-1} + b'_2 z^{-2} + \cdots + b'_n z^{-n}} \tag{28}$$

where $a''s$ and $b''s$ are the constants to be determined. The frequency-characteristic function of the digital control system as shown in Figure 4 can be written as

$$G_{d1}^{*}(j\omega) = \frac{D_2(z)\ \overline{G_{h0}G_1G_2}(z)}{1 + D_1(z)\ \overline{G_{h0}G_1}(z) + D_2(z)\ \overline{G_{h0}G_1G_2G_{c3}}(z)} \tag{29}$$

where

$$\overline{G_{h0}G_1G_2}(z) = Z\left[G_{h0}G_1G_2(s)\right] \tag{30}$$

$$\overline{G_{h0}G_1G_2G_{c3}}(z) = Z\left[G_{h0}G_1G_2G_{c3}(s)\right] \tag{31}$$

Let the pulse-transfer function in equations (30) and (31) be written in terms of real and imaginary parts as

$$\overline{G_{h0}G_1G_2}(e^{j\omega T}) = x_1(\omega) + jy_1(\omega) \tag{32}$$

$$\overline{G_{h0}G_1G_2G_{c3}}(e^{j\omega T}) = x_2(\omega) + jy_2(\omega) \tag{33}$$

and let

$$D_1(e^{j\omega T})\ \overline{G_{h0}G_1}(e^{j\omega T}) = x_3(\omega) + jy_3(\omega) \tag{34}$$

The transfer function $F_0(j\omega)$ of the continuous model relating C(s) and R(s) can also be written in terms of real and imaginary part as

$$F_0(j\omega) = R_0(\omega) + j\ S_0(\omega) \tag{35}$$

Substituting equations (28), (32), (33) and (34) into (29) and after some algebraic manipulation, the real and imaginary part of the numerator and denominator of $G_{d1}^*(j\omega)$ are given by

$$\phi = \sum_{i=0}^{m} a_i' \left[x_1(\omega) \cos i\omega T + y_1(\omega) \sin i\omega T\right] \tag{36}$$

$$\theta = \sum_{i=0}^{m} a_i' \left[-x_1(\omega) \sin i\omega T + y_1(\omega) \cos i\omega T\right] \tag{37}$$

$$\sigma = 1 + x_3(\omega) + \sum_{i=0}^{m} a_i' \left[x_2(\omega) \cos i\omega T + y_2(\omega) \sin i\omega T\right] + \sum_{i=1}^{n} b_i' \left[\left(1+x_3(\omega)\right) \cos i\omega T + y_3(\omega) \sin i\omega T\right] \tag{38}$$

$$\tau = y_3(\omega) + \sum_{i=0}^{m} a_i' \left[-x_2(\omega) \sin i\omega T + y_2(\omega) \cos i\omega T\right] + \sum_{i=1}^{n} b_i' \left[-(1+x_3(\omega) \sin i\omega T + y_3 \cos i\omega T\right] \tag{39}$$

After substituting equations (34) - (39), if the first derivatives of $E_m$ with respect to a''s and b''s are equated to zero, a set of linear algebraic equations for optimal digital controller parameters of $D_2(z)$ are obtained. These equations are written in the matrix form as

$$\begin{bmatrix} \underline{a}' \\ \underline{b}' \end{bmatrix} = \begin{bmatrix} A'_{ij} & C'_{ij} \\ C'^{T}_{ij} & B'_{ij} \end{bmatrix}^{-1} \begin{bmatrix} \underline{I}'_i \\ \underline{J}'_i \end{bmatrix} \tag{40}$$

where

$$A'_{ij} = \int_0^{\omega_s/2} \left[\left(R_0(\omega)-1\right)^2+S_0^2(\omega)\right]\left(x_1^2(\omega)+y_1^2(\omega)\right)(CS)\,d\omega \tag{41}$$

$$B'_{ij} = \int_0^{\omega_s/2} \left(R_0^2(\omega)+S_0^2(\omega)\right)\left[\left(1+x_3(\omega)\right)^2+y_3^2(\omega)\right](CS)\,d\omega \tag{42}$$

$$\begin{aligned} C'_{ij} = {} & \int_0^{\omega_s/2} \left(R_0^2(\omega)+S_0^2(\omega)\right)\left[\left(1+x_3(\omega)\right)\left(x_2(\omega)(CS)+y_2(\omega)(SN)\right)\right]d\omega \\ & +\int_0^{\omega_s/2} \left(R_0^2(\omega)+S_0^2(\omega)\right)\left[y_3(\omega)\left(y_2(\omega)(CS)-x_2(\omega)(SN)\right)\right]d\omega \\ & +\int_0^{\omega_s/2} \left[-\left(1+x_3(\omega)\right)+y_3(\omega)\right]\left[\left(R_0(\omega)x_1(\omega)+S_0(\omega)y_1(\omega)\right)(CS)\right]d\omega \\ & +\left[-\left(1+x_3(\omega)\right)+y_3(\omega)\right]\left[\left(R_0(\omega)y_1(\omega)-S_0(\omega)x_1(\omega)\right)(SN)\right]d\omega \end{aligned} \tag{43}$$

$$I'_i = -C_{i0} \tag{44}$$

$$J'_i = -B_{i0} \tag{45}$$

$$CS = \cos(i-j)\omega T$$

$$SN = \sin(i-j)\omega T$$

Equations (40) - (45) provide a design algorithm for the digital controller $D_2(z)$ which has been programmed on a digital computer and is available in the form of a subroutine. Once the digital controller $D_2(z)$ is designed, it (along with the digital controller $D_1(z)$ ) is then utilized for the design of digital controller $D_3(z)$.

(2) Digital controller in the feedback loop. The block diagram of the digital control system after replacing the continuous compensators $G_{c1}(s)$ and $G_{c2}(s)$ with already designed digital controllers and after replacing $G_{c3}(s)$ with yet to be designed digital controller $D_3(z)$ is shown in Figure 5.

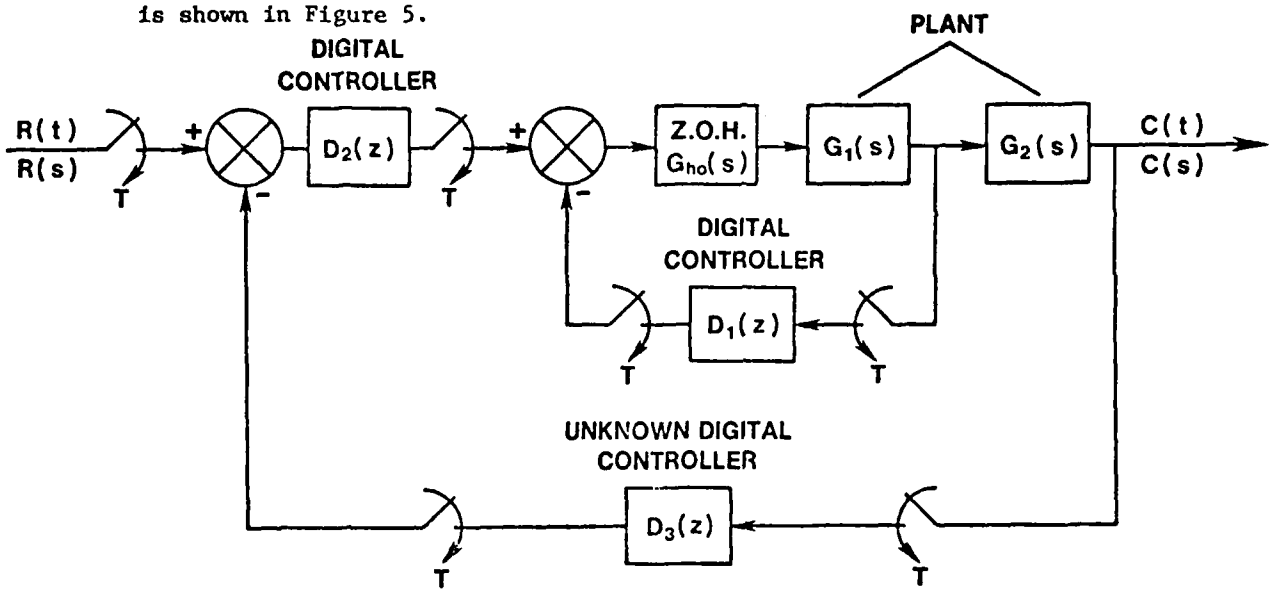



Figure 5. Digital Control system with unknown digital controller in the feedback loop.

The pulse transfer function of the digital controller $D_3(z)$ may be written as

$$D_3(z) = \frac{a_0'' + a_1''z^{-1} + a_2''z^{-2} + \cdots + a_m''z^{-m}}{1 + b_1''z^{-1} + b_2''z^{-2} + \cdots + b_n''z^{-n}} \tag{46}$$

where $a''$'s and $b''$'s are constants which are to be determined. The frequency-characteristic function of the digital control system shown in Figure 5 can be written as

$$G_{d2}^*(j\omega) = \left. \frac{D_2(z)\ \overline{G_{h0}G_1G_2}(z)}{1 + D_1(z)\ \overline{G_{h0}G_1}(z) + D_3(z)\ D_2(z)\ \overline{G_{h0}G_1G_2}(z)} \right|_{z\ =\ e^{j\omega T}} \tag{47}$$

Let

$$D_2(e^{j\omega T})\ \overline{G_{ho}G_1G_2}\ (e^{j\omega T}) = x_4(\omega) + j\ y_4(\omega) \tag{48}$$

Substituting equations (34), (46) and (48) into (47), and after some algebraic manipulation, the real and imaginary parts of the numerator and denominator of $G_{d2}^*(j\omega)$ are given by

$$\phi = x_4(\omega) + \sum_{i=1}^{n} b_i\left[x_4(\omega)\ \cos\ i\omega T + y_4(\omega)\ \sin\ i\omega T\right] \tag{49}$$

$$\theta = y_4(\omega) + \sum_{i=1}^{n} b_i\left[-x_4(\omega)\ \sin\ i\omega T + y_4(\omega)\ \cos\ i\omega T\right] \tag{50}$$

$$\sigma = 1 + x_3(\omega) + \sum_{i=1}^{n} b_i\left[\left(1+x_3(\omega)\right)\ \cos\ i\omega T + y_3\ \sin\ i\omega T\right]$$

$$+ \sum_{i=0}^{m} a_i\left[x_4(\omega)\ \cos\ i\omega T + y_4(\omega)\ \sin\ i\omega T\right] \tag{51}$$

$$\tau = y_3(\omega) + \sum_{i=1}^{n} b_i\left[-\left(1+x_3(\omega)\right)\ \sin\ i\omega T + y_3\ \cos\ i\omega T\right]$$

$$+ \sum_{i=0}^{m} a_i\left[-x_4(\omega)\ \sin\ i\omega T + y_4(\omega)\ \cos\ i\omega T\right] \tag{52}$$

After substituting equations (35) and (49) - (52) into (11), if the derivatives of $E_m$ with respect to a''s and b''s are equated to zero, we obtained the optimal parameters of digital controllers $D_3(z)$ which can be written in the matrix form as

$$\begin{bmatrix} \underline{a}'' \\ \underline{b}'' \end{bmatrix} = \begin{bmatrix} A'' & C'' \\ C''^T & B'' \end{bmatrix}^{-1} \begin{bmatrix} \underline{I}'' \\ \underline{J}'' \end{bmatrix} \tag{53}$$

where

$$A''_{ij} = \int_0^{\omega_s/2} \left(R_0^2(\omega)+S_0^2(\omega)\right)\left(x_4^2(\omega)+y_4^2(\omega)\right) \cos(i-j)\omega T \, d\omega \tag{54}$$

$$\begin{aligned} B''_{ij} = {} & \int_0^{\omega_s/2} \left(R_0^2(\omega)+S_0^2(\omega)\right)\left(\left(1+x_3(\omega)\right)^2+y_3^2(\omega)\right) \cos(i-j)\omega T \, d\omega \\ & + \int_0^{\omega_s/2} \left[x_4^2(\omega)+y_4^2(\omega)-2\left(1+x_3(\omega)\right)\left(R_0(\omega)x_4(\omega)+S_0(\omega)y_4(\omega)\right)\right] \cos(i-j)\omega T \, d\omega \\ & - \int_0^{\omega_s/2} 2y_3(\omega)\left(R_0(\omega)y_4(\omega)-S_0(\omega)x_4(\omega)\right) \cos(i-j)\omega T \, d\omega \end{aligned} \tag{55}$$

$$\begin{aligned} C''_{ij} = {} & \int_0^{\omega_s/2} \left(1+x_3(\omega)\right)\left(R_0^2(\omega)+S_0^2(\omega)\right)\left(x_4(\omega)\cos(i-j)\omega T+y_4(\omega)\sin(i-j)\omega T\right) d\omega \\ & + \int_0^{\omega_s/2} y_3(\omega)\left(R_0^2(\omega)+S_0^2(\omega)\right)\left(y_4(\omega)\cos(i-j)\omega T - x_4(\omega)\sin(i-j)\omega T\right) d\omega \\ & - \int_0^{\omega_s/2} \left(x_4^2(\omega)+y_4^2(\omega)\right)\left(R_0(\omega)\cos(i-j)\omega T+S_0(\omega)\sin(i-j)\omega T\right) d\omega \end{aligned} \tag{56}$$

$$I''_i = -C_{i0} \tag{57}$$

$$J_i = -B_{i0} \tag{58}$$

Equations (53)-(58) provide a design algorithm for the digital controller $D_3(z)$ which has been programmed on a digital computer and is available in the form of a subroutine. It is to be pointed out here that alongwith providing the optimal parameters of the digital controllers $D_1(z)$, $D_2(z)$ and $D_3(z)$; the algorithms also computes the frequency responses of the digital and continuous control systems of different loops. The stability of the digital control systems is also determined.

If the designer is not satisfied with the results and wants to improve the performance, the only change he needs to make is to increase the order of the controller. The algorithms go through the standard steps and find the optimal parameters of the new digital controllers. Thus the performance may be improved at the expense of increasing complexity.

If the designer wants to design a digital controller for a different frequency response, the only modification he has to make is to change the transfer function of the continuous model. Again, interacting with the computer, optimal digital controllers may be obtained. Thus the designer can obtain the desired solution by manipulating few parameters; the rest of the work is performed by the computer.

## IV. NUMERICAL EXAMPLE

The digitalization techniques, described in the previous section was applied to an analog flight controller[12] for the longitudinal YF-16 as shown in Figure 6. A listing of transfer functions of the aircraft flight at 30,000 ft at M = 0.6 can be found in Appendix A.

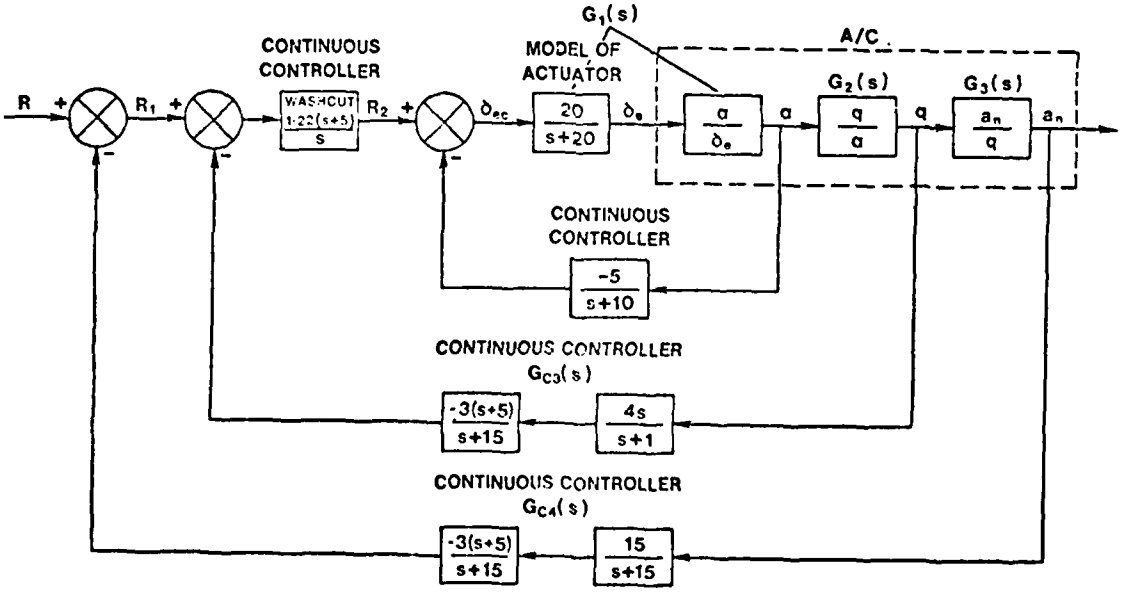



Figure 6. Analog YF-16 controller (M=0.6, h=30,000 ft)

The problem is to digitalize, i.e., to replace the continuous-time controllers by digital controllers while preserving the dynamic properties of the whole system. The block diagram of the digitally controlled YF-16 obtained by inserting a sampler at the input of the actuator and replacing continuous controllers by digital controllers is shown in Figure 7.

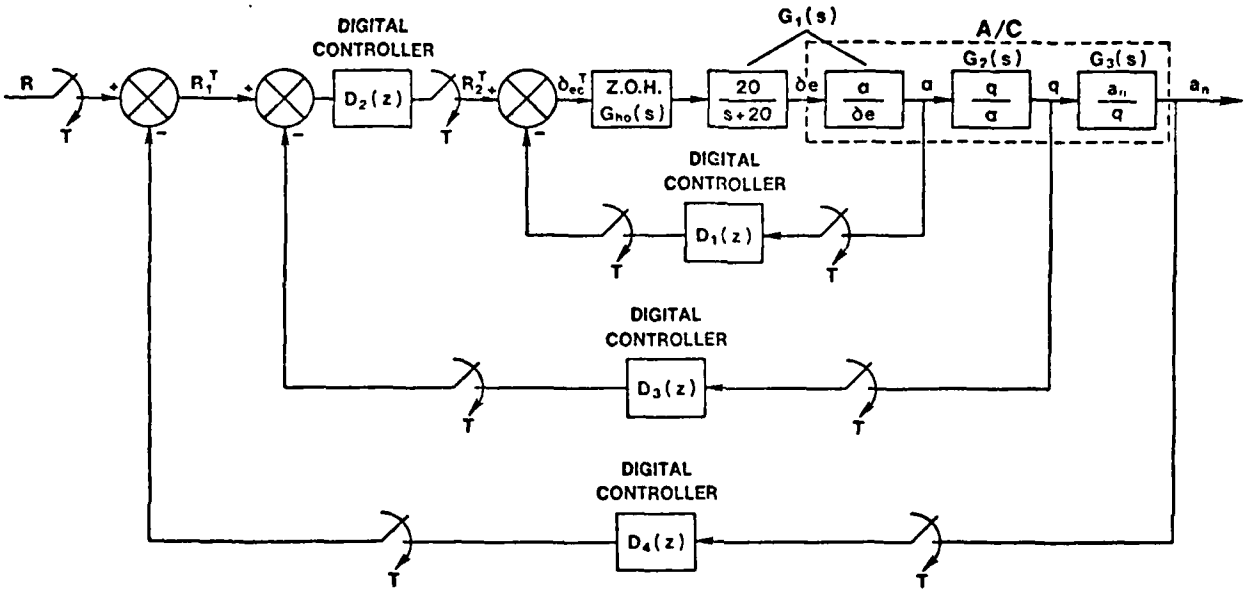



Figure 7. Digital YF-16 controller

$D_1(z)$ Controller: From Figure 6, the transfer function of the continuous model (innermost loop) for the design of digital controller $D_1(z)$ can be written as

$$F_1(s) = \frac{\alpha(s)}{R_2(s)} = \frac{G_1(s)}{1+G_{c1}(s)G_1(s)}$$

$$= -\frac{1.45s^4+162.1s^3+147.8s^2+24.53s+8.3}{s^6+30.95s^5+226.2s^4+127.7s^3+270.5s^2+3.75s+1.31} \qquad (59)$$

In view of the innermost loop of Figure 7, it is seen that

$$G_{ho}G_1(s) = \frac{1-e^{-ST}}{S} \frac{20}{S+20} \frac{\alpha}{\delta e} \tag{60}$$

Loading the z-transform of equation (60) alongwith equation (59) into the computer program for the algorithm implementing equations (23)-(27), the pulse-transfer functions of the first order digital controller $D_1(z)$ are given by

$T = 0.04$

$$D_1(z) = \frac{.3659(z - .7974)}{z - .8553} \tag{61}$$

$T = 0.1$

$$D_1(Z) = \frac{.4557(z - .7419)}{z - .7696} \tag{62}$$

$T = 0.15$

$$D_1(z) = \frac{.5113(z - .6151)}{z - .6065} \tag{63}$$

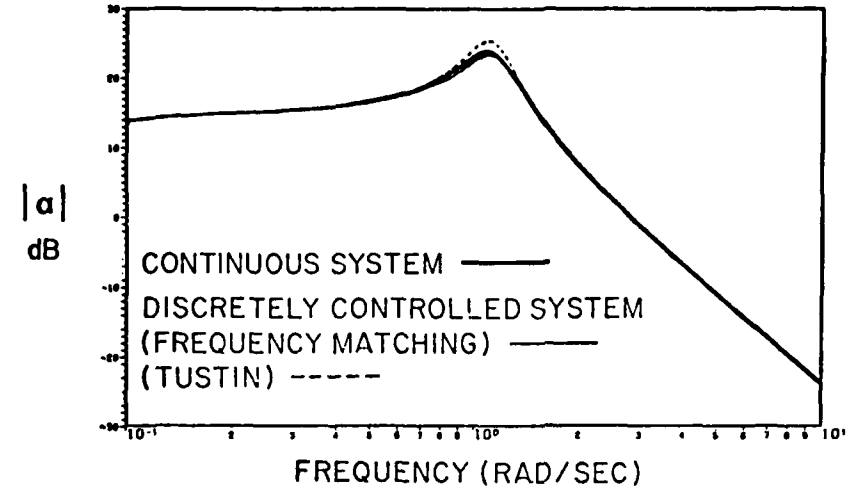
The frequency responses of the innermost loop of the digital control system shown in Figure 7 with the digital controller $D_1(z)$ given by equations (61)-(63) are shown in Figures 8, 9 and 10 respectively. It can be seen that both the magnitude and phase angle of $\alpha$ of the digital control system match those of the continuous model closely at low frequencies; whereas at high frequencies even though the magnitude matches closely, the phase angle does not. To improve this performance, a second-order controller can be designed using the same algorithm.

To compare these results with the method presented by Tabak[1], the continuous compensator $G_{c1}(s)$ was also digitalized using the Tustin transform

$$S = \frac{2}{T} \frac{z - 1}{z + 1} \tag{64}$$

The pulse-transfer functions of the digital controller $D_1(z)$ using this transformation are given by

T = 0.04



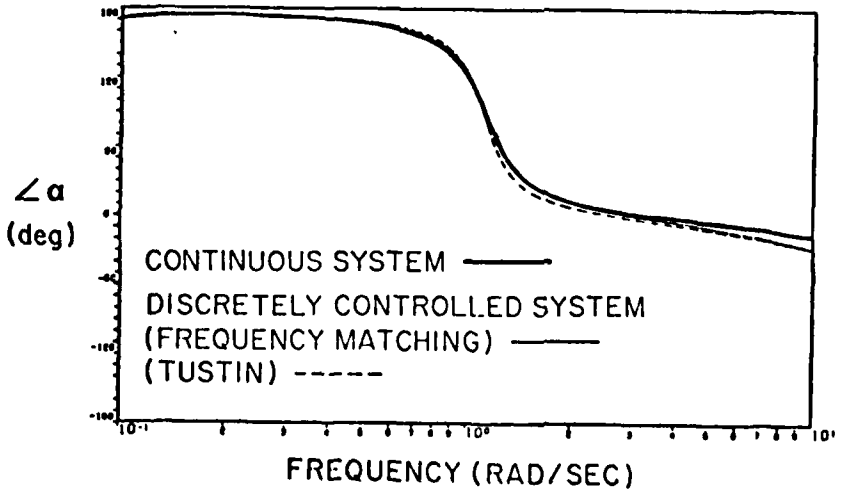
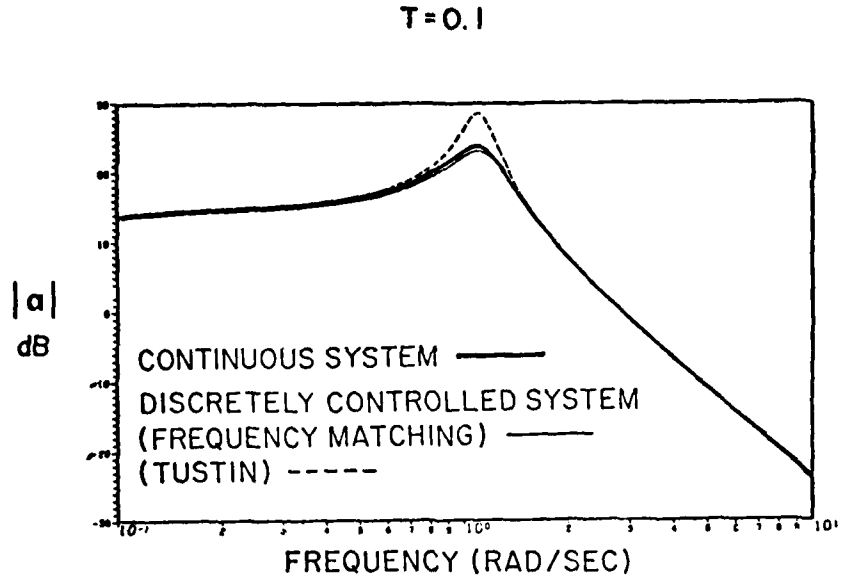




Figure 8. Frequency response of the innermost loop for a sampling frequency of 25 c/s



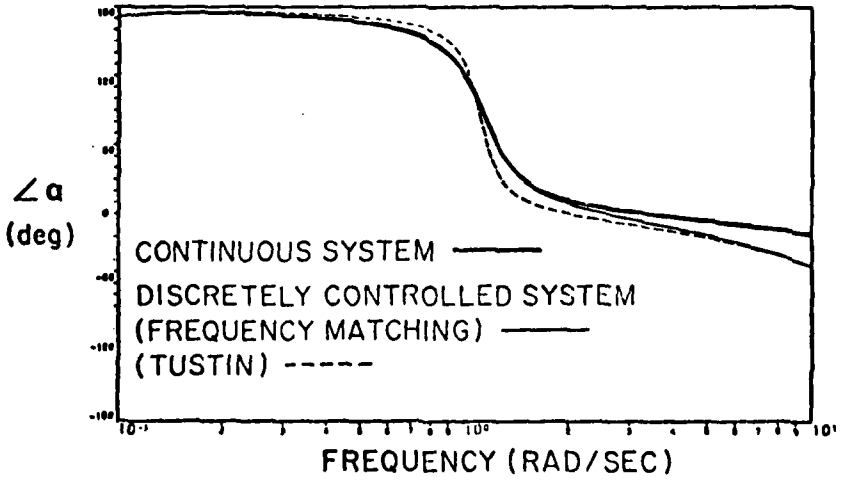




Figure 9. Frequency response of the innermost loop for a sampling frequency of 10 c/s

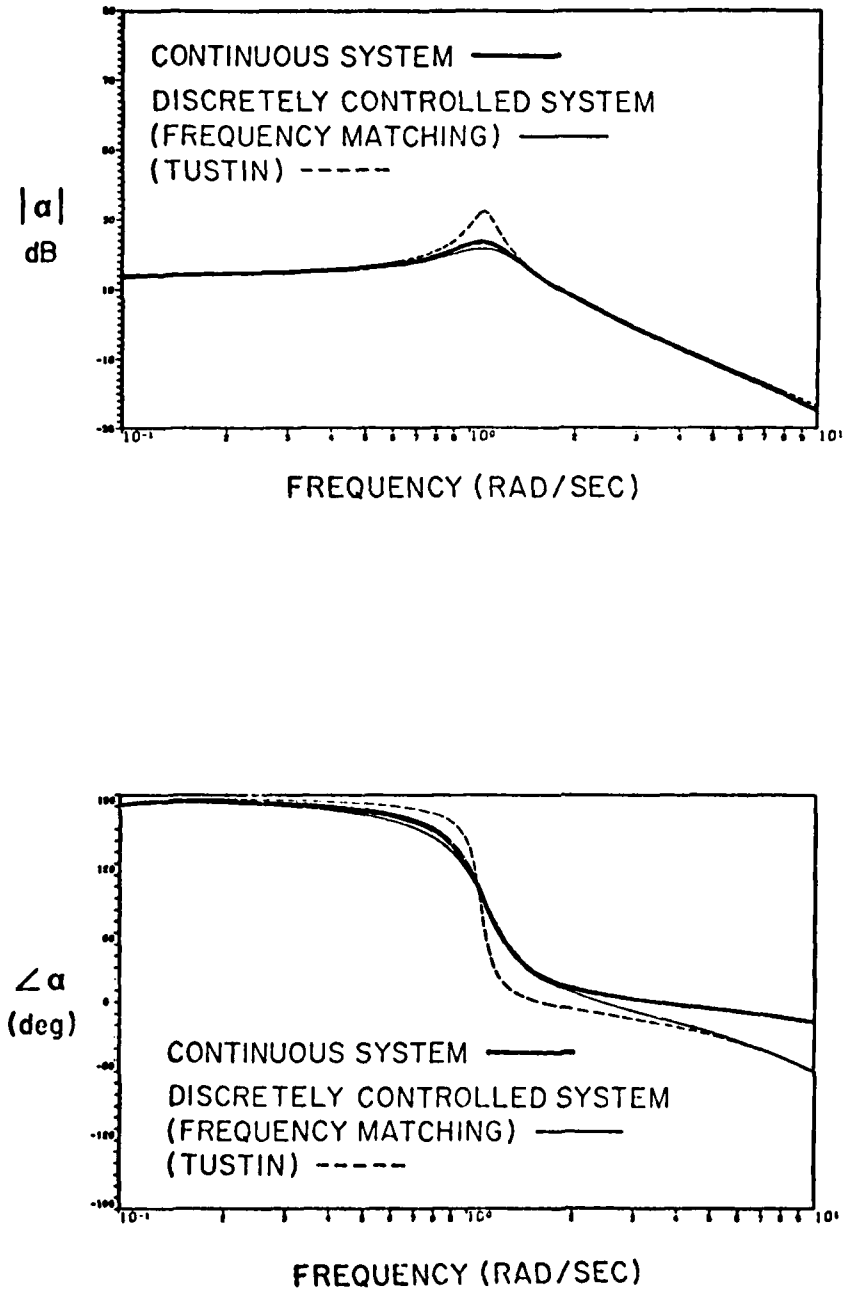



Figure 10. Frequency response of the innermost loop for a sampling frequency of 6.7 c/s

$T = 0.04$

$$D_1(z) = \frac{.083(Z+1)}{Z - .667} \tag{65}$$

$T = 0.1$

$$D_1(z) = \frac{.1667(Z+1)}{Z - .333} \tag{66}$$

$T = 0.15$

$$D_1(z) = \frac{.2143(Z+1)}{Z - .1428} \tag{67}$$

The frequency responses of the innermost loop of the digital control system shown in Figure 7 with the digital controller $D_1(z)$ given by equations (65)-(67) are shown in Figures 8, 9 and 10 respectively. It can be seen from these figures that at high sampling frequency (T=0.04), both the magnitude and phase angle of $\alpha$ match those of the continuous model closely but at low sampling frequencies (T=0.1 and 0.15), both the magnitude and phase angle of the frequency responses do not match well with that of the continuous model. Comparing these results with the frequency-matching method developed in this report reveals that the latter gives better results.

The pulse (width = 1 sec, strength = -1) responses of the continuous model and digital control systems obtained by replacing the continuous controller by the digital controller using both methods are shown in Figures 11, 12, and 13. It can be seen from these figures that the time responses of the digital control systems obtained by the frequency-matching method match those of the continuous model closely for all three sampling frequencies whereas the responses of the systems obtained using Tustin transform match well only at high sampling frequency (T=0.04)

$D_2(z)$ Controller: From Figure 6, the transfer function of the continuous model for the design of digital controller $D_2(z)$ can be written as

$$F_2(s) = \frac{q(s)}{R_1(s)} = \frac{G_{c2}(s)F_1(s)G_2(s)}{1+G_{c3}(s)G_{c2}(s)F_1(s)G_2(s)}$$

$$= -\frac{180S^6+.568x10^4S^5+.579x10^5S^4+.214x10^6S^3+.234x10^6S^2+.73x10^5S+629.9}{S^8+47S^7+925S^6+.86x10^4S^5+.35x10^5S^4+.75x10^5S^3+.33x10^5S^2+329\ 1S+19.6} \tag{68}$$

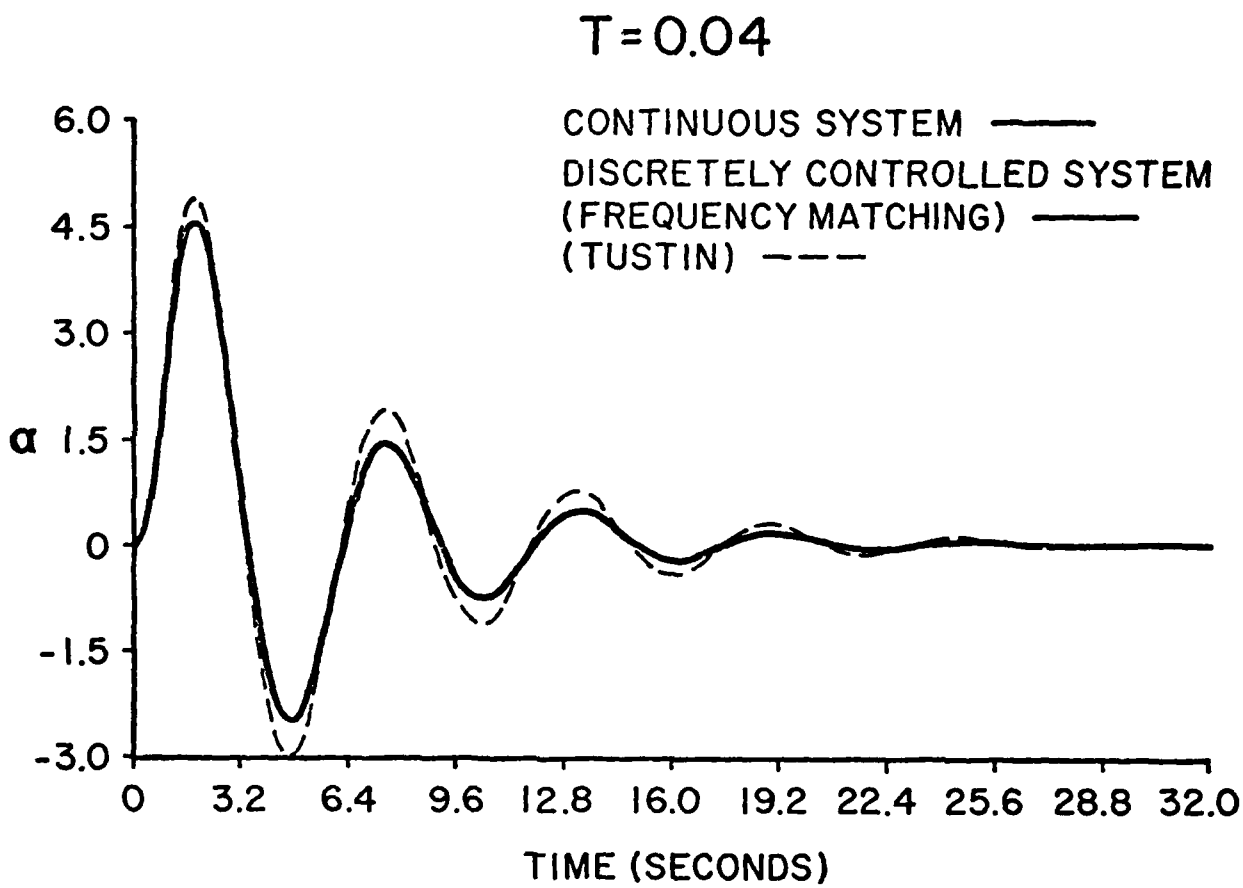



Figure 12. Pulse (width = 1 sec, strength = -1) response of the innermost loop for a sampling frequency of 25 c/s.

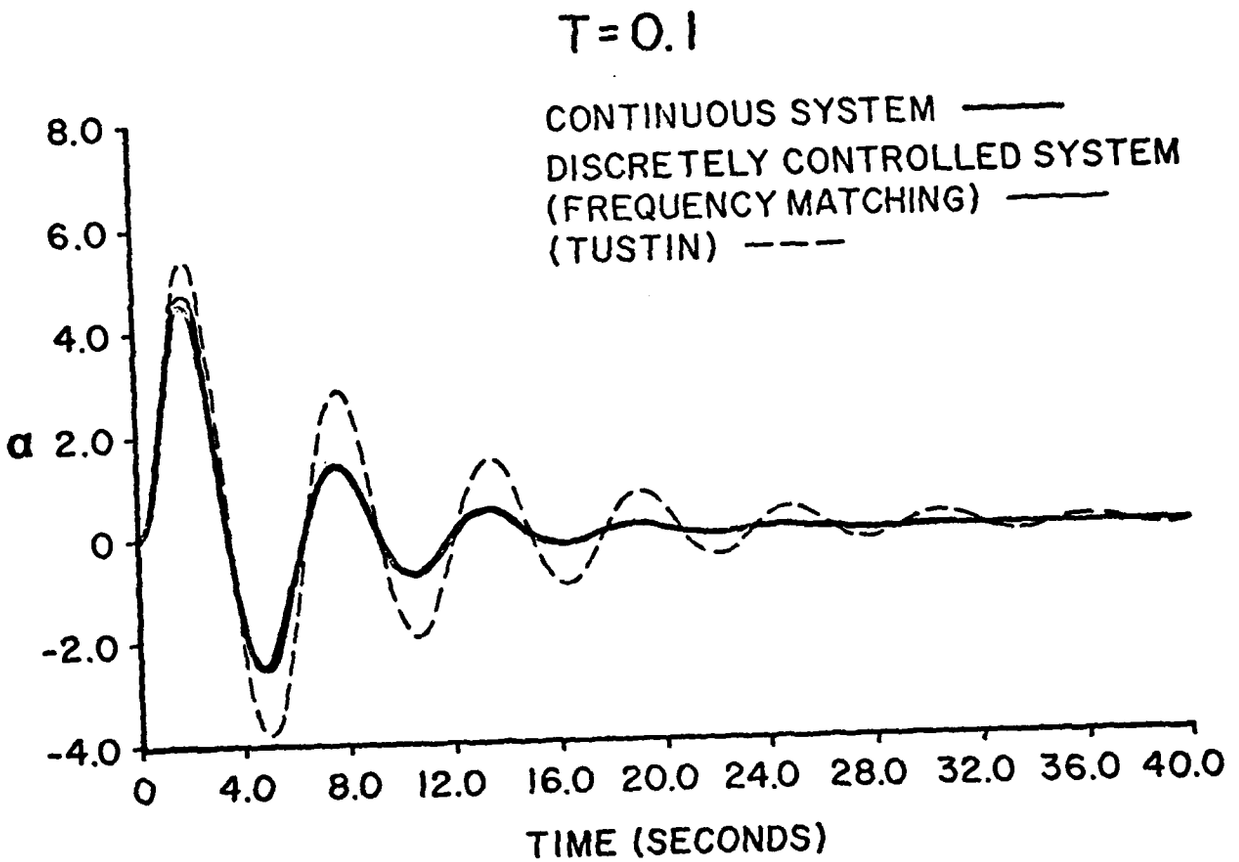



Figure 11. Pulse (width = 1 sec, strength = -1) response of the innermost loop for a sampling frequency of 10 c/s.

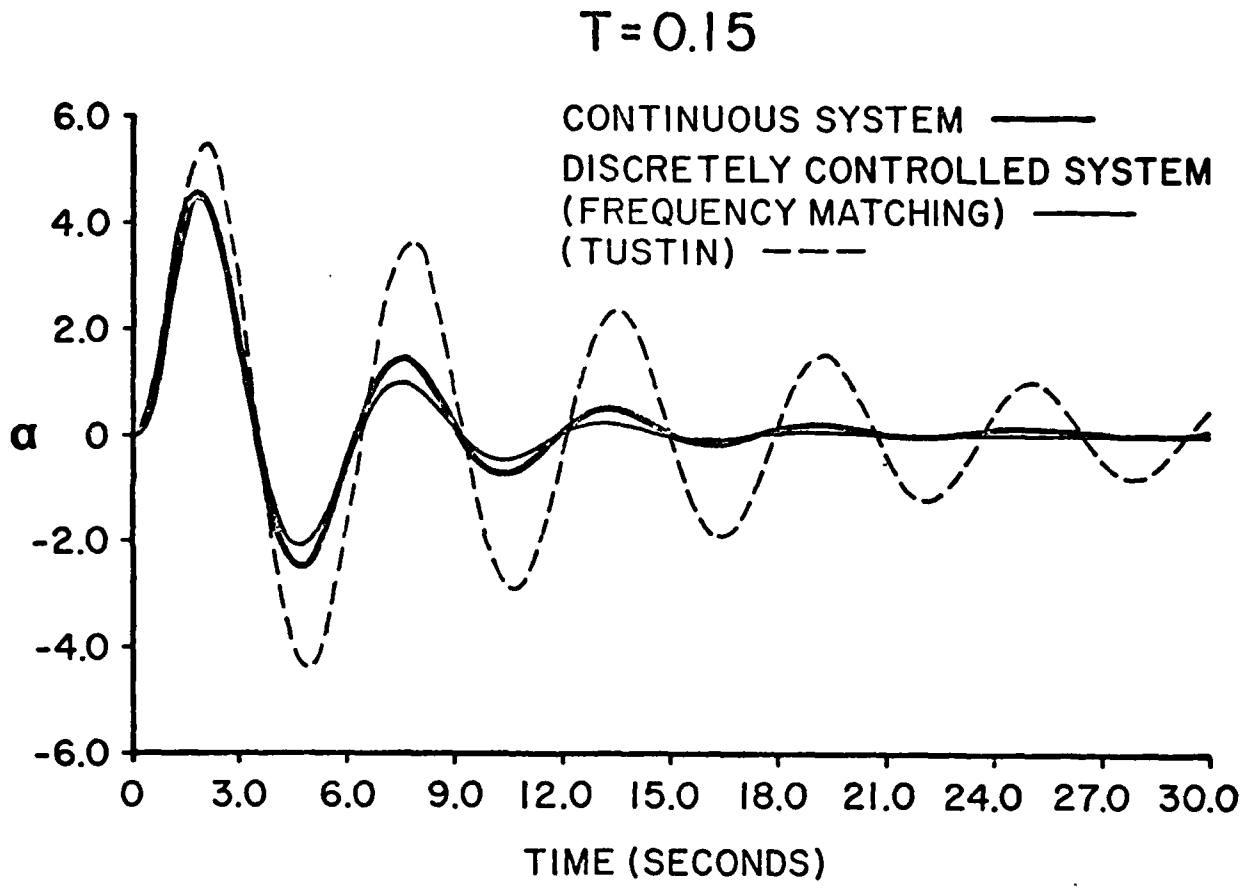



Figure 13. Pulse (width = 1 sec, stren-th = -1) response of the innermost loop for a sampling frequency of 6.7 c/s.

In view of Figure 4, it is seen that

$$G_{ho}G_1G_2(s) = \frac{1-e^{ST}}{S}\frac{20}{S+20}\frac{q}{\delta e} \tag{69}$$

$$G_{ho}G_1G_2G_{c3}(s) = -\frac{1-e^{-ST}}{S}\frac{24S(S+5)}{(S+1)(S+15)(S+20)}\frac{q}{\delta e} \tag{70}$$

Loading the z-transform of equations (60), (69) and (70), the pulse-transfer function of $D_1(z)$ (equations (61)-(63)) and equation (68) into the computer program for the algorithm implementing equations (40)-(45), the pulse-transfer functions of the first-order digital controller $D_2(z)$ are given by

$T = 0.04$

$$D_2(z) = \frac{1.38735(z-.80235)}{z-.9985} \tag{71}$$

$T = 0.1$

$$D_2(z) = \frac{1.699(z-.7086)}{z-.9995} \tag{72}$$

The pulse-transfer functions of $D_2(z)$ obtained by the Tustin transform are given by

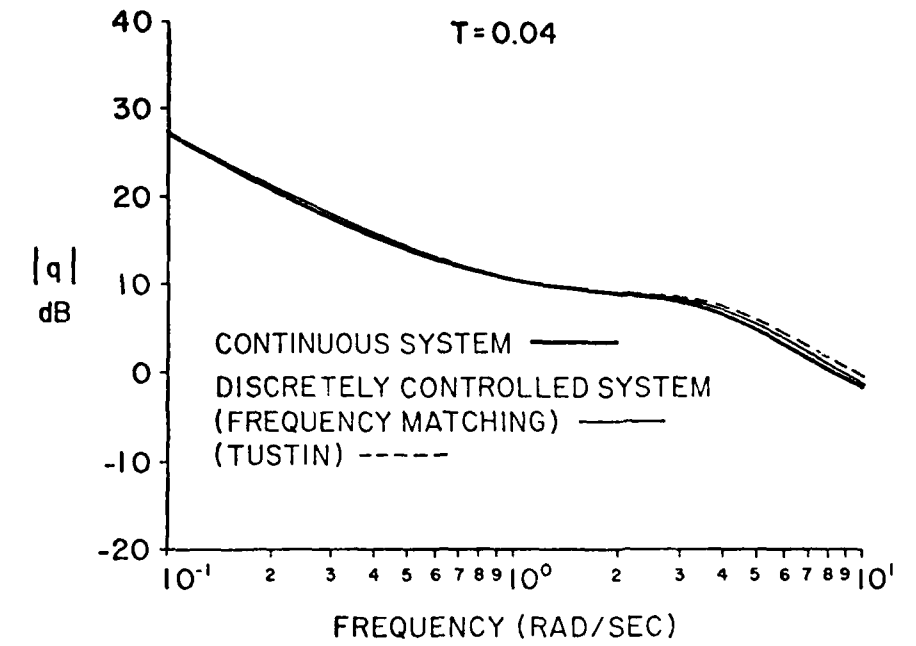
$T = 0.04$

$$D_2(z) = \frac{1.342(z-.8182)}{z-1} \tag{73}$$

$T = 0.1$

$$D_2(z) = \frac{1.525(z-0.6)}{z-1} \tag{74}$$

The frequency responses of the middle loop of the continuous system shown in Figure 6 and the digital control system shown in Figure 4 with digital controllers $D_2(z)$ given by equations (71)-(72) and (73)-(74) are shown in Figures 14 and 15. Comparing these results reveals that the digital controllers obtained by the frequency-matching method gives better results.



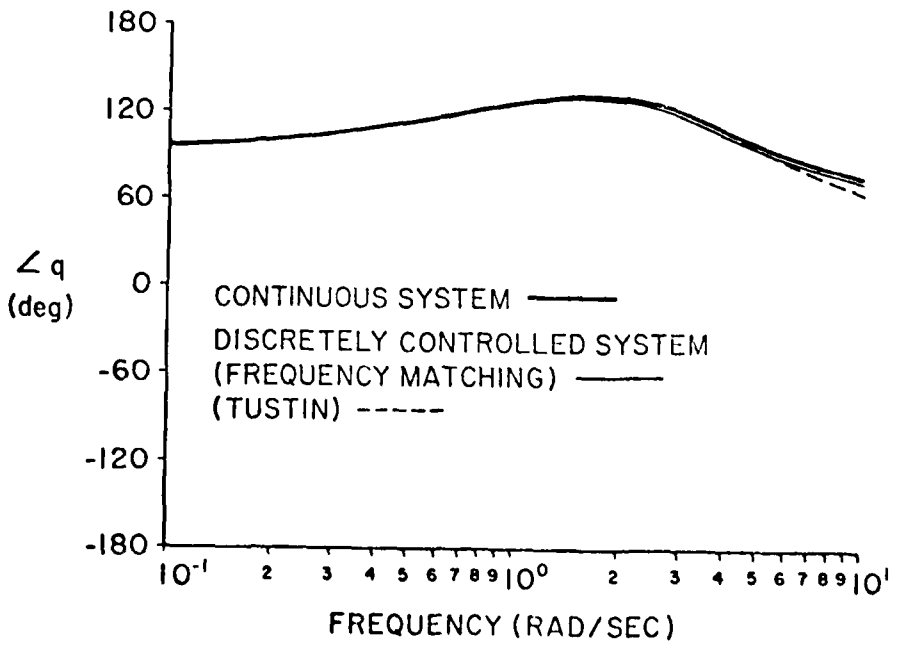




Figure 14. Frequency response of the continuous model (middle loop) and the digital control system shown in Figure 4.

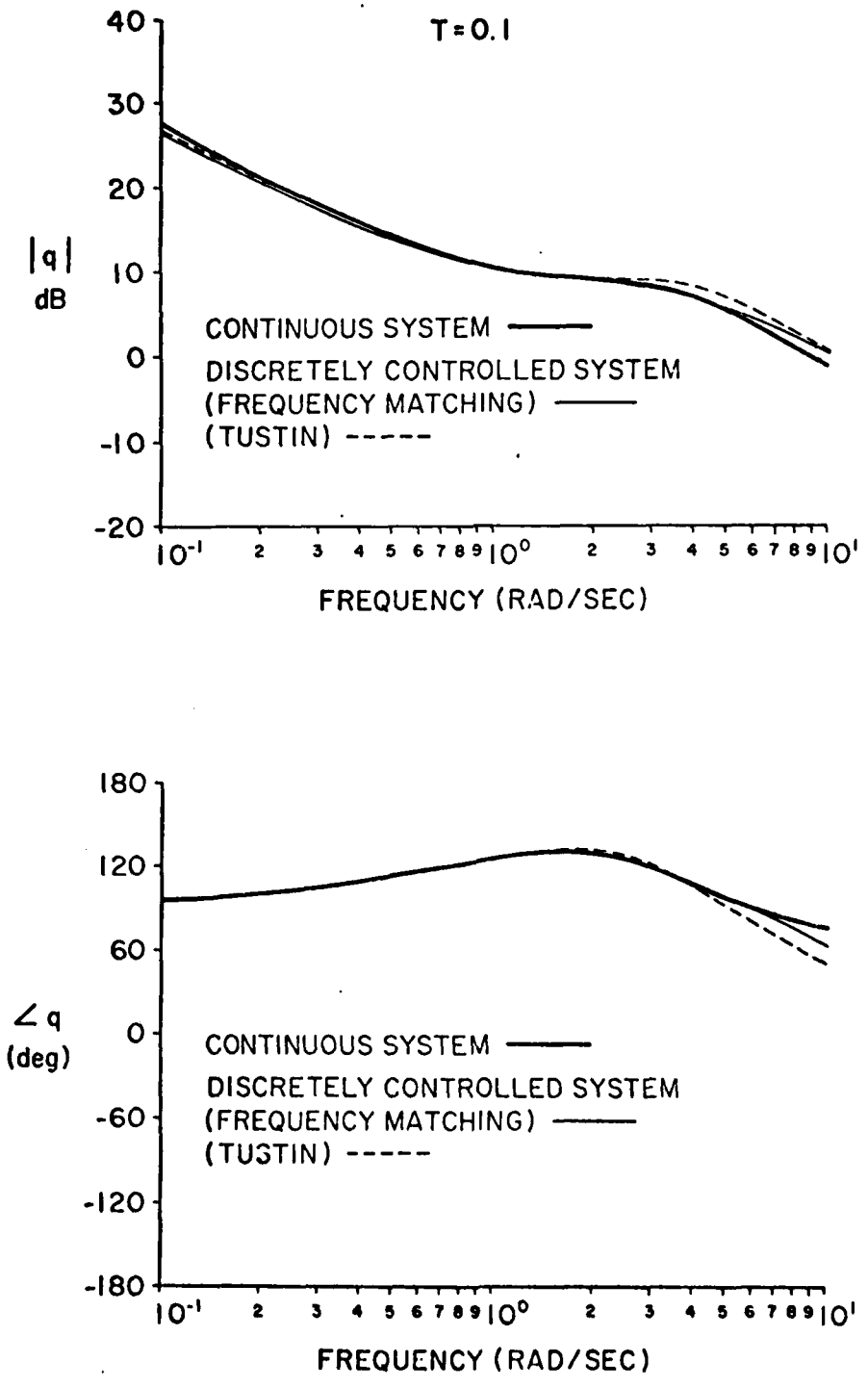



Figure 15. Frequency responses of the continuous model (middle loop) and the digital control system shown in Figure 4.

$D_3(z)$ Controller: (Refer to Figure 5) Loading the z-transform of equations (60) and (69), the pulse-transfer functions of $D_1(z)$ and $D_2(z)$ (equations (61)-(63) and equations (71)-(72)) and equation (68) into the computer program for the algorithm implementing equations (53)-(58), the pulse-transfer functions of the second-order digital controller $D_3(z)$ are given by

$T = 0.04$

$$D_3(z) = \frac{1.5433(z-.8512)(z-1)}{(z+.3876)(z+.9652)} \tag{75}$$

$T = 0.1$

$$D_3(z) = \frac{.9485z^2-1.625z+.677}{z^2-1.161z+.226} \tag{76}$$

The pulse-transfer functions of $D_3(z)$ obtained by the Tustin transform are given by

$T = 0.04$

$$D_3(z) = \frac{.995z^2-1.81z+.814}{z^2-1.5z+.517} \tag{77}$$

$T = 0.1$

$$D_3(z) = \frac{.816z^2-1.31z+.49}{z^2-1.05z+.13} \tag{78}$$

The frequency responses of the middle loop of the continuous system shown in Figure 6 and the digital control system shown in Figure 5 with digital controllers $D_3(z)$ given by equations (75)-(76) and (77)-(78) are shown in Figures 16 and 17. Comparison of the results in these figures demonstrates that the digital controllers obtained by the frequency-matching method give better results.

$D_4(z)$ Controller: From Figure 6, the transfer function of the continuous model for the design of digital controller $D_4(z)$ can be written as

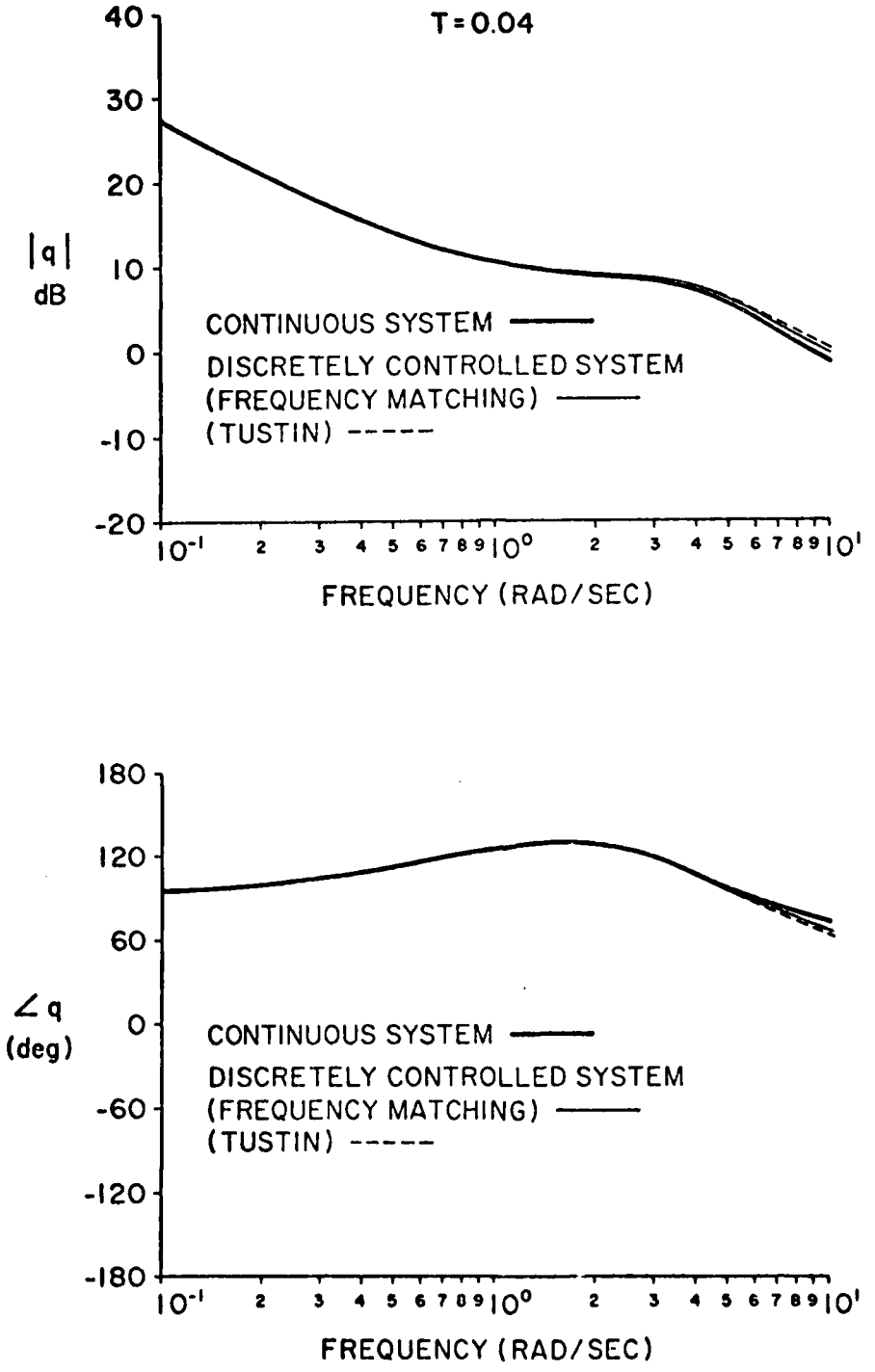



Figure 16. Frequency responses of the continuous model (middle loop) and the digital control system shown in Figure 5.

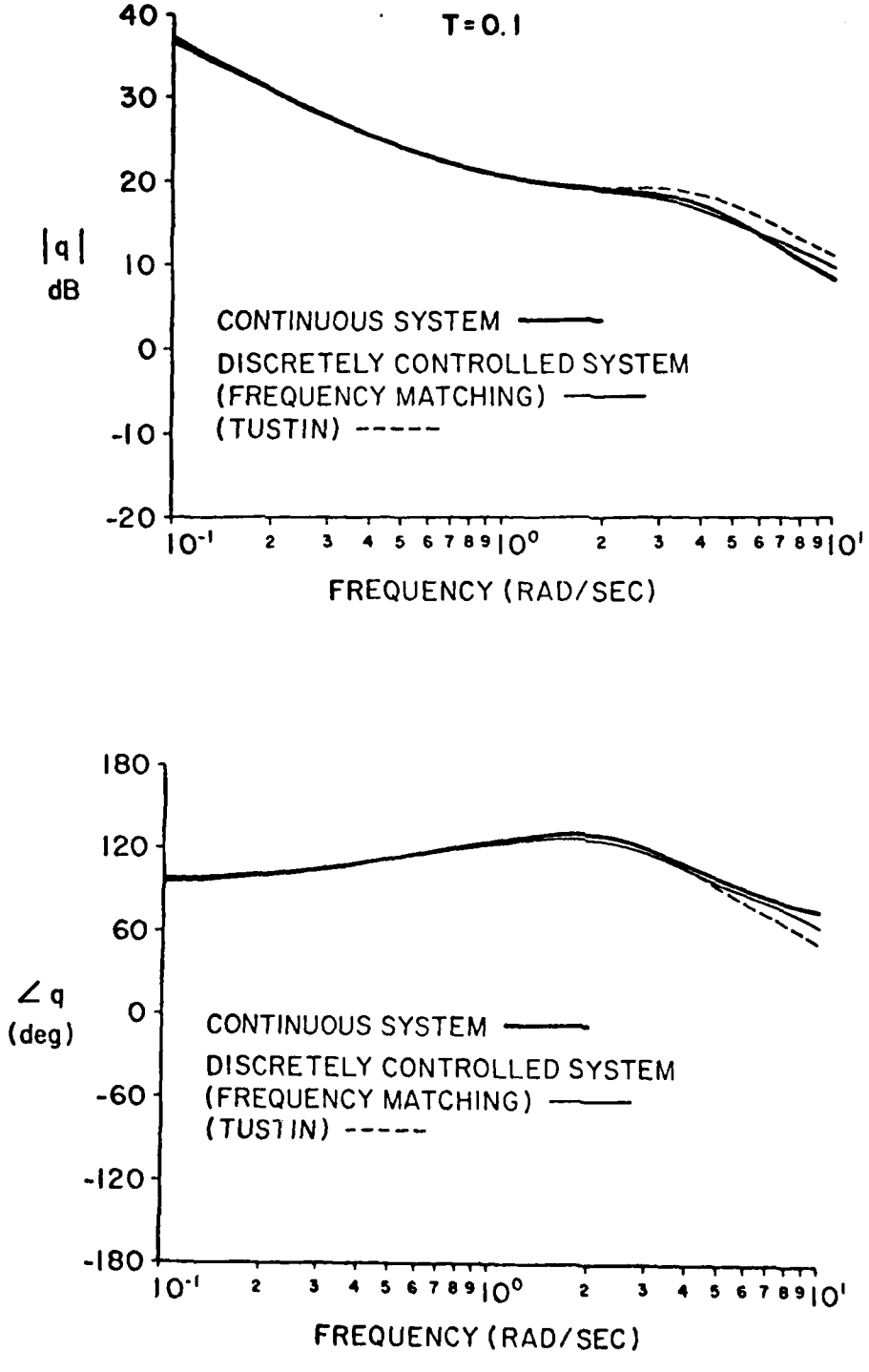



Figure 17. Frequency responses of the continuous model (middle loop) and the digital control system shown in Figure 5.

$$F_3(s) = \frac{a_n(s)}{R(s)} = \frac{F_2(s)G_3(s)}{1+G_{c4}(s)F_2(s)G_3(s)}$$

$$= -\frac{.649s^8+30.5s^7+559.9s^6+.5534\times10^4 s^5+.3754\times10^5 s^4+.1883\times10^6 s^3}{s^9+62s^8+187.2s^7+.2359\times10^5 s^6+.1711\times10^6 s^5+.6447\times10^6 s^4+.1373\times10^7 s^3}$$

$$\frac{+.4981\times10^6 s^2+.3417\times10^6 s-627.1}{+.1021\times10^7 s^2+.3466\times10^6 s-332.3} \quad (79)$$

The frequency-characteristic function of the digital control system shown in Figure 7 can be written as

$$G_d^*(j\omega) = \left.\frac{D_2(z)\overline{G_{h0}G_1G_2G_3}(z)}{1+D_1(z)\overline{G_{h0}G_1}(z)+D_3(z)D_2(z)\overline{G_{h0}G_1G_2}(z)+D_4(z)D_2(z)\overline{G_{h0}G_1G_2G_3}(z)}\right|_{z=e^{j\omega T}} \quad (80)$$

$$= \left.\frac{G_{N1}(z)}{1+G_{N2}(z)+D_4(z)G_{N2}(z)}\right|_{z=e^{j\omega T}} \quad (81)$$

where

$$G_{N1}(z) = D_2(z)\overline{G_{h0}G_1G_2G_3}(z) \quad (82)$$

$$G_{N2}(z) = D_1(z)\overline{G_{h0}G_1}(z)+D_3(z)D_2(z)\overline{G_{h0}G_1G_2}(z) \quad (83)$$

Let the pulse-transfer function in equations (82) and (83) be written in terms of real and imaginary part as

$$G_{N2}(e^{j\omega T}) = x_3(\omega) + jy_3(\omega) \quad (84)$$

and

$$G_{N1}(e^{j\omega T}) = x_4(\omega) + jy_4(\omega) \quad (85)$$

Loading equations (84) and (85) alongwith equation (79) into the computer program for the algorithm implementing equations (53)-(58), the pulse-transfer functions of the second-order controller $D_4(z)$ are given by

T = 0.04

$$D_4(z) = \frac{1.9939z^2 - 3.7164z + 1.803}{z^2 - 1.8812z + .9577} \tag{86}$$

T = 0.1

$$D_4(z) = \frac{1.0356z^2 - 1.971z + .964}{z^2 - 1.919z + .947} \tag{87}$$

The pulse-transfer functions of $D_4(z)$ obtained by the Tustin transform are given by

T = 0.04

$$D_4(z) = \frac{.5858z^2 + .1065z - .479}{z^2 - 1.08z + .29} \tag{88}$$

T = 0.1

$$D_4(z) = \frac{.9184z^2 + .3606z - .54}{z^2 - .28z + .02} \tag{89}$$

The frequency responses of the continuous system shown in Figure 6 and the digital control system shown in Figure 7 with digital controller $D_4(z)$ given by equations (86)-(87) and (88)-(89) are shown in Figures 18 and 19. Comparison of these results demonstrates the superiority of the frequency-matching method over the Tustin transform method.

## V. RECOMMENDATIONS

In this project, an attempt has been made to develop a computer-aided method for digitalizing existing multi-loop continuous-data control systems. The numerical example considered shows that the performance of the digital control system obtained by this method is superior to the one obtained by Tustin transform.

The optimal parameters of the digital controllers are obtained by matching the frequency responses of the digital control system as closely as possible with that of the continuous models. So it is important that the frequency responses be calculated accurately. In this study, the frequency response of a digital control system is calculated by substituting $z=e^{j\omega T}$ in the overall pulse-transfer function.

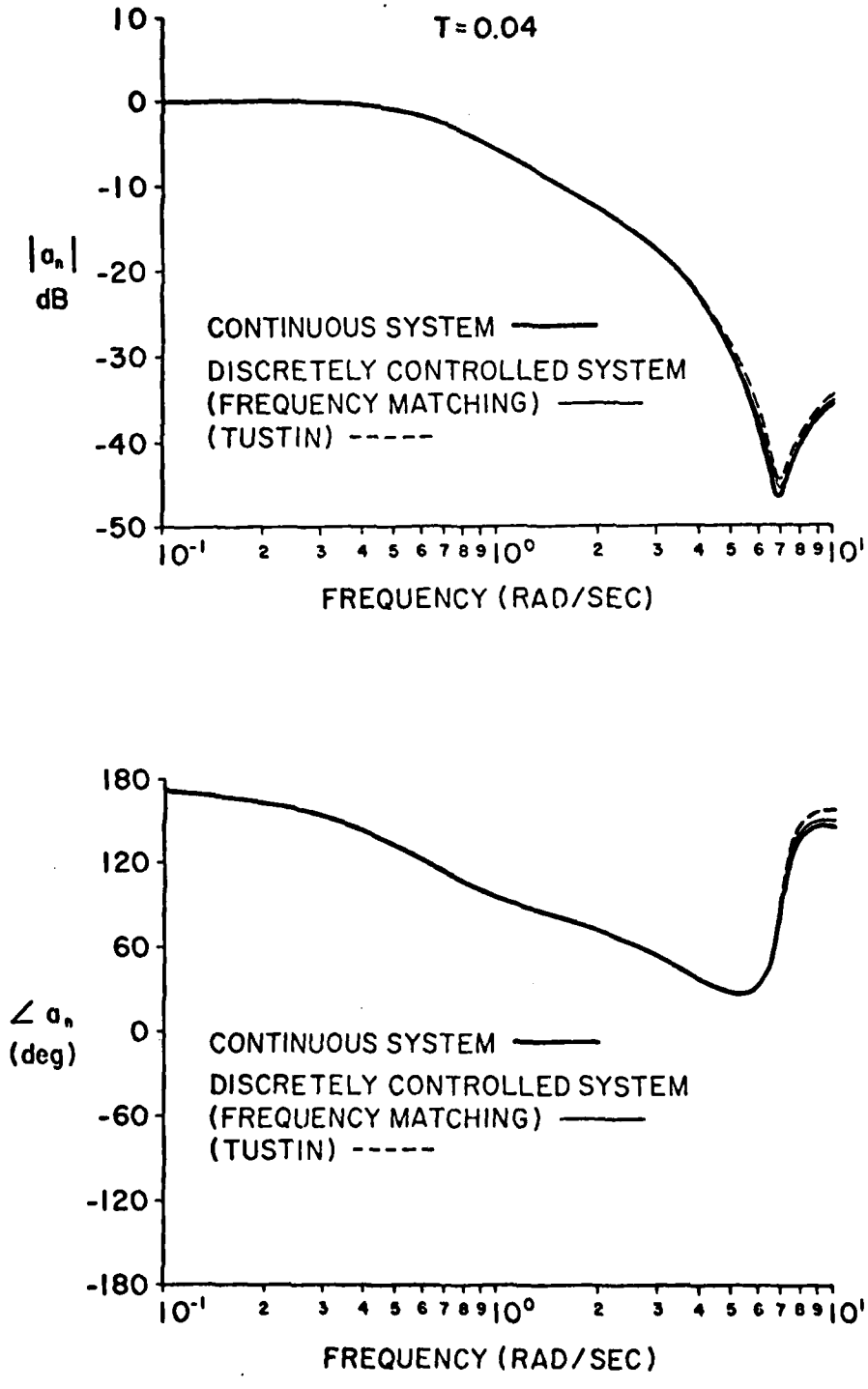
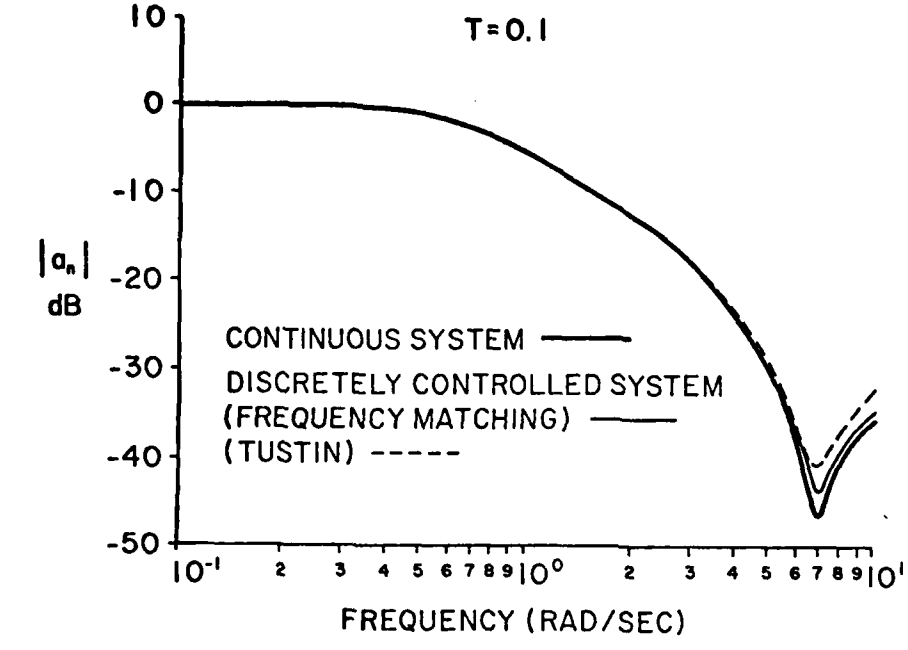



Figure 18. Frequency responses of the continuous model and the digital control system shown in Figures 6 and 7.



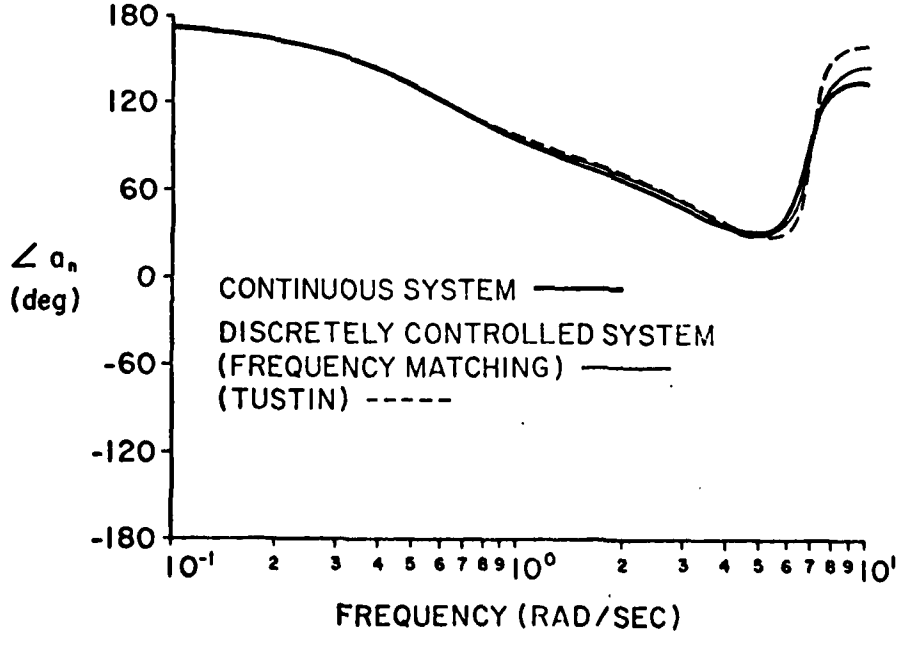




Figure 19. Frequency responses of the continuous model and the digital control system shown in Figures 6 and 7.

The multi-loop (high order) system employed as an example highlights the next problem that should be treated in this research area, that of accuracy. If the poles and zeros of a pulse-transfer function (which lie inside the unit circle for a stable system) are very close together, the frequency response obtained numerically by the above substitution is not accurate due to numerical inaccuracy in the z domain analysis. Because of this an incorrect set of digital controller coefficients are obtained. This problem was solved here by cancelling all the poles and zeros which were close together. This complicated the design process. Also by cancelling the poles and zeros, the accuracy problem still remains. Therefore, we need to use a different method other than cancelling the poles and zeros and one which can numerically determine the frequency response accurately.

I propose to do this by transforming the pulse-transfer function G(z) in the z-plane to G(W') in the W'-plane by making the substitution[10,11]

$$z = \frac{1 + W'T/2}{1 - W'T/2}$$

The frequency response will then be determined by substituting $W' \triangleq j\gamma = j\frac{2}{T}\tan\frac{\omega T}{2}$ in G(W'). By making this substitution, the unit circle is transformed into the infinite left half of the W -plane and this should help avoid the kinds of problems experienced during this project.

The results in this report show that even though the magnitude of the frequency response of the digital control system matched closely to that of the continuous model within the frequency range of interest, the phase angle begins to deviate at about 5 rad/sec. This problem results in a second recommendation for follow-on research. In order to match the phase angle of the digital control system to that of the continuous model at high frequency, both the magnitude and phase of the error should be minimized instead of only the magnitude as was done in this project.

I propose to do this by minimizing the real and imaginary part of the error between the transfer function of the continuous model and the frequency-characteristic function of the digital control system. The Goulb algorithm will be used to find the best estimate of the digital controller parameters.

## REFERENCES


1. D. Tabak, "Digitalization of Control Systems," Comput. Aided Des., Vol 3, No. 2, pp. 13-18, 1971.

2. B.C. Kuo, G. Singh and R.A. Yackel, "Digital Approximation of Continuous-Data Control Systems by Point-by-Point State Comparison," Comput. and Elect. Engng., Vol. 1, pp. 155-170, 1973.

3. R.A. Yackel, B.C. Kuo and G. Singh, "Digital Redesign of Continuous Systems by Matching of States at Multiple Sampling Periods," Automatica, Vol. 10, pp. 105-111, 1974.

4. G. Singh, B.C. Kuo and R.A. Yackel, "Digital Approximation by Point-by-Point State Matching with Higher-Order Holds," International Journal of Control, Vol. 20, No. 1, pp. 81-90, 1974.

5. E.C. Levy, "Complex-Curve Fitting, "I.R.E. Trans. Automatic Control, Vol. AC-4, pp. 37-43, 1959.

6. R. Kalman, "Design of a Self-Optimizing Control System," Trans. ASME, Vol. 80, pp. 468-478, 1958.

7. S.V. Rao and S.S. Lamba, "A New Frequency Domain Technique For the Simplification of Linear Dynamic Systems," International Journal of Control, Vol. 20, No. 1, pp. 71-79, 1974.

8. C.T. Mullis and R.A. Roberts, "The Use of Second-Order Information in the Approximation of Discrete-Time Linear Systems," IEEE Trans. On Acoustic, Speech and Signal Processing, Vol. 3, pp 226-238, 1976.

9. K.S. Rattan, "Computer-Aided Design of Sampled-Data Control System via Complex-Curve Fitting," Ph.D. dissertation, Univ. of Kentucky, 1975.

10. Gene F. Franklin and J. David Powell, Digital Control of Dynamic Systems, (Addison Wesley, 1980), p. 114.

11. R. F. Whitbeck and L.G. Hofman, "Analysis of Digital Flight Control Systems with Flying Quality Applications," Vol. II, Technical Report AFFDL-TR-78-115, 1978.

12. R.F. Whitbeck and Dennis G.J. Didalensky, "Multi-Rate Control Systems with Simulation Applications," Vol. I, Technical Report AFWAL-TR-80-, May 1980.

## APPENDIX A

## LISTING OF TRANSFER FUNCTIONS

In this appendix, the transfer functions of the aircraft model (M = 0.6, h = 30,000 ft) used in Section IV are provided.

$\alpha/\delta_e$

NUMERATOR

| I | NPOLY(I) | ZERO(I) |
|---|---|---|
| 1 | ( -1.449 )S** 3 | ( -.8003E-02) + J( -.7455E-01) |
| 2 | ( -147.6 )S** 2 | ( -.8003E-02) + J( .7455E-01) |
| 3 | ( -2.370 )S** 1 | ( -101.9 ) + J( 0. ) |
| 4 | ( -.8295 ) | |

DENOMINATOR

| I | DPOLY(I) | POLE(I) |
|---|---|---|
| 1 | ( 1.000 )S** 5 | ( 1.137 ) + J( 0. ) |
| 2 | ( 20.95 )S** 4 | ( -.9345E-02) + J( .7705E-01) |
| 3 | ( 16.71 )S** 3 | ( -.9345E-02) + J( -.7705E-01) |
| 4 | ( -46.66 )S** 2 | ( -2.071 ) + J( 0. ) |
| 5 | ( -.7820 )S** 1 | ( -20.00 ) + J( 0. ) |
| 6 | ( -.2837 ) | |

$q/\delta_e$

NUMERATOR

| I | NPOLY(I) | ZERO(I) |
|---|---|---|
| 1 | ( -147.6 )S** 3 | ( 0. ) + J( 0. ) |
| 2 | ( -79.39 )S** 2 | ( -.8816E-02) + J( 0. ) |
| 3 | ( -.6884 )S** 1 | ( -.5292 ) + J( 0. ) |
| 4 | ( 0. ) | |

DENOMINATOR

| I | DPOLY(I) | POLE |
|---|---|---|
| 1 | ( 1.000 )S** 5 | ( 1.137 ) + J( 0. ) |
| 2 | ( 20.95 )S** 4 | ( -.9345E-02) + J( .7705E-01) |
| 3 | ( 16.71 )S** 3 | ( -.9345E-02) + J( -.7705E-01) |
| 4 | ( -46.66 )S** 2 | ( -2.071 ) + J( 0. ) |
| 5 | ( -.7820 )S** 1 | ( -20.00 ) + J( 0. ) |
| 6 | ( -.2837 ) | |

$a_n/\delta_e$

NUMERATOR

| I | NPOLY(I) | | ZERO(I) | |
|---|---|---|---|---|
| 1 | ( -.5315 ) | S** 4 | ( 0. ) + J( | 0. ) |
| 2 | ( -.5314 ) | S** 3 | ( .1831E-02) + J( | 0. ) |
| 3 | ( -24.95 ) | S** 2 | ( -.5009 ) + J( | -6.833 ) |
| 4 | (.4567E-01 ) | S** 1 | ( -.5009 ) + J( | 6.833 ) |
| 5 | 0. ) | | | |

DENOMINATOR

| I | DPOLY(I) | | POLE(I) | |
|---|---|---|---|---|
| 1 | ( 1.000 ) | S** 5 | ( 1.137 ) + J( | 0. ) |
| 2 | ( 20.95 ) | S** 4 | ( -.9345E-02) + J( | .7705E-01) |
| 3 | ( 16.71 ) | S** 3 | ( -.9345E-02) + J( | -.7705E-01) |
| 4 | ( -46.66 ) | S** 2 | ( -2.071 ) + J( | 0. ) |
| 5 | ( -.7820 ) | S** 1 | ( -20.00 ) + J( | 0. ) |
| 6 | ( -.2837 ) | | | |

1980 USAF - SCEE SUMMER FACULTY RESEARCH PROGRAM

Sponsored by the

AIR FORCE OFFICE OF SCIENTIFIC RESEARCH

Conducted by the

SOUTHEASTERN CENTER FOR ELECTRICAL ENGINEERING EDUCATION

FINAL REPORT

# PHYSIOLOGICAL RESPONSES TO WEARING FIRE FIGHTER'S ENSEMBLE ON THE TREADMILL


| | |
|---|---|
| Prepared by: | Marvin L. Riedesel |
| Academic Rank: | Professor of Biology |
| Department and University: | Department of Biology, University of New Mexico |
| Research Location: | USAF School of Aerospace Medicine, Crew Protection Branch, Brooks Air Force Base, TX. |
| USAF Research Colleague: | Dr. Loren Myhre |
| Date: | July 29, 1980 |
| Contract No: | F49620-79-C-0038 |

# PHYSIOLOGICAL RESPONSES TO WEARING FIRE FIGHTER'S ENSEMBLE ON THE TREADMILL

by

Marvin L. Riedesel

## ABSTRACT

Twenty-three experiments conducted on three subjects describe considerable physiological cost to wearing the fire fighter's ensemble. The experiments involved variation in the work load, ambient temperature and clothing. Additional data are needed on two or three more subjects before the study can be published in the scientific literature. The data presented describe the wearing of the ensemble results in restricted evaporation of sweat, elevated body temperature, increased oxygen consumption and increased cardiovascular work.

## Acknowledgments

The author would like to thank the Air Force Systems Command, the Air Force Office of Scientific Research and the Southeastern Center for Electrical Engineering Education for providing financial support of my participation in the summer faculty research program at Brooks Air Force Base.

Dr. Loren Myhre and Dr. Sarah Nunneley provided outstanding encouragement, consultation and advisement. Col DeHart's sincere interest in my activities served as motivation. Dr. R. R. Burton and Col W. J. Sears as heads of the Crew Protection Branch created a comfortable atmosphere and encouraged co-operation and assistance by all persons in the branch. Capt D. M. Terrian, Lt R. Maldonado, Mr. Donald Tucker, MSgt Tom Crosby and AlC M. L. Faulkner were very patient in orientation, collaboration and providing technical assistance. Mr. David Atwood provided technical assistance and many hours of reducing data and consultation.

Mr. Tom Kay, Nuclear Medicine, Clinical Sciences, was very generous in providing guidance, laboratory facilities and equipment for the radioimmuno assay studies.

Col R. F. Ziegler, Lt Col D. K. Obeck, Capt R. C. Harvey and MSgt Biordo of the Veterinary Sciences Division were very cooperative and helpful in providing facilities, supplies and time.

## I. INTRODUCTION

From 1955 to 1959 I worked full time on the effects of thermal environment on industrial workers. Since then my research has been primarily in the field of comparative environmental physiology. My teaching assignment has involved mammalian physiology and environmental physiology. In recent years the interest of my students in human exercise physiology has increased. The summer faculty research program at Brooks Air Force Base provided me an opportunity to renew my "hands on" experience in assessment of the physiological responses of men to work and thermal stress.

The Air Force and more specifically the Crew Protection Branch, USAFSAM, Brooks Air Force Base, is concerned with a number of questions regarding fire fighting personnel. These questions include: What level of physical fitness should fire fighters maintain? To what extent will the insulation of the fire fighter's protective clothing limit heat loss generated during vigorous exercise? If a fire fighter needs to carry his own air supply, how much oxygen is needed and how much does the self-contained breathing apparatus add to the work load and oxygen need? The ideal situation would protect fire fighters and give them the capacity to be effective workers. This situation obviously requires a good match among thermal protection, adequate air supply, and physical fitness.

During the pre-summer visit and throughout the summer there were numerous topics of mutual interest discussed with various personnel at BAF Base. However, the major emphasis of my work was on the "Physiological Responses to Wearing Fire Fighter's Ensemble on the Treadmill."

## II. OBJECTIVES

The objectives set forth after the pre-summer visit were:

1. Participate in a study of the physiological responses of men wearing the complete fire fighter's protective ensemble (insulated garment and a self-contained breathing apparatus) while performing treadmill exercise in thermally (i) neutral and (ii) hot environments.
2. Endeavor to explore the feasibility of performing radioimmunoassay analyses for endorphin and prolactin on serum samples collected from men during and following prolonged exercise in the heat. If successful, a similar study will subsequently be conducted at the University of New Mexico following the same protocol

but studying female athletes in an attempt to relate endorphin and prolactin levels to menstruation and exercise-induced amenorrhea.

3. Familiarization with ongoing USAF physiological research programs, techniques, and instrumentation at the USAF School of Aerospace Medicine--this is to include active investigative involvement in such programs wherever possible.

*Additional goals and objectives set forth during the course of the* summer include:

Explore the feasibility of my conducting animal experiments at the Univ. of New Mexico which will parallel and complement studies being conducted at BAFB. The research topic of greatest potential may be "Effect of Oral Glycerol on Water Load Retention."

III. REPORT OF RESEARCH "Physiological Response to Wearing Fire Fighter's Ensemble on the Treadmill"

(1) Methods & Materials

*Aerobic capacity ($\dot{V}O_2$ max) measurements, performed* by the Clinical Sciences Division (SAM/BAF) were used in assigning standard work loads for the subjects in these experiments. The work loads assigned were calculated to require a given percent of each subject's $\dot{V}O_2$ max. This was accomplished by determining the oxygen consumption for each subject walking at a constant speed (3.3 mph) but at three different grades. The treadmill grades requiring 40 and 60% of $\dot{V}O_2$ max were then obtained by plotting the oxygen consumption against persent grade as illustrated in Figure 1. Similar graphs were constructed for each subject.

(a) Oxygen Consumption.

Analyses were made with an open system utilizing a dry gas meter and a Perkin Elmer medical gas analyzer. Exhaled air samples were collected between the 5th & 6th, 7th, & 8th, 12th & 13th, and 14th & 15th minute of each walk on the treadmill.

(b) Temperature.

All temperature measurements were made with thermistors. Rectal and skin temperatures were measured at one minute intervals throughout each experiment. Mean skin temperature was calculated by the method of Ramanathan[1].

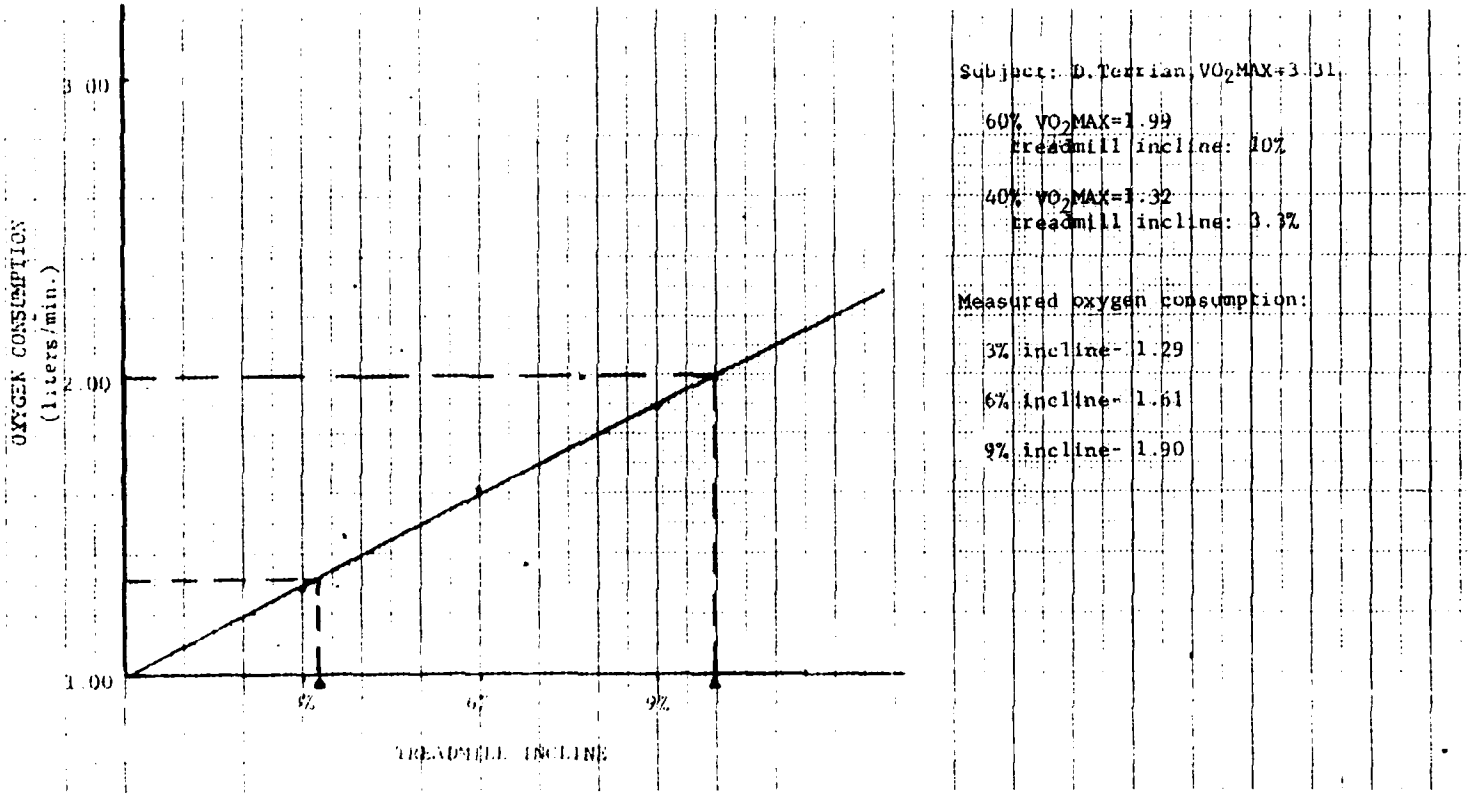



FIGURE 1 - GRAPH FOR DETERMINING TREADMILL GRADE FOR 40% AND 60% $\dot{V}O_2$ MAX.

(c) Heart Rate.

An ECG instrument provided continuous recording of heart rate during the exercise on the treadmill and the first 10 min of the post-exercise recovery period. The heart rate was recorded at 5 min-intervals at other times during the experiments.

(d) Sweat and Evaporation Measurements.

Periodic weighing to the nearest 5 g permitted measurement of sweat and evaporation. The weight change at each interval represented evaporation. The evaporation plus the weight gain of the clothing represented the sweat rate.

(e) Experimental Variables and Experimental Conditions.

EXPERIMENTAL VARIABLES

1. BUNKER versus GREENS
2. 40% MAXIMUM OXYGEN CONSUMPTION ($\dot{V}O_2$) vs 60% $\dot{V}O_2$
3. HOT versus COOL environments

| | Hot | Cool |
|---|---|---|
| d.b. | 40 C | 24 C |
| w.b. | 27 C | 18 C |
| Vapor Press. | 20 Torr | 12 Torr |
| globe | 48 C | 24 C |

EXPERIMENTAL CONDITIONS

Hot Bunker, 60% $\dot{V}O_2$ max
Cool Bunker, 60% $\dot{V}O_2$ max
Hot Bunker, 40% $\dot{V}O_2$ max
Cool Bunker, 40% $\dot{V}O_2$ max
Hot Greens, 60% $\dot{V}O_2$ max
Cool Greens, 60% $\dot{V}O_2$ max
Hot Greens, 40% $\dot{V}O_2$ max
Cool Greens, 40% $\dot{V}O_2$ max

(f) Protocol.

The protocol is presented in Table 1.

TABLE I EXPERIMENTAL PROTOCOL

| Greens: | Bunker: |
|---|---|
| weight in shorts<br>weight in greens | weight in shorts<br>weight in greens |
| Rest, 35 min. | Rest, 15 min. |
| weight in greens<br>weight in greens, boots, and socks | weight in greens<br>weight in bunker, boots, and gloves |
| | Rest, 20 min. |
| | weight in bunker, boots, and gloves |
| Walk on treadmill, 15 min.<br>collect expired gas: 6th, 8th, 13th, and 15th minutes | Walk on treadmill, 15 min., wearing SCBA<br>collect expired gas: 6th, 8th, 13th, and 15th minutes |
| weight in greens, boots, and socks | weight in bunker, boots, and gloves |
| Recovery, 10 min.<br>(seated on scale, without changing clothes) | Recovery, 10 min.<br>(seated on scale, holding hood and gloves, wearing bunker) |
| weight in greens, boots, and socks<br>weight in greens<br>weight in shorts | weight in bunker, boots, and gloves<br>weight in greens<br>weight in shorts |
| Recovery, 40 min.<br>(wearing greens only) | Recovery, 40 min.<br>(wearing only greens) |
| weight in greens<br>weight in shorts | weight in greens<br>weight in shorts |

(2) Results

Twenty-three experimental runs were conducted on three subjects during the 10 week summer session. Similar experiments will be conducted on two or three subjects after I leave BAFB. This report must be considered a preliminary report which justifies extension of the investigations.

At the higher work loads (60% $\dot{V}O_2$ max) the cost of wearing the Fire Fighter's Protection Ensemble (bunker) (Figure 2) was 0.7 liter/min (Table II). This extra cost of wearing the bunker ranged from 38 to 49% at the two work loads (Table II).

In all experiments the increase in rectal temperature was higher when wearing the bunker (Table III). A 39 C rectal temperature is considered the maximum safe upper limit in this laboratory. One subject had a 38.9 C rectal temperature during the recovery period after the walk.

A heart rate of 180 bts/min is the maximum safe upper limit in many industrial situations[2]. Wearing the bunker resulted in mean heart rates approaching the safe upper limit after only 15 min of work at 60% $\dot{V}O_2$ max (Table III).

Wearing the bunker resulted in an elevation of the sweat rate and markedly reduced the amount of sweat evaporated (Figure 3). While wearing the bunker in the hot environments the mean sweat rate was 4.5 times the evaporation rate during the walk plus the first 10 min of recovery.

(3) Discussion

From the data collected on three subjects with $\dot{V}O_2$ max values ranging from 44 to 47 ml $O_2$/kg $min^{-1}$, there is ample evidence that fire fighters should be in good to excellent physical condition. Activities such as climbing stairs while carrying fire extinguishing equipment could rapidly cause persons to have excessive elevations in heart rate and body temperature within 15 to 20 min.

The 0.7 liter/min increase in oxygen consumption (Table II) makes it necessary to warn subjects utilizing self containing breathing apparatus (SCBA) that exercise while wearing a bunker may deplete air supplies within a very limited period of time. The SCBA which will last a resting subject 30 min may last a working subject only 9 to 11 min.



FIGURE 2 - SKETCH OF SUBJECT WEARING FIRE FIGHTER'S ENSEMBLE (BUNKER)

## TABLE II OXYGEN CONSUMPTION DATA

| Experimental Condition | Oxygen Consumption liter/min | Cost of Bunker liter/min | Cost of Bunker % over greens |
|---|---|---|---|
| 60% $\dot{V}O_2$ max, Hot (n=2) | | | |
| Bunker | 2.33 | 0.72 | 44 |
| Greens | 1.61 | | |
| 60% $\dot{V}O_2$ max, Cool (n=3) | | | |
| Bunker | 2.53 | 0.70 | 38 |
| Greens | 1.83 | | |
| 40% $\dot{V}O_2$ max, Hot (n=1) | | | |
| Bunker | 1.76 | 0.58 | 49 |
| Greens | 1.18 | | |
| 40% $\dot{V}O_2$ max, Cool (n=2) | | | |
| Bunker | 1.80 | 0.55 | 44 |
| Greens | 1.25 | | |

## TABLE III RECTAL TEMPERATURE & HEART RATE

| Experimental Condition | Rectal Temp. Max. | Rectal Temp. End of Recovery | Maximum Heart Rate (beats/min) |
|---|---|---|---|
| 60% $\dot{V}O_2$ max, Hot (n=2) | | | |
| Bunker | 38.7 | 37.6 | 169 |
| Greens | 37.6 | 37.2 | 136 |
| 60% $\dot{V}O_2$ max, Cool (n=3) | | | |
| Bunker | 37.4 | 37.1 | 152 |
| Greens | 37.2 | 36.8 | 119 |
| 40% $\dot{V}O_2$ max, Hot (n=2) | | | |
| Bunker | 38.8 | 37.8 | 152 |
| Greens | 37.7 | 37.6 | 108 |
| 40% $\dot{V}O_2$ max, Cool (n=2) | | | |
| Bunker | 37.3 | 36.6 | 132 |
| Greens | 37.2 | 37.0 | 100 |

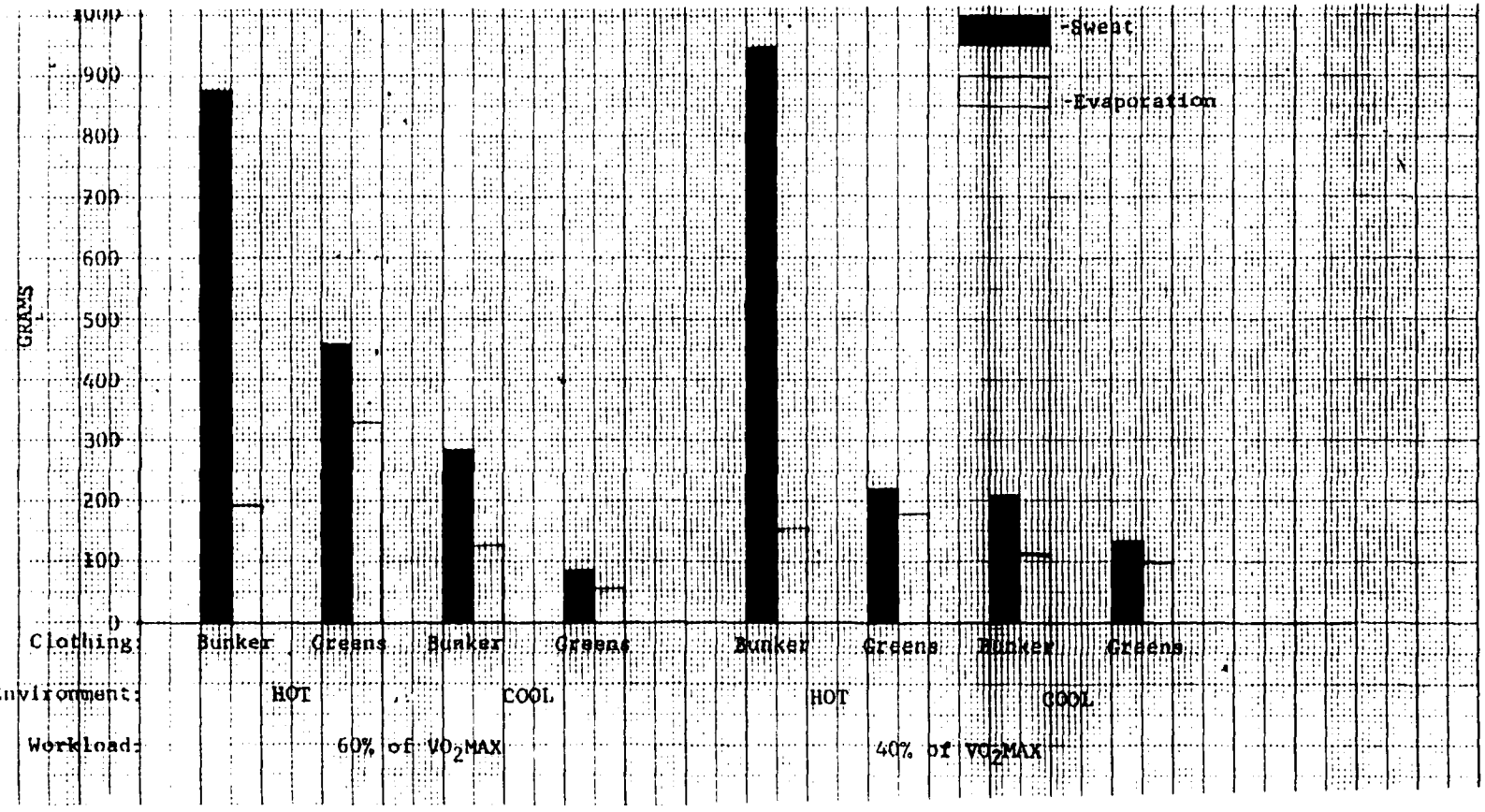



FIGURE 3 - MEAN SWEAT AND EVAPORATION DURING 15-MIN WALK AND FIRST 10 MIN OF RECOVERY

Fire fighters must realize that simply walking while wearing the bunker can be moderate to moderately heavy work. Working time for simple tasks may be limited to less than 15 min because of the 40 to 50% increase in the cost of work imposed by the bunker.

In each experiment the maximum rectal temperature occurred during the recovery period. Thus fire fighters must be advised not to continue working in the heat to near exhaustion because maximum body temperature is going to occur after they start resting from work in the heat. An exhausted fire fighter could readily become a heat stroke victim as heat generated in the working muscles is distributed throughout the body during the recovery period.

## IV. OTHER RESEARCH ACTIVITIES

(1) Plasma Endorphin and Prolactin Analyses

Approximately 5 to 8 work days were spent conducting 80 endorphin and 60 prolactin analyses on pooled plasma samples and individual plasma samples collected on marathon runners. Dr. Loren Myhre and Mr. Don Tucker are exploring the feasibility of continuing these studies at BAFB.

(2) Over hydration prior to heat exposure

Approximately 30 to 50 hr were spent consulting, reading and planning studies of glycerol administration as a method of overhydrating subjects. Aircrews of high-performance aircraft in warm climates frequently encounter heat stress and dehydration. Dehydration reduces cardiac output because of lowered plasma volume and reduces sweating. A minigrant proposal involving laboratory and field animals will be submitted in this research area to complement the human subject experiments planned at BAFB.

## V. RECOMMENDATIONS

Fire fighting personnel must be made aware of the necessity for maintaining good physical condition. Ventilation of the bunker would help promote evaporation and reduce elevation of body temperature. However, the cost of carrying ventilation equipment may offset the advantage gained from the extra ventilation.

## REFERENCES


1. N. L. Ramanthan, "A new weighting system for mean surface temperature of the human body", J. Appl. Physiol., 19:531-533, 1964.

2. Lucien Brouha, Physiology in Industry, Figure 3.24, Pergamon Press, 145 p. (1960).

1980 USAF - SCEEE SUMMER FACULTY RESEARCH PROGRAM

Sponsored by the

AIR FORCE OFFICE OF SCIENTIFIC RESEARCH

Conducted by the

SOUTHEASTERN CENTER FOR ELECTRICAL ENGINEERING EDUCATION

FINAL REPORT

# EVALUATION OF THE BOMB DAMAGE REPAIR COMPUTER CODE


Prepared by: Dr. Lawrence C. Rude

Academic Rank: Assistant Professor

Department and University: Department of Civil Engineering
Virginia Polytechnic Institute and
State University

Research Location: Engineering and Services Center
Tyndall AFB, Florida

USAF Research Colleague: Mr. Phil Nash



Date: September 9, 1980

Contract No: F49620-79-C-0038

# EVALUATION OF THE BOMB DAMAGE REPAIR COMPUTER CODE

by

Lawrence C. Rude

## ABSTRACT

An evaluation of the Bomb Damage Repair (BDR) Computer Code was completed. The evaluation consisted of outlining the structure and function of each subroutine and making a subjective appraisal. Comparisons between elastic solution of Boussinesq's equation for stresses and Steinbrenner's method of computing settlements were made. A section describing the use of the program is presented. A parameter study showing variations in crater repair is also presented.

In general the BDR computer code is a good finite element computer code. It has the capability of analyzing crater repairs, pavement structures and alternate launch and recovery surfaces. It has the capability for some non-linear material behavior as represented by Hardin's material laws, otherwise the program is a linear finite element program. The program contains axisymmetric and prismatic elements. The prismatic elements were considered to fall into a semi-analytic category and due care should be used regarding their use.

## ACKNOWLEDGEMENTS

The writer would like to thank and acknowledge the assistance of the Air Force Systems Command, the Air Force Office of Scientific Research, SCEEE and the Engineering and Service Center, Tyndall Air Force Base for the opportunity to work on this worthwhile project.

I would also like to thank Mr. Phil Nash and the men at the Computer Service Center at AFESC for their aid, advice and outstanding assistance in making this a very productive summer.

## I. INTRODUCTION

The Engineering and Services Laboratory at the Air Force Engineering and Services Center, Tyndall Air Force Base, Florida have been assigned the program to (a) develop materials, methods and equipment for the rapid repair of airfield pavements following a conventional enemy attack and (b) designs of alternate launch and/or recovery surface for aircraft operations that are independent of conventional runways and that will provide a redundancy. The final goal of the project is to provide, by 1986, the capability of a limited number of aircraft missions within one hour after a bombing via alternate surfaces and for a sustained aircraft operations within a few hours after an attack.

In conjunction with this goal, the use of analytical predictions to reduce the number of experimental tests has been permitted. Actual repairs will be constructed to validate the computer analysis. The repair designs for the spalls and craters include flexible and rigid pavements using asphalt and rapid setting cement, unsurfaced aggregate systems, and prefabricated structural caps over selected fill. Advanced material application is also included. For the alternate launch and recovery surfaces design concepts as stabilized soils, membranes, mats, reinforced earth and fabrics, and existing roads and highways are to be considered.

A computer program called the Bomb Damage Repair (BDR) Code is currently being developed. The program is a modification of existing codes called AFPAV and WINDAX previously developed by the Air Force for the analysis of pavements and bomb damage repair. The purpose of this project is to evaluate the new BDR computer code at its current developmental stage.

## II. OBJECTIVES

The prime goal of this study was to evaluate the Bomb Damage Repair Computer Code. To achieve this goal the theory and structure of the program was reviewed. An operational version of the current code was installed on a CDC 6600 and Cyber 176. Procedures for using the code were investigated. Comparisons with elastic solutions were

made to verify the accuracy of the program. Parameter studies were conducted to depict the effects of various types of crater repair.

## III. THEORY OF THE BDR CODE

### Introduction

The Bomb Damage Repair (BDR) computer program is a finite element program used to simulate repairs on cratered runways. It also may be used to represent conventional pavements and alternate launch/recovery surfaces. The program offers a selection of various single wheel and multiwheel aircraft wheel loads, linear and non-linear material behavior and axisymmetric or prismatic elements. The program is divided into three overlays to reduce its computer core requirements.

### Theory of Finite Element Method

The finite element method has been described (Desai and Christians, 1977) as comprising five steps: (1) discretization of the continuum, (2) selection of the element displacement function, (3) derivation of the element stiffness, (4) assemblage of the elements to form a continuum and (5) solution of the unknown quantities. The steps will be briefly reviewed to explain the finite element procedures used in the BDR code. More detailed information is available in many references and textbooks.

The first step involves discretization of a continuum. The continuum represents the engineering work to be analyzed. The discretization involves dividing the cross section into smaller continua which are called finite elements. The elements are often triangular or rectangular in shape. The elements are connected at nodal points located often at the corners.

The fundamental approach in the finite element method is to characterize the behavior of each element in terms of a prime unknown quantity at the node points. In the BDR code these unknown quantities are displacements. Secondary unknowns as stresses and strains within the element are calculated from the prime unknowns.

The resistance an element has to deformatize caused by applied forces at the nodal points is called stiffness. Once the stiffness of

of an element has been defined in terms of displacements, the individual elements are assembled to represent the behavior of the original continuum. The assembled elements provide a resistance to deformation at a given node. This stiffners at each node are the coefficients a system of simultaneous equations relating displacement and force. The displacements are solved using an appropriate numerical technique, e.g. Gauss elimination and back substitution.

Axisymmetric Element

The axisymmetric element used in the BDR code is a quadrilateral element. The element is formulated from sub-element triangular stiffness elements. The displacement within each triangular element is a priori assumed to be represented by a linear equation. In matrix notation the general form of the displacement equation $\{u\} = [M]\{\alpha\}$ where $\{u\}$ equals the displacement vector. [M] represents generalized coordinates and $\{\alpha\}$ represents unknown constants. The nodal displacements vector is related to the unknown coefficients by $\{\mu_i\} = [A]\{\alpha\}$ and $\{\alpha\} = [A^{-1}]\{\mu_i\}$ The triangular sub-elements are isoparametric elements in that an interpolation function $[N] = [A^{-1}]$ is the same expression used to define the coordinates of a point within the element. The use of interpolation functions precludes the need to invert [A].

The element strains are defined as $\{\epsilon\} = [B]\{\alpha\}$ where [B] is the proper differentiation of [A]. Since $\{\alpha\} = [A^{-1}]\{\mu_i\} = [N]$ $\{\epsilon\} = [B]\,[N]\{\mu_i\}$ . The stresses are defined by $\{\sigma\} = [C]\{\epsilon\}$ $\{\sigma\}$ equals the stress vector, $\{\epsilon\}$ represents the strain vector, and [C] contains the material laws for the element.

Using the principal of virtual work, the element stiffness can be obtained. A virtual nodal displacement $\{\bar{u}_i\}$ is produced in the element correspond the stresses $\{\sigma\}$ . The strains are in equilibrium with nodal forces $\{S_i\}$ . The external virtual work equals the internal virtual work. Expressed mathematically:

$$\{\mu_i\}^T [S_1] = \int_v \{\bar{\epsilon}\}^T \{\sigma\}\, dV \qquad V = \text{volume of element}$$

$$\{\bar{\epsilon}\}^T = \left[[B]\,[A^{-1}]\{\bar{u}_i\}\right]^T = \left[[B]\,[N]\{\bar{u}_i\}\right]^T$$

$$[S_1] = \int_v [N]^T [B]^T [C]\,[B]\, dV\, N$$

The stiffness matrix [K] for the element is defined as $[K] = [N^T] \int_V [B]^T [C] [B] \, dV \, [N]$.

The program performs the operations expressed in the above expression when it derives the axisymmetric stiffness matrix.

Prismatic Elements

The prismatic elements are applicable idealization a structural system whose (1) loading function is approximated by a periodic function, (2) longitudinal direction is infinite, (3) whose cross section does not vary in longitudinal direction and (4) whose material properties do not vary in the longitudinal direction. The prismatic elements are composed of four triangular elements.

The displacement function for the nodes is a function of three dimensions x, y, and z. The displacement function is assumed to vary as a periodic function in the longitudinal direction:

$$u(x,y,z) = \sum_{n=0}^{N} U_{xn}(x,y) \cos\frac{n\pi z}{L} + \sum_{m=1}^{M} U_{xm}(x,y) \sin\frac{m\pi z}{L}$$

$$v(x,y,z) = \sum_{n=0}^{N} U_{yn}(x,y) \cos\frac{n\pi z}{L} + \sum_{m=1}^{M} U_{ym}(x,y) \sin\frac{m\pi z}{L}$$

$$w(x,y,z) = \sum_{n=0}^{N} U_{zn}(x,y) \cos\frac{n\pi z}{L} + \sum_{m=1}^{M} U_{zm}(x,y) \sin\frac{m\pi z}{L}$$

u, v, w represent the displacements in the x, y, z direction respectively. In this manner the Fourier coefficients Uxn, Uxm, etc. are functions of x and y only and the deflection in the z direction is accounted for the Fourier expansion. L is the characteristic length.

To represent the prismatic solid elements the quadratic element needs only to be generated in two dimensions. The quadratic element is composed of four triangular elements. The displacement function is given below. The function specifies a linear variation of displacement.

$$U_{xn}(x,y) = \alpha_{1n} + \alpha_{2n} x + \alpha_{3n} y$$

$$U_{yn}(x,y) = \alpha_{4n} + \alpha_{5n} x + \alpha_{6n} y$$

$$U_{zn}(x,y) = \alpha_{7n} + \alpha_{8n} x + \alpha_{9n} y$$

Where the $\alpha$'s are the generalized coordinates.

In the BDR code, the matrix multiplication required for the derivation of the stiffness matrix has been previously worked out. The triangular stiffness is calculated directly. The global stiffness matrix is generated for each term of the Fourier series. The final solution is the superposition of the results of each term of the series.

Material Laws

The program has two options to define the [c] matrix relating stress and strain, $\{\sigma\} = [c]\{\epsilon\}$ . One option is to represent the material as a linear elastic material. For this option the [c] matrix as defined in the program is given below:

$$\{\sigma\} = \begin{Bmatrix} \sigma_{xx} \\ \sigma_{yy} \\ \sigma_{zz} \\ \sigma_{xy} \\ \sigma_{xz} \\ \sigma_{zx} \end{Bmatrix} \qquad \{\epsilon\} = \begin{Bmatrix} \epsilon_{xx} \\ \epsilon_{yy} \\ \epsilon_{zz} \\ \epsilon_{xy} \\ \epsilon_{xz} \\ \epsilon_{zx} \end{Bmatrix}$$

$$c(1,1) = \frac{E}{(1-2\upsilon)\ (1+\upsilon)} = c(2,2) = c(3,3)$$

$$c(1,2) = c(1,3) = c(2,1) = c(2,3) = c(3,2) = c(3,1)$$

$$= \frac{[E \times \upsilon \quad ]}{(1-2\upsilon)\ (1+\upsilon)}$$

$$c(4,4) = c(5,5) = c(6,6) = G = \frac{E}{2(1+\upsilon)}$$

This represents the subsurface as an isotropic material, e.g., when material properties are identical regardless of orientation of coordinate system.

Non-linear Material Behavior

The program uses a material characterization developed by B. O. Hardin as a non-linear representative. The law generalizes soil as a strain-hardening material. The program uses an solution scheme for selecting a secant shear modulus such that equilibrium and strain characteristics for each material are satisfied.

The program applies the aircraft loading on the first increment. The program redefines a secant shear modulus for each element based on

the strains from the previous step. The first step uses the initial tangent or maximum shear modulus.

Hardin discovered that for a given strain, cycle of loading and soil type the secant shear modulus can be computed from the normalized shear modulus:

$$G/G_{max} = \frac{1}{1 + \gamma_h} \qquad \text{Equation 1}$$

where $\gamma_h = \frac{\gamma}{\gamma_r}\left[1 + a \exp\left\{-\left(\frac{\gamma}{\gamma_r}\right)^{0.4}\right\}\right]$

$\gamma$ = shear strain

$\gamma_r$ = references strain

$$\gamma_r = \frac{\tau_{max}}{G_{max}}$$

$$a = \left\{\frac{3.85}{N} - .85\right\} T^{.25} \qquad \text{for clean sands}$$

$$= 1.6 \left\{\frac{(1 + .02\ S)\ T^{.2}}{N^{.6}}\right\} \qquad \text{for non-plastic soils with fines and low plasticity soils}$$

$$= \frac{0.2\ (1 + .02\ S)\ .75}{N^{.15}} \qquad \text{for high plasticity soils with liquid limit >50}$$

S = % saturation

N = number of cycles

T = time in minutes to reach normalized strain

From experimental studies

$$\gamma_r = \frac{G_{max}}{F^2 R^2}\left\{0.6 - .25\ (PI)^{.6}\right\} \qquad \text{Equation 2}$$

P.I. = plasticity index

$$F = \frac{(2.973 - e)^2}{(1 + e)}$$

R = 1100 for sands with less than 15% fines

= 1100 - GS for cohesive soils with more than 15% fines

If $C_1 = \frac{F^2\ (1100 - 6S)^2}{0.6 - .25\ (P.I.)^{.6}}$ then

$$\gamma_r = \frac{G_{max}}{C_1} \qquad \text{Equation 3}$$

$G_{max}$ can be computed from Young's modulus and Poisson's ratio by

$$G_{max} = \frac{E}{2(1+\nu)} \qquad \text{Equation 4}$$

or by

$$G_{max} = \frac{1230 \times (2.973 - e)^2}{(1 + e)} \times (O.C.R)^K \times \sqrt{\overline{\sigma_o}} \qquad \text{Equation 5}$$

where $e$ = void ratio
$O.C.R.$ = over consolidation ratio
$K$ = - .453 + .209 x In(P.I.)
$P.I.$ = plastic index
$\overline{\sigma_o}$ = geostatic stress

## IV. STRUCTURE OF THE BDR CODE

### Introduction

In this section the structure of the Bomb Damage Repair Code is presented. The structure is explained by the use of a flow chart and a table that briefly describes the function of each program and subroutine. A User's Manual is also presented.

### Structure of the BDR Code

The Bomb Damage Repair Code (BDR) is divided into three overlay programs. The overlays reduce the amount of core space required by the code. The AFCAN program generates input data for the AFPRE program and sets default valves. The AFPRE program generates AFPAV input data and generates the mesh for single wheel, multi-wheel loadings and identifies the crater. The AFPAV program is a general purpose finite element program using axisymmetric or prismatic elements for linear and non-linear layered systems. A schematic flow diagram of the program is presented in Figure 1. Table 1, briefly describes the subroutines in the BDR code. A representation of the mesh generated by the program is shown in Figure 2.

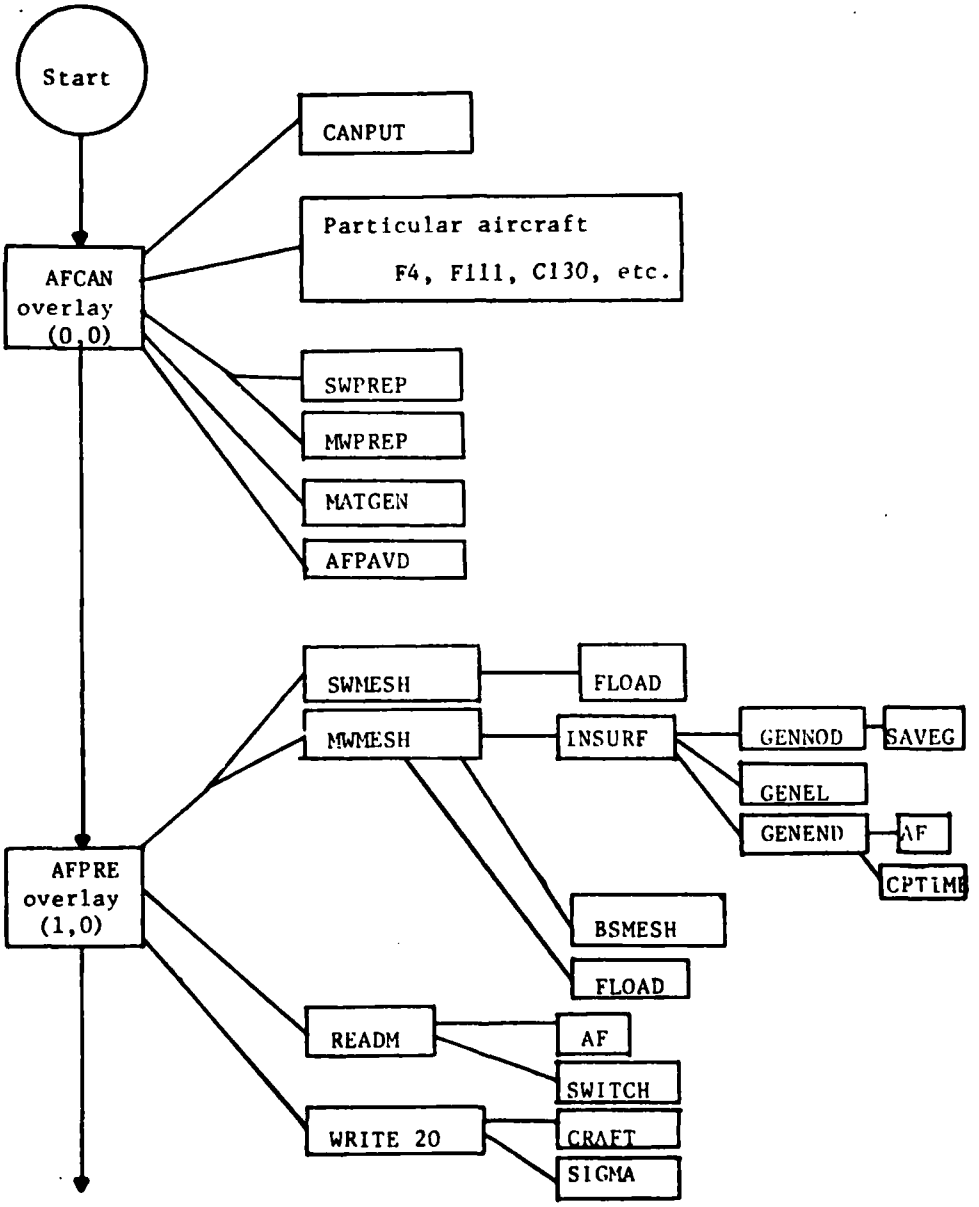



**Figure 1. Flow diagram for B.D.R. Code**

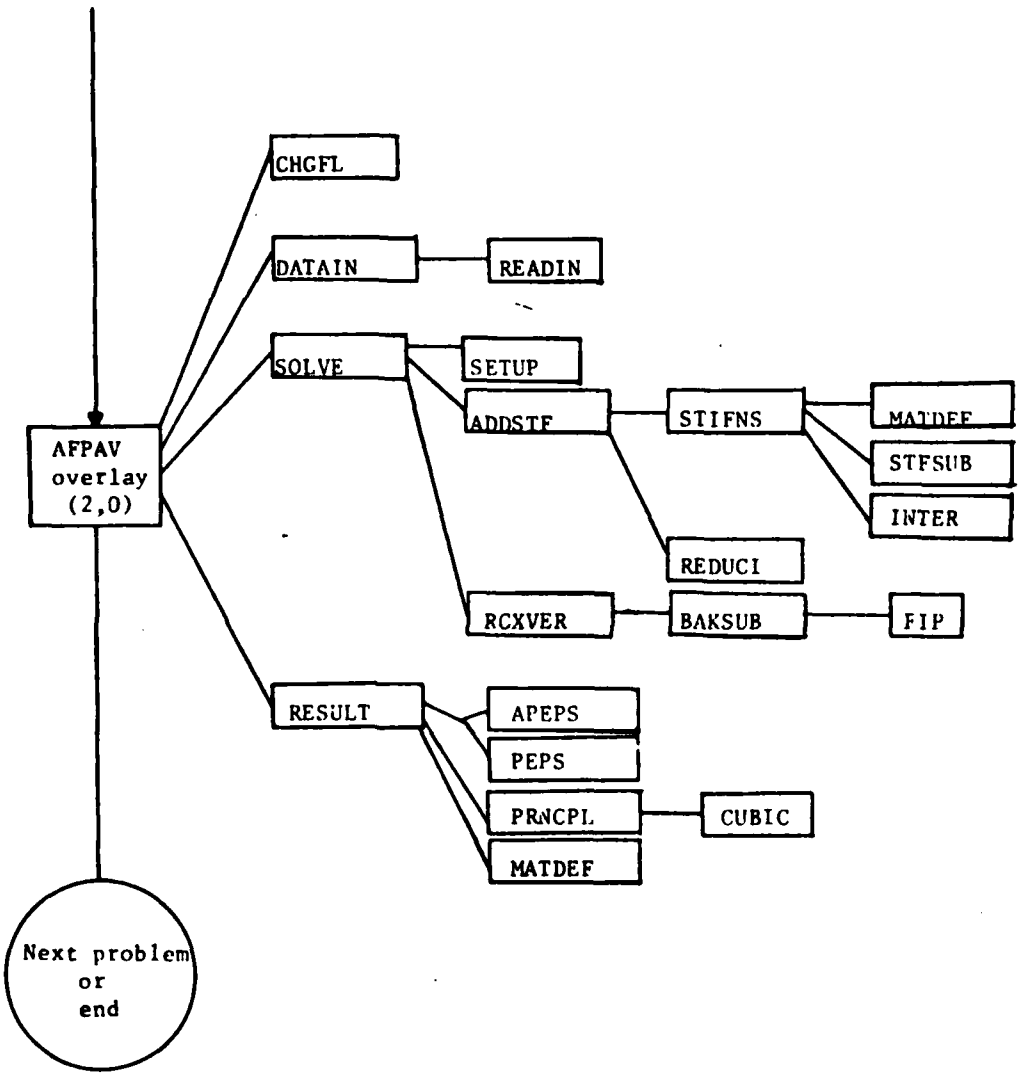



Figure 1. (continued)

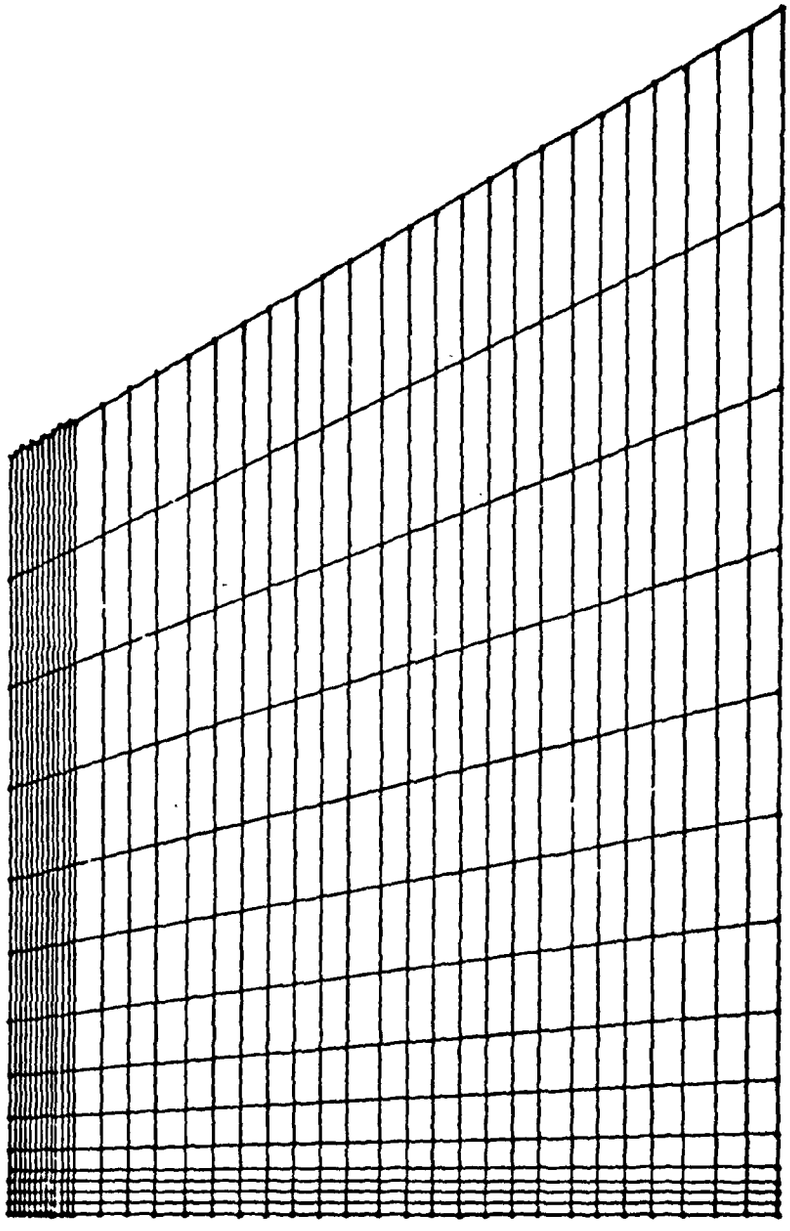


Figure 2. Example of generated mesh

TABLE 1: DESCRIPTION OF BDR SUBROUTINES

| NAME | PURPOSE | CALLED BY | CALLS TO |
|---|---|---|---|
| ADDSTF | System stiffness matrix generated into blocks | SOLVE | STIFNS |
| AF | Calculates area of triangle | GENEND<br>READM | |
| AFCAN | Executive program. Calls subroutines for (0,0) overlay and calls (1,0) and (2,0) overlays | | CANPUT<br>particular aircraft routines, F-4, B52, etc.<br>SWPREP<br>MWPREP<br>AFPAVD |
| AFPAV | Executive program for (2,0) overlay; sets up storage arrays | | |
| AFPAVD | Sets AFPAV parameters, defines start and stop points for element and node generation | | AFCAN |
| AFPRE | Sets storage array for mesh generation<br>Executive program for (1,0) overlay | | SLOMESH<br>MWMESH<br>READM<br>WRITZO |
| APEPS | Calculates strain for axi-symmetric elements | RESULT | |
| AI0 | Sets constants for A10 single wheel loading | AFCAN | |
| BAKSUB | Preforms back subsitution | REXOVR | |

TABLE 1: (Continued) DESCRIPTION OF BDR SUBROUTINES

| NAME | PURPOSE | CALLED BY | CALLS TO |
|---|---|---|---|
| BSMESH | Generates subgrade and base level mesh | MWMESH | |
| B1 | Sets controls for B1 multiwheel loading | AFCAN | |
| B52 | Sets controls for B52 multiwheel loading | AFCAN | |
| B57 | Sets controls for B57 single wheel loading | AFCAN | |
| B747 | Sets controls for B47 multiwheel loading | AFCAN | |
| CANPUT | Reads data cards. Checks layer thickness and concrete tensile strength | AFCAN | |
| CHGFL | Compares field length with that set up in common block array | AFPAV | |
| CPTIME | Returns current CP time | GENEND | |
| CRAFT | Defines boundary of crater and redefines material outside crater to native soil except for layer 1 | WRITE 20 | |
| CUBIC | Finds roots of rational cubic equation | PRNCPL | |

TABLE 1: (Continued) DESCRIPTION OF BDR SUBROUTINES

| NAME | PURPOSE | CALLED BY | CALLS TO |
|---|---|---|---|
| C5 | Sets constants for C5 multiwheel loading | AFCAN | |
| C9A | Sets controls for C9A multiwheel loading | AFCAN | |
| C130 | Sets constants for C130 multiwheel loadings | AFCAN | |
| C141 | Sets constants for wheel loading for C141 multi-wheel loading | AFCAN | |
| DATIN | Reads data input from AFPRE | AFPRE | READIN |
| ERROR | Error message subroutine | | |
| FIP | Binary control cards | BAKSUB | |
| FLOAD | Computes Fourier series terms and pressure loading | SWMESH<br>MWMESH | |
| F4 | Sets constants for wheel loading of F4 single wheel loading | AFCAN | |
| F15 | Sets controls for F15 single wheel loading | AFCAN | |
| F16 | Sets controls for F16 single wheel loading | AFCAN | |

TABLE 1: (Continued) DESCRIPTION OF BDR SUBROUTINES

| NAME | PURPOSE | CALLED BY | CALLS TO |
|---|---|---|---|
| F105 | Sets controls for F105 single wheel loading | AFCAN | |
| FB111A | Sets controls for FB111A single wheel loading | AFCAN | |
| INSURF | Call mesh generation routines | MWMESH | GENNOD<br>GENEL<br>GENEND |
| INTER | Performs numerical integration | STFSUB | |
| GENEL | Generates elements assigns connectivity and material identification | INSURF | |
| GENEND | Generates coordinates for unspecified nodes using Laplace generation, generates boundary condition data | INSURF | AF<br>CPTIME |
| GENNOD | Generates nodes along straight lines and along arcs (except Laplace generation) | INSURF | SAVEG |
| KC97 | Sets controls for KC97 multiwheel loading | AFCAN | |
| KC135 | Sets control for KC135 multiwheel loading | AFCAN | |

TABLE 1: (Continued) DESCRIPTION OF BDR SUBROUTINES

| NAME | PURPOSE | CALLED BY | CALLS TO |
|---|---|---|---|
| MATDEF | Defines material constitutive matrix | STFSUB<br>RESULT | |
| MATGEN | Determines material constants for linear and non-linear materials | AFCAN | |
| MWMESH | Generates mesh and displacement boundary conditions, calculates loads | AFPRE | INSURF |
| MWPREP | Computes mesh control parameter for multiwheel load, sets output control, generates surface region nodes and elements | AFCAN | |
| PEPS | Calculates strain for prismatic elements | RESULT | |
| PRNCPL | Computes principal components of stress | RESULT | CUBIC |
| READIN | Reads in list where solution is to be calculated and checks list | DATIN | |
| READM | Reads material properties, assigns gravity body forces, remembers nodes if requested | AFPRE | AF<br>SWITCH |
| REDUCI | Reduces block of equations by Gauss elimination | ADDSTF | |

TABLE 1: (Continued) DESCRIPTION OF BDR SUBROUTINES

| NAME | PURPOSE | CALLED BY | CALLS TO |
|---|---|---|---|
| RESULT | Outputs strains and stresses, calculates updated parameter for new stiffness calculation if requested | AFPAV | APEPS<br>PEPS<br>PRNCPL<br>MATDEF |
| RCXOVR | Any equation blocks on tape are recovered | SOLVE | BAKSUB |
| SAVEG | Lists nodes generated from input | GENNOD | |
| SETUP | Determines block size, band-width and equation positioning array | SOLVE | STIFNS<br>REDUCI |
| SIGMA | Calculates mean normal stress due to over burden | WRITE 20 | |
| SOLVE | Creates global stiffness matrix, nodal displacement coefficients and write solution to disk | AFPAX | SETUP<br>ADDSTF<br>RCXOVR |
| STIFNS | Forms quadrilateral element | ADDSTF | MATDEF<br>STFSUB |
| SWITCH | Changes node numbers | READM | |
| SWMESH | Generates nodes, boundary condition informative, Fourier coefficient, and loads for single wheel aircraft | AFPRE | FLOAD |

TABLE 1: (Continued) DESCRIPTION OF BDR SUBROUTINES

| NAME | PURPOSE | CALLED BY | CALLS TO |
|---|---|---|---|
| SWPREP | Computes control parameters for single wheel mesh and sets output locations | AFCAN | |
| T38 | Sets controls for T38 single wheel loading | AFCAN | |
| T43 | Sets constants for T43 multiwheel loading | AFCAN | |
| WRITE 20 | Initalizes AFPAV parameters, creates AFPAV input tape | AFPRE | CRAFT<br>SIGMA |

Input Data for Program

The following is a modified version of the User's Manual of the BDR Computer Code. Each problem requires four groups of cards for a particular job, additional problems may be solved at the same time by including additional sets of data. The program will terminate when an END is encountered.

A. Title and Solution Type Card (A8, 15A4, 2A2, 1X, A2, 4X, 1A)

| Column | Variable | Description |
|---|---|---|
| 1-8 | TITLE (1) | Aircraft Name (left Justified) F4, B52, F111, FB111A, B57, C130, C141, B747, B1, C5, T3, F105, KC135, C9A, F15, F16, KC97, T43, or A10. |
| 9-72 | TITLE (2) | Problem identification |
| 74-75 | LRWTP | Traffic type always use RR |
| 80 | SOLTYPE | Solution type<br>A = axisymmetric<br>P = prismatic |

NOTE: A suggested for crater repairs

B. Load Factors and Print Control Card (I2, F4.0, 2(1X,I1), 5X, F10.0, I5)

| Column | Variable | Description |
|---|---|---|
| 1-2 | NUMLAY | Number of materials maximum = 10 |
| 3-6 | PSI | Tire pressure 0 = default value |
| 8 | KPPRE | Print control for APRE output always = 1 |
| 10 | KPPAV | Print control for AFPAV always = 1 |
| 16-25 | WLOAD | Wheel load (lbs) 1 = default value |
| 26-30 | LCONCOP | Tensile strength of concrete |

C. Crater Profile Cards (6F, 10.0)

| | Column | Variable | Description |
|---|---|---|---|
| C1. | 1-10 | XCP(1) | X coordinate of point 1 (inches) |
| | 11-20 | YCP(2) | Y coordinate of point 2 (inches) |
| | 21-30 | XCP(2) | |
| | 31-40 | YCP(2) | |

| | Column | Variable |
|---|---|---|
| | 41-50 | XCP(3) |
| | 51-60 | YCP(3) |
| C2. | 1-10 | XCP(4) |
| | 11-20 | YCP(4) |
| | 21-30 | XCP(5) |
| | 31-40 | YCP(5) |
| | 41-50 | XCP(6) |
| | 51-60 | YCP(6) |

NOTE: Coordinates must begin at bottom of crater and progress vertically to crater edge XCP(1) must always equal 0, YCP(1) corresponds to the depth of the crater, XCP(6) corresponds to the crater radius and YCP(6) always equals 0. All X-coordinates must be positive and all Y-coordinates must be negative.

D. Material Property Cards (F4.0, 1X, A1, I1), F8.0, 1X, F3.2, 5X, F1.0, 5X, F10.3, F5.3, 2X, F3.0, 3I1)

| Column | Variable | Description |
|---|---|---|
| 1-4 | THICK | Material layer thickness (inches) |
| 6 | MATID | Material identification code<br>C = concrete<br>A = asphalt<br>L = crushed limestone<br>M = landing mat<br>F = fallback/pushback<br>P = compacted pushback<br>S = stabilized material<br>N = native material<br>B = base course<br>X = special material |
| 7 | MATCKSR | modulus generation option<br>0 = property (1) is input<br>1 = property (1) is generated from void ratio<br>2 = program default |

| Column | Variable | Description |
|---|---|---|
| 8-15 | PROPTY(1) | Young's modulus (psi) |
| 17-19 | PROPTY(2) | Poisson's ratio<br>0 = default value User value must be greater than 0 but less than 0.48 |
| 25 | STYPE | material type<br>0 = linear elastic material<br>1 = non-plastic with fines, low plasticity<br>2 = high plasticity, LL>50<br>3 = clean sands<br>4 = clean gravels, poorly graded sand/gravel mixtures<br>5 = well graded sand/gravel mixtures |
| 31-40 | WETPEN | wet unit weight (pcf) |
| 41-45 | WATCON | water content (percent) |
| 48-50 | P.I. | plasticity index (percent) |
| 51 | KHARDN | Type of Hardin law (for each element)<br>0 = shear modulus is a function of confining stress and shear strain and used to calculate new stiffness and stress output for each iteration.<br>1 = shear modulus is a function of station pressure and station strain and used to calculate stress output only |

| Column | Variable | Description |
|---|---|---|
| | | 2 = shear modulus is a function of the shear strain only and used for calculation of new stiffness and stress output |
| | | 3 = shear modulus is a function the maximum shear strain and used for calculation of new stiffness. |
| 52 | KGAMMA | shear strain calculation |
| | | 0 = shear strain used in stiffness matrix is the maximum of all station shear strains |
| | | 1 = shear strain used in stiffness matrix is minimum of station shear strain |
| 53 | KCPRESS | Confining Pressure Calculation |
| | | 0 = maximum of station pressures is used to calculate stiffness |
| | | 1 = average of station pressure is used to calculate stiffness pressure is used to calculate stiffness |

NOTE: Confining pressure is negative for compression. Tensile confining pressures (positive) are not permitted in stiffness calculation.

Material layers are input beginning at surface. A minimum thickness of the first five layers are 2", 4", 6", 10", 12" respectively. All layers must be represented by three or more finite element rows. No thickness requirement exists for the last layer (i.e., native material).

The KHARDN options 0, 1 apply to MATCKSR = 1 option only. The purpose of these options is to give loose material additional stiffness via consolidation due to trafficing. For MATID = S, C, A, M, F, X automatically default to linear materials. MATID = L, F, P, B can be linear materials or Hardin's law materials.

| Column | Variable | Description |
|---|---|---|
| 1-3 | TITLE(1) | End of data identification |

Repeat cards A through D for each problem. Only one E card is required per data deck.

AIRCRAFT DEFAULT VALUES

| Aircraft | Wheel Load (lbs) | Tire pressure ($lb/in^2$) |
|---|---|---|
| A10 | 20,600 | 213 |
| B1 | 40,500 | 195 |
| B52 | 67,100 | 285 |
| B57 | 27,700 | 152 |
| B747 | 41,600 | 204 |
| C5 | 30,100 | 115 |
| C9A | 25,800 | 148 |
| C130 | 41,900 | 95 |
| C141 | 37,400 | 180 |
| F4 | 27,000 | 265 |
| F15 | 23,400 | 260 |
| F16 | 15,000 | 275 |
| F105 | 23,400 | 220 |
| F111 | 47,000 | 150 |
| FB111A | 54,000 | 215 |
| KC97 | 44,500 | 180 |
| KC135 | 35,500 | 155 |
| T38 | 5,650 | 250 |
| T43 | 27,000 | 148 |

| | Material | Young's Modulus (psi) | Poisson's Ratio |
|---|---|---|---|
| C | Concrete | 3,000,000 | .15 |
| A | Asphalt | 700,000 | .43 |
| F | Fallback/pushback | 3,000 | .40 |
| P | Compacted pushback | 5,000 | .37 |
| L | Crushed Limestone | 100,000 | .25 |
| S | Stabilized material | 50,000 | .30 |
| M | Landing mat | 100,000 | 0.00 |

| | Material | Young's Modulus (psi) | Poisson's Ratio |
|---|---|---|---|
| N | Native material | 5,000 | .43 |
| B | Base course material | 10,000 | .30 |
| X | Special material | 5,000 | .40 |

If default values are used linear behavior is assumed unless variable "STYPE" is input.

Summary

The structure and the User's Manual for the BDR code was presented in this section. Changes in the code during the project were reflected in the discussion. It is hoped that such a presentation helps new users of the code.

## V. USE OF THE BDR CODE

### Introduction

The purpose of this section is to describe the application of the BDR code. The capabilities of the program are described. A scheme for its use is presented.

### Application

The Bomb Damage Repair Code is a linear finite element computer program. The program contains a heavily automated mesh generation capability that reduces the number of data cards to fourteen or less. The program offers the choice of two types of finite elements: an axisymmetric element or a prismatic element. The program generates the wheel loads due to fourteen different aircraft. Material properties are depicted as isotropic linear elastic or isotropic non-linear based on the work of B. O. Hardin. The program contains default values should the magnitude of wheel loads, tire pressure or material properties not be known to the user.

There are certain limitations in the use of the program. The prismatic elements represent a pavement structure better than a crater. One of the basic assumptions for the prismatic elements it that their properties do not vary in the longitudinal direction. This assumption is not satisfied in the idealization of the crater. Alternate launch and recovery cross sections seem to be well represented by the prismatic

element. Multiwheel aircraft wheel loads are applicable only if prismatic elements are selected.

The axisymmetric elements best represent the crater repairs. Selection of the axisymmetric case implies that the user is using the circular cylindrical coordinate system. The limitation of using these elements is that only single wheel aircraft may be loaded onto the mesh surface. Single wheel loadings are applied to the center of the cylindrical axis. Loading when applied away from cylindrical axis assume that loading is symmetrically applied about the central axis. Multiwheel aircraft can be used with the axisymmetrical elements when they are converted into equivalent single wheel loadings.

The user has the option of making all materials in the subsoil linear elastic if desired. In these cases, the variable NSTEPS in line number BDR 768 should be step equal to 1. If a multistep solution is desired to represent non-linear behavior of the subsoil NSTEPS = 3 should provide sufficient accuracy. By program default only materials with the following identification can be represented by Hardin's equations: compacted push back, crushed limestone, stabilized materials, native materials, and base course materials. The program requires all other materials to be considered as linear.

The program has limitations on the number and thickness of the material layers. The maximum number of materials is 10. The minimum thickness of the first five layers are 2, 4, 6, 10 and 14 inches respectively. Each individual layer should be represented by at least three rows of finite elements. There are no limitations imposed on the bottom layer. To reduce the size of the finite element grid, the total depth of all layers should be less than 144 inches. The thickness requirement is controlled by the variables ZONMIN defined in line BDR 211.

When the program first reads a new set of data cards the specified layer system is generated. The layers extend across the full width of the finite element mesh. If the coordinates of the crater have been input as all zero values, no alteration will be made to this layered system. If the coordinates of the crater are non-zero, e.g., all x-values

positive, and all y-values negative, the program alters the layered system. The program defines the crater profile by a step function. All materials, except for the top layer, that lie outside of the crater profile are changed to the native material. The top layer is unaltered and extends beyond the edge of the crater profile. If more than just the top layer are to be extended beyond the crater boundaries then line BDR 3622 should be changed. The program only allows for one native soil to exist outside the crater. Multi-layer native soil systems can be accomodated with major changes in the program.

The program has three control parameters that have a significant effect on the magnitude of the nodal displacements and element stresses. These parameters are KHARDN, KGAMMA, and KCPRESR. By varying these parameters, output values would change by a factor of nine. The large variance of these values resulted in changes in the use of Hardin's law in the MATDEF subroutine. The discussion below refers to the use of the KHARDN control parameter, after the MATDEF subroutine was changed to conform to a strict application of Hardin's law. The options of the initial version of the code were retained, but documentation to support their use has not been found in the initial literature review.

The KHARDN parameter controls the manner in which the stiffness of an element and stress output is computed. If KHARDN is less than two and MATCKSR = 1 the maximum shear modulus in Hardin's law is adjusted by the square root of the confining pressure. If KHARPN is greater or equal to 2 to maximum shear modulus is not adjusted. If KHARDN = 0 the stress output is computed using the adjust shear modulus and the element strains. If KHARDN = 1 the stress output is computed using the modified shear modulus and the principal shear strains. If KHARDN = 2 the stress output is computed using the element shear strain only. If KHARDN = 3 the stress output is determined using the principal shear stains.

The program gives the user the nodal displacements and element stresses due to one loading of the selected aircraft. The material responses are given for the aircraft applied symmetrically about the center of the crater. It does not give the residual or permanent

deflections. It does not give the accumulative residual displacements due to repeated aircraft loadings. The program considers the static application of the aircraft.

Use of the BDR Program

The finite element program is best used in a three phase scheme. In the first phase the geometry of the problem and the material properties of the native soil, push back material and compacted materials, etc., must be known. The geometry of the problem consists of determining the thicknesses and spatial arrangements of the native soil deposits, configuration of the crater, and runway materials. The second phase consists of selecting the finite element program that best models the field phenomenon. The third phase consists of field verification of the program by monitoring the behavior of the actual structure in the field.

The first phase must involve a soil exploration program at the specific site to be analyzed. Soil exploration itself can be divided into three phases: a reconnaissance phase, an exploration phase, and a testing phase. The reconnaissance phase involves gathering all information available about the site from geologic maps, previous drilling records, previous construction, aerial photograph, and a physical inspection of the site. The exploration phase consists of determining the depth of the soil layers, the extent of a particular soil deposit and mechanically testing the soil in the field. A large variety of equipment and techniques exists for this purpose and one has a choice of auger borings, standard penetration tests, undisturbed sampling, cone penetration, pressure meter testing, and a variety of seismic surveys. The testing phase can either be accomplished by insite testing of the soil or obtaining undistrubed samples and testing the soil in the laboratory to determine the constitutive properties required for input into the finite element program. Additional considerations will have to be given regarding the alteration of soil properties near the crater due to the bomb explosion. The properties of any concrete, bituminous, stabilized soil, fabrics and mats used should also be determined.

The soil and other repair materials have to be tested under conditions that exist in the field and under conditions that represent the drainage

conditions and the loading rate for the particular application. If the crater or runway is to be analyzed for static cases, then static or slow loadings should occur in the laboratory. If dynamic loadings are to be considered then dynamic testing of the soil should also occur. Secant nodulus may be required for materials that do not fall within those representative by Hardin's law.

In the third phase, instrumentation of an actual crater repair or runway should be done to verify the accuracy of the program, selection of the material properties, and the constitutive relations. All work should be inspected as they are completed to verify they are constructed in accordance with the design. Only a limited number of works would require full instrumentation. Instrumentation would include accurate determination of the densities, moisture contents, and layer thicknesses during construction. Samples of these materials should be retained for laboratory analysis. Settlement plates or settlement devices should be installed for measurement of displacements. Pressure cells that have been calibrated in the specific material in which they are placed should be used to record induced and over burdened pressures. Surface deflection should be made before, during and after application of the wheel load.

The BDR computer code can be used to analyze the repair of a cratered runway, an existing pavement, or an alternate launch/recovery surface. The axisymmetric finite element selection models the crater repairs based on a conceptual point of view than does the prismatic finite elements option. The prismatic finite elements best represent materials whose geometry and material properties do not vary in the longitudinal direction. The program gives the user the displacements, stresses and strains that are induced into the subsoil due to the presence of the aircraft. Residual stresses are not reported. The program will provide the best results if the materials to be used for a specific project are tested to provide input data for the program. Field instrumentation should be done to verify the programs computations.

Summary

In this section a discussion of the use of the BDR code has been presented. The axisymmetric elements model a crater repair conceptually

better than the prismatic elements. The use of Hardin's law is restricted to materials for which the law was derived. All other materials must be defined as linear elastic. The use of the KHARDN parameter was discussed.

Experimental documentation should be presented supporting the modification of Hardin's laws. It was suggested that the BDR program will yield its best results if it is used in conjunction with a subsurface exploratory program, a material testing program and monitoring of the engineering work.

## VI. CALCULATIONS USING THE BDR CODE

### Introduction

Initial evaluations of the BDR code were made by comparing the computer outputs with Boussinesq's solution for stresses in an elastic media and Steinbrenner's method of computing settlements of rectangular footings on elastic materials. Such comparison should indicate flaws in the concept and accuracy of the solution schemes. Additional computations were conducted representing the subsoil as an elastic material to indicate the sensitivity of the program to changes in the characteristic length and the number of cosine terms of the prismatic solution option. Parameter studies on crater repair were also done.

### Comparisons with Elastic Solutions

Figure 3 shows surface deflections for a F111 wheel loading for an elastic material 144 inches deep computed by the axisymmetric and prismatic solution scheme. The deflection computed by Steinbrenner's equations are also shown. The agreement between all three solutions appears to be very good.

Figures 4 and 5 show the comparison between the vertical stresses developed beneath the F111 wheel load and the Boussinesq solution for a uniformly loaded circular foundation. Figure 4 shows the axisymmetric computations and Figure 5 shows the prismatic computations. Agreement between the three solutions is acceptable.

Figure 6 and 7 depict the results of the study of the variation of the characteristic length. Figure 7 shows the surface deflections and Figure 6 shows the induced vertical stress beneath the wheel of

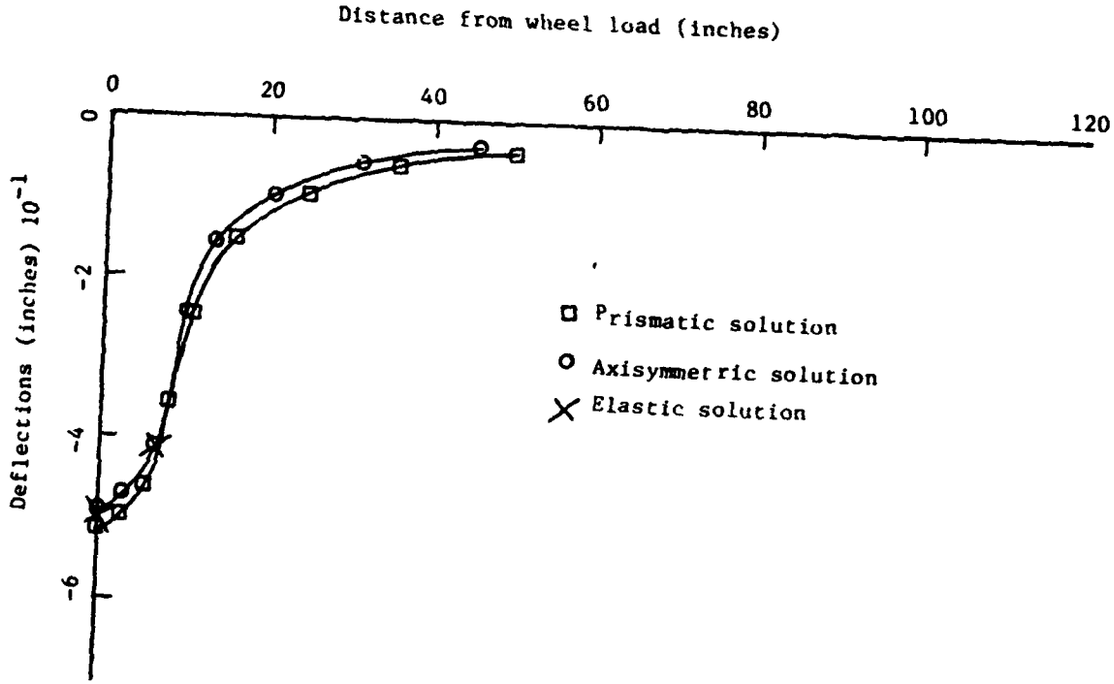



Figure 3. Surface deflection for F 111 on elastic subgrade

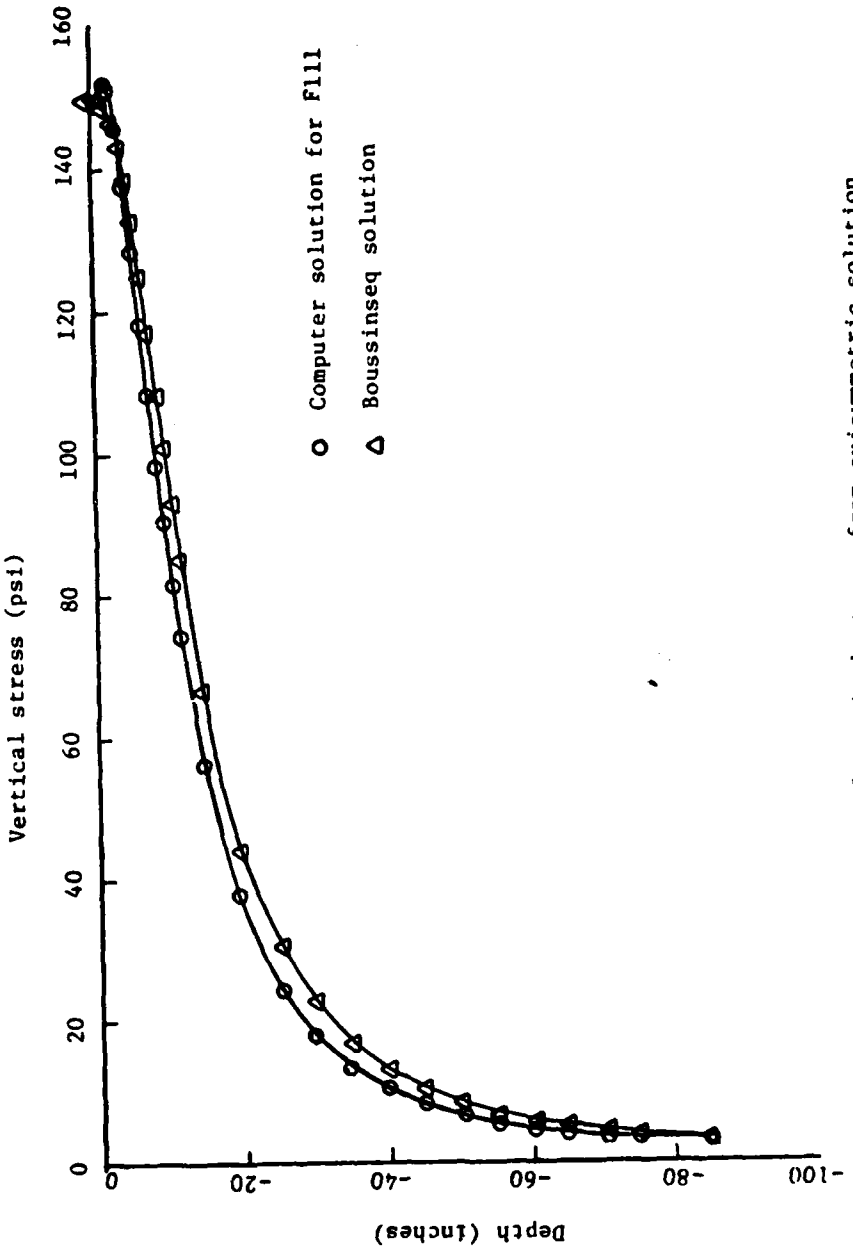



Figure 4. Comparison of vertical stress from axisymmetric solution and Boussinseq equation

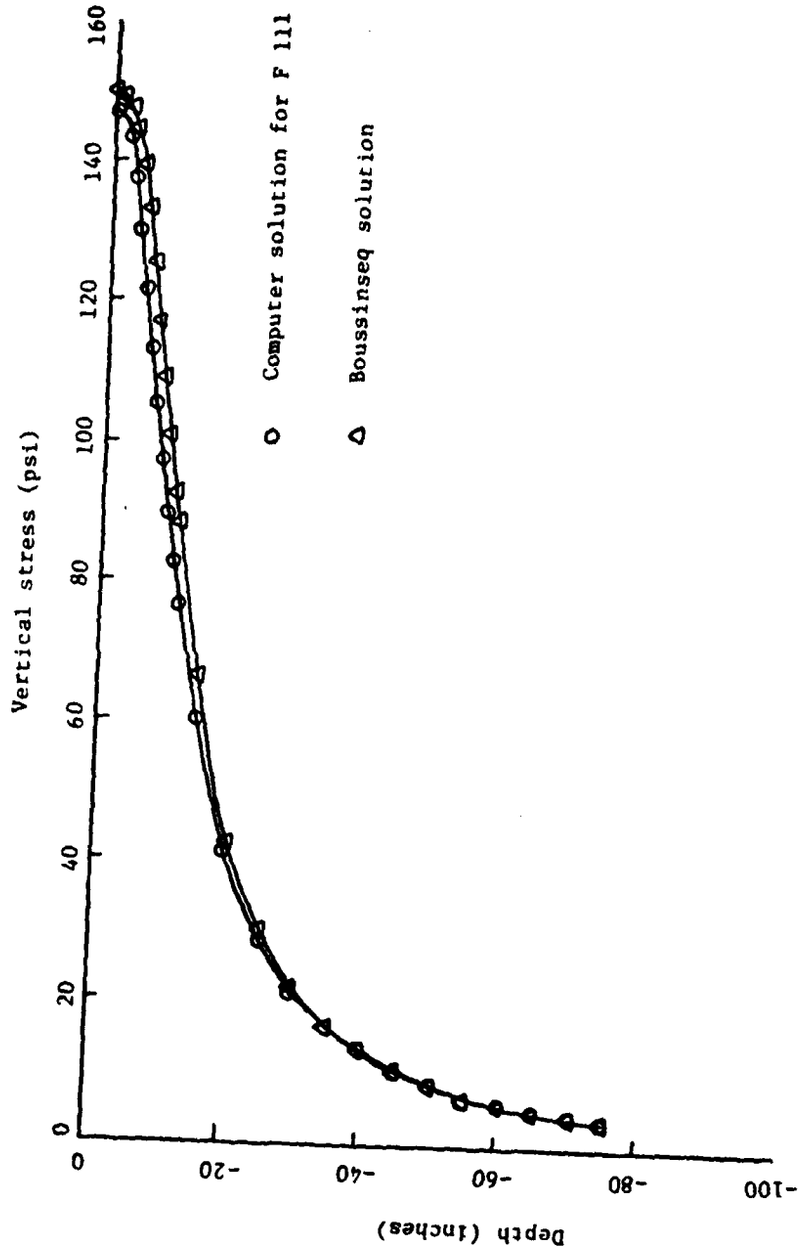



Figure 5. Comparison of vertical stress from prismatic solution and Boussinseq equation

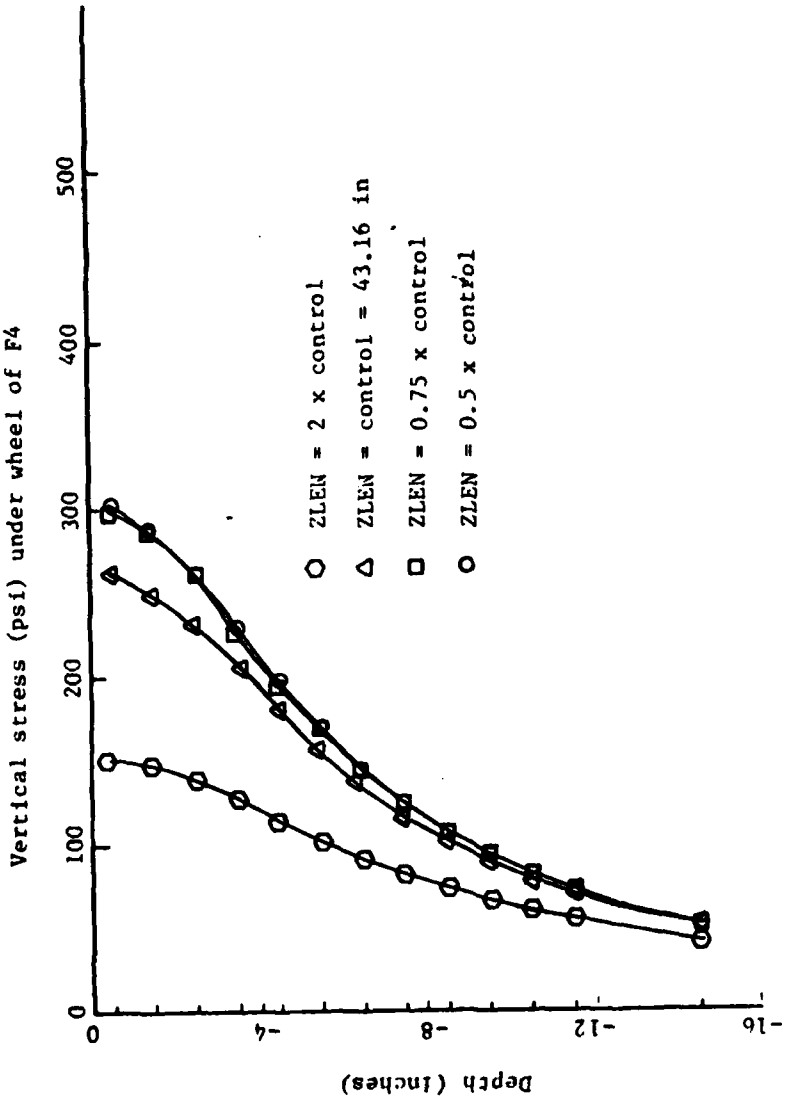



Figure 6. Variation of ZLEN for F4 plane on elastic media - vertical stress versus depth

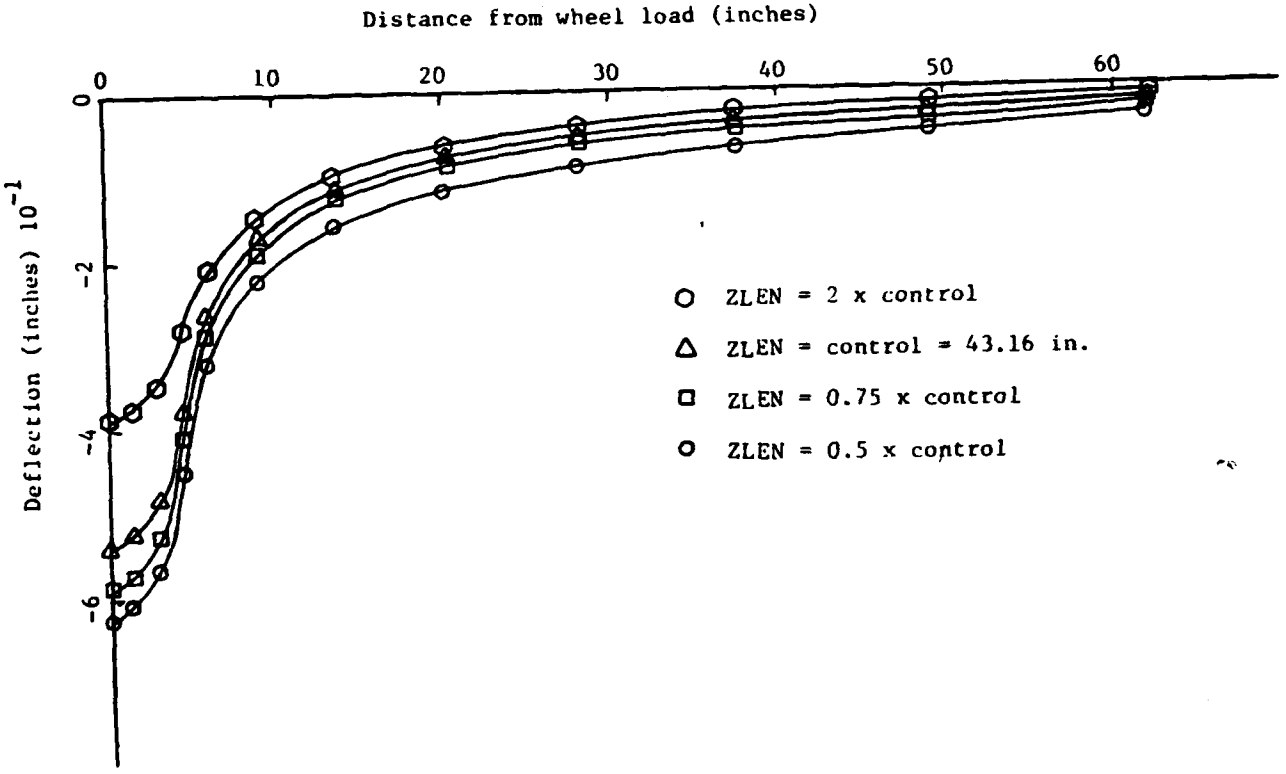



Figure 7. Variation ZLEN for F4 plane on elastic media - surface deflections versus distance from wheel load

an F-4. The characteristic length of 43.16 inches was used as the standard. Increasing the characteristic length by a factor of two resulted in a maximum reduction in vertical soil pressure by 42 percent and a maximum reduction in surface deflections by 27 percent. Decreasing the characteristic length by one half increased the vertical stress by as much as 18 percent and increased the vertical stresses by 15 percent.

Figure 8 and 9 depict the results of the effect of varying the number of cosine terms in the Fourier series for the prismatic solution. As with the previous study, the subsurface was made linearly elastic. The current number of cosine terms used by the BDR code for the F-4 aircraft is five. The results compare favorably with expected values. A reduction of the number of cosine terms to three reduces the surface deflections by 22 percent and the vertical soil pressure by 35 percent. Increasing the number of cosine terms to ten increases the surface deflections and vertical soil pressure by 6 percent and 13 percent respectively.

In conclusion, the number of cosine terms in the Fourier series has a significant effect on the BDR solution. The comparison with Boussinesq solutions indicate that the program runs correctly.

Comparison with Tyndall

A comparison was attempted for the test results determined at Tyndall AFB for a flush crushed limestone repair and the predicted output from the BDR code. The Tyndall tests results gave the deflections at various levels in the fill due to compaction and 1440 coverage of the F-4 loadcart. Deflection of the surface of the repair due to the 1440 coverages was also available. Since the BDR code gives deflections for one loading situation with the load still in place, there was little compatability for a comparison.

A graphic showing the computer predictions for one loading cycle as compared to the total surface deflections are shown in Figure 10. A real aircraft does not cross the same path along the repair in subsequent landings. In fact, the distribution of aircraft loadings is assumed to be distributed in a normal distribution across the runway. The spacing of the load in this fashion accounts for the gradual compression of a well repaired crater.

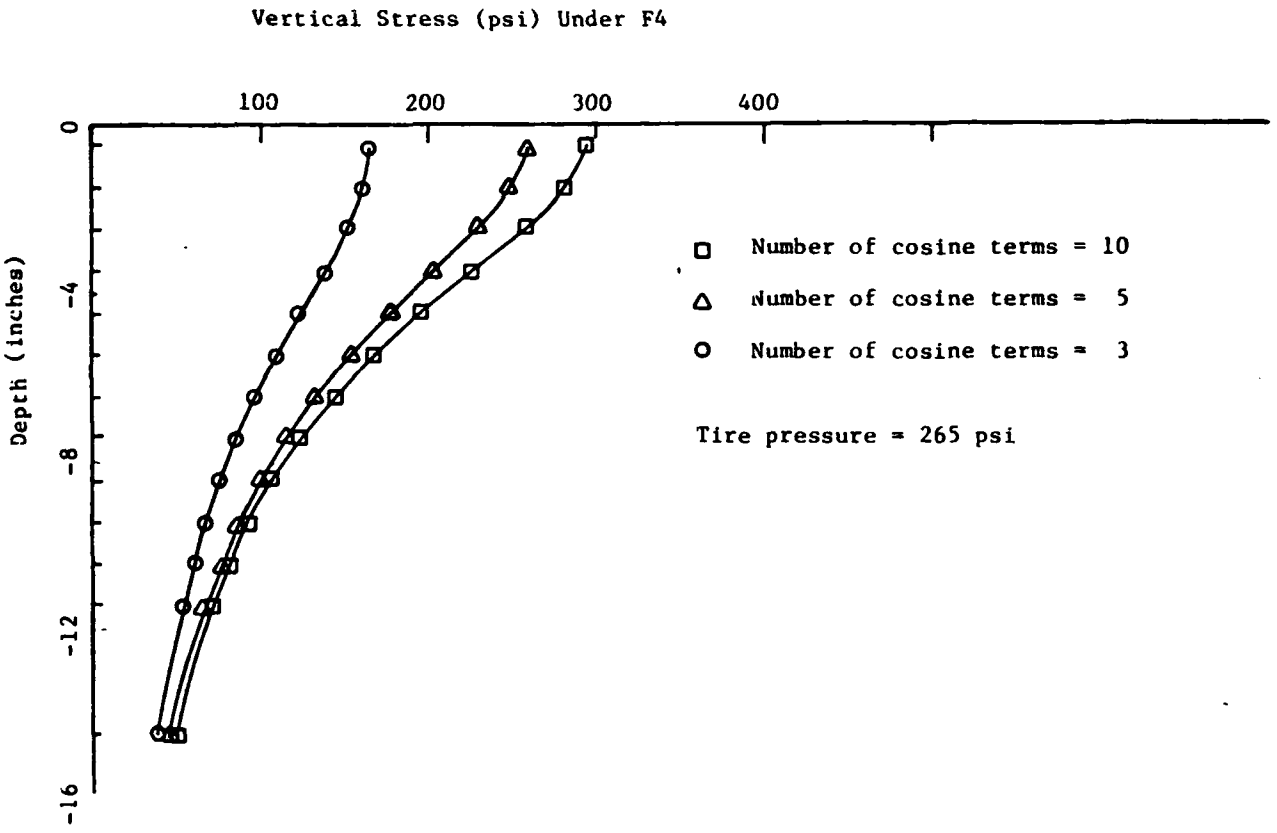



Figure 8. Variation in number of cosine terms for prismatic element solution - vertical stress versus depth

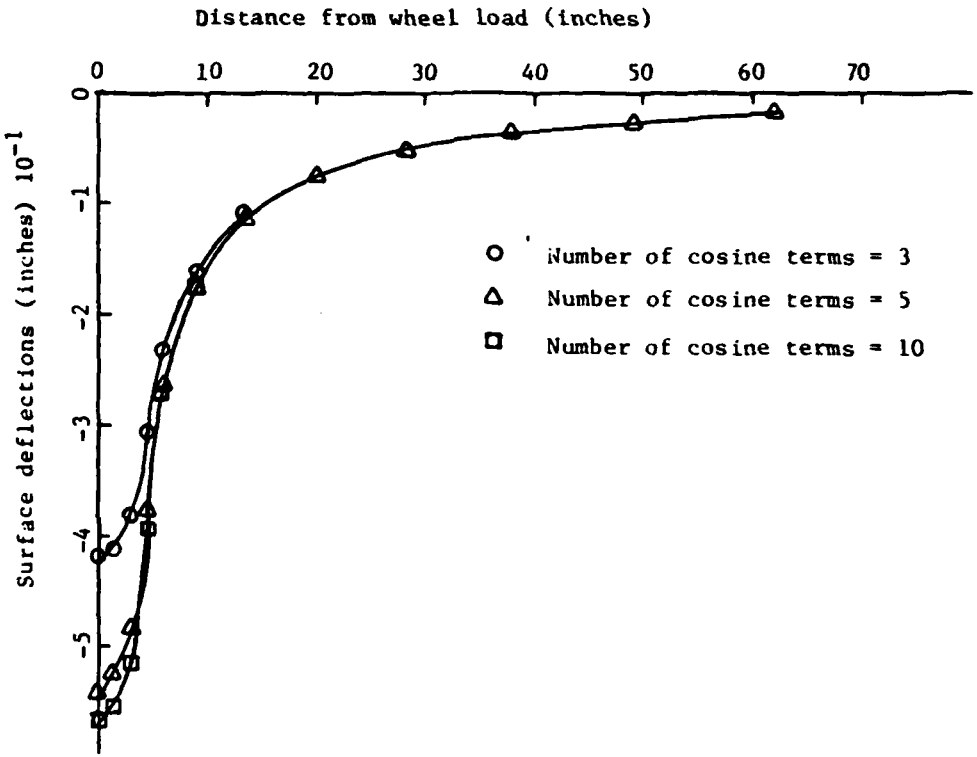



Figure 9. Variation number of cosine terms prismatic element solution - surface deflections versus distance from wheel load

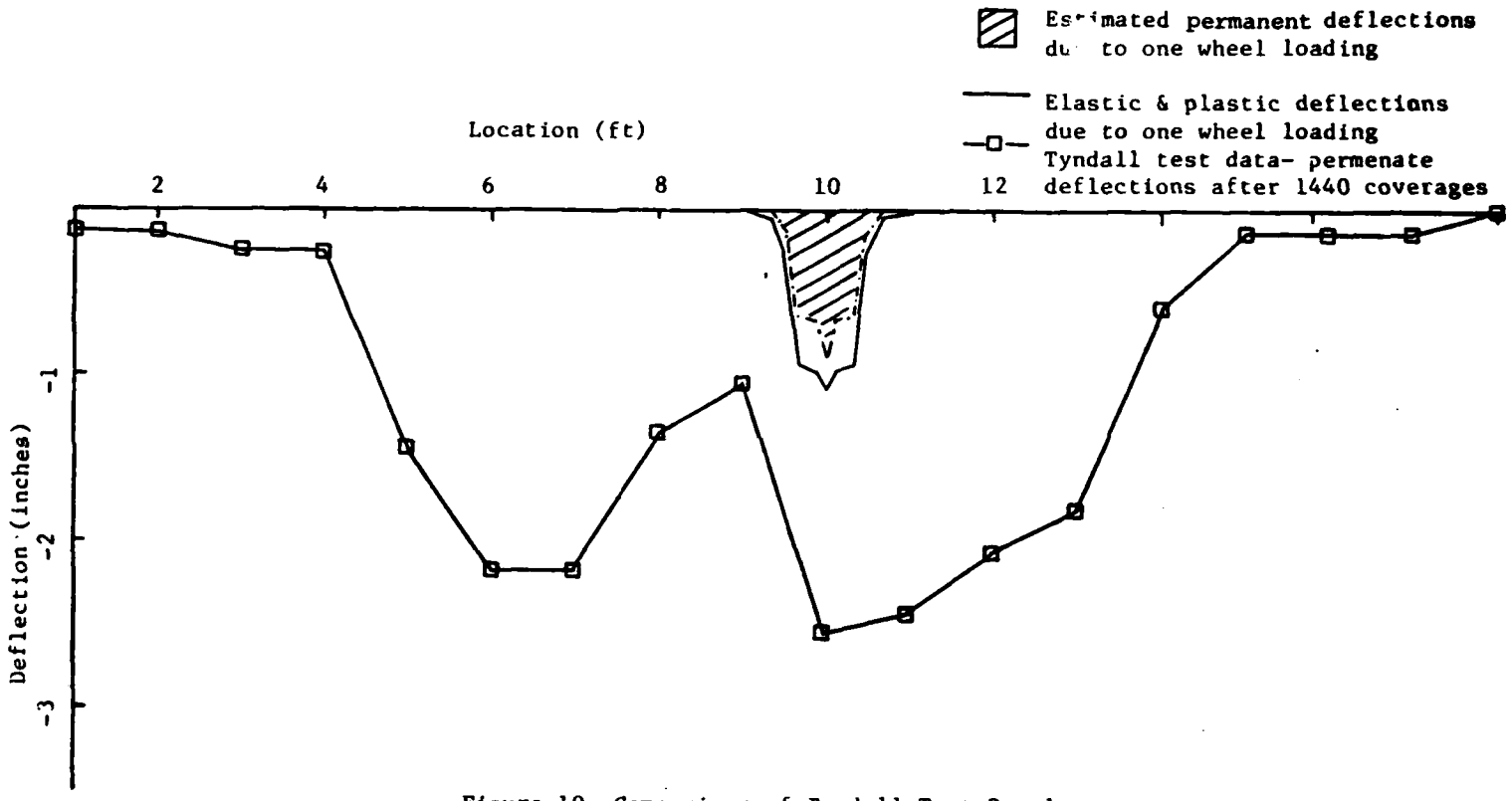



Figure 10. Comparisom of Tyndall Test Results and B.D.R. Code Results for Surface Deflections

In Figure 10 a comparison of the output of the BDR code and the Tyndall test results are shown. The test results consist of the permanent deflections of the repaired crater surface after a total of 1440 passes of a F-4 load cart. The data points were obtained by subtracting the elevation of the surface before and after the coverage were conducted.

The BDR computer output is depicted in two forms. The deflection caused by the wheel is shown by the solid line. Residual deflections were estimated by subtracting the first step using Hardin's soil model from the third step. The comparison of these results illustrates the fact that crater repair problem is an accumulative displacement problem caused by surface rutting by many different applications of an aircraft wheel at a variety of locations. At present the BDR code can give results for a single loading while the wheel load is still applied to the repair.

Parameter Studies

The computer program has the advantage that simulations can be performed without actually having to perform any field construction. The main ingredient for such simulations is that the geometry of the problem will be defined and that the material properties of the engineering work will be defined. The geometry including the dimensions and shapes of the structure is usually well defined. The material properties are well defined for engineering materials as steel and concrete but are not well known for soils. Each soil deposit should be thoroughly tested to determine its constitutive properties.

In the parameter study described below, two ficticious sites were selected. The original runway consisted of 12 inches of concrete and 12 inches of crushed stone overlaying either a hard clay or a medium stiff clay. Young's modulus and Poisson's ratio for the clays were selected from recommended values in Foundation Analyses and Design by J. E. Bowles. The purpose of the parameter study was to compare the increase in static deflections of an F-4 aircraft due to different expedient runway repairs. The cross section of the repaired runway is shown in Figure 11.

The parameter study consisted of varying the thickness of the the compacted crushed limestone and the push back debris from explosion.

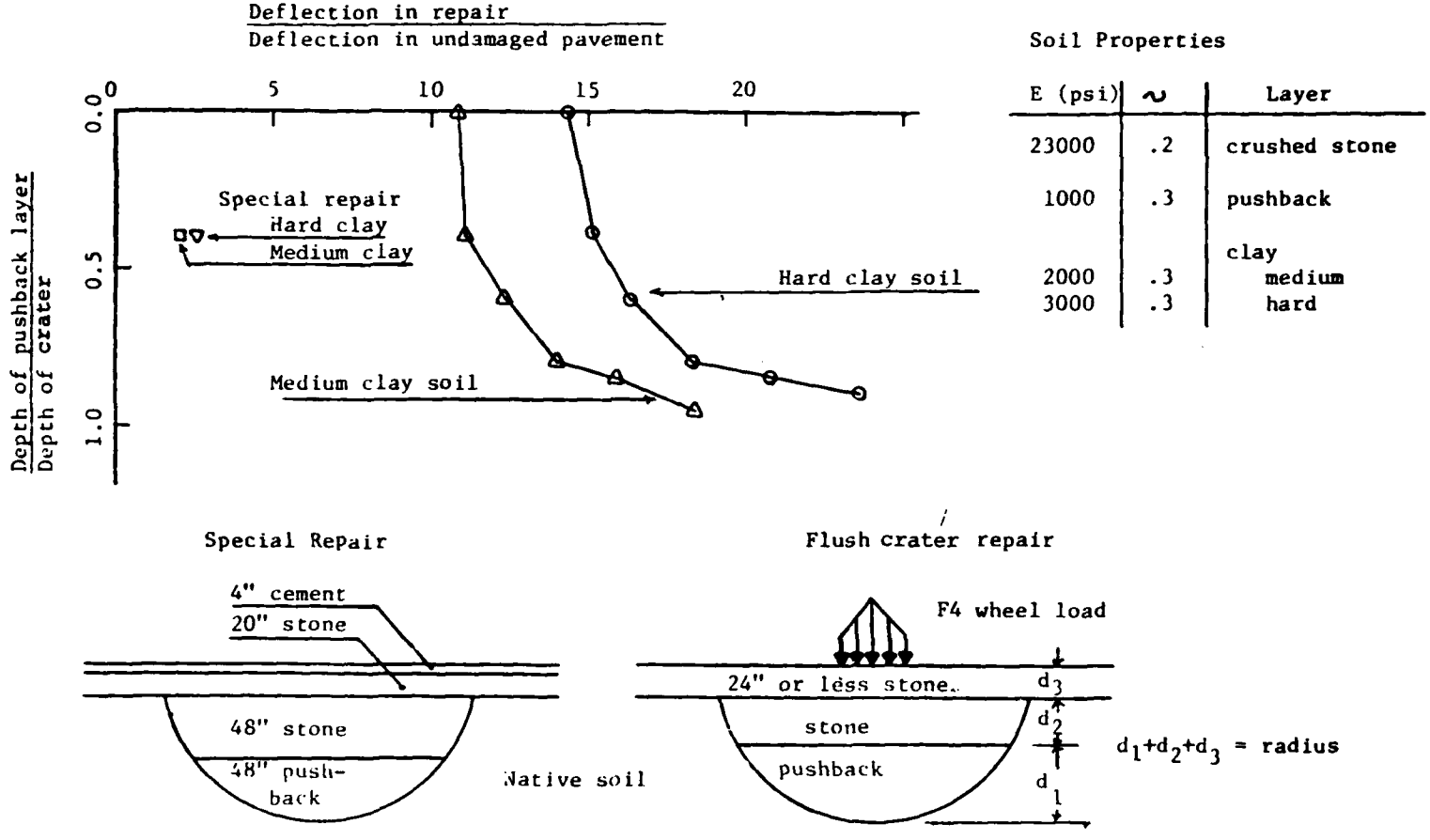


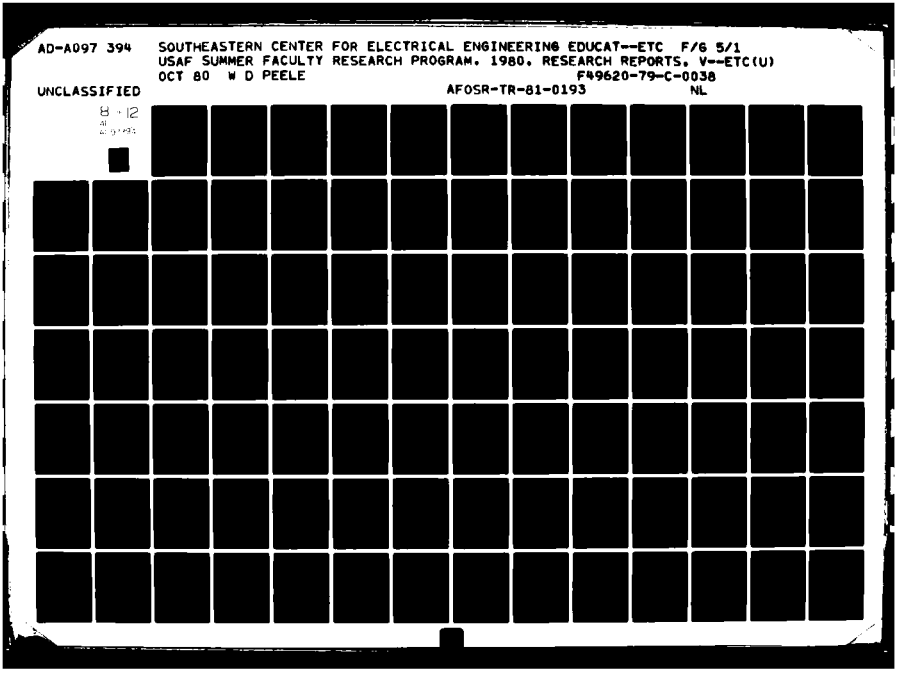

Figure 11. Increase in static deflections for

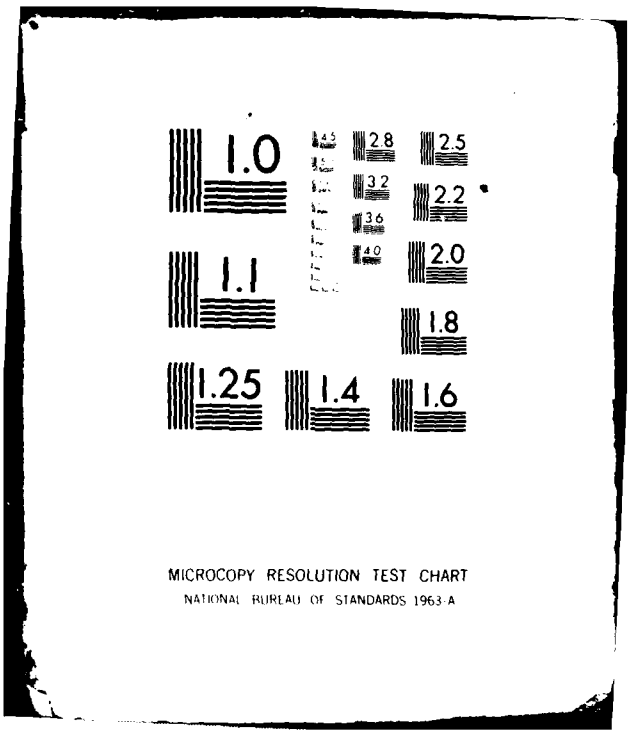
Various types of rapid runway repair

AD-A097 394 SOUTHEASTERN CENTER FOR ELECTRICAL ENGINEERING EDUCAT--ETC F/6 5/1
USAF SUMMER FACULTY RESEARCH PROGRAM, 1980, RESEARCH REPORTS, V--ETC(U)
OCT 80 W D PEELE F49620-79-C-0038

UNCLASSIFIED AFOSR-TR-81-0193 NL

8 - 12
81
DTIC




1.0
2.8
2.5
3.2
2.2
3.6
2.0
4.0
1.1
1.8
1.25
1.4
1.6
MICROCOPY RESOLUTION TEST CHART
NATIONAL BUREAU OF STANDARDS 1963-A

Notationally, we have

$$\delta^m * e(t) = e^m(t)$$

and

$$\delta^m_{\tau(t)} * e(t) = e^m(t-\tau(t))$$

where * denotes the convolution operator and $\delta^m$ denotes the m-th derivative of Dirac delta functiona. Throughout we are assuming that the distribution functions are measureable and have compact support on $[0,\tau]$.

Next, we define the convolution equations.

$$e_1(t) = \sigma * e_2(t)$$

$$e(t) = \ell * e_1(t) = \ell * \sigma * e_2(t)$$

The Laplace transform of the distribution $e_1(t)$ can be represented by a function

$$< e_1, e^{-st} > = \int_{-\infty}^{\infty} e_1(t)\ e^{-st}\, dt$$

It is assumed, however, that the distributions are of the finite order. In other words the distributions throughout have compact support. For details of such distribution function, we refer Schwartz [9]. Our objective here is to provide some background material rather than vigorous derivations. Next, we state a Theorem which establishes the properties of solutions of e(t). This result will be used later in the analysis of closed-loop pilot model.

Theorem 1. The solutions of the equation

$$e(t) = \ell * \sigma * e_2(t) = 0$$

are exponentially stable provided the transcendental polynomial $\ell(s)\sigma(s)$ satisfy the following conditions:

(i) $\text{Re}\,[L(s)\,\sigma(s)|_{\tau(t)=o}] \leq 0$

(ii) $L(w)\,\sigma(w) \neq 0$

Proof of Theorem 1. It is sufficient to show that the real parts of the roots of the transcendental polynomial

$$P(s;\tau(t)) = L(s) \cdot \sigma(s)$$
$$= \left( \sum_{i=o}^{m} a_i (t)\, s^i\, e^{-\tau(t)s} + \sum_{i=o}^{n} b_i (t) s^i \right)$$
$$\cdot (s^2 + 2\, \zeta_{sp}\, w_{sp}\, s + w_{sp}^2)\, (s^2 + 2\, \zeta_{ph}\, w_{ph}\, s + w_{ph}^2) = 0 \qquad (5)$$

are all negative for $\tau(t) \geq 0$. It is obvious that Re $\sigma(s) < 0$ provided $0 \leq \zeta_{sp} \leq w_{sp}$ and $0 \leq \zeta_{ph} \leq w_{ph}$.

To show that the real part of the transcendental polynomial $L(s;\tau(t))$ to be negative, we expand in the form

$$L(s;\tau(t)) = s^n + [a_{n-1}(t)\, e^{-\tau(t)s} + b_{n-1}(t)]\, s^{n-1}$$
$$+ [a_{n-2}(t)\, e^{-\tau(t)s} + b_{n-2}(t)]\, s^{n-2} + \cdots$$
$$+ [a_o(t)\, e^{-\tau(t)s} + b_o(t)] \qquad (6)$$

we have assumed that $m = n - 1$. If m is order less than n-1, we can set the coefficients $a_{n-1}$ etc. zero.

$$L(s;\tau(t)) = s^n + p_{n-1}(t)\, s^{n-1} + p_{n-2}(t)\, s^{n-2} + \cdots + p_o(t) \qquad (7)$$

where

$$p_{n-1}(t) = a_{n-1}(t)\, e^{-\tau(t)s} + b_{n-1}(t)$$
$$p_{n-2}(t) = a_{n-2}(t)\, e^{-\tau(t)s} + b_{n-2}(t)$$
$$\vdots \qquad \vdots \qquad \vdots$$
$$p_o(t) = a_o(t)\, e^{-\tau(t)s} + b_o(t)$$

Since, $|\exp[-\tau(t)s]| \leq 1$ for all $\tau(t) \geq 0$,

hence, when $\tau(t) \geq 0$ and $s \geq 0$, the coefficients $p_i(t)$, i=1,..., n are bounded. Let $\bar{p}$ denote a constant such that $\bar{p} = \max | p_i(t) |$ and let $D = \max [1, (n+1)\bar{p}] > 0$. We will now show that $1 \leq i \leq n$ under the assumptions of Theorem 1, all roots of $L(s;\tau(t))$ lie in the left half plane. To prove this, we consider two cases (i) region when $|s| \geq D$ and (ii) when $|s| < D$. Now suppose $|s| \geq D$, then

$$
\begin{aligned}
| L(s;\tau(t)) | &= | s^n + p_{n-1}(t)\, s^{n-1} + \ldots + p_o(t) | \\
&\geq | s |^n \left[ 1 - \frac{|p_{n-1}(t)|}{|s|} - \ldots - \frac{|p_o(t)|}{|s|^n} \right] \\
&\geq |s|^n \left[ 1 - \frac{n\bar{p}}{(n+1)\bar{p}} \right] > 0 \qquad (9)
\end{aligned}
$$

The last inequality follows from the fact that $|s| \geq D = (n+1)\bar{p} \geq 1$. Thus, in the domain $|s| \geq D$ and Re (s) > 0 the polynomial $L(s;\tau(t))$ possesses no root for any bounded $\tau(t) \geq 0$. Now suppose that $|s| < D$. From condition (i) of Theorem 1 roots of $e(s)\,\sigma(s)$ are all in the semi-plane Re (s) < 0 for $\tau(t) = 0$. Now when $\tau(t) \neq 0$, the only possibility for the characteristic roots to fall within Re(s) > 0 is that for $\tau(t) \neq 0$ the variable s runs along the imaginary axis on the s-plane from -D to D. But the comdition (ii) does not allow the roots to run along the imaginary axis of s-plane and therefore under our assumptions the characteristic roots must remain within the semi-plane Re(s) < 0. This completes the proof.

For the nonlinear model in fig. 2, the description of the system is obtained as

$$\ell * \sigma * e_2(t) + f(t,\ \rho * e_2(t)) = u(t);\ t \geq 0 \qquad (10)$$

To analyze stability of the functional equation (10), we shall construct a Lyapunov functional. The spectral factorization of the entire function plays an important role in the construction of this Lyapunov functional as can be seen later. We heavily depend upon the works of

Levin [4] who has shown that the entire function of exponential type has the spectral factorization. We state these results for our convenience.

Lemma 1. In order that an entire function F(s) of exponential type may be of class A it is necessary and sufficient that for some fixed $w > 0$ and for every $R > w$ the following inequality be valid:

$$\int_{-w}^{R} \frac{|n|\ F(w)\ F(-w)|}{w^2}\ dw < m_{f,\lambda}$$

where $M_{f,\lambda}$ is a constant.

Lemma 2. For an entire function F(s) of exponential type to have the representation

$$F(w) = \emptyset(w)\ \emptyset(-w)$$

Where $\emptyset(w)$ is an entire function of type $\frac{T}{2}$ ( $|\ \tau(t)\ | \leq T$) with zeros in the half-plane Re $s \geq 0$, if and only if F(s) belongs to class A and $F(w) \geq 0$.

We will now introduce our main results to establish asymptotic stability of the nonlinear system (10). The stability of largest invariant set is then derived from the application of the 'invariance principle'.

Theorem 2. Suppose assumptions of Theorem 1 and lemmas 1 and 2 hold, then there exists a Lyapunov functional $V(t,\emptyset)$ of (10) on $G \subset R$.

Theorem 3. Let the set E is defined by

$$E = \{ x_t : \dot{V}(t, x(\cdot)) = 0,\ x_t \in \bar{G} \}$$

and let $V(t, x(\cdot))$ be Lyapunov functional of (10) on G. If the solution $x(t_o, \emptyset_o)(t)$ of (10) is bounded and remains in G for all $t \geq 0$, then $x(t_o,\emptyset_o)(t) \to E$ as $t \to \infty$.

The proof of Theorems 2 and 3 will be completed during the follow-up research.

## V RECOMMENDATIONS

The results presented are concerned with a reasonably realistic model of an important type of control system. The effects of control system dynamics on fighter approach and landing longitudinal flying qualities for highly unstable aircrafts need very careful analysis. It is presumed that a fully-developed pilot-induced oscillations (PIO) will tax the pilot's ability to control it and thereby leave little or no margin for accomplishment of the primary piloting task. Even worse, it may be entirely beyond his control capabilities. In the later case, the only successful recovery technique is for the pilot to remove himself from the control loop either by clamping or releasing the control.

In the present summer research, we have considered the effects of variable lag and variable gain in the pilot model. Such formulation has been justified due to effect of wind shear and the neuromuscular system dynamics according to the available datas.

Another interesting problem of pure transport time-delays such as those associated with digital flight control systems should be treated in further research studies of NT-33 aircraft. Such problems are expected to be infinite-dimensional and I propose to do this by extending the present results of spectral factorization of finite-dimensional problem to infinite dimensional problem. It is expected that the present method can be extended to construct Lyapunov functionals for infinite-dimensional problems.

Part of the sketch of the proofs of summer research and its application to an existing result will be completed during the follow-up research. It is expected that the future course of research will

answer key questions concerning the pilot-induced oscillations of the systems, and provide an analytical basis for using a computer for further studies.

## REFERENCES


1. H. G. Warren and R. P. Harper, Jr., "In-Flight Simulation of the Light Weight Fighters", AIAA Paper No. 75-985, Aug. 1975
2. G. W. Hall, and R. W. Huber, "System Description and Performance Data for the USAF/Calspan Variable Stability T-33 Airplane," AFFDL-TR-70-71, July 1970
3. R. E. Smith, "Effects of Control System Dynamics on Fighter Approach and Landing Longitunal Flying Qualities", Vol. 1, AFFDL-TR-78-122, March 1978
4. B. J. Levin, "Distribution of Zeros of Entire Functions," Vol. 5. Translations of Mathematical Monographs, Rhode Island, American Math Soc., 1964
5. J. K. Hale and K. R. Meyer, "A Class of Functional Equations of Neutral Type" Mem. Amer. Math. Soc. No. 76, 1967
6. J. P. LaSalle, "The Stability of Dynamical Systems" CBMS Regional Conference Series, Mississippi State Univ. Dec. 1975
7. A. S. C. Sinha, "Invariance Principle in Power-System Analysis," 2nd International Symposium on Large Engineering Systems, Univ. of Waterloo, Waterloo, Ontario, May 1978
8. J. Hale, "Functional Differential Equations," Springer-Verlag, New York, 1971
9. L. Schwartz "Theorie des Distributions," Vol. I and II, Paris: Herman, 1966

10. McRuer, D. Graham, E. Krendel, and W. Reisner, Jr., "Human Pilot Dynamics in Compensatory Systems: Theory, Models and Experiments with Controlled Element and Forcing Function Variations", AFFDL-TR-65-15, July 1965

11. R. E. Magaleno, H. R. Jex and W. A. Johnson, "Tracking Quasi-Predictable Displays": Subjective Predictability Gradations Pilot Models for Periodic and Narrowband Inputs", NASA SP-215 Fifth Annual NASA-Univ. Conf. on Mannual Control,1969 pp. 391-428

12. R. H. Smith, "A Theory for Handling Qualities with Applications to MIL-F-8785B", AFFDL-TR-75-119 Oct. 1975

13. A. S. C. Sinha, "Global Asymptotic Stability of Certain Nonlinear Feedback Systems", Proc. IEEE 61, 1506-1507, 1973

1980 USAF - SCEE SUMMER FACULTY RESEARCH PROGRAM

Sponsored by the

AIR FORCE OFFICE OF SCIENTIFIC RESEARCH

Conducted by the

SOUTHEASTERN CENTER FOR ELECTRICAL ENGINEERING EDUCATION

# FINAL REPORT

# A MODEL AND POLDER TENSOR FOR MAGNETOSTATIC WAVE INTERACTIONS WITH METAL STRIPS


| | |
|---|---|
| Prepared by: | Charles V. Smith, Jr. |
| Academic Rank: | Professor |
| Department and University: | Electrical Engineering<br>The University of Texas at Arlington |
| Research Location: | Rome Air Development Center<br>Hanscom AFB, MA 01730 |
| USAF Research Colleague: | Mr. James C. Sethares |
| Date: | 21 September 1980 |
| Contract No.: | F49620-79-C-0038 |

# A MODEL AND POLDER TENSOR FOR MAGNETOSTATIC WAVE INTERACTIONS WITH METAL STRIPS

by

Charles V. Smith, Jr.

## ABSTRACT

A novel technology for microwave (1-20 GHz) signal processing based on magnetostatic wave propagation in epitaxial Yttrium Iron Garnet films and utilizing the concept of transversal filtering has been developing during the past four years. The continued development of this technology is strongly dependent on the generation of more sophisticated models for prediction of the interaction of magnetostatic waves with various individual elements of a transducer or reflecting array which forms the transversal filter. This work presents a proposed method for the formulation of a boundary value problem for metal strips which may be utilized in the calculation of reflection and transmission factor of various elements in a given device model and a derivation of a generalized Polder Tensor for application in such calculations. Recommendations are made for the further continuation of this work.

## ACKNOWLEDGMENTS

The author wishes to thank the Air Force Office of Scientific Research, the Air Force Systems Command, and Southeastern Center for Electrical Engineering Education for the appointment as a Summer Faculty Research Program Research Associate and SCEEE Fellow. The Rome Air Development Center personnel, in particular, Mr. J. C. Sethares, Dr. L. V. Taylor, Mr. M. Stiglitz and Dr. P. Carr, as well as all Hanscom AFB personnel made this a most enjoyable productive summer research experience for me and I convey to them warmest thanks for their support.

## I. INTRODUCTION

A need exists for a microwave (1-20GHz) analog signal processing technology with processing capabilities complementary to those developed in the past ten years with surface acoustic waves at VHF/UHF frequencies. In particular, tunable, narrow bandpass filters and wide band tunable matched filters and dispersive nondispersive delay lines can find significant applications in military microwave systems. A new technology, with the potential to realize these requirements, has been developing over the past four years. This technology is based on magnetostatic wave (MSW) propagation in epitaxial Yttrium Iron Garnet (YIG) and utilizes the concept of transversal filtering which has been so effectively applied in Surface Acoustic Wave (SAW) devices.

Surface acoustic wave (SAW) devices, which perform very effectively in the VHF/UHF range as sophisticated analog signal processors, have significant problems as the operating frequency is increased above 1GHz. For a material such as quartz the attenuation can be in excess of 100dB/μsec at 10GHz and the wavelength is of the order of 0.1μm making SAW devices in this frequency range of very limited usefulness and exceedingly difficult to fabricate. Bulk acoustic delay lines work well in this frequency range; however, complex signal processing is not practical since the signal cannot be easily accessed during propagation as in SAW.[1]

Magnetostatic Waves (MSW) are slow, dispersive, magnetically dominated electromagnetic waves which propagate in magnetically biased ferrite materials at microwave frequencies (typically 1-20GHz in Yttrium iron garnet).[2] Essential to recent development of MSW devices has been development of low linewidth loss, high quality Yttrium iron garnet (YIG) ($Y_3Fe_5O_{12}$) grown on gadolinium gallium garnet (GGG) substrates as epitaxial films. The growth technology utilized is a result of magnetic bubble domain research and is highly developed.[3] Such films offer lower MSW propagation loss than SAW on Lithium Niobate at 3GHz and less than 12db/μsec at 10GHz.

MSW propagation in a free ferrite slab has been extensively considered, including the effect of ground planes in close proximity.[1]

Several propagation modes are possible, two of which are of particular interest for device applications. First, the magnetostatic surface wave (MSSW), in which the bias field $\bar{H}$ is perpendicular to the direction of wave propagation and in the plane of the film. For this wave the propagation is highly anisotropic in the film plane and the energy is confined near one surface of the film depending on the direction of propagation. Second, the magnetostatic forward volume mode (MSFVW) characterized by the fact that the bias field is perpendicular to the plane of the ferrite slab. The wave has approximately isotropic propagation characteristic in the plane of the slab volume with energy distributions resembling those found in rectangular pipe waveguides. The lowest order distribution dominates and is easily excited. Both MSSW and MSFVW modes are tunable by bias field adjustment and in principle, any wavelength can be obtained at any frequency. Thus, a filter designed to work at a specific wave length can be made to work at any frequency for which a bias field can be provided and the ferrite saturated. Typically, group velocities are in the range 3-300 km/sec and wave numbers in the range $10\text{-}10^3$ $cm^{-1}$; thus, transducer and periodic structure dimensions permit easy fabrication by standard photolithographic, microelectronic techniques. Propagation delays of several hundred nanoseconds per cm are typical of these devices.

## II. OBJECTIVES

The continued development of MSW devices for microwave signal processing by nonrecursive transversal filtering is strongly dependent on the generation of more sophisticated models for prediction of the interaction of the MSW with various individual elements in a transducer or reflecting array. To date, the basic modeling approach has been to suitably interconnect or cascade equivalent transmission line models of the various elements within a device to obtain a model to predict the overall device performance such as is done in SAW work.[4] Such an approach is still valid and may also be developed to produce synthesis procedures; however, the validity of this modeling is limited in no small way by the requirement to define the equivalent elements of the transmission line model. The initial MSW device work has

applied various approaches of limited validity and sophistication for the determination of the required model parameters. The initial results for simple device considerations were most encouraging; however, recent experimental results indicate a need to further upgrade parameter determinations so the model predictions have sufficient accuracy for development of MSW devices beyond feasibility demonstration toward usuable protype microwave system devices.

One candidate for use as an element in an array or transducer which is presently receiving a great deal of attention is a conducting metal strip which is placed either directly on or dielectrically spaced from the surface of the ferrite film (usually YIG) which acts as a propagation structure for the MSW. Such metal strips have a number of significant advantages for use as elements in MSW device fabrication. For example, the forming and placement of such strips is a well developed art in microelectronics fabrication technology; further, the ability to modify individual element currents by the simple procedures of variation of end interconnections and electrical loads gives rise to a wide selection of possible elements for device applications.

It is the objective of this present work to formulate a model and begin its solution as far as possible during the allotted research period. As part of this effort a generalization of the Polder Tensor will be made.

## III. DISCUSSION OF APPROACH

In order to more accurately predict the interaction of these metal strips with the MSW waves, a general boundary value problem or a group of such problems must be formulated and solved. The basic geometry of the situation for a single strip is shown schematically in the section of figure 1. This schematic is applicable

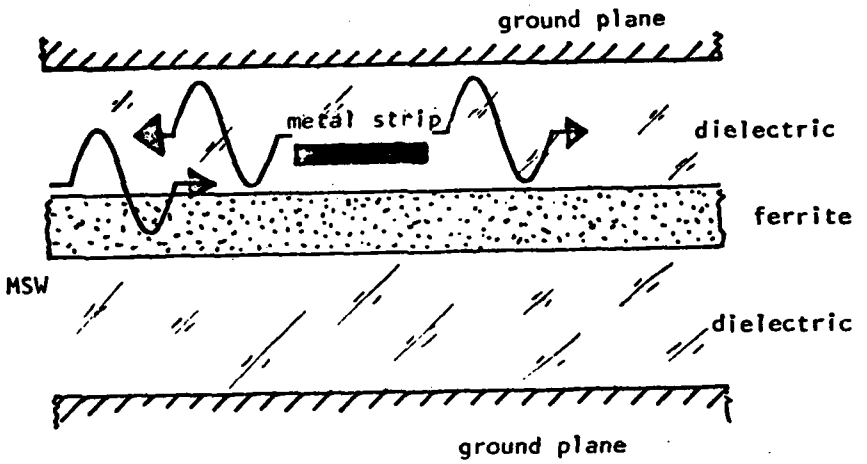



Figure 1 A schematic section of a metal strip element in s MSW device.

for both oblique and normal incidence elements and assumes the transverse aspect ratio of the ferrite film propagation medium is sufficiently large so edge effects may be neglected (films of this size are routinely grown in the laboratory). The finite thickness of the metal strip is an important parameter in determination of the coupling and loss associated with an element; unfortunately, this aspect of the geometry greatly complicates any proposed boundary value problem modeling by introducing a number of "sharp" edges as well as multiple regions. In order to have a more tractable model it is proposed to treat the strip as two edges separated by a transmission region and to retain the finite strip thickness only for the transmission region. The solution for this transmission region model has been achieved for some limiting cases and needs only to generalized to be applied in the proposed manner. For the edges, it is necessary to determine transmission and reflection factors for MSW incident from both sides (i.e., strip and nonstrip). This must be done for both normal and oblique incidence. This modeling assumes that the edges of the strip act as independent reflectors; one desirable prediction from the boundary value problem would be the limit on the equivalent strip width in the propagation direction for this assumption to apply. By focusing attention on the interaction of the MSW with the strip edges and neglecting the finite strip thickness a boundary value problem geometry consisting of six effective regions and only one "sharp" edge may be treated as shown in figure 2. With these assumptions and choice of boundary value problem geometry, the parameter determination is

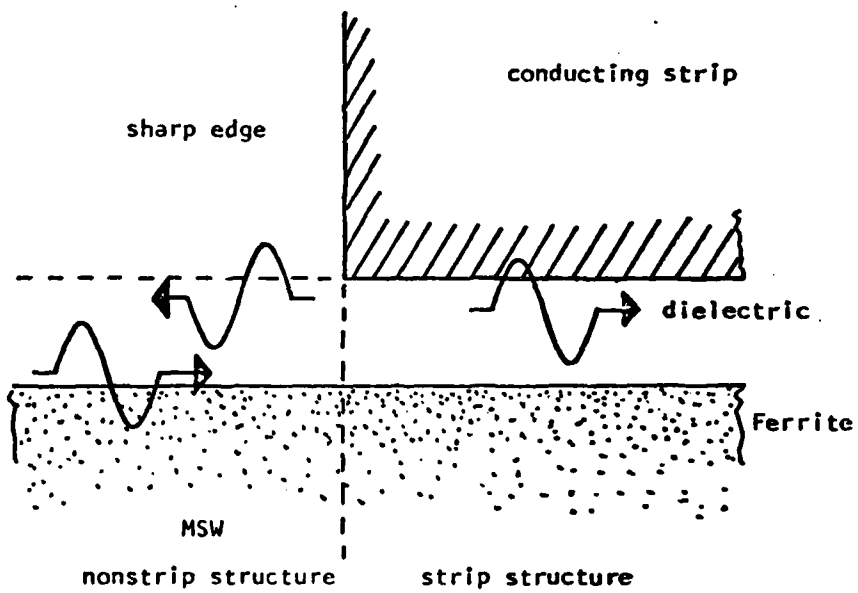



Figure 2. Boundary value problem geometry for the calculation of transmission and reflection factors at a metal strip edge.

reduced to application of a straight forward but somewhat lengthy and complex mathematical procedure.[5,6] Basically, the transverse variation and propagation structures must be determined. From these fundamental modes in the two propagation structures a common set of normal modes must be constructed. Next the desired reflection-transmission problem is set up by picking an incident MSW and writing the general solutions for transmitted and reflected waves in terms of the normal mode set. The application of the boundary conditions to be satisfied by the MSW fields at the interface of the nonstrip and strip propagation structures leads to an infinite set of linear simultaneous equations which relate the mode amplitudes of the transmitted, reflected and incident wave. The solution of this infinite set is uniquely determined if an edge condition is applied to the set. For this problem, the edge condition is essentially the energy of MSW field in the vicinity of the edge remains finite. In principle, this procedure yields a unique solution for the model amplitudes of the transmitted and reflected waves in terms of the incident wave amplitude. With these values in hand it is a straight forward step to calculate transmission and reflection factors; there are a number of formats which could be utilized at this juncture. It is not known at this time if this proposed boundary value problem leads to an infinite set of modal amplitude equations which have an exact analytic solution. An analytic solution is desirable from a number of points of view; however, if such a solution is not possible then either approximate methods such as trunction or iteration may be applied to achieve results of sufficient accuracy for model parameter determination. The truncation solution would, at this time, appear to be the most desirable approximation method; particularly, since a clever choice of the set of normal modes might allow the modeling accuracy to be achieved with only a few modes.

## IV. GUIDED MSW PROPAGATION - THE GENERALIZED POLDER TENSOR

The development of the general magnetostatic equations for a ferrite medium has been considered in detail in various texts.[7,8,9,10,11,12] The usual magnetic equations of Ampere's law, the solenoid law and the constituent relation (in MKS units) are coupled with a magnetic spin

$$curl\ \bar{H} = 0 \qquad (1)$$

$$div\ \bar{B} = 0 \tag{2}$$

$$\bar{B} = \mu_0(\bar{H} + \bar{M}) \tag{3}$$

equation of motion in terms of the magnetization where $\gamma$ = 2.8 GHz/kOe

$$(d\bar{M}_T/dt) = -\gamma \bar{M}_T \times \bar{H}_T + \alpha(\bar{M}_T/M_T) \times (d\bar{M}_T/dt) \tag{4}$$

is the gyromagnetic ratio and $\alpha$ is a Gilbert damping factor. For the remaining regions in the layered propagation the usual Maxwell equations will be used along with an assumption of a linear isotropic media. Since interest is limited to exploitation of this propagation for microwave communications devices, a "small signal" linear operation is desirable. In such a model the magnetization is eliminated by introduction of a Polder or a complex permeability tensor relating small signal complex amplitudes.

The Polder tensor, in the form presently available in the literature, was first developed by D. Polder in 1949.[13] In developing such a tensor, the basic idea is to eliminate the material variables such as the magnetization from the model and focus attention on the electromagnetic quantities. This procedure produces a tensor constituent relation between the small signal complex amplitudes representing the magnetic induction $\bar{b}$ and intensity $\bar{h}$; the components of this relating tensor are then identified as the desired complex permeability or Polder tensor.

In the analysis of the electromagnetic models for these MSW devices two problems arise whish provide motivation for this generalization of the Polder tensor. First, for MSW propagation in planar slabs different orientations of the bias field relative to the film or slab normal and the propagation direction correspond to different modes of propagation with technically exploitable properties which are significant in their differences. To date the use of Polder's original formulation requires each of these modes to be treated by separate analysis. The generalized Polder tensor presented in this work promotes a single analysis in which the film normal and propagation direction are set and the various modes of

of interest achieved by suitable specification of the bias field orientation. A further benefit is the possibility of studying general bias field orientation MSW propagation characteristics. The second problem presently under consideration is the fact that the bias field most likely will not be exactly aligned producing various beam steering effects[14] in MSW devices. Such steering may be detrimental or helpful in any particular situation; however, the presented generalized Polder tensor will allow analysis of such effects following the method of Addison, Auld and Wilkinson.[15]

The dynamics of the magnetic spins in the ferrite is usually modeled in a phenomenological way as there is no complete understanding of the various physical mechanism underlying such factors as damping. Various models are discussed by Lax and Button.[8] The equation of motion to be used in this present work is a modified form of the Landau-Lifshitz phenomenological model due to Gilbert. For electron spins the Gilbert equation of motion is given by equation (4) where $\bar{M}_T$ is the total magnetization, $\bar{H}_T$ is the total local magnetic intensity. For ferrites with low propagation loss $\alpha$ must, in some sense, be small and the damping could be considered as a perturbation type effect.

Application of electromagnetic wave propagation in thin ferrite films to a realization of microwave communications devices for analog signal processing generally requires linear system behavior; thus, it is important to consider a small signal theory of device performance. Since the nonlinearities occur only in the mechanical equation of motion only this equation need to be linearized to obtain small signal equations. Assuming exp ($j\omega t$) dependence for "small" signal quantities equation (4) yields

$$j\omega \bar{m} = -\gamma \bar{M} \times \bar{h} - \gamma \bar{m} \times \bar{H} + j\omega\alpha(\bar{M}/M) \times \bar{m} \quad (5)$$

where $\omega$ us the radian frequency, upper case variables are equilibrium quantities and lover case variables are corresponding complex amplitudes of the small signal quantities. Equation (2) may be further consolidated by noting that $\bar{M}$ and $\bar{H}$ must be parallel (if anisotropy is neglected) and writing

$$j\omega \bar{m} = -\omega_M \bar{\nu} \times \bar{h} + \omega_R \bar{\nu} \times \bar{m} \quad (6)$$

where $\bar{\nu}$ is a unit vector in the direction of $\bar{M}$ and $\bar{H}$, $\omega_M = \gamma M$, $\omega_o = \gamma H$

and $\omega_R = \omega_o + j\omega\alpha$.

In the derivation of the generalized Polder tensor the magnetization $\bar{m}$, which represents a material quantity, is eliminated from the electromagnetic constituent relation by use of the equation of motion. There are various forms of the electromagnetic constituent relation; for example the SI system or rationalized MKSA system where

$$\bar{b} = \mu_o(\bar{h} + \bar{m}) \tag{7}$$

The Gaussian system or unrationalized CGS system where

$$\bar{b} = \bar{h} + 4\pi\bar{m} \tag{8}$$

and the Heaviside-Lorentz system or rationalized CGS system where

$$\bar{b} = \bar{h} + \bar{m} \tag{9}$$

These are the most widely utilized forms; however, there are a number of other forms which occur in the existing literature. For this work the SI or rationalized MKSA system will be used.

On examination it is seen that equation (6) may be considered to represent a system of three linear algebraic equations in terms of a suitable set of components of $\bar{m}$ as the three unknowns. The solution of this system for the components of $\bar{m}$ as functions of the components of $\bar{h}$ permits an identification of the components of the complex susceptibility tensor $\bar{\bar{X}}$ where

$$\bar{m} = \bar{\bar{X}} \cdot \bar{h} \tag{10}$$

With this result in hand a simple substitution obtains the Polder tensor as

$$\bar{\bar{\mu}} = \mu_o(\bar{\bar{I}} + \bar{\bar{X}}) \tag{11}$$

where $\bar{\bar{I}}$ is an identity tensor and $\mu o = 4\pi\ (10^{-7})$ hy/m is the free space permeability.

To effect this solution in a general orthogonal coordinate system the linearized spin equation of motion is written in terms of components using index notation (16); this gives

$$j\omega m^p = \epsilon^{pqn}\, \nu_q\, (\omega_R\, m_n - \omega_M\, h_n) \tag{12}$$

where it is to be noted that indices are Roman lower case super or subscripts and upper case subscripts are not indices but simply identifiers. Consider arranging the solution into the form

$$m^p = X^p_g \, h^g \tag{13}$$

so the complex susceptability $X^p_g$ may be determined. Recalling the relationship between associated tensors and using in equation (12) gives

$$(\jmath\omega\delta^p_s - \omega_R \epsilon^{pgr} \nu_g g_{rs}) m^s = -\omega_M \epsilon^{pgr} \nu_g g_{rt} h^t \tag{14}$$

where $\delta^p_s$ is a Kronecher delta, $g_{ij}$ are components of the metric tensor for the coordinate system and $\epsilon^{ijk}$ are components of the permutation tensor. For linear the algebraic system

$$a^p_s x^s = b^p \tag{15}$$

the cofactor of $a^r_i$ is

$$A^i_r = (\epsilon^{ijk} \epsilon_{rst} a^s_j a^t_k)/2 \tag{16}$$

and

$$a^m_r A^i_m = A \delta^i_r \tag{17}$$

where A is the determinant of $a^r_i$ (i.e., $A = \det(a^r_i) = |a^r_i|$ Assuming $a^r_i$ is nonsingular and solving yields

$$x^k = (A^k_p b^p)/A \tag{18}$$

Clearly, $(A^k_p/A)$ is the tensor relating the vector $b^p$ to the vector $x^k$. Applying these ideas to the present system, identify

$$a^r_i = \jmath\omega\delta^r_i - \omega_R \epsilon^{ruv} \nu_u g_{vi} \tag{19}$$

and calculate

$$A^i_r = [(\jmath\omega)^2 \delta^i_r + \jmath\omega\omega_R \epsilon^{imn} \nu_m g_{nr} + (\omega_R)^2 \nu_r \nu^i] \tag{20}$$

and

$$A = \jmath\omega[(\omega_R)^2 - \omega^2] \tag{21}$$

With these quantities the complex magnetic susceptability $X^i_j$ can be written as

$$X^i_j = (-\omega_M A^i_p \epsilon^{pqr} \nu_q g_{rj}) / A \qquad (22)$$

and performing the indicated operations obtains

$$X^i_j = [\omega_M \omega_R (\delta^i_j - \nu_j \nu^i) - j\omega\omega_M \epsilon^{iqr} \nu_q g_{rj}] / [(\omega_R)^2 - \omega^2] \qquad (23)$$

For SI units (i.e., rationalized MKSQ units) the Polder tensor is

$$\mu^i_j = \mu_0 \{[(\omega_R)^2 + \omega_M \omega_R - \omega^2] \delta^i_j - \omega_M \omega_R \nu_j \nu^i - j\omega\omega_M \epsilon^{iqr} \nu_q g_{rj}\} / (\omega_R^2 - \omega^2) \qquad (24)$$

This result is valid for any curvilinear coordinate system and represents the components of the Polder tensor as a mixed tensor of second rank.

## V. PHYSICAL COMPONENTS FOR SPECIAL CASES

Since it is known that the electromagnetic theory equations lead to the Helmholtz equation which is simply separable only in some orthogonal curvilinear coordinates, it is useful to restrict the remainder of these considerations to such coordinates and the corresponding physical components of $\mu^i_j$. Further, most technical research effort is presently focused on exploitation of LPE-YIG for microwave signal processing so rectangular Cartesian coordinates are of particular significance. In this section explicit expressions for the Polder tensor physical components are given for three cases; general orthogonal curvilinear coordinates, rectangular Cartesian with $\bar{\nu}$ along the z-axis (i.e., Polder's case) and rectangular Cartesian with $\bar{\nu}$ in an arbitrary direction. For this work the lower case Greek letter as shown in figure 3 $\alpha$, $\beta$, $\gamma$ will represent the physical components corresponding respectively to the curvilinear indices 1, 2, 3. From equation (24) the physical components in a general orthogonal curvilinear coordinate system are found to be

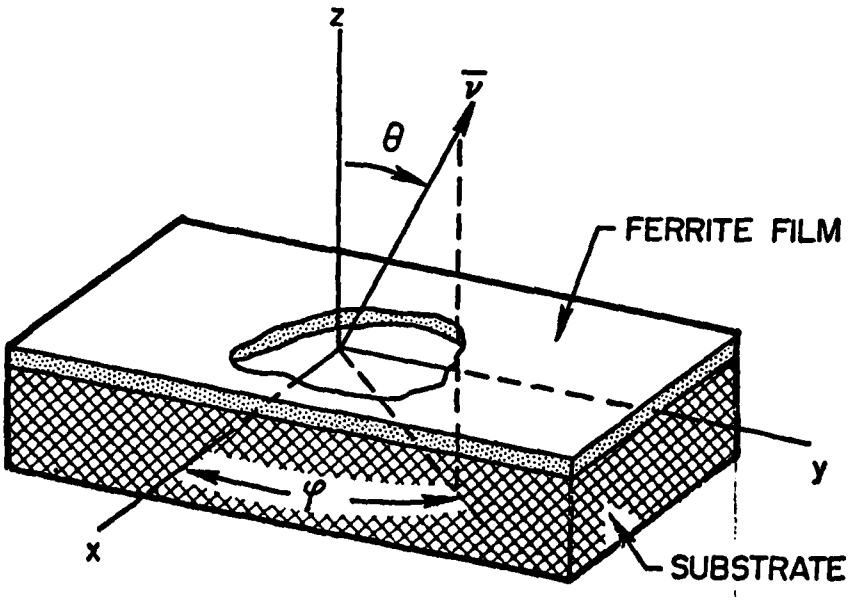



Figure 3 - A schematic representation showing an arbitrary orientation of the unit vector $\bar{\nu}$ along the bias direction relative to a YIG film.

$$\mu_{\alpha\alpha} = \mu_0 \left[ \omega_R^2 + (1-\nu_\alpha^2)\omega_M\omega_R - \omega^2 \right]/(\omega_R^2-\omega^2)$$

$$\mu_{\alpha\beta} = \mu_0 \left[ -\omega_M\omega_R\nu_\alpha\nu_\beta + j\omega\omega_M\nu_\gamma \right]/(\omega_R^2-\omega^2)$$

$$\mu_{\alpha\gamma} = \mu_0 \left[ -\omega_M\omega_R\nu_\alpha\nu_\gamma - j\omega\omega_M\nu_\beta \right]/(\omega_R^2-\omega^2)$$

$$\mu_{\beta\alpha} = \mu_0 \left[ -\omega_M\omega_R\nu_\alpha\nu_\beta - j\omega\omega_M\nu_\gamma \right]/(\omega_R^2-\omega^2)$$

$$\mu_{\beta\beta} = \mu_0 \left[ \omega_R^2 + (1-\nu_\beta^2)\omega_M\omega_R - \omega^2 \right]/(\omega_R^2-\omega^2) \qquad (25)$$

$$\mu_{\beta\gamma} = \mu_0 \left[ -\omega_M\omega_R\nu_\beta\nu_\gamma + j\omega\omega_M\nu_\alpha \right]/(\omega_R^2-\omega^2)$$

$$\mu_{\gamma\alpha} = \mu_0 \left[ -\omega_M\omega_R\nu_\alpha\nu_\gamma + j\omega\omega_M\nu_\beta \right]/(\omega_R^2-\omega^2)$$

$$\mu_{\gamma\beta} = \mu_0 \left[ -\omega_M\omega_R\nu_\beta\nu_\gamma - j\omega\omega_M\nu_\alpha \right]/(\omega_R^2-\omega^2)$$

$$\mu_{\gamma\gamma} = \mu_0 \left[ \omega_R^2 + (1-\nu_\gamma^2)\omega_M\omega_R - \omega^2 \right]/(\omega_R^2-\omega^2)$$

In passing note that this tensor for a lossless case is Hermitian as should be expected. To obtain Polder's original form from these results note that $\alpha$, $\beta$, $\gamma$ correspond respectively to x, y, z and that $\nu_x = \nu_y = 0$, $\nu_z = 1$; thus,

$$\mu_{xx} = \mu_o \left[ \omega_R^2 + \omega_M \omega_R - \omega^2 \right] / \left( \omega_R^2 - \omega^2 \right)$$

$$\mu_{xy} = \mu_o \left[ j\omega\omega_M \; / \; \left( \omega_R^2 - \omega^2 \right) \right]$$

$$\mu_{xz} = 0$$

$$\mu_{yx} = \mu_o \left[ -j\omega\omega_M \; / \; \left( \omega_R^2 - \omega^2 \right] \right.$$

$$\mu_{yy} = \mu_o \left[ \omega_R^2 + \omega_M \omega_R - \omega^2 \right] / \left( \omega_R^2 - \omega^2 \right) \qquad (26)$$

$$\mu_{yz} = 0$$

$$\mu_{zx} = 0$$

$$\mu_{zy} = 0$$

$$\mu_{zz} = \mu_o$$

Another case of technical interest is that of arbitrary orientation for $\bar{\nu}$ and rectangular Cartesian coordinates. In the present formulation the components of $\bar{\nu}$ must also be resolved relative to this defining coordinate system; however, it is useful to specify the components of $\bar{\nu}$ relative to spherical coordinates using the usual definitions of angles relative to the rectangular system. From a different point of view the required components of $\bar{\nu}$ are obtained from this latter set by a suitable tensor transformation. Making again the previous identification of $\alpha$, $\beta$, $\gamma$ with x, y, z and noting $\nu_\alpha = \sin\theta \cos\varphi$, $\nu_\beta = \sin\theta \sin\varphi$, $\nu_\gamma = \cos\theta$ substitution obtains

$$\mu_{xx} = \mu_0 \left[ \omega_R^2 + (1 - \sin^2\theta \cos^2\varphi)\omega_M\omega_R - \omega^2 \right] / (\omega_R^2 - \omega^2)$$

$$\mu_{xy} = \mu_0 \left[ -\omega_M\omega_R \sin^2\theta \sin\varphi\cos\varphi + j\omega\omega_M \cos\theta \right] / (\omega_R^2 - \omega^2)$$

$$\mu_{xz} = \mu_0 \left[ -\omega_M\omega_R \sin\theta\cos\theta\cos\varphi - j\omega\omega_M \sin\theta\sin\varphi \right] / (\omega_R^2 - \omega^2)$$

$$\mu_{yx} = \mu_0 \left[ -\omega_M\omega_R \sin^2\theta \sin\varphi\cos\varphi - j\omega\omega_M \cos\theta \right] / (\omega_R^2 - \omega^2) \qquad (27)$$

$$\mu_{yy} = \mu_0 \left[ \omega_R^2 + (1 - \sin^2\theta \sin^2\varphi)\omega_M\omega_R - \omega^2 \right] / (\omega_R^2 - \omega^2)$$

$$\mu_{yz} = \mu_0 \left[ -\omega_M\omega_R \sin\theta\cos\theta\sin\varphi + j\omega\omega_M \sin\theta\cos\varphi \right] / (\omega_R^2 - \omega^2)$$

$$\mu_{zx} = \mu_0 \left[ -\omega_M\omega_R \sin\theta\cos\theta\cos\varphi + j\omega\omega_M \sin\theta\sin\varphi \right] / (\omega_R^2 - \omega^2)$$

$$\mu_{zy} = \mu_0 \left[ -\omega_M\omega_R \sin\theta\cos\theta\sin\varphi - j\omega\omega_M \sin\theta\cos\varphi \right] / (\omega_R^2 - \omega^2)$$

$$\mu_{zz} = \mu_0 \left[ \omega_R^2 + \sin^2\theta\,\omega_M\omega_R - \omega^2 \right] / (\omega_R^2 - \omega^2)$$

## VI. FERRITE LINEWIDTH ΔH AND THE GILBERT DAMPING FACTOR X

The ferrite linewidth ΔH is usually defined as the difference in field values at constant frequency where the imaginary part of the diagonal components of Polder's form of the complex susceptability attains half the resonant value. For this case these imaginary parts of the diagonal components are

$$Im(X_{xx}) = Im(X_{yy}) = -\omega_M\omega\alpha \left[ \omega_o^2 + \omega^2(1+\alpha^2) \right] / \left\{ \left[ \omega_o^2 - \omega^2(1+\alpha^2) \right]^2 + (2\omega_o\omega\alpha)^2 \right\} \qquad (28)$$

Clearly, the Gilbert damping factor α, which appears explicitly in these expressions, is related to the experimentally determined linewidth. For small damping, which must prevail for useful microwave device material, the resonance occurs approximately at the Lamour frequency; that is

$$\omega \simeq \omega_o \qquad (29)$$

at resonance as shown in figure 4. Again for small damping the maximum value is

$$\left| Im(X_{xx}) \right|_{\omega=\omega_o} \simeq \omega_M / (2\omega\alpha) \qquad (30)$$

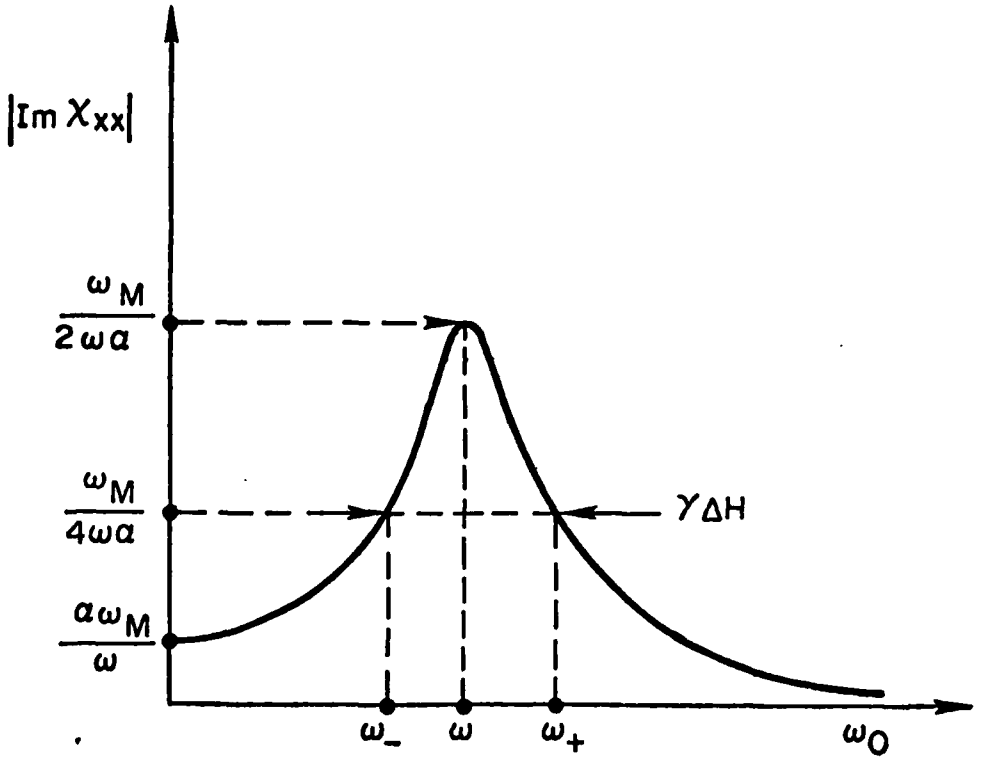



Figure 4 - A sketch of $|\mathrm{Im}(\chi_{xx})|$ versus $\omega_o$ (i.e, variation of bias field) with frequency $\omega$ fixed. The half peak amplitude width is identified as $\gamma$ times the material linewidth $\Delta\bar{H}$.

and the half amplitude values for this approximation occur at

$$\omega_{\pm} = \omega(1 \pm \alpha) \tag{31}$$

The difference is defined as the linewidth; thus,

$$\gamma \Delta H = 2\omega\alpha \tag{32}$$

or

$$\Delta H = (2\alpha/\gamma)\omega \tag{33}$$

To check the assumption of small $\alpha$, take as values from figure 2-20 of von Aulock (7) $\Delta H = 0.50e$ at 3GHz. From these values and equation (30) it is found

$$\alpha \simeq 3.7\,(10^{-5}) \tag{34}$$

which strongly satisfies the assumption of small damping.

## VII. SUMMARY AND RECOMMENDATIONS

At this juncture the present work may be summarized as follows: first, a method has been proposed for the formulation of a boundary value problem to be utilized in the calculation of reflection and transmission factors for magnetostatic waves incident on metal strips; and, second, a generalized Polder tensor has been derived to permit examination of the various propagation modes corresponding to a given bias field orientation. The following recommendations are made with the objective of bringing the present effort to a fruitful conclusion; first, the modes of propagation should be identified and the reflection and transmission factors determined in terms of suitable superpositions of these modes; and, second, numerical results should be computed with emphasis on generating simple, closed form approximations for the reflection and transmission factors which may be used in MSW device modeling.

## REFERENCES


1. J. H. Collins et al, 1977 Ultrasonics Symp Proc., IEEE Cat. No. 77 CH 1264 1SU, 541-552, 1977.

2. R. W. Damon and J. R. Eshbach, J. Phys. Chem. Solids, 19, 308-320, 1961.

3. H. J. Levinstein, et al, Appl. Phys. Lett., 19, 486-488, 1971.

4. E. K. Sittig and G. A. Coquin, IEEE Trans. SU, SU-15, 111-119, 1968.

5. J. Meixner, "The Behavior of Electromagnetic Fields at Edges," Inst. Math Sci. Res. Dept EM-72, New York University, New York, New York, Dec. 1954.

6. R. Mittra and S. W. Lee, Analytic Techniques in the Theory of Guided Waves, The MacMillan Company, New York, New York, 1971.

7. W. H. von Aulock, Ed., Handbook of Microwave Ferrite Materials, Academic Press, New York, New York, 1965.

8. B. Lax and K. J. Button, Microwave Ferrites and Ferrimagnetics, McGraw Hill, New York, New York, 1962.

9. G. T. Rado and H. Suhl, Eds., Magnetism Vol. 1, Academic Press, New York, New York, 1963.

10. H. P. J. Wijn, Ed., Encyclopedia of Physics, Springer-Verlag, Berlin, 1966.

11. A. H. Morrish, The Physical Principles of Magnetism, John Wiley and Sons, New York, New York, 1965.

12. J. Helszajn, Principles of Microwave Ferrite Engineering, Wiley Interscience, London, 1969.

13. D. Polder, "On The Theory of Ferromagnetic Resonance," Phil. Mag., 40, 1949, p. 99.

14. C. V. Smith, Jr., J. M. Owens, T. J. Mears II and N. D. Parikh, IEEE Trans. Mag., MAG-15, 1979, p. 1738.

15. R. C. Addison, B. A. Auld and J. H. Wilkinson, Proc. IEEE, 55, 1967, p. 68.

16. I. S. Sokolnikoff, Tensor Analysis, John Wiley & Sons, Inc., New York, 1951.

1980 USAF - SCEEE SUMMER FACULTY RESEARCH PROGRAM

Sponsored by the

AIR FORCE OFFICE OF SCIENTIFIC RESEARCH

Conducted by the

SOUTHEASTERN CENTER FOR ELECTRICAL ENGINEERING EDUCATION

# FINAL REPORT

# OPTIMAL CONTROL OF THE HEL BEAM


| | |
|---|---|
| Prepared by: | J. Eldon Steelman |
| Academic Rank: | Associate Professor |
| Department and | Electrical and Computer Engineering |
| University: | New Mexico State University |
| Research Location: | Advanced Laser Technology Division |
| | Advanced Beam Control Branch |
| | Air Force Weapons Laboratory |
| | Kirtland AFB, NM |
| Research Associate: | Lt Col James A. Dillow |
| Date: | August 15, 1980 |
| Contract No: | F49620-79-C-0038 |

# OPTIMAL CONTROL OF THE HEL BEAM

by

J. Eldon Steelman

## ABSTRACT

The optimal control of the deformable mirror in a High Energy Laser is required to offset the turbulence in the atmosphere. Computer models suitable for finding the optimal control of each of the first five optical modes treated separately were developed. A detailed study of the tilt and control system model indicates that a Kalman estimator and an optimal control can provide satisfactory system response. Further research in this area is suggested.

## ACKNOWLEDGEMENTS

The author would like to thank the Air Force Systems Command, the Air Force Office of Scientific Research, and the Southeastern Center for Electrical Engineering Education for funding and administering an outstanding program. He would like to thank Dr. Guenther and Mr. Ungvarsky for their assistance and their interest in the program. He would also like to express his appreciation to Capt Hal McIntire, Mrs. Pat Simari, Dr. Arnold Elsbernd, and Mr. Don Evey for providing computer assistance. The author would also like to thank Ms. Hoover for typing this report. Further, he would like to thank the staff of Air Force Weapons Laboratory for making the laboratory such a pleasant place to work.

The author would like to thank Lt Col James A. Dillow for suggesting this area of research and for his guidance. Lt Col Dillow exemplifies the scientific and management skills desired in a scientific officer and working with him has been a pleasure.

## I. INTRODUCTION:

The optimal control of the deformable mirror in a High Energy Laser (HEL) (see Figure 1) is required to offset the turbulence in the atmosphere. This research effort seeks the best control system for the HEL as a function of the signal to noise ratio and the number of detector sub-apertures. The number of sub-apertures is important because more sub-apertures allow the estimation of higher order optical effects and the potential for better control. However, increasing the number of sub-aperture decreases the signal-to-noise ratio.

The primary tool used in this determination was computer modeling. Kleinman's routines (References 1 through 5) were used to determine the optimal continuous control and the gain of a continuous Kalman estimator. Kleinman's routines were also used to find the overall system step response and overall system covariance matrix.

## II. OBJECTIVES OF THE RESEARCH EFFORT:

The objective of this project was to determine the control system for the deformable mirror which minimized the effects of atmospheric turbulence. The best control system was sought as a function of signal-to-noise ratio and number of sub-apertures. The project goal was to make this determination for the first five optical modes. A basic assumption was that each optical mode could be estimated separately and linearly.

## III. ATMOSPHERIC TURBULENCE:

The distortion induced in the laser beam by atmospheric turbulence can be described in terms of its effect on the various optical modes (tilt, focus, astigmatism, etc.). The effect on each optical mode can be modeled by a three state variable model driven by a Gaussian random variable (References 6 and 7).

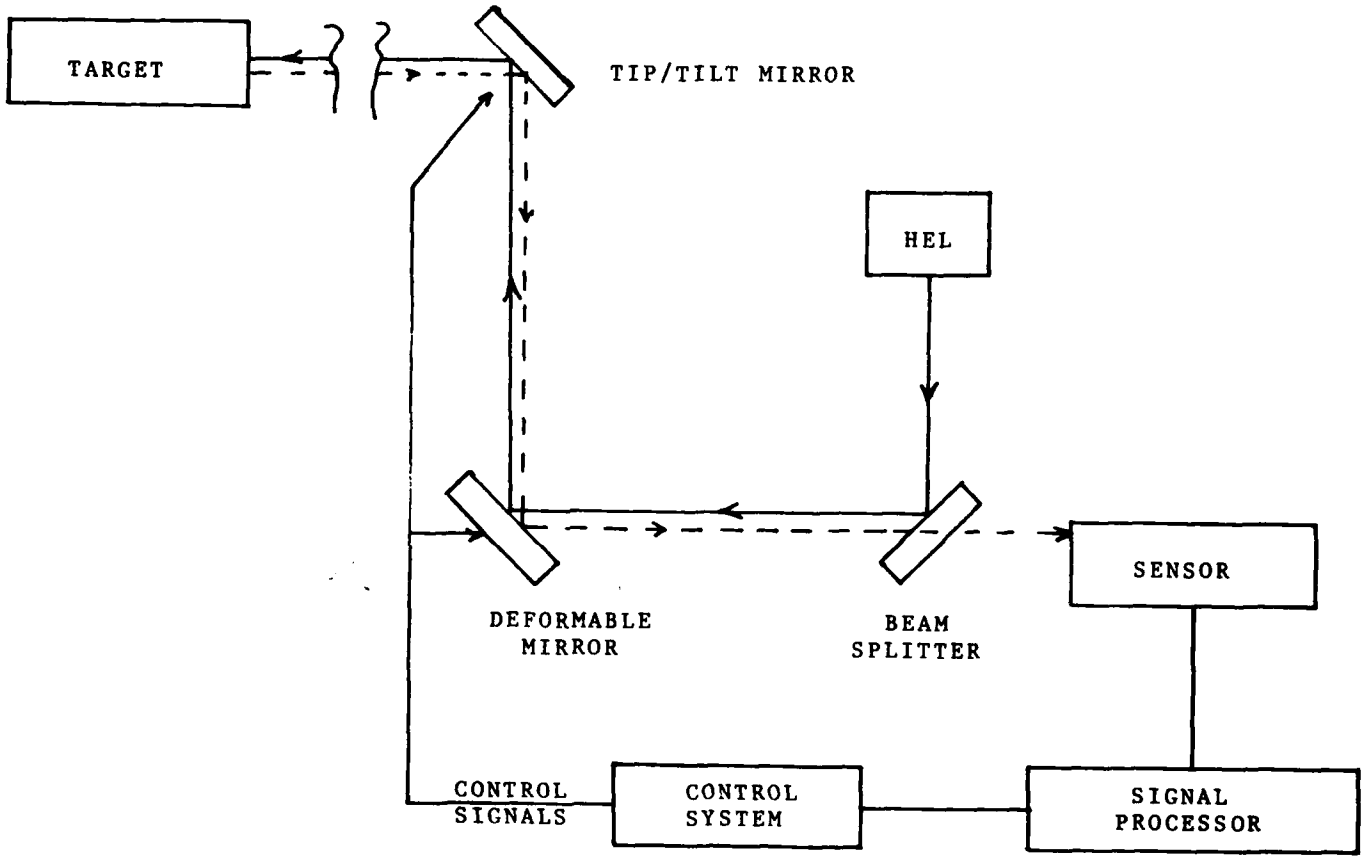



FIGURE 1. SIMPLIFIED HEL CONTROL SYSTEM

Let $x_1 = v_x$ = random effect on optical mode

$x_2$ = turbulence model state

$x_3$ = turbulence model state

Then the state model is

$$\dot{x}_1 = -a x_1 + b x_2 \quad (1)$$

$$\dot{x}_2 = -b x_2 + c x_3 \quad (2)$$

$$\dot{x}_3 = -c x_3 + v_t \quad (3)$$

where

$$E \left| v_t(t)\, v_t(t+T) \right| = k \delta(t) \quad (4)$$

Values of k, a, b, and c for the first five optical modes are given in Table I (Reference 7).

| Mode | k | a | b | c |
|---|---|---|---|---|
| x | $2.6 \times 10^{-7}$ | 47.10 | 2200 | 2200 |
| y | $2.4 \times 10^{-7}$ | 47.10 | 2200 | 2200 |
| $x^2 + y^2 - R^2/2$ | $3.3 \times 10^{-8}$ | 94.20 | 3350 | 3350 |
| $x^2 - y^2$ | $5.4 \times 10^{-8}$ | 41.80 | 2576 | 2576 |
| xy | $6.0 \times 10^{-10}$ | 4.710 | 73.30 | 2932 |

Table 1. Parameters for Turbulence Model.

NOTE: Mode xy has a zero at .0523 radians/sec which will be neglected.

## IV MIRROR AND CONTROL SYSTEM MODEL:

The mirror tilt and control system are represented by three state variables.

Let $x_4$ = mirror tilt (5)

$x_5$ = mirror tilt rate (6)

$x_6$ = integral of error $(x_1 - x_4)$ (7)

Finally, the mirror drive is a force driver such that

$$\dot{x}_4 = x_5 = u \tag{8}$$

The complete tilt system model is

$$\begin{bmatrix} \dot{x}_1 \\ \dot{x}_2 \\ \dot{x}_3 \\ \dot{x}_4 \\ \dot{x}_5 \\ \dot{x}_6 \end{bmatrix} = \begin{bmatrix} -a & a & 0 & 0 & 0 & 0 \\ 0 & -b & b & 0 & 0 & 0 \\ 0 & 0 & -c & 0 & 0 & 0 \\ 0 & 0 & 0 & 0 & 1 & 0 \\ 0 & 0 & 0 & 0 & 0 & 0 \\ 1 & 0 & 0 & -1 & 0 & 0 \end{bmatrix} \begin{bmatrix} x_1 \\ x_2 \\ x_3 \\ x_4 \\ x_5 \\ x_6 \end{bmatrix} + \begin{bmatrix} 0 \\ 0 \\ 0 \\ 0 \\ 1 \\ 0 \end{bmatrix} u + \begin{bmatrix} 0 \\ 0 \\ v_t \\ 0 \\ 0 \\ 0 \end{bmatrix} \tag{9}$$

The covariance matrix for the noise is

$$Q_t = k \delta_{33}$$

As a first approximation, the remaining four optical modes will be modeled by the same general equation. The different values from Table 1 will be used in equations (9) and (10).

## V. SYSTEM OBSERVATION MATRIX:

The quantity $y_1$ is measured by the detector.

$$y_1 = x_1 - x_4 + v_1 \tag{11}$$

Observability requires that $x_6$ also be measured

$$y_2 = x_6 + v_2 \tag{12}$$

Other measurements will be selected as required for adequate system performance.

## VI. OPTIMAL CONTROL SYSTEM DESIGN:

The classical infinite time optimal control problem minimizes a cost function (Reference 8).

$$V = \int_0^\infty (x^t Qx + u^t Ru)\, dt \tag{13}$$

The minimization of V produces the control in terms of P, the solution to a Ricatti equation

$$PA + A^t P - P\, \underline{b}\, R^{-1}\, \underline{b}^t\, P + Q = 0 \tag{14}$$

(Kleinman's subroutine MRIC solves this equation.)

The optimal control is

$$\underline{u}^* = -R^{-1}\, \underline{b}^t\, P \tag{15}$$

The optimal control can be required to have a prescribed stability by replacing A by ( $\alpha$ + A).

The steady state output covariance matrix is the solution of the linear variance matrix (Reference 9)

$$AP + PA^t + B\, Q_i\, B^t = 0 \tag{16}$$

where P is the output covariance matrix,

A and B are system matrices,

$Q_i$ is the input covariance matrix.

(Kleinman's subroutine MLINEQ solves this equation.)

## VII. KALMAN STATE ESTIMATOR[2]

If the basic plant is described by

$$\underline{x} = A\,\underline{x} + B\,\underline{u} + \underline{v}_x \tag{17}$$

$$\underline{y} = M\,\underline{x} + \underline{v}_m \tag{18}$$

The Kalman estimator is

$$\underline{x}_e = A\,\underline{x}_e + B\,\underline{u} + k_e\,(M\,\underline{x}_e - \underline{y}) \tag{19}$$

Desired control law

$$\underline{u} = \underline{u}_{ext} + F\,\underline{x} \tag{20}$$

Actual control law

$$\underline{u} = \underline{u}_{ext} + F\,\underline{x}_e \tag{21}$$

Defining

$$\underline{e} = \underline{x} - \underline{x}_e \tag{22}$$

yields a new system with doubled dimension

$$\begin{bmatrix} \underline{x} \\ \underline{e} \end{bmatrix} = \begin{bmatrix} A + B\,F & -B\,F \\ 0 & A + k_e\,M \end{bmatrix} \begin{bmatrix} \underline{x} \\ \underline{e} \end{bmatrix} + \begin{bmatrix} B \\ 0 \end{bmatrix} u_{ext} + \begin{bmatrix} \underline{v}_x \\ \underline{v}_x + k_e\,\underline{v}_m \end{bmatrix} \tag{23}$$

The matrix $k_e$ is the Kalman gain. It is given by

$$k_e = - P M^t R_m^{-1} \tag{24}$$

where $R_m$ is the covariance of $\underline{v}_m$.

P is the solution to (Reference 8)

$$P A^t + A P - P M^t R_m^{-1} M P + Q_n = 0 \tag{25}$$

$Q_n$ is the covariance of $\underline{v}_x$.

R is the covariance of $\underline{v}_m$.

The input covariance for equation (23) is

$$\text{cov} \begin{bmatrix} \underline{v}_x \\ \underline{v}_x + k_e \underline{v}_m \end{bmatrix} = E \left\{ \begin{matrix} \underline{v}_x \\ \underline{v}_x + k_e \underline{v}_m \end{matrix} \quad \underline{v}_x^t \; \underline{v}_x^t + \underline{v}_m^t \; k_e^t \right\}$$

Thus,

$$\text{cov} \begin{bmatrix} \underline{v}_x \\ \underline{v}_x + k_e \underline{v}_m \end{bmatrix} = \begin{bmatrix} Q_n & Q_n \\ Q_n & Q_n + k_e R_m k_e^t \end{bmatrix} \tag{26}$$

The (2,2) term can be further simplified by substituting equation (24).

$$k_e R_m k_e^t = P M^t R_m^{-1} R_m (R_m^{-1})^t M P$$
$$= P (M^t R_m^{-1} M) P$$

Thus, the (2,2) term becomes

$$Q_n + k_e R_m k_e^t = Q_n + P (M^t R_m^{-1} M) P \tag{27}$$

One set of measurements satisfying the observability requirement is

$$\begin{bmatrix} y_1 \\ y_2 \\ y_3 \end{bmatrix} = \begin{bmatrix} 1 & 0 & 0 & -1 & 0 & 0 \\ 0 & 0 & 0 & 1 & 0 & 0 \\ 0 & 0 & 0 & 0 & 0 & 1 \end{bmatrix} \underline{x} + \underline{v}_m \tag{28}$$

## VIII. COMPUTER PROGRAMS

The primary product of this research effort was four main computer programs. All four of these share some segments; nevertheless, each program will be discussed separately. All of these programs are in the system files with ID = ARAAJES.

A. PROGRAM IAKLMNM4 (cy = 5). (See Appendix A for a listing and sample output.)

This is an interactive program which requires that Kleinman's routines be "ATTACHed" and 'LIBRARYed". The program also requires input data in file TAPE 5.

The program reads:

1. A matrix (6 card images, 6 values per image).
2. X vector (not used)(1 card of 6 values).
3. B vector (1 card of 6 values).
4. U vector (not used) (1 card of 6 values).
5. M matrix (4 cards, 6 values per card).
6. Q matrix (6 cards, 6 values per card).
7. ALPHA (single value from a card).
8. R (single value from a card).
9. SGMTURB, SGMILS4, SGMM2, SGMM3, SGMM4 (5 values on one card).

After reading this information, the program forms the AT (A transpose), the QNMAT, and the SKLMN matrices. The program uses Kleinman's subroutine MRIC to calculate the Kalman gain and the transpose of the Kalman estimator system matrix. The program then forms QPLSRSR, the input covariance for the Kalman estimator operating on the error vector of equation (23). The program calculates and prints the eigenvalues for the system. The program outputs the error covariance matrix from MRIC (RKLMN) and the error covariance matrix from MLINEQ (COVARX). A comparison of these two results indicates the quality of the RKLMN solution. The Kalman section ends by requesting a pointer for the next step in the computation. If the user desires, one of the measurement sigmas or the tolerance for MRIC or the tolerance for MLINEQ may be changed and the Kalman section repeated.

If the user chooses to go to the optimal control section, the program calculates the optimal control based on the input Q, R, and ALPHA. After the optimal control calculation, the program calculates and prints the eigenvalues for the optimal system. The user is then allowed to change Q, R, or ALPHA or to proceed to the covariance calculation.

This program will run on MFY or MFB.

B. PROGRAM COVARTST (cy = 3). (See Appendix B for a listing and sample output.) This program includes all of IAKLMN (cy = 5). Additionally, it has three more features.

1. The program substitutes RKLMN and COVARX back into equation (16). The result should be zero and examination of the output matrices provides a further indication of the quality of the solutions.

2. The program forms the 12 by 12 system matrix DV for the optimal system and the Kalman estimator combined. (See equations (17) through (24).) This DV matrix is written on TAPE 7 and portions of it are also printed.

3. The program forms the 12 by 12 input covariance matrix Q12. The Q12 matrix is the input covariance matrix for the 12 by 12 system. The Q12 matrix is written on TAPE 7 and portions of it are also listed.

COVARTST must be followed by EGNMLN12, which calculates the overall output covariance matrix and the sigma of the error $(x_1 - x_4)$. (This segmenting of programs is due to the dimensioning of Kleinman's routines. It is not absolutely required because the 12 by 12 version of equation (16) can be reduced to 6 by 6 equations. However, this approach was the quickest path to an answer.)

This program will run on MFY or MFB.

C. PROGRAM EGNMLN12 (cy = 5). (See Appendix C for a listing and sample output.)

This program dimensions Kleinman's routines appropriately for a 12 by 12 system. The program operates on TAPE 7 written by COVARTST and calculates the eigenvalues and output covariance matrix for the 12 by 12 system. As checks, the eigenvalues must be the same and the covariance out for the Kalman section must be the same (as the 6 by 6 case).

This program will run on MFY or MFB.

D. PROGRAM KRASTP (cy = 9). (See Appendix D for a listing and sample output.) This program is a non-interactive version of IAKLMN4 for the CRAY-1 computer. Additionally, this program uses IMSL routine DVERK to calculate the time response of the 12 by 12 system due to a unit change in $x_3$. The program also uses plotting package DISSPLA to plot $x_1$, $x_1 - x_4$, $x_7$ $(x_1 - x_{1\ est})$, and $x_{10}$ $(x_4 - x_{4\ est})$. The required input data is the last portion of the file.

KRASTP generates a Gould plot which is processed by the system without further user intervention. KRASTP also creates a printer plot which the user must process with METALIB routines CRAMET and DIRECT in order to create a usable plot file. (The printer plot allows the user to get a quick look at plots. The Gould always takes one night to produce the plot and occasionally takes several days.)

Program KRAX1IC is the same as KRASTP except that the system is excited by an initial condition in $x_1$.

Program KRAX7IC is the same as KRASTP except for a smaller step size and an initial condition in $x_7$ $(x_1 - x_{1\ est})$.

Program KRAX10IC is the same as KRAX7IC except for an initial condition in $x_{10}$ $(x_4 - x_{4\ est})$.

## IX. RESULTS AND CONCLUSIONS:

The model for the single channel case was completed and tested. The Q, R and for the cost function of Section VI were chosen to produce a system response near 500 Hz with a damping ratio near 0.707. The selected set of Q, R, and are

$$Q = \begin{bmatrix} .1E+10 & 0 & 0 & -.1E+10 & 0 & 0 \\ 0 & 0 & 0 & 0 & 0 & 0 \\ 0 & 0 & 0 & 0 & 0 & 0 \\ -.1E+10 & 0 & 0 & .1E+10 & 0 & 0 \\ 0 & 0 & 0 & 0 & 50 & 0 \\ 0 & 0 & 0 & 0 & 0 & .5E+16 \end{bmatrix} \qquad (29)$$

$$R = 1.05E-05 \qquad (30)$$

$$ALPHA = 47.0 \qquad (31)$$

For these values of Q, R, and $\alpha$ , the three controllable eigenvalues are -2312 and -2231 ± j2206 (see Appendix A, B, or D). The eigenvalues associated with the turbulence model are uncontrollable.) The pair of complex eigenvalues correspond to a natural frequency of 499.3 Hz and a damping ratio of 0.711. Further, if the sigma of the turbulence is 1, the sigma of the error $(x_1 - x_4)$ is 0.00527. (This value assumes that all states are observable.)

The Separation Theorem (Reference 8) allows the Kalman Filter calculation to be made separately. The set of parameters chosen to use for system response studies is shown in Table 2.

| | SIGMAS | | |
|---|---|---|---|
| INPUT | MEASUREMENTS | | |
| TURBULENCE | $x_1 - x_4$ | $x_4$ | $x_6$ |
| 1.0 | .87E-4 | .1379E-5 | .1E-8 |

Table 2. Parameter for System Response Studies

This set of parameters yields the following set of eigenvalues.

(for MRIC tolerance of .2E-4)

Eigenvalues:

-5736 ± j13600

-13711 ± j5575

-252 ± j4.56

Next, Kalman section was combined with the optimal control section to produce the overall error ($x_1 - x_4$) sigma of 0.02279 (see Appendix C).

Finally, the time response was calculated for various excitations. Figure 2 shows the response of $x_4$ due to an input of 2200 for u(3). This input produced final values of 1 for $x_1$, $x_2$, $x_3$ and $x_4$. Figure 3 shows the error for this same case. Note that the maximum excursion is less than 6.E-4. For this same case, the estimated quantities track the actual quantities with no error (see printout of final x in Appendix D).

The next set of time responses are for an initial condition in $x_1$. Figure 4 is the response of $x_4$ to this initial condition and Figure 5 is the error response ($x_1 - x_4$). Again, the estimated quantities track the actual quantities with no error.

The next set of time responses are for an initial condition in $x_{10}$ ( $= x_4 - x_{4\ est}$ ). Figure 6 is the response of $x_4$ to this initial condition and Figure 7 is the error response. Figures 8 and 9 show the estimation error for this case.

The final set of time responses are for an initial condition in $x_7$ ( $= x_1 - x_{1\ est}$ ). Figure 10 is the response of $x_4$ to this initial condition and Figure 11 is the error response. Figures 12 and 13 show the estimator error. Note (Figure 13) that the scale for $x_4 - x_{4\ est}$ is much smaller than the other scales.

All of these results indicate that the system response is satisfactory for this particular set of parameters. Thus, further study of this system is merited.

X UNRESOLVED PROBLEMS: During this research some problems have arisen which remain unresolved.

A. Sensitivity to MRIC Tolerance

The dominant poles in the Kalman estimator are a function of the tolerance used in subroutine MRIC (see Table 3). The input noise for this case is shown in Table 2.

FIGURE 2 X4 FOR U(3)=2200

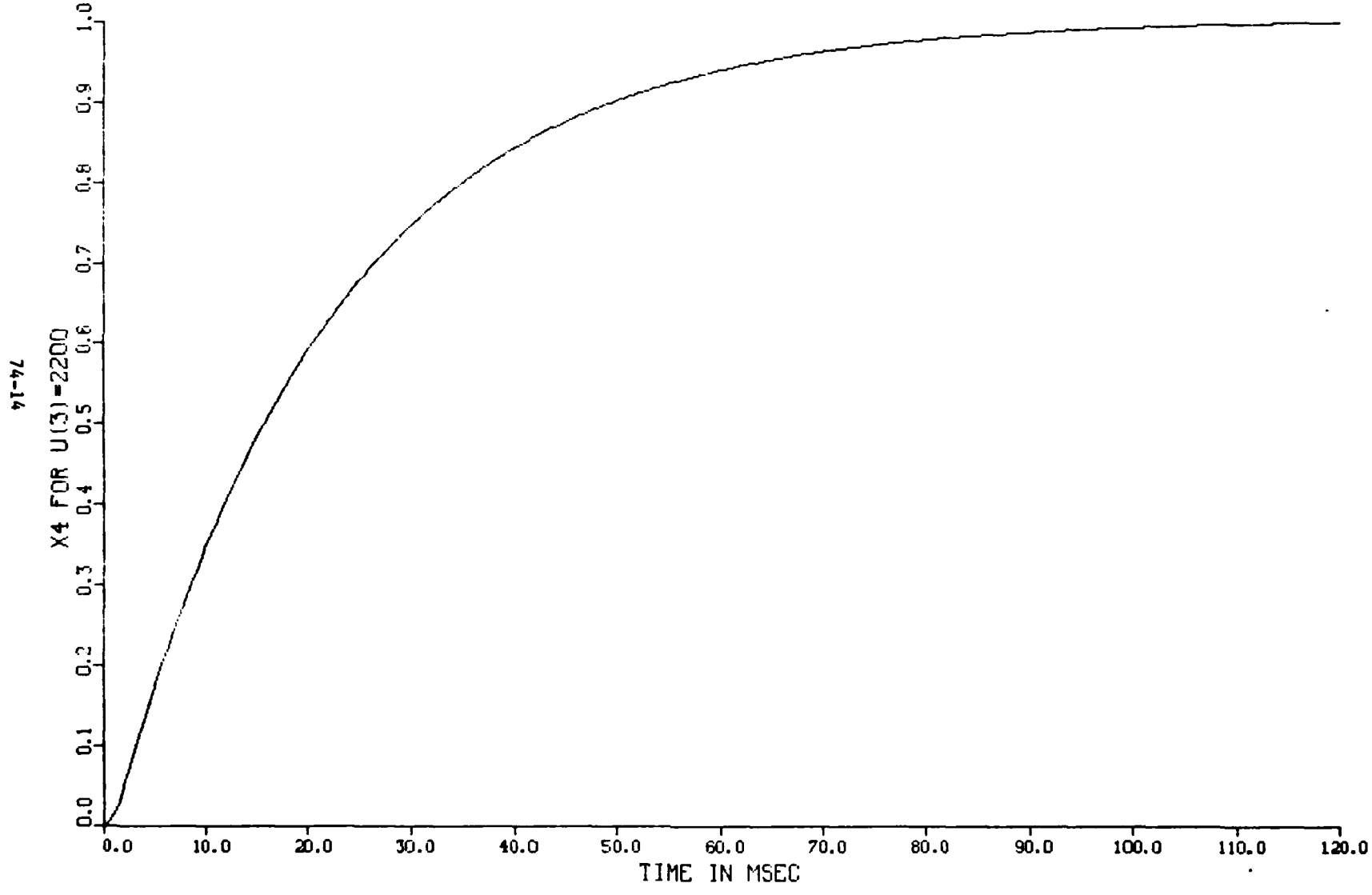


FIGURE 3 X1-X4 FOR U(3)=2200

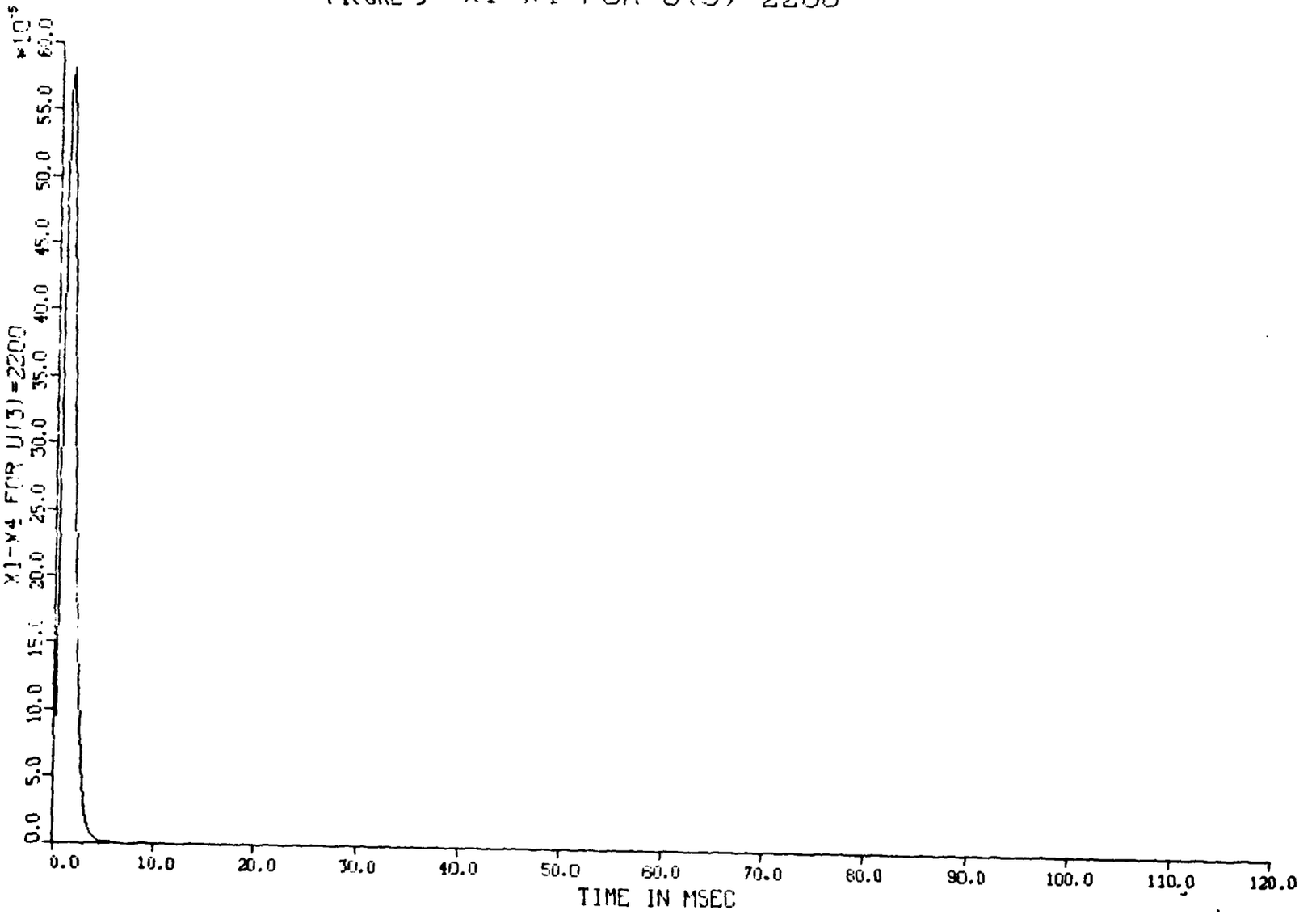


FIGURE 4 X4 FOR X1(0)=1

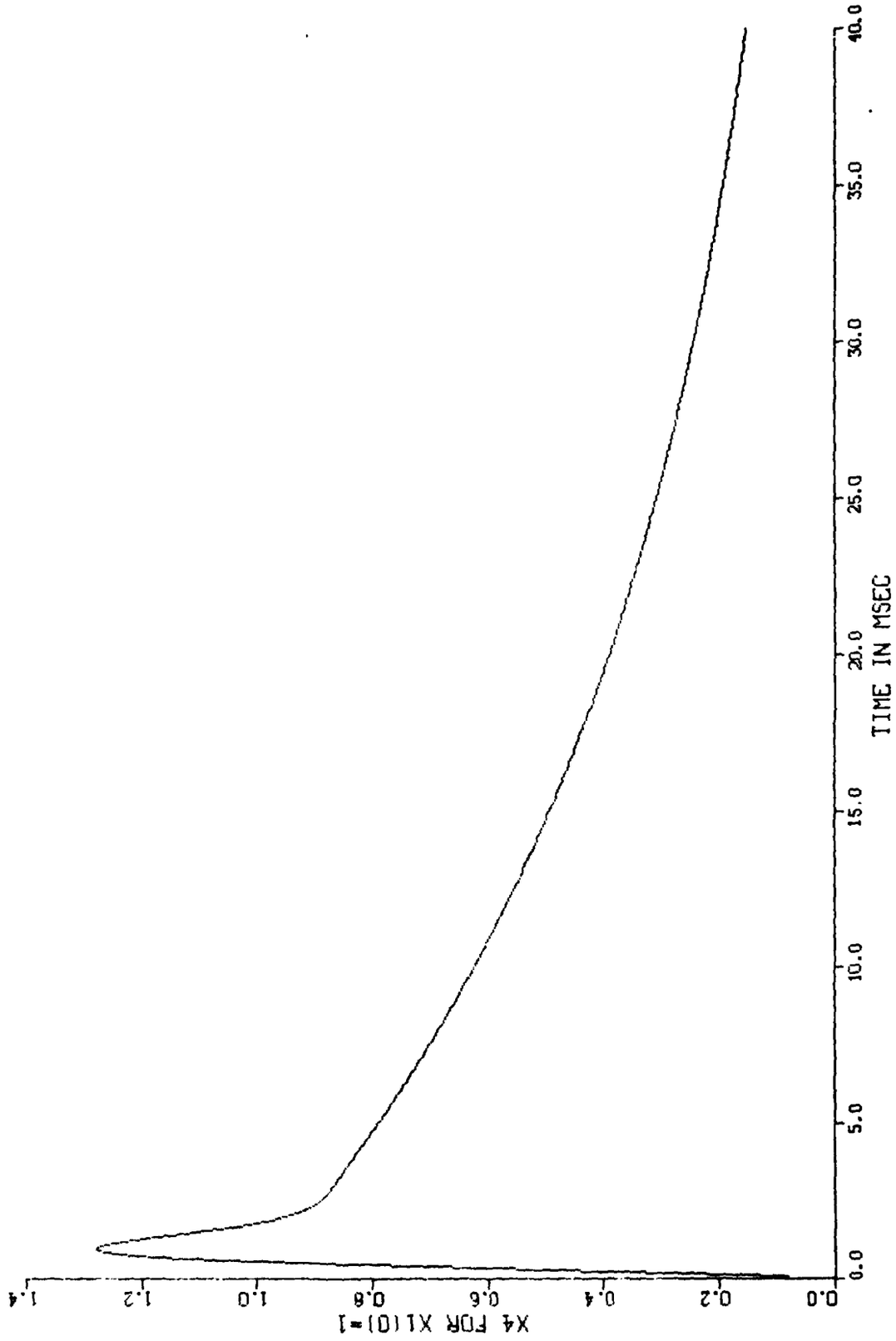


FIGURE 5 X 1-X4 FOR X1(0) = 1

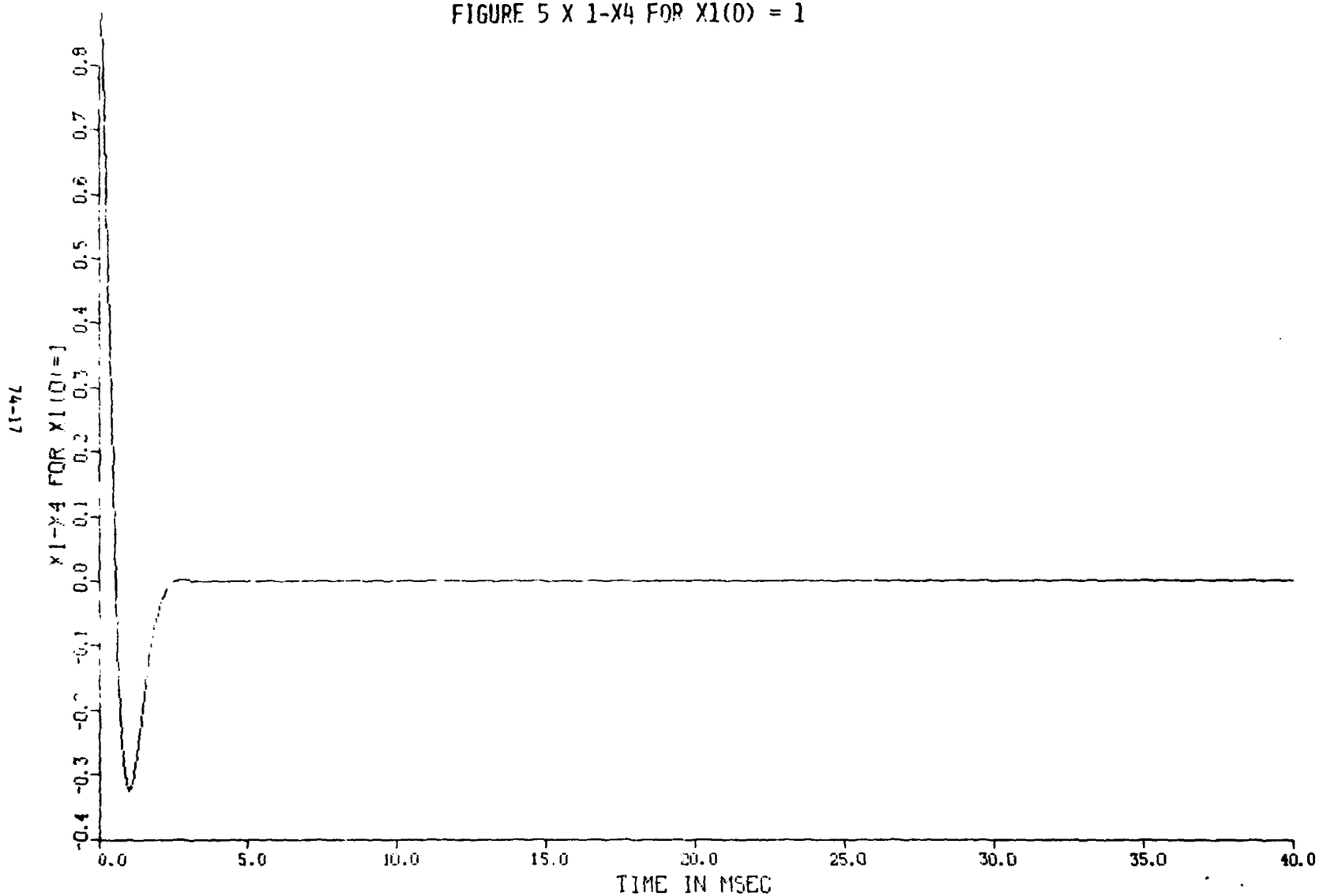


FIGURE 6 AS FOR X10ID.=100

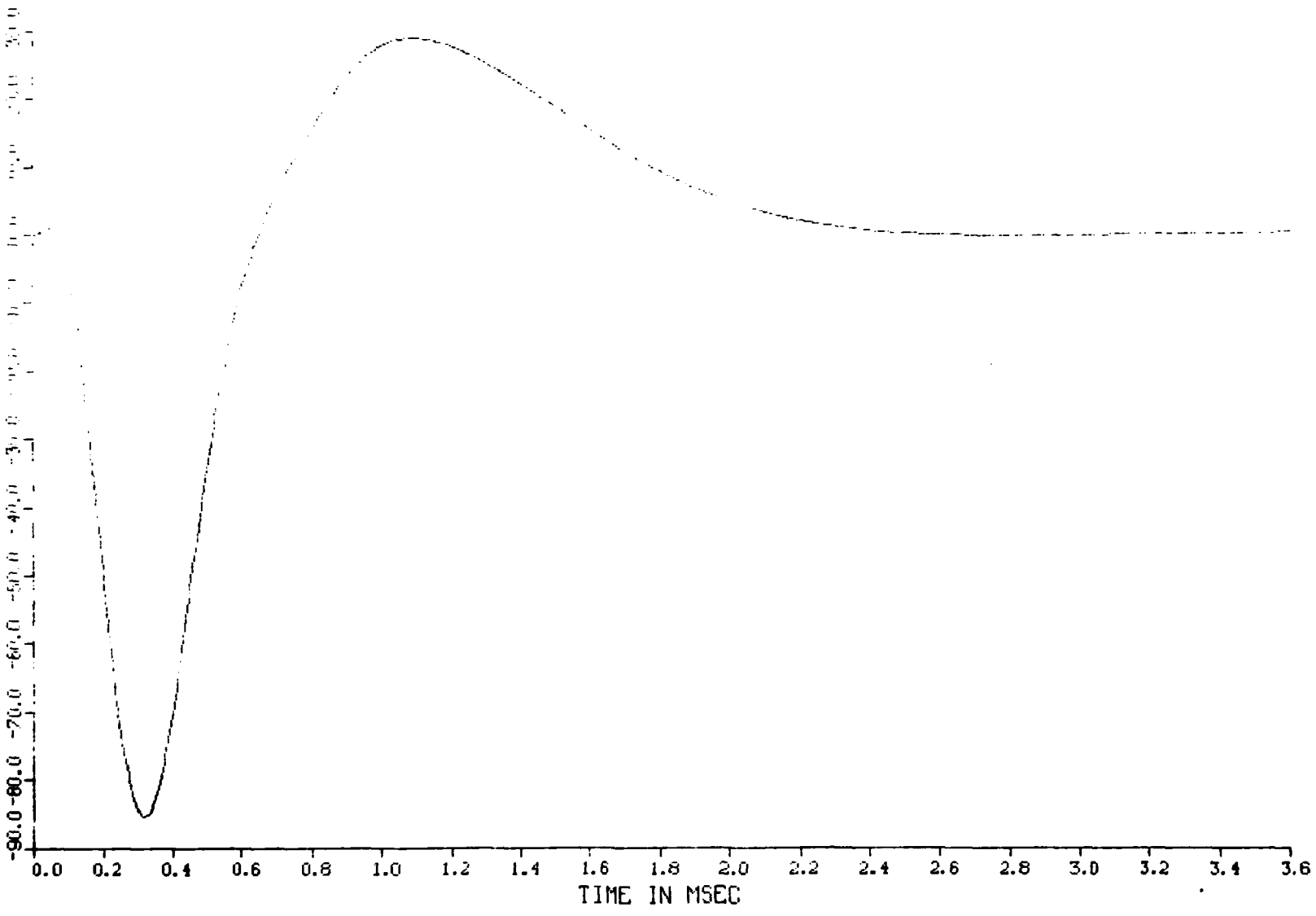


FIGURE 7

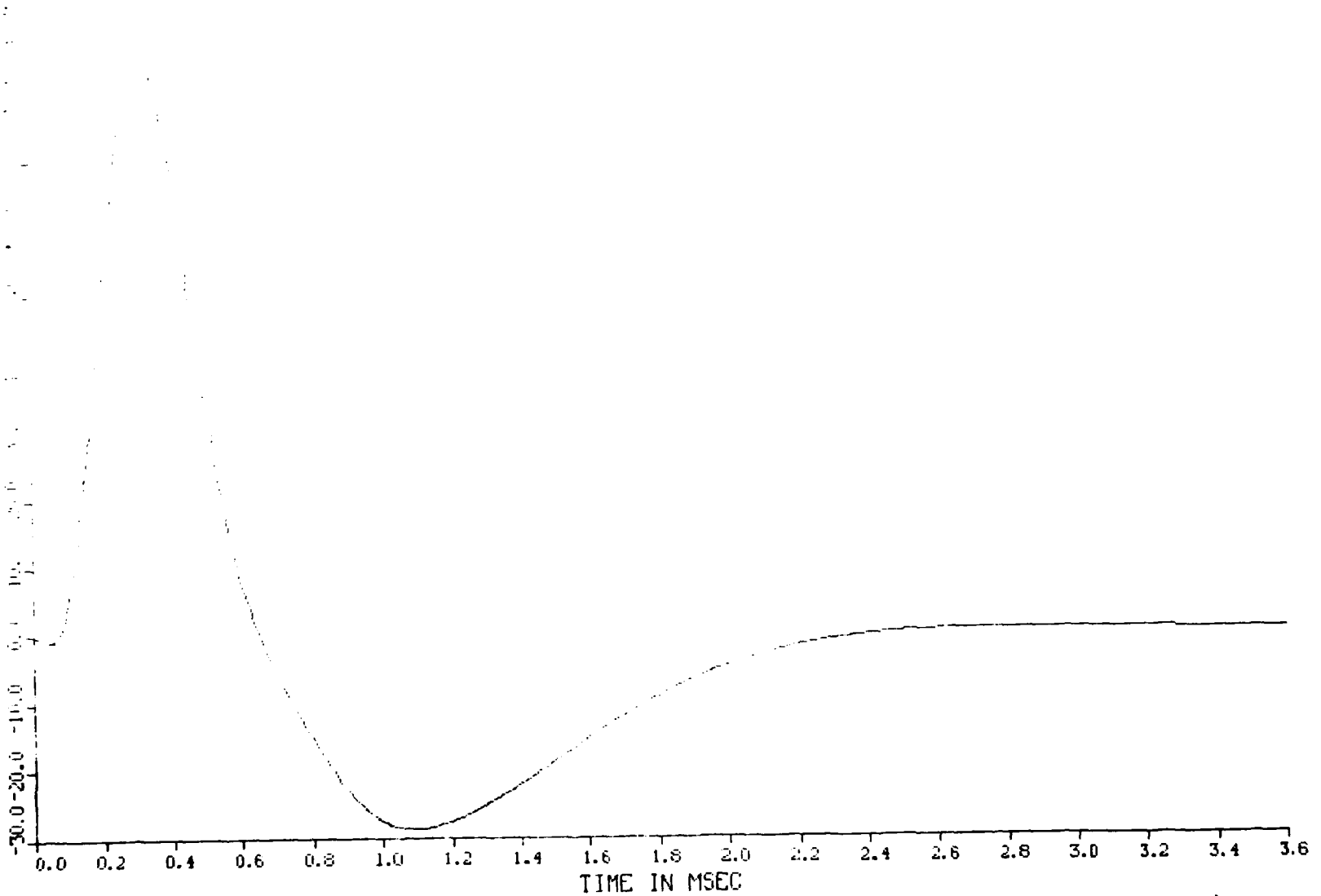

-30.0
-20.0
0.0
0.2
0.4
0.6
0.8
1.0
1.2
1.4
1.6
1.8
2.0
2.2
2.4
2.6
2.8
3.0
3.2
3.4
3.6
TIME IN MSEC

FIGURE 8 X4-X4EST FOR X1(0)=100

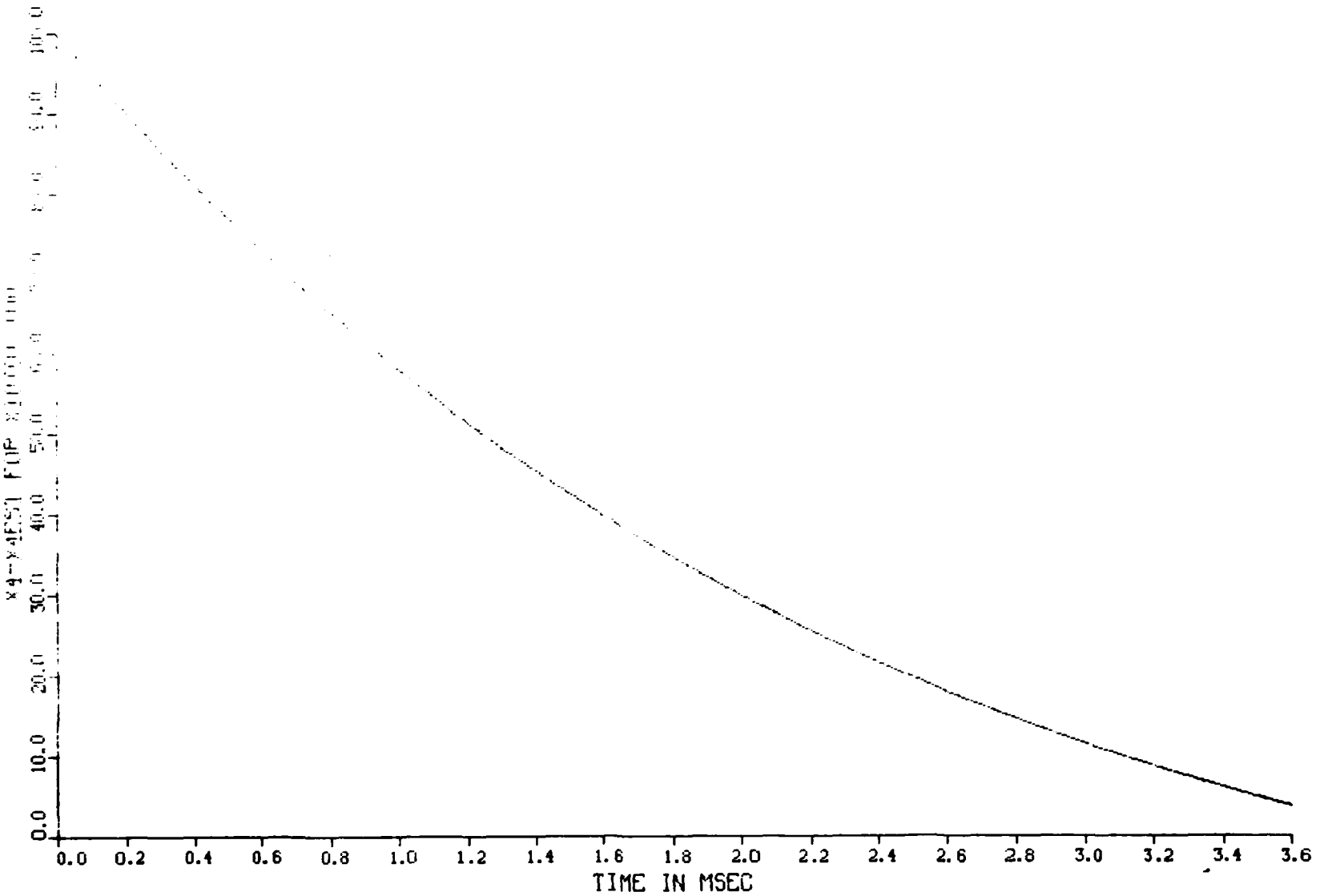


FIGURE 9 XI-XIENT FOR X(50)=100

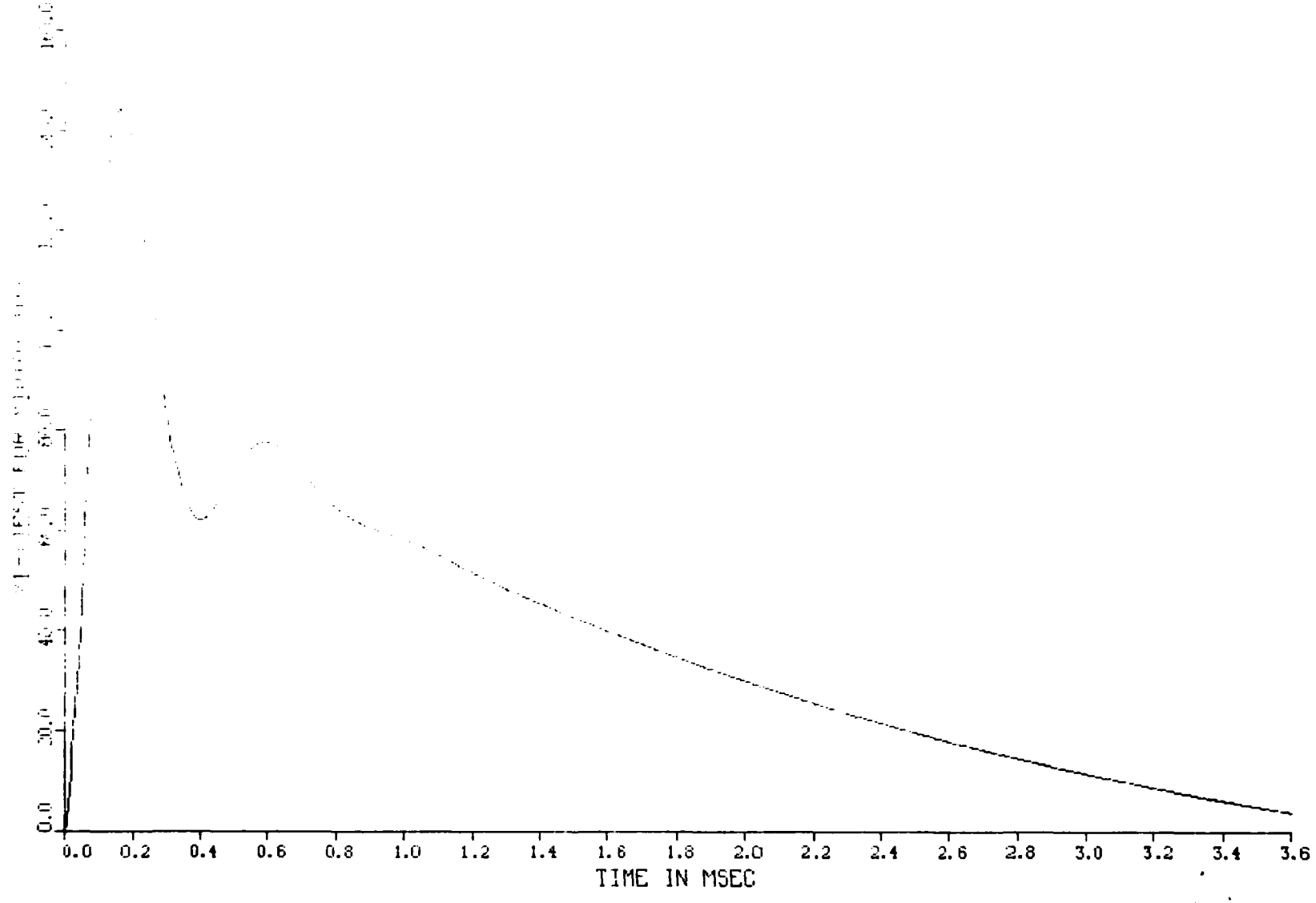


FIGURE 10 X4 FOR X7(0)=1000

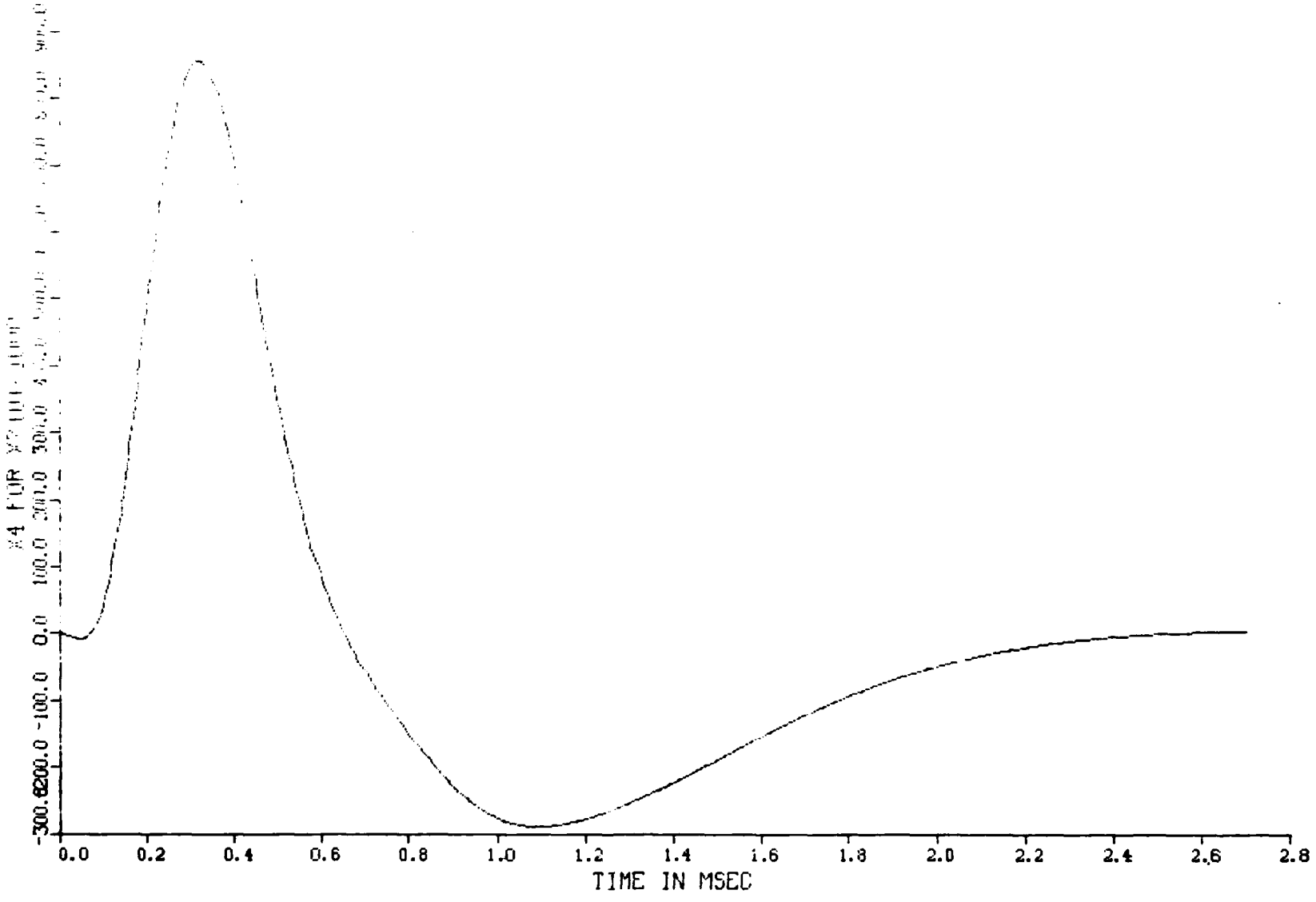


FIGURE 11 X1-X4 FOR X7(0)=1000

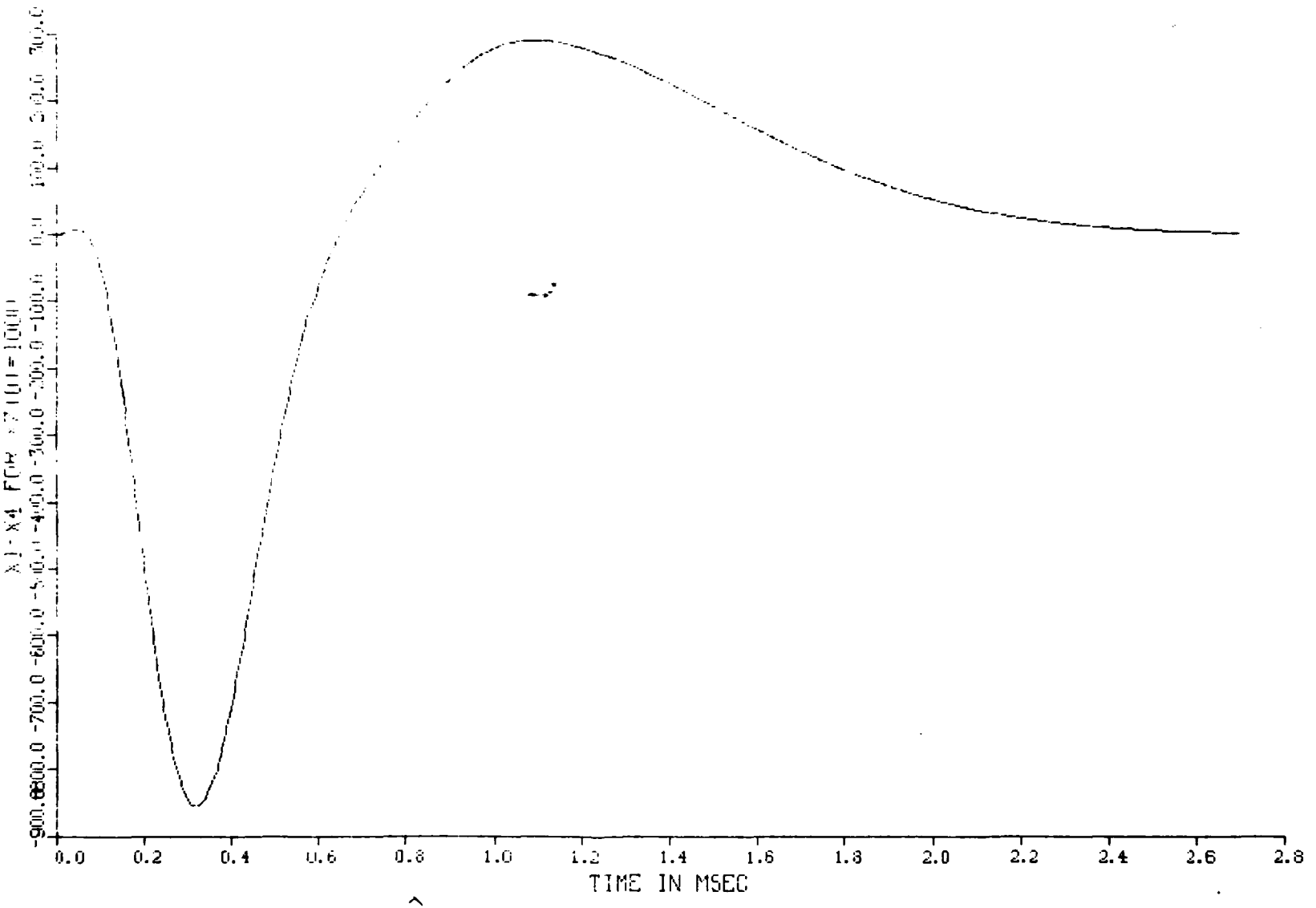


FIGURE 12 X1-X1EST FOR X7.01=1000

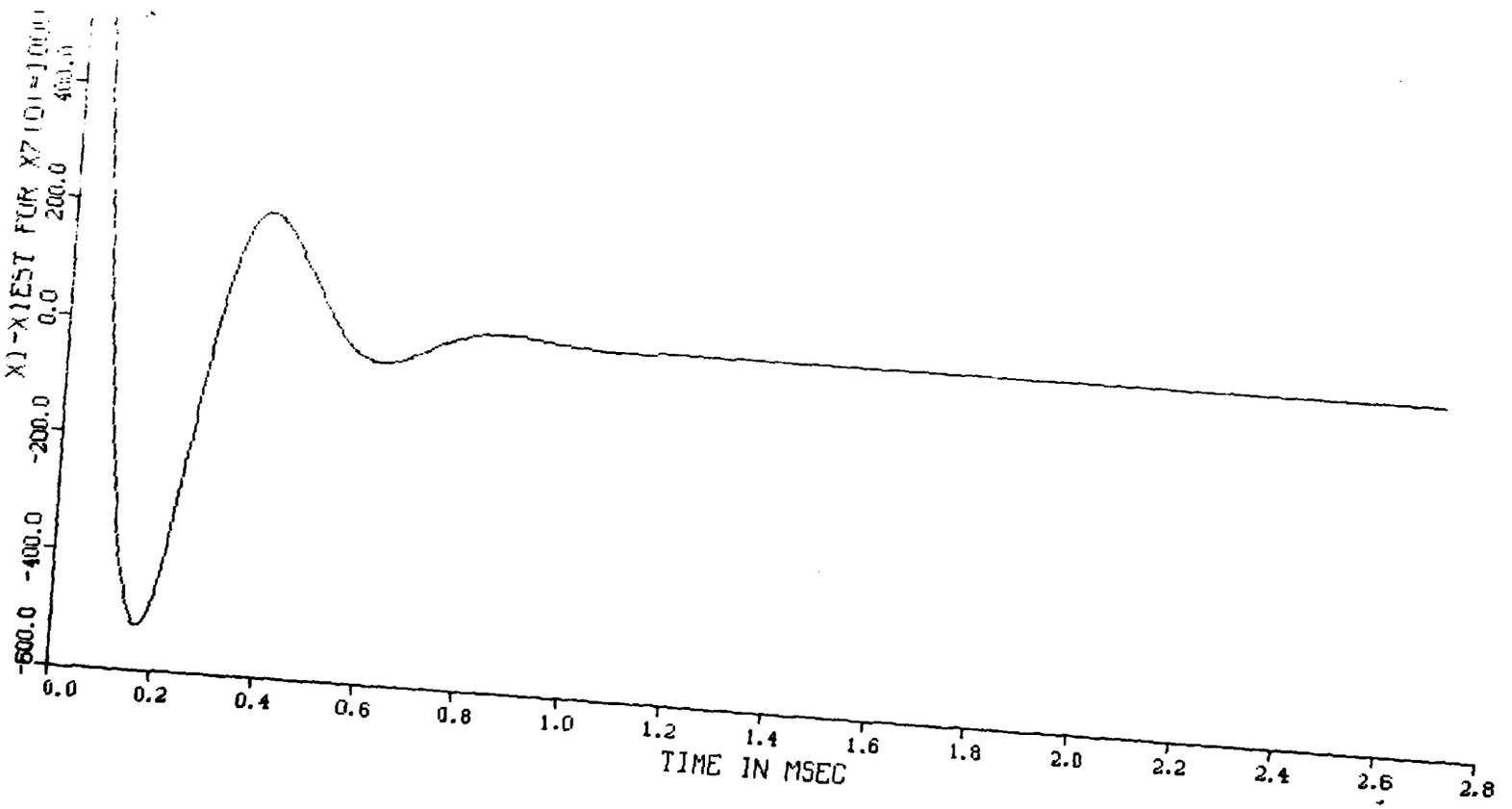
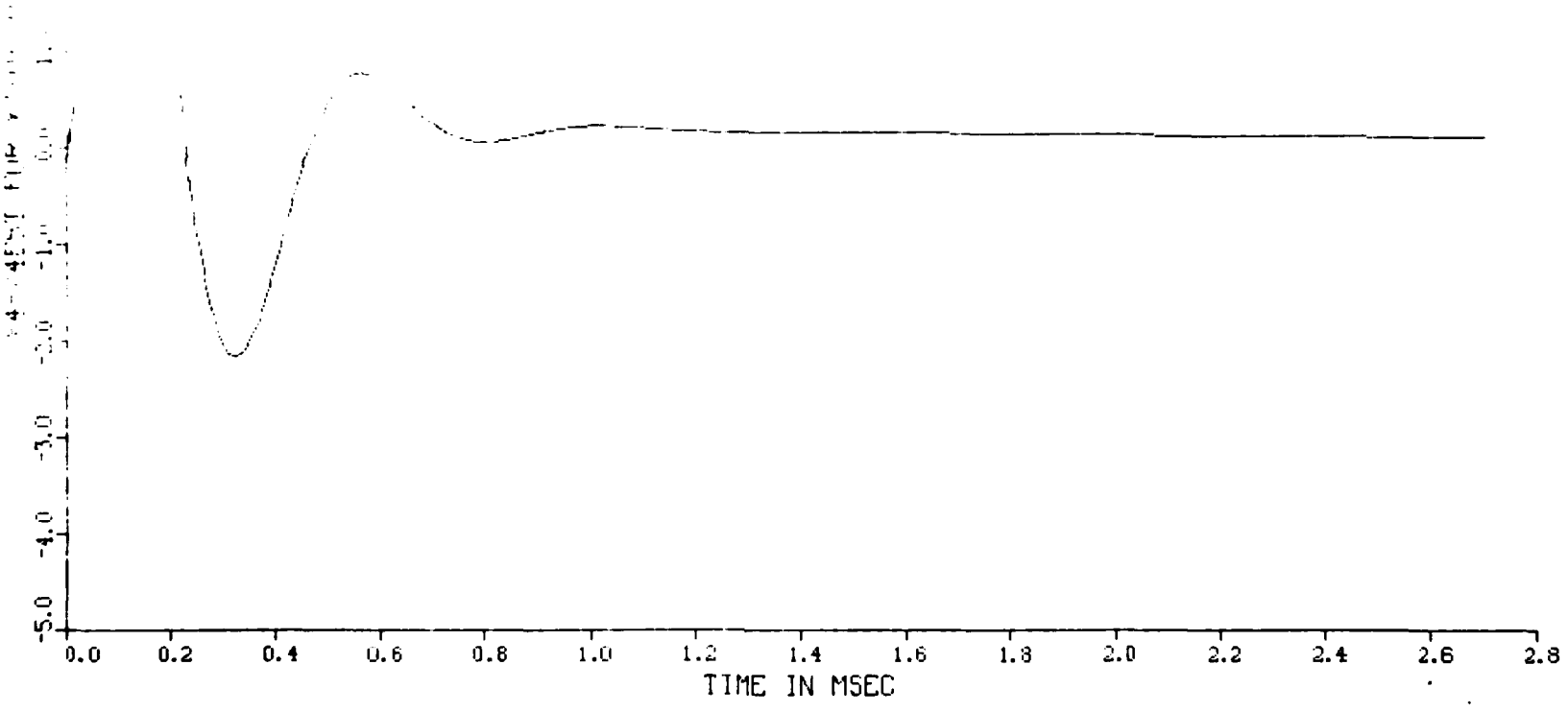


FIGURE 13


-5.0
-4.0
-3.0
-2.0
-1.0
0.0
0.0
0.2
0.4
0.6
0.8
1.0
1.2
1.4
1.6
1.8
2.0
2.2
2.4
2.6
2.8
TIME IN MSEC

| TOLERANCE | DOMINANT POLES | ITERATIONS |
|---|---|---|
| .2E -4 | -252.5 ± j4.56 | 29 |
| .4E -6 | -157.8 ± j83.55 | 30 |
| .4E -7 | - 49.6 ± j39.1 | 33 |
| .2E -7 | - 34.8 ± j27.9 | 34 |

Table 3. DOMINANT POLES FOR VARIOUS TOLERANCES.

When most of these runs were made, that portion of the program which calculated the error sigma was faulty. One approach to resolving this problem would be to rerun the program with these values and observe the behavior of the error sigma. The largest tolerance which produces a stable error sigma should be satisfactory.

B. Sensitivity to Scale.

Examination of equation (27) indicates that all sigmas can be multiplied by a constant without changing the Kalman estimator result. However, multiplying the sigmas of Table 2 by .11E-5 and using the default tolerance of .1E-02 resulted in MRIC running 89 iterations and increasing the tolerance to 0.1 before convergence. In this case, decreasing the tolerance decreased the number of iterations and produced the same 4 non-dominant poles as the original input data of Table 2.

C. Appropriate Noise Values.

The values of Table 2 were selected to give adequate system response. The appropriate noise values are unknown. Further, even if the noise values for one operture were known, the appropriate noise levels for the higher modes is unknown.

## XI RECOMMENDATIONS:

The results of this research indicate that this approach to mirror control is feasible. I recommend that this research be continued. The objectives of the research should include a test of the assumption that each optical mode can be estimated separately.

## REFERENCES


1. D. L. Kleinman, "On an Iterative Technique for Ricatti Equation Computations," IEEE Trans. on Automatic Control, Vol AC-13, No. 1, February 1968.
2. D. L. Kleinman, "An Easy Way to Stabilize a Linear Constant System," IEEE Trans. on Automatic Control, Vol AC-15, No. 6, December 1970.
3. P. G. Smith, "Numerican Solution of the Matrix Equation $AX + X^tA^t + B = 0$," IEEE Trans. on Automatic Control, Vol AC-16, No. 3, June 1971.
4. J. H. Wilkinson and C. Peters, "Eigenvectors of Real and Complex Matrices by LR and QR Triangularizations," Numer. Math., Vol 16, pp. 181-204, 1970.
5. B. Rush, W. R. Burrus, and C. Schneeberger, "A Simple Algorithm for Computing the Generalized Inverse of a Matrix," Communications of the ACM, Vol 9, No. 5, May 1966.
6. L. E. Mabius and Sol Gully, "An Optimal Control Design for the Large Pointing System," AFWL Document TR-1252-1, 12 March 1979.
7. D. P. Glasson and D. K. Guha, "Advanced Adaptive Optics Control Techniques," AFWL Document TR-78-8, January 1979.
8. B. D. O. Anderson and J. B. Moore, Linear Optimal Control, Prentice Hall, Englewood Cliffs, New Jersey, 1971.
9. Arthur Gelb (Editor), Applied Optimal Estimation, M.I.T. Press, Cambridge, Massachusetts, 1974.

```
      PROGRAM MAIN(INPUT,OUTPUT,TAPE5,TAPE6=OUTPUT)
C  SINGLE CHANNEL CASE AUGUST 02 1410
C USES KLEINMAN'S ROUTINES
C  USES MRIC TO CALCULATE KALMAN GAIN.
C  REQUIRES MEASUREMENT MATRIX 4 BY 6.
C  USES MRIC TO CALCULATE OPTIMAL CONTROL.
C  CALCULATES EIGENVALUES OF Z(=A-S*P)
C  USES MLINEQ TO CALCULATE THE COVARIANCE OF OUTPUT X VECTOR.
C  REQUIRES INPUT IN FILE TAPE5 & INPUT FROM TERMINAL.
      REAL X(6),XDOT(6),C(24),W(6,9),TEMP(6,6),ZT(6,6),M(4,5),P(6,4),
     * Q(6,6),S(6,6),COM1(6,6),COM2(6,6),COVARX(6,6),ZK(6,6),A(6,6),
     * AT(6,6),B(6),UNIT(6,6),RR(6),RI(6),QNMAT(6,6),SKLMN(6,6),
     * RKLMINV(4,4),ZKT(6,6),RKLMN(6,6),RKOPT(6,6),UPLSRSR(6,6)
      EXTERNAL FCN
      COMMON/FCNCOM/Z(5,6),U(6)
      COMMON/MAIN1/NDIM,NDIM1,COM1
      COMMON/MAIN2/COM2
      COMMON/INOU/KIN,KOUT,KPUNCH
C THIS COMMON AREA IS REQUIRED FOR KLEINMAN'S ROUTINES
      DATA QNMAT/36*0./
      DATA RKLMINV/16*0./
      N=6
      NDIM=6
      NDIM1=NDIM+1
      MDIM=4
      KIN=5
      KOUT=6
      KPUNCH=7
      REWIND 5
      WRITE(6,599)
  599 FORMAT(2X,22HPROGRAM= IAKLMNM4,CY=5 )
      DO 10 I=1,NDIM
   10 READ(5,500)(A(I,J),J=1,NDIM)
  500 FORMAT(6E12.5)
      READ(5,500)(X(I),I=1,N)
      READ(5,500)(B(I),I=1,NDIM)
      READ(5,500)(U(I),I=1,N)
      DO 9 I=1,MDIM
    9 READ(5,500)(M(I,J),J=1,NDIM)
      DO 12 I=1,NDIM
   12 READ(5,500)(Q(I,J),J=1,NDIM)
      READ(5,500)ALPHA
      READ(5,500)R
      READ(5,500)SGMTURB,SGM1LSM,SGMM2,SGMM3,SGMM4
      WRITE(6,600)
  600 FORMAT(9X,15HTHE A MATRIX IS)
      DO 60 I=1,NDIM
      DO 19 K=1,NDIM
   19 AT(K,I)=A(I,K)
   60 WRITE(6,610)(A(I,J),J=1,NDIM)
  610 FORMAT(6(1X,E12.5))
      WRITE(6,880)
  880 FORMAT(6X,15HTHE M MATRIX IS )
      DO 4 I=1,MDIM
    4 WRITE(6,610)(M(I,J),J=1,NDIM)
      TOLMLIN=1.E-7
      TOLMRIC=2.E-5
   31 QNMAT(3,3)=(4.*(SGMTURB**2)*A(2,3)*(A(1,2)*A(2,3))**2)/
     * (A(1,2)*(A(1,2)*2.*A(2,3)))
C      IAKLMNM4
```

```
      WRITE(6,900)SGMTJRB,QNMAT(3,3)
  900 FORMAT(4X,8HSGMTJRB=,E12.5,  3X,
     * 13H  QNMAT(3,3)=,E12.5)
      WRITE(6,847)SGM1LS4,SGMM2,SGMM3
  847 FORMAT(4X,8HSGM1LS4=,E12.5,3X,6HSGMM2=,E12.5,3X,6HSGMM3=,E12.5)
      WRITE(6,837)SGMM4
  837 FORMAT(4X,6HSGMM4= ,E12.5)
      WRITE(6,901)TOLMLIN,TOLMRIC
  901 FORMAT(4X,8HTOLMLIN=,E12.5,10H  TOLMRIC=,E12.5)
      RKLMINV(1,1)=1./SGM1LS4**2
      RKLMINV(2,2)=1./SGMM2**2
      RKLMINV(3,3)=1./SGMM3**2
      RKLMINV(4,4)=1./SGMM4**2
C  NOW CALCULATE P=M TRANSPOSE*RKLMINV.
      DO 53 I=1,NDIM
      DO 59 J=1,MDIM
      TEMP=0.
      DO 55 K=1,MDIM
   55 TEMP=TEMP+M(K,I)*RKLMINV(K,J)
   59 P(I,J)=TEMP
   53 CONTINUE
C  NEXT CALCULATE MT*RKLMINV*M
      DO 3 I=1,NDIM
      DO 2 J=1,NDIM
      TEMP=0.
      DO 1 K=1,MDIM
    1 TEMP=TEMP+P(I,K)*M(K,J)
    2 SKLMN(I,J)=TEMP
    3 CONTINUE
      T3=0.
      ITBASE=32
      CALL MRIC(NDIM,AT,SKLMN,QNMAT,RKLMN,ZKT,TOLMRIC,T3,ITBASE)
C  THE KALMAN RICATTI EQUATION OPERATES ON A TRANSPOSE
C   S YIELDS THE TRANSPOSE OF THE CLOSED LOOP SYSTEM ZKT.
      CALL TRANS2(NDIM,NDIM,ZKT,ZK)
C  THE CLOSED LOOP SYSTEM MATRIX IS ZK
      WRITE(6,810)
  810 FORMAT(6X,22HTHE KALMAN Z MATRIX IS )
      DO 67 I=1,NDIM
   67 WRITE(6,610)(ZK(I,J),J=1,NDIM)
      CALL EGNO(ZK,RR,RI,UNIT,0)
      CALL MAT3A(NDIM,NDIM,RKLMN,SKLMN,TEMP)
C  FORMS TEMP=RKLMN*SKLMN*RKLMN
      CALL MADD1(NDIM,NDIM,QNMAT,TEMP,QPLSRSR,1.)
C  FORMS QPLSRSR=QNMAT+RKLMN*SKLMN*RKLMN
C  QPLSRSR IS THE INPUT COVARIANCE FOR KALMAN ESTIMATOR
      WRITE(6,611)
  611 FORMAT(9X,20HTHE RKLMN MATRIX IS    )
      DO 69 I=1,NDIM
   69 WRITE(6,610)(RKLMN(I,J),J=1,NDIM)
      CALL PREP(ZK,QPLSRSR,ZKT,COVARX,UNIT,TEMP)
      WRITE(6,820)
  820 FORMAT(6X,37HTHE COVARIANCE MATRIX AFTER KALMAN IS )
C   RKLMN SHOULD BE THE COVARIANCE OF X AFTER KALMAN!!!
      CALL MLINEQ(NDIM,ZKT,TEMP,COVARX,TOLMLIN)
      DO 68 I=1,NDIM
   68 WRITE(6,610)(COVARX(I,J),J=1,NDIM)
C      IAKLMNM4
```

```
      SGMERR=SQRT(COVARX(1,1)+COVARX(4,4)-2.*COVARX(1,4))
      WRITE(5,791)SGMERR
   37 WRITE(6,891)
  891 FORMAT(4X,5HENTER ,/,4X,
     + 18H1 FOR NEW SGM1LS4 ,/,4X,
     + 18H2 FOR NEW SGMTURB  ,/,4X,
     + 17H3 FOR NEW TOLMLIN ,/,4X,
     + 19H4 FOR NEW TOLMRIC  ,/,4X,
     + 17H5 FOR NEW SGMM2  ,/,4X,
     + 16H6 FOR NEW SGM3  ,/,4X,
     + 16H7 FOR NEW SGM4  ,/,4X,
     + 31H8 FOR OPTIMAL CONTROL SEGMENT  )
      READ*,IPOINT
      IF(IPOINT.GT.8)GO TO 99
      GO TO (36,38,41,44,47,48,49,39)IPOINT
   36 WRITE(6,851)
  851 FORMAT(6X,10HSGM1LS4=  )
      READ*,SGM1LS4
      GO TO 31
   38 WRITE(6,853)
  853 FORMAT(6X,10HSGMTURB=  )
      READ*,SGMTURB
      GO TO 31
   41 WRITE(6,999)
  999 FORMAT(6X,10HTOLMLIN=  )
      READ*,TOLMLIN
      GO TO 31
   44 WRITE(6,998)
  998 FORMAT(6X,10HTOLMRIC=  )
      READ*,TOLMRIC
      GO TO 31
   47 WRITE(6,991)
  991 FORMAT(6X,8HSGMM2=  )
      READ*,SGMM2
      GO TO 31
   48 WRITE(6,989)
  989 FORMAT(6X,8HSGMM3=  )
      READ*,SGMM3
      GO TO 31
   49 WRITE(6,849)
  849 FORMAT(6X,8HSGMM4=  )
      READ*,SGMM4
      GO TO 31
   39 WRITE(6,630)
  630 FORMAT(9X,15HTHE B VECTOR IS)
      WRITE(6,610)(B(I),I=1,NDIM)
   13 WRITE(6,690)
  690 FORMAT(9X,15HTHE Q MATRIX IS)
      DO 62 I=1,6
   62 WRITE(6,610)(Q(I,J),J=1,NDIM)
   15 WRITE(6,670)ALPHA
  670 FORMAT(9X,9H ALPHA IS ,E12.5)
   16 RINV=1./R
      WRITE(6,601)RINV
  601 FORMAT(9X,6HRINV= ,E12.5)
      DO 70 I=1,NDIM
      DO 80 J=1,NDIM
      UNIT(I,J)=0.
   80 S(I,J)=B(I)*RINV*B(J)
   70 UNIT(I,I)=1.
C     IAKLMNM4
```

```
C  S=B*RINV*BTRANSPOSE
      DO 90 I=1,NDIM
   90 A(I,I)=A(I,I)+ALPHA
C  THIS ALLOWS AN UPPER BOUND ON MAT FREQ OF EACH SV
      TOLMRIC=0.
C  SETTING TOLMRIC.LT.1.E-15,RESULTS IN MRIC SETTING TOL=1.E-3
      WRITE(6,730)TOLMRIC
  730 FORMAT(9X,9HTOLMRIC= ,E12.5)
      T3=0.
C  SETTING T3=0. ALLOWS MRIC TO CALCULATE T3 INTERNALLY.
      WRITE(6,740)T3
  740 FORMAT(9X,4HT3= ,E12.5)
      ITBASE=0
C  IF ITBASE=0,MAXIT=30+N IF ITBASE.NE.0,MAXIT=ITBASE+N
      WRITE(6,750)ITBASE
  750 FORMAT(9X,8HITBASE= ,I2)
      CALL MRIC(NDIM,A,S,Q,RK,Z,TOLMRIC,T3,ITBASE)
      DO 33 I=1,NDIM
      Z(I,I)=Z(I,I)-ALPHA
   33 A(I,I)=A(I,I)-ALPHA
C  THESE SUBTRACTIONS CANCEL THE ADDITION OF STATEMENT 90.
C  INPUTS ARE A,S,&Q. OUTPUTS ARE RK&Z(=A-S*RK)
C  P IS THE SOLUTION TO THE RICCATI EQUATION.
C  Z IS THE CLOSED LOOP SYSTEM WITH OPT S.V. FEEDBACK.
      WRITE(6,699)
  699 FORMAT(9X,30HTHE 5TH ROW OF THE Z MATRIX IS )
   95 WRITE(6,610)(Z(5,J),J=1,NDIM)
      CALL EGNO(Z,RR,RI,UNIT,0)
   73 WRITE(6,780)
  780 FORMAT(9X,5HENTER,/,9X,16H1 FOR COVARIANCE ,/,9X,
     + 15H2 FOR NEW ALPHA ,/,9X,
     + 13H3 FOR NEW Q'S ,/,9X,
     + 12H4 FOR NEW R )
      READ*,IPOINT
      IF(IPOINT.LT.1.OR.IPOINT.GT.4)GO TO 99
      GO TO (98,17,23,29)IPOINT
   17 WRITE(6,782)
  782 FORMAT(3X,12HENTER ALPHA )
      READ*,ALPHA
      IF(ALPHA.LT.0.)GO TO 98
      GO TO 15
   23 WRITE(6,784)
  784 FORMAT(3X,38HENTER ROW&COL OF Q OR 0 0 TO EXECUTE. )
      READ*,I,J
      IF(I.EQ.0)GO TO 13
      IF(I.GT.NDIM)GO TO 98
      WRITE(6,785)I,J
  785 FORMAT(3X,8HENTER Q(,I1,1H,,I1,2H)  )
      READ*,Q(I,J)
      Q(J,I)=Q(I,J)
      GO TO 23
   29 WRITE(6,786)
  786 FORMAT(3X,8HENTER R )
      READ*,R
      IF(R.LE.0.)GO TO 98
      GO TO 16
   98 CALL PREP(Z,QMAT,ZT,COVARX,UNIT,TEMP)
      CALL MLINEQ(NDIM,ZT,TEMP,COVARX,TOLMLIN)
C     IAKLMNM4
```

```
      WRITE(6,792)
  792 FORMAT(9X,22HTHE COVARIANCE OF X IS)
      DO 43 I=1,NDIM
   43 WRITE(6,610)(COVARX(I,J),J=1,NDIM)
      SGMERR=SQRT(COVARX(1,1)+COVARX(4,4)-2.*COVARX(1,4))
      WRITE(6,791)SGMERR
  791 FORMAT(9X,8HSGMERR= ,E12.5)
      WRITE(6,777)
  777 FORMAT(7X,5HENTER,/,7X,
     + 26H1 TO REPEAT KALMAN SECTION ,/,7X,
     + 35H2 TO REPEAT OPTIMAL CONTROL SECTION,/,7X,
     + 10H3 TO EXIT )
      READ*,IPOINT
      IF(IPOINT.LT.1.OR.IPOINT.GE.3)GO TO 99
      GO TO(37,73,99)IPOINT
   99 STOP
      END
      SUBROUTINE EGVO(Z,RR,RI,UNIT,IZERO)
      COMMON/MAIN1/NDIM,NDIM1,COM1
      COMMON/MAIN2/COM2
      COMMON/INOU/KIN,KOUT,KPUNCH
      REAL Z(6,6),RR(6),RI(6),UNIT(6,6)
      CALL EIGEN(NDIM,Z,RR,RI,UNIT,IZERO)
      WRITE(6,769)
  769 FORMAT(11X,9HREAL PART,5X,24HIMAG PART OF EIGENVALUES )
      DO 40 I=1,NDIM
   40 WRITE(6,770)RR(I),RI(I)
  770 FORMAT(9X,E12.5,3X,E12.5)
      RETURN
      END
      SUBROUTINE PREP(Z,QNMAT,ZT,COVARX,UNIT,TEMP)
      REAL Z(6,6),QNMAT(6,6),ZT(6,6),COVARX(6,6),UNIT(6,6),TEMP(6,6)
      DO 40 I=1,6
      DO 41 J=1,6
      ZT(J,I)=Z(I,J)
      COVARX(I,J)=0.
      UNIT(I,J)=0.
   41 TEMP(I,J)=QNMAT(I,J)
   40 UNIT(I,I)=1.
      RETURN
      END
```

```
..
 PROGRAM= IAKLMNM4,CY=5
        THE A MATRIX IS
 -.47100E+02    .47100E+02   0.            0.            0.            0.
 0.            -.22000E+04    .22000E+04   0.            0.            0.
 0.             0.           -.22000E+04   0.            0.            0.
 0.             0.            0.           0.             .10000E+01   0.
 0.             0.            0.           0.            0.            0.
  .10000E+01    0.            0.          -.10000E+01    0.            0.
     THE M MATRIX IS
  .10000E+01    0.            0.          -.10000E+01    0.            0.
 0.             0.            0.           .10000E+01    0.            0.
 0.             0.            0.           0.            0.            0.
 0.             0.            0.           0.            0.             .10000E+01
   SGMTURB=   .10000E+01      QNMAT(3,3)=   .21214E+06
   SGM1LS4=   .87000E-04    SGMM2=   .13790E-05    SGMM3=   .10000E+02
   SGMM4=   .10000E-08
   TOLMLIN=   .10000E-06  TOLMRIC=   .20000E-04

RICCATI SOLN IN 29 ITERATIONS
     THE KALMAN Z MATRIX IS
 -.18678E+04    .47100E+02   0.             .13164E+04   0.            -.55238E+09
 -.46496E+06   -.22000E+04    .22000E+04    .46338E+06   0.            -.11194E+12
 -.14352E+07    0.           -.22000E+04    .14346E+07   0.            -.28916E+12
  .18443E-03    0.            0.           -.50501E+03    .10000E+01    .33142E+02
  .30153E-01    0.            0.           -.63780E+05   0.             .53176E+04
  .92702E+00    0.            0.           -.92700E+00   0.            -.32626E+05
          REAL PART      IMAG PART OF EIGENVALUES
         -.57363E+04      .13600E+05
         -.57363E+04     -.13600E+05
         -.13711E+05      .55753E+04
         -.13711E+05     -.55753E+04
         -.25251E+03      .45630E+01
         -.25251E+03     -.45630E+01
        THE RKLMN MATRIX IS
  .13782E-04    .35193E-02    .10863E-01    .95895E-09    .12106E-06    .55238E-09
  .35193E-02    .11094E+01    .43294E+01    .29989E-08    .41431E-06    .11194E-06
  .10863E-01    .43294E+01    .25668E+02    .11380E-08    .11464E-06    .28916E-06
  .95895E-09    .29989E-08    .11380E-08    .96035E-09    .12129E-06   -.33142E-16
  .12106E-06    .41431E-06    .11464E-06    .12129E-06    .17947E-04   -.53176E-14
  .55238E-09    .11194E-06    .28916E-06   -.33142E-16   -.53176E-14    .32626E-13
     THE COVARIANCE MATRIX AFTER KALMAN IS
  .13782E-04    .35193E-02    .10863E-01    .59994E-09    .60604E-07    .55238E-09
  .35193E-02    .11094E+01    .43294E+01    .17703E-08    .20909E-06    .11194E-06
  .10863E-01    .43294E+01    .25668E+02    .12882E-08    .15173E-06    .28916E-06
  .59994E-09    .17703E-08    .12882E-08    .60026E-09    .60643E-07   -.91899E-17
  .60604E-07    .20909E-06    .15173E-06    .60643E-07    .76588E-05   -.11199E-14
  .55238E-09    .11194E-06    .28916E-06   -.91899E-17   -.11199E-14    .32626E-13
        SGMERR=    .37123E-02
  ENTER
  1 FOR NEW SGM1LS4
  2 FOR NEW SGMTURB
  3 FOR NEW TOLMLIN
  4 FOR NEW TOLMRIC
  5 FOR NEW SGMM2
  6 FOR NEW SGMM3
  7 FOR NEW SGMM4
  8 FOR OPTIMAL CONTROL SEGMENT  8
```

```
        THE B VECTOR IS
 0.             0.             0.             0.              .10000E+01   0.
        THE Q MATRIX IS
  .10000E+10   0.             0.            -.10000E+10   0.             0.
 0.             0.             0.             0.             0.             0.
 0.             0.             0.             0.             0.             0.
-.10000E+10   0.             0.              .10000E+10   0.             0.
 0.             0.             0.             0.              .50000E+02   0.
 0.             0.             0.             0.             0.              .50000E+16
         ALPHA IS  .47000E+02
        RINV=    .95238E+05
        TOLMPIC=  0.
        T3=  0.
        ITBASE=  0
GRAMMIAN IS 6X 6 OF RANK  3

RICCATI SOLN IN 14 ITERATIONS
        THE 5TH ROW OF THE Z MATRIX IS
  .19930E+08    .21298E+06    .84523E+05  -.20247E+08  -.67745E+04    .22763E+11
          REAL PART      IMAG PART OF EIGENVALUES
         -.22313E+04      .22063E+04
         -.22313E+04     -.22063E+04
         -.23119E+04     0.
         -.47099E+02     0.
         -.22000E+04     0.
         -.22000E+04     0.
        ENTER
        1 FOR COVARIANCE
        2 FOR NEW ALPHA
        3 FOR NEW Q'S
        4 FOR NEW R 1

        THE COVARIANCE OF X IS
  .10000E+01    .10000E+01    .50530E+00    .10006E+01    .71247E+00    .12059E-05
  .10000E+01    .24107E+02    .24107E+02    .98552E+00    .10970E+04    .14953E-04
  .50530E+00    .24107E+02    .48214E+02    .48688E+00    .10711E+04    .83711E-05
  .10006E+01    .98552E+00    .48688E+00    .10013E+01   -.17211E-10    .12059E-05
  .71247E+00    .10970E+04    .10711E+04   -.17211E-10    .52217E+05    .67526E-03
  .12059E-05    .14953E-04    .83711E-05    .12059E-05    .67526E-03    .15466E-10
        SIGMERR=    .52722E-02
      ENTER
      1 TO REPEAT KALMAN SECTION
      2 TO REPEAT OPTIMAL CONTROL SECTION
      3 TO EXIT 3

     STOP
      8.947 CP SECONDS EXECUTION TIME
COMMAND-
```

```
      PROGRAM MAIN(INPUT,OUTPUT,TAPE5,TAPE6=OUTPUT,TAPE7)

C  SINGLE CHANNEL CASE AUGUST 12 1114
C USES KLEINMAN'S ROUTINES
C  USES MRIC TO CALCULATE KALMAN GAIN.
C  REQUIRES MEASUREMENT MATRIX 4 BY 6.
C  USES MRIC TO CALCULATE OPTIMAL CONTROL.
C  CALCULATES EIGENVALUES OF Z(=A-S*P),
C  USES MLINEQ TO CALCULATE THE COVARIANCE OF OUTPUT X VECTOR.
C  REQUIRES INPUT IN FILE TAPE5 & INPUT FROM TERMINAL.
C  OUTPUTS THE DV & Q12 MATRIX ON TAPE7.
C  MUST BE FOLLOWED BY EGNMLN12.
      REAL X(6),XDOT(6),C(24),W(6,9),TEMP(6,6),ZT(6,6),M(4,6),P(6,4),
     + Q(6,6),S(6,6),COM1(6,6),COM2(6,6),COVARX(6,6),ZK(6,6),
     + A(6,6),B(6),UNIT(6,6),RR(6),RI(6),QNMAT(6,6),SKLMN(6,6),
     + Z(6,6),U(6),RKLMINV(4,4),AT(6,6),ZKT(6,6),DV(12,12),Q12(12,12),
     + RKOPT(6,6),RKLMN(6,6),GPLSRSR(6,6)
      COMMON/MAIN1/NDIM,NDIM1,COM1
      COMMON/MAIN2/COM2
      COMMON/INOU/KIN,KOUT,KPUNCH
C THIS COMMON AREA IS REQUIRED FOR KLEINMAN'S ROUTINES
      DATA QNMAT/36*0./
      DATA RKLMINV/16*0./
      DATA DV/144*0./
      DATA Q12/144*0./
      N=6
      NDIM=6
      NDIM1=NDIM+1
      MDIM=4
      NDV=12
      NHALF=NDV/2
      NHALF1=NHALF+1
      KIN=5
      KOUT=6
      KPUNCH=7
      REWIND 5
      WRITE(6,599)
  599 FORMAT(2X,27HPROGRAM=  COVARTST    ,CY=3    )
      DO 10 I=1,NDIM
   10 READ(5,500)(A(I,J),J=1,NDIM)
  500 FORMAT(6E12.5)
      READ(5,500)(X(I),I=1,N)
      READ(5,500)(B(I),I=1,NDIM)
      READ(5,500)(U(I),I=1,N)
      DO 9 I=1,MDIM
    9 READ(5,500)(M(I,J),J=1,NDIM)
      DO 12 I=1,NDIM
   12 READ(5,500)(Q(I,J),J=1,NDIM)
      READ(5,500)ALPHA
      READ(5,500)R
      READ(5,500)SGMTURB,SGM1LS4,SGMM2,SGMM3,SGMM4
      WRITE(6,600)
  600 FORMAT(9X,15HTHE A MATRIX IS)
      DO 60 I=1,NDIM
      DO 19 K=1,NDIM
   19 AT(K,I)=A(I,K)
   60 WRITE(6,610)(A(I,J),J=1,NDIM)
  610 FORMAT(6(1X,E12.5))
C     COVARTST
```

```
      WRITE(6,880)
  880 FORMAT(6X,15HTHE M MATRIX IS )
      DO 4 I=1,MDIM
    4 WRITE(6,610)(M(I,J),J=1,NDIM)
      TOLMLIN=2.E-5
      TOLMRIC=2.E-5
   31 QNMAT(3,3)=(4.*(SGMTURB**2)*A(2,3)*(A(1,2)+A(2,3))**2)/
     + (A(1,2)*(A(1,2)+2.*A(2,3)))
      WRITE(6,900)SGMTURB,QNMAT(3,3)
  900 FORMAT(4X,8HSGMTURB=,E12.5,  3X,
     + 13H  QNMAT(3,3)=,E12.5)
      WRITE(6,847)SGM1LS4,SGMM2,SGMM3
  847 FORMAT(4X,8HSGM1LS4=,E12.5,3X,6HSGMM2=,E12.5,3X,6HSGMM3=,E12.5)
      WRITE(6,837)SGMM4
  837 FORMAT(4X,6HSGMM4= ,E12.5)
      WRITE(6,901)TOLM_IN,TOLMRIC
  901 FORMAT(4X,8HTOLMLIN=,E12.5,10H  TOLMRIC=,E12.5)
      RKLMINV(1,1)=1./SGM1LS4**2
      RKLMINV(2,2)=1./SGMM2**2
      RKLMINV(3,3)=1./SGMM3**2
      RKLMINV(4,4)=1./SGMM4**2
C  NOW CALCULATE P=M TRANSPOSE*RKLMINV.
      DO 53 I=1,NDIM
      DO 59 J=1,MDIM
      TEMP=0.
      DO 55 K=1,MDIM
   55 TEMP=TEMP+M(K,I)*RKLMINV(K,J)
   59 P(I,J)=TEMP
   53 CONTINUE
C  NEXT CALCULATE MT*RKLMINV*M
      DO 3 I=1,NDIM
      DO 2 J=1,NDIM
      TEMP=0.
      DO 1 K=1,MDIM
    1 TEMP=TEMP+P(I,K)*M(K,J)
    2 SKLMN(I,J)=TEMP
    3 CONTINUE
      T3=0.
      ITBASE=32
      CALL MRIC(NDIM,AT,SKLMN,QNMAT,RKLMN,ZKT,TOLMRIC,T3,ITBASE)
C  THE KALMAN RICATTI EQUATION OPERATES ON A TRANSPOSE
C   & YIELDS THE TRANSPOSE OF THE CLOSED LOOP SYSTEM ZKT.
      CALL TRANSI(N,ZKT,ZK)
C  THE CLOSED LOOP KALMAN SYSTEM MATRIX IS ZK
      WRITE(6,810)
  810 FORMAT(6X,22HTHE KALMAN Z MATRIX IS )
      DO 67 I=1,NDIM
   67 WRITE(6,610)(ZK(I,J),J=1,NDIM)
      CALL MAT3A(N,N,R(LMN,SKLMN,TEMP)
C  FORMS TEMP=RKLMN*SKLMN*RKLMN
      CALL MADD1(N,N,GVMAT,TEMP,QPLSRSR,1.)
C  FORMS QPLSRSR=QNMAT+RKLMN*SKLMN*RKLMN
C  QPLSRSR IS THE INPUT COVARIANCE MATRIX FOR KALMAN ESTIMATOR.
      WRITE(6,607)
  607 FORMAT(9X,22HTHE QPLSRSR MATRIX IS  )
      DO 79 I=1,N
   79 WRITE(6,610)(QPLSRSR(I,J),J=1,N)
      CALL ECNO(ZK,RR,RI,UNIT,0)
C     COVARTST
```

```
      WRITE(6,601)
  601 FORMAT(9X,20HTHE RKLMN MATRIX IS    )
      DO 69 I=1,N
   69 WRITE(6,610)(RKLMN(I,J),J=1,N)
      WRITE(6,604)
  604 FORMAT(9X,30HZK*RKLMN*RKLMN*ZKT*QPLSRSR IS    )
      CALL CVRTST(RKLMN,ZK,ZKT,QPLSRSR,TEMP,N)
C  FORMS TEMP=ZK*RKLMN*RKLMN*ZKT*QPLSRSR
   32 CALL PREP(ZK,QPLSRSR,ZKT,COVARX,UNIT,TEMP)
C  PREP SETS TEMP=QPLSRSR & ZKT=ZK TRANSPOSE.
      WRITE(6,820)
  320 FORMAT(6X,37HTHE COVARIANCE MATRIX AFTER KALMAN IS )
C      RK SHOULD BE THE COVARIANCE OF X AFTER KALMAN!!!
      CALL MLINEQ(NDIM,ZKT,TEMP,COVARX,TOLMLIN)
      DO 68 I=1,NDIM
   68 WRITE(6,610)(COVARX(I,J),J=1,NDIM)
      SGMERR=SQRT(COVARX(1,1)+COVARX(4,4)-2.*COVARX(1,4))
      WRITE(6,791)SGMERR
      WRITE(6,605)
  605 FORMAT(9X,32HZK*COVARX*COVARX*ZKT*QPLSRSR IS    )
      CALL CVRTST(COVARX,ZK,ZKT,QPLSRSR,TEMP,N)
C  FORMS TEMP=ZK*COVARX*COVARX*ZKT*QPLSRSR & OUTPUTS IT
   37 WRITE(6,891)
  891 FORMAT(4X,5HENTER ,/,4X,
     + 18H1 FOR NEW SGM1LS4 ,/,4X,
     + 18H2 FOR NEW SGMTURB  ,/,4X,
     + 17H3 FOR NEW TOLMLIN ,/,4X,
     + 19H4 FOR NEW TOLMRIC   ,/,4X,
     + 17H5 FOR NEW SGMM2   ,/,4X,
     + 16H6 FOR NEW SGMM3  ,/,4X,
     + 16H7 FOR NEW SGMM4   ,/,4X,
     + 31H8 FOR OPTIMAL CONTROL SEGMENT    )
      READ*,IPOINT
      IF(IPOINT.GT.8)GO TO 99
      GO TO (36,38,41,44,47,48,49,39)IPOINT
   36 WRITE(6,851)
  851 FORMAT(6X,10HSGM1LS4=    )
      READ*,SGM1LS4
      GO TO 31
   38 WRITE(6,853)
  853 FORMAT(6X,10HSGMTURB=    )
      READ*,SGMTURB
      GO TO 31
   41 WRITE(6,999)
  999 FORMAT(6X,10HTOLMLIN=    )
      READ*,TOLMLIN
      GO TO 32
   44 WRITE(6,998)
  998 FORMAT(6X,10HTOLMRIC=    )
      READ*,TOLMRIC
      GO TO 31
   47 WRITE(6,991)
  991 FORMAT(6X,8HSGMM2=    )
      READ*,SGMM2
      GO TO 31
   48 WRITE(6,989)
  989 FORMAT(6X,8HSGMM3=    )
      READ*,SGMM3
      GO TO 31
C     COVARTST
```

```
   49 WRITE(6,849)
  849 FORMAT(6X,6HSGMM4=    )
      READ*,SGMM4
      GO TO 31
   39 WRITE(6,630)
  630 FORMAT(9X,15HTHE B VECTOR IS)
      WRITE(6,610)(B(I),I=1,NDIM)
   13 WRITE(6,690)
  690 FORMAT(9X,15HTHE Q MATRIX IS)
      DO 62 I=1,6
   62 WRITE(6,610)(Q(I,J),J=1,NDIM)
   15 WRITE(6,670)ALPHA
  670 FORMAT(9X,9H ALPHA IS ,E12.5)
   16 RINV=1./R
      WRITE(6,603)RINV
  603 FORMAT(9X,6HRINV= ,E12.5)
      DO 70 I=1,NDIM
      DO 80 J=1,NDIM
      UNIT(I,J)=0.
   80 S(I,J)=B(I)*RINV*B(J)
   70 UNIT(I,I)=1.
C  S=B*RINV*BTRANSPOSE
      DO 90 I=1,NDIM
   90 A(I,I)=A(I,I)+ALPHA
C  THIS ALLOWS AN UPPER BOUND ON WAT FREW OF EACH SV
      TOLMRIC=0.
C  SETTING TOLMRIC.LT.1.E-15.RESULTS IN MRIC SETTING TOL=1.E-3
      WRITE(6,730)TOLMRIC
  730 FORMAT(9X,9HTOLMRIC= ,E12.5)
      T3=0.
C  SETTING T3=0. ALLOWS MRIC TO CALCULATE T3 INTERNALLY.
      WRITE(6,740)T3
  740 FORMAT(9X,4HT3= ,E12.5)
      ITBASE=0
C  IF ITBASE=0,MAXIT=30+N IF ITBASE.NE.0,MAXIT=ITBASE+N
      WRITE(6,750)ITBASE
  750 FORMAT(9X,8HITBASE= ,I2)
      CALL MRIC(NDIM,A,S,Q,RKOPT,Z,TOLMRIC,T3,ITBASE)
      DO 33 I=1,NDIM
      Z(I,I)=Z(I,I)-ALPHA
   33 A(I,I)=A(I,I)-ALPHA
C  THESE SUBTRACTIONS CANCEL THE ADDITION OF STATEMENT 90.
C  INPUTS ARE A,S,XJ. OUTPUTS ARE RK&Z(=A-S*RK)
C  RK IS THE SOLUTION TO THE RICCATI EQUATION.
C  Z IS THE CLOSED LOOP SYSTEM WITH OPT S.V. FEEDBACK.
      WRITE(6,699)
  699 FORMAT(9X,30HTHE 5TH ROW OF THE Z MATRIX IS )
   95 WRITE(6,610)(Z(5,J),J=1,NDIM)
      CALL EGNO(Z,RR,RI,UNIT,0)
   73 WRITE(6,780)
  780 FORMAT(9X,5HENTER,/,9X,16H1 FOR COVARIANCE ,/,9X,
     + 15H2 FOR NEW ALPHA ,/,9X,
     + 13H3 FOR NEW Q'S ,/,9X,
     + 12H4 FOR NEW R )
      READ*,IPOINT
      IF(IPOINT.LT.1.OR.IPOINT.GT.4)GO TO 99
      GO TO (98,17,25,29)IPOINT
C     COVARTST
```

```
 17 WRITE(6,782)
782 FORMAT(3X,12HENTER ALPHA )
    READ*,ALPHA
    IF(ALPHA.LT.0.)GO TO 98
    GO TO 15
 23 WRITE(6,784)
784 FORMAT(3X,38HENTER ROW&COL OF Q OR 0 0 TO EXECUTE. )
    READ*,I,J
    IF(I.EQ.0)GO TO 13
    IF(I.GT.NDIM)GO TO 98
    WRITE(6,785)I,J
785 FORMAT(3X,8HENTER Q(,I1,1H,,I1,2H)  )
    READ*,Q(I,J)
    Q(J,I)=Q(I,J)
    GO TO 23
 29 WRITE(6,786)
786 FORMAT(3X,8HENTER R )
    READ*,R
    IF(R.LE.0.)GO TO 98
    GO TO 16
    CALL PREP(Z,QNMAT,ZT,COVARX,UNIT,TEMP)
 98 CALL MLINEQ(NDIM,ZT,TEMP,COVARX,TOLMLIN)
    WRITE(6,792)
792 FORMAT(9X,22HTHE COVARIANCE OF X IS)
    DO 43 I=1,NDIM
 43 WRITE(6,610)(COVARX(I,J),J=1,NDIM)
    SGMERR=SQRT(COVARX(1,1)+COVARX(4,4)-2.*COVARX(1,4))
    WRITE(6,791)SGMERR
791 FORMAT(9X,8HSGMERR= ,E12.5)
    WRITE(6,777)
777 FORMAT(7X,5HENTER,/,7X,
   + 26H1 TO REPEAT KALMAN SECTION ,/,7X,
   + 35H2 TO REPEAT OPTIMAL CONTROL SECTION,/,7X,
   + 28H3 TO WRITE DV & Q12 ON TAPE7  )
    READ*,IPOINT
    IF(IPOINT.LT.1.OR.IPOINT.GE.4)GO TO 99
    GO TO(37,73,51)IPOINT
C   THIS SECTION FORMS THE DV & Q12 MATRICES FOR OPT SYSTEM & ESTIMATOR.
C   UPPER LEFT OF DV IS THE CLOSED LOOP OPTIMAL MATRIX.
C   UPPER RIGHT OF DV IS -BKT.
C   LOWER RIGHT OF DV IS THE CLOSED LOOP KALMAN ESTIMATOR.
C   THE UPPER LEFT OF Q12 IS THE QNMAT MATRIX.
C   THE UPPER RIGHT OF Q12 IS THE QNMAT MATRIX.
C   THE LOWER LEFT OF Q12 IS THE QNMAT MATRIX.
C   THE LOWER RIGHT OF Q12 IS THE QPLSRSR MATRIX.
C   ALL OTHER AREAS IN DV  REMAIN ZEROS.
 51 DO 100 I=1,NHALF
    INHALF=I+NHALF
    DO 110 J=1,NHALF
    JNHALF=J+NHALF
    Q12(I,J)=QNMAT(I,J)
    Q12(INHALF,JNHALF)=QPLSRSR(I,J)
    Q12(I,JNHALF)=QNMAT(I,J)
    Q12(INHALF,J)=QNMAT(I,J)
C   BOTH Q12 & QNMAT ARE SYMETRIC
    TMP=Z(I,J)
    DV(I,J)=TMP
    DV(I,JNHALF)=A(I,J)-TMP
110 DV(INHALF,JNHALF)=ZK(I,J)
100 CONTINUE
C       COVARTST
```

```
      WRITE(6,826)
  826 FORMAT(9X,35HTHE UPPER LEFT OF THE DV MATRIX IS  )
      DO 140 I=1,NHALF
  140 WRITE(6,610)(DV(I,J),J=1,NHALF)
      WRITE(6,327)
  327 FORMAT(9X,36HTHE UPPER RIGHT OF THE DV MATRIX IS  )
      DO 150 I=1,NHALF
  150 WRITE(6,610)(DV(I,J),J=NHALF1,NDV)
      DO 120 I=1,NDV
  120 WRITE(7,838)(DV(I,J),J=1,NDV)
  838 FORMAT(12E12.5)
      DO 130 I=1,NDV
  130 WRITE(7,838)(Q12(I,J),J=1,NDV)
      WRITE(6,824)
  824 FORMAT(9X,34HTHE 11TH ROW OF THE DV MATRIX IS  )
      WRITE(6,610)(DV(11,I),I=1,NDV)
      WRITE(6,825)
  825 FORMAT(9X,35HTHE 11TH ROW OF THE Q12 MATRIX IS  )
      WRITE(6,610)(Q12(11,I),I=1,NDV)
      WRITE(6,823)
  823 FORMAT(3X,32HNOW PROCESS TAPE7 WITH EGNMLN12.  )
   99 STOP
      END
      SUBROUTINE EGNO(Z,RR,RI,UNIT,IZERO)
      COMMON/MAIN1/NDIM,NDIM1,COM1
      COMMON/MAIN2/COM2
      COMMON/INOU/KIN,KOUT,KPUNCH
      REAL Z(6,6),RR(6),RI(6),UNIT(6,6)
      CALL EIGEN(NDIM,Z,RR,RI,UNIT,IZERO)
      WRITE(6,769)
  769 FORMAT(11X,9HREAL PART,5X,24HIMAG PART OF EIGENVALUES )
      DO 40 I=1,NDIM
   40 WRITE(6,770)RR(I),RI(I)
  770 FORMAT(9X,E12.5,3X,E12.5)
      RETURN
      END
      SUBROUTINE PREP(Z,QNMAT,ZT,COVARX,UNIT,TEMP)
      REAL Z(6,5),QNMAT(6,6),ZT(6,6),COVARX(6,6),UNIT(6,6),TEMP(6,6)
      DO 40 I=1,6
      DO 41 J=1,6
      ZT(J,I)=Z(I,J)
      COVARX(I,J)=0.
      UNIT(I,J)=0.
   41 TEMP(I,J)=QNMAT(I,J)
   40 UNIT(I,I)=1.
      RETURN
      END
C     COVARTST
```

```
      SUBROUTINE CVRTST(RKLMN,ZK,ZKT,QPLSRSR,TEMP,N)
      REAL RKLMN(6,6),ZK(6,6),ZKT(6,6),QPLSRSR(6,6),TEMP(6,6)
      COMMON/MAIN1/NDIM,NDIM1,COM1
      COMMON/MAIN2/COM2
      COMMON/INOU/KIN,KOUT,KPUNCH
      CALL EQUATE(TEMP,QPLSRSR,N,N)
C  SETS TEMP=QPLSRSR
      CALL MMULS(RKLMN,ZKT,N,N,N,TEMP)
C  FORMS TEMP=RKLMN*ZKT+TEMP
      CALL MMULS(ZK,RKLMN,N,N,N,TEMP)
C  FORMS TEMP=ZK*RKLMN+RKLMN*ZKT+QPLSRSR
C  TEMP SHOULD BE CLOSE TO ZERO IF RKLMN IS THE COVARIANCE MATRIX
      DO 76 I=1,N
   76 WRITE(6,610)(TEMP(I,J),J=1,N)
  610 FORMAT(6(1X,E12.5))
      RETURN
      END
```

```
 PROGRAM=  COVAPTIT   ,CY=3
        THE A MATRIX IC
 -.47100E+02   .47100E+02  0.            0.            0.            0.
 0.           -.22000E+04   .22000E+04  0.            0.            0.
 0.            0.           -.22000E+04  0.            0.            0.
 0.            0.            0.           0.            .10000E+01   0.
 0.            0.            0.           0.            0.           0.
  .10000E+01   0.            0.          -.10000E+01    0.           0.
     THE M MATRIX IC
  .10000E+01   0.            0.          -.10000E+01    0.           0.
 0.            0.            0.           .10000E+01    0.           0.
 0.            0.            0.           0.            0.           0.
 0.            0.            0.           0.            0.            .10000E+01
   IGMTURB=  .10000E+01     ONMAT(3,3)=  .21214E+06
   IGM1LG4=  .87000E-04   IGMM2=  .13790E-05   IGMM3=  .10000E+02
   IGMM4=  .10000E-08
   TOLMLIN=  .20000E-04  TOLMPIC=  .20000E-04

PICCATI IOLN IN 29 ITERATIONI
     THE KALMAN G MATRIX IC
 -.18678E+04   .47100E+02  0.            .13164E+04   0.           -.55238E+0
 -.46496E+06  -.22000E+04   .22000E+04   .46238E+06   0.           -.11194E+12
 -.14352E+07   0.           -.22000E+04   .14346E+07   0.           -.28916E+12
  .18443E-03   0.            0.          -.50501E+03    .10000E+01   .33142E+02
  .30153E-01   0.            0.          -.63780E+05   0.            .5317GE+04
  .92702E+00   0.            0.          -.92700E+00   0.           -.32626E+05
        THE OPLICIP MATRIX IC
  .33022E+06   .68244E+02   .17950E+03   .46343E-06   -.57809E-04   -.19023E-04
  .68244E+02   .14164E+05   .37421E+05  -.28447E-05   -.51013E-03   -.39041E-12
  .17950E+03   .37421E+05   .31135E+06  -.11012E-04   -.17926E-02   -.10227E-01
  .46343E-06  -.28447E-05  -.11012E-04   .48499E-06    .61251E-04   -.11994E-11
  .57809E-04  -.51012E-03  -.17926E-02   .61251E-04    .77356E-02   -.19226E-04
  .19023E-04   .39041E-02   .10227E-01  -.11994E-11   -.19226E-04    .11043E-0
         REAL PART      IMAG PART OF EIGENVALUE
        -.57363E+04      .13600E+05
        -.57363E+04     -.13600E+05
        -.13711E+05      .55753E+04
        -.13711E+05     -.55753E+04
        -.25251E+03      .45630E+01
        -.25251E+03     -.45630E+01
        THE KALMN MATRIX IC
  .13782E+04   .35193E+02   .10863E+01   .95895E+03    .12106E-06    .55233E-0
  .35193E+02   .11094E+01   .43294E+01   .29994E+02    .41431E-06    .11194E-0
  .10863E+01   .43294E+01   .25663E+02   .11330E+03    .11496E-06    .28916E-0
  .95895E+03   .29994E+02   .11330E+04   .96035E+03    .12129E-06   -.33142E-1
  .12106E-06   .41431E-06   .11496E-06   .12129E-06    .17947E-04   -.53176E-14
  .55233E-04   .11194E-06   .28916E-06  -.33142E-16   -.53176E-14    .32626E-13
       CI*KALMN+KALMN*CIT+OPLICIP IC
 -.85024E-06  -.84825E-06   .87611E-05  -.24629E-06   -.43947E-04   -.20459E-12
 -.84825E-06  -.28783E-05   .29709E-04  -.83487E-06   -.14914E-03   -.69447E-12
  .87611E-05   .29709E-04  -.30664E-03   .86230E-05    .15404E-02    .71547E-11
 -.24629E-06  -.83487E-06   .86230E-05  -.24241E-06   -.43304E-04   -.20135E-12
 -.43947E-04  -.14914E-03   .15404E-02  -.43304E-04   -.77356E-02   -.35966E-1
 -.20459E-12  -.69449E-12   .71547E-11  -.20135E-12   -.35966E-10   -.16726E-1
     THE COVARIANCE MATRIX AFTER KALMAN IC
  .13782E+04   .35193E+02   .10863E+01   .59444E+03    .60604E-07    .55233E-0
  .35193E+02   .11094E+01   .43294E+01   .17703E+03    .20604E-06    .11194E-0
  .10863E+01   .43294E+01   .25663E+02   .12882E+03    .15173E-06    .28916E-0
  .59444E+03   .17703E+03   .12882E+03   .60026E+04    .60643E-07   -.91894E-17
  .60604E-07   .20604E-06   .15173E-06   .60643E-07    .76568E-05   -.11194E-14
  .55233E-04   .11194E-06   .28916E-06  -.91894E-17   -.11194E-14    .32626E-13
        IGMERR=   .37123E-02
       CI*COVARI*CIT+OPLICIP IC
  .35527E-14   .18190E-11  -.36380E-11  -.14853E-13   -.36286E-12   -.30161E-17
  .22737E-11   .18626E-08   .47730E-08  -.49800E-11   -.14279E-09   -.49209E-15
 -.36380E-11   .36089E-08   .27474E-07  -.25593E-10   -.79821E-09   -.36617E-14
 -.14853E-13  -.49800E-11  -.25593E-10  -.33082E-14   -.23446E-17   -.55451E-13
 -.36286E-12  -.14279E-09  -.79821E-09  -.22983E-17   -.17976E-15   -.11424E-14
 -.30161E-17  -.49209E-15  -.36617E-14  -.55451E-13   -.11424E-14   -.25144E-13
```

```
        THE B VECTOR IS
 0.             0.             0.             0.             .10000E+01   0.
        THE Q MATRIX IS
  .10000E+10   0.             0.            -.10000E+10   0.             0.
 0.             0.             0.             0.             0.           0.
 0.             0.             0.             0.             0.           0.
-.10000E+10   0.             0.             .10000E+10   0.             0.
 0.             0.             0.             0.             .50000E+02   0.
 0.             0.             0.             0.             0.            .50000E+16
         ALPHA IS  .47000E+02
        RINV=    .95238E+05
        TOLMRIC=  0.
        T3=  0.
        ITBASE=  0
GRAMMIAN IS 6X 6 OF RANK  3

RICCATI SOLN IN 14 ITERATIONS
        THE 5TH ROW OF THE Z MATRIX IS
  .19930E+08    .21298E+06    .84523E+05   -.20247E+08   -.67745E+04    .22763E+11
          REAL PART      IMAG PART OF EIGENVALUES
         -.22313E+04      .22063E+04
         -.22313E+04     -.22063E+04
         -.23119E+04     0.
         -.47099E+02     0.
         -.22000E+04     0.
         -.22000E+04     0.
        ENTER
        1 FOR COVARIANCE
        2 FOR NEW ALPHA
        3 FOR NEW Q'S
        4 FOR NEW R 1

        THE COVARIANCE OF X IS
  .10000E+01    .10000E+01    .50530E+00    .10006E+01    .71247E+00    .12059E-05
  .10000E+01    .24107E+02    .24107E+02    .98552E+00    .10970E+04    .14953E-04
  .50530E+00    .24107E+02    .48214E+02    .48688E+00    .10711E+04    .83711E-05
  .10006E+01    .98552E+00    .48688E+00    .10013E+01    .39671E-09    .12059E-05
  .71247E+00    .10970E+04    .10711E+04    .39671E-09    .52217E+05    .67526E-03
  .12059E-05    .14953E-04    .83711E-05    .12059E-05    .67526E-03    .15466E-10
        SGMERR=    .52722E-02
      ENTER
      1 TO REPEAT KALMAN SECTION
      2 TO REPEAT OPTIMAL CONTROL SECTION
      3 TO WRITE DV & Q12 ON TAPE7  3

        THE UPPER LEFT OF THE DV MATRIX IS
 -.47100E+02    .47100E+02   0.             0.             0.             0.
 0.            -.22000E+04    .22000E+04   0.             0.             0.
 0.             0.            -.22000E+04   0.             0.             0.
 0.             0.             0.             0.             .10000E+01   0.
  .19930E+08    .21298E+06    .84523E+05   -.20247E+08   -.67745E+04    .22763E+11
  .10000E+01   0.             0.            -.10000E+01   0.             0.
        THE UPPER RIGHT OF THE DV MATRIX IS
 0.             0.             0.             0.             0.           0.
 0.             0.             0.             0.             0.           0.
 0.             0.             0.             0.             0.           0.
 0.             0.             0.             0.             0.           0.
-.19930E+08   -.21298E+06   -.84523E+05    .20247E+08    .67745E+04   -.22763E+11
 0.             0.             0.             0.             0.           0.
        THE 11TH ROW OF THE DV MATRIX IS
 0.             0.             0.             0.             0.           0.
  .30153E-01   0.             0.            -.63780E+05   0.            .53176E+04
        THE 11TH ROW OF THE Q12 MATRIX IS
 0.             0.             0.             0.             0.           0.
  .57809E-04   -.51012E-03   -.17926E-02    .61251E-04    .77356E-02   -.19226E-0
  NOW PROCESS TAPE7 WITH EGNMLN12.
     STOP
      9.115 CP SECONDS EXECUTION TIME
COMMAND-
```

```
      PROGRAM MAIN(INPUT,OUTPUT,TAPE5,TAPE6=OUTPUT,TAPE7)
C  SINGLE CHANNEL CASE AUGUST 12 1541
C  USES KLEINMAN'S ROUTINES
C  OPERATES ON 12 BY 12 MATRICES WITH MLINEQ & EIGEN.
C  INCLUDES X AND X-XEST IN THE X VECTOR.
C  CALCULATES RESPONSE DUE TO INITIAL CONDITION.
C  CALCULATES EIGENVALUES OF DV MATRIX( OPTIMAL SYSTEM & KALMAN EST).
C  USES MLINEQ TO CALCULATE THE COVARIANCE OF OUTPUT X VECTOR.
C  REQUIRES INPUT IN FILE TAPE7.
      REAL X(12),XDOT(12),C(24),W(12,9),Q12(12,12),DVT(12,12),
     + RR12(12),RI12(12),UNIT12(12,12),TEMP12(12,12),COVAR12(12,12),
     + COM1(12,12),COM2(12,12)
      EXTERNAL FCN
      COMMON/FCNCOM/DV(12,12),U(12)
      COMMON/MAIN1/NDIM,NDIM1,COM1
      COMMON/MAIN2/COM2
      COMMON/INOU/KIN,KOUT,KPUNCH
C THIS COMMON AREA IS REQUIRED FOR KLEINMAN'S ROUTINES
      DATA DV/144*0./
      DATA UNIT12(12,12)/144*0./
      DATA Q12/144*0./
      N=12
      NHALF=N/2
      NHALF1=NHALF+1
      NDIM=12
      NDIM1=NDIM+1
      KIN=5
      KOUT=6
      KPUNCH=7
      REWIND7
      WRITE(6,599)
  599 FORMAT(2X,25HPROGRAM= EGNMLN12    ,CY=5 )
      DO 120 I=1,N
  120 READ(7,510)(DV(I,J),J=1,N)
  510 FORMAT(12E12.5)
      DO 130 I=1,N
  130 READ(7,510)(Q12(I,J),J=1,N)
      WRITE(6,826)
  826 FORMAT(9X,35HTHE UPPER LEFT OF THE DV MATRIX IS    )
      DO 140 I=1,NHALF
  140 WRITE(6,610)(DV(I,J),J=1,NHALF)
  610 FORMAT(6(1X,E12.5))
      WRITE(6,827)
  827 FORMAT(9X,36HTHE UPPER RIGHT OF THE DV MATRIX IS    )
      DO 150 I=1,NHALF
  150 WRITE(6,610)(DV(I,J),J=NHALF1,N)
      WRITE(6,828)
  828 FORMAT(9X,35HTHE LOWER RIGHT OF THE DV MATRIX IS    )
      DO 160 I=NHALF1,N
  160 WRITE(6,610)(DV(I,J),J=NHALF1,N)
      WRITE(6,829)
  829 FORMAT(9X,43HTHE LOWER LEFT OF THE DV MATRIX IS ZEROS.  )
C     EGNMLN12
```

```
      WRITE(6,831)
  831 FORMAT(9X,50HTHE UPPER LEFT,UPPER RIGHT,& LOWER LEFT OF Q12 IS )
      DO 170 I=1,NHALF
  170 WRITE(6,610)(Q12(I,J),J=1,NHALF)
      WRITE(6,832)
      DO 180 I=NHALF1,N
  180 WRITE(6,610)(Q12(I,J),J=NHALF1,N)
  832 FORMAT(9X,37HTHE LOWER RIGHT OF THE Q12 MATRIX IS   )
      CALL EGNO12(N,DV,RR12,RI12,UNIT12,IZERO)
      CALL TRANS2(N,N,DV,DVT)
      CALL EQUATE(TEMP12,Q12,N,N)
      TOLMLIN=1.E-7
      CALL MLINE1(NDIM,DVT,TEMP12,COVAR12,TOLMLIN)
      WRITE(6,834)
  834 FORMAT(9X,42HTHE UPPER LEFT OF THE COVAR12 MATRIX IS   )
      DO 190 I=1,NHALF
  190 WRITE(6,610)(COVAR12(I,J),J=1,NHALF)
      WRITE(6,835)
  835 FORMAT(9X,43HTHE LOWER RIGHT OF THE COVAR12 MATRIX IS   )
      DO 201 I=NHALF1,N
  201 WRITE(6,610)(COVAR12(I,J),J=NHALF1,N)
      WRITE(6,836)
  836 FORMAT(9X,42HTHE LOWER LEFT OF THE COVAR12 MATRIX IS   )
      DO 210 I=NHALF1,N
  210 WRITE(6,610)(Q12(I,J),J=1,NHALF)
      WRITE(6,837)
  837 FORMAT(9X,31HTHE COVAR12 MATRIX IS SYMMETRIC     )
      SGMERR=SQRT(COVAR12(1,1)+COVAR12(4,4)-2.*COVAR12(4,1))
      WRITE(6,791)SGMERR
  791 FORMAT(9X,8HSGMERR=  ,E12.5)
   99 STOP
      END
      SUBROUTINE EGNO12(N,DV,RR12,RI12,UNIT12,IZERO)
      COMMON/MAIN1/NDIM,NDIM1,COM1
      COMMON/INOU/KIN,KOUT,KPUNCH
      REAL DV(12,12),RR12(12),RI12(12),UNIT12(12,12)
      DO 30 I=1,N
   30 UNIT12(I,I)=1.
      CALL EIGEN(NDIM,DV,RR12,RI12,UNIT12,IZERO)
      WRITE(6,769)
  769 FORMAT(11X,9HREAL PART,5X,24HIMAG PART OF EIGENVALUES )
      DO 40 I=1,N
   40 WRITE(6,770)RR12(I),RI12(I)
  770 FORMAT(9X,E12.5,3X,E12.5)
      RETURN
      END
      EGNMLN12
```

```
C( PROGRAM= EGNMLN12   ,CY=5
        THE UPPER LEFT OF THE DV MATRIX IS
 -.47100E+02   .47100E+02   0.            0.            0.            0.
  0.           -.22000E+04   .22000E+04   0.            0.            0.
  0.            0.           -.22000E+04   0.            0.            0.
  0.            0.            0.           0.            .10000E+01    0.
  .19930E+08    .21298E+06    .84523E+05  -.20247E+08   -.67745E+04    .22763E+11
  .10000E+01    0.            0.          -.10000E+01    0.            0.
        THE UPPER RIGHT OF THE DV MATRIX IS
  0.            0.            0.           0.            0.            0.
  0.            0.            0.           0.            0.            0.
  0.            0.            0.           0.            0.            0.
  0.            0.            0.           0.            0.            0.
 -.19930E+08   -.21298E+06   -.84523E+05   .20247E+08    .67745E+04   -.22763E+11
  0.            0.            0.           0.            0.            0.
        THE LOWER RIGHT OF THE DV MATRIX IS
 -.18678E+04    .47100E+02   0.            .13164E+04    0.           -.55238E+0
 -.46496E+06   -.22000E+04    .22000E+04    .46338E+06    0.           -.11194E+1
 -.14352E+07   0.            -.22000E+04    .14346E+07    0.           -.28916E+1
  .18443E-03   0.            0.           -.50501E+03    .10000E+01    .3314E+02
  .30153E-01   0.            0.           -.63780E+05    0.            .5317E+04
  .92702E+00   0.            0.           -.92700E+00    0.           -.32686E+05
        THE LOWER LEFT OF THE DV MATRIX IS ZERO.
        THE UPPER LEFT,UPPER RIGHT,& LOWER LEFT OF Q12 IS
  0.            0.            0.           0.            0.            0.
  0.            0.            0.           0.            0.            0.
  0.            0.            .21214E+06   0.            0.            0.
  0.            0.            0.           0.            0.            0.
  0.            0.            0.           0.            0.            0.
  0.            0.            0.           0.            0.            0.
        THE LOWER RIGHT OF THE Q12 MATRIX IS
 .33022E+00    .68244E+02    .17950E+03    .46343E-06    .57809E-04    .19026E-04
 .68244E+02    .14168E+05    .37421E+05   -.28447E-05   -.51013E-03    .3904?E-03
 .17950E+03    .37421E+05    .31135E+06   -.11012E-04   -.17986E-02    .10227E-01
 .46343E-06   -.28447E-05   -.11012E-04    .48499E-06    .61251E-04   -.11999E-11
 .57809E-04   -.51013E-03   -.17986E-02    .61251E-04    .7735?E-02   -.19226E-0
 .19026E-04    .39041E-03    .10227E-01   -.11999E-11   -.19226E-09    .11043E-0
          REAL PART      IMAG PART OF EIGENVALUE
         -.28312E+04     .28062E+04
         -.28312E+04    -.28062E+04
         -.23121E+04     0.
         -.47044E+02     0.
         -.22000E+04     0.
         -.22000E+04     0.
         -.57362E+04     .13600E+05
         -.57362E+04    -.13600E+05
         -.13711E+05     .55762E+04
         -.13711E+05    -.55762E+04
         -.25250E+03     .46088E+01
         -.25250E+03    -.46088E+01
        THE UPPER LEFT OF THE COVAR12 MATRIX IS
 .99993E+00    .99993E+00    .50529E+00    .10026E+01    .23151E+01    .33973E-0
 .99993E+00    .24107E+02    .24107E+02    .95347E+00    .11714E+04    .5944?E-0
 .50529E+00    .24107E+02    .48214E+02    .42102E+00    .9?625E+03    .3?3?3E-0
 .10026E+01    .95347E+00    .42102E+00    .10058E+01   -.9816?E-10    .33973E-0
 .23151E+01    .11714E+04    .9?625E+03   -.9816?E-10    .65310E+05    .31594E-0
 .33973E-05    .59445E-04    .3?30?E-04    .33973E-05    .31594E-02    .19010E-0
        THE LOWER RIGHT OF THE COVAR12 MATRIX IS
 .13783E-04    .35196E-02    .10863E-01    .59994E-04    .60604E-07    .55241E-0
 .35196E-02    .11095E+01    .43297E+01    .17706E-03    .20911E-06    .11195E-0
 .10863E-01    .43297E+01    .25669E+02    .12883E-03    .15178E-06    .28916E-0
 .59994E-04    .17706E-03    .12883E-03    .60026E-04    .60643E-07   -.91909E-1
 .60604E-07    .20911E-06    .15178E-06    .60643E-07    .76583E-09   -.11199E-1
 .55241E-04    .11195E-06    .28916E-06   -.91909E-17   -.11199E-14    .32627E-1
        THE LOWER LEFT OF THE COVAR12 MATRIX IS
  0.            0.            0.           0.            0.            0.
  0.            0.            0.           0.            0.            0.
  0.            0.            .21214E+06   0.            0.            0.
  0.            0.            0.           0.            0.            0.
  0.            0.            0.           0.            0.            0.
  0.            0.            0.           0.            0.            0.
        THE COVAR12 MATRIX IS SYMMETRIC
        SUMEPS=    .22794E-01
```

```
SEJ,STCRA.
ACCOUNT,STEELMAN,              .,ARAA,8212.
JOB.
REWIND,DN=$OUT.
DISPOSE,DN=$OUT,DC=PR,TID=MX2CM,DEFER.
CFT,E=0,ON=BXZ.
ACCESS,DN=DISSPLA,ID=ADPSBOB.
ACCESS,DN=METALIB,ID=ADPSBOB.
ACCESS,DN=KRSTL,ID=ARAAJES.
LDR,LIB=DISSPLA:METALIB:IMSLLIB:KRSTL,SET=NGINDEF,MAP=ON.
REWIND,DN=FT99.
COPYD,I=FT99,O=FT98.
ACCESS,DN=METAOUT,ID=ADPSBOB.
METAOUT,I=FT99,O=PLOT1,FC=G1,FID=SEJ.
DISPOSE,DN=PLOT1,TID=GMFMY.
METAOUT,I=FT98,O=PLOT2,FC=F8,FID=SEJ.
DISPOSE,DN=PLOT2,DC=PR,TID=MX2VR.
EXIT.
DUMPJOB.
DEBUG,TRACE,BLOCKS.
      PROGRAM MAIN(INPUT,OUTPUT,TAPE5=INPUT,TAPE6=OUTPUT,TAPE99=0)
C  SINGLE CHANNEL CASE AUGUST 02 1454
C  USES KLEINMAN'S ROUTINES
C  OPERATES ON 6 BY 6 MATRICES WITH MLINEQ & MRIC.
C  INCLUDES X AND X-XEST IN THE X VECTOR.
C  PLOTS RESPONSE DUE TO INITIAL CONDITION.
C  USES MRIC TO CALCULATE KALMAN GAIN.
C  REQUIRES MEASUREMENT MATRIX 4 BY 6.
C  USES MRIC TO CALCULATE OPTIMAL CONTROL.
C  CALCULATES EIGENVALUES OF Z(=A-S*P)
C  USES MLINEQ TO CALCULATE THE COVARIANCE OF OUTPUT X VECTOR.
      REAL X(12),XDOT(12),C(24),W(12,9),TEMP(6,6),ZT(6,6),M(4,6),P(6,4),
     * Q(6,6),S(6,6),COM1(6,6),COM2(6,6),COVARX(6,6),ZK(6,6),
     * A(6,6),B(6),JNIT(6,6),RR(6),RI(6),QNMAT(6,6),SKLMN(6,6),Z(6,6),
     * RKLMINV(4,4),AT(6,6),ZKT(6,6),TMSEC(400),X4(400),DIF(400),
     * X1LSEST(400),X4LSEST(400),QPLSRSR(6,6),RKOPT(6,6),RKLMN(6,6)
      EXTERNAL FCN
      COMMON/FCNCOM/DV(12,12),U(12)
      COMMON/MAIN1/NDIM,NDIM1,COM1
      COMMON/MAIN2/COM2
      COMMON/INOU/KIN,KOUT,KPUNCH
C THIS COMMON AREA IS REQUIRED FOR KLEINMAN'S ROUTINES
      CALL META
C  CALL META INITIALIZES DISSPLA
      DATA QNMAT/36*0./
      DATA RKLMINV/16*0./
      DATA DV/144*0./
      N=12
      NHALF=N/2
      NHALF1=NHALF+1
      NDIM=6
      NDIM1=NDIM+1
      MDIM=4
      KIN=5
      KOUT=6
      KPUNCH=7
      WRITE(6,591)
  591 FORMAT(1H1)
C  GO TO TOP OF NEW PAGE
C     KRASTP
```

```
      WRITE(6,599)
  599 FORMAT(25H/ PROGRAM= KRASTP ,CY=9  )
      DO 10 I=1,NDIM
   10 READ(5,500)(A(I,J),J=1,NDIM)
  500 FORMAT(6E12.5)
      READ(5,500)(X(I),I=1,N)
      READ(5,500)(B(I),I=1,NDIM)
      READ(5,500)(U(I),I=1,N)
      DO 9 I=1,MDIM
    9 READ(5,500)(M(I,J),J=1,NDIM)
      DO 12 I=1,NDIM
   12 READ(5,500)(Q(I,J),J=1,NDIM)
      READ(5,500)ALPHA
      READ(5,500)R
      READ(5,500)SGMTURB,SGM1LS4,SGMM2,SGMM3,SGMM4
      READ(5,500)DT
      WRITE(6,600)
  600 FORMAT(9X,15HTHE A MATRIX IS)
      DO 60 I=1,NDIM
      DO 19 K=1,NDIM
   19 AT(K,I)=A(I,K)
   60 WRITE(6,610)(A(I,J),J=1,NDIM)
  610 FORMAT(6(1X,E12.5))
      WRITE(6,620)
  620 FORMAT(9X,17HTHE INITIAL X IS  )
      WRITE(6,610)(X(I),I=1,NHALF)
      WRITE(6,621)
  621 FORMAT(9X,21HTHE INITIAL X-XEST IS  )
      WRITE(6,610)(X(I),I=NHALF1,N)
      WRITE(6,880)
  880 FORMAT(6X,15HTHE M MATRIX IS )
      DO 4 I=1,MDIM
    4 WRITE(6,610)(M(I,J),J=1,NDIM)
      TOLMLIN=1.E-7
      TOLMRIC=2.E-5
   31 QNMAT(3,3)=(4.*(SGMTURB**2)*A(2,3)*(A(1,2)+A(2,3))**2)/
     * (A(1,2)*(A(1,2)+2.*A(2,3)))
      WRITE(6,900)SGMTURB,QNMAT(3,3)
  900 FORMAT(4X,8HSGMTURB=,E12.5,  3X,
     * 13H  QNMAT(3,3)=,E12.5)
      WRITE(6,847)SGM1LS4,SGMM2,SGMM3
  847 FORMAT(4X,8HSGM1LS4=,E12.5,3X,6HSGMM2=,E12.5,3X,6HSGMM3=,E12.5)
      WRITE(6,837)SGMM4
  837 FORMAT(4X,6HSGMM4= ,E12.5)
      WRITE(6,901)TOLMLIN,TOLMRIC
  901 FORMAT(4X,8HTOLMLIN=,E12.5,10H  TOLMRIC=,E12.5)
      RKLMINV(1,1)=1./SGM1LS4**2
      RKLMINV(2,2)=1./SGMM2**2
      RKLMINV(3,3)=1./SGMM3**2
      RKLMINV(4,4)=1./SGMM4**2
C  NOW CALCULATE P=M TRANSPOSE*RKLMINV.
      DO 53 I=1,NDIM
      DO 59 J=1,MDIM
      TMP=0.
      DO 55 K=1,MDIM
   55 TMP=TMP+M(K,I)*RKLMINV(K,J)
   59 P(I,J)=TMP
   53 CONTINUE
C     KRASTP
```

```
C  NEXT CALCULATE MT*RKLMINV*M
      DO 3 I=1,NDIM
      DO 2 J=1,NDIM
      TMP=0.
      DO 1 K=1,MDIM
    1 TMP=TMP+P(I,K)*M(K,J)
    2 SKLMN(I,J)=TMP
    3 CONTINUE
      T3=0.
      ITBASE=32
      CALL MRIC(NDIM,AT,SKLMN,QNMAT,RKLMN,ZKT,TOLMRIC,T3,ITBASE)
C  THE KALMAN RICATTI EQUATION OPERATES ON A TRANSPOSE
C   & YIELDS THE TRANSPOSE OF THE CLOSED LOOP SYSTEM ZKT.
      CALL TRANS2(NDIM,NDIM,ZKT,ZK)
C  THE CLOSED LOOP SYSTEM MATRIX IS ZK
      WRITE(6,810)
  810 FORMAT(6X,22HTHE KALMAN Z MATRIX IS )
      DO 67 I=1,NDIM
   67 WRITE(6,610)(ZK(I,J),J=1,NDIM)
      CALL EGNO(ZK,RR,RI,UNIT,0)
      CALL MAT3A(NDIM,NDIM,RKLMN,SKLMN,TEMP)
C  FORMS TEMP=RKLMN*SKLMN*RKLMN
      CALL MADD1(NDIM,NDIM,QNMAT,TEMP,QPLSRSR,1.)
C  FORMS QPLSRSR=QNMAT+RKLMN*SKLMN*RKLMN
C  QPLSRSR IS THE INPUT COVARIANCE FOR KALMAN ESTIMATOR
      WRITE(6,601)
  601 FORMAT(9X,20HTHE RKLMN MATRIX IS    )
      DO 69 I=1,NDIM
   69 WRITE(6,610)(RKLMN(I,J),J=1,NDIM)
      CALL PREP(ZK,QPLSRSR,ZKT,COVARX,UNIT,TEMP)
      WRITE(6,820)
  820 FORMAT(6X,37HTHE COVARIANCE MATRIX AFTER KALMAN IS )
C   RKLMN SHOULD BE THE COVARIANCE OF X AFTER KALMAN!!!
      CALL MLINEQ(NDIM,ZKT,TEMP,COVARX,TOLMLIN)
      DO 68 I=1,NDIM
   68 WRITE(6,610)(COVARX(I,J),J=1,NDIM)
      SGMERR=SQRT(COVARX(1,1)+COVARX(4,4)-2.*COVARX(1,4))
      WRITE(6,791)SGMERR
      WRITE(6,591)
C  GO TO TOP OF NEXT PAGE
      WRITE(6,630)
  630 FORMAT(1H/,8X,15HTHE B VECTOR IS)
      WRITE(6,610)(B(I),I=1,NDIM)
      WRITE(6,671)
  671 FORMAT(9X,15HTHE U VECTOR IS )
      WRITE(6,610)(U(I),I=1,N)
   13 WRITE(6,690)
  690 FORMAT(9X,15HTHE Q MATRIX IS)
      DO 62 I=1,6
   62 WRITE(6,610)(Q(I,J),J=1,NDIM)
   15 WRITE(6,670)ALPHA
  670 FORMAT(9X,9H ALPHA IS ,E12.5)
   16 RINV=1./R
      WRITE(6,680)RINV
  680 FORMAT(9X,6HRINV= ,E12.5)
C     KRASTP
```

```
      DO 70 I=1,NDIM
      DO 80 J=1,NDIM
      UNIT(I,J)=0.
   80 S(I,J)=B(I)*RINV*B(J)
   70 UNIT(I,I)=1.
C  S=B*RINV*BTRANSPOSE
      DO 90 I=1,NDIM
   90 A(I,I)=A(I,I)+ALPHA
C  THIS ALLOWS AN UPPER BOUND ON NAT FREQ OF EACH SV
      TOLMRIC=0.
C  SETTING TOLMRIC.LT.1.E-15,RESULTS IN MRIC SETTING TOL=1.E-3
      WRITE(6,730)TOLMRIC
  730 FORMAT(9X,9HTOLMRIC= ,E12.5)
      T3=0.
C  SETTING T3=0. ALLOWS MRIC TO CALCULATE T3 INTERNALLY.
      WRITE(6,740)T3
  740 FORMAT(9X,4HT3= ,E12.5)
      ITBASE=0
C  IF ITBASE=0,MAXIT=30+N IF ITBASE.NE.0,MAXIT=ITBASE+N
      WRITE(6,750)ITBASE
  750 FORMAT(9X,8HITBASE= ,I2)
      CALL MRIC(NDIM,A,S,Q,RKOPT,Z,TOLMRIC,T3,ITBASE)
      DO 33 I=1,NDIM
      Z(I,I)=Z(I,I)-ALPHA
   33 A(I,I)=A(I,I)-ALPHA
C  THESE SUBTRACTIONS CANCEL THE ADDITION OF STATEMENT 90.
C  INPUTS ARE A,S,&Q. OUTPUTS ARE RK&Z(=A-S*RK)
C  P IS THE SOLUTION TO THE RICCATI EQUATION.
C  Z IS THE CLOSED LOOP SYSTEM WITH OPT S.V. FEEDBACK.
      WRITE(6,699)
  699 FORMAT(9X,30HTHE 5TH ROW OF THE Z MATRIX IS )
   95 WRITE(6,610)(Z(5,J),J=1,NDIM)
      CALL EGNO(Z,RR,RI,UNIT,0)
   98 CALL PREP(Z,QNMAT,ZT,COVARX,UNIT,TEMP)
      CALL MLINEQ(NDIM,ZT,TEMP,COVARX,TOLMLIN)
      WRITE(6,792)
  792 FORMAT(9X,22HTHE COVARIANCE OF X IS)
      DO 43 I=1,NDIM
   43 WRITE(6,610)(COVARX(I,J),J=1,NDIM)
      SGMERR=SQRT(COVARX(1,1)+COVARX(4,4)-2.*COVARX(1,4))
      WRITE(6,791)SGMERR
  791 FORMAT(9X,8HSGMERR= ,E12.5)
C  THIS SECTION FORMS THE DV MATRIX FOR OPTIMAL SYSTEM & ESTIMATOR.
C  UPPER LEFT OF DV IS THE CLOSED LOOP OPTIMAL MATRIX
C  UPPER RIGHT OF DV IS -BKT
C  LOWER LEFT REMAINS ZEROS
C  LOWER RIGHT OF DV IS CLOSED LOOP KALMAN ESTIMATOR
   51 DO 100 I=1,NHALF
      INHALF=I+NHALF
      DO 110 J=1,NHALF
      JNHALF=J+NHALF
      TMP=Z(I,J)
      DV(I,J)=TMP
      DV(I,JNHALF)=A(I,J)-TMP
  110 DV(INHALF,JNHALF)=ZK(I,J)
  100 CONTINUE
C     KRASTP
```

```
      WRITE(6,623)
  623 FORMAT(9X,16HTHE DV MATRIX IS  )
      DO 111 I=1,N
  111 WRITE(6,629)(DV(I,J),J=1,N)
  629 FORMAT(12E11.4)
      TOLDV=.1E-6
      NW=12
      IND=1
      T=0.
C  DT WAS READ IN EARLIER
      DO 30 I=1,400
      TF=T+DT
      CALL DVERK(N,FCN,T,X,TF,TOLDV,IND,C,NW,W,IER)
C  DVERK NORMALLY EXITS WITH T REPLACED BY TF
      X4(I)=X(4)
      DIF(I)=X(1)-X(4)
      X1LSEST(I)=X(7)
      X4LSEST(I)=X(10)
      TMSEC(I)=1000.*TF
   30 CONTINUE
      WRITE(6,633)DT
  633 FORMAT(9X,4HDT= ,E12.5)
      WRITE(6,640)TF
  640 FORMAT(9X,7HAT TF=  ,F7.4)
      WRITE(6,650)
  650 FORMAT(9X,10HFINAL X IS )
      WRITE(6,610)(X(I),I=1,N)
      CALL BGNPL(1)
      CALL PAGE(14.,11.)
      CALL TITLE(18HX4 FOR U(3)=2200  ,18,12HTIME IN MSEC,12,
     + 18HX4 FOR U(3)=2200  ,18,11.,7.)
      CALL GRAF(0.,5HSCALE,TMSEC(400),0.,5HSCALE,1.)
      CALL CURVE(TMSEC,X4,400,0)
      CALL ENDPL(1)
      CALL BGNPL(2)
      CALL PAGE(14.,11.)
      CALL TITLE(21HX1-X4 FOR U(3)=2200  ,21,12HTIME IN MSEC,12,
     + 21HX1-X4 FOR U(3)=2200  ,21,11.,7.)
      CALL GRAF(0.,5HSCALE,TMSEC(400),0.,5HSCALE,6.E-4)
      CALL CURVE(TMSEC,DIF,400,0)
      CALL ENDPL(2)
      CALL BGNPL(3)
      CALL PAGE(14.,11.)
      CALL TITLE(24HX1-X1EST FOR U(3)=2200  ,24,12HTIME IN MSEC,12,
     + 24HX1-X1EST FOR U(3)=2200  ,24,11.,7.)
      CALL GRAF(0.,5HSCALE,TMSEC(400),-1.E-6,5HSCALE,1.E-6)
      CALL CURVE(TMSEC,X1LSEST,400,0)
      CALL ENDPL(3)
      CALL BGNPL(4)
      CALL PAGE(14.,11.)
      CALL TITLE(24HX4-X4EST FOR U(3)=2200  ,24,12HTIME IN MSEC,12,
     + 24HX4-X4EST FOR U(3)=2200  ,24,11.,7.)
      CALL GRAF(0.,5HSCALE,TMSEC(400),-1.E-6,5HSCALE,1.E-6)
      CALL CURVE(TMSEC,X4LSEST,400,0)
      CALL ENDPL(4)
      CALL DONEPL
   99 STOP
      END
C     KRASTP
```

```
      SUBROUTINE EGVO(Z,RR,RI,UNIT,IZERO)
      COMMON/MAIN1/NDIM,NDIM1,COM1
      COMMON/MAIN2/COM2
      COMMON/INOU/KIN,KOUT,KPUNCH
      REAL Z(6,6),RR(6),RI(6),UNIT(6,6)
      CALL EIGEN(NDIM,Z,RR,RI,UNIT,IZERO)
      WRITE(6,769)
  769 FORMAT(11X,9HREAL PART,5X,24HIMAG PART OF EIGENVALUES )
      DO 40 I=1,NDIM
   40 WRITE(6,770)RR(I),RI(I)
  770 FORMAT(9X,E12.5,3X,E12.5)
      RETURN
      END
      SUBROUTINE PREP(Z,QNMAT,ZT,COVARX,UNIT,TEMP)
      REAL Z(6,6),QNMAT(6,6),ZT(6,6),COVARX(6,6),UNIT(6,6),TEMP(6,6)
      DO 40 I=1,6
      DO 41 J=1,6
      ZT(J,I)=Z(I,J)
      COVARX(I,J)=0.
      UNIT(I,J)=0.
   41 TEMP(I,J)=QNMAT(I,J)
   40 UNIT(I,I)=1.
      RETURN
      END
      SUBROUTINE FCN(N,T,X,XDOT)
      REAL X(12),XDOT(12)
      COMMON/FCNCOM/DV(12,12),U(12)
      DO 10 I=1,12
      TEMP=0.
       DO 20 J=1,12
   20  TEMP=DV(I,J)*X(J)+TEMP
   10 XDOT(I)=TEMP+U(I)
      RETURN
      END
-47.10        47.10         0.            0.            0.            0.
 0.      E+00-2.200  E+03 2.200  E+03 0.      E+00 0.      E+00 0.      E+00
 0.      E+00 0.      E+00-2.200  E+03 0.      E+00 0.      E+00 0.      E+00
 0.           0.            0.            0.            1.            0.
 0.           0.            0.            0.            0.            0.
 1.           0.            0.           -1.            0.            0.
 0.0          0.            0.            0.            0.            0.          X
 0.           0.0           0.00          0.000         0.000         .0          X
 0.           0.            0.            0.            1.            0.          B
 0.           0.            2200.         0.            0.            0.          U
 0.           0.            0.            0.            0.            0.          U
 1.           0.            0.           -1.            0.            0.          M
0.            0.            0.            1.            0.            0.          M
 0.           0.            0.            0.            0.            0.          M
 0.           0.            0.            0.            0.            1.          M
      .1E+10  0.            0.                -.1E+10   0.            0.
 0.           0.            0.            0.            0.            0.
 0.           0.            0.            0.            0.            0.
    -.1E+10   0.            0.                .1E+10    0.            0.
 0.           0.            0.            0.              50.         0.
 0.           0.            0.            0.            0.                    .5E+15
 46.             ALPHA
 1.05   E-05  R
 1.     E+00 .87    E-04 1.379  E-06 1.      E+01 .1      E-08  SIGMAS
 3.     E-04 DT
```

```
PROGRAM= KRASTP ,CY=9
      THE A MATRIX IS
-0.47100E+02  0.47100E+02  0.00000E+00  0.00000E+00  0.00000E+00  0.00000E+00
 0.00000E+00 -0.22000E+04  0.22000E+04  0.00000E+00  0.00000E+00  0.00000E+00
 0.00000E+00  0.00000E+00 -0.22000E+04  0.00000E+00  0.00000E+00  0.00000E+00
 0.00000E+00  0.00000E+00  0.00000E+00  0.00000E+00  0.10000E+01  0.00000E+00
 0.00000E+00  0.00000E+00  0.00000E+00  0.00000E+00  0.00000E+00  0.00000E+00
 0.10000E+01  0.00000E+00  0.00000E+00 -0.10000E+01  0.00000E+00  0.00000E+00
      THE INITIAL X IS
 0.00000E+00  0.00000E+00  0.00000E+00  0.00000E+00  0.00000E+00  0.00000E+00
      THE INITIAL X-XEST IS
 0.00000E+00  0.00000E+00  0.00000E+00  0.00000E+00  0.00000E+00  0.00000E+00
    THE M MATRIX IS
 0.10000E+01  0.00000E+00  0.00000E+00 -0.10000E+01  0.00000E+00  0.00000E+00
 0.00000E+00  0.00000E+00  0.00000E+00  0.10000E+01  0.00000E+00  0.00000E+00
 0.00000E+00  0.00000E+00  0.00000E+00  0.00000E+00  0.00000E+00  0.00000E+00
 0.00000E+00  0.00000E+00  0.00000E+00  0.00000E+00  0.00000E+00  0.10000E+01
  SGMTURB= 0.10000E+01      QNMAT(3,3)= 0.21214E+06
  SGM1LS4= 0.87600E-04   SGMM2= 0.13790E-05   SGMM3= 0.10000E+02
  SGMM4= 0.10000E-08
  TOLMLIN= 0.10000E-06  TOLMRIC= 0.20000E-04

RICCATI SOLN IN 29 ITERATIONS
    THE KALMAN Z MATRIX IS
-0.18678E+04  0.47100E+02  0.00000E+00  0.13164E+04  0.00000E+00 -0.55233E+09
-0.46496E+06 -0.22000E+04  0.22000E+04  0.46338E+06  0.00000E+00 -0.11194E+12
-0.14352E+07  0.00000E+00 -0.22000E+04  0.14346E+07  0.00000E+00 -0.28916E+12
 0.18443E-03  0.00000E+00  0.00000E+00 -0.50501E+03  0.10000E+01  0.33142E+02
 0.30153E-01  0.00000E+00  0.00000E+00 -0.63780E+05  0.00000E+00  0.53176E+04
 0.92702E+00  0.00000E+00  0.00000E+00 -0.92700E+00  0.00000E+00 -0.32626E+05
        REAL PART     IMAG PART OF EIGENVALUES
       -0.57363E+04   0.13600E+05
       -0.57363E+04  -0.13600E+05
       -0.13711E+05   0.55753E+04
       -0.13711E+05  -0.55753E+04
       -0.25251E+03   0.45630E+01
       -0.25251E+03  -0.45630E+01
       THE RKLMN MATRIX IS
 0.13782E-04  0.35193E-02  0.10863E-01  0.95895E-09  0.12106E-06  0.55238E-09
 0.35193E-02  0.11094E+01  0.43294E+01  0.23989E-08  0.41431E-06  0.11194E-06
 0.10863E-01  0.43294E+01  0.25668E+02  0.11380E-08  0.11464E-06  0.28916E-06
 0.95895E-09  0.29939E-08  0.11380E-08  0.96035E-09  0.12129E-06 -0.33142E-16
 0.12106E-06  0.41431E-06  0.11464E-06  0.12129E-06  0.17947E-04 -0.53176E-14
 0.55238E-09  0.11194E-06  0.28916E-06 -0.33142E-16 -0.53176E-14  0.32626E-13
    THE COVARIANCE MATRIX AFTER KALMAN IS
 0.13782E-04  0.35193E-02  0.10863E-01  0.59994E-09  0.60604E-07  0.35238E-09
 0.35193E-02  0.11094E+01  0.43294E+01  0.17703E-08  0.20909E-06  0.11194E-06
 0.10863E-01  0.43294E+01  0.25668E+02  0.12882E-08  0.15173E-06  0.28916E-06
 0.59994E-09  0.17703E-08  0.12882E-08  0.60026E-09  0.60643E-07 -0.91900E-17
 0.60604E-07  0.20909E-06  0.15173E-06  0.60643E-07  0.76588E-05 -0.11199E-14
 0.35238E-09  0.11194E-06  0.28916E-06 -0.91900E-17 -0.11199E-14  0.32626E-13
      SGMERR= 0.37123E-02
```

```
        THE S VECTOR IS
 0.00000E+00  0.00000E+00  0.00000E+00  0.00000E+00  0.10000E+01  0.00000E+00
        THE U VECTOR IS
 0.00000E+00  0.00000E+00  0.22900E+04  0.00000E+00  0.00000E+00  0.10000E+00
 0.00000E+00  0.00000E+00  0.00000E+00  0.00000E+00  0.00000E+00  0.00000E+00
        THE Q MATRIX IS
 0.10000E+10  0.00000E+00  0.00000E+00 -0.10000E+10  0.00000E+00  0.00000E+00
 0.00000E+00  0.00000E+00  0.00000E+00  0.00000E+00  0.00000E+00  0.00000E+00
 0.00000E+00  0.00000E+00  0.00000E+00  0.00000E+00  0.00000E+00  0.00000E+00
-0.10000E+10  0.00000E+00  0.00000E+00  0.10000E+10  0.00000E+00  0.00000E+00
 0.00000E+00  0.00000E+00  0.00000E+00  0.00000E+00  0.50000E+02  0.00000E+00
 0.00000E+00  0.00000E+00  0.00000E+00  0.00000E+00  0.00000E+00  0.50000E+16
        ALPHA IS 0.46000E+02
        RINV=  0.9523dE+05
        TOLMRIC=  0.00000E+00
        I3=  0.00000E+00
        ITBASE=  0
GRAMMIAN IS 6X 6 OF RANK  3

RICCATI SOLN IN 14 ITERATIONS
        THE 5TH ROW OF THE Z MATRIX IS
 0.19917E+08  0.21284E+06  0.84482E+05 -0.20234E+08 -0.67714E+04  0.22743E+11
          REAL PART      IMAG PART OF EIGENVALUES
        -0.22303E+04     0.22863E+04
        -0.22303E+04    -0.22863E+04
        -0.23108E+04     0.00000E+00
        -0.47099E+02     0.00000E+00
        -0.22000E+04     0.00000E+00
        -0.22000E+04     0.00000E+00
        THE COVARIANCE OF X IS
 0.10000E+01  0.10000E+01  0.50530E+00  0.10006E+01  0.71435E+00  0.12091E-05
 0.10000E+01  0.24107E+02  0.24107E+02  0.98548E+00  0.10970E+04  0.14991E-04
 0.50530E+00  0.24107E+02  0.48214E+02  0.48683E+00  0.10710E+04  0.83922E-05
 0.10006E+01  0.98548E+00  0.48683E+00  0.10013E+01  0.21239E-10  0.12091E-05
 0.71435E+00  0.10970E+04  0.10710E+04  0.21239E-10  0.52220E+05  0.67708E-03
 0.12091E-05  0.14991E-04  0.83922E-05  0.12091E-05  0.67708E-03  0.15547E-10
        SGMERR=  0.52800E-02
        THE QV MATRIX IS

 0.4710E+02 0.4710E+02 0.0000E+00 0.0000E+00 0.0000E+00 0.0000E+00 0.0000E+00 0.0000E+00 0.0000E+00 0.0000E+00 0.0000E+00 0.0000E+00
 0.0000E+00-0.2200E+04 0.2200E+04 0.0000E+00 0.0000E+00 0.0000E+00 0.0000E+00 0.0000E+00 0.0000E+00 0.0000E+00 0.0000E+00 0.0000E+00
 0.0000E+00 0.0000E+00-0.2200E+04 0.0000E+00 0.0000E+00 0.0000E+00 0.0000E+00 0.0000E+00 0.0000E+00 0.0000E+00 0.0000E+00 0.0000E+00
 0.0000E+00 0.0000E+00 0.0000E+00 0.0000E+00 0.1000E+01 0.0000E+00 0.0000E+00 0.0000E+00 0.0000E+00 0.0000E+00 0.0000E+00 0.0000E+00
 0.1992E+08 0.2128E+06 0.8448E+05-0.2023E+08-0.6771E+04 0.2274E+11-0.1992E+08-0.2128E+06-0.8448E+05 0.2023E+08 0.6771E+04-0.2274E+11
 0.1000E+01 0.0000E+00 0.0000E+00-0.1000E+01 0.0000E+00 0.0000E+00 0.0000E+00 0.0000E+00 0.0000E+00 0.0000E+00 0.0000E+00 0.0000E+00
 0.0000E+00 0.0000E+00 0.0000E+00 0.0000E+00 0.0000E+00 0.0000E+00 0.0000E+00-0.1868E+04 0.4710E+02 0.0000E+00 0.1316E+04 0.0000E+00-0.5524E+09
 0.0000E+00 0.0000E+00 0.0000E+00 0.0000E+00 0.0000E+00 0.0000E+00 0.0000E+00-0.4650E+06-0.2200E+04 0.2200E+04 0.4634E+06 0.0000E+00-0.1119E+12
 0.0000E+00 0.0000E+00 0.0000E+00 0.0000E+00 0.0000E+00 0.0000E+00 0.0000E+00-0.1435E+07 0.0000E+00-0.2200E+04 0.1435E+07 0.0000E+00-0.2892E+12
 0.0000E+00 0.0000E+00 0.0000E+00 0.0000E+00 0.0000E+00 0.0000E+00 0.0000E+00 0.1844E-03 0.0000E+00 0.0000E+00-0.5050E+03 0.1000E+01 0.3314E+02
 0.0000E+00 0.0000E+00 0.0000E+00 0.0000E+00 0.0000E+00 0.0000E+00 0.0000E+00 0.3015E-01 0.0000E+00 0.0000E+00-0.6378E+05 0.0000E+00 0.5318E+04
 0.0000E+00 0.0000E+00 0.0000E+00 0.0000E+00 0.0000E+00 0.0000E+00 0.0000E+00 0.9270E+00 0.0000E+00 0.0000E+00-0.9270E+00 0.0000E+00-0.3263E+05
        DT=  0.36000E-03
        AT TF=  0.1200
        FINAL X IS
 0.99633E+00  0.10000E+01  0.10000E+01  0.99633E+00  0.17266E+00  0.45173E-06
 0.00000E+00  0.00000E+00  0.00000E+00  0.00000E+00  0.00000E+00  0.00000E+00
```

1980 USAF - SCEEE SUMMER FACULTY RESEARCH PROGRAM

Sponsored by the

AIR FORCE OFFICE OF SCIENTIFIC RESEARCH

Conducted by the

SOUTHEASTERN CENTER FOR ELECTRICAL ENGINEERING EDUCATION

FINAL REPORT

# A STUDY OF SELECTED FACTORS RELATING TO HUMAN RESOURCE MANAGEMENT IN THE AIR FORCE


| | |
|---|---|
| Prepared by: | Dr. Philip Tolin |
| Academic Rank: | Associate Professor |
| Department and *University:* | Department of Psychology<br>Central Washington University |
| Research Location: | Air Force Human Resources Laboratory,<br>Manpower and Personnel Division,<br>Force Utilization Branch |
| USAF Research Colleague: | Dr. Jeffrey E. Kantor |
| Date: | August 22, 1980 |
| Contract Number: | F49620-79-C-0038 |

# A STUDY OF SELECTED FACTORS RELATING TO HUMAN RESOURCE MANAGEMENT IN THE AIR FORCE

by

Philip Tolin

## ABSTRACT

This report describes several activities performed in conjunction with the USAF - SCEEE Summer Faculty Research Program. The major effort involved preparation of a USAF Human Resources Laboratory Technical Report describing the characteristics of accessions of CYs 1977 - 1979. Other projects involved work preparatory to the development of an exit interview survey instrument, assessment of the predictive efficiencies of alternative subscales of the History Opinion Inventory, a content analysis of comments related to pilot stress, and a preliminary literature review dealing with fighter pilot selection.

## Acknowledgement

I would like to express my thanks to the Air Force Systems Command, the Air Force office of Scientific Research, and the Southeastern Center for Eletrical Engineering Education for providing the opportunity to spend an interesting summer at the Air Force Human Resources Laboratory, Brooks AFB TX 78235. I have been impressed with the competence and professionalism of the scientists at the laboratory and I am grateful for their hospitality. In particular, I would like to thank Drs. Jeffrey Kantor, Malcolm Ree, Charles Weaver, and Joe Ward for their roles in making this experience both professionally stimulating and personally rewarding.

## I. INTRODUCTION

In order to ensure the maintenance of an effective military force, Air Force manpower planners periodically must receive information describing the characteristics of first-term enlisted personnel. Since the termination of draft-motivated enlistments in 1973, such reports have acquired additional importance as Air Force planners have been concerned with the possibility of changes in the aptitude and ability levels of first-term accessions and with the fulfilment of the social obligation to maintain equality of opportunity for women and for members of racial and ethnic minorities.

During the 1970's a series of reports were written documenting accession characteristics. The last such report (Leisey & Vitola, 1979) dealt with enlistees who entered the Air Force between January, 1975 and June, 1977, and described trends over that time in aptitude test scores, mental ability levels, education levels, minority representation, the utilization of women, and regional differences in accession characteristics. The present summer research effort involved the development of a similar report covering the calendar years 1977-1979.

A second factor of importance to manpower planners is the prediction and minimization of attrition. The Air Force Human Resources Laboratory (AFHRL) has sponsored a considerable amount of research designed to determine the usefulness of a number of measures as predictors of attrition. While the prediction equations generated by these studies have been somewhat successful in predicting attrition rates among enlisted personnel, it is clear that additional work is needed to identify reasons for leaving the Air Force that are given by attriting personnel. Specifically, it appears that a questionnaire to be administered during an exit interview would provide important information concerning sources of difficulty and irritation encountered by persons leaving the Air Force.

The Summer Faculty research effort described in this report originally was planned around the dual objectives of preparing an accessions report and developing a suitable exit interview instrument. Due to circumstances beyond the control either of this writer or AFHRL colleagues, the latter project was suspended after several weeks of preliminary work, described below. Work subsequently began on three other formal tasks. Work on each of these projects was not extensive; brief descriptions of these efforts, as well as efforts undertaken on an informal basis, are described below.

## II OBJECTIVES

The specific research assignments arrived at during the pre-summer visit were as follows: (a) to participate in the preparation of a technical report on the quality and characteristics of Air Force accessions for calendar years 1977 - 1979, to summarize, tabulate, and interpret data comparing year-by-year accessions against such criteria as educational level, age, mental ability and aptitude, racial/ethnic group, sex, etc.; and to describe the implications of the research findings for Air Force management's concern regarding whether the quality, quantity, and favorable characteristics of individuals who enlisted in the draft era are being sustained in the draft-free era; and (b) to participate in research on reasons for attrition among first-term airmen, with the goal of developing a survey instrument to be used in conducting exit interviews with separating enlistees to identify factors contributing to attrition.

As noted above, the second assignment was dropped after several weeks. Activities which replaced that project involved the begining of a literature search on fighter pilot selection, the examination of the relative efficacies of various predictors of attrition, and the identification of sources of fighter pilot stress during combat. Several informal projects which were undertaken in an effort to gain a wide variety of experiences related to human reources management. These efforts are described below.

## III. ACCESSIONS REPORT

The examination of data describing first-term accession characteristics in calendar years 1977 - 1979 resulted in the preparation of an AFHRL technical report. Data collected on all recruits who entered the Air Force during these years were obtained from the Processing and Classification of Enlistees (PACE) files maintained by the Technical Services Division of the Air Force Human Resources Laboratory, Air Force Systems Command. These data included age, sex, education level, racial/ethnic identification, geographic area of enlistment, Armed Services Vocational Aptitude Battery (ASVAB) scores, and Armed Forces Qualification Test (AFQT) scores.

Educational data were divided into the following categories: 11 or fewer years, 12 years completed (high school graduation or GED equivalent), 13-15 years completed, or 16 or more years completed. Racial/ethnic classification followed the definitions given by the Office of Management and Budget: White, Black, Oriental, Hispanic, Indian, and Other.

The ASVAB is an instrument that is used to assess an appliant's eligibility to enlist in the Air Force and suitability for classification in specific career fields. The ASVAB yields four aptitude indexes which are predictive of success in technical school: Mechanical aptitude, Administrative aptitude, General aptitude, and Electronics aptitude. Performance on the AFQT is described in terms of centile ranks which are converted to mental ability categories.

The data presented and analyzed in the technical report may not be released without clearance and, hence, cannot be discussed at this time. The technical report, when published by AFHRL, will describe the 1977 - 1979 data and compare these with data reported previously.

## IV. EXIT INTERVIEW INSTRUMENT

The second planned project involved the development of a questionnaire designed to identify factors contributing to attrition. Toward that end, a literature search was conducted. Books and a large number of articles relating to the issue of employee turnover and morale were read. A computer-aided literature search of the ERIC and Psychological Abstracts data bases was conducted, with specific reference to reports dealing with attrition, termination, failure, and morale of enlisted personnel. Work Unit summaries and military technical report summaries for the last 10 years were obtained from the Defense Technical Information Center, Defense Logistics Agency. Many technical reports were obtained and read.

After 2-3 weeks of such activity, interspersed with some of the preparation of the technical report described above, I was able to meet with individuals attached to the Manpower and Personnel office at Randolph Air Force Base, where it was disclosed that work had recently been completed on an exit questionnaire and that data collection was scheduled to begin shortly. Upon consultation with my supervisor at AFHRL, it was agreed that it would be inappropriate to continue with this project.

## V. OTHER ASSIGNED PROJECTS

Following termination of the exit interview project, I became involved in three additional assigned projects.

(A) In 1972, Air Force medical personnel developed a screening procedures, the History Opinion Inventory (HOI), which is useful in identifying recruits likely to have problems in adapting to a military

environment. Research at the AFHRL suggested that the HOI was moderately effective in the prediction of involuntary separations during an individual's first term.

Subsequent to the original research on the HOI, enlistment standards became more stringent, and the utility of the HOI as a predictor of attrition became uncertain. Therefore, a group of 1975 accessions was tested to provide more current data on the effectiveness of the procedure and to provide a basis for a decision regarding implementation.

Data had been collected and a number of statistical analyses had been run on the computer prior to my involvement with the project. My effort involved evaluation of several multiple linear regression analyses and the development of a series of "hit" tables to determine the relative efficacies of the full HOI and certain subscales of the HOI in the prediction of attrition, using alternate definitions of attrition, for male and female enlistees, both separately and altogether. As was the case for the research described above, these data may not be released without approval.

(B) Another research effort undertaken at the request of the Section Chief involved the performance of a content analysis of comments made by Viet Nam combat pilots concerning sources of stress. The data had been collected as part of a larger study dealing with stress, and the comments had been made in conjunction with completion of an extensive questionnaire dealing with stress. The comments revealed many sources of stress that had not been suggested by the questionnaire data. As with the data mentioned above, this information ultimately will be made public in an approved technical report.

(C) The Air Force method for selecting those who will become fighter pilots is based upon recommendation by their instructors, on their successful completion of Undergraduate Pilot Training, and on their expressed preference for flying fighters as opposed to tankers, bombers, or transport planes. Certain foreign pilot training programs and several research efforts have suggested that personal characteristics may be important determiners of successful fighter pilot performance. A few of these characteristics have been identified, but most have been isolated only anecdotally. Additional work involving the development of a suitable screening device appears to be warranted.

Prior to the developement of a screening instrument or battery of instruments to predict effectiveness as a fighter pilot, it is necessary to survey the relevant literature. Toward the end, a literature search was

initiated to identify variables that might be worth pursuing. Among these variables are personal characteristics, such as self-esteem, assertiveness, aggressiveness, willingness to take risks, cognitive style, and others; as well as decision making abilities, particularly under stress, and interpersonal abilities related to effective crew coordination. Perceptual-motor and cognitive tasks also were sought which potentially relate to suitable pilot placement.

## VI. INFORMAL PROJECTS

A personal goal for the summer effort was to sample a variety of related areas, to discuss research and ideas with highly qualified behavioral scientists, to read and study, to assist in the conduct of as many research projects as possible, and, in general, to learn as much as possible in a brief period of time. Much of the activity, therefore, is difficult to document. For example, I read a large number of Air Force technical reports dealing with many aspects of manpower procurement, retention, and utilization. I discussed ongoing and planned research with a number of AFHRL scientists and with colleagues at Randolph and Lackland Air Force Bases. I viewed many hours of video tapes of a course dealing with task analysis that had been conducted at AFHRL prior to my arrival, and I participated in what amounted to a short informal class on linear modeling and policy specification.

This extensive reading and interaction with colleagues has been most valuable, both personally and professionally. I have developed a great appreciation for the manpower and personnel research being conducted by the Air Force and I have gained a great deal of practical, as well as academic, insight into the field. This will result in major changes in a number of my courses and in the development of research projects, which will involve several students.

## VII. RECOMMENDATIONS

The varied projects described in this report do not lend themselves to recommendations regarding implementation of results. The impact of this work will be felt strongly in several classes that I teach. The practical insights that I have gained will translate into major changes in courses dealing with personnel and industrial psychology, research design, and statistics. It has become evident to me that work being done at the HRL in the areas of linear modeling, judgment analysis, and policy capturing has the potential to

liberate behavioral scientists from many of the restrictive limitations of traditional research designs and statistical tests based on the analysis of variance model.

At this time, it is expected that follow-on research will involve the development of a screening test to predict fighter pilot effectiveness. As indicated previously, work is needed to develop methods to predict which candidates have the greatest potential to develop into successful fighter pilots and which have the greatest potential for flying other types of aircraft. My goal is to attempt to develop a perceptual-motor task which will assess a candidate's ability to react quickly to a series of unpredictable events and which will provide, in addition to latency and accuracy measures common to such tasks, an analysis of performance using the methods of the Theory of Signal Detection. Such an analysis would provide information concerning the individual's ability to discriminate relevant and irrelevant events under a variety of conditions and the individual's decision criterion, which may be taken as a measure of impulsivity.

## REFERENCES

1. Leisey, S.A., and Vitola, B.M. "Characteristics of Air Force Accessions: January 1975 to June 1977." AFHRL-TR-76-74, Brooks AFB, TX: Air Force Human Resources Laboratory, January 1979.

2. Guinn, N., Johnson, A.L., an Kantor, J.E., "Screening for Adaptability to Military Service." AFHRL-TR-75-30. Brooks AFB, TX: Air Force Human Resources Laboratory, May 1975.

3. Guinn, N., Kantor, J.E., and Vitola, B.M. "Effectiveness of Adaptability Screening." AFHRL-TR-78-38. Brooks AFB, TX: Air Force Human Resources Laboratory, August 1978.

1980 USAF-SCEEE SUMMER FACULTY RESEARCH PROGRAM

Sponsored by the

AIR FORCE OFFICE OF SCIENTIFIC RESEARCH

Conducted by the

SOUTHEASTERN CENTER FOR ELECTRICAL ENGINEERING EDUCATION

# FINAL REPORT

# PROTON INDUCED NUCLEAR EVENTS IN SILICON


| | |
|---|---|
| Prepared by: | William P. Tucker |
| Academic Rank: | Associate Professor |
| Department and University: | Department of Physics, Florida A & M University |
| Research Location: | Air Force Geophysics Laboratory, Hanscom AFB, MA |
| USAF Research Colleague: | P.J. McNulty, R.C. Rothwell |
| Date: | 3 SEPT 1980 |
| Contract No: | F49620-79-C-0038 |

# PROTON INDUCED NUCLEAR EVENTS IN SILICON

by

William P. Tucker

## ABSTRACT

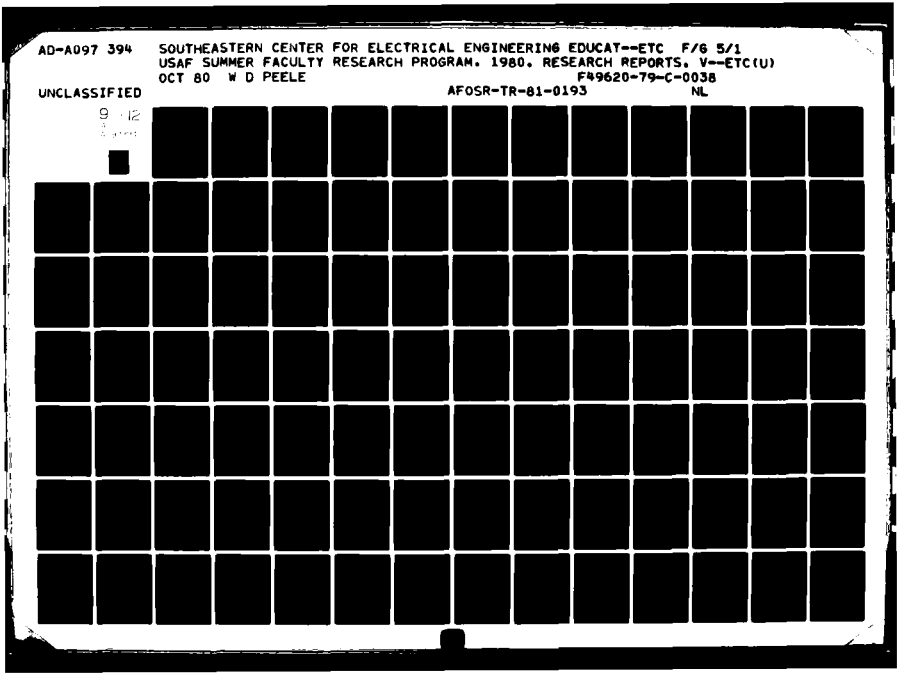
A direct result of the rapid advancements in the miniturization of electronic circuitry (in particular computer memory devices) is a marked increse in the susceptibility of these devices to the deleterious effects of high and low energy charged particles.

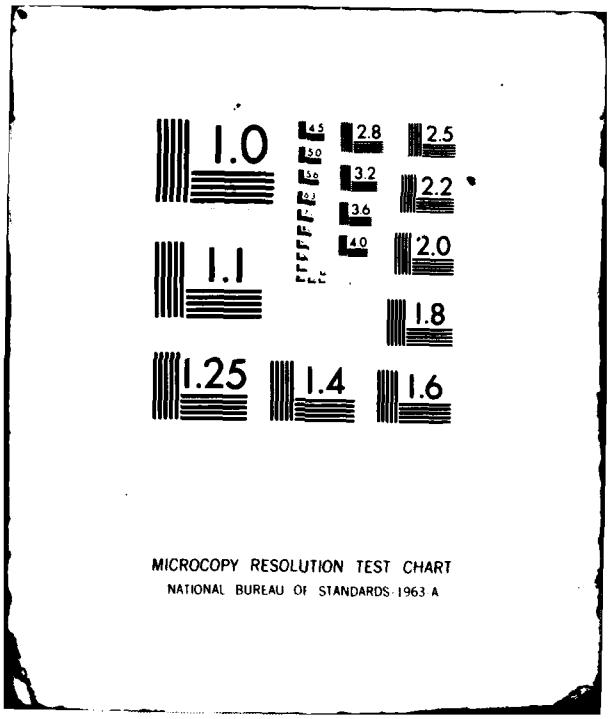
In various types of Random Access Memory (RAM) devices the high and low Z particles cause soft errors (zeroes converted into ones and vice-versa) or logic upsets. In this work one of the mechanisms, nuclear recoil, principally responsible for soft errors is investigated by irridating various thicknesses of silicon with protons whose energies range from 51 to 158 MeV. The spectra of the energy deposited within the silicon slab is thus revealed.

AD-A097 394 SOUTHEASTERN CENTER FOR ELECTRICAL ENGINEERING EDUCAT--ETC F/G 5/1
USAF SUMMER FACULTY RESEARCH PROGRAM, 1980, RESEARCH REPORTS, V--ETC(U)
OCT 80 W D PEELE F49620-79-C-0038

UNCLASSIFIED AFOSR-TR-81-0193 NL

9 12




1.0
1.1
1.25
1.4
1.6
1.8
2.0
2.2
2.5
2.8
3.2
3.6
4.0
4.5
5.0
5.6
6.3
MICROCOPY RESOLUTION TEST CHART
NATIONAL BUREAU OF STANDARDS-1963-A

## ACKNOWLEDGEMENTS

The author would like to convey thanks to the Air Force Systems Command, the Air Force Office of Scientific Research, and the Southeastern Center for Electrical Engineering Education for providing the opportunity to spend a very worthwhile and interesting summer at the Air Force Geophysics Laboratory, Hanscom AFB, MA. I would like to acknowledge the laboratory, in particular the Plasmas, Particles and Fields Branch for its hospitality and outstanding working conditions.

Finally, I would like to thank Dr. Peter J. McNulty of Clarkson College of Technology, Dr. Paul L. Rothwell and Dr. G. Kenneth Yates, both of AFGL for their kind assistance, without which this work would not have been accomplished.

Additionally, the advice and help of A. Koehler of the Harvard Cyclotron are greatly appreciated.

I. INTRODUCTION: Because of the Air Force's increasing use of Large Scale Integrated and Very Large Scale Integrated and Very Large Scale Integrated (LSI and VLSI, respectively) RAM devices in space bourn systems (e.g., missiles and satellites), charged particle induced errors in these devices have generated a considerable degree of interest at this facility and, indeed, throughout the entire electronic industry.

This particular research effort is an extension of the now established efforts of McNulty, Rothwell, et al[1] to explain the physical mechanisms responsible for energetic charged particle induced soft errors in various types of LSI RAM devices. Since such devices are fabricated from silicon, it seemed resonable[2] to pursue the processes involved in particle induced errors by systematically studying the manner in which these particles interact with silicon. The experimental technique[2] employed to obtain data for analysis is one in which thin ( ~3 - 100 μm) silicon wafer diode detectors (by EG & G Oretec) are exposed to a beam of energetic protons (developed by the Harvard Cyclotron), some of which interact inelastically with the silicon nuclei, giving rise to fast and slow secondaries and recoiling residual nuclear fragments. There is ample reason[2] to believe that the residual recoiling nuclei are the prime contributors to soft errors in various types of static and dynamic RAMs.

When protons at energies greater than about 30 MeV enter silicon, several different types of inelastic scattering proceses can ensue. Principally, nucleons in the target nucleus are excited, leading to a cascade of intra-nuclear fast nucleons, some of which may be ejected from the nucleus or be captured and, thus, leave the nucleus in an excited state. The de-excitation of the target nucleus can occur in several stages over a period of about $10^{-16}$ sec, a time short in comparison with that required for the initial excitation ( $\sim 10^{-21}$ sec), please see Fig. 1.

The excited nucleus loses energy by emitting various types of particles, (alpha, deuterons, etc.) all of which contribute to the recoil momentum of the residual nucleus. During the time of transit ( $\sim 10^{-12}$ sec) of the recoiling nucleus, many electron-hole pairs (3.6 ev/pair) are created, contributing substantially to the phenomenon of logic upset in LSI, and especially VLSI RAM devices. The work of other investigators[3] (Greiner et al.) suggests that the recoiling nuclear fragments represent a significant fraction of the energy deposited in the crystal. Model calculations using results of Greiner et al.,[3] Silberberg, Tsao[4] and G.E. Ferrell[5] are in progress and will be presented for publication at a later date. This summer's effort resulted in the completion of some of the experimental work (data acquisition) and the initial stages of the analysis.

II. OBJECTIVES OF THE RESEARCH EFFORT: The principle objective of this project was to gain insight into the physical processes that lead to proton induced logic upsets (soft errors) in LSI and VLSI Memory devices. Since the recoiling fragments of the initial target nuclei (silicon) are believed to contribute substantially to the upset events, it was decided that more information (up to now, non-existent) on the inelastic processes involving silicon nuclei and protons was needed. We, therefore, began to acquire the experimental data with which model calculations can be compared and thus enable us to make more definitive statements about the mechanisms involved.

To this end, the task for this summer was to: a) Calibrate and test newly acquired (from Ortec) silicon surface barrier detectors of various thicknesses (2, 10, 50 and 100 μm). b) Expose the detectors to protons of energies ranging from 51 to 158 MeV. c) Complete the initial data reduction and determine the energy deposition spectra.

It should again be noted that additional data reduction and analysis are in progress and will be submitted to an appropriate journal for publication.

III. EXPERIMENTAL PROCEDURES: The calibration of the silicon surface barrier detector is a relatively straight forward procedure. A very precisely known source (in this case, AM 241 which has a strong alpha peak at 5.5 MeV) of charged nuclear particles (e.g., $\alpha$ particles) is used to determine the signal level that can be expected for a given amount of energy deposited in the structure of the detector (silicon). This information is then used to calibrate the output of the multichannel analyzer (see Fig 2).

The proton scattering experiments were carried out at the Harvard Cyclotron, a facility capable of delivering a 2 mm diameter beam of 158 MeV (maximum) protons. The experimental configuration is shown in Figure 3. In this experiment, the detectors (97 μm; 2.8 μm) were each given four different exposures at beam energies of 51, 91, 130 and 158 MeV. The above energies were achieved by inserting lucite and coper degraders into the path of the 158 MeV stream of particles. This practice tended to increase the background of secondary particles (eminating from the degraders), making it necessary to carry out additional experiments using an aperature plug between the degraders and the detectors. This resulted in the establishment of background levels that were used to determine the true energy deposition spectra.

The silicon surface barrier detectors (in the form of diode slabs) were each subjected to a bias voltage of sufficient strength to make them fully depleted (total separation of electrons and holes). The protons (up to $10^6$/min) entered the biased detector, underwent inelastic collisions with silicon nuclei which underwent evaporative fragmentation, recoiled and, in so doing, created electron hole pairs in the fully depleted zone of the detector. The strong bias field quickly swept the resultant charge out of the depletion zone and into the charge coupled pre-amplifier. The pre-amplifier output was shaped and fed into the multi-channel analyzer. The resulting spectra minus the background represents the spectra of the energies deposited in the slab.

## IV. RESULTS

Using the results of the AM 241 calibration experiments the multi-channel analyzer output was divided into 1 MeV bins (6.94 channels/MeV). Histograms of the energy spectra (counts Vs. energy) were prepared and are shown in Figures 4-7. The results shown here are for the 97 μm detector. Due to equipment failures the data on the 2.8 and 8.7 μm detectors were not sufficiently complete to permit complete analysis.

However, the 97 μm data is quite significant in that, to our knowledge, such an experiment had (previous to this work) never been carried out.

The 97 μm data appears to be in substantial agreement with those of McNulty, et al.[2] where a 21 μm detector was exposed at the same energy levels. Moreover, the 97 μm data relative to that for 21 μm shows a longer high energy tail, a result which supports the belief that many fast secondaries tend to escape thinner detectors.

## V. RECOMMENDATIONS:

From the above results an obvious recommendation follows.

The work on the thinner detectors must be completed in order to fully establish the validity of the statement that the high energy tail of the energy deposition spectra decreases as a function of thickness.

The current state of the art in the microelectronics field has advanced to the point where component structures can be fabricated within linear dimension of only a few microns. It is, therefore, likely that different parts of a chip will exhibit vastly different susceptibilities to logic upset. Such differences may be due to the particular technique used to fabricate the device and/or the variations in types of materials used to develop the various discrete regions of a given chip. In order to determine where the vulnerabilities to logic upsets of a given VLSI device lie, it will be necessary to employ particle accelerators capable of confining a beam to linear dimension that do not exceed the intercomponent dimensions ( ~1μm) of a device. Hopefully, the use of now existing microbeam accelerator will be used to verify the radiation hardness of the rapidly developing VLSI devices in the very near future.

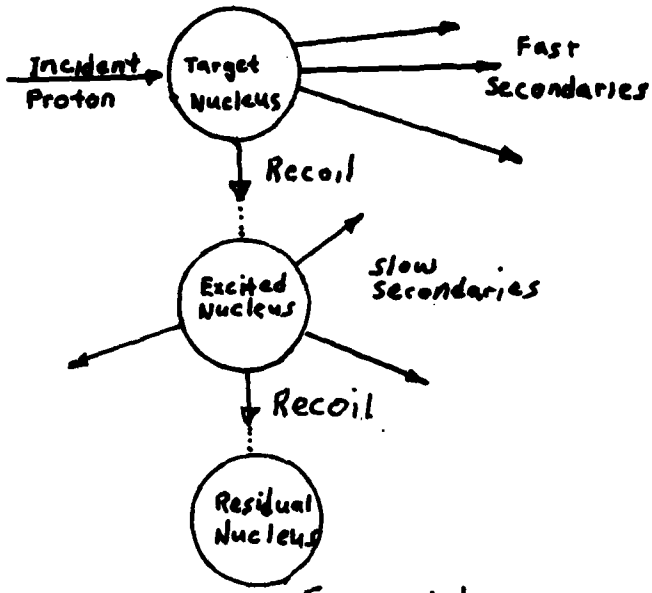



FIGURE 1 - Nuclear Fragmentation

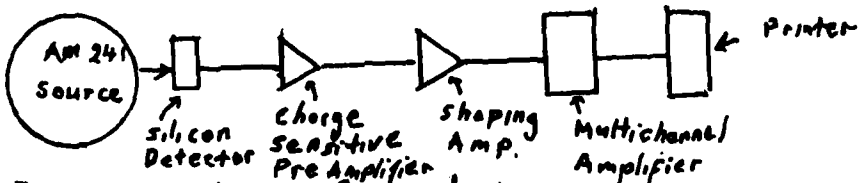



Figure 2 - Detector Calibration

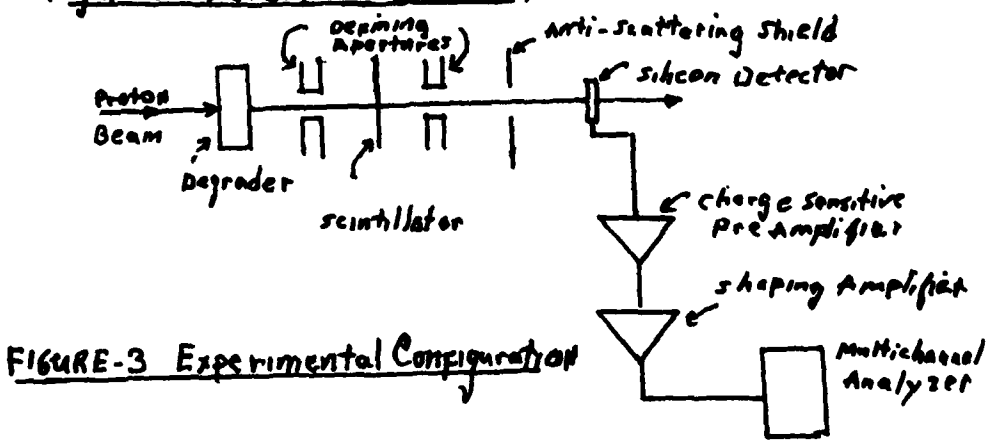



FIGURE-3 Experimental Configuration

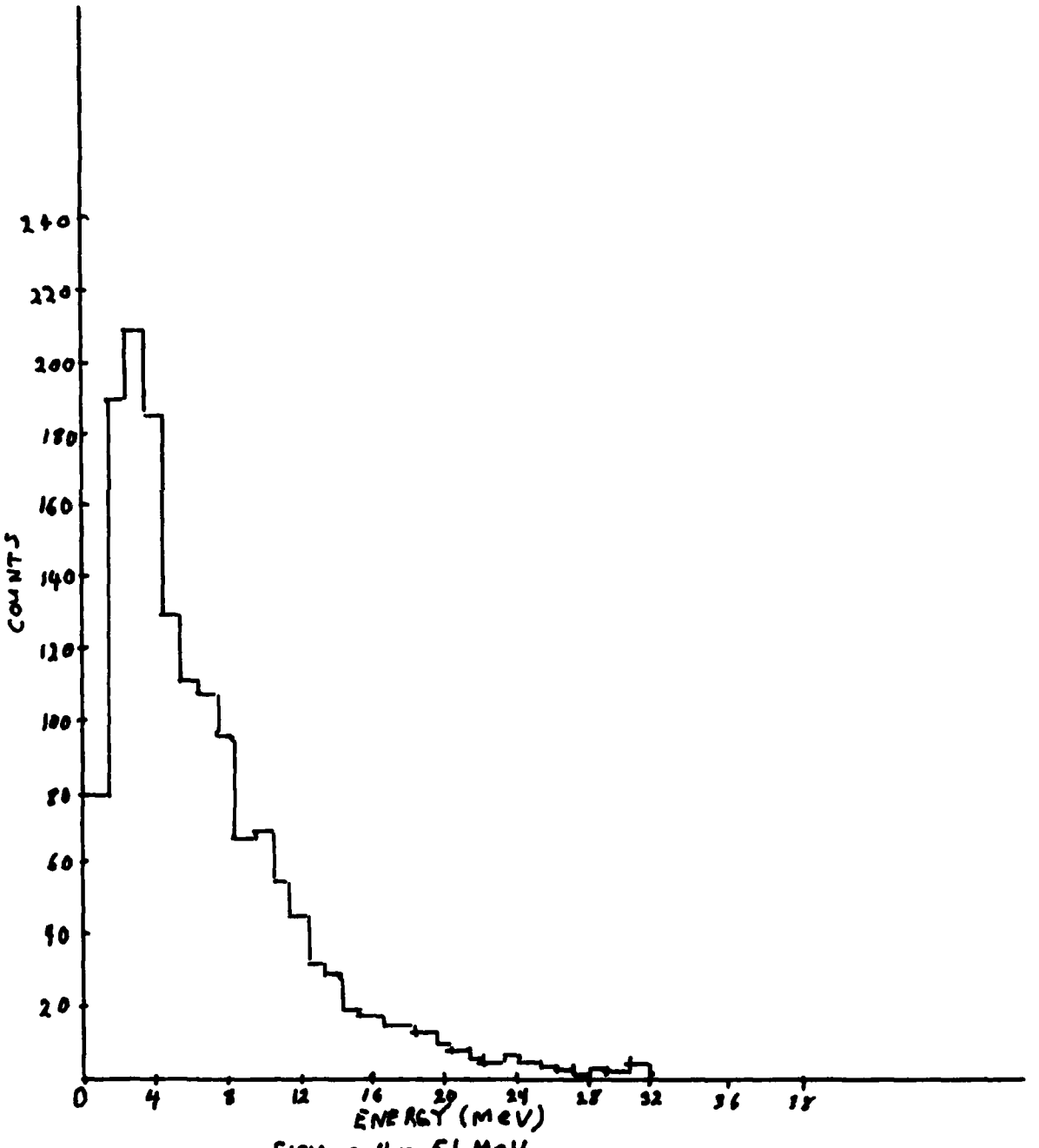



Figure 4 - 51 MeV

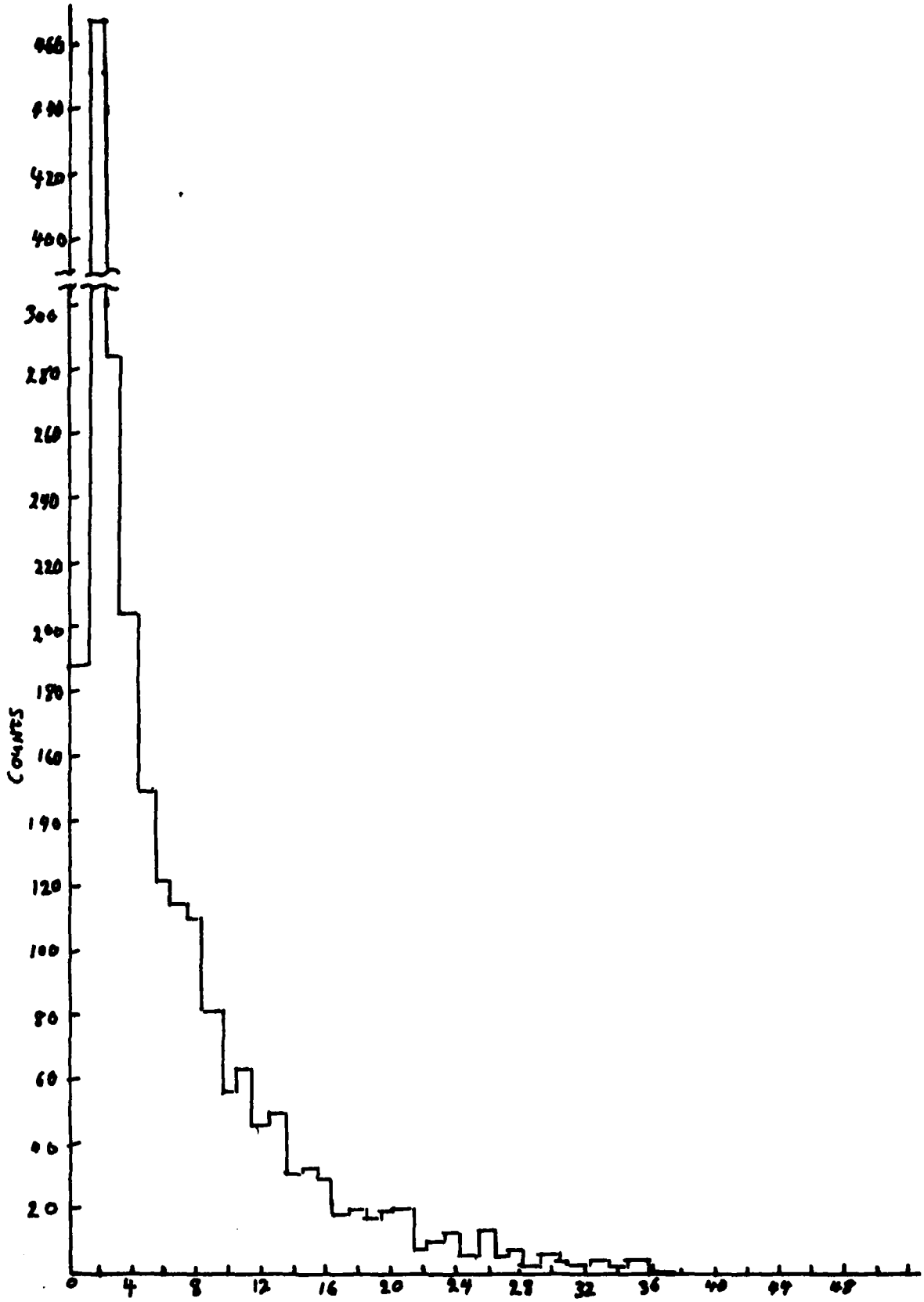



Figure 5-91MeV

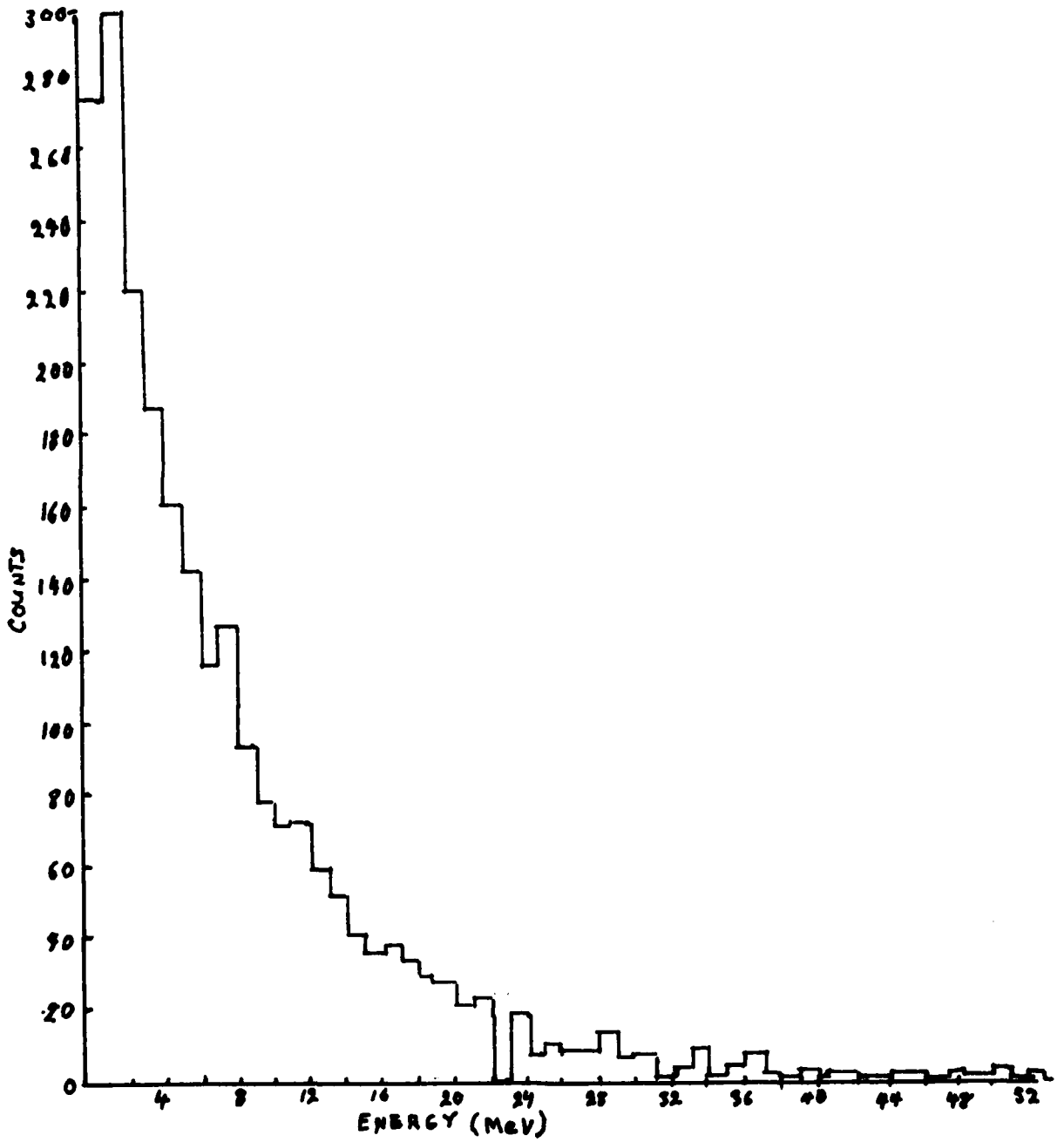



Figure 6- 130 MeV

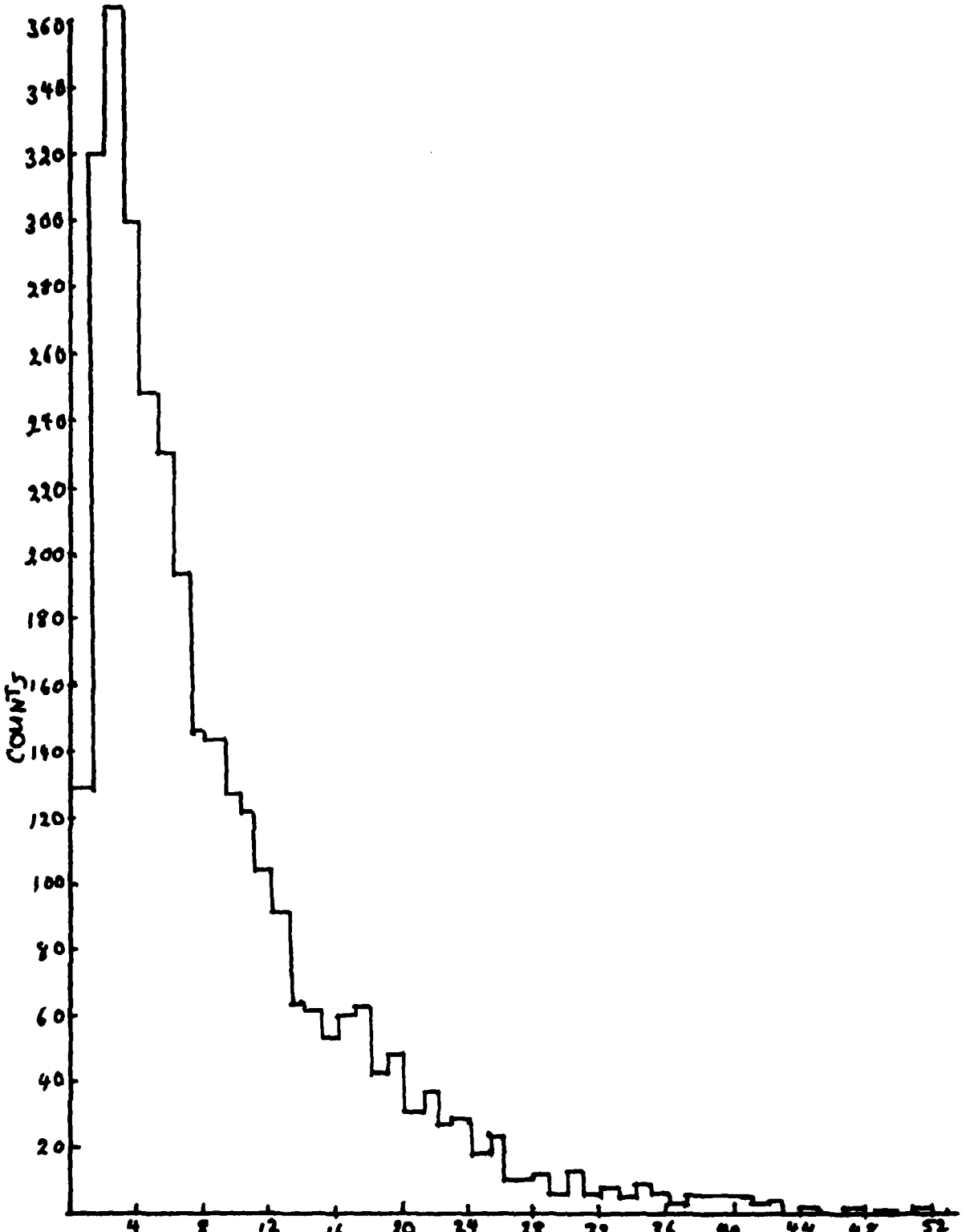



Figure 7 - 158 MeV

## REFERENCES


1. R.C. Wyatt, P.J. McNulty, P. Toumbas, P.L. Rothwell, and R.C. Filz, "Soft Errors Induced by Energetic Protons" IEEE Trans. Nucl. Sci. NS-26, 4905 (1979).

2. P.J. McNulty, G.E. Ferrell;, R.C. Wyatt, P.L. Rothwell, and R.C. Filz, "Upset Phenomena Induced by Energetic Protons and Electrons, Proc. IEEE, 1980 Annual Conference on Nuclear and Space Radiation Effects, Cornell University, Ithaca, N.Y., July 1980, pp C-2.

3. D.E. Greiner, P.J. Lindstron, H.H. Heckman, B. Cork, and F.S. Beiser, "Momentum Distribution of Isotopes Produced by Fragmentation of Relativistic $^{12}C$ and $^{16}O$ Projec.iles" Phys. Rev. Lett., 35, 152 (1975).

4. R. Silberberg, and C.H. Tsao, "Partial Cross Sections in High-Energy Nuclear Reactions, and Astrophysical Applications. I. Targets with $Z \leq 28$" Astrophysical Journal Supplement, 25, 315 (1973).

5. John N. Bradford, "Nonequilibrium Radiation Effects in VLSI", IEEE Trans. on Nucl. Sci., NS-25 (5), pp 1144-1195, Oct 1978.

6. Private Communication
   G.E. Farrell, Summer 1980.

1980 USAF - SCEEE SUMMER FACULTY RESEARCH PROGRAM

Sponsored by the

AIR FORCE OFFICE OF SCIENTIFIC RESEARCH

Conducted by the

SOUTHEASTERN CENTER FOR ELECTRICAL ENGINEERING EDUCATION

FINAL REPORT

# A MODEL FOR THE THERMAL DECOMPOSITION OF TNT; THEORETICAL REACTION PROFILES


Prepared by: Professor Almon G. Turner

Academic Rank: Professor

Department and University: Department of Chemistry, University of Detroit

Research Location: Frank J. Seiler Research Laboratory, USAF Academy, Colorado

USAF Research Colleague: Dr. Larry P. Davis



Date: August 15, 1980

Contract No: F49620-79-C-0038

# A MODEL FOR THE THERMAL DECOMPOSITION OF TNT; THEORETICAL REACTION PROFILES

by

Almon G. Turner

## ABSTRACT

The molecule 1-nitropropylene has been investigated as a model system for the simulation of the thermal decomposition of TNT. Two distinct types of reaction mechanisms were considered: Intramolecular Mechanisms and Bimolecular Mechanisms. Intramolecular mechanisms investigated include an oxidative hydrogen atom transfer to form the diradical aci nitropropylene and an oxidative oxygen atom insertion reaction to form 1-nitro-3-hydroxy propylene. Semi empirical molecular orbital calculations (MNDO and MINDO/3) were carried out to obtain a reaction profile for these mechanisms, and indicated that the oxygen atom insertion reaction should lead to the reaction products, methyl nitrite and acetylene. This is not in accord with experiment. The profile for the oxidative hydrogen atom transfer was found to reproduce many of the features known for the thermal decomposition of TNT.

Bimolecular mechanisms considered included an oxidative hydrogen atom transfer from one nitropropylene molecule to another to form the 1-nitropropylene radical and the aci form of nitropropylene and an intermolecular oxidative insertion reaction to form 1-nitro-3-hydroxy propylene and 1-nitroso propylene. Preliminary reports are given for these bimolecular mechanisms.

## Acknowledgements

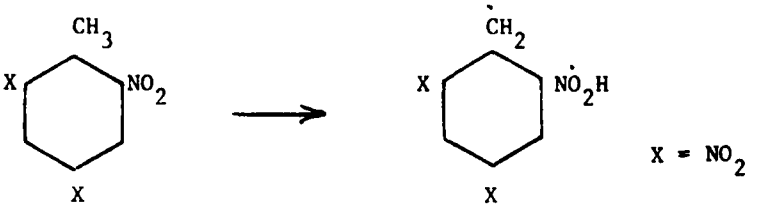
The author would like to thank the Air Force Systems Command, the Air Force Office of Scientific Research and the Southeastern Center for Electrical Engineering Education for financial support via a Summer Faculty Research Program Fellowship. He should like to acknowledge the hospitality extended to him by the members of the Frank J. Seiler Research Laboratory, USAF Academy.

He should particularly like to acknowledge the cooperation of Capt Larry P. Davis for introducing him to the area of the chemical decomposition of explosives and for the many helpful discussions held in this area.

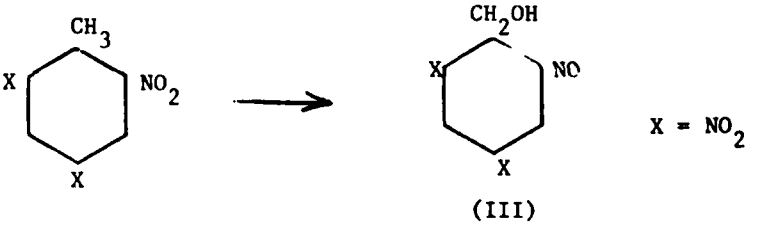
I. INTRODUCTION:

A large number of experimental studies have been carried out in an effort to obtain an understanding of the thermal decomposition of trinitrotoluene (TNT)[1]. These studies have resulted in the proposal of four different possible reaction mechanisms for the process[2]. The mechanisms proposed are:

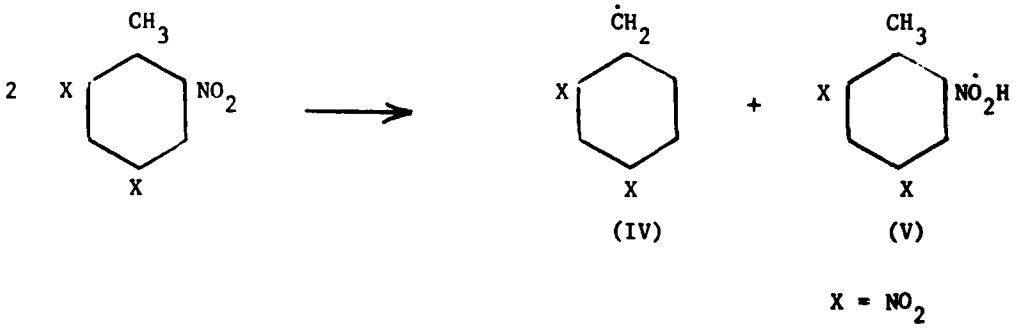
a. Intramolecular Oxidative Hydrogen Atom Transfer.



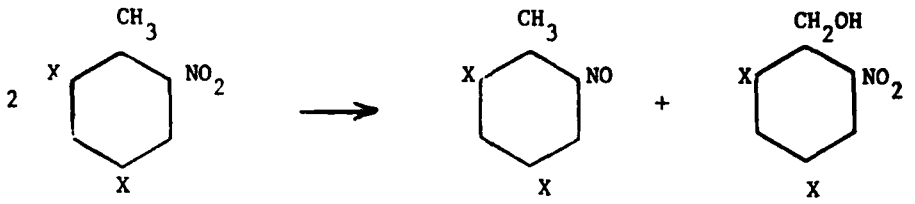

b. Intramolecular Oxidative Oxygen Atom Transfer.




c. Intermolecular Oxidative Hydrogen Atom Transfer.



d.




(VI) (VII)

X = $NO_2$

Recent advances in semiempirical molecular orbital methods (MNDO, MINDO/3) have demonstrated that the standard enthalpies of formation, $\Delta H_f^\circ$, can be calculated with some confidence for small molecules[3]. These same methods have been utilized to study reaction mechanisms for elementary processes of the type which occur in the above mechanisms[4]. The shear size of the TNT molecules prohibits an exhaustive investigation of the proposed mechanisms by the MNDO method. Accordingly it would be advantageous to find a smaller molecular system which might possess the salient features of TNT, and could thus be used to model the mechanisms proposed above. The author has suggested that the 1-nitropropylene molecule might be suitable for these purposes. The research reported below is concerned with the use of 1-nitropropylene to model the thermal decomposition of TNT.

## II. OBJECTIVES

The main purpose of this research was to ascertain the extent to which mechanisms analogous to those listed above but studied in the system 1-nitropropylene can be used to model the decomposition of TNT. Specific objectives were:

(1) To study the thermodynamics of the proposed reactions and compare the results to the corresponding values for the TNT system.

(2) To obtain reaction profiles for each of the proposed mechanisms and to identify the transition state for each of the mechanisms. Successful identification of a transition state enables one to calculate

the energy of activation for the process, which in turn can be compared to results obtained from the experimental study of the decomposition.

## III. THEORETICAL METHODS

The principal method employed to study the decomposition of 1-nitropropylene was the MNDO (Modified Neglect of Differential Overlap) molecular orbital method of Dewar et. al.[3,4]. The method was applied in its "closed shell" form to those mechanisms which did not involve radical species, while it was combined with the method of configuration interaction to treat radical species[5]. 3 x 3 configuration interaction was carried out using the ground state configuration and the two configurations obtainable from it using the two lowest unoccupied molecular orbitals obtained from the ground state calculation.

## IV. THERMODYNAMIC STUDIES

The specified chemical reaction (mechanisms) studied were:

i. Intramolecular Hydrogen Atom Transfer

$CH_3CHCHNO_2 \longrightarrow \cdot CH_2CHCHNO_2H$

1-nitropropylene (I) ACI-nitropropylene (II)

ii. Intramolecular Oxygen Atom Transfer

$CH_3CHCHNO_2 \longrightarrow HOCH_2CHCHNO$

1-nitroso-3-hydroxy propylene (III)

iii. Intermolecular Hydrogen Atom Transfer

$2\ CH_3CHCHNO_2 \longrightarrow \cdot CH_2CHCHNO_2$ (IV) + $CH_3CHCHNO_2H$ (V)

iv. Intermolecular Oxygen Atom Transfer

$2\ CH_3CHCHNO_2 \longrightarrow CH_3CHCHNO$

1-nitrosopropylene (VI)

$+\ HOCH_2CHCHNO_2$

1-nitro-3-hydroxy propylene (VII)

The ground state energies and heats of formation were calculated for species I - VII and the corresponding heats of reaction calculated. The 1-nitropropylene molecule was calculated in a geometry where the nitro

group was rotated about the carbon atom so as to have it in the same conformation that it would have were it a part of a TNT molecule. The energy of the true ground state form (unrotated) was found to be 18.10 Kcal/mole. The energy of the rotated "TNT like" form was calculated to be 18.99 Kcal/mole. The results of these calculations are shown below.

Calculated Standard Heats of Formation

| Mechanism | Reactant | Product(s) | $\Delta H_f^\circ$ | TNT Case |
|---|---|---|---|---|
| i | 18.99 | 33.50 | +14.51 | 16.6 |
| ii | 18.99 | -30.32 | -49.31 | -49.9 |
| iii | 37.98 | IV 48.63; V 8.88 | 19.53 | 16.8 |
| iv | 37.98 | VI 12.45; VII 022.98 | -48.51 | -52.4 |

The experimental activation energy for the initiation step in the decomposition of TNT is known to be 40-46 Kcal/mole. Since the $\Delta H_f^\circ$ for the reaction is a lower bound for the corresponding activation energy all the above mechanisms are possible. The corresponding enthalpy changes have been calculated for three of the four mechanisms in the case of TNT. The values are given in the last column of the table. Note the relative order of agreement is good. On the basis of thermodynamics the 1-nitropropylene system seems to reflect the same energetic behavior as the TNT system.

## V. INTRAMOLECULAR HYDROGEN ATOM TRANSFER MECHANISM

Optimization of the ground state energy of aci nitropropylene yielded a value of 33.50 Kcal/mole for the heat of formation of the product molecule. The hydrogen atom transfer was initially viewed by using the hydrogen atom oxygen atom distance as the reaction coordinate. The distance varies from 3.73 Å in 1-nitropropylene to 0.95 Å in product aci form. A reaction profile was calculated along this path at values for the reaction coordinate of 3.73, 3.27, 2.77, 2.27, 1.77, 1.50, 1.40, 1.35, 1.30, 1.25, 1.20, 1.175, 1.15, 1.125, 1.10, 1.00, 0.95 Å. A maximum was obtained in the vicinity $d_{O-H}$ = 1.20 where $\Delta H_f^\circ$ = 81.4 Kcal/mole, which corresponds to an activation energy of 62.4 Kcal/mole. The product state was identified at a heat of formation of about 27.4 Kcal/mole and did not correspond geometrically

to the aci form of 1-nitropropylene. Attempts were made to start from this new product state and back calculate to the initial state. These attempts were unsuccessful.

The next series of calculations performed consisted of starting the reaction profile in the product state and attempting to find a path which would lead to the starting material. This was done by defining the reaction coordinate to be the hydrogen atom - methyl carbon atom distance. This distance varies from 3.234 Å to 1.497 Å in the reactant. Points were calculated at values of 3.20, 3.00, 2.50, 2.00, 1.75, 1.60, 1.50, 1.40, 1.35, and 1.30 Å. A profile was obtained with a maximum energy of 86.3 Kcal/mole corresponding to an activation energy of 52.8 Kcal/mole occurring at $d_{C-H}$ = 1.37 Å. An attempt was made to reverse the calculation and it was found that the path was not reversible, the reverse path leading to a new maxima in energy in excess of 76 Kcal/mole. The two profiles intersected at about 1.59 Å with an energy of about 69 Kcal/mole. Application of the MINDO/3 method led to the same basic results. From these calculations it was concluded that neither the hydrogen - oxygen atom distance nor the hydrogen atom - methyl carbon atom distance was a suitable reaction coordinate. It is probably necessary to use both. In addition as the molecule proceeds from reactant to product a considerable readjustment occurs in the $H_3C_1-C_2=C_3-N_4$ framework. The $C_1-C_2$ and $C_3-N_4$ bonds are shortened considerably, while a lengthening occurs in the $C_2-C_3$ bond. Accordingly, a series of calculations were carried out for $d_{O-H}$ distances of 0.96, 1.00, 1.10, 1.20, 1.70, 1.40, and 1.50 where the $C_1-C_2=C_3-N$ framework was fixed at values which corresponded to one third, one half, and two thirds of the way along the progression from starting material to product material. The results of these calculations are in Table 1. Listed are the $\Delta H_f^\circ$'s and the algebraic sign of $dE/dX$.

Table 1 **GRID MOVING FROM REACTANT TO PRODUCT**

| | $d_{O-H}$ | | | | | | |
|---|---|---|---|---|---|---|---|
| | 0.96 | 1.00 | 1.10 | 1.20 | 1.30 | 1.40 | 1.50 |
| Starting Material | 62.6- | 63.8+ | 91.6- | 81.8- | 71.5- | 61.8- | 53.0- |
| 1/3 | 42.9- | 43.7+ | 52.0+ | 83.1- | 73.4- | 64.0- | 55.4- |
| 1/2 | 76.6- | 37.4+ | 45.7+ | 85.8- | 76.8- | 67.8- | 59.3- |
| 2/3 | 32.6- | 33.7+ | 45.6+ | 89.3- | 81.2- | 72.4- | 64.0- |
| Product Material | 27.6- | 28.4+ | 36.9+ | 56.1+ | 96.8- | 88.9- | 81.1- |

The line delineates the region of the hypersurface where maxima are located.

The largest maxima being in the region of $120 < d_{O-H} < 1.30$ with the geometry being virtually TNT or product like. Calculations were then performed to test the reversibility of the reaction coordinate $d_{O-H}$. Starting with the TNT like geometry (two thirds) at $d_{O-H} = 1.10$, $d_{O-H}$ was allowed to increase to 1.20, 1.30 and 1.40. At each point a lower energy form was found. This indicated that the $C_1$-$C_2$ = $C_3$-N framework must also be relaxed.

A grid search was conducted by performing calculations which start with a TNT like geometry and allowing $d_{O-H}$ to vary from 1.00 to 1.60 and at the same time allowing $d_{C-H}$ to vary from 1.20-1.80. The results are shown in Table 2.

Table 2 **GRID SEARCH HYDROGEN ATOM TRANSFER**

| | | $d_{O-H}$ | | | |
|---|---|---|---|---|---|
| | | 1.00 | 1.20 | 1.40 | 1.60 |
| | 1.20 | 119.9- | 84.0- | 61.8- | 48.0- |
| | 1.40 | 86.5- | 83.5- | 72.0- | 63.3- |
| $d_{C-H}$ | 1.60 | 66.2- | 78.9+ | 91.2- | 88.2- |
| | 1.80 | 54.9+ | 72.1+ | 108.2+ | 110.5- |
| | 2.00 | | | | |

The solid line in the table defines points in the hypersurface along which maxima occur.

Calculations were next carried out by starting with the product like geometries for $d_{O-H}$ equal to 1.00 and attempting to proceed to the TNT like geometries for each C-H distance. It appears that some points of lower energy can be located in this manner.

In summary, the location of transition state for this mechanism is particularly difficult and involves a great deal of trial and error calculation. It is felt that a transition state is being approached asymptotically but the calculation points to the severe need for an analytical approach to the problem.

## VI. INTRAMOLECULAR OXYGEN ATOM TRANSFER MECHANISM

A calculation of the optimized ground state energy of the product molecule, 1-nitroso-3-hydroxy propylene yielded a standard enthalpy of formation of -30.32 Kcal/mole. The methyl carbon-oxygen atom distance was employed as a reaction coordinate and it was allowed to vary from 3.73 Å (starting material) to 1.40 Å (product material). A reaction profile was obtained which showed an activation energy of 96 Kcal/mole and a maximum present at $d_{C-O}$ = 1.75 Å. An examination of the product state ($\Delta H_f^\circ$ = 21.71 Kcal/mole) showed it to consit of molecular acetylene, $C_2H_2$; and methyl nitrite, $CH_3ONO$. A rerun of the calculation using configuration interaction led to new transition state of a higher heat of formation than that calculated previously. As such, it was not pursued further. An attempt was made to establish a reaction profile in the direction product to reactant. It also led to a higher activation energy.

## VII. INTERMOLECULAR MECHANISMS

Work was just being initiated on these mechanisms as the period of my fellowship came to end. Planary calculations were begun on a mechanism in which the 1-nitropropylene molecules were stacked end to end with the hydrogen atom to be transferred of one molecule located symmetrically between the two oxygen atoms of the nitro group of the second molecule. The distance from the oxygen atom of the second molecule to the methyl carbon atom of the first molecule was used as a reaction coordinate. These efforts are continuing at the present time.

## VIII. AN ANALYTICAL APPROACH

The principal difficulties encountered in these studies seems to be the recognition of what to use for a reaction coordinate in a given mechanism. The reaction coordinate is generally not a simple atom-atom distance, bond angle or dihedral angle but rather it is expressible as a linear combination of those atom-atom distances, bond angles and dihedral angles which change markedly as one proceeds from reactant to product. As such, it can be uniquely identified once it is recognized what internal coordinates (bond distance - bond angle basis) enter into it. One way to proceed would be to do a few planary calculations to identify which internal coordinates, $|q|$ enter the reaction coordinate, $\phi$ and then solve the required set of linear equations to identify the reaction coordinate. Explicitly, let

$$\phi = \sum_i a_i q_i \qquad i = 1, n \tag{1}$$

Consider the energy as a function of $\phi$,

$$E = E(\phi) \tag{2}$$

Since we are always seeking a transition state, E is a maximum for such a state, we can write

$$E = X\phi^2 + Y\phi + Z \tag{3}$$

and we know that $X < 0$ and $Y > 0$. The reaction coordinate must belong to one of the irreducible representations of the point group which is appropriate to the transition state geometry.

From a set of $n^2$ values for the $|q|$ one can calculate $n^2$ values of the energy $\varepsilon$. Since the energy is a quadratic function of the $|q|$ we can write

$$\begin{aligned} \varepsilon_1 &= b_{11}q_{11}^2 + b_{12}q_{12}^2 + \cdots b_{1n}q_{1n}^2 + b_{1o}q_{11} + b_{2o}q_{12} + b_{no}q_{1n} + b_1 \\ &\vdots \\ \varepsilon_{n2} &= b_{11}q_{n1}^2 + b_{12}q_{n2}^2 + b_{1n}q_{n,n}^2 + b_{10}q_{n,1} + b_{no}q_{n,n} + b_1 \end{aligned} \tag{4}$$

The linear equations (4) can be solved to obtain the coefficients $|b|$. These coefficients in turn are related to coefficients $|a|$ of equation (1). Namely

for quadratic terms

$$b_{ij} = X\, a_i a_j \tag{5}$$

for linear terms

$$b_{io} = Y_{ai} \tag{6}$$

and

$$b_1 = Z \tag{7}$$

From eqn. (6) we in effect know the coefficients $|a|$ to within the normalization constant Y. If we redefine the norm of the space spanned by the reaction coordinate, we can calculate the $|a|$ and then obtain our reaction coordinate.

## IX. RECOMMENDATIONS

On the basis of the above research the following recommendations can be made:

1. That the grid search method employed in part V be continued until a transition state is obtained which will reversibly interconnect reaction and product for the intramolecular hydrogen atom transfer mechanism.
2. That the intramolecular oxygen atom transfer be rejected as a possible reaction path in the initiation of the thermal decomposition of TNT.
3. That the analytical approach (part VIII) to finding a reaction coordinate be tested in the context of a known reaction mechanism and if successful then used to pursue the study of the bimolecular mechanisms of part VII.
4. That the questions concerned with the effects of overcompleteness and undercompleteness in the choice of the set of variables $|q|$ be investigated on the analytical approach (part VIII).

## REFERENCES


1. For representative studies see:

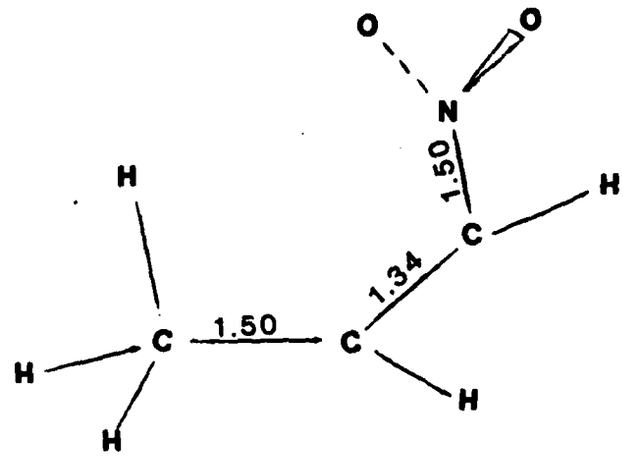
R. Robertson, J. Chem. Soc. 119, 1 (1921); Trans. Far Soc. 44, 977 (1948); M. A. Cook and A. B. Taylor, Ind. Eng. Chem. 48, 1090 (1956); J. C. Dacons, M. J. Kamlet, and D. V. Sickman, NAVORD Rept. 6831 (1970); J. C. Dacons, H. C. Horst, and M. J. Kamlet, J. Phys. Chem. 74, 3035 (1970); R. N. Rogers, Anal. Chem. 39, 730 (1967); J. M. Rosen and J. C. Dacons, Explosivstoffe, 11 250 (1968); J. W. Beckmann, J. S. Wilkes, and R. R. McGuire, Thermchim. Acta, 19, 111 (1977); S. A. Shackelford, J. S. Wilkes, and J. W. Beckmann, J. Org. Chem. 42, 4201 (1977).

2. R. M. Guidry and L. P. Davis, Proc. of the Ninth Annual Pittsburg Conference, American Instrument Society, Volume 9, Modeling and Simulation, Page 331, 1978.

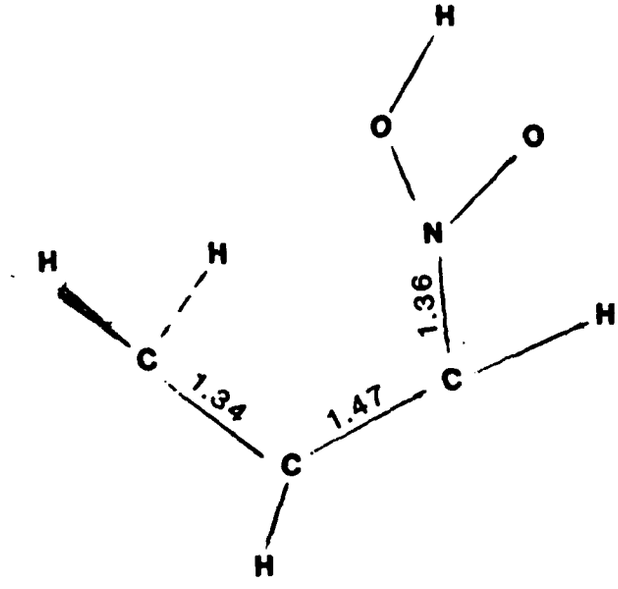
3. R. C. Bingham, M. J. S. Dewar, and D. H. Lo, J. Amer. Chem. Soc. 97, 1285 (1975).

4. M. J. S. Dewar and W. Thiel, J. Amer. Chem. Soc. 99, 4899 (1977).

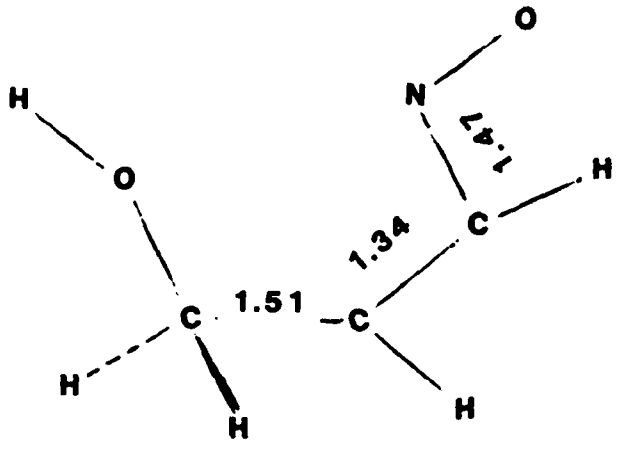
5. The open shell structure of radical species necessitates the inclusion of neighboring configurations of the same spin multiplicity. We assume that we are operating at a "near" Hartree Fock level of approximation and include only configurations obtainable from the parent configuration by "two electron jumps".




GEOMETRY OF 1- NITROPROPYLENE




GEOMETRY OF "acl" NITROPROPYLENE




**GEOMETRY OF 1-NITROSO-3-HYDROXY PROPYLENE**

1980 USAF - SCEEE SUMMER FACULTY RESEARCH PROGRAM

Sponsored by the

AIR FORCE OFFICE OF SCIENTIFIC RESEARCH

Conducted by the

SOUTHEASTERN CENTER FOR ELECTRICAL ENGINEERING EDUCATION

FINAL REPORT

# IMPROVEMENT OF TRAJECTORY TRACKING ACCURACY OF INSTRUMENTATION SHIPS: A FEASIBILITY STUDY


| | |
|---|---|
| Prepared by: | Dr. V. Vemuri |
| Academic Rank: | Associate Professor |
| Department and University: | Department of Computer Science<br>State University of New York |
| Research Location: | Eastern Space and Missile Center<br>Range Systems and Navigation |
| USAF Research Colleague: | Mr. Steve Andrews |
| Date: | August 15, 1980 |
| Contract No. | F49620-79-C-0038 |

# IMPROVEMENT OF TRAJECTORY TRACKING ACCURACY OF INSTRUMENTATION SHIPS: A FEASIBILITY STUDY

by

V. Vemuri

## ABSTRACT

The question of the feasibility of improving metric accuracy of radar data obtained from instrumentation ships is investigated. It is argued that major sources of error are tracking, navigation and stabilization. Using available data as a guide, it is argued that substantial improvements in metric accuracy are attainable if the present auto-tracking is upgraded to on-axis tracking with a Kalman-type filter in the tracking loop. It is also recommended that a simulation study be conducted to gain better insight into the nature of navigational and stabilization errors. These two recommendations are considered to be most cost-effective within the constraints of the mission under study.

## ACKNOWLEDGEMENTS

The author would like to thank the Air Force Systems Command, the Air Force Office of Scientific Research and the Southeastern Center for Electrical Engineering Education for providing him with the opportunity to spend a useful summer at the Eastern Space and Missile Center (ESMC), Patrick AFB, FL. He would like to thank the people at ESMC, in particular, those associated with RSN for their hospitality.

Although several people went out of their way to help the author in formulating the ideas presented here, particular mention must be made of Steve Andrews (USAF), Walt Elenburg (RCA), and Charles Miller (USAF) for their collaboration and guidance. Further, they read an initial draft of this report and helped the author in identifying and correcting several errors. Finally, the author gratefully acknowledges all the help he received from Connie Pelligra for typing this report.

## I. INTRODUCTION

The USNS General H. H. Arnold and USNS General H. S. Vandenberg, operated by the Air Force Systems Command, Eastern Space and Missile Center (ESMC), are two Advanced Range Instrumentation Ships (ARIS) designed to gather precision data on missile reentry bodies and penetration aids.[1] The primary mission of these ships is to collect metric and signature data during the midcourse and reentry phases of a ballistic missile's flight. These instrumentation ships play a significant role because they constitute a flexible expansion of a missile test range beyond the coverage capabilities of land based instrumentation. Therefore, these ships play a crucial role in tracking the terminal segment of a reentry vehicle's (RV) trajectory that, very often, falls in remote ocean areas.

Although there are differences, each ARIS in general, and H. S. Vandenberg in particular, is equipped with advanced instrumentation to gather radar, telemetry, optical, opto-radiometric, navigation, and meteorological data. Typically, during a trajectory mission, an ARIS collects data on:

(1) Metric information such as range, azimuth and elevation of the RV.
(2) Signature information such as radar cross section.
(3) The ship's location and heading.
(4) Other relevant telemetry, optical and meteorological variables.

Following a tracking mission, the collected data are processed, off-line, (i.e., in a post-test environment) to obtain accurate estimates of metric and signature information. These estimates are required to accurately characterize an RV's flight from its "penetration point" (i.e., the point at which the RV enters the atmosphere) to the "splash point" (i.e., the point where the RV hits the ocean surface).

Engineers and scientists at the Eastern Space and Missile Center recognized the need for improving the accuracy of metric information derived from data collected by radar trackers aboard the instrumentation ships. Toward this end, they embarked on a modernization program aimed at upgrading various systems on ARIS. For example, plans are underway to upgrade the Timing System[2], the Communications System[3], the computer hardware, and so on. In this context, the author of this report was asked TO INVESTIGATE THE VARIOUS ALTERNATIVES THAT MIGHT LEAD TO AN IMPROVEMENT IN TRAJECTORY TRACKING ACCURACY THAT IS SUFFICIENT

TO MEET THE MORE STRINGENT TEST REQUIREMENTS OF CURRENT AND UPCOMING MISSILE SYSTEMS. This statement, therefore, is taken as the goal of this research.

This report, therefore, is the result of a feasibility study. The recommendations made at the end of this report constitute a plan to reach the goal.

## II. OBJECTIVES

Although the instrumentation ships gather a wealth of data during a tracking mission, the scope of the goal statement is confined to a study of the acquisition and processing of metric data only; that is, data about range, azimuth and elevation of a RV. Even with this restriction, the scope is still too broad in the sense that it allows the possibility of including a host of competing alternative paths in reaching the stated goal. Some of these alternatives are considered extraneous to the major thrust of this research effort and are, therefore, eliminated forthwith from further consideration. Thus, no proposals for improving the electronics aboard the tracking ship are either made or considered. Similarly, no proposals to increase the number of tracking ships are either made or considered. In fact an attempt is being made to strike a balance between a desire for a thorough exploration of all possibilities and a desire to confine the effort to those alternatives that appear feasible. Included in the feasibility considerations are technical criteria such as practical realizability and compatibility with existing configurations, economic criteria such as development and maintenance cost and the management criterion, namely an ability to meet deadlines. In our pursuit to reach the goal within the framework of constraints articulated in the preceding paragraph, we propose to seek specific answers to the following broadly stated questions:

(1) Can we improve the metric accuracy of the instrumentation ships to meet the stringent test requirements of current and up-coming missile systems?

(2) If the answer to this question is in the affirmative, then to what extent can the accuracy be improved with the present configuration of the ship's instrumentation?

(3) If modifications to the present configuration are warranted, then can these modifications be made within reasonable time and cost constraints?

(4) If modifications are considered necessary, which of these modifications should be directed at improving the quality of the data acquisition phase and which toward improving the quality of the post-test data analysis phase?

(5) Whatever the modifications are, what would it take to actually implement them?

## III. DESCRIPTION OF A TYPICAL ARIS MISSION

To present the results of this research in a proper perspective, it is useful to review the salient steps of a typical mission.

Stated in a nutshell, the present tracking procedure consists of two broad phases: the on-board data acquisition phase and the off-board data processing phase. Preparatory to the data acquisition operations, first the longitudinal axis of the instrumentation ship is positioned roughly perpendicular to the plane of the trajectory of the RV. Then the location of the ship with respect to an earth-fixed geocentric (EFG coordinate) system is determined with the help of data provided by the ship's inertial navigation system (SINS) as well as from fixes obtained from an array of submerged transponders. Then, to lend a degree of stability to the observation platform, the ship is maintained on a linear course at a small constant velocity. Then the target is acquired by the radar and tracked in the so-called "auto-track" mode and the necessary data are recorded on digital and video tapes. This constitutes the end of the first phase.

Among all the data items collected during the data acquisition (or first) phase, only a few are of particular interest to us here. Those data items are navigation data (to determine the exact location and attitude of the ship at any time), metric data (to determine the range, elevation and azimuth of the target with respect to any desired coordinate system) and timing data (for synchronization purposes). These data items, recorded on digital tapes, will be referred to as raw mission data.

The second phase of the tracking procedure, called the data processing phase, takes the raw mission data as input and produces, as output, target position, velocity and acceleration relative to any desired fixed point and any fixed reference system. That is, the output of this phase is the required metric data about the RV's trajectory. This phase is conducted off-line in a post-test environment.

## IV. DISCUSSION ON PRESENT EFFORTS TO IMPROVE METRIC ACCURACY

The purpose of this section is to identify and comment on some of the problems being encountered in the context of accuracy improvement. Engineers at ESMC

(representing USAF, Pan Am, RCA) are addressing these problems systematically and thoroughly. Their approach is based on an identification of all possible sources of error, classification into categories (significant, insignificant; biased, random; and so on), and charaterization in terms of variables that can be controlled. This approach led to a satisfactory charaterization of the behavior of some of the errors. For example, engineers at ESMC appear to be fairly happy with their ability to control the errors due to, say, nonorthogonality of antenna axes, antenna droop, refraction and RF optical errors. This is understandable because such errors are common with all (land based and shipboard) radar trackers and most of the technical personnel have rich experience in this area.

The problem gets a little complex while studying the performance of shipboard radars. A new class of errors enter the picture here. A case in point are errors introduced due to our inability to estimate accurately the position and attitude of the ship on the ocean surface. Position simply means the coordinates of the ship in the EFG (earth fixed geocentric) coordinate system. Attitude refers to two aspects of ship motion: roll and pitch relative to the local vertical, and heading relative to north. In this report, we would like to refer to position and heading errors as navigational errors and errors due to roll and pitch as stabilization errors. In addition to these errors, we also have to deal with flexure errors, that is, errors caused by bending and flexing of the ship's body. Some effort is already under way to minimize the effect of these errors. For example, attempts are being made to minimize navigational errors by supplementing SINS with position data obtained from submerged transponders. Similarly, attempts are being made to minimize flexure errors by redesigning the physical layout of some of the instruments.

This investigator feels that all the above cited measures are necessary but not sufficient. This feeling is based on the assumption that there always exists residual errors; to assume that we can identify, characterize, and compensate each and every source of residual error is unrealistic. There is no suggestion here to indicate that the present approach of correcting major errors on an individual basis be abandoned. What is being suggested here is to supplement the present effort with a good tracking procedure that explicitly recognizes the need to compensate the residual errors during the data acquisition phase.

The development of good tracking procedures for shipboard radars is not a trivial matter. The difficulty arises because the errors associated with the range, azimuth and elevation (say in the EFG coordinate system) are an aggregate of residual errors from all sources cited above. To gain an insight into the nature and magnitude of these aggregate residual errors, it is useful to digress and inspect the magnitudes of these errors resulting from the tracking procedures currently in use at ESMC.

The present data acquisition system on H. S. Vandenberg, for example, uses the autotracking procedure. The monopulse radar in an autotrack mode is essentially a simple closed loop control system in which the radar receiver feeds the control signal directly to the radar sensors. In other words, there is no predictive capability in the autotracking mode. Improved performance can be obtained if the loop is closed through a computer so that the computer can be used to anticipate the RV's position from past data. This is the basic idea of on-axis tracking. The Eastern Test Range used this on-axis concept as early as 1967 to control the ground based radar (the AN/FPQ-13) at Grand Bahama Island. The Western Test Range also used the on-axis concept for its ground based radar at Kaena Point, Hawaii.[4]

The on-axis concept can be used at several levels of sophistication. Even the most primitive type of on-axis tracking is an order of magnitude better than the simple autotracking. Indeed, the on-axis procedure used in Grand Bahama Island and Kaena Point radar trackers (namely, the $\alpha$-$\beta$ tracking) is relatively primitive. Nevertheless, it is apparently giving satisfactory performance. For example, it is claimed that the above two, as well as other ground based radars using $\alpha$-$\beta$ tracking, are giving an accuracy of $\pm$ 6 ft. in linear measurements and $\pm$ $(1/2^{20})$ x $2\pi$ radians ($\simeq$ 0.006 milliradians) in angle measurements.[5] In contrast, the autotracked radars on H. S. Vandenberg are committing errors of up to $\pm$ 1500 ft. in range and $\pm$ 0.5 milliradians in angle measurements.[6] Two possible reasons for the poor quality of metric information from H. S. Vandenberg are: (a) measurements are taken from a moving, unstable platform, namely the ship; and (b) the radar trackers on the ship are using autotracking rather than on-axis tracking. A useful question that should be answered at this stage is: What part of the error is caused by the moving, unstable platform and what part by autotracking? For example, 1 mr of ship roll, it is observed, produces about one inch of C-band antenna movement but can introduce

up to 1000 ft of RV position error at pierce point.[7] However, it is dangerous to conclude (from what is stated so far) that 2/3 of the range error is due to an unstable platform and only 1/3 due to autotracking; other factors, such as navigational errors, also play a role in this context. For example, it appears that the uncertainty in this ship's location could be of the order of ± 1500 ft. The precise impact of this error on metric information is unclear.

This digression (the preceding three paragraphs) confirms the general qualitative feeling that tracking, stabilization and navigational problems are major problems to be solved. However, we do not yet have any quantitative measures of the contribution of each of these to the total observed error. Until we can develop quantitative estimates of the error contributions from each of these sources, we will not be in a strong position to decide where we should put our resources to meet our goal. Toward this end, we developed in the next section, some quantitative estimates of the order of magnitude improvements that can be made by improving tracking. We do not have information to help us make analogous estimates insofar as navigation and stabilization errors are concerned. In Section VI, we proposed that a simulation study be conducted to gain better insight into navigation and stabilization errors.

## V. SPECTRUM OF FUTURE POSSIBILITIES

The limited scope of the discussion in the preceding four sections is not sufficient to completely reveal the complexity of a trackingmission. Nevertheless, the success of a mission depends upon the coordinated operation of a number of subsystems. Modification of one subsystem or one operational procedure could create a ripple effect demanding modifications in other systems. As the scope, as outlined in Section II, of this effort is somewhat limited, it is not possible to address all these ripple effects. By the same token, they cannot be ignored either. In this section, we intend to propose some modifications and briefly touch upon some of the possible ripple effects.

A. Possible Modifications to Tracking. The radar trackers on H. S. Vandenberg now use autotracking. Engineers at ESMC recognized a decade ago the inadequacy of autotracking and the desirability of on-axis tracking.[3, 9] In fact, Reference 9 gives the figures shown in Table 1 to illustrate the advantage of on-axis tracking over autotracking. The reference did not mention the filter used in the on-axis algorithm. However, there is reason to believe

that it probably was an $\alpha$-$\beta$ filter; definitely not a Kalman filter.

Table 1

A comparison of orbital residuals from echo track of the satellite Pegasus performed by Radar 12.15 at Ascension in February 1974.

| Variable | Autotracking | On-Axis | Absolute Improvement | % Improvement (Approximate) |
|---|---|---|---|---|
| Elevation errors | 0.22 mr | 0.044 mr | 0.176 | 80% |
| Range error | 33.5 ft | 10.5 ft | 23.0 | 69% |

Inspection of Table 1 reveals that accuracy improvements of the order of 70 - 80% can be attained by replacing autotracker with a simple $\alpha$-$\beta$ tracker. Furthermore, in Reference 4 (page 1.5), it was estimated that a nine-variable Kalman filter has the potential of giving a 30% improvement in real-time tracking accuracy over an $\alpha$-$\beta$ filter. Admittedly, these two estimates were made in the context of ground based radars. In spite of this knowledge, it is surprising that ESMC did not initiate plans to upgrade tracking procedures on ARIS until the 1980s. There are two frequently quoted reasons for this delay. First, that the ARIS were originally designed to gather signature data and the desire to use them for metric data gathering is an afterthought. Second, that everything possible is being done to correct errors due to various sources and that there is nothing much to be gained by overhauling the tracking procedure. The first of the above implies that there is a change in mission requirements and the second reflects a lack of strong conviction. Nevertheless, plans are under way to explore the possibility of replacing autotracking with on-axis $\alpha$-$\beta$ tracking. This is definitely a step in the right direction, although not a decisive one. The author feels that this line of thinking should be pursued more aggressively by going all the way to a Kalman-type tracker rather than stop in midstep with an $\alpha$-$\beta$ tracker. If there are some practical reasons for a reluctance to go all the way for a full-blown Kalman tracker, there exist some suboptimal Kalman trackers for consideration. There are even optimal $\alpha$-$\beta$ trackers that are equivalent to Kalman trackers in their performance.[10]

Without going into detailed analyses of the advantages and disadvantages of Kalman filters in general, let us briefly look into the ripple effects of on-axis traking in the context of a typical ARIS mission. At present, most of the metric information is being derived by off-line processing of data in a post test environment. On-axis tracking (be it $\alpha$-$\beta$ or Kalman variety) is an on-line, real-time procedure. This implies that there is a need for an additional computer, on-board, dedicated to on-axis tracking. This computer should be supplied with navigation data, in addition to the usual tracking data. This, in turn, means that we cannot afford the luxury of waiting for the splash point to occur in order to determine the ship's location. That is, we have to make navigation independent of tracking but not vice versa.

A second possible side effect has to do with data processing operations such as the editing of raw data and accuracy of encoders. For example, Kalman filters tend to be sensitive to the editing scheme used. Also, if a lot of effort is going to be expended in improving the accuracy of data gathered, corresponding attention should be paid in maintaining this accuracy in digitizing and encoding this information. Toward this end the UNIVAC 1219 type computer with a standard word length may not be sufficient. A computer with a 32-bit word length and 64K of storage is probably needed for any sophisticated scheme.

A third side effect of on-axis tracking is the need to perform the computations on-line although this is not at all a requirement of the mission.

B. Possible Modifications to Navigation. There is a general feeling at ESMC that the impact of navigational errors on metric accuracy are not as severe as those of tracking and stabilization errors. This is predicated on the assumption that the coordinates of the splash point can always be determined fairly accurately and the ship's location with respect to the splash point can therefore be derived because the ship is generally not too far from the splash point. As noted earlier, this implies that the ship's location can be accurately determined after the mission, not before or during the mission because the splash point is the terminal point of the RV trajectory. But the accuracy of on-axis tracking depends, to some extent, on advance knowledge of ship's position. Thus, to make the on-axis tracking really useful, we must look for ways to determine the ship's position and heading by methods that do not depend upon data derived from the trajectory. This is an interesting side effect of using on-axis tracking. Therefore, either we have to determine ship's position only from ship's

inertial navigation system (SINS) or supplement it with some other system. One possibility is to explore the possibility of using the Navstar Global Positioning System (GPS) currently under development by the Department of Defense. The GPS system can be used to get both time and position information precisely. In fact, the GPS system is being considered in Timing Modernization Plan.[2] If it is going to be used to get timing information, one may as well use it to get position data also. Presumably, the cost involved in using the GPS system is in building a GPS receiver.[11]

Alternatively, one can take advantage of the similarity between the problem of tracking the position of an RV in space and the problem of tracking the position of a ship on ocean surface. As both problems involve the observation of a moving object with imperfect instruments and subsequently filtering the noisy data, the same procedure, with appropriate modification, can be used in both cases.[12-14] This strategy has the aesthetic appeal of depending on a uniform procedure to solve a broad class of problems in the mission. Such a streamlined procedure, that keeps the number of new things to be learned to a minimum, vastly improves the efficiency of people who design and maintain these facilities.

C. The Platform Stabilization Problem. A possible solution to the platform stabilization problem appears to be a little more difficult. Although Kalman-type approaches were proposed in the past by several investigators to solve analogous problems, their applicability to the present problem needs to be investigated. A simulation approach appears to offer an ideal compromise here. The simulator would take sea state, wind and ship velocity as inputs and produces expected pitch, roll and yaw as outputs.[15, 16] The results of this simulation can be used to predict errors due to ship motion.

## VI. RECOMMENDATIONS

Analyses in the preceding sections can now be used to answer the questions raised in Section II of this report.

(1) It is possible to improve the accuracy of metric measurements by a substantial margin. There is sufficient evidence in published literature for this possibility.

(2) If the objective is to achieve as much of this improvement as possible with minimum change in the ship's instrumentation, then the best course of action is to replace autotracking with on-axis tracking. This option would probably require a minicomputer dedicated to tracking. Although an exact

estimate of the size of the computer depends upon the type of filter used in the on-axis tracking, an educated guess would be a machine with 48-64K of memory size with 32-bit word length.

(3) If the on-axis tracking idea is acceptable, then this investigator feels that a serious effort at implementing a Kalman-type filter be initiated. In trying to implement a Kalman-type filter, consideration should be given to a determination of the type of suboptimal filter that best suits the needs of this project. In view of the time and cost constraints, the possibility of developing an optimized - filter (that is, one whose performance is equivalent to a Kalman filter) for possible implementation on modern microcomputers should not be ignored.

(4) Once the above idea is adopted, it is important to realize that now we are dealing with the so-called embedded computer systems. The reliability and maintainability of such embedded computer systems very much depends upon the quality of software support. Toward this end, it is strongly recommended that all future software development efforts follow modern ideas of software engineering; that is, ideas such as top-down design and structured programming.

(5) The author also feels that the short range objective of improving the quality of metric data from H. S. Vandenberg should not be allowed to cloud the long range objective of maintaining the concept of using ARIS as a flexible expansion of a missile test range. In this context, it is extremely useful to conduct a simulation study to determine how the various aspects of a ship's motion influence the overall accuracy.

(6) Finally, regardless of whatever action is being taken insofar as ARIS are concerned, it is important that all personnel concerned with RV tracking at ESMC be encouraged to get abreast with the developments in technology. Recent advancements, and some not so recent, in guidance and control, computer simulation, distributed processing and software engineering are revolutionizing thinking in these areas.

## REFERENCES


1. ARIS Orientation Manual, prepared by Pan American Airways and RCA International Services Corporation, Patrick Air Force Base, FL, June 1971.

2. ESMC Ships Timing Modernization Plan, prepared by Communications/ Timing Systems of Pan American Airways, Inc., Patrick Air Force Base, FL, Second Revision, 18 December 1979.

3. USNS Redstone External Communications Modernization Plan, prepared by Pan American Airways, Inc., Patrick Air Force Base, FL, 14 December 1979.

4. R. L. Barkeley, et al, SAMTEC On-Axis Radar Study, TRW Technical Report No. 20966-6001-TO-00, July 1972.

5. Private conversation with Mr. Jerry Brubaker, ESMC.

6. Private conversation with Mr. W. Elenberg, RCA at ESMC.

7. Private conversation with Mr. W. Elenberg, RCA at ESMC.

8. L. B. Rice, ARIS Closed Loop Tracking, Special Report 81-SR-70-2, RCA International Service Corporation, Missile Test Project, Patrick Air Force Base, FL, 29 January 1970.

9. A Compilation of Papers Presented at the On-Axis Software Conference, Technical Report No. ETR-TR-74-01, Directorate of Range Operations, Patrick Air Force Base, FL, September 1974.

10. C. C. Schooler, "Optimal $\alpha$-$\beta$ Filters for Systems with Modeling Inaccuracies," IEEE Trans. Aerospace and Electronic Systems, Vol. AES-11, No. 6, pp 1300-1306, November 1975.

11. P. S. Noe and K. A. Myers, "A Position Fixing Algorithm for Low-Cost GPS Receiver," IEEE Trans. Aerospace and Electronics, Vol. AES-12, No. 2, pp 295-297, March 1976.

12. A. G. Lindgren and K. F. Gong, "Position and Velocity Estimation via Bearing Observations," IEEE Trans. Aerospace and Electronic Systems, Vol. AES-14, No. 4, pp 564-577, July 1978.

13. S. F. Schmidt, "Application of State Space Methods to Navigation Problems," in Advances in Control Systems, Vol. 3, pp 293-340, 1966.

14. C. A. Darmon, "A Ship Tracking System Using Kalman-Schmidt Filter," in Agard Lecture Series No. 82, Practical Aspects of Kalman Filtering Implementation, NATO Advisory Group for Aerospace Research and Development, 1976.

15. P. Kaplan and T. P. Sargent, Theoretical Study of the Motions of an Aircraft Carrier at Sea, Oceanics, Inc., Technical Industrial Park, Plainville, N. Y., January 1965.

16. W. A. Johnson, Analysis of Aircraft Carrier Motions in a High Sea State, STI 137-3, Systems Technology Inc., Hawthorne, CA, March 1969.

1980 USAF - SCEE SUMMER FACULTY RESEARCH PROGRAM

Sponsored by the

AIR FORCE OFFICE OF SCIENTIFIC RESEARCH

Conducted by the

SOUTHEASTERN CENTER FOR ELECTRICAL ENGINEERING EDUCATION

# FINAL REPORT

# A COMPARATIVE STUDY OF ORGANIZATIONAL STRUCTURES IN AIR FORCE MAINTENANCE ORGANIZATIONS USING A MACRO MODEL: POMO VRS 66-1


| | |
|---|---|
| Prepared by: | Larry C. Wall, Ph.D. |
| Academic Rank: | Assistant Professor |
| Department and University: | Department of Management<br>New Mexico State University |
| Research Location: | Air Force Human Resources Laboratory<br>Advanced Systems Division<br>Maintenance Performance Branch<br>(AFHRL/LRLM)<br>Wright-Patterson AFB, Ohio |
| USAF Research Colleague: | Mr. Robert C. Johnson |
| Date: | August 8, 1980 |
| Contract No: | F49620-79-C-0038 |

# A COMPARATIVE STUDY OF ORGANIZATIONAL STRUCTURES IN AIR FORCE MAINTENANCE ORGANIZATIONS USING A MACRO MODEL: POMO VRS 66-1

by

Larry C. Wall

## ABSTRACT

A historical analysis of the evolution of maintenance organization structures provides clues for understanding the two different organizational structures which are currently used by Air Force Maintenance organizations. Relying on the literature in the area of organizational theory, a macro model of performance in maintenance organizations was developed. The model was then utilized to compare and contract maintenance performance under the two different structural arrangements. After organizational behavior had been described, twenty one hypotheses were derived in order to compare performance. Several potential data collection instruments were discussed as to their feasibility for collecting data. No actual data was gathered; however, each hypothesis was discussed and a prediction as to its likely acceptance or rejection was made. Several recommendations for further research were proposed.

## ACKNOWLEDGEMENTS

The author would like to thank the Air Force Systems Command, the Air Force Office of Scientific Research, and the Southeastern Center for Electrical Engineering Education for providing him the opportunity to spend an enlightening and educationally stimulating summer at the Air Force Human Resources Laboratory at Wright-Patterson Air Force Base.

The author would particularly like to thank Robert Johnson of the Air Force Human Resources Laboratory for the direction and supportive encouragement which he provided. A special thanks is also extended to Richard Weimer of the Air Force Human Resources Laboratory who shared freely of his time and experience. In the process of conducting this research, I have learned a great deal about maintenance, management, and the Air Force. For this knowledge I am very thankful. I hope that I also have contributed.

## I. INTRODUCTION

The Air Force is a dynamic, growing, and ever changing organization. While cognizant and concerned about accomplishing its current goals, the Air Force is proactively searching for new ways and methods for improving its functioning. Technological weapon system innovations are perhaps more noticeable to the public as indicators of organizational change and development, other innovations are, however, equally important. Air Force policy relative to personnel activities reflect a greater awareness and concern for the plight of the individual airman who often experiences extreme frustration when confronted with the overwhelming military bureaucracy. The Air Force is increasingly concerning itself with environmental issues. Recently these issues have complicated and made belligerent the once positive or, at worst, benign relationships between the Air Force and its social environment. Specifically, special interest groups whose demands were once ignored or shuffled are being given fair consideration. Mutually satisfactory solutions are being sought as the Air Force strives to fulfill its mission in a manner which minimizes friction between itself and the larger society of which it is a part. Many other illustrations could be cited as evidence for increased organization wide concern by the Air Force.

The maintenance operation is one area in the Air Force where improved organizational functioning through better human relations, new managerial philosophies, and meaningful organizational adaptation is being displayed. In 1977 after several years of study and experimentation, the Air Force introduced the Production Oriented Maintenance Organization (POMO) Structure. The intent of this program was to increased the productivity of the maintenance organization. This increased productivity would result from increased utilization of personnel as well as better utilization of their skills. Further increased job skills and a team climate within the maintenance shop would add to overall productivity. Finally, productivity would be increased as a result of the decentralization which occurs. The POMO structure has been completely adopted by AAC, TAC, PACAF, and USAFE. Other commands have expressed varying degrees of interest in

experimenting with or adopting this approach, but have not changed to the new structure.[1]

The development and implementation of new methodologies designed to improve productivity must be continued. The costs of a modern, well-equipped, and properly maintained Air Force are continually increasing. Concurrently, resources are becoming much more difficult to obtain. These factors combined to make the implementation of planned organizational change of crucial importance to the Air Force. Careful study and analysis of these changes must be made prior to implementation. Further, periodic followup studies are essential to insure that desired outcomes are being obtained.

Change is a universal characteristic of organizations and as such should be anticipated. However, planned change should have an objective of improved organizational functioning. Change is psychologically uncomfortable and typically leads to disruption of morale and productivity. Secondly, if the change is unsuccessful in improving organizational performance, there is a tendency among organizational participants to distrust future change efforts. Finally, it would be naive and unwise to assume that simple single variable solutions are appropriate for complex multivariable problems. Change will occur and must be carefully planned if it is to have a constructive impact upon an organization.

POMO is a significant organizational change which has been implemented into several Air Force maintenance organizations. It would be impossible to assess if the change were adequately researched prior to implementation. After three years in operation, however, it seems appropriate to assess whether this change has accomplished its stated objectives. POMO is an intuitively appealing approach to maintenance management. The relevant question, however, is what impact has this change had upon the personnel working in and the productivity of a maintenance operation. The intent of this paper is to provide the background and the framework for answering this question.

## II. OBJECTIVES

The objective of this report is to build a model of maintenance organization performance. This model could then be utilized to compare

a maintenance operation under a traditional 66-1 organization structure with a maintenance operation utilizing a POMO structure. The second objective is the derivation of testable hypotheses from the model.

In order to accomplish these objectives the following steps will be taken. First, a brief historical analysis of Air Force maintenance will be conducted. The purpose of this analysis is to discover reasons for the developments of both the 66-1 and POMO structures. The second step is the evaluation of literature available in the field of organizational theory. This review will note organizational characteristics and variables which impact upon organizational performance and individual performance within the organization. A model of maintenance performance containing these variables will then be constructed. The fourth step will elaborate potential data collection instruments which could be employed to collect data for the evaluation of the hypotheses. The final section will provide some recommendations and conclusions about likely consequences of structural changes such as POMO. These conjectures, while unsupported by empirical evidence, have value in designing future research activities.

## III. HISTORICAL BACKGROUND

The maintenance operation in the Air Force has evolved and grown with the changing nature and sophistication of the aircraft and equipment. Early in the history of aviation the pilot was responsible for the bulk of the maintenance performance on the aircraft. As the machinery became more complex the need for more capable and skilled mechanics emerged. WWI saw the development of master mechanics. These individuals were responsible for and capable of handling almost any maintenance problem which the aircraft might face. Even in these early years, however, specialists were required to repair and maintain specialized equipment such as radios, cameras, armament, etc.[2]

The expansion of the Air Forces during WWII brought drastic changes to the maintenance operation. In the four year period from 1940 - 1944, over 170,000 military aircraft were produced in the U.S. and Canada. This drastic increase in the number of aircraft and successive technological advancements being built into the aircraft

made maintenance a more difficult task. The large number of people and machines as well as the importance of the task, made training of master mechanics an impossibility. Consequently maintenance personnel were trained in specialty areas. This approach to job design allowed the maintenance operation to be performed very capably. At the same time it was possible to quickly train the large influx of relatively unskilled individuals. The effectiveness of this approach is demonstrated by the fact that peak employment reached approximately 750,000 in a few short years, technological advancements were significant, and the maintenance operation performed well.[3]

With the cessation of wartime activities a corresponding drop in maintenance personnel occurred. By 1947 the number of maintenance personnel had been reduced to some 56,000 individuals. The structural arrangements that had worked so effectively during wartime were carried forward into a peacetime environment. This viewpoint was perhaps best depicted by SAC Regulation 66-12 published in 1949 by the Strategic Air Command. The thrust of this document was the emphasis placed upon specialization and strong centralized control. The document and the whole concept of specialization and centralization received much support from SAC Command. This support is clearly demonstrated in a report published in 1956 in which the performance of different SAC wings on two different SAC bases was compared. Two wings on each base were identified and using established criteria, one was classified as a high performer while the other was classified as a low performer. While performance on a multitude of variables was studied, two results which emerged are of particular interest. First, the exercise of authority (that is more active executive and coordinative groups) was positively related to wing performance. Secondly, when the work situation was unambiguous and the production workers were able to see clearly what the executive branch desired, they were more willing to perform. Hence, the conclusion emerges that the centralization of maintenance activities is conducive to effective maintenance. Further, the specialization of the job (unambiguous nature of work to be performed) leads to increased maintenance effectiveness. Thus support was found for a more centralized control structure and specialization of the tasks to be performed.[4]

This philosophy was also prevalent throughout the rest of the Air Force. In 1956, Headquarters USAF prescribed a uniform maintenance philosophy with the publication of AFM 66-1. Although optional when first introduced, by 1959 application of this structural arrangement was mandatory. The intended purpose of the document was to provide for a uniform maintenance posture throughout the Air Force. This uniformity would help minimize the transfer problem as personnel are shifted to different duty stations and commands. However, as latitude of implementation was given to the major commands the maintenance structure was strongly influenced by a variety of command unique philosophies and practices. In late 1971 steps were taken to provide increased homogenity within the Air Force maintenance structure and activities with the implementation of Project RIVET RALLY. The goal of this project was the reaffirmation of standardized organizational structure, standard procedures, specialization, and central control throughout the Air Force. All deviations previously granted to the various commands were cancelled, and command latitude necessary for program implementation was sharply reduced.[5]

There have been numerous changes to the AFM 66-1 as indicated by the previous discussion. Figure 1 depicts current Air Force structure utilizing the 66-1 approach.[6]

- - - -

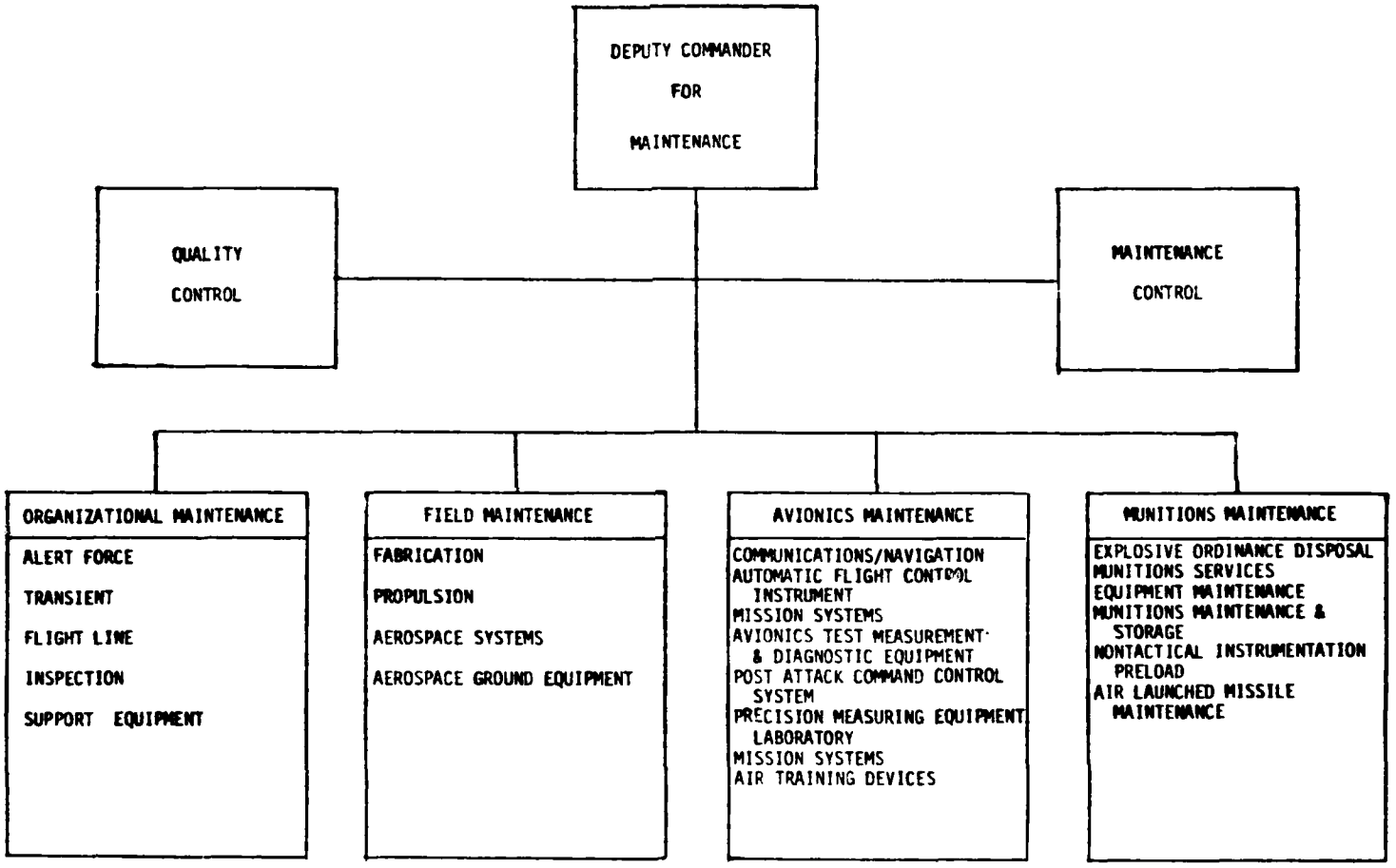



Figure 1: Maintenance Organization Structure (Ref)

unstated policy of the Air Force is the tendency to rely on labor rather than machines. This makes the operation labor intensive and very expensive. As indicated above, maintenance is performed through the utilization of many specialists. As the aircraft have become more sophisticated it has become necessary to employ even more specialists. Thus a particular maintenance operation requires the coordination of several specialists each responsible for only one particular area of activity. Nonavailability of a specialist or disagreement as to what part of the aircraft is actually malfunctioning can lead to serious delays in the repair of an aircraft. Further, dual responsibilities both in the shop and on the flightline can lead to lessened performance, especially in the shop where work is likely to be interrupted. A final policy is the orientation in maintenance activities toward maximum organic selfsufficiency. This sufficiency is possible by relying upon the repair cycle concept. This concept enables a weapon system to be maintained at a high state of operational readiness on a base by base level. This concept is very costly in terms of equipment, inventory levels, and appropriately skilled personnel because of the duplication involved.[7]

These implied policies have resulted in a number of problems which adversely affect goal accomplishment within the maintenance operation.[8] The first set of problems might be labeled production problems, and come in several categories. The first category is time lost while doing base or squadron details and in non-maintenance training. Thus productivity is lower because worktime is taken for activities that do not result in maintenance output. A recent study by Drake, et. al.,[9] estimates that maintenance personnel working on Army helicopters spend 4 to 5 hours in maintenance activities on a typical work day. A second category of lost time is work done which is unnecessary. Much time may be lost through excessive inspections of aircraft. Still more time is lost through the use of unreliable components which result in unnecessary troubleshooting and repair. A final category of production problems are those which result from a lack of group solidarity and cohesiveness. Maintenance teams are composed of specialists from various shops brought together to solve a particular maintenance problem. After the problem is solved the

specialists return to their respective shops. The short duration of the maintenance activity does not allow group identities to form. Often, shop objectives and parocial interests can overshadow group integrity resulting in reduced maintenance productivity.

A second problem stems from the repair cycle concept. Because needed parts, components, facilities, or skills are not always available, long delays are typical in the maintenance process. In an effort to reduce delays there is often a tendency toward increased cannibalization. This policy only serves to increased the amount of effort expended by the maintenance personnel. Personnel must expend effort taking a part off one aircraft only to place it on a second. Further, when the replacement part arrives it must be placed on the first aircraft. This type of problem, long delays, typically impairs operational readiness. A final type of problem has to do with employment related matters. The large number of specialists categories, inhibits organizational flexibility. A large quantity of technicians must be deployed to support even limited size dispersals. Not only must people be deployed but so must their equipment and tools. These two factors combine to result in expensive and complex logistical support problems.

In 1973 facing declining budgets and skyrocketing costs, both acquisitional and operational, a new program was developed. The Maintenance Posture Improvement Program was designed to improve all areas of equipment maintenance and to identify potential manpower and other resource savings. One of the innovative structural programs to evolve from the MIPP activities was Production Oriented Maintenance Concept (POMC). Because of its success this new structural arrangement was instituted into selected MAJCOMs in 1977. Currently, a number of Air Force Commands are using or have evaluated the potential for employing the POMC concept under the name Production Oriented Maintenance Organization or POMO. The organization structure of a POMO organization is depicted graphically in Figure 2.[10]

- - - -

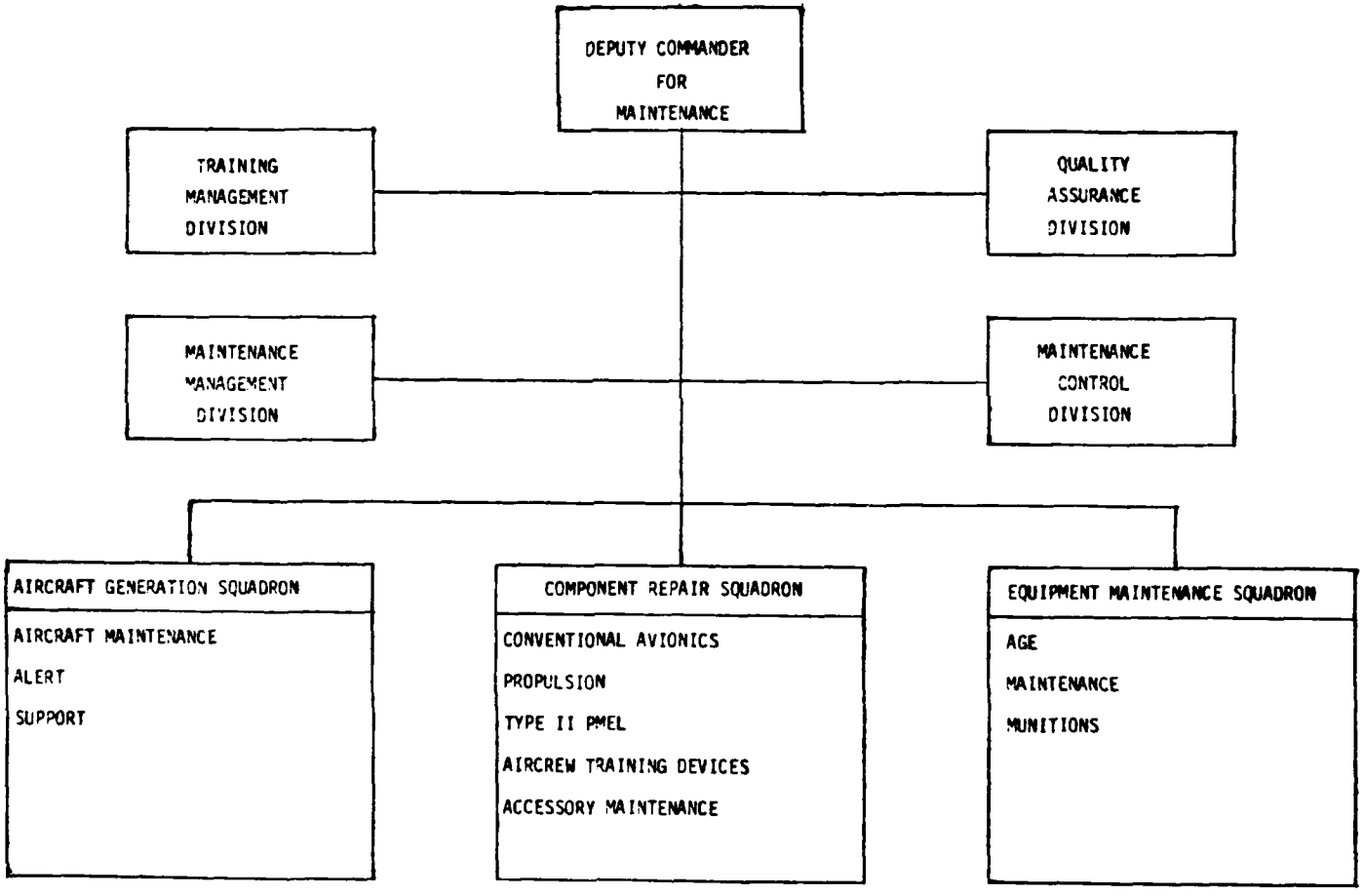



Figure 2 : Maintenance Organization Structure, 66-5 POMO

structure was modified to include the three squadrons depicted in Figure 2. Under the POMO arrangement, the DCM is left with the same basic mission responsibilities and support requirements which were held under the more centralized approach. However, the implementation of these responsibilities was significantly altered. Also note that two additional staff functions were created in the POMO structure. A brief description of Figure 2 is appropriate.

The Aircraft Generation Squadron (AGS) became the key squadron for carrying out maintenance for the wing. The AGS is responsible for all maintenance which is performed on the aircraft. This squadron is further subdivided into Aircraft Maintenance Units (AMUs). These AMUs correspond directly to the individual aircraft squadrons which comprise the wing. The AMU is a smaller organization within a larger organization and is designed to provide group solidarity and personal identification with an aircraft or a small number of aircraft.

The next squadron shown on the figure is the Component Repair Squadron (CRS). The CRS performs a significant portion of the off equipment maintenance which is directly related to the aircraft being supported. Thus, in reality the CRS is subordinate to and supportive of the AGS. This squadron performs many of the functions previously handled by the Avionics and Field maintenance squadrons which existed under a 66-1 structure.

The final component of the POMO structure is the Equipment Maintenance Squadron (EMS). This squadron is responsible for the remainder of equipment maintenance which was not assigned to the CRS. This squadron, like the CRS, also performs some of the old Field Maintenance functions as well as most of the functions of the Munitions Squadron of a 66-1 organization. This squadron is also subordinate to and supportive of the AGS.

The implementation of a POMO organization structure reflects a change in direction and policy for maintenance operations with the Air Force. These changes are not always clearly laid out but rather are subtle in their application. Further the effect of these changes are not easily measured or even known. The first change is a shift in emphasis from efforts by an individual to the efforts of a group. The

group becomes the focal point for determining organizational effectiveness. The second change is movement toward a more holistic approach. Emphasis is placed upon total system support (aircraft) as opposed to support of individual aircraft systems. Third, there is an increased level of autonomy for both supervisors and workers. Individuals lower in the hierarchy are given more freedom to make decisions about how their specific job is to be conducted. Fourth, and closely related, there is an increased amount of delegation of authority for decision making to both flight line and shop personnel. A fifth change is the effort expended to enhance worker identification with the mission of the maintenance organization. This is done by assigning AMUs to specific aircraft and by relying on the group processes mentioned above. The final change is a realignment of duty responsibilities and training requirements. This will allow for both greater utilization of the personnel available and provide more flexibility for the organization as it pursues its goals.[12]

The above mentioned changes in direction and policy are clearly seen when one looks at the POMO operation. It should also be clear that the POMO concept is intended as a radical organizational change from the 66-1 structure. Evans and Ferraro in a recent study provide significant insight into factors behind the development of this new structure.[13]

The first and probably most significant factor is the modernization of the tactical air fleet. With the addition of the A-10, F-15, and F-16 aircraft, the Air Force has obtained a new wave of technologically sophisticated aircraft built utilizing a modular approach to construction and maintenance. For the first time the possibility of organizing around an on equipment/off equipment became highly plausible.

A second factor contributing to the development of POMO is really a combination of several related items. First TAC experienced an inventory increase of 200 aircraft bringing its total inventory for aircraft to 1800. Secondly, to be better prepared for war contingencies and to more closely simulate actual war conditions, an increased sortie rate was established. Specifically, the sortie rate requirements under contingency operations was raised from 1.2 to 3.0 sorties

per day per aircraft. A third item was that manpower resources could be expected to remain constant. Thus TAC was faced with more work as a result of more aircraft and increased production requirements without additional people to do the work. Finally for the first time maintenance requirements for spare parts were fully funded by Congress. This gave the logistics manager tremendous flexibility in supporting operational requirements of the consolidated maintenance organization.

The POMO organizational structure offers several advantages over the traditional 66-1 structure. In a recent article by Townsend,[14] he noted several. First and foremost, it increases sortie production. This occurs for several reasons, but primarily, increased productivity is the result of the cross utilization of maintenance personnel. Maintenance personnel operate within their own job category, but also provide support for related activities. In addition all personnel are trained in routine but necessary aircraft maintenance duties such as launching, recovering, and towing aircraft. A second advantage noted is that the system gets people closer to the job. This is done by actually assigning specialists to the flightline or at least near to it. This reduces delays caused by the complexity of the specialist dispatch system used in a centralized maintenance shop. This closeness to the flightline has an additional intangible benefit noted by Anderton.[15] Quoting experienced maintenance personnel, Anderton stated that reliance upon the centralized maintenance system resulted in an inability for maintenance workers to personally identify with a specific aircraft. This often results in a lower quality of work performed, as the specialist works on black boxes rather than on an airplane. A third advantage to the POMO structure is noted by Nelson[16] who states that the POMO structural arrangement returns decision making authority to junior level officers and senior level NCOs. Utilizing this structure, maintenance control is no longer charged with directing and controlling the entire maintenance effort. Instead, maintenance control is responsible for all scheduled on equipment maintenance and monitoring pertinent unscheduled maintenance. The remaining maintenance responsibility is delegated to branch chiefs and crew chiefs, who are held responsible for sortie production. These three advantages or

changes are designed to increase both the productivity and the flexibility of the aircraft maintenance organization.

To summarize, POMO is a significant organizational change in the maintenance organizations of the Air Force. The change is intended to improve performance and indicates significant departure from standard policies by the Air Force. Before evaluating this change further, a model of organizational functioning will be constructed.

## IV. ORGANIZATIONAL VARIABLES

The third section of this report will discuss some of the key organizational or macro variables and assess their impact upon the maintenance organization. Macro variables may be defined as those variables which impact upon a given organization regardless of the particular individuals currently composing that organization. That is, these variables influence individual behavior yet are independent of individual actions. The organization is the unit of analysis. That is not to say that people are unimportant. They are crucial for the organization to be successful or even to survive. However, individual actions at a given point in time are constrained by many factors. These factors are often beyond the immediate control of the individuals who comprise the organization. Thus these factors serve to delineate an arena within which individual behavior occurs. A careful analysis of the arena is necessary if individual and organizational performance is to be properly assessed. Ten macro variables will now be discussed. This discussion will be followed by the development of a model of maintenance performance, and a description of the maintenance operation using the macro variables.

### SYSTEMS THEORY

The first and perhaps most significant macro variable is the systems theory paradigm. This model has revolutionized theorizing in the social sciences, particularly the study of organizations. While a detailed discussion of systems theory is beyond the scope of this study several key implications will be noted. According to Kast and Rosenzweig, a system is defined as "an organized unitary whole consisting of two or more interdependent parts, components, or subsystems;

and delineated by identifiable boundaries from its environmental supra-system."[17] This definition implies a state of continual interaction between the system and its environment. The first issue raised by the definition which needs further clarification is the dilemma between the openness and closedness of the system. The more open the system the greater the interaction and boundary permiability. The more closed the system the less interaction and the more rigid are the system boundaries. Most systems can be plotted along a continuum between totally open and totally closed. Organizations are socially contrived (man made) systems and are nearer the open end of the continuum. Systems are neither totally open nor totally closed but rather have elements of both. They need to be open in order for survival to be insured by determining what outputs the environment desires from the organization. This determination requires interaction between the organization and the environment. However, in order for an organization to operate in a rational manner, it must close itself to environmental influences. This closed perspective allows the organization to link means to ends as relationships between variables become stable, knowable, and quantifiable. Thus organizations need to be at the same time both open and closed.

A second issue which may be derived from the above definition is equifinality. This term refers to the idea that there are multiple means to the same ends within an organization. Thus an organization can use a variety of resources and techniques to accomplish a desired goal. Further, there is not only one right way or method for accomplishing a particular goal, there may be many appropriate methods.

## GOALS

The second macro level variable to be analyzed and discussed is the goalsetting process and the goals which emerge from it. All organizations have goals or a desired state of affairs which the organization attempts to realize.[18] When talking about goals it is easy to assume much more about the organization than is actually true. To illustrate some of the problems utilizing goals to describe organizational functioning, a maintenance operation will be used. Some typical goals of a maintenance organization might include a certain

level of sortie proficiency, a given percentage of reenlistment among first term airmen, a reduction in damaged parts resulting from maintenance activities, an increase in organizational morale, or maybe all of these. While not an exhaustive or maybe even representative list of goals, three problems of using goals emerge which are of relevance to this discussion. First, it is evident that maintenance organizations like most other organizations have multiple goals. Further as is true in all organizations, some of these goals are in conflict with each other. For example, increased sortie proficiency may actually lead to a reduction in organizational morale because of the extra demands made upon maintenance personnel. A second issue results from the first. Given a multiplicity of goals and conflict between them, an organization can never be fully effective. It is simply impossible to accomplish all of the goals which the organization establishes. Finally, as the maintenance organization strives to meet the demands placed on it by an environmental constituent (accomplishes one of its goals) and thus be considered effective by that constituent group, it is likely to be viewed as ineffective or even dangerous by other environmental constituents. Returning to the example of the goal for increased sortie proficiency, this third issue can be illustrated. In order for a particular maintenance organization to attain a greater sortie proficiency it may be necessary to make a change in operation, or organizational structure, or actual work activities. Thus airmen may have to work longer hours, work more productively, work in unfamiliar AFSCs (AFSCs other than the one originally trained for) or a combination of all these factors. As the maintenance unit accomplishes this goal and is assessed effective by the wing commander other constituents may have differing viewpoints. The logistics system may feel that the maintenance unit is placing too many demands upon their support system. The training system may argue that the training being provided airmen is not appropriately being utilized, and hence the maintenance organization is ineffective.

There are two other problems commonly associated with the use of goals. First there is the difference between official and operative goals. Official goals are the general purposes of the organization found in public statements and other authoritative reports and

documents. Operative goals are those ends actually sought by the organization as evidenced by their day to day activities.[19] There may or may not be congruence between these two types of goals. In the case of incongruence the obvious problem emerges as to which goal to utilize in measuring effectiveness of the organization.

The final problem relevant to the discussion of goals is concerned with the concept of goal displacement. Goal displacement is the development of clearly different goals from those professed at the outset. That is, an organization has an official and operative goal A. During the course of pursuing goal A, however, goal A is displaced by goal B as the operative goal even though it remains the official goal of the organization. There have been a number of explanations of this phenomenon. The most insightful is called the goals-means hierarchy. The hierarchy develops in the following manner. After a general goal is established by an organization, it is necessary to transform the goal into successively more specific subgoals in order for the goal to be implemented at lower levels within the organizations. Thus means to overall goal accomplishment become goals at lower levels in the organization. Further, lower levels lose perspective of the overall goals of the organization. Environmental constituents interacting with lower levels of the organization accurately observe that the organization has lost sight of its goals; the means have become the goals.

## ORGANIZATIONAL SIZE

The next macro variable to be considered, the size of the organization, has multiple implications for organizational performance. Before looking at the impact of size on organizational performance a conceptual problem relating to the accurate measurement of organizational size needs to be resolved. The issue is what variable to use in order to measure size; number of employees, amount of assets, sales volume, etc. Although still unresolved, the high correlations reported between various measures of organizational size give assurance that most approaches employed will result in reasonably accurate measures.

The size of an organization has been researched to better understand its impact upon structural arrangements and upon individual performance. It is intuitively appealing to think of a direct casual

relationship existing between size and organizational structure, the larger the organization the more structure one is likely to encounter. There is research which supports this viewpoint.[20,21] However, there is equally valid research which indicates an opposite point of view, size and structure are unrelated. Hall, Haas, and Johnson conclude in a study of varied organizational types, that neither complexity nor formalization can be implied from organizational size.[22] Size may well be correlated with structural differentiations but one cannot say that size generated or caused these differentiations.

The impact of size upon the individual is also an important consideration. A large organization presents many unknowns for the individual. The size of the organization is probably one of the first things a person notices about an organization. However, size has probably little effect on the actual performance of an individual. Research does not support a hypothesis of lessened productivity or satisfaction among workers in large organizations. The explanation may well lie in the role played by the informal organization. Or the impact of the large organization may be moderated by the contemporary society in which we exist. Society today is dominated by large organizations and our life styles and value systems have changed to reflect this reality. The mere existence of a large organization does not generate the anxiety and stress that it once did.

## TECHNOLOGY

One of the most important macro variables to be considered is technology. Technology as used in this study is not synonymous with automation. Rather it is a more inclusive term which includes automation as well as the procedures and the knowledge about the process being studied. A number of technological typologies or classification schemes have been developed to better understand technological impacts upon organizations. One of the more interesting typologies was developed by Thompson.[23] He stated that all organizations can be categorized as predominantly employing one type of technology. They may use other types as well, but rely primarily on one type to accomplish their key mission. The first category of technology is labeled long linked or assembly line production. The second type of technology is

mediating. Here the organization links clients or customers who are or wish to become interdependent. The final type is labeled intensive technology. Here a variety of techniques are drawn upon to achieve a change in an object. But which techniques are used and the order in which they are applied is dependent upon feedback received from the object being changed.[24]

While it is obvious that organizations employ different types of technology it may not be clear that interdepartmental relations are related to the type of technology employed in the organization. Thompson also notes three categories of relationships. The first is called pooled dependence which is best expressed by the attitude "We're all in this together." All of the departments are indirectly dependent on all of the others for overall organizational success. However, the actions of one department do not directly impinge upon the actions of another. A second type of relationship is labeled sequential. As the name implies, the outputs of one department serve as inputs to the next department. For example, B cannot begin working until A has completed its tasks and C cannot begin until B is finished and so forth. The dependencies are obviously much greater in this type of an arrangement than in pooled. The third relationship has the greatest number of dependencies. Under this relationship the output of A is the input for B but unlike sequential dependency, the output of B is the input for A. Thus the two departments have a reciprocal relationship. For example, the output of a flight squadron is aircraft in need of maintenance. The output of the maintenance organization is maintained aircraft which are operationally ready.

Each grouping is a more inclusive coupling of the departments making up the organization. That is, not only does the maintenance organization have a reciprocal relationship with operations, there are also sequential and pooled relationships as well. The type of technology employed and the relationships between departments have tremendous impact upon the nature of the job tasks found in the organization and upon the individuals who are members of that organization.[25]

## COMPLEXITY

Complexity is another macro variable that influences organizational and human performance. As in the case of the size of the organization, complexity is one of the first characteristics that is noticed by an individual when initially encountering an organization. Further, an organization may be complex or different parts of the organization may vary in the amount of complexity which they possess. There are three elements of complexity. The first is horizontal differentiation, or the subdivision of the tasks performed by the organization. These tasks may be subdivided in two basic ways. The first is to give highly trained specialists a rather comprehensive range of activities to perform, i.e., the use of professionals responsible for the completion of an entire operation. The second approach is to minutely subdivide the tasks so that nonspecialists can perform them. This latter approach is clearly seen in assembly line situations. Hage defines complexity in terms of the amount of horizontal differentiation found in an organization. He states that the greater the number of occupations in an organization and the longer the period of training required, the more complex the organization.[26]

The second element of complexity is vertical differentiation or the depth of the hierarchy. This element is more straight forward and more easily quantifiable than the horizontal element. The usual approach is to simply count the number of levels in the hierarchy between the highest and lowest positions. The more levels there are, the more complex the organization. One limiting assumption needs to be noted. It is assumed that authority is distributed in accordance with the level in the hierarchy. If this assumption does not hold, a misleading viewpoint emerges. For instance, if an organization contains many levels, yet authority is concentrated at the top of the organization, it would not be as complex as the number of levels would indicate. A final element comprising complexity is spatial dispersion. This dispersion can take place either horizontally, vertically, or in both directions. The more physically separated are activities and power centers, the more complex the organization. It should be obvious that these elements can and often do covary. Thus

organizations are seen to exist on a continuum from low complexity to high complexity as the organization adds an increasing number of occupational specialties, hierarchial levels, and geographic locations.

## FORMALIZATION

Another macro variable is formalization. Formalization is defined as the rules and procedures which are developed to handle the contingencies faced by the organization. It can be measured by the proportion of codified jobs and the range of variation that is tolerated within the rules defining the jobs. Formalization varies along a continuum from low to high. The smaller the proportion of codified jobs and the wider the variation allowed in performing those tasks, the less formalized the organization.

Before looking at the impact of formalization on organizational performance, one significant methodological question needs to be resolved. The issue is how should formalization be measured. The easiest approach involves a straight forward enumeration of the rules and procedures which exist in an organization. However, the simple fact that the rule was written down is no assurance that the rule is enforced. And if a sizeable proportion of the written rules are not enforced, the question of whether the organization is formalized has not been answered. In such a situation, it would appear that the organization is not formalized and the rules are merely procedural formalities or useless relics left behind as the contingencies facing the organization have changed.

To overcome the deficiencies associated with simply counting the number of rules, a second approach utilizes individual member's perceptions of the formalization of the organization. In other words, formalization is defined as the extent to which individuals perceive the organization to be formalized. As would be expected these two approaches yield somewhat different results. The activities which occur in an organization are often very different from what official statements of the organization would lead one to believe. One will recall the discussion concerning the difference between official and operative goals. The same findings would be appropriate relative to rule enforcement within an organization. The formal system is useful,

however, as it prescribes the parameters from which any deviation that does occur can be measured. Further, the formal system serves as a starting point from which actual behavior in the organization begins.

There are two closely related topics which are of interest to the discussion of formalization. The first has to do with conflict which is frequently noted between formalization and professionalization. As will be recalled from the discussion of complexity, the use of professionals is one way to horizontally differentiate an organization. The professional brings to the organization a set of behaviors or guidelines learned in another organization. These guidelines prepare the individual to accomplish certain job tasks and to exhibit learned behavior patterns. When rules and regulations, i.e., formalization, is imposed upon the professional the issue of redundancy becomes a problem. The professional feels that the formalization is telling him/her to act in a way in which he/she has already been trained to act. This situation is often an uncomfortable one for the professional as he/she is made to feel less than a professional by the imposition of rules which serve to reduce or eliminate professional discretion.[27]

The second related topic to formalization is the creation of roles within the organization and the resulting role behavior. In a book by Kahn et al the notion of roles in an organizational setting is discussed. They argue that positions are created within an organization by the nature of the tasks to be performed and interactions required of the position by other positions in the organization. Further, the nature of the tasks and required interactions elicit certain behaviors from the individuals who occupy those positions. The extent to which the expectations about how a particular role is to be played are formalized is an important determinant of how the role will be played and how the individual will react to his/her siutation in the organization.[28] The study of role behavior is an extremely useful technique for examining the relationship between an individual and the organization. It provides one of the more useful methodologies for combining macro and micro variables into a workable model of organizational performance. However there are still other macro variables to be analyzed.

## CENTRALIZATION

Centralization is a macro variable which is defined as the extent to which power distributions are determined in advance by the organization. The amount of centralization varies from organization to organization and can be applied to individuals or units, or more commonly to levels in the organization, or to both. In measuring the degree of centralization within an organization, it is necessary to determine where in the organization decision making is occurring. If most decision making occurs at the top of the organization, the organization is considered to be centralized. Care must be taken, however, before over generalizing. If lower level personnel are making decisions, but the decisions have been "programmed" by organizational policies, the organization remains centralized. The related area of evaluation clarifies this point. If individual behavior is evaluated by people at the top of the organization, regardless of where decisions are made in that organization, it is still centralized. This is true because the evaluators are able to influence the behavior displayed. The degree of centralization in an organization and its appropriateness depend on several variables already discussed, notably size and technology. Further, the environment and the power structure also have significant influences on the amount of centralization. Centralization and formalization provide insight into the attitudes which the organization has of its personnel. In essence a highly centralized organization indicates an attitude that the personnel employed do not have the insight or ability to make organizationally rational decisions. Consequently, decisions must be made at higher levels in the organization.[29]

## POWER

As noted above, centralization is influenced by a number of other macro variables including power. In fact it is not at all difficult to explain centralization patterns within many organizations by using this macro variable alone. Although power has been defined in a number of ways, Richard Emerson provides a most insightful definition. He suggests that power resides implicitly in another's dependency. That is, to the extent that A depends upon B for goal accomplishment or gratification, B has power over A. Thus power is the obverse of

of dependency.[30] If a person or organization has no dependencies they are free to behave as they choose. Conversely complete dependency of an individual or organization would be synonymous with powerlessness. Most if not all individuals and organizations fall somewhere between the two extremes. Thus power is a variable which varies from individual to individual, from situation to situation, and from organization to organization. The amount of power is not fixed for all time within an organization, it can expand or contract. A final definitional note about power is that it is an act. Power is something that is used or exercised. This implies that the recipient in a power relationship is crucial in determining if a power act has occurred. If the recipient views an act as a power act, he/she will respond on that basis, regardless of the intent of the actor.

There are many different categorizations of the types of power reported in the research literature. Probably the most widely utilized typology was developed by French and Raven.[31] Their typology is built upon the relationship between the powerholder and the power recipient. They state that there are five types of power relationships found in organizations. The first type of power is labeled reward power and is dependent upon the powerholder's ability to reward the power recipient. This type of power is useful only when the reward offered is desired by the recipient. The same social relationship exists when the second type of power, labeled coersive power, is employed. Coersive power is the ability of the powerholder to punish the power recipient. Given the same social relationship, the difference between these two types of power lies in the perceptions and motives of the recipient. One recipient may view a particular act as an opportunity for reward while another views the same act as being punitive. The third type, legitimate power, occurs when the recipient acknowledges that the powerholder has the right to influence him and as a follower has an obligation to follow the directions given. The fourth type of power is called referent power. When a power recipient identifies with the powerholder and strives to behave like him/her, the powerholder is exercising referent power. This power relationship is subtle and the powerholder may or may not know that this type of power is being utilized. The final category of power is expert power, or power attributed to the

powerholder on the basis of specialized knowledge. The power recipient believes that the powerholder has access to relevant information whic the power recipient does not possess. All of these types of power can be found in organizations and except for referent power are also or can be made part of the official authority system of the organization.

As mentioned previously, power varies. There have been a number of studies conducted to ascertain why power resides in a particular subsystem of an organization, and the flow of power through an organization. Several studies have supported the notion that power within an organization is lodged with the subsystem that is most capable of dealing with the most important contingencies faced by the organization. The organizational unit that is able to cope and control the critical functions of an organization gains a strategic advantage over other units. This advantage is utilized to improve the subsystem's power position and to ensure a greater share of the organizational rewards. Further, power has a self perpetuating effect. Once an organizational unit gains power, it seeks to maintain it, and usually has the resources to do so.[32]

Power is a significant macro variable whose impacts upon organizational performance can be clearly observed. However, the power structure in an organization is limited by several factors. First, while the amount of power in an organization varies from situation to situation, it does not vary much. Factors leading to an increase or decrease in power are typically not sudden or rapid in their impact. A second limiting factor is that at any given point in time the amount of power within the organization is fixed. If one subsystem gains X amount of power, then another subsystem or group of subsystems must lose an identical amount. Finally, external factors can influence which organizational units gain and which subsystems lose power. An example from industry makes clear this point. As a result of the creation of the National Labor Relations Board (NLRB) by the Federal government, the labor relations and personnel specialties gained tremendous power in business organizations. Much of this power came at the expense of the line supervisor who lost tremendous latitude and discretion in the performance of his duties. The impetus for this change in power relationships came from an external source, the

federal government.

## LEADERSHIP

The next macro variable to be discussed is often viewed as a micro variable. For purposes of this study, the leadership behavior to be analyzed is the behavior of the person in the top position in the organization and the impact of this behavior upon organizational performance. Leadership is often cited as the key variable in explaining and understanding organizational behavior. While a change in leadership offers an extremely easy solution for dealing with organizational problems, such an approach is more likely to coverup the problems plaguing an organization than it is to provide a workable solution. As should be evident, leadership is only one of the variables influencing organizational performance. Leadership is important, in some situations even critical, but in most situations it is heavily constrained by many of the variables previously discussed.

Leadership is defined by Etzion, "... as the ability, based on personal qualities of the leader, to elicit the follower's voluntary compliance in a broad range of matters."[33] Leadership is different from power in that a leader changes followers preferences while a powerholder simply imposes preferences upon the power recipients. In an organizational setting, leadership is a combination of occupying a high position and displaying behavior which meets the expectations which the followers have for that position in a particular situation.

The impact of leadership on the organization is not at all clear. Little direct evidence exists as to the effect that top level leaders have on organizational performance because little research has been conducted on top level leadership. Studies of leadership at the supervisory level are at best confusing because of the myriad of dependent variables employed. Evidence seems to indicate that supportive leadership leads to more positive attitudinal responses on the part of subordinates. Further, some research evidence does suggest that greater productivity is associated with supportive supervision. However, there is an equally substantial amount of research literature which reports no difference, or even less productivity when supportive leadership styles are employed. As should be evident, other macro

variables such as the technology utilized by the organization, the number of professionals employed, or the level of formalization have the potential to limit the impact which the leadership variable by itself can have upon organization performance.

The arguments presented above relative to the impact of this macro variable are contrary to widely accepted viewpoints of the human relations school of management. Perrow, Hall, and Thompson offer insightful critiques of this school of thought to the interested reader.

## ENVIRONMENT

The final macro variable to be discussed is the environment which surrounds the organization. For ease of discussion, it is desirable to think of the environment as existing on two levels. The first level is the general environment which contains conditions likely to affect all organizations, for example, the state of the economy, demographic changes, etc. The second level is the specific environment of an organization which contains other organizations and individuals with which the first organization interacts.

Hall notes seven general conditions which affect most organizations.[34] While not all of the conditions are equally critical or even relevant to every organization, each condition has the ability to become critical. The first condition is technological innovation. Technology is a macro variable which has already been discussed. The reason for including it again is that most technological innovations occur outside older established organizations and industries. Organizations do not exist in a vacuum. It is important that established organizations be aware of and responsive to technological innovations if they are to continue to survive. The organization may choose to change and adopt the new technology, or it may choose to ignore the innovation, or may even try to squelch the innovation. However, if the organization is going to act, it must be aware of the technological occurrences taking place in its environment.

Legal conditions are the second set of environmental conditions affecting most organizations. The organization must be aware of existing laws which serve as constraints to organizational action.

Further, the organization should be aware of trends in the interpretation of existing laws or in the legislation of new laws. The third environmental condition is closely related to the legal condition and is referred to as the political situation. This is a particularly important condition for public spector organizations. Laws which affect their operation and the resources necessary for their operation are strongly influenced by the political leanings of the party in power.

Economic conditions also affect all organizations. Changing economic conditions can serve as a significant constraint or opportunity for a given organization. An organization must evaluate its priorities and trim excess fat in recessionary periods. Conversely during boom times, many activities are undertaken which are only remotely related to the primary mission of the organization.

The fifth factor, demographic conditions, also affects all organizations, as all organizations are comprised of people. As the population served fluctuates, an organization must respond to these changes. Demographic fluctuations also impact upon the organization's ability to obtain appropriate human resources. The general ecological situation also must be considered by the organization. This condition includes the social ecological system as well as the physical environment of an organization. This condition obviously varies from one organization to another.

The final of the seven conditions is the cultural condition. Unlike the previous conditions which are much more readily measurable, cultural conditions are not. The lack of quantifiability does not reduce the significance of this condition to the organization. Numerous cross cultural studies have come to very similar conclusions; the culture surrounding an organization has a major impact on the way the organization operates. While few question the general impact of culture on an organization, little can be said as to how much or how strong the impact will be. For example it appears that the more routine and standardized the technology, the less the impact of cultural factors. Further, the impact of culture is not a constant; it varies over time, and even over geographic regions of the same country. The conclusion is softened, the culture influences organizations within

it, but the extent of that influence is not readily determinable.

The specific environment of an organization might be referred to as the organization set. It is composed of organizations and individuals in interaction with a particular focal organization. These environmental constituents make specified demands upon the focal organization which must be attended to if the organization is to survive and prosper. Further, the organization set includes similar organizations with whom the focal organization must compete for scarce resources. The focal organization may also use the similar organizations as a basis for comparing its own progress as well as a source for new ideas and innovations.

The general and specific environments of an organization place strong limitations on the performance of an organization. In fact, one might be led to conclude that an organization is a helpless pawn at the mercy of every environmental whim. This conclusion is erroneous. Organizations exist in a reciprocal relationship with their environments, both specific and general. Organizations strive to maximize the benefit received by the organization whenever it engages in environmental interaction. Further, organizations are themselves technological innovators, they seek to change laws and influence politics, they have drastic impacts upon the state of the economy and their own ecological system, they influence demographics and modify the culture around them. Thus to a considerable degree organizations seek to mold their environment to fit them. They do not simply adjust to environmental demands. While the environment is seeking to bring about changes in the organization, the organization is concurrently seeking to modify the environment.[35]

In an effort to summarize the information presented in this section, the following formula has been developed. The formula is intended to describe the relationships between the variables discussed.

$$\text{Organizational Performance} = f\ (S, L, P, G, OS)^{St:T \text{ and } E}$$

Where

S = Organizational structure (a construct consisting of centralization, complexity, formalization, and the size of the organization)

L = Leadership

P = Power structure

G = Goal setting process and resulting goals

OS = Other subsystems

T = Technology

E = Environment

Graphically these same relationships are depicted in Figure 3.

- - - - - - - - - - - - - - - - - - - - - - - - - - - - - - - - - - - - - - - -

INSERT FIGURE 3 ABOUT HERE

- - - - - - - - - - - - - - - - - - - - - - - - - - - - - - - - - - - - - - - -

The purpose of the formula and the graph is to emphasize that performance within an organization is constrained and guided by a number of variables. Many of these variables may be beyond the control of the individuals whose activities they regulate. Using the macro variables just discussed, the information from the previous section, and Figure 3, the operations of a maintenance organization will now be discussed.

The first variable in the model to be examined is the systems concepts. The maintenance operation is a subsystem of a larger system, the Air Force. It exists in a close reciprocal relationship with the operations subsystem. Further, the maintenance subsystem interacts with numerous other subsystems (personnel, training, recruitment, logistics, etc.) This list is obviously not exhaustive but rather

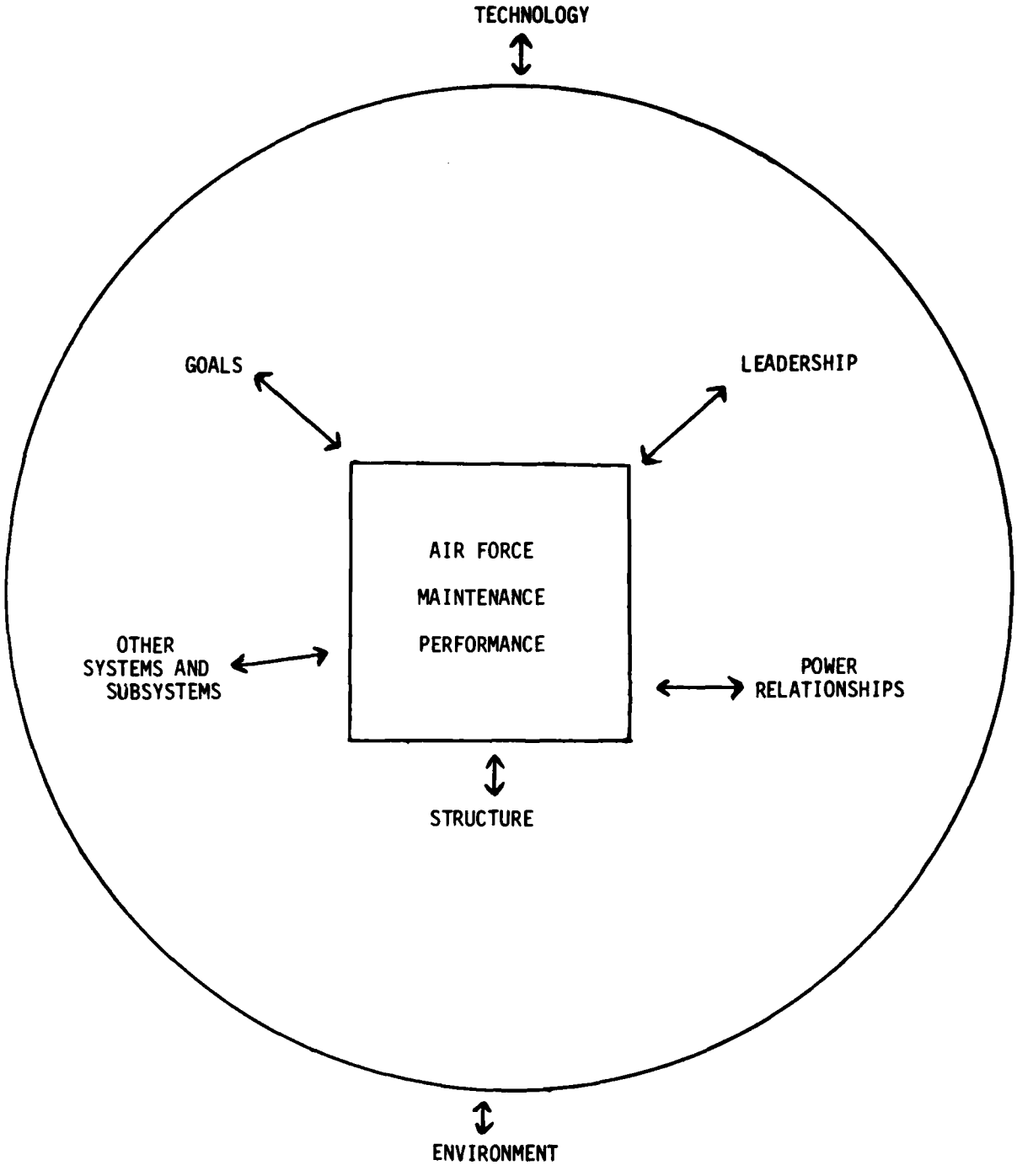



Figure 3: Macro Variables Influencing Organizational Performance

intended to be illustrative of the numerous interactions between the maintenance subsystem and other subsystem organizations. The actions of these subsystems heavily constrain the actions of the maintenance subsystem. For instance, the quality of the personnel employed, or the availability of spare parts would directly impact upon the effectiveness of the maintenance subsystem but are beyond its control. Thus while the maintenance subsystem is seeking closure, the number of dependencies preclude much movement in that direction. Finally, it should be noted that in spite of the many efforts at creating uniformity by higher level managerial systems, maintenance subsystems still retain individual differences.

The goals of the maintenance subsystem also influence its overall performance. While there is not direct evidence to indicate substantial difference between official and operative goals, some amount of goal displacement would be expected. As the goals pass down the hierarchical chain, there is a strong possibility that they will become modified significantly. This modification influences the outcomes generated by this subsystem, especially at the base level. It is also likely that multiple conflicting goals exist within the maintenance subsystem which makes the measurement of performance most difficult

The third variable is the structure of the maintenance organization. This variable is a combination of four closely related variables: centralization, complexity, formalization, and size. The size of the maintenance subsystem is probably not a significant variable. At the base level, most maintenance organizations vary from 20-200 organizational members. While the subsystem would not be classified as a small group, it is not large enough to encounter interaction problems typical of larger organizations.

The maintenance subsystem would be classified as highly complex. There are typically four or five vertical levels within the maintenance subsystem at the base level. There are as many as twenty four occupational specialties (horizontal categories) on a base in the maintenance organization. Finally, the maintenance operation is physically dispersed, being divided into multiple shops as well as being on the flightline. All three of these dimensions serve to make the structure

very complex.

The structure is also very formalized. There are plethora of rules, regulations, and procedures detailing the activities to be performed. Many of the regulations are imposed by the maintenance subsystem itself, while others come from higher levels. Because of the fragmentation of the work performed and the usage of nonprofessional personnel, the need for a large number of rules and regulations to coordinate the work becomes necessary.

Finally, the centralization within the maintenance subsystem should be noted. The Air Force, like other military organizations maintains structured and highly codified hierarchies of authority, responsibility, and accountability. The maintenance subsystem reflects these relationships in its operation. Authority, decision making, and evaluation all reside at or near the top of the organization. Hence the maintenance operation would be classified as being centralized. The maintenance subsytem is highly structured resulting from a high degree of centralization, complexity, and formalization.

A fourth variable in the model are the power relations which exist between the maintenance subsystems and other subsystems in the Air Force. As noted, power is the absence of dependencies. Further, the maintenance subsystem was noted as being dependent upon numerous other subsystems. For example, the maintenance subsystem is dependent upon recruitment and training for the quality of people which they get. Further they are dependent upon logistics to supply them with needed repair components, and upon the budgetary committees who decide how many resources are allocated to maintenance. These few examples serve to illustrate some of the dependencies of the maintenance subsystem. The maintenance subsystem is not without power. It exists in a reciprocal relationship with the operations subsystem. Consequently, if the aircraft have not been maintained then they cannot be flown. Thus the maintenance operation does have a certain amount of power.

To summarize, the maintenance subsystem has power but is also severely constrained by numerous dependencies. One of these dependencies that is often overlooked is the role of tradition. Tradition has played and continues to play a significant role in power relationships

within the Air Force. It is interesting and somewhat surprising that the majority of Air Force Staff level leadership comes from the operational rather than the maintenance subsystems. As will be recalled, once a subsystem has gained power it is not easily taken away nor given up.

The next variable which has direct impact upon the performance of the maintenance subsystem is leadership. even though the maintenance subsystem is not large, the leader (DCM) may have difficulty positively affecting performance at the base level. The impact of quality leadership may be muted by the constraints imposed by the other macro variables. Secondly, the transitory nature of the individuals in the DCM position serve to lessen the impact which a single individual can have. Quality leaders are an important necessary condition to bring about improved performance but this variable is not sufficient to guarantee increased productivity.

The final two variables are more general in nature. In similar manner to the other macro variables discussed, they directly influence the performance of the maintenance organization. They also directly influence the other macro variables. This is not to imply that no interaction occurs between the variables previously discussed. Obviously, there are significant relationships between many of the macro variables. However, technology and the environment are likely to have a greater impact upon other macro variables. Figure 3 has been drawn to reflect the greater impact of technology and the environment. The reader should bear in mind, however, that performance is influenced by all of these variables, and their relationship to each other.

The environment has tremendous influence on the maintenance subsystem's performance. Today the environment is usually viewed more as a constraint rather than an opportunity for the maintenance organization. For example, the political, the economic, and the ecological conditions all are imposing significant barriers to maintenance performance. The continuing political attitude toward reduced government spending has restricted funds available. The inflationary trends in the economy make the funds that are available less valuable in terms of the amount of resources which can be purchased. Finally, the

ecological environmental factors have been playing an increasingly important role. The energy shortage and the dumping of nuclear wastes serve as two examples of these problems. The legal and demographic conditions are for the most part benign in their influence on maintenance performance. Some of the newer governmental regulations such as OSHA and EEO are having some impact on the maintenance operation however. Although the impact of cultural conditions on the maintenance subsystem is somewhat mixed, this area seems to offer some opportunities. There currently seems to be a more favorable view of the military than the attitude held five to ten years ago. This shift in values provides an excellent opportunity for the maintenance subsystem as well as other Air Force subsystems to increase the amount of resources obtained from the environment. Further it may be possible to channel favorable cultural support into other areas of environmental interaction.

The final variable included in the model is technology and technological innovations. As with the environment, changes in technology directly influence maintenance performance and the appropriateness of the other macro variables. The maintenance operation would be classified as an organization utilizing an intensive technology. Further, maintenance exists in a reciprocal relationship with operations. The technological sophistication of the weapon systems which must be maintained is highly complex and continually increasing in complexity. The training requirements are becoming increasingly stringent and the problems of skill or knowledge obsolesence have not been adequately assessed. Organizational action may be approaching the limit of its capability when working in this advanced technological mode. In any event, the technology of the weapon systems and the technology of the maintenance procedures required to maintain these weapon systems place significant constraints on the performance of the maintenance subsystem.

The next section of this report contains some hypotheses that could be analyzed to compare mainteance productivity under a POMO structure with that under the traditional 66-1 structure.

## V. SELECTED HYPOTHESES

The central premise throughout this paper is that POMO was introduced as a methodology for improving organizational performance of Air Force maintenance units. On the whole, the liturature available about POMO would lead one to conclude that these suggested changes have been successful in accomplishing their objectives. POMO is a change strategy which would be categorized as job enrichment. This managerial technique was initially developed by Frederick Herzberg.[36] Job enrichment is an attempt to provide more meaningful work for the employee. Many organizational change and development strategies can be traced to this significant work. A recent study by Hackman expands on the concept by describing an enriched job. Hackman states that meaningful work occurs when an individual worker's job has task significance and requires skill variety, has increased autonomy and responsibility, and the worker is provided knowledge about his/her results.[37] It would appear that the intent of the POMO structure is to provide for these job characteristics.

If the POMO structure had implemented the above job changes and if these changes are the relevant factors influencing satisfaction and organizational performance then job satisfaction and productivity should increase. To determine if these changes have occurred, the following hypotheses are proposed for evaluation. The hypotheses will be grouped into two groups. The first group will be related to the attitudes and behaviors of the maintenance personnel. Many organization behavior theorists argue that there exists a strong relationship between job satisfaction and productivity. The second group contains hypotheses which relate directly to productivity. In the first group, each hypothesis will be presented, then discussed, and finally a prediction as to its expected acceptance or rejection will be made.

H:I a. Aircraft maintenance personnel will perceive a greater sense of participation in decision making under the POMO structure.

b. The actual amount of participative decision making occurring will be greater under the POMO structure.

One of the advantages claimed by the proponents of POMO is that

decision making responsibilities will be placed in the hands of lower level management, i.e., squadron leaders and crew chiefs. Thus it would seem reasonable to expect that more participation by airmen in decision making would occur. From the viewpoint of the macro model, however, evaluation of performance still remains in the top levels of the organization. Hence decisions are still made at that level and the hypothesis will be rejected.

H:II Aircraft maintenance personnel wll perceive greater autonomy for their work group under the POMO structure.

A POMO structure is designed to provide for delegation of authority to lower organizational levels. Further AMUs created within the AGS are intended to bring about group identity and solidarity. If this is true then the work groups should perceive greater control over their own activities. As noted in the macro model, however, the maintenance subsystem is dependent upon a number of other subsystems. At the same time dependencies also exist within the maintenance organization between the three main squadrons comprising POMO. Both the CRS and the EMS are subordinate to the AGS with respect to the coordination and timing of many of their operations. Hence, it is unlikely that maintenance personnel working in these two squadrons would feel that their work unit has more autonomy. Therefore, with two of the three squadrons likely to be experiencing less rather than more autonomy, the hypothesis will be rejected.

H:III a. There will be greater reliance upon reward and legitimate power relationships when the POMO structure is utilized.

b. There will be less reliance upon coercive power relationships when the POMO structure is utilized.

With an increase in responsibility and autonomy comes a corresponding decline in the need by the powerholders to use force in order to gain compliance. The airmen recognize that they are being treated in a mature fashion and respond accordingly. Consequently, only rarely

will coercive power be required. The acceptance of this hypothesis is dependent upon the validity of three assumptions. First, it must be assumed that airmen want additional responsibilities. Secondly, it must be assumed that delegation has taken place and some power equalization has occurred. Third, it must be assumed that the rewards offered are those desired by the airmen. If these assumptions are not met, the hypothesis will be rejected. It would be difficult to demonstrate the validity of these assumptions. In fact one would have to ignore substantial available data to accept the first and last assumptions. Therefore, the hypothesis will be rejected.

H:IV Under the POMO structure, aircraft maintenance personnel will tend to perceive of themselves as professionals.

This hypothesis is designed to test the notion that the POMO structure provides for increased skill variety. Under POMO the AGS does have broadened skill requirements for the airmen assigned to it. Further, POMO provides for the cross utilization of maintenance personnel in other AFSCs as needs arise. The definition of a professional used in the macro model was a specialist capable of completing an entire task by relying upon a variety of skills. POMO is designed to enhance the professionalization of maintenance personnel so this hypothesis will probably be accepted. The one qualification that should be noted is that this skill diversification may only be occurring in the AGS.

H:V Aircraft maintenance personnel will perceive the work environment as being less formalized under the POMO structure.

This hypothesis is likely to be rejected. The primary reason that this rejection is likely to occur can be explained in the following manner. The perceptual approach to formalization measures formalization by assessing the airmen's perceptions of the extent to which rules and regulations are being enforced. While many job related rules were eliminated with the implementation of POMO, others were created in their place. The POMO structure has no mechanisms to either encourage

or discourage rule enforcement. Hence it is unlikely that POMO could help reduce formalization, perceived or actual, in the maintenance organization.

H:VI Under the POMO structure, aircraft maintenance personnel will perceive an increased freedom in making job related decisions.

The intent of POMO is to simplify the maintenance organizational structure. One of the key advantages associated with POMO is that it reduces the coordination necessary between various specialties required to perform a particular maintenance operation. From the discussion of the macro model it will be recalled that formalization is defined as the extent to which jobs are codified and the amount of latitude in conducting one's job. POMO has provided no conditions for recodifying jobs nor has it suggested ways to increase flexibility in performing a particular job. Thus it would be predicted that the maintenance organization remains highly formalized under POMO and the hypothesis is rejected.

H:VII The increased size of the maintenance squadrons operating under the POMO structure will result in a higher rate of maintenance technician manhours consumed in direct labor.

Because of the smaller number of maintenance squadrons under the POMO structure, the number of airmen per squadron will increase. The literature on size and its impacts upon organizational performance is not conclusive. Consequently, this prediction is somewhat tenuous. The hypothesis will be accepted.

H:VIII Under the POMO structure aircraft maintenance personnel perceive a greater contribution to overall goal accomplishment.

As previously noted, under the POMO structure decentralization of decision making will occur. Research literature provides adequate support for the notion that participation in goal setting leads to increased satisfaction and goal accomplishment. If the airmen are

actually involved in the decision making process one would expect to find support for this hypothesis. However, as noted in the discussion under the first hypothesis, delegation of decision making is unlikely to occur. Therefore, it is predicted that this hypothesis will be rejected.

H:IX Aircraft maintenance personnel will perceive a stronger group identity under the POMO structure.

One of the major thrusts of POMO is the increase in group solidarity, cohesiveness, and identity. The structural arrangement is intended to promote a team type atmosphere. This will occur as maintenance personnel identify with a whole weapons system, i.e., a particular plane, as opposed to subsystems comprising the aircraft. This identification is particularly likely in the AGS, but will occur less readily in the other two squadrons. The technology employed and the formalization regarding transfers, placement, and training procedures may reduce this identification. The prediction for this hypothesis is mixed; for the AGS it will be accepted; for the other two squadrons it will be rejected.

H:X Under the POMO structure, maintenance personnel will experience higher levels of job satisfaction.

The POMO structure is designed to enrich the jobs of maintenance personnel. If this enrichment occurs, one of the key benefits will be increased job satisfaction of the airmen. Their enriched jobs will provide a sense of accomplishment and contribution to the overall tasks of the maintenance operation. The jobs will require the exercise of more skills and will provide feedback for self evaluation. All of these factors contribute to more meaningful work and more satisfied airmen. This hypothesis and the three which follow are closely related. Thus, where job satisfaction is high, interpersonal and group relations tend to be good, perceived productivity is high, and leadership is evaluated in a positive manner. This hypothesis states

that the POMO arrangement provides the necessary changes in maintenance jobs which will result in increased job satisfaction. From the macro model viewpoint this hypothesis will be rejected. The job enrichment approach ignores several key variables, notably the environment and technology. Further, the relationships with other subsystems, and the power arrangements within the organization are discounted. It is highly unlikely that job satisfaction can be improved without addressing these macro factors.

H: XI Perceived work group relations among aircraft maintenance personnel will be improved under the POMO structure.

As noted above, when job satisfaction is high there is a tendency toward good interpersonal relationships among work group members. Further, group identity tends to promote positive intra-group relationships. Literature about POMO structure gives no indication of potential intergroup relationship problems. However, it will be recalled that the CRS and EMS are subordinate to the AGS. While the subordination is only implied the potential for conflict exists. Further, the complexity of the organization and the technology employed serve to make the formation of cohesive groups more difficult. Consequently, the relationship between groups is likely to be unimproved and the hypothesis will be rejected.

H: XII Under the POMO structure, perceived work productivity will be higher among aircraft maintenance personnel.

The organization behavior literature argues that job satisfaction leads to higher productivity. Some theorists argue that this relationship is actually reversed; that is, productivity leads to job satisfaction. In either event, given high job satisfaction there is likely to be increased productivity. In the analysis of hypothesis X, the likelyhood of high job satisfaction was questioned. The same arguments would be appropriate to this analysis as to whether the changes instituted by POMO lead to increased perceptions of productivity. Thus the hypothesis would be rejected.

H: XIII a. Aircraft maintenance personnel will exhibit a more positive attitude toward the organizational leader (DCM) under the POMO structure.

b. Organizational leaders (DCMs) under the POMO structure will experience higher levels of job satisfaction.

Assuming that maintenance personnel experience higher levels of job satisfaction, better group relations, and perceived productivity, it follows that they would view leadership more positively. Concurrently, if productivity and morale are both high it is likely that the DCM will be more satisfied with the job which he/she is doing. However, given the discussions of the previous three hypotheses, there is no reason to believe that the assumptions will be met. It is unlikely that maintenance employees under a POMO structure have more positive attitudes toward their leaders. Further job satisfaction for the DCM is not likely to be positively related to the POMO structure. Hence this hypothesis will be rejcted.

H:XIV The percentage of first-term maintenance airmen who will re-enlist will be higher under the POMO structure.

This is the last of the attitudinal and behavioral hypothesis to be evaluated. If the POMO structure results in all of the positive job related factors mentioned in the above hypotheses, this hypothesis will be accepted. Higher reenlistment rates would be expected if the jobs are meaningful and provide the airmen with a psychologically rewarding work opportunity. If the macro model is valid however, this hypothesis will be rejected. The reason this rejection is likely is because the POMO structure has done little to influence the variables which contribute most directly to organizational activity. The POMO structure is a whitewash intended to cover serious organizational flaws. After working within the system for a short while, the airman is able to detect that the POMO structure has not accomplished its intended objectives. Faced with empty promises rather than substantive organizational changes, the airman chooses not to reenlist. This hypothesis will likely be rejected.

The final group of hypotheses attempt to provide answers to questions concerning actual output of maintenance organizations using the POMO structure. Each hypothesis is concerned with a slightly different measure of maintenance productivity. However, the reasons for acceptance or rejection of each hypothesis is likely to be the same. Therefore, all seven of these hypotheses will be listed. Then the likelyhood of accepting or rejecting all of the hypotheses will be discussed.

H:XV The percentage of operational aircraft will be higher under the POMO structure.

H:XVI The percentage of aircraft which are not flyable due to maintenance will be less under the POMO structure.

H:XVII The percentage of aircraft which are not flyable due to non-availability of repair parts will be less under the POMO structure.

H:XVIII The percentage of aircraft which are flown as scheduled will be higher under the POMO structure.

H:XIX The percentage of aircraft aborts will be less under the POMO structure.

H:XX The number of aircraft maintenance actions which require cannibalization of repair parts from another aircraft will be lower under the POMO structure.

H:XXI The percentage of available maintenance technician man-hours consumed in direct labor will be less under the POMO structure.

This last group of hypotheses were taken from a study conducted by Foster and Olson.[38] The output of the maintenance organization is readily measurable, serviced aircraft. But there are numerous methods of reporting the service provided, hence a need for multiple hypotheses. One would expect to find a high level of correlation between

these measures and uniformity in the acceptance or rejection of the proposed hypotheses. There are two reasons why these seven hypotheses are all predicted to be rejected. First the Foster study could find no support for the hypotheses and rejected all of them.[39] Secondly, and more significantly, the POMO structural arrangement is an attempt to change some of the micro variables within a maintenance organization. No conclusive results exist today which link changes in micro variables to changes in productivity of the organization. The POMO structural arrangement gives only limited attention to the problems created by a couple of the macro variables, centralization and complexity, and ignores the others completely. The intent of the POMO structure is to increase the productivity of the maintenance organization. It is predicted however, that productivity has not increased and may well have decreased as a result of the implementation of POMO. The hypotheses will be rejected.

This section has presented twenty one hypotheses which may be tested in order to compare aircraft maintenance under a POMO structure with the maintenance performed under a traditional 66-1 structure. Each hypothesis has been discussed and a prediction as to its likely acceptance or rejection has been made. The next step in the research project is the selection or development of a research instrument.

## VI. POTENTIAL RESEARCH INSTRUMENTS

In a research undertaking of this nature there are basically two methods for obtaining a research instrument. The first is to utilize existing instruments. The second method is to develop new ones or to make modifications to existing questionnaires. Given the standardized nature of the research questions, existing questionnaires would provide the most efficient results. Therefore, the procedure recommended in this study is to utilize existing questionnaires making minor modifications where necessary.

There are two major sections of the instrument that would be employed to collect data. The first section contains general classification type questions such as rank, experience in job, duty location, etc. This information allows the data to be categorized so that comparisons between category types can be made. The second section

contains questions intended to capture the attitudes, perceptions, and intended behaviors of the respondents. This section would be further subdivided into divisions containing questions relevant to the particular attitudes or perceptions of interest. For example, the instrument would have divisions pertaining to a respondent's attitude toward job satisfaction, the freedom felt to perform the work assigned, the quality of interpersonal relationships, or the perceived capabilities of the organization's leadership.

There are numerous instruments which have been developed which could be utilized to gather the necessary data to test the hypotheses. Four different instruments were discovered during the course of the library research. The first is a 71 item questionnaire developed by Noyes and Parker.[40] This particular instrument would require substantial modification and therefore will not be utilized. A second instrument was the one developed by Foster and Olson.[41] This instrument could be utilized but would need to be expanded in several areas. Either of the last two instruments seem to have the flexibility and coverage necessary for this study. The first such instrument was developed by Hamilton. The study was conducted at the request of the Air Force LG and had as an objective the determination of job related attitudes of maintenance personnel. The 159 item questionnaire adequately meets the data requirements of this study.[42] The final instrument was developed to better assess organizational effectiveness. This 165 item questionnaire could also readily be employed to collect data for this study.[43]

To assess the actual productivity differences between POMO and 66-1 maintenance operations another set of data will need to be collected. Data from standard reports of aircraft maintenance activity and from the wing management should provide the necessary information. Some information may need to be obtained from personnel offices, as well. The data should be fairly standard and should not pose any significant data collection problems.

The actual determination of which instrument to employ is not necessary at this time. Proven instruments are available whose validity and reliability could be readily determined.

## VII SUMMARY

It is appropriate at this point to provide a brief summarization of this report. Faced with ever rising costs and diminishing supplies of quality resources, the Air Force is becoming increasingly aware of the need for efficiency of operation. This concern is particularly evident in the areas relating to the human resource, where new programs for improving satisfaction and productivity are prevalent. In 1977 one such program, POMO, was implemented into the maintenance organization of TAC. This job enrichment program was designed to improve the productivity of maintenance personnel by a reorganization of the maintenance structure. Further, the program was intended to provide decentralization of decision making, increased identification with a small group, and increased coordination between work groups.

Maintenance organization performance was then discussed by relying upon organizational theory to develop a macro model. It was the purpose of the model to depict factors which influence organizational performance but which may be beyond the control of individuals who currently comprise the maintenance organizations. The maintenance organization was then described by relying on the variables included in the model. The next step in the study was the development of twenty one hypotheses which could be evaluated in order to compare maintenance performance under the POMO structure and maintenance under the 66-1 structure. The final section of the report examined potential instruments for collecting data to evaluate the hypotheses.

Since no data has been collected, the following conclusion is tenuous. Based on the organization theory literature and the macro performance model developed, the usefulness of the POMO structure is questionable. Organizational changes which do not take into account significant organizational variables are doomed to failure. It is the contention of this report that the POMO structure failed to deal with these variables. POMO's impact upon maintenance productivity is likely to be negligible or perhaps even negative.

## VIII. RECOMMENDATIONS

There are three recommendations which emerge from this study. The first is a reminder of the necessity to carefully evaluate new programs

before they are implemented. It is imperative to avoid simplistic single variable solutions to complex multivariable problems. Typically these solutions treat only the symptoms and miss the real problem. Not only do they miss the problem, frequently they serve to mask the real problems facing the organization. This is not a recommendation to cease efforts to improve organizational functioning. But problems plaguing modern complex organizations are rarely solved with single variable approaches.

The second recommendation is the empirical assessment of the proposed hypotheses. The hypotheses are not without value as they are currently written. They are useful for guiding further research. However, they would provide much more information if they were empirically tested. It is the intent of the author to implement this recommendation through a follow-up mini grant. It is the contention of this paper that the POMO has not accomplished its objectives of increased productivity within the maintenance organization. This contention requires substantiation with empirical data.

The final recommendation is of importance if significant improvements in maintenance organizational performance is to occur. In fact, most subsystems in the Air Force would likely improve their performance if this suggestion is implemented. From a macro model viewpoint, several organizational variables require the attention of the Air Staff. Changes in these variables offer the greatest potential for increasing the sagging reenlistment rates and enhancing productivity. These changes, however, are very complex and will have ramifications throughout the Air Force. For example, one method of dealing with the complexity variable would be the creation of master technicians. That is, assume that a maintenance technician has no desire to move into supervisory positions. Then the question becomes, is it desireable to force the individual into making such a move through the up or out method of promotion. Another example is the number of rules, procedures, and guidelines which govern all aspects of the work arena. While no one would discount the necessity of some rules and guidelines the issue today is an over abundance of rules. The question could be raised as to whether the Air Force has become so formalized as to effectively squelch individual initiative and creativity. A final

example will make clear the importance of attending to the macro variables proposed in this report. The technology employed by the Air Force has become increasingly sophisticated. This sophistication requires a subsequent upgrading of maintenance personnel and increased input by the maintenance organization in Air Force level decision-making. However, the power structure in the Air Force and high level Air Force leadership continue to reflect the importance attached to the operations subsystem. This is not to say that operations is unimportant. Rather it is simply an attempt to note that this subsystem is disproportionately represented in high level leadership and decision-aking.

The implementation of these or similar changes will be difficult. The complexity of the changes will preclude simplistic approaches. The magnitude of the problems can not overwhelm high level decision makers to the point of inactivity. Rather careful attention to the revitalization of the organization must continue. The task is unending, but the reward of organizational survival is worth the effort expended.

## REFERENCES


1. Townsend, G.E., "Air Force Maintenance - Issues and Challenges for the Eighties," Air Force Magazine, Vol. 63, pp. 56-61, Jan 1980.
2. Halsell, L.H., Alternative Aircraft Maintenance Management, Research Study, Air Command and Staff College, Air University, p. 6, 1977.
3. Ibid, p. 7.
4. Ferris, A.L., "Studies in the Organization of Maintenance: Authority Patterns in High- and Low- Performance Wings," Symposium on Electronics Maintenance, sponsored by Advisory Panel on Personnel and Training Research, pp. 175-192, 1955.
5. Halsell, pp. 8-11.
6. Air Force Regulation 66-1, Maintenance Management (Washington, Department of the Air Force, 1980.)
7. Keller, G.B., A Restructured Maintenance System, Research Study, Air War College, Air University, pp. 19-24, 1975.
8. Ibid, pp. 28-30.
9. Drake, K.L., M.S. Sanders, W.H. Crooks, and G. Weltman, Comparative Studies of Organizational Factors in Military Maintenance, Cybernetics Technology Office, (ADA 050403), pp. 3-15-3-18, 1977.
10. Air Force Regulation 66-5, Production Oriented Maintenance Organization, (Washington, Department of the Air Force, 1979.)
11. Foster, D.J. and J.C. Olsen, A Comparative Evaluation of the Effect of the Implementation of the Production Oriented Maintenance Organization (POMO) on Aircraft Maintenance, Master's Thesis, Air Force Institute of Technology, Air University, pp. 2-11, 1978.
12. Ibid, pp. 28-40.
13. Evans, B.M. and A. Ferraro, A Study Into the Relationships Between Air Force Logistics Doctrine and Maintenance Posture Improvement Program Policies, Master's Thesis, Air Force Institute of Technology, Air University, 1979.

14. Townsend, pp. 56-58
15. Anderton, D.A., "POMO and POST: Keystones of TAC Readiness," Air Force Magazine Vol. 62, pp. 46-50, Jan 1979.
16. Nelson, W.R., "Production Oriented Maintenance Organization POMO A New Concept," Aerospace Safety,Vol. 33, pp. 2-4, March 1977.
17. Kast, F.E. and J.E. Rosenzweig, Organization and Management: A Systems and Contingency Approach, (New York, McGraw-Hill Book Company, 1979), pp. 98.
18. Etzioni, A., Modern Organizations (Englewood Cliffs, N.J., Prentice-Hall, Inc., 1964).
19. Hall, R.H., Organizations:Structures and Process,(Englewood Cliffs, N.J., Prentice-Hall, Inc., 1977).
20. Anderson, T. and S. Workov, "Organizational Size and Functional Complexity," American Sociological Review, Vol. 26, pp. 21-30, February 1961.
21. Frost, P.J., N.F. Crandall, T.A. Mohoney, and W. Weitzel, Organization Size as an Influence on Organization Behavior, Personnel and Training Research Programs, Office of Naval Research (NR 151-323) pp. 12-16, 1971.
22. Hall, R.H., J.E. Haas and N.J. Johnson, "Organizational Size, Complexity, and Formalization," American Sociological Review, Vol. 32, pp. 501-513, December, 1967.
23. Thompson, J., Organizations in Action, (New York:McGraw-Hill Book Company, 1967).
24. Ibid, pp. 15-18
25. Ibid, pp. 51-65.
26. Hage, J., "An Axiomatic Theory of Organizations," Administrative Science Quarterly, Vol. 10, pp. 292-303, December 1965.
27. Hall, pp. 152-172
28. Kahn, R.L., D.M. Wolfe, R.P. Quinn, J.D. Snoek, and R.A. Rosenthal, Organizational Stress:Studies in Role Conflict and Ambiguity, (New York:John Wiley & Sons Inc., 1964), pp. 20-33.
29. Hall, pp. 181-193.

30. Emerson, R.M. "Power Dependence Relations," American Sociological Review, Vol. 27, pp. 28-34, February 1962.

31. French, J.R.P. and B. Raven, "The Bases of Social Power," in D. Cartwright and A. Zander, eds., Group Dynamics (New York: Harper and Row, Publishers, 1968), pp. 259-269.

32. Perrow, C., Complex Organizations:A Critical essay, (Glenview, Illinois:Scott, Foresman and Company, 1972), pp. 58-60.

33. Etzioni, A. "Dual Leadership in Complex Organizations," American Sociological Review, Vol. 30, pp. 680-691, October 1965.

34. Hall, pp. 303-332.

35. Perrow, pp. 199-202.

36. Herzberg, F., The Managerial Choice:To be Efficient and to be Human, (Homewood, Illinois:Richard D. Irwin, Inc., 1976).

37. Hackman, J.R., G. Oldham, G.R. Hanson, and K. Purdy, "A New Strategy for Job Enrichment," California Management Review, pp. 57-71 Summer 1975.

38. Foster and Olson, pp. 18-20

39. Ibid, pp. 68-83.

40. Noyes, C.J. and T.E. Parker, Organizational Variables in an Air Force Program Environment, Master's Thesis, Air Force Institute of Technology, Air University, pp. 168-179, 1978.

41. Foster and Olson, pp. 132-149

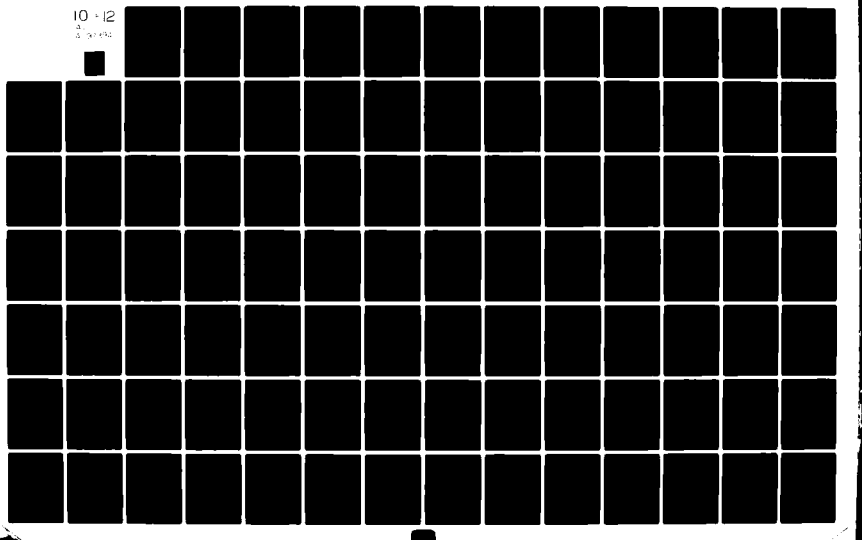
42. Hamilton, C., Maintenance Career Field Survey, USAF-SCN-79-146, AFMPC/MPLYPS, San Antonio, TX, pp 1-19, 1979.

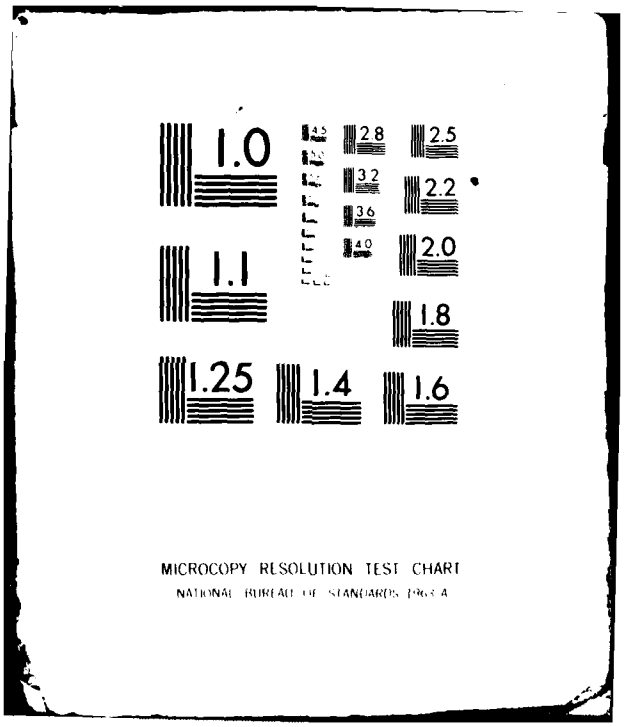
43. Hendrix, W.H. Organizational Assessment Indices of Effectiveness, AFHRL-TR-79-46, pp. 19-30, 1979.

AD-A097 394 SOUTHEASTERN CENTER FOR ELECTRICAL ENGINEERING EDUCAT--ETC F/6 5/1
USAF SUMMER FACULTY RESEARCH PROGRAM, 1980. RESEARCH REPORTS. V--ETC(U)
OCT 80 W D PEELE F49620-79-C-0038

UNCLASSIFIED AFOSR-TR-81-0193 NL

10 12




1.0
1.1
1.25
1.4
1.6
1.8
2.0
2.2
2.5
2.8
3.2
3.6
4.0
MICROCOPY RESOLUTION TEST CHART
NATIONAL BUREAU OF STANDARDS 1963-A

1980 USAF - SCEEE SUMMER FACULTY RESEARCH PROGRAM

Sponsored by the

AIR FORCE OFFICE OF SCIENTIFIC RESEARCH

Conducted by the

SOUTHEASTERN CENTER FOR ELECTRICAL ENGINEERING EDUCATION

FINAL REPORT

# EVALUATION OF R&D PROGRAM ON COMPUTATION FOR SIMULATION


| | |
|---|---|
| Prepared by: | Marshall Waller |
| Academic Rank: | Assistant Professor |
| Department and University: | College of General Studies<br>George Washington University |
| Research Location: | Air Force Human Resources Laboratory<br>Williams Air Force Base, Arizona |
| USAF Research Colleague: | Warren E. Richeson<br>Chief, Systems Engineering Branch, OTF |
| Date: | August 8, 1980 |
| Contract No. | F49620-80-C-0038 |

# EVALUATION OF R&D PROGRAM ON COMPUTATION FOR SIMULATION

By

Professor Marshall Waller

## ABSTRACT

An evaluation of the AFHRL R&D Program on Computation for Simulation was performed by examining the design and performance characteristics of the Advanced Simulator for Pilot Training, by reviewing the Air Force Systems Command current research objectives in science and technology, and by coordinating, formatting and analyzing project research data.

## ACKNOWLEDGEMENT

The author would like to thank the Air Force Systems Command, the Air Force Office of Scientific Research, and the Southeastern Center for Electrical Engineering Education for providing him with the opportunity to spend a very worthwhile and interesting summer at the Air Force Human Resources Laboratory, Williams Air Force Base, Arizona.

I would especially like to thank the Chief and Assistant Chief of the Systems Engineering Branch, Mr. Warren E. Richeson and Major John Kiselyk, for their advice and help in my work.

## I. INTRODUCTION

The responsibility for R&D in flying training technology for the AF Human Resources Laboratory resides with the Operations Training (OT) Division at Williams AFB, AZ. The scope of the OT program is significant in terms of personnel, funds and facilities. OT develops, tests, and evaluates newly developed hardware, software, procedures and techniques for improving all phases of USAF flying training programs.

The major research tool of the Division is the Advanced Simulator for Pilot Training (ASPT). This research simulator, provides operational replicas of the F-16 and A-10 aircraft, and is used for research and training 24 hours per day, 7 days per week. This simulator provides OT and the AF with the latest state-of-the-art in flying training simulation. There are considerable computer peripherals associated with the real-time simulation, particularly for image generation and force cuing simulation.

This report discusses my efforts, as an Assistant Professor of Mathematics and as a Flight Instructor, to become familiar with the organization, functioning, technical aspects and state-of-the-art represented by the HRL OT Division at Williams AFB, AZ. Within the time constraint of ten weeks, I approached this task in three areas: I became as familiar as possible with the ASPT; I studied the broader research objectives in science and technology of the Air Force System Command (of which HRL is a part); and I gathered, formatted and analyzed R&D data on Computation for Simulation as part of a report for the Engineering Branch.

## II. OBJECTIVES OF THE RESEARCH EFFORT

There were three objectives in this research effort:

A. To become familiar with the design and performance characteristics of the Advanced Simulator for Pilot Training (ASPT) as they relate to the A-10 and F-16 aircraft, plus learning and observing the organization and functions of the Operations Training Division of the Human Resources Laboratory at Williams AFB, AZ

B. To study the Air Force System Command's (AFSC) current research objectives in science and technology, particularly in the Electronics Technical Subarea.

C. To gather, format and report on R&D data pertaining to Computation for Simulation.

## III. ACCOMPLISHING THE OBJECTIVES

A. I became familiar with the ASPT by conference with scientists and engineers in the OT Division; by reading extensively through reports which are part of the files of the Division; and by being present at briefings and meetings pertaining to the history, development and to the on-going business of the Division. I was given full freedom to discuss any matter with military, civil service or contractor personnel. As a pilot, I also benefitted from observing other pilots training in the ASPT, as well as from flying them myself.

B. I studied the AFSC research objectives in science and technology by reviewing the 1980 Research and Planning Guide. This document of nearly 300 pages identified research needed by the AF in the mid and long-term. The seven technical areas covered in some detail were Life Sciences, Material, Geophysics, Aerospace Vehicles, Propulsion and Power, Weaponry, and Electronics. The apparent threading of mathematical support throughout all these subareas was of particular interest to me.

C. I volunteered for the opportunity to gather, format and report on data pertaining to Computation for Simulation. (My Effort Focal Point for this summer faculty research program, Mr. Warren E. Richeson, was Chairman of the SubTAG on this subject, and was also a member of the steering group for the overseeing Technology Advisory Group for Simulation).

In this effort I was able to talk to, correspond with, and interact with all eighteen SubTAG members, each a distinguished scientist or engineer representing the state of computation for simulation R&D in the Army, Navy, Air Force and Maritime Service.

D. In addition to the foregoing, I attended several scientific colloquia which were sponsored by the Division while I was in residence.

## IV. DISCUSSION OF OBSERVATIONS

In my opinion, the OT Division is a well-managed, funds-conscious, efficient and effective organization, fully accomplishing the missions assigned to it by the Human Resources Laboratory Headquarters at Brooks AFB, Texas. The personnel all seem hard-working and conscientious. The history, development, objectives, past accomplishments and plans for the Division are well documented in detail, and are known to all appropriate organizational elements. I found the technical and training missions of the Division being accomplished with particular care and comprehensiveness.

My review of the research and technology objectives of the AFSC will be continued when I return to my University, in order to determine if elements of the University may wish to submit proposals to the AF for pertinent research efforts.

## V. RECOMMENDATIONS. I recommend that the:

A. OT Division continue with its present and future plans for AF utilization of ASPT, improved by state-of-the-art technology in research and training.

B. AFSC Research Planning Guide (TR 80-01) continue to be given the widest possible distribution in Industry and Universities this year and in the future.

C. SimTAG and the computational SubTAG continue to update compendia of R&D information yearly, if possible.

## REFERENCES


AFSC Regulation 12-1, "Research and Development Case Files", 1979.

Flying Training Division, AF Human Resources Laboratory, "Simulation Research for Flying Training", April, 1978.

AF Human Resources Laboratory, "Operations Training Division" (Draft), April, 1980.

Hq AFSC, "Research Planning Guide (Research Objectives)", TR 80-01, February, 1980.

AF Office of Scientific Research, "Flight and Technical Training, Review of AF-Sponsored Basic Research" (USAF Academy Symposium) Directorate of Life Sciences, Bolling AFB, DC, March, 1980.

US Army Missile Command, "Low Altitude Radar Simulation Techniques" (Draft), Missile Intelligence Agency, Redstone Arsenal, Ala., January, 1980.

Various recent pamphlets, brochures, unpublished briefings, and manuscripts pertaining to the AF Human Resources Laboratory, generally undated.

Large file of charters, missions, minutes, and plans pertaining to the DoD Simulation Technology Advisory Group and its SubTAGs, dated 1978-1980.

1980 USAF - SCEEE SUMMER FACULTY RESEARCH PROGRAM

Sponsored by the

AIR FORCE OFFICE OF SCIENTIFIC RESEARCH

Conducted by the

SOUTHEASTERN CENTER FOR ELECTRICAL ENGINEERING EDUCATION

FINAL REPORT

# THE ASSESSMENT OF HUMAN FACTORS IN COMMAND, CONTROL AND COMMUNICATION SYSTEMS: APPLICATION OF NON-PARAMETRIC RELATIVE OPERATING CHARACTERISTICS


| | |
|---|---|
| Prepared by: | Dr. Rik Warren |
| Academic Rank: | Visiting Professor |
| Department and University: | Department of Psychology<br>Ohio State University |
| Research Location: | Air Force Human Resources Laboratory, Logistics Research Division, Ground Operations Section |
| USAF Research Colleague: | Dr. Larry Reed |
| Date: | September 15, 1980 |
| Contract No: | F49620-79-C-0038 |

# THE ASSESSMENT OF HUMAN FACTORS IN COMMAND CONTROL AND COMMUNICATION SYSTEMS: APPLICATION OF NON-PARAMETRIC RELATIVE OPERATING CHARACTERISTICS

by

Rik Warren

ABSTRACT

The problem of the assessment of human factors in command, control and communication systems is considered. Previous attempts at producing a practical quantitative method have failed and the reasons are discussed. The key to assessment is to conceive of a commander as a decision maker. The worth of a system is determined by its impact on a commander's decisions. Command decisions may be evaluated by signal detection theory. This theory provides two classes of performance indices: one of decision making quality irrespective of bias effects and one of inherent bias. Practical problems in applying classical methods are discussed and new methods and non-parametric indices are shown to be of operational value. The importance of assessing bias effects in $C^3$ decision making is stressed.

## Acknowledgement

The author would like to thank the Air Force Systems Command, the Air Force Office of Scientific Research and the Southeastern Center for Electrical Engineering Education for providing him with the opportunity to spend the summer at the Air Force Human Resources Laboratory, Logistics Research Division, Wright-Patterson AFB, OH. He would like to acknowledge the laboratory for its hospitality.

Finally, he would like to thank Dr. Larry Reed and Bert Cream of the Ground Operations Section. Walt Johnson, a visiting graduate student from Ohio State University and summer office-mate deserves a special thank-you.

## I. INTRODUCTION

Command, control and communication systems are becoming more sophisticated and prevalent in today's Air Force operations, but they are also becoming more costly. Hence, a major concern is their cost-effectiveness. But intelligent determination of cost-effectiveness requires an objective assessment methodology. This need for assessment was recognized early[1] and there followed several attempts at developing an assessment methodology.[2,3,4,5,6]

The success or failure of a $C^3$ system is intimately bound to the performance characteristics of the human operators who use the system and this is expecially true as the system increases in complexity. As Conley[7] points out: "At the present level of technology there is a limit to the complexity of a $C^2$ system which can be produced without a human playing an integral part in the process." This immediately implies that the human factors aspects of $C^2$ and $C^3$ systems must be carefully consideredin the design of a system for the system to succeed. But determining the human factors contributions to $C^3$ systems also requires and objective, quantitative assessment methodology.

This need has also been recognized and human performance research that may relate to the design and operation of $C^3$ systems has been reviewed[8,9,10] and attempts have been made to integrate the findings and make recommendations for $C^3$ operations.[11,12] However, much remains to be done in the area of the assessment of $C^3$ systems in general and Human Factors in $C^3$ systems in particular as evidenced by recent reviews on the state of the art.[13,14,15] In spite of much effort, no adequate assessment methodology exists today that is practical or useful. Why is this so? And what can be done to acheive this goal?

One possible reason for the poor state of the art is the inordinate degree of complexity inherent in the hardware, organizational, human, and task factors that are the essence of $C^3$ systems. The complexity level is all too real and hence the appeal to complexity is not all

that gratuitous, but such appeals must be taken as challenges rather than as excuses else they grow tiresome. Another possible reason for the poor state of the art is that there is conceptual confusion and this, as Wittgenstein[16] points out, rather than the alleged complexity or immaturity of a field may be the real culprit impeding progress.

Conceptual confusions may arise in several areas. Of particular interest here are the definition of a $C^3$ system, the identification of the users of the system, and the nature of the tasks involved. As will be discussed, there are problems with the existing definitions or conceptualizations of what $C^3$ systems are and this lack of specificity or preciseness of the concept of $C^3$ system may account for some of the measurement problems. Our understanding of who the users are is also incomplete and and understanding of the nature of the tasks to which $C^3$ systems are applied will also influence our ability to assess the degree of success or failure of a system.

The problem of the degree of success or failure of a system is further exacerbated by still another source of conceptual confusion, namely, the question of what constitutes good or poor performance. Performance on a large class of tasks is not simply two-fold catagorizable as "right" or "wrong": Modern Signal Detection Theory has caused a revolution in psychology and the theory of assessment by reconceptualizing "right" and "wrong" each into two varieties. Although many areas of psychology have benefitted from the new conceptualization,[18] many areas have not due to the difficulty of applying classical signal detection theory to them. However, new techniques have emerged that will help extend the benefits of signal detection approaches to such areas. In particular, the assessment of $C^3$ systems and human performance in $C^3$ systems could benefit from application of the new technology.

## II. OBJECTIVES

The main objective of this project was to help clarify some of

the conceptual confusions that have hindered the development of a satisfactory, quantitative and operationally useful assessment methodology for $C^3$ systems in general and human factors in $C^3$ systems in particular. The particular areas of conceptual confusion that may profitably be explored were identified in the introduction, namely:

(1) The problem of definition of command and control and also command, control and communication systems;

(2) The problem of the identification and role of the human users of a C3 system;

(3) The problem of the identification and explication of the nature of the tasks to which C3 systems are applied, and;

(4) The problem of determining what constitutes good and poor performance.

This last problem deserves amplification since a main objective of this paper is to suggest the desireability of using non-parametric signal detection theory indices of performance for assessing human factors in $C^3$ systems. Specifically, signal detection theory stresses the ubiquity of bias effects in system performance in addition to a system's performance being "correct" or "incorrect". Fortunately, although paradoxically, the theory provides bias free indices of performance as well as indices of bias. Unfortunately, signal detection methods have required very many areas that would otherwise benefit from the theoretical advantages. However, there are now available more efficient TSD indices that promise to be of practical significance for general system assessment. This paper will thus explore the problem of how to apply these methods and benefit from their power.

## III. PROBLEM OF A $C^3$ SYSTEM DEFINITION

In order to discuss the assessment of human factors in $C^3$ systems,

it is first necessary to know what such a system is. Although there is an official Department of Defense Definition,[19] there is no simple and satisfactory definition of a command, control, and communication system, let alone the command and control part of $C^3$, as evidenced by the numerous discussions and attempts at definition.[4,9,20] Nickerson, Adams and Pew,[9] in their background notes for a recent set of major workshops on human factors in command, control and communication systems, have provided a working definition (p. 1): "For our purposes a command, control and communication system is a system, the function of which is to direct the activity of some organizational or operational entity." This is obviously too broad a definition and they immediately begin to narrow down the scope of the definition by considering examples of the class of systems that have received the appelation, namely, those in "space flight, commercial air traffic control, law enforcement, disaster releif management, and industrial production" (pp. 1-2) and especially, defense related systems.

After reveiwing the official Department of Defense definition of command and control - "the exercise of authority and direction by duly designated authorities (p. 2)" - they proceed to discuss a key feature of a $C^3$ system: Bidirectional flow of information to and from a commander/controller. The supporting communication systems tend to be very complex with a crucial dependence on sophisticated electronic sensors and computer processing of and display of information. The simple definition does not require computer technology and indeed a simple system such as one based on indian smoke signals would technically qualify as a $C^3$ system. However, at least implicit is the requirement of advanced electronics and computer display as evidenced by another type of definition - that by example and enumeration. Both Nickerson, Adams and Pew[9] and expecially Parsons and Perry[4] provide extensive lists of $C^3$ systems. Presumeably, these

systems are to serve as examplars and all entail sophisticated electronic technology.

These examplars and working definitions enable some progress on $C^3$ system development to be sure, but design and use of $C^3$ systems will remain more art than science until an adequate and explicit theory and defintion of $C^3$ emerges. Likewise without a guiding theory, the assessment of the human factors contribution will remain less than optimal. How do you assess what is done without knowing what ought to be done?

## Purpose of $C^3$ Systems and Goals of Assessment

To properly define and intelligently assess a $C^3$ system, it is necessary to know what the purpose or intended function of the system is. The assessment is then simply a measure of how well the system is performing its function. For purpose of this paper, the function of a $C^3$ system is simply to assist a human user to perform better in a command and control situation than he would without the system. More specifically, Nickerson, Adams and Pew[9] state that "The fundamental purpose of a $C^3$ system is to optimize the quality of command decisions and the timeliness with which they are made and communicated" (p. 21).

## Focus on Human Factors and Scope

The operational goals of timeliness and quality of command and control decisions can, of course, be influenced by hardware factors but the direct assessment of hardware as hardware is not in the domain of this paper. Human factors assessment is, in a sense, an indirect assessment of the hardware base since a hardware configuration that is inoperable, or more likely, less than optimally operable by its user is inefficient, and therefore bad, no matter how sophisticated it components.

What is being assessed then is not the functioning of the hardware as such but rather the performance and contribution of the human user and operators in the context of the whole system configuration. By the context of the whole system configuration is meant that any system variable/aspect that may impact on a user's perfomrance is partially a function of (a) the decisions to be made, (b) the actions to be taken, (c) the information display quality, quantity and rates, and (d) formal and informal lines of communication.

This is one of many possible dissection of a $C^3$ system. How long should such lists be and what should be included in them? Nickerson, Adams and Pew[9] (pp. 21-22) argue that:

> "From a human factors point of view, therefore, two fundamental questions to consider about any $C^3$ system at any level of functioning are these: (1) What information should be presented to the user, and (2) How should that information be represented?. . .Indeed, the basic human factors problem in $C^3$ systems is not so much that of identifying what areas of psychological research are relevant - because they all are - but that of determining what specific research findings (including potential findings) could have truely significant impact on the degree to which these systems meet the needs of their users."

This last phrase "needs of their users" is very crucial for assessment. The problem of identification of needs is obvious, but the problem of identification of users is more subtle. A $C^3$ system does not impact equally on all its users and not all users equally effect the performance of the $C^3$ system. Who are the users?

## IV. THE PROBLEM OF THE IDENTIFICATION OF THE USER

In general, the class of $C^3$ systems to be considered will have three classes of components: (1) the executive user or the commander user, (2) none or more subordinate or support users, and (3) the hardware. The executive user or the commander is a single person with the final command/control authority and responsiblity for the use of the system. The subordinate users may themselves form a positional network or hierarchy. Their function is to operate the system hardware and to to request, seek and pass on information either with or without some modification or processing on their part. There is no attempt here to assess the functioning of the hardware as such. The executive and subordinate users are, of course, humans and it is their performance within the system context that is to be assessed.

For purposes of this paper, the function of a $C^3$ system may be more precisely defined as that of simply assissting a Commander-user to perform better in a command and control situation than he would without the system. Notice that for purposes of assessment, the executive-user is not considered a part of the $C^3$ system. The focus of the assessment problem should be on the performance of this user, the commander, or more specifically on the relative performance of the commander-user with versus without the system or as compared to with another system.

The commander-user's performance thus becomes the key to the assessment of a particular $C^3$ system: A particular system's worth is measured by its impact and only by its impact on the the commander-user. The technical elegance, complexity or primitiveness of a $C^3$ system is totally irrelevant to its worth. The worth of a system is to be measured only by its degree of meeting its goal and that goal is to make a commander perform better.

The point to be emphasized here is that there is a profound distinction to be made between the performance of the commander and

the performance of the subordinate users.

What can be said of the performance of the subordinate users? All human factors consideration with respect to the subordinate users are to be ultimately adjudged by their impact on the ultimate user, the commander. An assessment program that concentrates, for example, on the effects of console design or data transmission rates is doomed to irrelevance if there is no appreciable effect on the commander. But this too has a subtle implication: Subordinate user factors that do not result in a decrement in a commander's performance may provide an intelligent basis for cost-cutting programs. For example, if a color coded CRT screen of a subordinate radar operator does not result in better performance by a commander then any money spent on the color CRTs in wasted no matter how much the subordinate operator's own performance or job satisfaction is improved.

This last point raises the distinction between local and global measures of performance. There is no guarantee that improvements in local subcomponents will have any appreciable effect in the overall performance of the commander. Relevant here is also the question of interaction among components and sub-users. There is no guarantee that interaction effects among components or sub-users will result in improved performance by a commander. What is being presented here is <u>not</u> a case against the attempt to asses and improve local sub-components but rather a cautionary note and reminder that there is <u>one</u> legitimate criterion for assessing the performance of a local sub-component or user, namely, the impact on the commander. Local user benefits are not, of themselves, sufficient justification for making recommendations about $C^3$ systems.

The assessment question now becomes: How to assess the commander's performance?

## V. THE PROBLEM OF THE NATURE OF THE TASK

In order to evaluate a commander's performance in a useful way, it is necessary to define and delimit his task so that a quantitative assessment is possible. There are, of course, many subtasks that a commander is expected to complete successfully and an evaluation may be rendered on each. It is easy enough to make lists of the various subtasks and to devise performance measures for each. This may be termed microassessment and is an inherently locally oriented evaluation strategy.

Another approach is to look for the most general invariences or commonalities across all tasks. That is the approach taken here since any advances in such assessment would then have braod application and generality. The most general conception of a commander's task is that of the commander as a decision maker. This conception of a commander as a decision maker has been strongly preshadowed in the previous sections.

The emphasis on the commander as a decision maker means that some very powerful evaluation techniques may be introduced. How good a decision maker is a commander operating within the context of a particular $C^3$ system?

## VI. THE PROBLEM OF DEFINING GOOD AND BAD PERFORMANCE

The framework for the evaluation of decision making that is being advocated here is that of signal detection theory (SDT or TSD). Many areas of modern psychology have been shown to be analyzable and to profit by this approach.[17,18] Since the standard methodology of classical signal detection theory is well known,[17,18,21] it is not

necessary to review the techniques in detail here, but a few points deserve discussion.

Signal detection theory distinguishes between two types of correct decision and two types of incorrect decision. A person may be correct by deciding in favor of an appropriate alternative, a "hit", or by deciding against an inappropriate alternative, a "correct rejection". A person may be incorrect by deciding in favor of an inappropriate alternative, a "false alarm", or by deciding against an appropriate alternative, a "miss". A person's hit and false alarm rates are jointly determined by the person's decision making ability or true sensitivity and also by the person's bias. Bias is a tendancy to generally decide in favor or against an alternative irrespective of the evidence and may be seen as a tendancy to be "trigger happy" or "gun shy". Bias is, according to the theory, determined jointly by a person's concept of the likelihood of an alternative being correct, the "prior odds", and the relative costs and benefits of each consequence of a decision, the "payoff matrix".

A principal claim of signal detection theory is that bias is unbiquitous. All decision making is inherently tainted by bias effects. Although bias may never be eliminated, it can be numerically indexed and placed under experimenter control, for example, by explicitly manipulating the payoff matrix.

The effect of varying bias may be seen in the "relative operating characteristic" or ROC curve which is a plot of hit rate versus false alarm rate as bias is varied. A trigger happy decision maker will have many hits but at the expense of many false alarms. A gushy decision maker will make few false alarms but at the expense of very few hits. Hence, a high hit rate or low false alarm rate are not, in themselves, a reasonable measure of true decision making ability or performance. Both hit and false rates must be simultaneously

considered: A high hit rate at the expense of a high false alarm rate may be as poor decision making performance as that resulting in a low false alarm rate accompanied by a low hit rate.

The index of bias-independent decision making performance in classical signal detection theory is termed d' and the index of bias is called beta. Although these indices were very useful in numerous psychophysical and decision making areas, they are not without their drawbacks.

One drawback to the extension of signal dectection techniques to many areas that could benefit is the tremendous time inefficiency of the experimental procedures: Ideally several hundred trials would be used to determine one value of d' and beta per person. Even under experimental situations that permit one trial per every few seconds, the methodology is inordinately cumbersome, time-consuming and fatiguing for subjects. In a typical study, so many sessions are required that so few subjects and so few performance measures per subject are obtained that the results are not further analyzable by analysis of variance or by multiple regression-multiple correlation techniques and therefore this important step in research must be foresaken.

A second drawback to classical signal detection techniques is that the d' index is rarely computed correctly when data are obtained by the popular rating scale method since the standard curve fitting techniques are mathematically inappropriate.[22,23] Unfortunately, the correct maximum likelihood procedure is not widely known and practiced by psychologists. This correct procedure requires a mathematical technique that is also unfamiliar and therefore avoided by most psychologists.

A third drawback is that even if maximum likelihood computational methods were used, the underlying parametric assumptions of classical

d' and beta indices (equal variance and normal distributions) are rarely, if ever, met. This vulnerability to assumption failure is true also of any of the other d' procedures in addition to the rating scale procedure. In sum, the classical signal detection indices are often computed using inappropriate techniques and even when computed correctly, empirically untenable assumptions are made to justify the use of these indices. Hence, the potential benefits of using this very sophisticated theory are called into question or at least diluted by the problems of flawed empirical measures when the theory is applied and also by the simple inabiliity to even apply the theory to many research areas.

However, there are now available non-parametric signal detection indices that simultaneously avoid the problems introduced by inappropriate computational procedures and failures to meet equal variance and normal distribution assumptions. In addition, the new methods are relatively stable and tolerant of data from just a few trials. The non-parametric measure of sensitivity is the area under the relative operating characteristic curve. This may efficiently be used with few trials if the rating procedure is used and the computational methods are simple and straightforward.[21,24,25] There are several non-parametric indices of response bias[21,26,27] but the B" of reference 27 and the B of reference 21 seem the most promising.

## VII. RECOMMENDATIONS

Non-parametric signal detection methods are data-efficient and may be applied profitably in many areas of human factors assessment in $C^3$ systems. Two distinct but complementary assessment areas to benefit from this approach are:

One. The performance of individual users may be measured and compared. This comparison may be within a user (for example, learning

and fatigue effects), or between users (individual differences in decision skill or bias).

Two. Entire $C^3$ systems or their components may be assessed. The performance of an entire system is acheived by comparing average performance of several equivalent groups using different systems or by comparing a particular user's performance on different systems.

Modifications to a system are here considered to produce different systems. Hence, the effects of system modification can be assessed using the same techniques as for entirely different systems.

Of special value is that signal detection methods provide two independent measures of performance, one indexes the quality of decision making irrespective of bias factors and the other indexes bias.

A possible area of future research combines timeliness and bias analyses. For example, Sidorsky[28] found that perceived advantage-disadvantage in a command and control situation markedly effects quality of performance. Two possible bias hypotheses are that a commander who perceives himself to be at a disadvantage performs poorly because (a) he becomes too conservative or "gun shy", thereby requiring much information for a decision and hence acting too late, or (b) he becomes too liberal ("grabbing at straws") and acts too soon or risky without sufficient information. These are not the only possibilities but they are worthy of investigation.

In conclusion, ROC methods permit the assessment of a particular user's bias, but more importantly, it is recommended that research be conducted on $C^3$ situations that may induce general shifts in bias across commanders.

## REFERENCES


1. R.L. Chapman, J.L. Kennedy, A. Newall and W.C. Biel,"The systems research laboratory's air defense experiments," Management Sci., Vol. 5, pp. 250-269, 1959.

2. R.B. Davis and R.A. Behan, "Evaluating system performance in simulated environments," in R.M. Gagne (Ed.), Psychological principles in system development, New York: Holt, Rinehart & Winston, 1962.

3. J.J. Keenan, T.C. Parker and H.P. Lenzycki, "Concepts and practices in the assessment of human performance in Air Force systems," Tech. Rep. AMRL-TR-69-100, Aerospace Medical Research Laboratory, Wright-Patterson AFB, Sept. 1969.

4. S.M. Parsons and W.E. Perry, "Concepts for command and control systems," Tech. Memo. TM-WD-227/000/00, Falls Church, Va.: System Development Corp., December, 1960.

5. J.F. Jacobs, "Practical evaluation of command and control systems," Report MP-7, Bedford, Mass., MITRE Corp., 1963.

6. [illegible] Finley, F.A. Mackler, C.A. Gainer and W.T. Roe, "Development of an analysis and evaluation methodology for command and control: First technical report (U)," Canoga Park, Ca.: ANSA Information Corp., March 1974.

7. R.E. Caley, "Military command and control ($C^2$)," Signal, January 1978, pp. 14-17.

8. A.B. Nickerson, R.J. Adams, R.W. Pew, J.A. Swets, S.A. Fidell, R.E. Pearrer, R.B. Yntema and D.M. Green, "The $C^3$-system user (Vol.1)," Report No. 3433, Cambridge, Mass.: Bolt, Beranek and Newman, Feb. 1977.

9. A.B. Nickerson, R.J. Adams, R.W. Pew, J.A. Swets, S.A. Fidell, R.E. Pearrer, R.B. Yntema and D.M. Green, "The $C^3$-system user (Vol.2)," Report No. 3434, Cambridge, Mass.: Bolt, Beranek and Newman, Feb. 1977.

10. [illegible] Harvey and [illegible] Atwood, "Human factors in computer systems: A review of the literature," Tech. Rep. SAI-79-111-DEN, Englewood, Col.: Science Applications, Inc., September, 1979.

11. A.R. Tolcott, "Human factors in command and control," The technical cooperation program: Subgroup C - Behavioral Sciences, Technical Panel [illegible]-4, April 1979.

12. [illegible] Smith, "Requirements definition and design guidlines for the man-machine interface in $C^3$ system aquisition," Tech. Rep. No. [illegible]-3656, Bedford, Mass., MITRE Corp. December, 1979.

13. D.A. Topmiller, "Man-machine $C^3$ simulation studies in the Air Force," in C.P. Tsokos and R.M. Thrall (Eds.), Decision information, New York: Academic Press, 1979.

14. J.A. Welch, Maj. Gen., "State of the art of $C^2$ assessment," Proc. for quantitative assessment of utility of command and control systems, McLean, Va.: MITRE Corp., January 1980.

15. MITRE, Proc. for quantitative assessment of utility of command and control systems, McLean, Va.: MITRE Corp., January 1980.

16. L. Wittgenstein, Philosophical investigations (Trans. G.E.M. Anscombe), New York: Macmillan, 1953.

17. D.M. Green and J.A. Swets, Signal detection theory and psychophysics, New York: Wiley, 1966.

18. R.E. Pastore and C.J. Scheirer, "Signal detection theory: Considerations for general application," Psych. Bull., Vol. 81, pp.945-958, 1974.

19. Dept. of Defense Directive 5100.30, 2 December 1971.

20. A.B. Yeates, D.J. Shanahan and B.B. Wise, "Defining and measuring $C^2$," Milit. Electronics/Countermeasures, May 1980, p. 40 and June 1980, pp.28-34.

21. D.McNicol, A primer of signal detection theory, London: Allen & Unwin, 1972.

22. R.J. Dorfman and E. Alf, "Maximum likelihood estimation of parameters of signal detection theory - a direct solution," Psychometrika, Vol. 33, pp.117-124, 1968.

23. R.D. Dorfman and E. Alf, "Maximum likelihood estimation of parameters of signal-detection theory and determination of confidence intervals - Rating method data," J. Math. Psych., Vol. 6, pp.487-496, 1969.

24. I. Pollack and W.A. Norman, "A non-parametric analysis of recognition experiments," Psychon. Sci., Vol.1, pp. 125-126, 1964.

25. I. Pollack, W.A. Norman and L. Galanter, "An efficient non-parametric analysis of recognition memory," Psychon. Sci., Vol. 1, pp327-328, 1964.

26. W. Hodos, "Nonparametric index of response bias for use in detection and recognition experiments," Psych. Bull., Vol. 74, pp. 351-354, 1970.

27. J.B. Grier, "Nonparametric indexes for sensitivity and bias: Computing formulas," Psych. Bull., Vol. 75, pp. 424-429, 1971.

28. M.E. Sharkey, "Some determinants of computer-aided decision effectiveness," Proc. of the 80th Ann. Conv. of the Am. Psych. Asso., pp. 697-698,1972.

1980 USAF - SCEEE SUMMER FACULTY RESEARCH PROGRAM

Sponsored by the

AIR FORCE OFFICE OF SCIENTIFIC RESEARCH

Conducted by the

SOUTHEASTERN CENTER FOR ELECTRICAL ENGINEERING EDUCATION

FINAL REPORT

# THE EFFECT OF ROTATION, NOISE AND SIMILITUDE ON IMAGE MOMENTS AND MOMENT INVARIANTS


| | |
|---|---|
| Prepared by: | Dr. David H. Williams |
| Academic Rank: | Assistant Professor |
| Department and University: | Department of Electrical Engineering<br>The University of Texas at El Paso |
| Research Location: | Air Force Weapons Laboratory |
| USAF Research Colleague: | Lt. Col. Carey O'Bryan |
| Date: | August 22, 1980 |
| Contract No.: | F49620-79-C-0038 |

# THE EFFECT OF ROTATION, NOISE AND SIMILITUDE ON IMAGE MOMENTS AND MOMENT INVARIANTS

by

David H. Williams

## ABSTRACT

Previous investigations have described two-dimensional moment invariant functions that are theoretically invariant to object orientation, and therefore useful for computer location and recognition of objects in digital images. In a real system, however, anomalies such as noise, computation errors, and less than perfect resolution of the object are present that would cause these functions not to be totally invariant. The objective of this study was to determine how these functions behave when faced with a limited number of such anomalies. The results indicate that moment invariants are very sensitive to the number and configuration of the object pixels, and to computation error introduced by discrete integration.

## ACKNOWLEDGEMENTS

The author would like to thank the Air Force Systems Command, the Air Force Office of Scientific Research, and the Southeastern Center for Electrical Engineering Education for a very interesting and productive summer at the Air Force Weapons Laboratory, Kirtland AFB, New Mexico. He would also like to thank the personnel of the Beam Control Systems Branch for their assistance and hospitality; with special thanks to Lt. Col. Carey O'Bryan for his help and guidance, and many helpful discussions about this investigation.

## I. INTRODUCTION

Pattern recognition and digital image processing techniques for computer recognition of objects have many applications that are of great significance to the Air Force. One such method, originally described by Hu[1.] in 1962, is that of two dimensional moment invariants. This method is attractive since moment invariant functions which two-dimensionally describe an object can be constructed that are (theoretically) invariant to object size, translation, and rotation. Thus, if the shape of the object does not vary these functions will be independent of its orientation, and may be used to recognize and to determine spatial characteristics of the object, without further processing.

Dudani et al[2.] extended the use of two-dimensional moment invariants to include the recognition of objects in a three dimensional space for aircraft identification. His techniques are currently being implemented in the Navy AUASAM and the Air Force IPAAACS tracking systems. Teague has performed further investigations[3.,4.] to apply moment invariants to automatic image analysis, and for target aimpoint selection, and just recently, the theory of moment invariants has been expanded to include three-dimensional moment invariants.[5.]

Moment invariants are functions constructed from two-dimensional central moments. The $(p + q)$th order two-dimensional (raw) moment is defined as:

$$M_{pq} = \int_{-\infty}^{\infty} \int_{-\infty}^{\infty} X^p Y^q \rho(X,Y) dX dY \qquad (1)$$

where

$p,q = 0,1,2,\text{---}$

$\rho(X,Y)$ = the density distribution of the object.

and

$$\bar{X} = \frac{M_{10}}{M_{00}}$$

$$\bar{Y} = \frac{M_{01}}{M_{00}}$$

$$\overline{XY} = \frac{M_{11}}{M_{00}} \qquad (2)$$

$$\overline{X^2} = \frac{M_{20}}{M_{00}}$$

etc.

Since raw moments are affected by translation, they can be referenced to the object centroid position $\bar{X},\bar{Y}$ to eliminate this variation. This defines the two-dimensional central moments:

$$\mu_{pq} = \int_{-\infty}^{\infty}\int_{-\infty}^{\infty} (X-\bar{X})^p (Y-\bar{Y})^q \rho(X,Y)\,d(X-\bar{X})\,d(Y-\bar{Y}) \qquad (3)$$

From this expression, the polynomials in X and Y can be expanded[3] to relate the central moments, to the raw moments:

$$\mu_{pq} = \sum_{r=0}^{p}\sum_{s=0}^{q} \binom{p}{r}\binom{q}{s}(-\bar{X})^{p-r}(-\bar{Y})^{q-s} M_{pq} \qquad (4)$$

where $\binom{n}{k}$ denotes a binomial coefficient.

Hu[1] has shown that the following combinations of central moments are invariant to rotation, and furthermore, since they are formed from central moments, they are also invariant to translation:

$$M_1 = (\mu_{20} + \mu_{02})$$

$$M_2 = (\mu_{20} - \mu_{02})^2 + 4\,\mu_{11}^2$$

$$M_3 = (\mu_{30} - 3\mu_{12})^2 + (3\mu_{21} - \mu_{03})^2$$

$$M_4 = (\mu_{30} + \mu_{12})^2 + (\mu_{21} + \mu_{03})^2$$

$$\begin{aligned} M_5 = {} & (\mu_{30} - 3\mu_{12})\,(\mu_{30} + \mu_{12}) \\ & \cdot \left[(\mu_{30} + \mu_{12})^2 - 3\,(\mu_{21} + \mu_{03})^2\right] \\ & + (3\mu_{21} - \mu_{03})\,(\mu_{21} + \mu_{03}) \\ & \cdot \left[3(\mu_{30} + \mu_{12})^2 - (\mu_{21} + \mu_{03})^2\right] \end{aligned} \tag{5}$$

$$\begin{aligned} M_6 = {} & (\mu_{20} - \mu_{02}) \left[(\mu_{30} + \mu_{12})^2 - (\mu_{21} + \mu_{03})^2\right] \\ & + 4\mu_{11}(\mu_{30} + \mu_{12})\,(\mu_{21} + \mu_{03}) \end{aligned}$$

$$\begin{aligned} M_7 = {} & (3\mu_{21} - \mu_{03})\,(\mu_{30} + \mu_{12}) \\ & \cdot \left[(\mu_{30} + \mu_{12})^2 - 3(\mu_{21} + \mu_{03})^2\right] \\ & - (\mu_{30} - 3\mu_{12})\,(\mu_{21} + \mu_{03}) \\ & \cdot \left[3(\mu_{30} + \mu_{12})^2 - (\mu_{21} + \mu_{03})^2\right] \end{aligned}$$

$M_7$ is invariant in magnitude only, and changes sign under reflection when a mirror image occurs.

Central moments can also be made invariant to similitude (size) changes. Given the transformation in scale:

$$X' = \alpha X$$
$$Y' = \alpha Y \tag{6}$$

where $\alpha$ is a constant scale factor, the following expression[1] relates the change in the central moments due to the variation in scale:

$$\mu'_{pq} = \alpha^{p+q+2} \mu_{pq} \tag{7}$$

The new value, $\mu'_{pq}$, can then be rescaled back to the original value, $\mu_{pq}$, by dividing by $\alpha$ raised to the proper power. Note that if $\alpha$ is known it can be used directly, or can be determined by taking the ratio:

$$\alpha = \left(\frac{\mu'_{00}}{\mu_{00}}\right)^{\frac{1}{2}} \tag{8}$$

Using these values, the central moments can be calculated and compensated for variations in similitude. The compensated central moments are then used to calculate the moment invariants which are invariant to changes in similitude, rotation and translation.

Dudani[2] described an alternate approach to compensate the moment invariants for variations in similitude. A radius of gyration,

$$r = \left(\mu_{20} + \mu_{02}\right)^{\frac{1}{2}} \tag{9}$$

and B, the distance along the optical axis are calculated and used to normalize the moment invariants as follows:

$$
\begin{aligned}
M_1' &= r \cdot B = M_1^{\frac{1}{2}} \cdot B \\
M_2' &= M_2 / r^4 \\
M_3' &= M_3 / r^6 \\
M_4' &= M_4 / r^6 \\
M_5' &= M_5 / r^{12} \\
M_6' &= M_6 / r^8 \\
M_7' &= M_7 / r^{12}
\end{aligned}
\tag{10}
$$

Applying this method, the central moments are calculated as usual to form the moment invariants. The moment invariants are then normalized to compensate for variations in similitude.

## II. OBJECTIVES

In the previous section, functions were described that are theoretically invariant to similitude, rotation, and translation. In a real system, however, anomalies are present that would cause these functions not to be totally invariant. Two such problems are the presence of noise, and less than perfect resolution of the object. Imaging devices inject noise into the signal during image formation and transmission, and the formation of a digital image involves the mapping of the intensity values of an object onto an integer coordinate

plane with less than perfect resolution. Also, roundoff errors, and errors in computation are present. Since the defining papers[1-5] do not address these issues, the main purpose of this investigation was to determine how these functions behave under these circumstances. It appeared likely that some moment invariants would be more sensitive to these anomalies than others, and therefore would be less useful for object location and identification.

To support this investigation, both general and special purpose digital image processing software was developed. For brevity, however, and since this software is installation dependent, only the general processing methods are discussed.

## III. The Effect of Noise on Moments and Moment Invariants

In order to determine the effect of noise on moments, and moment invariants, the image shown in Figure 1 was processed. (This image was originally generated by Michael Teague for other applications.) Each background pixel (picture element) in the image has an intensity value of zero, and each object pixel has the value of 80. To determine the effect of noise on the moment invariants, the object was rotated in 90 degree increments, after which uniformly distributed random noise with a zero mean was added to the object. No noise was added to the background pixels, since in practice, the image is normally thresholded to separate the object from the background. The noise was added in 5% increments, in a range from 0 to 25%, relative to the intensity range of the image. (As an example, noise uniformly distributed between -4 and +4 is specified as 10%.)

The effect of noise on the zeroth through second order moments is shown in Figure 2, and tabulated in Table I. The moments are specified only for the unrotated object, since these values vary with rotation. $M_{00}$ decreased with increasing values of noise, indicating that the noise did not have a zero mean as expected. (With a zero mean, $M_{00}$ would tend to vary randomly around the zero noise value.)

The other moment values decreased slightly with increasing noise, with the largest variation of .767% given by $M_{02}$. These results indicate that noise alone does not significantly change the moment values. The central moments exhibited similar variations, and are not shown separately.

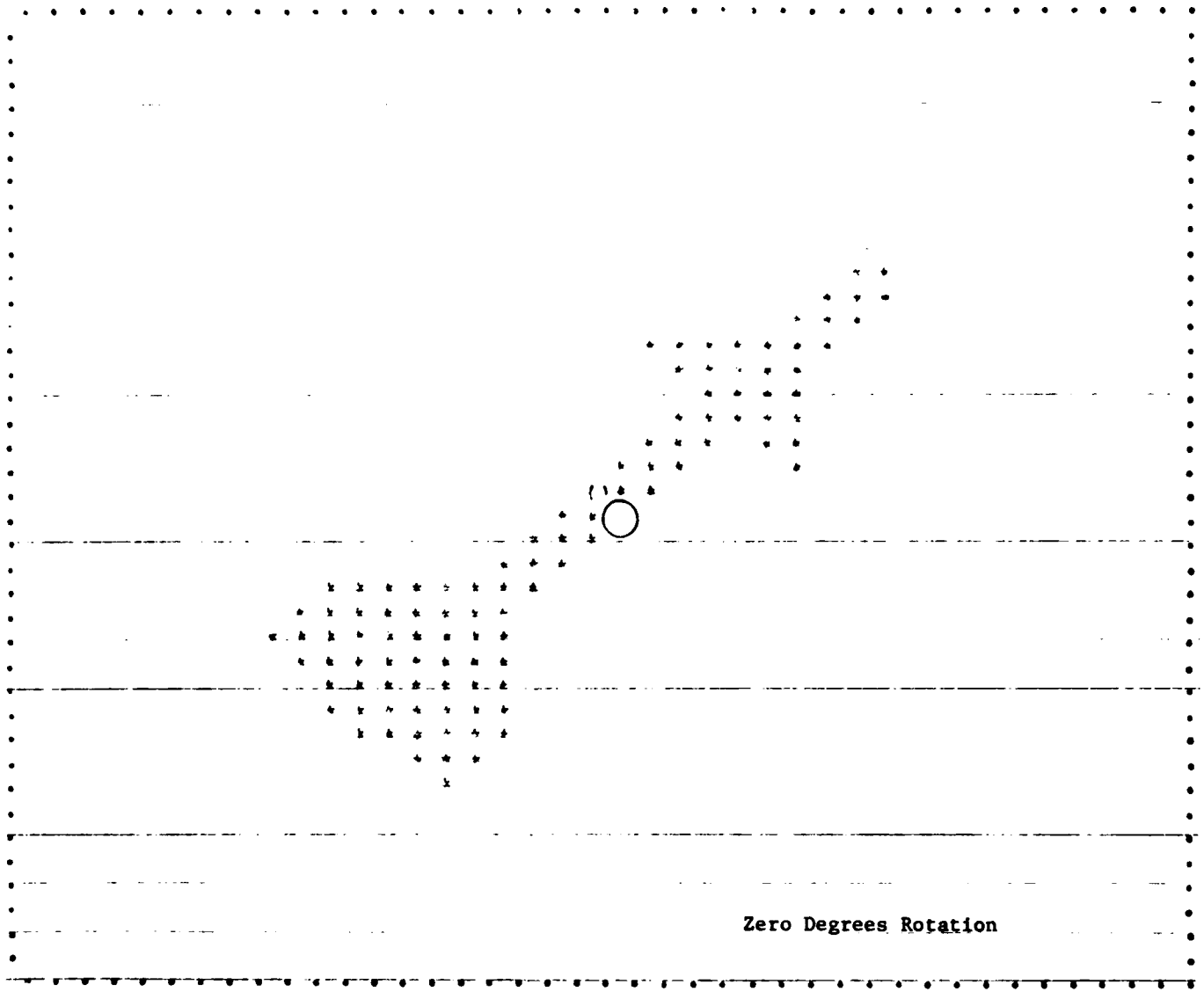



Figure 1. Test Image for Rotation with Noise. (Missing Pixel is circled.)

Figure 2a) Response of Zeroth Order Moment to Noise

Figure 2b) Response of First Order Momenta to Noise

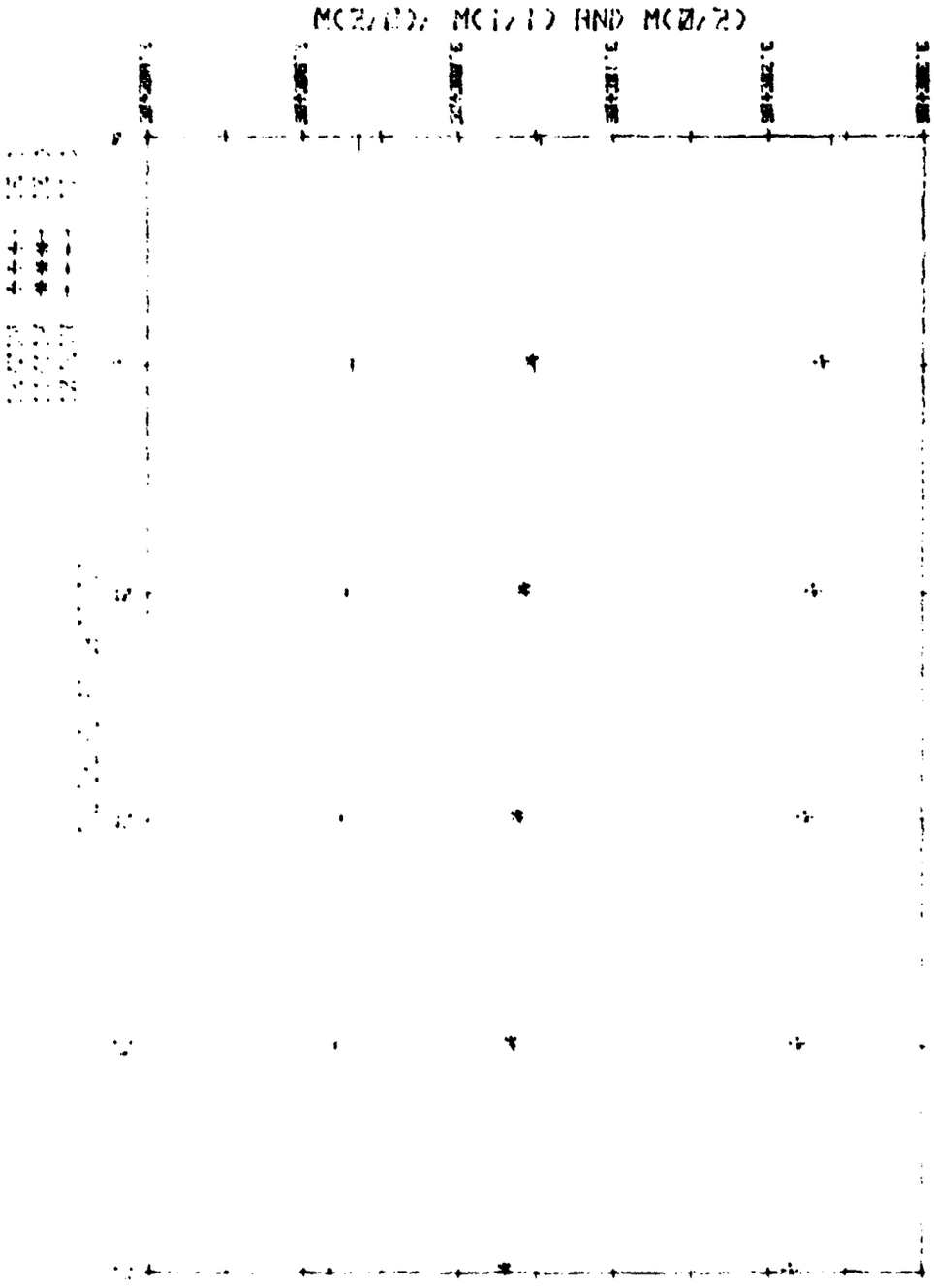


Figure 2c) Response of Second Order Moments to Noise

| | Maximum Error (%) |
|---|---|
| $M_{00}$ | .412 |
| $M_{10}$ | .506 |
| $M_{01}$ | .565 |
| $M_{20}$ | .644 |
| $M_{11}$ | .708 |
| $M_{02}$ | .767 |

Table I. Maximum Error of Raw Moments Due to Noise

The effect of rotation with noise on the moment invariant functions is shown in Figure 3, and tabulated in Table II. For zero noise, each invariant (except $M_7$) intercepts the M axis at two locations, once for zero and 180 degrees of rotation and once for 90 and 270 degrees of rotation. This resulted from the object having one less pixel in the former two cases, a situation that is common in real data. The lower moments, exhibited minimum change between intercepts, while excluding $M_7$, $M_5$ exhibited the largest error with a variation of 8%. The maximum effect of noise, defined as the maximum error between the zero noise value and another noise value at the same rotation was also given by $M_5$ and was 5.9%.

The maximum error caused by both the difference in the number of pixels, and the addition of noise is given by the maximum difference between the zero noise value at zero degrees rotation, and any other value. These values are also tabulated in Table II. The error from both sources are not additive and partially cancel each other. The maximum error (exclusive of $M_7$) is again exhibited by $M_5$, however, with a value of 9.2%.

$M_7$, exhibited anomalous behavior in every respect. For the zero noise case, there were four intercepts with the $M_7$ axis:

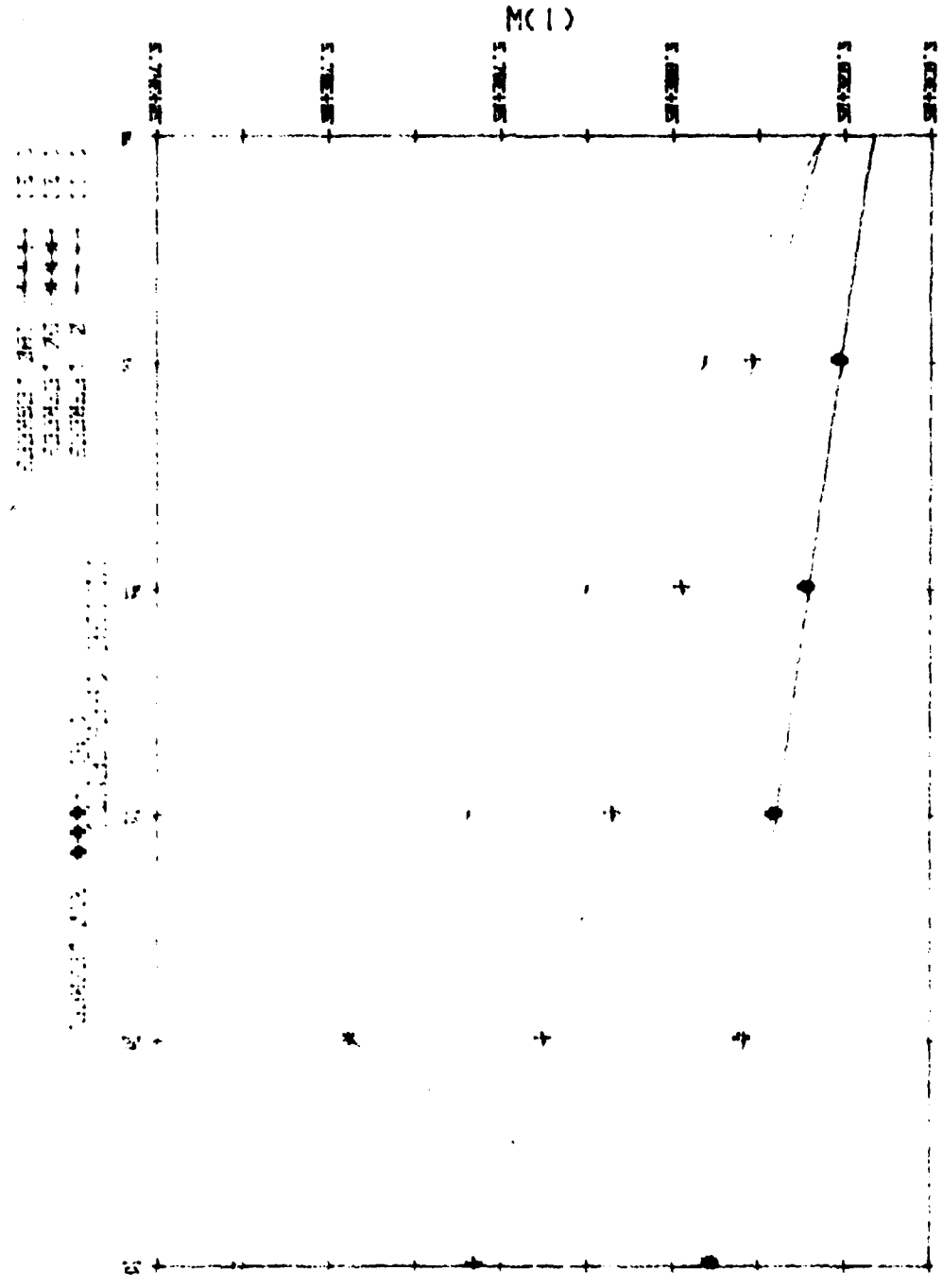



Figure 3a) $M_1$ as a Function of Noise and Rotation

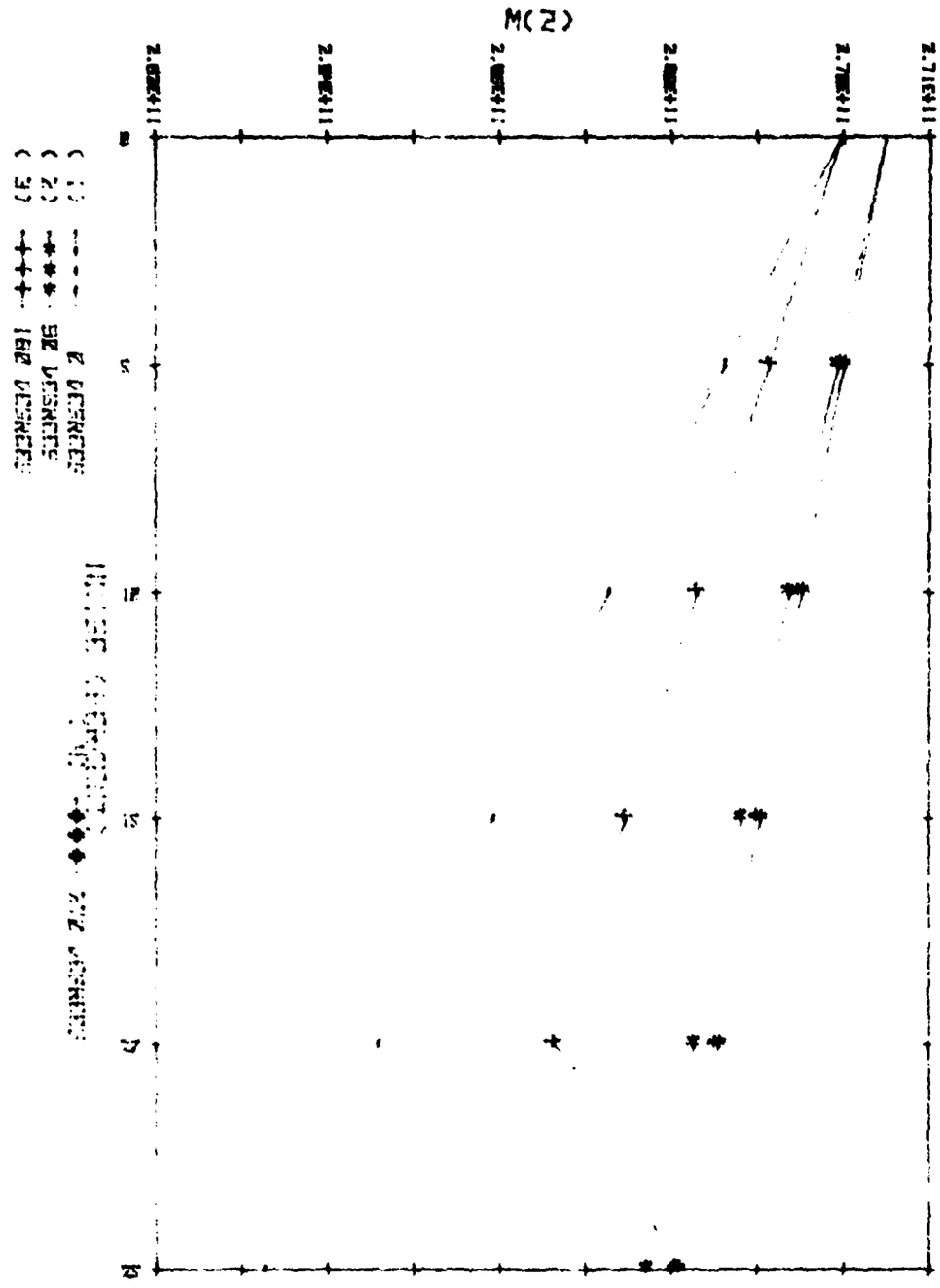



Figure 3b) $M_2$ as a Function of Noise and Rotation

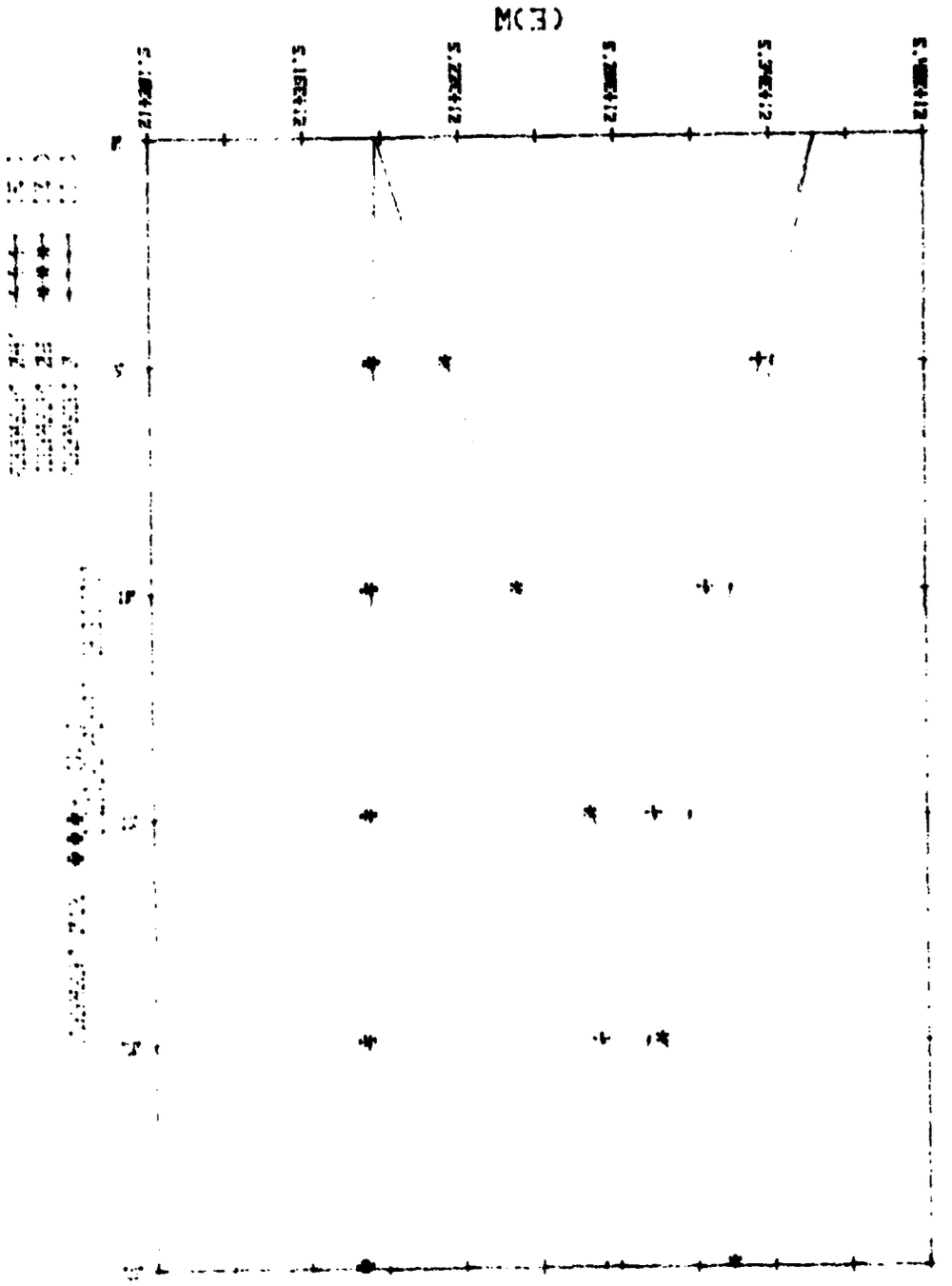



Figure 3c) $M_3$ as a Function of Noise and Rotation

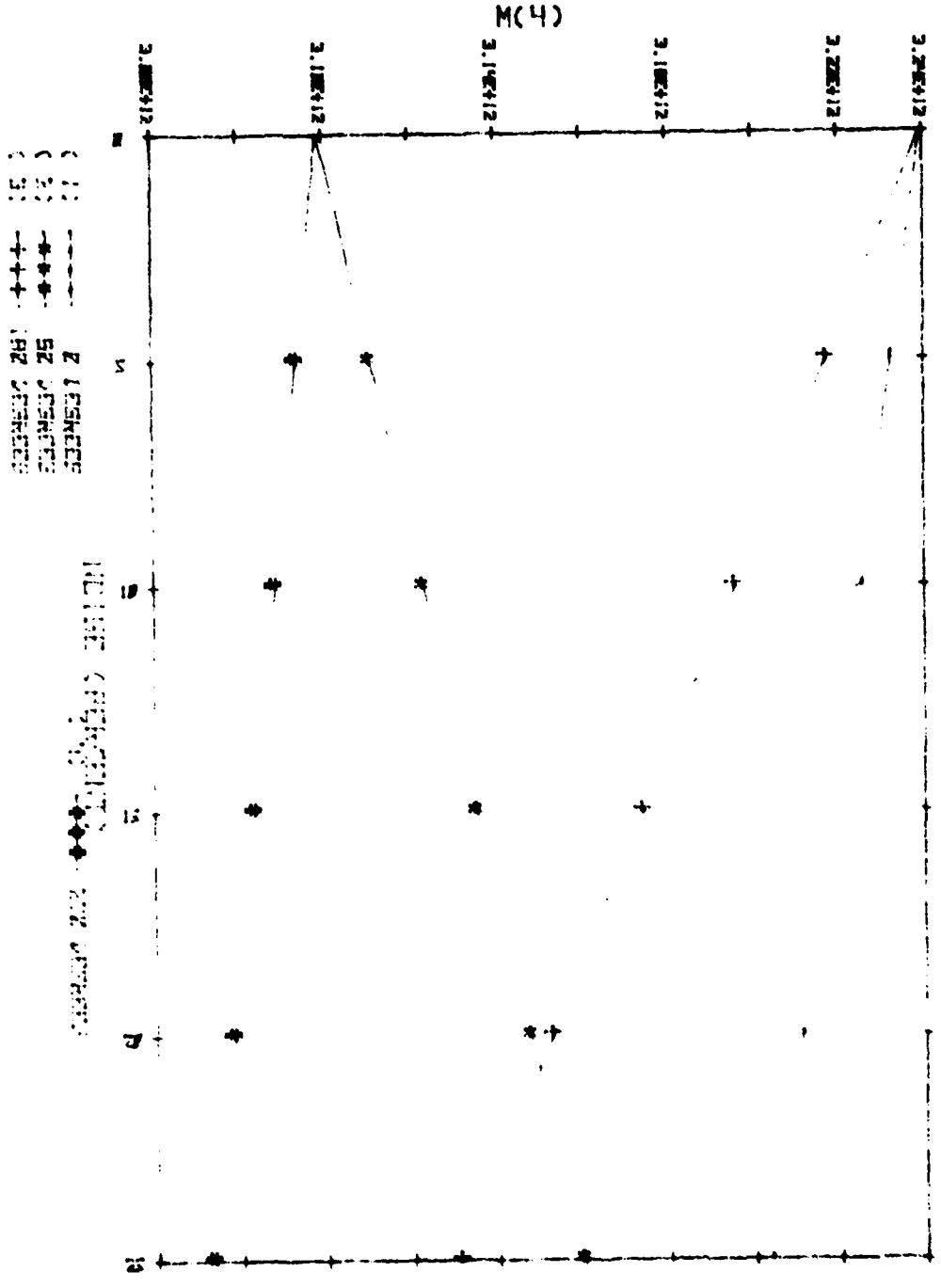



Figure 3d) $M_4$ as a Function of Noise and Rotation

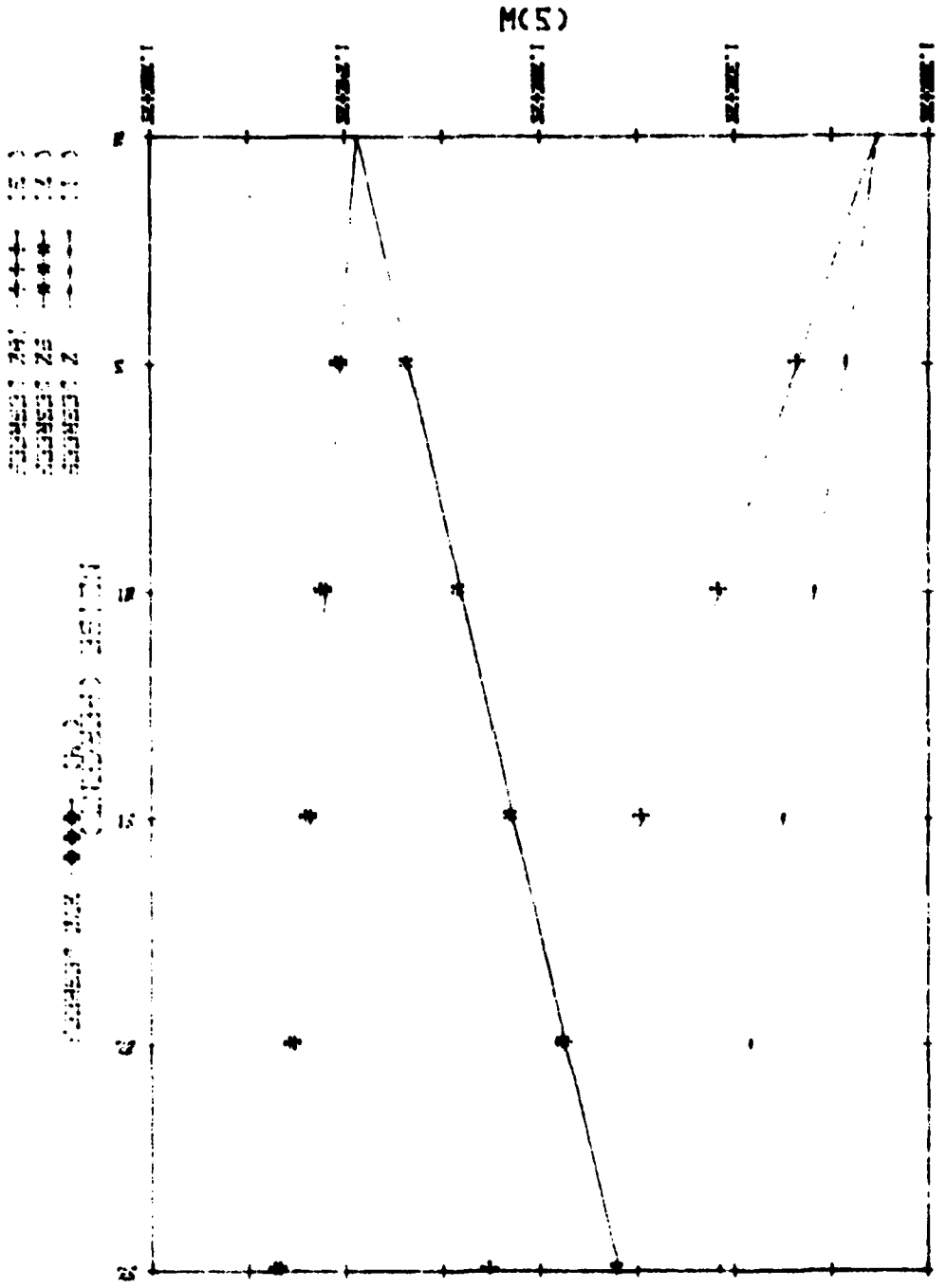



Figure 3e) $M_5$ as a Function of Noise and Rotation

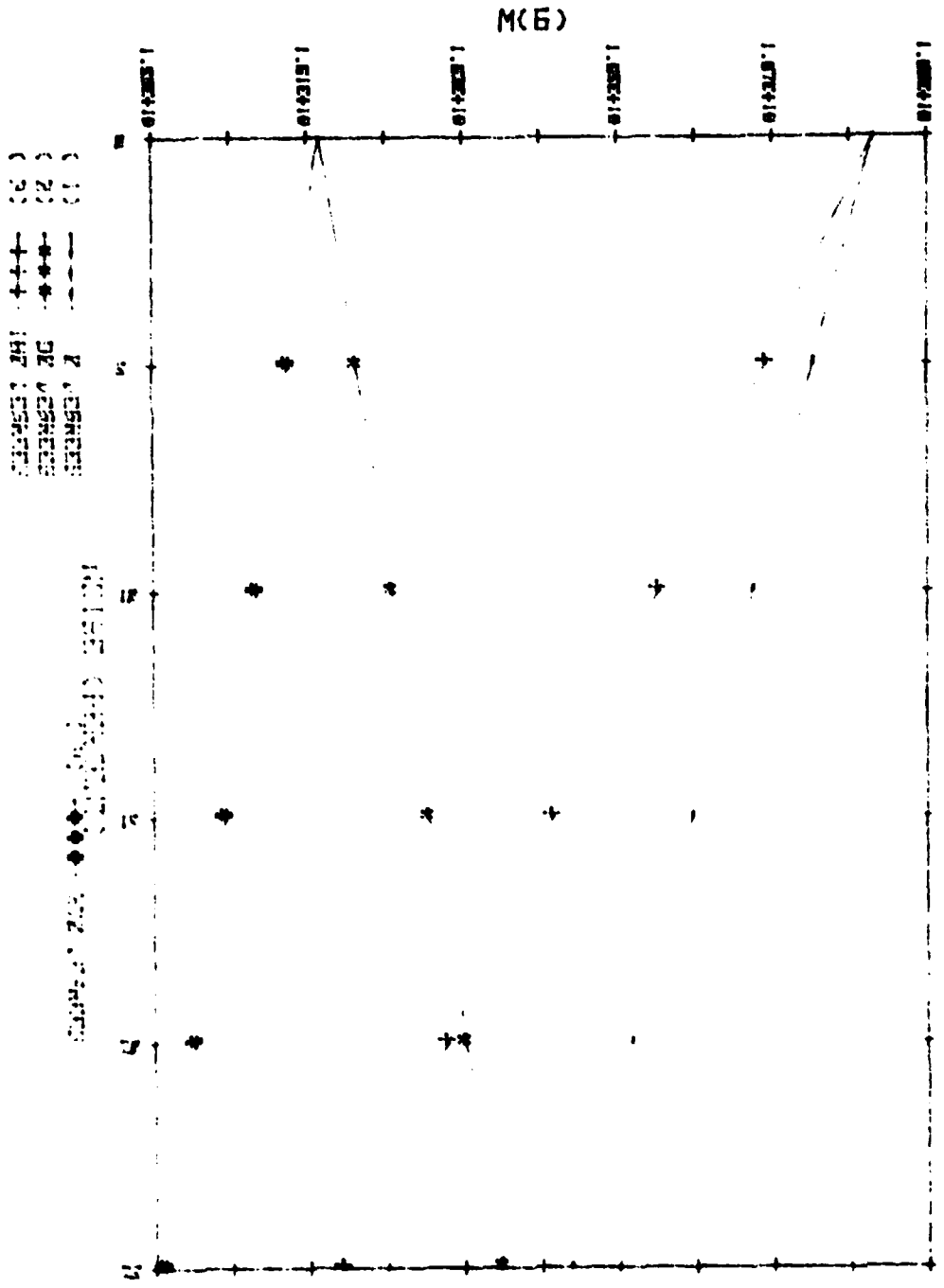



Figure 3f) $M_6$ as a Function of Noise and Rotation

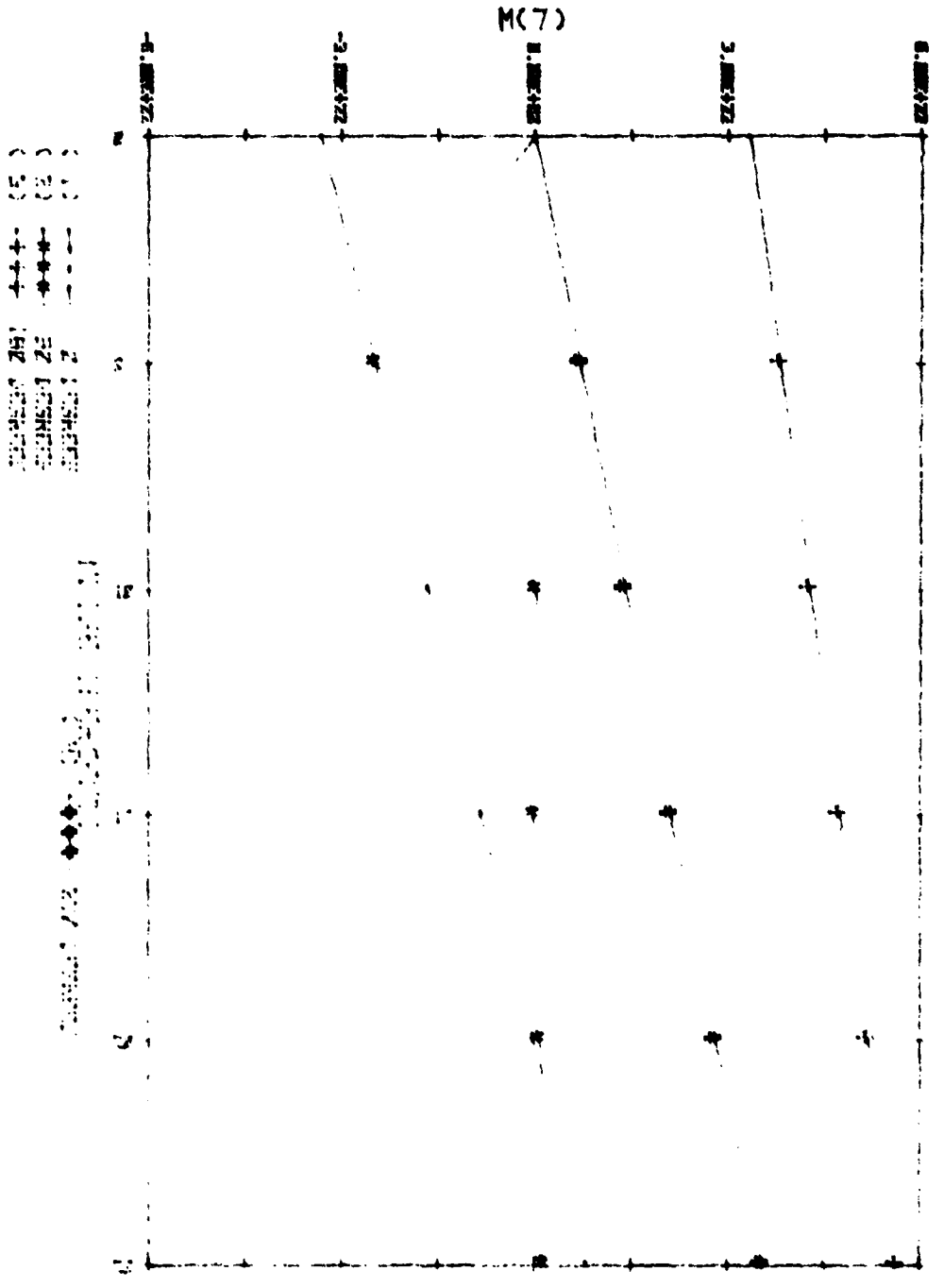



Figure 3g) $M_7$ as a Function of Noise and Rotation

$\pm$ .33($10^{23}$), -.62 ($10^{12}$) and -.20 ($10^{13}$).

These values illustrate that $M_7$ is very sensitive during rotation, even without noise.

What causes this large variation? There appears to be two possible causes. First, is the change in the number of pixels during rotation, which may explain the large variation where no noise was present.

| | Maximum Pixel Error (%) | Maximum Noise Error (%) | Maximum Combined Noise and Pixel Error (%) |
|---|---|---|---|
| $M_1$ | .08 | 1.1 | 1.1 |
| $M_2$ | .10 | 3.3 | 3.3 |
| $M_3$ | 3.17 | 1.4 | 3.1 |
| $M_4$ | 4.30 | 3.7 | 5.2 |
| $M_5$ | 8.00 | 5.9 | 9.2 |
| $M_6$ | 4.10 | 3.8 | 5.4 |
| $M_7$ | —— | —— | —— |

Table II The Effect of Noise and Pixel Error on the Moment Invariants

A second cause appears to be that of integration error. For these calculations, a modified form of the rectangular rule was employed. This is the same method that is employed by the AUASAM system. This technique forms the exact integration only for $M_{00}$, and has increasing error for higher order central moments. Since $M_7$ is dependent on the higher order central moments, it is possible that the error for these values do not cancel, contributing to the large variation.

In conclusion, it was found that the raw and central moments did not vary significantly with noise. The moment invariants did vary, however, due to noise, the number of pixels, and perhaps due to integration error. $M_5$ and $M_7$ exhibited the greatest sensitivity due to these causes, and do not appear to be useful for invariant functions in real systems.

## IV. THE EFFECT OF SIMILITUDE ON MOMENT INVARIANTS

The test images shown in Figure 4 were processed to determine how changes in object size affected the moment invariants. First, the data picture with a scale factor of one was formed and used to generate the other images via a reduction in scale. Note that even though the reduced images are formed from the same master copy, they are not "exact" reproductions. Furthermore, as the scale factor is reduced, (i.e., .2) the resolution of the object is diminished.

Three computation methods were tested to determine their effect in compensating for changes in similitude. The moment invariants that were calculated using these methods were compared against the uncompensated values as shown in Figure 5. (For some invariants, the values were normalized so that the different techniques could be compared on the same graph). No noise was added during the processing.

The first method, denoted as Dudani in Figure 5, used the radius of gyration, r, and the distance, along the optical axis, B (calculated as $B = 1/SF$ where SF is the image scale factor), to normalize the image invariants, as specified in equations 9 and 10. The second method, denoted as Hu SF, employed the value $\alpha = SF$ for the calculations given in equation 7. For the last method, denoted as Hu SQRT in Figure 5, $\alpha$ was formed from the square root of the ratio of the zeroth order moments as shown in equation 8.

The results show that none of the methods performed well, although all of the compensation methods gave more uniform results than the uncompensated values. Because of the large variations, no error analysis was performed. $M_2$ calculated using Dudani's method was the only quantity that was invariant. In general, the Hu SF method exhibited the best results for $M_1$ and $M_3$, and Dudani's method gave the most uniform results for $M_2$ and $M_4$ through $M_6$.

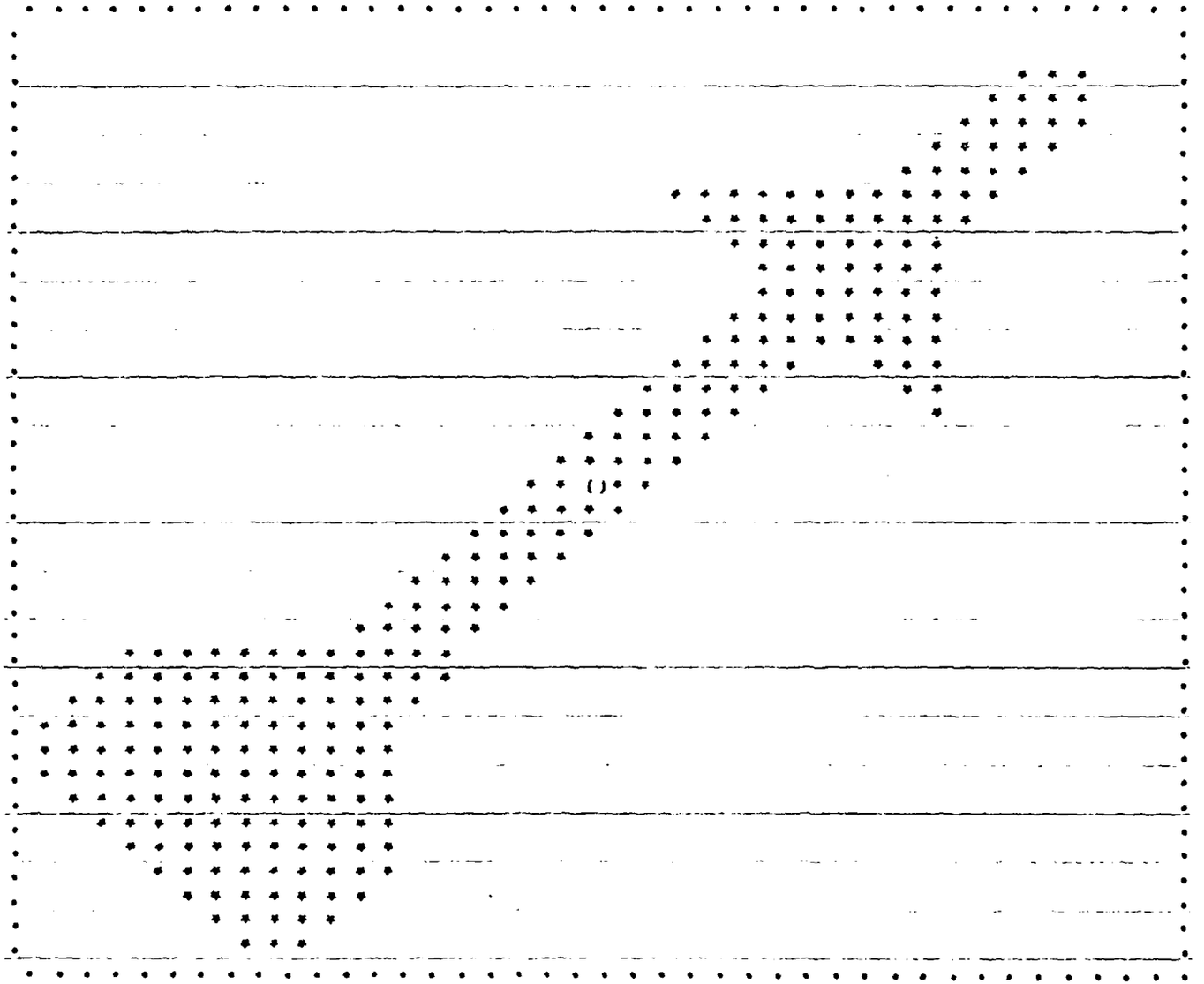


Figure 4a) Similitude Test Image, Scale Factor (SF) = 1

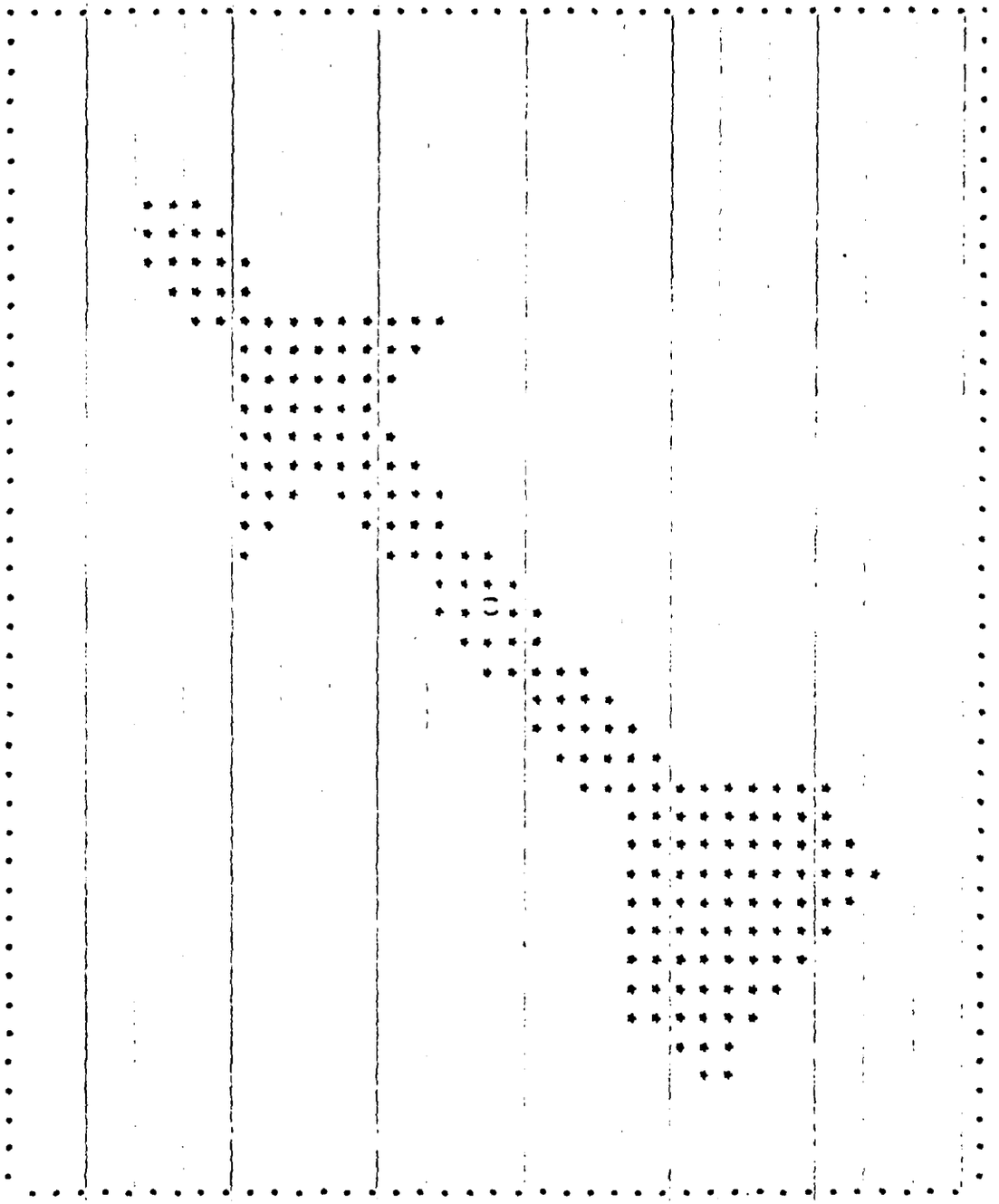


Figure 4b) Similitude Test Image SF = .8

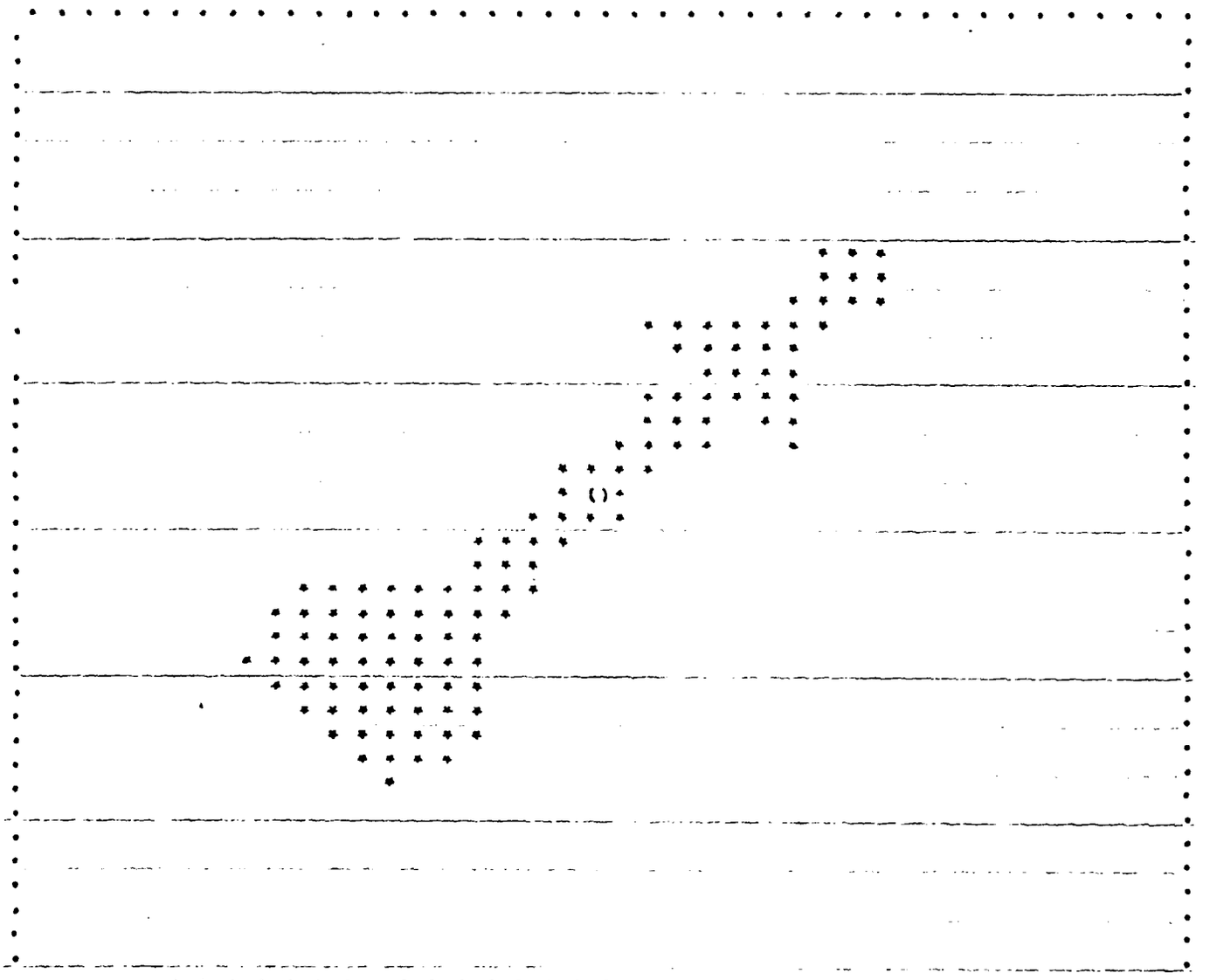


Figure 4c) Similitude Test Image, SF = .6

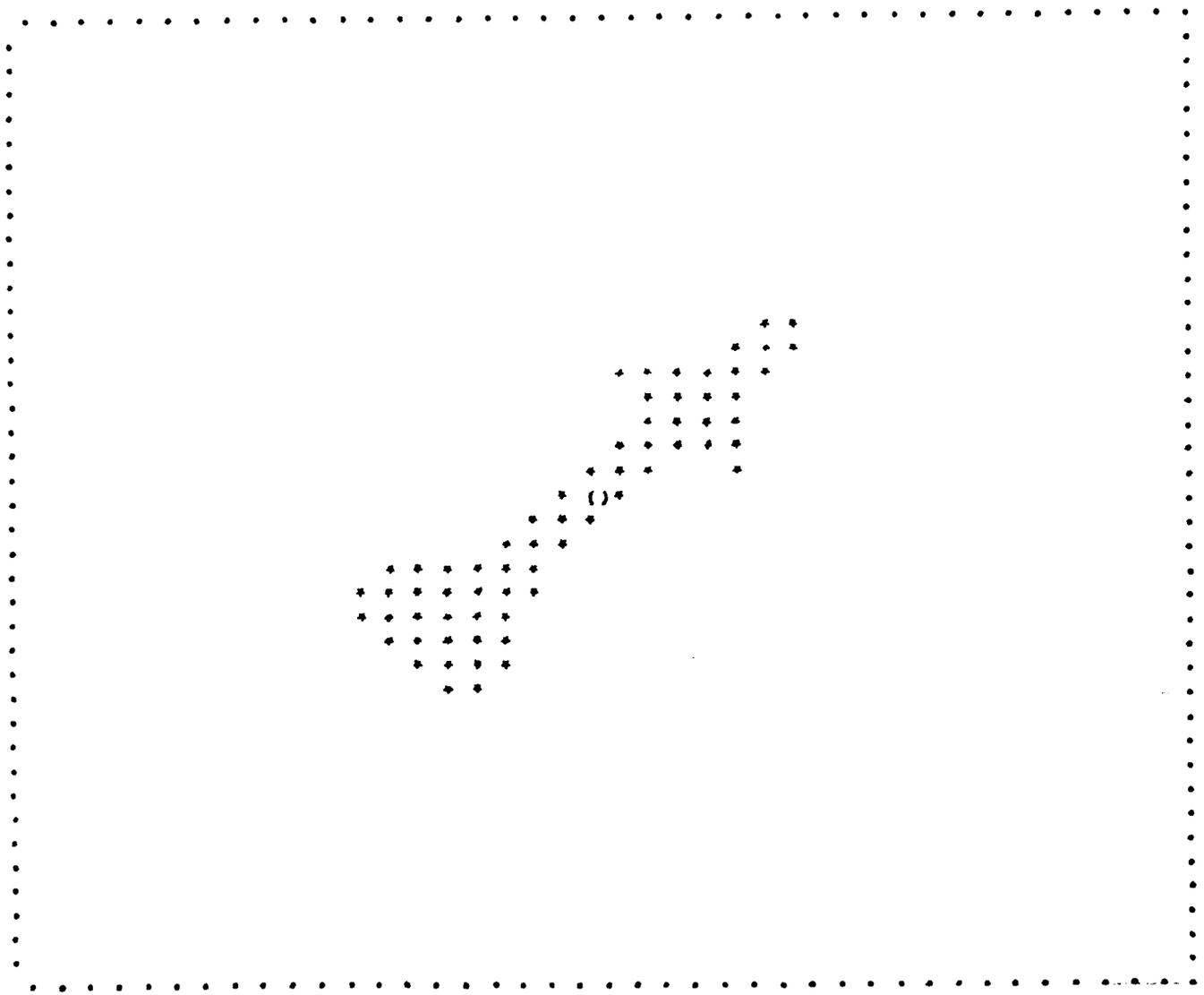


Figure 4d) Similitude Test Image SF = .4

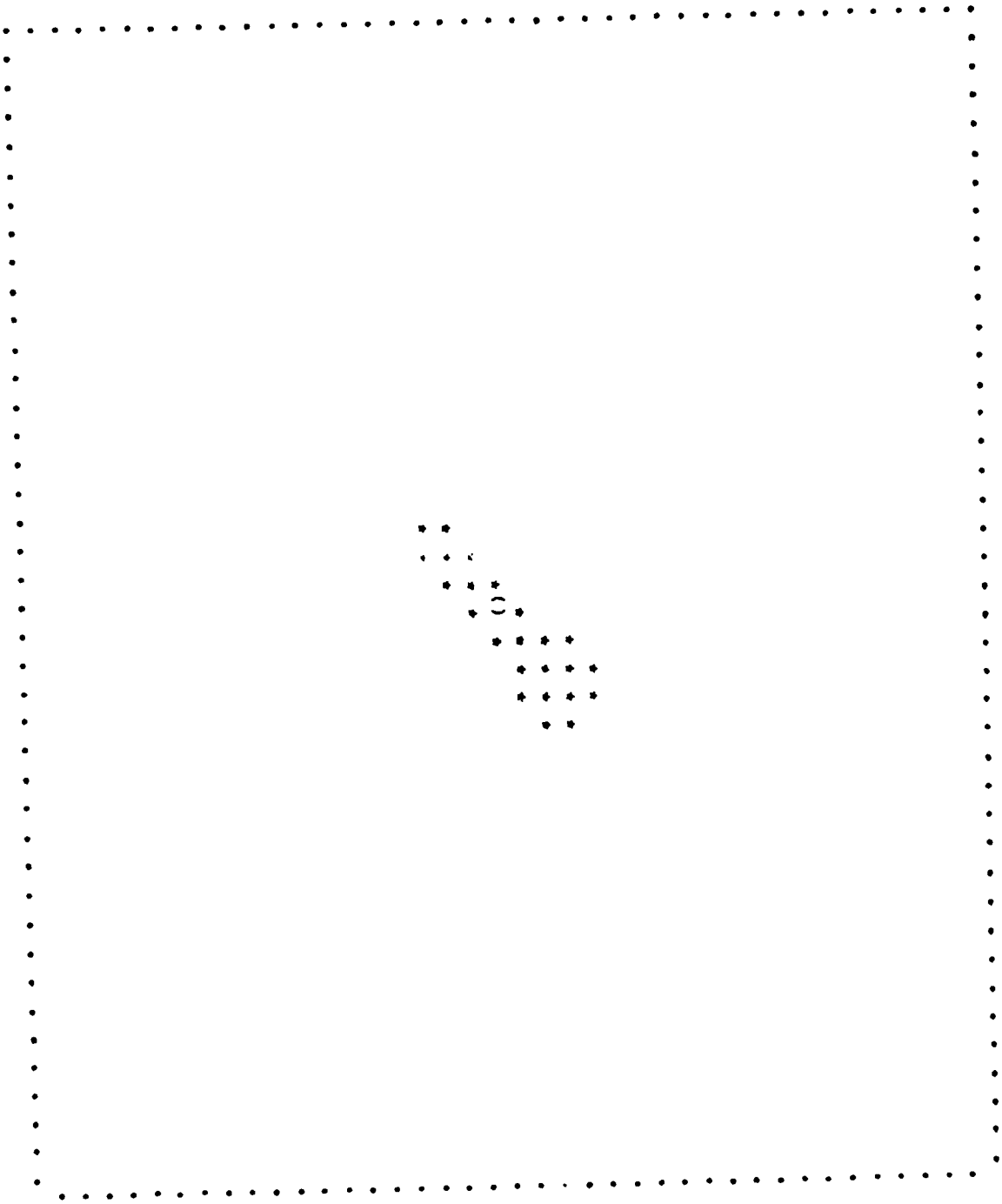


Figure 4e) Similitude Test Image SF = .2

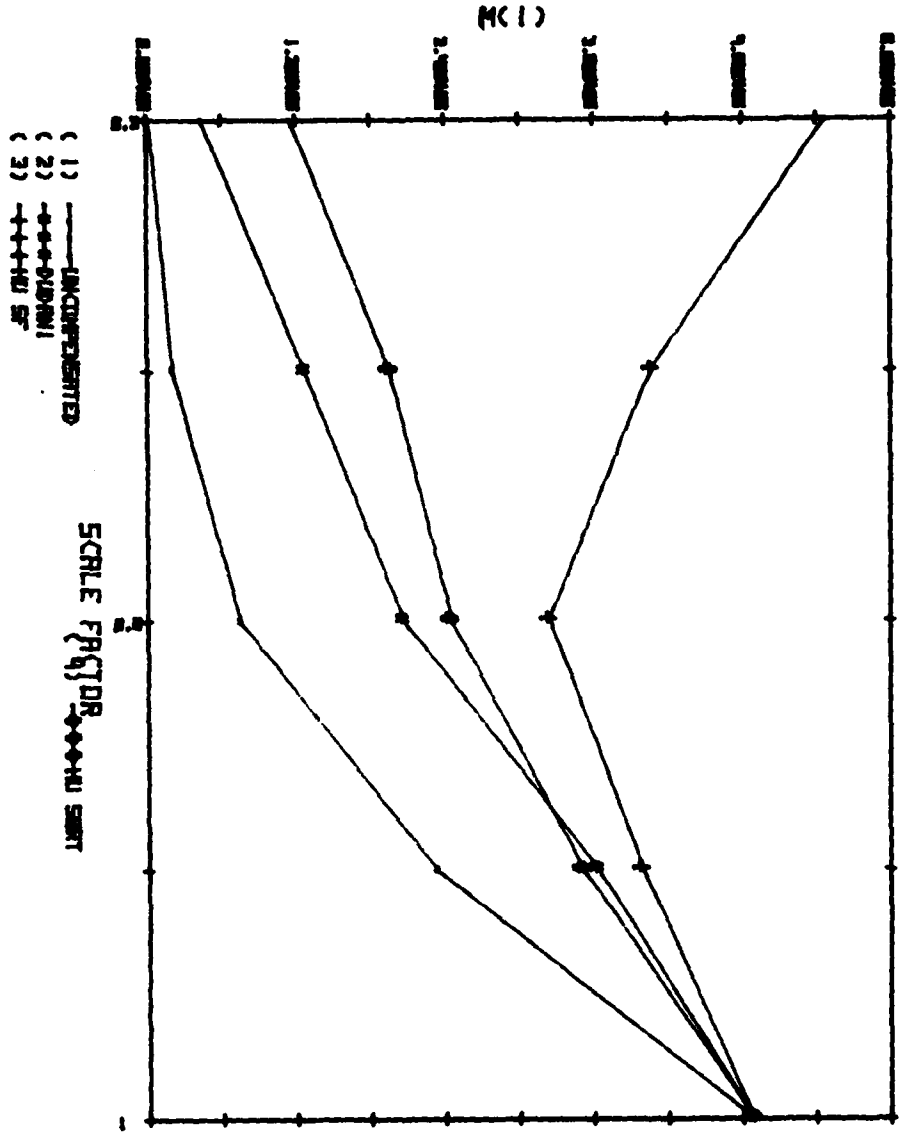



Figure 5a) $M_1$ as a Function of Similitude

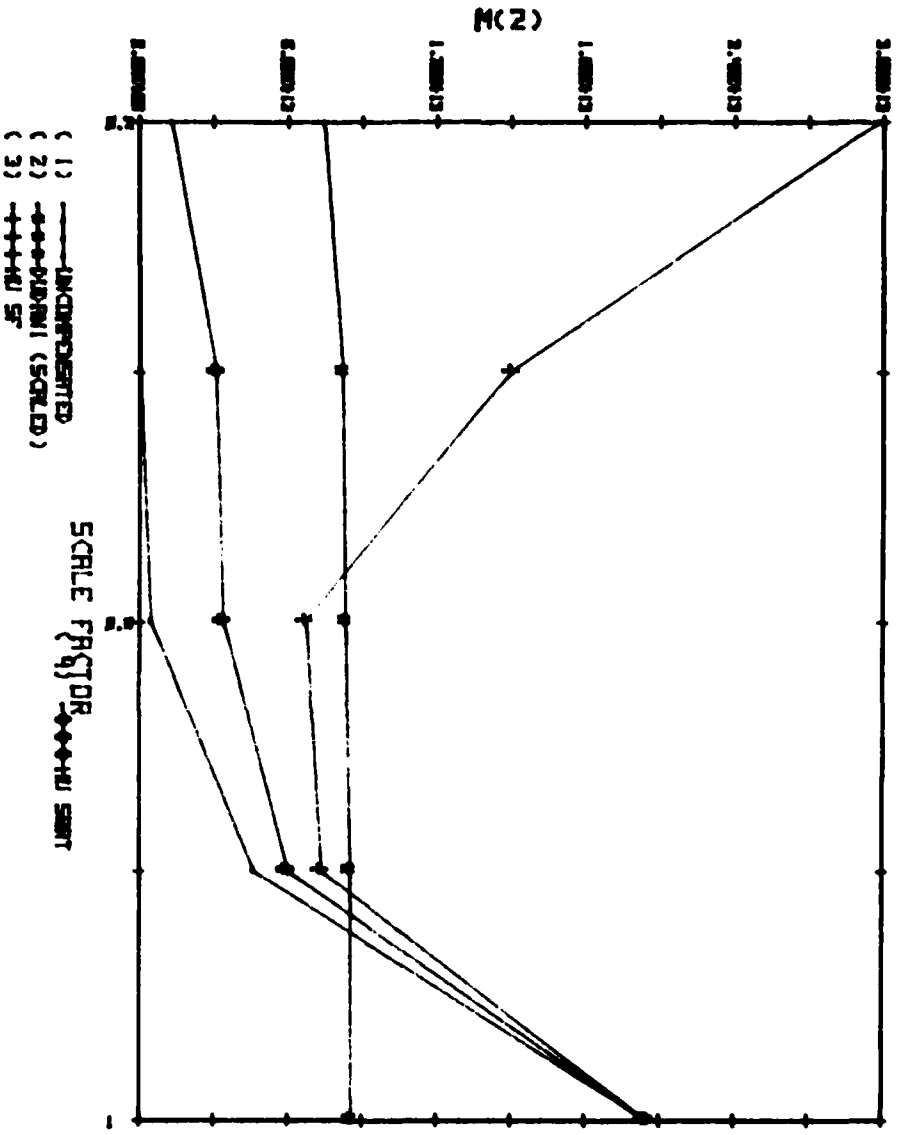



Figure 5b) $M_2$ as a Function of Similitude

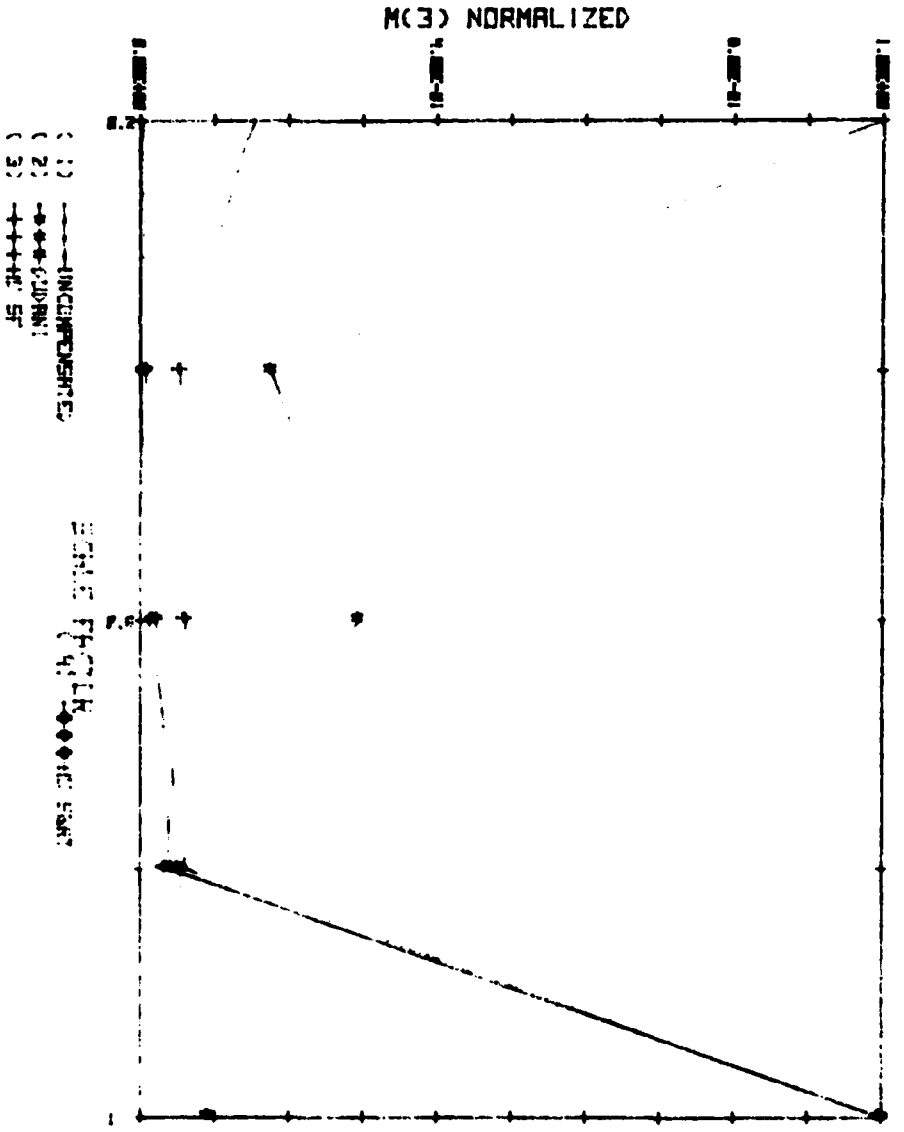



Figure 5c) $M_3$ as a Function of Similitude

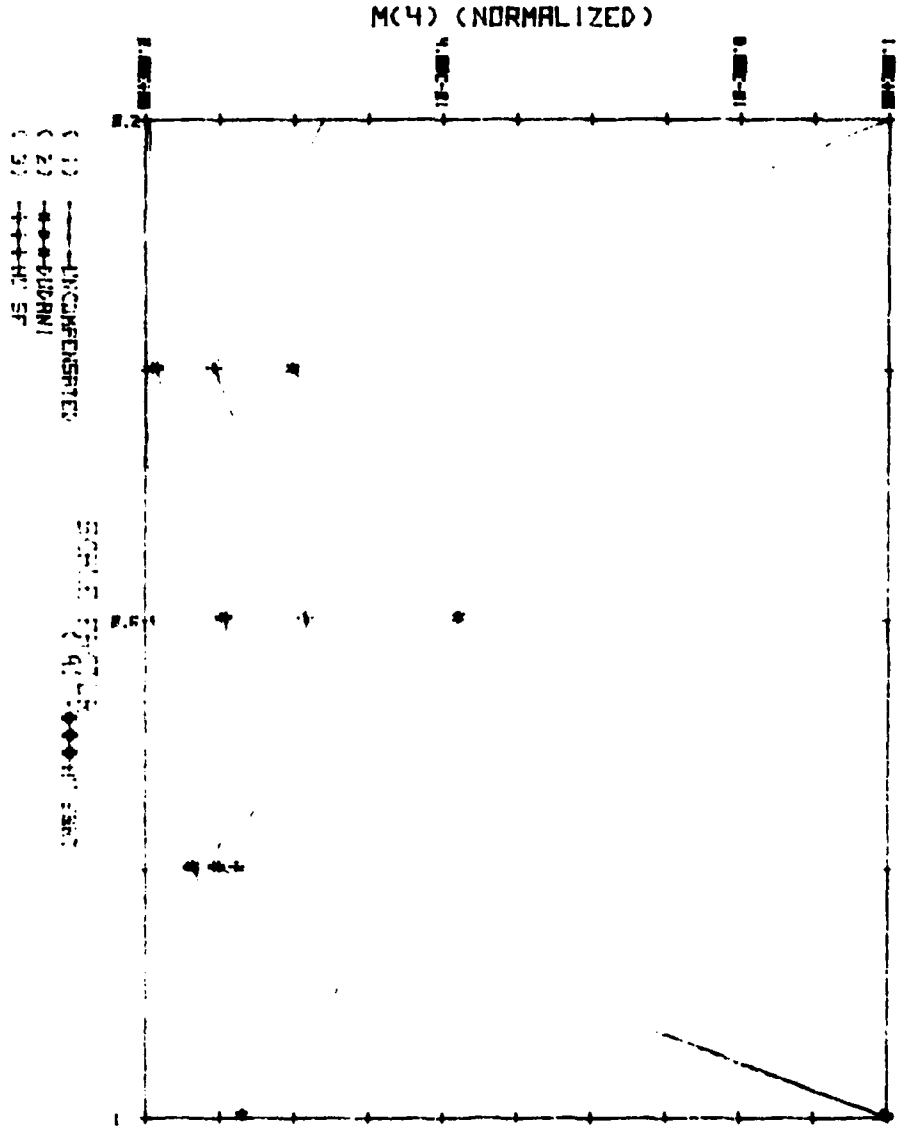



Figure 5d) $M_4$ as a Function of Similitude

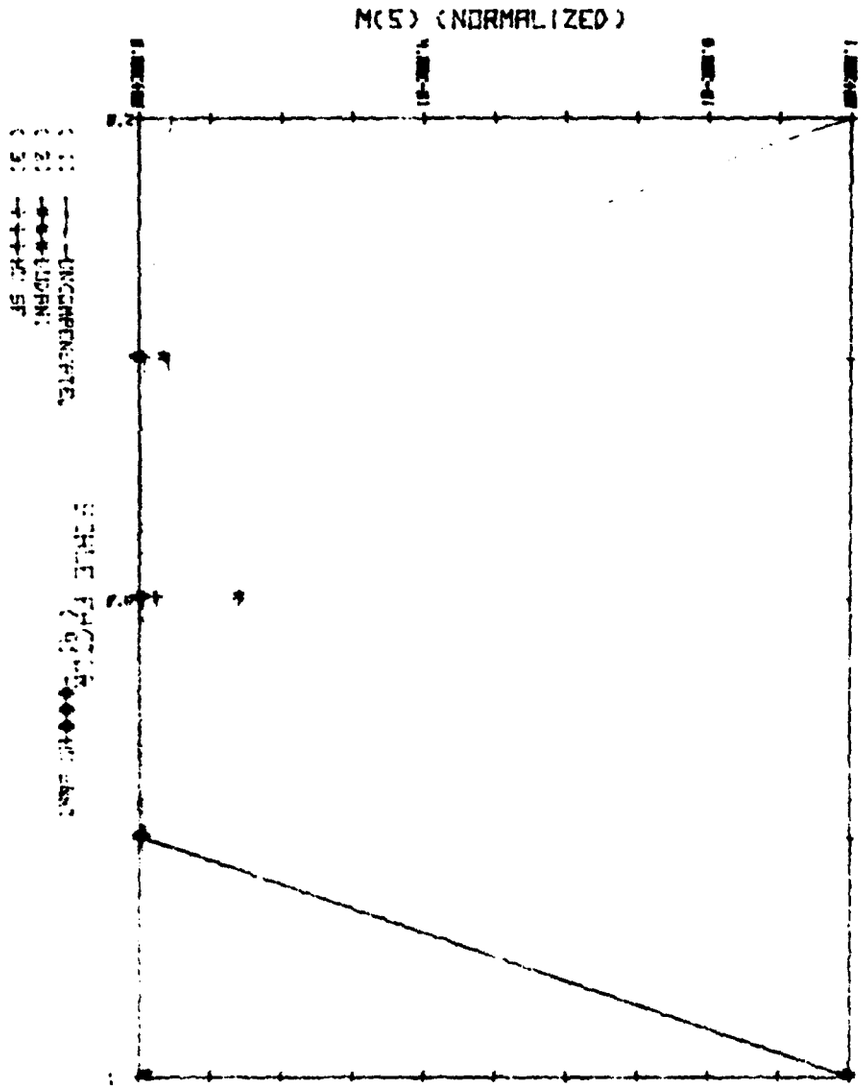



Figure 5e) $M_5$ as a Function of Similitude

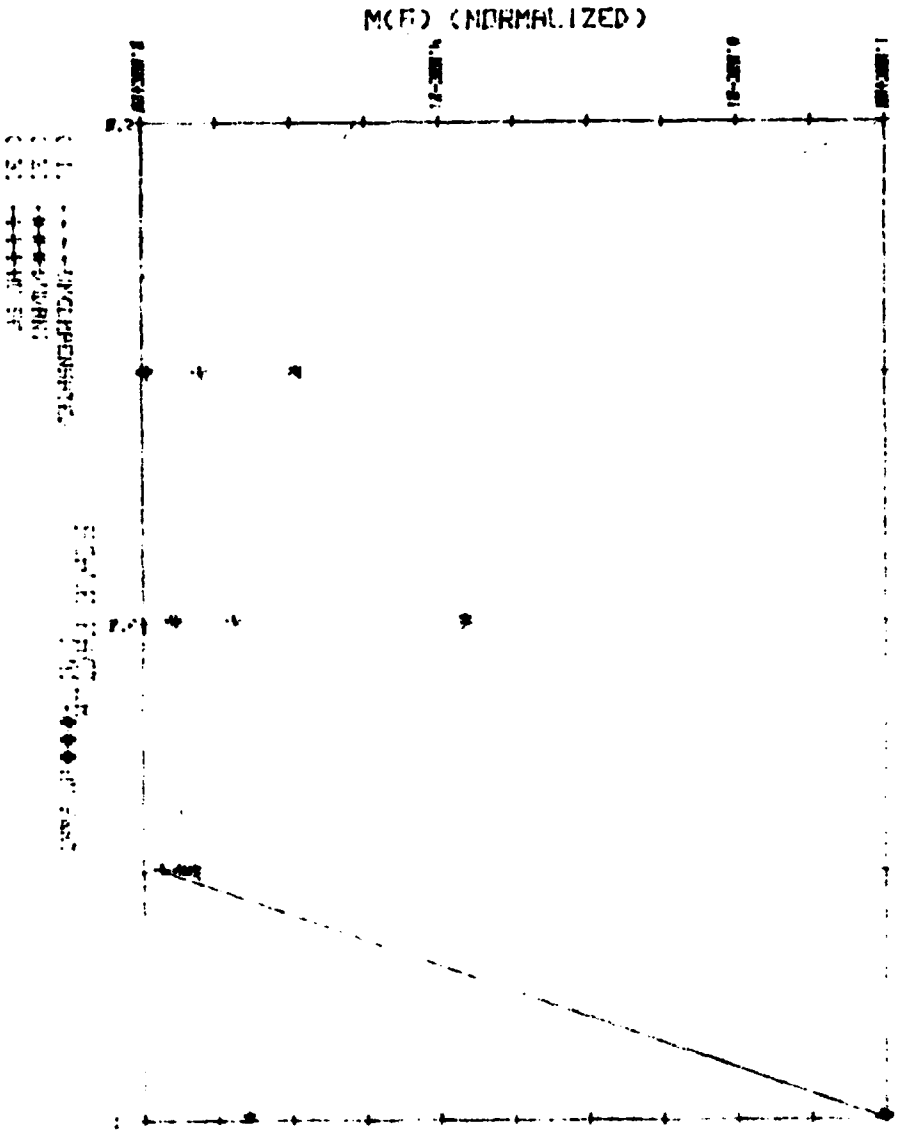



Figure 5f) $M_6$ as a Function of Similitude

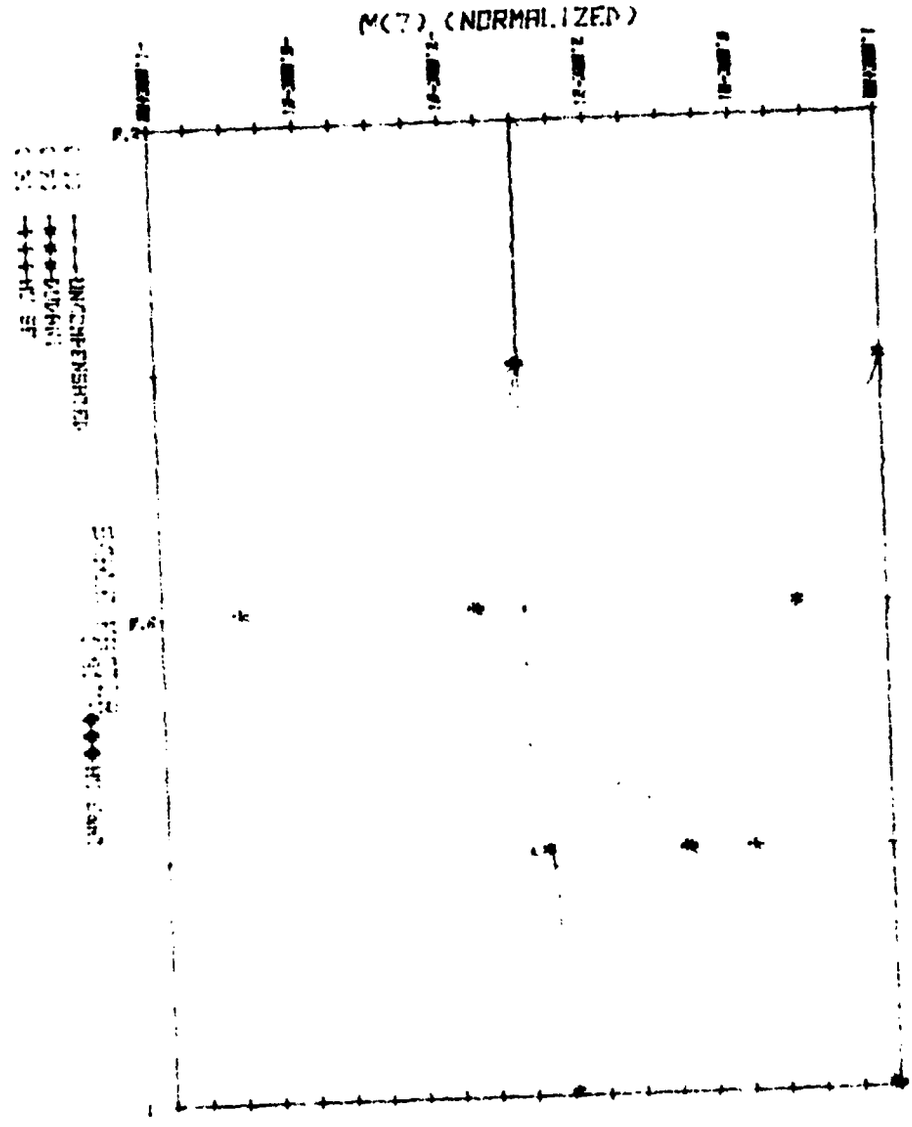



Figure 5g) $M_7$ as a Function of Similitude

One reason that the compensated values were not invariant was the lack of correspondence between the object dimensions, as modified by the scale factor, and the object area. If an object is reduced by a scale factor of .8, with infinite coordinate resolution, the number of pixels which specify the object area are reduced by .64. This cannot occur exactly with a digital image, however, because the object coordinates are mapped onto an integer valued coordinate plane. For the test image, reduction of the object by SF = .8 caused a reduction in area of only .70. (This value can be readily determined from $\mu_{00}$). As a result, the ratio of the zeroth moments, and the radius of gyration do not map into a straight line from .2 to 1. as shown in Figure 6, and therefore cannot exactly compensate for the variation in similitude.

As shown in Figure 5g), $M_7$ again exhibited anomalous behavior during these processes, including both under and over compensation by the same method. It is not known whether this was caused by the previous problem, or by computation errors that result from the error in integration. Since $M_7$ contains the largest number of higher order central moments however, it seems likely that the latter is the cause.

These results again illustrate that the moment invariants, and invariant processing methods appear to be very sensitive to the number of object pixels, and perhaps also to computation errors introduced during integration. The effect of diminished resolution was not observed in the results, because of the large changes introduced by these problems.

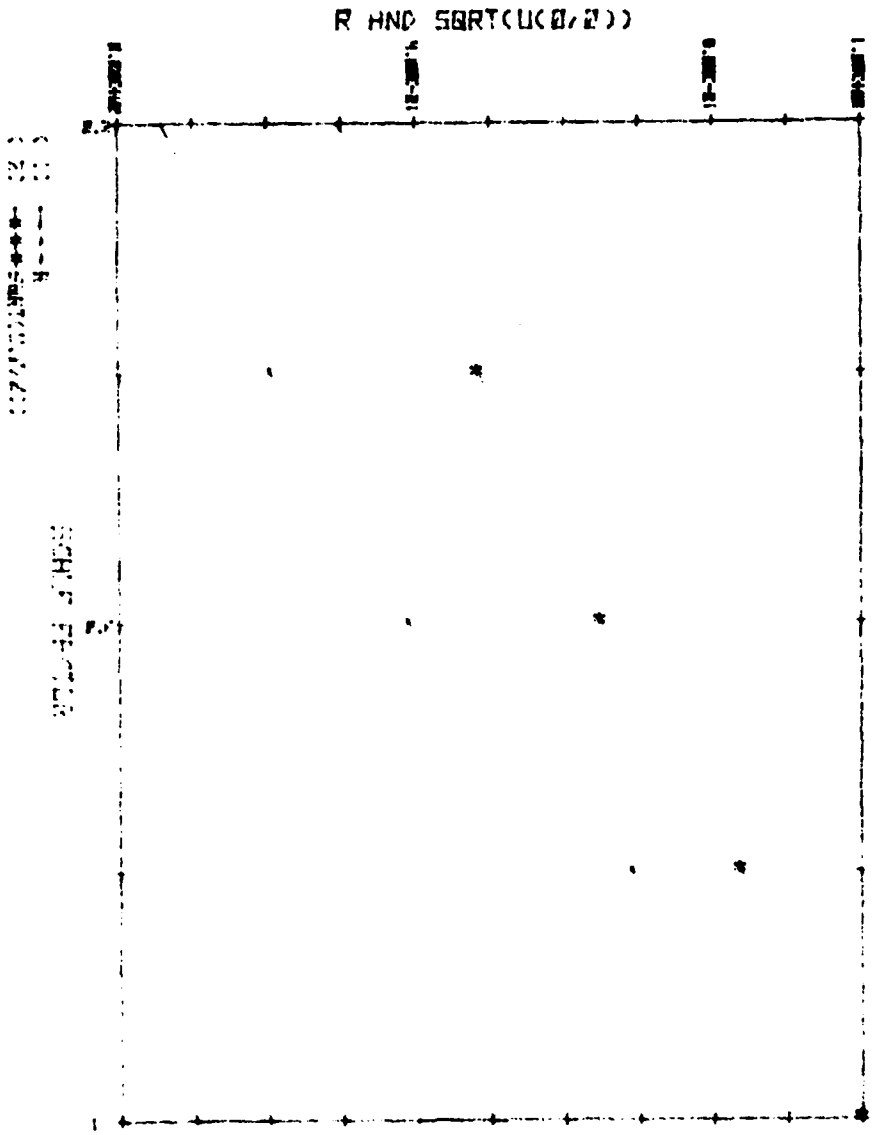



Figure 6 r and $(\mu_{00}'/\mu_{00})^{1/2}$ as a Function of the Scale Factor

## V. RECOMMENDATIONS

The results of the previous sections indicate that moment invariants were very sensitive to the number and configuration of the object pixels, and to computation errors introduced by discrete integration. In fact, these effects caused variations of the invariant values that were larger than those caused by noise, or by diminished resolution of the object. In view of this it is recommended that a further study be made to isolate these effects from each other, and from other errors, and to determine the contribution of each effect to changes in the central moments and moments invariants. Integration errors can be checked by taking an object that is exactly integrable, two dimensionally, such as a rectangle or an ellipse, and comparing the exact and computed values for the central moments and moment invariants. The objective here is to determine a more accurate and yet computationally effective method to calculate the central moments. The sensitivity to the pixel configuration can be determined by the addition or removal of one or more pixels from various locations relative to the centroid position. Intuitively, it appears that addition or removal of pixels will have a greater effect as they move away from the centroid. The objective of this study would be to determine techniques (i.e., an interpolation method) that would reduce this variation, as it relates to the moment invariants.

## References


1. Ming-Kuei Hu, "Visual Pattern Recognition by Moment Invariants," IRE Transaction on Information Theory, Vol. IT-8, February 1962, pp. 179-187.

2. Sahibsingh A. Dudani, Kenneth J. Breeding, and Robert B. McGhee, "Aircraft Identification by Moment Invariants," IEEE Transactions on Computers, Vol. C-26, No. 1, January 1972, pp. 39-45.

3. Michael R. Teague, "Automatic Image Analysis via The Method of Moments", Laser Digest, AFWL, Kirtland AFB, NM, Summer 1979, pp. 29-43.

4. Michael R. Teague, "Image Moments Invariants and Designation of Aimpoint on Extended Targets," Laser Digest, AFWL, Kirtland AFB, NM, Summer 1979, pp. 44-65.

5. Firooz A. Sadjadi and Ernest L. Hall, "Three Dimensional Moment Invariants," IEEE Transactions on Pattern Analysis and Machine Intelligence, Vol. PAMI-2, No. 2, March 1980, pp. 127-136.

1980 USAF - SCEE SUMMER FACULTY RESEARCH PROGRAM

Sponsored by the

AIR FORCE OFFICE OF SCIENTIFIC RESEARCH

Conducted by the

SOUTHEASTERN CENTER FOR ELECTRICAL ENGINEERING EDUCATION

FINAL REPORT

# EVALUATION OF DEPOT MAINTENANCE COST ALLOCATION IN VAMOSC II


| | |
|---|---|
| Prepared by: | Dr. Paul L. Williams, Jr. |
| Academic Rank: | Assistant Professor |
| Department and University: | Department of Mathematical Sciences<br>University of Wisconsin at Superior |
| Research Location: | Air Force Logistics Command<br>Directorate of Management Sciences<br>Management Sciences Division (XRSM) |
| USAF Research Colleague: | Dr. William E. Dickison |
| Date: | 8 August 1980 |
| Contract No: | F49620-79-C-0038 |

# EVALUATION OF DEPOT MAINTENANCE COST ALLOCATION IN VAMOSC II

by

Paul L. Williams, Jr

## ABSTRACT

As the operating and support costs become a larger part of the life cycle costs for a weapon system it becomes more important for those costs to be visible for management use. The Air Force Visibility and Management of Operating and Support Cost II system is a project to satisfy that need. This report is an evaluation of the depot maintenance portion of that system. All costs are not recorded by weapon system so an allocation procedure must be used. The model, data base, computer implementation and output product were evaluated. Ninety-five to ninety-eight percent of the depot costs are available for allocation; eighty percent are actually distributed. Discrepancies in the allocation ratios were found and one computer program produced erroneous output for FY79. There is a need for improved documentation. Suggestions for allocating more of the costs are made.

## ACKNOWLEDGMENTS

The author would like to thank the Air Force Systems Command, the Air Force Office of Scientific Research and the Southeastern Center for Electrical Engineering Education for providing the opportunity to investigate Air Force Logistics in the Management Sciences Division (XRSM) at Wright-Patterson Air Force Base. In particular, special thanks are due Dr. William E. Dickison, XRSM Chief, for his guidance and support in this study and to Hugh Hunsaker for his patience and willingness to answer questions and provide background information.

Many others were helpful by supplying information for the study. Included in that list are Robert DeSanty, Rolf Hagton, Clark Oursler, and William Wysinski. Dan Danishek, SCEEE coordinator at WPAFB, was most helpful in making the summer an enjoyable one.

## I. INTRODUCTION

The operating and support costs of a weapon system must be visible when management decisions concerning that system are made. The Department of Defense has published goals for cost visibility. The Visibility and Management of Operating and Support Costs system is the Air Force's effort to satisfy those goals. The Weapon System Support Cost subsystem is one part of that system. Depot maintenance costs make up about 15 percent of all the costs rolled up in that subsystem for a given weapon system. This report is the results of a study that was made to evaluate the depot maintenance portion of the Weapon System Support Cost subsystem.

The evaluation is complicated by the fact that some operating support costs are not reported by weapon system. Different techniques using various independent variables have been devised for allocating maintenance costs. Some are not applicable because they depend on known values of the maintenance costs. Since one constraint on the project is that no new data sources are to be used, the choice of a technique depends on what information is available and the selection of appropriate algorithms.

The evaluation procedure consists of an assessment of the model used to allocate the costs, an assessment of the data base, an assessment of the computer implementation of the model and a determination of the adequacy of the output product.

## II. OBJECTIVE

The main objective of this project was to devise a procedure to evaluate the Weapon System Support Cost subsystem of VAMOSC II. That procedure was used to evaluate and validate the depot maintenance portion of the subsystem. Recommendations based on the study were to be made.

## III. HISTORICAL SUMMARY

The following summary of the events leading up to the project that is partially evaluated in this report is offered to identify some of the terms/acronyms used and to place the project in the proper perspective.

During a period of austere budgets all appropriations come under greater scrutiny. Operating and support (O&S) costs for weapon systems are no exception. Peacetime budgets have shown an increasing percentage of the total defense budget being devoted to O&S. Visible O&S costs by weapon system make it possible to measure and evaluate trends, to identify shifting demands and to focus management attention on critical resource demands of new systems. In the early 1970s this was impossible because accounting systems identified cost organizationally and functionally rather than by weapon systems. In January of 1974 the DOD Weapon System Support Cost Visibility Group was established to develop a systematic plan for identifying DOD O&S support cost by weapon system. The DOD Management by Objective 9-2 publication contains guidelines for achieving the goals of quantifying appropriate weapon system cost. There are three main objectives (6):

a. To develop service-peculiar O&S cost management information systems which provide the capability of identifying O&S costs by weapon system.

b. To expand weapon system O&S cost systems to obtain detailed data on weapon system subsystem and replacement component maintenance costs.

c. To standardize O&S costs and make the costs compatible with the Uniform Depot Cost Accounting System.

Guidelines for the implementation of methods to achieve these goals were released. The Cost Analysis Improvement Group (CAIG) published the "Operating and Support Cost Estimate for Aircraft System Development Guide." Its purpose was to provide a framework for review of new weapon systems. In October of 1975 DOD 7220.29-H was released. It contained guidelines for uniform cost accounting at all depot maintenance activities of DOD. Its provisions are applicable to all depot maintenance work done on operational weapon systems. A data record is required for each type of maintenance work as specified in the document.

To satisfy these requirements the Air Force developed the Operating and Support Cost Reporting (OSCR) system. It was later named the Operating Support Costing and Reporting (OSCAR) system. In phase I of that development data for four aircraft systems were manually processed. The computerized version for all active aircraft systems was completed by January 1976. The first years' data were for FY75. Subsequent data were added to the basic data base. An OSCAR document states, "The Air Force, viewing the task as a pilot effort, proceeded on the premise that sole reliance had to be placed upon existing data sources, identification of O&S cost to weapon systems could be accomplished without recourse to the establishment of a new appropriation accounting system, and the pilot O&S costs system would be confined to the total weapon system and not its subsystem or major components". By April 1976 O&S costs by weapon system were available on a limited basis within a 24 hour period.

Another effort, Weapon System Cost Retrieval System (WSCRS), was operational in 1978. Whereas OSCAR was developed as a management information system, WSCRS was developed as a data retrieval system. Both systems use the H036B depot maintenance file.

In order to avoid duplication and to centralize effort toward Visibility and Management of Operating and Support Cost (VAMOSC) the VAMOSC II project was begun in 1978. A contract was let

to Information Spectrum Incorporated to develop and deliver system specifications by February 1979. One constraint was that no new data collection system was to be incorporated in the project. There are four subsystems associated with the VAMOSC II project. The first, VAMOH, is used to make necessary data conversions so that the input data for the other subsystems is in the most useful format. The other subsystems are the Component Support Cost Subsystems (CSCS), the Communication-Electronic (C-E) subsystem, and the Weapon System Support Cost (WSSC) subsystem.

Responsibility for the planning and execution of the VAMOSC project was assigned to AFLC in May 1979. The office of VAMOSC was created to oversee that responsibility.

AFLC/XRSM was assigned the task of validating the WSSC subsystem. The statement of task in the study proposal is to

a. Investigate the algorithms used in the program logic for adequacy, consistency and appropriateness in view of the current O&S cost methodology.

b. Investigate sources of data used for the program logic for precision and accuracy with a view for those data elements that are captured by the source data system instead of feeder data systems.

c. Investigate the current and proposed output products with a view towards satisfying the table of accounts promulgated by the Cost Analysis Improvement Group.

d. Make recommendations for changes resulting from the above study areas, as appropriate.

One aspect of the WSSC subsystem is depot maintenance. Costs incurred at the five ALC's and at the electronics facility in Newark must be allocated to weapon systems. This report is the

result of the validation/evaluation study of the depot maintenance aspect of the WSSC subsystem.

## IV. TECHNIQUES OF ALLOCATING COST

Two basic types of models can be used to make cost estimates where actual costs are not available. A parametric model "uses historical information from other programs correlated with performance characteristics such as weight, speed, range, as the basis for estimating the cost of a new system" (4). The other type, called the industrial engineering model, depends on an in-depth analysis of the necessary work methods involved. It can be used as development progresses and more information becomes available. Ordinarily, an industrial engineering model would be used to estimate depot maintenance cost on operational weapon systems.

The Uniform Cost Accounting System used at the maintenance depots is such that some costs can be identified with a particular weapon system. In order to satisfy the requirements of VAMOSC II a valid procedure must be developed to allocate the other costs. Various allocation algorithms may be considered.

Simple relationships may be used. For example, the Army found that empty weight of helicopter was the best predictor of maintenance cost (4). As an alternative, acquisition costs could be used if it is reasonable to assume that expensive weapon systems would be more costly to maintain than less expensive ones. Maintenance costs for a given weapon system would, it would seem, depend on the amount of usage that the weapon system receives and/or the relative size of that weapon system as compared to other systems. Consequently, one algorithm might be

$$\text{Weapon System Cost} = (C_1 + C_2 * \text{FHR} + C_3 * \text{PHR}) * \text{Depot cost}$$

where FHR = flying hour ratio for the weapon system

PHR = possessed hour ratio for the weapon system

$C_1$, $C_2$ and $C_3$ are constants that may be zero

Depot cost = the cost to be distributed

Alternate forms of this linear relationship may be used. For example, annual prorated cost for overhaul may be expressed as a + bx where x represents the annual flying hours; a and b are constants.

As more experience is obtained with a given weapon system, other algorithms may be used. The simplest would be to use the average of historical data. However, if accurate data by weapon system is not available then this approach cannot be used. Mean-Time-Between-Failures may be useful as a estimator. The costing community may establish standard factors which have been determined with experience (3).

More complex algorithms can also be devised. For example, the Navy Aircraft O&S Cost Model uses the function (10)

$$\text{Component rework/FH} = a * (\text{MMH})^b * (\text{GTOW})^c$$

where MMH = maintenance manhours

GTOW = gross take-off weight

a, b and c are constants to be determined

Obviously, this expression is meaningless unless accurate values for the independent variables are available to determine the constants.

The choice of algorithm to be used depends on the data that is available and on the experience that has been accumulated.

## V. DESCRIPTION OF WSSC SUBSYSTEM (DEPOT MAINTENANCE)

A diagram illustrating the depot maintenance data processing procedures is given Figure 1. The H036 system is used to merge and sort data from the Air Logistics Centers (ALCs) into a useful format. To reduce the number of distinct Mission Design Series (MDS) some similar ones with low activity are grouped together. This gives a standard MDS (STD-MDS). Some STD-MDS's represent a single MDS; others will represent a group. The VAMOH subsystem accumulates flying and possessed hour information for the STD-MDS's under consideration. One program of WSSC (PIPNO of Function 1) accumulates the possessed hours (PH) and flying hours (FH), by organization/MDS and by MDS alone. Another program (PIPTO of Function 8) then produces the cost records by organization/MDS and Work Breakdown Structure (WBS) and by MDS and WBS. The WBS's used are Airframe, Engine, Avionics, and Other.

## VI. EVALUATION RESULTS

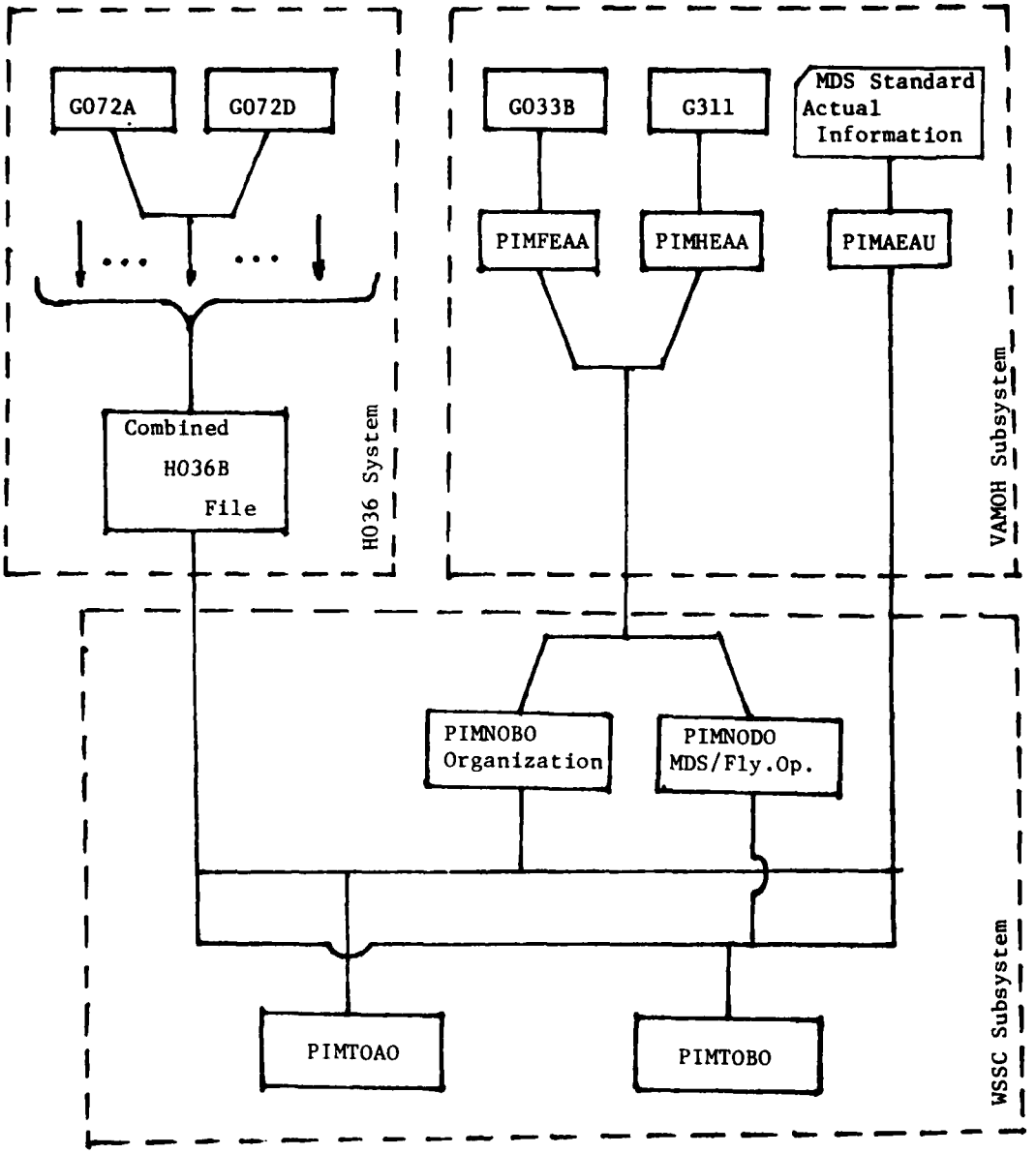
Five steps will be used to evaluate the subsystem.

1. Determination of the Purpose of the Subsystem.

The depot maintenance costs are to be allocated in such a manner that the costs actually incurred by a given STD-MDS are reflected as accurately as possible.

2. Assessment of the Model.

The report "Understanding and Evaluation Life Cycle Cost Models" (3) gives steps for the assessment of a model. Section 4.4.7 of the WSSC Subsystem Specifications (9) outlines the procedures to process depot maintenance data. Details are not given in that description, so it is impossible to give a complete assessment. For example, the End Item Identifiers (EII)




DEPOT MAINTENANCE COST DATA PROCESSING

FIGURE 1

that are used on ALC records may be MDS's, Type Model Series (TMS) for engines, National Stock Numbers (NSN), or some other designation. The WSSC description does not specify how the different types of records are to be processed. Allocations are to be made using the "Standard- Flying Ratio "which is the average of the FH and PH ratios for a given STD-MDS. The reasoning behind the choice of that ratio is not explained.

The H036C subsystem has been developed to produce a Depot Operations Cost File on magnetic tape. Costs are given by MDS and WBS. The subsystem also produces a 200 page listing of depot costs. Each page has the depot maintenance costs for a given STD-MDS broken out by WBS. The output is that which is specified in WSSC specifications C-69 and C-72.

The algorithms used in H036C are probably quite similar to those intended for WSSC. Comments made hereafter in this report will refer to the H036C subsystem as if it were the depot maintenance part of WSSC.

If the EII is a STD-MDS costs are allocated totally to that weapon system. If the EII is a TMS then flying hours for aircraft employing that engine are used to allocate the cost. In this case, the ratio for a given STD-MDS is equal to the engine flying hours accumulated by that STD-MDS divided by the total engine flying hours accumulated by all aircraft using that engine. No costs are allocated to a weapon system if the ratio is less than 1/200. A similar allocation procedure is used if the EII is an NSN. Applications for NSNs are determined from D041. Applicable costs that cannot be associated with any particular one of the MDS or TMS are allocated to all SDT-MDS's under consideration using the ratio of flying hours for that STD-MDS divided by the worldwide flying hours for all weapon systems.

3. Assessment of the Data Base.

The WSSC specifications indicates that two files, G033B and G311, will be used to roll up flying hours and possessed hours. Developers of the subsystem are already aware that all necessary information is available in G033B. It is assumed that subsequent specifications will incorporate that change.

Overhead, with general and administrative (G&A) costs, are included in each record of the H036A file. A routine audit to reconcile the ledger at each ALC with the general account shows agreement within 2-5%. The H036B subsystem is used to merge files from the 5 ALCs and Newark. No cost manipulations are made except that in some cases standard costs have been associated with labor items. It can be assumed, then, that 95 to 98 percent of the costs actually incurred are included in H036B. During processing some of the records in H036B file may be deleted. Records associated with work that was not done for the Air Force, work with a work performance code not included, and work not done on aircraft can be deleted. Of the remaining records, some cannot be processed because it is impossible to identify the EII with any of the STD-MDS, TMS or NSN under consideration. That may be intentional or it may be the results of an error in recording information. Results from H036C for FY79 indicate that approximately 20% of the costs cannot be processed because of the inability to match the identifier number.

4. Assessment of the Implementation of the Model.

The output from H036C for FY79 was used as a guide in the study of the programs of H036C. As was indicated, some records are immediately deleted because they do not represent the costs that should be included. These records represented about 18% of total costs represented by all records. Taking

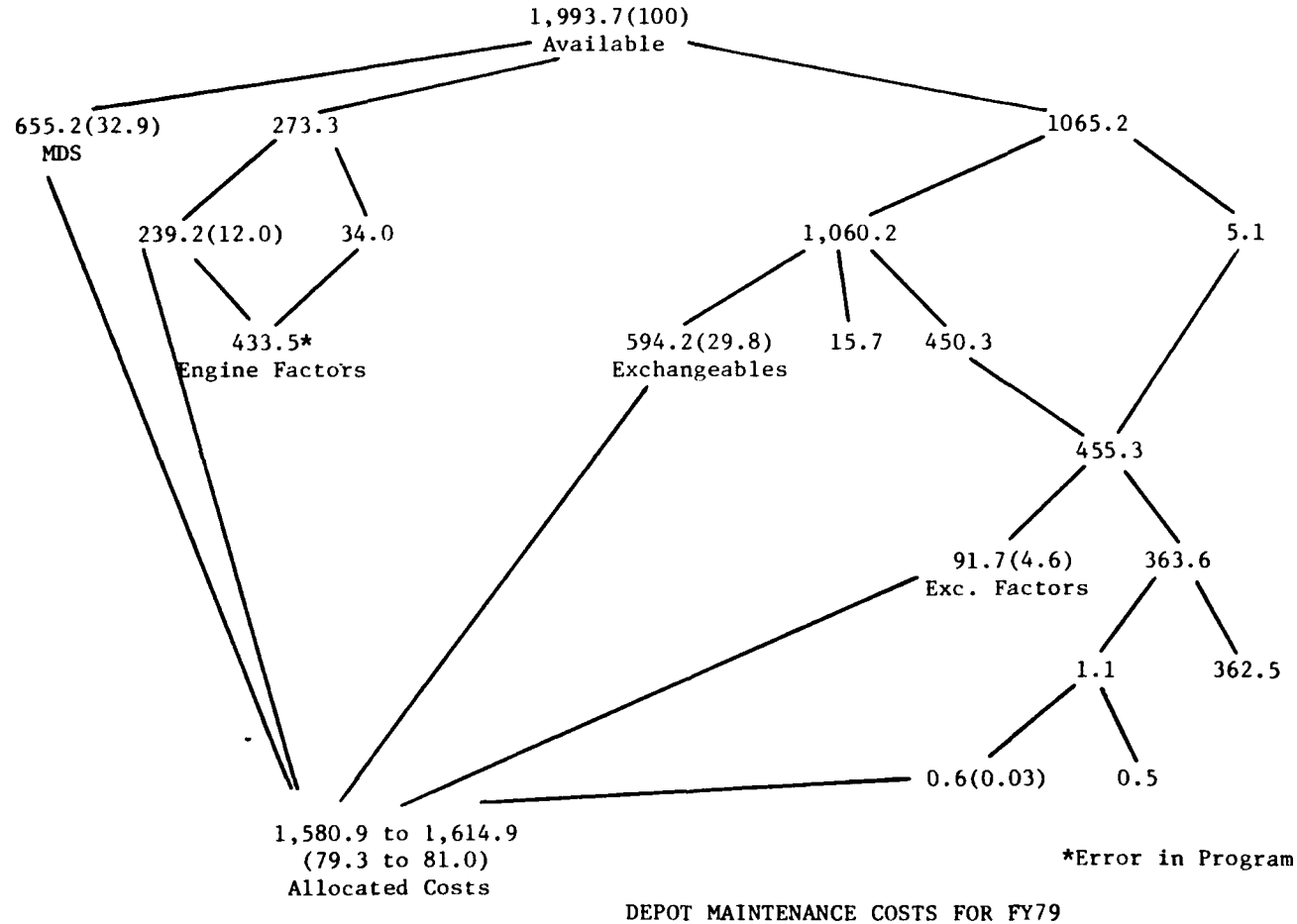
the remaining records, it is of interest to see how those costs were allocated. The distribution is illustrated in Figure 2. One error is evident. The intent of program LVPBF is a second attempt at prorating engine costs which initially could not be matched. Those costs were to be included in the engine factor file. The costs that were distributed (204,268,330) exceeded the costs available (34,026,011). The error could have been caused by faulty card input or by the program itself. The cards seem to be in order. Otherwise, H036C programs seem to be working as expected.

5. Determination of Adequacy of Output.

The output from the depot maintenance part of WSSC satisfies the first objective of MBO 9-2 to a large extent. Labor and material cost estimates for the work breakdown categories are visible by weapon system. The second objective is not appropriate. It will be under consideration in subsystem CSCS. The H036 system conforms to DOD- 7220.29H specifications for uniform cost accounting so the third objective is satisfied.

The report described on page D-1 for DOD use conforms to CAIG Cost Development Guide (13) except for the fact that no "Software Updates" is included. That item was not included in the 1974 edition of the Guide. It could very well be a justifiable O&S cost but there is no category in the H036 system that would supply that information. The CAIG Cost Development Guide is not clear how some costs, such as those for avionics, should be reported.

The report described on page D-2 for USAF use specifies depot maintenance costs in categories corresponding to the WBS used in H036. Therefore, the depot maintenance part of that report follows smoothly from the WSSC subsystem.




*Error in Program (See Text)

DEPOT MAINTENANCE COSTS FOR FY79
Millions of Dollars (Percent)

Figure 2

## VII. DISCUSSION OF EVALUATION

Since 95 to 98% of depot maintenance costs are represented in the records of H036B the main problem is in allocating those costs to the proper weapon system. If the output from the program LVPBF had been correct then at most 34 million dollars would have been added to the engine factor file. If that had been the case then of the 1,994 million dollars to be allocated, approximately 9043.6 million (47.3%) would have been assigned without prorating; 671.3 million (33.7%) assigned with prorating and 379.1 million (19.0%) could not be allocated. If a greater percentage of the depot costs are to be assigned to weapon systems then a technique must be devised so that more of the EII can be recognized and the corresponding cost realistically allocated.

Whether or not the amount of improvement (0.03% of the total) realized by using programs LVPCF and LVPCH is worthwhile should be studied. Computer time is probably not a factor since the programs are only run annually.

Some questions have been raised concerning the parts cost found in D041. That should not cause a problem in this system since only utilization information from D041 is used.

Since a given component (engine, radar unit, etc.) may be used on several STD-MDS's it will always be necessary to prorate repair costs on those components to appropriate weapon systems. Flying hours and/or possessed hours information is available and is probably the most useful. There is a difference in the application of this information for OSCAR, WSSC, and H036C. OSCAR (and WSCRS) uses 65% of the FH ratio and 35% of the PH ratio for some costs and uses the FH ratio alone for the others. The WSSC specification uses the average of the FH and PH ratios. H036C uses the FH ratio alone. Naturally, if the FH ratio is equal to the PH ratio for a STD-MDS then results of the three

methods would be the same. In an effort to determine what differences might be expected the FH and PH for all weapon systems in January 1980 were studied. The information for weapon systems having the greatest difference in ratios is given in Figure 3. These ratios can be used with FY79 data as follows to determine the effect.

Depot Cost for MDS = prorated costs + non-prorated costs

= (ratio * amount to be distributed) + non-prorated costs

Non-prorated costs = Depot Cost for MDS - ratio * amount to be distributed

For FY79 the amount allocated was approximately 670 million dollars. The FY79 depot costs for the C141 and F4 were used with H036C ratios to find the non-prorated costs for each. These values were used to find what the depot costs would have been if the other models had been used. The results are given in Figure 4. The relative change in going from H036C to OSCAR or WSSC for the C141 data is approximately 20%, for the F4 it is approximately 5%.

If H036C is used as the depot maintenance part of WSSC then the System Specifications will have to be rewritten to include those algorithms. The proportions of FH and PH ratios to be used in the model must be selected and should periodically be reviewed. The WSSC specifications will also have to explicitly indicate how the uniform cost accounting categories are to be rolled up to produce the CAIG report (D-1) for DOD.

## VIII. RECOMMENDATIONS

As the development of the WSSC (VAMOSC II) subsystem progresses it will be necessary to supply accurate documentation to ensure that later revisions do not destroy the integrity of the system. The operation of program LVPBF of H036C must be

FLYING AND POSSESSED HOUR RATIOS

(PERCENT) FOR COST ALLOCATION

| MISSION DESIGN | FLYING HOUR RATIO | POSSESSED HOUR RATIO | OSCAR[1] RATIO | WSSC[1] RATIO | H036C[1] RATIO |
|---|---|---|---|---|---|
| C 141 | 8.8 | 2.7 | 6.7 | 5.8 | 8.8 |
| F-4 | 12.4 | 17.5 | 14.2 | 15.0 | 12.4 |

1. OSCAR RATIO = 0.65 FH ratio + 0.35 PM ratio
   WSSC RATIO = 0.5 FH ratio + 0.5 PM ratio
   H036C RATIO = FH ratio

FIGURE 3

ALLOCATED COSTS (MILLIONS)

| MISSION DESIGN | NON-PRORATED COSTS | COSTS IN H036C | COSTS IN OSCAR | COSTS IN WSSC |
|---|---|---|---|---|
| C 141 | 26.04 | 85.0 | 70.9 | 64.9 |
| F-4 | 183.62 | 266.7 | 278.8 | 284.1 |

FIGURE 4

corrected. It may be that the cost allocated by that program are relatively small. There are errors of estimation associated with allocating costs in a system of this kind. If the costs allocated by programs LVPBF and LVPCF/LVPCH are small compared with the expected error then the possible omission of those programs should be considered.

In FY79 about 20% of the depot maintenance available costs were not allocated to any weapon system by H036C. A detailed study of the records representing those costs possibly would reveal how that percentage could be reduced.

The goals of DOD MBO 9-2 will not be completely achieved until all operating and support costs are included. The WSCRS system has been extended and it now includes condemnation costs. These costs are obtained from the D041 file. Preliminary runs indicate that the magnitude of the condemnation costs are similar to those of depot maintenance as given by H036C. They are costs that should not be overlooked. Some efforts have been instigated to replace H036C with WSCRS. Before that is done a comparative study should be performed. There is a distinct difference in philosophy between H036C and WSCRS. The H036C system takes costs from the H036B file and allocates them, as much as possible, to appropriate weapon systems. The WSCRS system, on the other hand, starts with a weapon system, uses D041 to find parts/components used on that system, and then uses H036B to assign the costs. The outputs from the two systems would be similar if costs from the same records of H036B are used. There is no guarantee that that is the case. The comparative study could determine which of the two philosophies is the most realistic and then that one should be used. In either case, condemnation costs from D041 could be incorporated.

The results of this subsystem would be more useful if sensitivity information was included. A range of values for the depot

maintenance costs for a given weapon system would be most useful. This may be included as part of the historical data base section of the VAMOSC II project. It should be a part of the system at some level.

## REFERENCES


1. H. L. Eskew, T. P. Frazier, and P. T. Heilig, "An Operating and Support Cost Model for Aircraft Carriers and Surface Combatants," Defense Documentation Center AD-A044744, September 1977.

2. G. D. Luker, G. N. Stanard and J. E. Thomas, "AVSCOM Maintenance Operating and Support Cost Model," Defense Logistics Studies Information Exchange Document LD 38739A, February 1977.

3. B. S. Mills, "Understanding and Evaluating Life Cycle Cost Models (Second Edition)," Defense Logistics Studies Information Exchange Document LD 45159A, March 1977.

4. A. D. Stament and C. R. Wilbourn, "Cost Estimating Relationships: A Manual for the Army Material Command," Defense Documentation Center Document AD 742810, May 1972.

5. A. A. Yawitz, "Flying Hours Utilized to Estimate Dollar Amounts of Selected Army Aircraft Fiscal Activities," Defense Logistics Studies Information Exchange Document LD 46140A, July 1979.

6. AFLC/ACRCC, "Cost by Weapon System Analysis," WPAFB, August 1978.

7. AFLC/ACVMS, "Monthly Aerospace Vehicle Status/Utilization Report," A-G033B-MSU-M3-MM1, January 1980.

8. AFLC/ACVRF, "Visibility and Management of Operating and Support Costs System II - Functional Description," 3 June 1980.

9. AFLC/ACVRF, "Visibility and Management of Operating and Support Costs System II - Weapon System Support Cost Subsystem Specification," 3 June 1980.

10. Office of Chief of Naval Operations, "Naval Aircraft Operating and Support Cost Model," Defense Logistics Studies Information Exchange Document LD 32472MB, March 1978.

11. Office of the Comptroller of the Army, "Operating and Support Costing Guide - Army Weapon Systems," Defense Logistics Studies Information Exchange Document LD 33144A, December 1974.

12. DOD 7220.29-H, "Department of Defense Depot Maintenance and Maintenance Support Cost Accounting and Production Reporting Handbook," October 1975.

13. DOD/CAIG, "Aircraft Operating and Support Cost Development Guide," 26 November 1979.

1980 USAF - SCEEE SUMMER FACULTY RESEARCH PROGRAM

Sponsored by the

AIR FORCE OFFICE OF SCIENTIFIC RESEARCH

Conducted by the

SOUTHEASTERN CENTER FOR ELECTRICAL ENGINEERING EDUCATION

FINAL REPORT

# AN ANALYSIS OF THE PLANNED MULTIFUNCTION-MULTIBAND AIRBORNE RADIO SYSTEM (MFBARS) OPERATIONAL IMPACT STUDY: A MARKETING PERSPECTIVE


| | |
|---|---|
| Prepared by: | E.P. WINKOFSKY |
| Academic Rank: | ASSISTANT PROFESSOR |
| Department and University: | DEPARTMENT OF MANAGEMENT SCIENCE<br>VIRGINIA POLYTECHNIC INSTITUTE AND STATE UNIVERSITY |
| Research Location: | AIR FORCE WRIGHT AERONAUTICAL LABORATORIES,<br>*AVIONICS LABORATORY, SYSTEM AVIONICS DIVISION,*<br>INFORMATION TRANSMISSION BRANCH, RADIO SYSTEMS GROUP |
| USAF Research Colleague: | MAJOR ROBERT CORTEZ |
| Date: | AUGUST 13,1980 |
| Contract No. | F49620-79-C-0038 |

# AN ANALYSIS OF THE PLANNED MULTIFUNCTION-MULTIBAND AIRBORNE RADIO SYSTEM (MFBARS) OPERATIONAL IMPACT STUDY: A MARKETING PERSPECTIVE

by

E.P. WINKOFSKY

## ABSTRACT

In order to transition technological advancements, research laboratories must have the support of an appropriate operating command. The generation of such support requires the development of a suitable marketing strategy. This report develops such a strategy for MFBARS. It identifies the benefits of the MFBARS concept and the data necessary to support these benefits. In addition, future efforts inside and outside the lab needed to generate this data are detailed, and appropriate base-line documents are delineated. These efforts are then analyzed in terms of their responsiveness to the questions of the MFBARS Operational Impact Study.

## ACKNOWLEDGMENTS

The author would like to thank the Air Force Systems Command, the Air Force Office of Scientific Research and the Southeastern Center for Electrical Engineering Eductation for the opportunity to be an SFRP Associate. This has been a very fruitful and rewarding endeavor. I would like to also thank the members of the AFWAL Avionics Laboratory and the Aerospace Medical Research Laboratory without whose assistance this effort would not have been possible. In particular, Major Robert Cortez, Captain Dennis Hamme, Mr. Darlow Botha, Mr. Robert Harris and Captain Thomas Hall have been very supportive and helpful throughout the ten weeks. A special thanks to Mrs. Betty Hoover who had the unenviable task of providing me with secretarial support.

I. INTRODUCTION:

The Multifunction-Multiband Airborne Radio System (MFBARS) Program developed two conceptual architectures to integrate communication, navigation, and identification (CNI) functions. Since either of these designs if implemented would affect aircraft operations, it is appropriate to study these effects. Thus, the overall purpose of the planned MFBARS Operational Impact Study (OIS) is to "analyze the operational impact of the MFBARS concept on mission effectiveness and the requirements of operational and maintenance personnel " [1, p.19]. The initial impetus for this effort were the comments of Willis H. Ware, Chairman, ASA Committee of the Air Force Studies Board [2]. He was concerned that the MFBARS concept "be set in a system context that is pertinent to the aircraft, the operational needs of the crew, and the needs of the operational and maintenance personnel" [2, p.2]. His comments and this program were designed to ensure that the MFBARS concept is not developed in a vacuum without regard to the user community.

The need for an impact study is further emphased in ITT's Final Technical Report on MFBARS [3]. They divided an operational impact study into nine tasks [3, p.6-7]:

1. Refine mission analysis/flight profiles for the system evaluation.
2. Refine pilot interface and control concepts.
3. Refine interface concepts, e.g., DAIS, INS, cockpit displays, etc.
4. Refine threat analyses/system vulnerabilities, i.e., EW, and physical.
5. Refine packaging, reliability, survivability concepts.
6. Develop preliminary logistics support concepts, e.g., spares, maintenance, training, etc.
7. Refine logistic support concepts.
8. Refine LCC, DTC analyses.
9. Develop preliminary system facility concepts.

These tasks were considered to be important to the development of a simulation model to evaluate the MFBARS system. In addition, these tasks are important in themselves in that they demonstrate the implications of the MFBARS program.

With this type of support for an operational impact study as background, the Class D&F specifies that the program address these key issues:

a. What will be the actual CNI requirements for aircraft of the 1990s?
b. What will the MFBARS concept do to help solve the pilot saturation problem?
c. To what extent will pilot functions need to be automated in order to

make this workable?

d. What will be the impact of the MFBARS concept on mission procedures?

e. What are the MFBARS control and display requirements?

f. How should system availability needs be satisfied? This must include such concepts as fault recognition, fault isolation, fault tolerance, design-for-repair, built-in-test, MTBFs and MTTRs.

g. What is an appropriate life cycle support concept? [1, p.19]

As described above, the scope of this program is very broad and ambitious. Since this study like most studies will be funds-limited, it is critical that the appropriate emphasis be placed on each of these questions. Thus, the criticality of each question should be explored, and relevant baseline studies should be identified. In this manner, the OIS can be focused on the most significant knowledge gaps.

## II. OBJECTIVES OF THE RESEARCH EFFORT:

The objectives of the summer research effort were threefold:

1. Identify appropriate baseline studies for the planned MFBARS Operational Impact Study.
2. Identify the major information gaps that should be addressed in the OIS, and
3. Identify methodologies for filling the identified gaps.

Within the process of meeting these objectives, it became apparent that an implicit purpose of the OIS was to make MFBARS and the Integrated Communication Navigation Identification Avionics (ICNIA) Program (MFBARS advanced development continuation) more saleable. In order for ICNIA to proceed to engineering development, it must be sold to a product division and the user. An OIS could provide information to assist in this transition. The recognition of this aspect of the OIS gave a somewhat different slant to the summer research effort and this final report.

To successfully market a product, the producer must match the products benefits with the user's needs. Thus, AAAD must fully recognize MFBARS/ICNIA's benefits and communicate how these benefits address some of the user's needs. This report is an attempt to develop an initial marketing strategy for MFBARS/ICNIA.

To accomplish this objective this report will:

1. Identify the benefits of MFBARS:

2. Identify the data necessary to support these benefits;
3. Identify the tasks required to generate this data;
4. Identity appropriate baseline studies and methodologies for these tasks;
5. Discuss how these tasks respond to the key issues of the original OIS; and
6. Provide, in appendix form, various recommendations of the author concerning avionics modeling and a possible mini-grant opportunity.

## III. THE BENEFITS OF MFBARS:

The benefits of the MFBARS/ICNIA concept have been delineated in a number of sources [2,3,4,5]. These benefits can be summarized as follows:

1. A savings in weight, volume, and power;
2. A savings in production cost;
3. A savings in life-cycle-costs;
4. An improvement in functional reliability; and
5. A lengthening of the product life cycle.

Some of these benefits are rather obvious. For example, the functions that MFBARS is to replace currently require 19 line replaceable units (LRUs) and approximately 7.4 cubic feet while weighing 472 lbs [3]. The ITT architechture at this stage would require 4 LRUs and approximately 2.6 cubic feet while weighing 215 lbs [3]. It is noted that these figures are preliminary estimates and are presented only to demonstrate the order of magnitude of savings. Similar figures could be determined for power. In any case, integration certainly will provide significant savings in this area.

The next two benefits are related to standarization benefits. Standardization across aircraft will mean longer production runs. The fixed costs will be spread over a larger number of units, and other economies of scale are possible. Thus, there should be a lower acquisition cost. Standardization should also reduce logistic and maintenance costs. Service training may need to be less extensive. This, combined with built-in-tests (BIT), may provide more effective maintenance procedures, the lack of which is becoming a very critical DOD problem. Inventory costs should be reduced since one standard radio would be on all aircraft or at least a large number of aircraft.

MFBARS should also provide improved functional reliabilty. From a very simple viewpoint, the fact that there will be fewer parts in the system will increase the total system reliabilty. Also, MFBARS is to be reprogrammable,

i.e., its subfunctions ahould be multifunctional. The system will have gradual degradation failure modes that will ensure that the functional capability exists even though a particular subfunction may have failed.

MFBARS will have by design a longer life cycle than other radio systems. First it is being developed using advanced technology that should be state-of-the-art in the 1990s. This is an attempt to eliminate the instant obsolescence that often occurs on long term system development efforts. Second, the system is to be flexible. That is to say, its modularity will allow for future incorporation of additional system requirements as they are developed. This will be possible due to the software dependence of the system and its access to the entire spectrum from 2 MHz to 2000 MHz.

IV. FUTURE EFFORTS TO SUPPORT MFBARS BENEFITS:

A. Weight, Volume, and Power Savings: The previous Section showed that there are substantial savings in this area. As the MFBARS/ICNIA concept becomes more crystallized, these savings should become more exact. The ICNIA System Definition Studies are required to "develop an approach to physical partitioning of the system architecture components" [6, p. 3]. This partitioning task should provide additional information concerning the physical attributes of the ICNIA System.

Although the proposed ITT ICNIA architecture would fit into four LRUs, it is unlikely that the system would be encased in such a manner. Such deployment of the system would make it highly vulnerable during various mission segments. Thus, it is likely that it will be divided into smaller units. The physical characteristics of these units will be important considerations for any planned installment of ICNIA. This information concerning size, weight, and power is vital to supporting the benefits of MFBARS and also the planning of its introduction into aircraft.

B. Production Cost Savings: The contractors of the ICNIA System Definition Studies are required to provide the necessary input parameters to drive the Programmed Review of Information Costing and Evaluation (PRICE) models [6]. PRICE is an RCA software package of cost-predicting models. The basic PRICE or PRICE-H model estimates hardware development and production costs. PRICE-L estimates hardware logistics support costs or life cycle costs, and PRICE-S estimates software development costs [7]. All three of these models have been used to analyze the two MFBARS architectures [3, 7, 8].

Basic PRICE's cost estimates are "based upon physical parameters such as quantity, size, weight, power consumption, environmental specification, type

of packaging, and level of integration; and schedule parameters such as months to first prototype, manufacturing rate, and amount of new design" [9, p.A1]. Besides development and production costs, PRICE-H can also estimate MTBF and MTTR for the hardware units.

PRICE-L's inputs are supplied in part by PRICE-H and in part by the user. The major user inputs are deployment characteristics. These include the number of locations at which equipment is installed, the number of locations at which they can be maintained, the number of locations where spares are stocked, equipment usage, and length of support period [10]. The remaining user inputs are user selected program constants.

"The PRICE-S model inputs include the size of a computer program (in machine-level, executable, deliverable instructions), program applications, percentages of new design and code, project complexity and hardware constraints" [7, p.I-2]. The model outputs software cost and schedule estimates plus "automatic sensitivity and schedule effect analyses, together with monthly cost and progress summaries to support budgeting, risk analysis and project tracking" [11, p.1].

The PRICE models will be useful for comparing the two candidate architectures. In addition, the models will provide information concerning the order of magnitude of production costs from a hardware and software prespective. The utilization of the PRICE package results compared with the baseline [3] should provide the necessary data to support production cost savings.

C. Life Cycle Cost Savings: There are a number of software packages available to evaluate a system from a LCC view. However, to this point there is no one overall model (such as PRICE-H for hardware costs) that is considered the "best" [12]. This Section will review the available packages and make recommendations concerning future tasks.

1. PRICE-L: As stated above, the PRICE-L inputs will be generated during the System Definition projects. A unique feature of PRICE-L is its ability to consider alternative maintenance concepts. The available options are listed in Table 1. The output of the model is primarily program cost. This cost is partitioned into development, production, and support costs which are further subdivided into equipment, support equipment, manpower, supply, supply administration, contract support, and other cost. In addition, the program provides "values for the inherent and operational availability; the number of test sets used at each maintenance level and their

1. LRU discard at failure.
2. LRU repair at Organization. Module discard.
3. LRU repair at Intermediate. Module discard.
4. LRU repair at Depot. Module discard.
5. LRU repair at Organization. Module repair at Intermediate.
6. LRU repair at Organization. Module repair at Depot.
7. Repair LRU to piece part at Intermediate.
8. LRU repair at Intermediate. Module repair at Depot.
9. Repair LRU to piece part at Depot.
10. Repair LRU to piece part at Organization.
11. On-equipment repair to module. Module discard.
12. On-equipment repair to module. Module repair at Organization.
13. On-equipment repair to module. Module repair at Intermediate.
14. On-equipment repair to module. Module repair at Depot.
15. LRU repair at Contractor Depot. Module discard.
16. On-equipment repair to module. Module repair at Contractor Depot.
17. LRU repair at Organization. Module repair at Contractor Depot.
18. LRU repair at Intermediate. Module repair at Contractor Depot.
19. Repair LRU to piece part at Contractor Depot.

29. On-equipment repair to non-repairable module.
30. On-equipment repair to non-repairable part.

Notes: 1. Cases 29 and 30 are predetermined by the design of the hardware.

2. In addition to the 19 basic concepts above, algebra is available to define nine additional concepts. All 28 may be "mixed" arithmetically to construct customized maintenance concepts. A typical mixed concept might be one which called for 20% of concept no. 4, and 80% of concept no. 8.

TABLE 1: PRICE-L MAINTENANCE CONCEPTS [10, p.3]

utilization fraction, and the required supply quantities, both initial and balance consumed of LRUs, modules (per type) and parts (per type)" [10, p.4].

2. SAVE: System Avionics Value Estimation (SAVE) is a "collection of five special-purpose computerized logistics-and-support cost models integrated within an interactive framework" [13, p.1073]. The models included are CACE, LCC-2, GEMM and MOD-METRIC.

1. CACE "aggregates the cost to operate and support a squadron of aircraft at the base level" [14, p.9].
2. LSC addresses support costs such as spares, support equipment, on-equipment maintenance, etc.
3. LCC-2 quantifies life-cycle cost of a subsystem including procurement and installation costs and life-time support costs [14].
4. GEMM considers "life-cycle cost of a subsystem that can be specified down to its piece-parts (components)" [13, p.1075].
5. "MOD-METRIC is a mathematical model used to analyze a multi-item, multi-echelon, multi-identure inventory system for recoverable items" [14, p.14]. Information concerning these models and their input requirements can be found in [14].

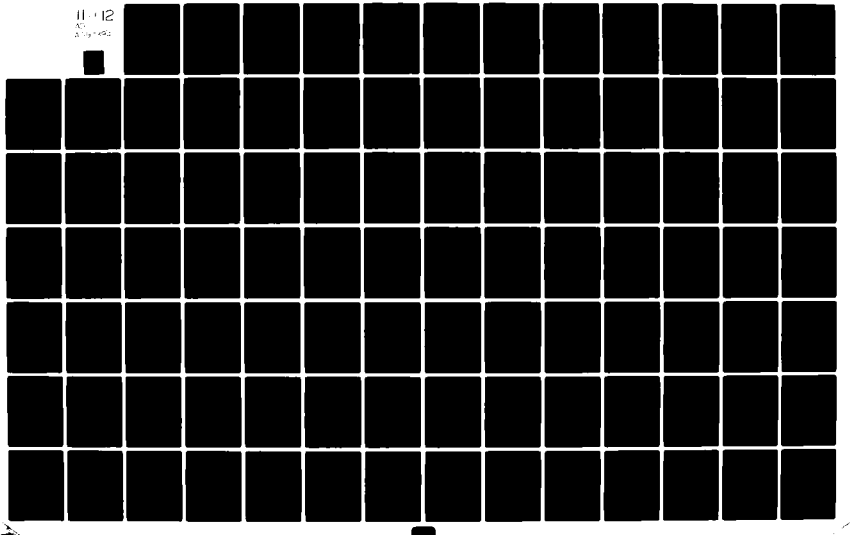
The SAVE package requires extensive data input. Considering the generation effort involved and the uncertainty of the data, it is probably not a worthwhile endeavor to use SAVE at this phase of the MFBARS/ICNIA study. SAVE provides a rich amount of unique output from a somewhat micro view. However, MFBARS's level of uncertainty requires a more macro approach. This group of models could be used to study ICNIA as the project becomes more certain and the data becomes more firm.

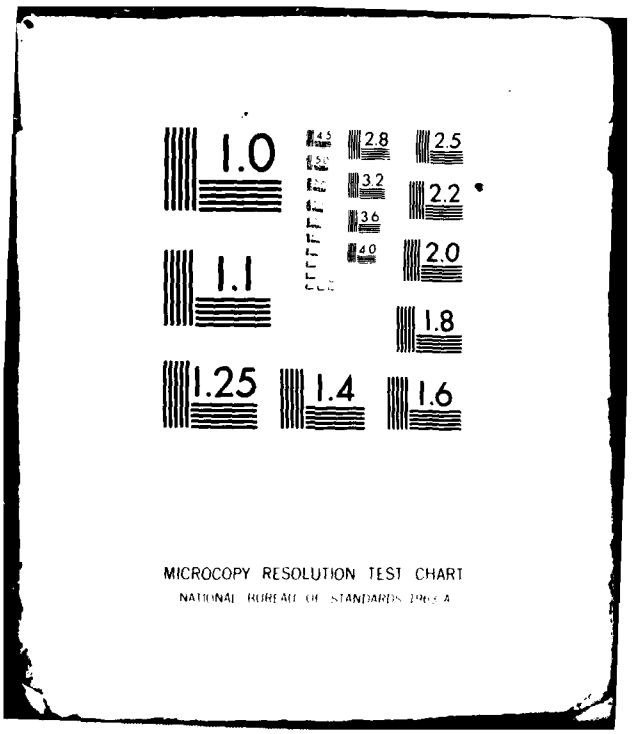
3. ALPOS: The Avionics Laboratory Predictive Operation and Support (ALPOS) cost model predicts "in the conceptual/early design phase various drivers on elements of LCC for avionics LRUs "[15]. Inputs to the model include hardware, physical design parameters, e.g., price, volume, weight, etc., and aircraft deployment information [12]. The possible outputs of ALPOS are listed in Table 2.

ALPOS has been used on MFBARS data and is less difficult to run than some of the SAVE models. In addition, its data requirements are rather similar to PRICE-L's. Since the effort would seem minimal, it is recommended that the model be used on the System Definition data sets.

AD-A097 394 SOUTHEASTERN CENTER FOR ELECTRICAL ENGINEERING EDUCAT--ETC F/G 5/1
USAF SUMMER FACULTY RESEARCH PROGRAM, 1980, RESEARCH REPORTS, V--ETC(U)
OCT 80 W D PEELE F49620-79-C-0038

UNCLASSIFIED AFOSR-TR-81-0193 NL




1.0
1.1
1.25
1.4
1.6
1.8
2.0
2.2
2.5
2.8
3.2
3.6
4.0
MICROCOPY RESOLUTION TEST CHART
NATIONAL BUREAU OF STANDARDS 1963-A

| | |
|---|---|
| 1. | Total Maintenance Manhours (MMH)/Operating Hour (OH) |
| 2. | Unsheduled MMH/OH |
| 3. | Shop MMH/OH |
| 4. | Total Logistic Support Cost (LSC)/OH |
| 5. | Field LSC/OH |
| 6. | Depot Repair Cost/Unit |
| 7. | Training Costs/OH |
| 8. | MTBF (Mean Time Between Failures) |
| 9. | MTBMA (Mean Time Between Maintenance Actions) |
| 10. | Spares Quantities |
| 11. | Subsystem MTBF & MTBMA |
| 12. | Subsystem MMH/OH & LSC/OH |
| 13. | Annual LSC |
| 14. | Annual Training Cost |
| 15. | Annual Support Equipment Costs |
| 16. | Total Annual Costs |
| 17. | Non-Recurring Spares Costs |
| 18. | Non-Recurring Support Equipment Cost |

TABLE 2: ALPOS OUTPUT DATA [15].

4. STEP: The Standardization Evaluation Program (STEP) was developed as part of the Standardization Potential Across Navigation Systems (SPANS) study [4]. For a particular aircraft and avionics suite, the program determines the mission complete success probability, the avionics life-cycle cost for the aircraft, and the total avionics life-cycle cost across all considered aircraft [16]. The input data to STEP can be divided into four categories: standard cost factors, aircraft/mission data, avionics equipment data, and equipment suite definitions. A more detailed delineation of these requirements is provided in Tables 3-7. How STEP may be used in the evaluation of module commonality programs such as MFBARS is discussed in [16]. STEP is currently being updated by The Analytic Sciences Corporation (TASC) and is expected to be on-line in September 1980.

As can be seen from an examination of Tables 3-7, the input requirements of STEP are rather formidable. However, most of this data, unlike the SAVE requirements, is deployment sensitive and not avionic suite sensitive. Thus, the uncertainty associated with the MFBARS architecture will have a minimal effect.

MFBARS is expected to have LCC benefits that, in part, are derived from standardization. The STEP model is designed to quantify this type of cost savings. It seems rather obvious then that STEP should be used to analyze the MFBARS concept. Thus, it is recommended that this be done based on available data and/or the System Definition data. Due to reliability and cost consideration, probably only the latter effort is needed.

5. Conclusions: To this point it has been recommended that various software models (PRICE-H, PRICE-L, PRICE-S, ALPOS, and STEP) be used to analyze the MFBARS/ICNIA system. Except for PRICE-S each of these models require information concerning either the number of systems to be produced or the detailed deployment and support of these systems. In order to fulfill either of these data requirements, the market for ICNIA must be identified. To date this has not been done. The market may range from only being installed in the next generation of aircraft to being retrofitted in every F-15, F-16, A-10, F-4, and EF-111. Thus, it is recommended that a detailed retrofit analysis be designed and implemented. More information concerning this proposed study will be presented in Section VI of this report.

D. Reliability Improvement: The expected improved reliability that ICNIA will provide is its significant mission benefit. Since the subfunctions are to be reprogrammable, it may be possible to maintain functional capability in the light of partial system failure. How this gradual degradation failure approach is to be

| | |
|---|---|
| 1. | Total Number of Base Locations |
| 2. | Total Number of CONUS Base Locations |
| 3. | Availabilty Objective Allocation Factor |
| 4. | I-Level Repair Turnaround Time (hours) |
| 5. | Resupply Time to CONUS Located Bases (hours) |
| 6. | Resupply Time to Overseas Located Bases (hours) |
| 7. | Depot Stock Safety Factor (standard deviations) |
| 8. | Shipping Time to Depot from CONUS Bases (hours) |
| 9. | Shipping Time to Depot from Overseas Bases(hours) |
| 10. | D-Level Repair Turnaround Time (hours) |
| 11. | I-Level Labor Rate for Maintenance (dollars/hour) |
| 12. | I-Level Materials Consumption Rate (dollars/hours) |
| 13. | D-Level Labor Rate for Maintenance (dollars/hours) |
| 14. | D-Level Materials Consumption Rate (dollars/hour) |
| 15. | Support Equipment Operation and Maintenance Cost (% of SE acquisition cost/year) |
| 16. | Packaging and Shipping Cost - CONUS (dollars/pound) |
| 17. | Packaging and Shipping Cost - Overseas (dollars/pound) |
| 18. | Exponent of Production Learning Curve for Electronic Equipment |
| 19. | Exponent of Production Learning Curve for Radar Equipment |
| 20. | Exponent of Production Learning Curve for Inertial Equipment |
| 21. | Exponent of Production Learning Curve for Support Equipment |
| 22. | Depot Working Hours/Month/Shift |
| 23. | Number of Depot Work Shifts |
| 24. | Support Equipment Utilization Factor (utilizable hours/hour) |
| 25. | Ratio of Nonhardware Acquisition Cost to First Unit Cost |

TABLE 3: STANDARD COST FACTOR DATA [17, p.2-5]

| | |
|---|---|
| 1. | Initial Year of Installation/Retrofit Program |
| 2. | Installation/Retrofit Rate (aircraft/month) |
| 3. | Aircraft Service Life (years) |
| 4. | Total Number of Aircraft |
| 5. | Number of Aircraft Base Locations |
| 6. | Base Location Indices |
| 7. | Aircraft/Base Location |
| 8. | Number of Mission Types |
| 9. | Number of Mission Phases |
| 10. | Mission Success Probability Objective |
| 11. | Missions Flown per Month |
| 12. | Aircraft Reliability K-Factor |
| 13. | Aircraft Availability Objective |

TABLE 4: AIRCRAFT/MISSION DATA [17, p.2-9]

| | |
|---|---|
| 1. | Projected Availability Date (year) |
| 2. | Technology Type (Electronics-1, Radar-2, Inertial-3) |
| 3. | Failure Rate (failure/hour) |
| 4. | Accumulated Operating Hours |
| 5. | Present Unit Acquisition Cost |
| 6. | Present Production Quantity |
| 7. | Development Cost |
| 8. | Initial Inventory Introduction Switch |
| 9. | Reliability Growth Factor (Slope of Duane Curve) |
| 10. | Number of Line Replaceable Units |
| 11. | Number of Shop Replaceable Units |
| 12. | Number of Piece-Parts |
| 13. | LRU Cost (Fraction of Total Equipment Cost) |
| 14. | LRU Failure Rate (Fraction of Equipment Failure Rate) |
| 15. | Fraction of Repairs Performed at I-Level |
| 16. | Base Repair Time (manhours) |
| 17. | Depot Repair Time (manhours) |
| 18. | Weight (pounds) |
| 19. | Peak Depot Return Rate (returns/hour) |
| 20. | Current Level of Depot Squares |
| 21. | I-Level SE Line Item Index |
| 22. | D-Level SE Line Item Index |

TABLE 5: AVIONICS EQUIPMENT DATA [17, p.2-15]

| |
|---|
| 1. SE Development Cost (dollars) |
| 2. SE Inventory Introduction Switch |
| 3. SE Unit Acquisition Cost (dollars) |
| 4. SE Production Quantity |
| 5. Current Usage Rate (hours/month) |
| 6. Current Depot Quantity |
| 7. Number of Bases with SE Positioned |
| 8. SE Base Location Indices |

TABLE 6: SUPPORT EQUIPMENT DATA [17, p.2-17]

1. Aircraft Index
2. Number of Subsystems in Suite
3. Number of Nonredundant Subsystem Options
4. Equipment Indices for Nonredundant Options
5. Number of Redundant Subsystem Options
6. Number of Redundant Equipments in Option
7. Equipment Indices for Redundant Options
8. Subsystem Operating Time
9. Mission Failure Probability Given Subsystem Failure

TABLE 7: EQUIPMENT SUITE DEFINITION DATA [17, p.2-21]

implemented is part of the System Definition phase of ICNIA. Yet, there still is a need to support quantitatively, if possible, this expected mission benefit. One approach to quantification might be the use of the Avionics Evaluation Program (AEP). AEP is a collection "of seven detailed avionics performance assessment models all driven by a common interactive software package. AEP provides an efficient means for performing trade-off analyses among cost, reliability, maintainability, and performance of avionic configurations" [18, p. 31-1]. Programs included in this package are: Air-to-Ground Mission Analysis, Target Acquisition, Weapon Delivery, Communications, Survivability, Air-to-Air Mission Analysis and Dogfight Analysis [19]. Since AEP was developed for and maintained by the Avionics Lab, it seems to be a likely candidate to assist in the evaluation of the mission benefit of MFBARS. To evaluate this candidate it is necessary to determine its output capabilities and its input requirements.

The Air-to-Ground Mission Analysis Program provides an example of the required inputs and the available outputs. The following information is required to set up the program [18, 19]:

1. The mission must be defined in terms of the target, threat, and weapons.
2. The flight profile is defined using waypoints to describe flight segments.
3. A suite of hardware (black boxes) describing the complete aircraft is itemized. Reliability and maintenance data are provided for each black box.
4. The required mission functions are selected (typical functions include navigation, navigation update, target acquisition, weapon delivery, survivability, communications, refueling, etc.).
5. For each function, the primary and backup modes of operation must be defined. A mode is defined by specifying the performance capability (if applicable) and assigning the hardware black boxes required to operate in that mode.

"The output is composed of statistics describing the mission events for the selected number of Monte Carlo trials" [18, p. 31-1], and includes:

1. Targets destroyed
2. Mission aborts
3. Aircraft losses

4. Targets detected
5. Average number of attack passes/target
6. Mission costs, and
7. Statistical summary of ground servicing and maintenance activities [18, 19].

The inputs listed above provide the general package requirements. Each of the other models necessitate some additional inputs, however, in most cases, this is merely mode selection or scenario specification. Obviously, the other models provide additional outputs concerning their specific areas. For more detail see [18, 19] or [20] which is a study of the F-16 using AEP.

The use of AEP to evaluate the MFBARS reliability improvement at this point would probably be premature. The data input requirements are substantial, and many of these values are still rather uncertain for MFBARS. Therefore, the results from AEP would be suspect since the output cannot be any better than the input. AEP, however, has extensive capabilities and would provide strong quantitative support for the program. The use of AEP should be reconsidered at or near the end of the System Definition phase of ICNIA.

Although the use of sophisticated software may not be warranted at this point, the concept of functional reliability needs to be further explored. This area may provide an opportunity for a follow-on study to the Summer Faculty Research Program under a mini-grant. Such a possibility will be examined in Appendix B of this report.

E. Life Cycle Lengthening: As discussed in Section III, MFBARS is to have a longer life cycle due to its advanced technology and reconfigurability. Quantitative support for this benefit is probably the most difficult to generate. First, experts can attempt to forecast the technology state-of-the-art in the 1990s but no one can obviously be certain. Second, since no new radio functions have been identified, the reconfigurability effect is difficult to measure.

In order to substantiate the system reconfigurability of MFBARS, the System Definition contractors are tasked to specify how this capability will be operationalized. This is certainly a first step in supporting this benefit. As ICNIA develops, opportunities may appear which will allow for a more detailed examination of this capability. However, this benefit may be one that can only be supported by its innate attractiveness.

V. RESPONSIVENESS TO THE OIS:

This Section is devoted to analyzing the original OIS and determining the appropriate response to this key issue. The already proposed efforts will be

examined to determine what if any issues they address. Finally, whatever new tasks are required will be identified. Appropriate baselines and methodologies for these new tasks will be specified.

Section I listed the seven key issues that were to be addressed in the OIS. These issues can be divided into three areas of concern: CNI requirements, pilot-control/display interface, and availability needs.

A. CNI Requirements: There are a number of studies that directly or indirectly relate to CNI requirements. A portion of this literature will be reviewed to demonstrate what information is readily available. What gaps and tasks remain is discussed at the conclusion of this Section.

1. Requirements analysis for MFBARS: The Requirements Analysis for a Multifunction Multiband Airborne Radio System final report prepared by ARINC Research Corporation summarizes the expected mid-to-late 1980's requirements that will affect the design of a MFBARS. In particular, it addresses the requirements for communication, navigation, and identification (CNI) equipment and identifies them by their source [21, p. 1-1]. The report considers the following aircraft: F-15A, F-16A/B, A-10, FAC-X, F-4G, ATF, FOI, RF-X and EF-111A. Tables 8 and 9 are reproductions of two tables from this report. They identify various functions and pieces of equipment that are expected to be on the studied aircraft in the mid 1980s. Table 9 in particular identifies the functions or capabilities that MFBARS will have to accommodate if there is to be no degradation of performance. However, in addition to overall functions, it is imperative to know the time-phasing of these functions in order to determine the hardware requirements. The Requirements Study also provides this type of information.

Tables 10-14 have been adapted from [21, pp. 3-19 - 3-22]. This information according to the authors was obtained from the SPANS study [4]. For the SPANS study, twelve mission profiles were evaluated. See Table 15. Only five of the twelve, however, were detailed in [21]. Tables 10-14 identify what specific functions are used during various mission segments, and thus provide significant inputs for the development of MFBARS.

2. Adaptive multifunction antenna (AMA) program: The AMA efforts of the Reference Systems Branch (AAAN) of the Systems Avionics Division are closely related to the MFBARS/ICNIA Program. Two efforts which are the most relevant to the MFBARS OIS are the GPS/JTIDS threat study and an impact analysis study.

The threat study's purpose was to define jamming threats to the Global Positioning System (GPS) and the Joint Tactical Information Distribution System (JTIDS) for the 1990s with an emphasis on threats to high performance antennas. This

| | Functions | F-15A | F-16A/B | EF-111A | A-10A/B | F-4G | FAC-X (A-10) | ATF | POI (F-15) | RF-X |
|---|---|---|---|---|---|---|---|---|---|---|
| C | UHF | ARC-164 (2) | ARC-164 | ARC-164 | ARC-164 | ARC-164 | X | X | ARC-164 | X |
| C | VHF-AM | - | ARC-186 | - | 807A | - | X | - | - | - |
| C | VHF-FM | - | - | - | ARC-131 | - | X | - | - | - |
| C | HF | - | - * | ARC-112 | ARC-154* | - | X | X | - | X |
| C | Crypto | KY-28 | KY-28 | KY-28 | KY-28/58 | KY-28 | X | X | KY-28 | X |
| C | JTIDS | X | X | X | X | X | X | X | X | X |
| C | SEEK TALK | X | X | X | X | X | X | X | X | X |
| N | INS | ASN-109 | GRN-2400 | ASQ-20 | X | ASN-63 | X | X | ASN-109 | X |
| N | TACAN | ARN-118 | ARN-118 | ARN-118 | ARN-118 | ARN-118 | ARN-118 | X | ARN-118 | X |
| N | ILS | ARN-112 | ARN-108 | ARN-58 | ARN-108 | - | ARN-108 | X | ARN-112 | - |
| N | UHF/ADF | OA-8639/ARD | - | ARA-50 | OA8697/ARD | - | OA-8697/ARD | X | OA-8639/ARD | X |
| N | HUD | AVQ-20 | X | - | X | - | X | X | AVQ-20 | X |
| N | Navigation Radar | - | X | - | - | - | - | - | - | - |
| N | Radar Altimeter | - | - | APN-167 | - | APN-155 | - | - | - | X |
| N | TFR | - | - | APQ-110 | - | - | - | X | - | X |
| N | Radar Beacon | - | - | - | UPN-25 | UPN-25 | UPN-25 | X | - | - |
| N | OMEGA | - | - | - | - | - | - | X | - | - |
| N | GPS | X | X | X | X | X | X | X | X | X |
| N | MLS | X | X | X | X | X | X | X | X | X |
| I | IFF Transponder | APX-101 | APX-101 | APX-64 | APX-101 | ASQ-19 | APX-101 | X | APX-101 | X |
| I | IFF Interrogator | APX-76 | - | - | - | APX-76 | - | X | APX-76 | X |
| I | IFF Crypto | KIT-1A | KIT-1A | KIT-1A | KIT-1A | KIT-1A | KIT-1A | X | KIT-1A | X |
| I | Automatic Altitude Reporting | - | - | - | AAV-19 | - | AAV-19 | X | - | X |

*Weight, space, volume allocations.

X: Equipment set planned but designation unknown.
-: No equipment planned.

TABLE 8: CNI FUNCTIONS [21, p. 2-15]

| Aircraft | Avionics | | | | | | | | | | | | | | | | | | | | |
|---|---|---|---|---|---|---|---|---|---|---|---|---|---|---|---|---|---|---|---|---|---|
| | UHF Radio | Secure Speech (SEEK TALK) | VHF AM Radio | VHF FM Radio | HF Radio | JTIDS | ILS | VOR | UHF/DF | Radar Beacon | TACAN (as a discrete unit) | GPS | Doppler | INS | Radar Altimeter | CAS | Radar | MLS | IFF Trans. | IFF Int. | IFF Crypto |
| A-10A/B | 1 | 1 | 1 | 1 | 1 | 1 | 1 | X | 3 | 2 | 3 | 1 | X | 1 | 2 | 1 | 2 | 1 | 1 | X | 1 |
| ATF | 1 | 1 | 2 | 2 | 2 | 1 | 1 | X | X | X | 3 | 1 | X | 1 | X | 1 | 1 | 1 | 1 | 1 | 1 |
| EF-111A | 1 | 1 | 2 | 2 | 2 | 1 | 1 | X | 3 | X | 3 | 1 | X | 1 | 1 | 1 | 1 | 1 | 1 | X | 1 |
| F-4G | 1 | 1 | 2 | 2 | X | 1 | 1 | 3 | 3 | X | 3 | 1 | X | 1 | 1 | 1 | 1 | 1 | 1 | 1 | 1 |
| F-15A | 1 | 1 | 2 | 2 | 1 | 1 | 1 | X | 3 | X | 3 | 1 | X | 1 | X | 1 | 1 | 1 | 1 | 1 | 1 |
| F-16A/B | 1 | 1 | 1 | 2 | 1 | 1 | 1 | X | 3 | X | 3 | 1 | X | 1 | X | 1 | 1 | 1 | 1 | 1 | 1 |
| FAC-X | 1 | 1 | 1 | 1 | 1 | 1 | 1 | X | 3 | 1 | 3 | 1 | X | 1 | 1 | 1 | 1 | 1 | 1 | X | 1 |
| FOI | 1 | 1 | 1 | 2 | 1 | 1 | 1 | X | 3 | X | 3 | 1 | X | 1 | X | 1 | 1 | 1 | 1 | 1 | 1 |
| RF-X | 1 | 1 | 1 | 1 | 1 | 1 | 1 | X | 3 | X | 3 | 1 | X | 1 | 1 | 1 | 1 | 1 | 1 | 1 | 1 |

1 - ROC, Avionics Planning Baseline, or similar Air Force planning document states installation requirement.

2 - Assumed requirement (based on AF "wants", unofficial requirements, or trends).

3 - Probable demodification.

X - No installation.

TABLE 9: CNI REQUIREMENTS [21, p. 2-17]

| Mission Phase: |
|---|
| Segment 1 - React |
| Segment 2 - Take off, accelerate, climb, turn to heading |
| Segment 3 - Climb and dash to intercept area, steer to achieve optimum attach position |
| Segment 4 - Acquire target, engage in combat |
| Segment 5 - Break off, regain altitude |
| Segment 6 - Inbound cruise |
| Segment 7 - Descend, approach, land |
| **Avionics Required:** |
| Segment 1 - Communications |
| Segment 2 - Communications, GPS, TACAN, Altimeter, CAS |
| Segment 3 - GPS, TACAN, Altimeter, JTIDS, CAS, IFF |
| Segment 4 - GPS, JTIDS, IFF |
| Segment 5 - GPS, Altimeter, JTIDS |
| Segment 6 - GPS, TACAN, Altimeter, JTIDS, CAS, ADF, IFF |
| Segment 7 - Communications, GPS, TACAN, JTIDS, ILS, CAS, ADF |

TABLE 10: AIR SUPERIORITY - AIR DEFENSE POINT INTERCEPT MISSION [8, p. 3-19]

| |
|---|
| Mission Phases:<br>Segment 1 - React<br>Segment 2 - Take off, accelerate, climb, turn to heading<br>Segment 3 - Rendezvous with prime mission aircraft<br>Segment 4 - Cruise to target area<br>Segment 5 - Intercept threat or descend and strafe<br>Segment 6 - Break off and escape<br>Segment 7 - Inbound cruise<br>Segment 8 - Descend, approach, land |
| Avionics Required:<br>Segment 1 - Communications<br>Segment 2 - Communications, GPS, TACAN, Altimeter, JTIDS, CAS<br>Segment 3 - Communications, GPS, TACAN, Altimeter, JTIDS, CAS<br>Segment 4 - GPS, JTIDS, IFF<br>Segment 5 - GPS, Altimeter, JTIDS, IFF<br>Segment 6 - GPS, JTIDS, IFF<br>Segment 7 - GPS, TACAN, Altimeter, JTIDS, CAS, ADF, IFF<br>Segment 8 - Communications, GPS, TACAN, JTIDS, ILS, CAS, ADF |

TABLE 11: AIR SUPERIORITY - ESCORT/INTERCEPT MISSION [8, p. 3-20]

| |
|---|
| Mission Phases:<br>Segment 1 - React<br>Segment 2 - Take off, accelerate, climb, turn to heading<br>Segment 3 - Dash to FEBA<br>Segment 4 - Dash to target area<br>Segment 5 - Attack<br>Segment 6 - Escape<br>Segment 7 - Inbound cruise<br>Segment 8 - Descend, approach, land |
| Avionics Required:<br>Segment 1 - Communications<br>Segment 2 - Communications, GPS, TACAN, Altimeter, JTIDS, CAS<br>Segment 3 - GPS, JTIDS, IFF<br>Segment 4 - GPS, Altimeter, JTIDS, IFF<br>Segment 5 - GPS, Altimeter, JTIDS, IFF<br>Segment 6 - GPS, JTIDS, IFF<br>Segment 7 - GPS, TACAN, Altimeter, JTIDS, CAS, ADF, IFF<br>Segment 8 - Communications, GPS, TACAN, JTIDS, ILS, CAS, ADF |

TABLE 12: ATTACK - DEFENSIVE STRIKE MISSION [8, pp. 3-20 & 3-21]

Mission Phases:

Segment 1 - React

Segment 2 - Take off, accelerate, climb, turn to heading

Segment 3 - Rendezvous

Segment 4 - Cruise to target area

Segment 5 - Dash to target

Segment 6 - Attack

Segment 7 - Escape

Segment 8 - Inbound cruise

Segment 9 - Descend, approach, land

Avionics Required:

Segment 1 - Communications

Segment 2 - Communications, GPS, TACAN, Altimeter, JTIDS, CAS

Segment 3 - Communications, GPS, TACAN, Altimeter, JTIDS, CAS

Segment 4 - GPS, Altimeter, JTIDS, IFF

Segment 5 - GPS, Altimeter, JTIDS, IFF

Segment 6 - GPS, Altimeter, JTIDS, IFF

Segment 7 - GPS, JTIDS, IFF

Segment 8 - GPS, TACAN, Altimeter, JTIDS, CAS, ADF, IFF

Segment 9 - Communications, GPS, TACAN, JTIDS, ILS, CAS, ADF

TABLE X: ATTACK - PREPLANNED ATTACK [21, p. 3-21]

Mission Phases:

Segment 1 - React

Segment 2 - Take off, accelerate, climb, turn to heading

Segment 3 - Cruise to loiter station

Segment 4 - Loiter

Segment 5 - Attack Number 1

Segment 6 - Random navigation at low altitude (CAS only)

Segment 7 - Attack Number 2 (CAS only)

Segment 8 - Regain altitude

Segment 9 - Loiter, coordinate follow-up strike (FAC only)

Segment 10 - Inbound cruise

Segment 11 - Descend, approach, land

*Avionics Required:*

Segment 1 - Communications

Segment 2 - Communications, GPS, TACAN, Altimeter, JTIDS, CAS

Segment 3 - GPS, Altimeter, JTIDS, IFF

Segment 4 - GPS, Altimeter, JTIDS, IFF

Segment 5 - GPS, Altimeter, JTIDS, IFF

Segment 6 - GPS, Altimeter, JTIDS, IFF

Segment 7 - GPS, Altimeter, JTIDS, IFF

Segment 8 - GPS, Altimeter, JTIDS, IFF

Segment 9 - GPS, Altimeter, JTIDS, IFF

Segment 10 - GPS, TACAN, Altimeter, JTIDS, CAS, ADF, IFF

Segment 11 - Communications, GPS, TACAN, JTIDS, ILS, CAS, ADF

TABLE 14: ATTACK - CLOSE AIR SUPPORT [21, p. 3-22]

| MISSION AREA | MISSION PROFILES |
|---|---|
| Air Defense/Superiority | Air Defense Point Intercept (ADPI)<br>Escort Intercept (EI) |
| Attack | Close Air Support (CAS<br>Forward Air Control-Interim CAS (FAC)<br>Defensive Strike, Volatile Target (DS)<br>Preplanned Deep Strike (PPS) |
| Cargo/Transport | Intertheater Logistics (ILT)<br>Intratheater STOL/CTOL (IST)<br>Tanker, Tactical/Airlift (TTA)<br>Tanker, Strategic (TS) |
| Strategic Bomber | Strategic Bomber, Penetration (SBP)<br>Strategic Bomber, Standoff (SBS) |

TABLE 15: MISSION PROFILES [4, p. 3-2]

project was completed in January 1980, and the report entitled ECM Scenarios for JTIDS/GPS/INS Integration Studies [22] is currently being printed. The information contained in this document sets the environment for the mission profiles needed to identify aircraft CNI requirements.

The impact analysis is actually two studies. The first considers GPS/JTIDS while the second will consider IFF, SINCGARS, and SEEK TALK. The first study which was recently completed was intended to define representative mission profiles, the communication/navigation environment, and the communication/navigation data requirements. Three baseline missions were considered: Close Air Support (CAS), Deep Interdiction (DI), and Air Defense Point Intercept (ADPI). Each was "analyzed to determine the navigation and communication performance requirements during each mission segment" [23, p. iii].

Figures 1-3 are from this report and identify the mission segments for each of the three baseline scenarios. Figures 4 and 5 present the communication requirements for CAS and ADPI missions as a function of the distance from the Forward Edge of the Battlefield (FEBA). Similar information for the DI mission is presented on page 3-7 of [23]. However, this material is classified. Sections 4 and 5 of [23] are also classified and, thus, have not been reviewed for this analysis. It is recommended that these sections and the classified portions of Section 3 be reviewed to determine their relevance to the MFBARS OIS and other future efforts.

The second impact analysis study concerning additional CNI systems is to be completed near the end of FY80. It is expected that it will be similar in structure to the first study. Since these additional systems will be part of ICNIA, it is recommended that the report from this project be reviewed by AAAD-3 as soon as it is made available.

3. Visual display research: Three studies [24, 25, 26] regarding visual display requirements completed for the Aerospace Medical Research Laboratory (AMRL) could provide a third data base for the OIS's CNI question. The two unclassified documents will be briefly reviewed here and in more detail in Section IV B of this report.

The McDonnell Aircraft study considered three mission types: Close Air Support (CAS), Air Interdiction (AI), and Counter Air (CA). These missions are briefly described within the report itself [24, p. 21-22]. Like the previous studies these missions are broken down into segments. However, the level of detail in this case is much greater. Table 16 lists the phases that are considered in the missions. Figures 9-11 of the McDonnell report [24, pp. 30-31] identify

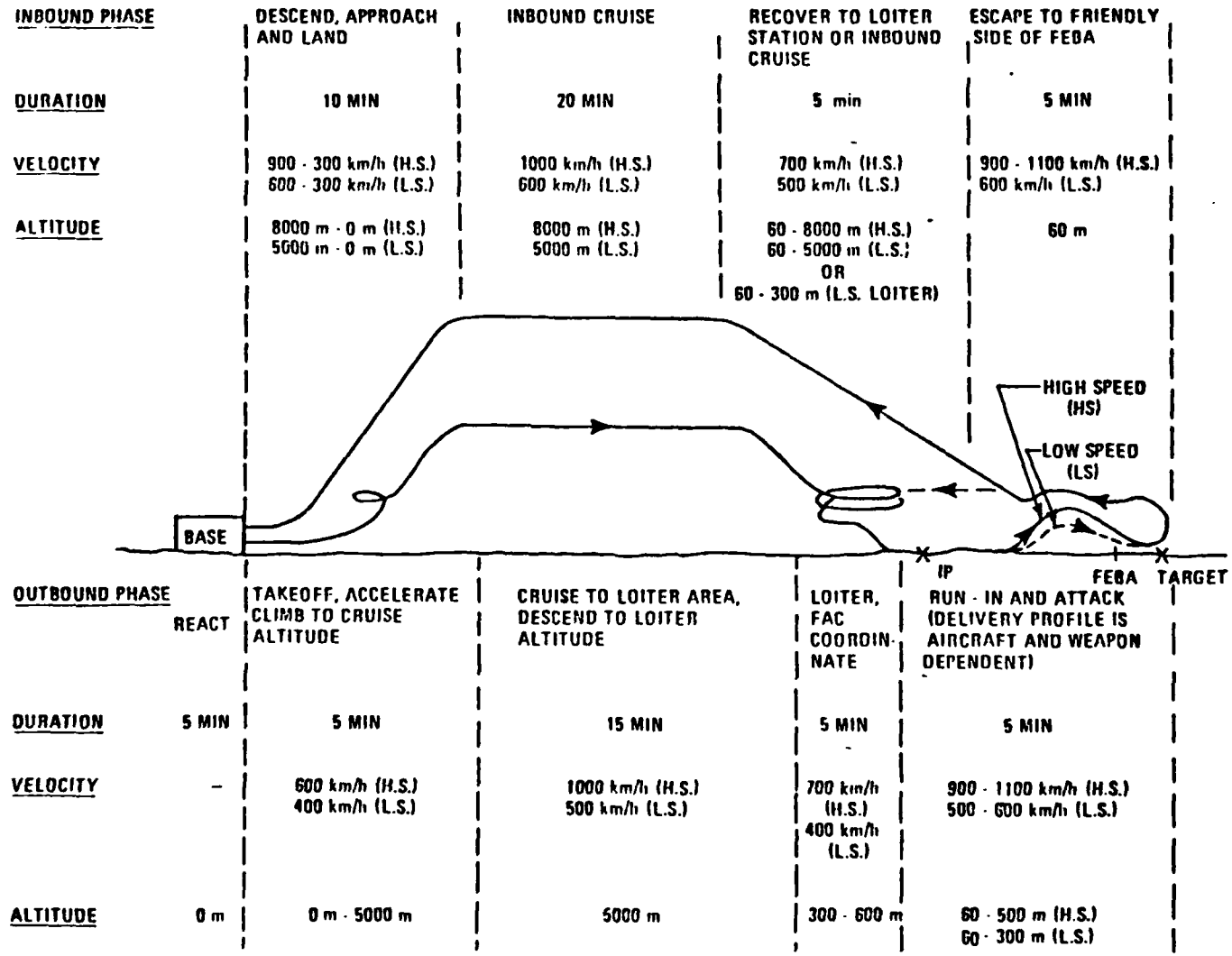



FIGURE 1: TYPICAL CLOSE AIR SUPPORT MISSION FLIGHT PROFILE [23, p. 2-2]

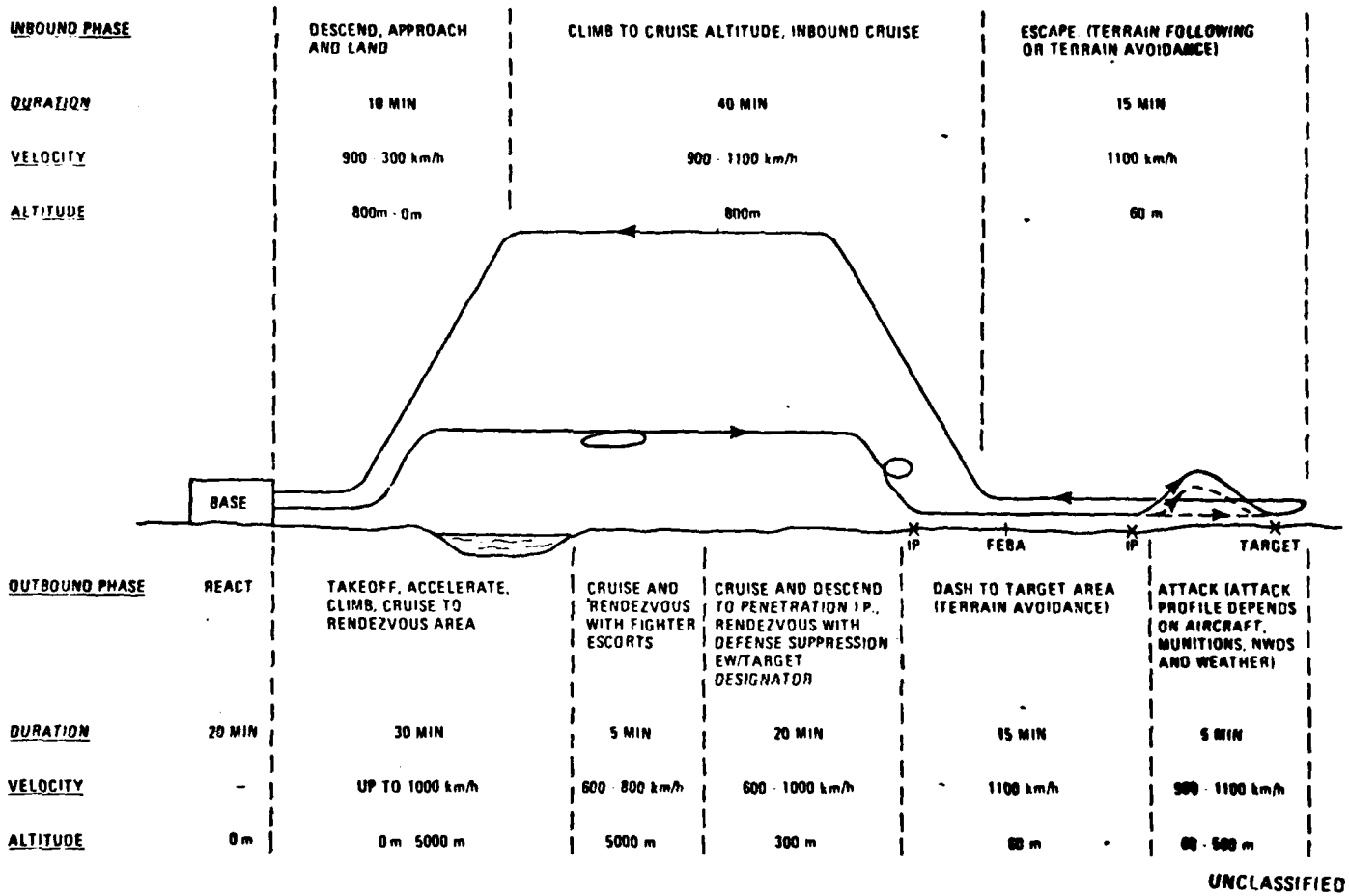



FIGURE 2: TYPICAL DEEP INTERDICTION MISSION FLIGHT PROFILE [23, p. 2-3]

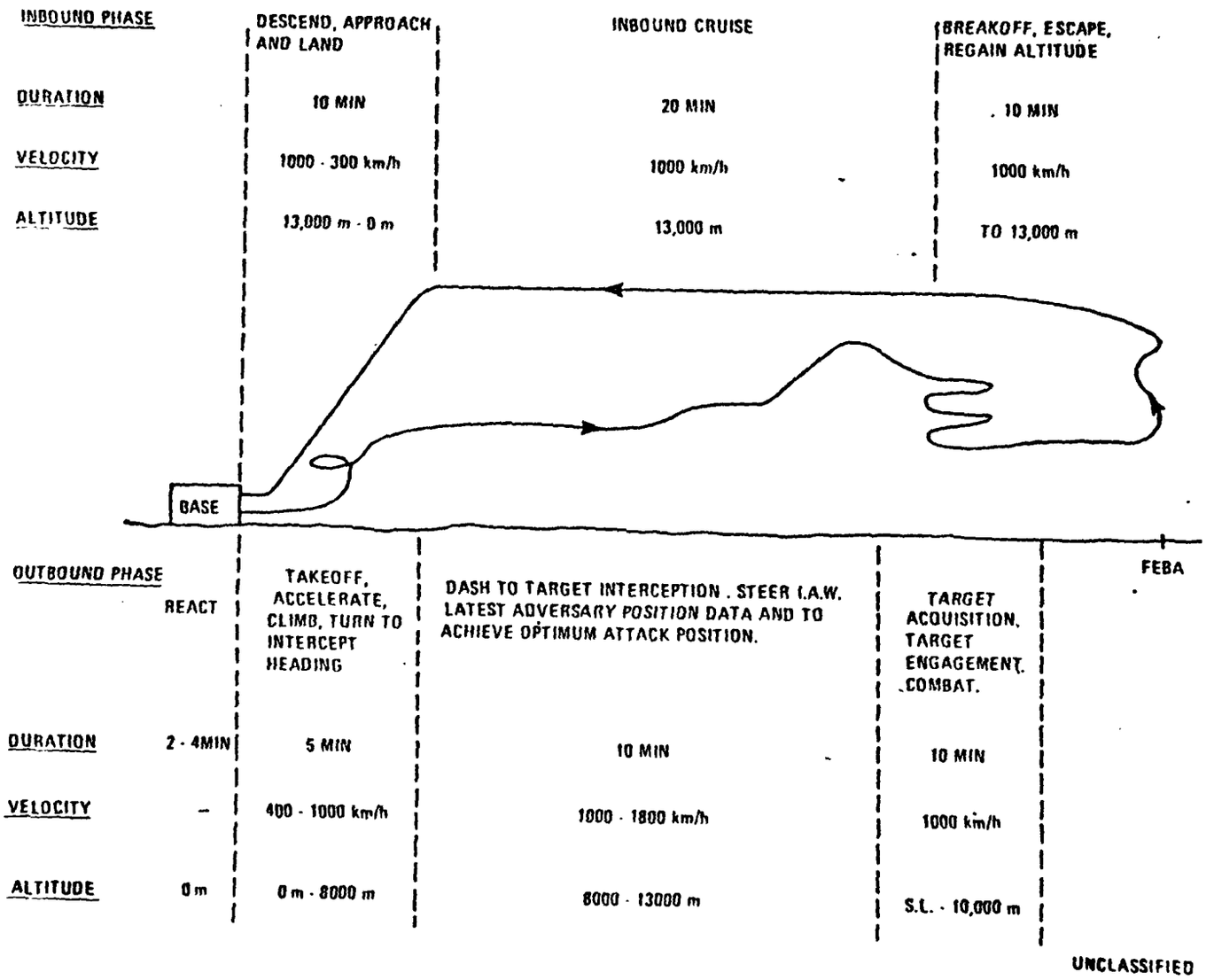



FIGURE 3: TYPICAL AIR DEFENSE POINT INTERCEPT FLIGHT PROFILE [23, p. 2-4]

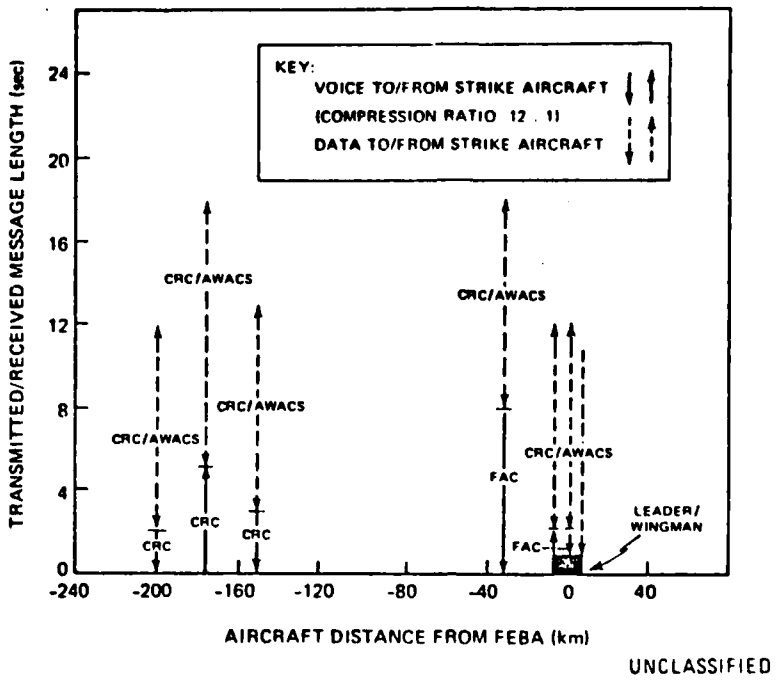



FIGURE 4: CAS AIRCRAFT COMMUNICATION REQUIREMENTS [23, p. 3-4]

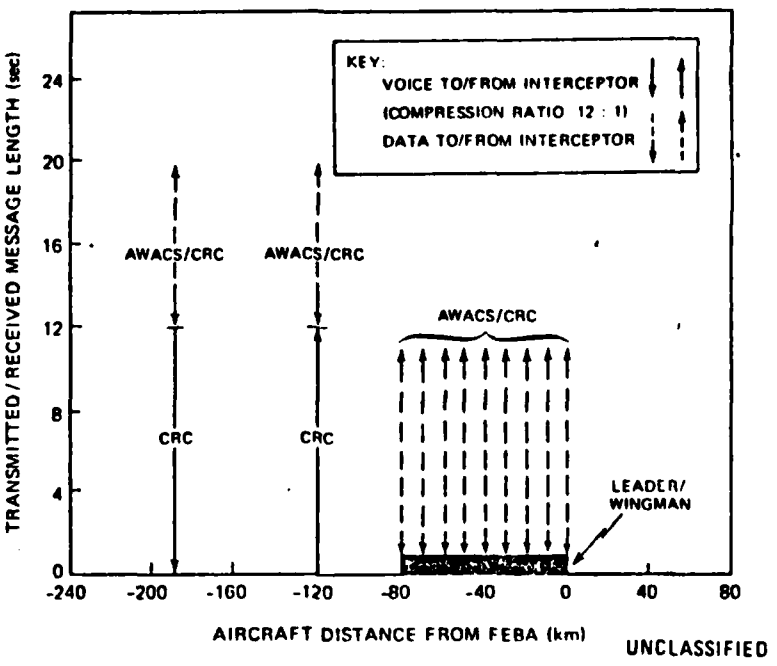



FIGURE 5: POINT INTERCEPT AIRCRAFT COMMUNICATION REQUIREMENTS [23, p. 3-10]

| |
|---|
| PREFLIGHT |
| Mission Planning |
| Preflight |
| Start and System Checks |
| Taxi |
| Arming |
| Takeoff |
| IN-FLIGHT |
| Climb to Level Off |
| Cruise |
| Loiter |
| Rendezvous and Air-to-Air Refueling (AAR) |
| Coordination |
| Mission Rendezvous |
| Penetration |
| Threat Warning |
| Detection |
| Location |
| Identification |
| Decision |
| Execution |
| Assessment |
| Termination |
| Egress |
| Cruise |
| Rendezvous and Air-to-Air Refueling (AAR) |
| Reengage |
| Return to Base |
| Descent |
| Approach |
| Landing |
| POST-FLIGHT |
| De-arm |
| Taxi |
| System Checks |
| Shutdown |
| Post Flight |
| Debrief |

TABLE 16: MISSION REQUIREMENTS: PHASES OF FLIGHT [24, p. 30]

which phases are relevant to the three scenarios. Appendix B [24, pp. 118-150] provides additional information describing the phases. Figures 25-27 [24, pp. 50-61] identify the crew information requirements for each of the phases. The information is categorized as required, frequently required, and additional value. Table 17 is a partial reproduction of one of these tables for the Close Air Support mission concerning communication and navigation information requirements. Other information requirements considered are listed in Table 18.

In reviewing the information requirements for the three missions, the report made the following observations [24, pp. 62-66]:

1. Time is one of the more important information requirements. Often airspeeds are used to compute time values and are not necessarily important in themselves.
2. Much information need not be displayed unless there is an emergency.
3. Information is needed prior to an actual event to assist in preparation.
4. Low and/or slow flight requires more information.
5. There is a need to interface the briefing room with the crew station.
6. The more uncertain a mission is, the more information flexibility is required.
7. More time-to-type information is required.

The Honeywell study [25] is a continutation of the study described above. They also considered three mission scenarios which are labeled as Close-Air Support (CAS), Deep Strike (DS), and Battlefield Interdiction (BI). These scenarios are detailed within the report [25, pp. 35-49]. Included in these specifications are possible targets, threats, weather, response time, flight profile, and weapons. The missions are divided into their phases, and functions utilized during these phases are identified. Table 19 is adapted from Figure 4 [25, p. 38] of the Honeywell report. Similar analyses are done for BI and CAS missions [25, pp. 42, 46]. In addition, the study does detailed task analyses of the pilot work load during various mission segments with two different cockpit designs [25, pp. 132-159, 176-202]. Tables 20 and 21 are examples of this type of analysis. This work will also be more fully analyzed in Section IV B.

4. Conclusion: The CNI requirements question can be subdivided into the following: (1) What CNI functions are used in a mission? (2) When are these functions used? In part they have been answered by the ARINC requirements study [21]. Tables 10-14 answer both of these questions for five mission scenarios. What remains is an expansion of this approach to additional scenarios and an up-dating

| | PRE-FLIGHT | | | | | IN-FLIGHT | | | | | | | | | | | | | | | | | | | | | | | POST-FLIGHT | | | | |
|---|---|---|---|---|---|---|---|---|---|---|---|---|---|---|---|---|---|---|---|---|---|---|---|---|---|---|---|---|---|---|---|---|---|
| | Mission Planning | Preflight | Start & System Checks | Taxi | Arming | Takeoff | Climb to Level Off | Cruise | Loiter | Rendezvous & AAR | Coordination | Mission Rendezvous | Penetration | Threat Warning | Detection | Location | Identification | Decision | Execution | Assessment | Termination | Egress | Cruise | Rendezvous & AAR | Reengage | Return to Base | Descent | Approach | Landing | De-Arm | Taxi | System Checks | Shutdown | Post Flight | Debrief |
| *COMMUNICATIONS* | | | | | | | | | | | | | | | | | | | | | | | | | | | | | | | | | | |
| Controlling Agency | 1 | | 2 | 1 | 1 | 1 | 2 | 2 | 2 | 1 | 1 | 1 | 2 | 2 | 1 | 1 | 1 | 1 | 1 | 1 | 1 | 1 | 2 | 1 | 1 | 1 | 1 | 1 | 1 | 1 | | | | |
| Aircraft Call Sign | 1 | | 1 | 1 | 2 | 2 | 2 | 2 | 2 | 1 | 1 | 1 | 2 | 1 | 2 | 2 | 2 | 2 | 2 | 2 | 2 | 2 | 2 | 1 | 1 | 2 | 2 | 2 | 2 | 1 | 2 | 2 | | |
| Authentication | 1 | | | | | | | | | 1 | 1 | 1 | | | | | | | 1 | | | | | 1 | 1 | 1 | | | | | | | | | |
| IFF/SIF | 1 | | 1 | 2 | | 1 | 1 | 1 | 1 | 1 | 1 | 1 | 2 | | | | | | | | | 1 | 1 | 1 | 1 | 1 | 1 | 1 | 1 | | | | | |
| Clearances | 1 | | 1 | 1 | 1 | 1 | 1 | 1 | 1 | 1 | 1 | 1 | 1 | 1 | 1 | 1 | 1 | 1 | 1 | 1 | 1 | 1 | 1 | 1 | 1 | 1 | 1 | 1 | 1 | 1 | 1 | 1 | 1 | |
| Secure Communication | | | | | | | | | | 1 | 1 | 1 | 1 | 1 | 1 | 1 | 1 | 1 | 1 | 1 | 1 | | | 1 | | | | | | | | | | |
| Frequencies | 1 | | 1 | 1 | 1 | 1 | 1 | 1 | 1 | 1 | 1 | 1 | 1 | 1 | 1 | 1 | 1 | 1 | 1 | 1 | 1 | 1 | 1 | 1 | 1 | 1 | 1 | 1 | 2 | 2 | 2 | 2 | | |
| Intercom | | | | | | | | | | | | | | | | | | | | | | | | | | | | | 2 | 2 | 2 | 2 | | |
| Navigation Aids Identifiers | | | | | | | | 2 | | | | | | | | | | | | | | | 2 | | | | | | | | | | | |
| Mission Reports | | | | | | | | 2 | 2 | 2 | 1 | 1 | 2 | 2 | 2 | 2 | 2 | 2 | 2 | 1 | 2 | 1 | 2 | 1 | 1 | 2 | 2 | 2 | 2 | | | | | 2 |
| *NAVIGATION* | | | | | | | | | | | | | | | | | | | | | | | | | | | | | | | | | | |
| *Course* | 1 | | | | | 1 | 1 | 1 | 1 | 1 | 1 | 1 | 1 | 1 | 1 | 1 | 1 | 1 | 1 | 1 | 1 | 1 | 1 | 1 | 1 | 1 | 1 | 1 | | | | | | 1 |
| Heading | | | 2 | 2 | | 1 | 1 | 1 | 1 | 1 | 1 | 1 | 1 | 1 | 1 | 1 | 1 | 1 | 1 | 1 | 1 | 1 | 1 | 1 | 1 | 1 | 1 | 1 | | 2 | 1 | | | 2 |
| Flight Path | | | | | | 1 | 1 | 1 | 1 | 1 | 1 | 1 | 1 | 1 | 1 | 1 | 1 | 1 | 1 | 1 | 1 | 1 | 1 | 1 | 1 | 1 | 1 | 1 | | | 2 | | | |
| Pitch Steering | | | 2 | | | 1 | 1 | 1 | 1 | 1 | 1 | 1 | 1 | 1 | 1 | 1 | 1 | 1 | 1 | 1 | 1 | 1 | 1 | 1 | 1 | 1 | 1 | 1 | | | 2 | | | |
| Bank Steering | | | 2 | | | 1 | 1 | 1 | 1 | 1 | 1 | 1 | 1 | 1 | 1 | 1 | 1 | 1 | 1 | 1 | 1 | 1 | 1 | 1 | 1 | 1 | 1 | 1 | | | 2 | | | |
| Glide Scope | | | 3 | 2 | | 3 | | | | | | | | | | | | | | | | | | | | 2 | 1 | 1 | | | 2 | | | |
| *Localizer* | | | 3 | 3 | | 3 | | | | | | | | | | | | | | | | | | | | 2 | 1 | 1 | 1 | | 2 | | | |
| Distance to Destination | 1 | | | 2 | | 3 | 1 | 1 | 1 | 1 | 1 | 1 | 1 | 1 | 1 | 1 | 1 | 1 | 1 | 1 | 1 | 1 | 1 | 1 | 1 | 1 | 1 | 1 | | | 2 | | | |
| Bearing to Destination | | | | 2 | | 1 | 1 | 1 | 1 | 1 | 1 | 1 | 1 | 1 | 1 | 1 | 1 | 1 | 1 | 1 | 1 | 1 | 1 | 1 | 1 | 1 | 1 | 1 | | | 2 | | | |
| *Destination Selected* | 1 | | 2 | 2 | | 1 | 1 | 1 | 1 | 1 | 1 | 1 | 1 | 1 | 1 | 1 | 1 | 1 | 1 | 1 | 1 | 1 | 1 | 1 | 1 | 1 | 1 | 1 | | | 2 | | | |
| Marker Beacon | | | | | | | | | | | | | | | | | | | | | | | | | | | 1 | 1 | | | 2 | | | |
| Present Position | 1 | | 1 | 2 | | | 1 | 1 | 1 | 1 | 1 | 1 | 1 | 1 | 1 | 1 | 1 | 1 | 1 | 1 | 1 | 1 | 1 | 1 | 1 | 1 | 1 | 1 | | | 1 | | | |
| Destination Offsets | 1 | | | 2 | | | 1 | 1 | 1 | 2 | 2 | 1 | 1 | 1 | 1 | 1 | 1 | 1 | 1 | 1 | 1 | 1 | 1 | 2 | 1 | 1 | 1 | 1 | | | 2 | | | |
| Magnetic Variation | 1 | | 1 | 3 | | | | | | | | | | | | | | | | | | | | | | | | | | | 2 | | | |
| Coordinates | | | 1 | 2 | | | | | | | | | | | | | | | | | | | | | | | | | | | 2 | | | |
| Navigation Point | 1 | | 1 | 2 | | | 1 | 1 | 1 | 1 | 1 | 1 | 1 | 1 | 1 | 1 | 1 | 1 | 1 | 1 | 1 | 1 | 1 | 1 | 1 | 1 | 1 | 1 | | | 1 | | | 1 |
| Planned Route of Flight | 1 | | 1 | 2 | | 1 | 1 | 1 | 1 | 1 | 1 | 1 | 1 | 1 | 1 | 1 | 1 | 1 | 1 | 1 | 1 | 1 | 1 | 1 | 1 | 1 | 1 | 1 | | | 1 | | | 1 |
| Holding Patterns | 2 | | | | | | | | 1 | 1 | | 1 | | | | | | | | | | | | | | 2 | 2 | 2 | 2 | | | | | | |
| Minimum Descent Altitude | | | | | | | | | | | | | | | | | | | | | | | | | | 3 | 2 | 1 | 1 | | | | | | |
| Missed Approach Point | | | | | | | | | | | | | | | | | | | | | | | | | | 3 | 2 | 1 | 1 | | | | | | |

1 = Required  2 = Frequently Required  3 = Additional Value

TABLE 17: CREW/INFORMATION REQUIREMENTS - CLOSE AIR SUPPORT [24]

| | |
|---|---|
| **Administration** | Time to Climb |
| Formation Call Signs | Time to Go |
| Flight Position | Control Times |
| Aircraft Assignment | Landing Time |
| Parking Spot | Rendezvous Time |
| Spare Procedures | Enroute Times |
| Aircraft Configuration | Time of Day |
| Frequencies | |
| IFF/SIF Procedures | **Caution and Warning Systems** |
| Weather | Master Caution |
| Regulations | Configuration Warning |
| | Operating Limitation Warning |
| **Airfield Status** | Primary Systems Fail |
| Airfield Description | Fuel Low |
| Landing Runway | Oxygen Low |
| Runway Length | Environmental Control System Warning |
| Barriers | Autopilot Disengaged |
| Approaches | Avionics Malfunctions |
| Missed Approach Instructions | Altitude Low |
| Airfield Elevation | Airspeed Low |
| Decision Height | |
| Parking Area | **Miscellaneous** |
| Taxi Routes | Fuel Off Loading |
| Arming Area | Gross Weight |
| De-Arming Area | Autopilot Submodes |
| Alternate Field | Aircraft Lighting |
| **Time** | **Flight Aids** |
| Briefing Time | Normal Checklists |
| Station Time | Emergency Checklists |
| Start Engine Time | Procedures |
| Flight Check-In-Time | Approach Aids |
| Taxi Time | Emergency Airfields |
| Takeoff Time | Personal Techniques |
| Air Refueling Contract Time | |
| Time on Target | |

TABLE 18a: FLIGHT INFORMATION REQUIREMENTS [24, pp. 50-53]

| |
|---|
| Altitude |
| Altitude Above Ground Level (AGL) |
| Altitude Above Mean Sea Level |
| Altimeter Setting |
| Command Altitude |
| Target Elevation |
| Minimum Enroute Safe Altitude |
| Terrain Altitude |
| Terrain Clearance |
| Velocity |
| Vertical Velocity |
| Rotation Speed |
| Takeoff Speed |
| Check Speeds |
| Climb Speed (Normal) |
| Climb Speed (Maximum Performance) |
| Maximum Range Cruise |
| Maximum Endurance |
| Maximum Range Descent |
| Approach Speed |
| Landing Speed |
| Maximum Safe Speed |
| Minimum Controllable Speed |
| Limitations |
| Corner Speed |
| True Airspeed |
| Angle of Attack (AOA) |
| Ground Speed |
| Wind Velocity and Direction |
| Turn Rate |
| Best Rate of Climb |
| Best Angle of Climb |
| Mach Number |
| Selected Speed |
| Emegency Airspeeds |
| Weapons Release Speeds |
| IAS |
| Systems |
| Fuel Flow |
| Fuel Remaining |
| Fuel Required to Destination |
| Fuel Management |
| Hydraulic |
| Electrical |
| Oxygen |
| Engine |
| Penetration Aids |
| AI Warning |
| SAM Warning |
| Threat Avoidance |
| Disposable Status |
| ECM Status |
| ECM Tactics |
| Mutual Support |
| Special Threat |
| Weapons Information |
| Ballistics |
| Weapons Envelope |
| Weapons Ready |
| Weapons Release |
| Weapons Remaining |
| Weapons Impact |
| Weapons Selected |
| Bombs Fall Time/Impact Point |
| Weapons Options Selected |

TABLE 18b: FLIGHT INFORMATION REQUIREMENTS [24, pp. 50-53]

| Weapons Delivery Selected |
|---|
| <u>Air-to-Air Target</u><br>Range<br>Bearing<br>Overtake<br>Altitude Differential<br>Target Turn Rate<br>Target Attitude<br>Identification<br>Target Altitude<br>In Range<br>Aim Point Breakaway |
| <u>Air-to-Ground Target Acquisition</u><br>Target Range<br>Target Bearing<br>Positive Target ID<br>Aim Point<br>Break Away (Pullup) |

TABLE 18c: FLIGHT INFORMATION REQUIREMENTS [24, pp. 50-53]

| Mission Phase | Functions |
|---|---|
| Take-Off and Accelerate to Optimum Climb | A/C Control, Visual Observation, Traffic Coordination |
| Climb to Cruise Altitude | A/C Control, Navigation Traffic Coordination |
| Rendezvous with Other Aircraft on Mission | A/C Control, Visual/ Sensor Search, Mission Coordination |
| Cruise | A/C Control, Navigation, Formation Flying, Threat Surveillance |
| Climb to Dash Altitude | A/C Control, Navigation, Formation Flying, Threat Surveillance |
| High Speed Ingress | A/C Control, Navigation, Formation Flying, Threat Surveillance |
| Target Search Using SAR | A/C Control, Navigation, Coord. Attack, Threat Surveillance, SAR Data Processing, Target Identification and Track |
| Weapon Delivery Using Boost/Glide Rocket | A/C Control, Designate Target, Launch Rocket, Threat Evaluation, Threat Designation, Launch Armament, Target Track Bomb Damage Assessment, Coordinate Attack |
| High Speed Withdrawal | A/C Control, Navigation, Threat Surveillance, Formation Flying |
| Descend to Cruise Altitude | A/C Control, Navigation, Threat Surveillance, Formation Flying |
| Cruise | A/C Control, Navigation, Threat Surveillance, Formation Flying |
| Descend to Air Field | A/C Control, Navigation, Traffic Coordination |
| Land | A/C Control, Visual Observation, Traffic Coordination, Landing Aid Operation |

TABLE 19: DEEP STRIKE MISSION PROFILE [17, p. 38]

Mission: Deep Strike

Phase: Ingress

1. Verify crossing FEBA.
2. Select next steerpoint.
3. Disengage autopilot.
4. Fly steering commands.
5. Monitor flight parameters.
6. Engage autopilot.
7. Turn TACAN to receive.
8. Turn radar to auto.
9. Verify threat warning system operational.
10. Verify ECM pod operational.
11. Check dispenser system status.
12. Adjust brightness of threat display.
13. Monitor external environment.
14. Monitor engine instruments.
15. Monitor fuel status.
16. Monitor navigation data.

TABLE 20: PILOT TASKS WITH F-16 SYSTEM CONCEPT [25, pp. 132-134]

| |
|---|
| **Mission: Deep Strike** |
| Phase: Ingress |
| 1. Verify crossing FEBA. |
| 2. Confirm waypoint passage. |
| 3. Monitor steering commands. |
| 4. Monitor flight parameters. |
| 5. Turn TACAN to receive. |
| 6. Turn radar to standby. |
| 7. Verigy threat warning system operational. |
| 8. Verify ECM system operational. |
| 9. Check dispenser system status. |
| 10. Adjust brightness of threat display. |
| 11. Monitor external environment. |
| 12. Monitor engine data. |
| 13. Monitor fuel status. |
| 14. Monitor navigation data. |

TABLE 21: PILOT TASKS WITH ATA SYSTEM CONCEPT [7, pp. 176-177]

of the ARINC effort.

This type of effort could be performed in-house. The SPAN [4] mission scenarios are available and were used in the AAAN effort [23]. With the ARINC results as a model, new CNI requirement tables could be developed taking into consideration the two AAAN impact analyses and the AAAN threat analysis [22].

This document will have design implications for ICNIA and should be made available to the System Definition contractors. The results will influence the hardware requirements and assist in analyzing failure modes. Thus, this effort will also impinge on the reliability and availability analyses.

It is assumed that this type of in-house effort will be sufficient to answer the CNI questions. If more detailed information about CNI requirements is deemed necessary, then the AMRL studies [24, 25, 26] provide a starting point. It is not expected that this will be required.

B. Pilot - Control/Display (C/D) Interface: Three of the seven key issues of the OIS concern the pilot interface with the C/D equipment. Thus, the issues of pilot saturation, pilot automation, and C/D requirements are evaluated together. Approaches to modeling this interface are addressed in Appendix A.

1. Visual display research: The visual display study [24] performed by McDonnell Aircraft for AMRL was, in part, concerned with display technology. It "explored the mission requirements, aircrew functions, current and projected weapons, crew information requirements and display technologies applicable to the 1985-1990 attack/fighter missions" [24, p. 13]. As presented previously, this study analyzed the Close Air Support, Air Interdiction, and Counter Air missions to determine their crew information requirements. This Section concentrates on the reports conclusions concerning C/D technology and requirements.

McDonnell Aircraft considered and evaluated seven display technologies: cathode ray tubes (CRTs), liquid crystals (LCs), plasma devices (PLD), light emitting diodes (LEDs), electroluminescence (EL), electro/mechanical devices (EMD), and laser displays (LD). These technologies were evaluated on the following criteria: resolution, brightness, contrast, display size, color, power requirements, thickness, weight, environment, aspect viewing, time constants, storage/refresh, reliability/maintainability, and technological status [24, p. 88]. Based on this evaluation the following options were identified for investigation:

> Option 1 - The cathode ray tube...is considered the first selection... It is expected that the CRT will retain its preeminence into 1985-1990 time period...

Option 2 - The plasma flat display panel is the leading contender to replace the CRT in the near term (0 to 5 years)...

Option 3 - Liquid crystal displays (LCD), while presented as a second choice to replace a CRT, may in fact become the first military cockpit replacement for a CRT as a result of the momentum generated by military funding of liquid crystal display development

Option 4 - Electroluminescence displays, with thin-film-transistor (TFT) picture elements, although considered speculative, are selected as a long-term replacement for the CRT [24, p. 89].

In addition to these technology options, two C/D configurations were recommended for further study [24, pp. 101-102].

The evaluation process was continued in the follow-up Honeywell report [25]. "This study demonstrates via example a methodology which will aid the cockpit designer in evolving and evaluating candidate integrated display options for advanced fighter aircraft" [24, p. 1]. This is a paper and pencil approach based on human task analysis. A result of this research was the development of an alternative system concept, the Advanced Technology Aircraft (ATA). The ATA cockpit configuration is shown in Figure 6.

An interesting aspect of this study is the data base they established for their analysis. One topic area covered in the data base accumulation was the projected post-1985 technology state-of-the-art options pertaining to cockpit synthesis and integration. A very briefly annotated outline of this assessment is presented below. More detail concerning this topic can be found in [25, pp. 61-109].

A. Display/Control Concepts
   1. Advanced Integrated Display Systems (AIDS) - A Naval program intended to integrate C/D equipment in post-1980 aircraft.
   2. Digital Avionics Information System (DAIS).
   3. F-18 Aircraft - This fighter/attack aircraft uses an AIDS type C/D configuration.
   4. Tactile Displays - These techniques include air jets, electromechanical vibrators, and electrodes. The pilot's anti-g suit holds the most promise for use as a tactile display.
   5. Virtual Image Display (VID).

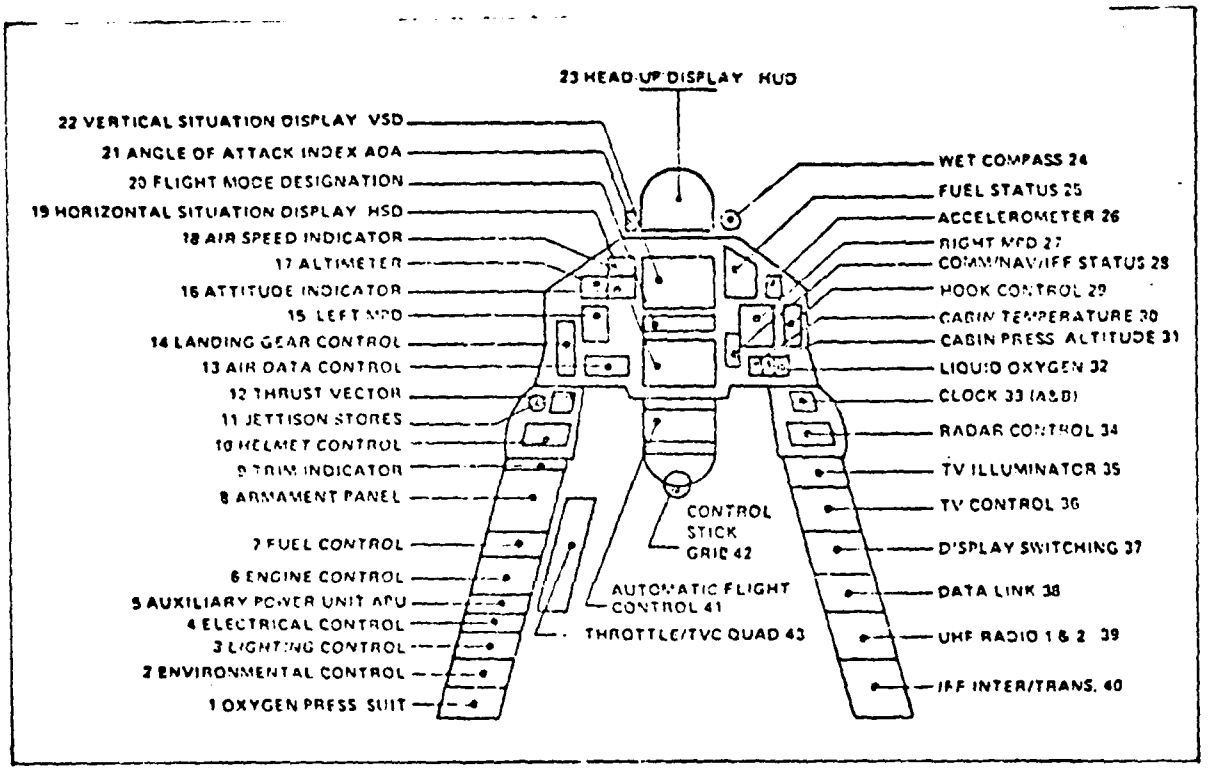



FIGURE 6: AIDS SINGLE-SEAT COCKPIT LAYOUT [25, p. 171]

B. Control Technology

1. Hands-on - Throttle-and-Stick (HOTAS) - Switches are placed on the stick and throttle to allow pilot control of various systems with minimal eye and hand movements.
2. Integrated Control System (ICS).
3. Visually Activated Switching System (VASS).

C. Avionics Concepts/Systems

1. Navigation Equipment (GPS, JTIDS, LORAN, INS, TACAN, TERCOM, MICRAD).
2. Communication (UHF, VHF/AM, VHF/FM, HF, JTIDS, IFF/SIF).
3. Electronic Warfare (EW) Systems.
4. Sensors and Target Acquisition Techniques.
5. Flight Control Systems.
6. Fire Control Systems.

The two reports discussed in this subsection are part of an on-going effort at AMRL. A continuation of the studies described above is currently in the planning stages. A draft statement of work has recently been completed for a project entitled "Fighter/Attack Crew Enhancement Study" [27]. The missions of concern in this study are Close Air Support, Air Interdiction and Counter Air in adverse environments. The two time periods of primary interest are 1985-1990 and 1990-1995. The study itself "will provide design techniques for configuring advanced cockpit alternatives at early stages of pre-design, apply those techniques in evolving design integration features to enhance tactical aircrew effectiveness for post-1985 fighter/attack missions" [27, p. 1].

2. Workload analysis: The concern over crew workload has in part been the driving force behind the studies described in the previous subsections. Other examples of this concern over crew workload are [28, 29, 30]. Thus, this effort to alleviate workload through system design is not new or unique to the MFBARS project. In fact, even in 1947, C/D configuration was considered a cause of many pilot errors [31]. There is, then, a rather substantial body of literature concerned with this question of workload and information saturation. A program is currently underway under the auspices of AMRL to develop "a standard technology for evaluating man-machine workload" [32]. The study includes the development of workload measures and a neuropsychological test battery. In addition, a workload task has been developed using the pilot's communications during F-16 air-to-air and A-10 air-to-ground missions. This work has been documented in a System Research Laboratory technical report entitled Tactile Communications Workload Tasks for R&D

Simulations, January, 1980 [32]. The workload program is to be completed at the end of FY84.

3. DAIS: The Digital Avionics Information System (DAIS) Program provides a third data base with which MFBARS should be consistent. The documentation associated with DAIS is rather substantial especially in the C/D area. Reference [33] is an annotated bibliography of the documents comprising the DAIS formal specification structure. A portion of the DAIS literature is discussed below.

DAIS has four principal elements:

1. A set of sensors that provide input data;
2. An information data bus that distributes information through the vehicle in a common format;
3. An information-processing system that performs data processing and storage; and
4. An information-presentation and control system that provides the crew all the information needed to conduct a mission in a timely fashion and also gives warning of any 'out-of-normal' conditions [34].

It is the last element that most directly applies to the interface question. An example of the C/D effort which was a part of DAIS is [35].

The DAIS Definition Study defined the core elements of the system which "consisted of processor ensemble, controls/displays, information transfer system, and software" [35, Abstract]. The study considered the Close Air Support and Air Superiority mission scenarios. The missions were defined; the flight segments identified; and the required avionic functions were listed. See Tables 22 and 23. These functions were partitioned into six avionic subsystems: Navigation and Weapon Delivery, Mission and Traffic Control, Instruments and A/C Systems, Penetration Aids, Armament Systems, and Controls and Displays [35, p. 27]. The report shows the controls and displays necessary to provide the pilot-machine interface for the other five subsystems for the two general mission scenarios. See Table 24.

The control and display requirements were analyzed in order to develop a simplified set of cockpit controls and displays. The following guidelines were used in developing the cockpit concept:

1. Pilot's role of systems manager.
2. Transition low-risk display technology to advanced displays.
3. Compatibility with DAIS redundancy approach.
4. Use separate imagery and status displays.
5. Use separate keyboard and functional controls.
6. Dedicated controls for flight safety.
7. Automated functions with manual override retained.

| Close Air-Support | Time | Ceiling | Visibility | Base | Terrain | Distance To Target (nmi) | Target | Defense Level | FAC Position | No. A/C | Flight Segments 1 | 2 | 3 | 4 | 5 | 6 | 7 | 8 | 9 | 10 | 11 | 12 | 13 |
|---|---|---|---|---|---|---|---|---|---|---|---|---|---|---|---|---|---|---|---|---|---|---|---|
| Preplanned | Day | High | High | MOB | Mt. | 150-200 | Tanks | High | Surface | 6 | X | X | X | X | X | X | X | X | X | X | X | X | X |
| Immediate | Day | Low | Low | SOB | Hills | 100-150 | Trucks | Low | Air | 4 | X | X | X | X | X | | | X | | X | X | X | X |
| Immediate | Night | High | High | FOB | Flat | 50-100 | Pers. | Med | Air | 4 | X | | | X | | | | X | | | X | | X |
| Preplanned | Night | M. Low | M. Low | MOB | Woods | 150-200 | Launcher | High | Surface | 2 | X | X | | X | X | | X | X | X | X | X | X | X |
| Immediate/Self-Defense | Dark | High | High | MOB | Hills | 150-200 | Bunker | High | -- | 2 | X | X | | X | X | | X | X | X | | X | X | X |
| Preplanned/Self-Defense | Day | Low | Low | MOB | Flat | 150-200 | Pers. | Med | -- | 4 | X | X | | X | X | X | | X | X | X | X | X | X |
| Preplanned EW | Night | High | Low | MOB | Hills | 150-200 | AA | High | -- | 2 | X | X | | X | X | | X | X | X | X | X | X | X |
| Air Superiority | | | | | | | | | | | | | | | | | | | | | | | |
| Fighter Sweep | Day | High | Med | MOB | -- | 150-200 | A/C | -- | -- | 6 | X | X | X | X | | X | X | X | X | | X | X | X |
| Escort | Day | Low | High | MOB | -- | 150-200 | A/C | -- | -- | 3 | X | X | X | X | | X | | X | | | X | X | X |
| Combat Air Patrol | Day | Med | Med | MOB | -- | 150-200 | A/C | -- | -- | 4 | X | X | X | X | X | X | | X | | | X | X | X |
| Air Defense | Day | High | High | FOB | -- | 50-100 | A/C | -- | -- | 4 | X | X | | | | | | X | | | | X | X |
| Air to Ground | Day | High | High | MOB | Flat | 150-200 | Trucks | -- | -- | 6 | X | X | X | X | X | | X | X | X | X | X | X | X |

*Flight Segments

1 Preflight and Takeoff
2 Climb after Takeoff
3 Rendezvous
4 Cruise Outbound
5 Descend
6 Loiter
7 Dash to Target
8 Combat
9 Dash from Target
10 Climb after Dash
11 Cruise to Base
12 Descend to Land
13 Land and Post Flight

MOB = Main Operations Base
FOB = Forward Operations Base
SOB = Satellit Operations Base

TABLE 22: CLOSE AIR-SUPPORT AND AIR SUPERIORITY SCENARIOS [35, pp. 23-24]

CAS FLIGHT SEGMENT*

| Functions | 1 | 2 | 3 | 4 | 5 | 6 | 7 | 8 | 9 | 10 | 11 | 12 | 13 |
|---|---|---|---|---|---|---|---|---|---|---|---|---|---|
| Navigation | X | X | X | X | X | X | X | X | X | X | X | X | X |
| Navigation Fix | | | | X | | | | X | | | X | | |
| Communications | X | | X | X | X | X | X | X | X | X | X | X | X |
| Flight Control | X | X | X | X | X | X | X | X | X | X | X | X | X |
| Air Data | X | X | X | X | X | X | X | X | X | X | X | X | X |
| Power Managements | X | X | X | X | X | X | X | X | X | X | X | X | X |
| Display/Control | X | X | X | X | X | X | X | X | X | X | X | X | X |
| Cent. Int. Test | X | X | X | X | X | X | X | X | X | X | X | X | X |
| EW/ECM | | | | | X | X | X | X | X | | | | |
| Target Acquisition | | | | | | | X | X | | | | | |
| Weapon Delivery | | | | | | | | X | | | | | |
| Damage Assessment | | | | | | | | X | X | | | | |
| Terrain Following | | | | | | | X | X | X | | | | |
| Stores Management | | | | | | | | X | | | | | |
| Landing Aids | | | | | | | | | | | | X | X |

AS FLIGHT SEGMENT*

| Functions | 1 | 2 | 3 | 4 | 5 | 6 | 7 | 8 | 9 | 10 | 11 | 12 | 13 |
|---|---|---|---|---|---|---|---|---|---|---|---|---|---|
| Navigation | X | X | X | X | X | X | X | X | X | X | X | X | X |
| Navigation Fix | | | | X | | | | | | | X | | |
| Communications | X | | X | X | X | X | X | X | X | X | X | X | X |
| Flight Control | X | X | X | X | X | X | X | X | X | X | X | X | |
| Air Data | X | X | X | X | X | X | X | X | X | X | X | X | X |
| Power Management | X | X | X | X | X | X | X | X | X | X | X | X | X |
| Energy Management | X | X | X | X | X | X | X | X | X | X | X | X | X |
| Display/Control | X | X | X | X | X | X | X | X | X | X | X | X | X |
| Cent. Int. Test | X | X | X | X | X | X | X | X | X | X | X | X | X |
| EW/ECM | | | | | X | X | X | X | X | | | | |
| Target Acquisition | | | | | | | X | X | | | | | |
| Weapon Delivery | | | | | | | | X | | | | | |
| Stores Management | | | | | | | | X | | | | | |
| Landing Aids | | | | | | | | | | | | X | X |

*FLIGHT SEGMENTS

| | | |
|---|---|---|
| 1 Preflight and takeoff | 5 Descend | 9 Dash from target |
| 2 Climb after takeoff | 6 Loiter | 10 Climb after dash |
| 3 Rendezvous | 7 Dash to target | 11 Cruise to base |
| 4 Cruise outbound | 8 Combat | 12 Descend to land |
| | | 13 Land and postflight |

TABLE 23: CAS AND AS FUNCTION REQUIREMENTS [35, p. 26]

| NAVIGATION AND WEAPON DELIVERY | PENETRATION AIDS | MISSION AND TRAFFIC CONTROL | ARMAMENT SYSTEMS | INSTRUMENTS AND A/C SYSTEMS |
|---|---|---|---|---|
| IMS Control | RHAW Control | Secure Speech Control | Pilot Control Stick | Horizontal Situation Indicator |
| Projected Map Display | RHAW Indicator Assembly | UHF Communications Control | Armament Release Panel | Attitude Direction Indicator |
| Head-up Display | Threat Display | VHF Communications Control | Armament Control Panel | Heading Mode Switch |
| FLR Display | ECM POD Control | TACAN Control | Miscellaneous Switches | Master Function Switch |
| FLR Control | Destruct Disarming Switch | IFS Control | Thumbwheel Encoder | Counting Acceleration Indicator |
| Tactical Computer Control | | UHF/ADF Control | Armament Advisory Lights Panel | Mach No./Airspeed Indicator |
| Radar Altimeter Indicator | | Intercom Control | Attack Mode Controls | True Airspeed Indicator |
| FLIR Display | | IFF Control | | Vertical Velocity Indicator |
| Air Navigation Multiplex Indicator | | Radar Beacon Control | | Approach Indexer |
| | | LORAN Control | | Caution Annunciator Panel |
| | | Marker Beacon Light | | Standby Attitude Indicator |
| | | | | Standby Attitude Erect Switch |
| | | | | Advisory Annunciator Panel |
| | | | | Approach Index Dimmer Control |
| | | | | AOA Indicator |
| | | | | AFCS Control |
| | | | | Beep Trim Switch |
| | | | | Landing Gear Position Indicator |
| | | | | Miscellaneous Warning Lights and Indicators |

TABLE 24: C/D REQUIREMENTS FOR CAS [35, pp. 35-36]

8. Variable gain controls.

9. Program-controlled symbol generator.

10. DAIS controls and displays as a maintenance tool [35].

Figure 7 shows the C/D elements, and Figure 8 identifies the functions performed by each C/D device. Figures 9 through 11 show various configurations of the multilayer control panels. The complete set of control configurations for CAS and AS missions are contained in Appendix C of [35]. The conclusions of this study concerning C/D were:

1. Multilayer cockpit control design is a viable approach.
2. Additional study is required to define scan converter requirements and architecture.
3. Digital display technology will be pacing item [35, p. 223].

A different type of information is provided in [36]. The purpose of this study was to establish a baseline for a DAIS LCC study. Part of the baseline was to identify the avionics hardware expected to be in a 1980 Close Air-Support Aircraft. Table 25 lists these pieces of equipment. It is provided here to demonstrate the DAIS approach to avionics.

Tables 26-28 and Figure 12 are adapted from [37]. This study specified the system requirements for four very specific missions. The Tables describe the missions, their sensor requirements, and the DAIS functional capabilities. The Figure demonstrates a portion of the DAIS symbology. This provided a base for simulation studies of the DAIS concept.

As part of the DAIS computer specification, the various types and sources of flight information were identified [38]. Navigation is responsible for keeping track of the aircraft state. This state is specified by latitude, longitude, wander angle, altitude, attitude and velocities. The sources of this information are the INS, air data sensors, and a navigation function such as TACAN. The algorithms used to compute the state data from the sources are described in the Appendix to [38].

A detail C/D document was developed for the B mission [39]. The document "defines and establishes the baseline interface between the controls and displays, pilot, and mission operations sequence to meet" mission requirements [39, p. 1]. The displays and pilot actions are detailed for the various DAIS master modes. Table 29 lists these modes. The displays presented during the Cruise mode are shown in Figures 13-18. Table 30 identifies the symbol types used on the moving map.

The required symbology update rates are provided in [40]. Table 31 reproduces this information. As in the previous study, information concerning message displays

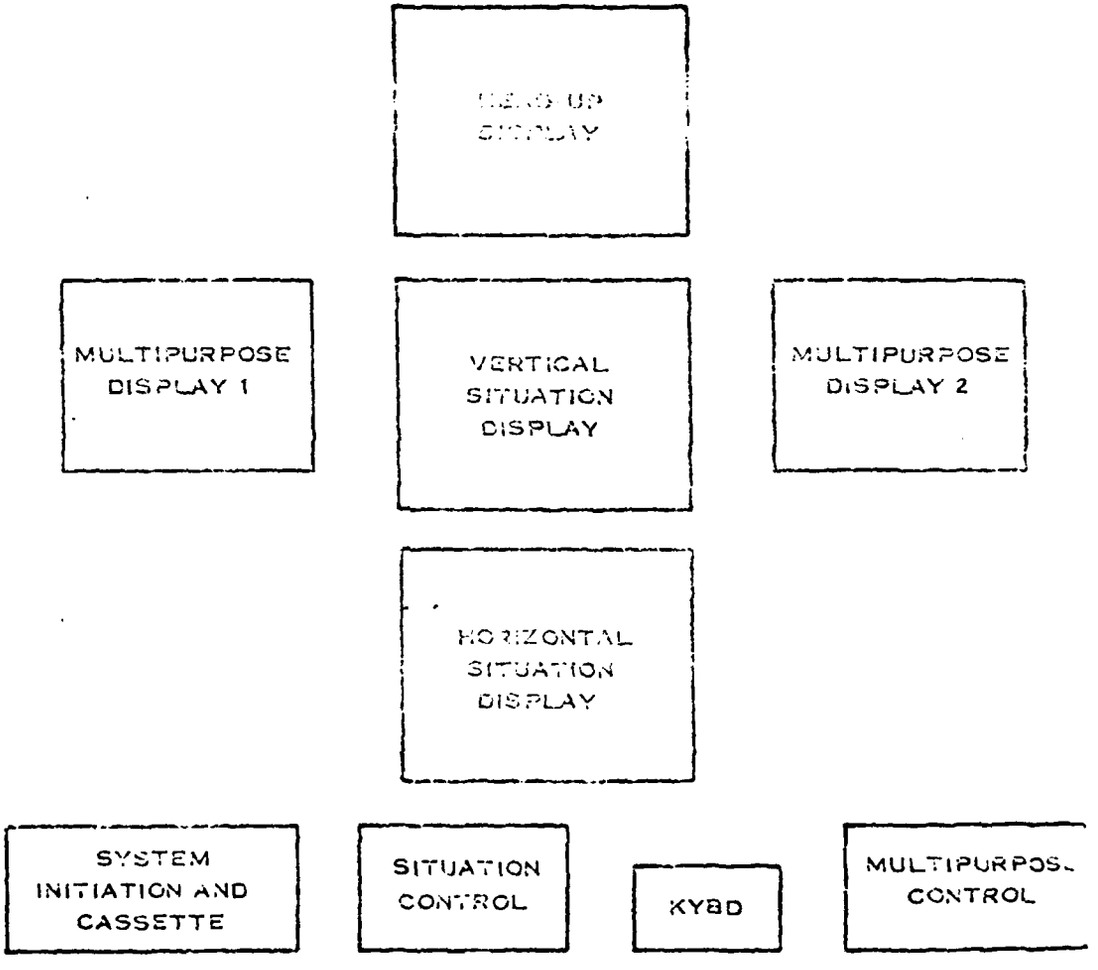



FIGURE 7: C/D ELEMENTS [35, p. 204]

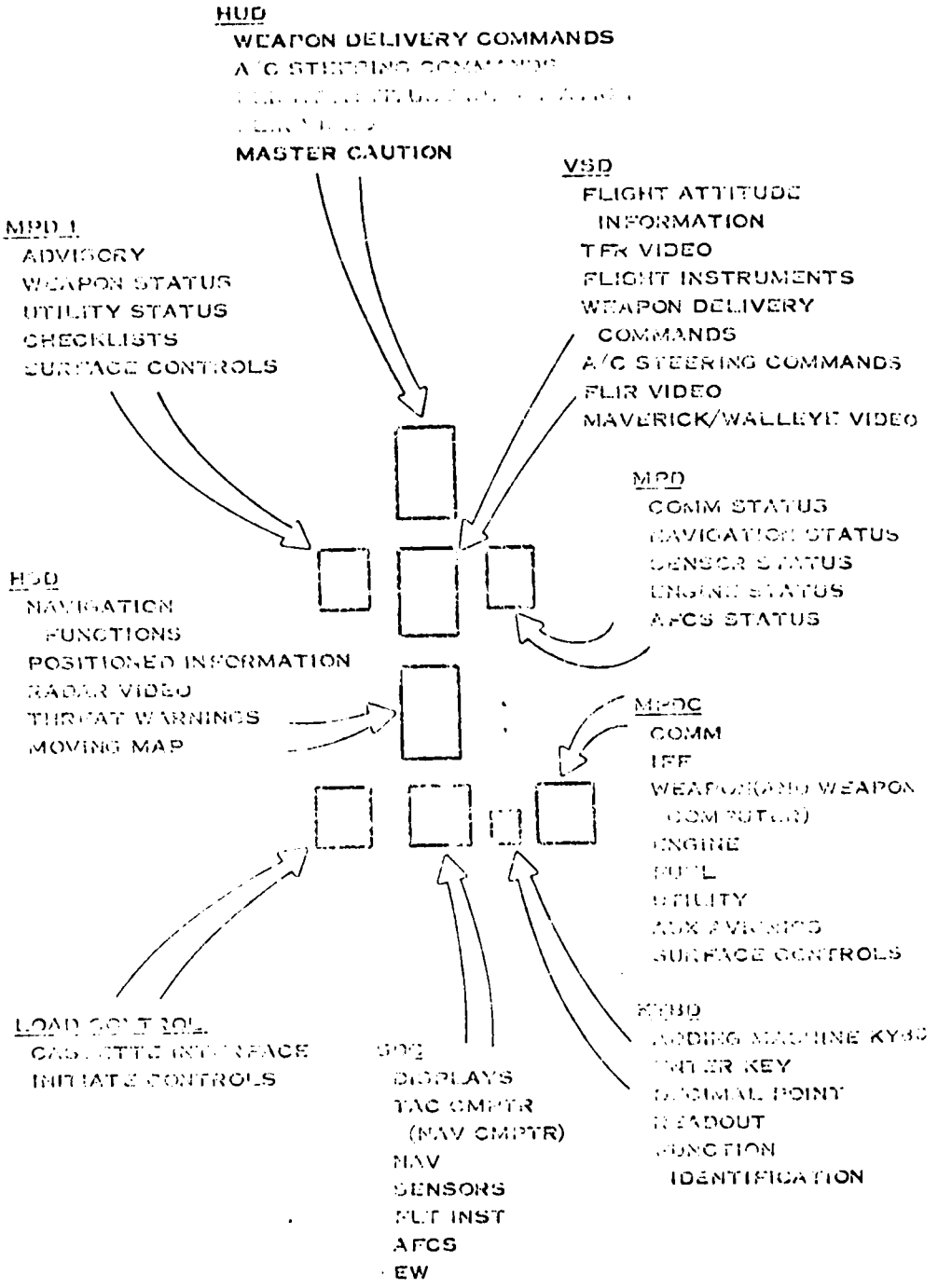



FIGURE 8: C/D FUNCTIONS [35, p. 196]

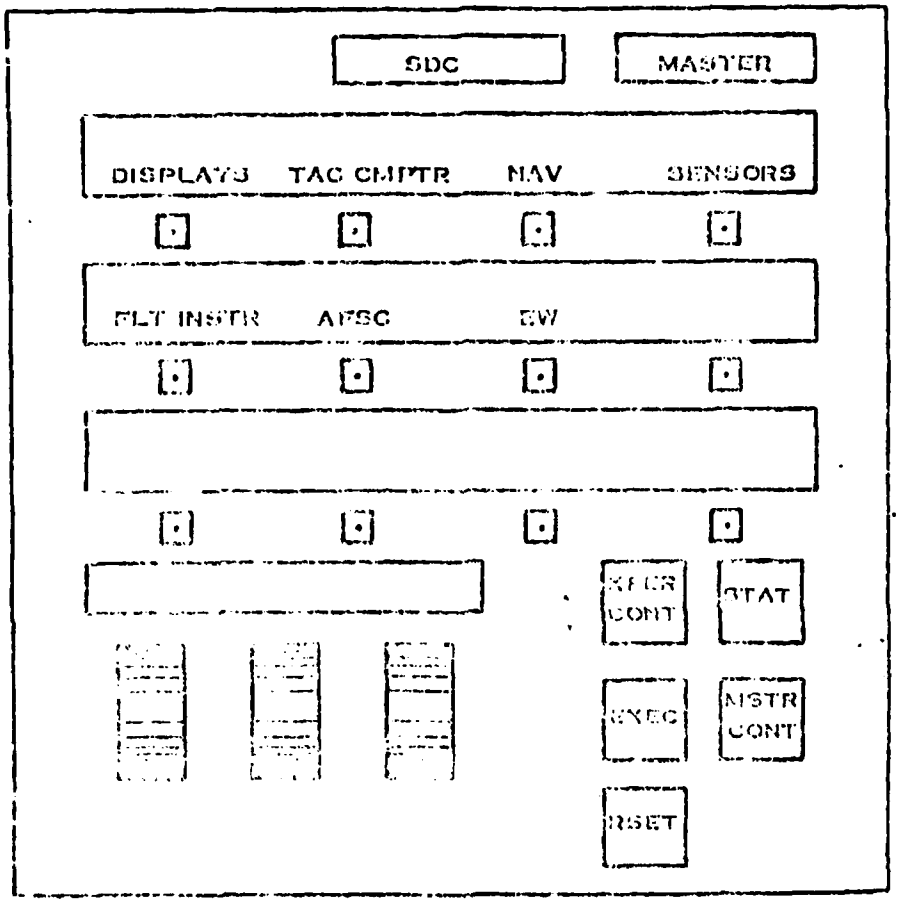



FIGURE 9: CONTROL PANEL CONFIGURATION
EXAMPLE 1 [35, p. 228]

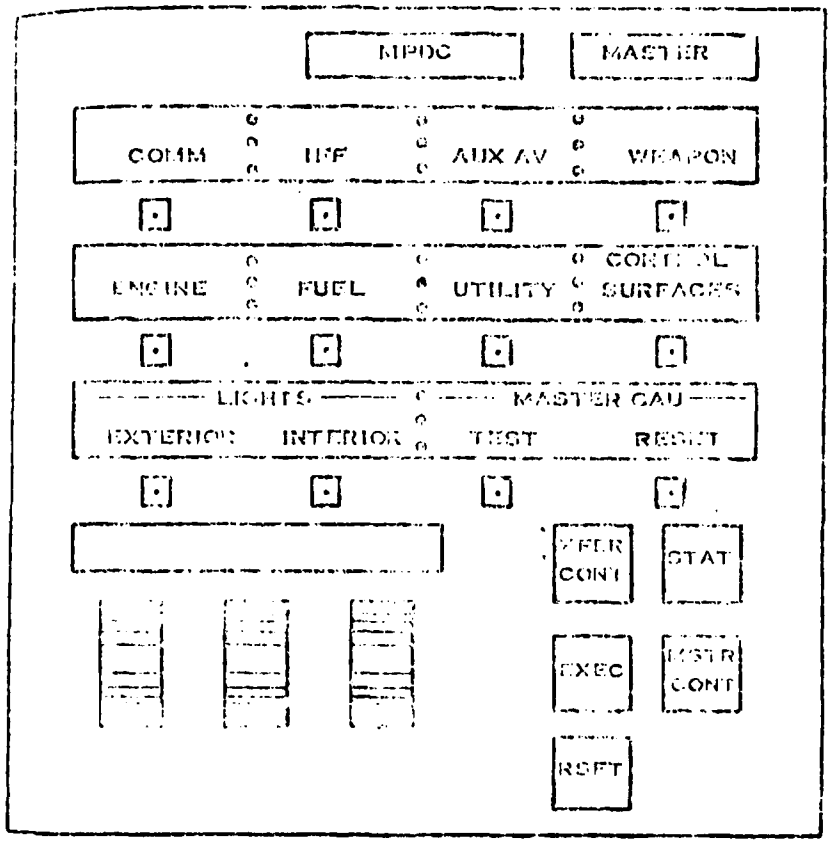



FIGURE 10: CONTROL PANEL CONFIGURATION

EXAMPLE 2 [35, p. 229]

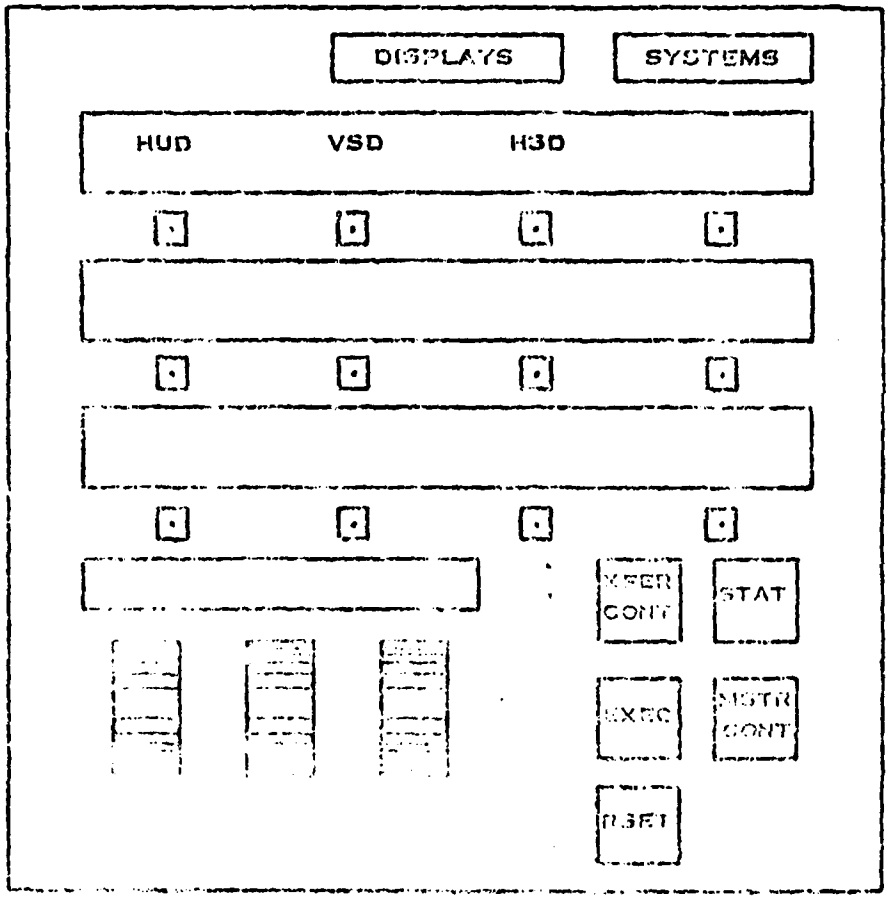



FIGURE 11: CONTROL PANEL CONFIGURATION

EXAMPLE 3 [35, p. 228]

| Function: NAVIGATION | | |
|---|---|---|
| Subsystem | Nomenclature | Aircraft |
| INS | ASN-109 | F-15A |
| UHF-ADF | OA-8638/ARD | F-15A, A-10A |
| TACAN | RT-1045/ARN | F-15A |
| ILS | R-2755/ARN | F-15A |
| ADC | ASK-6 | F-15 |
| Beacon | UPN-25 | A-10A |
| Radar Altimeter* | APN-194 | A-7E, F-14A |
| Function: COMMUNICATIONS | | |
| UHF | ARC-109 | F-15A |
| HF | ARC-123 | F-111A |
| VHF-FM | FM-622A | A-7D, A-10A |
| Secure Voice | TSEC/KY-28 | F-15A, A-10A |
| Intercom | AIC-18 | A-10A |
| Data Link | ASW-25A | A-7E |
| IFF | APX-101 | A-10A, F-15A |
| Function: COUNTERMEASURES | | |
| RHAW* | ALR-46 | A-7D, F-4E |
| IR Tail Warning* | AAQ-4 | RF-4C |
| Function: AIR-GROUND ATTACK | | |
| LTS | AAS-35 | A-10A |
| FLIR | AAS-28 | A-7D (test) |
| FLR | APQ-( ) | F-16A |
| Function: CONTROL & DISPLAY | | |
| HUD | AVQ-20 | F-15A |
| HSI | AWU-6/A | A-10A |
| ADI* | ARU-( ) | A-10A |
| MPDs | ** | ** |
| IMFK | ** | ** |
| MFCPs | ** | ** |

*Excluded from partitioning

**Not in "current" aircraft inventory but development is dictated via adoption of DAIS concept

TABLE 25: AVIONICS EQUIPMENT FOR 1980's CAS AIRCRAFT [36, p. 84]

| MISSION | TARGET | VISIBILITY/ WEATHER | WEAPONS | SENSORS FOR ATTACK | SPECIFIC MISSION FUNCTION |
|---|---|---|---|---|---|
| α | FIXED GROUND TARGET (BRIDGE) | NIGHT - CLEAR | MK-82 LDGP | NAV FLIR<br>LASER RANGER | POSITION UPDATE/TARGET ACQUISITION USING FLIR AND LASER |
| β | FIXED GROUND TARGET (BRIDGE) | NIGHT - CLEAR | MK-82 LDGP | NAV FLIR<br>LASER RANGER | SYSTEM STARTUP & RESTART<br>BACKUP NAVIGATION<br>STEERING CUES |
| γ | FIXED OR MOVING GROUND TARGETS | NIGHT - CLEAR | MK-82 LDGP | NAV FLIR<br>PAVE PENNY<br>LASER RANGER | POWER TRANSIENT<br>RECOVERY FROM MONITOR FAILURE<br>BACKUP TO MONITOR PROCESSOR<br>SYSTEM MASS MEMORY<br>C&D SWITCHOLOGY<br>IN-FLIGHT DITS FUNCTIONS<br>PAVE PENNY TARGET ACQUISITION<br>INTEGRATED NAVIGATION |
| δ | FIXED GROUND TARGET | NIGHT - CLEAR | MK-82 LDGP<br>AGM-65A (TV MAVERICK) | PAVE PENNY<br>VATS/PAVE TACK | C&D FAILURE RECOVERY<br>SYSTEM RECONFIGURATION<br>DITS PRE-FLIGHT/POST-FLIGHT FUNCTIONS<br>PAVE TACK AND MAVERICK |

TABLE 26: DAIS MISSIONS [37, p.11]

| | MISSION | | | |
|---|---|---|---|---|
| SENSOR | α | β | γ | δ |
| INS (SKN-2416) | X | X | X | X |
| NAV FLIR (AAQ-9) | X | X | X | X |
| Laser Ranger | X | X | X | X |
| Air Data Sensors | X | X | X | X |
| Radar Altimeter (APN-141) | X | X | X | X |
| ILS (ARN-58A) | X | X | X | X |
| TACAN, (ARN-118) | X | X | X | X |
| UHF (ARC-51) | X | X | X | X |
| Pave Penny (AAS-35) | | | X | X |
| Maverick Video | | | | X |
| VATS/Pave Tack | | | | X |

TABLE 27: DAIS SENSOR COMPLEMENT [37, p. 29]

| | MISSIONS | | | |
|---|---|---|---|---|
| | α | β | γ | δ |
| Navigation | | | | |
| Inertial/Baro-damped | X | X | X | X |
| TACAN Area Nav | | X | X | X |
| Dead-Reckoning | | X | X | X |
| Steering | | | | |
| Command Nav | X | X | X | X |
| Command Track | | X | X | X |
| Command Heading | | X | X | X |
| Command Altitude | | X | X | X |
| TACAN | X | X | X | X |
| ILS | X | X | X | X |
| Navigation Update | | | | |
| Flyover | X | X | X | X |
| HUD/Laser | X | X | X | X |
| FLIR/Laser | X | X | X | X |
| VATS/Pave Tack | | | | X |
| Acquisition/Cueing | | | | |
| Pilot/HUD | X | X | X | X |
| Pilot/FLIR | X | X | X | X |
| Pave Penny | | | X | X |
| VATS/Pave Tack | | | | X |
| Target (or OAP) Fix (Designation) | | | | |
| HUD/Laser | X | X | X | X |
| FLIR/Laser | X | X | X | X |
| Pave Penny/Laser | | | X | X |
| VATS/Pave Tack | | | | X |
| Communications | | | | |
| UHF | X | X | X | X |

TABLE 28: DAIS FUNCTIONAL CAPABILITY (ADAPTED FROM [37, p. 30, 31])

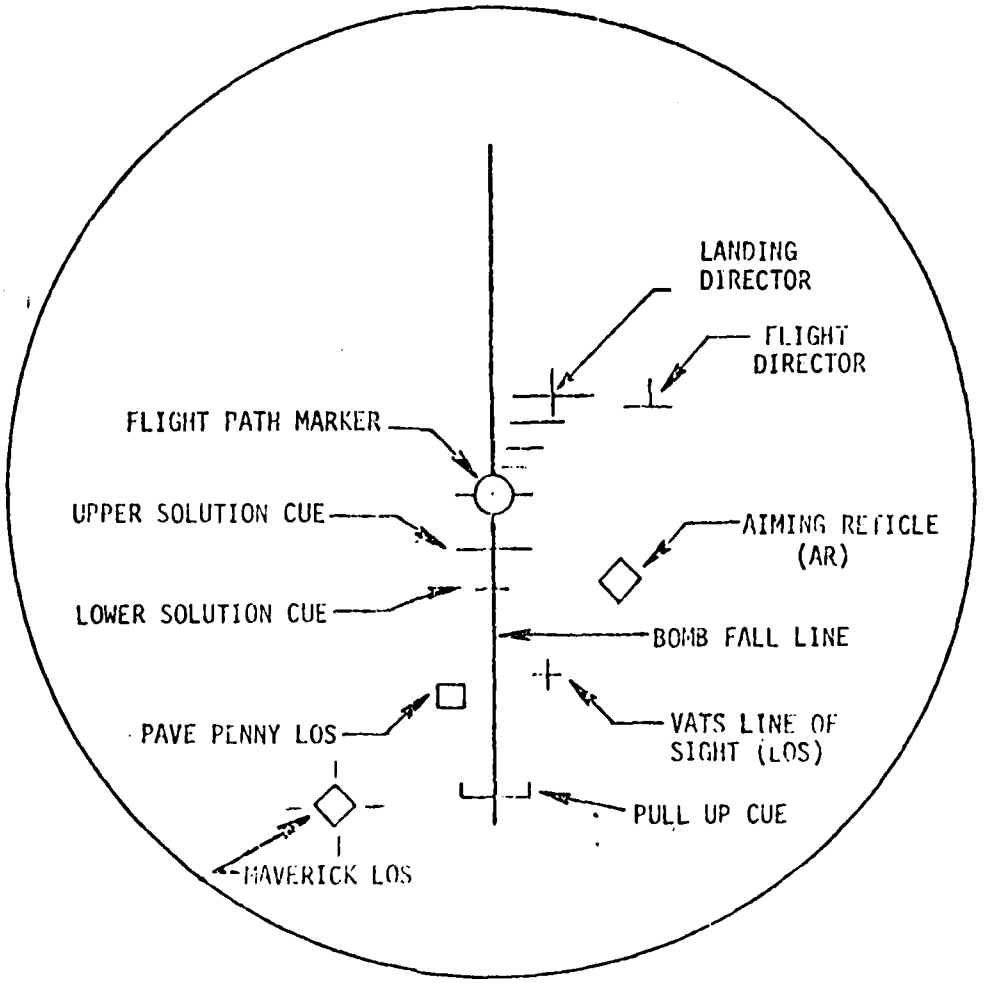



FIGURE 12: DAIS HUD SYMBOLOGY [37, p. 21]

| |
|---|
| 1. NULL |
| 2. PREFLIGHT |
| 3. TAKEOFF/CLIMB |
| 4. CRUISE |
| 5. TERRAIN FOLLOWING/TERRAIN AVOIDING |
| 6. APPROACH/LANDING |
| 7. PRECISION APPROACH |
| 8. NAV BOMB |
| 9. RADAR BOMB |
| 10. ANGLE RATE BOMBING SYSTEM |
| 11. MANUAL BOMB |
| 12. AIR/AIR |
| 13. CCIP/AUTO |
| 14. CCIP/MANUAL |
| 15. MISSED APPROACH |

TABLE 29: DAIS MASTER MODES [39]

| | | | |
|---|---|---|---|
| 1. | OXY SYS CHK | 6. | |
| 2. | FUEL CHK | 7. | |
| 3. | ENG INSTR CHK | 8. | |
| 4. | EXT TANKS CHK | 9. | |
| 5. | | 10. | ADV PAGE |

FIGURE 13: DAIS CRUISE MODE-IMFK CHECKLIST CONFIGURATION [39, p. 61]

| | | | |
|---|---|---|---|
| 1. | UHF CHNG<br>( 1 ) | 6. | |
| 2. | TCN CHNG<br>( 058X ) | 7. | |
| 3. | CMD HDG<br>( ) | 8. | |
| 4. | CMD ALT<br>( ) | 9. | |
| 5. | FLY TO<br>( ) | 10. | CRS SET<br>( ) |

FIGURE 14: DAIS CRUISE MODE-IMFK TAILORED FUNCTIONS CONFIGURATION [39, p. 62]

WP 99 315/120 1 55.4 M

PSN XX XX.XXN CRS SEL 315
XXX XX.XXE

NAV (Mode)
ILS XXX.X
TCN XXXX,XXX/XXX
UHF TRG 323.00

FIGURE 15: DAIS CRUISE MODE-MPD-2 FORMAT [39, p. 65]

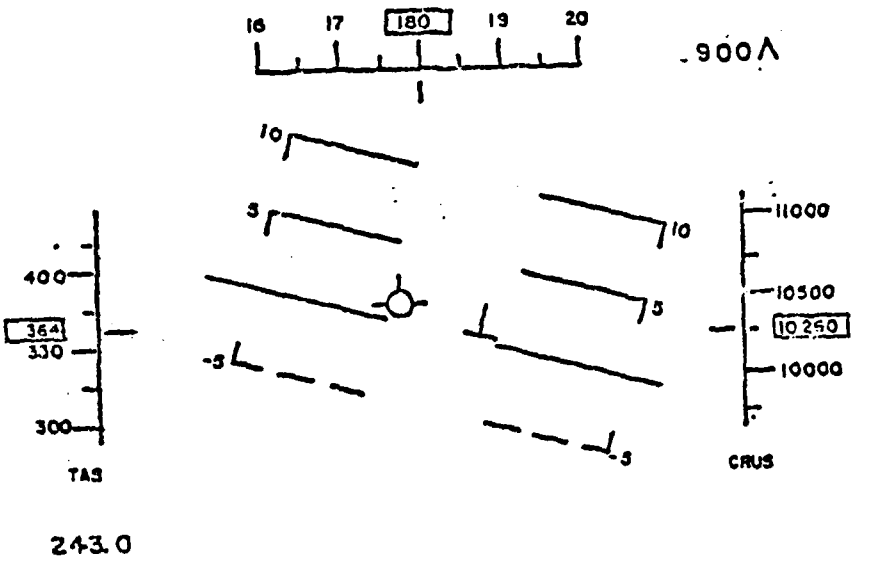



FIGURE 16: DAIS CRUISE-HUD DISPLAY [39, p. 66]

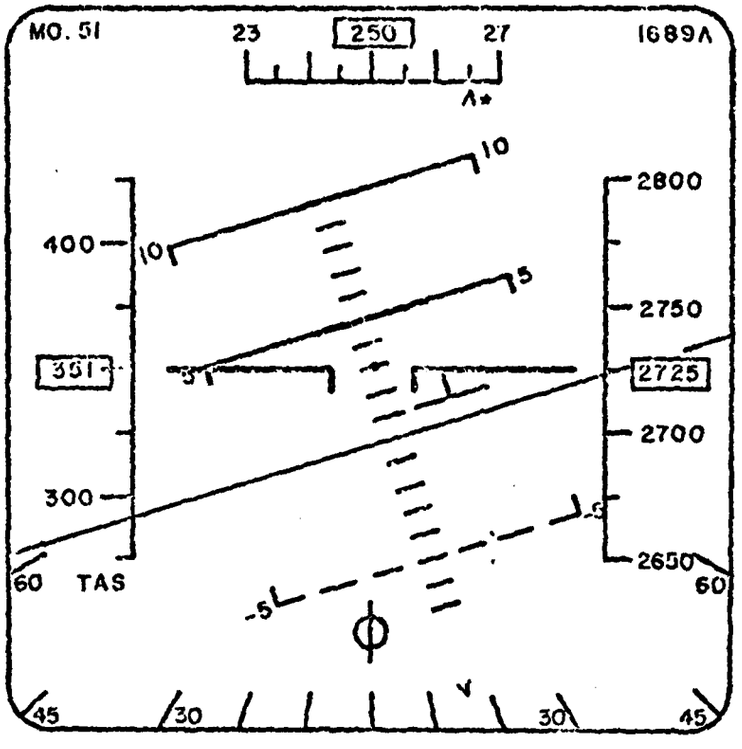



FIGURE 17: DAIS CRUISE MODE-VSD DISPLAY [39, p. 67]

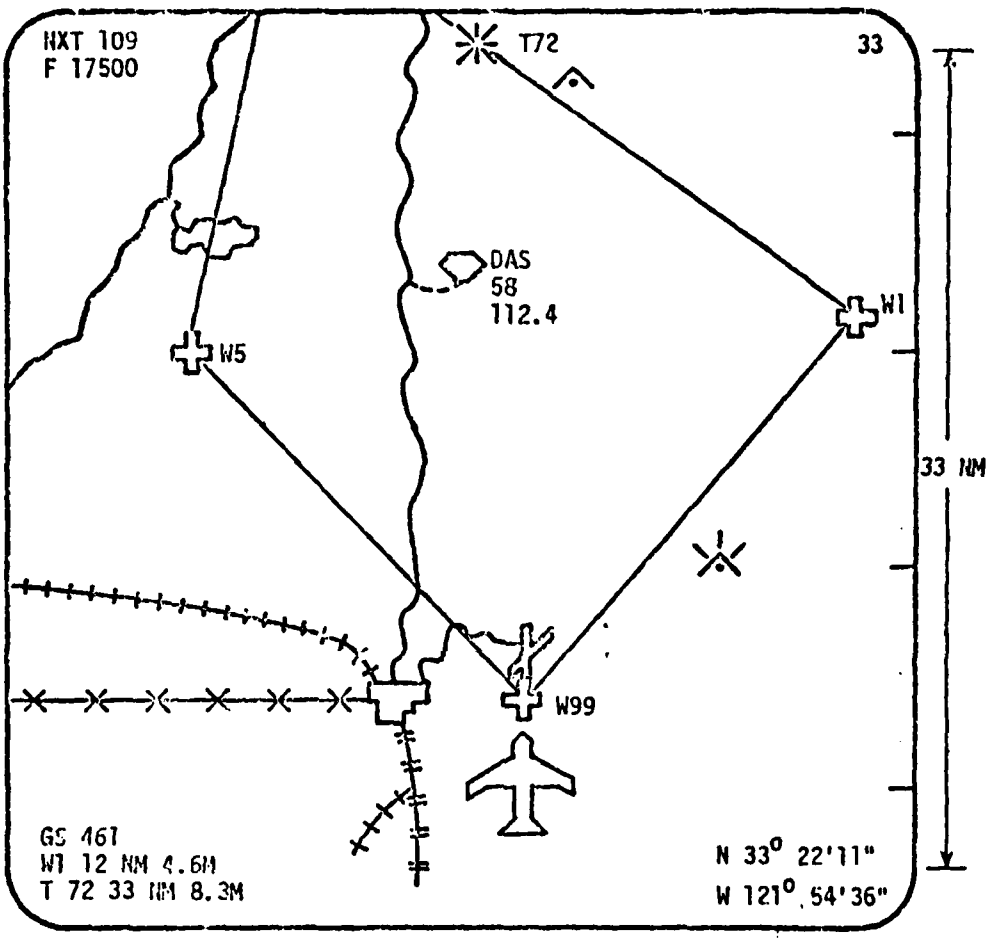



FIGURE 18: DAIS CRUISE MODE-HSD DISPLAY [39, p. 69]

1. VORTACS
2. Road Intersections
3. Bridges
4. Major Roads
5. Lakes
6. Coastlines
7. Obstructions (Lit and Unlit)
8. Waypoints
9. Rivers
10. Minor Roads
11. Urban Areas
12. Power Lines
13. Railroads

TABLE 30: MOVING MAP SYMBOL TYPES [39]

| HUD Update Rates | | Processor Time (MSEC) |
|---|---|---|
| 30 Hz: | Flight Path Scales & Marker | 3.00 |
| | Aiming Reticle | .19 |
| | In Range Cue | .19 |
| | Bomb Fall Line | .34 |
| | Upper and Lower Cues | .34 |
| | Pull Up Anticipation | .08 |
| | Flight Director | .22 |
| | Landing Director | .34 |
| 15 Hz: | NONE | |
| 7.5 Hz: | Altitude Scales | 3.5 |
| | Command/Hold Carets | .22 |
| | Airspeed Scale | 2.5 |
| | Heading Scale | 2.5 |
| | Angle of Attack | .07 |
| | Minimum Descent | .3 |
| | Decision Height | .3 |
| | Touch Down Zone Box | .3 |
| | Ground Elevation | .16 |
| | Breakaway Symbol | |
| 2 Hz: | Radar Altitude | .9 |
| | Warning Indicator | |
| | Acceleration | 1.7 |
| | Vertical Velocity | 1.0 |
| | Mach Number | 1.0 |
| | Weapon Select | |
| | Reconfigure | |
| | Wheels | |
| | Flaps | |
| | UHF Frequency or Channel | |
| | CAS/TAS | |
| Static: | Master Mode Acronym | 1.1 |

TABLE 31: SYMBOL UPDATE RATES FOR A-7D DYNAMICS [40, p. 7]

and formats as a function of the master mode is reviewed. In this case the information is more detailed. Appropriate information sources for the display information are suggested. Finally the interface messages between the mission software and the C/D are identified.

4. Recommendations: Given that the aircraft of the 1990s will have integrated controls and displays (DAIS, ATA, etc.) and the avionic suite described in [6], then MFBARS/ICNIA provides no new information capabilities. This is a very important point. MFBARS's mission benefits is in terms of increased functional reliability. It does not provide any new mission capability. Thus, C/D research that considered the avionic suite described in Table 32 are very relevant to MFBARS. ICNIA does not generate a new C/D question or capability.

For the integrated C/D aircraft of the 1990s, the C/D questions have been or will be answered by other studies. MFBARS's system interface for this aircraft is not with the pilot but rather with the mission control bus. The design of this interface is part of the System Definition Studies [6]. The contractor is to "design the functional interface between the ICNIA terminal and core integration system in accordance with MIL-STD-1553B. Consideration shall be given to signal flow in and out, partitioning of ICNIA and core control modes, and failure reporting" [6, Paragraph 4.2.5]. Thus, for the integrated C/D aircraft this information would answer the interface question.

If MFBARS will be retrofitted into aircraft without a fully integrated cockpit, then the C/D question again becomes relevant. In this situation ICNIA would have to have its own C/D or be retrofitted with an integrated cockpit. However, C/D research would be based on the results of the retrofit study; therefore, no such C/D efforts are being recommended at this time.

In order to improve information flow between various groups, it is recommended that working relations be developed between AAAN, AMRL, the Flight Dynamics Lab (FDL), and the Advanced System Avionics (ASA) Project which is continuing some of the DAIS efforts [41]. AMRL seems to be at the fore-front of display technology and information requirements. FDL maintains a DAIS cockpit and was involved in its development. It is important that these groups be fully aware of the MFBARS/ICNIA effort and that AAAD be fully aware of their efforts. Thus, if there are significant impacts in one direction or other, they will be recognized quickly. Also, these groups would be able to assist AAAD in directing any future C/D research if it becomes warranted in the future.

Although this report does not recommend such an effort, there does seem to be some organizational pressure for an ICNIA C/D effort. If such work is necessary,

then it is recommended that the research be done in-house. By utilizing the appropriate AMRL, FDL and especially DAIS information, one should be able to identify CNI display symbology, display messages, control requirements, update rates, and information sources. This would seem to be the most cost-effective way to respond to this pressure.

C. Availability Needs: The availability issue was further specified in the Request for Class D&F [1] to include fault recognition, fault isolation, fault tolerance, design for repair, built-in-test, MTBF and MTTR. These last two items (MTBF and MTTR) will be evaluated through the PRICE-H model. The other factors are to be considered in the System Definition projects [6].

Paragraph 4.2.4 of [6] specifies that "the contractor shall develop an approach to physical partitioning of system architecture components that includes redundancy and fault tolerant design concepts to enhance the reliability, availability, and survivability of the system, and facilitates ease of maintenance". Further, the contractor is to include "BIT function partitioning in the analysis and develop and justify a rationale for the lowest level of fault isolation" [6, Paragraph 4.2.4]. Paragraph 4.2.11 [6] also considers the abilities aspect of ICNIA. In addition, this Paragraph requires the contractors to consider possible logistic support concepts which is the last key issue of the OIS. Since MFBARS is a software radio, it raises different support issues or demands a different type of support. Investigation into this life cycle support concept is a required task of the System Definition studies.

Since the final two key issues of the OIS will be addressed as part of System Definition work, they cease to become efforts of the OIS. There certainly appears to be no reason why these tasks should be repeated. The above analysis does place added importance on these tasks. Thus, the selected contractors should be encouraged to devote adequate attention and resources to this analysis. These issues are too important to become mere secondary efforts.

VI. RECOMMENDATIONS: This section of the report summarizes the recommendations made throughout the body of this document and contains a few new recommendations. In addition, more detail will be provided concerning the proposed retrofit study.

1. The primary recommendation is that an in-depth retrofit study be initiated. Since the key issues of the OIS will be responded to by either of the two in-house efforts and the System Definition effort, the funds originally allocated to the OIS could be used in the retrofit study. Whether this study is called an OIS or something else is an organizational matter.

1. AN/ARC - 190 (HF)
2. AN/ARC - 115, - 131 (VHF)
3. AN/ARC - 164 (UHF)
4. AN/ARC - 171 (AFSATCOM)
5. AN/ARC - 108 (ILS/VOR)
6. AN/ARN - 118 (TACAN)
7. AN/APX - 76 - 101 (IFF)
8. JTIDS CLASS II TERMINAL
9. GPS HIGH DYNAMIC SET
10. SEEK TALK
11. SINCGARS

OPTIONS

12. ADAPTIVE HF/VHF
13. NATO IDENTIFICATION SYSTEM
14. DISCRETE ADDRESS BEACON SYSTEM

TABLE 32: BASELINE FUNCTIONAL REQUIREMENTS [6]

1. COCKPIT LAYOUT
2. AVAILABLE AVIONIC SPACE
   a. location
   b. size
   c. cooling method
   d. vibration
   e. possible candidates
3. ELECTRIC POWER SYSTEM
4. ENVIRONMENT CONTROL SYSTEM
5. CURRENT AVIONICS
   a. location
   b. size
   c. weight
   d. power
   e. cooling method
   f. mounting
6. ANTENNAS
   a. type
   b. location
7. INTERFACE DATA
   a. signal characteristics
   b. electrical characteristics
8. FUTURE MODIFICATIONS
9. DATA SOURCES

TABLE 33: ELEMENTS OF AVIONIC SUMMARY [42]

The retrofit results would have three impacts. First, many of ICNIA's benefits are due to standardization. If MFBARS will not be retrofitted, then these benefits would be limited in the near future. Standardization benefits would not occur until the next century. Second, the retrofit results will influence what C/D research is necessary. Once the market for MFBARS is established, the equipment with which MFBARS would need to be compatible would be identified. Third, on certain aircraft ICNIA may provide new functional capabilities since not all aircraft contain the avionic suite identified in Table 32. These added capabilities may be able to off-set some of the retrofit costs.

In the ARINC study [21] the potential market for MFBARS was the F-15, F-16, A-10, F-4G, and EF-111A. These would provide a starting point for the analysis. An additional document which should provide an excellent baseline is Avionics Interface Data Summaries: A-10A, EF-111A, F-4E, F-4G, F-15A, F-16A, F-111A, F-111E, F-111F, RF-4C [42]. Table 33 lists the elements detailed in this report. The study provides information concerning the space and environment in which MFBARS would be placed. In addition, the equipment with which it must interface is also identified.

The output of Retrofit Report should be a complete specification of ICNIA's market. It should identify the aircraft and whether the aircraft should receive the complete MFBARS or some portion of it. The report should also include a detailed analysis of the interface question. This would include consideration of controls and displays, partitioning and software requirements.

2. The System Definition data should be analyzed using the following software packages: PRICE-H, PRICE-L, PRICE-S, ALPOS and STEP. (Another additional example of STEP's ability is [43]).
3. A more accurate physical description of ICNIA will be available at the conclusion of the System Definition phase. This data will substantiate the claims of power, size, and weight savings of MFBARS. This support and the results generated in (2) should be combined into a single in-house document. This document would specify the physical and cost benefits of ICNIA. A single document would more effectively provide information to the potential users and make the preparation of the necessary briefings easier.

4. Avionics System Analysis and Integration Laboratory (AVSAIL) provides a very strong in-house simulation capability. These capabilities are detailed in [44]. Although still too early in ICNIA's life for strong consideration, AVSAIL and AEP (described in Section IV. D.) should be utilized when appropriate. Such capabilities should not be ignored in the marketing of ICNIA.
5. Through an in-house effort, the avionic function mission scenarios should be developed. This project should combine information from ARINC [21], SPANS [4] and AMA [22, 23]. This document will be very useful to future reliability work.
6. A formal liaison should be developed with AMRL, FDL, and ASA. This would keep all parties informed of state-of-the-art developments and provide a forum for technology transfer. In addition, this base would provide the experienced consultation that AAAD will need if future C/D work is required due to retrofit.
7. A formal liaison should be established with the Navy's Tactical Information Exchange System (TIES) Program. Since MFBARS and TIES have similar goals [45], the Air Force and Navy may learn from each others' efforts.
8. This report does not recommend the initiating of any C/D effort before the completion of the retrofit study. However, if the System Avionics Division or AAAD disagree with this recommendation, then a small in-house effort is suggested. The DAIS and AMRL studies provide valuable documentation. The in-house effort should emphasize the isolation of CNI data and display requirements.
9. The System Definition contractors should be closely monitored to ensure adequate response to the availability and logistic support issues. These could be major benefits of ICNIA. Thus, it is in AAAD's best interests that these concepts be fully and professionally examined.

The Retrofit Report and the other recommended tasks would provide a more firm basis upon which to do an indepth benefit analysis. This benefit analysis is essential if ICNIA is to be marketed to the users. It is certainly not too soon in ICNIA's development to consider its marketing strategy. Hopefully, this report has been of some assistance in developing an ICNIA market strategy.

## APPENDIX A

## MODELING THE PILOT - C/D INTERFACE

I. PURPOSE:

This appendix is devoted to detailing my efforts concerning models of the pilot-C/D interface. Previously, it was expected that the MFBARS OIS would be concerned with this topic. If a reasonably good model could be developed, this model could be used to analyze the interface problem. This analysis might be able to answer many of the interface questions and provide some guidance to the more expensive man-in-the-loop simulations that would follow.

This report, however, suggests that although the interface problem is an important issue, it is an issue that needs to be and is being analyzed by other groups. Thus, this appendix will probably have no direct bearing on the MFBARS OIS. It is presented here to give a more complete accounting of my efforts. This material may be general enough to be of use in analyzing the ICNIA-core avionics interface to be addressed in the System Definition study [6]. This possible application will be considered in the summary of this appendix.

II. BACKGROUND:

It has been stated that the C/D design problem is "one of providing the precise information needed, at the precise time needed, in the precise format needed for assimilation, and in the precise location needed" [24, p. 62]. Each of these are critical aspects of the C/D problem, but the emphasis here is on what information is needed. However, many of the models are general enough to consider the more expanded question.

The question of what information leads to consideration of human decision processes. Leedom, in a recent article, reviews modeling approaches to including the human in system simulations [46]. Obviously for the C/D system the human element is rather important. One way of including the human in system simulations is the man-in-the-loop approach. A second is through a simulation of human decision processes. This latter approach will be considered here.

In order to build a simulation of human decision processes, it would be advantageous to build it based on a well-recognized theory of human decision making. One such theory is the information processing approach to problem solving [47, 48]. In general, it assumes that "much human problem solving proceeds by erecting goals, detecting differences between present situation and goals, finding in memory or by search tools or processes that are relevant to reducing

differences of these particular kinds, and applying these tools and processes" [49, p. 403]. Certainly, this is a very broad basis and must be particularized to a specific problem situation. However, even when particularized, this approach provides more of a framework than an actual model that could be used to simulate human behavior. This framework has spawned a large number of simulation models [47] and is recommended as an approach to pilot-C/D interface modeling. As stated above, no modeling effort is required by the OIS; therefore, there will not be a follow-up to this recommendation.

The next two sections will identify two additional modeling approaches. Actually, these approaches are specific software packages. The two techniques will be briefly described and applications of the techniques will be cited.

III. SAINT:

Systems Analysis of Integrated Networks of Tasks (SAINT) "is a FORTRAN based, network-oriented, combined simulation language for modeling large, complex systems with continuous and discrete event components that interact and possess time varying properties" [50, Abstract]. Due to this combination of discrete and continuous events, the language is ideal for modeling the pilot-aircraft interface. The pilot performs discrete tasks as he flies the aircraft. The aircraft dynamics, on the other hand, are continuous. Thus, this language provides a tool for both of these component types to interact. SAINT has been used to evaluate the DAIS display concepts [51, 52], and additional information concerning SAINT is contained in [50, 53, 54, 55, 56, 57].

IV. HOS:

Human Operator Simulator (HOS) "is a digital computer program designed to simulate the complex interactions between man and equipment by modeling both the operating characteristics of the machine and the perceptual, cognitive and motor functions of the operator" [58, p. 39-3]. The simulated operator can: obtain information, remember information, perform mental calculations, make decisions, move a body part, manipulate a control, and relax [58]. The HOS model was initially developed to assist in the evaluation of new Naval airborne weapon systems with regard to displays, controls, labels, panels, etc. [59].

HOS has been used to simulate an open ocean convoy screening mission [58] and pursuit tracking [60]. It is propounded to be "a highly useful technique for the initial assessment of how well a trained operator will be able to perform his tasks in a specified crewstation under varying situational demands" [59, p. A-9]. Additional information about HOS can be found in [59].

V. SUMMARY:

This appendix has presented three approaches to modeling the human operator. The first approach is a rather general paradigm of human problem solving. It is a rather useful tool for analysis but would only lay the ground work for modeling. The SAINT and HOS packages provide the software to build human pilot simulations. Thus, they are capable of modeling the pilot-C/D interface. This information may also be useful in modeling other interfaces.

Part of the Systems Definition project is ICNIA-Core Partitioning [6]. The contractor will identify which functions will reside in the CNI terminal and which in the core avionics. This hardware network might be modeled through SAINT or a SAINT-like language to analyze the various system requirements. This analysis could assist in the partitioning effort.

## APPENDIX B

## FUTURE EFFORTS: RELIABILITY ANALYSIS

This rather brief appendix is devoted to discussing a possible mini-grant effort to follow the summer program.

I. BACKGROUND:

The concept of functional reliability is of major concern for ICNIA. Previously, each black box contained a single function. Thus, when this box failed, the function failed. In this situation the reliability of the black box and the reliability of the function were one and the same. Within the MFBARS system this one-to-one correspondence between functions and black boxes no longer exists. Therefore, a box may fail without any corresponding loss of function due to the reconfigurability of the system.

MTBF and MTTR are usual measures of reliability. Although these values are still important,there needs to be an approach to evaluate the increased functional reliability that is associated with MFBARS. Thus, a mini-grant effort could explore possible measures and develop an analytical tool to evaluate a proposed system.

II. METHODOLOGY:

At this point, detailed methodological development is premature. This Section, then, should be considered as preliminary.

The MFBARS/ICNIA system could be considered a network of inter-related pieces of hardware and software. Since the system is reconfigurable, there are multiple paths through the network. One tool for studying this network might be SAINT.

SAINT's appeal in this situation is due to its structure and physical availability. As stated in Appendix A, it is a network-based language and may be very useful in describing the ICNIA system. In addition, since SAINT was developed at WPAFB, it is available and well-supported at this facility. In-house support is often very helpful.

III. EXPECTED OUTPUT:

The results of this effort are expected to:

1. Provide measures for evaluating the functional reliability of MFBARS; and
2. Provide AAAD with a tool for analyzing various ICNIA configurations with respect to functional reliability.

## REFERENCES


1. Request for Class D&F, Avionics Technology, Project #2003 et al, Project Office: AFWAL/AAA

2. Ware, Willis H., Correspondence to General Alton D. Slay, (December 19, 1979).

3. ITT Avionics Division, Final Technical Report Modular Multifunction-Multiband Airborne Radio System (MFBARS), Preliminary Draft, Contract F33615-78-C-1518, (January 15, 1980).

4. Gates, R.K., and Shipp, R.F., Standardization Potential Across Navigation Systems (SPANS), The Analytic Sciences Corporation, AFAL-TR-77-188, (September, 1977).

5. Hamme, D., and Botha, D., "ICNIA Briefing to AF Studies Board", Andrews AFB, (December 19, 1979).

6. "ICNIA System Definition - Statement of Work", AFWAL/AAAD-3, (July, 1980).

7. Ferens, D.V., Advanced Development Cost Estimates for the Multi-Function Multi-Band Airborne Radio System (MFBARS), AFWAL/AAA-3, (October 2, 1979).

8. TRW, Defense and Space Group, MFBARS Radio Architecture Final Draft Technical Report, Contract No. F33615-77-C-1172, (March, 1980).

9. Freiman, F.R., PRICE - A Parametric Cost Modeling Methodology, RCA, Cherry Hill, N.J., (May, 1978).

10. Kaufman, G.A., The PRICE Life Cycle Cost Model, RCA, Cherry Hill, N.J., (March, 1978).

11. Freiman, F.R., and Park, R.E., PRICE Software Model - Version 3, RCA, Cherry Hill, N.J., (October, 1979).

12. Ferens, D.V., Drobot, N., Miller, D., and Thomas, J., "Hardware Logistic Support Cost Models: QUO VADIS?", Avionics Laboratory, System Evaluation Group, (February 12, 1980).

13. Harris, R.L., and Cork, T.R., "System Avionics Value Estimation (SAVE): A New Tool for Logistics and Support Cost Analyses", Proceeding of the IEEE 1978 National Aerospace and Electronics Conference, Vol III (May 16-18, 1978) pp. 1073-1077.

14. Cork, T.R., and Mulcahy, J.F., System Avionics Value Estimation (SAVE): An Aid for Avionics Logistics - and - Support-Cost Analyses, Battelle's Columbus Laboratories, AFAL/TR-77-179, (September, 1977).

15. Predictive Operations and Maintenance Cost Model, TRACE of AFAL-TR-79-1120 Westinghouse, Contract No. F33615-77-C-1105.

16. Gates, R.K., and Shipp, R.F., Avionics Standardization Potential Analysis, The Analytical Sciences Corporation, AFAL-TR-78-168, (November 30, 1978).

17. Gates, R.K., Standardization Evaluation Program (STEP) User Guide, The Analytical Sciences Corporation, Contract No. F33615-77-C-1167, (May 31, 1978).

18. Welp, D., Almquist, K. and Rainey, L. (editor), "Avionics Evaluation Program: Simulation Models for the Effectiveness Analysis of Avionics", Modeling and Simulation of Avionics Systems and Command, Control and Communications Systems, AGARD Conference Proceedings No. 268, NATO, (January, 1980), Paper #31.

19. Avionics Cost Effectiveness, AEP/SAVE Brochure, AFAL, System Avionics Division, Wright-Patterson AFB.

20. F-16 Air-to-Ground Baseline Study, AFWAL/AAAS-2, AFAL-TM-28-37 AAA-3, (October, 1978).

21. Chelson, P.O., Martinec, D.A., and Savisaar, A., Requirements Analysis for a Multifunction, Multiband Airborne Radio System (MFBARS), ARINC Research Corporation, AFAL-TR-7899, (July, 1978).

22. Greenspun, R., and Konop, P., ECM Scenarios for JTIDS/GPS/INS Integration Studies, C.S. Draper Laboratory, Report No. 024-09-702, (January, 1980), (SECRET).

23. The Analytic Sciences Corporation, GPS/JTIDS Operational Impact Analysis Study, TR-1426-5, Contract No. F04701-79-C-0030, (May 30, 1980).

24. Mills, G.S., Grayson, M.A., Jauer, R.A., Jr., and Loy, S.L., Research on Visual Display Integration for Advanced Fighter Aircraft, McDonnell Aircraft Company, AMRL-TR-78-97, AD-A069 605, (November, 1978).

25. Hanson, T.G., Jones, D., Macek, A.J., Peters, G.L., and Sanviz, J.H., Research on Visual Display Integration for Advanced Fighter Aircraft, Honeywell Systems and Research Center, AMRL-TR-78-118, AD-B035 580L, (January, 1979).

26. Hughes Aircraft, Research on Visual Display Integration for Advanced Fighter Aircraft, AMRL-TR-78-121, AD-C018280.

27. Kulwicki, P.V., "Fighter/Attack Crew Enhancement Study", Draft Statement of Work, AFAMRL/HEA, (May 15, 1980).

28. Nicholson, A.N., (editor), Simulation and Study of High Workload Operations, AGARD Conference Proceedings No. 146, NATO, (October, 1974).

29. Methods to Assess Workload, AGARD Conference Proceedings No. 216, NATO, (June, 1978).

30. Stringer, F.S. (editor), Optimization of Pilot Capability and Avionic System Design, AGARD Advisory Report No. 118, NATO, (November, 1978).

31. Fitts, P.M., and Jones, R.E., "Analysis of Factors Contributing to 460 Pilot-Error Experiences in Operating Aircraft Controls", Selected Papers on Human Factors in the Design and Use of Control Systems, H.W. Sinailso, (editor), New York: Dover Publications, Inc., (1961), pp. 332-358.

32. Operator Workload Assessment Research and Development Planning Summary, AMRL, Human Engineering Division, (September, 1979).

33. DAIS Documentation Descriptions: Specifications, Manuals, Plans and Drawings, MA 100 100B, (November 1, 1979).

34. List, B., "DAIS: A Major Crossroad in the Development of Avionic Systems", Astronautics & Aeronautics, (January, 1973), pp. 55-61.

35. Brodnax, C.T., A Conceptual Study for a Digital Avionics Information System (Approach II), Texas Instruments, Inc., AFAL-TR-73-427, (March, 1974).

36. Czuchry, A.J., Engel, H.E., Dowd, R., Baran, H.A., and Greene, R., Mid-1980's Digital Avionics Information System Conceptual Design Configuration, Dynamic Research Corporation, AFHRL-TR-76-59, (July, 1976).

37. O'Brien, Capt M.J., System Segment Specification for the Digital Avionics Information System Missions α, β, γ, δ, Type A, SA 100 100A, (December 15, 1978).

38. Holsapple, B.E., Computer Program Development Specification for DAIS Mission Software: OFP Applications, SA 201 305, Part I, (February 21, 1979).

39. Blair, J.L., DAIS Interface Control Document Mission Operation Sequence: Pilot/Controls & Displays/Interface with Applications Software (Mission B), SA 803 201 B, (June 18, 1979).

40. Garcher, J., Functional Interface Requirements Manual for DAIS Control and Display Subsystem, MA 802301, (December 1, 1979).

41. Krieg, G.R., "Advanced System Integration Demonstrator - Decision Unit Overview", AFAL/AAS, (January 11, 1980).

42. ARINC Research Corporation, Avionics Interface Data Summaries: AIDS, EF-111A, F-4E, F-4C, F-15A, F-16A, F-111A, F-111E, F-111F, RF-4C, ADA077388, (October, 1979).

43. Jolda, J.G., and Thomas, J.L., A Standardization Evaluation Potential Study of the Common Multi-Mode Radar Program, AFAL-TR-79-1195, (November, 1979).

44. Trainor, W.L., and Weber, Maj J.G., "AVSAIL: A Simulation and Support Laboratory for Digital Avionics Systems Integration and Verification", (1978).

45. Schoppe, W.J., "The Navy's Use of Digital Radio:, IEEE Transactions on Communications, Vol. COM-27, No 12, (December, 1979) pp. 1938-1945.

46. Leedom, D.K., "Representing Human Thought and Response in Military Conflict Simulation Models", Modeling and Simulation of Avionics Systems and Command, Control and Communication Systems, AGARD Conference Proceeding No. 268, NATO, (January, 1980), No. 5.

47. Simon, H.A., "Information Processing Models of Cognition", Annual Review of Psychology, Vol. 30, (1979), pp. 363-396.

48. Newell, A., and Simon, H.A., Human Problem Solving, Englewood Cliffs, N.J.: Prentice-Hall, (1972).

49. Newell, A., and Simon, H.A., "Computers in Psychology", Handbook of Mathematical Psychology, Luce, R.D., Bush, R.R., and Galanter, E., (eds.), New York: John Wiley & Sons, Inc (1963).

50. Chubb, G.P., "SAINT, A Digital Simulation Language for the Study of Manned Systems", AMRL, WPAFB.

51. Kuperman, G.C., and Seifert, D.J., "Development of a Computer Simulation Model for Evaluating DAIS Display Concepts" Proceedings of the Human Factors Society - 19th Annual Meeting, (October, 1975), pp. 347-353.

52. Kuperman, G.C., Hann, R.L., and Berisford, K.M., "Refinement of a Computer Simulation Model for Evaluating DAIS Display Concepts", Proceedings of the Human Factors Society - 21st Annual Meeting, (1977), pp. 305-310.

53. Wortman, D.B., Duket, S.D., Seifert, D.J., Hann, R.L., and Chubb, G.P., Simulation Using SAINT: A User-Oriented Instruction Manual, AMRL-TR-77-61, (July, 1978).

54. Duket, S.D., Seifert, D.J., Hann, R.L., and Chubb, G.P., Documentation for the SAINT Simulation Program, AMRL-TR-77-65, (June, 1978).

55. Duket, S.D., Seifert, D.J., Hann, R.L., and Chubb, G.P., Analyzing SAINT Output Using SPSS, AMRL-TR-77-64, (June, 1978).

56. Wortman, D.B., Duket, S.D., Seifert, D.J., Hann, R.L. and Chubb, G.P., The SAINT User's Manual, AMRL-TR-77-62 (June 1978).

57. Seifert, D.J., and Chubb, G.P., SAINT: A Combined Simulation Language for Modeling Large Complex Systems, AMRL-TR-78-48, (September, 1978).

58. Lane, N.E., Strieb, M.I., and Leyland, W., "Modeling the Human Operator: Applications to System Cost Effectiveness", Modeling and Simulation of Avionics Systems and Command, Control and Communication Systems, AGARD Conference Proceeding No. 238, NATO, (January, 1980), No. 39.

59. Strieb, M.I., and Wherry, R.J., Jr., An Introduction to the Human Operator Simulator, Analytics, TR-1400.02-D, Contract No. N62269-79-C-0235.

60. Lane, N.E., Strieb, M.I., and Wherry, R.J., Jr., "The Human Operator Simulator: Workload Estimation Using A Simulated Secondary Task", Methods to Assess Workload, AGARD Conference Proceedings No. 216, NATO, (June, 1978), No. 11.

1980 USAF - SCEEE SUMMER FACULTY RESEARCH PROGRAM

Sponsored by the

AIR FORCE OFFICE OF SCIENTIFIC RESEARCH

Conducted by the

SOUTHEASTER CENTER FOR ELECTRICAL ENGINEERING EDUCATION

FINAL REPORT

# APPLICATION OF RISK ANALYSIS IN THE ACQUISITION OF MAJOR WEAPON SYSTEMS


| | |
|---|---|
| Prepared by: | Dr. George H. Worm |
| Academic Rank: | Associate Professor |
| Department and: University: | Department of Industrial Management Clemson University |
| Research Location: | AFBRMC/RDCB, Wright-Patterson AFB, OH 45433 |
| USAF Research Colleague: | David Krahenbuhl, Lt Col; Bill Harris, Myron Bailey |
| Date: | August 1, 1980 |
| Contract No: | F49620-79-C-0038 |

# APPLICATION OF RISK ANALYSIS IN THE ACQUISITION OF MAJOR WEAPON SYSTEMS

by

Dr. George H. Worm

## ABSTRACT

An implementation of a statistical approach to cost risk analysis is developed in this paper. A general discussion of risk analysis is presented to familiarize the price analysis with the concepts involved and then forms are presented which allow for the implementation of a risk analysis. Appropriate definitions are given along with a step-by-step procedure. The results of the risk analysis are related to the effect of incentive contracts and several examples are presented.

## ACKNOWLEDGEMENTS

I would like to dedicate this work to the memory of Captain William L. Glover, who helped me greatly in the initial phases of this research. His death has affected me greatly and I will never forget him.

I would also like to thank Col Dean Martin, Lt Col David Krahenbuhl, Mr. Bill Harris, Mr. Myron Bailey, and all of the price analyst who gave freely of their time during my investigation. Also I would like to thank the staff of the Business Research Management Center.

This work was sponsored by the Air Force Systems Command, the Air Force Office of Scientific Research, and the Business Research Management Center.

## I. INTRODUCTION

During the development and procurement phases of acquiring a major defense weapon system, many decisions must be made concerning its performance, cost and scheduling. An important aspect of this decision making process is the analysis of uncertainty* which exists. Common approaches to analyzing uncertainty have in the past focused on the decision maker's intuition, on sensitivity analysis and on risk analysis. At the time of negotiating one of possibly many contracts, the focus is narrowed to the analysis of uncertainty inherent in the projection of cost involved in a contract. The cost of a specific contract and not the cost of the entire system acquisition is discussed here.

When the term risk analysis is used, three types of risk are generally implied. These types are technical risk, cost risk, and schedule risk. In the study of a large weapon system, all of these risks should be analyzed to determine which alternatives should be chosen in order to maximize the probability of having a successful program. When a specific contract for a program is being negotiated, the primary variable of interest is the cost risk. Important to note, however, is that the cost is *not independent of the amount* of technical and schedule risk. The technical and schedule risk are important factors in the estimation of the cost risk and hence the cost which should be negotiated.

For a major weapon acquisition both a price and cost analysis are required. These forms of analyses are methods of investigating historical data and projected costs in order to obtain independent estimates of costs from those provided by the contractor.

The cost analysis is an examination of individual cost elements to determine if the estimates approximate the dollars it should cost to perform the contract if the company operates with reasonable economy and efficiency. In the process of a cost analysis there are many uncertainties which may arise and which are not under the control of the government or the contractor. These uncertainties should be isolated in addition to

---

* Technically many authors differentiate between risk and uncertainty, but the terms will be used interchangeably in this paper.

the cost estimates during the cost analysis. It is important to note that throughout this paper the controllable factors which influence the cost during the performance of a contract are assumed to be at an economic and efficient level on both the part of the government and the contractor.

The price analysis, which is based on comparisons with similar products or earlier production, may provide additional information concerning the estimates and the amount of randomness which might be expected. The price and cost analysis provide the necessary subjective and objective information for a risk analysis. This includes not only the cost esimates but also the definition of random factors which are important influences on cost.

At ASD a price analyst has the responsibility of determining and negotiating a fair and reasonable cost and profit for a contract. Many of the cost elements may be estimated with some degree of certainty and will be referred to as non-random. Examples of non-random cost include negotiated overhead rates, wage rates and certain routine labor costs. Other cost elements will not be known or identifiable with certainty and will be referred to as random. The randomness in the cost elements may be caused by some factor affecting cost or may be totally unexplainable. Causes of randomness in cost elements include design, labor and material uncertainties concerning costs and amounts. The price analyst must still estimate the cost and negotiate a price for the contract. The purpose of this paper is to explain how risk analysis can be used to reflect the extent to which randomness affects total cost.

Random factors affecting cost are events which the contractor cannot control and which are known (or suspected) to impact one or more elements of a cost of the contract. These factors represent the element of risk involved in a contract, thus the term risk analysis.

Again, risk analysis is a procedure for analyzing how randomness affects the total cost. An analyst must identify the random, uncontrollable factors and assess the probability of different events occurring. Then using risk analysis, the distribution of the total cost is obtained. Results of a risk analysis may be useful to a price analyst in several ways. First, it will help to show possible actual costs which might occur and the probability that they will occur. Second, it may help in determining the type of contract to offer. Third, expected cost to the government

and expected profit can be determined. And fourth, actual cost can be bounded or given a range over which it will most likely occur.

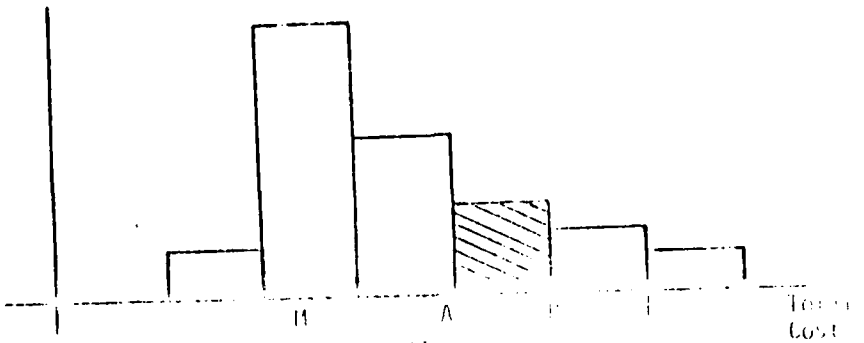
The remainder of this paper will discuss a procedure for risk analysis which avoids the use of simulation by applying some well known statistical properties. First, a structure for risk analysis is discussed which is then applied to a simple case. Second, a cost model is given which allows for a systematic and consistent method of estimating costs and arriving at a total cost. Third, a statistical approach to risk analysis is presented with the accompanying forms for performing the necessary calculations. Finally, examples are given to illustrate the results of a risk analysis.

## II. BACKGROUND FOR RISK ANALYSIS

For risk analysis the contract cost must be viewed as an unknown (at the time of cost and/or price analysis) which will be some specific dollar value in the future. That specific dollar value we will assume is the total cost recognized in the final settlement. If this cost was known with certainty and the profit was agreed upon, the price analyst would be out of business. However, since the cost is not known, the price analyst must estimate cost and degree of risk involved.

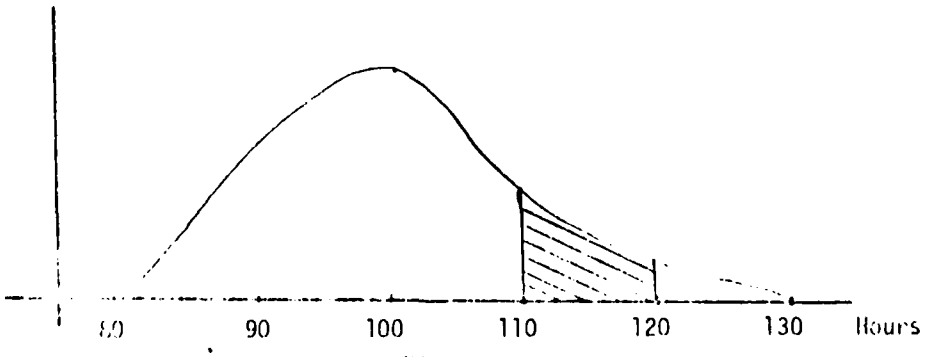
At the time of negotiation, the future actual cost, since unknown, must be estimated. Risk analysis does not exactly estimate the cost but rather estimates its distribution. A distribution is a pictorial representation of the probabilities of different true costs occurring in the final settlement. This distribution is the ultimate goal of risk analysis.

An example of the output of a risk analysis is shown in the graph in Figure 1. This is an example of a discrete distribution, which is simpler than a continuous distribution, and is used when there are discrete outcomes of the random factors. A discussion of a continuous distribution is given later in this section. The height of the curve represents the relative likelihood of occurrence at each cost level. However, the area under the curve gives us probabilities of the cost recognized at the final settlement being between two numbers. In Figure 1, the total area under the curve will always be one and the area shaded is the probability that the final actual cost will be between the two dollar figures "A" and "B." The cost denoted by "M" is sometimes referred to as the most likely value.




Discrete Distribution
Figure I

Appendix I gives a numerical example using discrete events. In the example we have only discussed factors which could have a finite number of outcomes. In most price analysis, however, the randomness is of a continuous type. For instance, the price analysis might estimate that the number of hours required for a contract are going to be between 80 and 130 hours and will most likely be 100. If the distribution of the hours required is continuous then a distribution of the form in Figure II is commonly used. A commonly used distribution for costs is known as a Beta distribution and has several favorable properties to be discussed later.




Continuous Distribution
Figure II

The analyst is only responsible for choosing the three points. He must choose the minimum, the most likely and the maximum. As with the discrete distribution, the total area is one square unit, and in Figure II the number of squared units in the shaded area is the probability that the hours required in the contract will actually be between 110 and 120.

If Beta distributions are used in specifying possible outcomes for the random factors, then the total cost distribution which is the output of the risk analysis is going to be continuous. The procedure described in step 5 of Appendix I is quite a bit more complex than for the discrete case because there are an infinite number of possibilities.

## III. COST MODEL

Common approaches used in risk analysis to handle continuous distributions are simulation and statistical analysis. Although the same basic approach as given in Appendix I is used in simulation, generally a computer is used to manage the calculations involved. Several computer programs for simulation can be found in the literature for performing risk analysis. In order to avoid customizing a risk analysis to a particular contract, a general cost model is given in this section. This cost model is an organization of all the cost subcomponents into a form which can be used in either a simulation study or a statistical analysis.

By applying some well known statistical properties to the cost model below, an alternative to simulation is employed. A general cost model is first described as a starting point for performing a risk analysis for a contract. The total cost is assumed to be comprised of the following subcomponents:

a) Material (MAT),
b) Material Overhead (MATOH),
c) Interdivision Transfer (IT),
d) Direct Engineering Labor (DEL),
e) Engineering Overhead (EOH),

f) Direct Manufacturing Labor (DML),

g) Manufacturing Overhead (MOH),

h) Other Costs (OC), and

i) General and Administrative Expenses (GAE).

In evaluation of a contract, each of these subcomponents are usually broken down further and are commonly interrelated as shown below, where P1 through P4 are specific percentage figures, and R1 and R2 are specific rates. The * is used to denote multiplication. The general cost model is:

MAT = Estimated Material Cost

MATOH = P1* MAT + Estimated Independent Material Overhead

IT = Estimated IT Cost

DEL = (Estimated Engineering Hours)* R1

EOH = P2*DEL + Estimated Independent Engineering Overhead

DML = (Estimated Manufacturing Hours)*R2

MOH = P3*DML + Estimated Independent Manufacturing Overhead

OC = Estimated Other Cost

SUBTOTAL = ST= MAT + MATOH + IT + DEL + EOH + DML + MOH + OC

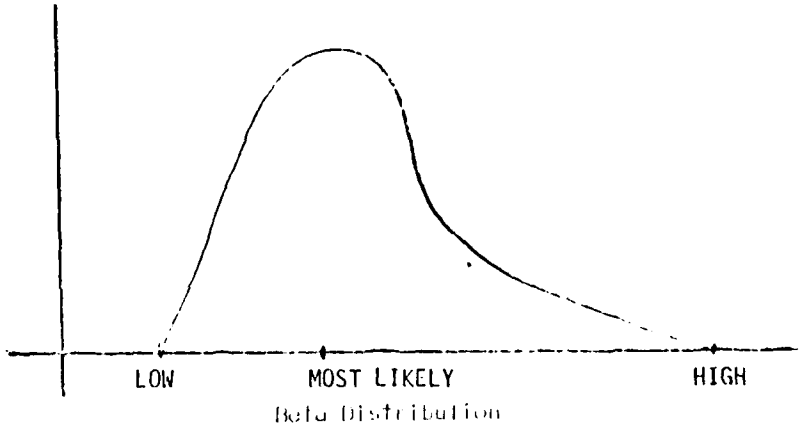
GAE = P4*ST

TOTAL COST = TC = ST + GAE

Even though we are showing the P's and R's as given quantities, they may be considered as random. If they are considered to be random, then a simulation or moments must be used rather than the statistical approach presented here.

Note that in this model eight estimates are needed to determine the total cost. A form for organizing the collection of data required for the risk analysis is given in Form I. The estimates requiring minimum, most likely, and maximum are assumed to be Beta distributed as shown in Figure III. The minimum, most likely, and maximum values must be supplied by the analyst. For each of the cost categories, either the cost ($) or hours must be estimated. The overhead categories are divided into two parts, the independent overhead cost and the overhead rate. The independent overhead cost is a cost which does not change when the direct cost

changes. Usually, the uncertainty in the independent overhead cost is due to future business conditions. The independent overhead cost is commonly allocated to the direct cost and then lumped with the overhead rate, however, it should be kept separate for a risk analysis. The overhead rate should reflect those costs which are directly proportional to the direct cost. It is assumed here that this rate is known with certainty. Using the Beta distribution implicitly assumes that the possible outcomes can be bounded in some finite range. For mature systems, this is not an unreasonable assumption. Appendix II discusses how these aggregate values can best be estimated.




Beta Distribution
Figure III

The formula for the mean (expected) and variance are theoretically based on the properties of the Beta distribution and have been widely used in statistics, risk analysis and scheduling (PERT). The formulas for calculating the Mean and Variance for a Beta distribution are:

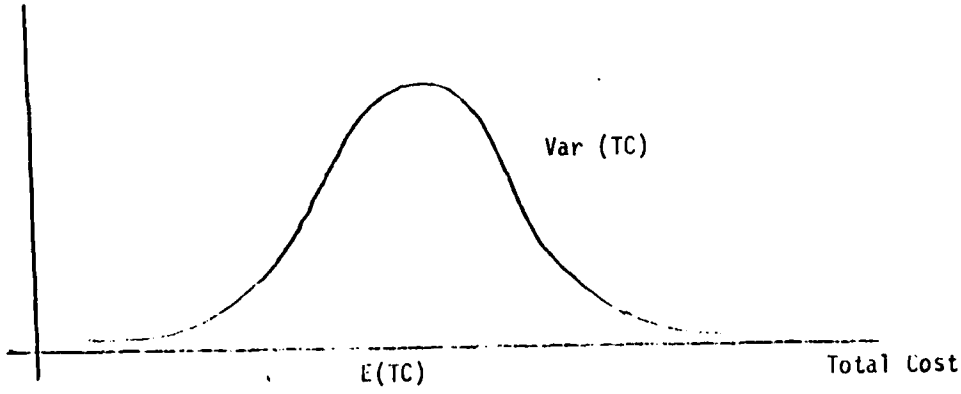
$$\text{Mean} = \frac{L + 4ML + H}{6}$$

and

$$\text{Variance} = \left(\frac{H-L}{6}\right)^2 ,$$

where H=maximum, L=minimum and ML=most likely. These calculations are actually approximations and are very good if the distribution is not too severely skewed ( ).

The theoretical justification for the use of a statistical method in performing risk analysis is presented in Appendix III. This involves rearranging the cost elements of the total cost so that the total cost is a sum of independent random variables. Using this fact the total cost is known to be normally distributed as shown in Figure IV. This means that only the mean (expected value, E(TC)) and variance, Var(TC) need to be determined in order to make statistical statements about the total actual cost. The next section discusses how the expected value and variance can be estimated from the estimates of the individual cost subcomponents.




Normal Distribution
Figure IV

IV. Statistical Procedure for Risk Analysis.

As mentioned above, several estimates are required and therefore need to be defined as closely as possible in order to develop good estimates of the actual cost. Figure V shows that there are many different costs involved from the beginning to the end of a contract. They are:

1. Actual,
2. Negotiated,
3. Objective,
4. Most Likely (estimated),
5. Minimum (estimated),
6. Maximum (estimated),
7. Expected (calculated), and
8. Confidence Intervals for Total Cost (calculated).

These eight costs are described below in order to avoid confusion. The costs 4, 5, and 6 are estimates required for a risk analysis and 7 and 8 are calculated in the risk analysis. The information provided by 7 and 8 should be helpful in the establishment of objectives and in the determination of the type of incentive contract to be used.

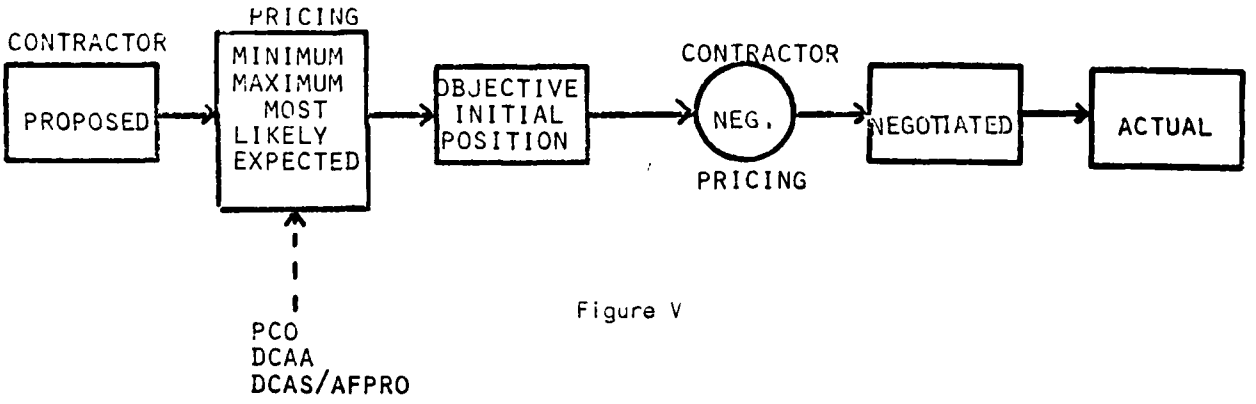



Figure V

1. Actual - The total dollars paid at the time of the final settlement. For incentive contracts the actual is the actual cost plus target profit plus share of underrun or less share of overrun.

2. Negotiated - The negotiated is the target cost, target profit, share and ceiling agreed upon. This will be the basis for the actual settlement as soon as the actual cost is known.

3. Objective - An Air Force goal established before negotiations as an acceptable final negotiated value. Using the proposal and field reports, a fair and reasonable target cost, target profit, ceiling and share are determined. The estimates should be realistic rather than accurate. Realistic assumes that the contractor is responsible for cost control and the creation of operational efficiencies but not necessarily the costs for which he has no control. Accurate estimates tend to encourage inefficiencies and higher prices because the government assumes all cost responsibility.

4. Most Likely - The most likely cost is that projected cost that a contractor may be expected to incur at the completion of the effort under normal, controllable conditions and represents estimated costs that will most likely occur. It does not include uncontrollable risks such as contingencies in the event a vendor does not deliver as scheduled or the quality required, or abnormal cost impacts due to catastrophic conditions. The most likely is an estimate of the actual cost developed using the contractor's proposal, field reports, etc. This estimate is the single <u>most</u> probable cost which might actually occur. There is a tendency to adjust this estimate based on the <u>less</u> probable costs which might occur, however, this adjustment <u>should not</u> be made in the most likely estimate. The most likely estimate should be the estimate of cost which will most likely be correct. Here we are not interested in getting close but are interested in the cost which has the highest probability of actually occurring. This estimate should assume efficencies and cost control on the part of the contractor.

Operationally the objective cost can be used as the most likely if the following guidelines are followed:

A. A predetermined level of efficiency and cost control is assumed for both the government and contractor.

B. The cost estimate is based on expected conditions under which the contractor will have to operate.

C. No adjustments are made to the most likely cost based on what "might" happen during the performance of the contract.

Note that for negotiations the most likely may or may not be the objective depending on the information obtained from the risk analysis.

5. Minimum - The minimum estimate of the actual cost should be the cost expected under the "best" possible conditions during the performance of the contract. The same level of efficiency and cost control as used for the most likely estimate should be assumed for the contractor's behavior. The reasons that the actual cost would be at the minimum are not controllable by the contractor and will be this low only because of chance. Be sure not to confuse this minimum with the least possible negotiated cost. Again, the estimate has nothing to do with what might happen during the negotiations but rather should reflect the least possible actual cost which might occur.

Operationally the minimum can be estimated by:

A. Assuming efficiency and cost control by the contractor during the performance of the contract. (i.e., What is fair and reasonable behavior on the contractor's part?)

B. Determining the best possible conditions (uncontrollable) which might exist during the performance of the contract and estimating the minimum cost.

Note that the actual cost might be lower than the minimum if the contractor performs more efficiently than assumed. The minimum defined here is for a given contractor's behavior and is the minimum over uncontrollable conditions.

6. Maximum - The maximum estimate of the actual cost should be the cost expected under the "worst" possible conditions during the performance of the contract. Again, the same level of efficiency and cost control should be assumed for the contractor's behavior. The maximum cost would not be due to poor performance by the contractor but would be high strictly because of chance. The maximum is not to be confused with the limits placed on the negotiator as his maximum position or the maximum approved position.

Operationally the maximum can be estimated by:

A. Assume efficiency and cost control by the contractor during the performance of the contract (i.e., What is fair and reasonable behavior on the contractor's part?)

B. Determining the worst possible conditions (uncontrollable) which might exist during the performance of the contract and estimating the maximum cost.

Note that the only reason the cost might be higher than the maximum is if there is poor contractor efficiency or cost control. The maximum defined here is for a given contractor's behavior and is the maximum over uncontrollable conditions.

7. Expected - The expected total cost is the average total cost which would occur if the contract were performed many times. This calculated cost may differ from the sum of the most likely cost because it incorporates the randomness involved in each of the cost subcomponents. Actually, the expected total cost is the sum of the expected cost for each subcomponent. From the estimates defined above in 4, 5, and 6 the expected cost can be calculated using a weighted average of those estimates. The formula which is commonly used weights the maximum and minimum equally and weights the most likely by a weight of four. That is:

$$\mu = \text{Expected Cost} = \frac{H + 4ML + L}{6}$$

No truely intuitive feel for this formula can be given, but by weighting the most likely four times as much as the maximum and minimum, the expected cost is pulled away from the midpoint between the maximum and minimum towards the most likely. This formula has been found to work well when the distribution of the cost is not too skewed. As mentioned earlier, the formula for expected cost is theoretically based on the properties of the Beta distribution and has been widely used in statistics, risk analysis, and scheduling (PERT).

The expected total cost will generally be in the center of the possible total costs which might occur. Note that the most likely is not necessarily in the center but is most probable. The expected cost takes into account possible high and (or) low costs which might occur.

8. Confidence intervals for total cost - Just as the expected cost is a measure of the center of the costs which might occur, the variance is a measure of the amount of dispersion in the cost. The variance of individual cost subcomponents can be estimated by dividing the range between the maximum and minimum by six and squaring the results, that is

$$\sigma^2 = \text{Variance} = \left(\frac{H - L}{6}\right)^2$$

The variance of the total cost is then the sum of the variance of the subcomponents. The expected value and variance then totally describe the total because the total is a sum of independent subcomponent costs. The total cost is therefore normally distributed.

A confidence interval is a range of costs which has an associated probability that the actual cost incurred will be in the range. Since the total cost is normally distributed these probability statements are as given below:

| STATEMENT | PROBABILITY |
|---|---|
| Total Incurred Cost $\leq \mu$ | .5 |
| Total Incurred Cost $\leq \mu + 1\sigma$ | .8413 |
| Total Incurred Cost $\leq \mu + 2\sigma$ | .9772 |
| Total Incurred Cost $\leq \mu + 3\sigma$ | .9987 |

For example, of all of the possible outcomes of the cost subcomponents, 84.13% would have a total cost of less than $u + 1\sigma$ or there is a probability of .8413 that the actual total cost incurred will be less than $u + 1\sigma$.

The following is a brief description of Forms I, II, and III which can be used as a risk analysis. The accuracy of probability statements depend on the accuracy of the estimates required. The theoretical considerations of the risk analysis are presented in Appendix III.

The purpose of DD Form 633 is to provide a standard format which the contractor submits to the Government a summary of incurred and estimated costs. Form I attached has the same cost categories but allows for uncertainty in the cost estimates. The only difference is the segmentation of overhead into independent overhead costs and overhead rates. The independent overhead cost does not depend on the direct cost and the overhead rates are the factor applied to the direct cost.

STEP 1: Complete the first three columns of Form I

The estimates required in Form I must be made by the price analyst and may require judgemental factors along with mathematical or other methods of cost estimation. It is assumed that the cost will turn out to be some where between the minimum and maximum bounds estimated. The overhead rates are assumed to be known with certainty.

STEP 2: Calculated last two columns of Form I

The formulas for calculating the mean and variance are supplied at the top of Form I.

STEP 3: Transfer values from Form I to the first two columns of Form II and III

STEP 4: Calculate third column of Forms II and III when multiplied by the factor shown.

The third column is the product of the first two and the totals provide an estimate of the Expected Total Cost, E(TC), and the variance of Total Cost, Var(TC).

The "true total cost" will be normally distributed with mean E(TC) and variance Var(TC). With these estimates of E(TC) and Var(TC) the following probability statements can be made.

| STATEMENT | | PROBABILITY |
|---|---|---|
| True Total Cost | $E(TC)$ | .5000 |
| True Total Cost | $E(TC) + \sqrt{Var(TC)}$ | .8413 |
| True Total Cost | $E(TC) + 2\sqrt{Var(TC)}$ | .9772 |
| True Total Cost | $E(TC) + 3\sqrt{Var(TC)}$ | .9987 |

The Forms I, II, and III can be used to find the expected total cost and the variance and probability statements can be made as above. In addition this information can be used to evaluate different incentive contracts by applying the formulas presented in Appendix III. Since these formulas are very difficult to use, a computer program is given in Appendix IV for calculating the expected profit and expected price for a given incentive contract.

Before discussing the use of this program the concept of expected profit and expected price need to be discussed. As we saw in the example in section II there are many methods of estimating the profit on a contract (see Methods 1-4). The expected profit weighs each possible profit by the probability of the corresponding cost occurring. The expected profit is an average profit if the contract were performed many times. The expected price is the average cost to the government if the contract were performed many times.

An example run of the program is given in Appendix V, where input supplied by the user is underlined and the response of the computer is not. The output in the example is self-explanatory. The high and low are computed at plus and minus 3 $\sqrt{Var(TC)}$. In other words we can be 99.7% confident that the profit and price will be between the high and low values.

Appendix VI is a listing of a computer program which can be used to perform the calculations involved in Forms I, II, and III. The output of the program is a suggested price ceiling and contractor share calculated from the risk analysis. Note that the incentive contract is suggested for contracts which have more than a five percent variation. An example run is given in Appendix VII. The inputs required in addition to the entries in Form I are the Weighted Guideline Method (WGM) profit and the cost risk used in the WGM. The program computes a ceiling and contractor's share based on the concept that $E(TC) + 3\sqrt{Var(TC)}$ is the point of total assumption and the corresponding profit should be the WGM profit less the cost risk.

The next section presents several examples of the use of Forms I, II, and III and discusses the conclusions which can be drawn from each analysis.

## V. EXAMPLES

The following examples are actual cases which have been negotiated or are in the process of being negotiated by ASD Pricing. The specifics concerning the companies and airframes involved are not disclosed here. The estimates in the first three columns of Form I were given by knowledgeable price analysts involved with the negotiations. Cost entries are in $1,000,000 or hours are in 1,000,000 hours. The wage rates are in dollars.

### Case 1

The information obtained from the price analyst for case one is shown in the first three columns of Case 1-I. The material, engineering and manufacturing overheads for this case were considered to be independent. It would be preferable to breakdown the overhead into two separate categories independent and rate applied to a base, however, this information was not available. The effect on the analysis of treating all of the overhead as independent is not extremely significant but will cause the confidence intervals to be tighter than if it were separated.

The hours for labor were not readily available, therefore, the cost of labor was used. This will not have any effect on the results of the analysis.

From the estimates provided, the last two columns of Case 1-I and forms Case 1-II and Case 1-III were completed. The analysis shows that the expected total cost is 38.0266 and the variance is .2877. The following probability statements can then be made.

| STATEMENT ($1,000,000) | PROBABILITY |
|---|---|
| Total Cost $\leq$ 38.0266 | .5000 |
| Total Cost $\leq$ 38.563 | .8413 |
| Total Cost $\leq$ 39.1 | .9772 |
| Total Cost $\leq$ 39.635 | .9987 |

Observe that there is a very small chance of the cost exceeding the expected by more than 4 percent, i.e. $(3\sqrt{Var(TC)}/E(TC))$. With this small risk most likely a FFP would be preferred. This information can be used to decide on the type of contract and to evaluate different share ratios and ceilings. For instance the following information was obtained using the computer program in appendix IV. The share for over and under runs was kept the same in this example.

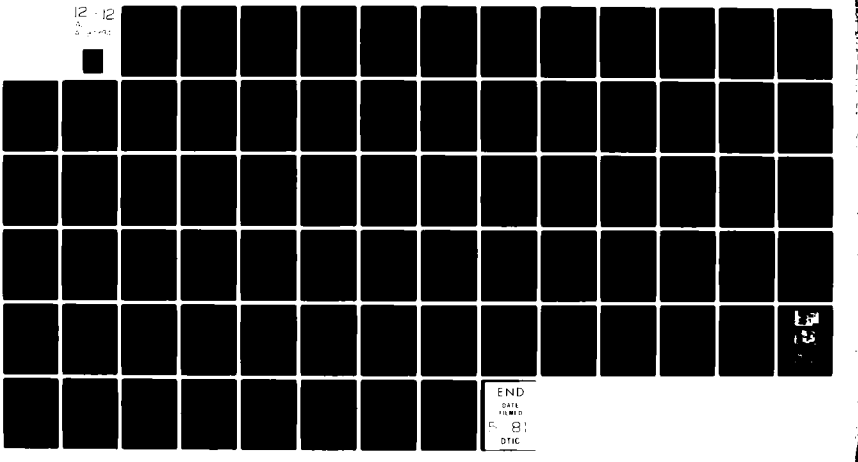
| TARGET COST | TARGET PROFIT | CONTRACTOR'S SHARE | CEILING | PROFIT EXPECTED | PRICE EXPECTED |
|---|---|---|---|---|---|
| 38.5 | 3.85 | .4 | 46. | 4.028 | 42.054 |
| 38.0 | 3.8 | .4 | 39.635 | 1.693 | 39.719 |
| 38.5 | 4.2 | .3 | 42. | 3.959 | 41.986 |
| 38.5 | 3.85 | .3 | 42. | 3.891 | 41.918 |
| 38 | 3.8 | .3 | 39.635 | 1.6725 | 39.699 |
| 38.5 | 4.2 | .4 | 42. | 3.961 | 41.989 |
| 38.5 | 4.2 | .3 | 46. | 4.329 | 42.356 |

Note that the expected profit and the expected price are all approximately the same, indicating that the FFP contract would be preferred as mentioned earlier. Although the second and fifth contracts appear to be less costly, the ceiling would be far to tight (approximately 104%).

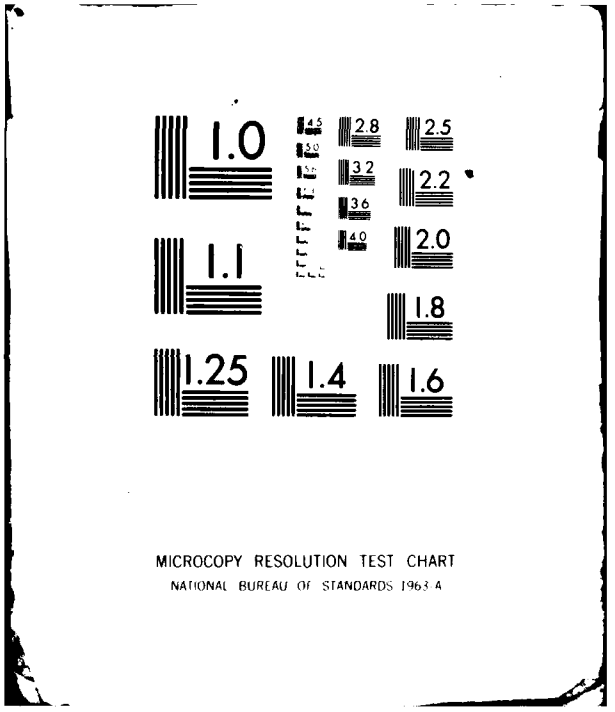
AD-A097 394 SOUTHEASTERN CENTER FOR ELECTRICAL ENGINEERING EDUCAT--ETC F/G 5/1
USAF SUMMER FACULTY RESEARCH PROGRAM, 1980, RESEARCH REPORTS, V--ETC(U)
OCT 80 W D PEELE F49620-79-C-0038

UNCLASSIFIED AFOSR-TR-81-0193 NL

12 12



END
DATE FILMED
5 81
DTIC


1.0
1.1
1.25
1.4
1.6
1.8
2.0
2.2
2.5
2.8
3.2
3.6
4.0
MICROCOPY RESOLUTION TEST CHART
NATIONAL BUREAU OF STANDARDS 1963-A

ESTIMATES FOR RISK ANALYSIS

($1,000,000)

| SUBCOMPONENTS | | ESTIMATES MINIMUM (L) | MOST LIKELY (ML) | MAXIMUM (H) | EXPECTED VALUE L + 4ML + H / 6 | | CALCULATED VALUE (E − L)² / 5 | |
|---|---|---|---|---|---|---|---|---|
| MATERIAL | COST | 7.9 | 8.0 | 8.1 | 8.0 | E(V1) | .0011 | Var V1 |
| MATERIAL OVERHEAD | INDEPENDENT | 1.2 | 1.3 | 1.4 | 1.3 | E(V2) | .0011 | Var V2 |
| RATE FOR MATERIAL | 0 P1 | | | | | | | |
| DIRECT ENGRG | COST | | | | | E(V3) | | Var V3 |
| DIRECT ENGRG LABOR | ~~cost~~ ~~HOURS~~ | 2.6 | 3.6 | 3.6 | 3.43 | E(V4) | .0279 | Var V4 |
| WAGE RATE | 1. R1 | | | | | | | |
| ENGRG OVERHEAD | INDEPENDENT | 4.1 | 5.6 | 5.6 | 5.35 | E(V5) | .0625 | Var V5 |
| RATE FOR ENGRG | 0 P2 | | | | | | | |
| MFG LABOR | ~~cost~~ ~~HOURS~~ | 3.9 | 4.6 | 4.7 | 4.5 | E(V6) | .0178 | Var V6 |
| WAGE RATE | 1. R2 | | | | | | | |
| MFG OVERHEAD | INDEPENDENT | 9.9 | 10.2 | 10.9 | 10.1 | E(V7) | .1111 | Var V7 |
| RATE FOR MFG | 0 P3 | | | | | | | |
| OTHER COSTS | COST | .66 | .68 | .68 | .6767 | E(V8) | .00001 | Var V8 |
| G&A EXPENSES | | | | | | | | |
| PERCENT OF SUBTOTAL | .14 P4 | | | | | | | |

85-22

FORM I

CASE 1-I

RISK ANALYSIS WORKSHEET (EXPECTED VALUE)

| | (COL 1) | | (COL 2) | (COL 3) = (COL 1) * (COL 2) |
|---|---|---|---|---|
| (1 + P1) | | E(V1) | 8.0 | 8.0 |
| | 1 | E(V2) | 1.3 | 1.3 |
| | 1 | E(V3) | | |
| (R1 + R1*P2) | | E(V4) | 3.43 | 3.43 |
| | 1 | E(V5) | 5.35 | 5.35 |
| (R2 + R2*P3) | | E(V6) | 4.5 | 4.5 |
| | 1 | E(V7) | 10.1 | 10.1 |
| | 1 | E(V8) | .6767 | .6767 |
| | | | TOTAL (COL 3) | 33.3567 |
| | | | (1 + P4) | 1.14 |
| | | | EXPECTED TOTAL COST = E(TC) = (1 + P4)* TOTAL (COL 3) | 38.03 |

FORM II

CASE I-II

RISK ANALYSIS WORKSHEET (VARIANCE)

| | (COL 1) | | (COL 2) | (COL 3) = (COL 1) * (COL 2) |
|---|---|---|---|---|
| $(1 + P1)^2$ | 1 | Var(V1) | .0011 | .0011 |
| | 1 | Var(V2) | .0011 | .0011 |
| | 1 | Var(V3) | | |
| $(R1 + R1*P2)^2$ | 1 | Var(V4) | .0278 | .0278 |
| | 1 | Var(V5) | .0625 | .0625 |
| $(R2 + R2*P3)^2$ | 1 | Var(V6) | .0178 | .0178 |
| | 1 | Var(V7) | .1111 | .1111 |
| | 1 | Var(V8) | .00001 | .00001 |
| | | | TOTAL (COL 3) | .22142 |
| | | | $(1 + P4)^2$ | $(1.14)^2$ |

VARIANCE OF TOTAL COST = Var(TC) = $(1 + P4)^2$ *TOTAL (COL 3) = .2874

FORM III

CASE I-III

Case 2

The information obtained from the price analyst for Case 2 is shown in the first three columns of Case 2-I. In this example the overheads were not considered to be independent and fringe benefits were a factor applied to labor. Note that the fringe rate was added to the overhead rate although it was in other costs originally.

From the estimates provided, the total cost using the minimum, most likely, and maximum were 18,579; 19,532; and 20,430 respectively. After completing Case 2-II and Case 2-III the resulting expected value and variance were 19,525 and 33,327. The following probability statements can then be made.

| STATEMENT ($1,000) | PROBABILITY |
|---|---|
| Total Cost $\leq$ 19,525 | .5 |
| Total Cost $\leq$ 19,707 | .8413 |
| Total Cost $\leq$ 19,890 | .9772 |
| Total Cost $\leq$ 20,072 | .9987 |

Note that the total cost obtained from the maximum positions 20,430 would be extremely improbable if the contractor is efficient and uses cost controls.

This case has very little uncertainty because the extreme case of 20,072 is only 2.8% ($3\sqrt{Var(TC)}/E(TC)$ larger than the expected cost. This would indicate a FFP type of contract would most likely be acceptable. The maximum gain or loss for the contractor for a FPIF contract would be his share of 2.8% of the expected cost. For instance, if the share ratio were 40% the contractor may gain or lose atmost (atmost means with probability less than .13%) 1.12% profit due to the uncertainty in this contract.

ESTIMATES FOR RISK ANALYSIS

($1,000)

ESTIMATES

| SUBCOMPONENTS | | MINIMUM (L) | MOST LIKELY (ML) | MAXIMUM (H) | EXPECTED VALUE $\frac{L + 4ML + H}{6}$ | | CALCULATED VARIANCE $\left(\frac{H - L}{6}\right)^2$ | |
|---|---|---|---|---|---|---|---|---|
| MATERIAL | COST | 8,367 | 8,867 | 9267 | 8,850.3 | E(V1) | 22,500 | Var |
| MATERIAL OVERHEAD | INDEPENDENT | | | | | E(V2) | | Var |
| RATE FOR MATERIAL | .045 P1 | | | | | | | |
| ENGRG ENGRS | COST | 1751 | 1905 | 2060 | 1,905.2 | E(V3) | 2,652.3 | Var |
| DIRECT ENGRG LABOR | HOURS | 34 | 39 | 45 | 39.16 | E(V4) | 3.4 | Var |
| LABOR RATE | 11.57 R1 | | | | | | | |
| ENGRG OVERHEAD | INDEPENDENT | | | | | E(V5) | | Var |
| RATE FOR ENGRG | .63 P2 String .4 | | | | | | | |
| DIRECT MFG LABOR | HOURS | 214 | 217 | 221 | 217.2 | E(V6) | 1.4 | Var |
| LABOR RATE | 11.03 R2 | | | | | | | |
| MFG OVERHEAD | INDEPENDENT | | | | | E(V7) | | Var |
| RATE FOR MFG | 1.14 P3 String .4 | | | | | | | |
| NEW COSTS | COST | 420 | 450 | 480 | 450 | E(V8) | 100 | Var |
| G&A EXPENSES | | | | | | | | |
| PERCENT OF SUBTOTAL | .0492 P4 | | | | | | | |

FORM I

CASE 2-I

RISK ANALYSIS WORKSHEET (EXPECTED VALUE)

| | (COL 1) | | (COL 2) | (COL 3) = (COL 1) * (COL 2) |
|---|---|---|---|---|
| (1 + P1) | 1.045 | E(V1) | 8,850.3 | 9,248.3 |
| | 1 | E(V2) | | |
| | 1 | E(V3) | 1,905.2 | 1,905.2 |
| (R1 + R1*P2) | 23.49 | E(V4) | 39.16 | 919.9 |
| | 1 | E(V5) | | |
| (R2 + R2*P3) | 28.02 | E(V6) | 217.2 | 6,085.9 |
| | 1 | E(V7) | | |
| | 1 | E(V8) | 450 | 450 |
| | | | TOTAL (COL 3) | 18,609.6 |
| | | | (1 + P4) | 1.0492 |
| | | | EXPECTED TOTAL COST = E(TC) = (1 + P4)* TOTAL (COL 3) | 19,525 |

FORM II

CASE 2 - II

RISK ANALYSIS WORKSHEET (VARIANCE)

| | (COL 1) | (COL 2) | (COL 3) = (COL 1) * (COL 2) |
|---|---|---|---|
| $(1 + P1)^2$ | 1.092 | Var(V1) 22,500 | 24,570 |
| | 1 | Var(V2) | |
| | 1 | Var(V3) 2,652.3 | 2,652.3 |
| $(R1 + R1*P2)^2$ | 551.78 | Var(V4) 3.4 | 1,876. |
| | 1 | Var(V5) | |
| $(R2 + R2*P3)^2$ | 784.9 | Var(V6) 1.4 | 1098.8 |
| | 1 | Var(V7) | |
| | 1 | Var(V8) 100 | 100 |
| | | TOTAL (COL 3) | 30,297 |
| | | $(1 + P4)^2$ | 1.1 |
| | | VARIANCE OF TOTAL COST = Var(TC) = $(1 + P4)^2$ *TOTAL (COL 3) | 33,327 |

FORM III

CASE 2 - III

Case 3

The information obtained from the price analysts for Case 3 is shown in the first three columns of Case 3-I. The overhead in this example could not be separated from the costs associated with material, engineering labor, and manufacturing labor. This is no problem in the analysis except for the difference which would occur if the independent overhead were kept separate.

The G&A is not a percent of the subtotal in this example and is treated differently. This example was used to illustrate that to handle special cases the forms may need to be adjusted.

The minimum most likely and maximum positions result in a total cost of 63.2, 66.1, and 71.55 (million) respectively. After completing Case 3-II and Case 3-III the resulting expected value and variance were 66.5 and .6013. The following probability statements can then be made.

| STATEMENT ($1,000,000) | PROBABILITY |
|---|---|
| True Cost $\leq$ 66.5 | .5 |
| True Cost $\leq$ 67.3 | .8413 |
| True Cost $\leq$ 68.1 | .9772 |
| True Cost $\leq$ 68.9 | .9987 |

Note that the most likely position is .4 million less than the expected cost. This would indicate that the most likely position is a little too low. Again in this example there is very little uncertainty. There is almost (probability less than .0013) no chance that the cost will vary more than 3.6% ($3\sqrt{Var(TC)}/E(TC)$ because of the uncertainty. It is of interest to note that the maximum position is 3.4 million more than 68.1 which will be exceeded with probability 1-.9772 = .0228.

ESTIMATES FOR RISK ANALYSIS

($1,000,000)

ESTIMATES

| COMPONENTS | | MINIMUM (L) | MOST LIKELY (ML) | MAXIMUM (H) | EXPECTED VALUE $\frac{L + 4ML + H}{6}$ | | CALCULATED VARIANCE $\left(\frac{H - L}{6}\right)^2$ | |
|---|---|---|---|---|---|---|---|---|
| MATERIAL | O.H. + COST | 39 | 40.2 | 42.1 | 40.3167 | E(V2) | .2669 | V2 |
| MATERIAL OVERHEAD | INDEPENDENT | | | | | E(V2) | | |
| RATE FOR MATERIAL | 0 P1 | | | | | | | |
| DIRECT LABOR | COST | | | | | E(V3) | | |
| DIRECT ENGRG LABOR | cost+oh HOURS | 1.5 | 1.6 | 1.95 | 1.6417 | E(V4) | .0056 | V4 |
| LAB RATE | 1 R1 | | | | | | | |
| ENGRG OVERHEAD | INDEPENDENT | | | | | E(V6) | | |
| RATE FOR ENGRG | 0 P2 | | | | | | | |
| DIRECT MFG LABOR | cost+OH HOURS | 13.9 | 15.0 | 17.1 | 15.1667 | E(V8) | .2844 | V8 |
| LABOR RATE | 1 R2 | | | | | | | |
| MFG OVERHEAD | INDEPENDENT | | | | | E(V7) | | |
| RATE FOR MFG | 0 P3 | | | | | | | |
| OTHER COSTS | COST | 5.3 | 5.7 | 6.5 | 5.7667 | E(V8) | .04 | V8 |
| G&A EXPENSES | | 3.5 | 3.6 | 3.9 | 3.633 | | .0044 | |
| PERCENT OF SUBTOTAL | 0 P4 | | | | | | | |

FORM I

CASE 3-I

RISK ANALYSIS WORKSHEET (EXPECTED VALUE)

| | (COL 1) | | (COL 2) | (COL 3) = (COL 1) * (COL 2) |
|---|---|---|---|---|
| (1 - P1) | 1 | E(V1) | 40.3167 | 40.3167 |
| | 1 | E(V2) | | |
| | 1 | E(V3) | | |
| (R1 + R1*P2) | 1 | E(V4) | 1.6417 | 1.6417 |
| | 1 | E(V5) | | |
| (R2 + R2*P3) | 1 | E(V6) | 15.1667 | 15.1667 |
| | 1 | E(V7) | | |
| | 1 | E(V8) | 5.7667 | 5.7667 |
| G+A | 1 | | 3.633 | 3.633 |
| | | | TOTAL (COL 3) | 66.525 1 |
| | | | (1 + P4) | 1 |
| | | | EXPECTED TOTAL COST = E(TC) = (1 + P4)* TOTAL (COL 3) | 66.525 1 |

FORM II

CASE 3-II

RISK ANALYSIS WORKSHEET (VARIANCE)

| | (COL 1) | | (COL 2) | | (COL 3) = (COL 1) * (COL 2) |
|---|---|---|---|---|---|
| $(1 + P1)^2$ | 1 | Var(V1) | .2669 | | .2669 |
| | 1 | Var(V2) | | | |
| | 1 | Var(V3) | | | |
| $(R1 + R1*P2)^2$ | 1 | Var(V4) | .0056 | | .0056 |
| | 1 | Var(V5) | | | |
| $(R2 + R2*P3)^2$ | 1 | Var(V6) | .2844 | | .2844 |
| | 1 | Var(V7) | | | |
| | 1 | Var(V8) | .04 | | .04 |
| G*A | 1 | | .0044 | | .0044 |
| | | | | TOTAL (COL 3) | .6013 |
| | | | | $(1 + P4)^2$ | 1 |
| | | | | VARIANCE OF TOTAL COST = Var(TC) = $(1 + P4)^2$ *TOTAL (COL 3) | .6013 |

FORM III

CASE 3-III

## VI. SUMMARY

In this paper an attempt has been made to provide and explain the necessary concepts for a risk analysis. Although the methodology is theoretically sound, the user should be aware of the following pitfalls in attempting to use the forms supplied here.

1. Preconceived definitions of terms used in this paper should be avoided. For the purpose of risk analysis the user should not already know the meaning of the following terms unless he has a strong background in statistics. The technical terms used here include:

   A. Risk analysis,

   B. Probability distribution,

   C. Maximum and minimum costs,

   D. Most likely costs,

   E. Expected cost,

   F. Variance,

   G. Actual total cost as a random variable, and

   H. Independent cost subcomponents.

2. Bias positions in estimates of costs will result in a bias risk analysis.

3. Contractor efficiency and cost control are not an issue in this analysis.

4. As more information becomes available the maximum, most likely, and minimum should be adjusted appropriately and the risk analysis repeated. Additional information will tend to reduce the amount of variability.

5. The risk factor used in the profit weighted guidelines should not be added in addition to the cost which is added because of a risk analysis.

6. This analysis should not be used if the total cost is dominated by one cost subcomponent. Good business sense should always be applied in defining objectives and risk analysis should be recognized as only an information tool for capturing the uncertainty in cost estimations. This tool helps the analyst to see what might happen in order to choose appropriate objects and/or contract types.

Risk analysis can be a very useful tool but the results should always be interpreted with common sense.

## Suggested Readings in Cost Risk Analysis


1. Dienemann, P. F., "Estimating Cost Uncertainty Using Monte Carlo Techniques," RM-4854-PR, The Rand Corporation. January, 1966.

2. Fisher, G. H., Cost Considerations in Systems Analysis, American Elsevier Publishing Company, New York.

3. Klein, Michael R., Treating Uncertainty in Cost Analysis: The Beta Distribution, U.S. Navy CNO Resource Analysis Group.

4. Murphy, E. L., Jr., "Statistical Methods of Measuring the Uncertainty of Cost Estimates," AD 718862, February, 1970.

5. Quade, E. S. and Boucher, W. I., System Analysis and Policy Planning--Application in Defense, American Elsevier Publishing Company, New York.

6. Schaefer, D. F., Husic, F. J. and Gutowski, M. F., "A Mote Carlo Simulation Approach to Cost--Uncertainty Analysis," AD 850054, March 1969.

7. Wilder, J. J., An Analytical Method of Cost Risk Analysis, Grumman Aerospace Corporation, PDR-OP-T77-12, June 1977.

## APPENDIX I

### Discrete Risk Analysis

In discussion of risk analysis, we are concerned with those factors which are random (i.e., which cannot be controlled) and which affect cost in some way. For instance, we are not sure how many labor hours will be required or how much scrap there will be. Once the randomness is determined, a risk analysis can be performed in the following way.

STEP 1 - Identify those random factors which would affect the cost of the contract. (A factor might be the number of hours required by the contract).

These factors should be as independent as possible. That is, the future outcome or value of one factor should not influence the outcome of another. If this is not the case then the dependence of one factor on another must be defined.

STEP 2 - Determine the specific outcomes which might occur for each factor and the probability of each occurring. (The outcomes of hours required could be "high" with probability .3 or "low" with probability .7).

STEP 3 - Break the total cost into subcomponents and define how these subcomponents are interrelated.

STEP 4 - Define which cost subcomponents would be affected by each factor and the magnitude of the effects for each possible outcome.

STEP 5 - The distribution of the total cost (e.g., Figure I) may be obtained by considering all possible combinations of the states of the factors, calculating the total cost and weighing these costs by the product of the probabilities of the specific outcomes occurring.

Using the above procedures one should make sure that "bias" and randomness are separated. If bias is included in a risk analysis, then it

should be recognized as such and not incorporated as part of the randomness. Risk analysis of a bias position can be performed, however, the end result will also be biased.

A simple example may help to explain exactly what is meant by the steps described in Section II for a discrete distribution. This example is oversimplified in order to demonstrate how a risk analysis could be performed. For the contract under consideration we have three cost subcomponents which are interrelated as follows:

1. Labor = hours times wage rate

Step 2. Materials
3

3. Overhead = Labor overhead plus General and Administrative (G&A)

Total cost is then Labor plus Materials plus Overhead. Note that a change in labor hours or wage rate affect Labor and also Overhead.

Suppose that for the contract under consideration, we expect the following:

| | | |
|---|---|---|
| Labor hours | = | 100 |
| wage rate | = | $10/hr |
| Labor Overhead | = | 150% Labor |
| materials | = | $5000 |
| G&A | = | $1000 |

Therefore the cost model above gives us:

Estimated Total Cost = $8,500

The factors which we have determined to affect the cost of this project are:

1. Uncertain estimate of hours

Step 2. Negotiated new wage rate with union
1

3. Reliability of supplier of materials

The outcomes of these factors are given below with their associated probabilities. Generally these probabilities are subjective estimates by the price analyst.

1. Uncertain estimate of hours

   a) 25% chance hours will be 80
   b) 50% chance hours will be 100 (expected)
   c) 25% chance hours will be 130

STEP 2

2. Negotiated wage rate with union

   a) 70% change low wage rate ($10) (expected)
   b) 30% chance high wage rate will occur ($11)

3. Reliability of supplier of materials

   a) 75% chance supplier will deliver ($5,000)(expected)
   b) 25% chance the materials will have to be purchased on open market ($6,000)

Note that the total of the probabilities under each factor total 100%. This must always be the case. The factors above will effect the cost in the following manner.

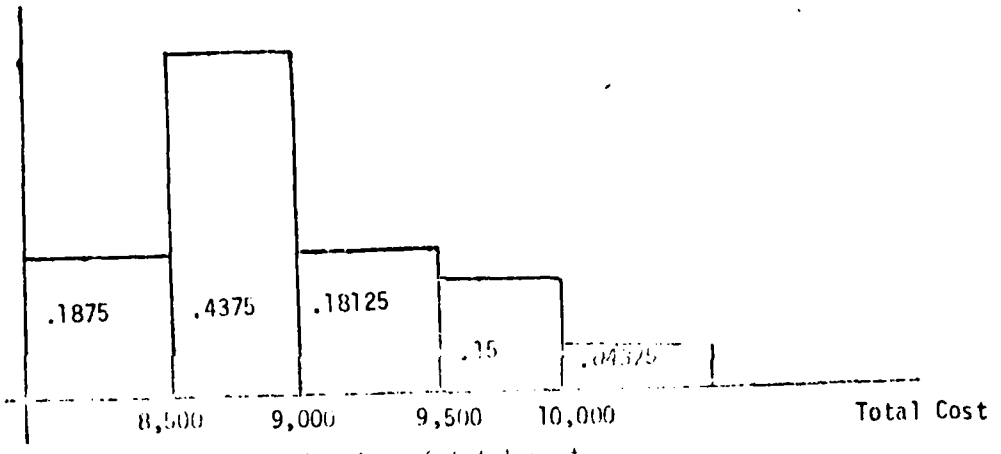
Factor 1 - the outcome of factor number 1 clearly is going to effect the total cost by the amount caused by changing the hours in the cost model defined in step 3.

Step 4

Factor 2 - Suppose that the low wage rate is $10/hr, but may have to be increased to $11/hr. The effect on total cost can be determined by changing the wage rate in model given in step 3.

Factor 3 - The current supplier will supply the material at $5,000, however, if he fails to do so then the materials will cost us $6,000. This will effect the material cost only.

The possible costs for this contract are given in Table I below with their associated probabilities. The resulting probability distribution for total cost of the project is shown in Figure VII. From this graph we can now make statements about the probability that the true final cost will be in different ranges. For instance, the probability that the total cost will be between $9,000 and $9,500 is .18125. Also, we can see that there is only a .04375 probability that the total cost will exceed $10,000. The most likely cost will be between $8,500 and $9,000.




Distribution of total cost
Figure VII

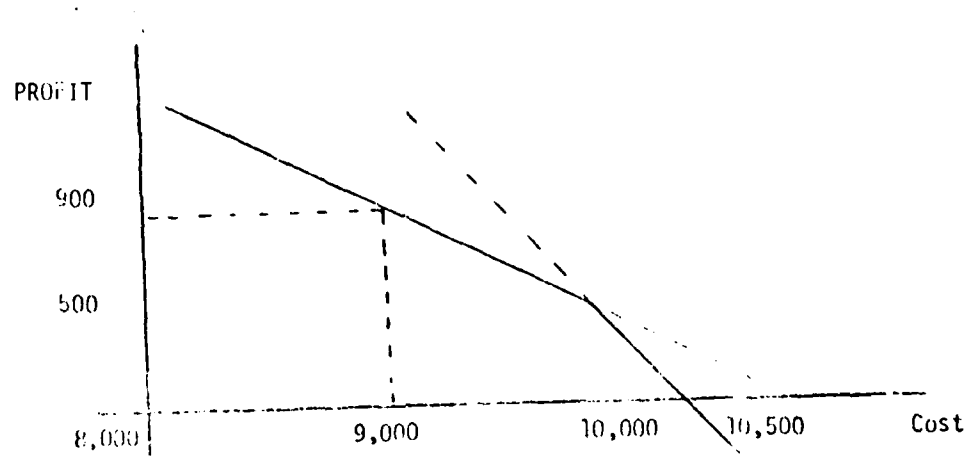
Expected cost is the cost which would occur on the average if this contract were executed many times. It is determined by weighing the total costs in Table I by the associated probability. In this case, the expected total cost is .05625 (8000) + .1125(8500) + . . . = $8,866.87.

*If we compare the information obtained above and in Figure VII to the* total cost using only what we expected, it is clear that our original estimate of the cost was too low ($8,500).

Let us now evaluate a Fixed Price Incentive Firm contract where

Target Cost = $9,000,
Target Profit = $ 900,
Price Ceiling = $10,250, and
Contractor Share = 30%.

See Figure VIII for the cost/profit graph.




FIXED PRICE INCENTIVE FIRM, COST-PROFIT GRAPH
Figure VIII

Several possible ways exist for determining the profit and the cost to the government which might be expected.

Method 1 - If we use our original estimates of the cost components the profit appears to be 900 + .3 (9,000 - 8,500) = 1,050. The corresponding cost to the government would be 8,500 + 1,050 = 9,550.

Method 2 - If we use the expected cost, the profit appears to be 900 + .3 (9,000 - 8,867) = 940. The corresponding cost to the government would be 8,867 + 940 = 9,807.

Method 3 - Using the same method as used to determine the expected cost, the expected profit can be determined by weighing each of the profits determined by the outcomes in Table 1 by the associated

probabilities. In this case, expected profit would be .05625 (900 + .3(9000-8000)) + .1125 (900 + .3(9000-8500)) + . . . = 996 and the expected cost to the government would be 8,867 + 996 = $9,863.

Method 4 - The best and worst possibilities and the probability of them occurring are given below.

| | BEST | WORST |
|---|---|---|
| Probability | .05625 | .04375 |
| Cost | 8,000 | 10,075 |
| Profit | 1,200 | 175 |
| Cost to Gov't | 9,200 | 10,250 |

The four methods above are used to show that different estimated costs to the government and different profits can be obtained. Method 1 is a common method which does not include the risk. Methods 3 and 4 are the method of determining the expected profit and cost to the government using risk analysis. In fact, if all of the randomness is contained in the three factors used and it were possible to perform this contract many times, the average profit per contract and the average cost to the government would be the expected values given in Method 3.

STATES

| FACTOR 1 | FACTOR 2 | FACTOR 3 | PROBABILITY | LABOR | MATERIAL | OVERHEAD | TOTAL COST |
|---|---|---|---|---|---|---|---|
| 1a | 2a | 3a | .05625 | 800 | 5,000 | 2,220 | 8,000 |
| 1b | 2a | 3a | .1125 | 1,000 | 5,000 | 2,500 | 8,500 |
| 1c | 2a | 3a | .05625 | 1,300 | 5,000 | 2,950 | 9,250 |
| 1a | 2b | 3a | .13125 | 880 | 5,000 | 2,320 | 8,200 |
| 1b | 2b | 3a | .2625 | 1,100 | 5,000 | 2,650 | 8,750 |
| 1c | 2b | 3a | .13125 | 1,430 | 5,000 | 3,145 | 9,575 |
| 1a | 2a | 3b | .01875 | 800 | 5,500 | 2,200 | 8,500 |
| 1b | 2a | 3b | .0375 | 1,000 | 5,500 | 2,500 | 9,000 |
| 1c | 2a | 3b | .01875 | 1,300 | 5,500 | 2,950 | 9,750 |
| 1a | 2b | 3b | .04375 | 880 | 5,500 | 2,320 | 8,700 |
| 1b | 2b | 3b | .0875 | 1,100 | 5,500 | 2,650 | 9,250 |
| 1c | 2b | 3b | .04375 | 1,430 | 5,500 | 3,145 | 10,075 |

TABLE I

## APPENDIX II

### Aggregated Estimates

Usually, the values required in Form I are not aggregated to the level required. It is necessary therefore to discuss how these aggregate estimates can be determined from much more detailed estimates. The procedures for aggregation are of two types. First is the estimation of maximum, most likely and minimums for a total, where the maximums, most likelies and minimums are estimated for each element of a total. Second is the estimate of aggregate rates or percentages.

For the first type, it would not be correct to estimate the maximum, most likely and minimum by simply adding the corresponding values from each element. For instance, Material may be composed of three elements such as

| | Minimum(L) | Most Likely(ML) | Maximum(H) |
|---|---|---|---|
| Subcontracted Items | 5,000 | 6,000 | 8,000 |
| Purchased Parts | 3,000 | 3,000 | 3,000 |
| Other Material | 10,000 | 12,000 | 16,000 |

Then rather than using the three corresponding totals 18,000, 21,000 and 27,000 and coming up with a mean of 21,500 and a variance of 2,250,000, we would find the mean and variance of each element and use the total, which would be a mean of 21,500 and a variance of 1,250,000. Remember that the mean and variance are calculated as

$$\text{Mean} = \frac{L + 4*ML + H}{6} \quad \text{and}$$

$$\text{Variance} = \left(\frac{H - L}{6}\right)^2 .$$

In mathematical form the mean and variance for a total of several elements is given by:

$$\text{Mean} = \sum_{i=1}^{n} \frac{L_i + 4*ML_i + H_i}{6}$$

$$\text{Variance} = \sum_{i=1}^{n} \left( \frac{H_i - L_i}{6} \right)^2 ,$$

where i denotes the $i^{th}$ element and n is the number of elements of the total. For this type of situation, the maximum, most likely and minimum are not needed since the mean and variance are already determined.

For the second type of aggregation, a weighted average could be used as the single rate or percentage needed. For instance, suppose that the labor hours are broken into two parts

| | Hours(H) | Rate(R) |
|---|---|---|
| Skilled | 300 | $11.00 |
| Non-Skilled | 500 | $ 8.00 |

Then the weighted average rate would be (300*11 + 500*8)/(300 + 500) or 9.125. *Note that when this rate is applied to the total hours we get the same as if the two rates were applied separately and then totaled.* Mathematically this could be expressed as

$$\text{Average Rate} = \sum_{i=1}^{n} H_i * R_i \Big/ \sum_{i=1}^{n} H_i ,$$

where i denotes the $i^{th}$ element and n is the number of elements. A weighted average percentage can be obtained in the same fashion.

## APPENDIX III

### STATISTICAL APPROACH

The approach used in this paper to perform risk analysis is the application of some well known statistical analysis to the cost model described in Section III. The statistical analysis approach is useful in the handling of continuous distribution problems.

The statistical concept used in this paper is one which states that the sum of independent random variables will be approximately normally distributed with a mean equal to the sum of the individual means and variance equal to the sum of the individual variances. Usually for more than four independent random variables this approximation is also very good.

If we rewrite our total cost model, we can get it into the form need. That is:

$$TC = \{(1+P1)*V1 + V2 + V4*(R1 + R1*P2) + V6*(R2 + R2*P3) + V5 + V3 + V7 + V8\} *(1 + P4)$$

where V1 = Material Cost
V2 = Independent Material Overhead
V3 = IT Cost
V4 = Engineering Hours
V5 = Independent Engineering Overhead
V6 = Manufacturing Hours
V7 = Independent Manufacturing Overhead
V8 = Other Costs

Using the notation E(V1) to represent the mean of variable V1 and Var (V1) to denote the variance of V1, the mean E(TC), and variance, Var (TC), of the total cost are:

$$E(TC) = \{(1+P1)*E(V1) + E(V2) + E(V4)*(R1+R1*P2) + E(V6)* (R2 + R2*P3) + E(V5) + E(V3) + E(V7) + E(V8)\} * (1+P4)$$

$$Var(TC) = \{(1+P1)^2*V(V1) + Var(V2) + Var(V4)*(R1+R1*P2)^2 + Var(V6)* (R2+R2*P3)^2 + Var(V5) + Var(V3) + Var(V7) + Var(V8)\} *(1 + P4)^2$$

The distribution of the total cost would thus be as given in Figure VI.

The normal distribution has the property that probability statements can be made using only the mean and variance. For instance, there is a 68% chance that the total cost will be between $E(TC) \pm \sqrt{Var(TC)}$ and a 95% chance that the total cost will be between $E(TC) \pm 2*\sqrt{Var(TC)}$.

In order to facilitate the calculation of E(TC) and Var(TC), two work sheets are provided in Forms II and III. The values needed for these worksheets can be taken from the form in Form I.

Once the mean and variance of the total cost have been determined, the distribution of the total cost is completely described since the total cost is normally distributed. The functional form of the normal distribution is:

$$f(c) = \frac{1}{\sqrt{2\pi}\sigma} e^{-\frac{(c-\mu)^2}{2\sigma^2}}$$

Where $\mu = E(TC)$ and $\sigma^2 = Var(TC)$. This distribution is then the completion of the risk analysis.

Let us now investigate the effect of risk on a Fixed Price Incentive Firm contract which is commonly used for contracts which have some risk but not enough to resort to a cost plus type contract. In particular, the expected profit and the expected cost to the government will be expressed in terms of the following variables:

TC = Target Cost

TP = Target Profit

PC = Ceiling Price

a = Contractor's share of underruns

b = Contractor's share of overruns

CC = Point of total assumption = $\frac{PC - (TC + TP)}{1-b} + TC$

and

f(c) = distribution of true total cost

A profit-cost graph for a Fixed Price Incentive Firm contract is presented in Figure VI. The line segments to the left of TC, between TC and CC and to the right of CC are given in terms of the cost (C) as

L1 = TP + a(TC - C)

L2 = TP - b(C - TC) and

L3 = PC - C.

Thus, the expected profit is given by:

$$E(\text{Profit}) = \int_{TC-3\sigma}^{TC} L1\, f(c)dc + \int_{TC}^{CC} L2\, f(c)\, dc + \int_{CC}^{TC+3\sigma} L3\, f(c)dc$$

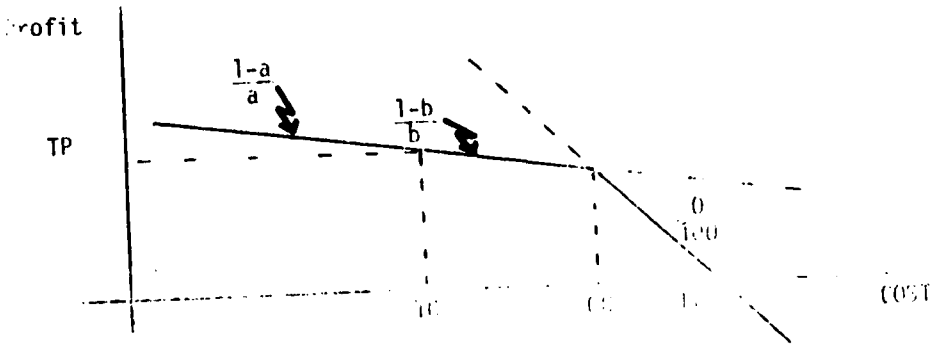
Of course if CC is greater than TC + 3$\sigma$, then the last term is dropped.

The expected cost to the government is then

E(TC) + E(Profit).

Note that the Normal distribution has been truncated at plus or minus 3$\sigma$ since it is extremely unlikely that the cost will be outside of that range.

A computer program is provided for the calculations necessary for comparing different incentive plans. This program accepts as input TC, TP, $\sigma$, a, b, and PC, and prints the expected profit and cost to the government. Also the high and low profits and cost to the government are printed. The computer program use Gaussion Quadrature as a numerical integration technique for calculation of the expected profit.




Fixed Price Incentive Firm, Constraint Graph
Figure 6

APPENDIX IV

```
AGGREGATE PROFIT VS PRICE
DIMENSION A(12),I(12),X1(12),X2(12),X3(12),F1(12),F2(12),F3(12)
DIMENSION A0(12),PI(12),SIG(12),X(12),F(12),AN(12)
DATA A/.2588,.3333,.3831,.4511,.5117,.5774,.6511,.7211,.7911,
1.8583,.9211,.9789/
DATA A0/.2588,.3333,.3831,.4511,.5117,.5774,.6511,.7211,.7911,
1.8583,.9211,.9789/
DATA PI/3.14159/
DATA SIG/.239,.1691,.1381,.1196,.1069,.0976,.0904,.0845,.0795,
1.0753,.0717,.0686/
DATA AN/.0472,.0856,.1155,.1444,.1889,.2076,.2134,.1889,.1444,
1.1155,.0856,.0472/
DO 1 I=1,12
1 I(I)=I
C(A,B,I)=(A+B)/2.+(B-A)/2.*I
F(A,B,SIG,X)=(B-A)/2./SQRT(6.28)/SIG*EXP(-(X-A0)**2/(2.*SIG**2))
N=12
PRINT,'INPUT MEAN, STD DEV, TARGET PROFIT'
PRINT,' AND A GUESS AS TO PRICE'
INPUT,AM,SIG,TC,TP
PRINT,' '
PRINT,'INPUT MEAN(S) AND STD DEV(S) OF ',' ',' PORTFOLIO ',' '
PRINT,' '
PRINT,' '
INPUT,A,
PRINT,' '
C=(C2-C1*3*C1)/(C1-3)
PRINT,'COMPANY MAY PAY ',' ',' ',' '
A1=C1-3.*S1
A2=C1
A3=C2
IF(A3.GT.AM+3.*SIG)A3=AM+3.*SIG
B1=A1
B2=A2
B3=A3
EPROF=0
DO 21 I=1,N
X1(I)=C(A1,B1,I(I))
X2(I)=C(A2,B2,I(I))
X3(I)=C(A3,B3,I(I))
F1(I)=F(A1,B1,AM,SIG,X1(I))
F2(I)=F(A2,B2,AM,SIG,X2(I))
F3(I)=F(A3,B3,AM,SIG,X3(I))
DO 2 I=1,N
EPROF=EPROF+((TP+A*(TC-X1(I)))*F1(I)+(TP-6*(X2(I)-TC))*F2(I))*AN(I)
IF(X2.GE.AM+3*SIG)GO TO 2
EPROF=EPROF+(PC-X3(I))*AN(I)*F3(I)
2 CONTINUE
EPROF=EPROF+AM
IF(A1+3*S1.EQ.A2.OR.A2.GT.PC)GOTO4
PRI=TP-A*((AM+3*SIG)-TC)
GO TO 5
4 PRIGH=(PC-AM-3.*SIG)
5 PRON=TP+A*(TC-AM+3.*SIG)
PRIGH=AM+3.*SIG+PRIGH
PRON=AM-3.*SIG+PRON
PRINT 6,EPROF,PRIGH
6 FORMAT(' ',F12.5,' EXPECTED PROFIT ',F12.5,' EXPECTED PRICE ',F12.5)
PRINT 7,PRIGH,PRON
7 FORMAT(' ',' HIGH COST ',F12.5,' PROFIT ',F12.5,' PRICE ',F12.5)
PRINT 8,PRON
8 FORMAT(' ',' LOW COST ',F12.5,' PROFIT ',F12.5,' PRICE ',F12.5)
GO TO 20
END
```

RUN

APPENDIX VI

```
WORM3       09:17PDT    07/30/80

100 DIMENSION A(8,5),ETC(5)
110 REAL MOR, MWR, MGOR
120 PRINT, 'THIS PROGRAM WAS WRITTEN TO PERFORM THE NECESSARY'
130 PRINT, 'CALCULATIONS FOR A RISK ANALYSIS BY GEORGE WORM, 1980'
140 PRINT, 'THE LINES REQUIRING THREE INPUTS END WITH L, ML, H'
150 PRINT, 'MATERIAL COST L, ML, H'
160 INPUT, A(1,1), A(1,2), A(1,3)
170 PRINT, 'MATERIAL OVERHEAD INDEPENDENT L, ML, H'
180 INPUT, A(2,1), A(2,2), A(2,3)
190 PRINT, 'MATERIAL OVERHEAD RATE%'
200 INPUT, MOR
210 MOR=MOR/100.
220 PRINT, 'INTERDIV TRSFRS L, ML, H'
230 INPUT, A(3,1), A(3,2), A(3,3)
240 PRINT, 'DIRECT ENGRG LABOR (HOURS OR COST) L,ML,H'
250 INPUT, A(4,1), A(4,2), A(4,3)
260 PRINT, 'ENGRG WAGE RATE (ENTER ONE IF LABOR IS COST AND NOT HOURS)'
270 INPUT, EWR
280 PRINT, 'ENGRG OVERHEAD INDEPENDENT L, ML, H'
290 INPUT, A(5,1), A(5,2), A(5,3)
300 PRINT, 'ENGRG OVERHEAD RATE%'
310 INPUT, EOR
320 EOR=EOR/100.
330 PRINT, 'DIRECT MFG LABOR (HOURS OR COST) L, ML, H'
340 INPUT, A(6,1), A(6,2), A(6,3)
350 PRINT, 'MGT WAGE RATE (ENTER ONE IF LABOR IN COST AND NOT HOURS'
360 INPUT, MWR
370 PRINT, 'MFG OVERHEAD INDEPENDENT L, ML, H'
380 INPUT, A(7,1), A(7,2), A(7,3)
390 PRINT, 'MFG OVERHEAD RATE%'
400 INPUT, MGOR
410 MGOR=MGOR/100.
420 PRINT, 'OTHER COSTS L, ML, H'
430 INPUT, A(8,1), A(8,2), A(8,3)
440 PRINT, 'G AND A EXPENSE (PERCENT OF SUBTOTAL)%'
450 INPUT, GAE
460 GAE=GAE/100.
470 DO1I = 1,8
480 A(I,4) = (A(I,1) + 4. * A(I,2) + A(I,3))/6
490 1 A(I,5) = ((A(I,3) - A(I,1))/6.) **2
500 DO 2 I=1,4
510 ETC(I)=(1.+MOR)*A(1,I)+A(2,I)+A(3,I)+EWR*(1.+EOR)*A(4,I)+A(5,I)
520 ETC(I)=ETC(I)+MWR*(1.+MGOR)*A(6,I)+A(7,I)+A(8,I)
530 2 ETC(I)=ETC(I)*(1.+GAE)
540 ETC(5)=(1.+MOR)**2*A(1,5)+A(2,5)+A(3,5)+(EWR+EWR*EOR)**2*A(4,5)
550 ETC(5)=ETC(5)+A(5,5)+(MWR+MWR*MGOR)**2*A(6,5)+A(7,5)+A(8,5)
560 TSL = ETC(4) + 3. * SQRT (ETC(5))
570 RATIO = 3. * SQRT (ETC(5))/ETC(4)
580 IF (RATIO .GT. .05) GO TO 3
590 PRINT, 'SINCE VARIABILITY IS SMALL FFP IS RECOMMENDED'
600 TP = 0
610 CR = 0
620 GO TO 4
630 3 PRINT, 'SINCE VARIABILITY IS MORE THAN 5 PERCENT FPIF IS RECOMMENDED
```

```
640 RATIO=RATIO*100.
650 39 PRINT 5, ETC(4)
660 PRINT, 'INPUT WGM PROFIT (PERCENT)'
670  5 FORMAT (' EXPECTED TOTAL COST IS',F10 .2)
680 INPUT, TP
690 TP=TP/100.
700 PRINT 6, TSL
710 6 FORMAT (' RISK ANALYSIS COST (UPPER LIMIT) IS',F10.2)
720 PRINT, 'INPUT COST RISK USED IN WGM (PERCENT)'
730 INPUT, CR
740 CR=CR/100.
750 4 PRINT 7
760 7 FORMAT (30X,'ESTIMATES FOR RISK ANALYSIS',///)
770 PRINT 8
780 8 FORMAT (2X, 'ELEMENTS', 41X, 'MOST')
790 PRINT 9
800 9 FORMAT (39X, 'MINIMUM', 4X, 'LIKELY', 3X, 'MAXIMUM')
810 PRINT 10, (A(1,I), I = 1,3)
820 10 FORMAT (' MATERIAL',23X,'COST',3F10.2)
830 PRINT 11, (A(2,I), I=1,3)
840 11 FORMAT (' MGT OVERHEAD', 11X,' INDEPENDENT', 3F10.2)
850 PRINT 12, MOR
860 12 FORMAT (2X, 'RATE FOR MATERIAL' F6.3)
870 PRINT 13, (A(3,I), I=1,3)
880 13 FORMAT (' INTERDIV TRSFRS', 16X, 'COST', 3F10.2)
890 PRINT 14, (A(4,I), I=1,3)
900 14 FORMAT (' DIRECT ENGRG LABOR', 12X, 'HOURS' 3F10.2)
910 PRINT 15, EWR
920 15 FORMAT (2X, 'WAGE RATE', F14.3)
930 PRINT 16, (A(5,I), I=1,3)
940 16 FORMAT (' ENGRG OVERHEAD', 10X, 'INDEPENDENT', 3F10.2)
950 PRINT 17, EOR
960 17 FORMAT(2X,'RATE FOR ENGRG',F9.3)
970 PRINT18,(A(6,I),I=1,3)
980 18 FORMAT (' DIRECT MFG LABOR', 14X, 'HOURS', 3F10.2)
990 PRINT 19, MWR
1000 19 FORMAT (2X, 'WAGE RATE', F14.3)
1010 PRINT 20, (A(7,I), I=1,3)
1020 20 FORMAT (' MFG OVERHEAD', 12X, 'INDEPENDENT', 3F10.2)
1030 PRINT 21,MGOR
1040 21 FORMAT (2X, 'RATE FOR MFG', F11.3)
1050 PRINT 22, (A(8,I), I=1,3)
1060 22 FORMAT (' OTHER COST', 21X, 'COST', 3F10.2)
1070 PRINT 23,GAE
1080 23 FORMAT (' G&A EXPENSE', F14.4,//////)
1090 PRINT 24
1100 24 FORMAT (10X, 'SUMMARY, CEILING/SHARE COMPUTATION')
1110 PRINT25,ETC(1)
1120 25 FORMAT (/ ' SUMMARY, MINIMUM COST', 24X,F10.2)
1130 PRINT 26, ETC(2)
1140 26 FORMAT (/ ' SUMMARY, MOST LIKELY COST', 20X,F10.2)
1150 PRINT 27, ETC(3)
1160 27 FORMAT (/ ' SUMMARY, MAXIMUM COST', 24X,F10.2)
1170 PRINT28,ETC(4)
1180 28 FORMAT (/ ' EXPECTED TOTAL COST, E(TC)',19X, F10.2,1X, 'EXCEEDE
                                                    W/PROB OF 50%')
```

```
1190 PRINT 29, TSL
1200 29 FORMAT (/ ' RISK ANALYSIS COST, RAC', 22X,F10.2,1X, 'EXCEEDED W/PROB
1210 IF(TP.EQ.0) GO TO 31                                    OF 1% OR LESS')
1220 WP=TP-CR
1230 WPD=TSL*WP
1240 PRINT 30, WPD
1250 30 FORMAT (/ ' WARRANTED PROFIT' 29X,F10.2)
1260 TPD=TP*ETC(4)
1270 PRINT 32, TPD
1280 32 FORMAT (/ ' TARGET PROFIT', 32X,F10.2)
1290 CP=TSL+WPD
1300 PRINT33,CP
1310 33 FORMAT (/ ' CEILING PRICE', 32X,F10.2)
1320 PRINT34,RATIO
1330 34 FORMAT (/ ' PERCENT DIFFERENCE BETWEEN RAC AND OBJECTIVE', 1X,F10.2,
1340 PRINT 35                                                    %')
1350 35 FORMAT (//, ' SHARING COMPUTATION:')
1360 DUMM=TPD-WPD
1370 PRINT 36, DUMM
1380 36 FORMAT (/, 4X, 'WGM PROFIT LESS WARRANTED PROFIT', 9X,F10.2)
1390 DUM=TSL-ETC(4)
1400 PRINT 37,DUM
1410 37 FORMAT (/,4X,'RISK ANALYSIS COST LESS OBJECTIVE COST', 3X,F10.2)
1420 CS=DUMM/DUM*100.
1430 PRINT 38, CS
1440 38 FORMAT (/, 4X, 'CONTRACTORS SHARE' 24X,F10.2,'%')
1450 31 PRINT, 'TO CHANGE WGM PROFIT OR RISK, (TYPE 0 FOR YES, 1 FOR NO)'
1460 INPUT, ANS
1470 IF (ANS.EQ.0) GO TO 39
1480 STOP
1490 END
```

APPENDIX VII

```
OLD WORM3


READY
RUN-20

WORM3        09:12 PDT     07/30/80

THIS PROGRAM WAS WRITTEN TO PERFORM THE NECESSARY
CALCULATIONS FOR A RISK ANALYSIS BY GEORGE WORM, 1980
THE LINES REQUIRING THREE INPUTS END WITH L, ML, H
MATERIAL COST L, ML, H?8400 9000 12000

MATERIAL OVERHEAD INDEPENDENT L, ML, H?0 0 0

MATERIAL OVERHEAD RATE%?5

INTERDIV TRSFRS L, ML, H?1700 1800 2300

DIRECT ENGRG LABOR (HOURS OR COST) L,ML,H?85 95 115

ENGRG WAGE RATE (ENTER ONE IF LABOR IS COST AND NOT HOURS)?11.5

ENGRG OVERHEAD INDEPENDENT L, ML, H?0 0 0

ENGRG OVERHEAD RATE%?70

DIRECT MFG LABOR (HOURS OR COST) L, ML, H?200 230 290

MGT WAGE RATE (ENTER ONE IF LABOR IN COST AND NOT HOURS?11

MFG OVERHEAD INDEPENDENT L, ML, H?0 0 0

MFG OVERHEAD RATE%?170

OTHER COSTS L, ML, H?400 450 500

G AND A EXPENSE (PERCENT OF SUBTOTAL)%?10

SINCE VARIABILITY IS MORE THAN 5 PERCENT FPIF IS RECOMMENDED
EXPECTED TOTAL COST IS  23161.60
INPUT WGM PROFIT (PERCENT)?12
```

RISK ANALYSIS COST (UPPER LIMIT) IS 25514.65
INPUT COST RISK USED IN WGM (PERCENT)?5

ESTIMATES FOR RISK ANALYSIS

| ELEMENTS | | MINIMUM | MOST LIKELY | MAXIMUM |
|---|---|---|---|---|
| MATERIAL | COST | 8400.00 | 9000.00 | 12000.00 |
| MGT OVERHEAD | INDEPENDENT | 0.00 | 0.00 | 0.00 |
| RATE FOR MATERIAL 0.050 | | | | |
| INTERDIV TRSFRS | COST | 1700.00 | 1800.00 | 2300.00 |
| DIRECT ENGRG LABOR | HOURS | 85.00 | 95.00 | 115.00 |
| WAGE RATE 11.500 | | | | |
| ENGRG OVERHEAD | INDEPENDENT | 0.00 | 0.00 | 0.00 |
| RATE FOR ENGRG 0.700 | | | | |
| DIRECT MFG LABOR | HOURS | 200.00 | 230.00 | 290.00 |
| WAGE RATE 11.000 | | | | |
| MFG OVERHEAD | INDEPENDENT | 0.00 | 0.00 | 0.00 |
| RATE FOR MFG 1.700 | | | | |
| OTHER COST | COST | 400.00 | 450.00 | 500.00 |
| G&A EXPENSE 0.1000 | | | | |

SUMMARY, CEILING/SHARE COMPUTATION

| | |
|---|---|
| SUMMARY, MINIMUM COST | 20373.93 |
| SUMMARY, MOST LIKELY COST | 22427.07 |
| SUMMARY, MAXIMUM COST | 28887.37 |
| EXPECTED TOTAL COST, E(TC) | 23161.60 EXCEEDED W/PROB OF 50% |
| RISK ANALYSIS COST, RAC | 25514.65 EXCEEDED W/PROB OF 1% OR LESS |
| WARRANTED PROFIT | 1786.03 |
| TARGET PROFIT | 2779.39 |
| CEILING PRICE | 27300.67 |
| PERCENT DIFFERENCE BETWEEN RAC AND OBJECTIVE | 10.16% |

SHARING COMPUTATION:

| | |
|---|---|
| WGM PROFIT LESS WARRANTED PROFIT | 993.37 |
| RISK ANALYSIS COST LESS OBJECTIVE COST | 2353.05 |
| CONTRACTORS SHARE | 42.22% |

ASD/PMF CASE NO. _____

DATE _____

ESTIMATES FOR RISK ANALYSIS

ESTIMATES

| COMPONENTS | | MINIMUM (L) | MOST LIKELY (ML) | MAXIMUM (H) | EXPECTED VALUE $\frac{L + 4ML + H}{6}$ | CALCULATED VARIANCE $\left(\frac{H - L}{6}\right)^2$ |
|---|---|---|---|---|---|---|
| MATERIAL | COST | | | | E(V1) | Var(V1) |
| MATERIAL OVERHEAD | INDEPENDENT | | | | E(V2) | Var(V2) |
| RATE FOR MATERIAL | P1 | | | | | |
| INTERDIV TRSFRS | COST | | | | E(V3) | Var(V3) |
| DIRECT ENGRG LABOR | HOURS | | | | E(V4) | Var(V4) |
| WAGE RATE | R1 | | | | | |
| ENGRG OVERHEAD | INDEPENDENT | | | | E(V5) | Var(V5) |
| RATE FOR ENGRG | P2 | | | | | |
| DIRECT MFG LABOR | HOURS | | | | E(V6) | Var(V6) |
| WAGE RATE | R2 | | | | | |
| MFG OVERHEAD | INDEPENDENT | | | | E(V7) | Var(V7) |
| RATE FOR MFG | P3 | | | | | |
| OTHER COSTS | COST | | | | E(V8) | Var(V8) |
| G&A EXPENSES | | | | | | |
| PERCENT OF SUBTOTAL | P4 | | | | | |

85-56

FORM I

RISK ANALYSIS WORKSHEET (EXPECTED VALUE)

| | (COL 1) | (COL 2) | (COL 3) = (COL 1) * (COL 2) |
|---|---|---|---|
| (1 + P1) | _____ | E(V1) _____ | _____ |
| 1 | _____ | E(V2) _____ | _____ |
| 1 | _____ | E(V3) _____ | _____ |
| (R1 + R1*P2) | _____ | E(V4) _____ | _____ |
| 1 | _____ | E(V5) _____ | _____ |
| (R2 + R2*P3) | _____ | E(V6) _____ | _____ |
| 1 | _____ | E(V7) _____ | _____ |
| 1 | _____ | E(V8) _____ | _____ |
| | | TOTAL (COL 3) | _____ |
| | | (1 + P4) | _____ |
| | | EXPECTED TOTAL COST = E(TC) = (1 + P4)* TOTAL (COL 3) | _____ |

FORM II

RISK ANALYSIS WORKSHEET (VARIANCE)

| | (COL 1) | | (COL 2) | (COL 3) = (COL 1) * (COL 2) |
|---|---|---|---|---|
| $(1 + P1)^2$ | _____ | Var(V1) | _____ | _____ |
| | 1 | Var(V2) | _____ | _____ |
| | 1 | Var(V3) | _____ | _____ |
| $(R1 + R1*P2)^2$ | _____ | Var(V4) | _____ | _____ |
| | 1 | Var(V5) | _____ | _____ |
| $(R2 + R2*P3)^2$ | _____ | Var(V6) | _____ | _____ |
| | 1 | Var(V7) | _____ | _____ |
| | 1 | Var(V8) | _____ | _____ |
| | | | TOTAL (COL 3) | _____ |
| | | | $(1 + P4)^2$ | _____ |

VARIANCE OF TOTAL COST = Var(TC) = $(1 + P4)^2$ *TOTAL (COL 3) _____

FORM III

1980 USAF - SCEEE SUMMER FACULTY RESEARCH PROGRAM

Sponsored by the

AIR FORCE OFFICE OF SCIENTIFIC RESEARCH

Conducted by the

SOUTHEASTERN CENTER FOR ELECTRICAL ENGINEERING EDUCATION

FINAL REPORT

# PULSED PLASMA PLUME MODELING STUDY


| | |
|---|---|
| Prepared by: | Daniel W. Yannitell |
| Academic Rank: | Associate Professor |
| Department and University: | Mechanical Engineering Department<br>Louisiana State University |
| Research Location: | Air Force Rocket Propulsion Laboratory, Propulsion Analysis Division, Plume Technology Branch |
| USAF Research Colleagues: | Dr David M. Mann 1Lt Ronald P. Furstenau |



| | |
|---|---|
| Date: | 15 August 1980 |
| Contract No: | F49620-79-C-0038 |

# PULSED PLASMA PLUME MODELING STUDY

by

Daniel W. Yannitell

## ABSTRACT

The present state of knowledge relevant to the theoretical modeling of the exhaust plume of a solid teflon pulsed plasma thruster is examined. A phenomenological description of the sequence of events which occur during a single pulse of the thruster is given, followed by a discussion of existing analytical models and experimental investigation of the complex processes involved. Emphasis is placed on the uncertainties in the modeling and the difficulties involved in interpretation of experimental test-chamber data. Areas in which current information is inadequate are discussed, and suggestions are offered regarding further research deemed necessary to improve current understanding of the plume and its possible effects on spacecraft.

## Acknowledgement

The author would like to thank the Air Force Systems Command, the Air Force Office of Scientific Research, and the Southeastern Center for Electrical Engineering Education for the sponsorship of this research. He is also grateful to the Air Force Rocket Propulsion Laboratory and, in particular, the Propulsion Analysis Division for its hospitality and support.

Special thanks are due to Lt Ronald Furstenau, his principal collaborator, and Dr David Mann, Chief of the Plume Technology Branch, for their encouragement and assistance, without which this research could not have been accomplished.

In addition the author wishes to acknowledge very helpful discussions with Dr Robert Vondra of the Liquid Rocket Division, Dr Ronald Dawbarn of the Arnold Engineering Development Center, and Drs Martin Begun and Dominic Palumbo of the Fairchild Republic Company.

Finally, thanks are extended to the laboratory staff, especially Mrs Carol Maples, technical librarian, and Mrs Julie Casper, the branch secretary.

## I. INTRODUCTION:

The pulsed-plasma thruster (PPT) has several characteristics which would seem to make it ideally suited for attitude control and station keeping on long life satellites. The high specific impulse (1500-2000 sec) means a small amount of "fuel" will provide a large total impulse. The small reproducible impulse bit (~5 mlb-sec) will allow precise adjustments. In addition, the simplicity of design, lack of tanks, valves, etc., will provide high reliability.

Some aspects of the PPT, however, are of serious concern to satellite designers, and many of these concerns are associated with the highly energetic, ionized exhaust plume and its interaction with both satellite surfaces and communication transmissions. Some of these concerns are reflected in Reference 1. "More data is needed relative to ..... plume effects" (pg 11) and "the present data base does not extend into sufficiently high divergence angle regimes and into sufficiently dilute flow portions of the plume to allow the usual (and required) form of an interactive effects analysis." (pg 67).

It is thus necessary to develop as complete a characterization of the plume as possible. In addition to detailed experimental mapping of the plume of the thruster in its present state of development, a theoretical model which would predict the effect of design changes is needed.

Both experimental and theoretical investigations have been actively pursued, but the picture is far from complete. Vacuum chamber tests have been beset with serious diagnostic difficulties; and mathematical modeling presents additional problems, not the least of which is the lack of sufficient reliable data with which to correlate the model. Reference 2 presents an overview of experimental investigations prior to 1977, including an extensive bibliography.

## II. OBJECTIVES OF THE RESEARCH EFFORT

The main objective of this project was to determine the physics relevant to modeling the exhaust flow of the pulsed plasma thruster. Specific subtasks were to:

(1) Review past and present experimental programs designed to characterize the pulsed plasma exhaust flow.

(2) Review relevant literature on high current, ablative discharge processes to determine state-of-the-art in modeling these processes.

(3) Review theories/models for highly ionized, high velocity flowfields. Determine relevance to pulsed plasma flowfield.

(4) From comparison of available data/theories, determine if the global mechanisms for ionization/acceleration for pulsed plasma (E x B) are appropriate.

(5) Determine physical processes which must be modeled in detail to describe the pulsed plasma exhaust flowfield, with special emphasis on those effects yielding flows into the backflow (behind exit plane) region.

(6) Recommend experimental/theoretical directions for future work.

This report summarizes the results of these investigations, although the organization does not follow the above objectives in order.

Section III provides a phenomenological description of the processes that comprise a single pulse of the thruster. This description is based on interpretation of a considerable amount of data, and some conjecture.

Section IV outlines and describes the basic components of a complete PPT exhaust model, and Section V presents a discussion of the "state-of-the-art" for each component. That discussion includes a review of experimental investigations with which the analytical models must be correlated. Finally, Section VI suggests further reasearch necessary to "fill the gaps" in the model presented.

## III. PHENOMENOLOGY OF THE PULSE

Although a single firing of the PPT takes only about 30 μsec, it consists of a rather complicated sequence of events. Figure 1 (taken from Reference 3) shows the basic features of the device. The model currently being tested incorporates some design changes, but these are not essential to the understanding of the process. This section describes the process of a single firing in a sequential manner.

During the 5-6 seconds between firings the capacitor bank is charged to 2-3 kV, which potential is also imposed across the gap between the thruster electrodes. No discharge can occur because of the space vacuum between the electrodes. The firing then proceeds as follows:

(1) The ignitor plug is fired (by closing its circuit). This vaporizes a minute amount of teflon (sometimes referred to as the microplasma) which provides sufficient matter between the electrodes to support the main discharge arc. This process requires only nanoseconds.

(2) The main circuit discharges across the face of the teflon fuel rods. The voltage in the circuit drops to zero and becomes negative, while the current rises to a peak value of many thousands of amperes and falls to zero, in about 3 μsec. Practically all of the capacitor energy (several hundred joules) is delivered in this short pulse. The history of the circuit variables is shown in Figure 2 (also from Reference 3).

(3) The distribution of this sudden burst of energy is not fully understood. It is known that a large portion (~30%) is lost in the capacitor circuit. A very small fraction of this energy is used to heat the teflon surface to the depolymerizing state or even to dissociate the resulting gas into free carbon and fluorine. The bulk of this energy is absorbed through ionization and heating of the plasma to ten of thousands of degrees, and establishment of strong magnetic fields (several Teslas).

(4) Through coupling between the field and the plasma, some of this magnetic field energy is converted to plasma kinetic energy as the Lorentz force accelerates the plasma out through the exhaust cone, thus producing the thrust. Only a few percent of the initial capacitor energy is converted to plasma kinetic energy.

(5) Subsequent to this initial discharge the circuit variables cycle through positive and negative values for several more microseconds. During this time a small amount (a few joules) of energy is transferred back and forth between the plasma and the capacitor circuit. The Lorentz force also changes direction, as revealed by analysis of the electric and magnetic fields.

(6) The plasma is thus accelerated out of the inter-electrode gap in relatively discreet "blobs" or plasmoids". This effect is best seen by high speed photography[3]. The timing of at least the first two plasmoids corresponds well with the field reversals. The reversing Lorentz force alternately holds hot plasma against the teflon surface, which thus continues to ablate, and then accelerates the next plasmoid

out as exhaust. In the "cooldown" later portion of the process the gas produced is only slightly ionized (energy transfer is small) and the acceleration of the gas may well be accomplished primarily by ordinary gas dynamic pressure rather than electromagnetic effects.

It seems appropriate at this point to make some conjectures which seem to be supported by experimental evidence, but have not been completely verified.

(1) The tremendous amount of energy available during the formation of the first plasmoid suggests that it should be highly ionized and accelerated to a very high exhaust velocity. Ample evidence of the existence of doubly and even triply ionized C and F atoms in the plume has been found spectroscopically.[4,5] Experimental data indicate velocities of these multiply ionized species as high as 50-60 ($10^3$) m/s. A small fraction (~10%) of the mass ablated per pulse, travelling at these velocities, could account for virtually all of the thrust.

(2) The second and subsequent blobs are characterized by high ambient temperatures (decreasing with time) but small energy transfer from the capacitor circuit. The "fuel" thus continues to ablate, but ionization is much lower. In fact, data on the time of peak luminosity of ionized C and F in the PPT indicate that most, if not all, of the ionization occurs during the first current pulse; the intensity of emissions (in the 2100-7300Å range) of all ions observed falling to 10% of peak values within 1.6 μs.[4] As the fields are also decreasing, acceleration is much smaller, electromagnetic effects become less and less important.

(3) The "plasma" produced during this cooldown phase is really more like an ordinary gas. Velocities are small (thus contributing little to the thrust) and the expansion of this gas into the vacuum of space is probably governed by ordinary gas-dynamic phenomena.

(4) The initial plasmoid velocity is quite well collimated by the strong fields. Several measurements indicate an expansion cone half-angle of 40° or less.[5,6,7,8] Subsequent blobs are less directional, however. Toward the end of the cooldown period (tens of microseconds after ignition) the thruster is producing a neutral gas of heavier molecules (CF, $C_2F_4$, etc). This gas expands in all directions, including into the backflow region (>90° off the thrust axis). It is likely that this "cool" gas provides essentially all of the backflow.

## IV. ANALYTICAL MODEL OVERVIEW

Figure 3 shows the essential components of a complete exhaust model. Internal and external refer to regions between and away from the electrodes, respectively. An arrow indicates that the results of one component are necessary as input to another, while a double headed arrow indicates a coupling requiring simultaneous solution. Since experimental programs providing correlative data have been, and will continue to be, performed in test chambers of finite size, the chamber interactions have been included.

Thus, it is necessary to somehow model the ablation-ionization chemistry in order to provide input (formation rates and concentrations of various species) for the plasma dynamics model. The plasma flow is inherently coupled to the electromagnetic field which, in turn, is coupled to the circuit variables of voltage and current. These components must therefore be treated together.

The most important output of the internal model is the physical output of the PPT itself; i.e., the temporal variations of species concentrations and velocities at the exit plane of the electrodes. As long as the flow is supersonic and super-Alfvenic these conditions do not affect the internal model, and they become input for the external model.

The main component of the external model is the plume model. It must accept the exit plane data and describe the expansion of this fast moving gas (or plasma) into the vacuum of space. If, however, it must be correlated with test chamber experiments, it should be coupled with a chamber effects model. An alternative to this coupling would be to use the chamber effects model to eliminate those effects from the experimental data, if possible.

Finally, the effects of the plume on spacecraft surfaces (by deposition) and on various transmissions (radio frequency, microwave, etc.) must be modeled. These effects are lumped into the contamination model in the diagram. It has been assumed above that these effects are one-way, and that the plume can be investigated without considering the spacecraft and its transmissions.

## V. MODEL COMPONENTS

This section considers the components of the model of Section IV. It reviews existing theoretical and experimental studies with emphasis on difficulties encountered and gaps in current understanding.

### A. Internal Model

Much effort has been expended on development of analytical models of the internal processes. An early study[9] concentrated on the electric circuit, treating the plasma as a circuit element with varying resistance and inductance. This resulted in the ability to predict thrust and efficiency, and in an enhanced understanding of the device.

The most extensive internal analysis is presented in Reference 10, which also provides correlative experimental data. This model is described very briefly in the following paragraphs.

Ablation rate is assumed proportional to the square of the current flowing through the discharge. This assumption is based on the observation that the total mass ablated per pulse correlates linearly with the total integral of the square of the current. This conclusion does not follow rigorously, but no better assumption suggests itself.

Complete dissociation of the ablated gas into carbon and fluorine is assumed to occur immediately, but ionization rates are assumed finite. Although it is known that the energy required for the dissociation is a very small fraction of that available during the first current pulse, it is likely that heavier molecules will remain during the cooldown phase. Also, ionization rates are unknown at this time, and some average must be assumed. Evidence of multiply charged ions appears very early in the pulse; the ultraviolet emissions from these species peak within half a microsecond.[4] These emissions also decay very quickly, within the time span of the initial current pulse. Emissions from singly charged ions and neutrals peak later and decay more slowly.

The plasma dynamics component of this model assumes a continuum fluid flow between the electrodes (which is appropriate in view of the rather high particle density-on the order of $10^{17}$ $cm^{-3}$). The field and flow variables are coupled in the magneto-gas dyanmic equations, and the external (capacitor) circuit is coupled with the field.

It was found that the numerical analysis became unstable due to the low density (and thus extremely high Alfvén wave speed) at the leading edge of the plasma. This was corrected by defining the plasmoid front and matching the solution there with free space electromagnetic wave propagation. This correction could not be applied, however, to the low density region between the first and second plasmoid, and thus the numerical procedure becomes unstable shortly after the plasmoid separation begins.

Reference 10 also provides the bulk of the available experimental data on the internal processes, including maps of the electric current density and magnetic field at several times. These data were taken from an 82 joule thruster. As yet no corresponding data from the larger 750 joule thruster are available, and problems in obtaining this information are foreseen due to arcing between the electrodes and the diagnostic tools.[11]

Qualitatively, the model described is in agreement with the experimental data, until the instability manifests itself. Uncertainties in important parameters, however, prevented real quantitative correlation. The most serious knowledge gaps probably stem from the ablation-ionization model, since uncertainties in density and degree of ionization produce an even greater uncertainty in the plasma conductivity, collision effects, etc. More experimental data are definitely needed. Other uncertainties exist with initial and boundary conditions.

B. External Model

A theoretical plume model is presented in Reference 12. The computational method used is the direct simulation Monte Carlo technique developed by Bird.[13] The technique has been shown to work well over a broad range from continuum to free molecular flows of dilute gases.

The plasma is modeled as a three species gas of neutrals and ions (both of which are assigned a mass equal to the weighted average of carbon and fluorine in the teflon) and electrons. The number of ions is assumed equal to that of electrons (thus not accounting for multiply charged ions), and the chemistry is assumed frozen; i.e., the gas species maintain their identity in a collision. Neutral-neutral, ion-neutral, and ion-electron collisions are modeled by power law forces.

Boundary conditions for the model are straightforward. Molecules enter the computational domain at the thruster exit plane with assumed density and velocity distributions. The remainder of the boundary consists of empty cells (the vacuum of space) or cells into which a small number of molecules have progressed. Molecules which share a cell with fewer than some predetermined number are considered collision free.

Although the inlet boundary conditions (at the thruster exit plane) are easy to apply, they are probably the major source of uncertainty in the model. It was found (as expected) that inlet conditions drastically affected the results. The inlet conditions used were not really representative of the actual thruster exhaust. For example; only singly charged ions were considered (probably invalid for the first plasmoid). The initial assumption of spatially uniform inlet conditions naturally produced a symmetric plume. Although adjustment of inlet conditions produced a qualitatively more realistic plume, further trial and error adjustment are probably not justified, especially in view of the very large computer times required. (The ten complete runs needed for statistically significant averages required over six hours of computer time to establish the plume for the first 27 μsec after firing[14]). Thus, as mentioned above, a more accurate internal model must be developed (and experimentally verified) to provide the input for the plume model before it can be developed further.

The above discussion points out some of the difficulties associated with the theoretical plume model, but equally important problems arise in the collection of experimental data with which such a model must be correlated. Experimental studies of PPT plumes are presented in References 2, 4, 5, 6, 7, 8, 9 and 12. The following paragraphs are by no means a complete discussion of these studies, but rather are intended to emphasize the difficulties involved in interpretation of the data.

Plume diagnostic problems arise primarily from the interactive effects of the chamber in which the testing is performed. Even the largest, cryogenically cooled chambers are not free of these problems, and the separation of the chamber interactions from the thruster produced effects is not yet possible.

The first emission from the PPT consists of intense radiation. Reference 4

and 5 document radiation in the visible and ultraviolet range, and tests from a related device[15] suggest that VUV radiation may be even more intense (spectroscopic study of the VUV emissions from the PPT are currently underway at AEDC). This radiation, upon impact with the chamber walls or with any instrumentation, appears to release an intense electron shower.[5] These chamber-provided electrons compromise the data from instruments such as Faraday cups, Langmuir probes, etc., (For example, this mechanism could be the source of the initial negative Faraday cup current reported in Reference 8 page 108).

The next PPT emission is the highly energetic first plasmoid. Upon impact, this plasmoid not only releases a secondary shower of electrons, but also sputter-erodes the impacted surfaces. Surfaces near the thruster axis, as far as a meter from the exit plane, clearly show this plume scrubbing action.[7] Reflected exhaust material and sputtered matter comprise the facility backscatter, which may well be significantly greater than the primary flow in regions parallel to or behind the exit plane (those regions of paramount importance to contamination studies). The magnitude of this problem becomes apparent when it is remembered that any open device such as quartz crystal microbalance (QCM), which must be exposed to many pulses to collect enough mass to register, "sees" the facility background for several seconds between each firing, and the primary flow for less than a millisecond per pulse.

A serious study of facility backscatter is reported in Reference 7 and 8. The tests were performed in the MOLSINK at the Jet Propulsion Laboratory, a fairly large, cryogenically cooled vacuum chamber. These reports contain a considerable amount of useful data but, in the opinion of the present author, some significant effects were neglected in the backscatter model used to correct the backflow measurements. These include the possibility that the dense central portion of the plume reacts at least in part as a fluid (rather than a stream of discrete particles) upon impact with surfaces along the thruster axis, and the strong possibility of multiple collisions. Not only will the more energetic particles probably survive more than one wall (or instrument) reflection, but reflected particles reentering the dense portion of the plume will likely produce significant scattering.

A further complication in chamber effects modeling is the deposit of material on the chamber walls, which can be re-introduced into the chamber

atmosphere when impacted by the plume. This deposit may consist of various materials either from the thruster exhaust, or formed by chemical reaction of exhaust material with available surface material. In a current investigation[5] it is reported that all horizontal surfaces (even those behind the thruster) collect carbon flakes which apparently settle out between pulses. Also, mass spectroscopy of the chamber atmosphere indicates the presence of hydrogen compounds (HF with warm walls and $CHF_3$ with cold walls), supporting the contention that chemical reactions occur in the chamber or on its walls. Obviously, more investigation is necessary if we are to understand the facility interactions.

Little has been said here about the contamination model. Until more is known about the true amount and nature of the material comprising the backflow it is not possible to assess its effect on spacecraft surfaces. One possible contaminant has just been reported.[5] It consists of a currently unknown matrix (liquid teflon?) impregnated with carbon flakes and copper spheres, captured on glass slides extending but slightly beyond the thruster exhaust cone. Thus, copper eroded from the electrodes and carbon flakes may be present in the backflow.

## VI. RECOMMENDATIONS

From the above discussions, the opinions of this author regarding the need for further research are probably apparent. This section presents some specific recommendations.

Obviously, the ultimate experimental investigation should be performed in space where there is no test chamber to interfere with the measurements. This is especially true of backflow measurements which may be completely overshadowed by chamber induced phenomena. As space testing is not likely in the near future, the following suggestions are offered.

First, emphasis should be placed on gaining a more complete picture of the internal processes as described above. Investigation of the exhaust by emission spectroscopy should continue. This should include not only extension of the range into the VUV as currently planned[11], but also investigation of the time dependence of the intensity of at least some of the identified emissions. This would provide information concerning the

rates of formation and neutralization of the various ion species, which are necessary for the ablation-ionization model. Also, if the arcing problem mentioned in Section V can be solved, it would be very helpful in evaluating the plasma flow model if the electric and magnetic fields between the electrodes could be mapped.

Probably most crucial to the development of a plume model is the accurate determination of the space-time variations in species densities and velocities at the electrode exit plane. This would provide the necessary data base to verify the internal model, as well as the input for the external plume model.

The theoretical plasma dynamics model[10] described in Section V-A is very promising. The numerical stability problem must be addressed, and it is possible that three dimensional effects must be considered to allow the sideways expansion of the plasma, especially for the side-fed thruster now being tested.

External plume investigation should also be continued, but these should be coupled with studies of the plume chamber interactions. Attempts to minimize backscatter, such as the baffle system being developed[16] and, possibly, charged grids to suppress secondary electrons, are necessary, but may never succeed in eliminating the problem. This materially reduces the number of available diagnostic tools. Instruments sensitive to a single pulse are recommended, and only signals received prior to the possible arrival of chamber-induced effects should be deemed accurate. Further development of nonintrusive spectroscopic and interference (scattering) diagnostics is needed.

Although direct backflow measurements are highly desirable from the application standpoint, these data are the most difficult to obtain in a test chamber, as the densities are expected to be very small and the facility backscatter will dominate the signals. In addition, these data provide little input to the model development. This is not meant to minimize the importance of backflow studies, which are necessary for verification of the model. For the present, the results reported in Reference 8 are the best available, but cannot be considered conclusive, and are probably over-estimates of the backflow.

The Monte Carlo model discussed in Section V-B is very powerful, and would probably produce the desired results if the input were better defined.

However, it may be found necessary to increase the number of species considered, which would further increase the already extreme computer time required. It is possible, however, that a simpler model would suffice if indeed the initial plasmoid is so collimated as to contribute negligibly to the backflow and subsequent portions are basically neutral. In this case, perhaps the dense first plasmoid can be treated as a continuum, and later portions as a nearly collisionless gas. Further development of the plume model should probably await the results of the exit plane mapping.

One final observation seems appropriate. It would seem to be worthwhile to investigate the possibility of redesigning the thruster to produce a more uniformly ionized exhaust; i.e., decreasing the number of multiply charged ions in the first plasmoid and increasing the ionization of late emissions. This should increase fuel efficiency and decrease backflow. One possibility might be the use of segmented electrodes and multiple current discharges to avoid dumping all of the capacitor energy in such a short time.

## REFERENCES


1. M. Huberman, S. Zafran, M. H. Gran, R. Pieper, J. M. Sellen, "Mission Integration Study for Solid Teflon Pulsed Plasma Millipound Propulsion System", AFRPL-TR-80-37, June 1980.

2. J. K. Hartman, "Solid Teflon Propulsion Contamination Investigation", USAF-ASEE Summer Faculty Research Program Final Report, Aug 1977.

3. D. J. Palumbo and M. Begun, "Plasma Acceleration in Pulsed Ablative Arc Discharges - Interim Report", AFOSR-TR-76-0738, May 1976.

4. K. I. Thomassen and R. J. Vondra, "Exhaust Velocity Studies of a Solid Teflon Pulsed Plasma Thruster", J. Spacecraft and Rockets, 9, 1, Jan 1972.

5. R. Dawbarn, R. L. McGuire, L. L. Price, and K. L. Krist, "Evaluation of Pulsed Plasma Engines Operating in a Vacuum Test Cell (Status Report)", AEDC-TMR-80-V12, July 1980.

6. W. J. Guman and M. Begun, "Pulsed Plasma Plume Studies", AFRPL-TR-77-2, Mar 1977.

7. L. C. Pless, L. K. Rudolph, D. J. Fitzgerald, "Plume Characterization of a One-Millipound Solid Teflon Pulsed Plasma Thruster - Phase I", AFRPL-TR-78-63, Oct 1978.

8. L. C. Pless, L. R. Rudolph, D. J. Fitzgerald, "Plume Characterization of a One-Millipound Solid Teflon Pulsed Plasma Thruster - Phase II", AFRPL-TR-79-60, Sept 1979.

9. R. Vondra, K. Thomassen and A. Solbes, "Analysis of Solid Teflon Pulsed Plasma Thruster", Journal of Spacecraft and Rockets, Vol. 7, Dec 1970.

10. D. J. Palumbo and M. Begun, "Plasma Acceleration in Pulsed Ablative Arc Discharges - Final Report', AFOSR-TR-77-0623, April 1977.

11. R. Dawbarn, personal communication, July 1980.

12. D. J. Palumbo and M. Begun, "Experimental and Theoretical Analysis of Pulsed Plasma Exhaust Plumes", AFOSR-TR-78-1242, 1978.

13. G. A. Bird, Molecular Gas Dynamics, Clarendon Press, Oxford, 1976.

14. D. J. Palumbo, personal connumication, July 1980.

15. B. A. Norton and E. R. Wooding, "A Versatile Pulsed Plasma Light Source Operating in the Vacuum Ultraviolet to Visible Wavelength Region", Journal of Scientific Instruments, 1977.

16. R. Dawbarn, "Pulsed Plasma Plume Contamination", AEDC Project Plan, Project No. V34M-28, Mar 1979.

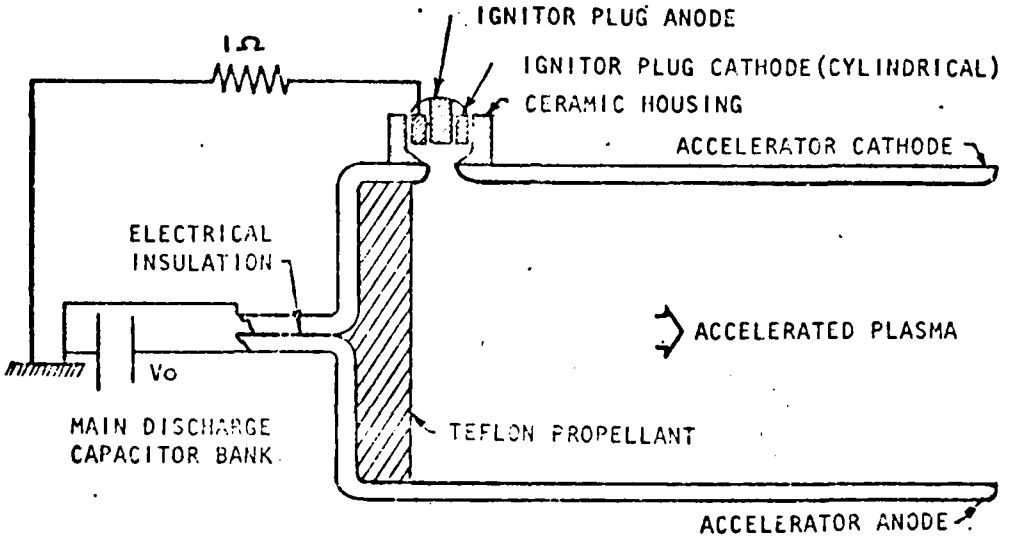



Figure 1. Schematic Cross-Section of Pulsed Ablative Accelerator

(Copied from Reference 3)

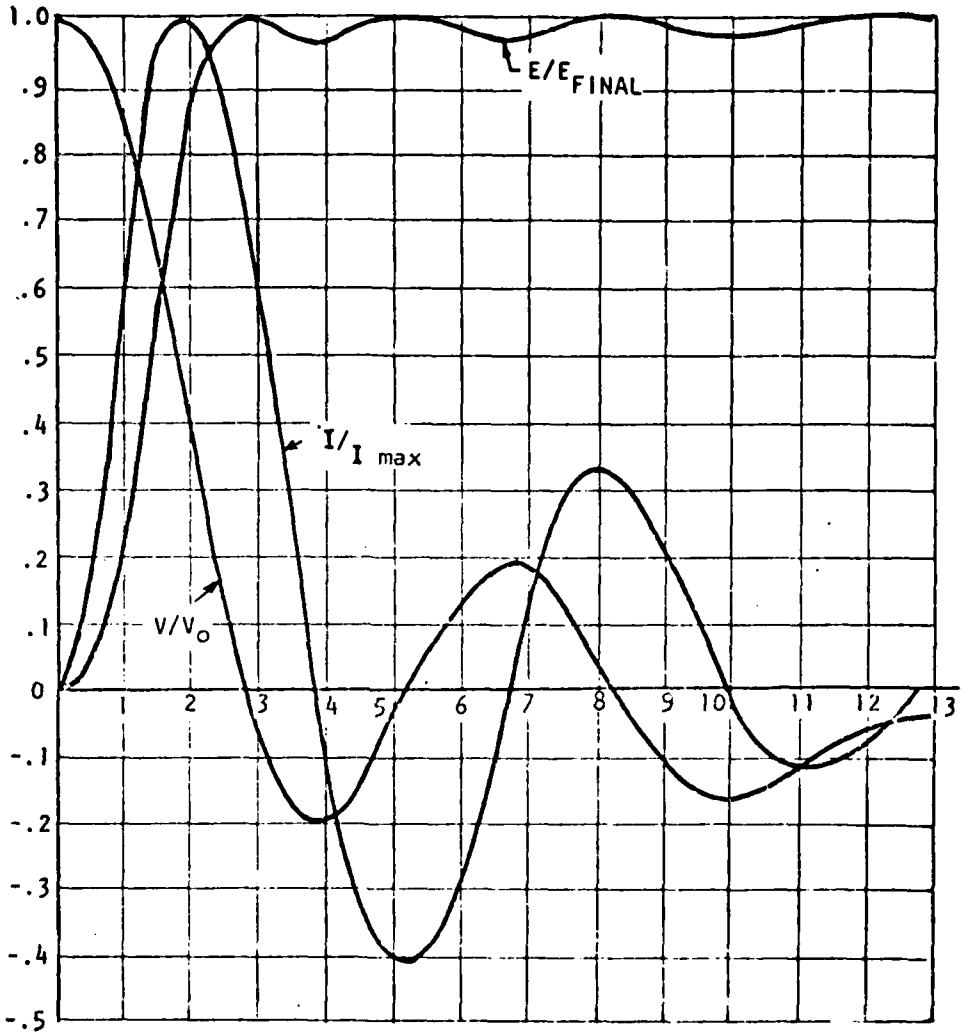



Figure 2. DISCHARGE CURRENT, VOLTAGE, AND ENERGY INPUT AS A FUNCTION OF TIME

$V_o$=3kV $I_{max}$=29.9kA $E_{FINAL}$=76.3J $E_o$=81.9J

(Copied from Reference 3)

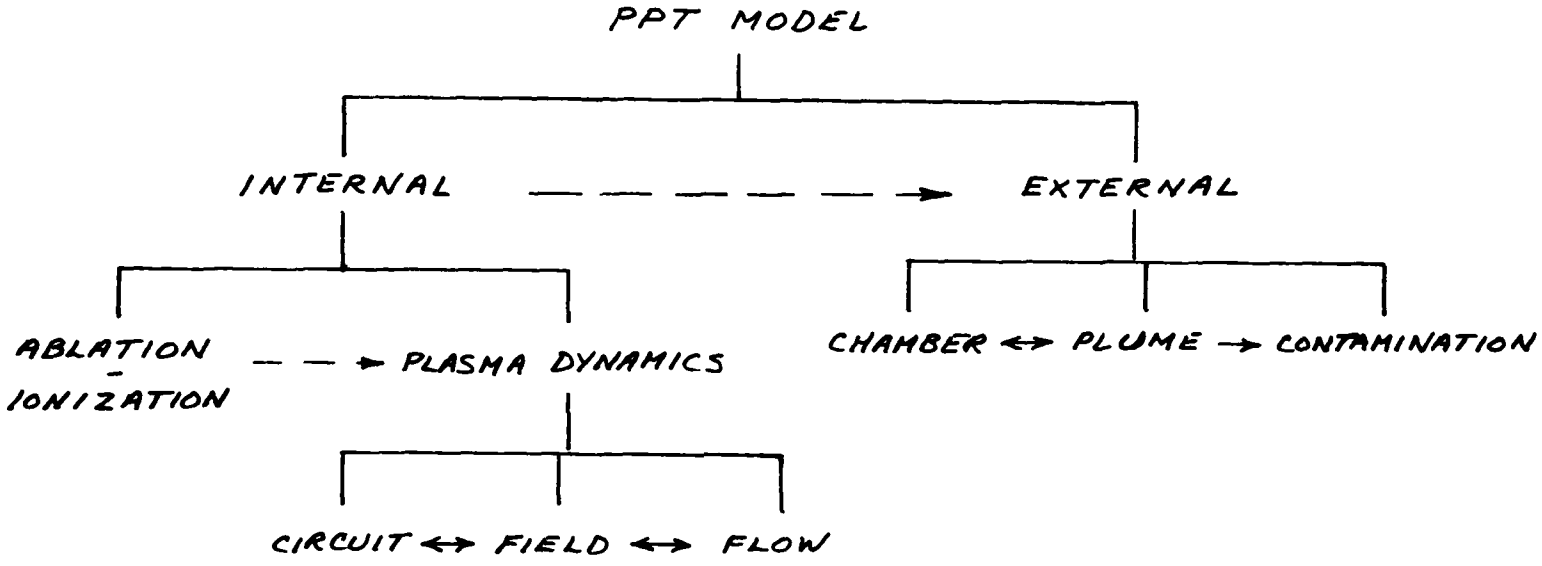



FIGURE 3

MODEL COMPONENTS

1980 USAF - SCEEE SUMMER FACULTY RESEARCH PROGRAM

Sponsored by the

AIR FORCE OFFICE OF SCIENTIFIC RESEARCH

Conducted by the

SOUTHEASTERN CENTER FOR ELECTRICAL ENGINEERING EDUCATION

# FINAL REPORT

# ANALYSIS OF EYE MOVEMENTS IN TARGET TRACKING AND DETECTION TASKS


| | |
|---|---|
| Prepared by: | Yehoshua Y. Zeevi |
| Academic Rank: | Associate Professor |
| Department and University: | Department of Aeronautics and Astronautics<br>Massachusetts Institute of Technology |
| Research Location: | Air Force Human Resources Laboratory/<br>Operations Training Division<br>Williams Air Force Base, Arizona 85224 |
| USAF Research Colleague: | Dr Thomas M. Longridge |
| Date: | August 4, 1980 |
| Contract No: | F49620-79-C-0038 |

# ANALYSIS OF EYE MOVEMENTS IN TARGET TRACKING AND DETECTION TASKS

by

Yehoshua Y. Zeevi

## ABSTRACT

Preliminary experiments were conducted to determine and compare the effects of static and dynamic noise on target tracking and detection performance. It was found that saccadic latency increases as static masking noise is introduced. It was also shown that dynamic noise of the same spatial frequency content has a significantly more detrimental effect than static noise on subjects' target detection performance as manifested by longer saccadic reaction time and higher misses and false alarm rate. These results are discussed as they relate to hypotheses concerning the dynamic characteristics of channels involved in the early stages of visual information processing. The data were also consistent with previous findings in demonstrating that target luminance has a substantial effect on saccadic latency. This effect becomes even more pronounced in the presence of noise.

These results, corroborated by other studies concerning critical band masking and target detection, have important implications concerning design and specifications of ASPT in simulation of air-to-air and air-to-ground combat and evasion tasks.

## ACKNOWLEDGEMENT

This research was supported by the Air Force Systems Command, Air Force Office of Scientific Research, and the Air Force Human Resources Laboratory, Operations Training Division, Williams Air Force Base.

I wish to thank the AFOSR and the Southeastern Center for Electrical Engineering Education for awarding me the Summer Faculty Fellowship and for providing me the opportunity to spend a most stimulating and productive summer with the AFHRL Laboratory at Williams AFB, Arizona.

Finally, I wish to thank the staff of AFHRL Laboratory and in particular its Chief, Colonel R. C. Needham; my research colleagues, Dr T. M. Longridge and Dr R. S. Kellogg for their hospitality and help in setting up the Eye Movement Laboratory, and also Dr J. C. De Maio of AFHRL for his assistance and collaboration in the experiments.

## I. INTRODUCTION

Technological advances in wide field-of-view computer generated imagery (CGI) representation of visual scenes in flight simulators have not been supported by concomitant development of objective quantitative measures and techniques for assessing pilot's performance. As one strives to develop necessary perceptual fidelity and enriched visual scenes with limited CGI resources, the question arises, what are the important display characteristics that contribute to minimally acceptable levels of behavioral fidelity? Specifically, objective behavioral measures are required in evaluation of the generated imagery.

It is apparent from various studies that when the visual scene subtends a wide angle, as is the case in both actual flight and the Advanced Simulator for Pilot Training (ASPT), eye movements are required for the detection and tracking of a target and/or for the recognition of a visual pattern (1,2). Such eye movements externalize some aspects of information processing in the visual system, and as such may provide some important objective measures of pilots' performance as well as of the utility of displayed visual information. Indeed, recent studies, albeit exhibiting obvious shortcomings, indicate that analysis of eye movements may provide important information concerning pilot scanning behavior (for example see papers presented at the 1977 AGARD symposium on "Guidance and control design consideration for low altitude and terminal, area flgiht").

The performance of most visual tasks requires extensive oculomotor scanning. Target acquisition is carried out by extremely fast and precise jumps called saccades. When a subject is instructed to fixate on a point target, and the target is suddenly shifted laterally to a new position, about 200 msec elapse between the shift of the target and the onset of saccadic eye movement towards the new position (3, 4). This effect, known as saccadic latency, is dependent on a variety of factors, such as target luminance and contract (5); it is also known that practice and target predictability may shorten it (4, 6), whereas fatigue may lengthen it (7).

The present research is concerned with the measurement of saccadic eye movement for the assessment of subjects' performance, and evaluation of display characteristics relevant to simple target detection and saccadic tracking tasks. (Dual target paradigms involving time-sharing tasks

spanning the near periphery are also being investigated and will be addressed in a separate report). The research reported herein concerns the question of whether dynamic noise is more effective than its static counterpart, characterized by the same spatial frequency content, in masking point targets in tracking and detection tasks.

## II. OBJECTIVES

The need for an objective means for assessing pilots' visual performance, and for evaluation of behaviorally relevant display characteristics requires implementation of eye and head movement measurement technology in flight simulators. In addition, efforts are currently underway to develop an eye-slaved helmet mounted display for implementation in ASPT. These developments have inspired interest at the Air Force Resources Laboratory of Williams AFB in physiological and technological aspects of eye movement research.

Therefore, the first objective of this project was to develop an in-house eye movement research capability which would serve as an intergral part of a newly established basic research laboratory. This facility would contribute to the development of in-house expertise in eye movement, so that once a helmet mounted TV oculometer is introduced in the ASPT, it will be utilized more efficiently.

Once our endeavor to set up an eye movement research facility proved to be successful, we selected a many-faceted research problem which (a) was relevant to CGI and flight simulation and (b) could be investigated outside the ASPT. As such, our second objective was to determine and compare the effects of static and dynamic noise on target detection and tracking as assessed by the probability of correct responses and their reaction times.

## III. METHOD

The experimental setup for eye movement measurements in target detection and tracking tasks, and its schematic representation are shown in Fig. 1 and Fig 2, respectively. The choice of this specific experimental configuration as well as the research problem and methodology selected were constrained by the availability of appropriate equipment. Eye movements

were recorded using a modified Gulf and Western Model 200 EyeTrac (Fig. 1). Only monocular movements of the left eye were recorded; the right eye was covered by a white patch which served as a light diffuser.

The video monitor, which is part of the EyeTrac system, served both as the point-of-gaze and target display. As such it could be used in secondary visual feedback (2VFB) experiments (8, 9, 10), in which the point-of-gaze is displayed to the observer in addition to a point target. In the experiments described below, however, the 2VFB was not implemented other than for calibration purposes.

Targets were generated on a dual beam oscilloscope, mounted sideways to allow driving two targets independently via the vertical amplifiers using signal generators. This permits having dual target paradigms involving time sharing tasks where the primary target may, for example, be slowly moving thereby eliciting smooth pursuit whereas the secondary target may appear abruptly at various eccentricities, the task being one of detection and acquisition. Such dual tasks are currently under investigation and will be pursued in a follow-up research program.

The target stimuli were transmitted via a TV-camera and superimposed on the video point-of-gaze display unit (VD in Fig. 1) so as to have an effective diameter of $0.4^{o}$ on the video display.

Masking field was generated by projection of a polarized texture slide and was superimposed on the visual axis by means of a beam splitter. As indicated in Fig. 2, this was superimposed in a rather awkward way, because of the lack of a rear projection screen, to avoid glare. For the same reason, the video display was oriented somewhat obliquely and as such gave rise to a symmetric left vs right response. Masking dynamics were generated by rotating a polarizer situated in front of the masking field projector. It is estimated that most of the texture spatial spectrum was below $1^{c}$/deg.

Target generator signal and eye movement response were recorded on a strip chart recorder at a paper speed of 10mm/sec.

## IV. RESULTS AND DISCUSSION

In this report we summarize results of experiments involving tracking of the primary target only, alternating between two fixed positions which

were separated by $18^{0}$ symmetrically with respect to the egocentric axis (Table 1). Whereas target positions were fixed in all experiments covered by this report, and as such may have affected predictive control of eye movement, timing of target transition was either periodic or aperiodic (indicated by P/AP in Table 1). These kind of stimulus conditions resulted in false alarm transitions to the right position in the absence of target transition. This phenomenon was even more pronounced once masking noise was superimposed and appeared to subserve the function of exploratory glimpses (see examples in Fig. 3).

Data summarized in Table 1 and Fig. 4 demonstrate that as target luminance decreases, saccadic latency increases; note that in most cases the variability is much smaller at higher luminance. This is consistent with previous findings (5) and should be taken into consideration in the design of ASPT. The effect of target luminance on saccadic latency is further substantiated once masking noise is introduced. This too is consistent with a previous result demonstrating that noise masking is more effective than coherent masking at the same contrast level (11, 12). However, this study was concerned with detection and masking of spatial frequency whereas our study is devoted to point target detection and tracking.

The dynamic aspect of vision is too often overlooked and most vision research has been dedicated to processing of spatial information. However, information flow in both actual flight and flight simulators is obviously dynamic as are the characteristics of noise generated by display systems. It is therefore important to compare the masking effects of static and dynamic noise on target detection and tracking. The results of Table 1 and Fig. 5 clearly demonstrate that compared with static noise, dynamic noise of the same spatial spectrum and contrast has a significantly more detrimental effect on subjects performance. This effect is manifested by both longer reaction time (subjects DA and CH) and higher rate of misses and false alarms. This should be expected in view of the fact that visual channels at the preprocessing stages are endowed with spatio-temporal characteristics (13) and as such are likely to mediate the corresponding spatio-temporal masking effects on saccadic latency (14).

## V. RECOMMENDATIONS

Current developments in state-of-the-art visual display technology focus on the implementation of eye-slaved imagery for air-to-air and air-to-surface weapons delivery training. Consequently, it becomes increasingly important to establish the range of effective stimulus parameters for visual cuing. Given the present results concerning saccadic latency as a function of stimulus intensity and background masking, it is recommended that future research concentrate on establishing the critical bandwidths for spatio-temporal masking. Also, it is important to determine how these critical frequencies are related to target size, and what the effects of target eccentricity are on detection, since it is known that both resolution and temporal frequency characteristics vary with target eccentricity (15).

Finally, this study suggests that visual tasks with which the pilot is confronted can be fruitfully studied outside of ASPT. It is, therefore, recommended that efforts to establish a basic visual research laboratory at AFHRL be expanded, and that the present study be replicated therein with fighter pilots.

## REFERENCES


1. A. L. Yarbus, Eye Movements and Vision, Plenum Press. New York, 1967.

2. J. W. Senders, D. F. Fisher and R. A. Monty, Ed's., Eye Movements and Higher Psychological Functions, Lawrence Erlbaum Assoc., Publishers, Hillsdale, N.J., 1978.

3. G. Westheimer, "Eye Movement Responses to Horizontally Moving Visual Stimulus, " Arch. Ophthalmol. Vol. 52, pp. 932-971. 1954.

4. L. Stark, G. Vossius and L. R. Young, "Predictive Control of Eye Tracking Movements, "IRE Trans. Human Factors Electron. Vol. 3, pp. 52-57, 1962

5. L. L. Wheeless, G. H. Cohen and R. M. Boynton, "Luminance as a Parameter of the Eye-Movement Control System, "J. Opt. Soc. Am., Vol. 57, pp. 394-400, 1967.

6. R. B. Hackman, "An Experimental Study of Variability in Ocular Latency, "J. Exp. Psychol., Vol. 27, pp. 548-558, 1940.

7. W. R. Miles, "The Reaction Time of the Eye," Psychol. Monog, Vol 47, pp. 268-293, 1963.

8. Y. Y. Zeevi, E. Peli and L. Stark, "Study of Eccentric Fixation with Secondary Visual Feedback," J. Opt. Soc. Am., Vol. 69, pp.669-675, 1979.

9. Y. Y. Zeevi and E. Peli, "Latency of Peripheral Saccades," J. Opt. Soc. Am., Vol. 69, pp. 1274-1279, 1979.

10. E. Peli and Y. Y. Zeevi, "Multiple Feedback Loops in Eye Movement Control," Proc. XII International Conf. Med. and Biol. Engineering, Jerusalem, August 1979.

11. C. F. Stromeyer and B. Julesz, "Spatial Frequency Masking in Vision-Critical Band and Spread of Masking." J. Opt. Soc. Am., Vol. 62, pp. 12-21, 1972.

12. R. E. Kronauer and C. F. Stromeyer, Personal Communication, 1980.

13. H. Gafni and Y. Y. Zeevi, "A Model for Separation of Spatial and Temporal Information in the Visual System," Biol. Cybernetics, Vol. 28, 73-82, 1977.

14. Y. Y. Zeevi, J. C. De Maio and T. M. Longridge, "Spatio-temporal Masking Effects on Saccadic Latency," to be submitted to J. Opt. Soc. Am.

15. T. Fukuda, "Relation Between Flicker Fusion Threshold and Retinal Eccentricity," Percept Motor Skills, Vol 49, pp. 3-17, 1979.

TABLE 1

Saccadic Latency in Tracking of Periodic (P) and Aperiodic (AP) Targets Masked by Static (ST) or Dynamic (DY) Texture Patterns. Luminance (L) is Given in Foot-Lamberts.

| S | L | P/AP | NOISE | $\bar{X}$ | 95% INT | N |
|---|---|---|---|---|---|---|
| DA | 6.6 | P | NO | 252 | 213-291 | 35 |
| DA | 6.6 | AP | NO | 336 | 292-380 | 40 |
| DA | 11.0 | P | NO | 209 | 198-220 | 41 |
| DA | 11.0 | P | ST | 370 | 323-417 | 47 |
| DA | 11.0 | P | DY | 447 | 403-491 | 68 |
| DA | 11.0 | AP | NO | 232 | 214-250 | 40 |
| DA | 11.0 | AP | ST | 433 | 379-487 | 37 |
| DA | 11.0 | AP | DY | 519 | 458-580 | 55 |
| DA | 15.0 | P | DY | 230 | 211-249 | 34 |
| DA | 15.0 | AP | ST | 271 | 255-287 | 76 |
| DA | 15.0 | AP | DY | 302 | 286-318 | 79 |
| CH | 6.6 | P | NO | 318 | 303-335 | 65 |
| CH | 6.6 | AP | NO | 394 | 346-442 | 35 |
| CH | 6.6 | AP | ST | 570 | 472-668 | 47 |
| CH | 6.6 | AP | DY | 582 | 513-651 | 41 |
| CH | 9.2 | P | DY | 381 | 347-415 | 60 |
| CH | 11.0 | P | NO | 255 | 228-282 | 66 |
| CH | 11.0 | AP | NO | 316 | 291-341 | 68 |
| CH | 15.0 | AP | ST | 276 | 263-289 | 88 |
| CH | 15.0 | AP | DY | 305 | 289-321 | 77 |
| JK | 6.6 | P | NO | 273 | 252-294 | 33 |
| JK | 6.6 | AP | NO | 406 | 355-457 | 33 |
| JK | 11.0 | P | NO | 227 | 216-238 | 66 |
| JK | 11.0 | AP | NO | 279 | 266-292 | 85 |
| JD | 6.6 | P | NO | 275 | 234-316 | 52 |
| JD | 6.6 | AP | NO | 336 | 305-367 | 44 |
| JD | 11.0 | P | NO | 231 | 216-246 | 104 |
| JD | 11.0 | AP | NO | 234 | 226-242 | 104 |

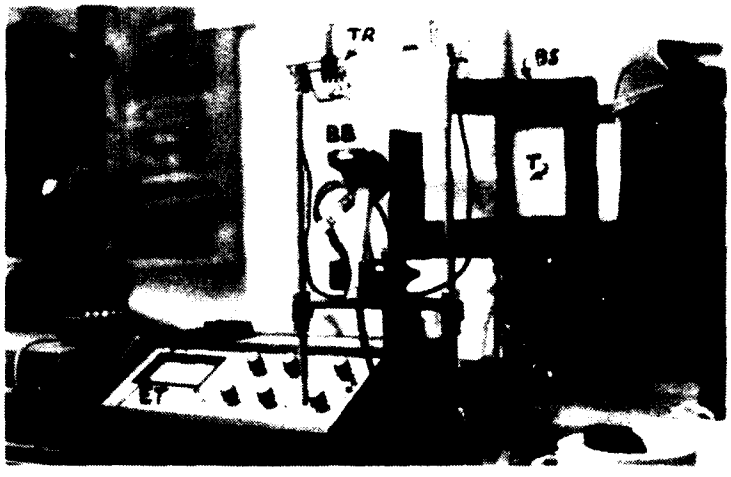
Fig. 1 - Laboratory for eye movement measurements setup at AFHRL, Williams AFB.
TR - transducer, BB-bite bar, T-target,
BS - beam splitter, VD - video display,
RP - rotating polarizer, NP - noise projector,
TG - target generator, TG - target display,
TVC - TV camera, ET - Model 200 Eye Trac.

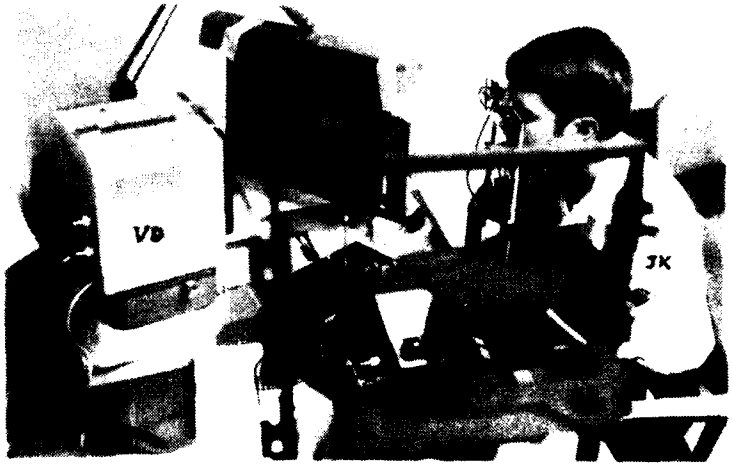
Fig. 2 - Schematic diagram of the setup for eye movement measurements in target detection and tracking tasks.

Fig. 3 - Examples of false alarms and misses in tracking aperiodic target masked by noise.

Fig. 4 - Saccadic latency in tracking periodic (circles) and aperiodic (squares) point target vs. target luminance.

Fig. 5 - Saccadic latencies in tracking periodic (a) and aperiodic targets (b) masked by noise. (Circles target above, X's - target masked by static noise, squares - target masked by dynamic noise)



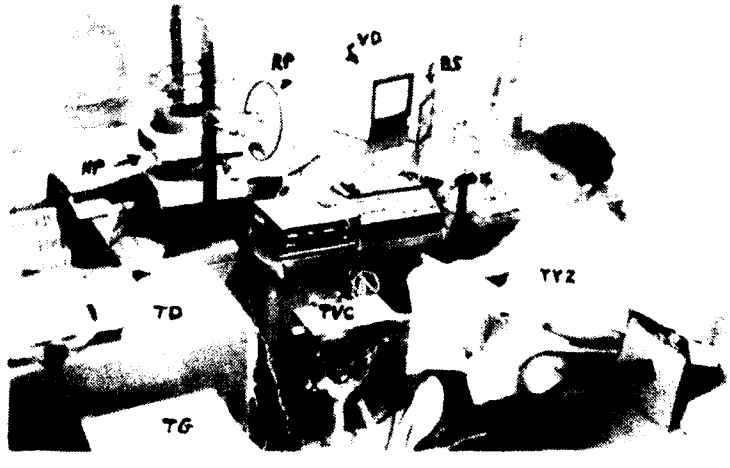




Fig. 1

87-12

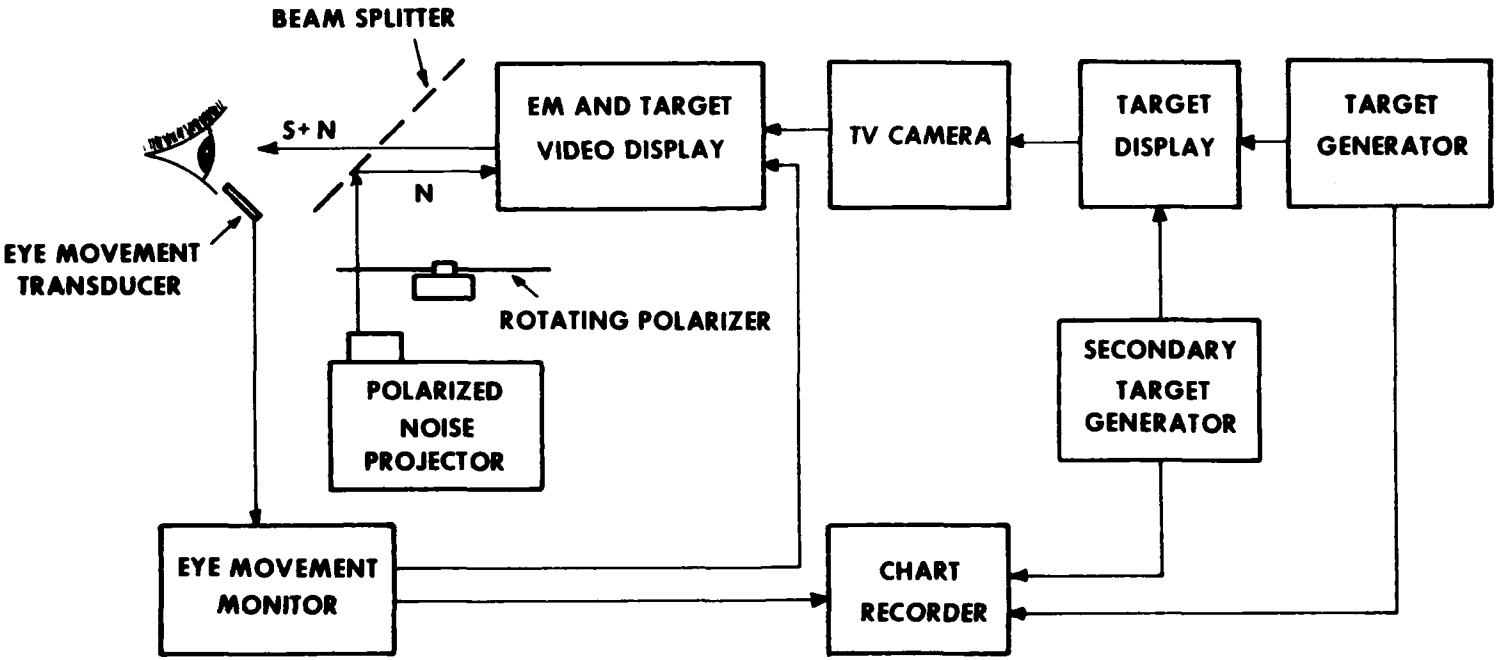

BEAM SPLITTER
S+N
N
EM AND TARGET VIDEO DISPLAY
TV CAMERA
TARGET DISPLAY
TARGET GENERATOR
EYE MOVEMENT TRANSDUCER
ROTATING POLARIZER
POLARIZED NOISE PROJECTOR
SECONDARY TARGET GENERATOR
EYE MOVEMENT MONITOR
CHART RECORDER

Fig. 2

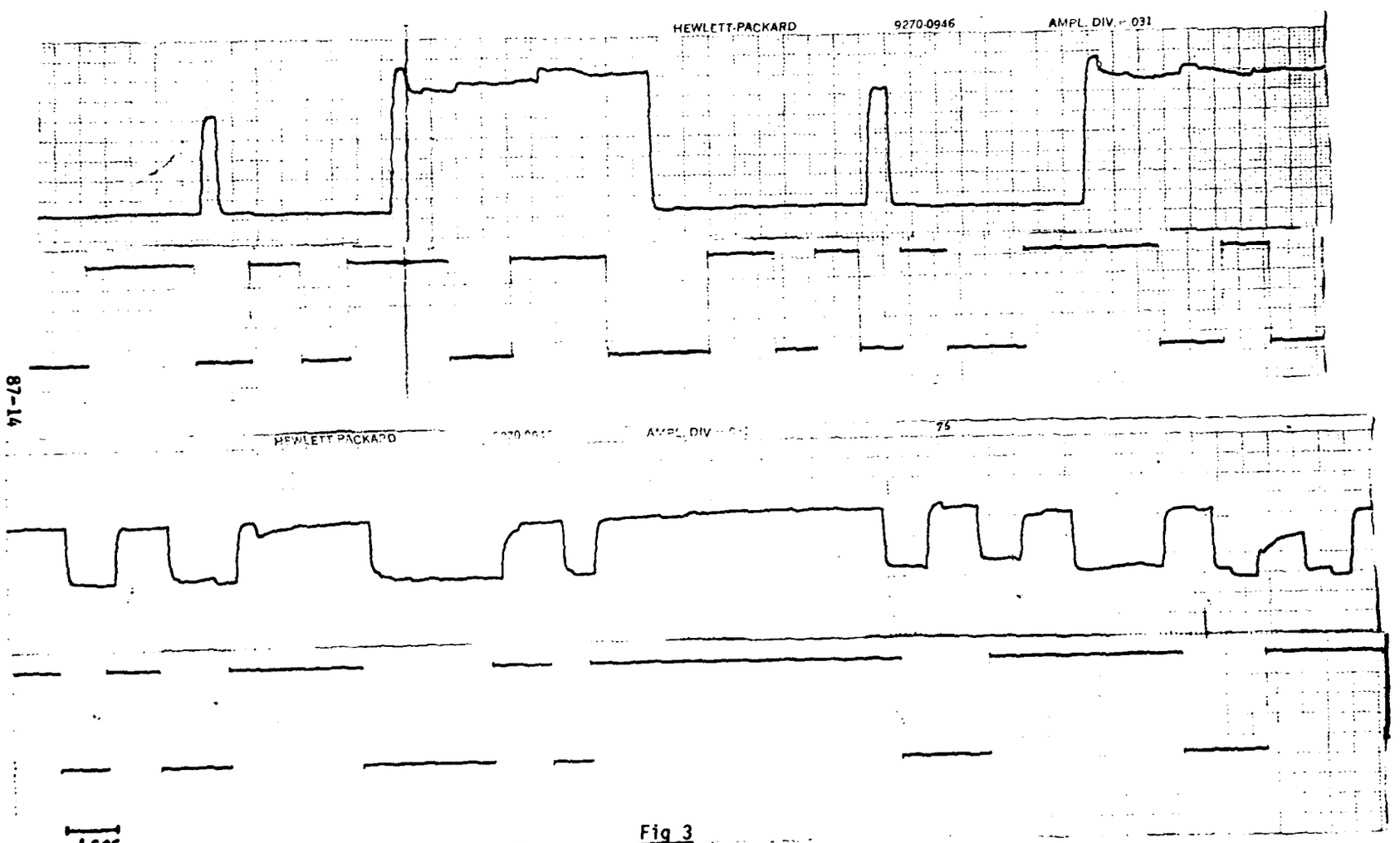

HEWLETT-PACKARD
9270-0946
AMPL. DIV. - 031
87-14
HEWLETT PACKARD
75
1sec.

Fig 3

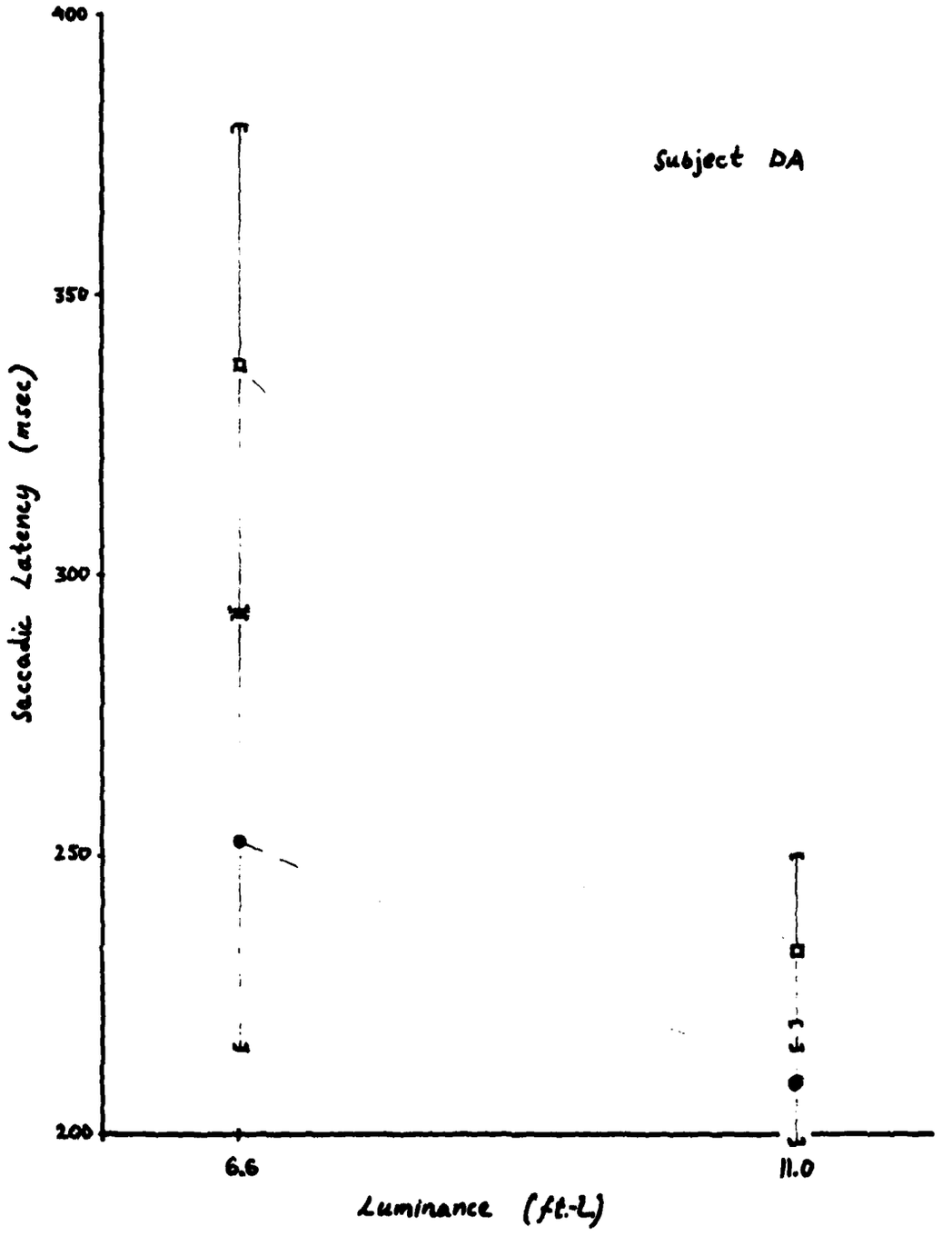

Subject DA
400
350
300
250
200
Saccadic Latency (msec)
6.6
11.0
Luminance (ft.-L)

Fig. 4a.
87-15

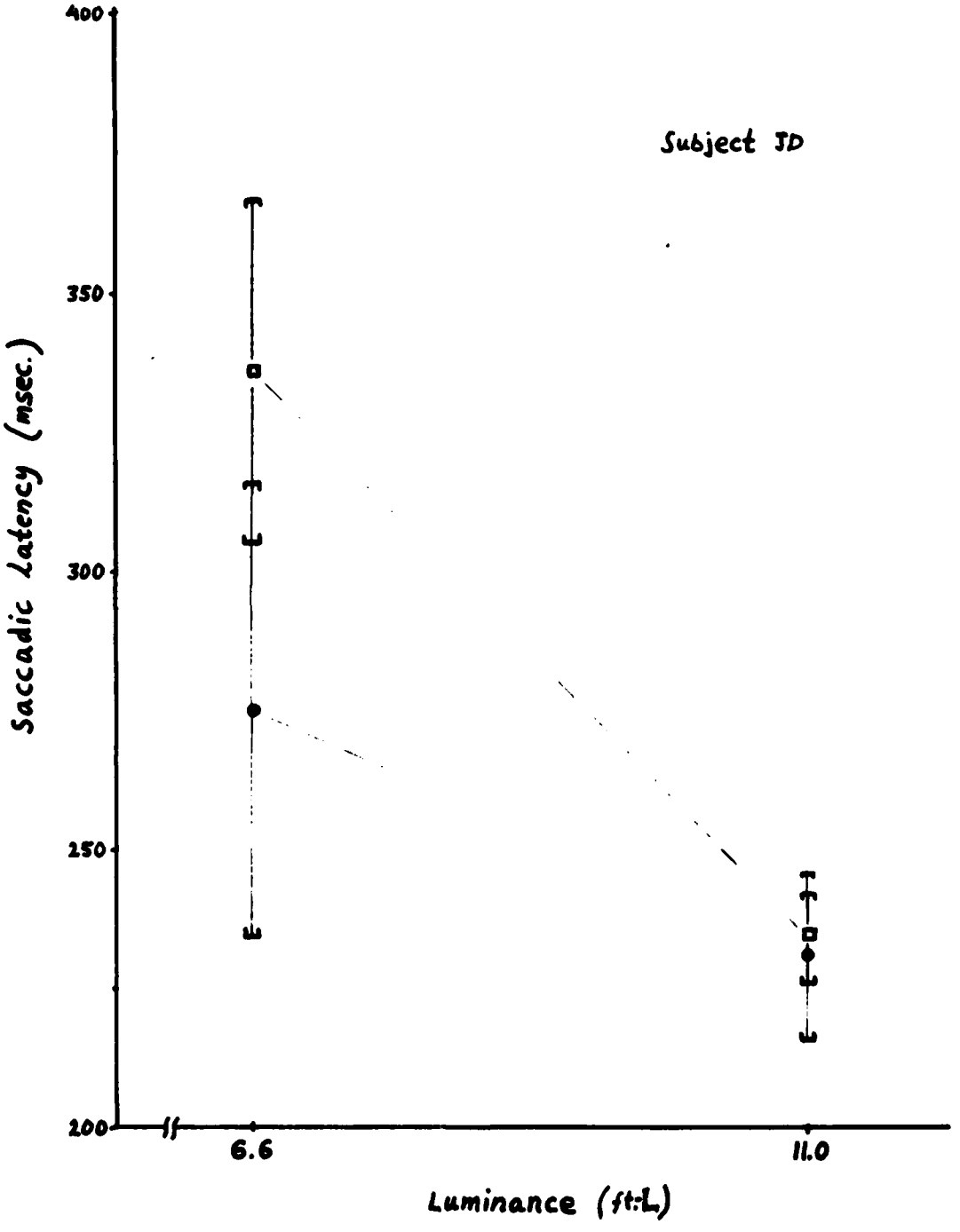

Subject JD
400
350
300
250
200
Saccadic Latency (msec.)
6.6
11.0
Luminance (ft-L)

Fig. 4b
87-16

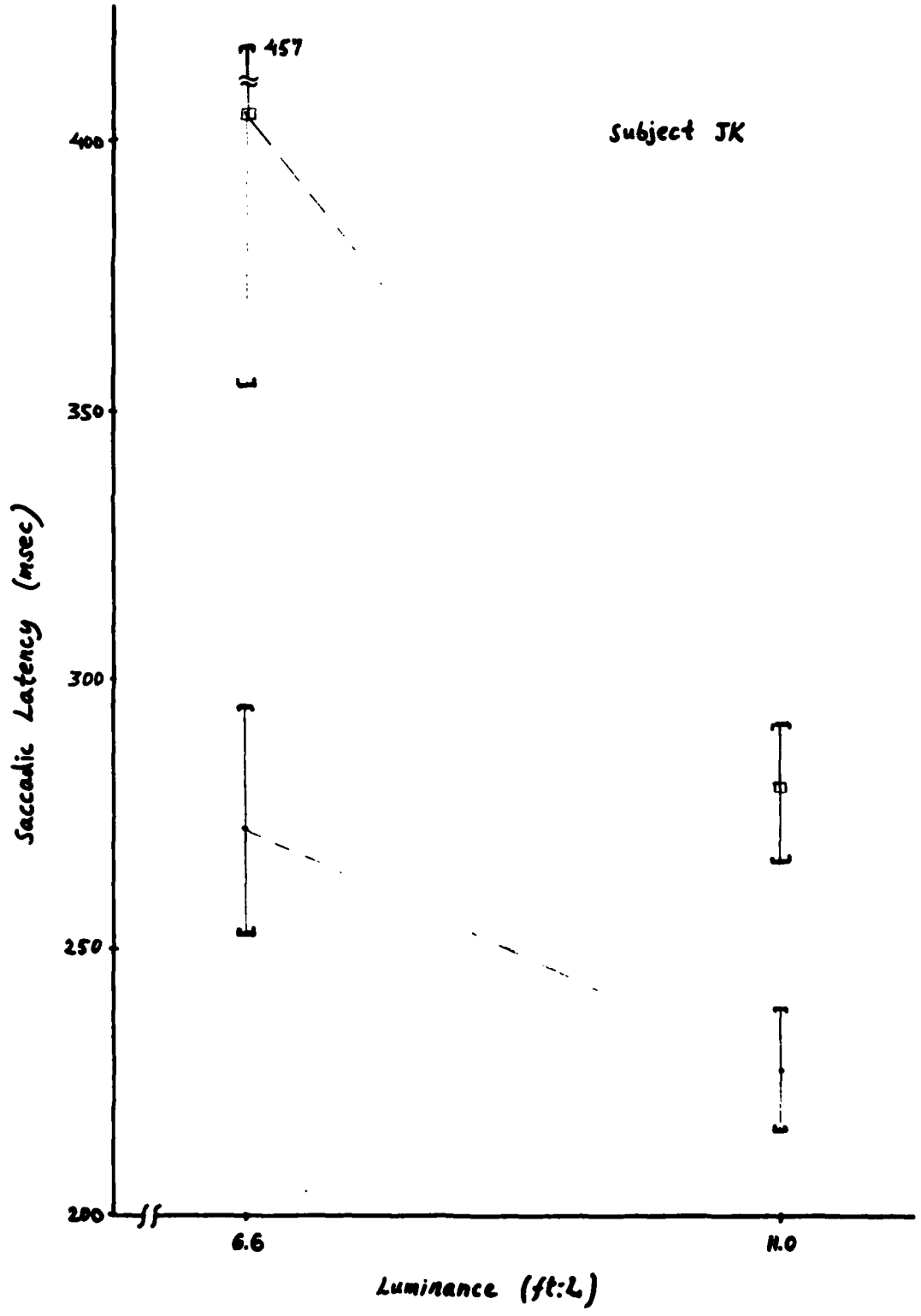

457
Subject JK
400
350
300
250
200
Saccadic Latency (msec)
6.6
11.0
Luminance (ft:L)

Fig 4c
87-17

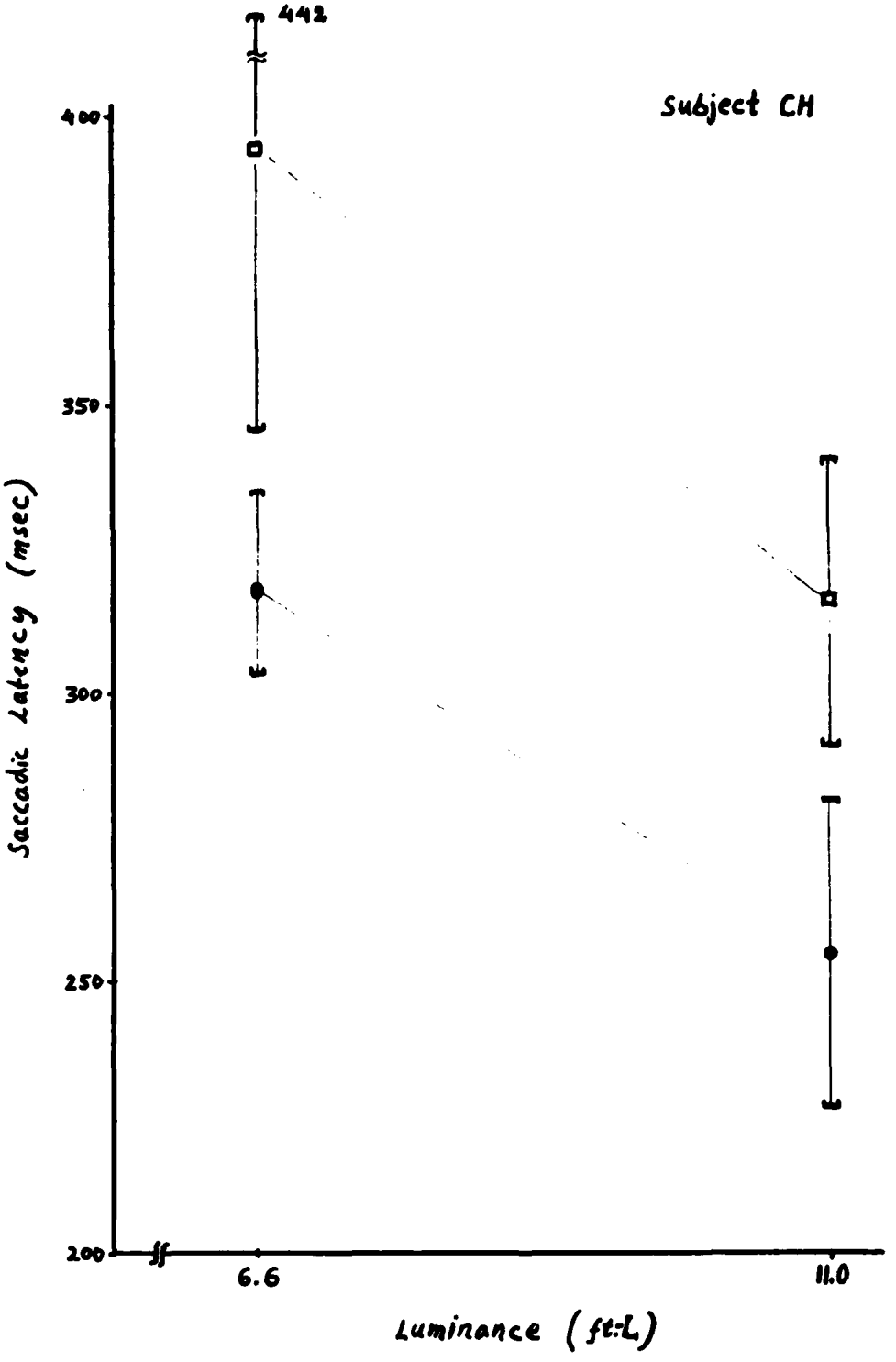

442
Subject CH
400
350
300
250
200
Saccadic Latency (msec)
6.6
11.0
Luminance (ft:L)

Fig 4d

87-18

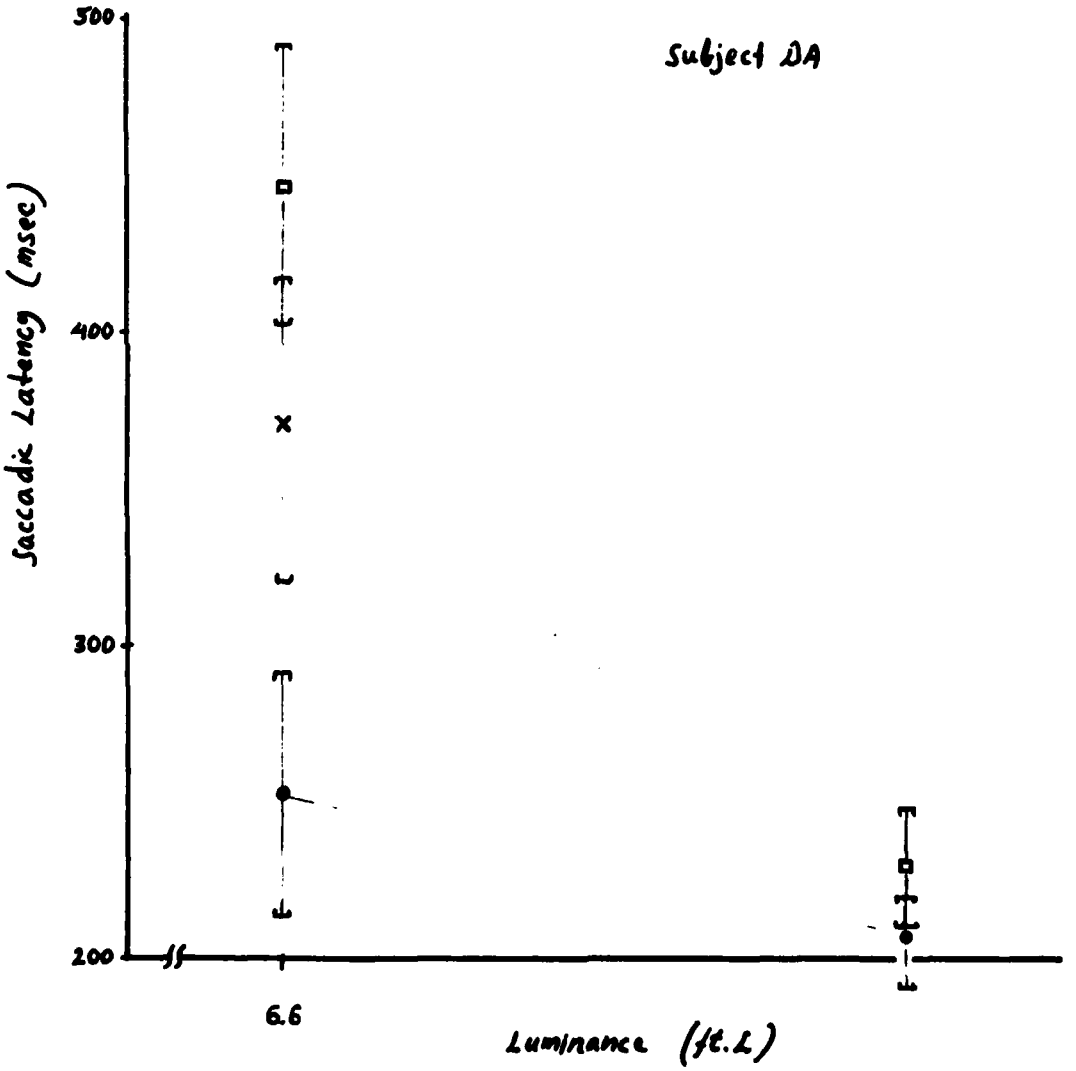

Subject DA
500
400
300
200
Saccadic Latency (msec)
6.6
Luminance (ft.L)

Fig. 5a
87-19

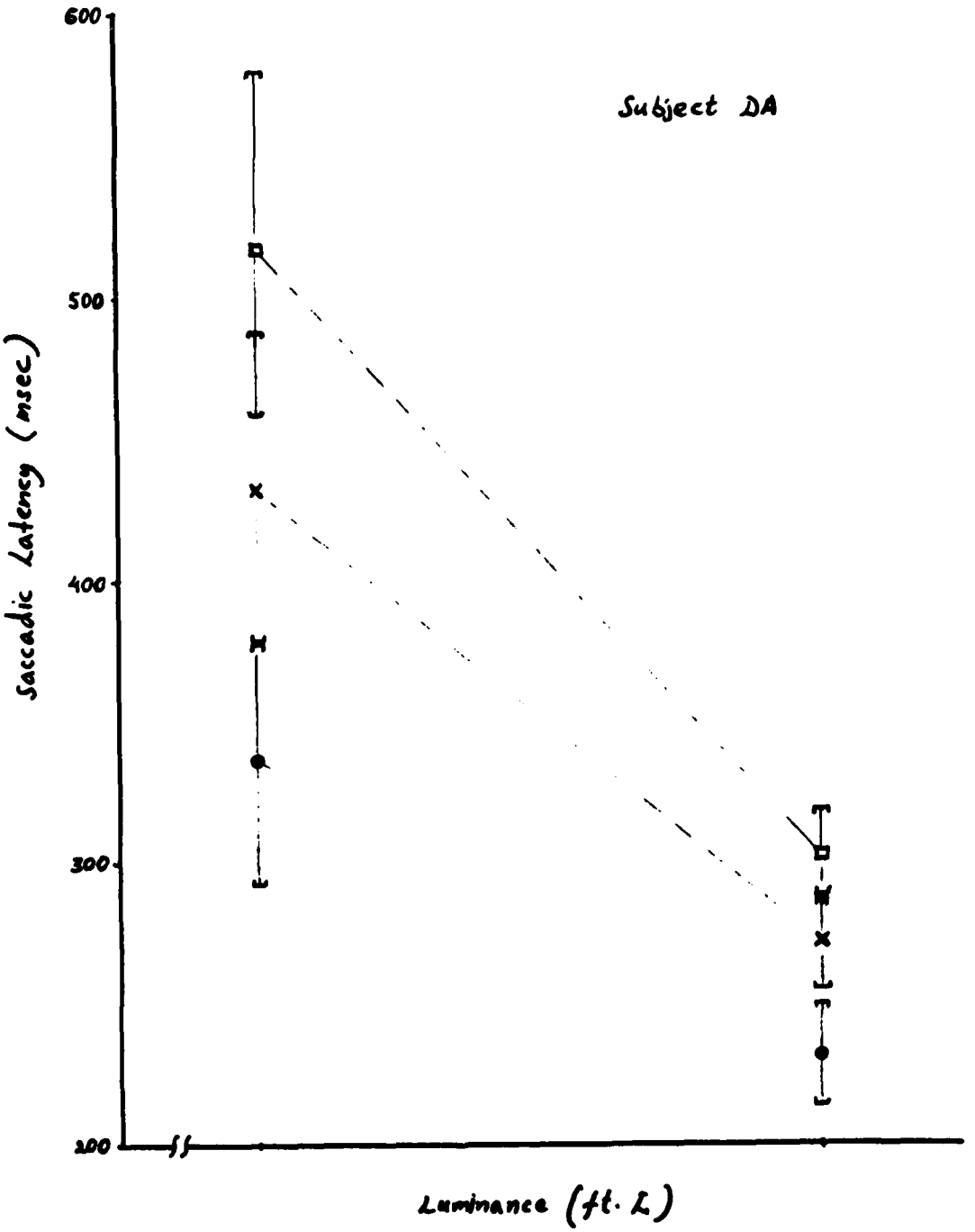
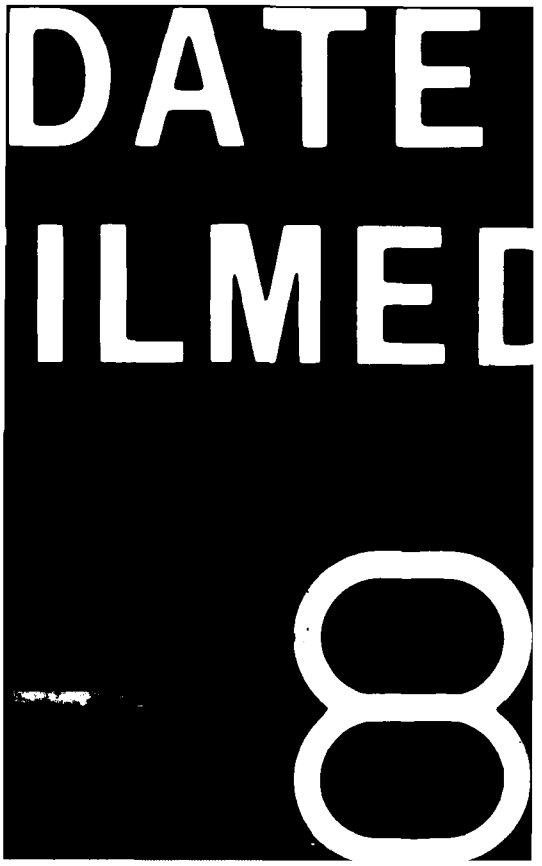

Subject DA
600
500
400
300
200
Saccadic Latency (msec)
Luminance (ft. L)

Fig. 5b
87-20


DATE
ILMED
8